UNIVERSITAT DE BARCELONA

Morfología del sistema digestivo y larvicultura del centollo (*Maja brachydactyla*, Balss 1922)

Diego Castejón Bueno

Aquesta tesi doctoral està subjecta a la llicència ***Reconeixement- NoComercial – SenseObraDerivada 3.0. Espanya de Creative Commons***.

Esta tesis doctoral está sujeta a la licencia ***Reconocimiento - NoComercial – SinObraDerivada 3.0. España de Creative* Commons**.

This doctoral thesis is licensed under the ***Creative Commons Attribution-NonCommercial-NoDerivs 3.0. Spain License***.

MORFOLOGÍA DEL SISTEMA DIGESTIVO Y LARVICULTURA DEL CENTOLLO (*Maja brachydactyla*, Balss 1922)

Tesis Doctoral

DIEGO CASTEJÓN BUENO

Marzo 2018

Programa de Doctorado de Biodiversidad (Universidad de Barcelona)

Institut de Recerca i Tecnologia Agroalimentàries (IRTA)

Institut de Ciències del Mar (ICM-CSIC)

MORFOLOGÍA DEL SISTEMA DIGESTIVO Y LARVICULTURA DEL CENTOLLO (*Maja brachydactyla*, Balss 1922)

Memoria presentada por

DIEGO CASTEJÓN BUENO

para optar al grado de Doctor por la Universidad de Barcelona

Barcelona, Marzo de 2018

El doctorando,

Fdo. Diego Castejón Bueno

Dirección	Codirección	Tutoría
Dr. Guillermo Guerao Serra	Dra. Guiomar Rotllant Estelrich	Dr. Enric Ribes Mora

A mis padres, Diego y Pepita

A Montse

La elaboración de una Tesis Doctoral no es una tarea solitaria. Su elaboración ha sido posible gracias a la ayuda y colaboración de muchísimas personas, que han permitido desde la financiación inicial hasta la redacción final y publicación de los artículos científicos. Las palabras no bastan para agradecer a todos aquellos que me han ayudado durante estos años.

La financiación fue posible gracias a la concesión de una beca para la formación de personal investigador en los centros de investigación agraria y alimentaria INIA-CCAA (FPI-INIA). Dicha beca, así como la propia Tesis, han estado financiadas en el marco del proyecto «Optimización del cultivo larvario de *Maja brachydactyla*: parámetros ambientales y nutrición» de código RTA2011-00004-00-00. Su subvención fue aprobada por el Instituto Nacional de Investigación y Tecnología Agraria y Alimentaria (INIA) y el Ministerio de Economía y Competitividad del Gobierno de España. En este marco también debo agradecer a Julián Barrera por toda su ayuda con los trámites asociados a esta beca.

No hay palabras suficientes para agradecer a Guillermo Guerao, Guiomar Rotllant y Enric Ribes por haber apostado por mí, así como por sus enseñanzas, ayuda y consejos. Más allá de su papel de director y co-directora, Guillermo ha sido un mentor inestimable en mi camino iniciático en el mundo larvario de los decápodos y Guiomar un enfoque distinto pero necesario a la hora de apuntalar los trabajos. Enric, más allá de su papel de tutor en la Universidad de Barcelona, es piedra angular de los estudios que han profundizado en la morfología de estos animales. También quiero darle las gracias a Gabriela Torres y Luis Giménez de la School of Ocean Sciences (Bangor University, Reino Unido) por su buena acogida en Menai Bridge, así como su ayuda en la realización de análisis tanto bioquímicos como estadísticos. A la Dra. María Font i Furnols de las instalaciones IRTA de Monells (Girona) y al Dr. Javier Alba-Tercedor de la Universidad de Granada, por su inestimable colaboración para reconstruir mediante modelos virtuales de tomografía la anatomía de estos animales. La labor de todos ellos en la redacción de los artículos de investigación ha sido clave. También quiero darles las gracias a Piero G. Giulianini, Alberto Pallavicini y Chiara Manfrin de la Università di Trieste (Italia) por acogerme en el bello paraje de Trieste y por sus enseñanzas en el ámbito de la transcriptómica, así como el muestreo, manejo, disección y anatomía del cangrejo de río americano *Procambarus clarkii*.

También quería darle las gracias a Joan Navarro del Institut de Ciències del Mar (ICM-CSIC) por darme la oportunidad de darle los últimos toques a la Tesis trabajando desde dicho centro, así como a Joan Baptista Company del mismo lugar por financiarme la impresión de la versión física de la presente memoria.

Desde los primeros años de la década del 2010, la investigación nacional tuvo que enfrentarse a una difícil situación derivada de la crisis económica que inició la década. Una de sus consecuencias fue la disolución de varios grupos de investigación. Por ello, estoy agradecido con Dolors Furones y Alicia Estévez por permitirme continuar con la realización de esta Tesis en el centro IRTA de Sant Carles de la Ràpita, así como por facilitarme en lo posible, dadas las circunstancias, las tareas de investigación. Quería agradecer a Karl B. Andree y al profesor Peter Mather por su ayuda en la corrección lingüística de determinados artículos, así como a Enric Gisbert, Ignasi Gairin y Neil Duncan por los consejos dados y buenos momentos.

La ayuda del personal técnico del centro IRTA de Sant Carles de la Ràpita ha sido crucial durante todos estos años. Debo darles las gracias a Marta Sastre y Olga Bellot por sus enseñanzas y consejos en relación a las técnicas y tareas de laboratorio. También agradecer a Mari Pau Balague y Noelia Gras por su ayuda en el mismo. A David Carmona, Esteban Hernández, Glòria Macià, Iván Costa, Josep Lluís Celades, Magda Monllaó, Rafael Gras, Sandra Molas y Xavier Ingla. Por ocuparse de los adultos y ayudarme con la instalación del sistema experimental diseñado para el cultivo larvario, gracias a ellos pude contar con un área estupenda para emprender los cultivos a pequeña escala. Tampoco me olvido de Josep Cid por el soporte informático brindado. Así como de Anna Salleras, a la que no atormentaré más con la búsqueda de aquellas *rarae aves* de las bibliografía. También agradecer al cuerpo administrativo, David Vallès, Maite Caballer, María Jesus Belvis y Romina Ventura, nuestra primera línea de defensa frente a las complicaciones de la burocracia.

Las tareas de microscopía electrónica han sido posibles gracias al personal de los Centres Científics i Tecnològics de la Universitat de Barcelona (CCiTUB) del Hospital Clinic, Adriana Martínez, Almudena García, José Manuel Rebled y Rosa Rivera. Gracias chic@s por tan estupenda ayuda y mejor trabajo, sé que os lo puse difícil con las larvas.

Y como no, a mis queridos compañeros de venturas y desventuras, algunos de ellos becarios en su día y doctores hoy. Gracias a ellos vivir en Sant Carles de la Ràpita realmente mereció la pena, imposible olvidar a Almudena Martínez, Ana Genua, Carles Alcaraz, Cindy Campoverde, Diana Garibo, Elvira Fatsini, Kruno Bonacic, Lucía Soliño, María García-Altares, Maria Rey, Mohamed Abdelmoneam, Nuria Salas, Xavier Benito y Zohar Ibarra. ¡Y las geniales salidas bicheras de Pere Josa! A todos ellos debo recordarles por todos aquellos buenos momentos y recuerdos inolvidables.

A Montse García, por estar siempre ahí y apoyarme en los buenos y malos momentos.

Por supuesto, a mis padres. Diego y Pepita. Por básicamente... todo.

Moltes gràcies a tots!!!

Realizar esta Tesis ha requerido contactar con el pasado, incluso he tenido que retrotraerme a trabajos realizados hace casi dos siglos, cuya calidad no deja de asombrarme. Pero en realidad, nuestras raíces son mucho más antiguas, algunas ya aparecen en la Grecia Clásica. Incluso en el caso de la carcinología, esa actividad científica que intenta entender la biología de los pancrustáceos no insectos, tiene apéndices en contacto con aquella cultura. Sin ir más lejos, el filósofo griego Aristóteles describió de forma somera varias especies de decápodos y realizó una de las primeras clasificaciones de este grupo. Este contacto con el pasado se conserva hoy día, ya que diversos géneros de braquiuros toman su nombre directamente de los mitos clásicos: *Scylla* y *Charybdis*, terribles monstruos que guardaban el Estrecho de Mesina y a las que Odiseo tuvo que hacerles frente; *Menippe*, *Panopeia* y *Xantho*, criaturas míticas del Mar Mediterráneo llamadas ninfas y nereidas y bendición de marineros; *Parthenope*, una de las sirenas que murió al no conseguir hechizar a Odiseo con su canto; *Dorippe*, madre del soberano Hellen; *Eriphia*, una de las Nisíades o ninfas del Monte Nisa, las cuales cuidaron al dios Dioniso durante su infancia. Incluso el propio cangrejo *Karkinos* / *Cancer* fue una criatura comandada por Hera, que murió al enfrentarse a Heracles mientras este combatía a la Hidra de Lerna, a su muerte se convirtió en elemento del Zodiaco.

El centollo conserva este contacto con el pasado. Hoy los zoólogos lo llamados *Maja*, derivado de *Maia*, nombre por el que probablemente era conocido por algunas gentes de la Grecia Clásica. Maia también era un ser mítico de ese pasado lejano. De un modo u otro, los científicos siempre tenemos una forma de recordar de dónde venimos.

Maia la de vivaz mirada, por Atlas engendrada, la más excepcional en belleza de entre sus siete hermanas de violáceos cabellos, las llamadas Pléyades.

Simónides (s. VI-V AEC)

Maia, la Ninfa de hermosos bucles […], ella, la diosa venerable. En su modestia evitó la compañía de los bendecidos dioses ocultándose en el interior de una oscura gruta. Allí en la penumbra se unía el Crónida a la Ninfa de hermosos rizos en la negrura de las noches, inadvertidos para dioses inmortales y hombres mortales. […]

Entonces cuando la décima Luna se alzó en el cielo, ella dio a luz y notables prodigios habrían de suceder. […] Yo le bendigo, descendiente de Zeus y *Maia*.

Homero (s. VII-IV AEC)

ÍNDICE DE CONTENIDO

1. INTRODUCCIÓN GENERAL 1

1.1 Etimología. 3

1.2 Taxonomía y filogenia 4

1.3 Biología del Centollo, *Maja brachydactyla* Balss, 1922 18

1.4 Bibliografía 33

2. OBJETIVOS Y ESTRUCTURA. 47

3. INFORME DEL DIRECTOR. 51

4. BLOQUE 1. LARVICULTURA. INTRODUCCIÓN. 57

4.1 Importancia económica del centollo 59

4.2 Centollo como especie acuícola. Experiencias 64

4.3 Objetivos del BLOQUE 1 70

4.4 Diseño experimental del BLOQUE 1 73

4.5 Bibliografía 83

5. The Effects of Temperature and Salinity on the Survival, Growth and Duration of the Larval Development of the Common Spider Crab *Maja brachydactyla* (Balss, 1922) (Brachyura: Majidae) 91

6. Influence of temperature and light regime on the larval development of the common spider crab *Maja brachydactyla* Balss, 1922 (Brachyura: Majidae) 131

7. Factors influencing successful settlement of the common spider crab *Maja brachydactyla* Balss, 1922 (Brachyura: Majidae): impacts of individual vs conspecific culture, adult exudates and settlement substrates 171

8. BLOQUE 1. LARVICULTURA. DISCUSIÓN 197

8.1 Parámetros ambientales óptimos de cultivo larvario 200

8.2 Sobre el asentamiento y el cultivo de juveniles 204

8.3 Conclusiones y nuevas preguntas 214

8.4 Bibliografía 216

9. BLOQUE 2. SISTEMA DIGESTIVO. INTRODUCCIÓN.....229

9.1 Sistema Digestivo de los decápodos. Caracteres generales. 231

9.2 Anatomía interna del centollo: antecedentes.....236

9.3 Objetivos del BLOQUE 2 241

9.4 Diseño experimental aplicado en el BLOQUE 2.....244

9.5 Bibliografía.....263

10. Exploring the internal morphology of the larvae digestive system of *Maja brachydactyla* Balss, 1922 using micro computed tomography: Assessment of spatial resolution 275

11. Morphology and ultrastructure of the esophagus during the ontogeny of the spider crab *Maja brachydactyla* (Decapoda, Brachyura, Majidae) 327

12. Foregut morphology and ontogeny of the spider crab *Maja brachydactyla* (Brachyura, Majoidea, Majidae) 367

13. Morphology of the stomach cuticle during the ontogeny of the spider crab *Maja brachydactyla* (Decapoda, Brachyura, Majidae).....407

14. Morphology and ontogeny of the midgut gland ("hepatopancreas") of the Atlantic spider crab *Maja brachydactyla* Balss, 1922 (Brachyura, Majidae) 451

15. Histology and ultrastructure of the adult and larval midgut gland ("hepatopancreas") of the Atlantic spider crab *Maja brachydactyla* Balss, 1922 (Brachyura, Majidae).....493

16. Morphology and ontogeny of the midgut tract in the spider crab *Maja brachydactyla* (Brachyura, Majidae) 545

17. Morphology and ontogeny of the midgut caeca in the spider crab *Maja brachydactyla* (Brachyura, Majidae).....581

18. Morphology and ontogeny of the hindgut tract in the spider crab *Maja brachydactyla* (Brachyura, Majidae) 615

19. BLOQUE 2. SISTEMA DIGESTIVO. DISCUSIÓN 651

19.1 Iniciación en el estudio anatómico de las larvas de decápodos 654

19.2 Sobre los derivados del ectodermo y endodermo 661

19.3 Sistema digestivo adulto y larvario: semejanzas y diferencias 667

19.4 El sistema digestivo durante el desarrollo larvario 676

19.5 El estómago y especializaciones de la cutícula 677

19.6 Micro-espinas y setas en los órganos derivados del ectodermo 689

19.7 Glándulas de roseta, más preguntas que respuestas 698

19.8 Células M de la órgano perigástrico como posibles células basales 706

19.9 Actividad secretora en el sistema digestivo 710

19.10 Conclusiones y nuevas preguntas 721

19.11 Bibliografía 725

20. CONCLUSIONES 745

21. ANEXO: ARTÍCULOS PUBLICADOS 749

INTRODUCCIÓN GENERAL

"No group of plants or animals on the planet exhibits the range of morphological diversity seen among the extant Crustacea"

Joel W. Martin & George E. Davis 2001

1.1 Etimología.

Cangrejo. Término derivado del término latino «*cancer*», el cuál deriva del término griego «*karkínos*». Desde los tiempos de Hipócrates este nombre no solo ha referido una enfermedad, sino también a los seres que han bautizado a la misma (Cortés, 2010). El «*karkínos*», el cangrejo, evoca la imagen mental de un animal de cuerpo duro y aplanado, de aspecto más o menos cuadrangular, ojos saltones sostenidos por un largo pedúnculo, veloces patas y armado con fuertes tenazas. Resulta fácil imaginar a estos animales marinos correteando entre las rocas donde rompe el oleaje. La presente Tesis Doctoral también está dedicada a un cangrejo, pero no puede ser más diferente a esta imagen mental. También de cuerpo duro y robusto, su tamaño es enorme, el caparazón tiene forma de pera y está tachonado de espinas y tubérculos, sus ojos de reducidas dimensiones se alojan muy juntos en un pequeño rostro, es un animal que no será encontrado correteando entre las rocas de la playa ya que habita a gran profundidad. Estamos hablando de ese cangrejo conocido como centollo, animal especialmente valorado en la gastronomía ibérica.

El centollo, al menos la especie que habita el Mar Mediterráneo, ya era conocido en la antigüedad. El filósofo griego Aristóteles (siglo IV a.e.c.) hace referencia a ella usando el nombre de «*maia*», "el más grande" de todos los cangrejos, en sus obras latinizadas como *Historia Animalium* y *Partibus Animalium*. En la actual era informática sigue siendo un animal reconocido a nivel europeo recibiendo diversos nombres comunes. En lengua castellana se le conoce como «*centollo* / *centolla*» indistintamente del sexo del animal, nombre muy similar al término «*santola*» por el que es conocido en lengua portuguesa (Arias García et al., 2013). Sin embargo, el origen de los términos «*centollo* / *centolla*» es incierto. Barriuso Fernández (1986) menciona una antigua propuesta del diccionario de la lengua española, la cual postula que este término podría provenir de los término latinos «*centum-oculus*», de significado "cien ojos", como posible referencia de los tubérculos y espinas del caparazón. La Real Academia Española (RAE) y Barriuso Fernández (1986) proponen otra posibilidad: podría derivar del antropónimo celta «*Cintullus* / *Kintuollos*», de significado "principal y grande", término que en la Gascuña del medievo originaría el antropónimo «*Centot*», por el que también se aludía a esta especie de cangrejo debido a su gran tamaño. Arias García et al. (2013) afirman que el término «*centollo* / *centolla*» sufre variaciones en otras áreas de habla castellana, como «*zantollo*» (Punta Umbría, Málaga), «*zantolla*» (Málaga) y «*zontollo*» (Roquetas); en otros lugares (Sanlúcar de Barrameda, El Puerto de Santa María y Sancti Petri) los juveniles pueden ser llamados «*ladillas*» por su relativo "parecido" con el insecto parásito *Pthirus pubis*. Si el caparazón está cubierto de algas u otros epífitos también puede ser llamado «*pelón* / *peluda*» (Barriuso Fernández, 1986).

En las poblaciones bañadas por el Mar Cantábrico es llamado «*centollu*», «*pelosu*» y «*peludu*». También «*peaña*» aunque este término es compartido con la nécora *Necora puber* (Linnaeus, 1767) (Barriuso Fernández, 1986). En euskera es el «*txangurro* / *txangurru*» que ha sido castellanizado a «*changurro*». En lengua catalana los nombres más populares son «*cranca*» (denominación genérica de la hembra del cangrejo) y «*cabra de mar*», quizás debido a las espinas del rostro. Se le conoce como «*araignée de mer*» en lengua francesa, «*spinous spider crab*» en lengua inglesa, «*Atlantische seespinne*» en lengua alemana y «*grote spinkrab*» en lengua neerlandesa, todos ellos nombres que significan "araña de mar" como referencia a su cuerpo globoso y largas patas que le dan cierto parecido a una araña (Arias García et al., 2013; Fransen y Türkay, 2007).

1.2 Taxonomía y filogenia.

La siguiente clasificación taxonómica combina las bases de datos "World Register of Marine Species" (WoRMS) y "National Center for Biotechnology Information" (NBCI), así como la revisión publicada por Ortega-Hernández (2016).

Especie: *MAJA BRACHYDACTYLA* Balss, 1922

- Sinonimias: *Maja gigantea* Baudouin, 1906; *Mamaia queketti* Stebbing, 1908

Género: *MAJA* Lamarck, 1801

Subfamilia: MAJINAE Samouelle, 1819

Familia: MAJIDAE Samouelle, 1819

Superfamilia: MAJOIDEA Samouelle, 1819

Subsección: HETEROTREMATA Guinot, 1977

Sección: EUBRACHYURA Saint Laurent, 1980

Infraorden: BRACHYURA Linnaeus, 1758

Suborden PLEOCYEMATA Burkenroad, 1963

Orden: DECAPODA Latreille, 1802

Clase: MALACOSTRACA Latreille, 1802

Subfilo: PANCRUSTACEA Zrzavý & Štys, 1997 o TETRACONATA Dohle, 2001

Clado: EUARTHROPODA Lankester, 1904

Clado: ECDYSOZOA A.M.A. Aguinaldo et al., 1997

Clado: METAZOA Haeckel, 1874

Género Maja. Los miembros del género *Maja* Lamarck, 1801 son comúnmente conocidos como cangrejos araña, son habitantes comunes del Atlántico Oriental, el mar Mediterráneo y las costas del Indo-Pacífico Occidental. Son cangrejos de caparazón típicamente piriforme, si bien en ciertas especies es subcircular o subrectangular. La superficie dorsal es rica en espinas y tubérculos. Suelen presentar un par de espinas en el rostro, una desarrollada espina post-orbital formando una depresión en el lado interno donde encaja la córnea y tres pares de espinas alargadas en la mitad anterior del caparazón. Las antenas tienen un segmento basal cuadrado (igual de ancho que largo) y un flagelo antenal corto y delgado. Las patas locomotoras suelen ser cortas (Davie et al., 2015; Ng y Richer De Forges, 2015).

El nombre *Maja* es herencia directa de la primera alusión bibliográfica de este género, originaria del filósofo griego Aristóteles (siglo IV a.e.c.). Este animal aparece en dos tratados latinizados como *Historia Animalium* y *Partibus Animalium*, obras que describen y clasifican numerosos grupos animales con términos que serían heredados por las ciencias zoológicas. En lo que refiere al animal objeto de estudio en esta Tesis, Aristóteles describe un tipo de cangrejo llamado «*Maia*» como "el más grande" del grupo, que "vive en el mar" difiriendo de otros cangrejos "que viven habitualmente cerca de la orilla", "las patas son muy delgadas", "los ojos se encuentran en la línea media y juntos" difiriendo de otros cangrejos donde "[los ojos] se encuentran inmediatamente tras la parte anterior y alejados entre sí" (Cresswell, 1883; Ogle, 1912; Voultsiadou y Vafidis, 2007). El nombre «*maia*» ha sido traducido como "partera" (Voultsiadou y Vafidis, 2007), aunque en la mitología griega «*Maia*» también fue la mayor de las Pléyades y madre del dios Hermes, esta entidad mítica fue asociada con las "madres lactantes" y la diosa madre de la tierra «*Gaia*». En cualquier caso, es posible que «*Maia*» fuese simplemente el nombre local/común que le dieron a este animal en aquel tiempo y lugar.

Otra obra de gran interés histórico y zoológico es el tratado "*De reliquis animalibus exanguibus*, *utpote de mollibus*, *crustaceis*, *testaceis* & *zoophytis*", del naturalista italiano Ulisse Aldrovandi (1522-1605). Esta obra describe la morfología externa de la especie mediterránea *Maja squinado* con gran nivel de detalle y la ilustra con magníficas planchas (ver Figura 1.2.1 y 1.2.2). Las impresionantes matrices xilográficas empleadas aún se conservan en el Museo di Palazzo Poggi (Bolonia, Italia). Las planchas de Aldrovandi referidas a esta especie están rotuladas con las palabras «*Pagurus venetorum mas / faemina*» traducido como "cangrejo veneciano macho / hembra", mientras que el rótulo «*Cancer maia alius*» quizás pueda traducirse "otro cangrejo *Maia*", en ese sentido sus ilustraciones incluyen varias especies de braquiuros que por su aspecto pueden identificarse como majoideos, cuyo aspecto físico recuerda a *Maja squinado*. Es llamativo que el nombre por el que se conoce este género haya perdurado por más de dos mil años, siendo su uso recurrente a través de los siglos.

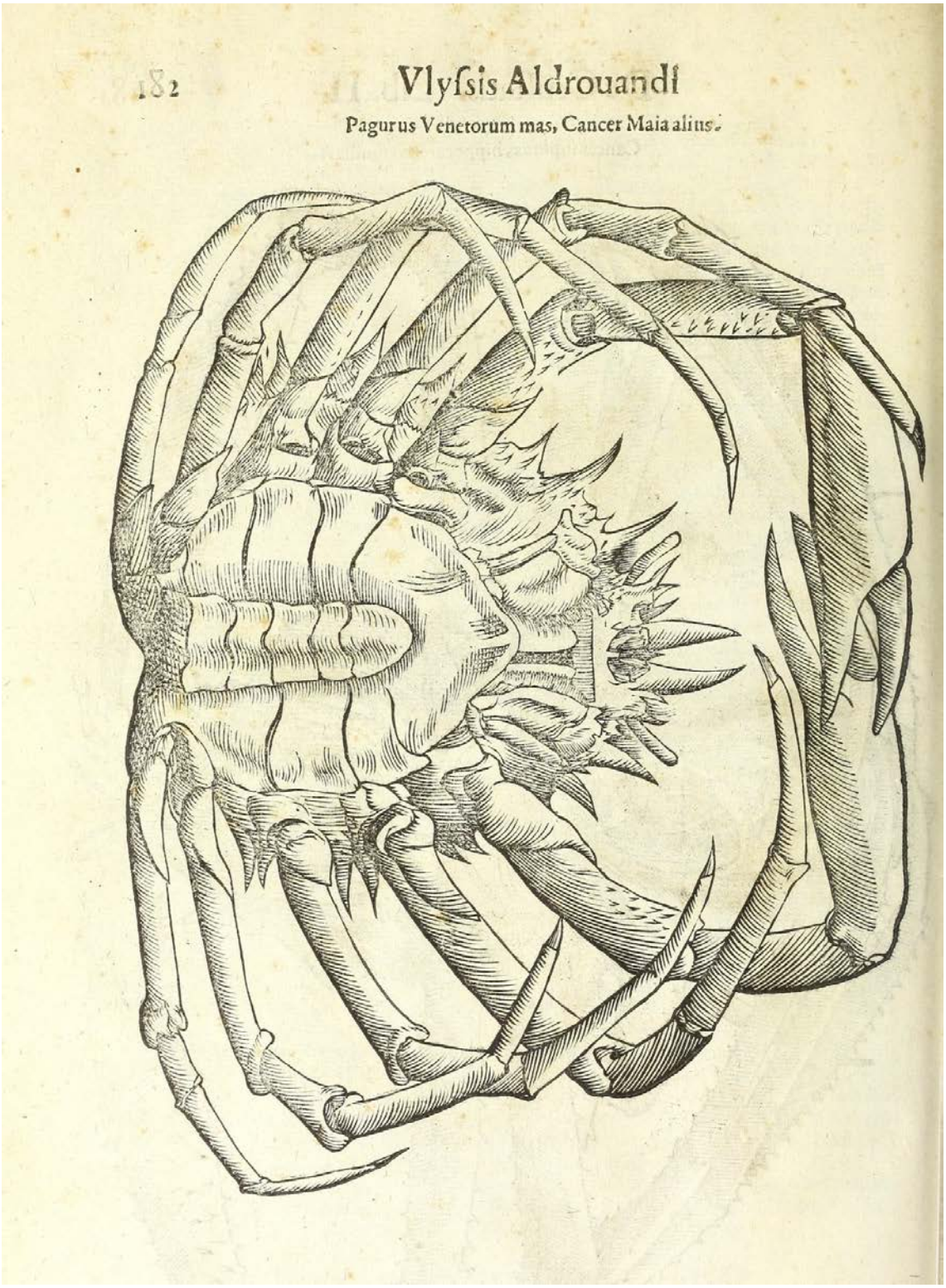

Fig. 1.2.1. Centollo mediterráneo *Maja squinado*, macho (nótese el estrecho pleon y los desarrollados quelípedos). Plancha publicada por el naturalista italiano Ulisse Aldrovandi (1522-1605) en el tratado "*De reliquis animalibus exanguibus*, *utpote de mollibus*, *crustaceis*, *testaceis* & *zoophytis*". Cortesía del Getty Research Institute, Los Ángeles (84-B28717).

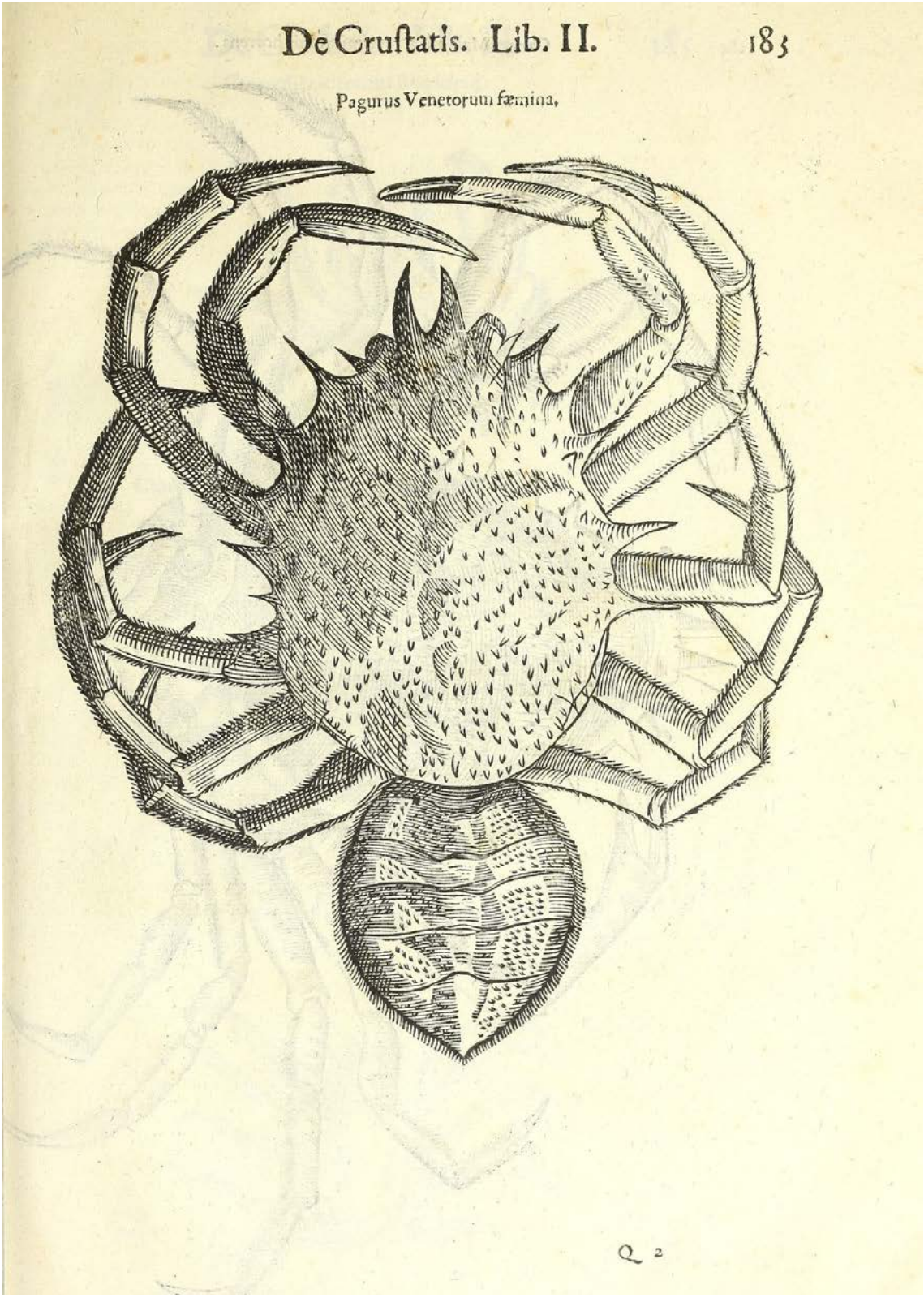

Fig. 1.2.2. Centollo mediterráneo *Maja squinado*, hembra (nótese el pleon redondeado y los quelípedos más pequeños y delgados). Plancha publicada por el naturalista italiano Ulisse Aldrovandi (1522-1605) en el tratado "*De reliquis animalibus exanguibus*, *utpote de mollibus*, *crustaceis*, *testaceis* & *zoophytis*". Cortesía del Getty Research Institute, Los Ángeles (84-B28717).

La reciente revisión del género *Maja* realizada por Ng y Richer De Forges (2015) reparte las entonces consideradas especies de májidos en 10 géneros distintos, quedando este género únicamente con cuatro especies, tres de ellas aceptadas hasta entonces: *M. brachydactyla* Balss, 1922; *M. squinado* (Herbst, 1788); y *M. crispata* Rissso, 1827; mientras que *Maja squinado* var. *capensis* Ortmann 1984 (sinonimia de *Maja capensis* Ortmann, 1894) es introducida como *Maja cornuta* (Linnaeus, 1758). Tradicionalmente el centollo ha sido considerado como una única especie denominada *Maja squinado* (Herbst, 1788), cuya amplia distribución abarcaba las costas europeas y africanas del Océano Atlántico y Mar Mediterráneo. Fue posteriormente cuando algunos carcinólogos apreciaron sutiles diferencias entre las poblaciones atlánticas y mediterráneas. Balss (1922) fue el primero en destacar que los especímenes atlánticos diferían de los mediterráneos en base a dos rasgos principales: en los atlánticos la superficie dorsal del caparazón es un poco más rica en espinas y setas ahorquilladas, mientras que los dos segmentos terminales o distales de los pereiópodos (propodio y dáctilo) son algo más cortos y anchos. Este último rasgo es el que da nombre a esta especie: «*brachydactyla*» es un término compuesto derivado del griego que significa "dedos" («*dáktylos*») "cortos" («*brachy*»).

Por su parte, el nombre «*squinado*» deriva de un antiguo término provenzal usado para denominar una o varias especies locales de braquiuros. Ya en el siglo XVI el naturalista francés Pierre Belon (1555) asoció el cangrejo «*maia*» de los griegos con el cangrejo «*squinado*» de Marsella, nombre que posiblemente refiere a las espinas del caparazón (ver Figura 1.2.3):

> "Les anciens Grecs one dict Maia. Ceulx de Marſeille, a cauſe des picquerons qu'il ha ſur le doz, ainſi que la Langouſte, es pluſieurs poils enſes ongles, l'ont nommee Squinade, a la ſimilitude du serrant, auquel on rend le lin plus delié."

Camus (1783), en su revisión de la obra de Aristóteles *Historia Animalium*, toma las palabras de Belon para asociar nuevamente el cangrejo «*maia*» del filósofo griego con el cangrejo «*ſquinade* / *ſquinado*» de Marsella: "*suivant Belon*, *le Cancre Maia eſt la ſquinade des Marſeillois*", mencionando el nombre «*squinado*» como un término usado para designar a este cangrejo en la Provenza, equivalente al «*araignée de mer*» por el que se le conocía en lengua francesa. No mucho más tarde, el naturalista alemán Johann F. W. Herbst (1788) establecería el taxón *Cancer squinado* en su descripción del mismo (ver Figura 1.2.4), mencionando que «*Squinado*» es el nombre que tiene esta especie en la Provenza: "*in der Provence heifst er* Squinado*, auch* Gritta*,* Squaranchon*,* Grampella".

Fig. 1.2.3. Centollo mediterráneo *Maja squinado*. Imagen de la obra "*La nature et diversité des poissons, avec leurs pourtraicts, représentez au plus près du naturel*", página 378, del naturalista francés Pierre Belon (1517-1564). Cortesía de la Blibiothèque nationale de France (BnF).

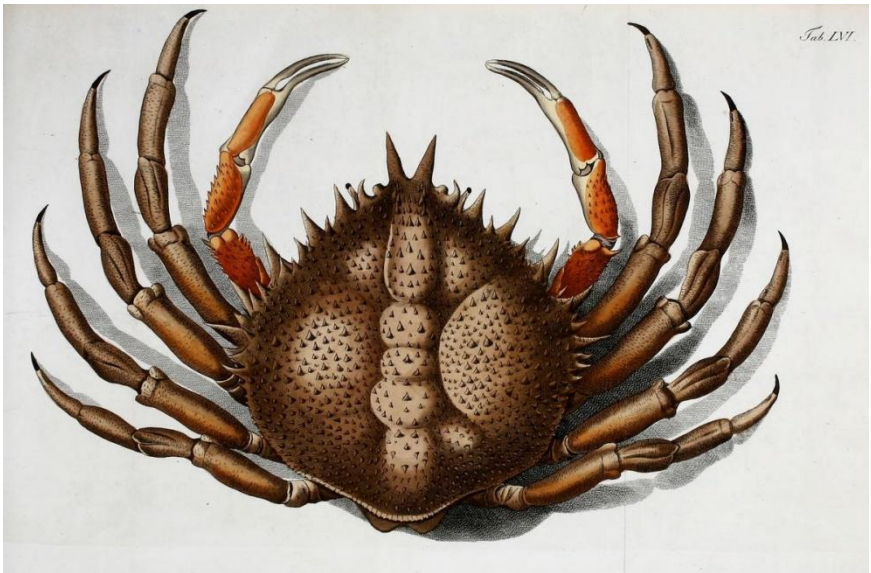

Fig. 1.2.4. Centollo mediterráneo *Maja squinado*. Imagen publicada en la obra del naturalista alemán Johann Friedrich Wilhelm Herbst (1743-1807), "*Versuch einer Naturgeschichte der Krabben und Krebse: nebst einer systematischen Beschreibung ihrer verschiedenen Arten. Bd. 3*, Berlin und Gottlieb August Lange, 1782-1804". Cortesía de Biodiversity Heritage Library (BHL). Versión digital realizada por Smithsonian Libraries. | www.biodiversitylibrary.org

El primer autor en considerar las poblaciones atlánticas y mediterráneas como especies distintas fue Neumann (1998) en su revisión del género *Maja*. Observó que las poblaciones atlánticas presentan un rostro más corto, espinas de la línea media más cortas y anchas, mientras que el gonopodio tiene el extremo distal redondeado (en lugar de anguloso) con transición al proceso terminal gradual (en lugar de abrupta). Por estos rasgos Neumann (1998) consideró que las poblaciones mediterráneas debieran agruparse en una especie y las poblaciones atlánticas en otra especie diferente, la especie mediterránea conservó el nombre original *Maja squinado*, mientras que la especie atlántica heredó el nombre dado originalmente como subespecie por Balss (1922), siendo llamada *Maja brachydactyla*. El estudio de Sotelo et al. (2008) basado en la secuenciación de los genes mitocondriales 16S y citocromo oxidasa tipo I (COI) de *M. brachydactyla* y *M. squinado* muestra que ambas especies están genéticamente diferenciadas. Un estudio posterior publicado por Guerao et al. (2011) aportó nuevas diferencias morfológicas entre *M. brachydactyla* y *M. squinado*: la proporción que existe entre la distancia de las espinas antero-orbitales y la longitud total del caparazón difiere significativamente ente ambas poblaciones; en el aspecto genético *M. brachydactyla* y *M. squinado* presentan distintos patrones de restricción (enzimas HpyCH4V y Ase I) en el gen mitocondrial citocromo oxidasa tipo I (COI) permitiendo una rápida identificación molecular.

El género *Maja* es relativamente antiguo. Se han recuperado miembros de este género en el Plioceno de la Península Itálica (Varola, 1981). Garassino et al. (2012), en su extensivo estudio dedicado a la fauna de decápodos del Plioceno Temprano (Zancliense, 5,3-3,6 millones de años) hallados en la cantera de La Serra (Toscana, Italia), describe la presencia de *Maja squinado*, cuyo registro fósil consiste en un caparazón completo y en un caparazón deformado. Más recientemente, Pasini y Garassino (2014) describen un fósil que consiste en un único dáctilo derecho, catalogado como *Maja* cf. *Maja squinado* y datado en el Plioceno Temprano de la localidad de Cheglio (Varese, Italia). Estos datos coinciden con los estudios moleculares, que datan en 9.6 millones de años la separación del clado *M. squinado* + *M. crispata* del clado *M. brachydactyla*, mientras que la separación de *M. squinado* y *M. crispata* en especies distintas se ha calculado en 600.000 años (Sotelo et al., 2009).

Familia Majidae. De acuerdo a la clasificación realizada por Davie et al. (2015), la familia Majidae Samouelle, 1819 es la más rica en especies de la superfamilia Majoidea. Mientras que en otras familias se han descrito menos de 100 especies: Epialtidae MacLeay, 1838 (89 especies, 52 géneros), Inachidae MacLeay, 1838 (35 géneros, 192 especies), Inachoididae Dana, 1821 (12 géneros, 43 especies), Mithracidae MacLeay 1838 (13 géneros, 60 especies), y Oregoniidae Garth, 1958 (9 géneros, 34 especies); en la familia Majidae se han descrito más de 125 especies distribuidas en 31 géneros, estas especies se han repartido en tres subfamilias: Eurynolambrinae Števčić 1994; Majinae Samouelle, 1819; y Planoterginae Števčić 1991. El registro fósil de esta familia se extiende al Mioceno y Eoceno, cerca del límite con el periodo Cretácico (Feldmann, 2016; McLay et al., 1995). Recientemente han sido recuperados en México unos fósiles de braquiuros que parecen ser májidos, de ser correcta esta clasificación el origen de los májidos podría adelantarse hasta el Cretácico Tardío (Maastrichtiense, 72-66 millones de años), siendo anteriores al evento de gran extinción que puso término a dicho periodo (Vega et al., 2016; Vega et al., 2006).

Superfamilia Majoidea. El carácter monofilético de la superfamilia Majoidea es apoyada por la morfología de los adultos, la presencia de setas ahorquilladas, el desarrollo larvario abreviado con dos estadios de zoea y uno de megalopa, así como la existencia de una muda terminal previa a la maduración sexual (Davie et al., 2015; Hultgren y Stachowicz, 2008). Ng et al. (2008) indican que existe una tendencia a reconocer ocho familias de majoideos: Majidae Samouelle, 1919; Epialtidae MacLeay, 1838; Inachidae MacLeay, 1838; Mithracidae MacLeay 1838; Inachoididae Dana, 1821; Pisidae Dana, 1851; Tychiidae Dana, 1851; y Oregoniidae Garth, 1958. Sin embargo, los mismos autores mencionan la necesidad de revisar la taxonomía del grupo, ya que está poco estudiada en relación a su gran biodiversidad.

Brösing et al. (2007) propuso que Majoidea no pertenece a la sección 'Eubrachyura' en base a la estructura de los osículos del estómago. Los estudios moleculares no respaldan esta proposición, ya que sitúan a la superfamilia Majoidea en el taxón 'Heterotremata', el cual pertenece a 'Eubrachyura' (Ahyong et al., 2007; Bracken et al., 2009; Spears et al., 1992; Tsang et al., 2014). Los estudios moleculares difieren al fechar el origen del grupo, desde el límite Pérmico-Triásico (Porter et al., 2005), hasta el periodo Cretácico (Tsang et al., 2014). Como apoyando esta última datación, los fósiles más antiguos de esta superfamilia datan del periodo Cretácico: *Priscinachus elongatus*, datado en el periodo Cenomaniense (100,5-93,9 millones de años) y recuperado en Francia (Breton, 2009); así como las especies *Cretamaja granulata* y *Koskobilius postangustus*, datadas en el periodo Albiense (113-100,5 millones de años), y recuperadas en la cantera de Koskobilo de la localidad de Alsasua (Navarra, España), estos fósiles son caparazones casi completos (Klompmaker, 2013).

Infraorden Brachyura. El término «*brachyura*» es un término compuesto derivado del griego que significa "cola" («*ourá*») "corta" («*brachy*»), en referencia al reducido tamaño del pleon. El taxón Brachyura, o braquiuros, engloba a los "verdaderos cangrejos", taxón distinto al de los "cangrejos ermitaños" y "cangrejos de porcelana", pertenecientes al infraorden Anomura, o anomuros (Scholtz, 2014). La primera descripción del infraorden Brachyura suele atribuirse a Latreille, sin embargo Ng et al. (2008) destaca que el primer autor en describir el clado y crear el término 'Brachyuri' fue Linneo. Las revisiones más recientes apuntan 7.250 especies descritas de braquiuros (Davie et al., 2015), repartidas en 98 familias, que han colonizado hábitats marinos, dulceacuícolas y terrestres (Tsang et al., 2014). La mayoría de carcinólogos considera al taxón Brachyura como monofilético, de acuerdo a los estudios basados en la morfología de adultos, larvas y sistema reproductor (Ng et al., 2008), la biología molecular (Bracken et al., 2009; Tsang et al., 2014), la estructura de los espermatozoides (Jamieson, 1994) y la organización de los osículos del estómago (Brösing et al., 2007).

Guinot (1977) propuso la que sería una de las clasificaciones más exitosas del taxón Brachyura, basada en la posición de los poros sexuales o *gonoporos*, establece tres grupos: 'Podotremata' (los gonoporos femeninos y masculinos abren en la coxa), 'Heterotremata' (los gonoporos femeninos abren en el esternón y los masculinos en la coxa) y 'Thoracotremata' (los gonoporos femeninos y masculinos abren en el esternón). De acuerdo a varias revisiones taxonómicas 'Heterotremata + Thoracotremata' forman el clado 'Eubrachyura', el cuál sería clado hermano de 'Podotremata'. Mientras que la monofilia de 'Eubrachyura' no suele ser discutida, entorno a 'Podotremata' existe un clima de debate acerca del carácter braquiuro de algunos de sus miembros (Ahyong et al., 2007; Brösing et al., 2007; Davie et al., 2015; Jamieson, 1994; Ng et al., 2008; Tavares, 2003; Tsang et al., 2014).

Tsang et al. (2014) usando datos moleculares han datado el origen de los braquiuros en el Jurásico Temprano (180 millones de años). En ese sentido, durante los últimos años han sido descritas varias especies fósiles de las familias Tanidromitidae Schweitzer & Feldmann, 2008 y Longodromitidae Schweitzer & Feldmann, 2009. Sin representantes vivos actuales, dichas familias se han clasificado como Dromiacea (Fraaije et al., 2013; Schweitzer y Koppka, 2011; Starzyk, 2013), un taxón que los datos moleculares sitúan en una posición basal respecto al resto de braquiuros (Ahyong et al., 2007; Tsang et al., 2014). Del periodo Jurásico se han datado otros fósiles de braquiuros, como *Eoprosopon klugi* Förster, 1986 y *Homolus auduini* Eudes-Deslongchamps, 1835, pertenecientes a la actual familia Homolodromiidae (Schweitzer y Feldmann, 2010). El género *Imocaris* Schram & Mapes, 1984 del Carbonífero (359-299 millones de años) es muy interesante, si se confirma que son braquiuros, adelantaría el origen de estos en más de 100 millones de años (Schram, 2009).

Orden Decapoda. El término «*decapoda*» es un término compuesto derivado del griego que significa "diez" «*déka*» "pies" «*poús*», en referencia a la presencia habitual de cinco pares de pereiópodos bien desarrollados, de función marchadora y/o prensil si terminan en quelas o pinzas. Este grupo animal en el año 2009 contaba con 14.756 especies repartidas en 2.725 géneros, de los cuáles los braquiuros constituían el 46 % (De Grave et al., 2009). La taxonomía de los decápodos suele ser objeto de controversia, así taxones tradicionales como "Reptantia" y "Natantia" son rechazados actualmente (Toon et al., 2009). El consenso actual divide a los decápodos en los subórdenes Dendrobranchiata Spence Bate, 1888 y Pleocyemata Burkenroad, 1963 (Poore, 2016; Toon et al., 2009; Tsang et al., 2008). El suborden Dendrobranchiata incluye a las gambas y langostinos de las superfamilias Penaeoidea Rafinesque, 1815 y Sergestoidea Dana, 1852 (Toon et al., 2009; Tsang et al., 2008). Por su parte, el suborden Pleocyemata incluye a todos los demás decápodos: los infraórdenes Achelata Sholtz & Richter 1995; Anomura MacLeay, 1838; Astacidea Latreille, 1802; Axiidea Saint Laurent, 1979; Brachyura Linnaeus, 1758; Caridea Dana, 1852; Gebiidea de Saint Laurent, 1979; Glypheidea Winkler, 1883; Polychelida Sholtz & Richter 1995; y Stenopodidea Bate, 1888 (De Grave et al., 2009; Poore y Türkay, 2015). La monofilia de dichos infraordenes está avalada por los estudios genéticos (Bracken et al., 2009; Tsang et al., 2008). Sin embargo, la posición de Caridea es controvertida: podría tratarse de un taxón basal de los Pleocyemata (Tsang et al., 2008), un taxón perteneciente a Dendrobanchiata (Bracken et al., 2009), o un taxón basal a todos los demás decápodos, "Dendrobranchiata + Pleocyemata" (Toon et al., 2009). En ese sentido son necesarios nuevos estudios morfológicos y moleculares para resolver esta situación (De Grave et al., 2009).

El origen de los decápodos es un problema cuya solución está todavía por esclarecer, no existe consenso acerca del taxón hermano de este grupo y los fósiles son muy derivados, por lo que reconocer formas basales es difícil (Schram, 2009). Uno de los decápodos más antiguos conocidos es *Palaeopalaemon newberryi* Whitfield, 1880, hallado en Norteamérica y datado en el Devónico Superior (Fameniense, 372-358,9 millones de años), se considera un decápodo demasiado avanzado como para esclarecer los orígenes de este grupo (Schram, 2009; Schram et al., 1978). En los últimos años se han descrito nuevos fósiles de decápodos datados en el Fameniense: *Tealliocaris walloniensis* sp. nov de Bélgica (Gueriau et al., 2014b) y *Aciculopoda mapesi* sp. nov de Estados Unidos (Feldmann y Schweitzer, 2010), todos estos fósiles permiten anclar el origen de los decápodos en el periodo Devónico. También del Fameniense, Angustidontidae Cooper, 1936 es una familia extinta de malacostráceos pelágicos que según algunos autores es grupo hermano de Decapoda, difiriendo de estos por tener 1-2 pares de maxilípedos en lugar de 3 y 7-6 pares de pereiópodos en lugar de 5, sus maxilípedos están transformados en largos apéndices raptores(Gueriau et al., 2014a).

Clase Malacostraca. El origen etimológico de este clado se remite a los tratados *Historia Animalium* y *Partibus Animalium* de Aristóteles. Dichas obras mencionan un grupo animal bautizado como «*malakostrakos*», cuyo significado es concha («*ostrakon*») blanda («*malako*»), describe a aquellos "animales no sanguíneos" que "tienen externamente sus partes duras e internamente sus partes blandas y carnosas" pero cuyas partes duras "son susceptibles a contusión". Con este último detalle Aristóteles los diferencia de los «*testacea*»: bivalvos y gasterópodos. Como ejemplos de «*malakostrakos*» Aristóteles menciona los «*carabi* / *karabi*» (langostas), «*astaci*» (bogavantes y cangrejos de río), «*carides* / *karides*» (langostinos y gambas) y a los «*carcini* / *karkini*» (cangrejos). Para profundizar más, es posible consultar la traducción de dichos documentos realizada por Cresswell (1883) y Ogle (1912), disponibles de forma libre en medios digitales. La revisión realizada por Voultsiadou y Vafidis (2007) es también un trabajo muy interesante, relaciona los animales mencionados por Aristóteles con taxones modernos. Curiosamente, la clasificación de Aristóteles es más cercana a la actual clasificación de los decápodos que a la de los malacostráceos propiamente dichos. Richter y Scholtz (2001) enumeran los cinco caracteres independientes que apoyan la monofilia de este grupo: ocho segmentos torácicos y siete segmentos abdominales (dependiendo del taxón pueden estar fusionados o reducidos); *gonoporos* femeninos en el sexto segmento torácico y masculinos en el octavo segmento torácico; sistema digestivo anterior cuyo estómago se divide en cámara anterior y posterior; la primera antena o anténula es birrámea; el estadio de nauplius presenta una banda de crecimiento posterior formada por un anillo de 19 células.

La clase Malacostraca comprende más de 28.000 especies descritas (Richter y Scholtz, 2001) y está generalmente aceptado que son un grupo monofilético (Martin y Davis, 2001; Richter et al., 2009; Richter y Scholtz, 2001). Por el contrario, la sistemática interna y filogenia del grupo es otra historia, existiendo tantas versiones de los árboles filogenéticos y los rangos de los taxones como autores los han estudiado (Martin y Davis, 2001; Richter y Scholtz, 2001). Dada esta complejidad, a continuación será presentada una aproximación fruto de revisiones relativamente recientes (Martin y Davis, 2001; Richter et al., 2009; Richter y Scholtz, 2001). La subclase Phyllocarida Packard, 1879 (Leptostraca Claus, 1880 como único orden vivo) sería la más basal y taxón hermano de "Hoplocarida + Eumalacostraca". Hoplocarida Calman, 1904 tiene un único orden: Stomatopoda Latreille, 1817. Eumalacostraca Grobben, 1892 engloba al resto del grupo: Peracarida Calman, 1904 (órdenes Amphipoda Latreille, 1816; Cumacea Krøyer, 1846; Isopoda Latreille, 1817; Lophogastrida Sars, 1870; Mictacea Bowman et al., 1985; Mysida Haworth, 1825; Spelaeogriphacea Gordon, 1957; Tanaidacea Dana, 1849 y Thermosbaenacea Monod, 1927); Eucarida Calman, 1904 (ordenes Decapoda Latreille, 1802 y Euphausiacea Dana, 1852) y Syncarida Packard, 1885 (ordenes Bathynellacea Chappuis, 1915 y Anaspidacea Calman, 1904).

Subfilo Pancrustacea (Tetraconata). «*Pancrustacea*», de reciente creación deriva del griego "todos" «*pan*» y del latín "los crustáceos" «*crustacea*». «*Tetraconata*» de significado "cuatro conos" fue creado por Dohle (2001) en base a la estructura de los omatidios compartida por insectos y "crustáceos". «*Crustacea*» deriva del latín «*crusta*» y significa "costra / corteza". El propio Plinio el Viejo (25 a.e.c. - 25 e.c.) utiliza «*crustata*» para describir aquellos animales "de cuerpos duros" (Scarborough, 1992). Pancrustacea y Tetraconata son fruto de una "reciente" revolución en la taxonomía tradicional de los "crustáceos" debida a los datos aportados por la biología molecular. Resumiendo la nueva situación: "Hexapoda Latreille, 1825 + Branchiopoda Latreille, 1817 + Remipedia Yager, 1981" formarían un taxón monofilético y hermano del taxón "Malacostraca Latreille, 1802 + Cirripedia Burmeister, 1834" (Aleshin et al., 2009; Regier et al., 2005; von Reumont et al., 2012). Esto sitúa a los hexápodos en el seno de los tradicionales "crustáceos" rompiendo la antigua asociación de hexápodos y miriápodos. Así los "crustáceos" tradicionales quedan como grupo "parafilético" (Aleshin et al., 2009; Regier et al., 2005) y Pancrustacea (Tetraconata) como "monofilético" (Mallatt et al., 2004; Regier et al., 2005). En relación a los taxones restantes que no han sido mencionados: la posición de Copepoda Milne Edwards, 1840 es incierta, tal vez grupo hermano de "Hexapoda + Branchiopoda" (Aleshin et al., 2009) o bien de "Malacostraca + Cirripedia" (Regier et al., 2005; von Reumont et al., 2012). En el caso de Ostracoda Latreille, 1802 tanto su posición como su monofilia son discutidos (Regier et al., 2005; von Reumont et al., 2012). El taxón Pancrustacea representa la mayor parte de la biodiversidad conocida del planeta. Brusca y Brusca (2003) menciona casi 70.000 especies de crustáceos y casi un millón de especies descritas de hexápodos.

Los pancrustáceos son un grupo antiguo donde las formas avanzadas aparecen temprano en el registro fósil. Por ejemplo, del Lagerstätten de Herefordshire (Silúrico, 425 millones de años), proceden *Cinerocaris magnifica* gen. et sp. nov. (Briggs et al., 2004) y *Cascolus ravitis* gen. et sp. nov.(Siveter et al., 2017), este último bautizado de ese modo en honor al divulgador y naturalista sir David Attenborough. Dichos fósiles destacan por ser filocáridos, el grupo más basal de malacostráceos con representantes vivos (Richter y Scholtz, 2001). Los pancrustáceos son comunes en el registro fósil de los últimos 500 millones de años (Zhang et al., 2007). Si bien en la provincia de Yunnan (China) ha sido recuperado un fósil aún más antiguo: *Yicarisdianensis* gen. et sp. nov. (Zhang et al., 2007), datado en el Cámbrico (Atdabaniense, 550-530 millones de años), posee caparazón cefálico, ojos compuestos y apéndices birrámeos con epipoditos, siendo considerado un animal próximo a los branquiópodos y remipedios. Otro grupo interesante son los Phosphatocopina Müller, 1964: pequeños artrópodos datados en 520-490 millones de años cuyo cuerpo está protegido por un caparazón bivalvo similar al de los ostrácodos, poseen ojos pedunculados y apéndices birrámeos, (Siveter et al., 2001; Zhang y Pratt, 2012), se les considera grupo hermano de Pancrustacea (Maas y Waloszek, 2005).

Filo Euarthropoda. El nombre «*euarthropoda*» es un término compuesto derivado del griego que significa "verdaderos" «*eu*» "pies" «*póus*» "articulados" «*árthron*», referencia a las extremidades segmentadas de estos animales. Son un grupo difícil a nivel de taxonomía y filogenia que ha dado lugar a diversas interpretaciones. Por ello, para evitar confusiones solo nos basaremos en la revisión publicada por Ortega-Hernández (2016). Euarthropoda lo forman "Chelicerata Heymons, 190 + Myriapoda Latreille, 1802 + Pancrustacea Zrzavý&Štys, 1997", donde Chelicerata sería grupo hermano de "Myriapoda + Pancrustacea" (Edgecombe, 2010; Giribet y Edgecombe, 2012). Las sinapomorfías del grupo incluyen una boca ínfera, cerebro formado por tres segmentos, exoesqueleto esclerotizado y apéndices artropodizados, es decir, cubiertos por un exoesqueleto rígido y articulado (Brusca y Brusca, 2003; Ortega-Hernández, 2016). Ortega-Hernández (2016) descarta el empleo del filo 'Arthropoda von Siebold, 1848' original al considerarlo impreciso por incluir a tardígrados y excluir a onicóforos; pero recomienda el uso de 'Panarthropoda Nielsen, 1995', constituido por "Euarthropoda Lankester,1904 + Onychophora Grube, 1853 + Tardigrada Spallanzani, 1777". Es un taxón monofilético (Garey, 2001; Halanych, 2004), cuyas sinapomorfías incluyen un cerebro ganglionar dorsal, cuerpo organizado en metámeros, y apéndices marchadores terminados en "uñas" y con musculatura segmentada (Ortega-Hernández, 2016).

Los subfilos de euartrópodos actuales descienden de los llamados "euartrópodos basales superiores", de afinidades filogenéticas inciertas y datados en el Cámbrico Temprano (520 millones de años), son los "megaqueiranos", "fuxianhuiidos" y "formas bivalvas cámbricas" (Budd y Telford, 2009; Edgecombe, 2009; 2010; Ortega-Hernández, 2016). Son animales de cuerpo cubierto por un exoesqueleto rígido y articulado, cabeza formada por dos o más segmentos, primer par de apéndices diferenciado y apéndices post-orales birrámeos (Ortega-Hernández, 2016). Los "megaqueiranos" incluyen a *Megacheira* Hou & Bergström, 1997 y similares, se caracterizan por su escudo cefálico fusionado con los segmentos de los ojos, de los apéndices raptores y de tres pares de apéndices anteriores; el tronco es uniforme con apéndices birrámeos foliáceos (Chen et al., 2004). Los "fuxianhuiidos" incluyen a *Fuxianhuia* Hou, 1987 y similares, la cabeza se compone de dos segmentos: anterior con ojos y posterior con antenas, de este parte un corto escudo libre sobre los primeros segmentos troncales; el tronco es uniforme con apéndices birrámeos de aspecto foliáceo (Bergström et al., 2008; Budd y Telford, 2009; Edgecombe, 2009; Waloszek et al., 2005; Yang et al., 2013). Las "formas bivalvas cámbricas" incluyen a *Canadaspis* Novozhilov in Orlov 1960 y similares, la cabeza se compone de dos segmentos: anterior con ojos y posterior con apéndices diferenciados en antenas o apéndices raptores, un caparazón bivalvo protege la cabeza y el tronco anterior, los apéndices (birrámeos) solo están presentes en los segmentos anteriores del tronco, y el telson termina en un par de cercos alargados o furcas (Edgecombe, 2010; Legg et al., 2012; Yang et al., 2016).

Los "euartrópodos basales superiores" descienden de los "euartrópodos basales inferiores", los cuales incluyen a Radiodonta Collins, 1996, *Opabinia* Walcott, 1912 y "lobopodios" (Budd y Telford, 2009; Edgecombe, 2009; 2010; Ortega-Hernández, 2016). Los Radiodonta son un grupo diverso cuyo exponente más famoso es *Anomalocaris* Whiteaves, 1892, presentes desde el Cámbrico Temprano hasta el Ordovícico Temprano (542- 472 millones de años), son los primeros en tener un caparazón cefálico y apéndices anteriores esclerotizados y articulados (Budd y Telford, 2009; Edgecombe, 2010; Ortega-Hernández, 2016). Los Radiodonta tienen una cabeza con ojos compuestos y pedunculados, un "cono oral" alrededor de la boca ínfera y apéndices raptores; de tronco uniforme y segmentado, presenta apéndices foliáceos imbricados entre sí (Daley y Edgecombe, 2014; Van Roy y Briggs, 2011; Xianguang et al., 2006). *Opabinia* Walcott, 1912 es un taxón del Cámbrico Medio (509-497 millones de años) de Burgess Shale, posee una cabeza con cinco ojos pedunculados y compuestos que proyecta un único apéndice frontal alargado terminado en pinza; el tronco uniforme y segmentado presenta apéndices foliáceos (Budd, 1996; Edgecombe, 2010; Ortega-Hernández, 2016; Zhang y Briggs, 2007). No existe ni en Radiodonta (Daley y Edgecombe, 2014; Van Roy et al., 2015), ni en *Opabinia* (Zhang y Briggs, 2007), evidencia de apéndices birrámeos o de apéndices locomotores ventrales. El taxón Lobopodia Snodgrass, 1938 comprende animales cuyo patrón corporal consiste en una región cefálica bulbosa con boca anterior, cuerpo vermiforme y anillado, y apéndices tubulares anillados terminados en "uñas". Desde inicios del Cámbrico presentan una gran diversidad en la forma y longitud de los apéndices, así como diversos tipos de proyecciones corporales filiformes, espinas, escleritos y/o placas a lo largo del cuerpo (Dzik, 2011; Liu et al., 2008; Ortega-Hernández, 2016; Yang et al., 2015). Especies como *Miraluolishania haikouensis* Liu et al. 2004 y *Onychodictyon ferox* Hou, Ramsköld & Bergström, 1991 son muy interesantes ya que presentan ojos y un par de apéndices similares a antenas en la región cefálica (Dzik, 2011; Ou et al., 2012).

Superfilo Ecdysozoa. El término «*ecdysozoa*» es un término compuesto que proviene del griego, de significado "animal" «*zôion*» "que se desnuda / que se quita [algo]" «*ekdusis*». Es una referencia a la ecdisis o muda, proceso por el que la cutícula o exoesqueleto que recubre el cuerpo de estos animales es eliminada y sustituida por una nueva. Este taxón se debe a Aguinaldo et al. (1997), los cuales demostraron por técnicas moleculares que "Euarthropoda Lankester, 1904 + Kinorhyncha Reinhard 1881 + Loricifera Kristensen, 1983 + Nematoda Rudolphi, 1808 + Nematomorpha Vejdovsky, 1886 + Onychophora Grube, 1853 + Priapulida Delage & Hérouard, 1897 + Tardigrada Spallanzani, 1777" son un único taxón monofilético. Este resultado ha sido confirmado por numerosos estudios posteriores (Dunn et al., 2014; Dunn et al., 2008; Garey, 2001; Halanych, 2004; 2016; Mallatt et al., 2004).

1.3 Biología del Centollo, *Maja brachydactyla* Balss, 1922.

El centollo presenta un marcado dimorfismo sexual. Los machos tienen los quelípedos relativamente más largos y gruesos, mientras que el pleon es estrecho. En las hembras el pleon es ancho y redondeado, con aspecto de domo abombado (Figura 1.2.1 y 1.2.2). Las tallas también varían con el sexo y la distribución geográfica. En el Canal de La Mancha la longitud del caparazón de los machos varía entre 152 y 162 mm con un máximo de 210 mm (Kergariou, 1971), el ancho entre 85 y 200 mm (Pawson, 1995), y el peso entre 1200 a 1500 gramos con un máximo de 4 kg (Kergariou, 1971); en las hembras la longitud oscila entre 122 y 141 mm con un máximo de 180 mm (Kergariou, 1971), el ancho entre 70 y 175 mm (Pawson, 1995), y el peso entre 500 a 900 gramos con un máximo de 1,8 kg (Kergariou, 1971). En Irlanda, la longitud de los machos varía entre 130 y 179 mm, con mínimos de 100 mm y máximos de 219 mm; en las hembras varía entre 120 y 140 mm, raramente superando los 150 mm (Rodhouse, 1984). En el Adriático Norte la longitud de los machos varía entre 113 y 149 mm, mientras que en las hembras varía entre 113 y 133 mm (Le Foll, 1993). En la costa de Galicia las capturas muestran una variación en la longitud total del caparazón entre 132,5 mm y 191,3 mm (Verísimo, 2015). En la costa de Asturias el rango de tallas se distribuye desde los 90 hasta los 210 mm, pero las tallas más habituales se engloban entre 120 y 140 mm (García-Flórez y Fernández-Rueda, 2003).

Fig. 1.3.1. Centollo, *Maja brachydactyla* Balss, 1922. Macho adulto.

El caparazón es descrito como piriforme u ovoide, más redondeado en los especímenes de mayor tamaño. La superficie dorsal es convexa, como en otros májidos, posee gran número de espinas y tubérculos (Fig. 1.3.1). El rostro presenta un par de espinas pseudo-rostrales largas, ligeramente curvadas y proyectadas hacia delante a modo de "cuernos". Cada región supra-orbital presenta una extensión estrecha que termina en una espina antero-orbital afilada y ligeramente curvada hacia arriba. En sentido antero-posterior, las espinas localizadas en los márgenes del caparazón son: una espina intercalar corta y robusta rozando la base de la espina post-orbital; espina post-orbital como la más larga espina del caparazón con extremo afilado; espina hepática larga y afilada con dos espinas accesorias basales; tres espinas laterales largas, con espinas y tubérculos intercalados de menor longitud. La línea media del cuerpo presenta hasta siete espinas, ligeramente más largas que las adyacentes: tres gástricas, dos sub-gástricas, una cardiaca y una intestinal. También se han descrito una espina localizada en cada región branquial del caparazón (Fig. 1.3.2). La articulación basal de las antenas es muy ancha y posee un par de espinas. El caparazón y los pereiópodos están cubiertos por setas ahorquilladas con forma de garfio (Neumann, 1998; Ng y Richer De Forges, 2015).

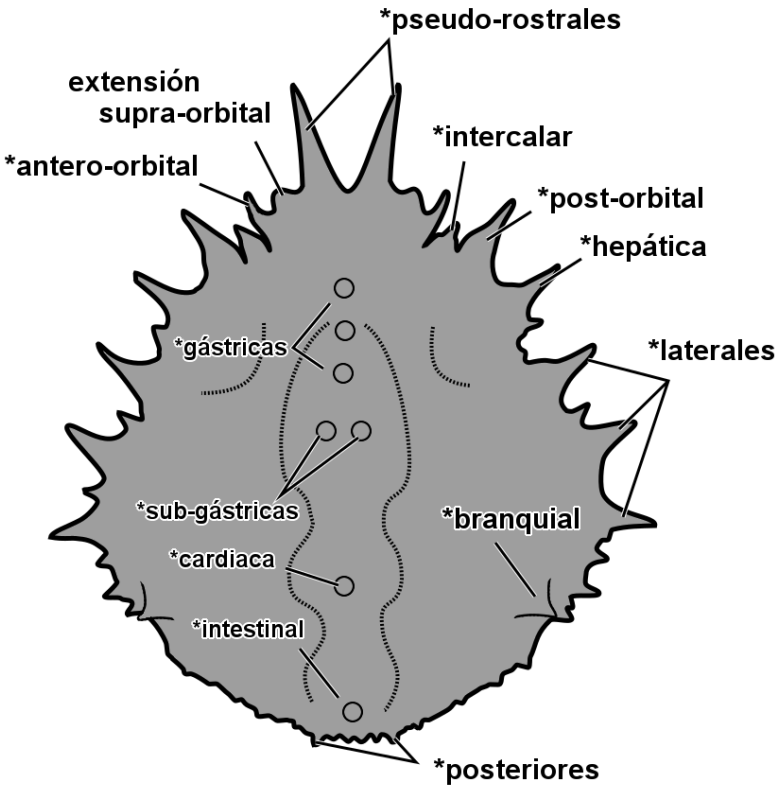

Fig. 1.3.2. Centollo, *Maja brachydactyla* Balss, 1922. Esquema del caparazón, indicando la distribución de las principales espinas localizadas en el mismo (marcadas con asterisco, *) y la extensión supra-orbital. La nomenclatura ha sido empleada de acuerdo con la revisión de Ng y Richer De Forges (2015).

1.3.1 Muda terminal

En la mayoría de decápodos, incluyendo otros braquiuros, el crecimiento no se detiene una vez alcanzada la madurez sexual y las mudas prosiguen después de alcanzado el estadio adulto. En el centollo y otros májidos esta situación no ocurre. En el centollo el desarrollo de los juveniles se caracteriza por dos fases: una primera fase de crecimiento y una segunda fase de maduración sexual tras la cual el crecimiento se detiene (Corgos et al., 2011). De modo que la muda previa a la madurez sexual será la última muda, por ello recibe el nombre de «muda terminal» o «muda puberal» (Corgos et al., 2011; Fahy, 2001; González-Gurriarán et al., 1993). Se ha calculado que los juveniles realizan la muda terminal cuando tienen 2 a 3 años de edad (González-Gurriarán et al., 1995; Le Foll, 1993). La muda terminal está acompañada de modificaciones en la morfología externa. El cambio más evidente es el aumento de tamaño corporal, dado que la muda terminal es la última muda realizada en la vida del animal, esta muda determina la talla máxima del ejemplar (González-Gurriarán et al., 1993). Este aumento de tamaño, en valores porcentuales representa entre un 26-27 % (González-Gurriarán et al., 1995) y un 29 % (Le Foll, 1993). Dichos valores son inferiores al 31 % observado en mudas anteriores (González-Gurriarán et al., 1995), si bien según otros autores el incremento de tamaño en dichas mudas varía del 10 al 20 % en cada una (Fahy y Carroll, 2009). Es posible que las variaciones en el crecimiento varíen en relación a la zona de estudio.

La muda terminal también genera cambios asociadas a los caracteres sexuales secundarios: en los machos el tamaño relativo de los quelípedos se incrementa entre un 40 y un 110 %, dicho aumento de tamaño posiblemente refleja su uso durante la cópula, consistente en aferrar y manipular a las hembras (Corgos y Freire, 2006; Sampedro et al., 1999). Nosotros también hemos observado que estos animales extienden los quelípedos como mecanismo de intimidación, tanto frente a miembros de su misma especie como frente otras especies. Por ello no parece descartable que sean útiles para combatir por las hembras con otros machos así como para rechazar a otros machos durante la cópula. En las hembras la muda terminal aumenta la anchura relativa del pleon. La forma plana del pleon juvenil cambia a una estructura abombada con forma de domo, dicho cambio está asociado a su función como cámara de incubación de las puestas, las cuales permanecen adheridas a los pleópodos de la madre durante la incubación (Le Foll, 1993; Sampedro et al., 1999). La muda terminal tiene lugar en verano: con temperaturas elevadas ocurre entre finales de junio y julio, mientras que con temperaturas más bajas ocurre entre julio y agosto (González-Gurriarán et al., 1995).

1.3.2 Maduración gonadal, incubación y estrategia reproductora

El desarrollo de las gónadas femeninas sucede poco después de la muda terminal. En ese sentido, González-Gurriarán et al. (1993), Rotllant et al. (2007) y Verísimo (2015) han caracterizado varias etapas del desarrollo gonadal. En la etapa I las gónadas son de color blanco crema y los ovocitos tienen un diámetro medio de 264 µm. En la etapa II el color varía entre crema pálido y anaranjado claro, el diámetro medio es de 453 µm y poseen vitelo en desarrollo. En la etapa III el color es naranja y los ovocitos tienen un diámetro medio de 673 µm. En la etapa IV las gónadas tienen un color naranja brillante y ocupan un gran volumen de la cavidad del cefalotórax, mientras que los ovocitos alcanzan un diámetro de 845 µm.

Entre los meses de julio y octubre más del 90 % de las hembras se hallan en la etapa I de maduración gonadal. Entre los meses de noviembre y diciembre, coincidiendo con la migración hacia aguas profundas, alrededor de dos tercios de las hembras se encuentran en la etapa II y el tercio restante en la etapa III, en diciembre hasta un quinto de las hembras se encuentra en la etapa IV. Desde diciembre hasta mayo gradualmente todas las hembras maduran alcanzando la etapa IV de maduración (Corgos y Freire, 2006; González-Gurriarán et al., 1998; González-Gurriarán et al., 1993). En los machos la maduración se sucede de forma diferente, ocurriendo la maduración fisiológica una o dos mudas antes de la muda terminal y la maduración funcional después de la misma (Corgos y Freire, 2006).

En la costa de Galicia la cópula ocurre entre enero y marzo, mientras que en condiciones de cultivo se ha observado entre octubre y diciembre, y ocasionalmente entre mayo y junio. Las hembras pueden aparearse sucesivamente con varios machos (González-Gurriarán et al., 1993). La presencia de hembras ovígeras, aquellas que tienen puestas en proceso de incubación adheridas a los pleópodos, se prolonga desde enero hasta octubre, con un porcentaje residual del 8 % desde diciembre hasta enero (González-Gurriarán et al., 1998; González-Gurriarán et al., 1993). El máximo pico de hembras ovígeras sucede de abril a junio (González-Gurriarán et al., 1993), si bien hasta el 75 % de las hembras son ovígeras en el periodo comprendido entre marzo y septiembre (González-Gurriarán et al., 1998). Se ha calculado que en las costas gallegas las hembras podrían realizar hasta tres puestas sucesivas anuales (Freire et al., 2002), si bien en condiciones de cultivo se ha demostrado que las hembras pueden realizar de 3 a 5 puestas anuales con un periodo de interpuesta de 4 a 5 días (Iglesias et al., 2002). Los periodos en los que las hembras son ovígeras y el número de puestas anuales varía con la distribución de la especie. En las aguas del Canal de la Mancha las hembras ovígeras aparecen desde abril hasta noviembre, con un pico máximo en junio (Kergariou, 1971; Pawson, 1995), pudiendo realizar dos desoves anuales (Pawson, 1995): el primer desove ocurre a principios de

mayo y la eclosión entre la segunda mitad de junio y la primera de julio, dos meses más tarde; tres o cuatro días después se produce el segundo desove, la eclosión ocurre un mes y medio después, requiriendo menos tiempo debido al aumento de la temperatura (Kergariou, 1971). Más al norte, en las pesquerías irlandesas de Magharees, las hembras ovígeras aparecen desde marzo - abril hasta agosto con un máximo en mayo (Fahy, 2001), observándose un único desove anual (Fahy, 2001; Rodhouse, 1984). Todos estos datos sugieren que el número de desoves anuales tiende a decrecer con la latitud.

Verísimo (2015) indica que la fecundidad de *M. brachydactyla* es muy variable: entre 125.000 y 540.000 huevos por puesta, variando el peso seco de esta entre 10 y 44 gramos. Kergariou (1971), estudiando las poblaciones del litoral sur de las Islas Británicas, calculó que el tamaño de la puesta varía entre 45.000 y 400.000 huevos (Kergariou, 1971). Individualmente, el volumen y peso seco de cada huevo también varía, entre 0,15 y 0,26 mm^3 y entre 74 y 116 µg, respectivamente (Verísimo, 2015; Verísimo et al., 2011). Se ha determinado que el número de huevos por puesta está positivamente correlacionado con el tamaño y peso corporal de la hembra (Kergariou, 1971; Verísimo, 2015; Verísimo et al., 2011), pero estos factores no influyen al tamaño y peso individual de los huevos (Verísimo, 2015; Verísimo et al., 2011). Su variación se debe a las dos estrategias reproductoras de esta especie. Durante los meses hibernales (diciembre a marzo), cuando las condiciones ambientales son más desfavorables, se favorece una estrategia de tipo K: las puestas son más reducidas en número pero los huevos son de mayor tamaño y peso, de ese modo las larvas disponen de más recursos nutricionales para sobrevivir condiciones de escasez de recursos. Por el contrario, durante los meses estivales (mayo a septiembre), cuando las condiciones ambientales son más favorables y el alimento abundante, se favorece una estrategia de tipo r: las puestas tienen mayor número de huevos pero estos son de menor tamaño y peso. El cambio de un tipo de estrategia a otra es gradual (Verísimo, 2015; Verísimo et al., 2011). El menor número de huevos durante el periodo hibernal en comparación con el estival ha sido confirmado por otros estudios (Rotllant et al., 2015). El periodo de incubación ha sido determinado en condiciones de cultivo, este fluctúa de 34 a 62 días, la reducción del periodo ocurre con el incremento de temperatura. Entre 1 y 6 días después de la eclosión las hembras son capaces de realizar una nueva puesta, de modo que bajo estas condiciones el número de puestas consecutivas oscila entre 1 y 4 a lo largo del año (González-Gurriarán et al., 1998; González-Gurriarán et al., 1993). Esto puede ocurrir gracias a la maduración paralela de nuevos oocitos mientras sucede la incubación de las puestas (González-Gurriarán et al., 1998). La tasa de eclosión puede verse afectada por las condiciones ambientales: p. e. una salinidad elevada (38 psu) en comparación con la normal (34 psu) reduce significativamente la tasa de eclosión (Rotllant et al., 2015).

1.3.3 Desarrollo larvario y post-larvario

El desarrollo larvario de *M. brachydactyla* incluye, como es típico en los miembros de la superfamilia Majoidea, tres estadios: dos de la fase zoea (zoea I y zoea II) y uno de la fase megalopa. El desarrollo incluye dos mudas metamórficas: al final de la fase zoea (la muda de zoea II a megalopa) y la muda de megalopa a primer juvenil (Fig. 1.3.3A-E). Los estadios de zoea son pelágicos, mientras que el estadio de megalopa es una etapa transicional entre un modo de vida pelágico y un modo de vida bentónico (Clark, 1986; Guerao et al., 2008; Guerao et al., 2012; Lebour, 1927). Tras el estadio de megalopa tiene lugar la metamorfosis a primer juvenil, el cuál es una versión en miniatura de los adultos con un estilo de vida bentónico (Fig. 1.3.3.1F). En condiciones de cultivo la duración de la fase de zoea es de 9 a 11 días a 18 ± 2 °C (Guerao et al., 2008), mientras que el desarrollo larvario puede completarse en 16-18 días a dicha temperatura (Andrés et al., 2008). En condiciones naturales, se ha calculado que las larvas de centollo completan la fase de zoea, el estilo de vida pelágico, en un periodo de 2 a 3 semanas dependiendo de la temperatura. Debido a la corta duración del desarrollo larvario, si las larvas se encuentran en un área cuyas corrientes son poco importantes, se sospecha que las larvas se distribuirán principalmente de forma local (Pawson, 1995).

Durante el desarrollo larvario el crecimiento en longitud y anchura es linear, mientras que el peso seco se dobla en relación al anterior estado larvario (Tabla 1).

Tabla 1. *M. brachydactyla*. Distintos estadios larvarios (ZI, zoea I; ZII, zoea II; Mg, megalopa) y primer juvenil (Jv). Crecimiento en tamaño (LC, longitud del caparazón; AC, anchura del caparazón; en milímetros) y peso seco (PS; en µg). Valores establecidos como media ± desviación estándar. Tabla publicada originalmente por Andrés et al. (2008).

	ZI	ZII	Mg	Jv
LC (mm)	0,57 ± 0,06	1,12 ± 0,05	1,55 ± 0,09	2,05 ± 0,09
AC (mm)	0,46 ± 0,04	0,90 ± 0,05	1,04 ± 0,10	1,51 ± 0,09
PS (µg)	94 ± 14	191 ± 33	389 ± 54	627 ± 152

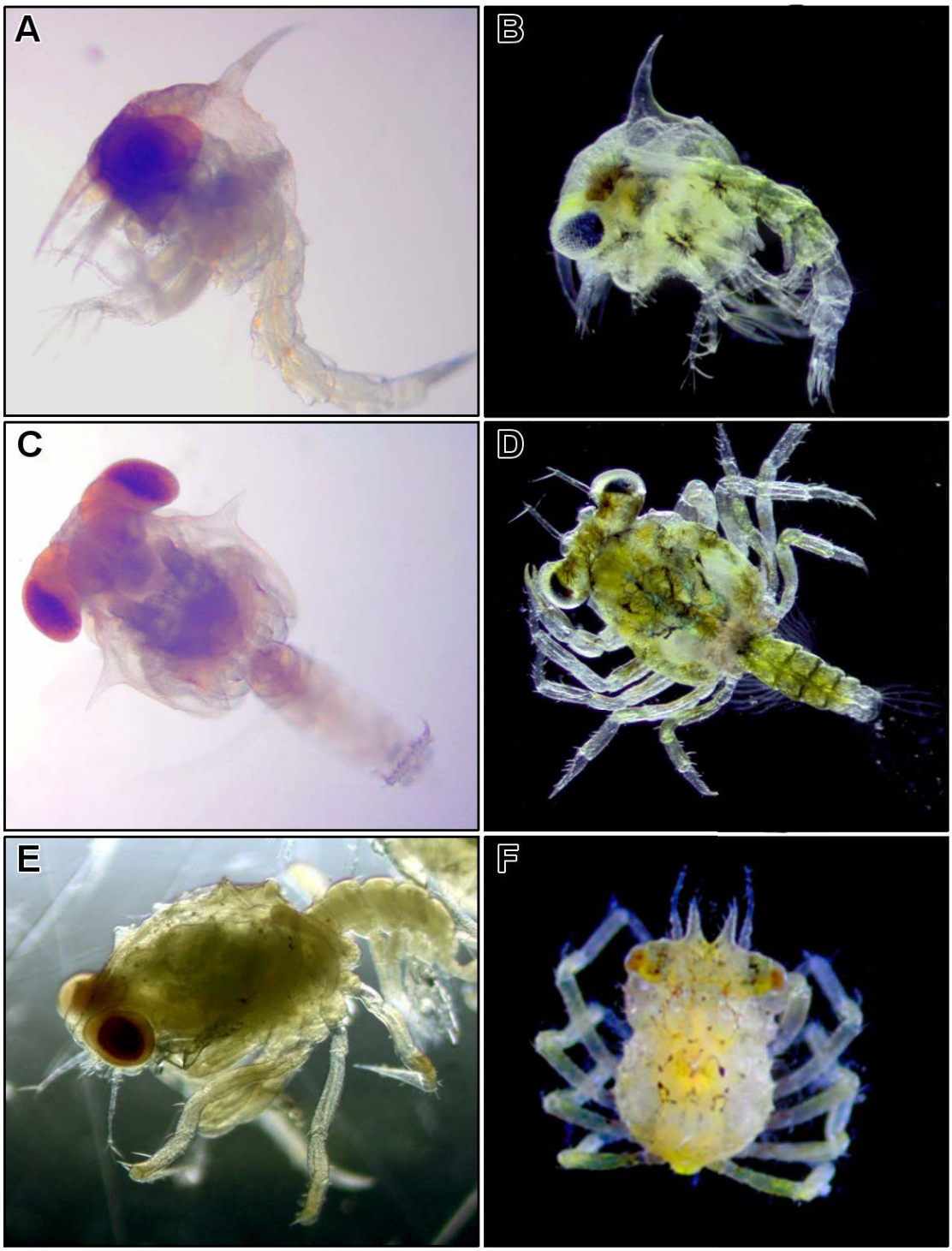

Fig. 1.3.3. Centollo atlántico, *Maja brachydactyla* Balss, 1922. Muestra de todos los estadios larvarios: Zoea I: vista lateral (A). Zoea II: vista lateral (B) y vista dorsal (C). Megalopa: vista dorsal (D) y vista lateral (E). Primer juvenil: vista dorsal (E).

Con la muda metamórfica a primer juvenil tiene lugar el asentamiento. Este es un proceso que ocurre en animales bentónicos con estadios larvarios pelágicos, definiéndose el asentamiento como el paso de un estilo de vida pelágico a uno bentónico y generalmente implica el inicio de la vida post-larvaria o juvenil (Pawlik, 1992). En *M. brachydactyla* este proceso ocurre desde finales de primavera hasta otoño, sospechándose que ocurre en tres oleadas en zonas rocosas cuya profundidad es inferior a 5-10 metros (Freire et al., 2002). Cuando los juveniles alcanzan una talla de 65 a 105 mm al cabo de 12-18 meses, se sucede una migración a fondos blandos (ej. arenas) situados entre 5 y 15 metros de profundidad (Fahy y Carroll, 2009; Freire et al., 2002).

Durante la fase juvenil se llegan a diferenciar ambos sexos observando el desarrollo de los pleópodos y la aparición de los gonoporos (Guerao y Rotllant, 2009b). El aspecto de los pleópodos durante el estadio de juvenil 1 es indiferenciado en relación al sexo, observándose un par de pleópodos en los pleonitos 2-6. La diferenciación comienza en el estadio juvenil 4: en las hembras los pares de pleópodos de los pleonitos 2 al 5 se transforman en birrámeos e incrementan gradualmente de tamaño en las subsecuentes mudas; por el contrario en los machos el número de pleópodos queda reducido a dos pares localizados en los pleonitos 1 y 2. Los gonoporos también aparecen en el estadio 4. La localización de los gonoporos varía con el sexo, como es característico entre los Heterotremata: en los machos se localizan en la coxa del quinto pereiópodo, mientras que en las hembras se localizan en el esternón del sexto pereionito, a la altura del tercer pereiópodo (Guerao y Rotllant, 2009a).

La longevidad natural de *M. brachydactyla* es incierta. Los cálculos y aproximaciones difieren según el autor. Así, Bodin et al. (2007) calcula una longevidad de entre 5 y 8 años, mientras que Le Foll (1993) menciona que podrían llegar a vivir hasta 7 años. En condiciones de cautiverio, ha sido posible mantener a las hembras adultas durante un periodo de casi dos años (Simeó et al., 2015).

1.3.4 Distribución y hábitat.

La distribución de *M. brachydactyla* es muy amplia (Fig. 1.3.4), abarcando la costa occidental del Océano Atlántico, desde el Sáhara occidental hasta el Mar del Norte (D'Udekem d'Acoz, 1999; Pawson, 1995), el cual debe ser el límite de su distribución ya que no ha sido citada en el Mar Báltico (Le Foll, 1993; Pawson, 1995). Según la revisión de Le Foll (1993, pág. 37-40), en el Mar del Norte es una especie rara, aunque ha sido citada en las costas de Alemania, Países Bajos y Bélgica. Le Foll (1993) y Pawson (1995) coinciden en considerarla una especie común en el Canal de la Mancha, apareciendo en la costa sur de las Islas Británicas y la costa norte y noreste de Francia. A mayor latitud, es una especie presente en el Mar de Irlanda, siendo citada en la costa este de Irlanda y la costa oeste de Inglaterra, incluyendo la Isla de Man (Le Foll, 1993; Pawson, 1995). A menor latitud es muy común, existiendo un amplio consenso acerca de su presencia en la costa atlántica de España, Portugal, Marruecos y Sáhara Occidental (Abelló et al., 2014; D'Udekem d'Acoz, 1999; Le Foll, 1993); así como las Islas Canarias y las Islas Azores (D'Udekem d'Acoz, 1999). Si bien, Le Foll (1993) también reporta citas de esta especie en las costas de Senegal, Guinea, Guinea-Bissau, Ghana, Gabón, Angola y Namibia; estas consisten en unos pocos ejemplares capturados entre los años '50 y '70, por lo que es preciso confirmar la presencia de *M. brachydactyla* en dichas costas, o si por el contrario se trata de otra especie. Recientemente, *M. brachydactyla* también ha sido citada en el Mar de Alborán, el extremo occidental del Mar Mediterráneo (Abelló et al., 2014).

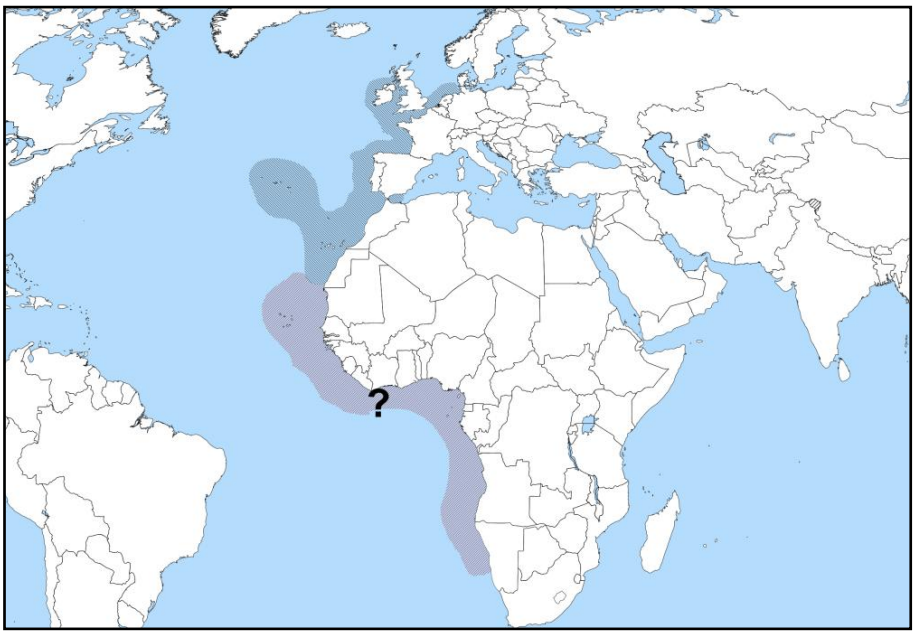

Fig. 1.3.4. Centollo, *Maja brachydactyla* Balss, 1922. Mapa de la distribución de la especie. Basado en las citas deLe Foll (1993), Pawson (1995), D'Udekem d'Acoz (1999) y Abelló et al. (2014). La presencia de la especie en la costa suroccidental de África debe ser confirmada.

El centollo *M. brachydactyla* es una especie con una marcada segregación espacial entre las poblaciones de adultos y juveniles. En la rías gallegas (A Coruña, Arousa) los juveniles y subadultos habitan aguas costeras de la plataforma continental a una profundidad de entre 1 y 10 metros, el hábitat es una combinación de fondos rocosos profusos en vegetación intercalados con fondos arenosos (Bernárdez et al., 2000; Bernárdez et al., 2003a; Freire et al., 1999; González-Gurriarán et al., 1993; González-Gurriarán y Freire, 1994), si bien el hábitat preferente parecen ser fondos rocosos con una profundidad media de 4 metros (Hines et al., 1995). En el litoral francés el hábitat de los juveniles suele estar formado por arenas y gravas, arenas y fangos, y fondos de Maërl, término por el que se definen formaciones de algas rojas coralinas (Le Foll, 1993). Los juveniles de *M. brachydactyla* son animales sedentarios y gregarios que suelen permanecer entorno la misma área (Corgos et al., 2011; Corgos et al., 2002), llegando a formar "guarderías" (Le Foll, 1993). En el Canal de La Mancha las guarderías comprenden fondos formados por roca y grava alternados con arenas o fango, localizados a una profundidad inferior a 20 metros (Latrouite y Le Foll, 1989; Pawson, 1995). Corgos et al. (2011) distingue entre ejemplares de "tipo rocoso" con caparazón rojizo y presencia de epibiontes, y ejemplares de "tipo arenoso" con caparazón claro y carente de epibiontes. Los autores han observado que los especímenes de "tipo rocoso" liberados en fondos arenosos pierden gradualmente los epibiontes (tiempo medio de 43 días) y la coloración (tiempo medio de 62 días), por lo que ambos tipos se corresponden con aclimataciones a diferentes ambientes. Freire et al. (2009) muestra que los juveniles no se establecen en un hábitat concreto sino que están continuamente desplazándose entre fondos rocosos y arenosos. La abundancia de juveniles decrece a partir de diciembre - enero hasta alcanzar un mínimo en agosto, coincidiendo con la muda terminal. Durante el otoño la abundancia de juveniles tiende a incrementarse debido al reclutamiento (Corgos et al., 2011).

El hábitat de los ejemplares adultos varía estacionalmente. Durante la época hibernal los adultos habitan fondos marinos profundos; en la costa gallega suelen ser capturados a profundidades de entre 15 y 40 metros (González-Gurriarán et al., 1993), pero también se han capturado en aguas de 100 metros de profundidad (Freire y González-Gurriarán, 1998). Durante la época de la migración hacia aguas someras (de septiembre a enero), en la Ría de A Coruña las capturas se producen a profundidades de entre 50 y 200 metros (Corgos et al., 2011); mientras que de enero a mayo la mayor tasa de capturas ocurre en fondos rocosos poco profundos de alrededor de 7 metros de profundidad media (Corgos et al., 2011; Freire et al., 1999). En la costa francesa del Canal de la Mancha, durante los meses hibernales se localizan en las zonas más profundas del canal (de hasta 100 metros); durante los meses de febrero y marzo se suelen localizar en fondos de entre 40 y 60 metros de profundidad; mientras que en primavera y verano se aproximan a la costa, colonizando fondos de entre 0 y 30 metros (Le Foll, 1993).

En la costa británica, los adultos habitan sustratos duros de estructura rocosa y coralina en la época hibernal, y sustratos blandos como arenas y praderas de hierbas marinas en la época estival (Kergariou, 1971). En el Mar de Iroise (costa occidental de la Bretaña Francesa) se suelen localizar en fondos profundos carentes de macrófitos durante la época hibernal y en fondos arenosos (principalmente las hembras en periodo de reproducción) poblados por Laminariales (Bodin et al., 2007). En la Bahía de Kilkieran (Irlanda), como en la costa gallega, durante la época estival los adultos habitan aguas someras de 3 a 27 metros de profundidad, habitando fondos rocosos intercalados con fondos arenosos y ricos en conchas y gravas (Rodhouse, 1984).

Le Foll (1993) menciona que existe una notable variación en la proporción de sexos de las capturas de *M. brachydactyla*, la cual podría representar una notable heterogeneidad espacial de ambos sexos. De modo similar, Fahy (2001) ha observado que en la pesquería de Magharees (Irlanda) el cociente número de machos/número de hembras cambia desde 3,09 en mayo a 0,77 en junio, postulando que este cambio puede deberse a una variación del patrón migratorio entre sexos. Similares resultados fueron obtenidos por Rodhouse (1984), la proporción de sexos alcanza su valor máximo en favor de los machos entre junio y julio, pero súbitamente este cae a mínimos durante agosto y septiembre. Guerao et al. (2016) analizaron los isótopos estables del caparazón de individuos procedentes de la costa de Galicia, revelando una mayor riqueza de $\delta^{13}C$ en el exoesqueleto de las hembras, un isótopo asociado a una mayor ingesta de macrófitos. Dado que *M. brachydactyla* tiene una dieta oportunista, los autores sugieren que tal diferencia puede deberse a que las hembras habitan aguas más someras que los machos durante el periodo previo a la muda terminal, las cuales son más ricas en macrófitos. Sin embargo, el estudio previo de Bodin et al. (2007) no encontró diferencia en la proporción de isótopos estables $\delta^{13}C$ y $\delta^{15}N$ en el músculo de ambos sexos. Aunque estos datos apoyan la hipótesis opuesta: machos y hembras habitan (o cohabitan) hábitats similares, estas diferencias también pueden explicarse por el hecho de que Bodin et al. (2007) estudiaron tejido corporal y Guerao et al. (2016) caparazón.

1.3.5 Comportamiento migratorio.

Los patrones de dispersión de los individuos varían entre juveniles y adultos: sedentarismo y gregarismo en los juveniles, así como comportamiento migratorio y dispersión durante la etapa adulta. Solo entre mediados y finales de verano tanto adultos como juveniles muestran un comportamiento similar: ambos permanecen en aguas someras (6,5 metros de media en juveniles y 9,5 metros de media en adultos) realizando desplazamientos cortos (aproximadamente 100-160 metros) sin una dirección determinada (Bernárdez et al., 2003a; b).

Los juveniles de *M. brachydactyla* son animales sedentarios de desplazamientos cortos, con tendencia a permanecer en el mismo área sin alcanzar poblaciones cercanas (Corgos et al., 2011; Corgos et al., 2002). Los juveniles suelen permanecer en un territorio de 150 a 580 metros de diámetro, incrementándose temporalmente hasta los 1000 metros. Mediante estudios basados en técnicas de marcaje se ha descubierto que los juveniles no suelen alejarse del punto de su liberación, así más del 50 % de los individuos recuperados no se habían alejado más de 200 metros de dicho punto (Corgos et al., 2010). Las técnicas de telemetría han demostrado que los juveniles tienden a desplazarse 10 metros diarios sin dirección determinada (González-Gurriarán y Freire, 1994; Hines et al., 1995).

Los adultos, por su parte, son animales con comportamiento migratorio. En la costa de Galicia el inicio de la migración desde fondos someros hacia fondos profundos comienza a finales de octubre e inicios de noviembre, este inicio puede prolongarse hasta enero en algunos ejemplares (Freire et al., 2002; Freire et al., 1999; González-Gurriarán et al., 2002). Es una migración que parece requerir cortos espacios de tiempo, observándose recorridos de 500 metros en 5-7 días con descensos en profundidad de hasta 9 metros diarios, llegando a descender de 13 a 54 metros de profundidad al final de la migración (Freire y González-Gurriarán, 1998; Freire et al., 1999; González-Gurriarán y Freire, 1994; González-Gurriarán et al., 2002; Hines et al., 1995). En el caso de las hembras la migración otoñal coincide con el final de la época reproductora. De acuerdo a los estudios de marcado y recaptura, en un corto periodo de tiempo (entre 4 y 16 días) las hembras descienden desde una profundidad media de 12 metros hasta una profundidad media de 63 metros, con un máximo de 96 metros, atravesando distintas zonas térmicas y sustratos (Freire y González-Gurriarán, 1998). Al año siguiente sucede una migración en sentido inverso, desde aguas profundas hacia aguas someras, que en el caso de las hembras coincide con la época de desove (Freire et al., 1999). Los machos adultos no participan en esta migración hacia aguas someras, sino que permanecen en los hábitats de invierno (Freire et al., 2002). La migración hacia aguas someras tiene su inicio a finales de noviembre, coincidiendo con individuos que aún no han iniciado su migración hacia aguas

profundas (Freire et al., 1999). La mayoría de las hembras adultas migran entre junio y febrero, después de la cópula (Freire et al., 2002). Son capaces de ascender hasta 12 metros diarios, hasta alcanzar una profundidad media de 7 metros (Freire et al., 1999).

En el Canal de La Mancha la situación es similar. Desde septiembre a enero ocurre la migración hacia fondos profundos que exceden los 40-50 metros (registrándose hasta 80 metros en algunos casos), donde los adultos pasarán la mayor parte invierno. Durante este periodo los animales experimentan una movilidad media de 1,5-3 kilómetros mensuales (Kergariou, 1971; Latrouite y Le Foll, 1989; Le Foll, 1993; Pawson, 1995), aunque también se han registrado desplazamientos de hasta 32 Km para ambos sexos, con una media de 5 Km por mes (Latrouite y Le Foll, 1989). La migración afecta a tantos individuos que no es posible recapturar individuos adultos en aguas someras durante el invierno (Kergariou, 1976). Dichas migraciones no solo implican un desplazamiento en profundidad y alejamiento de la costa, también se combinan con largos movimientos paralelos a la misma (Latrouite y Le Foll, 1989; Pawson, 1995). Al año siguiente, entre abril y junio, los adultos retornan a aguas someras (no necesariamente las áreas de "guardería" donde permanecieron durante su etapa juvenil) de profundidad media inferior a 20 metros, donde permanecen hasta junio y agosto (Kergariou, 1971; Le Foll, 1993; Pawson, 1995); siendo posible volver a capturar adultos en áreas cercanas a la costa durante la primavera y el verano (Kergariou, 1976). Las técnicas de marcaje y recaptura también muestran esta tendencia en la costa irlandesa, donde las capturas de adultos en aguas someras se incrementan en primavera, el pico se alcanza en verano y disminuye en otoño (Rodhouse, 1984).

No está claro que fenómeno/s actúa/n como estímulo que provoca el inicio de la migración. No se ha encontrado relación entre los movimientos migratorios y los ciclos mareales. Sin embargo, parece existir cierta relación con los cambios de temperatura a nivel de microhábitat. De modo que se ha postulado que los cambios térmicos en las masas de agua del fondo marino podrían desencadenar los distintos movimientos migratorios (Freire et al., 1999; González-Gurriarán et al., 2002). Por otro lado, ha sido observado que la muda terminal es un factor que altera el comportamiento de los animales, determinante a la hora de desencadenar la migración. Poco después de la muda terminal, el comportamiento de los nuevos adultos es muy similar al de su previa etapa como juveniles sedentarios, permaneciendo en los mismos fondos y desplazándose cortas distancias sin una dirección determinada. Sin embargo, poco después estos nuevos adultos inician la migración hacia aguas profundas, como se ha descrito previamente (Freire y González-Gurriarán, 1998; Freire et al., 1999; González-Gurriarán y Freire, 1994; González-Gurriarán et al., 2002; Hines et al., 1995).

1.3.6 Nicho ecológico y dieta.

Los miembros de la superfamilia Majoidea son conocidos como "cangrejos araña" y "cangrejos decoradores". El primer nombre refiere a su aspecto físico, generalmente globoso y con largas patas, recordando a dicho animal terrestre. El segundo nombre es una referencia a su habilidad única para camuflarse (Fig. 1.3.5). Como bien explica la revisión de Guinot y Wicksten (2015), el caparazón dorsal y los pereiópodos de estos braquiuros está poblado por setas en forma de gancho (o ahorquilladas) con gran adherencia. Utilizadas a modo de velcro, estas setas permiten al animal "disfrazarse" cubriendo su cuerpo (caparazón dorsal y pereiópodos) con elementos del entorno inmediato, lo cual permite simultáneamente ocultar al animal y repelar a los depredadores si dicho material incluye organismos tóxicos. De modo adicional, el caparazón de estos animales tiende a ser cubierto por epibiontes, organismos sésiles que crecen sobre el caparazón, los cuáles pueden contribuir al enmascaramiento (Guinot y Wicksten, 2015; Parapar et al., 1997). Parapar et al. (1997) describen estos organismos en *M. brachydactyla*, identificando hasta 309 taxones: algas (83 especies), anélidos (46 especies), cnidarios (44 especies), pancrustáceos (36 especies), moluscos (30 especies), ascidias (23 especies), poríferos (20 especies), briozoos (10 especies), equinodermos (6 especies) y picnogónidos (3 especies); los poliquetos, isópodos y anfípodos son herbívoros y depredadores que viven entre los anteriores. La distribución y abundancia de estos organismos varía con la región del exoesqueleto del animal (caparazón dorsal y ventral, región anterior y posterior, patas), la edad (individuos con mudas periódicas frente aquellos que han realizado la muda terminal), el hábitat (los fondos someros permiten el crecimiento de algas, los fondos profundos favorecen a los cnidarios), entre otros factores (Fernández et al., 1998; Parapar et al., 1997).

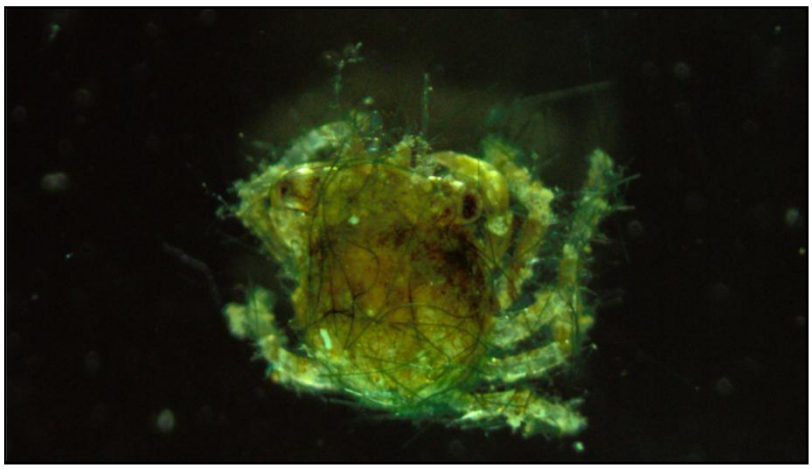

Fig. 1.3.5. Centollo, *Maja brachydactyla* Balss, 1922. Primer juvenil mostrando algunas algas adheridas al caparazón dorsal.

Los estudios realizados en la Ría de Arousa (Galicia, España) basados en el contenido estomacal demuestran que la dieta de *M. brachydactyla* es muy diversa, incluye varias especies de macrófitos (*Corallina* spp., *Cystoseira* spp., *Laminaria* spp., Phaeophyta, Rhodophyta y otras no identificadas), poríferos, corales, anélidos poliquetos, briozoos, quitones (*Acanthochiton acrinitus*), gasterópodos (*Bittium* spp., Trochiidae y otros sin identificar), bivalvos (*Mytilus* sp. y otros), pancrustáceos diversos (balánidos, peracáridos y diversos decápodos, incluyendo anomuros y braquiuros), holoturoideos (*Aslia lefevrei*), equinoideos (*Paracentrotus lividus* y otras especies sin identificar), ofiuroideos, ascidias e incluso teleósteos. El contenido estomacal más frecuente (de ocurrencia superior al 30 % de los estómagos) incluye algas como *Corallina* y laminariáceas, gasterópodos como *Bittium* sp. y tróquidos, equinodermos como *Aslia lefevrei*, así como materia orgánica indeterminada. El mayor peso seco del contenido estomacal corresponde con laminariáceas, bivalvos, equinodermos y ascidias solitarias. No se encontraron diferencias significativas entre el contenido estomacal de machos y hembras, resultando además muy similar entre la época hibernal y estival (Bernárdez et al., 2000; Freire et al., 2009; Kergariou, 1974). Se ha sugerido que la dieta está condicionada por la disponibilidad del alimento, especialmente su abundancia y movilidad, por lo que *M. brachydactyla* es una especie de hábitos alimentarios oportunistas, con preferencia sobre especies sésiles o con movilidad reducida (Bernárdez et al., 2000; Kergariou, 1974). Es una especie que ingiere gran cantidad de materia vegetal, pero no es descartable que en este caso la nutrición provenga principalmente de los epibiontes que crecen sobre los macrófitos, en lugar de los macrófitos propiamente dichos.

1.4 Bibliografía.

Abelló P, García Raso JE, Guerao G, Salmerón F. 2014. *Maja brachydactyla* (Brachyura: Majidae) in the western Mediterranean. Marine Biodiversity Records 7(e77).

Aguinaldo AMA, Turbeville JM, Linford LS, Rivera MC, Garey JR, Raff RA, Lake JA. 1997. Evidence for a clade of nematodes, arthropods and other moulting animals. Nature 387(6632):489-493.

Ahyong ST, Lai JCY, Sharkey D, Colgan DJ, Ng PKL. 2007. Phylogenetics of the brachyuran crabs (Crustacea: Decapoda): The status of Podotremata based on small subunit nuclear ribosomal RNA. Molecular Phylogenetics and Evolution 45(2):576-586.

Aleshin VV, Mikhailov KV, Konstantinova AV, Nikitin MA, Rusin LY, Buinova DA, Kedrova OS, Petrov NB. 2009. On the phylogenetic position of insects in the Pancrustacea clade. Molecular Biology 43(5):804-818.

Andrés M, Estévez A, Anger K, Rotllant G. 2008. Developmental patterns of larval growth in the edible spider crab, *Maja brachydactyla* (Decapoda: Majidae). J Exp Mar Biol Ecol 357(1):35-40.

Arias García AM, Torre García M, Fijo León MI, Arias Drake AM. 2013. IctioTerm. Base de datos terminológicos y de identificación de especies pesqueras de las costas de Andalucía. *Maja brachydactyla* (Balss, 1922).

Balss H. 1922. Crustacea VII: Decapoda Brachyura (Oxyrhyncha und Brachyrhyncha) und geographische Ubersicht fiber Crustacea Decapoda. In: Michaelsen W, editor. Beiträige zur Kenntnis der Meeresfauna Westafrikas. Hamburg: Friederichsen and Co. p 69-110.

Barriuso Fernández E. 1986. El léxico de la fauna marina en los puertos pesqueros de Asturias central. Principado de Asturias, Consejería de Educación Cultura y Deportes: Instituto de Estudios Asturianos (C.S.I.C.).

Belon P. 1555. La nature et diversité des poissons, avec leurs pourtraicts, représentez au plus près du naturel Estienne C, editor. Paris.

Bergström J, Hou X, Zhang X, Clausen S. 2008. A new ciew of the Cambrian arthropod *Fuxianhuia*. GFF 130(4):189-201.

Bernárdez C, Freire J, González-Gurriarán E. 2000. Feeding of the spider crab *Maja squinado* in rocky subtidal areas of the Ría de Arousa (north-west Spain). Journal of the Marine Biological Association of the United Kingdom 80(01):95-102.

Bernárdez C, González-Gurriarán E, García-Calvo B, Corgos A, Freire J. 2003a. Movements of juvenile and adult spider crab (*Maja squinado*) in the Ría da Coruña. In: Spedicato MT, Lembo G, Marmulla G, editors. Aquatic telemetry: advances and applications Proceedings of the Fifth Conference on Fish Telemetry held in Europe. Ustica, Palermo, Italy: FAO/COISPA. p 295.

Bernárdez C, González-Gurriarán E, García-Calvo B, Corgos A, Freire J. 2003b. Movements of juvenile and adult spider crab (*Maja squinado*) in the Ría da Coruña (N-W Spain). In: Spedicato MT, Lembo G, Marmulla G, editors. Aquatic telemetry: advances and applications. Ustica, Italy: Proceedings of the Fifth Conference on Fish Telemetry held in Europe. p 295.

Bodin N, Le Loc'h F, Hily C, Caisey X, Latrouite D, Le Guellec A-M. 2007. Variability of stable isotope signatures (δ13C and δ15N) in two spider crab populations (*Maja brachydactyla*) in Western Europe. J Exp Mar Biol Ecol 343(2):149-157.

Bracken HD, Toon A, Felder DL, Martin JW, Finley M, Rasmussen J, Palero F, Crandall KA. 2009. The Decapod Tree of Life: Compiling the data and moving toward a consensus of Decapod Evolution. Arthropod Systematics & Phylogeny 67(1):99-116.

Breton G. 2009. Description of *Priscinachus elongatus* n. gen., n. sp., and Priscinachidae n. fam. for the earliest spider crab (Crustacea, Decapoda, Majoidea), from the French Cretaceous (Cenomanian). Geodiversitas 31(3):509-523.

Briggs DEG, Sutton MD, Siveter DJ, Siveter DJ. 2004. A new phyllocarid (Crustacea: Malacostraca) from the Silurian Fossil–Lagerstätte of Herefordshire, UK. Proceedings of the Royal Society of London Series B: Biological Sciences 271(1535):131-138.

Brösing A, Richter S, Scholtz G. 2007. Phylogenetic analysis of the Brachyura (Crustacea, Decapoda) based on characters of the foregut with establishment of a new taxon. Journal of Zoological Systematics and Evolutionary Research 45(1):20-32.

Brusca RC, Brusca GJ. 2003. Invertebrates, 2nd Edition. 922 p.

Budd GE. 1996. The morphology of *Opabinia regalis* and the reconstruction of the arthropod stem-group. Lethaia 29(1):1-14.

Budd GE, Telford MJ. 2009. The origin and evolution of arthropods. Nature 457(7231):812-817.

Camus M. 1783. Histoire des animaux d'Aristote, avec la traduction francoise, par M. Camus, avocat au Parlement, censeur royal, etc, Volumen 2. Desaint V, editor.

Clark PF. 1986. The larval stages of *Maja squinado* (Herbst, 1788) (Crustacea: Brachyura: Majidae) reared in the laboratory. Journal of Natural History 20(4):825-836.

Corgos A, Bernárdez C, Sampedro P, Verísimo P, Freire J. 2011. Spatial structure of the spider crab, *Maja brachydactyla* population: Evidence of metapopulation structure. Journal of Sea Research 66(1):9-19.

Corgos A, Bernárdez C, Verísimo P, Freire J. 2002. Population dynamics of *Maja squinado* in the Ría de A Coruña (Galicia, NW Spain), using mark-recapture experiments. 8th Colloquium Crustacea Decapoda Mediterranea. Corfu, Greece.

Corgos A, Freire J. 2006. Morphometric and gonad maturity in the spider crab *Maja brachydactyla*: a comparison of methods for estimating size at maturity in species with determinate growth. ICES Journal of Marine Science: Journal du Conseil 63(5):851-859.

Corgos A, Sánchez N, Freire J. 2010. Dynamics of the Small-Scale Spatial Structure of a Population of the Spider Crab *Maja brachydactyla* (Decapoda: Majidae). Journal of Shellfish Research 29(1):25-36.

Cortés F. 2010. Cáncer. Diccionario médico-biológico, histórico y etimológico. Ediciones Universidad Salamanca.

Cresswell R. 1883. Aristotle's history of animals: in ten books. London: George Bell & Sons. 372 p.

Chen J, Waloszek D, Maas A. 2004. A new ‗great-appendage‘ arthropod from the Lower Cambrian of China and homology of chelicerate chelicerae and raptorial antero-ventral appendages. Lethaia 37(1):3-20.

D'Udekem d 'Acoz C . 1999. Inventaire et distribution des crustacés décapodes de l 'Atlantique nord - oriental, de la Méditerranée et des eaux contine ntales adjacentes au nord de 25 °N. naturels CP, editor. Paris: Muséum national d'histoire naturelle, Service du patrimoine naturel. 383 p.

Daley AC, Edgecombe GD. 2014. Morphology of *Anomalocaris canadensis* from the Burgess Shale. Journal of Paleontology 88(1):68-91.

Davie PJF, Guinot D, Ng PKL. 2015. Phylogeny of Brachyura. In: Castro P, Davie PJF, Guinot D, Schram F, Von Vaupel Klein C, editors. Treatise on Zoology - Anatomy Taxonomy Biology The Crustacea Volume 9 Part C: Brill, Leiden and Boston. p 922-979.

De Grave S, Pentcheff ND, Ahyong ST, Chan T-Y, Crandall KA, Dworschak PC, Felder DL, Feldmann RM, Fransen CHJM, Goulding LYD, Lemaitre R, Low MEY, Martin JW, Ng PKL, Schweitzer CE, Tan SH, Tshudy D, Wetzer R. 2009. A Classification of Living and Fossil Genera of Decapod Crustaceans. Raffles Bulletin of Zoology Supplement No. 21:1-109.

Dohle W. Are the insects terrestrial crustaceans? A discussion of some new facts and arguments and the proposal of the proper name 'Tetraconata' for the monophyletic unit Crustacea + Hexapoda; 2001. Société entomologique de France. p 85-103.

Dunn CW, Giribet G, Edgecombe GD, Hejnol A. 2014. Animal phylogeny and its evolutionary implications. Annual Review of Ecology, Evolution, and Systematics 45(371-395).

Dunn CW, Hejnol A, Matus DQ, Pang K, Browne WE, Smith SA, Seaver E, Rouse GW, Obst M, Edgecombe GD, Sorensen MV, Haddock SHD, Schmidt-Rhaesa A, Okusu A, Kristensen RM, Wheeler WC, Martindale MQ, Giribet G. 2008. Broad phylogenomic sampling improves resolution of the animal tree of life. Nature 452(7188):745-749.

Dzik J. 2011. The xenusian-to-anomalocaridid transition within the lobopodians. Bollettino della Società Paleontologica Italiana 50(1):65-74.

Edgecombe GD. 2009. Palaeontological and molecular evidence linking Arthropods, Onychophorans, and other Ecdysozoa. Evolution: Education and Outreach 2(2):178-190.

Edgecombe GD. 2010. Arthropod phylogeny: An overview from the perspectives of morphology, molecular data and the fossil record. Arthropod Structure & Development 39(2-3):74-87.

Fahy E. 2001. The Magharees spider crab *Maja squinado* fishery in 2000. Irish Fisheries Investigations 9. 21 + appendix p.

Fahy E, Carroll J. 2009. Vulnerability of male spider crab *Maja brachydactyla* (Brachyura: Majidae) to a pot fishery in south-west Ireland. Journal of the Marine Biological Association of the United Kingdom 89(7):1353-1366.

Feldmann RM. 2016. *Antarctomithrax thomsoni*, a new genus and species of crab (Brachyura; Majidae) from the La Meseta Formation (Eocene) of Seymour Island, Antarctica. Journal of Paleontology 68(1):174-176.

Feldmann RM, Schweitzer CE. 2010. The oldest shrimp (Devonian: Famennian) and remarkable preservation of soft tissue. Journal of Crustacean Biology 30(4):629-635.

Fernández L, Parapar J, González-Gurriarán E, Muíño R. 1998. Epibiosis and ornamental cover patterns of the spider crab *Maja squinado* on the Galician coast, Northwestern Spain: influence of behavioral and ecological characteristics of the host Journal of Crustacean Biology 18(4):728-737.

Fraaije RHB, van Bakel BWM, Guinot D, Jagt JWM. 2013. A new Middle Jurassic (Bajocian) homolodromioid crab from northwest France; th earliest record of the Tanidromitidae. Boletín de la Sociedad Geológica Mexicana 65(2):249-254.

Fransen C, Türkay M. 2007. *Maja brachydactyla* Balss, 1922. World Register of Marine Species.

Freire J, Bernárdez C, Corgos A, Fernández L, González-Gurriarán E, Sampedro MP, Verísimo P. 2002. Management strategies for sustainable invertebrate fisheries in coastal ecosystems of Galicia (NW Spain). Aquatic Ecology 36(1):41-50.

Freire J, Carabel S, Verísimo P, Bernárdez C, Fernández L. 2009. Patterns of juvenile habitat use by the spider crab *Maja brachydactyla* as revealed by stable isotope analyses. Sci Mar 73(1):39-49.

Freire J, González-Gurriarán E. 1998. New approaches to the behavioural ecology of decapod crustaceans using telemetry and electronic tags. In: Lagardère J-P, Anras M-LB, Claireaux G, editors. Advances in Invertebrates and Fish Telemetry: Proceedings of the Second Conference on Fish Telemetry in Europe, held in La Rochelle, France, 5–9 April 1997. Dordrecht: Springer Netherlands. p 123-132.

Freire J, González-Gurriarán E, Bernárdez C. 1999. Migratory patterns in the spider crab *Maja squinado* using telemetry and electronic tags. ICES Annual Science Conference Theme Session AA ICES CM 1999/AA: 14.

Garassino A, Pasini G, De Angeli A, Charbonnier S, Famiani F, Baldanza A, Bizzarri R. 2012. The decapod community from the Early Pliocene (Zanclean) of ―La Serra" quarry (San Miniato, Pisa, Toscana, central Italy): sedimentology, systematics, and palaeoenvironmental implications. Annales de Paléontologie 98(1):1-61.

García-Flórez L, Fernández-Rueda P. 2003. Parámetros biológicos del centollo, *Maja brachydactyla* (Brachyura: Majidae), procedente de capturas comerciales en la zona central de Asturias (España) y su aplicación a la gestión pesquera. Naturalia Cantabricae 2:45-52.

Garey JR. 2001. Ecdysozoa: The Relationship between Cycloneuralia and Panarthropoda. Zoologischer Anzeiger - A Journal of Comparative Zoology 240(3):321-330.

Giribet G, Edgecombe GD. 2012. Reevaluating the Arthropod Tree of Life. Annual Review of Entomology 57(1):167-186.

González-Gurriarán E, Fernández L, Freire J, Muiño R. 1998. Mating and role of seminal receptacles in the reproductive biology of the spider crab *Maja squinado* (Decapoda, Majidae). J Exp Mar Biol Ecol 220(2):269-285.

González-Gurriarán E, Fernández L, Freire J, Muiño R, Parapar J. 1993. Reproduction of the spider crab *Maja squinado* (Brachyura: Majidae) in the southern Galician coast (NW Spain). International Council for the Exploration of the Sea: Shellfish Committe ICES C.M. 1993/K:19.

González-Gurriarán E, Freire J. 1994. Movement patterns and habitat utilization in the spider crab *Maja squinado* (Herbst) (Decapoda, Majidae) measured by ultrasonic telemetry. J Exp Mar Biol Ecol 184(2):269-291.

González-Gurriarán E, Freire J, Bernárdez C. 2002. Migratory patterns of female spider crabs *Maja squinado* detected using electronics tags and telemetry. Journal of Crustacean Biology 22(1):91-97.

González-Gurriarán E, Freire J, Parapar J, Sampedro MP, Urcera M. 1995. Growth at moult and moulting seasonality of the spider crab, *Maja squinado* (Herbst) (Decapoda: Majidae) in experimental conditions: implications for juvenile life history. J Exp Mar Biol Ecol 189(1):183-203.

Guerao G, Andree KB, Froglia C, Simeó CG, Rotllant G. 2011. Identification of European species of *Maja* (Decapoda: Brachyura: Majidae): RFLP analyses of COI mtDNA and morphological considerations. Sci Mar 75(1):129-134.

Guerao G, Pastor E, Martin J, Andrés M, Estévez A, Grau A, Duran J, Rotllant G. 2008. The larval development of *Maja squinado* and *M. brachydactyla* (Decapoda, Brachyura, Majidae) described from plankton collected and laboratory-reared material. Journal of Natural History 42(33-34):2257-2276.

Guerao G, Rotllant G. 2009a. Post-larval development and sexual dimorphism of the spider crab *Maja brachydactyla* (Brachyura: Majidae). Sci Mar 73:797-808.

Guerao G, Rotllant G. 2009b. Survival and growth of post-settlement juveniles of the spider crab *Maja brachydactyla* (Brachyura: Majoidea) reared under individual culture system. Aquaculture 289(1-2):181-184.

Guerao G, Rotllant G, Gisbert E, Uyà M, Cardona L. 2016. Consistent habitat segregation between sexes in the spider crabs *Maja brachydactyla* and *Maja squinado* (Brachyura), as revealed by stable isotopes. Sci Mar 80(1):103-110.

Guerao G, Simeó CG, Anger K, Urzúa Á, Rotllant G. 2012. Nutritional vulnerability of early zoea larvae of the crab *Maja brachydactyla* (Brachyura, Majidae). Aquatic Biology 16(3):253-264.

Gueriau P, Charbonnier S, Clément G. 2014a. Angustidontid crustaceans from the Late Devonian of Strud (Namur Province, Belgium): insights into the origin of Decapoda. Neues Jahrbuch für Geologie und Paläontologie - Abhandlungen 273(3):327-337.

Gueriau P, Charbonnier S, Clément G. 2014b. First decapod crustaceans in a Late Devonian continental ecosystem. Palaeontology 57(6):1203-1213.

Guinot D. 1977. Propositions pour une nouvelle classification des Crustacés Décapodes Brachyoures. Comptes rendus hebdomadaires des séances de l'Académie des Sciences (D) 285:1049-1052.

Guinot D, Wicksten MK. 2015. Camouflage: carrying behaviour, decoration behaviour, and other modalities of concealment in Brachyura. In: Castro P, Davie PJF, Guinot D, Schram F, Von Vaupel Klein C, editors. Treatise on Zoology - Anatomy, taxonomy, biology: Brill, Leiden and Boston. p 582-638.

Halanych KM. 2004. The new view of animal phylogeny. Annual Review of Ecology, Evolution, and Systematics 35:229-256.

Halanych KM. 2016. How our view of animal phylogeny was reshaped by molecular approaches: lessons learned. Organisms Diversity & Evolution 16(2):319-328.

Herbst JFW. 1788. Versuch einer Naturgeschichte der Krabben und Krebse : nebst einer systematischen Beschreibung ihrer verschiedenen Arten Berlin and Stralsund: Bei Gottlieb August Lange.

Hines AH, Wolcott TG, González-Gurriarán E, González-Escalante JL, Freire J. 1995. Movement patterns and migrations in crabs: telemetry of juvenile and adult behaviour in *Callinectes sapidus* and *Maja squinado*. Journal of the Marine Biological Association of the United Kingdom 75(1):27-42.

Hultgren KM, Stachowicz JJ. 2008. Molecular phylogeny of the brachyuran crab superfamily Majoidea indicates close congruence with trees based on larval morphology. Molecular Phylogenetics and Evolution 48(3):986-996.

Iglesias J, Sánchez FJ, Moxica C, Fuentes L, Otero JJ, Pérez JL. 2002. Datos preliminares sobre el cultivo de larvas y juveniles de centolla *Maja squinado* Herbst, 1788 en el Centro Oceanográfico de Vigo del Instituto Español de Oceanografía. Boletín del Instituto Español de Oceanografía 18(1-4):25-30.

Jamieson BGM. 1994. Phylogeny of the Brachyura with particular reference to the Podotremata: evidence from a review of spermatozoal ultrastructure (Crustacea, Decapoda). Philosophical Transactions of the Royal Society of London Series B: Biological Sciences 345(1314):373-393.

Kergariou G. 1971. L'Araignee de Mer, *Maia squinado* L., sur le littoral de Bretagne. Science et Pêche 205:12-19.

Kergariou G. 1974. Régime alimentaire de Maia squinado. Conseil International pour l'Exploration de la Mer ICES CM (International Council for the Exploration of the Sea Shellfish and Benthos Committee); 1974/K:36.

Kergariou G. 1976. Premiers résultats obtenus par marquage de l'araignée de mer, *Maia squinado*, déplacements, mortalité par pêche. Conseil International pour l'Exploration de la Mer ICES CM (International Council for the Exploration of the Sea Shellfish and Benthos Committee); 1976/K:14.

Klompmaker AA. 2013. Extreme diversity of decapod crustaceans from the mid-Cretaceous (late Albian) of Spain: Implications for Cretaceous decapod paleoecology. Cretaceous Research 41:150-185.

Latrouite D, Le Foll D. 1989. Donnees sur les migrations des crabes tourteau *Cancer pagurus* et les araignees de mer *Maja squinado*. Océanis 15(2):133-142.

Le Foll D. 1993. Biologie et exploitation de l'araignée de mer *Maja squinado* Herbst en Manche Ouest [Doctoral Dissertation]. Plouzane (France): Université de Bretagne Occidentale. 517 p.

Lebour MV. 1927. Studies of the Plymouth Brachyura. I. The rearing of crabs in captivity, with a description of the larval stages of *Inachus dorsettensis*, *Macropodia longirostris* and *Maia squinado*. Journal of the Marine Biological Association of the United Kingdom 14(3):795-821.

Legg DA, Sutton MD, Edgecombe GD, Caron J-B. 2012. Cambrian bivalved arthropod reveals origin of arthrodization. Proceedings of the Royal Society B: Biological Sciences.

Liu J, Shu D, Han J, Zhang Z, Zhang X. 2008. Origin, diversification, and relationships of Cambrian lobopods. Gondwana Research 14(1–2):277-283.

Maas A, Waloszek D. 2005. Phosphatocopina – ostracode-like sister group of Eucrustacea. Hydrobiologia 538(1):139-152.

Mallatt JM, Garey JR, Shultz JW. 2004. Ecdysozoan phylogeny and Bayesian inference: first use of nearly complete 28S and 18S rRNA gene sequences to classify the arthropods and their kin. Molecular Phylogenetics and Evolution 31(1):178-191.

Martin JW, Davis GE. 2001. An updated classification of the recent crustacea. Los Angeles, California: Natural History Museum of Los Angeles County.

McLay CL, Feldmann RM, MacKinnon DI. 1995. New species of Miocene spider crabs from New Zealand, and a partial cladistic analysis of the genus *Leptomithrax* Miers, 1876 (Brachyura: Majidae). New Zealand Journal of Geology and Geophysics 38(3):299-313.

Neumann V. 1998. A review of the *Maja squinado* (Crustacea: Decapoda: Brachyura) species-complex with a key to the eastern Atlantic and Mediterranean species of the genus. Journal of Natural History 32(10-11):1667-1684.

Ng PKL, Guinot D, Davie PJF. 2008. Systema Brachyurorum: Part I. An annotated cheklist of extant brachyuran crabs of the world. The Raffles Bulletin of Zoology 17:1-268.

Ng PKL, Richer De Forges B. 2015. Revision of the spider crab genus *Maja* Lamarck, 1801 (Crustacea: Brachyura: Majoidea: Majidae), with descriptions of seven new genera and 17 new species from the Atlantic and Indo-West Pacific. Raffles Bulletin of Zoology 63:110-225.

Ogle W. 1912. De Partibus Animalium. In: Smith JA, Ross WD, editors. The Works of Aristotle. Oxford: Clarendon Press.

Ortega-Hernández J. 2016. Making sense of ‗lower‘ and ‗upper‘ stem-group Euarthropoda, with comments on the strict use of the name Arthropoda von Siebold, 1848. Biological Reviews 91(1):255-273.

Ou Q, Shu D, Mayer G. 2012. Cambrian lobopodians and extant onychophorans provide new insights into early cephalization in Panarthropoda. Nature Communications 3(1261).

Parapar J, Fernández L, González-Gurriarán E, Muíño R. 1997. Epibiosis and masking material in the spider crab *Maja squinado* (Decapoda: Majidae) in the Ría de Arousa (Galicia, NW Spain). Cahiers de Biologie Marine 38(4):221-234.

Pasini G, Garassino A. 2014. Report of *Maja* cf. *Maja squinado* (Herbst, 1788) (Crustacea, Brachyura, Majidae) from the Early Pliocene of Cheglio (Varese, northern Italy). Natural History Sciences Atti della Società Italiana di Scienze Naturali e del Museo Civico di Storia Naturale in Milano 1(2):139-144.

Pawlik JR. 1992. Chemical ecology of the settlement of benthic marine invertebrates. Oceanography and Marine Biology: An Annual Review 30(273-335).

Pawson MG. 1995. Biogeographical identification of English Channel fish and shellfish stocks. Lowestoft: Ministry of Agriculture, Fisheries and Food Directorate of Fisheries Research: Fisheries Research Technical Report, Nº 99. 72 p.

Poore G. 2016. Decapoda. World Register of Marine Species (WoRMS). .

Poore G, Türkay M. 2015. Pleocyemata. World Register of Marine Species (WoRMS). .

Porter ML, Pérez-Losada M, Crandall KA. 2005. Model-based multi-locus estimation of decapod phylogeny and divergence times. Molecular Phylogenetics and Evolution 37(2):355-369.

Regier JC, Shultz JW, Kambic RE. 2005. Pancrustacean phylogeny: hexapods are terrestrial crustaceans and maxillopods are not monophyletic. Proceedings of the Royal Society B: Biological Sciences 272(1561):395-401.

Richter S, Møller OS, Wirkner CS. 2009. Advances in crustacean phylogenetics. Arthropod Systematics & Phylogeny 67(2):275-286.

Richter S, Scholtz G. 2001. Phylogenetic analysis of the Malacostraca (Crustacea). Journal of Zoological Systematics and Evolutionary Research 39(3):113-136.

Rodhouse DM. 1984. Experimental fishing for the Spider crab, *Maia Squinado*: sea and laboratory trials. Journal of the Marine Biological Association of the United Kingdom 64(2):251-259.

Rotllant G, González-Gurriarán E, Fernández L, Benhalima K, Ribes E. 2007. Ovarian maturation of the multi-spawning spider crab *Maja brachydactyla* (Decapoda: Majidae) with special reference to yolk formation. Marine Biology 152(2):383-394.

Rotllant G, Simeó CG, Macià G, Estévez A. 2015. High environmental salinity reduces the reproductive potential of the spider crab *Maja brachydactyla* (Decapoda, Majidae). Marine Ecology 36(3):496-505.

Sampedro MP, González G, E., Freire J, Muiño R. 1999. Morphometry and sexual maturity in the spider crab *Maja squinado* (Decapoda: Majidae) in Galicia, Spain. Journal of Crustacean Biology 19(3):578-592.

Scarborough J. 1992. Medical and Biological Terminologies: Classical Origins: University of Oklahoma Press.

Scholtz G. 2014. Evolution of crabs - history and deconstruction of a prime example of convergence. Contributions to Zoology 83(2):87-105.

Schram F. 2009. On the origin of Decapoda. In: Martin JW, Crandall KA, Felder DL, editors. Decapod Crustacean Phylogenetics: CRC Press. p 3-13.

Schram FR, Feldmann RM, Copeland MJ. 1978. The Late Devonian Palaeopalaemonidae and the earliest decapod crustaceans. Journal of Paleontology 52(6):1375-1387.

Schweitzer CE, Feldmann RM. 2010. The oldest Brachyura (Decapoda: Homolodromioidea: Glaessneropsoidea) known to date (Jurassic). Journal of Crustacean Biology 30(2):251-256.

Schweitzer G, Koppka J. 2011. Decapods (Crustacea: Brachyura) from the Jurassic of Germany and Lithuania, with descriptions of new species of *Planoprosopon* and *Tanidromites*. Neues Jahrbuch für Geologie und Paläontologie - Abhandlungen 260(2):221-235.

Simeó CG, Andrés M, Estévez A, Rotllant G. 2015. The effect of male absence on the larval production of the spider crab *Maja brachydactyla* Balss, 1922. Aquaculture Research 46(4):937-944.

Siveter DJ, Briggs DEG, Siveter DJ, Sutton MD, Legg D. 2017. A new crustacean from the Herefordshire (Silurian) Lagerstätte, UK, and its significance in malacostracan evolution. Proceedings of the Royal Society B: Biological Sciences 284(1851).

Siveter DJ, Williams M, Waloszek D. 2001. A Phosphatocopid crustacean with appendages from the Lower Cambrian. Science 293(5529):479-481.

Sotelo G, Morán P, Posada D. 2008. Genetic identification of the northeastern Atlantic spiny spider crab as *Maja brachydactyla* Balss, 1922. Journal of Crustacean Biology 28(1):76-81.

Sotelo G, Morán P, Posada D. 2009. Molecular phylogeny and biogeographic history of the European *Maja* spider crabs (Decapoda, Majidae). Molecular Phylogenetics and Evolution 53(1):314-319.

Spears T, Abele LG, Kim W. 1992. The monophyly of brachyuran crabs: a phylogenetic study based on 18s rRNÅ. Systematic Biology 41(4):446-461.

Starzyk N. 2013. Jurassic crabs: new characters of carapace diagnostic to known tanidromitid species. Neues Jahrbuch für Geologie und Paläontologie - Abhandlungen 269(2):173-187.

Tavares M. 2003. A new theorical approach for the stuy of monophyly of the Brachyura (Crustacea: Decapoda) and its impact on the Anomura. Memoirs of Museum Victoria 60(1):145-149.

Toon A, Finley M, Staples J, Crandall K. 2009. Decapod phylogenetics and molecular evolution. In: Martin JW, Crandall KA, Felder DL, editors. Decapod Crustacean Phylogenetics: CRC Press. p 15-29.

Tsang LM, Ma KY, Ahyong ST, Chan TY, Chu KH. 2008. Phylogeny of Decapoda using two nuclear protein-coding genes: Origin and evolution of the Reptantia. Molecular Phylogenetics and Evolution 48(1):359-368.

Tsang LM, Schubart CD, Ahyong ST, Lai JCY, Au EYC, Chan T-Y, Ng PKL, Chu KH. 2014. Evolutionary history of true crabs (Crustacea: Decapoda: Brachyura) and the origin of freshwater crabs. Molecular Biology and Evolution 31(5):1173-1187.

Van Roy P, Briggs DEG. 2011. A giant Ordovician anomalocaridid. Nature 473(7348):510-513.

Van Roy P, Daley AC, Briggs DEG. 2015. Anomalocaridid trunk limb homology revealed by a giant filter-feeder with paired flaps. Nature 522(7554):77-80.

Varola A. 1981. Crostacei decapodi neogenici della Peninsola Salentina (Italia). Thalassia Salentina 2:3-51.

Vega FJ, Feldmann RM, Sour-Tovar F. 2016. Fossil crabs (Crustacea: Decapoda) from the Late Cretaceous cárdenas Formation, east-central Mexico. Journal of Paleontology 69(2):340-350.

Vega FJ, Nyborg TG, Perrilliat MDC. 2006. Mesozoic and Tertiary Decapod Crustacea from Mexico. In: Vega FJ, Nyborg TG, Perrilliat MDC, Montellano-Ballesteros M, Cevallos-Ferriz SRS, Quiroz-Barroso SA, editors. Studies on Mexican Paleontology. Dordrecht: Springer Netherlands. p 79-100.

Verísimo P. 2015. Implicaciones de la composición bioquímica y la condición energética de la centolla, *Maja brachydactyla* (Balss, 1922), en su ciclo reproductivo. Doctoral Thesis: Universidade da Coruña. 266 p.

Verísimo P, Bernárdez C, González-Gurriarán E, Freire J, Muino R, Fernández L. 2011. Changes between consecutive broods in the fecundity of the spider crab, *Maja brachydactyla*. ICES J Mar Sci 68(3):472-478.

von Reumont BM, Jenner RA, Wills MA, Dell'Ampio E, Pass G, Ebersberger I, Meyer B, Koenemann S, Iliffe TM, Stamatakis A, Niehuis O, Meusemann K, Misof B. 2012. Pancrustacean Phylogeny in the Light of New Phylogenomic Data: Support for Remipedia as the Possible Sister Group of Hexapoda. Molecular Biology and Evolution 29(3):1031-1045.

Voultsiadou E, Vafidis D. 2007. Marine invertebrate diversity in Aristotle's zoology. Contributions to Zoology 76(2):103-120.

Waloszek D, Chen J, Maas A, Wang X. 2005. Early Cambrian arthropods—new insights into arthropod head and structural evolution. Arthropod Structure & Development 34(2):189-205.

Xianguang H, Bergström J, Jie Y. 2006. Distinguishing anomalocaridids from arthropods and priapulids. Geological Journal 41(3-4):259-269.

Yang J, Ortega-Hernandez J, Butterfield NJ, Zhang X-g. 2013. Specialized appendages in fuxianhuiids and the head organization of early euarthropods. Nature 494(7438):468-471.

Yang J, Ortega-Hernández J, Gerber S, Butterfield NJ, Hou J-b, Lan T, Zhang X-g. 2015. A superarmored lobopodian from the Cambrian of China and early disparity in the evolution of Onychophora. Proceedings of the National Academy of Sciences 112(28):8678-8683.

Yang J, Ortega-Hernández J, Lan T, Hou J-b, Zhang X-g. 2016. A predatory bivalved euarthropod from the Cambrian (Stage 3) Xiaoshiba Lagerstätte, South China. Scientific Reports 6:27709.

Zhang X-g, Pratt Brian R. 2012. The first stalk-eyed Phosphatocopine crustacean from the Lower Cambrian of China. Current Biology 22(22):2149-2154.

Zhang X-g, Siveter DJ, Waloszek D, Maas A. 2007. An epipodite-bearing crown-group crustacean from the Lower Cambrian. Nature 449(7162):595-598.

Zhang X, Briggs DEG. 2007. The nature and significance of the appendages of *Opabinia* from the Middle Cambrian Burgess Shale. Lethaia 40(2):161-173.

OBJETIVOS y ESTRUCTURA

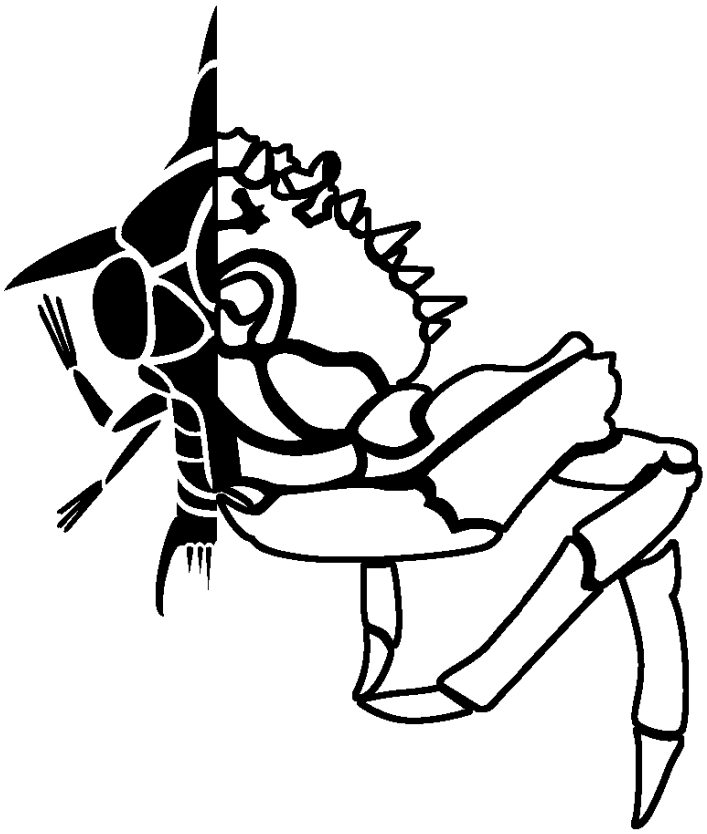

2.1 Objetivos.

La presente Tesis parte del proyecto INIA RTA2011-00004-00-00, cuyos objetivos principales nacen de un objetivo primario que podríamos considerar de carácter aplicado: convertir a *Maja brachydactyla* en una especie de cultivo acuícola, es decir, en una especie más de la creciente industria de la acuicultura. La razón de este potencial deriva principalmente de dos factores independientes: su valor comercial y sus características biológicas. Dichas características ya han sido descritas en el capítulo anterior, de modo resumido estas incluyen una elevada fecundidad, rápido desarrollo (l8 meses a talla comercial), desarrollo larvario abreviado y dieta generalista/oportunista.

Como se expondrá con mayor detalle en capítulos posteriores, estudios previos han permitido obtener un conocimiento básico de la reproducción, cultivo larvario y nutrición de *M. brachydactyla*. Sin embargo, dichos avances no son suficientes para rentabilizar su cultivo. Todavía es preciso optimizar el cultivo larvario y en especial solventar la elevada mortalidad, principalmente durante el asentamiento. Asimismo, el avance en la mejora nutricional de esta especie fácilmente puede quedar estancado, ya que se desconoce su anatomía digestiva. Por ello, los principales objetivos de este proyecto pretenden avanzar en tales direcciones:

1) conocer el efecto de la temperatura y del fotoperiodo en el desarrollo larvario (duración, supervivencia y composición bioquímica en cada estadio)

2) determinar el efecto del substrato y de substancias biogénicas en la inducción de la metamorfosis (asentamiento de las megalopas)

3) describir en detalle la morfología (histología y citología) del aparato digestivo de las larvas y primer juvenil, determinando los cambios ontogénicos a lo largo del desarrollo

Aunque el objetivo final (o a largo plazo) pueda considerarse aplicado, este solo puede lograrse mediante investigación de carácter básico. En este punto entran los mencionados objetivos del proyecto. Sin embargo, dado su carácter dispar, los distintos objetivos han requerido metodologías de estudio diferentes y se han obtenido resultados que no pueden discutirse en conjunto. Por esa razón, ha sido preciso subdividir la presente memoria en dos bloques principales: BLOQUE 1 dedicado al cultivo larvario y BLOQUE 2 dedicado al estudio del sistema digestivo. Cada bloque cuenta con su propio capítulo de introducción, que detalla los antecedentes, metodología de estudio empleada y objetivos precisos; cada bloque también cuenta con su propio capítulo de discusión, donde los resultados obtenidos en los distintos capítulos del bloque son comentados de modo global, asumiendo una perspectiva de conjunto.

Teniendo esto en cuenta, los objetivos de cada bloque son resumidos a continuación.

2.2 BLOQUE 1. Larvicultura.

Este bloque engloba los objetivos 1 y 2, ya que en conjunto incluyen metodologías aplicadas al cultivo larvario. De forma adicional, los objetivos de este bloque fueron expandidos para estudiar la influencia de la salinidad sobre el desarrollo larvario. Este tipo de estudios resulta interesante no solo porque aporta información que podría llegar a aplicarse en un hipotético cultivo de escala industrial, sino que permite averiguar los límites de tolerancia larvaria a distintos parámetros ambientales, así como sus requerimientos para el asentamiento. Por ello, este tipo de estudios aporta datos que podrían ayudar a entender la biología de la etapa larvaria de esta especie, incluyendo el nicho ecológico que ocupan en el medio externo, lo cual es muy interesante ya que apenas hay datos sobre la biología larvaria de *M. brachydactyla*. De forma adicional, la información obtenida puede contrastarse con datos obtenidos en otras especies de braquiuros, enriqueciendo la información disponible en este grupo animal.

2.3 BLOQUE 2. Sistema Digestivo.

Este bloque engloba el objetivo 3, ya que se trata de un estudio en detalle del aparato digestivo de esta especie. Este objetivo ha sido expandido para incluir la morfología (histología y citología) del aparato digestivo de los especímenes adultos. Si bien los juveniles y adultos son similares en cuanto a su morfología externa, resultará interesante comprobar si esta situación también se corresponde con su anatomía interna. Como se verá en el capítulo introductorio de este bloque, el conocimiento del sistema digestivo es útil para el desarrollo de dietas (naturales o artificiales) que optimicen el cultivo de las especies acuícolas. Sin embargo, más allá de este punto, cabe decirse que existen muy pocos datos acerca de la anatomía del aparato digestivo de los decápodos durante los estadios larvarios, de tal forma que los escasos estudios disponibles tienden a ser poco detallados. Personalmente, considero que esta falta de información es motivo por sí solo para estudiar con detalle dichos órganos. El carácter exploratorio de la ciencia básica debería de ser razón por si sola para llevarla a cabo, más aún cuando se trata de estructuras corporales tan importantes como los distintos órganos que conforman el sistema digestivo de un grupo animal dado.

Como ha sido comentado anteriormente, los antecedentes, objetivos, metodología empleada, resultados y discusión de cada uno de dichos bloques, serán explicados con detalle en los siguientes capítulos.

INFORME DEL DIRECTOR

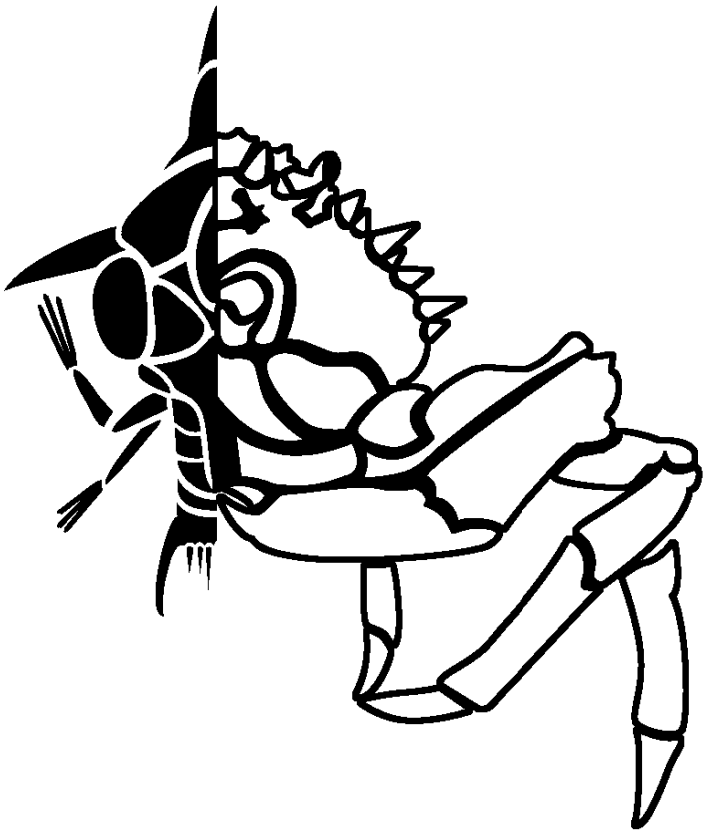

INFORME DEL DIRECTOR

Como director de la tesis doctoral **'Morfología del sistema digestivo y larvicultura del centollo (*Maja brachydactyla*, Balss 1922)'** realizada por **Diego Castejón Bueno**, presento el siguiente informe sobre la contribución del doctorando en las publicaciones en coautoría que componen la tesis:

BLOQUE 1. Capítulo 5. D. Castejón, G. Rotllant, L. Giménez, G. Torres y G. Guerao (2015). The effects of temperature and salinity on the survival, growth and duration of the larval development of the common spider crab *Maja brachydactyla* (Balss, 1922) (Brachyura: Majidae). *Journal of Shellfish Research*, 34 (3): 1073–1083.

Contribución del doctorando: Planificación del trabajo, participación en el diseño de los experimentos, mantenimiento de los acuarios, toma de datos, realización de los análisis, búsqueda bibliográfica y redacción del manuscrito.

Acerca de la revista: De acuerdo con la última edición disponible del *Journal Citation Reports* (*JCR*) correspondiente a 2017, *Journal of Shellfish Research* tuvo en el año 2015 un índice de impacto de 0.829, encontrándose en la posición 37 de 52 (3º cuartil) en el área de pesquerías (*Fisheries*) y en la posición 78 de 108 (3º cuartil) en biología de medios acuáticos (*Marine & Freshwater Biology*). Según *SCImago Journal & Country Rank* (*SJR*), esta revista se encontraba en la posición 104 de 199 (3º cuartil) en el área de las ciencias acuáticas (*Aquatic Sciences*).

BLOQUE 1. Capítulo 6. D. Castejón, G. Rotllant, L. Giménez, G. Torres y G. Guerao (2018). Influence of temperature and light regime on the larval development of the common spider crab *Maja brachydactyla Balss*, 1922 (Brachyura: Majidae). *Aquaculture Research* (Submitted, Under Review).

Contribución del doctorando: Planificación del trabajo, participación en el diseño de los experimentos, mantenimiento de los acuarios, toma de datos, realización de los análisis, búsqueda bibliográfica y redacción del manuscrito.

Acerca de la revista: De acuerdo con la última edición disponible del *Journal Citation Reports* (*JCR*) correspondiente a 2017, *Aquaculture Research* tuvo en el año 2016 un índice de impacto de 1.461, encontrándose en la posición 23 de 50 (2º cuartil) en el área de pesquerías (*Fisheries*). Según *SCImago Journal* & *Country Rank* (*SJR*), esta revista se encuentra en la posición 88 de 199 (2º cuartil) en el área de las ciencias acuáticas (*Aquatic Sciences*).

BLOQUE 2. Capítulo 11. D. Castejón, G. Rotllant, E. Ribes, M. Durfort y G. Guerao (2018). Morphology and ultrastructure of the esophagus during the ontogeny of the spider crab *Maja brachydactyla* (Decapoda, Brachyura, Majidae). *Journal of Morphology* (Submitted, Accepted).

Contribución del doctorando: Planificación del trabajo, participación en el diseño de la parte experimental (disecciones, preparación y observación de muestras), mantenimiento de los acuarios, toma de datos e imágenes, búsqueda bibliográfica y redacción del manuscrito.

Acerca de la revista: De acuerdo con la última edición disponible del *Journal Citation Reports* (*JCR*) correspondiente a 2017, *Journal of Morphology* tuvo en el año 2016 un índice de impacto de 1.655, encontrándose en la posición 7 de 21 (2º cuartil) en el área de anatomía y morfología (*Anatomy & Morphology*). Según *SCImago Journal* & *Country Rank* (*SJR*), esta revista se encuentra en la posición 52 de 367 (1º cuartil) en el área de las ciencias animales y zoología (*Animal Science and Zoology*).

BLOQUE 12. Capítulo 12. D. Castejón, G. Rotllant, E. Ribes, M. Durfort y G. Guerao (2015). Foregut morphology and ontogeny of the spider crab *Maja brachydactyla* (Brachyura, Majoidea, Majidae). *Journal of Morphology*, 276: 1109–1122.

Contribución del doctorando: Planificación del trabajo, participación en el diseño de la parte experimental (disecciones, preparación y observación de muestras), mantenimiento de los acuarios, toma de datos e imágenes, búsqueda bibliográfica y redacción del manuscrito.

Acerca de la revista: De acuerdo con la última edición disponible del *Journal Citation Reports* (*JCR*) correspondiente a 2017, *Journal of Morphology* tuvo en el año 2015 un índice de impacto de 1.521 de acuerdo, encontrándose en la posición 6 de 21 (2º cuartil) en el área de anatomía y morfología (*Anatomy & Morphology*). Según *SCImago Journal & Country Rank* (*SJR*), esta revista se encontraba en el número 48 de 370 (1º cuartil) en el área de las ciencias animales y zoología (*Animal Science and Zoology*).

BLOQUE 2. Capítulo 14. D. Castejón, G. Rotllant, E. Ribes, M. Durfort y G. Guerao (2018). Morphology and ontogeny of the midgut gland ("hepatopancreas") of the Atlantic spider crab Maja brachydactyla Balss, 1922 (Brachyura, Majidae). *Arthropod Structure & Development* (Submitted, Under Review).

Contribución del doctorando: Planificación del trabajo, participación en el diseño de la parte experimental (disecciones, preparación y observación de muestras), mantenimiento de los acuarios, toma de datos e imágenes, búsqueda bibliográfica y redacción del manuscrito.

Acerca de la revista: De acuerdo con la última edición disponible del *Journal Citation Reports* (*JCR*) correspondiente a 2017, *Arthropod Structure & Development* tuvo en el año 2016 un índice de impacto de 1.546, encontrándose en la posición 29 de 93 (2º cuartil) en entomología (*Entomology*). Según *SCImago Journal & Country Rank* (*SJR*), esta revista se encuentra en la posición 29 de 132 (1º cuartil) en el área de la entomología (*Insect Science*).

BLOQUE 2. Capítulo 15. D. Castejón, G. Rotllant, E. Ribes, M. Durfort y G. Guerao (2018). Histology and ultrastructure of the adult and larval midgut gland ("hepatopancreas") of the Atlantic spider crab Maja brachydactyla Balss, 1922 (Brachyura, Majidae). *Arthropod Structure & Development* (Submitted, Under Review).

Contribución del doctorando: Planificación del trabajo, participación en el diseño de la parte experimental (disecciones, preparación y observación de muestras), mantenimiento de los acuarios, toma de datos e imágenes, búsqueda bibliográfica y redacción del manuscrito.

Acerca de la revista: De acuerdo con la última edición disponible del *Journal Citation Reports* (*JCR*) correspondiente a 2017, *Arthropod Structure & Development* tuvo en el año 2016 un índice de impacto de 1.546, encontrándose en la posición 29 de 93 (2º cuartil) en entomología (*Entomology*). Según *SCImago Journal & Country Rank* (*SJR*), esta revista se encuentra en la posición 29 de 132 (1º cuartil) en el área de la entomología (*Insect Science*).

De la misma manera se informa que ninguno de los coautores participantes de los trabajos que componen esta tesis ha utilizado, implícita o explícitamente, estos trabajos para la elaboración de su propia tesis doctoral.

Barcelona,

Dr. Guillermo Guerao Serra

BLOQUE 1.

LARVICULTURA. INTRODUCCIÓN

"There is still a need to establish commercially relevant techniques for the mass production of crab larvae"

Galley et al. 2011

4.1 Importancia económica del centollo atlántico.

El centollo, *Maja brachydactyla*, es una especie de gran importancia comercial. Desde una perspectiva general, de acuerdo a la documentación publicada en el año 2007 por el entonces Ministerio de Medio Ambiente y Medio Rural y Marino, el consumo anual de marisco en España (incluyendo moluscos y crustáceos, tanto frescos como congelados) fue entorno 375 mil t (MARM, 2007). En el año 2015 dicho consumo fue de 310,5 mil t con un valor comercial de 2.500 millones de euros (Mercasa, 2016). En España el consumo nacional de marisco es próximo a su producción total (incluyendo pesca y acuicultura, tanto productos frescos como congelados), con una producción anual entre los años 2013 y 2015 que osciló entre 245 y 315 mil t, de las que solo entre el 5 y el 8 % se corresponden con la producción nacional de crustáceos. De modo que España es un importador neto de crustáceos. Según los datos oficiales publicados por el Ministerio de Agricultura y Pesca, Alimentación y Medio Ambiente, desde 2010 hasta 2015 España ha importado una media anual de 188 mil t de crustáceos, limitándose las exportaciones a una media de 12 mil t (MAPAMA, 2016).

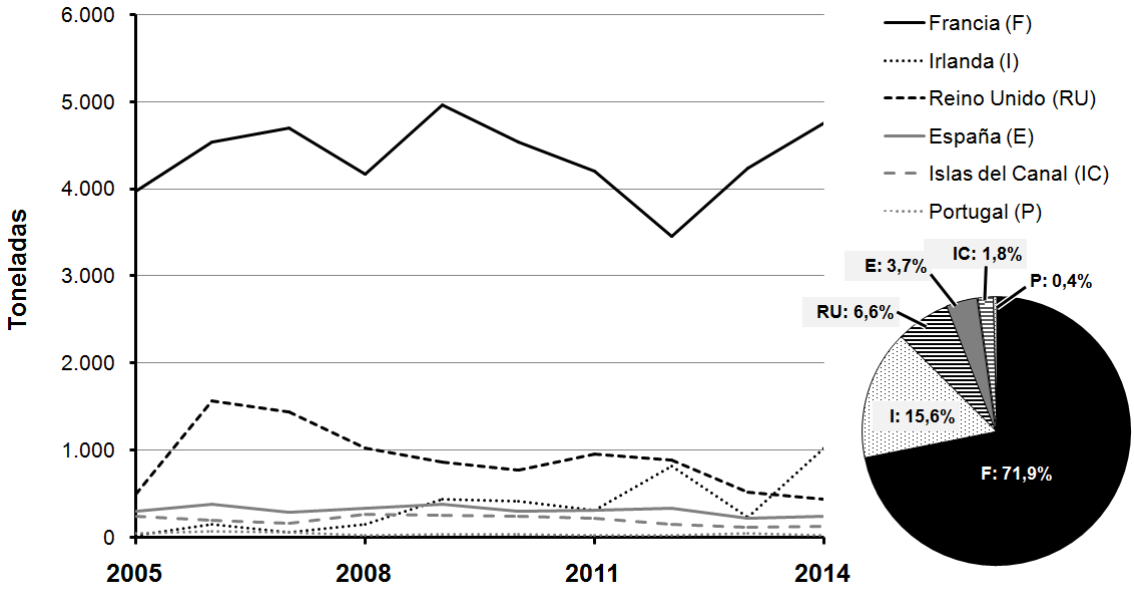

Fig. 4.1.1. Centollo (spider crabs). Total de capturas por países y año de acuerdo a la información publicada por la FAO (2014). Más del 90 % de las capturas mundiales de centollo es realizada por Francia, Irlanda y Reino Unido. El gráfico circular refleja el porcentaje de captura por países durante el año 2014. Gráficas de elaboración propia.

El papel de España como importador de neto crustáceos también se refleja en la situación comercial del centollo. La información publicada por la FAO (2014) refleja que *M. brachydactyla* es una especie de gran importancia comercial cuyas principales pesquerías, por orden de importancia, se localizan en las costas atlánticas de Francia, Irlanda, Reino Unido, España, las Islas del Canal y Portugal (Fig. 4.2.1). También se registran capturas en Dinamarca, pero a diferencia de los países anteriormente mencionados estas capturas no son registradas todos los años y representan un porcentaje residual si se compara con el resto de países. A nivel mundial, el volumen anual de capturas registrado entre los años 2005 y 2014 osciló entre 5.030 y 6.943 t. Durante el mismo periodo de tiempo, a nivel nacional las capturas oscilaron entre 216 y 379 t, representando dicho porcentaje entre el 2,85 y el 4,25 % de la producción mundial. Por el contrario, más del 90 % de la producción mundial se reparte entre Francia, Reino Unido e Irlanda. De hecho, en el año 2014 solo Francia e Irlanda realizaron el 71,9 y el 15,6 % del total mundial de capturas, respectivamente (Fig. 4.1.1). Por estas razones el centollo consumido en España es mayoritariamente un producto de importación, siendo los principales proveedores Francia y Reino Unido, los cuales representan entre el 60 y el 70 % de las importaciones (Illescas et al., 2007).

Los datos estadísticos aportados por la Consellería do Mar a través de la "Plataforma Tecnolóxica da Pesca" (https://www.pescadegalicia.gal/estadisticas/), perteneciente a la Xunta de Galicia, son mostrados de forma gráfica como el total de capturas mensuales realizadas durante el periodo de tiempo comprendido entre el año 2012 y el año 2016, así como la oscilación del precio en lonja del kilo de centollo en el mismo periodo de tiempo, usando los datos relativos a 49 lonjas distribuidas a lo largo de la costa gallega (Fig. 4.1.2). Estos datos muestran que las capturas se concentran desde finales de noviembre / inicios de diciembre hasta inicios de junio/julio, coincidiendo con la ventana temporal donde la pesca de esta especie no está vedada. Las actividad pesquera se concentra principalmente durante los meses de noviembre y diciembre, coincidiendo con la etapa final de la migración otoñal de la especie (González-Gurriarán et al., 2002), así como con la cercanía y celebración de las festividades navideñas, donde el centollo adquiere un gran valor gastronómico. Esta situación explicaría porque el pico de captura tiene lugar durante los meses de noviembre y diciembre, oscilando entre 60 y 135 t mensuales, mientras que el resto del año (salvo excepciones) las capturas suelen ser inferiores a 15 t mensuales.

Durante el mes de diciembre el precio medio en lonja suele oscilar entre 10 y 15 €/Kg, sin embargo en muchas localidades pueden alcanzarse precios superiores a 20 €/Kg. Por esta razón, de modo habitual los especímenes capturados durante el mes de noviembre suelen ser mantenidos en cetárea para su posterior venta en las mencionadas fechas. Durante el resto del año el precio medio de venta en lonja suele mantenerse en 9-15 €/Kg. De todos modos, el precio de venta oscila de forma importante entre localidades, llegando el precio máximo a ser de tres a cinco veces mayor que el precio mínimo aún en la misma época del año (Fig. 4.1.2). En Asturias la pesquería del centollo también resulta importante, siendo la principal especie de malacostráceo en número de capturas y la segunda en valor económico (García-Flórez y Fernández-Rueda, 2003).

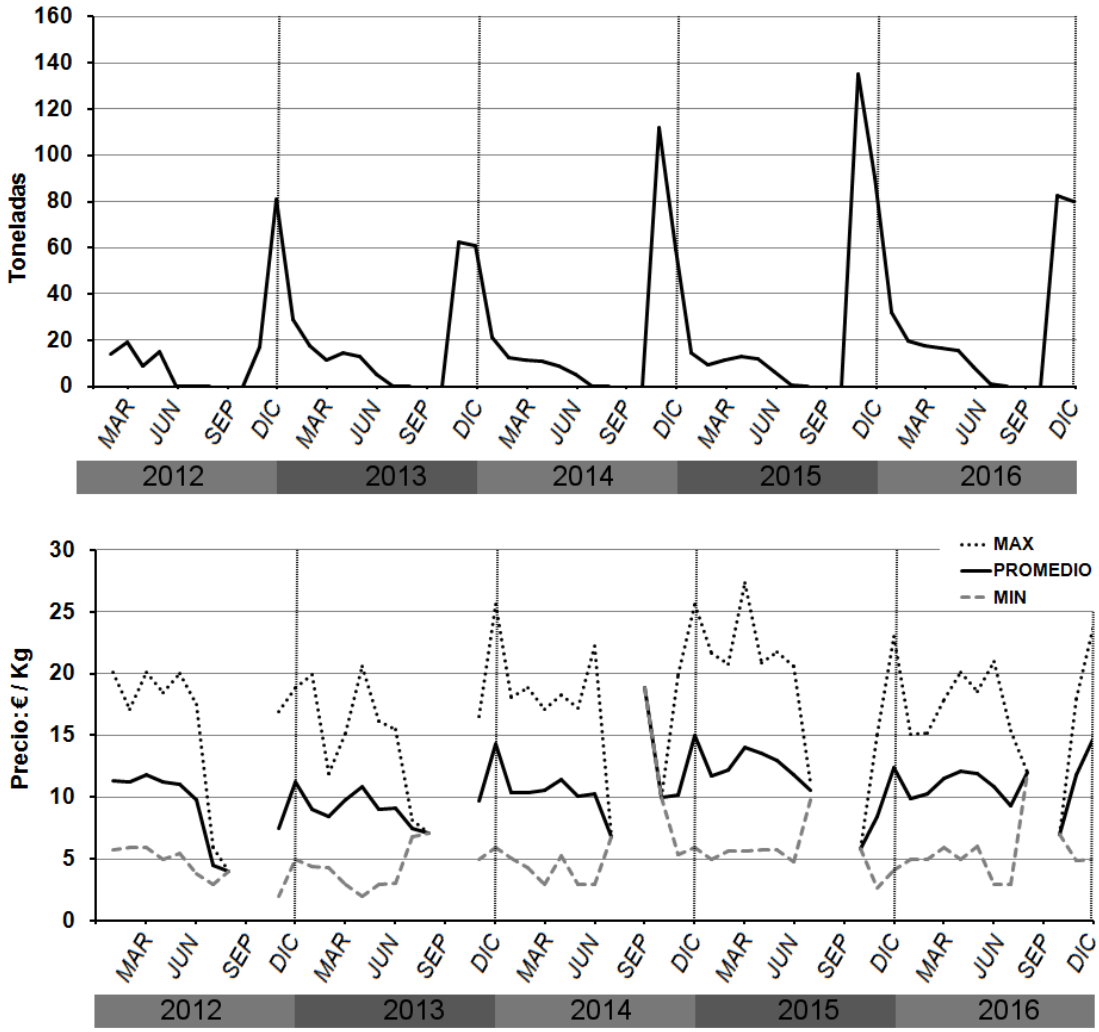

Fig. 4.1.2. Centollo. Galicia. Total de capturas y oscilación del precio de venta en lonja (precio máximo, MAX; medio, PROMEDIO; y mínimo, MIN), por meses. Información oficial obtenida a través de la "Plataforma Tecnolóxica da Pesca", Xunta de Galicia. Gráficas de elaboración propia.

En la década de los 90 la flota pesquera de centollo en Galicia se componía de aproximadamente 300 barcos, cuyas actividades eran realizadas en aguas próximas a la costa con una profundidad variable entre los 15 y los 40 metros (González-Gurriarán et al., 1993). Dicha flota supone una importante presión para la especie. Freire et al. (2002) expone que el centollo está sufriendo una importante sobreexplotación en la costa gallega, dicha afirmación se sostiene por tres premisas principales: (1) especies de la misma área que fueron históricamente importantes actualmente no son sino capturas residuales (como el bogavante *Homarus gammarus*, la langosta *Palinurus elephas*, y el besugo *Pagellus bogavareo*); (2) actualmente existe una reducción significativa de las capturas de centollo en comparación con las que eran realizadas entre los años 1940 y 1960; (3) las capturas de la época actual suponen más del 90 % del reclutamiento de la especie, de modo que entre mayo y junio menos del 10 % de las hembras primíparas llega a reproducirse con éxito. Por lo tanto, el establecimiento de un periodo de veda se hace necesario para evitar el agotamiento de la pesquería, suponiendo el incumplimiento de dicha veda graves daños para la especie (González-Gurriarán et al., 2002). En ese sentido, la resolución del 19 de mayo de 2016 por la que se aprueba el Plan de Gestión del Centollo y del Buey 2016-2017 por la Xunta de Galicia, publicada en el Diario Oficial de Galicia (DOG, Núm. 103, pág. 21.101) el 1 de junio de 2016, establece el periodo de veda para la pesca del centollo atlántico durante el año 2016 como sigue: en la provincia de Pontevedra desde el 4 de junio hasta el 27 de noviembre, en la provincia de A Coruña desde el 2 de julio hasta el 27 de noviembre, y en la provincia de Lugo desde el 2 de julio hasta el 4 de diciembre, decretándose que fuera del periodo de veda la cuota máxima de captura fuese 35 kg por barco y día, añadiéndose 35 kg/día por cada tripulante enrolado y a bordo.

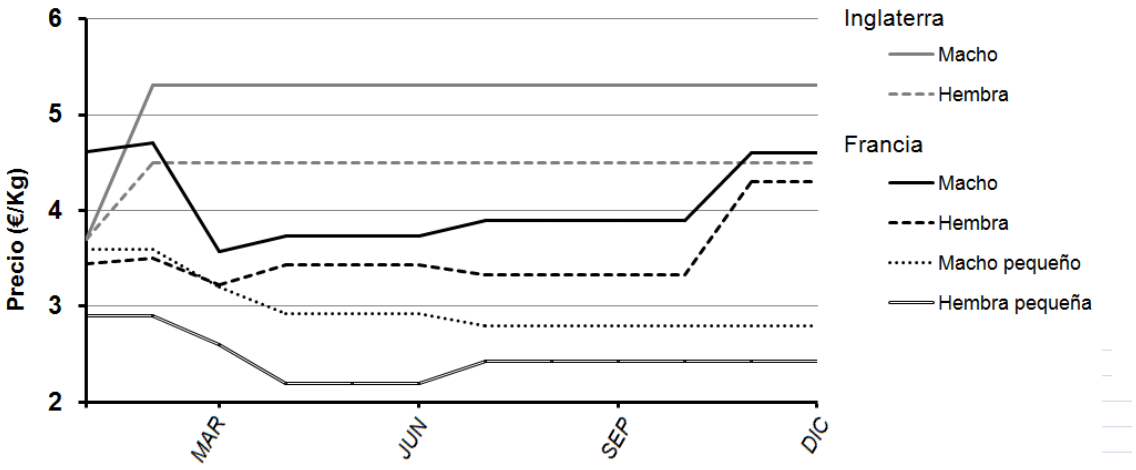

Fig. 4.1.3. Centollo. Precio en Francia y Reino Unido durante el año 2016, según datos del Departamento de Pesca y Acuicultura de la FAO (Globefish, 2016). Gráficas de elaboración propia.

En numerosos países europeos (Francia, Inglaterra e Irlanda) el declive de las pesquerías de bogavante (*Homarus gammarus*) y langosta (*Panulirus* sp.) durante las décadas de 1950 y 1960 impulsó la búsqueda de especies pesqueras alternativas como el buey de mar (*Cancer pagurus*) y centollo (*M. brachydactyla*), ambos especies de braquiuros (Fahy, 2001; Fahy y Carroll, 2009; Le Foll, 1993). Como consecuencia, la presión pesquera fue trasladada sobre estas especies. En el caso de la Bretaña Francesa la presión sobre las pesquerías de centollo, derivada de la caída de los rendimientos pesqueros de bogavante y langosta, ya alcanzó el nivel de sobreexplotación entre los años 1970 y 1980 (Le Foll, 1993). Según los estudios realizados en el Golfo Normando Bretón, la principal pesquería de centollo del litoral francés, las actividad pesquera llevada a cabo desde noviembre hasta mayo es capaz de capturar entre el 70 y el 80 % del reclutamiento de la especie (Kergariou y Veron, 1981; Le Foll, 1993). Los ensayos de marcado y recaptura confirman esta alta mortalidad, de todos los especímenes adultos marcados solo el 11 % llega a recapturarse al año siguiente, el 1,5 % dos años después, y ningún espécimen en periodos posteriores (Latrouite y Le Foll, 1989). Este resultado señala una importante presión pesquera, que en última instancia está llevando a la reducción de los rendimientos pesqueros (Le Foll, 1993).

Una situación similar se ha observado en Irlanda. Mientras que durante la década de 1970 el incremento de los rendimientos pesqueros promovió las exportaciones a países como España (Fahy, 2001; Fahy y Carroll, 2009), la situación ha cambiado en las últimas décadas. Desde 1981 la pesquería de Magharees es una de las más importantes pesquerías irlandesas dedicadas al centollo. De forma paralela al caso anterior, desde finales de los años 80 y durante la década de los 90 el rendimiento de dicha pesquería ha ido decreciendo paulatinamente reportándose una drástica reducción en las capturas (Fahy, 2001; Fahy y Carroll, 2009).

En los países europeos el precio mercantil del centollo atlántico varía con la talla, oscilando a lo largo del año de acuerdo a los informes publicados por la unidad «Globefish», perteneciente al Departamento de Pesca y Acuicultura de la FAO (Fig. 4.1.3). Durante el año 2016, en el Reino Unido el precio se mantuvo relativamente constante durante todo el año, con un precio de 5,30 y 4,50 €/Kg por machos y hembras, respectivamente. Mientras tanto, en Francia el precio de los especímenes adultos osciló entre 4,70 y 3,57 €/Kg en machos y entre 3,33 y 4,30 €/Kg en hembras, registrándose un ligero aumento de precio durante los meses de noviembre y diciembre. Las tallas pequeñas son menos valoradas, teniendo un precio que osciló entre 2,80 y 3,60 €/Kg en machos y entre 2,20 y 2,90 €/Kg en hembras (Globefish, 2016).

4.2 Centollo como especie de cultivo acuícola. Experiencias.

El consumo per cápita mundial de productos pesqueros aumentó desde un promedio de 9,9 kg desde 1960 hasta 18,4 kg en el año 2009. Este aumento del consumo, junto al incremento de la población mundial, supone una mayor demanda de productos pesqueros a nivel mundial. En este escenario la acuicultura, entendida como la producción de animales acuáticos (marinos y dulceacuícolas), ha ido adquiriendo un papel cada vez más importante. Desde el año 2006 hasta el año 2011 la producción de la acuicultura aumentó desde $47 \cdot 10^6$ t hasta $64 \cdot 10^6$ t, pasando de representar del 34,5 al 41,3 % de la producción mundial de productos pesqueros (FAO, 2012). El papel de la acuicultura es aún más importante si se considera que su producción se ha multiplicado por doce en las últimas décadas (1980-2010), mientras que en el mismo periodo de tiempo la producción pesquera parece haberse estancado (Fig. 4.2.1).

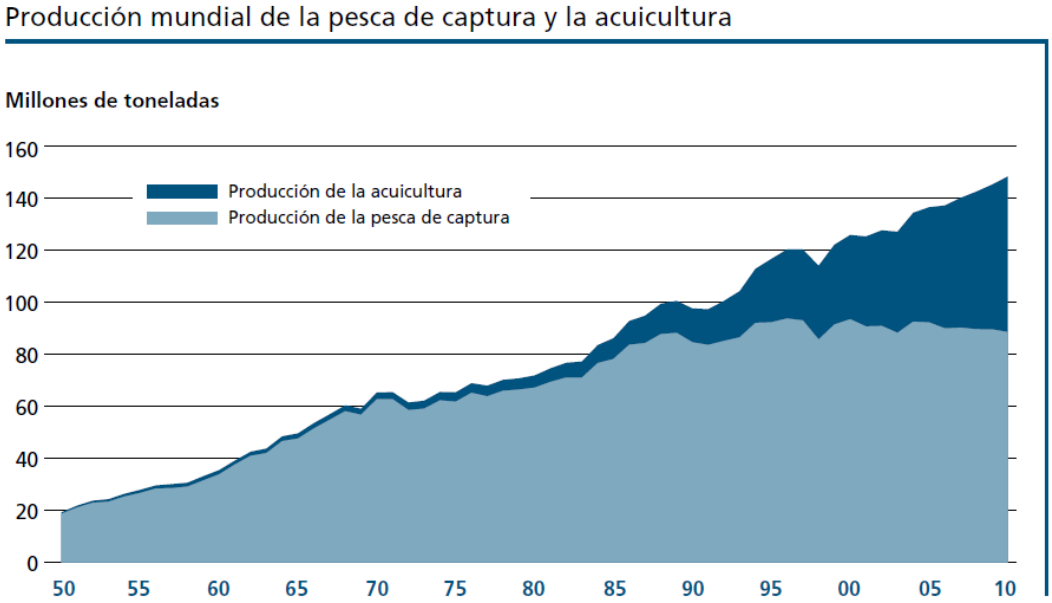

Fig. 4.2.1. Producción mundial de productos pesqueros. Imagen publicada originalmente en FAO (2012). El Estado Mundial de la Pesca y la Acuicultura. Roma: Departamento de Pesca y Acuicultura de la FAO. Imagen publicada por cortesía de FAO.

En este escenario la acuicultura de crustáceos juega un papel reducido en términos de producción pero elevado en términos económicos. Entre los años 2008 y 2009 representó $5 \cdot 10^6$ t y $22\text{-}24 \cdot 10^9$ dólares, en otros términos: el 5 % de la producción y el 23 % del valor económico de la acuicultura a nivel mundial (Bondad-Reantaso et al., 2012). La principal producción acuícola de crustáceos son los peneidos con más del 60 % de la producción, mientras que los braquiuros apenas superan el 4 % (Bondad-Reantaso et al., 2012; FAO, 2012). La producción de la acuicultura en España entre los años 2013 y 2015 aumentó desde las 226 hasta las 294 mil

t, alcanzando un valor superior a los $500 \cdot 10^6$ euros. La mayoría de esta producción está representada por el cultivo de moluscos (77,6 %) y peces (22,3 %). En ese sentido el cultivo de crustáceos representa un valor marginal, con una producción en el 2015 poco mayor de 200 t con un valor ligeramente superior al millón de euros (MAPAMA, 2016).

De acuerdo a la información publicada en el capítulo 1 (1.3 Ciclo biológico del centollo), *Maja brachydactyla* tiene numerosas características que la convierten en una especie potencialmente interesante desde el punto de vista de la producción acuícola. Dichas características incluyen: es una especie fácil de reproducir en condiciones de cautiverio, pueden obtenerse varias puestas anuales (entre 1 y 5 puestas por hembra), la fecundidad es muy elevada (entre 125.000 y 540.000 huevos por puesta) y el desarrollo larvario es abreviado, formado por tres estadios larvarios que pueden ser completados en 16-18 días. Debido a estas características, así como por su elevado valor comercial, se han llevado a cabo numerosas investigaciones que en conjunto forman parte del desarrollo de las técnicas y conocimientos necesarios para la producción acuícola de esta especie.

4.2.1 Stock de reproductores: mantenimiento, cópula y puesta

Las técnicas desarrolladas a partir de investigaciones realizadas en años anteriores han permitido el mantenimiento con éxito de un stock de reproductores durante uno o dos años. Los requisitos necesarios para ello son relativamente sencillos de cumplir teniendo en cuenta la tecnología actual. La relación de sexos (machos: hembras) puede variar de 1:3 a 1:6, siendo importante que exista una mayor proporción de hembras que de machos en un mismo tanque. Como tanques de cultivo que han dado buenos resultados se han empleado tanques cilíndricos, compuestos por fibra de vidrio y poliéster, de 2.000 L de capacidad. Estos tanques están conectados a una unidad de recirculación de agua con una tasa de renovación del agua de 65 m^3 h^{-1}. La temperatura y salinidad deben ser mantenidas a 18 °C y 34-36 psu, respectivamente. La dieta puede estar basada en mejillón (*Mytilus* sp.) fresco y congelado ofrecido diariamente *ad libitum*, así como cangrejo congelado (*Liocarcinus depurator*) una o dos veces por semana (Guerao y Rotllant, 2009a; Guerao et al., 2012; Rotllant et al., 2010).

González-Gurriarán et al. (1993) menciona que la cópula ocurre en el medio natural en dos intervalos: entre los meses de octubre-diciembre y entre los meses de mayo-junio. Dado que las hembras almacenan esperma en los receptáculos seminales, es posible obtener hembras adultas con capacidad de producir puestas viables sin necesidad de copular en condiciones de cultivo. Sin embargo, es relativamente sencillo obtener nuevas cópulas en tales condiciones, ya que el único requisito es mantener machos y hembras habitando el mismo tanque de cultivo en las condiciones previamente descritas, sin requerimientos especiales o adicionales. La cópula

sucede sin ningún comportamiento de cortejo previo o "de guarda" una vez finalizada esta (González-Gurriarán et al., 1998), durante la cópula el macho sujeta fuertemente a la hembra con los quelípedos (Sampedro et al., 1999), mientras ambos animales enfrentan su zona ventral (González-Gurriarán et al., 1998).

En condiciones de cultivo las hembras de centollo son capaces de realizar varias puestas consecutivas en una misma temporada de cría, pueden sucederse de 1 a 4 puestas anuales con un periodo de interpuesta de 1 a 6 días (González-Gurriarán et al., 1998; González-Gurriarán et al., 1993), o bien de 3 a 5 puestas anuales con un periodo de interpuesta de 4 a 5 días (Iglesias et al., 2002). El periodo de incubación también ha sido determinado en condiciones de cultivo, fluctuando entre 34 a 62 días (González-Gurriarán et al., 1998), o bien entre 30 y 40 días (Iglesias et al., 2002), mencionándose en ambos casos una temperatura ambiental de 16-18 °C. Los ciclos de puesta en condiciones de cultivo siguen el patrón observado en condiciones naturales, no siendo posible inducir la puesta en épocas del año distintas a las del ciclo natural mediante alteraciones del fotoperiodo (Simeó et al., 2009). Una vez la puesta es realizada, esta es fijada a los pleópodos de la hembra y parcialmente ocultada por la parte ventral del abdomen de la misma. Una vez fijada a los pleópodos la puesta es incubada, cuidada y protegida por la hembra hasta el momento de la eclosión. El estado de maduración de la puesta puede determinarse mediante observación visual, como ha sido descrito en el capítulo anterior. La calidad de la puesta no es constante y es afectada por las condiciones de cautiverio. Andrés et al. (2010b) observaron una importante reducción en la cantidad de vitaminas A y E, aminoácidos esenciales (Lys, Val, e His) y elementos traza (Cu e Fe), en larvas recién eclosionadas a finales de año en comparación con larvas recién eclosionadas a inicios de ese mismo año. Los autores sugieren que estos datos podrían indicar un déficit nutricional debido a la dieta del stock de reproductores en condiciones de cautiverio.

4.2.2 Cultivo larvario

El cultivo larvario tampoco parece requerir condiciones complejas o que requieran una extraordinaria inversión considerando la tecnología actual. Las experiencias realizadas hasta ahora demuestran que las larvas pueden ser cultivadas, desde el momento de la eclosión, en cilindros de PVC de 35 L cerrados basalmente por una malla de 150 µm. Dichos cilindros fueron alojados en tanques de 1500 L, provistos de aireación y conectados a una unidad de recirculación de agua. Las condiciones ambientales fueron: temperatura de 18 °C, salinidad de 36 psu y fotoperiodo natural con 12 h de luz. La dieta más exitosa consistió en estadios larvarios tempranos de *Artemia* sp. (generalmente nauplii y metanauplii), los cuales pueden ser enriquecidos con fitoplancton (*Isochrysis* sp., *Tetraselmis* sp.) o con emulsiones comerciales

(Andrés et al., 2008; Andrés et al., 2007; Guerao y Rotllant, 2009a; b; Rotllant et al., 2010). En estas condiciones, desde la eclosión hasta el estadio de megalopa la supervivencia puede alcanzar el 35 % (Guerao y Rotllant, 2009a; b). Este protocolo también permite el cultivo larvario de la especie mediterránea *Maja squinado*, de modo que en este caso hasta un 25 % de las larvas recién eclosionadas llegó a alcanzar el estadio de megalopa (Guerao y Rotllant, 2010). La densidad óptima de cultivo larvario se ha calculado entre 10 y 50 larvas L^{-1}, no recomendándose densidades iguales o superiores a 100 larvas L^{-1} debido al incremento de mortalidad (Andrés et al., 2007). Una técnica alternativa puede emplear el cultivo a pequeña escala, que por sus dimensiones puede considerarse una herramienta útil para la investigación. Las condiciones ambientales de salinidad, temperatura y fotoperiodo, así como de densidad larvaria y dieta, pueden ser las mismas que las anteriormente descritas. Sin embargo, este cultivo es realizado en vasos de precipitados con 50 mL de agua marina, cada uno de ellos empleado como réplica en condiciones experimentales (Guerao et al., 2012).

La alimentación durante los estadios larvarios es fundamental. Numerosos estudios han demostrado que las larvas de centollo atlántico son depredadores activos desde su eclosión (estadio de zoea I). Si desde ese momento son mantenidas en condiciones de inanición no serán capaces de alcanzar el siguiente estadio larvario (zoea II), sucediéndose en 6 días la mortalidad media y en 11 días la mortalidad total (Rotllant et al., 2010). Si el periodo de inanición dura 5 días o más, las larvas son incapaces de recuperarse aunque reciban alimento, muriendo en un plazo máximo de 10-11 días (Guerao et al., 2012; Rotllant et al., 2010). Sin embargo, si el periodo de inanición es inferior a 5 días, las larvas son capaces de recuperarse y completar el desarrollo larvario (Rotllant et al., 2010). En el caso opuesto, si las larvas recién nacidas son alimentadas durante 2 días desde el momento de la eclosión y posteriormente son sometidas a un régimen de inanición, serán capaces de alcanzar el siguiente estadio larvario. Dicha situación no se observa si el periodo inicial de alimentación es inferior a 2 días (Guerao et al., 2012). La densidad de la presa viva afecta a la condición y supervivencia larvaria, recomendándose al menos 60 metanauplii de *Artemia* por cada larva de *M. brachydactyla*. Mientras que las dietas enriquecidas parecen promover el crecimiento larvario, el aporte de alimento no vivo (como fragmentos de poliquetos) no muestra ningún efecto en el desarrollo (Andrés et al., 2007). Las larvas de centollo también pueden consumir dietas artificiales administradas como material particulado (100-250 μm), pero es un tipo de dieta mucho más ineficiente que las basadas en alimento vivo (Andrés et al., 2011).

Sin embargo, el uso de dietas artificiales aún requiere de investigación y desarrollo antes de aplicarse en el cultivo larvario de *M. brachydactyla*. Desde un punto de vista nutricional, desde el momento de la eclosión las larvas cuentan con la batería enzimática requerida para procesar y asimilar las presas ingeridas (Andrés et al., 2010c): proteínas (pepsina, tripsina, quimotripsina), carbohidratos (amilasa, quitinasa) y lípidos (esterasa), cuya actividad aumenta durante el desarrollo larvario. La composición corporal de las larvas sufre pocos cambios durante el desarrollo. La mayor transformación ocurre a nivel de los requerimientos de aminoácidos esenciales: en las larvas recién eclosionadas los más importantes son Leu, Lys, Val y Thr; en estadios más avanzados los aminoácidos Leu y Val mantienen su importancia pero la proporción de Lys y Thre se reduce significativamente. Por su parte, el aminoácido Arg se vuelve esencial en juveniles (Andrés et al., 2010a).

Una vez establecido el cultivo larvario, es posible realizar un seguimiento preciso del estado de desarrollo de las larvas, incluso en periodos de intermuda. Las distintas etapas que se suceden durante los periodos de intermuda (distinguidas a continuación mediante letras, de A hasta D), pueden determinarse mediante la observación del telson: A-B, postmuda, la epidermis tiene apariencia esponjosa; C, intermuda, la epidermis aparece rígida y gruesa; D_{0-1}, premuda temprana y media, la epidermis y setas se separan de la cutícula externa; D_2, premuda tardía, puede observarse la nueva cutícula debajo de la cutícula precedente (Guerao et al., 2010).

4.2.3 Asentamiento y cultivo post-larvario

El «asentamiento» puede considerarse uno de los factores de mayor importancia que afectan al reclutamiento de especies costeras y marinas cuyo desarrollo larvario es la etapa dispersiva de la especie (Giménez, 2010; Pawlik, 1992; Rodríguez et al., 1993). El asentamiento es generalmente definido como la transición desde una vida larvaria planctónica hasta una fase juvenil bentónica (Pawlik, 1992). En los braquiuros esta transición sucede con la metamorfosis desde megalopa a primer juvenil, dicho momento es crítico y su éxito condiciona la supervivencia posterior de los individuos (Anger, 2001; 2006). Esta situación es también relevante en el centollo. Palma et al. (2008) han observado que tanques de 40 litros de capacidad y fondo plano es requisito suficiente para obtener juveniles con una supervivencia ligeramente superior al 10 % desde el estadio de zoea. La dieta de los juveniles es similar a la adulta: mejillón, cangrejo, pescado congelado y macroalgas (Iglesias et al., 2002). La mayor parte de la mortalidad ocurre asociada a la muda (> 90 %), bien por episodios asociados al canibalismo o bien por el estrés asociado a la misma (Domingues y Alaminos, 2008).

Más interesante es el trabajo publicado por Iglesias et al. (2002), donde se realizaron dos tipos de experiencias con el objetivo de obtener juveniles: técnicas de cultivo intensivo y semi-intensivo. El cultivo intensivo empleó tanques de 2.000 y 10.000 L de capacidad con 10.000 y 30.000 zoeas en cada uno, respectivamente. La dieta consistió en una combinación de nauplius de *Artemia* y *Chlorella* sp., obteniéndose al cabo de 16-18 días un total de 800 y 4.000 juveniles, respectivamente. Los juveniles obtenidos en estas condiciones fueron trasladados a tanques de 500 L donde alcanzaron los 32 ± 7 mm de longitud en 9 meses con una tasa de supervivencia del 0,7 %. La experiencia de cultivo semi-intensivo fue llevada a cabo en tanques rectangulares exteriores de 225 m^3. En esta experiencia los adultos se mantuvieron en cajas flotantes. La dieta consistió en fito y zooplancton producido de forma natural en los tanques de cultivo, así como nauplii y metanauplii de *Artemia* que fueron añadidos diariamente. En estas condiciones se obtuvieron 5.000 juveniles al cabo de 40 días. Los juveniles obtenidos en estas condiciones fueron trasladados a tanques de 500 L donde alcanzaron 65 ± 7 mm de longitud en 9 meses con una tasa de supervivencia del 66 %.

Posteriormente, Domingues y Alaminos (2008) emplearon bandejas de 0,28 m^2 (80 x 35 x 15 cm) para estudiar la influencia de la densidad sobre el engorde de los juveniles. Para ello, se utilizaron juveniles de dos meses de edad a densidades de 11 y 50 individuos m^{-2}. La supervivencia fue menor en condiciones de densidad elevada, si bien no se pudo determinar si el canibalismo ocurrió con animales vivos tras el proceso de muda o bien tras la muerte de estos a consecuencia del estrés de la muda. En un estudio paralelo con una densidad de 32 individuos m^{-2}, no se encontró ninguna diferencia en supervivencia y crecimiento en ausencia y presencia del macroalga *Ulva lactuca*, no siendo esta útil ni como alimento complementario o refugio. Alaminos (2011) realizó otra experiencia de cultivo con celdillas individuales de tres tamaños distintos: pequeñas (6 x 8 cm), medianas (12 x 16 cm) y grandes (35 x 27 cm), mostrando que el crecimiento de los juveniles no difiere durante los primeros 60 días entre los distintos tratamientos. Sin embargo, a partir de los 90 días aparecieron diferencias significativas en longitud y peso entre las celdillas pequeñas y grandes, con mayor talla y número de mudas en estas últimas, pero no se detectaron diferencias significativas en la supervivencia. En estas condiciones, la muda terminal y maduración sexual tiene lugar a los 405 ± 38 días de edad (Alaminos, 2011). El crecimiento de los juveniles es acompañado de cambios morfológicos, adquiriendo los caracteres sexuales secundarios en el estadio 4 (Guerao y Rotllant, 2009a), como vimos en el capítulo anterior.

Guerao y Rotllant (2009b; 2010) mostraron otro sistema de cultivo de juveniles basado en tanques de metacrilato unidos paralelamente entre sí e individualmente compuestos por 12 celdas (40 x 50 x 45 mm), los tanques están conectados a un sistema de recirculación de agua

que renueva el 20 % del agua dos veces por semana. En estas condiciones el 45 % de las megalopas realizó la metamorfosis hasta primer estadio de juvenil y los juveniles crecieron desde el estadio 1 hasta el estadio 8 en 117,5 ± 7,5 días, alcanzando un tamaño aproximado de 15 mm y un peso de 1 gramo (Guerao y Rotllant, 2009b). Este sistema de cultivo también puede ser aplicado a la especie mediterránea *M. squinado*. Sin embargo, el éxito fue menor ya que menos del 20 % de las megalopas sobrevivió a primer juvenil y solo el 5,8 % alcanzó el estadio 8 en 154 ± 10 días, con una talla de 14 mm y 0,75 gramos (Guerao y Rotllant, 2010).

4.3 Objetivos del BLOQUE 1.

La producción de juveniles en etapa de pre-engorde, es una etapa crítica en la producción de especies de interés acuícola. En ese sentido, el desarrollo de técnicas de producción de juveniles en condiciones controladas, no dependientes de la obtención de stocks silvestres, es un requisito fundamental y necesario para la producción exitosa de una especie, ya que de ese modo se evita la incertidumbre inherente a la captura de stocks silvestres y permite el desarrollo de técnicas de selección genética para mejorar la especie cultivada (Browdy, 1998). En el caso de los decápodos braquiuros, el primer paso para evitar la dependencia hacia el medio natural es el desarrollo de técnicas de producción de cultivo larvario y producción de juveniles en condiciones de cautividad (Zmora et al., 2005). La producción de juveniles en la industria acuícola suele tener por objetivos la obtención de ejemplares con talla de pre-engorde para su posterior engorde en instalaciones propias. Sin embargo, en los braquiuros se ha desarrollado como alternativa la producción de juveniles con objeto de repoblar pesquerías locales en situación de declive debido a la sobrepesca (Hamasaki et al., 2011; Hamasaki et al., 2002; Kogane et al., 2007; Zmora et al., 2005).

En los braquiuros, quizás las etapas más críticas del desarrollo larvario son aquellas que dan lugar a grandes cambios en la morfología corporal: la metamorfosis desde el último estadio de zoea al estadio de megalopa y la metamorfosis de la megalopa al estadio de primer juvenil. En ese sentido, se han reportado importantes mortalidades durante la muda al estadio de megalopa en el portúnido *Scylla serrata* (Hamasaki et al., 2002) y en el oregónido *Chionoecetes opilio* (Kogane et al., 2007); así como una mortalidad elevada a partir del estadio de megalopa en el portúnido *Callinectes sapidus* (Zmora et al., 2005). La mayoría de las causas de mortalidad no se han logrado identificar, pero entre las identificadas destacan las infecciones bacterianas y fúngicas, así como el "Síndrome de Muerte asociada a la Muda", en la que los ejemplares mueren durante el proceso de muda sin poder liberarse de la antigua exuvia o inmediatamente tras realizar esta última muda (Hamasaki et al., 2011).

En el caso del centollo, *M. brachydactyla*, tal y como ha sido descrito en el apartado anterior, numerosas experiencias han demostrado que el cultivo larvario y el engorde de juveniles pueden ser llevado a cabo en condiciones de cultivo. Sin embargo, a pesar de los estudios previos, los parámetros ambientales óptimos (temperatura, iluminación, salinidad y requisitos de asentamiento) son poco conocidos en esta especie. Dichos parámetros se incluyen entre los más influyentes en el desarrollo larvario de los decápodos, de modo que es prioritario conocer qué combinaciones de los mismos permiten aumentar la supervivencia, reducir el tiempo de desarrollo y en definitiva, incrementar la productividad.

De modo que puede afirmarse que el estudio de estos factores ambientales es un elemento clave de cara al cultivo de una especie, asimismo conocer dichos parámetros puede proporcionarnos algunas pistas sobre la ecología de esta especie en el medio natural.

Temperatura. La temperatura es uno de los factores más influyentes sobre la duración y supervivencia durante el desarrollo larvario. Los braquiuros, como muchos otros invertebrados, son animales poiquilotermos cuya temperatura corporal varía paralelamente con la temperatura ambiental, influyendo en la velocidad de los procesos metabólicos y fisiológicos. En términos de cultivo acuícola, la consecuencia más inmediata es la posibilidad de acelerar la velocidad de desarrollo mediante aumentos de temperatura, como ha sido constatado en numerosas especies de braquiuros (Anger, 1991; 2001; Baylon y Suzuki, 2007; Costlow et al., 1960; Costlow Jr et al., 1966; Hernández et al., 2012; Lárez et al., 2000; Minagawa, 1990; Nagaraj, 1992; Nurdiani y Zeng, 2007; Ong y Costlow, 1970). Por el contrario, una temperatura excesivamente alta puede llegar a causar la muerte (Valdes et al., 1991; Vargo y Sastry, 1977). Adicionalmente, la temperatura puede tener efectos sinérgicos con otros factores ambientales como la salinidad y la intensidad lumínica y fotoperiodo (Anger, 2003; Baylon y Suzuki, 2007; Reed, 1969). Por esa razón uno de los objetivos del presente trabajo fue determinar la temperatura óptima (o rango de temperaturas) de cultivo para esta especie, así como determinar la sinergia de la temperatura con otros factores ambientales.

Salinidad. La salinidad es otro de los factores ambientales que tienen una influencia importante sobre el desarrollo larvario de los decápodos. Si es superado el rango de tolerancia salina de una especie, entonces ocurre una respuesta de estrés que afecta principalmente a la supervivencia y en menor medida a la duración de los estadios larvarios, además condiciones salinas inadecuadas pueden tener efectos perniciosos sobre el proceso de muda causando deformaciones en los individuos (Anger, 2003; Torres et al., 2011). Entre los braquiuros, se distinguen dos estrategias frente a las condiciones salinas del medio: especies eurihalinas con una elevada capacidad para tolerar amplios rangos de salinidad, y especies estenohalinas con rangos muy estrechos de tolerancia salina. Las primeras suelen corresponderse con especies que

habitan ambientes donde pueden ocurrir amplios cambios de salinidad en cortos periodos de tiempo como estuarios y áreas costeras, mientras que las segundas suelen habitar aguas oceánicas abiertas donde los cambios salinos son de menor magnitud (Torres et al., 2011). Visto que la salinidad tiene una gran influencia sobre el ciclo biológico de una especie dada, es fundamental conocer el rango de salinidad en el que la especie puede ser mantenida en condiciones de cultivo, así como la salinidad óptima para el mismo (Anger, 2003; Torres et al., 2011).

Iluminación. La luz es un factor ambiental con una importante influencia sobre los estadios larvarios pelágicos de numerosas especies marinas, incluyendo especies cuya fase adulta es sésil (Thorson, 1964). Estas etapas larvarias, especialmente la de edad más temprana, suelen mostrar un marcado fototactismo positivo en condiciones de baja y mediana intensidad, así como fototactismo negativo con alta intensidad luminosa (Forward Jr, 1974; Thorson, 1964). La luz facilita la orientación de los organismos en el medio acuático (Thorson, 1964). En numerosas especies del plancton la luz contribuye a la orientación en las migraciones verticales diarias en la columna de agua (Forward, 1976); mientras que en las etapas larvarias del braquiuro *Rhithropanopeus harrisii* la luz inhibe el desplazamiento vertical mientras que en condiciones de oscuridad muestran una geotaxis negativa, de ese modo la luz actúa como un regulador de las migraciones nocturnas hacia aguas superficiales (Forward et al., 1984). En condiciones de cultivo, se ha observado que otras especies de braquiuros ven reducida su supervivencia en condiciones de oscuridad total (Cottens et al., 2014). Por lo tanto, sería interesante determinar las condiciones de iluminación óptimas, incluyendo fotoperiodo e intensidad lumínica, con el objetivo de obtener la mayor tasa de supervivencia y el menor tiempo de desarrollo posible.

Asentamiento. Por asentamiento se entiende la transición que sufren muchas especies de animales marinos desde una vida larvaria pelágica a una vida juvenil bentónica (Rodríguez et al., 1993), dicho proceso tiene efectos directos sobre la dinámica de reclutamiento y la demografía de las especies implicadas (Flores et al., 2002; Palma et al., 2006). En los braquiuros el asentamiento suele ser paralelo a la metamorfosis que tiene lugar finalizado el estadio de megalopa, cuya siguiente muda implica la aparición del primer estadio de juvenil y el comienzo del desarrollo post-larvario. El asentamiento es un proceso complejo donde tiene lugar la convergencia de factores cuyos efectos impactan a gran escala como el régimen de vientos y corrientes (Flores et al., 2002; Paula et al., 2003; Paula et al., 2001), y los ciclos lunares y mareales (Paula et al., 2001); así como factores con efectos a nivel de meso y micro-escala como el tipo de sustrato (Alberts-Hubatsch et al., 2014; Diele y Simith, 2007; Flores et al., 2002; Pardo et al., 2007), la presencia de sustancias asociadas al hábitat de los estadios post-

larvales (Forward et al., 2001), así como la presencia de sustancias excretadas por los adultos (Diele y Simith, 2007; Forward et al., 2001; Gebauer et al., 1998; Simith et al., 2010). La metamorfosis y el asentamiento tienen efectos directos sobre el subsecuente desarrollo post-larvario, así retrasos en el proceso de asentamiento pueden reducir la supervivencia durante los subsecuentes estadios de juvenil (Gebauer et al., 2003; Simith et al., 2013). En condiciones de cultivo, para los braquiuros el asentamiento es una etapa crítica que debe de ser tenida en cuenta. Por esa razón, se han planteado una serie de experimentos para determinar los requisitos básicos para optimizar la producción de juveniles en condiciones de cultivo.

4.4 Diseño experimental aplicado en el BLOQUE 1.

4.4.1 Stock de reproductores: recogida y mantenimiento

Durante la realización de esta Tesis Doctoral se obtuvieron dos stocks de reproductores. El primer stock fue adquirido a través de pescadores locales de la ciudad de A Coruña en el mes de diciembre del año 2012. Los especímenes fueron capturados en las aguas costeras de A Coruña mediante técnicas tradicionales, coincidiendo con la apertura de la temporada pesquera de esta especie. Desde su captura en el medio marino hasta que fueron recogidos por nosotros, los ejemplares fueron mantenidos en condiciones de cetárea con agua a temperatura ambiente y en inanición. El transporte es muy estresante para los decápodos (Lorenzon et al., 2008; Whiteley y Taylor, 1992). Existen dos estrategias básicas de transporte: 1) en contenedores con agua marina, y 2) en contenedores al aire libre con un elevado nivel de humedad (Lorenzon et al., 2008). En ambos tipos de transporte el estrés por si solo incrementa la actividad respiratoria independientemente de los niveles de oxígeno ambiental (Jouve-Duhamel y Truchot, 1985) y concurren situaciones de hipoxia e hipoxemia con incremento en la concentración de lactato, glucosa, amonio, pH y CO_2 en la hemolinfa (Lorenzon et al., 2008; Whiteley y Taylor, 1992). El transporte también puede causar daños físicos y una reducción del vigor y capacidad de reacción de los especímenes (Barrento et al., 2010). Se ha constatado que el uso de contenedores con agua puede aumentar la mortalidad a causa de una caída en la calidad del agua por el estrés y hacinamiento (Lorenzon et al., 2008). Por ello empleamos el transporte terrestre para llevar los especímenes hasta las instalaciones del Institut de Recerca i Tecnologia Agroalimentàries (IRTA). Una ventaja adicional del transporte terrestre mediante cajones son sus menores requerimientos económicos y materiales. Los especímenes se introdujeron en los tanques de mantenimiento inmediatamente a su llegada al centro.

El segundo stock fue adquirido a través de la empresa Cademar S. Coop. R. L. (Alcanar, Tarragona) en el mes de abril del año 2014. En este caso fueron especímenes de importación procedentes de aguas europeas, probablemente Irlanda de acuerdo con la información suministrada por dicha empresa. En este caso no tuvimos ningún control de los especímenes hasta su recogida. Sin embargo, pudo observarse que los animales habían sido transportados en cajas de cartón con paños húmedos, presumiblemente fueron mantenidos en contenedores de baja temperatura durante el trayecto. Como en el caso anterior, los especímenes se introdujeron en los tanques de mantenimiento inmediatamente a su llegada al centro.

Debido a su eficiencia, las condiciones de mantenimiento del stock de reproductores fueron muy similares a las descritas en estudios previos (Guerao y Rotllant, 2009a; Guerao et al., 2012; Rotllant et al., 2010), ver Figura 4.4.1. Se emplearon tanques de cultivo cilíndricos compuestos por fibra de vidrio y poliéster. La capacidad de cada tanque fue de 2.000 L. Los tanques se llenaron con agua de mar filtrada y conectados a un sistema de recirculación de agua, cuya tasa de renovación fue de 35 m^3 h^{-1}. Los parámetros ambientales fueron constantes durante todo el año: temperatura de 18 ± 1 °C, salinidad de 35 ± 1 psu, fotoperiodo de 24 horas con 12 horas diarias de luz, intensidad luminosa de 25 lux provista por tubos fluorescentes situados sobre los tanques. Se suministró oxígeno adicional mediante la incorporación de un aireador en el fondo del tanque. Con objeto de aumentar la superficie disponible para la movilidad de los animales, decidimos introducir una red de malla gruesa en posición vertical cuyas medidas abarcaron el diámetro y altura del tanque, posteriormente pudo observarse que los animales asiduamente se aferraban a dicha red. La dieta consistió en mejillón (*Mytilus* sp.), administrado fresco cinco veces por semana y congelado dos veces por semana, esporádicamente también se les dió cangrejo congelado (*Liocarcinus depurator*) una vez por semana. La dieta se ofreció *ad libitum* diariamente, los mejillones eran abiertos previamente a su suministro. Cada día fueron retirados los restos del día anterior. En dichas condiciones la mortalidad se incrementó hasta aproximadamente el 50 % durante la primera semana tras la llegada de los animales, pero durante el resto de la temporada de cría la mortalidad de los adultos fue un evento raro. Nosotros sospechamos que aquella mortalidad inicial fue consecuencia del estrés debido a la captura, mantenimiento en cetárea y el posterior transporte de los especímenes. De modo que los animales aclimatados a las condiciones de cultivo son poco vulnerables. La relación de sexos (machos: hembras) se estableció finalmente entre 1:6 y 1:5 con 6-7 individuos por tanque. Nosotros pensamos que la mayor proporción de hembras que de machos podría reducir el estrés de estas al reducir el ratio de cópulas forzadas por hembra. Una vez finalizado el periodo de aclimatación, los especímenes supervivientes pudieron ser mantenidos en dichas condiciones durante uno a dos años.

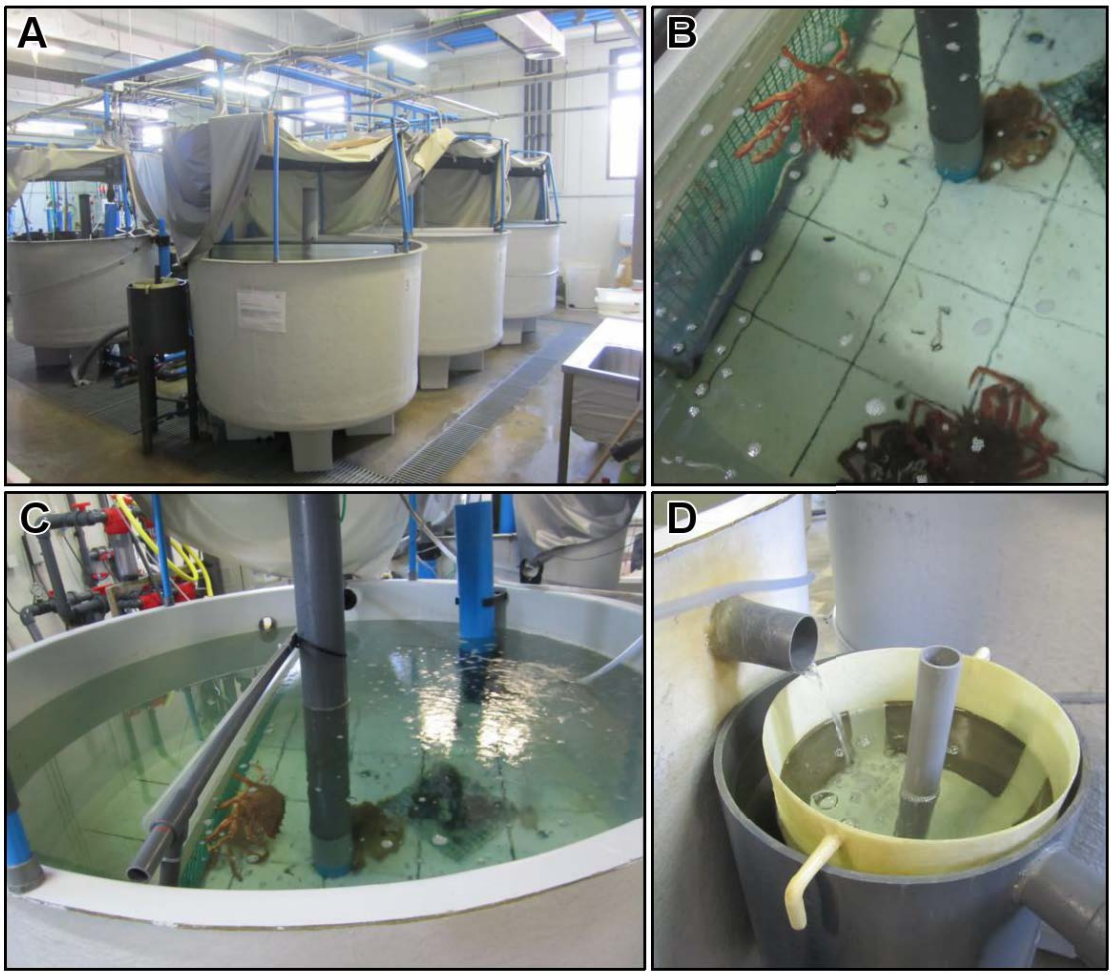

Figura 4.4.1. Instalaciones dedicadas al mantenimiento del stock de reproductores. A. Serie de tanques de 2.000 L de capacidad de fibra de vidrio y poliéster donde fueron alojados los adultos. B-C. Vista superior al interior de los tanques previamente mencionados, nótese la red que cruza el plano medio vertical de los tanques, los adultos suelen aferrarse a esta red. D. Colectores de 35 litros empleados para la recolección de las larvas recién eclosionadas, los tanques de reproductores desaguan directamente en estos colectores. Instalaciones del IRTA Sant Carles de la Ràpita, 2012-2016.

4.4.2 Cultivo larvario: diseño experimental

El diseño experimental empleado está basado en sistemas de cultivo utilizados a escala experimental para el estudio del desarrollo larvario de distintas especies de decápodos (Andrés et al., 2010d; Anger, 1991; 1995; Lebour, 1927; Messerknecht et al., 1991). Muchos de estos trabajos se basan en el cultivo individual de las larvas en recipientes de vidrio que permiten el seguimiento diario de los ejemplares, nuestro diseño es similar pero permite el cultivo simultáneo de varias larvas.

Fue empleado un set de acuarios de 200 L de capacidad (100 x 40 x 50 cm) vaciados y reutilizados como cámaras de cultivo. La temperatura de cada acuario fue mantenida constante mediante calentadores sumergibles controlados por termostato interno (Eheim Jäger, Finsterrot, Alemania), sumergidos en una capa de agua de 5-10 cm de altura. Esta capa de agua permitió distribuir homogéneamente la temperatura aprovechando al mismo tiempo el burbujeo de aire provisto por un sistema de aireación y el flujo de agua generado por los filtros Eheim Classic 350/2215 (Eheim GmbH & Co. KG, Plochinger, Alemania). El control de la temperatura fue diario empleando un medidor multi-parámetro portátil (precisión: 0,1°C; WTW ProfiLine Oxi 3210, Weilheim, Alemania), los calentadores fueron calibrados según necesidad. Las larvas de *M. brachydactyla* fueron cultivadas en el interior de vasos de precipitados de 600 mL que fueron dispuestos en el interior de los acuarios. Cada uno de los vasos de precipitados fue llenado con 500 mL de agua de mar filtrada, cuya salinidad fue de 35 ± 1 psu por norma general, excepcionalmente la salinidad varió por cuestiones experimentales.

El control de la salinidad se realizó empleando un refractómetro portátil (precisión: 1 psu, rango: 0–100 psu; Shenzhen Handsome Technology Co. Ltd., Guandong, China). La iluminación incidió desde la parte superior del acuario a una altura de 30 cm sobre la superficie de agua de los vasos de precipitados. De modo general, tanto el fotoperiodo como la intensidad lumínica se mantuvieron constantes, exceptuando los casos donde se modificó por cuestiones experimentales. Se mantuvo un fotoperiodo natural de 24 horas con 12 horas diarias de luz seguidas de 12 horas de oscuridad, el fotoperiodo fue controlado mediante temporizadores programables. La intensidad luminosa fue de 300 lux de intensidad y provista por tubos fluorescentes o de 1.000 lux de intensidad y provista por luces LED blancas (modelos LD65B 6.24 W y LD100B 14.40 W, ICA, España). La intensidad lumínica se midió empleando un luxómetro portátil (precision: 1 lx; Lx-101, Lutron Electronic Enterprise, Taipei, Taiwan). Este sistema está fotografiado y esquematizado en la Figura 4.4.2.

En relación a las larvas de *M. brachydactyla*, en todos los casos fueron recolectadas en un plazo máximo de 15 horas después de la eclosión. Previamente a la introducción de las larvas en los vasos de precipitados de cultivo, se recogieron con un vaso de precipitados adicional con objeto de seleccionar únicamente aquellas larvas con actividad nadadora, evitando realizar los experimentos con individuos que mostraran poco vigor tras la eclosión. La introducción de las larvas en los vasos de precipitados de cultivo se realizó sin aclimatación previa. De forma general, cada experimento constó de dos fases:

1. ***Cultivo de la fase de zoea***. Esta etapa englobó desde la etapa de zoea I en un plazo máximo de 15 horas tras la eclosión hasta la muda a megalopa. Siguiendo los trabajos publicados por Andrés et al. (2007, 2008), la densidad larvaria inicial se estableció en 60 zoeas L^{-1} (30 zoeas por vaso de precipitado).
2. ***Cultivo de la fase de megalopa***. Esta etapa englobó desde la etapa de megalopa en un plazo máximo de 15 horas tras la muda hasta la metamorfosis a primer juvenil. Debido al mayor tamaño de esta etapa larvaria, la densidad inicial de esta fase se estableció en 20 zoeas L^{-1} (10 zoeas por vaso de precipitado).

El mantenimiento diario de las larvas consistió en: registro, traslado, alimentación y preparación del material para el día siguiente. Estas actividades se detallarán a continuación:

1. ***Registro***. Fue contabilizado el número de larvas vivas, el número de larvas muertas, así como el número de individuos que mudaron con éxito al estadio de megalopa / juvenil según el caso. La muerte de los especímenes fue confirmada empleando una lupa binocular Nikon SMZ800. La falta de movimiento de los apéndices, la parálisis cardiaca y el blanqueamiento del cuerpo se utilizaron como criterios para catalogar al espécimen como fallecido.
2. ***Traslado***. La salubridad del cultivo fue mantenida mediante el traslado diario de las larvas a vasos de precipitados con agua limpia, pero cuyas condiciones ambientales imitaban las del vaso de procedencia: temperatura, salinidad, iluminación y las mismas larvas. El traslado se realizó cuidadosamente empleando pipetas Pasteur de plástico con el extremo anterior cortado.
3. ***Alimentación***. Una vez trasladas las larvas al vaso de precipitados de cultivo con agua limpia, fue incorporado el alimento. La dieta consistió en presa viva basada en nauplii y metanauplii de *Artemia* sp. (INVE Aquaculture Nutrition, Salt Lake UT) *ad libitum*. Los quistes de *Artemia* de los que procedió la alimentación diaria fueron dispuestos en condiciones adecuadas de eclosión 24 horas antes (Figura 4.4.3). No se precisó realizar enriquecimientos.

4. ***Preparación del material***. Cada día se prepararon los vasos de precipitados con agua limpia que serían empleados al día siguiente. Para ello los vasos retirados de la jornada recibieron dos lavados con agua dulce y después dos lavados con agua salada. Para que la temperatura de los vasos con agua limpia fuese similar a la de aquellos vasos que sustituirían al día siguiente, se situaron en los mismos acuarios donde se alojaron estos últimos.

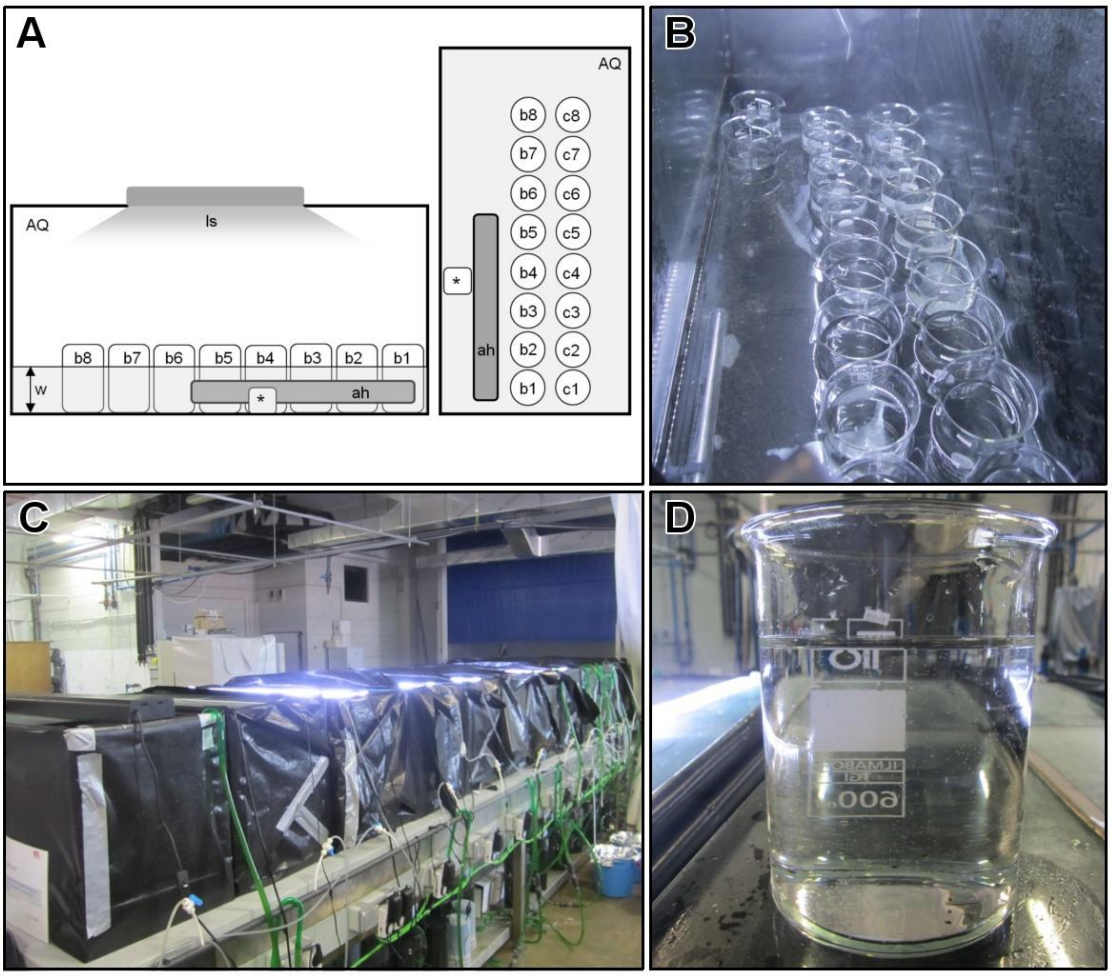

Figura 4.4.2. Diseño experimental empleado para el cultivo larvario. A. Esquema del diseño experimental (izquierda, vista lateral; derecha, vista superior): AQ, acuario; ah, calentador de agua; b1-b8, vasos de precipitados con larvas; c1- c8, vasos de precipitados con agua limpia preparados para su uso al día siguiente; ls, fuente de luz; w, columna de agua. B. Vista superior del interior de un acuario. C. Serie de acuarios empleados como cámaras de incubación en este diseño experimental. D. Vaso de precipitados empleado para el cultivo larvario. Instalaciones del IRTA Sant Carles de la Ràpita, 2012-2016.

Este diseño permite:

1. El seguimiento visual de las larvas es posible debido a la transparencia del vidrio. De modo que se puede observar la actividad de las larvas, advertir la presencia de especímenes muertos y mudas, así como el estado de la presa viva administrada como alimento.
2. Dadas las dimensiones de los vasos de precipitados, es posible capturar las larvas individualmente con objeto de hacer un recuento o ver su estado.
3. La presa viva no se acumula debido a las actividades diarias de limpieza y mantenimiento.
4. No existe acumulación de residuos debido a las actividades diarias de limpieza y mantenimiento.
5. Es posible recolectar de modo cuidadoso a las larvas y trasladarlas a vasos de precipitados con agua limpia y alimento fresco.

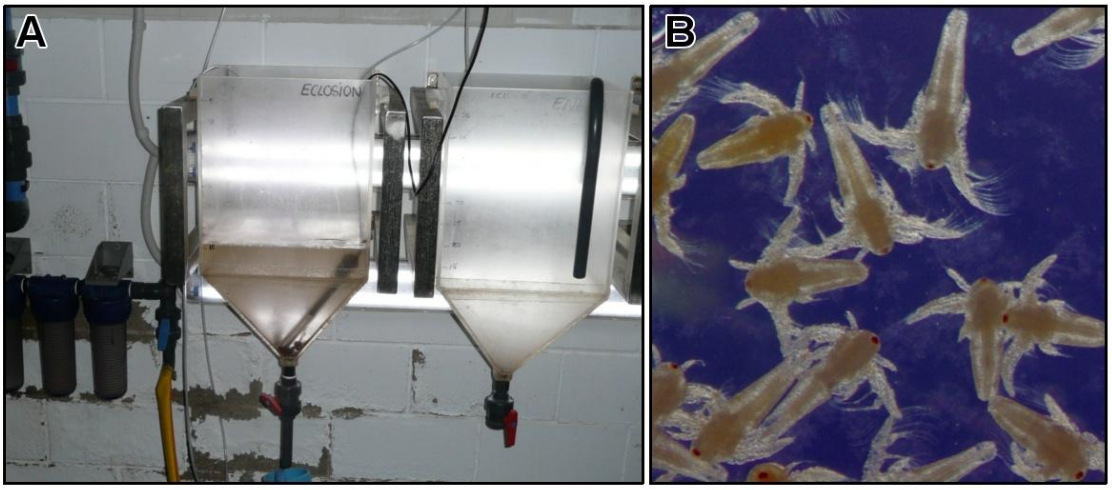

Figura 4.4.3. Alimentando a las larvas de centollo. A. Sistema empleado para eclosionar *Artemia* sp.: diariamente el tanque alojó 15 litros de agua de mar filtrada y alrededor de 5 gramos de quistes, en el interior del tanque fueron colocados un calentador de agua controlado por termostato (26-28 °C) y un aireador. La iluminación fue continua y provista por tubos fluorescentes. Mediante este sistema fueron obtenidas eclosiones cada 24 horas. B. Nauplii de *Artemia* sp. Instalaciones del IRTA Sant Carles de la Ràpita, 2012-2016.

El diseño previamente descrito fue ligeramente modificado para la realización de la serie de experimentos relacionados con el asentamiento, dado que estos requirieron un mayor número de tratamientos/réplicas. El principal cambio fueron las cámaras de cultivo, en lugar de los acuarios utilizamos una serie de tanques de 360 L (96 x 96 x 40 cm) conectados a un sistema de recirculación de agua con objeto de mantener una temperatura constante de 21 ± 1°C (Figura 4.4.4). Como en el diseño anterior, el cultivo fue realizado en vasos de precipitados, conservándose los mismos parámetros ambientales: salinidad (35 ± 1 psu, agua de mar filtrada), fotoperiodo (24 horas con 12 horas diarias de luz, temporizadores programables) e intensidad lumínica (1.000 lux, luces LED de iluminación blanca). La dieta también consistió en presas vivas (Figura 4.4.3): nauplii y metanauplii de *Artemia* sp. (INVE Aquaculture Nutrition, Salt Lake UT) *ad libitum* y fueron realizadas las mismas tareas diarias de mantenimiento.

Cada serie de experimentos (temperatura, iluminación, salinidad y asentamiento) requirió de sus propias particularidades, que consistieron en ligeras modificaciones del diseño básico descrito en este capítulo, las cuales fueron enfocadas hacia los distintos parámetros a estudiar. Estos cambios son detallados en sus respectivos capítulos.

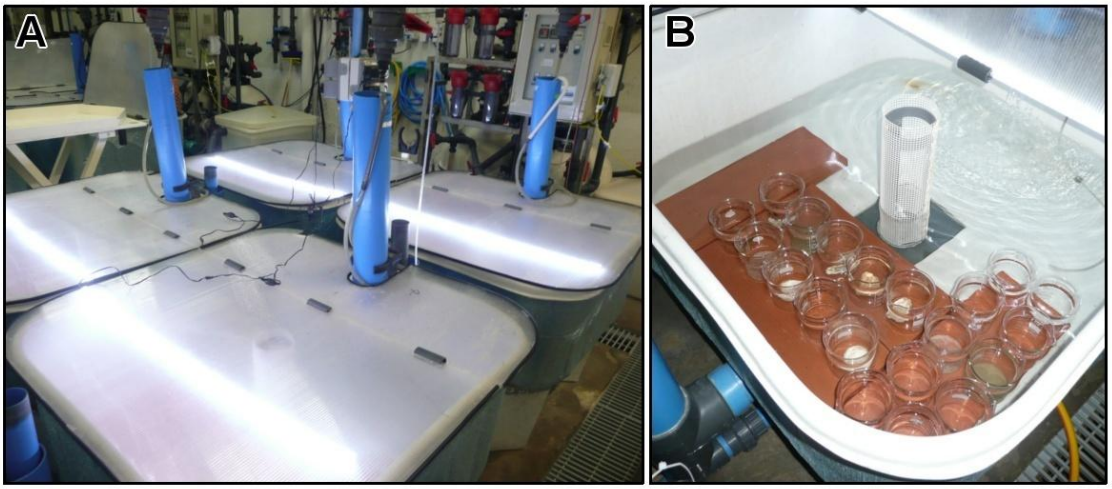

Figura 4.4.4. Sistema alternativo de cultivo larvario (modificación del sistema previo). A. Sistema de tanques de 360 litros empleados como cámaras de incubación. B. Vista superior al interior de los tanques. Instalaciones del IRTA Sant Carles de la Ràpita, 2012-2016.

4.4.4 Datos obtenidos y análisis estadístico

Los objetivos de las investigaciones de este bloque incluyen la determinación de los parámetros ambientales óptimos (temperatura, salinidad, iluminación y asentamiento) para el cultivo de los estadios larvarios de *M. brachydactyla*, desde la perspectiva del cultivo acuícola. Los datos más importantes para optimizar el cultivo larvario son la **supervivencia** y el **tiempo de desarrollo**. Desde un punto de vista productivo, es preciso obtener el máximo número de ejemplares con el tamaño / estadio de vida deseados en el menor tiempo posible. Por esa razón en cada experimento medimos la supervivencia y el tiempo de desarrollo desde la eclosión hasta la muda a megalopa, así como la supervivencia y el tiempo de desarrollo desde la muda de megalopa hasta la metamorfosis al primer estadio de juvenil. *M. brachydactyla* cuenta con dos estadios de zoea cuya identificación requiere el examen bajo lupa binocular. Dado que este procedimiento requiere el examen diario de cada larva durante el estadio de zoea en una gota de agua, se decidió estudiar el estadio de zoea en su conjunto para reducir al mínimo la manipulación y posible daño de las larvas, ya que todo estrés en las etapas tempranas puede tener consecuencias que pueden llegar a prolongarse durante todo el desarrollo larvario o bien manifestarse al final del mismo como un efecto latente (Pechenik, 2006).

Otras variables que fueron estudiadas fueron el **peso seco corporal** así como la **composición elemental (CHN)** de las larvas, entendida como la masa total y porcentaje de carbono (C), hidrógeno (H) y nitrógeno (N) que contienen sus cuerpos. El peso seco corporal es una variable indicativa de la ganancia de masa en los individuos, esta puede deberse al incremento en el contenido de materia orgánica como proteínas, lípidos o azúcares (entre otros); o bien debido a la acumulación de materia inorgánica como sales minerales, especialmente en el caparazón (Dillaman et al., 2012). La composición elemental en los crustáceos marinos, tantos adultos como larvas, es un reflejo de su composición bioquímica (Marc, 2006). De modo que el contenido en carbono e hidrógeno está principalmente representado por el contenido en proteínas (Marc, 2006), seguido del contenido en lípidos (Childress y Nygaard, 1974; Marc, 2006). Mientras que el contenido en nitrógeno es un reflejo de la abundancia de proteínas (Anger y Harms, 1990; Childress y Nygaard, 1974; Marc, 2006), y en menor medida quitina (Childress y Nygaard, 1974) y aminoácidos libres (Anger y Harms, 1990; Marc, 2006). Con estos valores algunos autores han establecido la ratio C/N como índice de la ratio entre lípidos/proteínas: la reducción en los valores de la ratio C/N podría considerarse un valor indicativo del cambio en la proporción corporal de lípidos (y carbohidratos) y proteínas (Anger y Dawirs, 1982; Anger y Harms, 1990). Esta información es valiosa para evaluar si los animales de cultivo están asimilando los nutrientes ingeridos o bien para determinar si a lo largo del ciclo vital ocurren cambios en la ratio de utilización de los recursos disponibles.

El procedimiento empleado para calcular la composición elemental fue realizado empleando protocolos estandarizados por diversas publicaciones (Anger y Dawirs, 1982; Anger y Harms, 1990; Ikeda, 1988; Ikeda y Kirkwood, 1989). Tras el muestreo, las larvas se lavaron cuidadosamente durante 10-20 segundos con agua destilada, a continuación se secaron sobre un filtro de metal y papel de filtro. Después las larvas fueron transferidas a cápsulas de estaño de uso especial para análisis micro-elemental cuyo peso era previamente conocido y anotado en una tabla. Una vez introducidas las larvas en el interior de las cápsulas de estaño, estas fueron cerradas y congeladas a -20 °C. La continuación del protocolo fue llevada a cabo en la School of Ocean Sciences (Bangor University, Bangor, Reino Unido). Las muestras fueron liofilizadas (Edwards Super Modulyo) durante 24 horas, a continuación el peso seco se determinó en una micro-balanza Mettler Toledo MX5 (precisión: 1 µg, capacidad: 5.1 g). Finalmente, las muestras fueron analizados en un Analizador Elemental CHNS-O (FlashEA 1112 Series).

Los análisis estadísticos fueron realizados empleando el software especializado en análisis estadístico R versión 3.2.0 (R Development Core Team, 2015). Todos los experimentos que estudiaron una única variable independiente (temperatura, salinidad, fotoperiodo, intensidad lumínica, tipo de sustrato) fueron analizados empleando la técnica de análisis ANOVA de una vía. Todos los experimentos que estudiaron la combinación de dos variables independientes (temperatura y salinidad, temperatura e intensidad lumínica) fueron analizados empleando la técnica de análisis ANOVA de dos vías tipo III, para ello tuvo que usarse el paquete de R «car 2.0-25» (Fox y Weisberg, 2011). Previamente al análisis estadístico ANOVA se comprobó que los residuos de los datos seguían una distribución normal (homocedasticidad) mediante el test de Shapiro-Wilk y que las varianzas eran homogéneas mediante el test de Levene. La aplicación de este último test requirió el uso del paquete de R «car 2.0-25» (Fox y Weisberg, 2011). Cuando dichas condiciones no fueron cumplimentadas se aplicó el test de Kruskal-Wallis para datos no paramétricos. La significancia estadística de los análisis fue establecida a partir de de un nivel crítico (α) de 0,05 para rechazar la hipótesis nula. Aquellos análisis que mostraron significancia estadística fueron analizados posteriormente mediante el análisis de Tukey-HSD con objeto de encontrar diferencias significativas entre grupos.

4.5 Bibliografía.

Alaminos J. 2011. Efecto del confinamiento en espacios reducidos sobre el crecimiento de juveniles de centollo, *Maja brachydactyla*, y su repercusión en la madurez. Revista de biología marina y oceanografía 46(2):219-230.

Alberts-Hubatsch H, Lee SY, Diele K, Wolff M, Nordhaus I. 2014. Microhabitat use of early benthic stage mud crabs, *Scylla serrata* (Forskål, 1775), in eastern Australia. Journal of Crustacean Biology 34(5):604-610.

Andrés M, Estévez A, Anger K, Rotllant G. 2008. Developmental patterns of larval growth in the edible spider crab, *Maja brachydactyla* (Decapoda: Majidae). J Exp Mar Biol Ecol 357(1):35-40.

Andrés M, Estévez A, Hontoria F, Rotllant G. 2010a. Differential utilization of biochemical components during larval development of the spider crab *Maja brachydactyla* (Decapoda: Majidae). Marine Biology 157(10):2329-2340.

Andrés M, Estévez A, Rotllant G. 2007. Growth, survival and biochemical composition of spider crab *Maja brachydactyla* (Balss, 1922) (Decapoda: Majidae) larvae reared under different stocking densities, prey:larva ratios and diets. Aquaculture 273(4):494-502.

Andrés M, Estévez A, Simeó CG, Rotllant G. 2010b. Annual variation in the biochemical composition of newly hatched larvae of *Maja brachydactyla* in captivity. Aquaculture 310(1-2):99-105.

Andrés M, Gisbert E, Díaz M, Moyano FJ, Estévez A, Rotllant G. 2010c. Ontogenetic changes in digestive enzymatic capacities of the spider crab, *Maja brachydactyla* (Decapoda: Majidae). J Exp Mar Biol Ecol 389(1-2):75-84.

Andrés M, Rotllant G, Sastre M, Estevez A. 2011. Replacement of live prey by formulated diets in larval rearing of spider crab *Maja brachydactyla*. Aquaculture 313(1-4):50-56.

Andrés M, Rotllant G, Zeng C. 2010d. Survival, development and growth of larvae of the blue swimmer crab, *Portunus pelagicus*, cultured under different photoperiod conditions. Aquaculture 300(1-4):218-222.

Anger K. 1991. Effects of temperature and salinity on the larval development of the Chinese mitten crab *Eriocheir sinensis* (Decapoda: Grapsidae). Marine Ecology Progress Series 72:103-110.

Anger K. 1995. Developmental biology of *Armases miersii* (Grapsidae), a crab breeding in supratidal rock pools. I. Facultative lecithotrophy of larval stages. Marine Ecology Progress Series 117:75-81.

Anger K. 2001. The Biology of Decapod Crustacean Larvae. Rotterdam: A.A. Balkema Publishers. 419 p.

Anger K. 2003. Salinity as a key parameter in the larval biology of decapod crustaceans. Invertebrate Reproduction & Development 43(1):29-45.

Anger K. 2006. Contributions of larval biology to crustacean research: a review. Invertebrate Reproduction & Development 49(3):175-205.

Anger K, Dawirs RR. 1982. Elemental composition (C, N, H) and energy in growing and starving larvae of *Hyas araneus* (Decapoda, Majidae). Fishery Bulletin 80(3):419-433.

Anger K, Harms J. 1990. Elemental (CHN) and proximate biochemical composition of decapod crustacean larvae. Comparative Biochemistry and Physiology Part B: Comparative Biochemistry 97B(1):69-80.

Barrento S, Marques A, Vaz-Pires P, Nunes ML. 2010. Live shipment of immersed crabs *Cancer pagurus* from England to Portugal and recovery in stocking tanks: stress parameter characterization. ICES Journal of Marine Science: Journal du Conseil 67(3):435-443.

Baylon J, Suzuki H. 2007. Effects of changes in salinity and temperature on survival and development of larvae and juveniles of the crucifix crab *Charybdis feriatus* (Crustacea:Decapoda:Portunidae). Aquaculture 269(1-4):390-401.

Bondad-Reantaso MG, Subasinghe RP, Josupeit H, Cai J, Zhou X. 2012. The role of crustacean fisheries and aquaculture in global food security: Past, present and future. Journal of Invertebrate Pathology 110(2):158-165.

Browdy CL. 1998. Recent developments in penaeid broodstock and seed production technologies: improving the outlook for superior captive stocks. Aquaculture 164(1–4):3-21.

Costlow JD, Bookhout CG, Monroe R. 1960. The Effect of Salinity and Temperature on Larval Development of *Sesarma cinereum* (Bosc) Reared in the Laboratory. Biological Bulletin 118(2):183-202.

Costlow Jr JD, Bookhout CG, Monroe R. 1966. Studies on the Larval Development of the Crab, *Rhithropanopeus harrisii* (Gould). I. The Effect of Salinity and Temperature on Larval Development. Physiological Zoology 39(2):81-100.

Cottens KF, Silva UAT, Ventura R, Ramos FM, Ostrensky A. 2014. Cultivo de larvas de *Ucides cordatus* (LINNAEU, 1763) sob diferentes intensidades luminosas. Arquivo Brasileiro de Medicina Veterinária e Zootecnia 66:1464-1470.

Childress JJ, Nygaard M. 1974. Chemical composition and buoyancy of midwater crustaceans as function of depth of occurrence off Southern California. Marine Biology 27(3):225-238.

Diele K, Simith DJB. 2007. Effects of substrata and conspecific odour on the metamorphosis of mangrove crab megalopae, *Ucides cordatus* (Ocypodidae). J Exp Mar Biol Ecol 348(1-2):174-182.

Dillaman RM, Roer R, Shafer T, Modla S. 2012. The Crustacean Integument: Structure and Function. In: Watling L, Thiel M, editors. The Natural History of the Crustacea, vol 1 Functional Morphology and Diversity: Oxford University Press. p 140-165.

Domingues P, Alaminos J. 2008. Efectos de la densidad de cultivo y de elementos de refugio en el crecimiento y supervivencia de juveniles de centollo, *Maja brachydactyla* (Balss, 1922). Revista de biología marina y oceanografía 43(1):121-127.

Fahy E. 2001. The Magharees spider crab *Maja squinado* fishery in 2000. Irish Fisheries Investigations 9. 21 + appendix p.

Fahy E, Carroll J. 2009. Vulnerability of male spider crab *Maja brachydactyla* (Brachyura: Majidae) to a pot fishery in south-west Ireland. Journal of the Marine Biological Association of the United Kingdom 89(7):1353-1366.

FAO. 2012. El Estado Mundial de la Pesca y la Acuicultura. Roma: Departamento de Pesca y Acuicultura de la FAO.

FAO. 2014. B-42 Crabs, sea-spiders. Capture production by species, fishing areas and countries or areas. In: FAO, editor. FAO yearbook Fishery and aquaculture statistics. Rome: FAO.

Flores AAV, Cruz J, Paula J. 2002. Temporal and spatial patterns of settlement of brachyuran crab megalopae at a rocky coast in Central Portugal Marine Ecology Progress Series 229:207-220.

Forward Jr RB. 1974. Negative phototaxis in crustacean larvae: Possible functional significance. J Exp Mar Biol Ecol 16(1):11-17.

Forward RB. 1976. Light and diurnal vertical migration: photobehavior and photophysiology of plankton. In: Smith KC, editor. Photochemical and Photobiological Reviews: Volume 1. Boston, MA: Springer US. p 157-209.

Forward RB, Cronin TW, Stearns DE. 1984. Control of diel vertical migration: Photoresponses of a larval crustacean. Limnology and Oceanography 29(1):146-154.

Forward RB, Tankersley RA, Rittschof D. 2001. Cues for Metamorphosis of Brachyuran Crabs: An Overview. American Zoologist 41(5):1108-1122.

Fox J, Weisberg S. 2011. An {R} Companion to Applied Regression. Thousand Oaks CA: Sage, Second Edition.

Freire J, Bernárdez C, Corgos A, Fernández L, González-Gurriarán E, Sampedro MP, Verísimo P. 2002. Management strategies for sustainable invertebrate fisheries in coastal ecosystems of Galicia (NW Spain). Aquatic Ecology 36(1):41-50.

García-Flórez L, Fernández-Rueda P. 2003. Parámetros biológicos del centollo, *Maja brachydactyla* (Brachyura: Majidae), procedente de capturas comerciales en la zona central de Asturias (España) y su aplicación a la gestión pesquera. Naturalia Cantabricae 2:45-52.

Gebauer P, Paschke K, Anger K. 2003. Delayed metamorphosis in decapod crustaceans: evidence and consequences. Revista Chilena de Historia Natural 76:169-175.

Gebauer P, Walter I, Anger K. 1998. Effects of substratum and conspecific adults on the metamorphosis of *Chasmagnathus granulata* (Dana) (Decapoda: Grapsidae) megalopae. J Exp Mar Biol Ecol 223(2):185-198.

Giménez L. 2010. Relationships between habitat conditions, larval traits, and juvenile performance in a marine invertebrate. Ecology 91(5):1401-1413.

Globefish. 2016. European Price Report. Food and Agriculture Organization of the United Nations (FAO) Fisheries and Aquaculture Policy and Economics Division Products, Trade and Marketing Branch Issue 1 - 12.

González-Gurriarán E, Fernández L, Freire J, Muiño R. 1998. Mating and role of seminal receptacles in the reproductive biology of the spider crab *Maja squinado* (Decapoda, Majidae). J Exp Mar Biol Ecol 220(2):269-285.

González-Gurriarán E, Fernández L, Freire J, Muiño R, Parapar J. 1993. Reproduction of the spider crab *Maja squinado* (Brachyura: Majidae) in the southern Galician coast (NW Spain). International Council for the Exploration of the Sea: Shellfish Committe ICES C.M. 1993/K:19.

González-Gurriarán E, Freire J, Bernárdez C. 2002. Migratory patterns of female spider crabs *Maja squinado* detected using electronics tags and telemetry. Journal of Crustacean Biology 22(1):91-97.

Guerao G, Rotllant G. 2009a. Post-larval development and sexual dimorphism of the spider crab *Maja brachydactyla* (Brachyura: Majidae). Sci Mar 73:797-808.

Guerao G, Rotllant G. 2009b. Survival and growth of post-settlement juveniles of the spider crab *Maja brachydactyla* (Brachyura: Majoidea) reared under individual culture system. Aquaculture 289(1-2):181-184.

Guerao G, Rotllant G. 2010. Development and growth of the early juveniles of the spider crab *Maja squinado* (Brachyura: Majoidea) in an individual culture system. Aquaculture 307(1-2):105-110.

Guerao G, Rotllant G, Anger K. 2010. Characterization of larval moulting cycles in *Maja brachydactyla* (Brachyura, Majidae) reared in the laboratory. Aquaculture 302(1-2):106-111.

Guerao G, Simeó CG, Anger K, Urzúa Á, Rotllant G. 2012. Nutritional vulnerability of early zoea larvae of the crab *Maja brachydactyla* (Brachyura, Majidae). Aquatic Biology 16(3):253-264.

Hamasaki K, Obata Y, Dan S, Kitada S. 2011. A review of seed production and stock enhancement for commercially important portunid crabs in Japan. Aquaculture International 19(2):217-235.

Hamasaki K, Suprayudi MA, Takeuchi T. 2002. Mass mortality during metamorphosis to megalops in the seed production of mud crab *Scylla serrata* (Crustacea, Decapoda, Portunidae). Fisheries Science 68:1226-1232.

Hernández JE, Palazón-Fernández JL, Hernández G, Bolaños J. 2012. The effect of temperature and salinity on the larval development of *Stenorhynchus seticornis* (Brachyura: Inachidae) reared in the laboratory. Journal of the Marine Biological Association of the United Kingdom 92(03):505-513.

Iglesias J, Sánchez FJ, Moxica C, Fuentes L, Otero JJ, Pérez JL. 2002. Datos preliminares sobre el cultivo de larvas y juveniles de centolla *Maja squinado* Herbst, 1788 en el Centro Oceanográfico de Vigo del Instituto Español de Oceanografía. Boletín del Instituto Español de Oceanografía 18(1-4):25-30.

Ikeda T. 1988. Metabolism and chemical composition of crustaceans from the Antarctic mesopelagic zone. Deep Sea Research Part A Oceanographic Research Papers 35(12):1991-2002.

Ikeda T, Kirkwood R. 1989. Metabolism and body composition of two euphausiids (*Euphausia superba* and *E. crystallorophias*) collected from under the pack-ice off Enderby Land, Antarctica. Marine Biology 100(3):301-308.

Illescas JL, Bacho O, Ferrer S. 2007. Análisis de las principales especies pesqueras comercializadas (y IV). Centollo o centolla. Distribución y Consumo 93:86 - 89.

Jouve-Duhamel A, Truchot J-P. 1985. Ventilatory responses to ambient oxygen in stressed and fully settled shore crabs *Carcinus maenas* (L.). J Exp Mar Biol Ecol 90(2):107-118.

Kergariou G, Veron G. 1981. Distribution de l'araignée de mer, *Maia squinado*, sur la pêcherie hivernale du Golfe Normano Breton. ICES, Shellfish Committee CM 1981/K:32: 9.

Kogane T, Dan S, Hamasaki K. 2007. Improvement of larval rearing technique for mass seed production of snow crab *Chionoecetes opilio*. Fisheries Science 73(4):851-861.

Lárez MB, Palazón-Fernández JL, Bolaños CJ. 2000. The effect of salinity and temperature on the larval development of *Mithrax caribbaeus* Rathbun, 1920 (Brachyura: Majidae) reared in the laboratory. Journal of Plankton Research 22(10):1855-1869.

Latrouite D, Le Foll D. 1989. Donnees sur les migrations des crabes tourteau *Cancer pagurus* et les araignees de mer *Maja squinado*. Océanis 15(2):133-142.

Le Foll D. 1993. Biologie et exploitation de l'araignée de mer *Maja squinado* Herbst en Manche Ouest [Doctoral Dissertation]. Plouzane (France): Université de Bretagne Occidentale. 517 p.

Lebour MV. 1927. Studies of the Plymouth Brachyura. I. The rearing of crabs in captivity, with a description of the larval stages of *Inachus dorsettensis*, *Macropodia longirostris* and *Maia squinado*. Journal of the Marine Biological Association of the United Kingdom 14(3):795-821.

Lorenzon S, Giulianini PG, Libralato S, Martinis M, Ferrero EA. 2008. Stress effect of two different transport systems on the physiological profiles of the crab *Cancer pagurus*. Aquaculture 278(1–4):156-163.

MAPAMA. 2016. Estadísticas Pesqueras. Noviembre 2016. Ministerio de Agricultura y Pesca, Alimentación y Medio Ambiente Secretaría General Técnica, Subdirección General de Estadística, Servicio de Estadísticas de la Pesca.

Marc V. 2006. Linking biochemical and elemental composition in freshwater and marine crustacean zooplankton. Marine Ecology Progress Series 327:233-246.

MARM. 2007. La Alimentación en España. Fichas de Consumo. Ministerio de Medio Ambiente y Medio Rural y Marino, Gobierno de España.

Mercasa. 2016. Alimentación en España. Producción, Industria, Distribución y Consumo. Distribución y Consumo.

Messerknecht I, Montu M, Anger K. 1991. Larval development and salinity tolerance of Brazilian *Eurytium limosum* (Say, 1818) (Brachyura: Xanthidae) reared in the laboratory. Meeresforschung 33:275-296.

Minagawa M. 1990. Influence of Temperature on Survival, Feeding and Development of Larvae of the Red Frog Crab, *Ranina ranina* (Crustacea, Decapoda, Raninidae). Nippon Suisan Gakkaishi 56(5):755-760.

Nagaraj M. 1992. Combined Effects of Temperature and Salinity on the Zoeal Development of the Crab *Liocarcinus puber* (Decapoda: Portunidae). Marine Ecology 13(3):233-241.

Nurdiani R, Zeng C. 2007. Effects of temperature and salinity on the survival and development of mud crab, *Scylla serrata* (Forsskål), larvae. Aquaculture Research 38(14):1529-1538.

Ong K-S, Costlow J. 1970. The effect of salinity and temperature on the larval development of the stone crab, *Menippe mercenaria* (Say), reared in the laboratory. Chesapeake Science 11(1):16-29.

Palma AT, Pardo LM, Veas R, Cartes C, Silva M, Manriquez K, Diaz A, Muñoz C, Ojeda FP. 2006. Coastal brachyuran decapods: settlement and recruitment under contrasting coastal geometry conditions. Marine Ecology Progress Series 316:139-153.

Palma J, Correia M, Andrade JP. 2008. Usefulness of flat bottom tanks on the settlement of spider crab (*Maja squinado*, Herbst) larvae. Aquaculture Research 39(9):1005-1008.

Pardo LM, Palma AT, Prieto C, Sepulveda P, Valdivia I, Ojeda FP. 2007. Processes regulating early post-settlement habitat use in a subtidal assemblage of brachyuran decapods. J Exp Mar Biol Ecol 344(1):10-22.

Paula J, Dornelas M, Flores AAV. 2003. Stratified settlement and moulting competency of brachyuran megalopae in Ponta Rasa mangrove swamp, Inhaca Island (Mozambique). Estuarine, Coastal and Shelf Science 56(2):325-337.

Paula J, Dray T, Queiroga H. 2001. Interaction of offshore and inshore processes controlling settlement of brachyuran megalopae in Saco mangrove creek, Inhaca Island (South Mozambique). Marine Ecology Progress Series 215:251-260.

Pawlik JR. 1992. Chemical ecology of the settlement of benthic marine invertebrates. Oceanography and Marine Biology: An Annual Review 30(273-335).

Pechenik JA. 2006. Larval experience and latent effects-metamorphosis is not a new beginning. Integrative and Comparative Biology 46(3):323-333.

R Development Core Team. 2015. R: A language and environment for statistical computing. Vienna, Austria: R Foundation for Statistical Computing.

Reed PH. 1969. Culture Methods and Effects of Temperature and Salinity on Survival and Growth of Dungeness Crab (*Cancer magister*) Larvae in the Laboratory. Journal of the Fisheries Research Board of Canada 26(2):389-397.

Rodríguez S, Ojeda FP, Inestrosa NC. 1993. Settlement of benthic marine invertebrates. Marine Ecology Progress Series 97:197-207.

Rotllant G, Moyano FJ, Andrés M, Estévez A, Díaz M, Gisbert E. 2010. Effect of delayed first feeding on larval performance of the spider crab *Maja brachydactyla* assessed by digestive enzyme activities and biometric parameters. Marine Biology 157(10):2215-2227.

Sampedro MP, González G, E., Freire J, Muiño R. 1999. Morphometry and sexual maturity in the spider crab *Maja squinado* (Decapoda: Majidae) in Galicia, Spain. Journal of Crustacean Biology 19(3):578-592.

Simeó CG, Estévez A, Rotllant G. 2009. Efecto del desplazamiento del fotoperiodo natural en la inducción y calidad de la puesta de la centolla, *Maja brachydactyla*. In: Beaz-Paleo D, Villarroel-Robinson M, Cárdenas-Rojas S, editors. XII Congreso Nacional de Acuicultura. Madrid: Ministerio de Medio Ambiente y Medio Rural y Marino. Sociedad Española de Acuicultura. Fundación Observatorio del Mar.

Simith DdJdB, Diele K, Abrunhosa FA. 2013. Carry-over effects of delayed larval metamorphosis on early juvenile performance in the mangrove crab *Ucides cordatus* (Ucididae). J Exp Mar Biol Ecol 440:61-68.

Simith DJB, Diele K, Abrunhosa FA. 2010. Influence of natural settlement cues on the metamorphosis of fiddler crab megalopae, *Uca vocator* (Decapoda: Ocypodidae). Anais da Academia Brasileira de Ciências 82(2):313-321.

Thorson G. 1964. Light as an ecological factor in the dispersal and settlement of larvae of marine bottom invertebrates. Ophelia 1(1):167-208.

Torres G, Giménez L, Anger K. 2011. Growth, tolerance to low salinity, and osmoregulation in decapod crustacean larvae. Aquatic Biology 12(3):249-260.

Valdes L, Alvarez-Ossorio MT, González-Gurriarán E. 1991. Influence of temperature on embryonic and larval development in *Necora puber* (Brachyura, Portunidae). Journal of the Marine Biological Association of the United Kingdom 71(4):787-789.

Vargo SL, Sastry AN. 1977. Acute temperature and low dissolved oxygen tolerances of brachyuran crab (*Cancer irroratus*) larvae. Marine Biology 40(2):165-171.

Whiteley NM, Taylor EW. 1992. Oxygen and acid-base disturbances in the hemolymph of the lobster *Homarus gammarus* during commercial transport and storage. Journal of Crustacean Biology 12(1):19-30.

Zmora O, Findiesen A, Stubblefield J, Frenkel V, Zohar Y. 2005. Large-scale juvenile production of the blue crab *Callinectes sapidus*. Aquaculture 244(1-4):129-139.

CHAPTER 5.

The Effects of Temperature and Salinity on the Survival, Growth and Duration of the Larval Development of the Common Spider Crab *Maja brachydactyla* (Balss, 1922) (Brachyura: Majidae)

Published in:

Journal of Shellfish Research 34 (3): 1073-7083

Impact factor: 0.829

The effects of temperature and salinity on the survival, growth and duration of the larval development of the common spider crab *Maja brachydactyla* Balss, 1922 (Brachyura: Majidae)

Diego Castejón[1]*, Guiomar Rotllant[2], Luis Giménez[3], Gabriela Torres[3], and Guillermo Guerao[4]

[1]Subprograma Cultius Aquàtics, IRTA, Ctra. de Pobre Nou, Km 5.5, Sant Carles de la Ràpita. 43540, Tarragona, Spain.

[2]Departament de Recursos Marins Renovables, Institut de Ciències Del Mar, CSIC, Passeig Marítim de la Barceloneta 37-49. Barcelona 08003, Spain

[3]School of Ocean Sciences, Bangor University, Menai Bridge, Anglesey, LL59 5AB, United Kingdom.

[4]PS Fabra i Puig 344, Barcelona. 08031, Spain.

Short title: *Maja brachydactyla* temperature salinity larvae

***Corresponding author**: Diego Castejón. E-mail: diego.castejon.dcb@gmail.com; phone: +34 681 154 398; postal address: Subprograma Cultius Aquàtics, IRTA, Ctra. Poble Nou, Km 5.5, Sant Carles de la Ràpita 43540, Tarragona, Spain.

Abstract.

The effect of temperature and salinity on the larval development of the common spider crab *Maja brachydactyla* Balss, 1922 were studied in the laboratory. Larvae were reared at different salinities (0 to 45) at constant temperature, and under 6 different combinations of temperature (18 and 21 °C) and salinity (30, 35 and 40). The survival and developmental time from newly hatched zoeae to the megalopa stage and from megalopa to the first juvenile stage was quantified; the 24 h median lethal salinity (LS_{50}) for first zoeal stage was calculated. Dry mass (DM), elemental body composition (CHN) and carbon: nitrogen ratio (C:N) were determined in both starved and nourished zoeae.

The lower and upper LS_{50} for *M. brachydactyla* first zoea in 24 h were 19.9 and 56.0, respectively; similar to other marine stenohaline brachyuran larvae. The megalopa stage was reached in a salinity range from 30 to 40. The highest survival rates to the first juvenile stage were observed at salinity: 35 and temperature: 21 °C. Salinity was the key parameter for the survival to first juvenile, while the temperature had a higher effect over the duration of the larval development. The greatest loss of DM and C:N in starving zoeae was observed at high salinity (45 and 55), while in nourished zoeae the greater loss in DM was observed at low salinity (25). No differences were found in DW or C:N during the megalopa stage. The culture and ecological implications of the salinity tolerance of *M. brachydactyla* larvae are discussed.

Keywords: *Maja brachydactyla*; Brachyura; growth; larval development; salinity; temperature

1. Introduction

The common spider crab *Maja brachydactyla* Balss, 1922 is a brachyuran widely distributed in the eastern Atlantic, from the southern British Isles to the western Sahara (including Azores and Canary Islands), and south-western Mediterranean (Abelló et al. 2014). This is a species of high commercial value whose main fisheries are located in France, United Kingdom, Ireland and Spain, with average of total annual captures of 5,600 and 7,000 tonnes between 2008 and 2012 (FAO 2012). This species shows an abbreviated larval development, consisting of a zoeal phase with two zoeal stages and a megalopa stage. The short larval duration makes *M. brachydactyla* a very attractive species for aquaculture (Guerao et al. 2008). Previous studies have covered the morphological description of larval stages and molt cycles (Guerao et al. 2008, Guerao & Rotllant 2010, Guerao et al. 2010), growth patterns (Andrés et al. 2008) and ontogenetic changes in biochemistry (Andrés et al. 2007, Andrés et al. 2010).

In the Galician coast (NW Iberian Peninsula), the larval release and recruitment of *M. brachydactyla* occur in nearshore waters (Corgos et al. 2011), where the larvae may be exposed to salinity fluctuations due to the coastal and estuarine influences (Cabanas et al. 1987, Gago et al. 2011). Since the salinity is one of the key factors affecting survival, growth, development and distribution of aquatic crustacean larvae (Charmantier 1998, Anger 2003, Torres et al. 2011), the study of the salinity tolerance during the larval development is interesting for inferring the ecological adaptations of the larvae in the field. The range of salinities for survival and development of crustacean larvae depends on the ability and range of the osmoregulatory capacity, driven by adaptations to osmotic stress that can change drastically during the ontogeny (Charmantier 1998, Charmantier et al. 2001). According to Anger (2003), if salinity

exceeds the tolerance range, there usually appears a stress response, characterized by reduced survival, prolongation of the developmental time, and a depression of the feeding and growth rates. Reductions in growth rates have also been correlated with the capacity to osmoregulate (Mikami & Kuballa 2007, Torres et al. 2011). In this sense, the precise knowledge of the range of salinity tolerance is necessary for both ecological and culture approaches.

Temperature is another factor with important implications for many ecological processes, including larval dispersal and mortality, population connectivity and recruitment dynamics (O'Connor et al. 2007). Temperature is known to have significant influence on survival, molting intervals and total duration of larval development (Anger 1983, Minagawa 1990, González-Ortegón & Giménez 2014). Many studies also have shown that temperature can modify the manner in which salinity can influence the survival and duration of the larval development of brachyuran species (Costlow Jr. et al. 1962, Costlow Jr. et al. 1966, Reed 1969, Baylon & Suzuki 2007, Nurdiani & Zeng 2007). Synergistic or other multiple stressors effects are likely to occur in coastal marine organisms as a consequence of natural variations in precipitation and estuarine discharge; they are currently an objective of intensive interest because variations caused by climate change and anthropogenic influence can also affect the capacity of organisms to cope with environmental stressors (González-Ortegón et al. 2013, Przeslawski et al. 2015). The larvae of *M. brachydactyla* develop in coastal waters where freshwater flux, evaporation, and thermal radiance create dynamic changes in temperature and salinity, all of which can cause multiple stressor effects; such effects are also of importance for the optimization of techniques in aquaculture.

Hence, the main objective of the present study was to determine the short and long term influence of salinity and the combined effects of temperature and salinity on larval development of *M. brachydactyla* to better understand the likely conditions for larval recruitment in the field and obtain valuable information for optimization of culture techniques.

2. Material and methods

2.1 Broodstock maintenance

The broodstock of *M. brachydactyla* was captured with commercial fishery boats in the NW Iberian Peninsula coast (Ría de A Coruña, Galicia, Spain) and transported to the Institut de Recerca i Tecnologia Agroalimentàries facilities (Sant Carles de la Ràpita, Tarragona, Spain) in December 2012. The broodstock was kept in 2000 L cylindrical tanks connected to a recirculation unit (renewal rate = 3.5 m^3 h^{-1}) maintained at controlled conditions of temperature (18 ± 1 °C), salinity (35 ± 1), photoperiod (12 h light: 12 h dark) and light intensity (25 lux, fluorescent lights). The broodstock was fed daily with a combination of fresh mussels (*Mytilus* sp. four times per week), frozen mussels (*Mytilus* sp, twice per week) and frozen crabs (*Liocarcinus depurator*, once per week).

2.2 Larval culture system

The designed larval culture system was a modification of a previous rearing system published by Anger et al. (1991) and Andrés et al. (2010) for experimental and small-scale culture of brachyuran larvae. Each experiment was carried out in 200 L aquaria (100 x 40 x 50 cm) used as incubation chambers (Fig. 1). Experimental glass beakers with 600 mL capacity were located inside each aquarium. The temperature was

maintained constant with calibrated submersible thermostat-controlled heaters (Eheim Jäger, Finsterrot, Germany) and distributed by an air lift. Daily the temperature was measured with portable meters (precision: 0.1 °C; WTW ProfiLine Oxi 3210, Weilheim, Germany). The aquaria were illuminated from above with 1000 lux LED lights; the light intensity was measured with a light meter (precision: 1 lux; Lx-101, Lutron Electronic Enterprise, Taipei, Taiwan). The photoperiod of 12 h light: 12 h dark was controlled with 24 hour programmable timers.

Low salinities were obtained by diluting filtered seawater with distilled water and higher salinities by adding sea salt (Natural Salt Mix, Oceanic™, Dallas, USA). The salinity of the experimental glass beakers was measured daily using a portable handheld salinity refractometer (precision: 1, range: 0 – 100; Shenzhen Handsome Technology Co. Ltd., Guandong, China). The glass beakers were filled with 500 mL of the test salinities according to each treatment.

The newly hatched larvae (ZI_0) were transferred by outflow pipe to special collectors (35 L fiberglass cylindro-conical baskets opened by 12 x 18 cm windows covered with 150 µm mesh). Only actively swimming zoeae of the same hatch within a maximum ca. 15 h after hatching were selected for the experiments.

Following Andrés et al. (2007; 2008), larvae were transferred to glass culture beakers at an initial density of 60 zoeae L^{-1} without prior adaptation, the experiment continued until all the larvae died or molted to megalopa. The newly molted megalopae (M_0) were transferred to new experimental glass beakers at an initial density of 20 megalopae L^{-1} and kept under the previous experimental conditions until all the animals died or reached the first juvenile instar (J_0). The confirmation of the death was carried

out using a Nikon SMZ800 stereomicroscope; the total lack of movement of appendages and the immobility of the heart were used as criteria.

The larvae were fed daily *ad libitum* with fresh *Artemia* sp. Kellogg, 1906 nauplii and metanauplii (INVE Aquaculture Nutrition, Salt Lake UT, USA). Living larvae were collected daily by carefully pipetting to reserve glass beakers previously prepared at the same temperature and salinity conditions.

2.3 Experiments

2.3.1 Acute osmotic stress tolerance. This first experiment used newly hatched zoeae in starving conditions to ascertain the range of salinity tolerance. We employed six salinity treatments ranging from 0 to 55 (0, 15, 25, 35, 45 and 55 ± 1) with four replicates per treatment. The total of living and dead specimens was counted after three days. Samples for DM and elemental body composition analysis were taken. The temperature was constant at 19.7 ± 0.2 °C.

2.3.2 Median lethal salinity in 24 h. In this second experiment newly hatched zoeae in starving conditions were used to obtain more detailed information on the range of tolerance. The upper and lower median lethal salinity (LS_{50}) were calculated through two separate experiments keeping larvae around the lower and upper range of tolerance: lower LS_{50} (15, 17, 19, 21, 23 and 25 ± 1); upper LS_{50} (51, 53, 55, 57, 59 and 61 ± 1). Three replicates per treatment were used. In both experimental sets the total of living and dead specimens were counted after 24 h. The temperature was maintained constant at 19.7 ± 0.1 °C.

2.3.3 Chronic effects of salinity on survival and growth. In this experiment we studied long term responses within the range of salinities (20 – 45) that were tolerated by the starving zoea I (six salinity treatments: 20, 25, 30, 35, 40 and 45 ± 1). The survival and developmental time were tested using four replicates per treatment; additional replicates for DM and elemental body composition analysis were used. The temperature was constant at 22 ± 1 °C. The following response variables were studied: (a) the duration of the zoeal phase, (b) the duration of the megalopa stage, (c) the survival to the megalopa stage and (d) the survival from the megalopa to the first juvenile stage. Since the differentiation between zoeae stages required the individual examination of the larvae under the stereomicroscope, we decided to focus our research in the zoeal phase to reduce the manipulation and potential damage of the larvae and increase the chances of survival until M_0 and J_0.

2.3.4 Combined effects of salinity and temperature on survival and growth. This experiment was used to understand how temperature may modulate the effect of salinity on survival and growth. The experiment used two temperature regimes: 18 and 21 ± 1 °C combined with three salinity levels: 30, 35 and 40 ± 1, giving a total of six temperature-salinity combinations. Four replicates per treatment were used. The response variables measured were as stated in the previous experiment.

2.4 Dry mass and elemental body composition

The dry mass (DM) and elemental body composition (Carbon, Hydrogen, Nitrogen; CHN) were analyzed in 2.3.1 and 2.3.3 experiments to study the acute and chronic effects of the salinity on the growth. Each treatment used 5 replicates per zoeae phase and megalopa stage. Each analysis (DM and CHN) required 5 zoeae and 3 megalopae, respectively. The zoeae were sampled as newly hatched (ZI_0) and in

intermolt (ZI_{2-3}), while the megalopae were sampled when newly molted (M_0). The larvae were gently rinsed in distilled water for 10-20 s and blotted dry on a metal sieve with filter paper. Subsequently, the larvae were transferred to pre-weighed tin capsules pressed for Elemental Microanalysis and stored at -20 °C.

Analyses of DM and CHN were carried out at the School of Ocean Sciences (Bangor University, Menai Bridge, UK) following standard techniques (D'Urban Jackson et al. 2014). Samples were freeze-dried in a vacuum drier (Edwards Super Modulyo) for 24 h and DM was determined with a Mettler Toledo MX5 microbalance (precision: 1 µg, capacity: 5.1 g). Elemental Analysis was performed using a CHNS-O Analyzer (FlashEA 1112 Series).

2.5 Statistical Analysis

The statistical treatment of the data was performed using R version 3.2.0 (R Development Core Team 2015). The median lethal salinity was calculated using a general linear model with the «dosing.p» function of the R package «MASS 7.3-4» (Venables & Ripley 2002). One way ANOVA was performed using salinity as factor. The combined effects of temperature and salinity were tested through two way Type III ANOVA applying R package «car 2.0-25» (Fox & Weisberg 2011). Comparisons between groups after finding significant differences were performed by Tukey's HSD test. Normality and homogeneity were tested by Shapiro-Wilk and Levene tests, respectively. Kruskal-Wallis test was carried out when the data did not show normality or homogeneity of variance. The critical level (α) to reject the null hypothesis was 0.05.

3. Results

3.1 Acute osmotic stress tolerance.

All larvae exposed to a salinity of 0 and 15 died in the first 24 hours. In the salinity range from 25 to 55 the survival was higher than 90 % without significant differences among treatments (Kruskal -Wallis: $X^2_3 = 2.76$, $p = 0.43$).

Salinity affected the dry mass and elemental body composition of the three day old zoeae (ANOVA: $F_{3,15} = 32.01$, $p < 0.001$). The stronger effect in decreasing dry mass was produced by the low salinity (25); while only a minor dry mass reduction was produced by the higher salinities, 45 and 55 (Table 1). Larvae reared at low and seawater salinity (35) showed higher percent carbon and nitrogen than larvae reared at extremely high salinities (C: $F_{3,14} = 200.9$, $p < 0.001$; N: $F_{3,14} = 169.9$, $p < 0.001$). The carbon content per individual also decreased at higher salinity, but the nitrogen content per individual did not vary between treatments (C: $F_{3,14} = 6.11$, $p < 0.01$; N: $F_{3,14} = 0.82$, $p = 0.51$). The C:N ratio indicated that at high and low salinity, the losses of C were proportionally larger than losses of N ($F_{3,15} = 79.19$, $p < 0.001$; Table 1).

3.2 Median lethal salinity in 24 h.

The lower LS_{50} was at 19.9, while the upper LS_{50} was at 56.0 (Fig. 2). The larvae exposed at 20 or lower salinities immediately sank passively to the bottom of the culture glass beakers; those larvae exposed at 56 or higher salinities remained swimming actively in the glass culture beakers until they died.

3.3 Chronic effects of salinity on survival and growth.

3.3.1 Survival and duration of larval development

Total mortality occurred after 24 hours at salinity 20, after five days at salinity 45 and after seven days at salinity 25, coinciding with the molt to megalopa stage (Fig. 3). The development until the megalopa stage only occurred in the salinity range from 30 to 40, but there were significant differences among treatments ($F_{2,9}$ = 16.52, $p < 0.001$). The highest survival was observed at salinity 35 (51.7 ± 11.4%), followed by salinity 30 (39.2 ± 9.6 %) and salinity 40 (11.4 ± 9.3 %; Fig. 3). The molt to zoea II occurred between the 3rd and 4th day of culture from hatching (salinity range from 25 to 45). The duration of the zoeal phase until M_0 was on average 7.1 ± 0.8 days, but significant differences among salinity treatments were not observed ($F_{2,8}$ = 0.64, p = 0.55).

The highest survival from megalopa to first juvenile occurred at salinity 35 (37.5 ± 4.8 %); and the average duration of the megalopa stage was 6.2 ± 1.1 days. High mortality rates were observed at other salinities (100 % of mortality at salinity 40; only one individual reached the juvenile stage at salinity 30 after 5 days of megalopa stage).

3.2.2 Growth and elemental body composition

Salinity had a significant effect on the larval growth and elemental body composition. Two day old zoeae showed a dry mass increment in all treatments except at salinity 25 ($F_{4,20}$= 12.12, $p < 0.001$; Table 2); the carbon and nitrogen content per individual also increased in all treatments except at 25 (C: $F_{4,20}$ 3.53, $p < 0.05$; N: $F_{4,20}$ = 3.58, $p < 0.05$). The percent carbon and nitrogen was significantly lower at salinity of 40 and 45 (C: $F_{4,20}$= 3.63, $p < 0.05$; N: $F_{4,20}$ = 4.70, $p < 0.01$). Although the C:N ratio

differed significantly among treatments ($F_{4,19} = 4.65$, $p < 0.01$), a general trend was not observed (Table 2).

Megalopa from different salinity treatments did not show significant differences in dry mass ($F_{2,11} = 0.719$, $p = 0.51$), carbon and nitrogen content per individual (C: $F_{2,11} = 2.02$, $p = 0.18$; N: $F_{2,11} = 2.51$, $p = 0.13$), percent nitrogen ($F_{2,11} = 3.05$, $p = 0.09$) or C:N ratio ($F_{2,11} = 1.16$, $p = 0.35$). Only the percent carbon showed a significant response, consisting in decreased levels at higher salinity ($F_{2,11} = 6.98$, $p < 0.05$; Table 3).

3.3 Combined effect of temperature and salinity.

3.3.1 Survival and duration of development

The two-way ANOVA showed a significant interaction between temperature and salinity on survival from hatching to the megalopa stage ($F_{2,18} = 5.26$, $p < 0.05$): survival decreased at salinity 30 and 40 with the temperature increment, but increased at salinity 35. The lowest survival occurred at the combination: salinity 40 and 18 °C (22.5 ± 22.3 %); but it doubled in the remaining temperature-salinity combinations (Fig. 4). Survival to the juvenile stage was significantly affected by salinity ($F_{2,18} = 11.54$, $p < 0.001$), but not by temperature ($F_{1,18} = 2.08$, $p = 0.16$) or the interaction of both ($F_{2,18} = 0.31$, $p = 0.73$); the highest survival occurred at salinity 35 (average 62.5 ± 21.2 %; Fig. 5). In most cases, mortality occurred at the time of metamorphosis: most individuals failed to metamorphose or metamorphosed with deformities (syndrome of molt cycle).

The duration of the zoeal phase was significantly affected by temperature ($F_{1,17} = 87.71$, $p < 0.001$), but not by salinity ($F_{2,17} = 1.06$, $p = 0.36$) or their interaction ($F_{2,17} = 0.95$, $p = 0.40$). The zoeal phase required less time at 21 °C (average 7.6 ± 0.7 days)

than at 18 °C (average 10.2 ± 1.0 days) to complete (Fig. 6).The duration of the megalopa was also affected by temperature ($F_{1,14} = 89.7$, $p < 0.001$), while salinity ($F_{2,14} = 1.62$, $p = 0.23$) and the interaction between temperature and salinity was not significant ($F_{1,14} = 2.58$, $p = 13$). The megalopa stage required less time to complete at 21 °C (average 6.0 ± 0.5 days) than at 18 °C (average 8.8 ± 1.0 days; Fig. 7).

4. Discussion

Our data showed that larvae of *M. brachydactyla* are strictly stenohaline. The acute stress restricted the salinity tolerance range from 20 to 56 and outside this range the larvae died in less than 24 hours. Larvae tolerated salinities of 25 and 45, but the growth rate was reduced and metamorphosis to megalopae did not occur. The most suitable range for development was between 30 and 40: larvae successfully metamorphosed to the first juvenile stage. Moreover, the highest survival from newly hatched zoeae to first juvenile stage was observed at salinity 35 ± 1. The duration of larval development was not affected by salinity. On the other hand, the highest temperature showed the shorter duration of the larval development (21 °C). In general terms, the larval culture of this species required a constant salinity at 35 ± 1. Contrary to other brachyuran species of interest for culture such as *Scylla serrata* (Nurdiani & Zeng 2007), the larval stages of *M. brachydactyla* were not tolerant to salinity levels below 30. These restrictions must be taken into account in the selection of sites or water sources for the culture of this species.

Previous studies which have focused on the osmoregulatory physiology of the majid crabs showed that generally they are osmoconformers or weak regulators with high sensitivity to variations in salinity (Dakin 1912, Drilhon 1935, Péqueux 1995). The vulnerability of *M. brachydactyla* to low salinity is also reflected in the decrement of

larvae production by adults (Rotllant et al. 2014) and a narrow range of acute salinity tolerance (LS_{50} in 24 h) in newly hatched zoeae (salinity range from 20 to 56). A similar LS_{50} range was observed in the larvae of other brachyurans such as the cancroid *Cancer irroratus* (salinity range from 15 to 46: Charmantier & Charmantier-Daures 1991) or the majoid *Chionoecetes opilio* (salinity range from 9.5 to 42.5: Charmantier & Charmantier-Daures 1995). Other brachyuran larvae have a broader salinity tolerance range: e.g. the grapsoid *Armases miersii* and the xanthoid *Rhithropanopeus harrisii* can complete the larval development in a salinity range from 5 to 35 (Anger 1996; Forward Jr. 2009), while the first zoeae of *Armases ricordi* tolerate a salinity range from 5 to 55 during six days (Diesel & Schuh 1998). These differences in the salinity tolerance range correspond to adaptations to fluctuations in the salinity in the field (Anger 2001). Larvae with a narrow salinity tolerance inhabit waters with oceanic influence (Bigford 1979, Charmantier & Charmantier-Daures 1995) while those with broader salinity tolerance usually inhabit environments with high salinity fluctuations, such as rocky pools or estuaries (Costlow Jr. et al. 1966, Anger 1995, Forward Jr. 2009). The Table 4 summarizes the relationship between the range of salinity tolerance of brachyuran larvae and their habitat. In some taxa there are specializations to some environments (e.g. estuarine environments in Grapsoidea and Portunoidea and nearshore/offshore in Majoidea); but exceptions are associated with habitat specialization (e.g. *Pachygrapsus transversus* in grapsoid or *Halicarcinus rostratus* in majoid crabs, see Table 4). Thus, we can hypothesize that the larval tolerance to salinity is more influenced by adaptations to field conditions than by the phylogeny.

The optimal salinity for the larval development of *M. brachydactyla* is 35 ± 1, coincides with the expected conditions for development in the field: the outer coast of Galicia (NW Iberian Peninsula) shows a constant salinity of ca. 35, whereas in the inner coast the salinity fluctuates between the 30 in winter and the 35 in summer due to estuarine influence (Cabanas et al. 1987, Corgos et al. 2011, Gago et al. 2011). Exposure of larvae to this estuarine influence cannot be discarded, since the zoeae are released in nearshore areas (Corgos et al. 2011) and they will be distributed by the marine currents as occurs with other brachyuran larvae (Peliz et al. 2007). From the standpoint of salinity, moderate to high survival would be expected since zoeae reached the megalopa stage at 30. Survival might be also maximized as a consequence of the time of release (spring and summer: Corgos et al. 2011), when the when fluctuations in salinity are reduced and the average salinity is nearest to the optimal range for this species (Gago et al. 2011).

When the larvae of *M. brachydactyla* were exposed to very low salinities (near or under the LS_{50}), their immediate reaction was immobilization and dropping to the bottom of the glass culture beakers as observed in other brachyurans (Anger 1985; Kannupandi et al. 2000; Baylon & Suzuki 2007). Anger (1985) suggested that this behavior would enable larvae to reach the lower waters layers, where salinity is higher. This strategy may be useful for *M. brachydactyla* larvae, since in the Galician coast the salinity increases with depth until reaching a maximum of 35.5 (Gago et al. 2011).

The likely salinity conditions at the settlement habitat are still unknown, but our experiments suggest that megalopa would not settle in very shallow habitats, characterized by low or variable salinity. Le Foll (1993) found that juveniles (carapace length > 50 mm) of *M. brachydactyla* (referred as *M. squinado*) inhabit sand, mud-sand,

gravel, rock and maërl seafloors, mainly at 15 meters depth; however, the habitat of younger juveniles was not found. Corgos et al. (2011) suggested that the recruitment may occur in more shallow habitats (< 5 meters depth). The same authors also noticed that both juveniles and adults inhabit seafloors with constant salinity around 35, in the range of optimal salinity as shown in the present study. Hence, we propose three possible hypotheses: (1) the megalopae avoid the estuarine influenced waters and their settlement occurs in coastal waters with oceanic characteristics; (2) since the settlement occurs during late spring and summer, the metamorphosis to first juvenile can take place in coastal waters with minimal estuarine influence (i.e. coinciding with a period when the drop in salinity is minimal); (3) the megalopae might tolerate short exposure to low salinity and they migrate shortly after metamorphosis into estuarine influenced coastal areas. To evaluate these hypotheses, the settlement habitat of *M. brachydactyla* in the field must be determined.

The temperature mainly influences the duration of the larval development of *M. brachydactyla*: the duration was significantly shorter at higher temperatures (21 vs 18 °C). Temperature increases the metabolic processes, accelerates the molting cycle and reduces the duration of larval development of brachyurans (Costlow et al. 1960, Costlow Jr. et al. 1966, Ong & Costlow 1970, Minagawa 1990, Anger 1991, Mene et al. 1991, Nagaraj 1992, Lárez et al. 2000, Anger 2001, Baylon & Suzuki 2007, Nurdiani & Zeng 2007, Spivak & Cuesta 2009, Hernández et al. 2012). Low salinities increased the duration of the larval development in some brachyuran species (Anger 1985, Mene et al. 1991, Minagawa 1992, Nagaraj 1992), however, we did not observe this phenomenon in *M. brachydactyla* larvae. Beside the cited studies, the salinity evokes comparatively weak effects over the duration of decapods as reviewed by Anger (2003).

The dry mass and elemental body composition of the zoeae of *M. brachydactyla* varied with the salinity. The larvae maintained at salinity 25 in starving conditions showed higher DM losses than the larvae maintained at salinity 35 although both groups maintained similar carbon levels. Since the carbon content is a reliable expression of the biomass content in the individuals (Anger & Dawirs 1982, Anger et al. 2000, Anger 2003), we can consider that the higher dry mass losses at salinity 25 could be explained by mineral losses. The larvae of another majoid, *Hyas araneus*, show important mineral depletion under low salinities, probably due to the depression in the mineral accumulation rate and the osmotic loss of mineral content (Anger 2003). In this sense, the higher dry mass and lower carbon and nitrogen percentages observed in the larvae maintained at salinity 45 and 55 could be explained by a mineral accumulation. On the contrary, well fed two day old larvae increased their dry mass in all the salinity treatments except at salinity 25, although similar values of percentage carbon and nitrogen were observed. Short exposures (ca. 50 % molt cycle) to low salinities may also cause reduction of dry mass, lipid and/or protein content in marine brachyuran larvae such as *Cancer pagurus* (Torres et al. 2002) or *Hyas araneus* (Anger 2003, Torres et al. 2011). Similar results were also reported in astacideans larvae such as *Homarus gammarus* and *Nephrops norvegicus* (Torres et al. 2002, Torres et al. 2011). A reduction of feeding (Minagawa 1992), and food conversion (Anger 2003, Torres et al. 2011) has been proposed as an explanation for the reduction in growth at low salinity.

The C:N ratio has been widely applied as an indicator of the lipid:protein ratio in the decapod larvae (Anger & Dawirs 1981, Anger & Dawirs 1982, Anger & Harms 1990, Anger et al. 1998, D'Urban Jackson et al. 2014), including *M. brachydactyla* (Andrés et al. 2008). Anger and Dawirs (1982) indicated that changes in the C:N ratio

indicate shifts in the relative amounts of lipids (plus carbohydrates) and proteins (plus free amino acids); and a decrease in the C:N ratio can be interpreted as a degradation in lipid contents and/or a protein accumulation. In starved zoeae the lowest C:N ratio occurred at salinity 55, intermediate values were observed at salinity 25 and 45. The reduction of the C:N ratio under unfavorable salinity conditions could be related with a degradation of the lipids due to extra energetic requirements. When larvae were fed, the C:N ratio did not show significant differences among the salinity concentrations tested.

In conclusion, the larvae of *M. brachydactyla* are stenohaline with a rather narrow range of salinities where complete larval development is achieved. Such narrow limits should restrict the timing and sites of larval settlement, duration of the period of metamorphosis in coastal areas, and the water sources useful for their culture. Extreme salinities (low or high), influence the dry mass and the elemental body composition of the developing larvae, while the temperature can interact with salinity to influence the survival during the zoeal phase.

5. Acknowledgements

The Spanish Ministry of Economy and Competitiveness funded bench fees through the INIA project (RTA2011-00004-00-00) to G.G. and a predoctoral fellowship to D.C. (FPI-INIA). The authors would like to thank Carles Alcaraz for his advice on the data analysis and Karl B. Andree for his improvement of the article. We thank hatchery technicians at IRTA in Sant Carles de la Ràpita (David Carmona, Glòria Macià, Magda Monllaó and Francesc X. Ingla) for the broodstock maintenance and the setup of the rearing culture system.

Table 1. Acute effects of salinity on growth under starving conditions in *Maja brachydactyla* zoeae I from ca. 15 hours after hatch (0 days) and in intermoult (3 days from hatch). Dry mass (DM, µg), carbon content (µg ind^{-1}), carbon percentage (%), nitrogen content (µg ind^{-1}), nitrogen percentage (%) and C:N ratio. Larvae were kept at constant 19.7 ± 0.2 °C. Values are expresed as average ± SD.

Age (days)	Salinity	DM (µg)	Carbon (µg ind^{-1})	Carbon (%)	Nitrogen (µg ind^{-1})	Nitrogen (%)	C:N ratio
0	-	104 ± 1	35.7 ± 0.3	34.4 ± 0.1	9.20 ± 0.05	8.85 ± 0.08	3.89 ± 0.03
3	25	91 ± 1^{a}	28.3 ± 0.3^{a}	31.3 ± 0.2^{a}	7.37 ± 0.10	8.14 ± 0.04^{a}	3.84 ± 0.02^{ab}
	35	93 ± 1^{b}	28.2 ± 0.4^{a}	30.2 ± 0.2^{b}	7.28 ± 0.12	7.80 ± 0.05^{b}	3.87 ± 0.01^{a}
	45	96 ± 2^{c}	28.0 ± 0.2^{ab}	29.2 ± 0.3^{c}	7.32 ± 0.05	7.64 ± 0.04^{c}	3.82 ± 0.01^{b}
	55	97 ± 1^{c}	27.4 ± 0.4^{b}	28.2 ± 0.1^{d}	7.34 ± 0.09	7.56 ± 0.01^{c}	3.73 ± 0.02^{c}

Different letters indicate significant difference ($P < 0.05$) among the treatments.

Table 2. Acute effects of salinity on growth under feeding conditions in *Maja brachydactyla* zoeae I from ca. 15 hours after hatch (0 days) and in intermoult (2 days from hatch). Dry mass (DM, µg), carbon content (µg ind^{-1}), carbon percentage (%), nitrogen content (µg ind^{-1}), nitrogen percentage (%) and C:N ratio. Larvae were kept at constant 22 ± 1 °C. Values are expresed as average ± SD.

Age (days)	Salinity	DM (µg)	Carbon (µg ind^{-1})	Carbon (%)	Nitrogen (µg ind^{-1})	Nitrogen (%)	C:N ratio
0	-	95 ± 1	30.6 ± 0.4	32.2 ± 0.3	8.01 ± 0.13	8.45 ± 0.10	3.82 ± 0.02
2	25	98 ± 3^{a}	32.1 ± 1.0^{a}	32.7 ± 0.4^{ab}	8.30 ± 0.26^{a}	8.45 ± 0.11^{ab}	3.87 ± 0.02^{ab}
	30	110 ± 4^{b}	36.5 ± 1.6^{ab}	33.2 ± 0.4^{a}	9.33 ± 0.41^{ab}	8.48 ± 0.09^{b}	3.91 ± 0.01^{a}
	35	110 ± 5^{b}	35.2 ± 2.5^{ab}	32.0 ± 0.7^{ab}	9.06 ± 0.56^{ab}	8.26 ± 0.15^{bc}	3.86 ± 0.02^{b}
	40	113 ± 2^{b}	35.6 ± 3.1^{ab}	31.5 ± 1.5^{b}	9.11 ± 0.73^{ab}	8.05 ± 0.32^{c}	3.91 ± 0.03^{a}
	45	118 ± 1^{b}	37.3 ± 2.9^{b}	31.5 ± 1.0^{b}	9.56 ± 0.70^{b}	8.08 ± 0.25^{ac}	3.90 ± 0.03^{ab}

Different letters indicate significant difference ($P < 0.05$) among the treatments.

Table 3. Chronic effects of salinity on growth under feeding conditions in *Maja brachydactyla* megalopae from ca. 15 hours after molt. Dry mass (DM, µg), carbon content (µg ind^{-1}), carbon percentage (%), nitrogen content (µg ind^{-1}), nitrogen percentage (%) and C:N ratio. Larvae were kept at constant 22 ± 1 °C. Values are expresed as average ± SD.

Salinity	DM (µg)	Carbon (µg ind^{-1})	Carbon (%)	Nitrogen (µg ind^{-1})	Nitrogen (%)	C:N ratio
30	168 ± 12	57.8 ± 4.4	34.3 ± 0.8^{a}	14.9 ± 1.0	8.82 ± 0.18	3.89 ± 0.07
35	171 ± 28	57.2 ± 10.1	33.4 ± 1.2^{ab}	15.0 ± 2.2	8.78 ± 0.36	3.81 ± 0.13
40	158 ± 8	50.9 ± 2.2	32.1 ± 0.8^{b}	13.3 ± 0.5	8.40 ± 0.34	3.83 ± 0.06

Different letters indicate significant difference ($P < 0.05$) among the treatments.

Table 4. Salinity tolerance in the larvae of the brachyuran clade. Saline range suitable for the larval development from newly hatched zoeae to first juvenile stage. The habitat of the larvae also was included.

Species	Family Superfamily	Saline range	Habitat	**References:**
Cardisoma armatum Herklots, 1851	Gecarcinidae Grapsoidea	15 to 35	Nearshore[M] Estuaries	(Cuesta & Anger 2005)
Cardisoma guanhumi Latreille, 1828	Gecarcinidae Grapsoidea	20 to 40	Nearshore[M] Estuaries	(Costlow & Bookhout 1968)
Aratus pisonii (H. Milne Edwards, 1837)	Grapsidae Grapsoidea	25 to 35*[a]	Nearshore[?M] Estuaries[?]	(Díaz & Bevilacqua 1986)
Pachygrapsus gracilis (Saussure, 1858)	Grapsidae Grapsoidea	28 to 34*[a]	Nearshore[?] Offshore[?]	(Brossi-Garcia & Rodrigues 1993)
Pachygrapsus transversus (Gibbes, 1850)	Grapsidae Grapsoidea	> 32 to 35*[a]	Nearshore[?] Offshore[?]	(Brossi-Garcia & Rodrigues 1997)
Armases (=*Sesarma*) *miersii* (Rathbun, 1897)	Sesarmidae Grapsoidea	15 to 45	Rocky pools	(Anger et al. 2000) (Schuh & Diesel 1995)
Armases ricordi (H. Milne Edwards, 1853)	Sesarmidae Grapsoidea	25 to 40	Nearshore[?M] Offshore[?M]	(Diesel & Schuh 1998)
Armases roberti (H. Milne Edwards, 1853)	Sesarmidae Grapsoidea	20 to 40	Nearshore[?M] Estuaries[?]	(Diesel & Schuh 1998)
Armases (=*Metasesarma*) *rubripes* (Rathbun, 1897)	Sesarmidae Grapsoidea	> 20 to 30*[a]	Nearshore[?M] Offshore[?M]	(Luppi et al. 2003)
Selatium (=*Sesarma*) *brockii* (De Man, 1887)	Sesarmidae Grapsosidea	> 20 to 30	Mangroves[?]	(Kannupandi et al. 2000)
Sesarma cinereum (Bosc, 1802)	Sesarmidae Grapsoidea	20 to 27	Nearshore[?M]	(Costlow et al. 1960) (Seiple & Salmon 1987)
Sesarma curacaoense De Man, 1982	Sesarmidae Grapsoidea	15 to 32	Rocky pools Mangroves	(Anger & Charmantier 2000) (Diesel & Schuh 1998)
Acmaeopleura parvula Stimpson, 1858	Varunidae Graposidea	> 27 to 34*[ab]	Nearshore Offshore	(Kim & Jang 1987)
Eriocheir sinensis H. Milne Edwards, 1853	Varunidae Grapsoidea	15 to 32[a]	Nearshore[M] Estuaries	(Anger 1991)
Neohelice (=*Chasmagnathus*) *granulata* (Dana, 1851)	Varunidae Grapsoidea	15 to 32*[a]	Nearshore[M] Estuaries	(Anger et al. 2008) (Charmantier et al. 2002)

Table 4 (continuation). Salinity tolerance in the larvae of the brachyuran clade. Saline range suitable for the larval development from newly hatched zoeae to first juvenile stage. The habitat of the larvae also was included.

Species	Family Superfamily	Saline range	Habitat	**References:**
Pseudohelice subquadrata (Dana, 1851) (referred as *Helice leachi*)	Varunidae Grapsoidea	15 to 25	Mangroves[?]	(Mia & Shokita 2002)
Uca rapax (S. I. Smith, 1870)	Ocypodidae Ocypodoidea	25 to 35*[a]	Nearshore[?M] Offshore[?M]	(Simith et al. 2014)
Uca subcylindrica (Stimpson, 1859)	Ocypodidae Ocypodoidea	0.08 to 45	Rainfall puddles	(Rabalais & Cameron 1985)
Uca tangeri (Eydoux 1835)	Ocypodidae Ocypodoidea	24 to 32*[a]	Nearshore[?M] Offshore[?M]	(Spivak & Cuesta 2009)
Uca vocator (J. F. W. Herbst, 1804)	Ocypodidae Ocypodoidea	10 to 30*[a]	Nearshore[?M] Offshore[?M]	(Simith et al. 2012)
Menippe mercenaria Say, 1818	Menippidae Xanthoidea	20 to 40[a]	Nearshore	(Ong & Costlow 1970)
Eurytium limosum (Say, 1818)	Panopeidae Xanthoidea	20 to 32[a]	Estuaries[?]	(Messerknecht et al. 1991)
Panopeus herbstii H. Milne-Edwards, 1834	Panopeidae Xanthoidea	20 to 31	Estuaries	(Costlow Jr. et al. 1962) (Dittel R. & Epifanio 1982)
Rhithropanopeus harrisii (Gould, 1841)	Panopeidae Xanthoidea	2.5 to 40	Estuaries	(Forward Jr. 2009)
Acheloüs (=Portunus) spinicarpus Stimpson, 1871	Portunidae Portunoidea	30 to 40	Nearshore Offshore	(Bookhout & Costlow Jr. 1974) (Brandão et al. 2015)
Callinectes sapidus (Rathbun, 1896)	Portunidae Portunoidea	20 to 31	Nearshore[M] Estuaries	(Costlow & Bookhout 1959) (Epifanio 1995)
Carcinus maenas (Linnaeus, 1758)	Portunidae Portunoidea	20 to 35*[ab]	Nearshore[M] Estuaries	(Nagaraj 1993)
Charybdis feriata (Linnaeus, 1758)	Portunidae Portunoidea	25 to 35	Nearshore Estuaries	(Baylon & Suzuki 2007) (Fowler et al. 2011)
Necora puber (Linnaeus, 1767)	Portunidae Portunoidea	30 to 35	Nearshore Offshore	(Choy 1991) (Mene et al. 1991) (Nagaraj 1992)
Scylla serrata (Forskål, 1775)	Portunidae Portunoidea	20 to 30	Nearshore Offshore	(Dan & Hamasaki 2011)
Cancer irroratus Say, 1817	Cancridae Cancroidea	25 to 35[a]	Nearshore Offshore	(Sastry 1970) (Bigford 1979)

Table 4 (continuation). Salinity tolerance in the larvae of the brachyuran clade. Saline range suitable for the larval development from newly hatched zoeae to first juvenile stage. The habitat of the larvae also was included.

Species	Family Superfamily	Saline range	Habitat	**References:**
Metacarcinus (=*Cancer*) *magister* (Dana, 1852)	Cancridae Cancroidea	20 to 30*[a]	Nearshore Offshore	(Reed 1969)
Halicarcinus rostratus (Haswell, 1882) (referred as *H. australis*)	Hymenosoma -tidae Majoidea	6.4 to 19.3[a]	Estuaries	(Lucas & Hodgkin 1970)
Hymenosoma orbiculare Desmarest, 1823	Hymenosoma -tidae Majoidea	21 to 42 ‰	Estuaries Nearshore	(Papadopoulos et al. 2006)
Stenorhynchus seticornis (Herbst. 1788)	Inachiae Majoidea	30 to 40[ab]	Nearshore[?] Offshore[?]	(Hernández et al. 2012)
Mithrax caribbaeus Rathbun, 1920	Mithracidae Majoidea	32 to 38[ab]	Nearshore Offshore	(Lárez et al. 2000)
Mithrax pleuracanthus Stimpson, 1871	Mithracidae Majoidea	30 to 35[a]	Nearshore Offshore	(Goy et al. 1981)
Mithrax verrucosus H. Milne-Edwards, 1832	Mithracidae Majoidea	25 to 35	Nearshore Offshore	(Rengel de Zambrano et al. 1993)
Chionoectes opilio (O. Fabricius, 1788)	Oregoniidae Majoidea	24 to 38[a]	Nearshore Offshore	(Yamamoto et al. 2015)
Hyas araneus (Linnaeus, 1758)	Oregoniidae Majoidea	25 to 35[a]	Nearshore Offshore	(Anger 1985)
Libinia emarginata Leach, 1815	Pisidae Majoidea	~30 ‰[a]	Nearshore Offshore	(Johns & Lang 1977)
Maja brachydactyla Balss, 1922	Majidae Majoidea	30 to 40	Nearshore[?] Offshore[?]	Present study

(*) The data only comprises the saline range suitable for the larval development from newly hatched zoeae to the megalopa stage. (a) Salinity higher than the highest suitable salinity was not tested. (b) Salinity lower than the lowest suitable salinity was not tested. (?) The habitat of the larvae is extrapolated from experimental data, confirmation with field data is required. (M) The larvae migrate from the hatching habitat (estuaries, mangroves, rivers or brackish waters) to nearshore and/or offshore waters, i.e. 'export strategy' (see Charmantier, Giménez et al. 2002).

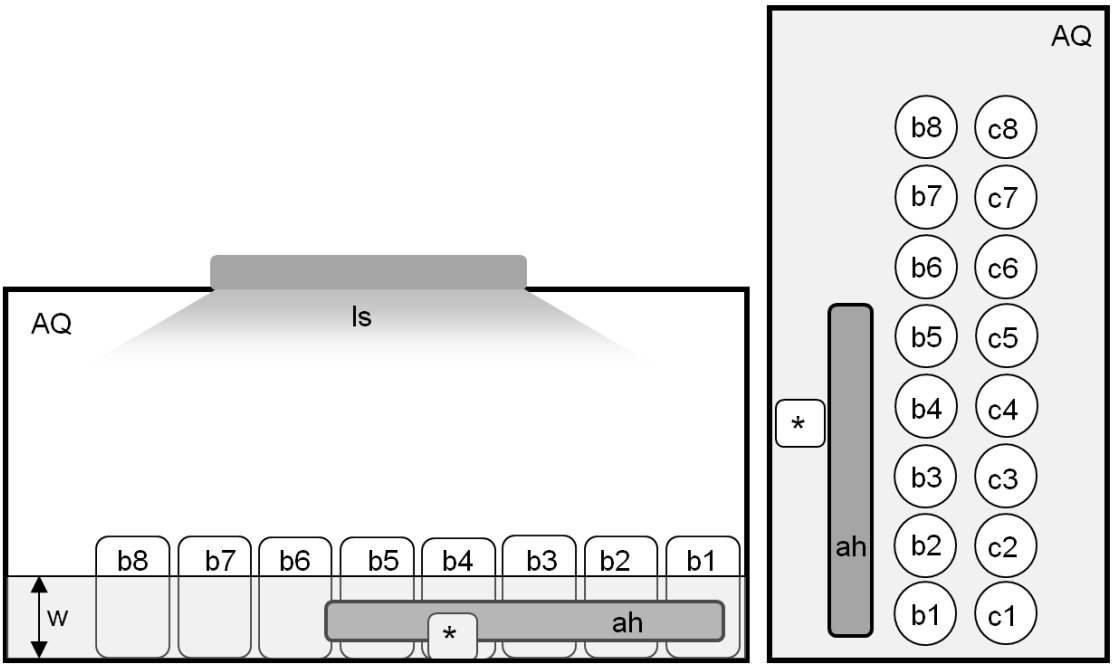

Figure 1. Experimental small-scale rearing system for *M. brachydactyla* larvae. Lateral view (left); upper view (right). Nomenclature: (AQ), 200 L aquarium (100 x 40 x 50 cm); (ah), submersible thermosthat-controlled heater; (b1 to b8), experimental glass beakers with larvae; (c1 to c8), reserve experimental vessels (without larvae, filled with clean filtered seawater); (ls), light source: LED lights; (w), water bath; (*) air lift.

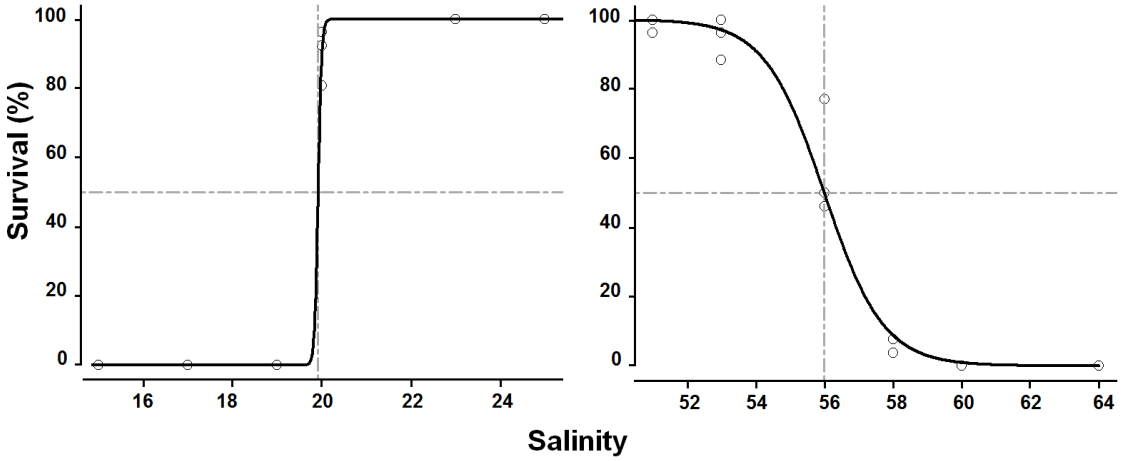

Figure 2. Median Lethal Salinity in *Maja brachydactyla*. Lower (left) and upper (right) median lethal salinity in newly hatched zoeae maintained during 24 hours in starvation at 19.7 °C.

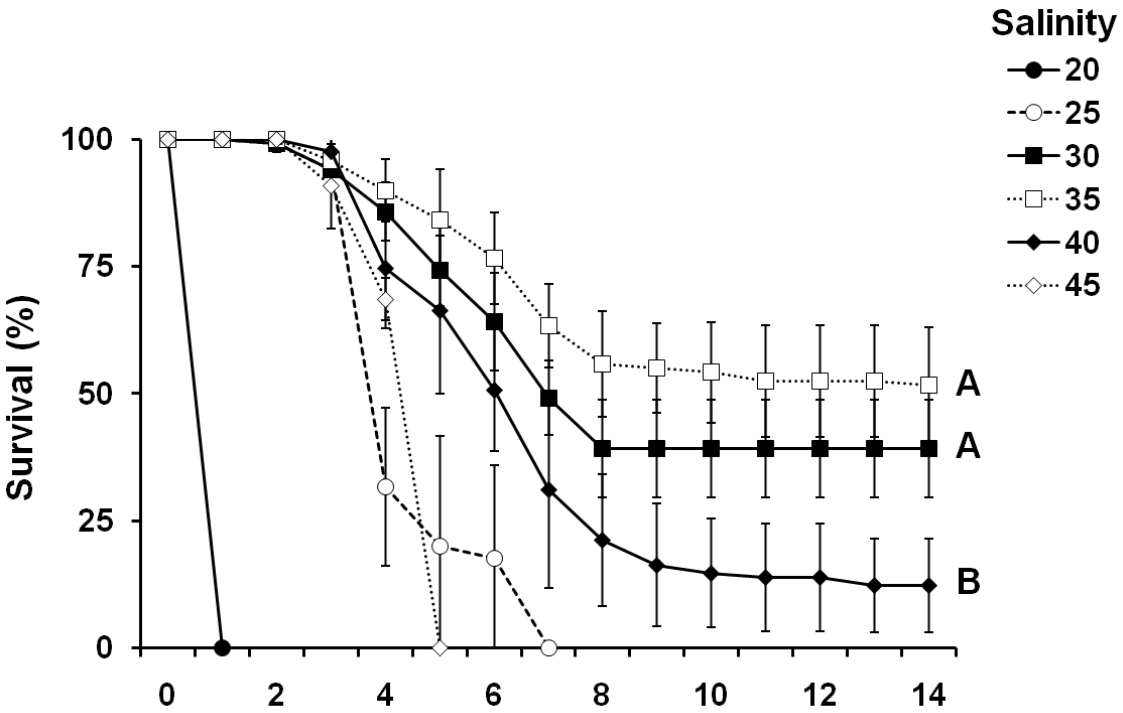

Figure 3. Chronic effect of the salinity on the survival to megalopa stage in *Maja brachydactyla*. Average survival (± SD) of the larvae from hatching to the megalopa stage at different salinity treatments at 22 °C (n = 4 per treatment). Different letters indicate significant differences among the treatments ($P < 0.05$) at the end of the experiment.

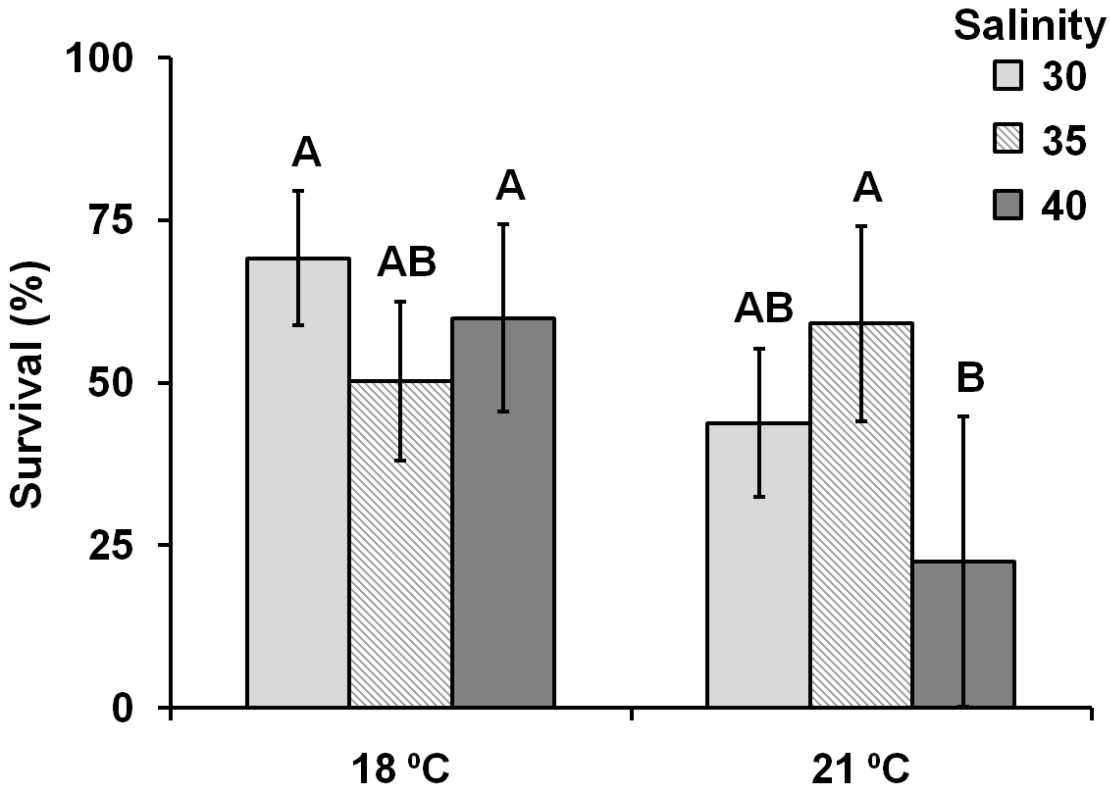

Figure 4. Combined effect of the temperature and salinity on the survival to megalopa stage in *Maja brachydactyla*. Average survival (± SD) of the larvae from hatching to the megalopa stage at different temperature (18 and 21 °C) and salinity (30, 35 and 40) combinations (n = 4 per temperature-salinity combination). Different letters indicate significant differences among the treatments ($P < 0.05$).

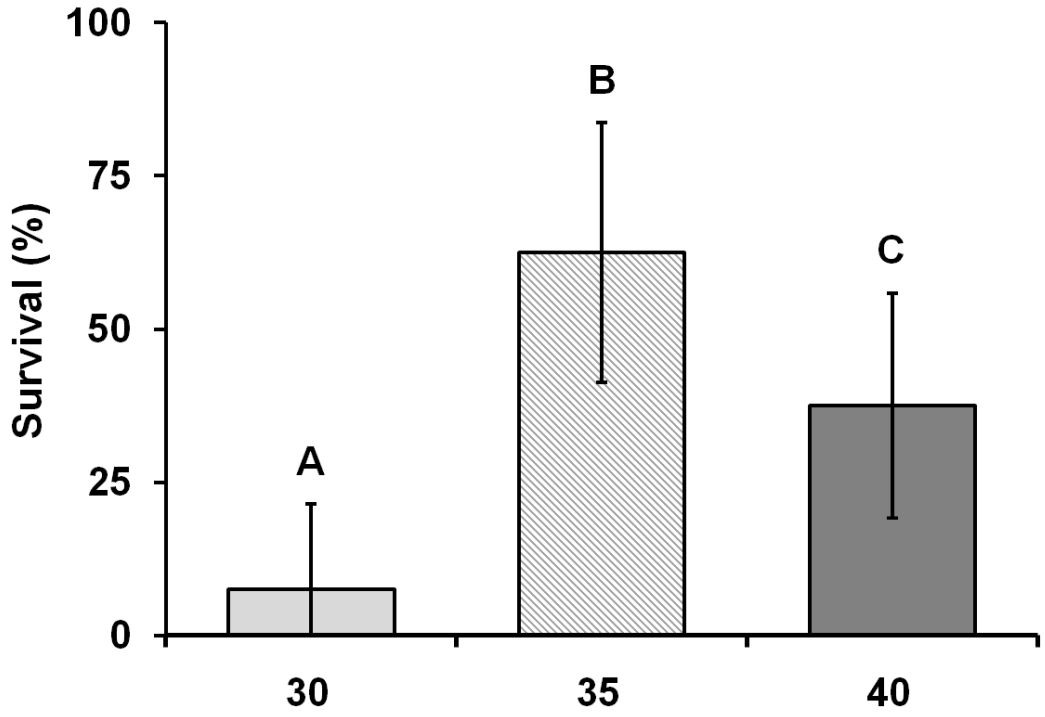

Figure 5. Combined effect of the temperature and salinity on the survival to juvenile stage in *Maja brachydactyla*. Average survival (± SD) of the larvae from megalopa to the juvenile stage at different salinity (30, 35, and 40) treatments (n = 8 per treatment). Different letters indicate significant differences among the treatments ($P < 0.05$).

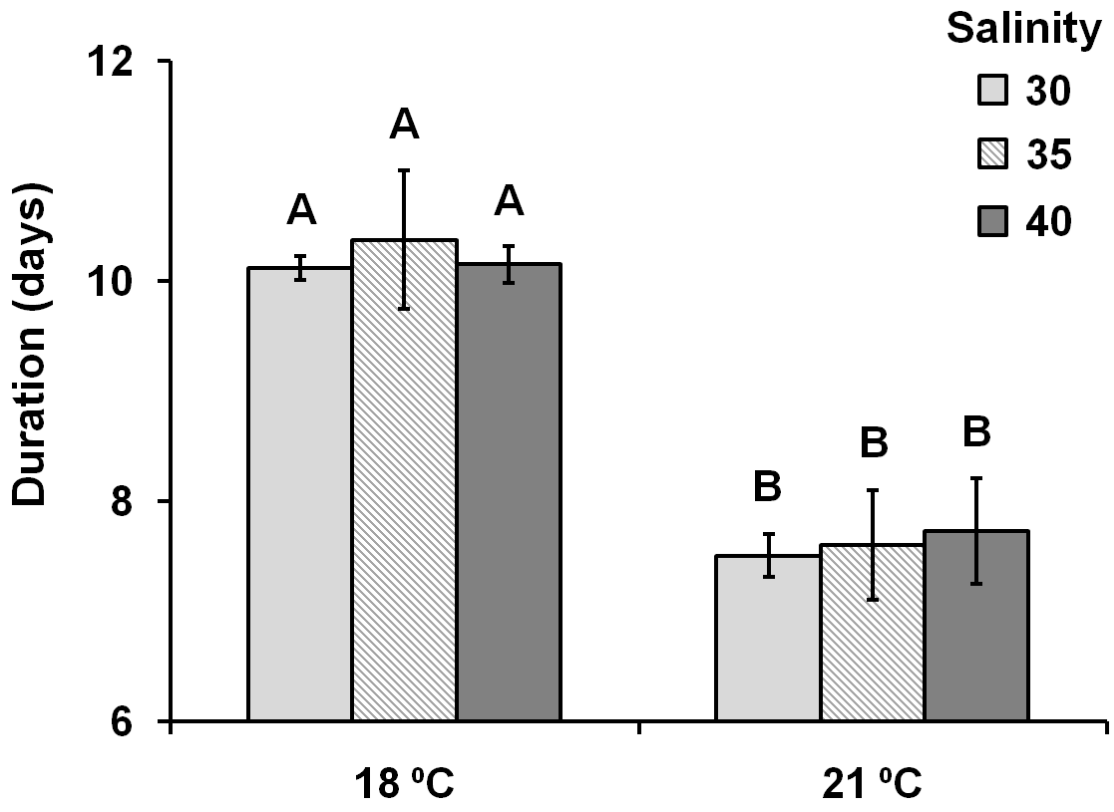

Figure 6. Effect of the temperature and salinity on the duration of the zoeal phase in *Maja brachydactyla*. Average developmental time (± SD) of the larvae from hatching to the megalopa stage at different temperature (18 and 21 °C) and salinity (30, 35 and 40) combinations (n = 4 per temperature-salinity combination). Different letters indicate significant differences among the treatments ($P < 0.05$).

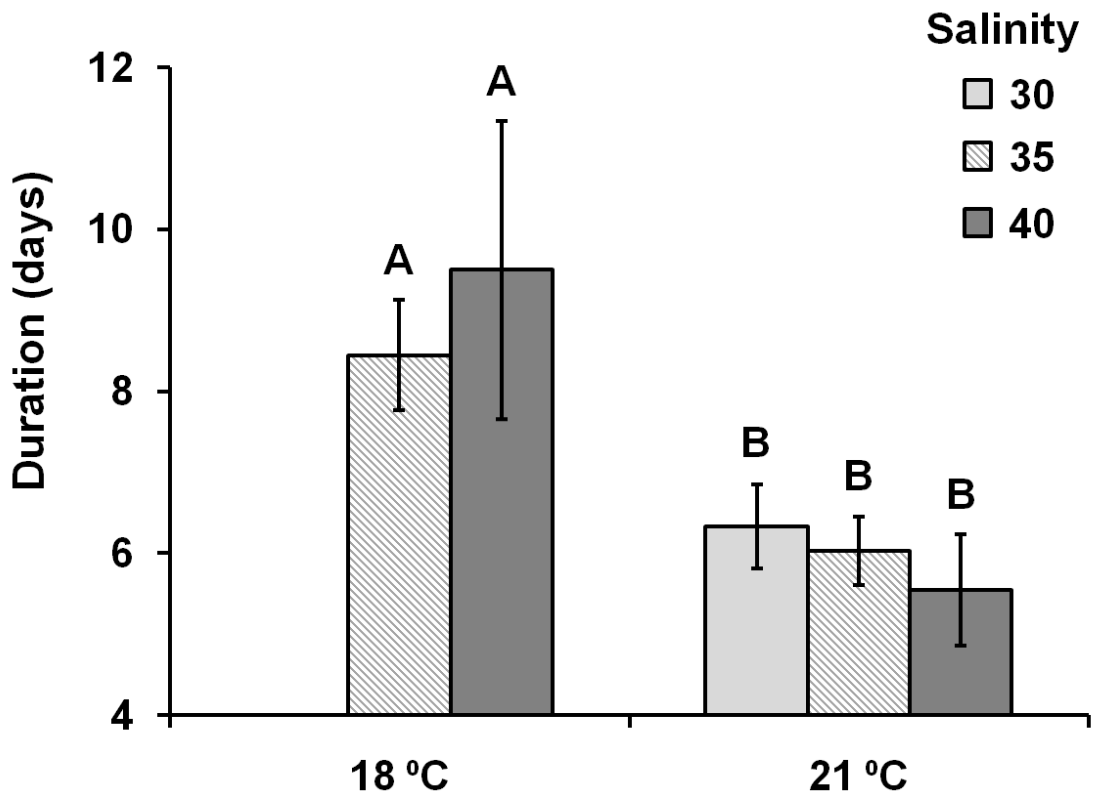

Figure 7. Combined effect of the temperature and salinity on the duration of the megalopa stage in *Maja brachydactyla*. Average developmental time (± SD) of the larvae from the megalopa to the juvenile stage at different temperature (18 and 21 °C) and salinity (30, 35 and 40) combinations (n = 4 per temperature-salinity combination). Different letters indicate significant differences among the treatments ($P < 0.05$).

6. References.

Abelló, P., J. E. García Raso, G. Guerao & F. Salmerón. 2014. *Maja brachydactyla* (Brachyura: Majidae) in the Western Mediterranean. Marine Biodiversity Records 7.

Andrés, M., A. Estévez & G. Rotllant. 2007. Growth, survival and biochemical composition of spider crab *Maja brachydactyla* (Balss, 1922) (Decapoda: Majidae) larvae reared under different stocking densities, prey:larva ratios and diets. Aquaculture 273:494-502.

Andrés, M., A. Estévez, K. Anger & G. Rotllant. 2008. Developmental patterns of larval growth in the edible spider crab, *Maja brachydactyla* (Decapoda: Majidae). J. Exp. Mar. Biol. Ecol. 357:35-40.

Andrés, M., A. Estévez, F. Hontoria & G. Rotllant. 2010. Differential utilization of biochemical components during larval development of the spider crab *Maja brachydactyla* (Decapoda: Majidae). Marine Biology 157:2329-2340.

Andrés, M., G. Rotllant & C. Zeng. 2010. Survival, development and growth of larvae of the blue swimmer crab, *Portunus pelagicus*, cultured under different photoperiod conditions. Aquaculture 300:218-222.

Anger, K. 1983. Temperature and the larval development of *Hyas araneus* L. (Decapoda: Majidae); extrapolation of laboratory data to field conditions. J. Exp. Mar. Biol. Ecol. 69:203-215.

Anger, K. 1985. Influence of salinity on larval development of the spider crab, *Hyas araneus*, reared in the laboratory. In: J. S. Gray & M. E. Christiansen, editors. Marine biology of polar regions and effects of stress on marine organisms. Chichester John Wiley & Sons. pp. 463–474.

Anger, K. 1991. Effects of temperature and salinity on the larval development of the chinese mitten crab *Eriocheir sinensis* (Decapoda: Grapsidae). Mar. Ecol. Prog. Ser. 72:103-110.

Anger, K. 1995. Developmental biology of *Armases miersii* (Grapsidae), a crab breeding in supratidal rock pools. I. Facultative lecithotrophy of larval stages. Marine Ecology Progress Series 117:75-81.

Anger, K. 1996. Salinity tolerance of the larvae and first juveniles of a semiterrestrial grapsid crab, *Armases miersii* (Rathbun). Journal of Marine Biology and Ecology 202:205-223.

Anger, K. 2001. The biology of decapod crustacean larvae. Rotterdam, A.A. Balkema Publishers.

Anger, K. 2003. Salinity as a key parameter in the larval biology of decapod crustaceans. Invertebrate Reproduction & Development 43:29-45.

Anger, K. & G. Charmantier. 2000. Ontogeny of osmoregulation and salinity tolerance in a mangrove crab, *Sesarma curacaoense* (Decapoda: Grapsidae). J. Exp. Mar. Biol. Ecol. 251:265-274.

Anger, K. & R. R. Dawirs. 1981. Influence of starvation on the larval development of *Hyas araneus* (Decapoda, Majidae). Helgoländer Meeresuntersuchungen 34:287-311.

Anger, K. & R. R. Dawirs. 1982. Elemental composition (C, N, H) and energy in growing and starving larvae of *Hyas araneus* (Decapoda, Majidae). Fishery Bulletin 80:419-433.

Anger, K. & J. Harms. 1990. Elemental (CHN) and proximate biochemical composition of decapod crustacean larvae. Comparative Biochemistry and Physiology Part B: Comparative Biochemistry 97B:69-80.

Anger, K., K. Riesebeck & C. Püschel. 2000. Effects of salinity on larval and early juvenile growth of an extremely euryhaline crab species, *Armases miersii* (Decapoda: Grapsidae). Hydrobiologia 426:161-168.

Anger, K., E. Spivak & T. Luppi. 1998. Effects of reduced salinities on development and bioenergetics of early larval shore crab, *Carcinus maenas*. J. Exp. Mar. Biol. Ecol. 220:287-304.

Anger, K., E. Spivak, T. Luppi, C. Bas & D. Ismael. 2008. Larval salinity tolerance of the South American salt-marsh crab, *Neohelice* (*Chasmagnathus*) *granulata*: physiological constraints to estuarine retention, export and reimmigration. Helgoland Marine Research 62:93-102.

Baylon, J. & H. Suzuki. 2007. Effects of changes in salinity and temperature on survival and development of larvae and juveniles of the crucifix crab *Charybdis feriatus* (Crustacea:Decapoda:Portunidae). Aquaculture 269:390-401.

Bigford, T. E. 1979. Ontogeny of light and gravity responses in rock crab larvae (*Cancer irroratus*). Marine Biology 52:69-76.

Bookhout, C. G., J. D. Costlow Jr. 1974. Larval development of *Portunus spinicarpus* reared in the laboratory. Bulletin of Marine Science 24:20-51.

Brandão, M. C., C. A. E. Garcia & A. S. Freire. 2015. Large-scale spatial variability of decapod and stomatopod larvae along the South Brazil Shelf. Continental Shelf Research 107:11-23.

Brossi-Garcia, A. L. & M. D. Rodrigues 1993. Zoeal morphology of *Pachygrapsus gracilis* (Saussure, 1858) (Decapoda, Grapsidae) reared in the laboratory. Invertebrate Reproduction & Development 24:197-205.

Brossi-Garcia, A. L. & M. D. Rodrigues. 1997. Zoeal morphology of *Pachygrapsus transversus* (Gibbes) (Decapoda, Grapsidae) reared in the laboratory. Revista Brasileira de Zoologia 14.

Cabanas, J. M., M. T. Nunes, M. L. Iglesias, N. González & R. Carballo. 1987. Oceanografía de la Bahía de La Coruña. Boletín. Instituto Español de Oceanografía 4:21-28.

Charmantier, G. 1998. Ontogeny of osmoregulation in crustaceans: A review. Invertebrate Reproduction & Development 33:177-190.

Charmantier, G. & M. Charmantier-Daures. 1991. Ontogeny of osmorregulation and salinity tolerance in *Cancer irroratus*; elements of comparison with *C. borealis* (Crustacea, Decapoda). Biological Bulletin 180:125-134.

Charmantier, G. & M. Charmantier-Daures. 1995. Osmoregulation and salinity tolerance in zoeae and juveniles of the snow crab *Chionoecetes opilio*. Aquatic Living Resources 8:171-179.

Charmantier, G., C. Haond, J. Lignot & M. Charmantier-Daures. 2001. Ecophysiological adaptation to salinity throughout a life cycle: A review in homarid lobsters. Journal of Experimental Biology 204:967-977.

Charmantier, G., L. Giménez, M. Charmantier-Daures & K. Anger. 2002. Ontogeny of osmoregulation, physiological plasticity, and larval export strategy in the grapsid crab *Chasmagnathus granulata* (Crustacea, Decapoda). Marine Ecology Progress Series 229:185-194.

Choy, S. C., 1991. Embryonic and larval biology of *Liocarcinus holsatus* and *Necora puber* (Crustacea: brachyura: portunidae). J. Exp. Mar. Biol. Ecol. 148:77-92.

Corgos, A., C. Bernárdez, P. Sampedro, P. Verísimo & J. Freire. 2011. Spatial structure of the spider crab, *Maja brachydactyla* population: Evidence of metapopulation structure. Journal of Sea Research 66:9-19.

Costlow, J. D. & C. G. Bookhout. 1959. The larval development of *Callinectes sapidus* Rathbun reared in the laboratory. The Biological Bulletin 116:373-396.

Costlow, J. D. & C. G. Bookhout. 1968. The effect of environmental factors on development of the land-crab, *Cardisoma guanhumi* Latreille. American Zoologist 8:399-410.

Costlow, J. D., C. G. Bookhout & R. Monroe. 1960. The effect of salinity and temperature on larval development of *Sesarma cinereum* (Bosc) reared in the laboratory. Biological Bulletin 118:183-202.

Costlow Jr., J. D., C. G. Bookhout & R. Monroe. 1962. Salinity-temperature effects on the larval development of the crab, *Panopeus herbstii*Milne-Edwards, reared in the laboratory. Physiological Zoology 35:79-93.

Costlow Jr., J. D., C. G. Bookhout & R. Monroe. 1966. Studies on the larval development of the crab, *Rhithropanopeus harrisii* (Gould). I. The effect of salinity and temperature on larval development. Physiological Zoology 39:81-100.

Cuesta, J.A. & K. Anger. 2005. Larval morphology and salinity tolerance of a land crab from West Africa, *Cardisoma armatum* (Brachyura: Grapsoidea: Gecarcinidae). Journal of Crustacean Biology 25:640-654.

D'Urban Jackson, T., G. Torres & L. Giménez. 2014. Survival and development of larvae of two decapod crustaceans under limited access to prey across a thermal range. J. Plank. Res. 36 (6):1476-1487.

Dakin, W. M. J. 1912. Aquatic animals and their environment. The constitution of the external medium, and its effect upon the blood. Internationale Revue der gesamten Hydrobiologie und Hydrographie 5:53-80.

Díaz, H. & M. Bevilacqua. 1986. Larval development of *Aratus pisonii* (Milne Edwards) (Brachyura, Grapsidae) from marine and estuarine environments reared under different salinity conditions. Journal of Coastal Research 2:43-49.

Diesel, R. & M. Schuh. 1998. Effects of salinity and starvation on larval development of the crabs *Armases ricordi* and *A. roberti* (Decapoda: Grapsidae) from Jamaica, with notes on the biology and ecology of adults. Journal of Crustacean Biology 18:423-436.

Dittel R., A. I. & C. E. Epifanio. 1982. Seasonal abundance and vertical distribution of crab larvae in Delaware Bay. Estuaries 5:197-202.

Drilhon, A. 1935. Etude biochimique de la mue chez les crustacés brachyoures (*Maïa squinado*). Annales de Physiologie et de Physicochimie Biologique 11:301-326.

Epifanio, C. E. 1995. Transport of blue crab (*Callinectes sapidus*) larvae in the waters of Mid-Atlantic States. Bulletin of Marine Science 57:713-725.

FAO. 2012. B-42 Crabs, sea-spiders. Capture production by species, fishing areas and countries or areas. In: FAO, editor editors. Fao yearbook. Fishery and aquaculture statistics. Rome: FAO.

Forward Jr., R. B. 2009. Larval biology of the crab *Rhithropanopeus harrisii* (Gould): A synthesis. The Biological Bulletin 216:243-256.

Fowler, A. E., N. V. Gerner, & M. A. Sewell. 2011. Temperature and salinity tolerances of Stage 1 zoeae predict possible range expansion of an introduced portunid crab, *Charybdis japonica*, in New Zealand. Biological Invasions 13:691-699.

Fox, J. & S. Weisberg. 2011. An {R} companion to applied regression. In. Thousand Oaks CA: Sage, Second Edition.

Gago, J., J. M. Cabanas, G. Casas & A. Miranda. 2011. Thermohaline measurements in the continental shelf zone of the NWIberian Peninsula, 1994–2006. Climate Research 48:219-229.

González-Ortegón, E., J. Blasco, L. Le Vay& L. Giménez. 2013. A multiple stressor approach to study the toxicity and sub-lethal effects of pharmaceutical compounds on the larval development of a marine invertebrate. Journal of Hazardous Materials 263, Part 1:233-238.

González-Ortegón, E. & L. Giménez. 2014. Environmentally mediated phenotypic links and performance in larvae of a marine invertebrate. Marine Ecology Progress Series 502:185-195.

Goy, J. W., C. G. Bookhout & J. D. Costlow Jr. 1981. Larval develoment of the spider crab *Mithrax pleuracanthus* Stimpson reared in the laboratory (Decapoda: Brachyura: Majidae). Journal of Crustacean Biology 1, 51-62.

Guerao, G., E. Pastor, J. Martin, M. Andrés, A. Estévez, A. Grau, J. Duran & G. Rotllant. 2008. The larval development of *Maja squinado* and *M. brachydactyla* (Decapoda, Brachyura, Majidae) described from plankton collected and laboratory-reared material. Journal of Natural History 42:2257-2276.

Guerao, G. & G. Rotllant. 2010. Development and growth of the early juveniles of the spider crab *Maja squinado* (Brachyura: Majoidea) in an individual culture system. Aquaculture 307:105-110.

Guerao, G., G. Rotllant & K. Anger. 2010. Characterization of larval moulting cycles in *Maja brachydactyla* (Brachyura, Majidae) reared in the laboratory. Aquaculture 302:106-111.

Hernández, J. E., J. L. Palazón-Fernández, G. Hernández & J. Bolaños. 2012. The effect of temperature and salinity on the larval development of *Stenorhynchus seticornis* (Brachyura: Inachidae) reared in the laboratory. Journal of the Marine Biological Association of the United Kingdom 92:505-513.

Johns, M. D. & W. H. Lang. 1977. Larval development of the spider crab *Libinia emarginata* (Majidae). Fishery Bulletin 75:831-841.

Kannupandi, T., G. Vijayakumar & P. Soundarapandian. 2000. Influence of salinity on larval development of the mangrove crab *Sesarma brockii* De Man. Indian Journal of Fisheries 47:343-348.

Kim, C. H. & I. K. Jang. 1987. The complete larval development of *Acmaeopleura parvula* Stimpson (Brachyura, Grapsidae) reared in the laboratory. Bull. Korean Fish. Soc. 20:543-560.

Lárez, M. B., J. L. Palazón-Fernández & C. J. Bolaños. 2000. The effect of salinity and temperature on the larval development of *Mithrax caribbaeus* Rathbun, 1920 (Brachyura: Majidae) reared in the laboratory. Journal of Plankton Research 22:1855-1869.

Le Foll, D. 1993. Biologie et exploitation de l'araignée de mer*Maja squinado*herbst en manche ouest. In: Ressources Halieutiques, IFREMER - Institut Français de Recherche pour l'Exploitation de la Mer. Plouzane (France): Université de Bretagne Occidentale. p. 517.

Lucas, J. S. & E. P. Hodgkin. 1970. Growth and reproduction of *Halicarcinus australis* (Haswell) (Crustacea, Brachyura) in the Swan Estuary Western Australia. II. Larval stages. Marine and Freshwater Research 21:163-173.

Luppi, T. A., E. D. Spivak & C. C. Bas. 2003. The effects of temperature and salinity on larval development of *Armases rubripes* Rathbun, 1897 (Brachyura, Grapsoidea, Sesarmidae), and the southern limit of its geographical distribution. Estuarine, Coastal and Shelf Science 58:575-585.

Mene, L., M. T. Alvarez-Ossorio, E. González-Gurrián & L. Valdés. 1991. Effects of temperature and salinity on larval development of *Necora puber* (Brachyura: Portunidae). Marine Biology 108:73-81.

Messerknecht, I., M. Montu & K. Anger. 1991. Larval development and salinity tolerance of Brazilian *Eurytium limosum* (Say, 1818) (Brachyura: Xanthidae) reared in the laboratory. Meeresforschung 33:275-296.

Mia, M. D. Y. & S. Shokita. 2002. Early life history of an estuarine grapsid crab, *Helice leachi* Hess. Indian Journal of Fisheries 49, 23-28.

Mikami, S. & A. V. Kuballa. 2007. Factors important in larval and postlarval molting, growth, and rearing. In: K. L. Lavalli & E. Spanier, editors. The biology and fisheries of the slipper lobster: CRC Press. pp. 91-110.

Minagawa, M. 1990. Influence of temperature on survival, feeding and development of larvae of the red frog crab, *Ranina ranina* (Crustacea, Decapoda, Raninidae). Nippon Suisan Gakkaishi 56:755-760.

Minagawa, M. 1992. Effects of salinity on survival, feeding and development of larvae of the red frog crab *Ranina ranina*. Nippon Suisan Gakkaishi 58:1855-1860.

Nagaraj, M. 1992. Combined effects of temperature and salinity on the zoeal development of the crab *Liocarcinus puber* (Decapoda: Portunidae). Marine Ecology 13:233-241.

Nagaraj, M., 1993. Combined effects of temperature and salinity on the zoeal development of the green crab, *Carcinus maenas* (Linnaeus, 1758) (Decapoda: Portunidae). Sci. Mar. 57:1-8.

Nurdiani, R. & C. Zeng. 2007. Effects of temperature and salinity on the survival and development of mud crab, *Scylla serrata* (Forsskål), larvae. Aquaculture Research 38:1529-1538.

O'Connor, M. I., J. F. Bruno, S. D. Gaines, B. S. Halpern, S. E. Lester, B. P. Kinlan & J. M. Weiss. 2007. Temperature control of larval dispersal and the implications for marine ecology, evolution, and conservation. Proceedings of the National Academy of Sciences 104:1266-1271.

Ong, K. S. & J. Costlow. 1970. The effect of salinity and temperature on the larval development of the stone crab, *Menippe mercenaria* (Say), reared in the laboratory. Chesapeake Science 11:16-29.

Papadopoulos, I., B. K. Newman, D. S. Schoeman & T. H.Wooldridge.. 2006. Influence of salinity and temperature on the larval development of the crown crab, *Hymenosoma orbiculare* (Crustacea: Brachyura: Hymenosomatidae). African Journal of Aquatic Science 31: 43-52.

Peliz, A., P. Marchesiello, J. Dubert, M. Marta-Almeida, C. Roy & H. Queiroga. 2007. A study of crab larvae dispersal on the Western Iberian shelf: physical processes. Journal of Marine Systems 68:215-236.

Péqueux, A. 1995. Osmotic regulation in crustaceans. Journal of Crustacean Biology 15:1-60.

Przeslawski, R., M. Byrne & C. Mellin. 2015. A review and meta-analysis of the effects of multiple abiotic stressors on marine embryos and larvae. Global Change Biology 21:2122-2140.

R Development Core Team. 2015. R: A language and environment for statistical computing. In. Vienna, Austria: R Foundation for Statistical Computing.

Rabalais, N. N. & J. N. Cameron. 1985. The effects of factors important in semi-arid environments on the early development of *Uca subcylindrica*. The Biological Bulletin 168:147-160.

Reed, P. H. 1969. Culture methods and effects of temperature and salinity on survival and growth of Dungeness crab (*Cancer magister*) larvae in the laboratory. Journal of the Fisheries Research Board of Canada 26:389-397.

Rengel de Zambrano, I., K. Chung, J. Bolaños & J. Fermín. 1993. El efecto de la interacción entre el cadmio, la salinidad y la temperatura sobre el desarrollo larval de *Mithrax verrucosus* Milne Edwards 1832 (Crustacea, Decapoda, Majidae). Ciencia 1, 13-25.

Rotllant, G., C. G. Simeó, G. Macià & A. Estévez. 2014. High environmental salinity reduces the reproductive potential of the spider crab *Maja brachydactyla* (Decapoda, Majidae). Marine Ecology:n/a-n/a.

Sastry, A. N., 1970. Culture of brachyuran crab larvae using a re-circulating sea water system in the laboratory. Helgoländer wissenschaftliche Meeresuntersuchungen 20:406-416.

Schuh, M. & R. Diesel. 1995. Effects of salinity, temperature, and starvation on the larval development of *Armases* (=*Sesarma*) *miersii* (Rathbun, 1897), a semiterrestrial crab with abbreviated development (Decapoda: Grapsidae). Journal of Crustacean Biology 15:205-213.

Seiple, W. H. & M. Salmon. 1987. Reproductive, growth and life-history contrasts between two species of grapsid crabs, *Sesarma cinereum* and *S. reticulatum*. Marine Biology 94:1-6.

Simith, D. d. J. d. B., A. S. de Souza, C. Maciel, F. Abrunhosa & K. Diele. 2012. Influence of salinity on the larval development of the fiddler crab *Uca vocator* (Ocypodidae) as an indicator of ontogenetic migration towards offshore waters. Helgoland Marine Research 66:77-85.

Simith, D. d. J. d. B., M. A. B. Pires, F. A. Abrunhosa, C. R. Maciel & K. Diele. 2014. Is larval dispersal a necessity for decapod crabs from the Amazon mangroves? Response of *Uca rapax* zoeae to different salinities and comparison with sympatric species. J. Exp. Mar. Biol. Ecol. 457:22-30.

Spivak, E. & J. A. Cuesta. 2009. The effect of salinity on larval development of *Uca tangeri* (Eydoux, 1835) (Brachyura: Ocypodidae) and new findings of the zoeal morphology. Sci. Mar. 73:297-305.

Torres, G., L. Giménez & K. Anger. 2002. Effects of reduced salinity on the biochemical composition (lipid, protein) of zoea 1 decapod crustacean larvae. J. Exp. Mar. Biol. Ecol. 277:43-60.

Torres, G., L. Giménez & K. Anger. 2011. Growth, tolerance to low salinity, and osmoregulation in decapod crustacean larvae. Aquatic Biology 12:249-260.

Venables, W. N. & B. D. Ripley. 2002. Modern applied statistics with s. In. New York, USA: Springer.

Yamamoto, T., T. Yamada, H. Fujimoto & K. Hamasaki. 2015. Effects of salinity on snow crab (*Chionoectes opilio*) larval survival and development under laboratory conditions. Journal of Shellfish Research 34:499-504.

CHAPTER 6.

Influence of temperature and light regime on the larval development of the common spider crab *Maja brachydactyla* Balss, 1922 (Brachyura: Majidae)

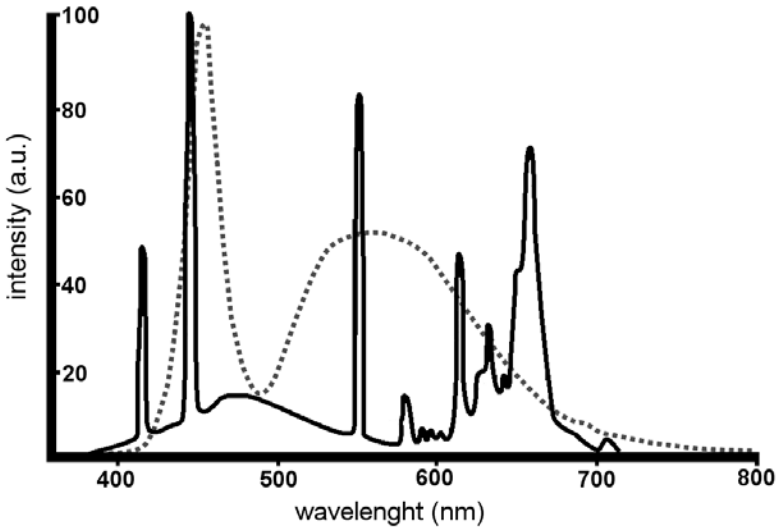

Influence of temperature and light regime on the larval development of the common spider crab *Maja brachydactyla* Balss, 1922 (Brachyura: Majidae)

Diego Castejón[1]*, Guiomar Rotllant[2], Luis Giménez[3], Gabriela Torres[3,5], and Guillermo Guerao[4]

[1]Cultius Aquàtics, IRTA, Ctra. de Poble Nou, Km 5.5, Sant Carles de la Ràpita 43540, Tarragona, Spain

[2]Departament de Recursos Marins Renovables, Institut De Ciències Del Mar, CSIC, Passeig Marítim de la Barceloneta 37-49, Barcelona 08003, Spain

[3]School of Ocean Sciences, Bangor University, Menai Bridge, Anglesey, LL59 5AB, United Kingdom.

[4]PS Fabra i Puig 344, Barcelona 08031, Spain.

[5]Present address: Alfred Wegener Institut, Helmholtz-Zentrum für Polar- und Meeresforschung, Biologische Anstalt Helgoland, 27498 Helgoland, Germany

Short title: Temperature and light influence on crab larval development

***Corresponding author**: Diego Castejón. E-mail: diego.castejon.dcb@gmail.com; phone: +34 681 154 398; postal address: Cultius Aquàtics, IRTA, Ctra. Poble Nou, Km 5.5, 43540 Sant Carles de la Ràpita, Tarragona, Spain.

Abstract.

The common spider crab *Maja brachydactyla* Balss, 1922 has a great potential for aquaculture because of the easy maintenance, high fecundity and short larval development. Temperature and light are important factors affecting production in the aquaculture industry as they can drive behavior and physiological responses of free-swimming larval stages. To optimize larval culture techniques, this study focused on the influence of temperature and light on larval survival and development, and elemental body composition. The experiments performed were: (1) temperature (15 to 30 °C), (2) photoperiod (0 to 24 daily light hours), (3) light intensity (0 to 3000 lx), (4) influence of light over metamorphosis and (5) combined effects of temperature (18 and 21 °C) and photoperiod (0 and 12 daily light hours). We found that the most suitable temperature, for aquaculture purposes, is 21 ± 1 °C. Larvae require light sources simulating the daily light cycle; those maintained at constant darkness showed lower survival and longer developmental time. The megalopae required longer to metamorphose when maintained at constant darkness during the zoeal phase than when reared under a light: dark regime. No interaction between temperature and light was found. Larvae reared in the absence of light showed lower dry mass, carbon and nitrogen content, and C:N ratio than larvae reared in the presence of light.

Keywords: Decapoda; larviculture; photoperiod; light intensity; elemental body composition

1. Introduction

Temperature is the most crucial factor influencing the production in the aquaculture industry and crustacean farming since it determines survival, metabolic activity, growth rate and time of development (Anger, 2001; Wickins & O'C Lee, 2002; Castejón, Rotllant, Giménez, Torres & Guerao, 2015). Light is another important factor affecting production in the aquaculture industry, due to its impact on biological cycles, feeding, growth, behavior or reproductive strategies (Boeuf & Le Bail, 1999; Villamizar, Blanco-Vives, Migaud, Davie, Carboni & Sánchez-Vázquez, 2011). However, the influence of light on crustacean farming receives little consideration (Wickins & O'C Lee, 2002). Light can drive behavior and physiological responses of free-swimming larval stages of crustacean species (Anger, 2001; Epifanio & Cohen, 2016). The photoperiod and intensity of light influence the feeding behavior (Viherluoto & Viitasalo, 2001; Minagawa, 1994; Rabbani & Zeng, 2005), growth rate (Minagawa, 1994; Hoang, Barchiesis, Lee, Keenan & Marsden, 2003; Ulikowski & Krzywosz, 2004); metabolic activity (Wang, Dong, Dong, Huang, Zhu & Mu, 2004), and also survival and duration of larval development (Minagawa, 1994; Rabbani & Zeng, 2005; Andrés, Rotllant & Zeng, 2010c). Light intensity also can affect the success of settlement and metamorphosis (Thorson, 1964). The effects of light can be modulated by various environmental factors (Epifanio & Cohen, 2016). In this sense, the light-response of larvae of many marine species, including some Decapoda, vary in relation to the temperature (Thorson, 1964; Anger, 2001).

To determine the light influence on the crustacean farming and specifically during the larval stages, we realized serial experiments on the common spider crab *Maja brachydactyla* Balss, 1922. It is a profitable resource whose main fisheries are located

in France, Ireland, Channel Islands and Spain (FAO, 2014). This species reproduces very easily in captivity and a single female can carry multiple and consecutive broods (González-Gurriarán, Fernández, Freire & Muiño, 1998). The female fecundity is also very high, varying from 100,000 to 500,000 eggs per female depending on environmental and animal conditions (Verísimo, Bernárdez, González-Gurriarán, Freire, Muino & Fernández, 2011; Rotllant, Simeó, Macià & Estévez, 2015). Larval development is abbreviated, comprising two zoeal stages (zoea I and zoea II) and one megalopal stage (Clark, 1986; Guerao, Pastor, Martin, Andrés, Estévez, Grau, Duran & Rotllant, 2008). Larvae can be cultured in captivity with a diet based on *Artemia* sp., requiring approximately two weeks to reach the first juvenile when reared at 21 °C (Castejón et al., 2015).

The profitable economic value, easy maintenance and reproduction, high female fecundity, short larval development, and feasible larval culture, are interesting features that give a great potential to *Maja brachydactyla* as an aquaculture species. This fact has been emphasized in a number of recent works focused on aspects of the reproductive biology (Rotllant, González-Gurriarán, Fernández, Benhalima & Ribes, 2007; Simeó, Kurtz, Rotllant, Chiva & Ribes, 2009; Simeó, Kurtz, Chiva, Ribes & Rotllant, 2010; Rotllant, Roque, Solé & Gisbert, 2013; Rotllant, Simeó, Macià & Estévez, 2014; Corgos & Freire, 2006; Figueiredo & Narciso, 2008), feeding strategy (Bernárdez, Freire & González-Gurriarán, 2000; Andrés, Estévez, Hontoria & Rotllant, 2010a; Andrés, Gisbert, Díaz, Moyano, Estévez & Rotllant, 2010b; Rotllant, Moyano, Andrés, Estévez, Díaz & Gisbert, 2010; Andrés, Rotllant, Sastre & Estevez, 2011; Guerao, Simeó, Anger, Urzúa & Rotllant, 2012), growth patterns (Andrés, Estévez & Rotllant, 2007; Guerao et al., 2008; Guerao & Rotllant, 2009b; Guerao & Rotllant,

2009a; Guerao, Rotllant & Anger, 2010; Domingues, Alaminos, García-Garrido, Hachero-Cruzado & Rosas, 2012), or other aspects of its production (Iglesias, Sánchez, Moxica, Fuentes, Otero & Pérez, 2002; Alaminos & Domingues, 2007; Domingues & Alaminos, 2008; Rotllant et al., 2013).

In the present study our objective was to determine the optimal combination of temperature and light conditions for the production of juveniles of *M. brachydactyla*. We therefore evaluated the effects of temperature, photoperiod, light intensity and photoperiod-temperature combinations on larval growth, survival and duration of larval development.

2. Material and methods

Broodstock maintenance

Adult specimens were captured in the Galician coast (North Spain) in December 2012, then were transported to the Institut de Recerca i Tecnologia Agroalimentàries facilities (Sant Carles de la Ràpita, Tarragona, Spain). The specimens were maintained in a sex ratio of six females per male and kept in 2,000 L cylindrical tanks connected to a recirculation unit (renewal rate = 3.5 m^3 h^{-1}). Animals were kept under constant conditions of temperature (18 ± 1 °C), salinity (35 ± 1), photoperiod (12 h light: 12 h dark) and light intensity (25 lx, fluorescent tubes), and fed with mussels and frozen crabs.

Larval culture system

Experiments were run in a culture system previously described in Castejón et al. (2015). The incubation chambers consisted of 200 L aquaria (100 x 40 x 50 cm), one per treatment. The larvae were cultured inside replicate 600 mL borosilicate glass

beakers filled with 500 mL of filtered seawater. Since the experiments required controlled conditions of illumination, the aquaria base and walls were covered with black plastic polyethylene sheets to prevent the influence of external light sources. The treatments of constant darkness were performed in a similar manner by totally covering the aquaria with the black sheets; while the treatments of light received illumination from above (0.4 m over the glass beakers). Fluorescent tubes (model 120 220 W, Beta Acuarios, Spain) and white LED lights (model LD65B 6.24 W and model LD100B 14.40 W, ICA, Spain) were used according to the experiment. The emission spectrum of the light sources was provided from the manufacturer (Fig. 1).

Fluorescent tubes were used to establish the most suitable temperature and photoperiod (see *Temperature* and *Photoperiod* experiments) following a previous photoperiod study (Andrés, Rotllant & Zeng 2010). In subsequent experiments LED lights were employed due to their versatility; for instance, the number of LED bulbs can be easily adjusted to modify light intensity; see *Light intensity*, *Photoperiod influence on megalopal settlement* and *Combined effects of light regime and temperature on survival and duration of the larval development* experiments. Light intensity was quantified with a light meter (precision: 1 lx; Lx-101, Lutron Electronic Enterprise, Taipei, Taiwan). Photoperiod was controlled with 24 hours programmable timers. During daily maintenance, larvae reared under constant darkness were exposed to the room illumination for 15 – 30 minutes every day; but the term “constant darkness” is used throughout the methods description for these treatments for simplicity. Salinity was constant at 35 ± 1, being measured using a portable handheld salinity refractometer (precision: 1, range: 0 – 100; Shenzhen Handsome Technology Co. Ltd., Guandong, China). To ensure that the temperature remained constant, calibrated submersible

heaters were used, controlled by an internal thermostat (Eheim Jäger, Finsterrot, Germany). In each aquarium, the heat distribution was carried out by water bath and an air lift. Temperature was measured daily with a portable meter (precision: 0.1 °C; WTW ProfiLine Oxi 3210, Weilheim, Germany).

Experimental design

Five different experiments were carried out to study different aspects of the effects of temperature and light. Larvae used in each experiment were obtained from the same hatch, but were not used in other experiments. Each experiment consisted in two phases:

1. The first phase started with newly hatched zoeae within maximally ca. 15 h after hatching that showed an active swimming activity and continued until all the larvae molted to megalopa or died. The larvae were transferred from the adult tanks to the culture glass beakers without prior adaptation. The initial density was 60 zoeae L^{-1} following Andrés, Estévez, Anger and Rotllant (2008).

2. The second phase started with newly molted megalopae within maximally ca. 15 h after molt that showed an active swimming activity and continued until all the larvae metamorphosed to first juvenile or died. Megalopa were transferred to the same conditions employed during the first phase, except for the special requirements of each treatment of the *Photoperiod influence on the megalopa settlement* experiment. The initial density was 20 megalopae L^{-1}.

Food consisted in fresh nauplii and metanauplii of *Artemia* sp. (INVE Aquaculture Nutrition, Salt Lake UT, USA) without enrichment. Water and food (*ad libitum*) were changed daily and dead larvae were discarded. The criteria used to

confirm death was the absence of appendage and heart movement employing a stereomicroscope.

The response variables were the proportion of survivors from hatching to megalopa and from megalopa to first juvenile stage, as well as the duration of the zoeal phase and megalopa stage. We did not study each separate zoeal stage in order to avoid, as much as possible, any effect of larval handling on survival. The main objective of our study was to determine the optimal conditions for the juvenile production. Survival is particularly low at metamorphosis to juvenile and may be influenced by stress effects experienced by zoeal stages.

To measure the survival and time of development four replicates were established per treatment in the *Temperature*, *Photoperiod* and *Light intensity* experiments (see below). Moreover, additional replicates were created to obtain samples for dry mass (DM) and elemental body composition analysis (CHN); the samples consisted on freshly hatched zoea I, inter-molt zoea I and early post-molt megalopae.

1. *Temperature experiment.* Larvae were reared in separate groups under six treatments: 15, 18, 21, 24, 27, and 30 ± 1 °C. Fluorescent tubes provided the illumination; photoperiod (12 h light: 12 h dark) and light intensity (300 lx) were maintained constant.

2. *Photoperiod experiment.* Five 24 h light: dark cycle regimes (0, 8, 12, 16 and 24 light hours) were employed. Fluorescent tubes provided the illumination; light intensity (300 lx) and temperature (21 ± 1 °C) were maintained constant.

3. *Light intensity experiment.* Four treatments with different light intensity (0, 300, 1000 and 3000 lx) were employed. The 0 lx treatment used a constant darkness photoperiod while the light treatments (from 300 to 3000 lx) used the same photoperiod

of 12 h light: 12 h dark. LED lights provided illumination. Temperature was kept constant at 21.0 ± 0.5 °C.

The following two experiments were carried out in order to better understand the influence of temperature and light on development, but samples for DM and CHN were not taken.

4. *Effect of photoperiod on development from megalopa to juvenile.* Only two light regimes were used: constant darkness (D: 0 lx; 0 h light: 24 h dark) and light: dark cycle (L: 1000 lx; 12 h light: 12 h dark). The choice of these regimes was based on previous experiments, where the most significant factor was presence (L) / absence (D) of light rather than light variations in photoperiod or intensity (see Results). These conditions were combined in four treatments: DD, DL, LD and LL (first letter: light regime used during the zoeal phase; second letter: light regime used during the megalopal stage). Six replicates per treatment were used. Temperature was maintained constant at 19.0 ± 0.5°C.

5. *Combined effects of light regime and temperature on survival and duration of the larval development.* Larvae were kept under two light regimes: constant darkness (D: 0 lx; 0 h light: 24 h dark) and light: dark cycle (L: 1000 lx; 12 h light: 12 h dark) combined with two temperatures: 18 and 21 ± 1 °C; giving a total of four light regime – temperature combinations. Four replicates per treatment were used during the zoeal phase. Due to technical problems, in the treatments „L – 18 °C" and „D – 21 °C" only two and three replicates during the megalopal stage were used, respectively.

Dry mass and elemental body composition analysis

The dry mass (DM) and elemental body composition (Carbon: Hydrogen: Nitrogen, CHN) were analyzed in the *Temperature*, *Photoperiod*, and *Light intensity* experiments. Larvae from the culture beakers were randomly mixed. In each experiment were sampled 25 newly hatched zoeae I before the start of the experiment, 25 inter-molt zoea I per treatment and 15 post-molt megalopae per treatment. In each experiment, the DM and CHN was determined realizing five analyses per larval phase and treatment, each analysis required 5 zoeae or 3 megalopae. The sampled larvae were carefully rinsed in distilled water for a few seconds and the excess of water was absorbed with filter paper. Then, larvae were introduced inside tin capsules and stored at -20 °C following Anger and Harms (1990). Samples were freeze-dried (vacuum drier: Edwards Super Modulyo) and the DM was determined (microbalance: Mettler Toledo MX5, precision: 1 µg, capacity: 5.1 g). The content of CHN was measured using a FlashEA 1112 Series Elemental Analyzer.

Statistical Analysis

Statistical analyses were performed using R software version 3.2.0 (R Development Core Team, 2015). Since each experiment was performed employing larvae from a different hatch, each experiment was analyzed separately to avoid hatch influence as confounding factor.

Survival and developmental time of the experiments 1 to 4, as well DM and CHN of the experiments 1 to 3, were analyzed by one-way ANOVA using temperature, photoperiod, light intensity, light regime, DM or carbon and nitrogen content or percentage as factor. Normality and homogeneity were verified by Shapiro-Wilk and Levene tests. The replication unit for the survival was the culture beaker. The

replication unit for the developmental time was the average duration per culture beaker, the lost of the replicate occurred when survival was zero. The replication unit for the DM and CHN were the analyses.

To analyze the combined effects of temperature and light regime we used a two-way Type III ANOVA (R package car 2.0-25 (Fox & Weisberg, 2011). The statistical significance was established with a critical level (α) of 0.05 to reject the null hypothesis. Significant treatment level effects after significant ANOVA were evaluated using the post-hoc Tukey-HSD test.

3. Results

Temperature

Survival and duration of larval development

The lowest survival, from hatching to megalopa stage, occurred at 30 °C (none specimen reached the seventh day: Fig. 2). Mortality was also very high at 27 °C with only 1.7 ± 1.9 % of the larvae reaching the megalopa. On the contrary, survival was significantly higher in the range from 15 to 21 °C ($F_{4,15} = 26.47$, $p < 0.001$). The highest survival was observed at 21 °C with 57.1 ± 2.8 % (Fig. 2). The duration of the zoeal phase significantly increased as temperature decreased ($F_{4,13} = 30.2$, $p < 0.001$): it was 14.9 ± 0.5 days at 15 °C, 11.6 ± 0.5 days at 18 °C, 9.1 ± 0.5 days at 21 °C, 8.6 ± 1.8 days at 24 °C and 8.5 ± 0.7 days at 27 °C (Fig. 3). Unfortunately, the effects of the temperature on the survival to first juvenile and the duration of the megalopal stage could not be analyzed due to low survival: 2 juveniles at 15 °C, 1 juveniles at 18 °C, 4 juveniles at 21 °C and 1 juvenile at 24 °C. The longest megalopa stage was observed at 15 °C (13.5 ± 0.7 days), and the shortest at 24 °C (6 days).

Biomass growth and elemental body composition

Temperature affected significantly all parameters studied in inter-molt zoea I. Dry mass was lower at 30 °C than from 15 to 24 °C ($F_{5,24}$= 10.41, $p < 0.001$). The same tendency was observed in C and N content per individual (C: $F_{5,24}$= 12.02, $p < 0.001$; N: $F_{5,24}$= 13.02, $p < 0.001$) and the C and N percentage per individual (C: $F_{5,24}$= 11.26, $p < 0.001$; N: $F_{5,24}$= 8.09, $p < 0.001$). The C:N ratio tend to be significantly lower at 30 °C than at a lower temperatures ($F_{5,24}$= 3.90, $p < 0.01$; Table 1).

Responses of megalopa biomass to temperature resembled those previously described for zoea I. Biomass decreased significantly at the highest temperature analyzed (24 °C; not enough survivors were available at 27 °C for body composition analysis). On the contrary, no significant differences were observed in the range: 15 - 21 °C. This pattern was found for DM ($F_{3,16}$= 8.97, $p < 0.01$), C and N content per individual (C: $F_{3,16}$= 11.27, $p < 0.001$; N: $F_{3,16}$= 15.38, $p < 0.001$), C and N percentage per individual (C: $F_{3,16}$= 10.26, $p < 0.001$; N: $F_{3,16}$= 9.45, $p < 0.001$). No significant differences on the C:N ratio were found from 15 to 24 °C treatments ($F_{3,16}$= 2.15, $p = 0.13$; Table 2).

Photoperiod

Survival and duration of larval development

Survival from hatching to megalopa was lower at constant darkness (0 L) or constant light (24 L) as compared to those treatments were larvae were reared under a light: dark cycle (from 8 to 16 L; $F_{4,15}$ = 5.30; $p < 0.01$; Fig. 4A). Survival from newly molted megalopa to first juvenile was also lower at constant darkness as compared to those treatments were the larvae were reared under a light: dark cycle or constant light

($F_{4,15}$ = 4.09; $p < 0.05$), but no significant differences were found in the range from 8 to 24 L (Fig. 4B).

The duration of the zoeal phase was longer at constant darkness (8.4 ± 0.5 days) than in those treatments where larvae were exposed to light: dark cycles (average 7.6 ± 0.3 days; $F_{4,15}$= 3.07; p = 0.049; Fig. 4C). The duration of the megalopal stage decreased in inverse proportion to the length of the light phase of the photoperiod ($F_{4,15}$= 19.88; $p < 0.001$; Fig. 4D).

Biomass growth and elemental body composition

Dry mass of zoea I varied with the photoperiod: it was higher at 8 and 12 L than at 16 and 24 L; the lowest values of DM occurred at constant darkness ($F_{4,20}$= 16.41, $p < 0.001$). The same tendency was observed in C and N content per individual (C: $F_{4,20}$= 19.95, $p < 0.001$; N: $F_{4,20}$= 21.15, $p < 0.001$) and C:N ratio ($F_{4,20}$= 11.71, $p < 0.001$). The lowest C and N percentage per individual occurred at constant darkness (C: $F_{4,19}$= 37.78, $p < 0.001$; N: $F_{4,20}$= 17.15, $p < 0.001$; see Table 3). By contrast, no significant effects of photoperiod were found on the dry mass and elemental body composition of early post-molt megalopae ($p > 0.05$, Table 4).

Light intensity

Survival and duration of larval development

Light intensity did not significantly affect survival during the zoeal phase ($F_{3,12}$= 2.21; p = 0.14; Fig. 5A) or from megalopae to first juvenile ($F_{3,10}$ = 2.61; p = 0.11; Fig. 5B). The duration of the zoeal phase was not significantly affected by light intensity ($F_{3,12}$= 3.13, p= 0.07; Fig. 5C). The duration of the stage of megalopa could not be analyzed statistically due to low number of individuals reaching the juvenile stage.

However, the longest duration was reported at constant darkness (8.0 days), being shorter under a light-dark cycle (6.1 ± 0.5 days).

Biomass growth and elemental body composition

Zoea I DM varied with the light treatment: it was significantly lower at constant darkness and increased in the presence of light ($F_{3,16}$= 7.94, $p < 0.05$). The same was observed for C and N content per individual (C: $F_{3,16}$= 5.89, $p < 0.01$; N: $F_{3,16}$= 4.24, $p < 0.05$) and C:N ratio ($F_{3,16}$= 11.40, $p < 0.001$). The percent of C and N did not show significant differences among treatments (C: $F_{3,16}$= 2.78, $p = 0.08$; N: $F_{3,16}$= 1.58, $p = 0.23$; Table 5).

Megalopae DM did not vary significantly with light intensity ($F_{3,16}$=1.10, $p = 0.38$), nor did the C or N content per individual (C: $F_{3,16}$=0.57; $p = 0.65$; N: $F_{3,16}$=0.67, $p = 0.58$), or the C:N ratio ($F_{3,16}$= 0.55, p= 0.66; Table 6). The percent of C and N was significantly higher at 300 lx as compared with the other treatments(C: $F_{3,16}$= 11.96, $p < 0.001$; N: $F_{3,15}$= 24.56, $p < 0.001$).

Effect of photoperiod on development from megalopa to juvenile

Survival from early post-molt megalopae to first juvenile was not affected by the light treatment experienced during the zoeal or the megalopal stage ($F_{3,20}$= 0.26, $p = 0.85$; Fig. 6A). The duration of the megalopal stage varied significantly depending on the light regime experienced during the megalopal stage and previous larval stages ($F_{3,19}$= 63.38, $p < 0.001$; Fig. 6B). The longest duration of the megalopal stage occurred when they were reared at constant darkness (average 9.2 ± 0.2 days), independently of the light conditions during the previous zoeal phase. The shortest duration (6.2 ± 0.3

days) of the megalopal stage occurred when larvae were exposed to a light: dark cycle during the whole larval development.

Combined effects of light regime and temperature on survival and duration of the larval development

There was no effect of temperature (T), light intensity (L) or their interaction (TxL) on survival from hatching to megalopa (T: $F_{1,12}$= 1.12, p = 0.30; L: $F_{1,12}$= 0.30, p = 0.60; TxL: $F_{1,12}$= 4.36, p = 0.06; Fig. 7A). The effect of temperature was significant on the survival from megalopa to first juvenile stage, where survival was higher at 21 ºC than at 18 °C, but no significant effect was observed with the light treatment or interacting with temperature (T: $F_{1,9}$ = 6.6, p < 0.05; L: $F_{1,9}$ = 1.4, p = 0.27; TxL: $F_{1,9}$ = 1.1, p = 0.33;Fig. 7B).

The duration of the zoeal development was affected by temperature but not by light treatment, either as a main factor on in interaction with temperature (T: $F_{1,10}$= 92.56, p < 0.001; L: $F_{1,10}$=3.13, p = 0.11; TxL: $F_{1,10}$=0.20, p = 0.66). The zoeal phase was shorter at 21 °C (8.8 ± 0.6 days) than at 18 °C (14.3 ± 1.5 days; Fig. 7C). The duration of the megalopal stage could not be analyzed statistically due to low number of individuals reaching the juvenile stage. On average the duration of the megalopa kept at 21 °C at constant darkness required 8.3 ± 2.3 days, and at light: dark cycle 6.0 ± 0.2 days (Fig. 7D). At 18 °C only one individual reached the juvenile stage at constant darkness (on day 13th) and three under a light: dark cycle (average = 9 ± 1 days).

4. Discussion

The optimal temperature for the larval culture of *M. brachydactyla* is 21 ± 1 °C. Lower temperatures cause an increase in the duration of larval development without a significant increment in survival, while higher temperatures significantly increase mortality without shortening the duration of the larval development. The suitable temperature range for aquaculture purposes is between 15 and 21 ºC These results support preliminary experiments (Castejón et al., 2015). This temperature range coincides or slightly surpass the temperature range measured in the coastal waters of the NW Iberian Peninsula (Gago, Cabanas, Casas & Miranda, 2011). Similar trends occur in other species that inhabit cold to temperate waters. The suitable temperature range for the larval development of the majoid *Hyas araneus* is between 6 and 12 °C (Anger, 1983); for the cancrid *Metacarcinus magister* (as *Cancer magister*) the optimal temperature is around 10 °C and the mortality increases concomitantly with the temperature (Reed, 1969; Sulkin & McKeen, 1989); while in *Cancer irroratus* the temperature ranged between 15 and 24 °C being the highest survival observed at 21 °C (Johns, 1981). By contrast, the species that inhabit tropical to warm temperate waters have an increased range for suitable temperatures. Majoids as *Stenorhynchus seticornis* (Hernández, Palazón-Fernández, Hernández & Bolaños, 2012), *Mithraculus forceps* and *M. sculptus* (Penha-Lopes, Rhyne, Lin & Narciso, 2005; Rhyne, Penha-Lopes & Lin, 2005) reach the first juvenile stage in a range from 25 to 28 °C. Similarly, the range for the larval culture of the portunid *Scylla serrata* was established between 25 and 30 °C (Hamasaki, 2003).

The present study also demonstrates that a light: dark cycle, independently of the duration of the light phase, is more suitable for the larval culture of *M. brachydactyla* than a constant regime of either light or darkness. The illumination should be provided by fluorescent or LED lights with intensities between 300 and 1000 lx, maintaining a photoperiod with 8 to 16 light hours. The megalopa stage is more sensitive to light conditions and the duration of this larval stage increases in the absence of light, as it has been observed in the brachyuran *Carcinus maenas* (Dawirs, 1982); so the light regime must be carefully monitored during this stage. The maintenance of a light: dark cycle and brighter light conditions also have been recommended for the larval culture of other brachyuran species (Minagawa, 1994; Gardner & Maguire, 1998).

Few studies have evaluated the influence of the light (or their absence) on the survival rate and duration of the brachyuran larval stages. In *M. brachydactyla* larval survival tends to be reduced by constant light or darkness. Similarly, larvae of *Ranina ranina* (Minagawa, 1994) and *Portunus pelagicus* (Andrés et al., 2010c) showed reduced survival rates to megalopa when reared under continuous darkness or light. In addition, larvae of *C. maenas* (Dawirs, 1982) and *Ucides cordatus* (Cottens, Silva, Ventura, Ramos & Ostrensky, 2014) showed lower survival to megalopa when reared under constant darkness. In *Sesarma reticulatum* the shortening of the light period increased mortality in developing larvae up to first juvenile (Costlow & Bookhout, 1962). Hamasaki, Ogiso, Dan and Kitada (2016) found that larvae of the anomuran *Birgus latro* cultured in a range from 0 to 24 hours of light showed a lower survival rate under constant darkness. On the other hand, the survival rate of *M. brachydactyla* larvae did not appear to be influenced by light intensity in the range 300 - 3000 lx; *U.*

cordatus larvae showed similar survival rates in the range: 210 - 710 lx (Cottens et al., 2014).

Megalopae of *M. brachydactyla* required longer to reach the first juvenile stage when reared under constant darkness during the zoeal phase. This influence of the conditions during previous stages over the megalopa development seems to be a latent effect (Pechenik, 2006), i.e. environmental conditions experienced at early stages affects development or other traits at later stages. Latent effects have been reported in decapod crustaceans in response to food limitation or osmotic stress (Giménez, 2006; Torres, Giménez & Anger, 2008; Giménez, 2010). Zoeae I, reared at constant darkness had lower dry mass, carbon and nitrogen content per individual, and C:N ratio than larvae reared in the presence of light. It is likely that lower larval quality caused by constant darkness led to compensatory effects at the megalopa stage, which may have also involved delaying the time of metamorphosis (*Photoperiod experiment*; Fig. 2C; Table 4).

Brachyuran larvae can be considered non-obligate visual feeders, since they can successfully complete the larval development in absence of light (Costlow & Bookhout, 1962; Cronin & Forward Jr, 1980; Dawirs, 1982; Minagawa, 1994; Gardner & Maguire, 1998; Andrés et al., 2010c). However, it is known that light stimulates swimming activity (Forward Jr, 1974; Forward Jr & Cronin, 1980; Cronin & Forward Jr, 1980), increasing the chances of prey encounter and consequently food intake (Andrés et al., 2010c; Rabbani & Zeng, 2005) as has been observed in *Pseudocarcinus gigas* (Gardner & Maguire, 1998), *R. ranina* (Minagawa, 1994) and *Rhithropanopeus harrisii* (Cronin & Forward Jr, 1980). Light intensity can influence food conversion efficiency, although the physiological mechanism still remains unknown. For instance,

Hoang et al. (2003) mentioned that the juveniles of the penaeid shrimp *Penaeus merguiensis* showed better food conversion efficiency at mid light intensities (750 lx) than at low light intensities (75 lx); while Wang et al. (2004) observed that the congeneric *Penaeus chinensis* have a better food conversion at low-mid light intensities (50 - 1,300 lx) than at high light intensities (5,500 lx). The authors hypothesized that at extremely high light intensity the animals spend more energy in respiration and excretion, retaining less energy for growth. By contrast, the larvae of *M. brachydactyla* exposed to the highest light intensity (3000 lx) did not show a detriment on the DM, C and N content per individual or C:N ratio. The better quality of *M. brachydactyla* larvae reared in presence of light (independently of the light source) could be a consequence of improved prey encounter and/or feeding rates stimulated by light exposition; or perhaps the highest light intensity we used was not enough to induce energy loss by excessive respiration and excretion.

To conclude, 21 ºC was the optimal temperature for the larval development of *M. brachydactyla*, while higher temperatures are not recommended due to associated higher mortality. The temperature have a stronger influence than the light over the larval development. The larvae survive and develop better under a light: dark cycle photoperiod with low to high light intensity; therefore continuous light or darkness periods must be avoided. Using light during the zoeal phase reduces the duration of the megalopa stage. Growth (measured using DM and elemental composition as proxies) is negatively influenced by darkness during larval development.

Acknowledgements

The Spanish Ministry of Economy and Competitiveness funded bench fees through the INIA project [grant number RTA2011-00004-00-00] to G.G and a predoctoral fellowship to D.C. [FPI-INIA]. The authors would like to thank Karl B. Andree for their comments that have greatly improved this manuscript. We thank hatchery technicians at IRTA in Sant Carles de la Ràpita (David Carmona, Glòria Macià, Magda Monllaó and Francesc X. Ingla) for their help in the broodstock maintenance and setup of the rearing culture system.

Table 1. *Maja brachydactyla*. Effects of the temperature (°C) on the dry mass and elemental body composition of zoeae I [from hatching (0 days) to intermolt (2 days)]. Dry mass (DM), carbon content per individual (C), carbon percentage (C %), nitrogen content per individual (N), nitrogen percentage (N %) and C:N ratio. Values are expresed as average ± SD.

Age (days)	Temp (± 1 °C)	DM (µg)	Carbon (µg ind^{-1})	Carbon (%)	Nitrogen (µg ind^{-1})	Nitrogen (%)	C:N ratio
0	-	99 ± 5	32.0 ± 0.4	32.5 ± 1.2	8.08 ± 0.09	8.20 ± 0.35	3.96 ± 0.03
2	15	114 ± 3^{ab}	35.0 ± 1.6^{ab}	30.6 ± 0.6^{ac}	8.72 ± 0.37^{ab}	7.64 ± 0.16^{ac}	4.01 ± 0.04^{ab}
	18	119 ± 8^{ab}	38.5 ± 3.8^{a}	32.2 ± 1.1^{ab}	9.39 ± 0.80^{a}	7.87 ± 0.15^{ab}	4.09 ± 0.06^{a}
	21	116 ± 4^{ab}	36.4 ± 2.4^{ab}	31.2 ± 1.0^{abc}	9.03 ± 0.41^{ab}	7.75 ± 0.12^{ab}	4.03 ± 0.09^{ab}
	24	123 ± 5^{a}	39.8 ± 2.7^{a}	32.4 ± 1.3^{b}	9.73 ± 0.56^{a}	7.94 ± 0.32^{a}	4.08 ± 0.08^{a}
	27	110 ± 8^{bc}	33.2 ± 3.1^{b}	30.2 ± 0.7^{cd}	8.32 ± 0.67^{bc}	7.59 ± 0.07^{bc}	3.99 ± 0.05^{ab}
	30	99 ± 1^{c}	28.6 ± 0.8^{c}	28.8 ± 0.4^{d}	7.27 ± 0.21^{c}	7.31 ± 0.13^{c}	3.94 ± 0.05^{b}

Different letters indicate significant differences ($P < 0.05$) among treatments.

Table 2. *Maja brachydactyla*. Effects of the temperature (°C) on the dry mass and elemental body composition of newly molted megalopae. Dry mass (DM), carbon content per individual (C), carbon percentage (C%), nitrogen content per individual (N), nitrogen percentage (N%) and C:N ratio. Values are expresed as average ± SD.

Temperature (± 1 °C)	DM (µg)	Carbon (µg ind^{-1})	Carbon (%)	Nitrogen (µg ind^{-1})	Nitrogen (%)	C:N ratio
15	205 ± 10^{a}	75.0 ± 4.3^{a}	36.6 ± 0.9^{a}	17.83 ± 0.63^{a}	8.71 ± 0.29^{a}	4.21 ± 0.12
18	200 ± 11^{a}	69.7 ± 6.0^{a}	34.8 ± 1.1^{ab}	17.10 ± 0.84^{a}	8.55 ± 0.21^{ab}	4.07 ± 0.17
21	193 ± 18^{ab}	65.9 ± 9.3^{a}	34.0 ± 2.2^{bc}	15.87 ± 1.82^{a}	8.20 ± 0.32^{bc}	4.14 ± 0.13
24	164 ± 13^{b}	52.4 ± 5.0^{b}	31.9 ± 0.9^{c}	13.04 ± 1.17^{b}	7.92 ± 0.18^{c}	4.02 ± 0.04

Different letters indicate significant differences ($P < 0.05$) among treatments.

Table 3. *Maja brachydactyla*. Effects of the photoperiod (L, light hours) on the dry mass and elemental body composition of zoeae I [from hatching (0 days) to intermolt (2 days)] reared at 21 °C. Dry mass (DM), carbon content per individual (C), carbon percentage (C %), nitrogen content per individual (N), nitrogen percentage (N %) and C:N ratio. Values are expresed as average ± SD.

Age (days)	Photoperiod (light hours)	DM (µg)	Carbon (µg/ind)	Carbon (%)	Nitrogen (µg/ind)	Nitrogen (%)	C:N ratio
0	-	118 ± 1	36.4 ± 0.5	30.8 ± 0.3	9.16 ± 0.07	7.74 ± 0.08	3.98 ± 0.03
2	0 L	122 ± 5^{a}	36.5 ± 2.0^{a}	30.0 ± 0.7^{a}	9.18 ± 0.50^{a}	7.54 ± 0.18^{a}	3.97 ± 0.03^{a}
	8 L	150 ± 4^{b}	50.8 ± 2.1^{bc}	33.9 ± 0.5^{b}	12.11 ± 0.39^{bc}	8.09 ± 0.06^{b}	4.20 ± 0.04^{bc}
	12 L	149 ± 4^{b}	52.6 ± 1.5^{b}	35.4 ± 0.3^{c}	12.41 ± 0.27^{b}	8.34 ± 0.12^{b}	4.24 ± 0.06^{c}
	16 L	135 ± 8^{c}	45.5 ± 4.1^{c}	33.5 ± 1.3^{bd}	11.10 ± 0.78^{c}	8.20 ± 0.15^{b}	4.09 ± 0.08^{ab}
	24 L	138 ± 9^{bc}	45.5 ± 4.7^{c}	32.3 ± 1.4^{d}	11.14 ± 0.90^{c}	8.05 ± 0.24^{b}	4.08 ± 0.10^{ab}

Different letters indicate significant difference ($p < 0.05$) among treatments.

Table 4. *Maja brachydactyla*. Effects of the photoperiod (L, light hours) on the dry mass and elemental body composition of newly molted megalopae reared at 21 °C. Dry mass (DM), carbon content per individual (C), carbon percentage (C%), nitrogen content per individual (N), nitrogen percentage (N%) and C:N ratio. Values are expresed as average ± SD.

Photoperiod (light hours)	DM (µg)	Carbon (µg/ind)	Carbon (%)	Nitrogen (µg/ind)	Nitrogen (%)	C:N ratio
0 L	189 ± 18	62.3 ± 2.6	33.1 ± 0.5	15.99 ± 0.52	8.50 ± 0.26	3.89 ± 0.08
8 L	201 ± 07	66.5 ± 1.2	33.0 ± 0.9	16.67 ± 0.15	8.28 ± 0.29	3.99 ± 0.09
12 L	206 ± 21	67.0 ± 3.1	32.5 ± 0.8	16.70 ± 0.66	8.11 ± 0.24	4.01 ± 0.09
16 L	201 ± 12	67.2 ± 3.4	33.4 ± 2.7	16.84 ± 0.75	8.37 ± 0.63	3.99 ± 0.07
24 L	196 ± 16	65.6 ± 2.2	33.6 ± 1.8	16.47 ± 0.42	8.44 ± 0.37	3.98 ± 0.08

Significant differences among treatments were not observed.

Table 5. *Maja brachydactyla*. Effects of the light intensity (lux) on the dry mass and elemental body composition of zoeae I [from hatching (0 days) to intermolt (2 days)] reared at 21 °C. Dry mass (DM), carbon content per individual (C), carbon percentage (C %), nitrogen content per individual (N), nitrogen percentage (N %) and C:N ratio. Values are expresed as average ± SD.

Age (days)	Light Intensity (lux)	DW (µg)	Carbon (µg/ind)	Carbon (%)	Nitrogen (µg/ind)	Nitrogen (%)	C:N ratio
0	-	87 ± 1	28.4 ± 0.5	32.5 ± 0.5	7.49 ± 0.10	8.57 ± 0.14	3.79 ± 0.06
2	0	106 ± 8[a]	32.9 ± 3.8[a]	31.0 ± 1.2	8.12 ± 0.91[a]	7.64 ± 0.29	4.05 ± 0.07[a]
	300	123 ± 6[b]	40.2 ± 3.2[b]	32.8 ± 1.2	9.58 ± 0.68[b]	7.82 ± 0.20	4.20 ± 0.08[b]
	1000	117 ± 6[ab]	37.3 ± 3.2[ab]	31.8 ± 1.4	8.85 ± 0.56[ab]	7.56 ± 0.16	4.21 ± 0.10[b]
	3000	124 ± 6[b]	40.8 ± 3.1[b]	32.8 ± 1.0	9.39 ± 0.65[ab]	7.56 ± 0.19	4.34 ± 0.05[c]

Different letters indicate significant difference ($p < 0.05$) among treatments.

Table 6. *Maja brachydactyla*. Effects of the light intensity (lux) on the dry mass and elemental body composition of newly molted megalopae reared at 21 °C. Dry mass (DM), carbon content per individual (C), carbon percentage (C %), nitrogen content per individual (N), nitrogen percentage (N %) and C:N ratio. Values are expresed as average ± SD.

Light Intensity (lux)	DW (µg)	Carbon (µg/ind)	Carbon (%)	Nitrogen (µg/ind)	Nitrogen (%)	C:N ratio
0	193 ± 17	61.3 ± 4.6	31.9 ± 1.5[a]	15.23 ± 0.89	7.93 ± 0.49[a]	4.02 ± 0.08
300	181 ± 14	65.2 ± 5.9	35.9 ± 0.7[b]	15.99 ± 0.80	8.83 ± 0.23[b]	4.07 ± 0.17
1000	194 ± 22	65.6 ± 8.5	33.7 ± 1.3[a]	15.95 ± 1.40	8.22 ± 0.28[c]	4.10 ± 0.19
3000	199 ± 10	65.3 ± 4.4	32.7 ± 0.6[a]	15.76 ± 0.51	7.91 ± 0.15[ac]	4.14 ± 0.14

Different letters indicate significant difference ($p < 0.05$) among treatments.

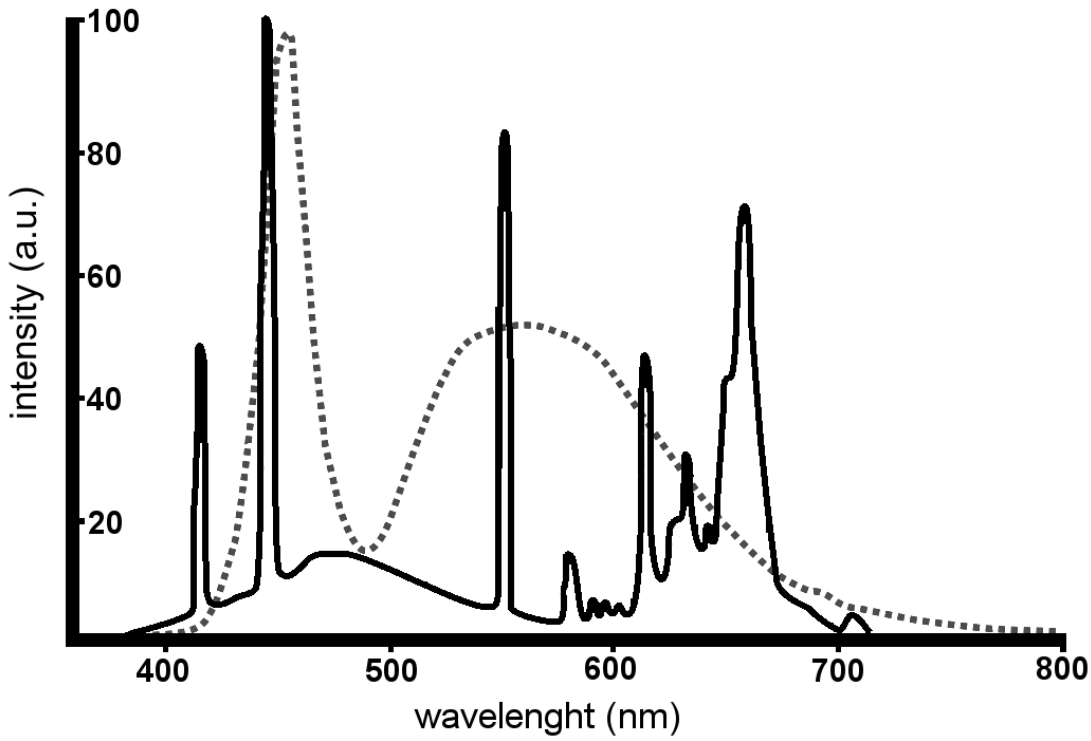

Figure 1. Emission spectra of the light sources employed in the experiments, provided by the manufacturer. Continuous line: fluorescent tubes. Dotted line: LED lights.

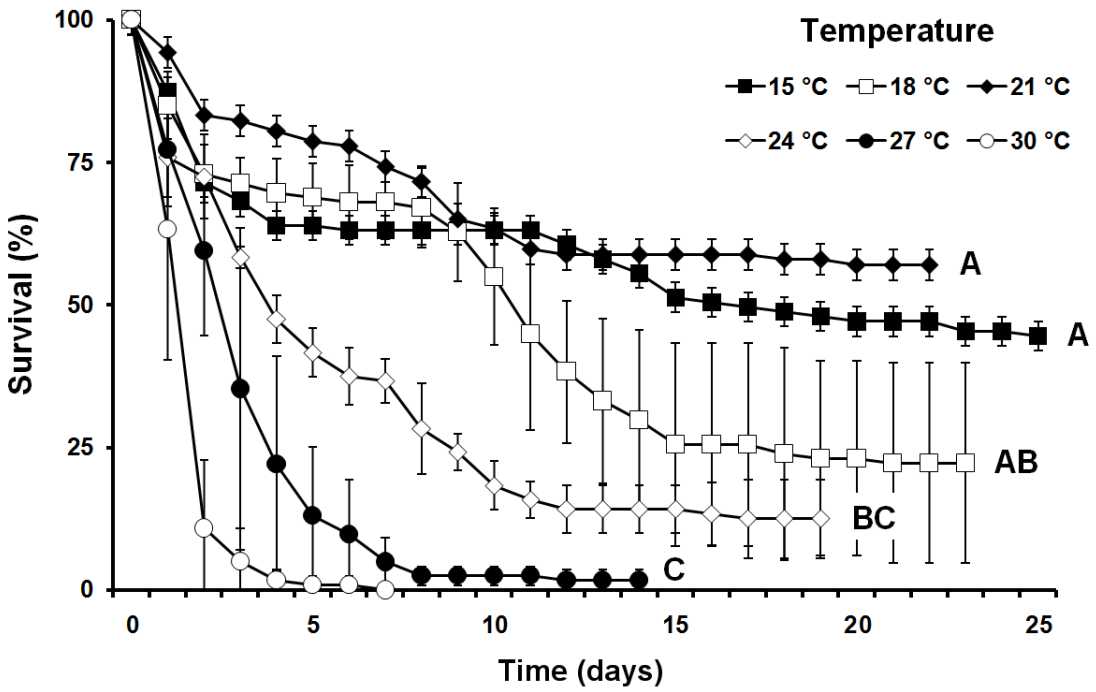

Figure 2. *Maja brachydactyla*. Effect of temperature on the survival to megalopa stage. Lines indicate the average survival (± SD) from hatching to megalopa (n = 4 per treatment) when reared at the following temperatures: 15 °C (black squares), 18 °C (white squares), 21 °C (black diamonds), 24 °C (white diamonds), 27 °C (black circles) and 30 °C (white circles). Different letters indicate significant differences ($p < 0.05$) at the end of the experiment.

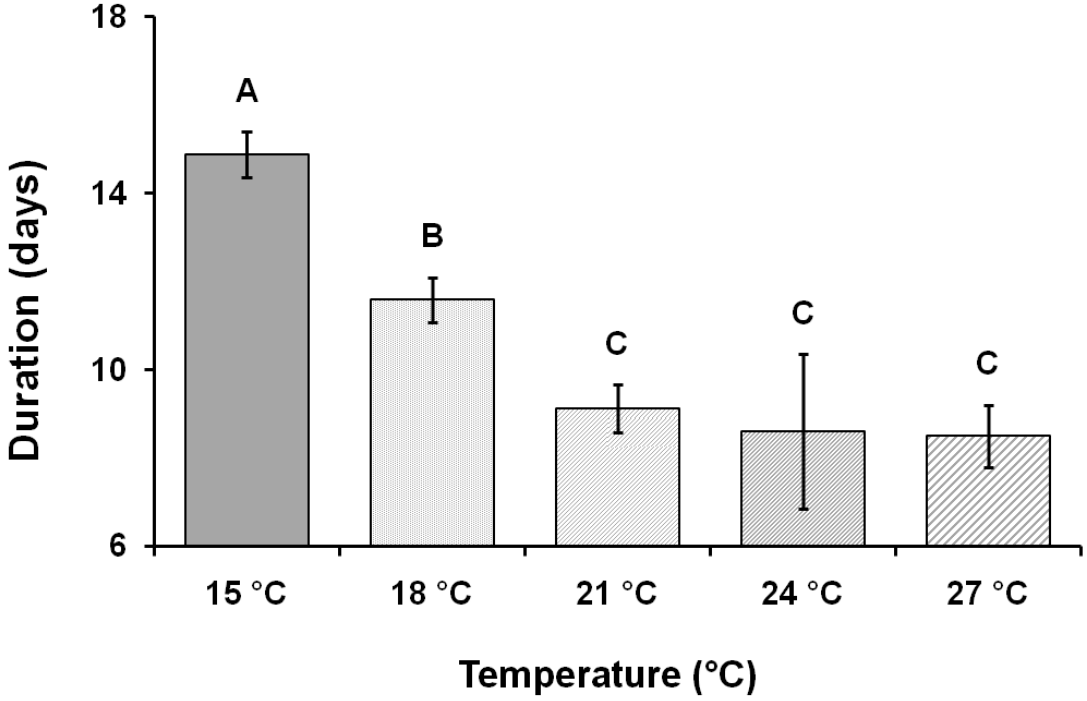

Figure 3. *Maja brachydactyla*. Influence of temperature on the duration of the megalopa stage.

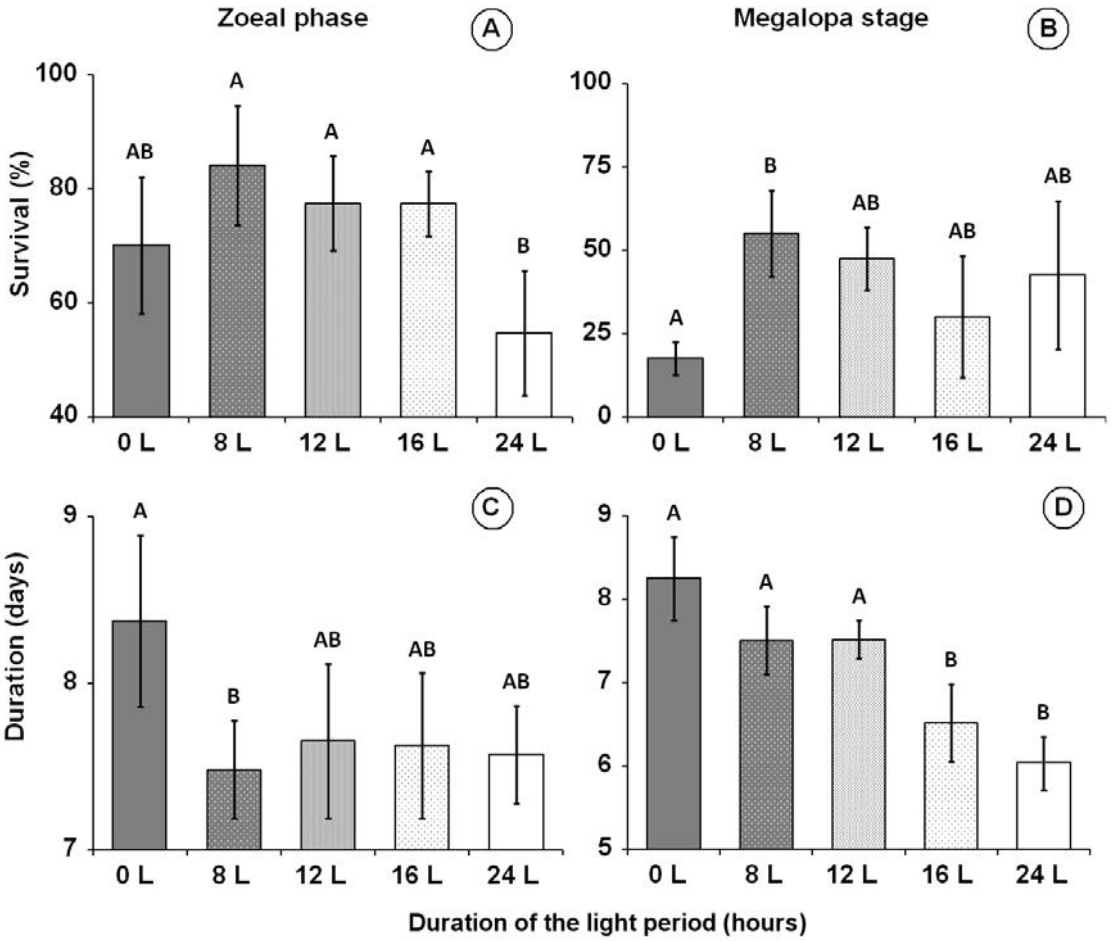

Figure 4. *Maja brachydactyla*. Influence of photoperiod (L, light hours) on survival and duration of the larval development. Survival from hatching to megalopa stage (n = 4 per treatment) (A). Survival from megalopa to first juvenile stage (n = 4 per treatment) (B). Duration of the zoeal phase (n = 4 per treatment) (C). Duration of the megalopa stage (n = 4 per treatment) (D). Bars show average ± SD. Different letters indicate significant differences ($p < 0.05$).

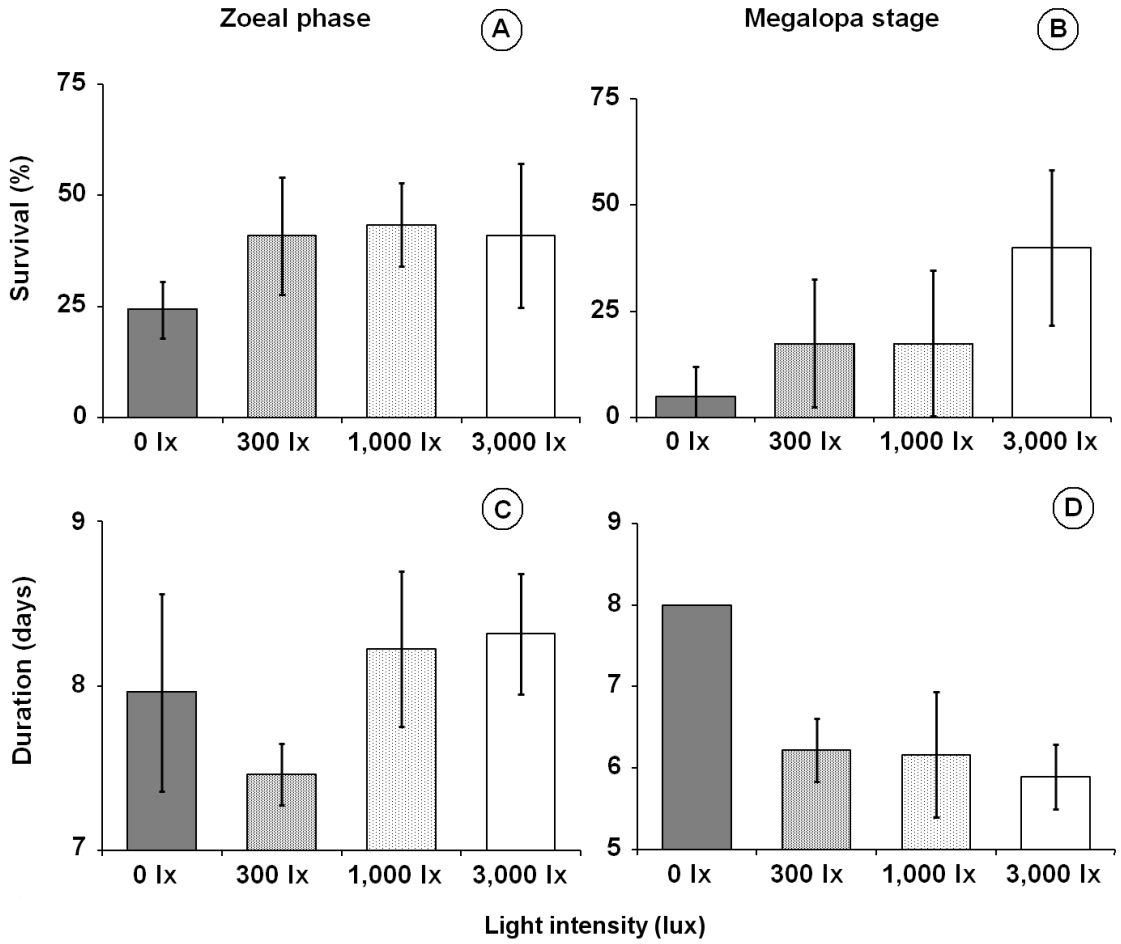

Figure 5. *Maja brachydactyla*. Influence of light intensity (lx, lux) on survival and duration of the larval development. Survival from hatching to megalopa stage (n = 4 per treatment) (A). Survival from megalopa to first juvenile (n = 2, 4, 4, 4) (B). Duration of the zoeal phase (n = 4 per treatment) (C). Duration of the megalopa stage (D). Bars show average ± SD. Different letters show significant differences ($p < 0.05$), except for panel D (no statistical analysis available).

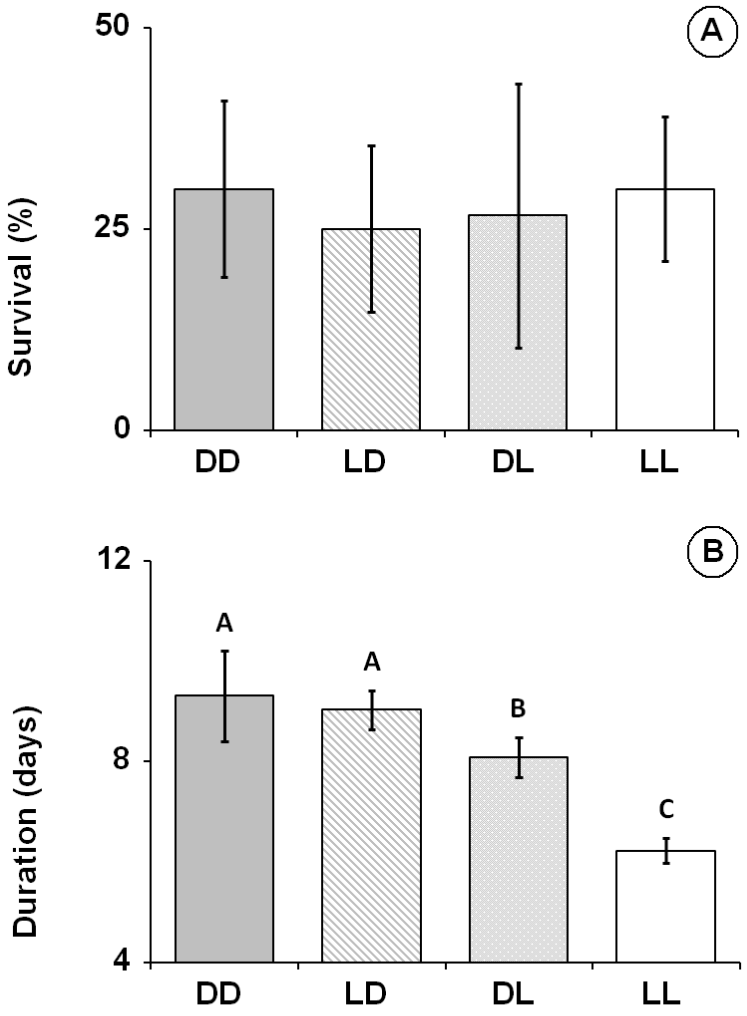

Figure 6. *Maja brachydactyla*. Effect of photoperiod on metamorphosis from megalopa to first juvenile. Survival from megalopa to first juvenile stage (n = 6 per treatment) (A). Duration of the megalopa stage (n = 6 per treatment) (B). Treatments: D = constant darkness, 0 light hours, 0 lx; L = 12 light hours, 1000 lx. First letter: treatment during the zoeal phase. Second letter: treatment during the megalopal stage. See section «Experimental design. Effect of photoperiod on development from megalopa to juvenile» for details. Bars show average ± SD. Different letters indicate significant differences ($p < 0.05$).

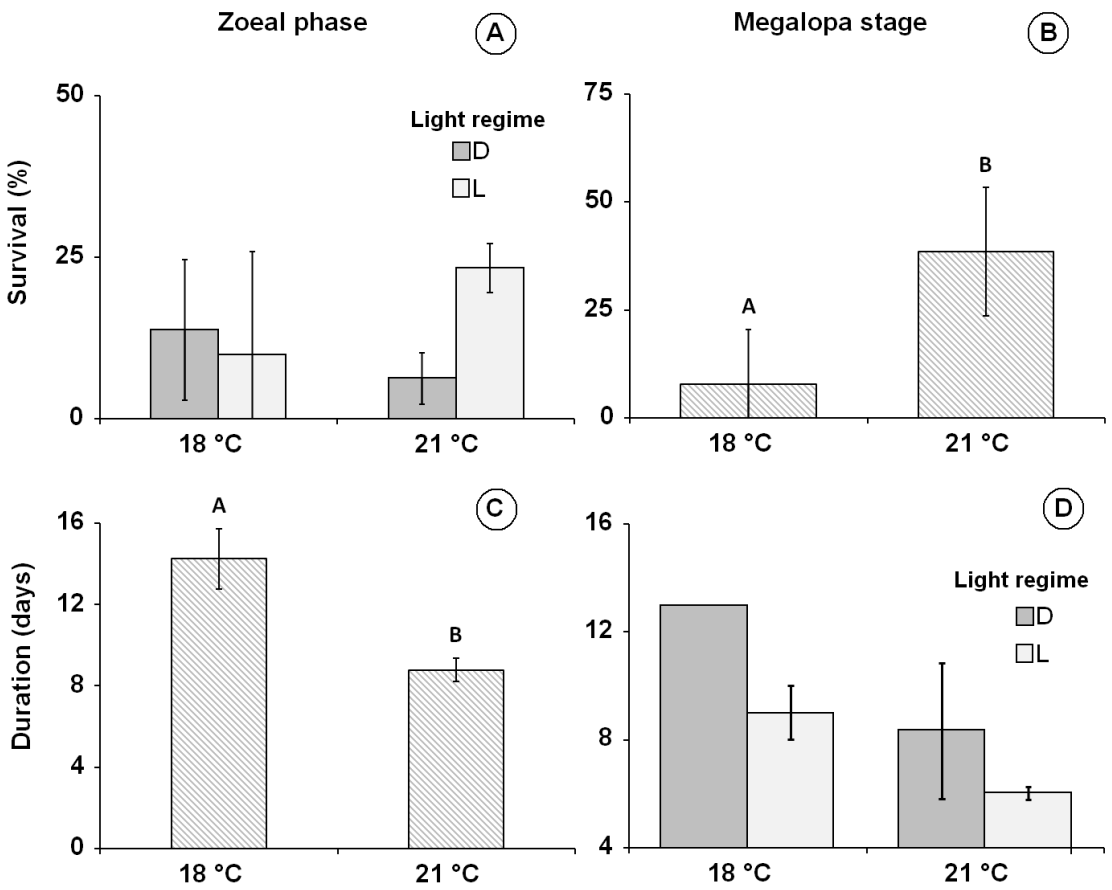

Figure 7. *Maja brachydactyla*. Influence of combined light intensity and temperature on survival and duration of the larval development. The graphs represents the results of the two-way ANOVA. Treatments: D = constant darkness, 0 light hours, 0 lx; L = 12 light hours, 1000 lx. Survival from hatching to megalopal stage (n = 4 per treatment) (A). Survival from megalopa to first juvenile stage (n = 6, 7 respectively), only temperature influence is showed (B). Duration of the zoeal phase (n = 6, 8, respectively), only temperature is showed (C). Duration of the megalopa stage (D). Bars show average ± SD. Different letters show significant differences ($p < 0.05$), except for panel D (no statistical analysis available).

6. Bibliography

Alaminos J., Domingues P. (2007) Efectos de la densidad de cultivo y dietas naturales y artificiales en el crecimiento, supervivencia y periodo de muda de juveniles de centollo, *Maja brachydactyla* In: *XI Congreso Nacional de Acuicultura*, Vigo (Pontevedra, Spain).

Andrés M., Estévez A., Anger K., Rotllant G. (2008) Developmental patterns of larval growth in the edible spider crab, *Maja brachydactyla* (Decapoda: Majidae). *Journal of Experimental Marine Biology and Ecology,* **357**, 35-40.

Andrés M., Estévez A., Hontoria F., Rotllant G. (2010a) Differential utilization of biochemical components during larval development of the spider crab *Maja brachydactyla* (Decapoda: Majidae). *Marine Biology,* **157**, 2329-2340.

Andrés M., Estévez A., Rotllant G. (2007) Growth, survival and biochemical composition of spider crab *Maja brachydactyla* (Balss, 1922) (Decapoda: Majidae) larvae reared under different stocking densities, prey:larva ratios and diets. *Aquaculture,* **273**, 494-502.

Andrés M., Gisbert E., Díaz M., Moyano F.J., Estévez A., Rotllant G. (2010b) Ontogenetic changes in digestive enzymatic capacities of the spider crab, *Maja brachydactyla* (Decapoda: Majidae). *Journal of Experimental Marine Biology and Ecology,* **389**, 75-84.

Andrés M., Rotllant G., Sastre M., Estevez A. (2011) Replacement of live prey by formulated diets in larval rearing of spider crab *Maja brachydactyla*. *Aquaculture,* **313**, 50-56.

Andrés M., Rotllant G., Zeng C. (2010c) Survival, development and growth of larvae of the blue swimmer crab, *Portunus pelagicus*, cultured under different photoperiod conditions. *Aquaculture,* **300**, 218-222.

Anger K. (1983) Temperature and the larval development of *Hyas araneus* L. (Decapoda : Majidae); extrapolation of laboratory data to field conditions. *Journal of Experimental Marine Biology and Ecology,* **69**, 203-215.

Anger K. (2001) *The Biology of Decapod Crustacean Larvae,* A.A. Balkema Publishers, Rotterdam.

Anger K., Harms J. (1990) Elemental (CHN) and proximate biochemical composition of decapod crustacean larvae. *Comparative Biochemistry and Physiology Part B: Comparative Biochemistry,* **97B**, 69-80.

Bernárdez C., Freire J., González-Gurriarán E. (2000) Feeding of the spider crab *Maja squinado* in rocky subtidal areas of the Ría de Arousa (north-west Spain). *Journal of the Marine Biological Association of the United Kingdom,* **80**, 95-102.

Boeuf G., Le Bail P.-Y. (1999) Does light have an influence on fish growth? *Aquaculture,* **177**, 129-152.

Castejón D., Rotllant G., Giménez L., Torres G., Guerao G. (2015) The effects of temperature and salinity on the survival, growth and duration of the larval development of the common spider crab *Maja brachydactyla* (Balss, 1922) (Brachyura: Majidae). *Journal of Shellfish Research,* **34**, 1073-1083.

Clark P.F. (1986) The larval stages of *Maja squinado* (Herbst, 1788) (Crustacea: Brachyura: Majidae) reared in the laboratory. *Journal of Natural History,* **20**, 825-836.

Corgos A., Freire J. (2006) Morphometric and gonad maturity in the spider crab *Maja brachydactyla*: a comparison of methods for estimating size at maturity in species with determinate growth. *ICES Journal of Marine Science: Journal du Conseil,* **63**, 851-859.

Costlow J.D., Bookhout C.G. (1962) The larval development of *Sesarma reticulatum* Say- Reared in the Laboratory. *Crustaceana,* **4**, 281-294.

Cottens K.F., Silva U.A.T., Ventura R., Ramos F.M., Ostrensky A. (2014) Cultivo de larvas de *Ucides cordatus* (LINNAEU, 1763) sob diferentes intensidades luminosas. *Arquivo Brasileiro de Medicina Veterinária e Zootecnia,* **66**, 1464-1470.

Cronin T.W., Forward Jr R.B. (1980) The Effects of Starvation on Phototaxis and Swimming of Larvae of the Crab *Rhithropanopeus harrisi*. *Biological Bulletin,* **158**, 283-294.

Dawirs R.R. (1982) Methodical aspects of rearing decapod larvae, *Pagurus bernhardus* (Paguridae) and *Carcinus maenas* (Portunidae). *Helgoländer Meeresuntersuchungen,* **35**, 439-464.

Domingues P., Alaminos J. (2008) Efectos de la densidad de cultivo y de elementos de refugio en el crecimiento y supervivencia de juveniles de centollo, *Maja brachydactyla* (Balss, 1922). *Revista de biología marina y oceanografía,* **43**, 121-127.

Domingues P., Alaminos J., García-Garrido S., Hachero-Cruzado I., Rosas C. (2012) Growth and survival of juvenile spider crabs, *Maja brachydactyla* (Balss, 1922), fed with fresh or frozen mussels. *Aquaculture Research,* **43**, 167-177.

Epifanio C.E., Cohen J.H. (2016) Behavioral adaptations in larvae of brachyuran crabs: A review. *Journal of Experimental Marine Biology and Ecology,* **482**, 85-105.

FAO (2014) B-42 Crabs, sea-spiders. Capture production by species, fishing areas and countries or areas. In: *FAO yearbook. Fishery and aquaculture statistics* (ed by FAO). FAO, Rome.

Figueiredo J., Narciso L. (2008) Egg volume, energy content and fatty acid a profile of *Maja brachydactyla* (Crustacea: Brachyura: Majidae) during embryogenesis. *Journal of the Marine Biological Association of the United Kingdom,* **88**, 1401-1405.

Forward Jr R.B. (1974) Negative phototaxis in crustacean larvae: Possible functional significance. *Journal of Experimental Marine Biology and Ecology,* **16**, 11-17.

Forward Jr R.B., Cronin T.W. (1980) Tidal Rhythms of Activity and Phototaxis of an Stuarine Crab Larva. *Biological Bulletin,* **158**, 295-303.

Fox J., Weisberg S. (2011) An {R} Companion to Applied Regression. Sage, Second Edition, Thousand Oaks CA.

Gago J., Cabanas J.M., Casas G., Miranda A. (2011) Thermohaline measurements in the continental shelf zone of the NW Iberian Peninsula, 1994–2006. *Climate Research,* **48**, 219-229.

Gardner C., Maguire G.B. (1998) Effect of photoperiod and light intensity on survival, development and cannibalism of larvae of the Australian giant crab *Pseudocarcinus gigas* (Lamarck). *Aquaculture,* **165**, 51-63.

Giménez L. (2006) Phenotypic links in complex life cycles: conclusions from studies with decapod crustaceans. *Integrative and Comparative Biology,* **46**, 615-622.

Giménez L. (2010) Relationships between habitat conditions, larval traits, and juvenile performance in a marine invertebrate. *Ecology,* **91**, 1401-1413.

González-Gurriarán E., Fernández L., Freire J., Muiño R. (1998) Mating and role of seminal receptacles in the reproductive biology of the spider crab *Maja squinado* (Decapoda, Majidae). *Journal of Experimental Marine Biology and Ecology,* **220**, 269-285.

Guerao G., Pastor E., Martin J., Andrés M., Estévez A., Grau A., Duran J., Rotllant G. (2008) The larval development of *Maja squinado* and *M. brachydactyla* (Decapoda, Brachyura, Majidae) described from plankton collected and laboratory-reared material. *Journal of Natural History,* **42**, 2257-2276.

Guerao G., Rotllant G. (2009a) Post-larval development and sexual dimorphism of the spider crab *Maja brachydactyla* (Brachyura: Majidae). *Scientia Marina,* **73**, 797-808.

Guerao G., Rotllant G. (2009b) Survival and growth of post-settlement juveniles of the spider crab *Maja brachydactyla* (Brachyura: Majoidea) reared under individual culture system. *Aquaculture,* **289**, 181-184.

Guerao G., Rotllant G., Anger K. (2010) Characterization of larval moulting cycles in *Maja brachydactyla* (Brachyura, Majidae) reared in the laboratory. *Aquaculture,* **302**, 106-111.

Guerao G., Simeó C.G., Anger K., Urzúa Á., Rotllant G. (2012) Nutritional vulnerability of early zoea larvae of the crab *Maja brachydactyla* (Brachyura, Majidae). *Aquatic Biology,* **16**, 253-264.

Hamasaki K. (2003) Effects of temperature on the egg incubation period, survival and developmental period of larvae of the mud crab *Scylla serrata* (Forskål) (Brachyura: Portunidae) reared in the laboratory. *Aquaculture,* **219**, 561-572.

Hamasaki K., Ogiso Y., Dan S., Kitada S. (2016) Survival, development and growth of larvae of the coconut crab, *Birgus latro*, cultured under different photoperiod conditions. *Aquaculture Research,* **47**, 2506-2517.

Hernández J.E., Palazón-Fernández J.L., Hernández G., Bolaños J. (2012) The effect of temperature and salinity on the larval development of *Stenorhynchus seticornis* (Brachyura: Inachidae) reared in

the laboratory. *Journal of the Marine Biological Association of the United Kingdom,* **92**, 505-513.

Hoang T., Barchiesis M., Lee S.Y., Keenan C.P., Marsden G.E. (2003) Influences of light intensity and photoperiod on moulting and growth of *Penaeus merguiensis* cultured under laboratory conditions. *Aquaculture,* **216**, 343-354.

Iglesias J., Sánchez F.J., Moxica C., Fuentes L., Otero J.J., Pérez J.L. (2002) Datos preliminares sobre el cultivo de larvas y juveniles de centolla *Maja squinado* Herbst, 1788 en el Centro Oceanográfico de Vigo del Instituto Español de Oceanografía. *Boletín del Instituto Español de Oceanografía,* **18**, 25-30.

Johns D.M. (1981) Physiological studies on *Cancer irroratus* larvae. I. Effects of temperature and salinity on survival, development rate and size. *Marine Ecology Progress Series,* **5**, 75-83.

Minagawa M. (1994) Effects of photoperiod on survival, feeding and development of larvae of the red frog crab, *Ranina ranina*. *Aquaculture,* **120**, 105-114.

Pechenik J.A. (2006) Larval experience and latent effects-metamorphosis is not a new beginning. *Integrative and Comparative Biology,* **46**, 323-333.

Penha-Lopes G., Rhyne A.L., Lin J., Narciso L. (2005) The larval rearing of the marine ornamental crab, *Mithraculus forceps* (A. Milne Edwards, 1875) (Decapoda: Brachyura: Majidae). *Aquaculture Research,* **36**, 1313-1321.

R Development Core Team (2015) R: A language and environment for statistical computing. R Foundation for Statistical Computing, Vienna, Austria.

Rabbani A.G., Zeng C. (2005) Effects of tank colour on larval survival and development of mud crab *Scylla serrata* (Forskål). *Aquaculture Research,* **36**, 1112-1119.

Reed P.H. (1969) Culture Methods and Effects of Temperature and Salinity on Survival and Growth of Dungeness Crab (*Cancer magister*) Larvae in the Laboratory. *Journal of the Fisheries Research Board of Canada,* **26**, 389-397.

Rhyne A.L., Penha-Lopes G., Lin J. (2005) Growth, development, and survival of larval *Mithraculus sculptus* (Lamark) and *Mithraculus forceps* (A. Milne Edwards) (Decapoda: Brachyura: Majidae): economically important marine ornamental crabs. *Aquaculture,* **245**, 183-191.

Rotllant G., González-Gurriarán E., Fernández L., Benhalima K., Ribes E. (2007) Ovarian maturation of the multi-spawning spider crab *Maja brachydactyla* (Decapoda: Majidae) with special reference to yolk formation. *Marine Biology,* **152**, 383-394.

Rotllant G., Moyano F.J., Andrés M., Estévez A., Díaz M., Gisbert E. (2010) Effect of delayed first feeding on larval performance of the spider crab *Maja brachydactyla* assessed by digestive enzyme activities and biometric parameters. *Marine Biology,* **157**, 2215-2227.

Rotllant G., Roque A., Solé M., Gisbert E. (2013) Assessment of the effects of confinement in the spider crab *Maja brachydactyla* Blass, 1922 broodstock. *Aquaculture Research,* **44**, 412-426.

Rotllant G., Simeó C.G., Macià G., Estévez A. (2014) High environmental salinity reduces the reproductive potential of the spider crab *Maja brachydactyla* (Decapoda, Majidae). *Marine Ecology*, n/a-n/a.

Rotllant G., Simeó C.G., Macià G., Estévez A. (2015) High environmental salinity reduces the reproductive potential of the spider crab *Maja brachydactyla* (Decapoda, Majidae). *Marine Ecology,* **36**, 496-505.

Simeó C.G., Kurtz K., Chiva M., Ribes E., Rotllant G. (2010) Spermatogenesis of the Spider Crab *Maja brachydactyla* (Decapoda: Brachyura). *Journal of Morphology,* **271**, 394-406.

Simeó C.G., Kurtz K., Rotllant G., Chiva M., Ribes E. (2009) Sperm ultrastructure of the spider crab *Maja brachydactyla* (Decapoda: Brachyura). *Journal of Morphology,* **271**, 407-417.

Sulkin S.D., McKeen G.L. (1989) Laboratory study of survival and duration of individual zoeal stages as a function of temperature in the brachyuran crab *Cancer magister*. *Marine Biology,* **103**, 31-37.

Thorson G. (1964) Light as an ecological factor in the dispersal and settlement of larvae of marine bottom invertebrates. *Ophelia,* **1**, 167-208.

Torres G., Giménez L., Anger K. (2008) Cumulative effects of low salinity on larval growth and biochemical composition in an estuarine crab, *Neohelice granulata*. *Aquatic Biology,* **2**, 37-45.

Ulikowski D., Krzywosz T. (2004) The impact of photoperiod and stocking density on the growth and survival of narrow-clawed crayfish (*Astacus leptodactylus* Esch.) larvae. *Archives of Polish Fisheries,* **12**, 81-86.

Verísimo P., Bernárdez C., González-Gurriarán E., Freire J., Muino R., Fernández L. (2011) Changes between consecutive broods in the fecundity of the spider crab, *Maja brachydactyla*. *Ices Journal of Marine Science,* **68**, 472-478.

Viherluoto M., Viitasalo M. (2001) Effect of light on the feeding rates of pelagic and littoral mysid shrimps: a trade-off between feeding success and predation avoidance. *Journal of Experimental Marine Biology and Ecology,* **261**, 237-244.

Villamizar N., Blanco-Vives B., Migaud H., Davie A., Carboni S., Sánchez-Vázquez F.J. (2011) Effects of light during early larval development of some aquacultured teleosts: A review. *Aquaculture,* **315**, 86-94.

Wang F., Dong S., Dong S., Huang G., Zhu C., Mu Y. (2004) The effect of light intensity on the growth of Chinese shrimp *Fenneropenaeus chinensis*. *Aquaculture,* **234**, 475-483.

Wickins J.F., O'C Lee D. (2002) *Crustacean Farming, Ranching and Culture, 2nd edition,* Wiley-Blackwell, Oxford.

CHAPTER 7.

On the settlement of the common spider crab *Maja brachydactyla* Balss, 1922 (Brachyura: Majidae): testing the conspecific culture, exudates and substrata

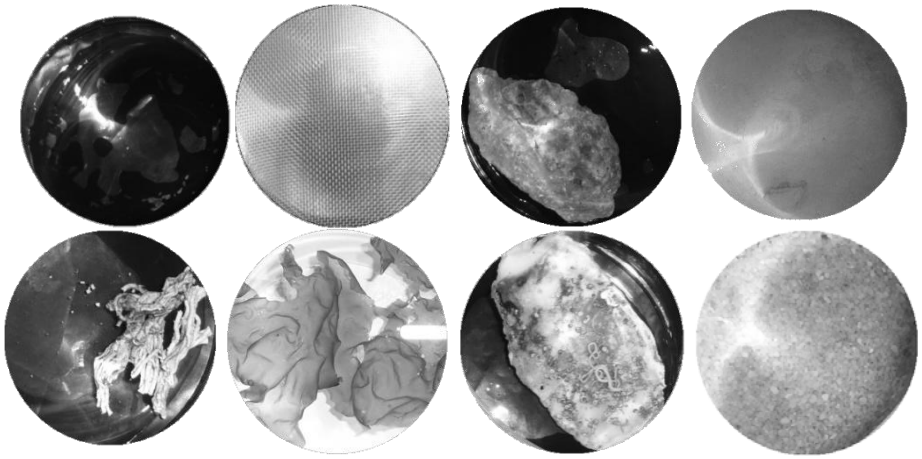

Factors influencing successful settlement of the common spider crab *Maja brachydactyla* Balss, 1922 (Brachyura: Majidae): impacts of individual vs conspecific culture, adult exudates and settlement substrates

Diego Castejón[1,2]*, Guiomar Rotllant[2], and Guillermo Guerao[3]

[1]Subprograma Cultius Aquàtics, IRTA, Ctra. de Pobre Nou, Km 5.5. 43540, Sant Carles de la Ràpita, Tarragona, Spain

[2]CSIC, Institut de Ciències del Mar, Passeig Marítim de la Barceloneta 37-49. 08003 Barcelona (Spain).

[3]PS Fabrai Puig 344. 08028 Barcelona (Spain).

Short title: *Maja brachydactyla* settlement conditions

***Corresponding author**: Diego Castejón. E-mail: diego.castejon.dcb@gmail.com; phone: +34 681 154 398; postal address: Institut de Ciències del Mar, Passeig Marítim de la Barceloneta 37-49. 08003 Barcelona (Spain).

Abstract.

The common spider crab *Maja brachydactyla* (Balss, 1922) is an important wild marine resource in many countries in the NE Atlantic region that also has potential in aquaculture. The larval cycle has been replicated successfully in captivity, with highest mortality evident during larval settlement and metamorphosis to first juvenile stages. As an approximation to understanding natural settlement requirements of this species, we examined the need for individual culture to produce first juveniles in the hatchery. In addition, we assessed whether presence of adult exudates and/or a number of different potential settlement substrates (natural vs. artificial) influenced settlement rates under laboratory conditions. Our data demonstrate that *M. brachydactyla* megalopae cultured in the presence of conspecifics showed higher survival rates and shorter time to juvenile metamorphosis stage when compared with under individual culture. Presence of adult exudates did not influence settlement rates or time to juvenile metamorphosis. Survival rates were not different between control conditions (absence of settlement substrate), artificial substrata (100 to 1,000 µm nylon mesh) or natural substrates except for "mud" substrate where no larvae survived to first juvenile stage in this treatment. Duration of the megalopa stage was also not influenced by type of settlement substrate added (natural or artificial) or to a control (no substrate). Results in the present study indicate that *M. brachydactyla* culture will not require provision of special requirements since communal larval rearing is an efficient and low cost viable strategy and specific larval settlement substrates are required to produce juveniles.

Keywords: *Maja brachydactyla*; megalopae; settlement; adult exudates; substrata

1. Introduction

It is widely currently acknowledged that 'larval settlement' is one of the major factors that influences effective natural recruitment of coastal marine species that possess a dispersive larval phase (Giménez, 2010; Pawlik, 1992; Rodríguez, Ojeda, Inestrosa, 1993). Settlement is generally defined as the overall transition from pelagic larval phase to benthic juvenile (Pawlik, 1992). So for species that display such complex life cycles it is important to understand how pre- and post settlement processes shape population persistence (Anger, 2001; 2006). Settlement can be a complex process that requires finding appropriate settlement sites and subsequent morphogenetic changes that are required for a new benthic lifestyle (Rodríguez, Ojeda, Inestrosa, 1993). Recognition of appropriate settlement sites for most marine species requires chemical and physical recognition systems that facilitate colonization of favourable juvenile habitat followed by stimulation of metamorphosis. For extensive reviews of these processes see Forward, Tankersley, Rittschof (2001) and Anger (2006).

Recognition of optimal settlement sites can include detection of the tridimensional shape of settlement structure (e.g. natural pebbles, mud etc.) and chemical compounds (e.g. conspecific odours, estuarine compounds etc.) associated with favourable post-larval habitat (Diele, Simith, 2007; Forward, Tankersley, Rittschof, 2001; Kopin, Epifanio, Nelson, Stratton, 2001; Welch, Rittschof, Bullock, Forward, 1997). Adult odour (referred to here as exudates) has been demonstrated to be one of the most important stimuli promoting metamorphosis to first juvenile stage in many brachyuran larvae (Andrews, Targett, Epifanio, 2001; Diele, Simith, 2007; Fitzgerald, Forward Jr, Tankersley, 1998; Forward, Tankersley, Rittschof, 2001; Gebauer, Walter, Anger, 1998; Gebauer, Paschke, Anger, 2002; Kopin, Epifanio,

Nelson, Stratton, 2001; Simith, Diele, 2008; Simith, Diele, Abrunhosa, 2010; Weber, Epifanio, 1996). Adult exudates therefore may act as a trigger for larvae to settle. For brachyuran species, settlement is closely linked with metamorphosis from megalopa stage to first juvenile stage (Forward, Tankersley, Rittschof, 2001). Delaying metamorphosis can affect post-larvae performance due to a requirement for additional energy for larval maintenance (Gebauer, Paschke, Anger, 2003; Simith, Diele, Abrunhosa, 2013) as occurs in some other animal phyla, including some vertebrates (Pechenik, 2006). Consequences resulting from delayed metamorphosis can also be observed at the population level (Giménez, 2006; 2010) and can also impact production in the aquaculture industry.

The common spider crab *Maja brachydactyla*(Balss, 1922) is a brachyuran that supports important wild fisheries in the European NE Atlantic region (FAO, 2014). This species has two pelagic zoeal stages and a single megalopa stage. It also has an intermediate pelagic-benthic lifestyle prior to metamorphosis to the first juvenile stage (Guerao, Rotllant, Anger, 2010; Guerao, Pastor, Martin, Andrés, Estévez, Grau, Duran, Rotllant, 2008). Benthic *M. brachydactyla* juveniles and adults are found mostly on sandy and rocky seafloor areas, although they can also use mud-sand, gravel and maërl substrate (Le Foll, 1993). Juveniles and adults are segregated spatially however, with juveniles usually inhabiting bottoms from 0 to 30 meters depth while adults migrate annually from 50 - 200 meters depth to less than 30 meters depth (Corgos, Sánchez, Freire, 2010; Corgos, Bernárdez, Sampedro, Verísimo, Freire, 2011; Le Foll, 1993). Currently, natural settlement and recruitment sites have not been defined nor has the habitat required by early juvenile stage (< 50 mm) (Corgos, Bernárdez, Sampedro, Verísimo, Freire, 2011; Le Foll, 1993).

Apart from a general ecological interest in understanding the settlement requirements of brachyuran species, the critical nature of developing efficient larviculture systems for the crustacean aquaculture industry will require developing and optimizing large-scale *in vitro* juvenile production technologies to allow farming (Browdy, 1998; Hamasaki, Obata, Dan, Kitada, 2011; Silva, Cottens, Ventura, Boeger, Ostrensky, 2012; Zmora, Findiesen, Stubblefield, Frenkel, Zohar, 2005). For these reasons, our objective here was to investigate the influence of adult exudates and different settlement substrates (natural vs. artificial) on larval settlement in the common spider crab,*M. brachydactyla*. We also examined if individual culture is required in the laboratory to allow larvae to reach the juvenile crab stage.

2. Materials and methods

2.1 Broodstock maintenance

Live *M. brachydactyla* broodstock were captured from the northwest Iberian Peninsula coast and transported to Sant Carles de la Ràpita (CADEMAR S.COOP.R.L., Tarragona, Spain), following which specimens were transferred to the Institut de Recerca i Tecnologia Agroalimentàries facilities located in Ebro Delta (Tarragona, Spain) in April 2014. The broodstock were housed in 2,000 L cylindrical tanks and maintained at a sex ratio of six females per male. Constant environmental parameters were maintained at: water renewal rate (3.5 m^3 h^{-1}), temperature (18 ± 1 °C, recirculation unit system), salinity (35 ± 1psu, filtered seawater), photoperiod (12 h light: 12 h dark, programmed timer) and light intensity (25 lux, fluorescent tubes). Adult diet consisted basically of fresh and frozen mussels (*Mytilus* sp.).

2.2 Larval culture system

The system employed for larviculture was a modification of a culture system employed previously for larval culture at a small scale under experimental conditions, see Castejón, Rotllant, Giménez, Torres, Guerao (2015). Larvae were reared in 600 mL glass beakers (filled with 500 mL of filtered seawater) placed inside 360 L tanks (96 x 96 x 40 cm) used as incubation chambers. Culture parameters employed were: temperature (21 ± 1 °C, recirculation unit system), salinity (35 ± 1psu, filtered seawater), photoperiod (12 h light: 12 h dark, programmed timers) and light intensity (1,000 lux, LED lights) were maintained as constants. Water temperature was measured daily with a portable meter (precision: 0.1 °C; WTW ProfiLine Oxi 3210, Weilheim, Germany). Larvae were transferred daily to beakers with fresh food (*Artemia* sp. Kellogg, 1906 nauplii and metanauplii fed *ad libitum*, INVE Aquaculture Nutrition, Salt Lake UT, USA) with clean water under the same environmental conditions. Larvae were maintained under these conditions until they reached megalopa stage.

Experiments were initiated using active and swimming megalopae within 15 h after their molt. In each experiment the megalopae employed were obtained from a single different brood. Experiments (except for the *Conspecific density* experiment, see below) were started with an initial density of 20 megalopae L^{-1} (10 megalopae per glass beaker) and this was continued until all had moulted to first juvenile stage or had died. In all experiments fordaily exchange of water and food, megalopae were transported in beakers with the same treatment conditions. Death of individuals was confirmed by absence of movement of their appendages and heart. Observations were conducted with a Nikon SMZ800 stereomicroscope.

2.3 Experimental design

Response variables studied in all experiments included; survival to first juvenile stage and duration of the megalopa stage. Four experiments were undertaken;

2.3.1 Conspecific density. Individual rearing has been recommended for studies of settlement in both Anomuran and Brachyuran taxa (Dawirs, 1982; Fernandez, Iribarne, Armstrong, 1994; Forward, Tankersley, Rittschof, 2001; Forward, De Vries, Rittschof, Frankel, Bischoff, Fisher, Welch, 1996). This approach however, is both expensive in time and the materials required from an aquaculture point of view. For this reason, we first evaluated the effectiveness of conspecific versus individual rearing of megalopa. We employed two treatments; 1) individual rearing - megalopae were reared individually in crystal dishes filled with 50 mL of seawater, with 100 replicates employed; 2) conspecific rearing -megalopae were reared in glass beakers filled with 500 mL of seawater with ten individuals added, ten replicates were used. Crystal dishes were used exclusively in this experiment to maintain the same relative volume of seawater per larvae as that used in the conspecific treatment.

2.3.2 Effect of adult exudates. In this experiment we studied the influence of the presence/absence of adult exudates in culture water. We used seawater obtained directly from the broodstock tank as source of adult exudates. Two treatments were employed; 1) Control - megalopae were reared in clean, filtered seawater; 2) Exudates treatment - megalopae were reared in seawater taken from the broodstock tank. Ten replicates per treatment were employed.

2.3.3 Nylon mesh as settlement substrate. Nylon mesh is a material easy to obtain that potentially facilitates megalopae crawling after settlement and metamorphosis to first juvenile stage. Earlier studies have used 35 L mesh bottom (150

µm) PVC baskets(Andrés, Estévez, Rotllant, 2007; Andrés, Estévez, Anger, Rotllant, 2008; Andrés, Rotllant, Sastre, Estevez, 2011; Guerao, Rotllant, 2009) and concluded that a mesh size of 500 µm appeared to improve juvenile survival (pers. comm.). In the current experiment this hypothesis was tested using white nylon mesh (7 x 15 cm) varying in mesh size as benthic substrate. Four treatments were employed;1) Control, - megalopae were reared without substrate; 2) mesh size -100 µm; 3) mesh size -500 µm; 4) mesh size -1,000µm. Prior to start of the experiment, all nylon mesh was first disinfected in bleach baths and then rinsed repeatedly in filtered seawater. Eight replicates were used per treatment.

2.3.4 Natural materials as substrate. This experiment investigated whether benthic substrate type influenced megalopa settlement and employed ten different substrate treatments. 1) Control - no substrate added. 2) Nylon mesh - nylon mesh (7 x 15 cm and 500 µm mesh size) was added as an example of an artificial substrate (this treatment also permitted corroboration of results obtained in the previous mesh size experiment). 3) Stone - small, coarse, sedimentary stones (6 ±1cm size) were added. 4) Sand- bottom of glass beakers were covered with a layer of coarse sand (1,700 ± 500 µm grain size) ca. 5 mm depth. 5) Mud - bottom of glass beakers were covered with a layer of mud (35 % of volume composed by 250 ± 80 µm grain size, 65 % remaining volume composed by smaller particles) ca. 5 mm depth. 6) Oyster (smooth) - shells of young oysters with a smooth and clean surface were added. 7) Oyster (fouled) - shells of young oysters with a coarse and fouled surface (calcareous tubes of annelids) were added. 8) Annelids + biofilms - set of calcareous tubes containing living annelids and covered by biofilms of micro-algae were added. 9) Chaetomorpha - living, filamentous blades of *Chaetomorpha* spp. were added 10) Ulva - living, laminar blades of *Ulva* spp.

were added. Prior to the start of the experiment, sand and nylon mesh were disinfected in bleach baths and then rinsed repeatedly with filtered seawater. Stone, mud and oyster shells were first sterilized by autoclaving. Annelid tubes covered in biofilms, as well as blades of *Chaetomorpha* spp. and *Ulva* spp. were added directly to glass beakers from a natural source. Five replicates were employed per treatment.

2.4 Statistical Analysis

In the *Conspecific density* experiment where only a single specimen was added to the test dishes, survival was either measured as either - 100 % or 0 %. For this reason, in this experiment, survival was analyzed using a Pearson's Chi-squared test with Yates' continuity correction; while duration of megalopa stage was analyzed using a Kruskal-Wallis test. Remaining experiments were analyzed using one-way ANOVA applying different treatments as the factor. We employed a Tukey-HSD test to assess the significance of differences observed among treatments. Normality and homogeneity were first checked using Shapiro-Wilk and Levene tests, respectively after survival data were transformed applying an arcsine of square root function. Kruskal-Wallis tests were applied when data did not show normality or homogeneity of variance. The critical level (α) to reject the null hypothesis was set at $P < 0.05$.

All statistical analyses were conducted in R version 3.2.0 (R Development Core Team, 2015). The R package «MASS 7.3-40» was also used for Pearson's Chi-squared tests (Venables, Ripley, 2002). The R package «car 2.0-25» (Fox, Weisberg, 2011) was used for Levene Tests.

3. Results

3.1 Conspecific density effect.

Survival to first juvenile stage under rearing with conspecifics doubled the survival rate compared with individual rearing. The difference however, was not significant ($X^2_1 = 2.83$, $p = 0.09$; Fig. 1). Duration of megalopa stage was significantly shorter under communal rearing with 6.4 ± 0.2 days (average ± SE) compared with individual rearing that required 7.5 ± 0.3 days ($X^2_1 = 5.82$, $p < 0.05$; Fig. 1).

3.2 Adult exudate effect.

No significant differences were observed for survival rate to first juvenile stage ($X^2_1 = 0.30$, $p = 0.58$) or duration of the megalopa stage ($X^2_1 = 0.07$, $p = 0.80$; Fig. 2) among treatments. Survival to first juvenile (average ± SE) was 14 ± 3 % and the duration of megalopa stage was 5.9 ± 0.2 days.

3.3 Nylon mesh effect.

The highest survival rate to first juvenile stage was 11 ± 2 % with the 500 µm mesh size, while in remaining treatments average survival rate ranged from 4 to 5 %, but there were no significant differences among remaining treatments ($X^2_3 = 5.96$, $p = 0.11$; Fig. 3). Duration of megalopa stage was also not different among treatments and averaged 7.3 ± 0.4 days (ANOVA: $F_{3,16} = 1.71$, $p = 0.21$; Fig. 3).

3.4 Natural materials effect.

Significant differences were evident for survival rate to first juvenile stage among treatments in this study ($p < 0.001$; Fig. 4). Highest survival rate was achieved in the sand treatment (80 ± 6 %), following which survival rate decreased among

treatments in the following way; *Ulva* (76 ± 5 %) > control (74 ± 7 %) > *Chaetomorpha* (68 ± 15 %) > annelids + biofilm (58 ± 7) > oyster (smooth) (54 ± 16 %) > nylon mesh (53 ± 6 %) > oyster (fouled) (44 ± 10 %) and > stone (38 ± 13 %). The remaining substrates (excepting mud) had spaces between the lower substrate surface and the bottom surface of the glass beakers, where dead megalopa were observed frequently. The lowest survival rate was evident in the mud treatment with 0 % at the third day and none individual reaching the first juvenile stage. Average duration of megalopa stage ranged from 5.8 ± 0.1 days in the sand treatment to 6.9 ± 0.2 days in the nylon mesh treatment, but no significant differences for average duration of megalopa were detected among treatments.

4. Discussion

Results of the present study confirm that *M. brachydactyla* can show high survival over a relatively short development cycle to metamorphosis when cultured with conspecifics under *in vitro* conditions in the laboratory. This contrasts with results of experiments on some other brachyuran species (e.g. *Callinectes sapidus*, *Metacarcinus magister* or *Carcinus maenas*) where co-culture resulted in very high mortality due to the competition among individual megalopa and high cannibalism rates (Dawirs, 1982; Fernandez, Iribarne, Armstrong, 1994; Forward, Tankersley, Rittschof, 2001; Forward, De Vries, Rittschof, Frankel, Bischoff, Fisher, Welch, 1996), and so culture practices for these species recommend that megalopa be reared separately. In the present study, higher survival rates and short time to metamorphosis under conspecific rearing support results of some earlier studies that have shown that *M. brachydactyla* can tolerate densities in a range from 10 to 100 larvae L^{-1}(Andrés, Estévez, Rotllant, 2007). Considering that individual culture requires more infrastructure and significantly higher

labour requirements than mass culture, good survival rates observed under mass culture for *M. brachydactyla* allowed us to use this more efficient approach in subsequent experiments in the current study . This has also been observed in certain other brachyuran species (Gebaueret al. 2002; Diele and Simith 2007; O'Connor 2007; Steinberg et al. 2007; Simith and Diele 2008; Steinberg et al. 2008).

Presence of adult exudates in culture water did not significantly influence survival rate to first juvenile stage or duration of the megalopa stage in the current study. Settlement is a multifactorial phenomenon that can involve both biological and physical factors (Eggleston, Armstrong, 1995; Émond, Sainte-Marie, Galbraith, Bêty, 2015; Figueiredo, Penha-Lopes, Narciso, Lin, 2008; Giménez, 2010; Rodríguez, Ojeda, Inestrosa, 1993). A factor that has been identified in certain brachyuran taxa to influence this process is presence of adult odors in culture water, where presence stimulates metamorphosis to first juvenile (Andrews, Targett, Epifanio, 2001; Diele, Simith, 2007; Fitzgerald, Forward Jr, Tankersley, 1998; Forward, Tankersley, Rittschof, 2001; Gebauer, Walter, Anger, 1998; Gebauer, Paschke, Anger, 2002; Kopin, Epifanio, Nelson, Stratton, 2001; Simith, Diele, 2008; Simith, Diele, Abrunhosa, 2010; Weber, Epifanio, 1996). Presence of adult exudates in culture water in the present study however, did not impact *M. brachydactyla* megalopa settlement rate. Potentially, this may reflect the observation that adult and early juveniles in the wild do not share the same habitats as has been observed for *Callinectes sapidus* or *Carcinus maenas* (Forward Jr, Frankel, Rittschof, 1994; Zeng, Naylor, Abello, 1997). Field studies have indicated that adult and juvenile *M. brachydactyla* are segregated spatially (Corgos, Sánchez, Freire, 2010; Corgos, Bernárdez, Sampedro, Verísimo, Freire, 2011; Le Foll, 1993). Corgos et al. (2011) postulated a scenario where juvenile recruitment occurs in

shallow coastal benthic areas of less than 5 meters depth, following which post-metamorphic individuals migrate to depths between 5 and 15 meters before migrating to greater depths when the adult stage is reached. So for *M. brachydactyla* juveniles in the wild, presence of adult odours in the water may not trigger settlement because juveniles and adults have different habitat requirements and so metamorphic juveniles do not have access to pheromonal cues from adults in the surrounding habitat that allow them to detect favourable settlement environments.

During experiments conducted for the study we observed the *M. brachydactyla* megalopae crawling over both the 500 and 1,000 μm nylon mesh, but they did not settle on the surfaces (we had expected that nylon mesh would provide an ideal surface for megalopae attachment facilitating settlement). The structure of artificial substrate has in some earlier studies been shown to influence larval settlement but not however, in brachyurans even where its tridimensional structure simulates real habitat (see Table 1 for more details).

Corgos, Bernárdez, Sampedro, Verísimo, Freire (2011) postulated that recruitment *M. brachydactyla* in occurs in shallow water with rocky bottoms after which approximately one year juveniles then move to depths between 5 and 15 meters. Le Foll (1993) reported that juveniles (carapace length of 50 mm or greater) mainly inhabit seafloors composed of gravels, rocks and/or maërls, while stable isotope analysis suggests that juveniles larger than 60 mm often move between sandy and rocky seafloors (Freire, Carabel, Verísimo, Bernárdez, Fernández, 2009). These observations led us to simulate this in captivity varying habitat form and different types of substrates, this was because habitat complexity has been shown to affect settlement in anomuran (Tapella, Romero, Stevens, Buck, 2009; Tapella, Sotelano, Romero, Lovrich, 2012) and

brachyuran species (Gebauer, Paschke, Anger, 2002; O'Connor, 2007; Steinberg, Krimsky, Epifanio, 2008) under laboratory conditions.

The highest megalopa mortality rate was observed when mud was used as a substrate with no individuals reaching first juvenile stage. In contrast, for the brachyuran *Neohelice granulata* (as *Chasmagnathus granulata*) metamorphosis to first juvenile stage is induced by presence of mud (Gebauer, Walter, Anger, 1998), as is the case with *Ucides cordatus* (Diele, Simith, 2007). These species naturally inhabit muddy benthic environments while *M. brachydactyla* juveniles and adults are found on sandy to rocky seafloors. Different experimental responses to the presence of mud substrate is likely to correspond with different effects of historical adaptation to their preferred benthic habitats. Moreover, when we observed mud attached to the body surfaces of *M. brachydactyla* megalopae high mortality rates may have resulted from impaired respiratory activity or perhaps toxicity of the attached material.. Larval mortality was also high when oyster shells, stones, annelid tubes or nylon mesh was used as substrate in the experiment even though we observed megalopae crawling over these surfaces or using them as refuges. We suggest that high mortality could be linked to the narrow spaces created between the glass of the beakers and the lower surface of the substrate, where larvae presumably can be trapped and/or damaged.

Higher survival rates were observed in those treatments that lacked narrow spaces i.e. in the control, coarse sand and algal substrate types with the highest survival rate observed in the control treatment confirming results of an earlier study that as a consequence had recommended flat bottom surfaces for settlement of *M. brachydactyla* larvae (Palma, Correia, Andrade, 2008). Earlier studies had also shown that *M. brachydactyla* juvenile survival was not influenced by presence of macroalgae

(Domingues, Alaminos, 2008). Rhyne et al. (2005) linked high settlement rate of a majid (*Mithraculus forceps*) regardless of benthic substrate type or specific chemical cues for settlement with their naturally wide distribution range. In parallel, *M. brachydactyla* also has an extensive natural distribution along the Atlantic northeastern European coast (Abelló, García Raso, Guerao, Salmerón, 2014)where there is a wide diversity in benthic substrates present where *M. brachydactyla* can complete metamorphosis rapidly from megalopa to juvenile stage. This would argue for potential for high flexibility in their settlement requirements.

Ability to produce high quality juveniles in hatcheries is one of the major requirements and constraints on developing many crustaceans for the aquaculture industry and can also impact restocking programs for species that have been over-fished (Browdy, 1998; Hamasaki, Obata, Dan, Kitada, 2011; Le Vay, Carvalho, Quinitio, Lebata, Ut, Fushimi, 2007; Planas, Cunha, 1999; Silva, Cottens, Ventura, Boeger, Ostrensky, 2012; Zmora, Findiesen, Stubblefield, Frenkel, Zohar, 2005). Our results demonstrate that production of *M. brachydactyla* juveniles in hatcheries is unlikely to require special infrastructure or technologies and can be accomplished successfully in relatively simple installations without a need for specific benthic substrates or chemical cues in larval settlement tanks. Moreover, juveniles can be produced in communal culture conditions reducing production costs significantly. The main factor that needs to be avoided is formation of narrow spaces between benthic settlement surfaces that can trap or damage larvae as the transform into the juvenile phase..

5. Acknowledgements

The Spanish Ministry of Economy and Competitiveness funded bench fees during the INIA project [grant number RTA2011-00004-00-00] to G.G and a predoctoral fellowship to D.C. [FPI-INIA]. We thank hatchery technicians at IRTA in Sant Carles de la Ràpita (David Carmona, Glòria Macià, Magda Monllaó and Francesc X. Ingla) for maintaining broodstock and the setup used for the culture rearing system. We are also grateful to Professor Peter Mather for the critical reading of the manuscript.

Table 1. Influence of artificial substrata on the settlement of brachyuran species on laboratory conditions. The substrata can influence the survival (S), duration of megalopa stage (D) or not influence in these parameters (-).

Species	Family Superfamily	Substrata	Influence	**References:**
Sesarma curacaoense De Man, 1982	Sesarmidae Grapsoidea	nylon gauges	S / -	(Gebauer, Paschke et al. 2002)
Hemigrapsus sanguineus (De Hann, 1835)	Varunidae Graposidea	nylon mesh	S / D	(O'Connor 2007) (Steinberg, Krimsky et al. 2008)
Neohelice (=*Chasmagnathus*) *granulata* (Dana, 1851)	Varunidae Grapsoidea	glass beds nylon gauze nylon threads	- / - - / - - / D	(Gebauer, Walter et al. 1998)
Uca pugnax (S. I. Smith, 1870)	Ocypodidae Ocypodoidea	glass beds	- / -	(O'Connor and Gregg 1998)
Ucides cordatus (Linnaeus, 1763)	Ocypodidae Ocypodoidea	nylon mesh	- / -	(Diele and Simith 2007)
Panopeus herbstii H. Milne Edwards,1834	Panopeidae Xanthoidea	plastic sheeting rock/shell mimic	- / - - / -	(Weber and Epifanio 1996)
Callinectes sapidus (Rathbun, 1896)	Portunidae Portunoidea	artificial plants	- / -	(Forward, De Vries et al. 1996)
Maja brachydactyla Balss, 1922	Majidae Majoidea	nylon mesh	- / -	Present study

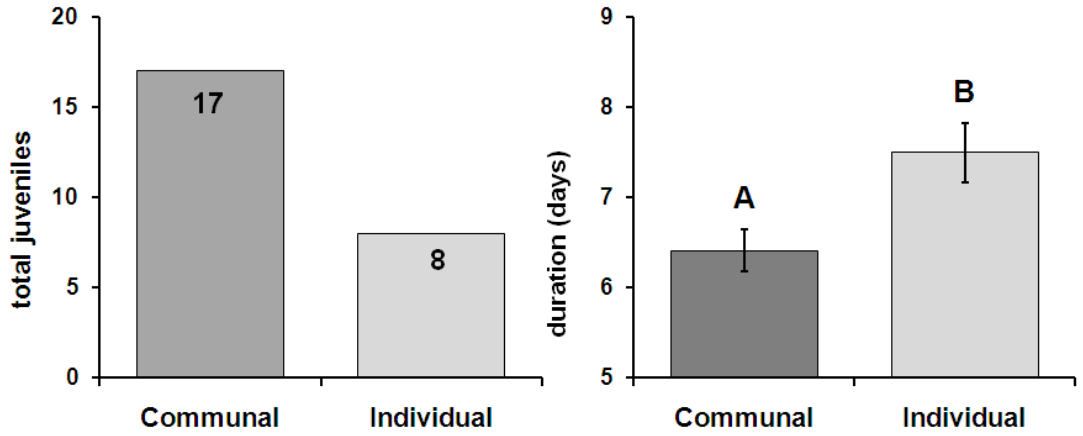

Figure 1. *Maja brachydactyla*. Communal rearing (10 megalopae per beaker, 10 replicates) and individual rearing (1 megalopae per crystallizer dish, 100 replicates). Survival to first juvenile stage (left) and duration of the megalopa stage (average ± SE, right).

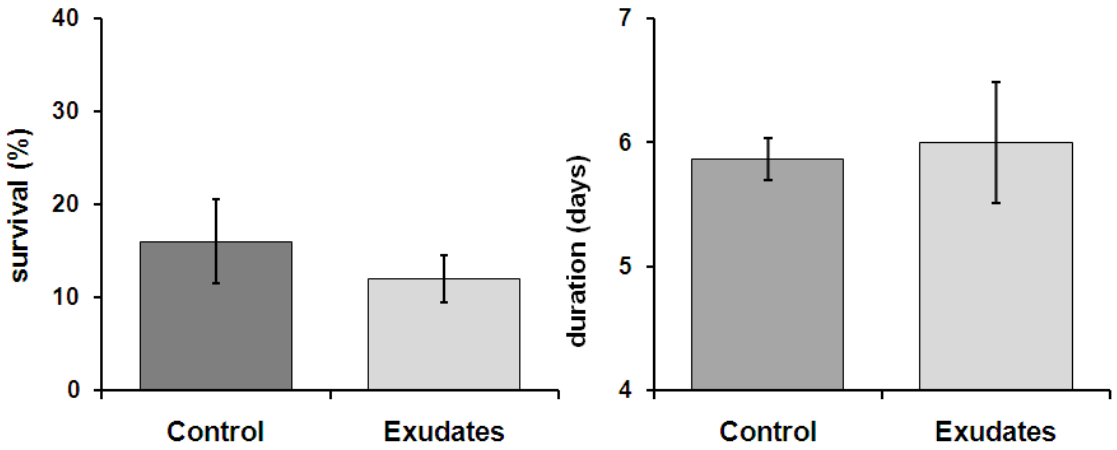

Figure 2. *Maja brachydactyla*. Influence of the adult exudates. Average survival (± SE) to first juvenile stage (left) and duration of the megalopa stage (right) in absence of adult exudates (control) and in presence of adult exudates (exudates).

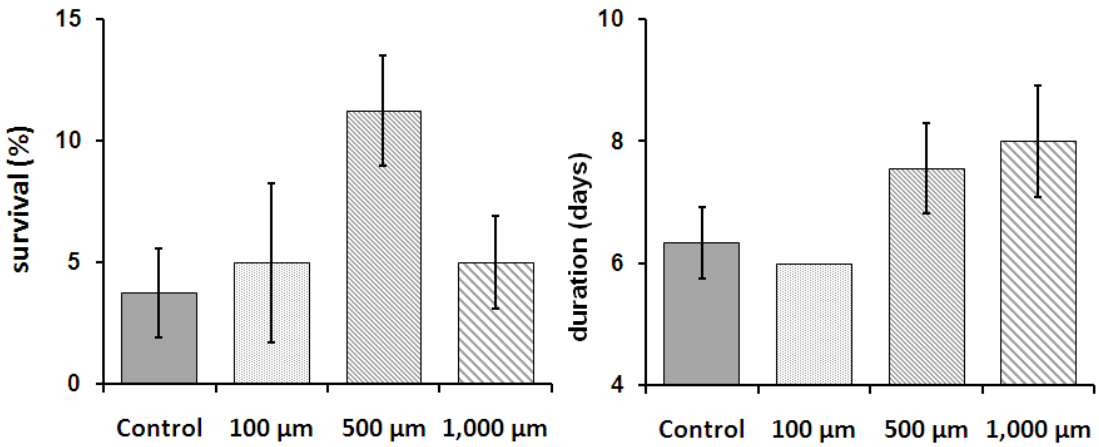

Figure 3. *Maja brachydactyla*. Nylon meshes as substrata. Average survival (± SE) to first juvenile stage (left) and duration of the megalopa stage (right). The control treatment indicates absence of substrate.

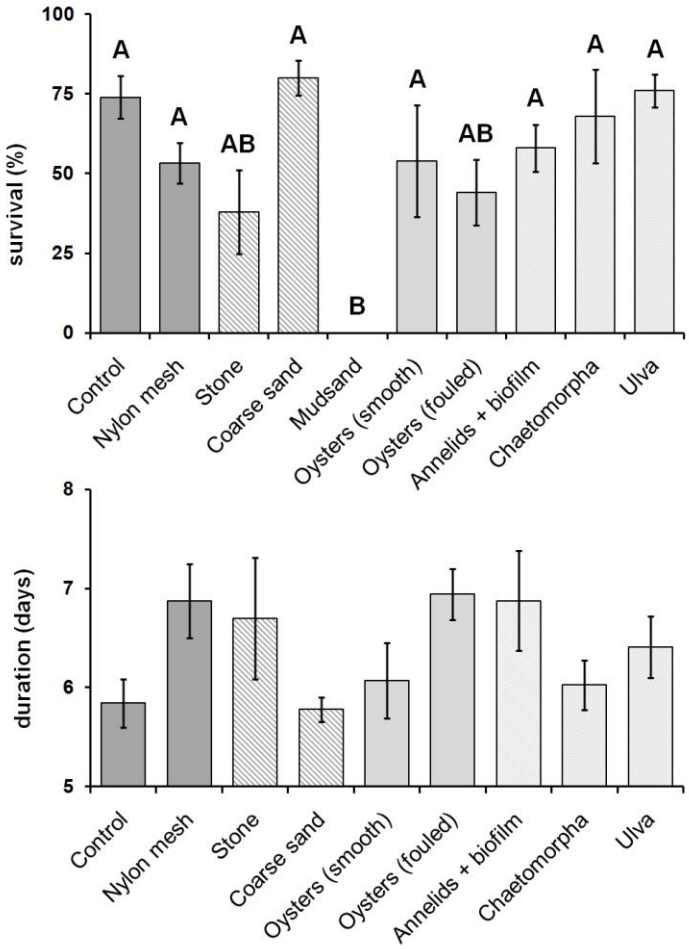

Figure 4. *Maja* brachydactyla. Natural materials as substrata. Average survival (± SE) to first juvenile stage (up) and duration of the megalopa stage (down). The control treatment indicates absence of substrate.

6. Bibliography

Abelló, P., García Raso, J.E., Guerao, G., Salmerón, F., 2014. *Maja brachydactyla* (Brachyura: Majidae) in the western Mediterranean. Marine Biodiversity Records. 7.

Andrés, M., Estévez, A., Rotllant, G., 2007. Growth, survival and biochemical composition of spider crab *Maja brachydactyla* (Balss, 1922) (Decapoda: Majidae) larvae reared under different stocking densities, prey:larva ratios and diets. Aquaculture. 273, 494-502.

Andrés, M., Estévez, A., Anger, K., Rotllant, G., 2008. Developmental patterns of larval growth in the edible spider crab, *Maja brachydactyla* (Decapoda: Majidae). J. Exp. Mar. Biol. Ecol. 357, 35-40.

Andrés, M., Rotllant, G., Sastre, M., Estevez, A., 2011. Replacement of live prey by formulated diets in larval rearing of spider crab *Maja brachydactyla*. Aquaculture. 313, 50-56.

Andrews, W.R., Targett, N.M., Epifanio, C.E., 2001. Isolation and characterization of the metamorphic inducer of the common mud crab, *Panopeus herbstii*. J. Exp. Mar. Biol. Ecol. 261, 121-134.

Anger, K., 2001. The Biology of Decapod Crustacean Larvae. A.A. Balkema Publishers, Rotterdam.

Anger, K., 2006. Contributions of larval biology to crustacean research: a review. Invertebrate Reproduction & Development. 49, 175-205.

Browdy, C.L., 1998. Recent developments in penaeid broodstock and seed production technologies: improving the outlook for superior captive stocks. Aquaculture. 164, 3-21.

Castejón, D., Rotllant, G., Giménez, L., Torres, G., Guerao, G., 2015. The effects of temperature and salinity on the survival, growth and duration of the larval development of the common spider crab *Maja brachydactyla* (Balss, 1922) (Brachyura: Majidae). Journal of Shellfish Research. 34, 1073-1083.

Corgos, A., Sánchez, N., Freire, J., 2010. Dynamics of the Small-Scale Spatial Structure of a Population of the Spider Crab *Maja brachydactyla* (Decapoda: Majidae). Journal of Shellfish Research. 29, 25-36.

Corgos, A., Bernárdez, C., Sampedro, P., Verísimo, P., Freire, J., 2011. Spatial structure of the spider crab, *Maja brachydactyla* population: Evidence of metapopulation structure. Journal of Sea Research. 66, 9-19.

Dawirs, R.R., 1982. Methodical aspects of rearing decapod larvae, *Pagurus bernhardus* (Paguridae) and *Carcinus maenas* (Portunidae). Helgoländer Meeresuntersuchungen. 35, 439-464.

Diele, K., Simith, D.J.B., 2007. Effects of substrata and conspecific odour on the metamorphosis of mangrove crab megalopae, *Ucides cordatus* (Ocypodidae). J. Exp. Mar. Biol. Ecol. 348, 174-182.

Domingues, P., Alaminos, J., 2008. Efectos de la densidad de cultivo y de elementos de refugio en el crecimiento y supervivencia de juveniles de centollo, *Maja brachydactyla* (Balss, 1922). Revista de biología marina y oceanografía. 43, 121-127.

Eggleston, D.B., Armstrong, D.A., 1995. Pre- And post-Settlement determinants of estuarine Dungeness crab recruitment. Ecological Monographs. 65, 193-216.

Émond, K., Sainte-Marie, B., Galbraith, P.S., Bêty, J., 2015. Top-down vs. bottom-up drivers of recruitment in a key marine invertebrate: investigating early life stages of snow crab. ICES Journal of Marine Science: Journal du Conseil. 72, 1336-1348.

FAO, 2014. B-42 Crabs, sea-spiders. Capture production by species, fishing areas and countries or areas. in: FAO (Ed.), FAO yearbook. Fishery and aquaculture statistics. FAO, Rome.

Fernandez, M., Iribarne, O., Armstrong, D., 1994. Ecdysial rhythms in megalopae and first instars of the Dungeness crab *Cancer magister*. Marine Biology. 118, 611-615.

Figueiredo, J., Penha-Lopes, G., Narciso, L., Lin, J., 2008. Effect of starvation during late megalopa stage of *Mithraculus forceps* (Brachyura: Majidae) on larval duration, synchronism of metamorphosis, survival to juvenile, and newly metamorphosed juvenile size. Aquaculture. 274, 175-180.

Fitzgerald, T.P., Forward Jr, R.B., Tankersley, R.A., 1998. Metamorphosis of the estuarine crab *Rhithropanopeus harrisii*: effect of water type and adult odor Marine Ecology Progress Series. 165, 217-223.

Forward Jr, R.B., Frankel, D.A.Z., Rittschof, D., 1994. Molting of megalopae from the blue crab *Callinectes sapidus*: effects of offshore and estuarine cues. Marine Ecology Progress Series. 113, 55-59.

Forward, R.B., Tankersley, R.A., Rittschof, D., 2001. Cues for Metamorphosis of Brachyuran Crabs: An Overview. American Zoologist. 41, 1108-1122.

Forward, R.B., De Vries, M.C., Rittschof, D., Frankel, D.A.Z., Bischoff, J.P., Fisher, C.M., Welch, J.M., 1996. Effects of environmental cues on metamorphosis of the blue crab *Callinectes sapidus*. Marine Ecology Progress Series. 131, 165-177.

Fox, J., Weisberg, S., 2011. An {R} Companion to Applied Regression. Sage, Second Edition, Thousand Oaks CA.

Freire, J., Carabel, S., Verísimo, P., Bernárdez, C., Fernández, L., 2009. Patterns of juvenile habitat use by the spider crab *Maja brachydactyla* as revealed by stable isotope analyses. Sci. Mar. 73, 39-49.

Gebauer, P., Walter, I., Anger, K., 1998. Effects of substratum and conspecific adults on the metamorphosis of *Chasmagnathus granulata* (Dana) (Decapoda: Grapsidae) megalopae. J. Exp. Mar. Biol. Ecol. 223, 185-198.

Gebauer, P., Paschke, K., Anger, K., 2002. Metamorphosis in a semiterrestrial crab, *Sesarma curacaoense*: intra- and interspecific settlement cues from adult odors. J. Exp. Mar. Biol. Ecol. 268, 1-12.

Gebauer, P., Paschke, K., Anger, K., 2003. Delayed metamorphosis in decapod crustaceans: evidence and consequences. Revista Chilena de Historia Natural. 76, 169-175.

Giménez, L., 2006. Phenotypic links in complex life cycles: conclusions from studies with decapod crustaceans. Integrative and Comparative Biology. 46, 615-622.

Giménez, L., 2010. Relationships between habitat conditions, larval traits, and juvenile performance in a marine invertebrate. Ecology. 91, 1401-1413.

Guerao, G., Rotllant, G., 2009. Post-larval development and sexual dimorphism of the spider crab *Maja brachydactyla* (Brachyura: Majidae). Sci. Mar. 73, 797-808.

Guerao, G., Rotllant, G., Anger, K., 2010. Characterization of larval moulting cycles in *Maja brachydactyla* (Brachyura, Majidae) reared in the laboratory. Aquaculture. 302, 106-111.

Guerao, G., Pastor, E., Martin, J., Andrés, M., Estévez, A., Grau, A., Duran, J., Rotllant, G., 2008. The larval development of *Maja squinado* and *M. brachydactyla* (Decapoda, Brachyura, Majidae) described from plankton collected and laboratory-reared material. Journal of Natural History. 42, 2257-2276.

Hamasaki, K., Obata, Y., Dan, S., Kitada, S., 2011. A review of seed production and stock enhancement for commercially important portunid crabs in Japan. Aquaculture International. 19, 217-235.

Kopin, C.Y., Epifanio, C.E., Nelson, S., Stratton, M., 2001. Effects of chemical cues on metamorphosis of the Asian shore crab *Hemigrapsus sanguineus*, an invasive species on the Atlantic Coast of North America. J. Exp. Mar. Biol. Ecol. 265, 141-151.

Le Foll, D., 1993. Biologie et exploitation de l'araignée de mer *Maja squinado* Herbst en Manche Ouest, Ressources Halieutiques, IFREMER - Institut Français de Recherche pour l'Exploitation de la Mer. Université de Bretagne Occidentale, Plouzane (France), pp. 517.

Le Vay, L., Carvalho, G.R., Quinitio, E.T., Lebata, J.H., Ut, V.N., Fushimi, H., 2007. Quality of hatchery-reared juveniles for marine fisheries stock enhancement. Aquaculture. 268, 169-180.

O'Connor, N.J., 2007. Stimulation of molting in megalopae of the Asian shore crab *Hemigrapsus sanguineus*: physical and chemical cues. Marine Ecology Progress Series. 352, 1-8.

O'Connor, N.J., Gregg, A.S., 1998. Influence of potential habitat cues on duration of the megalopal stage of the fiddler crab *Uca pugnax*. Journal of Crustacean Biology. 18, 700-709.

Palma, J., Correia, M., Andrade, J.P., 2008. Usefulness of flat bottom tanks on the settlement of spider crab (*Maja squinado*, Herbst) larvae. Aquaculture Research. 39, 1005-1008.

Pawlik, J.R., 1992. Chemical ecology of the settlement of benthic marine invertebrates. Oceanography and Marine Biology: An Annual Review. 30.

Pechenik, J.A., 2006. Larval experience and latent effects-metamorphosis is not a new beginning. Integrative and Comparative Biology. 46, 323-333.

Planas, M., Cunha, I., 1999. Larviculture of marine fish: problems and perspectives. Aquaculture. 177, 171-190.

R Development Core Team, 2015. R: A language and environment for statistical computing. R Foundation for Statistical Computing, Vienna, Austria.

Rhyne, A.L., Penha-Lopes, G., Lin, J., 2005. Growth, development, and survival of larval *Mithraculus sculptus* (Lamark) and *Mithraculus forceps* (A. Milne Edwards) (Decapoda: Brachyura: Majidae): economically important marine ornamental crabs. Aquaculture. 245, 183-191.

Rodríguez, S., Ojeda, F.P., Inestrosa, N.C., 1993. Settlement of benthic marine invertebrates. Marine Ecology Progress Series. 97, 197-207.

Silva, U.A.T.d., Cottens, K., Ventura, R., Boeger, W.A., Ostrensky, A., 2012. Different pathways in the larval development of the crab *Ucides cordatus* (Decapoda, Ocypodidae) and their relation with high mortality rates by the end of massive larvicultures. Pesquisa Veterinária Brasileira. 32, 284-288.

Simith, D.d.J.d.B., Diele, K., Abrunhosa, F.A., 2013. Carry-over effects of delayed larval metamorphosis on early juvenile performance in the mangrove crab *Ucides cordatus* (Ucididae). J. Exp. Mar. Biol. Ecol. 440, 61-68.

Simith, D.J.B., Diele, K., 2008. Metamorphosis of mangrove crab megalopae, *Ucides cordatus* (Ocypodidae): Effects of interspecific versus intraspecific settlement cues. J. Exp. Mar. Biol. Ecol. 362, 101-107.

Simith, D.J.B., Diele, K., Abrunhosa, F.A., 2010. Influence of natural settlement cues on the metamorphosis of fiddler crab megalopae, *Uca vocator* (Decapoda: Ocypodidae). Anais da Academia Brasileira de Ciências. 82, 313-321.

Steinberg, M., Krimsky, L., Epifanio, C., 2008. Induction of Metamorphosis in the Asian Shore Crab *Hemigrapsus sanguineus*: Effects of Biofilms and Substratum Texture. Estuaries and Coasts. 31, 738-744.

Tapella, F., Romero, M.C., Stevens, B.G., Buck, C.L., 2009. Substrate preferences and redistribution of blue king crab *Paralithodes platypus* glaucothoe and first crab on natural substrates in the laboratory. J. Exp. Mar. Biol. Ecol. 372, 31-35.

Tapella, F., Sotelano, M.P., Romero, M.C., Lovrich, G.A., 2012. Experimental natural substrate preference of southern king crab *Lithodes santolla* larvae. J. Exp. Mar. Biol. Ecol. 411, 70-77.

Venables, W.N., Ripley, B.D., 2002. Modern Applied Statistics with S. Springer, New York, USA.

Weber, J.C., Epifanio, C.E., 1996. Response of mud crab (*Panopeus herbstii*) megalopae to cues from adult habitat. Marine Biology. 126, 655-661.

Welch, J.M., Rittschof, D., Bullock, T.M., Forward, R.B., 1997. Effects of chemical cues on settlement behavior of blue crab *Callinectes sapidus* postlarvae. Marine Ecology Progress Series. 154, 143-153.

Zeng, C., Naylor, E., Abello, P., 1997. Endogenous control of timing of metamorphosis in megalopae of the shore crab *Carcinus maenas*. Marine Biology. 128, 299-305.

Zmora, O., Findiesen, A., Stubblefield, J., Frenkel, V., Zohar, Y., 2005. Large-scale juvenile production of the blue crab *Callinectes sapidus*. Aquaculture. 244, 129-139.

BLOQUE 1.

LARVICULTURA. DISCUSIÓN

"Larvae are fascinating animals!"

Klaus Anger 2001

En el presente primer bloque, los capítulos previos permiten describir y discutir los principales avances que se han logrado en relación al cultivo larvario de *Maja brachydactyla*. El principal objetivo era ajustar determinados parámetros ambientales, entre los que se incluyen la temperatura, salinidad, fotoperiodo e intensidad lumínica; con el deseo de lograr la máxima supervivencia desde la eclosión hasta el estadio de primer juvenil en el menor tiempo posible, optimizando de este modo el cultivo larvario o *larvicultura* de esta especie. Como ya se ha discutido, este estudio no solo se puede interpretar como ciencia básica, permitiéndonos tener una idea de las condiciones naturales en las cuáles prosperan dichos animales; sino que desde una perspectiva aplicada, estos datos permiten contribuir a maximizar la producción larvaria. En ese sentido, si bien los resultados obtenidos en el trabajo de asentamiento no nos permiten discernir qué tipo de ambiente favorece el asentamiento de las megalopas y por consiguiente, no nos otorga pistas acerca de dónde buscarlas en el medio natural; sí que nos permite comprobar de primera mano que, desde una perspectiva de producción acuícola, no se requieren condiciones especiales para obtener juveniles, cubriendo de ese modo los requisitos básicos de una *hatchery* de esta especie.

Sin embargo, dadas las limitaciones del formato artículo de los capítulos, hay ciertos detalles que no han podido ser comentados o discutidos. Por la misma razón, se dispone de información que no puede ser publicada en los capítulos previos por su falta de fortaleza empírica. Sin embargo dichos datos son interesantes por varias razones: pueden utilizarse para mejorar las condiciones de cultivo de *M. brachydactyla* y pueden servir de punto de inicio para futuros estudios que quieran profundizar en otros aspectos de la biología de esta especie.

De modo que este bloque resume aspectos no suficientemente comentados o discutidos, así como aquellos datos que no se han mostrado con anterioridad. También serán comentados de forma breve aquellos aspectos más importantes de los parámetros ambientales estudiados, así como los aspectos más importantes relativos al asentamiento y las vulnerabilidades del estadio de megalopa. Finalmente, se propondrán varias ideas para desarrollar la continuación natural a los presentes estudios: la optimización del engorde y producción de juveniles, empleando información adicional que ha sido obtenida mientras eran realizadas las experiencias de cultivo del presente estudio.

8.1 Parámetros ambientales óptimos de cultivo larvario.

Puede establecerse que los parámetros ambientales óptimos para el cultivo larvario del centollo, *Maja brachydactyla* Balss, 1922, incluyen: temperatura de 21 ± 1 °C, salinidad de 35 ± 1 psu, luces de tipo LED o tubos fluorescentes de luz blanca, fotoperiodo de 24 h de duración con un ciclo de luz-oscuridad. Estos parámetros permiten la mayor tasa de supervivencia hasta primer juvenil en el menor tiempo posible, siendo el desarrollo larvario completado en un lapso temporal de 12 a 14 días.

En los decápodos el desarrollo larvario abarca desde el momento de la eclosión hasta la metamorfosis a primer juvenil. Los estadios larvarios cambian en número y morfología entre los distintos taxones de decápodos (Anger, 2001; Martin et al., 2014; Williamson, 1969). En el caso de los braquiuros, estos se caracterizan por poseer dos fases larvarias: zoea y megalopa, ocasionalmente también se describe una fase temprana previa a la zoea denominada prezoea (Anger, 2001; Campbell and Fielder, 1987; Clark et al., 1998; Clark and Cuesta, 2015; Martin, 2014); aunque como apunta Martin (2014), la prezoea podría ser un artefacto debido a condiciones inadecuadas de incubación. La excepción a esta tendencia son los miembros de la familia Hymenosomatidae MacLeay, 1838, los cuales después del último estadio de zoea realizan directamente la metamorfosis a primer juvenil sin pasar por la fase intermedia de megalopa (Anger, 2001; Davie et al., 2015a; Rice, 1980).

Mientras que la fase de megalopa comprende un único estadio, la fase de zoea está formada por un número de estadios muy variable, generalmente de cuatro a seis en la mayoría de familias de braquiuros (Rice, 1980). En otros grupos puede extenderse hasta siete u ocho estadios, tal y como ocurre en portúnidos del género *Callinectes* (Bookhout and Costlow Jr, 1977; Costlow and Bookhout, 1959; Rice, 1980). Por el contrario, otros braquiuros tienen el desarrollo larvario abreviado, es decir, con un número reducido de estadios de zoea. Esta es la situación de nuestra especie objeto de estudio, *M. brachydactyla*, la cual cuenta únicamente con dos estadios de zoea, característica común a todos los miembros de la superfamilia Majoidea (Davie et al., 2015b; Hultgren and Stachowicz, 2008; Rice, 1980).

Desde el punto de vista del cultivo, un reducido número de estadios larvarios es una característica deseable debido a dos razones principales. La primera se basa en la vulnerabilidad del animal durante el proceso de muda, proceso durante el cual puede ocurrir la muerte del animal. La segunda razón radica en que un menor número de estadios larvarios acorta el tiempo de cultivo requerido para alcanzar la fase de juvenil. Por tanto, un menor número de estadios larvarios implica un aumento de la supervivencia y una reducción del tiempo de desarrollo.

En *M. brachydactyla* hemos observado que la velocidad de crecimiento se incrementa desde los 15 hasta los 24 ± 1 °C, siendo 21 ± 1 °C la temperatura óptima ya que se obtiene la mayor supervivencia asociada a un menor tiempo de desarrollo. Está actualmente aceptado que la temperatura acelera la tasa de desarrollo de forma aproximadamente lineal hasta que se alcanza la "temperatura óptima", a partir de la cual todo incremento adicional de temperatura reducirá rápidamente la supervivencia así como la tasa de desarrollo, hasta alcanzar la "temperatura máxima" o "temperatura letal" que implica la muerte de todos los individuos (Briere et al., 1999; Lactin et al., 1995; Logan et al., 1976). La misma situación se ha observado en *M. brachydactyla*, donde la supervivencia empieza a verse comprometida desde los 24 ± 1 °C, mientras que la "temperatura máxima o letal" se sitúa entre los 27 y los 30 ± 1 °C.

Esta aceleración de la tasa de crecimiento y desarrollo es asociada al incremento de la velocidad de los procesos metabólicos, causada por el incremento de la velocidad de las reacciones bioquímicas concomitante al incremento de la temperatura (Gillooly et al., 2001). El incremento de la velocidad de crecimiento asociado al aumento de la temperatura, reduciendo con ello la duración del desarrollo larvario (o bien de la duración de determinadas etapas larvarias en aquellos estudios que no han completado el desarrollo larvario), ha sido descrito en numerosas especies de braquiuros (Anger, 1991; 2001; Baylon and Suzuki, 2007; Costlow et al., 1960; Costlow Jr et al., 1966; Fagetti, 1969; Fagetti and Campodonico, 1971; Hernández et al., 2012; Lárez et al., 2000; Minagawa, 1990; Nagaraj, 1992; Nurdiani and Zeng, 2007; Ong and Costlow, 1970).

En la costa gallega las hembras ovígeras aparecen desde marzo hasta septiembre, con pico máximo entre abril y junio (González-Gurriarán et al., 1998; González-Gurriarán et al., 1993). Las hembras pueden realizar hasta tres puestas sucesivas anuales (Freire et al., 2002), el periodo de incubación podría oscilar de 34 a 62 días en condiciones de cultivo (González-Gurriarán et al., 1998; González-Gurriarán et al., 1993). Teniendo en cuenta estos datos es posible que la presencia de larvas tenga lugar entre los meses de abril a noviembre, durante este periodo la temperatura superficial de las aguas gallegas se mantiene alrededor de 14-16 °C con máximos estacionales entre mayo y agosto de 18-19 °C (Álvarez-Salgado et al., 2009; Doval et al., 1998; Gago et al., 2011), dichas temperaturas entran en el rango empleado para el cultivo de esta especie.

El equilibrio osmótico e iónico es clave para los procesos metabólicos y fisiológicos. De modo que una salinidad inadecuada afecta negativamente a la supervivencia, el crecimiento y la alimentación (Anger, 2003). El rango de tolerancia salina se relaciona con el hábitat: los animales estenohalinos tienen un rango de tolerancia muy estrecho ya que habitan ambientes de salinidad estable y homogénea donde los cambios de salinidad son fenómenos raros o inexistentes; mientras que los animales eurihalinos tienen un rango amplio ya que habitan ambientes cuya salinidad es muy variable a una escala temporal de horas a días, como estuarios o zonas costeras (Péqueux, 1995; Torres et al., 2011).

En ese sentido, la salinidad puede considerarse uno de los factores determinantes de la tasa de supervivencia en *M. brachydactyla*. De acuerdo a nuestros resultados, se trata de una especie marcadamente estenohalina con un rango muy estrecho de tolerancia salina, de 34 a 36 psu durante el desarrollo larvario, de modo que un cambio en 4-6 psu dispara la mortalidad en pocos días. Los adultos del género *Maja* también son animales estenohalinos osmoconformistas muy vulnerables a los cambios de salinidad (Péqueux, 1995), cuya hemolinfa posee una presión osmótica similar a la del medio externo (Dakin, 1912; Drilhon, 1935).

La salinidad de las aguas costeras de Galicia a una distancia costera de entre los 100 y 150 metros oscila entre las 34 y 36 psu, en un rango de profundidad de 0 a 40 metros (Doval et al., 1998; Gago et al., 2011). Dicho rango coincide con el rango de tolerancia salina, así como con el valor de salinidad óptima, que hemos observado en las etapas larvarias de *M. brachydactyla*. En aguas costeras localizadas cerca de la costa la salinidad puede decrecer estacionalmente por debajo de las 33 psu (Álvarez-Salgado et al., 2009; Gago et al., 2011). Esta caída en la salinidad suele ocurrir en época invernal por afluencia de las aguas dulces de los ríos (Cabanas et al., 1987). Parece improbable que esta salinidad pueda afectar a la supervivencia de los estadios larvarios de *M. brachydactyla*. En primer lugar, porque *a priori* no parece que coincidan la bajada estacional de salinidad con la presencia de alguno de los estadios larvarios. En segundo lugar, porque las larvas pueden evitar el nivel de salinidad subóptimo mediante la detención de la actividad natatoria y dejándose hundir pasivamente. Este comportamiento lo hemos observado bajo condiciones experimentales cuando las larvas son expuestas a baja salinidad. El mismo comportamiento ha sido observado en estadios larvarios de otras especies de braquiuros expuestos a baja salinidad, como *Charybdis feriata* (Baylon and Suzuki, 2007) o *Hyas araneus* (Anger, 1985); así como en zoeas del anomuro *Pagurus longicarpus* (Roberts, 1971). Anger (1985) ha sugerido que este comportamiento les permite alcanzar capas de agua más profundas, las cuáles suelen tener una salinidad más elevada.

El número de horas de luz y la intensidad lumínica parecen ser, de las variables estudiadas, las que menos afectan al cultivo larvario. En ese sentido, la supervivencia no se ve afectada significativamente ni por el número de horas de luz ni por una intensidad lumínica dentro del rango de 300-3000 lux, mientras que la duración del desarrollo larvario es acortado con el número de horas de luz pero no se ve afectado por la intensidad lumínica. La excepción es la exposición a un régimen de 24 h de luz, donde la supervivencia se ve reducida desde la eclosión hasta el estadio de megalopa. Esta situación se ha observado en otras especies de braquiuros como *Ranina ranina* (Minagawa, 1994) o *Portunus pelagicus* (Andrés et al., 2010d). Por otro lado, aunque en *M. brachydactyla* el régimen de 24 h de luz no parece afectar a la duración de la fase de zoea, en otros braquiuros como *Pseudocarcinus gigas* este régimen alarga la duración de esta fase (Dawirs, 1982; Gardner and Maguire, 1998) o la acorta como en *R. ranina* (Minagawa, 1994). En astacideos como *Homarus gammarus* la supervivencia decrece con el aumento de horas de luz (Aiken et al., 1981), mientras que en *Astacus leptodactylus* la supervivencia se incrementa ante la misma condición (Ulikowski and Krzywosz, 2004); en los carideos como *Palaemonetes argentinus* el aumento de horas de luz reduce la supervivencia (Díaz et al., 2003), pero la aumenta en *Macrobrachium rosenbergii* (Tidwell et al., 2001).

Aunque la influencia del régimen lumínico es baja, se podría decir que la ausencia de luz tiene un efecto mayor que cualquier fotofase: se reduce la supervivencia y aumenta la duración del desarrollo larvario. Algo similar ocurre con *Sesarma reticulatum* donde la supervivencia es menor en régimen de total oscuridad (Costlow and Bookhout, 1962). Esto no sucede en otras especies de braquiuros, en *P. gigas* y en *Carcinus maenas* la supervivencia no varía en condiciones de oscuridad total (Dawirs, 1982; Gardner and Maguire, 1998). En otros decápodos, los efectos de un régimen de oscuridad total son también muy variables, así en anomuros reduce la supervivencia de *Birgus latro* (Hamasaki et al., 2015) pero no la de *Pagurus bernhardus* (Dawirs, 1982). En astacideos, un régimen de oscuridad total retrasa el crecimiento de *Sagmariasus verreauxi* (Fitzgibbon and Battaglene, 2012), pero no el de *Jasus edwardsii* (Bermudes and Ritar, 2008).

Estos datos demuestran que la influencia de la luz (o su ausencia) sobre el desarrollo larvario de los decápodos es específico, encontrándose tendencias diferentes en taxones cercanos. Se desconoce qué proceso fisiológico está siendo influido por la luz (o por su ausencia). Se ha postulado que en ciertas especies la luz estimula la actividad natatoria (Cronin and Forward Jr, 1980; Forward Jr, 1974; Forward Jr and Cronin, 1980) y con ello la ingesta al incrementar la tasa de encuentro con presas (Andrés et al., 2010d; Rabbani and Zeng, 2005). También se ha propuesto que ciertas intensidades luminosas pueden estimular la conversión del alimento (Hoang et al., 2003). Sin embargo, todavía no hay datos concluyentes.

8.2 Sobre el asentamiento y el cultivo de juveniles.

El presente estudio ha demostrado que las megalopas de *M. brachydactyla* no necesitan un sustrato específico para realizar la metamorfosis a primer juvenil. Esto también se puede afirmar de otra manera, no se ha hallado un sustrato específico que induzca la metamorfosis a primer juvenil con mayor rapidez o mayor tasa de supervivencia que en la situación de control, la cual consistió en un tratamiento sin ningún tipo de sustrato. Tampoco hemos hallado que el agua procedente de los tanques del stock de reproductores, la cual contendría compuestos procedentes de dichos adultos, influya en la supervivencia y tiempo de desarrollo hasta la metamorfosis a primer juvenil, contrariamente a observaciones realizadas en otras especies de braquiuros. Otro resultado muy interesante es la demostración de que el desarrollo larvario puede completarse con mayor tasa de éxito en cultivos comunitarios, en lugar de cultivos individuales, con el consiguiente ahorro en tiempo de trabajo, materiales y personal. Lamentablemente, esta situación no se aplica al llamado desarrollo post-larvario, el engorde de juveniles hasta talla comercial, ya que estos muestran una marcada tendencia caníbal que obliga al cultivo individual. Esta situación y la posible estrategia comercial, en caso de desarrollarse intereses relativos al cultivo acuícola de esta especie, se discutirá posteriormente.

En ese sentido, las preguntas más inmediatas serían: ¿Por qué en muchos sustratos la supervivencia ha sido inferior al «control»? ¿Qué tienen en común los tratamientos que han obtenido un resultado equivalente al «control»?. Respondiendo a tales preguntas, una similitud entre los tratamientos «control», «arena gruesa», «*Chaetomorpha* sp.» y «*Ulva* sp.» es la carencia de obstáculos que puedan bloquear los desplazamientos de las megalopas (Fig. 8.2.1).

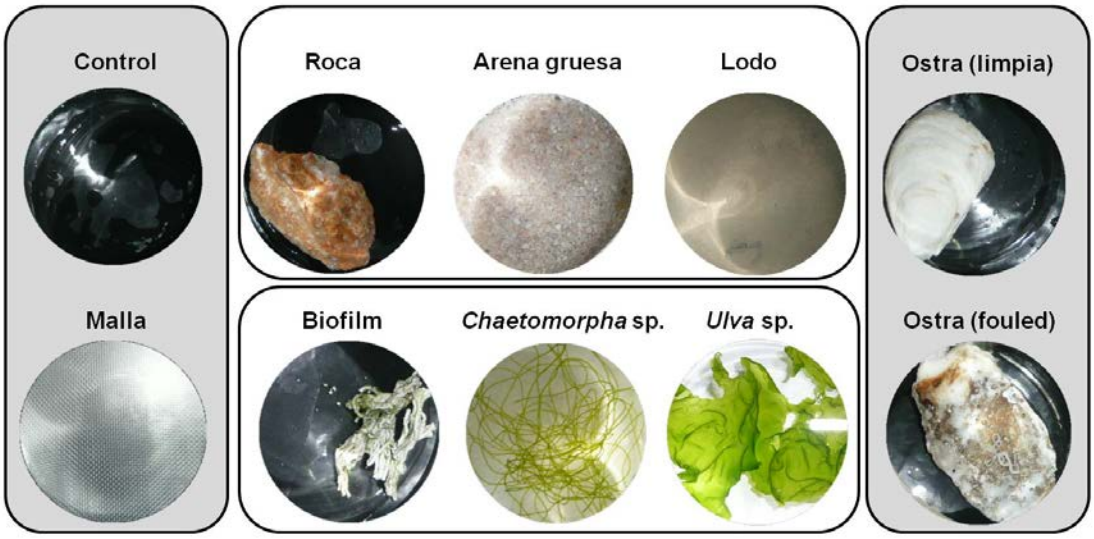

Figura 8.2.1. Sustratos empleados en los experimentos de asentamiento.

Por el contrario, el resto de tratamientos (exceptuando el tratamiento «lodo») poseen una zona de contacto contra el fondo del vaso de precipitados provista de irregularidades, las cuales pueden aprisionar a las megalopas. Desde mi punto de vista, esta zona de contacto pudo haber sido una trampa mortal para estas, ya que al quedar atrapadas no podrían alimentarse, sufrirían daños corporales y consumirían energía en sus intentos de liberación (en caso de realizarlos), lo que finalmente induciría a la muerte de los individuos. Esta situación explicaría porque la mayor parte de los cadáveres de megalopa se han hallado debajo de estos sustratos. Puede argumentarse que si ninguno de los sustratos favorece el proceso de asentamiento, es esperable obtener en todos ellos una supervivencia similar a la obtenida en el tratamiento «control» excepto si dichos sustratos provocan el efecto contrario: inhiben el asentamiento y/o incrementan la tasa de mortalidad. Por esta razón, el aumento de la mortalidad puede entenderse como la combinación de ausencia de estímulo para realizar el asentamiento (como es esperable en «control») combinado con factores que aumentan la tasa de mortalidad, en este caso el "aprisionamiento" de las larvas.

También se observó una mayor mortalidad en la experiencia de cultivo individual. En este ensayo fueron comparados dos tratamientos: cultivo comunal donde se situaron 10 megalopas en vasos de precipitados de 500 mL y cultivo individual donde se situó una única megalopa en un vaso cristalizador de 50 mL, empleándose en total 100 megalopas originadas de la misma puesta por cada tratamiento (Fig. 8.2.2). La razón de emplear distintos tipos de vasos de cultivo se debió a dos razones. La primera se justifica en el deseo de situar a las larvas en las mismas condiciones iniciales de volumen de agua, así al inicio del experimento cada megalopa dispondría de 50 mL de agua independientemente de su localización. La segunda es una razón práctica, no se disponían de suficientes recursos para poder disponer y situar 100 vasos de precipitados adicionales en condiciones de cultivo. Esta segunda razón explica por qué no pudo realizarse un tratamiento adicional de cultivo individual de megalopas en vasos de precipitados.

Tradicionalmente, el cultivo larvario de decápodos ha sido realizado de forma comunal (con pocos individuos) o individual en recipientes de vidrio o plástico de pequeñas dimensiones (Rice and Williamson, 1970). Generalmente, el cultivo individual suele recomendarse frente al comunal para evitar problemas derivados de la densidad (Forward et al., 2001). El cultivo comunal de *Callinectes sapidus*, *Metacarcinus magister* o *Carcinus maenas* da lugar a problemas de competencia y canibalismo que reducen la supervivencia y retrasan el desarrollo (Dawirs, 1982; Fernandez et al., 1994; Forward et al., 1996). Pese a ello, el cultivo comunal de las megalopas en laboratorio ha sido ampliamente aceptado en distintos diseños experimentales (Diele and Simith, 2007; Forward Jr et al., 1994; Forward et al., 1996; Gebauer et al., 2002; O'Connor, 2007; Simith and Diele, 2008; Steinberg et al., 2008; Steinberg et al., 2007).

Nosotros observamos mayor mortalidad y retraso en el desarrollo larvario en el cultivo individual. Esta situación quizás pueda ser debida al menor volumen de los vasos cristalizadores, lo que reduciría la libertad de movimiento y aumentaría el contacto con las paredes laterales y el fondo del recipiente. La permanencia en el fondo del recipiente también plantea un problema adicional en el ensayo de asentamiento, donde la mayor mortalidad fue presumiblemente debida al "aprisionamiento" de las larvas bajo ciertos sustratos. El fondo de los recipientes y tanques de cultivo puede considerarse la zona más insalubre de los mismos, ya que es donde se depositan los restos orgánicos (alimento, cadáveres, heces, mudas, etc.) convirtiéndose en una zona pobre en oxígeno donde pueden proliferar microorganismos potencialmente patógenos (Dugan et al., 1975; Genodepa et al., 2004; Philipose, 2009; Rice and Williamson, 1970), incluyendo bacterias, protozoos y hongos.

Según distintos autores, las larvas atrapadas en el fondo están expuestas a agua de baja calidad (rica en nitritos y pobre en oxígeno) y patógenos, este contacto también pueden dañar setas y apéndices, reduciendo la capacidad nadadora y eficiencia en la alimentación, lo que contribuye al incremento de la mortalidad (Calado et al., 2003; Calado et al., 2008; Dugan et al., 1975; Genodepa et al., 2004; Philipose, 2009; Rice and Williamson, 1970). Estos daños en las setas y apéndices nadadores también pueden producir heridas, las cuáles se han postulado como una posible vía de entrada de patógenos (Chinain and Vey, 1988; Luis-Villaseñor et al., 2012; Mohney et al., 1998). En nuestros cultivos larvarios de *M. brachydactyla*, de forma puntual también se han observado protozoos, posiblemente ciliados, infectando megalopas vivas y en apariencia consumiendo el tejido de las extremidades (Fig. 8.2.3). De forma más habitual, estos protozoos se han observado en cantidades más elevadas consumiendo cadáveres de larvas, por lo que no se descarta que en caso de infección actúen como patógenos oportunistas.

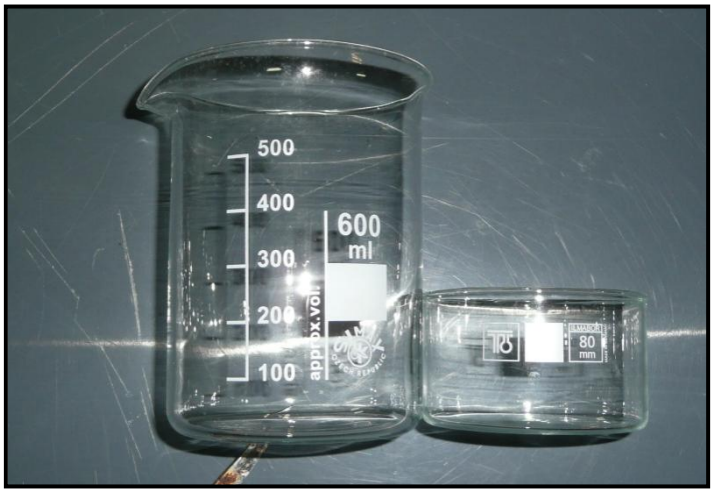

Figura 8.2.2. Recipientes empleados en el ensayo de cultivo comunal e individual. Derecha, vaso de precipitados, cultivo comunal. Izquierda, vaso cristalizador, cultivo individual.

Estudios anteriores realizados en *M. brachydactyla* determinaron que la supervivencia no se veía afectada en un rango que abarca entre 10 y 100 megalopas L^{-1} (Andrés et al., 2007). Por tanto, dado que en los ensayos enfocados en el asentamiento, incluyendo el ensayo de cultivo comunal, se empleó una densidad de 20 megalopas L^{-1}, esta es una densidad que entraría dentro del rango de tolerancia de esta especie.

No hemos observado que el uso de agua procedente del tanque de los adultos influya de algún modo sobre la tasa de metamorfosis o duración del estadio de megalopa. De acuerdo con la revisión de Forward et al. (2001), numerosos autores (ver Tabla 8.2.1) han reportado que la presencia de exudados (compuestos químicos denominados "olores" en otros estudios), producidos por adultos (tanto conespecíficos como congenéricos según la especie), son un estímulo que reducen la duración del estadio de megalopa y promueven la metamorfosis a primer juvenil. Dichos autores postulan que los exudados de los adultos actúan como un indicador de la presencia de un hábitat adecuado para los juveniles, ya que en dichas especies tanto adultos como juveniles coexisten en el mismo entorno. Esta atracción es acentuada por la presencia de productos característicos del hábitat de dichas especies, como ácidos húmicos en zonas de estuario o compuestos producidos por ciertos tipos de *biofilm* microbiano.

Por el contrario, en *M. brachydactyla* los exudados adultos no estimulan el asentamiento. Esta falta de estímulo ante la presencia de exudados, observada como una supervivencia hasta primer juvenil y una duración del estadio de megalopa que no difieren del tratamiento control, también ha sido observada en otras especies de braquiuros como *Callinectes sapidus* (Forward Jr et al., 1994), *Carcinus maenas* (Zeng et al., 1997) o *Menippe mercenaria* (Krimsky and Epifanio, 2008).

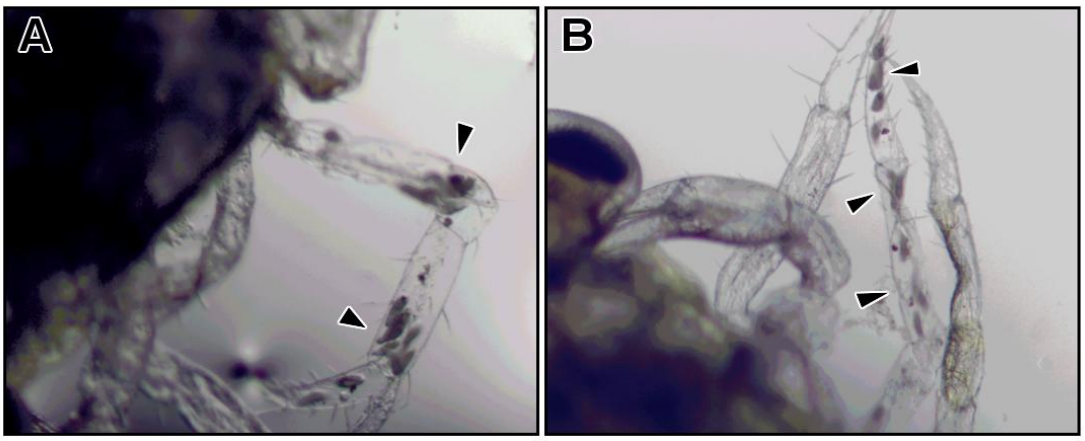

Figura 8.2.3. Megalopa de *M. brachydactyla* infectada por protozoos (puntas de flecha).

Se ha propuesto que en determinadas especies de braquiuros, los exudados producidos por los adultos no serían buenos indicadores de un hábitat adecuado para el desarrollo de los juveniles. Las hipótesis propuestas pueden resumirse en un único concepto: el hábitat de juveniles y adultos no coincide porque los adultos tienen un hábitat mucho más amplio o restringido que los juveniles, por ello los exudados adultos no pueden ser un buen indicativo de un hábitat adecuado para el desarrollo de los juveniles (Forward Jr et al., 1994; Zeng et al., 1997). En el caso de *M. brachydactyla* se puede considerar una situación similar: los exudados de los adultos no son un indicador adecuado dado que juveniles y adultos habitan entornos diferentes. Varios estudios realizados en *M. brachydactyla* muestran que adultos y juveniles forman poblaciones segregadas espacialmente (Corgos et al., 2011; Corgos et al., 2010; Le Foll, 1993). Corgos et al. (2011) resume esta idea postulando que el asentamiento debe de ocurrir a menos de 5 metros de profundidad, donde los juveniles permanecen hasta alcanzar 60 mm tras 12–18 meses de desarrollo, entonces migran hasta 5–15 metros de profundidad hasta que alcanzan la edad adulta, cuando realizan una nueva migración pero esta vez hacia aguas más profundas. Por tanto, dadas estas condiciones los exudados adultos no tendrían ningún significado como indicador de un buen lugar para el asentamiento de las megalopas.

Tabla 8.2.1. Especies de braquiuros donde se ha determinado que la presencia de exudados producidos por especímenes adultos estimula la metamorfosis al estadio de primer juvenil.

Especie	**Familia**	**Referencia**
Dyspanopeus sayi (Smith, 1869)	Panopeidae	(Kopin et al., 2001)
Panopeus herbstii H. Milne Edwards, 1834	Panopeidae	(Andrews et al., 2001; Kopin et al., 2001; Weber and Epifanio, 1996)
Rhithropanopeus harrisii (Gould, 1841)	Panopeidae	(Fitzgerald et al., 1998)
Minuca pugnax (Smith, 1870)	Ocypodidae	(O'Connor and Gregg, 1998)
Minuca vocator (Herbst, 1804)	Ocypodidae	(Simith et al., 2010)
Ucides cordatus (Linnaeus, 1763)	Ocypodidae	(Diele and Simith, 2007; Simith and Diele, 2008)
Sesarma curacaoense de Man, 1892	Sesarmidae	(Gebauer et al., 2002)
Hemigrapsus sanguineus (De Haan, 1835)	Varunidae	(Kopin et al., 2001)
Neohelice granulata (Dana, 1851)	Varunidae	(Gebauer et al., 1998)

Durante la realización de estos experimentos la supervivencia desde la eclosión hasta la metamorfosis a primer juvenil ha sido muy variable comparando condiciones de cultivo equivalentes (21 ± 1 °C, 35 ± 1 psu, 12 h luz: 12 h oscuridad, vaso de precipitados): desde inferior al 10 % hasta superior al 75 %. Esto también ocurre en el cultivo larvario de otras especies de braquiuros. Hamasaki et al. (2011) revisaron la supervivencia hasta el estadio de primer juvenil en distintas *hatcheries* para varias especies de braquiuros, observándose una gran variabilidad: en *Portunus trituberculatus* la supervivencia media y desviación estándar fue del 11.2 ± 12 % con un rango entre el 0 y el 80 %, en *Portunus pelagicus* la media fue del 11.2 ± 11.9 % con un rango entre el 0 y el 45 %, mientras que en *Scylla paramamosain* el valor medio fue del 9.4 ± 13.6 % con un rango entre el 0 y el 45 %. En *Scylla serrata* la revisión de diferentes estudios mostró que la supervivencia hasta primer juvenil oscila entre el 0 y el 90 % según las condiciones de cultivo (Genodepa et al., 2004). Mientras que en *Eriocheir sinensis* la supervivencia hasta megalopa también es muy variable, habitualmente es del 10–15 % pero puede alcanzar máximos del 30 al 50 % (Sui et al., 2011).

Numerosos factores pueden ser los responsables de esta oscilación en la supervivencia, distinguiéndose factores intrínsecos y extrínsecos. Entre los factores intrínsecos, se acepta que el tamaño y condición fisiológica y nutricional de las hembras ovígeras determina la condición nutricional de las puestas, a su vez determinante de la calidad de las larvas y el éxito del cultivo (Arcos et al., 2003; Arcos et al., 2005; Oniam et al., 2012; Palacios et al., 1999; Racotta et al., 2003; Wouters et al., 1999). Esta situación podría ocurrir en *M. brachydactyla*, demostrándose que tras un largo cautiverio las hembras realizan puestas de peor calidad nutricional (Verísimo, 2015), situación que se ha asociado a una dieta inadecuada y que origina larvas de peor calidad (Andrés et al., 2010b). Otro factor clave es el acervo genético de las larvas, el cual determinará desde su adaptabilidad a las condiciones de cultivo hasta su tasa de crecimiento, incluyendo la resistencia a las enfermedades (Benzie, 1997; Benzie, 2009).

La mayoría de los factores extrínsecos pueden ser controlados y regulados a lo largo de todo el cultivo, como los parámetros ambientales (temperatura, salinidad, iluminación, pH, oxígeno, niveles de nitritos y nitratos, etc.). Sin embargo, otros factores son más difíciles de controlar. La principal causa conocida de mortalidad son las infecciones por patógenos, muchas de ellas sin tratamiento conocido (Genodepa et al., 2004; Hamasaki et al., 2011; Sui et al., 2011). La alimentación inadecuada es otro factor que aumenta la mortalidad larvaria (Dan et al., 2013; Genodepa et al., 2004; Hamasaki et al., 2002; Holme et al., 2009; Sui et al., 2011). Sin embargo, puede afirmarse que todavía hay muchos elementos desconocidos en la larvicultura de decápodos. Por ejemplo, en relación al cultivo larvario de *S. serrata*, Hamasaki et al. (2011) menciona que se desconocen los causantes de la mortalidad larvaria en el 62 % de los casos.

Las experiencias de cultivo larvario de *M. brachydactyla* han permitido observar ejemplares que murieron antes, durante o después del proceso de muda de megalopa a primer juvenil, presentando habitualmente deformaciones en la forma del caparazón (Fig. 8.2.4). Este fenómeno es llamado "Síndrome de Muerte asociada a la Muda" (SMM, «*Molt/Moult Death Syndrome*» en inglés). En decápodos se ha reportado en astacideos (Bowser and Rosemark, 1981), braquiuros (Hamasaki et al., 2011; Nurdiani and Zeng, 2007; Romano and Zeng, 2006), carideos (Brock, 1993), esciláridos (Perry, 2001) y peneidos (Gong et al., 2004; Ye et al., 2009). Se caracteriza por la incapacidad de completar el proceso de muda, habitualmente se trata de la muda de zoea a megalopa o de megalopa a primer juvenil (Brock, 1993; Dan et al., 2013; Hamasaki et al., 2011; Nurdiani and Zeng, 2007). De causas desconocidas, tradicionalmente ha sido asociado a carencias nutricionales (Bowser and Rosemark, 1981; Coutteau et al., 1997; Dan et al., 2013; Wickins and O'C Lee, 2002). Según otros autores, una dieta excesivamente rica en ácidos grasos provoca un crecimiento anormal que termina repercutiendo en la muda (Hamasaki et al., 2011; Hamasaki et al., 2002). El SMM también ocurre en condiciones de salinidad (Gong et al., 2004; Romano and Zeng, 2006; Rouse and Kartamulia, 1992; Ye et al., 2009) o temperatura inadecuadas (Nurdiani and Zeng, 2007; Rouse and Kartamulia, 1992).

Durante el presente estudio el SMM ha sido observado aún con los parámetros ambientales optimizados. Andrés et al. (2009) estudiando la nutrición de *M. brachydactyla* ha asociado el SMM a un déficit de ácidos grasos en la dieta. En cualquier caso, no se puede descartar que el SMM simplemente sea un síntoma común a varias patologías de origen independiente o bien una patología compleja con múltiples causas. De todos modos, se trata de un problema que precisa ser profundizado en nuevos estudios.

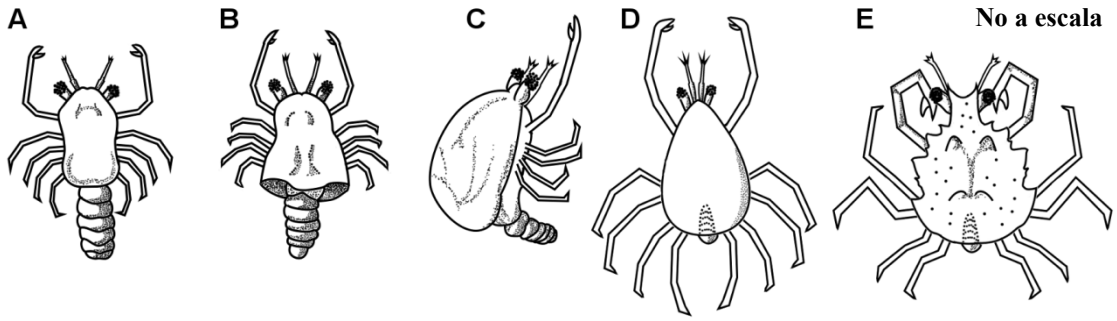

Figura 8.2.4. Diagramas del "Síndrome de Muerte asociado a la Muda" observados en *M. brachydactyla*. Megalopa sin deformaciones pre-muda (A). Megalopa "deformada" con caparazón inflado (B). Espécimen "deformado" y muerto en proceso de muda con caparazón inflado (C). Juvenil "deformado" con forma de "pera" y caparazón inflado (D). Juvenil sin deformaciones (E).

Estudios previos realizados en las instalaciones del IRTA de Sant Carles de la Ràpita señalan que el cultivo larvario intensivo de *M. brachydactyla* es posible mediante cilindros de 35 litros de PVC cerrados basalmente por una malla (150 µm), dichos cilindros son introducidos en tanques de 2000 L y conectados a un sistema de renovación de agua mediante inyección de aire (Andrés et al., 2010a; Andrés et al., 2007; Andrés et al., 2010c; Andrés et al., 2011; Guerao et al., 2008; Rotllant et al., 2008; Rotllant et al., 2010). Otro interesante sistema útil para el cultivo larvario son los *Planktonkreisels* o *Plankton Kreisels* (término compuesto derivado del alemán que significa "giroscopios de plancton"), los cuales consisten en tanques donde se eyecta un flujo de agua hacia las paredes laterales con objeto de mantener el agua en movimiento (Rice and Williamson, 1970). Basado en este sistema, Hughes et al. (1974) describe un diseño de tanques de base semiesférica con un tubo colector central, la base del tubo colector dispone de aberturas que proyectan el agua hacia la base del tanque generando una corriente rotatoria de agua que evita la deposición de material en el fondo. Aunque se pueden emplear tanques de base cónica (Dugan et al., 1975), se ha determinado que en estos la supervivencia es menor que en los de base esférica (Calado et al., 2008). Los *planktonkreisels* mantienen en suspensión los animales, partículas y residuos, paliando la aparición de lesiones y enfermedades (Calado et al., 2003; Calado et al., 2008) y favoreciendo la alimentación (Rice and Williamson, 1970). Desde mi punto de vista, en cuanto a la optimización del cultivo larvario intensivo de *M. brachydactyla* podría ser prometedor el uso de *planktonkreisels* (Fig. 8.2.5), ya que deberían permitir cultivar altas densidades larvarias conservando una supervivencia elevada.

El *Larvatron* es un sistema diseñado para el cultivo automatizado de larvas de decápodos cuyo prototipo fue ideado por Jackson et al. (1992). El prototipo incluye 200 recipientes de plástico de 1,5 litros conectados a un sistema de transporte, cada recipiente individual está conectado a un calentador y aireación. Un computador conectado a una serie de sensores se encarga de monitorizar automáticamente la temperatura y calidad del agua, mientras que unas bombas también automatizadas sustituyen el agua en condiciones inadecuadas por agua limpia con alimento. Este sistema de cultivo ha sido diseñado principalmente por motivos experimentales, con objeto de realizar experimentos multifactoriales que requieran una gran inversión en su gestión y mantenimiento y permite mantener numerosos recipientes de cultivo simultáneamente. Sin embargo, la principal desventaja del *larvatron* es la gran inversión inicial requerida para su montaje e instalación, también posee un mantenimiento complejo. Esto explicaría el bajo número de publicaciones que sostienen su diseño experimental en este sistema. También resulta ser un sistema inadecuado para la producción industrial de juveniles de braquiuros, incluyendo *M. brachydactyla*: su instalación es compleja y ocupa un gran volumen para una producción moderada de ejemplares.

En otras especies de braquiuros se han realizado experiencias de larvicultura empleando técnicas de cultivo de tipo extensivo o semi-extensivo, habilitando para ello estanques exteriores donde se cultivan larvas a densidad reducida. Las desventajas de estos sistemas son la menor densidad de cultivo y la falta de control sobre los factores ambientales, los cuales no están controlados sino sometidos a las fluctuaciones naturales; como ventaja, se afirma que los juveniles obtenidos tienen una mayor calidad y mejor precio en el mercado (Sui et al., 2011). Este tipo de cultivo también se ha aplicado en *M. brachydactyla*, demostrando que es posible tanto completar el desarrollo larvario como el engorde de juveniles, obteniéndose en 9,5 meses juveniles de 3,5 cm si estos procedían de cultivos intensivos y de 6,5 cm si procedían de cultivos semi-extensivos (Iglesias et al., 2002).

En relación al asentamiento, dado que el flujo de agua de un *planktonkreisel* impediría que las megalopas pudiesen asentarse en el fondo, además de acuerdo a nuestra experiencia y estudios previos se recomiendan fondos planos (Palma et al., 2008). Por ello, el siguiente paso del cultivo larvario debería de ser el traslado de las megalopas a tanques diseñados para este fin (Fig. 8.2.5). Los tanques de tipo "*raceways*" (o "canal de corriente rápida") son tanques rectangulares de varios metros de largo y escasa profundidad (habitualmente inferior a 1 metro), en los cuáles el agua sigue un circuito determinado. Estos tanques están acoplados a sistemas de aireación y filtración (Davis and Arnold, 1998; Mock et al., 1973; Rhodes et al., 1995).

La superficie del tanque varía dependiendo de los objetivos del productor, desde unos pocos metros cuadrados (Mock et al., 1973) hasta una hectárea (Rhodes et al., 1995). *A priori* serían tanques útiles para el cultivo de *M. brachydactyla* ya que ofrecen una gran superficie de fondo liso y poca profundidad, que permitiría el asentamiento y desarrollo de juveniles durante las primeras mudas. Los *raceways* se están utilizando ampliamente en la producción acuícola de de peneidos (Davis and Arnold, 1998; Mock et al., 1973; Rhodes et al., 1995; Samocha et al., 2002; Wickins and O'C Lee, 2002). En menor medida, este tipo de tanques también se ha utilizado para el engorde de juveniles de cangrejo de río (Ackefors, 2000; Jones, 1995) y de forma experimental en braquiuros del género *Menippe* (Duermit et al., 2015).

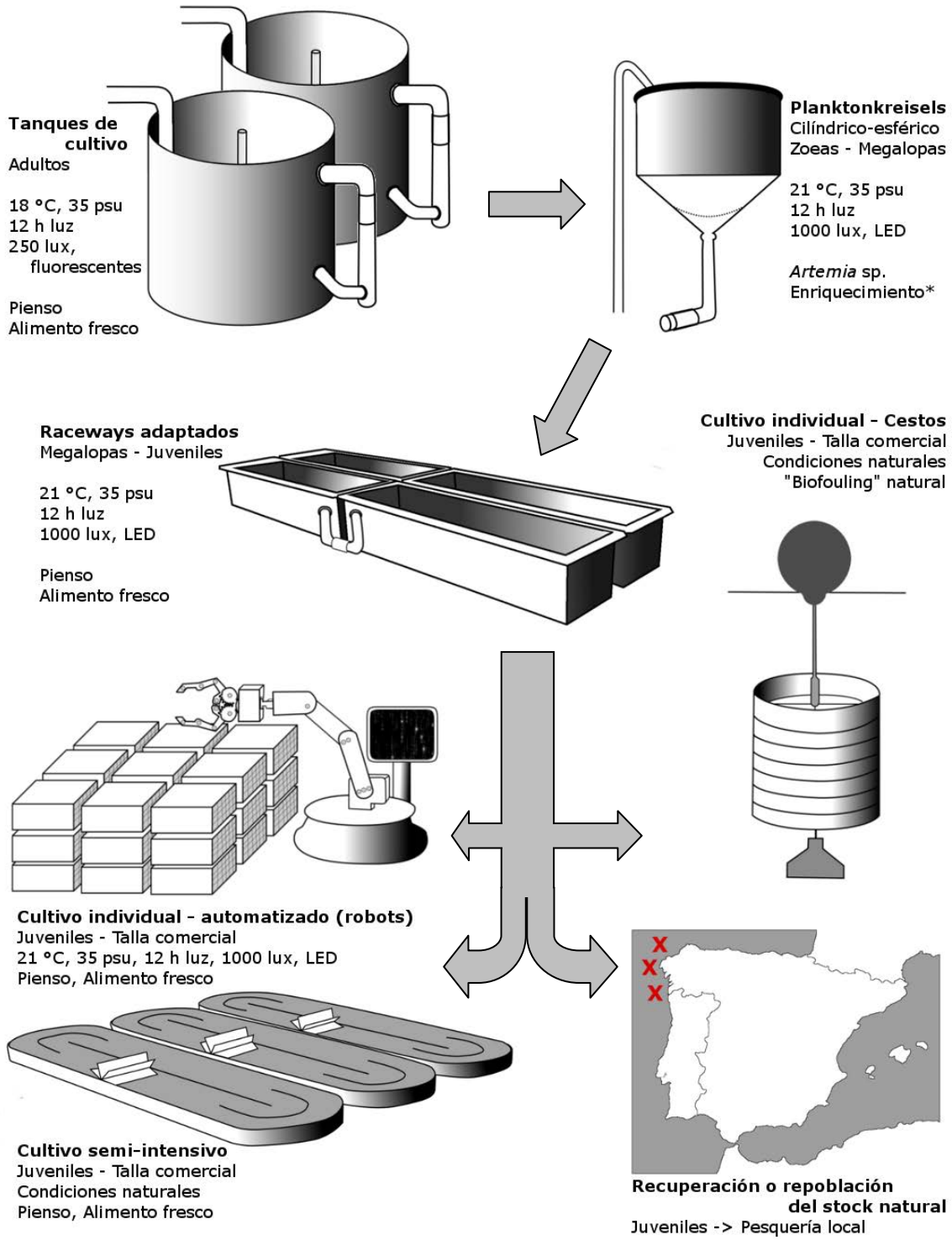

Figura 8.2.5. El cultivo de *M. brachydactyla*. Estrategias que podrían emplearse para el mantenimiento del stock de reproductores, posibles condiciones para el cultivo intensivo larvario y asentamiento de las megalopas (*raceways*) y cuatro estrategias que podrían ser útiles para el engorde de juveniles: cultivo individual automatizado o en cestos colgantes mediante boyas de la superficie del agua, cultivo extensivo en *raceways* adaptados o empleo de los juveniles para la recuperación de las poblaciones naturales.

8.3 Conclusiones y nuevas preguntas.

1. No ha sido posible desentrañar todas las facetas de la influencia de la luz sobre el desarrollo larvario. El fotoperiodo y la intensidad lumínica no son los únicos factores, ya que en los decápodos también pueden influir las longitudes de onda del rango del espectro visible (Guo et al., 2012), incluyendo el propio color del tanque (Luchiari et al., 2012; Rabbani and Zeng, 2005). Será interesante estudiar si la iluminación puede optimizarse cambiando el espectro de emisión de la fuente lumínica y/o el color de las paredes internas de los tanques.

2. Desconocemos cómo la luz (o su ausencia) influye sobre la fisiología de los braquiuros. Un primer paso puede darse con el estudio de los patrones hormonales y/o de producción enzimática en condiciones de presencia / ausencia de luz.

3. No hemos observado que ningún sustrato estimule el asentamiento. Eso no significa que no existan sustratos con dicha propiedad. Distintos estudios han demostrado que sustancias específicas del hábitat de los juveniles son capaces de producir dicho estímulo. Dado que en el presente estudio se emplearon sustratos procedentes del Mediterráneo, mientras que las larvas proceden de adultos de origen Atlántico, no es descartable que los sustratos mediterráneos no sean los adecuados para inducir el asentamiento. En ese sentido, futuros proyectos deberían de emplear sustratos de origen atlántico, especialmente aquellos procedentes de fondos inferiores a 5 metros de profundidad, donde se sospecha que ocurre el asentamiento de *M. brachydactyla*.

4. El estado de las hembras reproductoras podría influir sobre el éxito del cultivo larvario hasta la metamorfosis a primer juvenil. Demostrarlo requiere ensayos multifactoriales: hembra x origen de las mismas x condiciones de mantenimiento ("normales" y estresantes) x época del año. Es un experimento costoso dado el espacio que requiere para mantener a los reproductores, así como su duración y complejidad. Sin embargo, es necesario para entender hasta qué punto es preciso mantener al stock de reproductores en condiciones óptimas para obtener puestas de calidad que permitan una alta supervivencia hasta el estadio de juvenil.

5. Como ya ha sido comentado anteriormente, aunque los nauplios de *Artemia* sp. sirven como alimento vivo que permiten completar el desarrollo larvario de decápodos, podrían no ser el alimento ideal. Para optimizar la dieta sería útil probar con distintas técnicas específicas de enriquecimiento de *Artemia* sp. o bien otros alimentos vivos que pueda servir como suplemento alimenticio. Una pista podría obtenerse estudiando las comunidades con las que cohabitan las larvas de *M. brachydactyla* en el plancton.

6. El conocimiento de las patologías que afectan a los estadios larvarios de braquiuros en condiciones de cultivo es escaso, pero se incluyen infecciones víricas, bacterianas y fúngicas. Por lo tanto, se puede considerar que este es un campo de investigación apenas explorado.

7. El "Síndrome de Muerte asociada a la Muda" es una patología habitual pero cuyo origen es desconocido. Una tentativa de abordarla podría ser mediante un extenso registro de los individuos que han muerto debido a este problema, así como de las deformaciones asociadas, bajo distintas condiciones experimentales. El análisis multifactorial podría entonces elucidar las principales causas de este síndrome.

8. Se deberían de testear distintos tipos de tanques de cultivo con objeto de optimizar la producción de tipo intensivo y súper-intensivo. En especial la eficiencia de los *planktonkreisels*, los cuáles se han mostrado muy eficientes para el cultivo larvario de diversos decápodos. En cuanto al asentamiento, se pueden desarrollar *raceways* adaptados de modo que no tengan un flujo de agua de velocidad excesiva. Este tipo de tanques podría promover el asentamiento de las megalopas, si bien la densidad óptima para promover el asentamiento también tendrá que determinarse en condiciones experimentales.

9. En la Figura 8.2.5 se exponen distintas técnicas de engorde que podrían aplicarse para desarrollar la acuicultura de *M. brachydactyla* así como la repoblación de sus poblaciones naturales. Cada una de dichas estrategias merece su estudio por separado para poder determinar su viabilidad. La estrategia de repoblación además requerirá la introducción de juveniles durante varios años así como su seguimiento, con objeto de determinar realmente su eficiencia.

10. De acuerdo a nuestra experiencia los juveniles aceptan pienso como alimento, lo que permitiría desarrollar dietas artificiales que podrían sustituir al alimento fresco.

11. Se desconocen las condiciones óptimas de cultivo para conseguir el engorde de los juveniles de *M. brachydactyla* a largo plazo o hasta talla comercial. En ese sentido es precisa la realización de estudios enfocados en esta etapa vital.

12. La culminación de la producción de una especie acuícola es la mejora genética y la domesticación, proceso que en dichas especies ha requerido pocas generaciones una vez iniciados los programas de cría selectiva (Coman et al., 2005; Norman-López et al., 2016; Preston et al., 2004), los cuales han permitido adaptarlas a las condiciones de producción en cautividad, incrementando con ello de la eficiencia de la alimentación, la tasa de crecimiento y el peso corporal (Coman et al., 2005; Norman-López et al., 2016; Preston et al., 2004; Quinitio et al., 2011). Si se desea la producción rentable de *M. brachydactyla*, la domesticación debe ser el objetivo final a medio y largo plazo, de modo que pueda ser posible un ajuste recíproco entre técnicas de cultivo y especie. Por el contrario, si se pretende la repoblación de las poblaciones naturales debe evitarse cualquier intento de domesticación, puesto que los animales liberados no deben estar adaptados a las condiciones de cultivo sino al medio externo, siendo preciso imitar en lo posible las condiciones naturales y maximizar la diversidad genética.

8.4 Bibliografía.

Ackefors HEG. 2000. Freshwater crayfish farming technology in the 1990s: a European and global perspective. Fish and Fisheries 1(4):337-359.

Aiken DE, Martin DJ, Meisner JD, Sochasky JB. 1981. Influence of Photoperiod on Survival and Growth of larval American Lobster (*Homarus americanus*). Journal of the World Mariculture Society 12(1):225-230.

Álvarez-Salgado XA, Bode A, Castro CG, Gago J, Nogueira E, Pérez FF, Ríos AF, Rosón G, Varela M. 2009. Evidencias bioxeoquímicas do cambio climático. Galicia. Junta. p 24.

Andrés M, Estévez A, Hontoria F, Rotllant G. 2010a. Differential utilization of biochemical components during larval development of the spider crab *Maja brachydactyla* (Decapoda: Majidae). Marine Biology 157(10):2329-2340.

Andrés M, Estévez A, Rotllant G. 2007. Growth, survival and biochemical composition of spider crab *Maja brachydactyla* (Balss, 1922) (Decapoda: Majidae) larvae reared under different stocking densities, prey:larva ratios and diets. Aquaculture 273(4):494-502.

Andrés M, Estévez A, Rotllant G. 2009. Incidencia del síndrome de muerte en la muda en larvas de centollo, *Maja brachydactyla*, alimentadas con dietas artificiales. In: Beaz-Paleo D, Villarroel-Robinson M, Cárdenas-Rojas S, editors. XII Congreso Nacional de Acuicultura. Madrid. p 72-73.

Andrés M, Estévez A, Simeó CG, Rotllant G. 2010b. Annual variation in the biochemical composition of newly hatched larvae of *Maja brachydactyla* in captivity. Aquaculture 310(1-2):99-105.

Andrés M, Gisbert E, Díaz M, Moyano FJ, Estévez A, Rotllant G. 2010c. Ontogenetic changes in digestive enzymatic capacities of the spider crab, *Maja brachydactyla* (Decapoda: Majidae). J Exp Mar Biol Ecol 389(1-2):75-84.

Andrés M, Rotllant G, Sastre M, Estevez A. 2011. Replacement of live prey by formulated diets in larval rearing of spider crab *Maja brachydactyla*. Aquaculture 313(1-4):50-56.

Andrés M, Rotllant G, Zeng C. 2010d. Survival, development and growth of larvae of the blue swimmer crab, *Portunus pelagicus*, cultured under different photoperiod conditions. Aquaculture 300(1-4):218-222.

Andrews WR, Targett NM, Epifanio CE. 2001. Isolation and characterization of the metamorphic inducer of the common mud crab, *Panopeus herbstii*. J Exp Mar Biol Ecol 261(1):121-134.

Anger K. 1985. Influence of salinity on larval development of the spider crab, *Hyas araneus*, reared in the laboratory. In: Gray JS, Christiansen ME, editors. Marine biology of polar regions and effects of stress on marine organisms. Chichester John Wiley & Sons. p 463–474.

Anger K. 1991. Effects of temperature and salinity on the larval development of the Chinese mitten crab *Eriocheir sinensis* (Decapoda: Grapsidae). Marine Ecology Progress Series 72:103-110.

Anger K. 2001. The Biology of Decapod Crustacean Larvae. Rotterdam: A.A. Balkema Publishers. 419 p.

Anger K. 2003. Salinity as a key parameter in the larval biology of decapod crustaceans. Invertebrate Reproduction & Development 43(1):29-45.

Arcos FG, Ibarra AM, Palacios E, Vazquez-Boucard C, Racotta IS. 2003. Feasible predictive criteria for reproductive performance of white shrimp *Litopenaeus vannamei*: egg quality and female physiological condition. Aquaculture 228(1):335-349.

Arcos FG, Palacios E, Ibarra AM, Racotta IS. 2005. Larval quality in relation to consecutive spawnings in white shrimp *Litopenaeus vannamei* Boone. Aquaculture Research 36(9):890-897.

Baylon J, Suzuki H. 2007. Effects of changes in salinity and temperature on survival and development of larvae and juveniles of the crucifix crab *Charybdis feriatus* (Crustacea:Decapoda:Portunidae). Aquaculture 269(1-4):390-401.

Benzie JAH. 1997. A review of the effect of genetics and environment on the maturation and larval quality of the giant tiger prawn *Penaeus monodon*. Aquaculture 155(1):69-85.

Benzie JAH. 2009. Use and exchange of genetic resources of penaeid shrimps for food and aquaculture. Reviews in Aquaculture 1(3-4):232-250.

Bermudes M, Ritar AJ. 2008. Response of early stage spiny lobster *Jasus edwardsii* phyllosoma larvae to changes in temperature and photoperiod. Aquaculture 281(1-4):63-69.

Bookhout CG, Costlow Jr JD. 1977. Larval development of *Callinectes similis* reared in the laboratory. Bulletin of Marine Science 27(4):704-728.

Bowser PR, Rosemark R. 1981. Mortalities of cultured lobsters, *Homarus*, associated with a molt death syndrome. Aquaculture 23(1):11-18.

Briere J-F, Pracros P, Le Roux A-Y, Pierre J-S. 1999. A novel rate model of temperature-dependent development for arthropods. Environmental Entomology 28(1):22-29.

Brock JA. 1993. A synopsis of pathology, diseases, and production problemas of cultured *Macrobrachium*, with an emphasis on experiences in Hawaiian prawn farming. In: McVey JP, editor. CRC Handbook of Mariculture: Crustacean Aquaculture, Second Edition, Volumen 1: CRC Press. p 361-392.

Cabanas JM, Nunes Mt, Iglesias Mk, Gonzalez N, Carballo R. 1987. Oceanografía de la bahía de La Coruña. Boletín Instituto Español de Oceanografía 4(1):21-28.

Calado R, Narciso L, Morais S, Rhyne AL, Lin J. 2003. A rearing system for the culture of ornamental decapod crustacean larvae. Aquaculture 218(1-4):329-339.

Calado R, Pimentel T, Vitorino A, Dionísio G, Dinis MT. 2008. Technical improvements of a rearing system for the culture of decapod crustacean larvae, with emphasis on marine ornamental species. Aquaculture 285(1):264-269.

Campbell GR, Fielder DR. 1987. Occurrence of a prezoea in two species of commercially exploited portunid crabs (Decapoda, Brachyura). Crustaceana 52(2):202-206.

Clark PF, Calazans D, Pohle GW. 1998. Accuracy and standardization of brachyuran larval descriptions. Invertebrate Reproduction & Development 33(2-3):127-144.

Clark PF, Cuesta JA. 2015. Larval systematics of Brachyura. In: Castro P, Davie P, Guinot D, Schram F, Klein CV, editors. Treatise on Zoology - Anatomy Taxonomy Biology The Crustacea Volume 9 Part C 2 vols: Brill. p 981-1048.

Coman GI, Crocos PI, Arnold SJ, Keys SI, Preston NP, Murphy B. 2005. Growth, survival and reproductive performance of domesticated Australian stocks of the Giant Tiger Prawn, *Penaeus monodon*, reared in tanks and raceways. Journal of the World Aquaculture Society 36(4):464-479.

Corgos A, Bernárdez C, Sampedro P, Verísimo P, Freire J. 2011. Spatial structure of the spider crab, *Maja brachydactyla* population: Evidence of metapopulation structure. Journal of Sea Research 66(1):9-19.

Corgos A, Sánchez N, Freire J. 2010. Dynamics of the Small-Scale Spatial Structure of a Population of the Spider Crab *Maja brachydactyla* (Decapoda: Majidae). Journal of Shellfish Research 29(1):25-36.

Costlow JD, Bookhout CG. 1959. The Larval Development of *Callinectes sapidus* Rathbun Reared in the Laboratory. The Biological Bulletin 116(3):373-396.

Costlow JD, Bookhout CG. 1962. The larval development of *Sesarma reticulatum* Say- Reared in the Laboratory. Crustaceana 4(4):281-294.

Costlow JD, Bookhout CG, Monroe R. 1960. The Effect of Salinity and Temperature on Larval Development of *Sesarma cinereum* (Bosc) Reared in the Laboratory. Biological Bulletin 118(2):183-202.

Costlow Jr JD, Bookhout CG, Monroe R. 1966. Studies on the Larval Development of the Crab, *Rhithropanopeus harrisii* (Gould). I. The Effect of Salinity and Temperature on Larval Development. Physiological Zoology 39(2):81-100.

Coutteau P, Geurden I, Camara MR, Bergot P, Sorgeloos P. 1997. Review on the dietary effects of phospholipids in fish and crustacean larviculture. Aquaculture 155(1):149-164.

Cronin TW, Forward Jr RB. 1980. The Effects of Starvation on Phototaxis and Swimming of Larvae of the Crab *Rhithropanopeus harrisi*. Biological Bulletin 158:283-294.

Chinain M, Vey A. 1988. Experimental study of *Fusarium solani*: infections in *Astacus leptodactylus* and *Pacifastacus leniusculus* (Crustacea, Decapoda). Diseases of Aquatic Organisms 5:215-223.

Dakin WMJ. 1912. Aquatic animals and their environment. The Constitution of the external medium, and its effect upon the blood. Internationale Revue der gesamten Hydrobiologie und Hydrographie 5(1):53-80.

Dan S, Takeshima S, Ashidate M, Hamasaki K. 2013. Variations in larval morhpology and their relationships to survival during mass seed production by the swimming crab, *Portunus triberculatus* (Brachyura, Portunidae). Aquaculture 414-415:109-118.

Davie PJF, Guinot D, Ng PKL. 2015a. Anatomy and functional morphology of Brachyura. In: Castro P, Davie PJF, Guinot D, Schram F, Von Vaupel Klein C, editors. Treatise on Zoology - Anatomy Taxonomy Biology The Crustacea Volume 9 Part C: Brill. p 11-163.

Davie PJF, Guinot D, Ng PKL. 2015b. Phylogeny of Brachyura. In: Castro P, Davie PJF, Guinot D, Schram F, Von Vaupel Klein C, editors. Treatise on Zoology - Anatomy Taxonomy Biology The Crustacea Volume 9 Part C: Brill, Leiden and Boston. p 922-979.

Davis DA, Arnold CR. 1998. The design, management and production of a recirculating raceway system for the production of marine shrimp. Aquacultural Engineering 17(3):193-211.

Dawirs RR. 1982. Methodical aspects of rearing decapod larvae, *Pagurus bernhardus* (Paguridae) and *Carcinus maenas* (Portunidae). Helgoländer Meeresuntersuchungen 35:439-464.

Díaz AC, Sousa LG, Cuartas EI, Petriella AM. 2003. Growth, molt and survival of *Palaemonetes argentinus* (Decapoda, Caridea) under different light-dark conditions. Iheringia Série Zoologia 93(3):249-254.

Diele K, Simith DJB. 2007. Effects of substrata and conspecific odour on the metamorphosis of mangrove crab megalopae, *Ucides cordatus* (Ocypodidae). J Exp Mar Biol Ecol 348(1-2):174-182.

Doval MD, Nogueira E, Pérez FF. 1998. Spatio-temporal variability of the thermohaline and biogeochemical properties and dissolved organic carbon in a coastal embayment affected by upwelling: the Ría de Vigo (NW Spain). Journal of Marine Systems 14(1):135-150.

Drilhon A. 1935. Etude biochimique de la Mue chez les Crustacés Brachyoures (*Maïa Squinado*). Annales de Physiologie et de Physicochimie Biologique 11:301-326.

Duermit E, Kingsley-Smith PR, Wilber DH. 2015. The consequences of claw removal on stone crabs *Menippe* spp. and the ecological and fishery implications. North American Journal of Fisheries Management 35(5):895-905.

Dugan CC, Hagood RW, Frakes TA. 1975. Development of spawning and mass larval rearing techniques for brackish-freshwater shrimps of the genus *Macrobrachium* (Decapoda: Palaemonidae). St. Petersburg, Florida: Department of Natural Resources, Marine Research Laboratory.

Fagetti E. 1969. Larval development of the spider crab *Pisoides edwardsi* (Decapoda, Brachyura) under laboratory conditions. Marine Biology 4(2):160-165.

Fagetti E, Campodonico I. 1971. Desarrollo larval en el laboratorio de *Taliepus dentatus* (Milne Edwards) (Crustacea: Brachyura: Majidae: Acanthonychinae). Revista de Biología Marina y Oceanografía 14:1-14.

Fernandez M, Iribarne O, Armstrong D. 1994. Ecdysial rhythms in megalopae and first instars of the Dungeness crab *Cancer magister*. Marine Biology 118(4):611-615.

Fitzgerald TP, Forward Jr RB, Tankersley RA. 1998. Metamorphosis of the estuarine crab *Rhithropanopeus harrisii*: effect of water type and adult odor Marine Ecology Progress Series 165:217-223.

Fitzgibbon QP, Battaglene SC. 2012. Effect of photoperiod on the culture of early-stage phyllosoma and metamorphosis of spiny lobster (*Sagmariasus verreauxi*). Aquaculture 368-369(0):48-54.

Forward Jr RB. 1974. Negative phototaxis in crustacean larvae: Possible functional significance. J Exp Mar Biol Ecol 16(1):11-17.

Forward Jr RB, Cronin TW. 1980. Tidal Rhythms of Activity and Phototaxis of an Stuarine Crab Larva. Biological Bulletin 158:295-303.

Forward Jr RB, Frankel DAZ, Rittschof D. 1994. Molting of megalopae from the blue crab *Callinectes sapidus*: effects of offshore and estuarine cues. Marine Ecology Progress Series 113:55-59.

Forward RB, De Vries MC, Rittschof D, Frankel DAZ, Bischoff JP, Fisher CM, Welch JM. 1996. Effects of environmental cues on metamorphosis of the blue crab *Callinectes sapidus*. Marine Ecology Progress Series 131:165-177.

Forward RB, Tankersley RA, Rittschof D. 2001. Cues for Metamorphosis of Brachyuran Crabs: An Overview. American Zoologist 41(5):1108-1122.

Freire J, Bernárdez C, Corgos A, Fernández L, González-Gurriarán E, Sampedro MP, Verísimo P. 2002. Management strategies for sustainable invertebrate fisheries in coastal ecosystems of Galicia (NW Spain). Aquatic Ecology 36(1):41-50.

Gago J, Cabanas JM, Casas G, Miranda A. 2011. Thermohaline measurements in the continental shelf zone of the NW Iberian Peninsula, 1994–2006. Climate Research 48:219-229.

Gardner C, Maguire GB. 1998. Effect of photoperiod and light intensity on survival, development and cannibalism of larvae of the Australian giant crab *Pseudocarcinus gigas* (Lamarck). Aquaculture 165(1-2):51-63.

Gebauer P, Paschke K, Anger K. 2002. Metamorphosis in a semiterrestrial crab, *Sesarma curacaoense*: intra- and interspecific settlement cues from adult odors. J Exp Mar Biol Ecol 268(1):1-12.

Gebauer P, Walter I, Anger K. 1998. Effects of substratum and conspecific adults on the metamorphosis of *Chasmagnathus granulata* (Dana) (Decapoda: Grapsidae) megalopae. J Exp Mar Biol Ecol 223(2):185-198.

Genodepa J, Zeng C, Southgate PC. 2004. Preliminary assessment of a microbound diet as an Artemia replacement for mud crab, *Scylla serrata*, megalopa. Aquaculture 236(1):497-509.

Gillooly JF, Brown JH, West GB, Savage VM, Charnov EL. 2001. Effects of size and temperature on metabolic rate. Science 293(5538):2248-2251.

Gong H, Jiang DH, Lightner DV, Collins C, Brock D. 2004. A dietary modification approach to improve the osmoregulatory capacity of *Litopenaeus vannamei* cultured in the Arizona desert. Aquaculture Nutrition 10(4):227-236.

González-Gurriarán E, Fernández L, Freire J, Muiño R. 1998. Mating and role of seminal receptacles in the reproductive biology of the spider crab *Maja squinado* (Decapoda, Majidae). J Exp Mar Biol Ecol 220(2):269-285.

González-Gurriarán E, Fernández L, Freire J, Muiño R, Parapar J. 1993. Reproduction of the spider crab *Maja squinado* (Brachyura: Majidae) in the southern Galician coast (NW Spain). International Council for the Exploration of the Sea: Shellfish Committe ICES C.M. 1993/K:19.

Guerao G, Pastor E, Martin J, Andrés M, Estévez A, Grau A, Duran J, Rotllant G. 2008. The larval development of *Maja squinado* and *M. brachydactyla* (Decapoda, Brachyura, Majidae) described from plankton collected and laboratory-reared material. Journal of Natural History 42(33-34):2257-2276.

Guo B, Mu Y, Wang F, Dong S. 2012. Effect of periodic light color change on the molting frequency and growth of *Litopenaeus vannamei*. Aquaculture 362-363(0):67-71.

Hamasaki K, Obata Y, Dan S, Kitada S. 2011. A review of seed production and stock enhancement for commercially important portunid crabs in Japan. Aquaculture International 19(2):217-235.

Hamasaki K, Ogiso Y, Dan S, Kitada S. 2015. Survival, development and growth of larvae of the coconut crab, *Birgus latro*, cultured under different photoperiod conditions. Aquaculture Research:n/a-n/a.

Hamasaki K, Suprayudi MA, Takeuchi T. 2002. Mass mortality during metamorphosis to megalops in the seed production of mud crab *Scylla serrata* (Crustacea, Decapoda, Portunidae). Fisheries Science 68:1226-1232.

Hernández JE, Palazón-Fernández JL, Hernández G, Bolaños J. 2012. The effect of temperature and salinity on the larval development of *Stenorhynchus seticornis* (Brachyura: Inachidae) reared in the laboratory. Journal of the Marine Biological Association of the United Kingdom 92(03):505-513.

Hoang T, Barchiesis M, Lee SY, Keenan CP, Marsden GE. 2003. Influences of light intensity and photoperiod on moulting and growth of *Penaeus merguiensis* cultured under laboratory conditions. Aquaculture 216(1-4):343-354.

Holme M-H, Zeng C, Southgate PC. 2009. A review of recent progress toward development of a formulated microbound diet for mud crab, *Scylla serrata*, larvae and their nutritional requirements. Aquaculture 286(3-4):164-175.

Hughes JT, Shleser RA, Tchobanoglous G. 1974. A rearing tank for lobster larvae and other aquatic species. The Progressive Fish-Culturist 36(3):129-132.

Hultgren KM, Stachowicz JJ. 2008. Molecular phylogeny of the brachyuran crab superfamily Majoidea indicates close congruence with trees based on larval morphology. Molecular Phylogenetics and Evolution 48(3):986-996.

Iglesias J, Sánchez FJ, Moxica C, Fuentes L, Otero JJ, Pérez JL. 2002. Datos preliminares sobre el cultivo de larvas y juveniles de centolla *Maja squinado* Herbst, 1788 en el Centro Oceanográfico de Vigo del Instituto Español de Oceanografía. Boletín del Instituto Español de Oceanografía 18(1-4):25-30.

Jackson CJ, Pendrey RC, Rothlisberg PC. 1992. The Larvatron: a computer-controlled apparatus for rearing planktonic animals under experimental conditions Marine Ecology Progress Series 86(2):189-199.

Jones CM. 1995. Production of juvenile redclaw crayfish, *Cherax quadricarinatus* (von Martens) (Decapoda, Parastacidae) I. Development of hatchery and nursery procedures. Aquaculture 138(1):221-238.

Kopin CY, Epifanio CE, Nelson S, Stratton M. 2001. Effects of chemical cues on metamorphosis of the Asian shore crab *Hemigrapsus sanguineus*, an invasive species on the Atlantic Coast of North America. J Exp Mar Biol Ecol 265(2):141-151.

Krimsky LS, Epifanio CE. 2008. Multiple cues from multiple habitats: Effect on metamorphosis of the Florida stone crab, *Menippe mercenaria*. J Exp Mar Biol Ecol 358(2):178-184.

Lactin DJ, Holliday NJ, Johnson DL, Craigen R. 1995. Improved rate model of temperature-dependent development by arthropods. Environmental Entomology 24(1):68-75.

Lárez MB, Palazón-Fernández JL, Bolaños CJ. 2000. The effect of salinity and temperature on the larval development of *Mithrax caribbaeus* Rathbun, 1920 (Brachyura: Majidae) reared in the laboratory. Journal of Plankton Research 22(10):1855-1869.

Le Foll D. 1993. Biologie et exploitation de l'araignée de mer *Maja squinado* Herbst en Manche Ouest [Doctoral Dissertation]. Plouzane (France): Université de Bretagne Occidentale. 517 p.

Logan JA, Wollkind DJ, Hoyt SC, Tanigoshi LK. 1976. An analytic model for description of temperature dependent rate phenomena in arthropods 1. Environmental Entomology 5(6):1133-1140.

Luchiari AC, Marques AO, Freire FAM. 2012. Effects of substrate colour preference on growth of the shrimp *Litopenaeus vannamei* (Boone, 1931) (Decapoda, Penaeoidea). Crustaceana. p 789-800.

Luis-Villaseñor IE , Campa-Córdova AI , Ascencio-Valle FJ. 2012. Probiotics in larvae and juvenile Whiteleg Shrimp *Litopenaeus vannamei*. In: Rigobelo EC, editor. Probiotics. Rijeka: InTech. p Ch. 27.

Martin JW. 2014. 54. Brachyura. In: Martin JW, Olesen J, Høeg JT, editors. Baltimore: Johns Hopkins University Press. p 295-310.

Martin JW, Olesen J, Høeg JT. 2014. Atlas of Crustacean Larvae. Baltimore: Johns Hopkins University Press.

Minagawa M. 1990. Influence of Temperature on Survival, Feeding and Development of Larvae of the Red Frog Crab, *Ranina ranina* (Crustacea, Decapoda, Raninidae). Nippon Suisan Gakkaishi 56(5):755-760.

Minagawa M. 1994. Effects of photoperiod on survival, feeding and development of larvae of the red frog crab, *Ranina ranina*. Aquaculture 120(1â€“2):105-114.

Mock CR, Neal RA, Salser BR. 1973. A closed raceway for the culture of shrimp1. Proceedings of the annual workshop - World Mariculture Society 4(1-4):247-259.

Mohney LL, Poulos BT, Brooker JH, Cage GD, Lightner DV. 1998. Isolation and identification of *Mycobacterium peregrinum* from the Pacific White Shrimp *Penaeus vannamei*. Journal of Aquatic Animal Health 10(1):83-88.

Nagaraj M. 1992. Combined Effects of Temperature and Salinity on the Zoeal Development of the Crab *Liocarcinus puber* (Decapoda: Portunidae). Marine Ecology 13(3):233-241.

Norman-López A, Sellars MJ, Pascoe S, Coman GJ, Murphy B, Moore N, Preston N. 2016. Productivity benefits of selectively breeding Black Tiger shrimp (*Penaeus monodon*) in Australia. Aquaculture Research 47(10):3287-3296.

Nurdiani R, Zeng C. 2007. Effects of temperature and salinity on the survival and development of mud crab, *Scylla serrata* (Forsskål), larvae. Aquaculture Research 38(14):1529-1538.

O'Connor NJ. 2007. Stimulation of molting in megalopae of the Asian shore crab *Hemigrapsus sanguineus*: physical and chemical cues. Marine Ecology Progress Series 352:1-8.

O'Connor NJ, Gregg AS. 1998. Influence of potential habitat cues on duration of the megalopal stage of the fiddler crab *Uca pugnax*. Journal of Crustacean Biology 18(4):700-709.

Ong K-S, Costlow J. 1970. The effect of salinity and temperature on the larval development of the stone crab, *Menippe mercenaria* (Say), reared in the laboratory. Chesapeake Science 11(1):16-29.

Oniam V, Chuchit L, Arkronrat W. 2012. Reproductive performance and larval quality of blue swimming crab (*Portunus pelagicus*) broodstock, fed with different feeds. Songklanakarin Journal of Science & Technology 34(4):381-386.

Palacios E, Perez-Rostro CI, Ramirez JL, Ibarra AM, Racotta IS. 1999. Reproductive exhaustion in shrimp (*Penaeus vannamei*) reflected in larval biochemical composition, survival and growth. Aquaculture 171(3):309-321.

Palma J, Correia M, Andrade JP. 2008. Usefulness of flat bottom tanks on the settlement of spider crab (*Maja squinado*, Herbst) larvae. Aquaculture Research 39(9):1005-1008.

Péqueux A. 1995. Osmotic Regulation in Crustaceans. Journal of Crustacean Biology 15(1):1-60.

Perry LT. 2001. Relationships between culture conditions and moult death syndrome (MDS) in larval development of the bay lobsters *Thenus Orientalis* (Lund, 1793) and Thenus Indicus Leach, 1815 (Decapoda: Scyllaridae) [PhD Thesis]. Queensland, Australia: The University of Queensland. 160 p.

Philipose KK. 2009. Preliminary experiments on the culture of the banded coral shrimp *Stenopus hispidus* Oliver. In: Madhu K, Madhu R, editors. Winter School on Recent Advances in Breeding and Larviculture of Marine Finfish and Shellfish. Kerala, India: Central Marine Fisheries Research Institute. Indian Council of Agricultural Research.

Preston NP, Crocos PJ, Keys SJ, Coman GJ, Koenig R. 2004. Comparative growth of selected and non-selected Kuruma shrimp *Penaeus* (*Marsupenaeus*) *japonicus* in commercial farm ponds; implications for broodstock production. Aquaculture 231(1):73-82.

Quinitio ET, de la Cruz JJ, Eguia MRR, Parado-Estepa FD, Pates G, Lavilla-Pitogo CR. 2011. Domestication of the mud crab *Scylla serrata*. Aquaculture International 19(2):237-250.

Rabbani AG, Zeng C. 2005. Effects of tank colour on larval survival and development of mud crab *Scylla serrata* (Forskål). Aquaculture Research 36(11):1112-1119.

Racotta IS, Palacios E, Ibarra AM. 2003. Shrimp larval quality in relation to broodstock condition. Aquaculture 227(1):107-130.

Rhodes RJ, Sureshwaran S, Greene C, Browdy CL, Holloway JD, Samocha TM. 1995. Production effects of a greenhouse enclosed nursery system on the projected financial performance of a South Carolina marine shrimp farm: U. S. Government Printing Office (Gpo).

Rice AL. 1980. Crab zoeal morphology and its bearing on the classification of the Brachyura. The Transactions of the Zoological Society of London 35(3):271-372.

Rice AL, Williamson DI. 1970. Methods for rearing larval decapod crustacea. Helgoländer wissenschaftliche Meeresuntersuchungen 20(1):417-434.

Roberts MH. 1971. Larval development of *Pagurus longicarpus* Say reared in laboratory III. Behavioral responses to salinity discontinuities. The Biological Bulletin 140(3):489-501.

Romano N, Zeng C. 2006. The effects of salinity on the survival, growth and haemolymph osmolality of early juvenile blue swimmer crabs, *Portunus pelagicus*. Aquaculture 260(1):151-162.

Rotllant G, Moyano FJ, Andrés M, Díaz M, Estévez A, Gisbert E. 2008. Evaluation of fluorogenic substrates in the assessment of digestive enzymes in a decapod crustacean *Maja brachydactyla* larvae. Aquaculture 282(1–4):90-96.

Rotllant G, Moyano FJ, Andrés M, Estévez A, Díaz M, Gisbert E. 2010. Effect of delayed first feeding on larval performance of the spider crab *Maja brachydactyla* assessed by digestive enzyme activities and biometric parameters. Marine Biology 157(10):2215-2227.

Rouse DB, Kartamulia I. 1992. Influence of salinity and temperature on molting and survival of the Australian freshwater crayfish (*Cherax tenuimanus*). Aquaculture 105(1):47-52.

Samocha TM, Hamper L, Emberson CR, Davis AD, McIntosh D, Lawrence AL, Van Wyk PM. 2002. Review of some recent developments in sustainable shrimp farming practices in Texas, Arizona, and Florida. Journal of Applied Aquaculture 12(1):1-42.

Simith DJB, Diele K. 2008. Metamorphosis of mangrove crab megalopae, *Ucides cordatus* (Ocypodidae): Effects of interspecific versus intraspecific settlement cues. J Exp Mar Biol Ecol 362(2):101-107.

Simith DJB, Diele K, Abrunhosa FA. 2010. Influence of natural settlement cues on the metamorphosis of fiddler crab megalopae, *Uca vocator* (Decapoda: Ocypodidae). Anais da Academia Brasileira de Ciências 82(2):313-321.

Steinberg M, Krimsky L, Epifanio C. 2008. Induction of Metamorphosis in the Asian Shore Crab *Hemigrapsus sanguineus*: Effects of Biofilms and Substratum Texture. Estuaries and Coasts 31(4):738-744.

Steinberg MK, Epifanio CE, Andon A. 2007. A highly specific chemical cue for the metamorphosis of the Asian shore crab, *Hemigrapsus sanguineus*. J Exp Mar Biol Ecol 347(1-2):1-7.

Sui L, Wille M, Cheng Y, Wu X, Sorgeloos P. 2011. Larviculture techniques of Chinese mitten crab *Eriocheir sinensis*. Aquaculture 315(1):16-19.

Tidwell JH, Coyle S, Vanarnum A, Bright LA, McCathy M. 2001. The Effect of Photoperiod on Growth and Survival of Juvenile Freshwater Prawn, *Macrobrachium rosenbergii* in Nursery Tanks. Journal of Applied Aquaculture 11(4):41-47.

Torres G, Giménez L, Anger K. 2011. Growth, tolerance to low salinity, and osmoregulation in decapod crustacean larvae. Aquatic Biology 12(3):249-260.

Ulikowski D, Krzywosz T. 2004. The impact of photoperiod and stocking density on the growth and survival of narrow-clawed crayfish (*Astacus leptodactylus* Esch.) larvae. Archives of Polish Fisheries 12(1):81-86.

Verísimo P. 2015. Implicaciones de la composición bioquímica y la condición energética de la centolla, *Maja brachydactyla* (Balss, 1922), en su ciclo reproductivo. Doctoral Thesis: Universidade da Coruña. 266 p.

Weber JC, Epifanio CE. 1996. Response of mud crab (*Panopeus herbstii*) megalopae to cues from adult habitat. Marine Biology 126(4):655-661.

Wickins JF, O'C Lee D. 2002. Crustacean Farming, Ranching and Culture, 2nd edition. Oxford: Wiley-Blackwell. 464 p.

Williamson DI. 1969. Names of larvae in the Decapoda and Euphausiacea. Crustaceana 16(2):210-213.

Wouters R, Gomez L, Lavens P, Calderón J. 1999. Feeding enriched Artemia biomass to *Penaeus vannamei* broodstock: Its effect on reproductive performance and larval quality. Journal of Shellfish Research 18(2):651-656.

Ye L, Jiang S, Zhu X, Yang Q, Wen W, Wu K. 2009. Effects of salinity on growth and energy budget of juvenile *Penaeus monodon*. Aquaculture 290(1):140-144.

Zeng C, Naylor E, Abello P. 1997. Endogenous control of timing of metamorphosis in megalopae of the shore crab *Carcinus maenas*. Marine Biology 128(2):299-305.

BLOQUE 2.

SISTEMA DIGESTIVO. INTRODUCCIÓN.

"En ce qui concerne l'Anatomie de ces formes larvaires, notre ignorance est encore plus grande"

C. Schlegel 1911

9.1 Sistema Digestivo de los decápodos. Caracteres generales.

El sistema digestivo de los decápodos está subdivido en las regiones típicas del sistema digestivo de los pancrustáceos: digestivo anterior, digestivo medio y digestivo posterior. Tanto el digestivo anterior como el posterior son derivados ectodérmicos, ambos están delimitados por una cutícula continua con el exoesqueleto exterior, de modo que tanto la cutícula que reviste estos órganos internos como el exoesqueleto son mudados simultáneamente. Por su parte, los órganos del digestivo medio derivan del mesodermo y están delimitados por un epitelio simple carente de cutícula. El digestivo anterior abarca el esófago y el estómago. El digestivo medio está formado por el tracto digestivo medio, los ciegos asociados y la glándula digestiva (también llamada hepatopáncreas). El digestivo posterior se compone del tracto digestivo posterior y el ano (Brusca y Brusca, 2003; Ceccaldi, 1989; Davie et al., 2015; Felgenhauer, 1992). A continuación, se presentarán los distintos órganos que conforman el tracto digestivo así como una breve descripción de los mismos. Estos órganos serán estudiados individualmente y con mayor profundidad en los siguientes capítulos.

9.1.1 Digestivo anterior

El esófago de los decápodos es un tubo corto y vertical que une la boca con el estómago. El esófago presenta pliegues longitudinales que otorgan al lumen un aspecto de X o H en sección transversal (Erri Babu et al., 1982; Felgenhauer, 1992; Patwardhan, 1935; Trinadha Babu et al., 1989; Yonge, 1924). Como derivado del ectodermo embrionario, está cubierto por una cutícula continua con el exoesqueleto y el recubrimiento del estómago (Ceccaldi, 1989; Felgenhauer, 1992; Icely y Nott, 1992). Esta cutícula presenta dos tipos de estructuras: micro-espinas y poros. Elzinga y Hopkins (1994) y Elzinga (1998) han reportado micro-espinas en el esófago de numerosos taxa de artrópodos (incluyendo arácnidos, quilópodos y diversos grupos de pancrustáceos), pero su rol es desconocido. Los poros de los astacídeos son perforaciones de 1 a 8 μm de diámetro cuyo rol ha sido asociado a nervios sensores responsables de la peristalsis (Altner et al., 1986; Robertson y Laverack, 1979). El epitelio del esófago es simple y prismático, debajo de la lámina basal aparece una capa de tejido conectivo cuyo espesor varía entre diferentes taxones (Barker y Gibson, 1978; Dall, 1967; Erri Babu et al., 1982; Reddy, 1937; Sousa y Petriella, 2006; Trinadha Babu et al., 1989). El tejido conjuntivo puede presentar *glándulas de roseta*: agrupaciones globulares de células que rodean un fino canal central, estas glándulas participan en la secreción de sustancias mucosas que podrían actuar como lubricantes que facilitasen la ingesta del alimento (Barker y Gibson, 1978; Erri Babu et al., 1979; Erri Babu et al., 1982; Reddy, 1937; Trinadha Babu et al., 1989). El conectivo

está rodeado por gruesos paquetes de fibras musculares con tres tipos de orientaciones: fibras musculares circulares internas, fibras musculares longitudinales externas y fibras musculares dilatadoras que cruzan perpendicularmente el conectivo hasta alcanzar el epitelio; el rol de estos paquetes musculares es dilatar el lumen del esófago y permitir los movimientos peristálticos que permiten la ingestión del alimento (Ceccaldi, 1989; Erri Babu et al., 1979; Erri Babu et al., 1982; Felgenhauer, 1992; Icely y Nott, 1992).

El estómago es una estructura compleja unida anteriormente al esófago, posteriormente al tracto del digestivo medio y a la glándula digestiva o hepatopáncreas. El estómago puede subdividirse en una cámara anterior llamada estómago cardiaco y una cámara posterior llamada estómago pilórico, ambas cámaras están separadas por la válvula cardio-pilórica (Felgenhauer, 1992; Icely y Nott, 1992; Schaefer, 1970). El estómago presenta numerosos osículos, estas estructuras son engrosamientos de la cutícula endurecidos y calcificados de modo que forman una especie de armadura que soporta estructuralmente a este órgano (Alves et al., 2010; Brösing, 2010; 2014; Brösing et al., 2002; Brösing y Türkay, 2011; de La Barra et al., 2017; Hobbs y Hooper, 2009; Meiss y Norman, 1977). En los braquiuros se han descrito hasta 41 tipos de osículos (Brösing, 2010). Recientemente, dicho número se ha incrementado a 48 para ciertos miembros de la familia Trichodactylidae (Lima-Gomes et al., 2017). El estómago cardiaco presenta dorsalmente el molino gástrico, el cual está compuesto por un diente dorsal y dos pares de dientes laterales que derivan de osículos cuya cutícula está especialmente engrosada y endurecida, su función es moler el alimento ingerido. El estómago pilórico mantiene ventralmente a los filtros pilóricos, estructuras pares formadas por setas muy finas derivadas de la cutícula, este sistema de filtración permite que solo el material más fino pueda entrar en la glándula digestiva, mientras que el material rechazado es redirigido al tracto digestivo medio (Icely y Nott, 1992; Woods, 1995).

9.1.2 Digestivo medio

El tracto del digestivo medio de los decápodos es un órgano tubular cuyo extremo anterior está conectado con el estómago, los ciegos anteriores (si están presentes) y la glándula digestiva, mientras que el extremo posterior está conectado con el ciego posterior (si está presente) y con el tracto digestivo posterior (Barker y Gibson, 1977; 1978; Erri Babu et al., 1982; Hinton y Corey, 1979; Reddy, 1937; Yonge, 1924). El tracto digestivo medio está delimitado por un epitelio simple y prismático con ribete en cepillo que descansa sobre una lámina basal. En el tejido conectivo subyacente a la lámina basal aparece una banda continua de finos paquetes de fibras musculares circulares, seguida a poca distancia de una banda discontinua de finas fibras musculares longitudinales (Barker y Gibson, 1977; 1978; Erri Babu

et al., 1982; Hinton y Corey, 1979; Kaushik y Kumar, 1998; Reddy, 1937; Yonge, 1924). Las células epiteliales del tracto digestivo medio tienen el rol de secretar la membrana peritrófica, una secreción extracelular compuesta por un 3-13 % de quitina, así como una combinación de distintos tipos de proteínas, glicoproteínas y proteoglicanos (Lehane, 1997). Estos elementos se organizan formando membranas fibrilares que rodean al material presente en el lumen del tracto digestivo (Wang et al., 2012). La membrana peritrófica ha sido descrita en numerosos grupos de euartrópodos: pancrustáceos (incluyendo insectos), miriápodos y xifosuros (Lehane, 1997; Mets, 1962). Se ha sugerido que su principal función es envolver al material digerido para proteger a las células epiteliales de partículas abrasivas y patógenos (Martin et al., 2006; Wang et al., 2012).

Los ciegos del tracto digestivo medio son proyecciones dorsales y tubulares que surgen desde los extremos anterior y posterior del mismo tracto digestivo. Los ciegos anteriores suelen ser pares y son proyectados hacia el estómago, mientras que el ciego posterior suele ser impar y se proyecta hacia el tracto digestivo posterior (Erri Babu et al., 1982; Smith, 1978). En los decápodos, la longitud de estos ciegos es muy variable, desde proyecciones muy cortas en los astácidos (Factor, 1981; Hinton y Corey, 1979), hasta túbulos muy largos y enrollados sobre sí mismos en los braquiuros (Smith, 1978). El lumen de los ciegos está delimitado por un epitelio simple y prismático coronado por microvilli que descansa sobre una lámina basal, debajo de la cual se observa una delgada capa de tejido conjuntivo (Barker y Gibson, 1978; Erri Babu et al., 1982). Este tejido conjuntivo está asociado a fibras musculares muy finas que forman un entramado en forma de red (Davolos et al., 2010; Schmitz y Scherrey, 1983). La función de los ciegos del tracto digestivo sigue siendo desconocida, aunque se ha postulado un posible papel relacionado con la producción de enzimas digestivas (Holliday et al., 1980).

La glándula digestiva es tradicionalmente conocida como hepatopáncreas, si bien recientemente se ha propuesto denominarla órgano perigástrico (Cervellione et al., 2017b). Se trata de un órgano masivo que ocupa la mayor parte del volumen de la cavidad del cefalotórax. Se compone de dos mitades especulares que parten de la línea media del cuerpo, cada mitad está subdivida a su vez en dos o tres túbulos extendidos en dirección anterior, media y posterior. Cada uno de estos lóbulos se compone a su vez de una inmensa cantidad de cortos túbulos ciegos (Ceccaldi, 1989; Felgenhauer, 1992; Gibson y Barker, 1979; Loizzi, 1971; Van Weel, 1974; Vogt, 1996). El epitelio de la glándula digestiva es prismático y simple con ribete en cepillo, distinguiéndose cinco tipos celulares, cada una de los cuáles con un destacado rol en la funcionalidad de la glándula digestiva (Al-Mohanna y Nott, 1989; Al-Mohanna et al., 1985; Felgenhauer, 1992; Gibson y Barker, 1979; Icely y Nott, 1992; Loizzi, 1971; Longo y Díaz, 2015):

- Células E o "embrionarias". Localizas en el extremo distal de los túbulos, realizan procesos de división celular tras los cuales se diferencian en células R y F, posiblemente también en células M.
- Células R o "resortivas". Localizadas en la región distal, media y proximal de los túbulos, bajo microscopía óptica se caracterizan por su gran número de vacuolas lipídicas. Son células que sirven de almacén de lípidos y glucógeno.
- Células F o "fibrilares". Localizadas en la región distal, media y proximal de los túbulos, bajo microscopía óptica se caracterizan por su aspecto piramidal y la presencia de "estrías". Son responsables de la síntesis de enzimas digestivas.
- Células B o "ampulares". Localizadas en la región media y proximal de los túbulos, presentan una única y enorme vacuola que es liberada al lumen del túbulo mediante secreción apocrina/holocrina. Se asocian a procesos digestivos.
- Células M o "enanas". Se localizan a lo largo de todo el túbulo excepto en el extremo distal, son células muy pequeñas, adyacentes a la lámina basal no son capaces de alcanzar el lumen del órgano. Su función es desconocida.

El epitelio de la glándula digestiva descansa sobre una lámina basal, subyacente a la misma hay un delgado conjuntivo asociado a finas fibras musculares. Las fibras musculares forman una red compuesta por anillos espaciados longitudinalmente y unidos entre sí por fibras musculares longitudinales, formando un entramado muscular a modo de red cuadrangular (Barker y Gibson, 1978; Caceci et al., 1988; Ceccaldi, 1989; Loizzi, 1971).

9.1.3 Digestivo posterior

El tracto digestivo posterior es una estructura tubular que abarca desde la unión entre el tracto del digestivo medio y posterior hasta el ano (Ceccaldi, 1989; Felgenhauer, 1992; Herrera-Alvarez et al., 2000; Holdich, 1973; Smith, 1978). La longitud del tracto digestivo posterior de los decápodos varía entre distintos taxones, desde la mera longitud del sexto pleonito en algunos astacídeos marinos (Barker y Gibson, 1977; Yonge, 1924), hasta la mitad de la longitud del tracto digestivo post-estomacal en los braquiuros (Barker y Gibson, 1978; Erri Babu et al., 1982; Milne-Edwards, 1834b) y la casi totalidad del tracto digestivo post-estomacal en ciertos astacídeos dulceacuícolas, como los cangrejos de río (Chisaka et al., 1999; Komuro y Yamamoto, 1968). Como derivado del ectodermo embrionario, está cubierto por una cutícula continua con el exoesqueleto externo (Ceccaldi, 1989; Felgenhauer, 1992; Icely y Nott, 1992). El tracto digestivo posterior de los decápodos presenta pliegues longitudinales que recorren toda la longitud, el número de pliegues es variable pero los braquiuros conservan cinco pliegues

(Barker y Gibson, 1977; 1978; Huxley, 1880; Mykles, 1979; Pugh, 1962; Smith, 1978; Yonge, 1924). Elzinga y Hopkins (1995) y Elzinga (1998) han estudiado la superficie de la cutícula del tracto del digestivo medio y han reportado la presencia de micro-espinas en distintos taxones de euartrópodos (incluyendo arácnidos, diplópodos y pancrustáceos).

El papel de las micro-espinas es desconocido, se ha postulado que podrían ayudar a la excreción de las heces o bien sostener colonias de microorganismos simbiontes. El epitelio del tracto digestivo posterior es de tipo prismático y simple, este descansa sobre una lámina basal y tejido conjuntivo (Barker y Gibson, 1978; Erri Babu et al., 1982; Reddy, 1937). El tracto digestivo posterior de los braquiuros (Barker y Gibson, 1978) y astacídeos (To et al., 2004; Yonge, 1924; 1932) presenta glándulas de roseta muy similares a las descritas en el esófago. El tejido conjuntivo presenta una desarrollada capa de fibras musculares circulares. Los paquetes de musculatura longitudinal se localizan en el centro de los pliegues longitudinales y son necesarios para la excreción de las heces y la ingesta anal de agua (Barker y Gibson, 1977; 1978; Erri Babu et al., 1982; Komuro y Yamamoto, 1968; Reddy, 1937; To et al., 2004; Yonge, 1924).

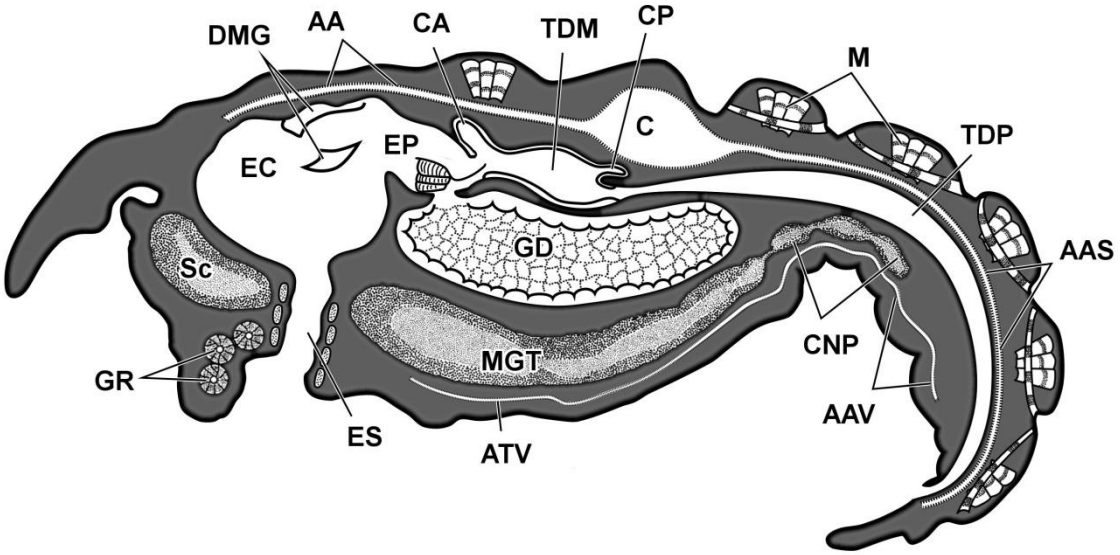

Fig. 9.1. Centollo, *Maja brachydactyla*. Esquema de la anatomía interna durante el estadio de megalopa. Abreviaciones: AA, arteria anterior; AAS, arteria abdominal superior; AAV, arteria abdominal ventral; ATV, arteria torácica ventral; C, corazón; CA, ciegos anteriores; CNP, cordón nervioso posterior; CP, ciego posterior; DMG, dientes del molino gástrico; EC, estómago cardiaco; EP, estómago pilórico; GD, glándula digestiva; GR, glándulas de roseta; M, musculatura; MGT, masa ganglionar torácica; Sc, sincerebro; TDM, tracto digestivo medio; TDP, tracto digestivo posterior.

9.2 Anatomía interna del centollo: antecedentes.

El "*Histoire naturelle des crustacés: comprenant l'anatomie, la physiologie et la classification de ces animaux*" es una obra que comprende tres volúmenes y un atlas laboriosamente detallado. Publicada entre 1834 y 1840, su autoría se debe al naturalista francés Henri Milne-Edwards. Desde el punto de vista de la presente Tesis, esta obra es especialmente relevante por dos razones. La primera, el primer volumen de esta obra presenta una detallada descripción de la morfología externa y la anatomía interna de los decápodos, incluyendo la descripción del sistema digestivo al inicio del segundo capítulo. La segunda razón, el atlas que forma parte de esta obra ilustra la anatomía interna de los decápodos de un modo excepcional, siendo uno de los animales elegidos como ejemplo los adultos del género *Maja*, mostrándose el sistema nervioso, circulatorio, branquial y digestivo (Fig. 9.2.1-9.2.3).

En lo que respecta al presente estudio, las ilustraciones de Milne-Edwards (1834b) relacionadas con el sistema digestivo son las más interesantes (Fig. 9.2.3). El esófago es un tubo corto, vertical y conectado a la pared ventral del estómago. El estómago aparece como un órgano complejo, se puede advertir la división entre la región cardiaca (globosa y expandida) y la región pilórica (estrecha y conectada con el tracto digestivo posterior), separadas por la válvula cardio-pilórica. Resulta especialmente interesante que hayan sido representados los osículos más desarrollados (urocárdico y pterocárdicos); así como el molino gástrico, compuesto por un diente dorsal derivado del osículo urocárdico y un par de dientes laterales molariformes derivados de los osículos pterocárdicos, cabe añadirse que dichos osículos reciben actualmente la misma denominación. La glándula digestiva (llamada "*foie*", hígado) destaca como una enorme masa visceral formada por cuantiosos tubos ciegos, está dividida en dos mitades en las que cada una presenta extensiones proyectadas en sentido anterior, medio y posterior. En cuanto al tracto digestivo post-estomacal, se divide entre un tracto digestivo medio ("*duodénium*", duodeno) corto y ancho, y un tracto digestivo posterior ("*rectum*", recto) largo y estrecho. En el extremo anterior del tracto digestivo medio aparecen un par de ciegos anteriores extremadamente largos y finos, mientras que en el extremo posterior del tracto digestivo medio, lindando con el tracto digestivo posterior, aparece un único ciego posterior largo y fino. Dichas observaciones serían corroboradas por posteriores estudios realizados en otros braquiuros, incluyendo la disposición de los osículos y el molino gástrico del estómago (Brösing, 2010; Brösing et al., 2007), la presencia de una enorme glándula digestiva formada por cuantiosos tubos ciegos de escasa longitud (Gibson y Barker, 1979; Vogt, 1996), un tracto digestivo post-estomacal dividido en una porción media y otra posterior (Felgenhauer, 1992; Icely y Nott, 1992), así como la presencia de un par de ciegos anteriores y un único ciego posterior (Smith, 1978). Por ello, este autor será un referente recurrente en los próximos capítulos.

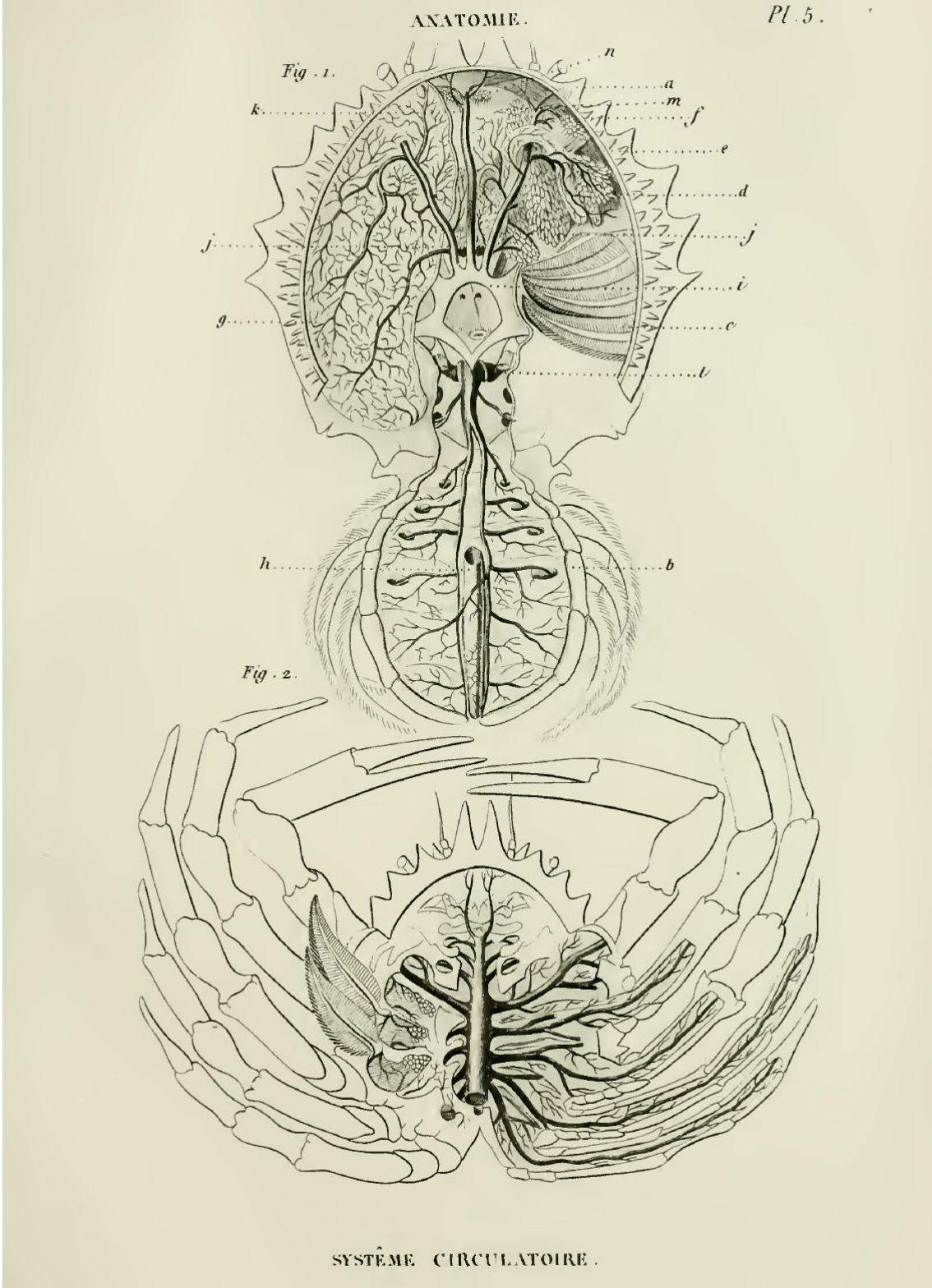

Fig. 9.2.1. Anatomía del género *Maja*. Adulto. Imagen publicada en la obra del naturalista francés Henri Milne - Edwards (1800-1885), "*Histoire naturelle des crustacés: comprenan tl'anatomie, la physiologie et la classification de ces animaux, Atlas*. Paris: Librairie encyclopédique de Roret, 1834-1840". Cortesía de Biodiversity Heritage Library (BHL). Versión digital realizada por Smithsonian Libraries. | www.biodiversitylibrary.org

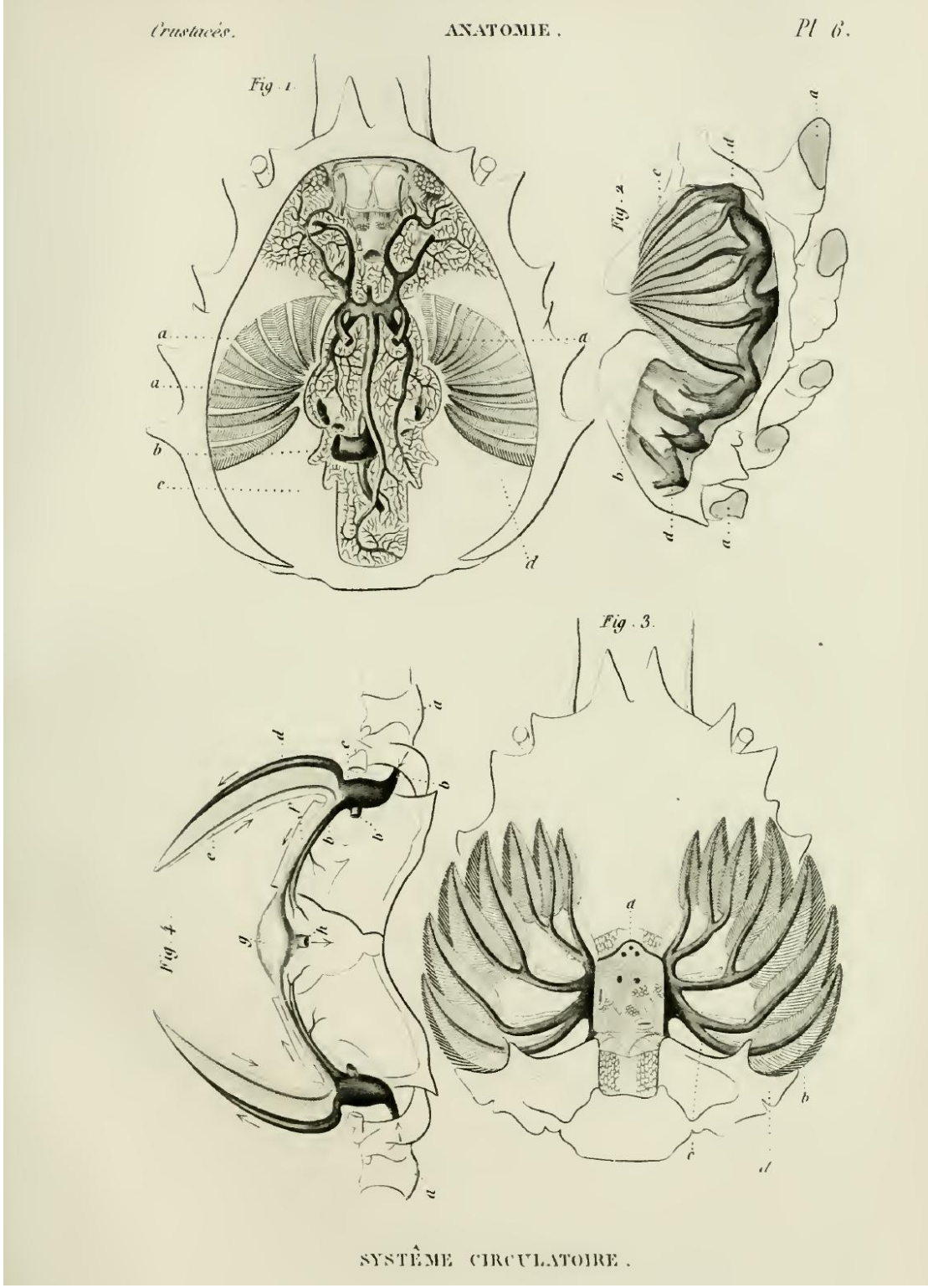

Fig. 9.2.2. Anatomía del género *Maja*. Adulto. Imagen publicada en la obra del naturalista francés Henri Milne - Edwards (1800-1885), "*Histoire naturelle des crustacés: comprenant l'anatomie, la physiologie et la classification de ces animaux, Atlas*. Paris: Librairie encyclopédique de Roret, 1834-1840". Cortesía de Biodiversity Heritage Library (BHL). Versión digital realizada por Smithsonian Libraries. | www.biodiversitylibrary.org

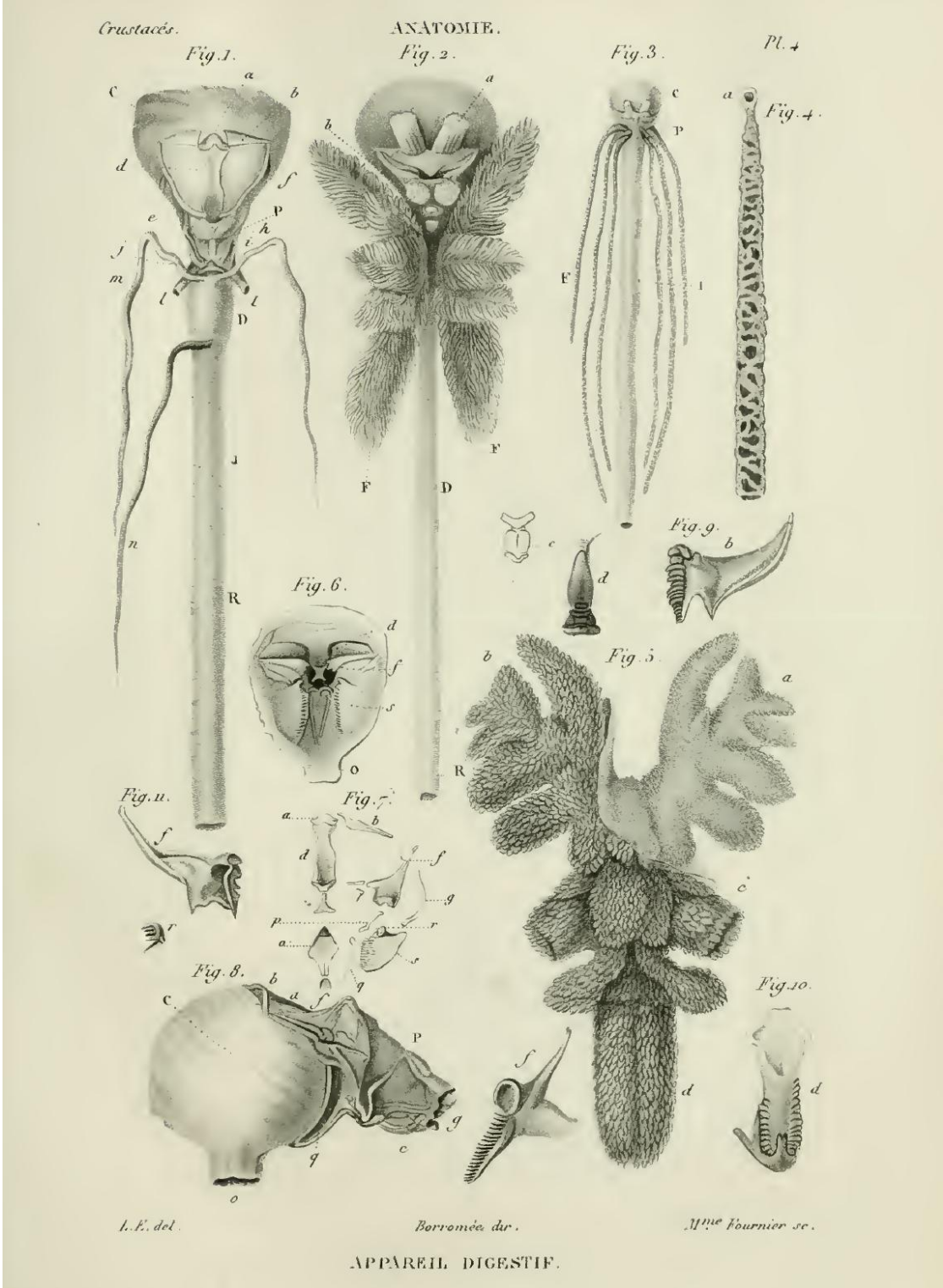

Fig. 9.2.3. Anatomía del género *Maja*. Adulto. Imagen publicada en la obra del naturalista francés Henri Milne - Edwards (1800-1885), "*Histoire naturelle des crustacés: comprenant l'anatomie, la physiologie et la classification de ces animaux, Atlas*. Paris: Librairie encyclopédique de Roret, 1834-1840". Cortesía de Biodiversity Heritage Library (BHL). Versión digital realizada por Smithsonian Libraries. | www.biodiversitylibrary.org

Después de Milne-Edwards, pocos estudios se han centrado en la anatomía interna del centollo u otras especies de májidos, en los que el estudio de su anatomía interna se estancó hasta las últimas décadas. En ese sentido, McGaw y Stillman (2010) utilizaron como modelo al cangrejo del kelp *Pugettia producta* (Randall, 1839) para describir brevemente la anatomía interna de este grupo. También de forma reciente ha resurgido el interés por el estudio de la anatomía interna de *Maja brachydactyla*, donde el creciente potencial de esta especie desde el punto de vista acuícola ha espoleado nuevas investigaciones. Los trabajos más importantes realizados sobre esta especie son los publicados por Rotllant et al. (2007), Simeó (2012) y Simeó et al. (2010; 2009a; 2009b), cuyo tema central fue el estudio del sistema reproductor. Más allá de las mencionadas publicaciones, no existen más trabajos centrados en la anatomía interna de esta especie durante la etapa adulta.

El único estudio centrado en la anatomía interna de los estadios larvarios del género *Maja* fue publicado por C. Schlegel (1911). Dicho estudio está enfocado en el primer estadio larvario (zoea I) y muestra que la anatomía interna de estos animales durante el primer estadio de zoea está lo suficientemente desarrollada como para englobar la mayoría de los sistemas de órganos observados en el adulto. Sin embargo, dichos órganos muestran una menor complejidad. El sistema digestivo presenta el esófago y el estómago delimitados por una cutícula. El esófago es un tubo corto, de lumen estrellado y rodeado de músculos constrictores. La región cardiaca del estómago carece de osículos y molino gástrico, pero la región pilórica posee un par de filtros ventro-laterales. La glándula digestiva ("*hépatopancréas*", "*organe entérique*") es una estructura multilobulada de gran volumen. El tracto digestivo medio ("*intestin*") es un túbulo sin cutícula, mientras que el tracto digestivo posterior ("*rectum*") tiene una estructura similar a la del esófago y está delimitado por una cutícula, el lumen es de forma estrellada y está rodeado de músculos constrictores.

9.3 Objetivos del BLOQUE 2.

La nutrición es un proceso clave que determina la supervivencia y el desarrollo de los organismos, este proceso también tiene una influencia directa sobre las transferencias de energía en las redes tróficas de los ecosistemas y sobre la dinámica de las poblaciones de productores y consumidores (Anger, 2001). El sistema digestivo es el responsable de la función nutricional, este sistema se encarga de la ingestión, digestión mecánica y química del alimento ingerido, absorción de nutrientes y excreción de residuos (Ceccaldi, 1989; Vogt, 1996). En los decápodos, el sistema digestivo es además responsable del almacenamiento de nutrientes, que serán utilizados, entre otras situaciones, durante la muda y post-muda (Ceccaldi, 1989). Por ello, el proceso digestivo no puede entenderse sin conocer la morfología y organización del sistema digestivo. La importancia de dicho sistema es tal que en función de las cualidades del hábitat y las preferencias alimentarias, el sistema digestivo de cada taxón posee características de tipo estructural y funcional únicas (Johnston, 2007). La estructura de dichos órganos, tanto a nivel de morfología como de histología, ha sido extensivamente estudiada en diversas especies de interés acuícola, incluyendo tanto teleósteos como decápodos (Zambonino-Infante et al., 2008).

En el caso de los decápodos, dichos estudios se remontan a más de un siglo (Huxley, 1880). El sistema digestivo de estos animales difiere considerablemente del de los vertebrados (Ceccaldi, 1989; Vogt, 1996). La morfología del sistema digestivo no es constante durante toda la vida del animal. En términos generales, dicho sistema es mucho más simple durante los primeros estadios larvarios, aunque se observan ciertas variaciones entre los distintos taxones: en Dendrobranchiata (larvas tipo nauplius) el sistema digestivo suele estar indiferenciado en el momento de la eclosión, mientras que en Pleocyemata (larvas tipo zoea) el sistema digestivo consta de órganos bien diferenciados dados sus mayores requisitos nutricionales (Anger, 2001; Ceccaldi, 1989). Al igual que sucede con el estadio adulto, estudiar los cambios ontogénicos ocurridos en el sistema digestivo durante el desarrollo larvario y juvenil, así como entender su forma y función, permitirá determinar los requerimientos alimentarios durante dichos estadios (Minagawa y Takashima, 1994). La descripción del sistema digestivo y su desarrollo ontogénico no solo es un tema de interés científico *per se*, este tipo de estudios son fundamentales para las empresas dedicadas a la producción acuícola. El conocimiento de la ontogenia del sistema digestivo es particularmente relevante para aquellas empresas productoras de juveniles pre-engorde, ya que un conocimiento profundo de los requerimientos nutricionales durante los estadios larvarios permite optimizar el esfuerzo productivo y reducir los cuellos de botella que suponen estos estadios (Zambonino-Infante et al., 2008).

A pesar del gran interés científico que despierta la morfología y fisiología del sistema digestivo de los decápodos, así como la gran cantidad de estudios enfocados en su organización tisular y celular, no todos los órganos han recibido la misma atención. Ciertos órganos, quizás por su enorme complejidad y/o gran volumen, han sido muy estudiados. Estos órganos incluyen al estómago (Brösing, 2010; 2014; Brösing et al., 2002; Brösing y Türkay, 2011; Kunze y Anderson, 1979; Meiss y Norman, 1977; Nakamura y Takemoto, 1986; Sharman et al., 2000; Suljak et al., 2010); la glándula digestiva o hepatopáncreas (Al-Mohanna et al., 1985; Bunt, 1968; Caceci et al., 1988; Cervellione et al., 2017a; Cuartas et al., 2002; Díaz et al., 2010; Gibson y Barker, 1979; Mykles, 1979; Nishida et al., 1995; Nunes et al., 2014; Papathanassiou y King, 1984; Ramadevi et al., 1990; Sousa y Petriella, 2007; Stanier et al., 1968; Storch y Anger, 1983; Van Weel, 1974); y el tracto digestivo medio (Barker y Gibson, 1977; 1978; Erri Babu et al., 1982; Mykles, 1979; Reddy, 1937; Sousa y Petriella, 2006). Dichos órganos han sido descritos en detalle a nivel morfológico, tisular y celular, empleando técnicas de microscopía óptica y electrónica. Por el contrario, otros órganos no han recibido tanta atención: el esófago ha sido considerado un órgano "sin nada destacable" (Milne-Edwards, 1834a) y ha sido descrito brevemente en publicaciones enfocadas en otros órganos (Barker y Gibson, 1977; 1978; Reddy, 1937; Sousa y Petriella, 2006); una situación similar ocurre con otros órganos como los ciegos asociados al tracto digestivo medio (Barker y Gibson, 1977; 1978; Holliday et al., 1980; Mykles, 1977; Smith, 1978); y el tracto digestivo posterior (Barker y Gibson, 1977; 1978; Erri Babu et al., 1982; Komuro y Yamamoto, 1968; Pugh, 1962). Dichos órganos suelen ser considerados estructuras "simples", por lo que han recibido poca atención por parte de los investigadores y, en comparación con el estómago y glándula digestiva, cuentan con un número de publicaciones mucho más limitado.

En el caso del sistema digestivo larvario la situación no es mucho mejor, puesto que apenas ha sido estudiado detalladamente. Esta afirmación puede parecer contradictoria con la realidad, dado el número existente de publicaciones centradas en la descripción y ontogenia del sistema digestivo larvario de numerosas especies de decápodos (Abrunhosa y Kittaka, 1997; Anger y Hayd, 2009; Factor, 1981; Lovett y Felder, 1989; 1990; Loya-Javellana et al., 1994; Lumasag et al., 2007; Muhammad et al., 2012; Tziouveli et al., 2011). Sin embargo, esta contradicción desaparece si tenemos en cuenta que la mayoría de dichos estudios describen el sistema digestivo por completo, basándose en observaciones de microscopia óptica y raramente de microscopía electrónica. Por ello, cada órgano es descrito de forma escueta y limitada, con poco nivel de detalle. Por ello, existen amplias lagunas en relación al conocimiento existente acerca del sistema digestivo de los decápodos durante sus estadios larvarios, así como su ontogenia.

Por ello, el segundo bloque de esta Tesis tiene por objetivo la descripción del sistema digestivo de *M. brachydactyla* Balss, 1922. No fue preciso el estudio de las piezas bucales de esta especie, así como la ontogenia de las mismas, puesto que ya han sido estudiadas (Guerao et al., 2008). En relación al estómago y glándula digestiva, dada su complejidad su estudio ha sido subdivido en dos tipos de publicaciones, una centrada en la morfología externa y otra en su histología y ultra-estructura. En lo que respecta a órganos tradicionalmente menos estudiados, como lo son el esófago, el tracto digestivo medio, los ciegos asociados al tracto digestivo medio y el tracto digestivo posterior; en el presente bloque se intenta profundizar en su morfología, histología, ultra-estructura y desarrollo ontogénico.

Para poder llevar a cabo estos estudios, dados los objetivos del proyecto y los limitados recursos disponibles, fueron empleadas técnicas de estudio tradicionales. La morfología externa fue estudiada mediante su observación en lupa binocular y microscopio electrónico de barrido. La estructura tisular fue estudiada mediante estudio histológico empleando tinciones tradicionales y observaciones de microscopía óptica. La ultra-estructura de los tejidos se estudió mediante microscopía electrónica de transmisión. La mayor innovación aplicada en este estudio fue el empleo de técnicas de tomografía y micro-tomografía computarizada, cuya realización hubiera sido imposible sin la colaboración de la Dra. María Font i Furnols del centro IRTA de Monells (Girona) y del Dr. Javier Alba-Tercedor de la Universidad de Granada. Dicha técnica permite reconstruir virtualmente los organismos en tres dimensiones a partir de su escaneo mediante rayos X. Esta reconstrucción tridimensional permite su exploración desde cualquier ángulo y corte, tanto a nivel externo como interno. La metodología aplicada para la realización de todas estas técnicas será detallada en el próximo apartado.

9.4 Diseño experimental aplicado en el BLOQUE 2.

9.4.1 Condiciones de cultivo

Los objetivos del presente bloque requirieron la obtención de especímenes de todos los estadios larvarios, del estadio de primer juvenil y adultos. Por ello, el stock de reproductores establecido con objeto de la realización del bloque anterior (ver "*2.4.1 Stock de reproductores: recogida y mantenimiento*", páginas 73-75), fue conservado para la realización del presente bloque. El estudio dedicado a la descripción de la morfología externa del estómago y el sistema de osículos (capítulo 10: "Foregut Morphology and Ontogeny of the Spider Crab *Maja brachydactyla* (Brachyura, Majoidea, Majidae)", empleó como material larvario los distintos estadios larvarios obtenidos mediante el sistema de cultivo en acuarios de 200 L, mientras que el material empleado en el resto de capítulos fue obtenido mediante el cultivo en tanques de 360 L (ver *2.4.2 Cultivo larvario: diseño experimental*, páginas 76-80). Con este sistema, fueron obtenidas larvas en el estadio de zoea II al cabo de tres días, en el estadio de megalopa al cabo de seis días, y en el estadio de primer juvenil al cabo de 12-13 días. En varias ocasiones, nuevos adultos fueron adquiridos mediante compra con el objetivo exclusivo de su disección.

9.4.2 Muestreo y disección de los especímenes

Con objeto de estudiar el sistema digestivo durante la etapa adulta, especímenes adultos adicionales al stock de reproductores hubieron de ser obtenidos. Estos especímenes se adquirieron a través de la empresa Cademar S. Coop. R.L. (Alcanar, Tarragona) y trasladados al centro de investigación IRTA de Sant Carles de la Ràpita. Los especímenes fueron introducidos en cajas de poliestireno que se colocaron durante un tiempo mínimo de 30 minutos en cámaras frigoríficas a 4-6 °C. La hipotermia como "anestésico" está aceptada en el manejo de diversas especies de invertebrados, dado que ralentiza su metabolismo y facilita su manipulación (Cooper, 2011), siempre y cuando se evite que tenga lugar la formación de cristales de hielo en los individuos (Kubaryk y Harper, 2001). De modo que, "algunos investigadores han recomendado el uso de hielo para reducir el metabolismo [...] permitiendo el subsecuente muestreo (con o sin recuperación) de los individuos" (Longshaw y Stebbing, 2016, página 334). Murray (2008) resume las técnicas de eutanasia que pueden aplicarse a los decápodos: los medios químicos incluyen compuestos como isoflurano, MS-222 y aceite de clavo, como alternativa se menciona el uso de la hipotermia. Cabe añadirse que las técnicas de anestesia y eutanasia de invertebrados están todavía poco desarrolladas, siendo aún requerida mucha investigación al respecto (Cooper, 2011; Murray, 2008).

La disección de las larvas fue llevada a cabo empleando agujas de disección elaboradas a partir de agujas hipodérmicas 25 G. Debido a su reducido tamaño, las tareas de disección se realizaron bajo una lupa binocular Nikon SMZ800. Por su parte, la disección de los ejemplares adultos fue realizada usando alicantes de punta plana. La técnica empleada para la disección de los adultos se describe en el apartado "*17.1 Iniciación en el estudio morfológico de las larvas de decápodos*", páginas 654-660.

El diseño del sistema de cultivo larvario en tanques de 360 L permitió disponer de un número suficiente de réplicas como para realizar muestreos diarios. En cada muestreo, entre el 15 y el 25 % de las larvas fueron fijadas en medio Davidson para su estudio histológico, el resto de larvas fueron fijadas en formaldehído al 4 % para su disección y estudio anatómico. Esporádicamente, como será detallado posteriormente, especímenes de los estadios zoea I, zoea II, megalopa y primer juvenil fueron fijados en paraformaldehído 2 % - glutaraldehído 2,5 % en tampón cacodilato (0,1 mol L^{-1} pH 7,4) para su uso en microscopía electrónica. De modo que, mientras que la disección de los adultos fue llevada a cabo con material fresco, en el caso de las larvas esta se llevó a cabo con material tanto fresco como fijado. Se decidió fijar un gran número de larvas previamente a su disección debido a que la fijación endurece los órganos permitiendo que sea más fácil separarlos de las estructuras cuticulares; diseccionar las larvas es una tarea que requiere tiempo y por ello, la fijación de los especímenes es imprescindible para conservarlos en el mejor estado posible durante los días que se invertirán en su disección; además, gracias a su menor tamaño la fijación y conservación de un gran número de larvas es una tarea asequible que permite disponer de un stock suficiente de animales para su estudio. Por el contrario, el gran tamaño de los adultos limita mucho el número de estos que puede ser fijado simultáneamente, debido al gran volumen de fijador requerido por espécimen (varios litros).

9.4.3 Estudio morfométrico: lupa binocular

El protocolo empleado en el estudio morfométrico de los órganos del sistema digestivo varió con el órgano y con el estadio del animal. El estudio del sistema digestivo de larvas, juveniles y adultos se realizó empleando órganos frescos y/o fijados en formaldehído 4%. Este compuesto es un fijador conocido desde hace décadas; reacciona con proteínas, ácidos nucleicos y polisacáridos formando puentes intra- e intermoleculares. Entre sus efectos macroscópicos se incluyen la preservación, endurecimiento, compactación y encogimiento de los tejidos. El encogimiento es un factor relevante en los estudios histológicos dada la alteración de los tejidos, pero tales efectos son mínimos para el estudio morfológico (Fox et al., 1985).

Digestivo anterior. La morfología externa del estómago fue estudiada siguiendo la metodología empleada en estudios previos sobre otras especies de braquiuros (Brösing, 2010; Brösing et al., 2002). Dado que el objetivo eran las estructuras cuticulares, fueron eliminados todos los elementos tisulares, celulares y extracelulares, con objeto de facilitar las observaciones evitando errores de interpretación. Con este fin, los estómagos una vez extraídos fueron sumergidos en una solución de hidróxido de potasio (KOH) al 10 %, la duración de este baño osciló entre 30 y 60 minutos en los adultos y entre 10 y 15 minutos en los estadios larvarios y juveniles. Empleando el mismo protocolo descrito por Brösing et al. (2002), tras la limpieza de los tejidos, los estómagos fueron sumergidos en una solución de Rojo de Alizarina S al 1 % y KOH al 10 % con objeto de teñir los osículos calcificados. El Rojo de Alizarina S es una antraquinona que tradicionalmente se ha usado como técnica histológica para demostrar la presencia de sales de calcio en los tejidos (Puchtler et al., 1969). Tal y como se describe en el capítulo "Foregut Morphology and Ontogeny of the Spider Crab *Maja brachydactyla* (Brachyura, Majoidea, Majidae)", se estudiaron: la morfología general del estómago (incluyendo molino gástrico, válvula cardio-pilórica y filtros pilóricos) y el número, forma y disposición de los osículos. Las observaciones del estómago adulto fueron realizadas empleando una lupa binocular Nikon SMZ800 conectada a una computadora y un programa de análisis de imagen (AnalySIS, SIS, Münster, Alemania; Fig. 9.4.2). Por su parte, las observaciones del estómago de juveniles y adultos fueron realizadas con un microscopio óptico (Leica LB30T 111/97, GmbH, Wetzlar, Alemania) conectado a una cámara digital Olympus DP70 de 12,5 megapíxeles (Olympus America, NY) con un programas de análisis de imagen (AnalySIS, SIS, Münster, Alemania; Fig. 9.4.4B).

Glándula digestiva. En los adultos la glándula digestiva es un órgano complejo formado por un gran número de túbulos ciegos, cuyo número fue calculado. Para ello la glándula digestiva de seis adultos fue extraída y pesada. Después se tomaron varias muestras de cada una de las glándulas, cada muestra fue pesada y el valor obtenido anotado, a continuación se fijaron en formaldehído 4 %. Una vez fijadas, el peso de cada una de las muestras fue medido de nuevo para calcular la variación relativa de peso debido al proceso de fijación. El siguiente paso fue la obtención de submuestras de un peso conocido (entre 15 y 60 mg) y el recuento de túbulos ciegos de dichas submuestras. Dado que los túbulos se quiebran muy fácilmente, para evitar errores solo se contó el número de ápices de túbulos ciegos. Una vez conocido el número de túbulos y corregido el peso debido a la fijación, se calculó la densidad de túbulos por unidad de peso y este valor fue extrapolado para conocer el número de túbulos en la glándula digestiva adulta. Las medidas de peso se realizaron en una balanza de precisión (Mettler Toledo AE200, rango: 0-205 g). Las observaciones fueron realizadas en una lupa binocular (Fig. 9.4.2).

La glándula digestiva es mucho más simple durante los estadios larvarios y del primer juvenil en comparación con el estadio adulto. Por lo que posteriormente a su extracción, fueron fotografiadas con la lupa binocular. Empleando el software de análisis de imagen AnalySIS se tomaron distintas medidas con objeto de estudiar el desarrollo de la glándula a lo largo del desarrollo larvario (Fig. 9.4.1).

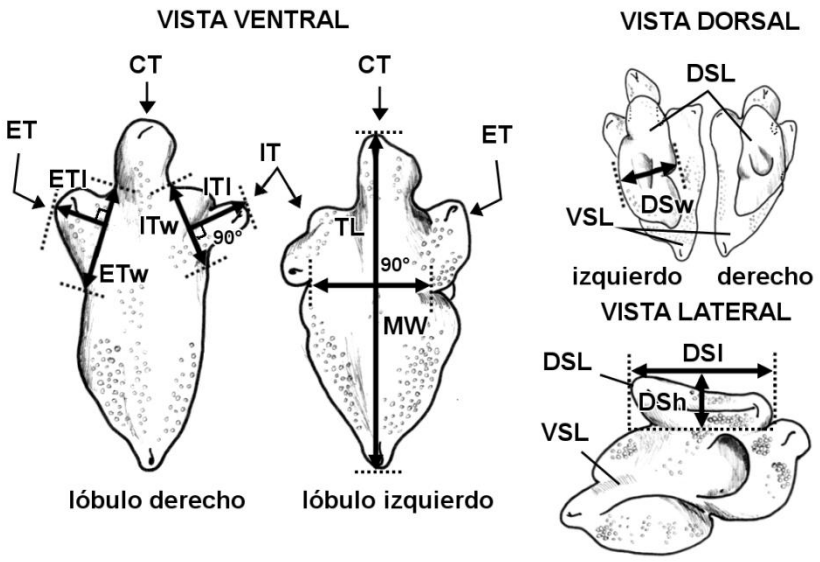

Fig. 9.4.1. *M. brachydactyla*. Esquema de la glándula digestiva larvaria, también conocida por el nombre de hepatopáncreas u órgano perigástrico de acuerdo con Cervellione et al. (2017b). Son destacados los sub-lóbulos ventrales (izquierda): longitud total (TL) y anchura máxima (MW); los túbulos laterales son diferenciados entre túbulos externos (ET) e internos (IT): longitud total (ETl e ITl), anchura máxima (ETw e ITw) y altura máxima (ETh e ITh). La anchura máxima se consideró la línea basal que separa dichos túbulos del túbulo central, mientras que la longitud se consideró la distancia perpendicular máxima entre la línea basal y el ápice del túbulo. También son destacados los sub-lóbulos dorsales (derecha): longitud total (DSl), anchura (DSw) y altura máximas (DSh).

Digestivo medio y posterior. En adultos, en todos los estadios larvarios (zoea I, zoea II y megalopa), así como en el primer juvenil fue estudiada y fotografiada la morfología externa de distintos órganos: tracto del digestivo medio y posterior, así como los ciegos asociados (un par de ciegos anteriores y un único ciego posterior). En todos los mencionados órganos fueron medidos la longitud total y el diámetro. Las observaciones del tracto digestivo medio y posterior fueron realizadas con una lupa binocular Nikon SMZ800 conectada a una computadora con un programa de análisis de imagen (AnalySIS, SIS, Münster, Alemania; Fig. 9.4.2); mientras que las observaciones de los ciegos asociados al digestivo medio fueron realizadas con un microscopio óptico (Leica LB30T 111/97, GmbH, Wetzlar, Alemania) conectado a una cámara digital Olympus DP70 de 12,5 megapíxeles (Olympus America, NY) y un programas de análisis de imagen (AnalySIS, SIS, Münster, Alemania; Fig. 9.4.4B).

Figura 9.4.2. Lupa binocular (Nikon SMZ800) y computador asociado empleado en el estudio de la morfología externa de los distintos órganos del sistema digestivo. Instalaciones del IRTA Sant Carles de la Ràpita, 2012-2016.

9.4.4 Estudio histológico: microscopía óptica

El material seleccionado para su estudio histológico difirió de acuerdo con el estadio de los especímenes. En el caso de los especímenes adultos el material seleccionado fueron porciones de los distintos órganos del sistema digestivo, dichas porciones fueron realizadas de modo que fuese posible estudiar el órgano desde diferentes orientaciones, siendo las más importantes las secciones longitudinales y transversales, si bien también se obtuvieron oblicuas de distintos ángulos. Por el contrario, durante los estadios larvarios y de primer juvenil el tamaño de los especímenes es el suficientemente pequeño como para permitir la observación de especímenes enteros, los cuales también fueron orientados como se ha descrito anteriormente.

La fijación es un proceso clave en microscopía óptica, consiste en la inmovilización de los elementos celulares y la detención del metabolismo celular, los procesos de degradación enzimática y la acción de bacterias y hongos. Bell y Lightner (1988) y Cervellione et al. (2017a) recomiendan en decápodos el uso del *fijador de Davidson*, una mezcla fijadora compuesta por etanol (96-100 %): agua de mar filtrada: formaldehído 37 %: glicina y ácido acético glacial, en proporción 3: 3: 2: 1: 1. Los autores recomiendan inyectar este fijador dentro de la cavidad del cefalotórax en especímenes juveniles y adultos, pero dado que en el presente estudio el material fijado son muestras de los órganos internos, este paso es innecesario.

Las muestras fijadas fueron conservadas en etanol 70 % hasta su posterior tratamiento. En la presente Tesis dicho periodo osciló entre 48 horas y un mes. El siguiente paso requirió infiltrar las muestras en parafina, con objeto de poder realizar un bloque del mismo material con una textura más o menos homogénea. Al tratarse de un compuesto no miscible en agua y alcoholes, es preciso deshidratar las muestras y embeberlas en un compuesto miscible con la parafina, para permitir que esta pueda infiltrarse en los tejidos. Para este proceso nosotros empleamos un procesador automático de tejidos (Myr, Spain), provisto de un brazo automático y una serie de cubetas con distintas soluciones (Fig. 9.4.3A). Este aparato permite procesar de forma automatizada y simultánea un gran número de muestras (hasta 50 en el presente caso). El brazo robot desplaza las muestras de una cubeta a otra, manteniéndolas sumergidas en soluciones durante un tiempo previamente programado.

Los tejidos fueron infiltrados siguiendo el siguiente protocolo de infiltración:

1. Etanol 70% durante 3 horas
2. Etanol 96% durante 1 hora
3. Etanol 100% durante 1 hora
4. Etanol 100% durante 1 hora
5. Solución 1:1 de etanol y xileno durante 1 hora
6. Xileno absoluto durante 1 hora
7. Xileno absoluto durante 1 hora
8. Parafina líquida durante 6 horas
9. Parafina líquida durante 6-12 horas

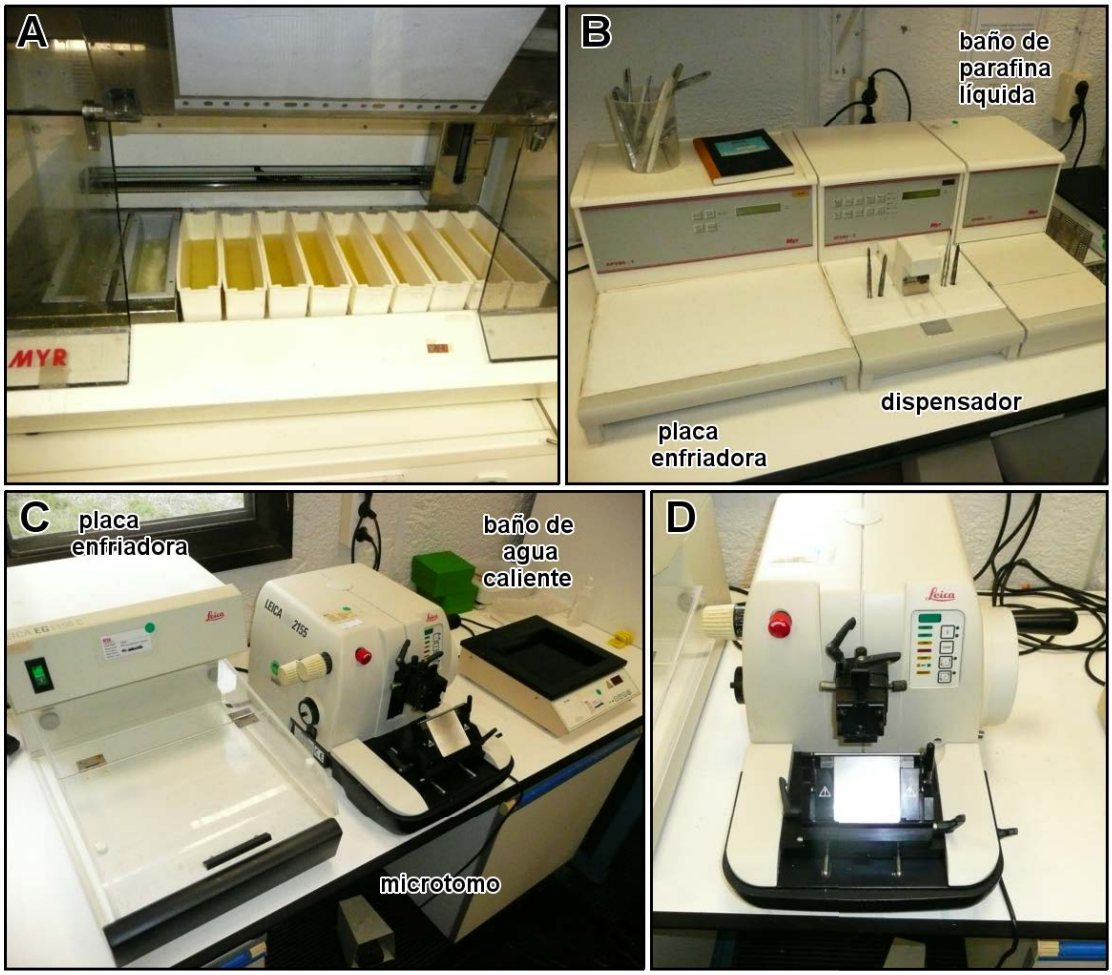

Figura 9.4.3. Procesando muestras histológicas. Procesador automático de tejidos (Myr, España). Infiltración automática de parafina (A). Procesador de muestra de parafina (AP208-1, AP208-2 and AP208-3; Myr, Spain) (B). Microtomo (Leica RM2155), placa enfriadora y baño de agua caliente (C). Microtomo (Leica RM2155) (D). Instalaciones del IRTA Sant Carles de la Ràpita, 2012-2016.

Una vez finalizada la infiltración de parafina, el siguiente paso fue obtener bloques de parafina sólida con las muestras embebidas dentro de tales bloques. Para ello empleamos un procesador de muestras de parafina (AP208-1, AP208-2 and AP208-3; Myr, Spain), que consta de: un baño de parafina líquida donde se introducen las muestras con parafina infiltrada desde el procesador de tejidos anterior; un dispensador que permite verter parafina líquida sobre una serie de moldes metálicos donde serán colocadas las muestras; y una placa enfriadora para solidificar rápidamente los moldes (Fig. 9.4.3B). El resultado final son bloques de parafina sólida con la muestra en su interior. A continuación, se realizaron cortes histológicos lo suficientemente finos como para ser observados bajo el microscopio óptico, para ello empleamos un microtomo (Leica RM2155) con el que fueron realizadas láminas de hasta 2 µm de espesor (Fig. 9.4.3C-D). Una vez obtenidas, las láminas fueron sumergidas en un baño de agua destilada a una temperatura de 36-38 °C, este baño elimina las arrugas que puedan presentar las láminas tras su obtención, ya que el calor expande y estira la parafina (Fig. 9.4.3C). Las láminas fueron recogidas con el portaobjetos y colocadas en el interior de un horno, donde fueron secadas durante 24-48 horas a 40 °C.

Con las muestras totalmente secas, fue posible comenzar con las técnicas de tinción. Las tinciones empleadas requieren que las muestras estén completamente hidratadas. Sin embargo, tras la desecación en el horno las muestras están embebidas en parafina y son impermeables al agua. Por ello, fue preciso eliminar la parafina y rehidratar las muestras. Con objeto de eliminar la parafina las muestras fueron inicialmente sumergidas en sendos baños de xileno 100 % durante 10 minutos por baño (para eliminar la parafina). A continuación, para rehidratarlas fueron sumergidas en baños de etanol 100 %, 90 % y 70 % de 5 minutos cada uno, antes de sumergirlos en un baño de agua destilada durante un mínimo de 5 minutos, completando la rehidratación (Fig. 9.4.4A).

Hematoxilina - Eosina (*HE*). La tinción de hematoxilina - eosina es actualmente una técnica de rutina de laboratorio de gran popularidad, utilizada para realizar observaciones de la estructura general de los tejidos, ya que permite diferenciar el citoplasma celular, los núcleos y los elementos extracelulares (Bancroft, 2008; Ross y Pawlina, 2016). La hematoxilina es un producto originario del árbol llamado palo de Campeche o palo de tinte, de nombre científico *Haematoxylon campechianum* Linnaeus y originario de México (Bancroft, 2008; Titford, 2005). La hematoxilina requiere de la presencia de un mordiente para unirse a los elementos celulares mediante la formación de un complejo hematoxilina-mordiente-elemento celular (Bancroft, 2008; Ross y Pawlina, 2016). En el presente estudio, utilizamos una solución comercial de hematoxilina de Mayer (Sigma-Aldrich) que incorpora mordiente y oxidante, permitiendo la tinción de las láminas inmediatamente a la hidratación de las mismas.

La eosina es un tinte ácido con carga negativa y soluble en alcohol, con afinidad por el citoplasma y fibras extracelulares (Bancroft, 2008; Ross y Pawlina, 2016). Nosotros empleamos eosina Y (Sigma-Aldrich), la cual que puede ser utilizada sin necesidad de preparar ninguna solución adicional. La combinación de ambos tintes (hematoxilina y eosina) permite diferenciar entre núcleo (violeta, violáceo azulado) y citoplasma (de coloración variable de rosado a violáceo anaranjado). El protocolo empleado para realizar esta tinción fue:

1. Solución de hematoxilina durante 5-6 min
2. Lavado con agua corriente (o destilada) durante 5-10 min
3. Solución de eosina durante 4-5 min
4. Primer paso de la deshidratación: etanol 96 %

Técnica de Schiff. También conocida como "*ácido periódico/peryódico de Schiff* " o por sus siglas en inglés "*PAS*". Desde hace varias décadas se trata de una técnica de tinción estandarizada para la detección de estructuras ricas en polisacáridos, las cuales quedan patentes con color rosado, estas incluyen: glucógeno, glicoproteínas, mucopolisacáridos y elementos tisulares como la lámina basal (Bancroft, 2008; Durfort i Coll, 2006; Ross y Pawlina, 2016). El *reactivo de Schiff* es fruto de la reacción de la pararosanilina (y otros compuestos similares) con el ácido sulfúrico (Bancroft, 2008). La solución comercial empleada (Sigma-Aldrich) consiste en una solución de ácido clorhídrico 0,25 M con metabisulfito de sodio ($Na_2S_2O_5$) al 4 % para generar ácido sulfúrico, así como pararosanilina al 1 % como reactivo principal. El *reactivo de Schiff* se asocia a los aldehídos libres, por ello un paso previo de esta técnica de tinción es el uso de ácido periódico (HIO_4), el cual oxida los grupos hidroxilo de los polisacáridos y los convierte en grupos aldehído (Bancroft, 2008; Durfort i Coll, 2006). Dada la especificidad del este reactivo, todos aquellos elementos carentes de grupos aldehído no son teñidos. Por ello, es preciso aplicar una tinción de contraste. En el presente estudio fue empleado el *azul de metileno*, un tinte de tipo básico con afinidad por elementos con carga negativa, incluyendo los ácidos nucleicos y grupos carboxilo, por ello con este tinte los núcleos quedan teñidos de un fuerte color azulado, mientras que el citoplasma destaca con un color azul claro. Por tanto, el protocolo empleado tras el proceso de hidratación fue:

1. Solución de ácido periódico / peryódico durante 15 min
2. Lavado con agua corriente (o destilada) durante 10 min
3. Solución de *reactivo de Schiff* durante 10 min
4. Lavado con agua corriente (o destilada) durante 5 min
5. Solución de azul de metileno 0,1 % durante 4 min
6. Serie de 5 lavados en agua corriente (o destilada) de 1 min cada uno
7. Primer paso de la deshidratación: etanol 100 %

Técnica de PAS & azul de alcián. Esta técnica es una variación de la anterior. En este caso, como paso previo al PAS fue realizada una tinción adicional con azul de alcián a pH 2,5. El azul de alcián es una molécula compleja que tiene gran afinidad por las sustancias mucosas ácidas, las cuáles son teñidas de color azul (Bancroft, 2008). Se trata de una tinción específica del pH: con un pH de 2,5 tiene especificidad por sustancias mucosas (glicoproteínas, proteoglicanos, sialomucinas y sulfomucinas) ricas en grupos carboxilo y sulfato; con un pH de 1,0 y 0,5 muestra afinidad únicamente por sustancias mucosas fuertemente sulfatadas (Lev y Spicer, 1964). Esta tinción se recomienda combinarla con PAS, de modo que las sustancias mucosas neutras son teñidas de color rosado por esta tinción, mientras que las sustancias mucosas ácidas son teñidas de azul por el azul de alcián. La combinación de técnicas puede considerarse un protocolo de amplio espectro para la detección de mucinas (Bancroft, 2008). Dado que ambas tinciones son específicas de mucinas, es preciso utilizar una tinción de contraste para distinguir el resto de elementos celulares. Para evitar enmascarar el tono azulado del azul alcián, en lugar de azul de metileno, como tinción de contraste se empleó hematoxilina de Mayer. El protocolo empleado fue:

1. Solución de azul alcián pH 2,5durante 10 min
2. Lavado con agua corriente (o destilada) durante 10 min
3. Solución de ácido periódico / peryódico durante 10 min
4. Lavado con agua corriente (o destilada) durante 10 min
5. Solución de reactivo de Schiff durante 8 min
6. Lavado con agua corriente (o destilada) durante 5 min
7. Solución de hematoxilina de Mayer durante 5-6 min
8. Lavado con agua corriente (o destilada) durante 5-10 min
9. Primer paso de la deshidratación: etanol 100 %

Tricrómico de Mallory. Los tricrómicos son técnicas especializadas en demostrar la presencia de músculo, fibras de colágeno, fibrina y eritrocitos, permitiendo distinguir entre dichos elementos mediante los distintos tintes empleados (Bancroft, 2008). Nosotros usamos la técnica desarrollada originalmente por Mallory (1900), de quien recibe el nombre. La versión actual, muy similar a la original, permite determinar la presencia de fibras de colágeno del tejido conectivo (azul), las fibras musculares (rojo), las fibras nerviosas (púrpura), el exoesqueleto (rojo) y los núcleos celulares (rojo); gracias a su combinación de tintes (Durfort i Coll, 2006). Esta tinción requiere como primer paso la aplicación de un sublimado corrosivo como mordiente (Durfort i Coll, 2006; Mallory, 1900), un elemento que actúa como fijador al formar un complejo entre el tinte, la estructura tisular y el propio mordiente (Ross y Pawlina, 2016).

El siguiente paso es la aplicación de fucsina ácida, tinte ácido derivado del trifenilmetano con afinidad por los aminoácidos básicos de las proteínas (Nielsen et al., 1998; Ross y Pawlina, 2016), permite la tinción de las fibras musculares y de colágeno, eritrocitos y núcleos celulares (Garvey, 1984; Ross y Pawlina, 2016). Tras un lavado rápido en agua destilada es necesaria la aplicación de ácido fosfomolíbdico, $H_3[P(Mo_3O_{10})_4] \cdot xH_2O$, este compuesto elimina la fucsina ácida del tejido conectivo, pero simultáneamente actúa como mordiente al fijar la fucsina ácida en las restantes estructuras (Bancroft, 2008; Mallory, 1900). Después de un lavado rápido es aplicada la *solución de Mallory*, cuya formulación permanece fiel a la original (Durfort i Coll, 2006; Mallory, 1900): orange G al 2 %, ácido oxálico al 2 % y azul de anilina al 0,5 %. El orange G es un tinte ácido de afinidades similares a las de la fucsina ácida, excepto que no tiñe las fibras de tejido conectivo (Ross y Pawlina, 2016); el azul de anilina es otro tinte ácido, pero debido a la presencia de orange G solo puede teñir el tejido conectivo; por su parte el ácido oxálico aumenta la intensidad del azul de anilina (Mallory, 1900). El último paso es el uso del diferenciador, una solución que reduce el nivel de tinción hasta que es posible visualizar las estructuras tisulares deseadas (Bancroft, 2008).

Así, el protocolo empleado fue:

1. Mordiente: solución de sublimado corrosivo (bicloruro de mercurio, $HgCl_2$) en saturación (entorno 6-10 %) durante 15 min
2. Lavado rápido en agua destilada
3. Solución de fucsina ácida 1 % durante 15 segundos
4. Lavado rápido en agua destilada
5. Solución de ácido fosfomolíbdico 1 % durante 1 min
6. Lavado rápido en agua destilada
7. Solución de Mallory durante 30-60 segundos
8. Lavado rápido en agua destilada
9. Diferenciador: azul de anilina 0,05 %, en etanol 96 %, durante 5-10 segundos
10. Primer paso de la deshidratación: etanol 96 %

Al finalizar el proceso de tinción, las láminas teñidas fueron sometidas a un proceso de deshidratación. Para ello fueron sumergidas en un baño de etanol 96 % seguido de dos baños de etanol 100 %, la duración de cada baño fue de 5 minutos. A continuación se sumergieron en dos baños de xileno 100 %, con una duración mínima de 5 minutos por baño. Una vez completado este proceso llegó el momento de cubrir las láminas con cubreobjetos (tamaños usados 20 x 20, 20 x 40 y 20 x 60 mm) con objeto de protegerlas. Para ello se utilizó medio de montaje, que permitió la adhesión del cubreobjetos al portaobjetos, con la lámina de tejido en medio. Antes de proceder a la observaciones, los portaobjetos se dejaron secar durante un mínimo de 24 horas a temperatura ambiente. Las observaciones histológicas fueron realizadas en un microscopio óptico (Leica LB30T 111/97) conectado a una cámara (Olympus DP70 1.45 Mpx; Olympus Corporation, Germany) con un software especializado en el análisis y manipulación de imágenes (DP Controller 2.1.1.83 and DP Manager 2.1.1.163; Olympus Corporation, Germany), ver Figura 9.4.4B.

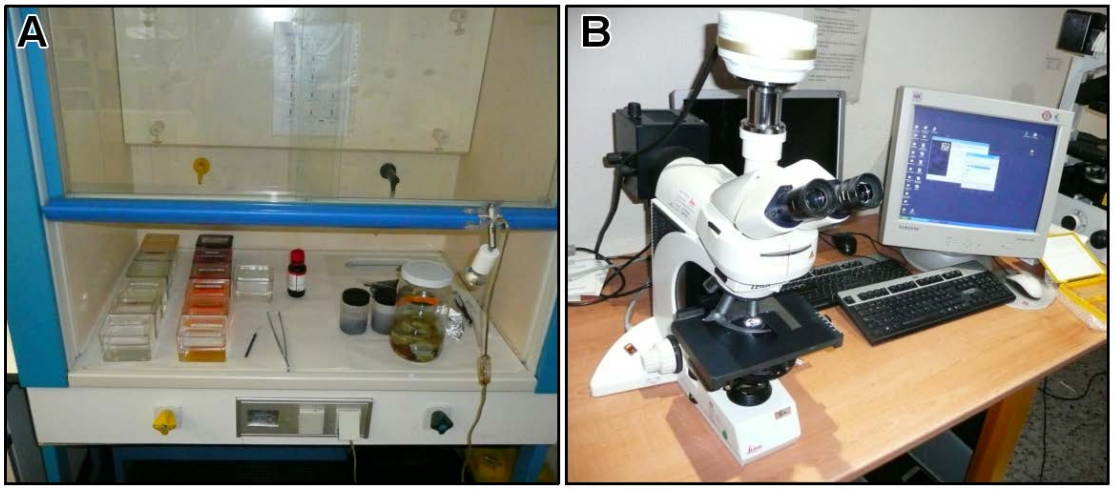

Figura 9.4.4. Tinción y observación de las muestras histológicas. Cámara de ventilación con cubetas que contienen algunos de los tintes empleados en el presente estudio (A). Microscopio óptico (Leica LB30T 111/97) y computador asociado, empleados para la realización de las observaciones histológicas (B). Instalaciones del IRTA Sant Carles de la Ràpita, 2012-2016.

7.3.5 Estudio ultra-estructural: microscopía electrónica

El estudio de los tejidos a nivel ultra-estructural requiere del uso de microscopía electrónica para obtener resoluciones de hasta 1 nm, permitiendo el estudio de la estructura de los orgánulos celulares y los elementos del citoesqueleto, la organización del citoplasma y núcleo, así como la morfología y especializaciones de las membranas (Ross y Pawlina, 2016). Es una técnica fundamental para el estudio detallado de los tejidos a nivel subcelular.

Debido a este nivel de detalle se requiere de un proceso de fijación que conserve la estructura de las células a nivel subcelular evitando artefactos y/o deformaciones (Ross y Pawlina, 2016). Desde el trabajo clásico de Karnovsky (1965), se han probado combinaciones de formaldehído/paraformaldehído y glutaraldehído (Bullock, 1984; McDowell y Trump, 1976). En el presente estudio se empleó una solución de paraformaldehído al 2% y glutaraldehído al 2,5% en tampón cacodilato (0,1 mol L^{-1} pH 7,4). El tamaño del material a fijar no debe ser superior a 3-4 mm (Karnovsky, 1965; McDowell y Trump, 1976), ya que el glutaraldehído es un fijador cuya velocidad de penetración es muy lenta (Bullock, 1984) y existe el riesgo de que las muestras se degraden antes de que el fijador haya tenido tiempo de penetrar y actuar en ellas. Debido a esta lenta velocidad de penetración, el glutaraldehído es empleado conjuntamente con paraformaldehído (Bullock, 1984). Ambos fijadores inmovilizan las proteínas mediante puentes cruzados (Bullock, 1984; Ross y Pawlina, 2016), el glutaraldehído también inmoviliza mediante puentes cruzados a los ácidos nucleicos, sin embargo estos fijadores no son eficientes fijando lípidos (Bullock, 1984). Por esa razón, se suele realizar un segundo proceso de fijación, o post-fijación, basado en el uso de tetraóxido de osmio (OsO_4). Este fijador tiene dos grandes cualidades: elevada electrodensidad y gran afinidad por los lípidos, especialmente fosfolípidos. Estas cualidades le permiten inmovilizar eficazmente las membranas plasmáticas elevando simultáneamente su electrodensidad y facilitando con ello su visualización. Por esta razón, el tetraóxido de osmio es el principal responsable de la calidad de las imágenes de microscopía electrónica (Bullock, 1984; Ross y Pawlina, 2016). Después de este proceso, el fijador debe eliminarse mediante una serie de lavados. El material puede conservarse en acetona absoluta tras un proceso de deshidratación.

El protocolo aplicado fue:

1. Solución de paraformaldehído 2 % - glutaraldehído 2,5 % en tampón cacodilato (0,1 mol L^{-1} pH 7,4) durante 2-4 horas a 4 °C
    - La disolución del paraformaldehído se llevó a cabo en agua bidestilada a 60-70 °C, en agitación, a la que se le añadieron gotas de NaOH hasta que la solución adquirió transparencia
2. Serie de 5 lavados en tampón cacodilato (0,1 mol L^{-1} pH 7,4) de 10 min a 4 °C
3. Post-fijación en tetraóxido de osmio 1-2 % en tampón cacodilato (0,1 mol L^{-1} pH 7,4) durante 1 hora y 30 min a 4 °C
4. Serie de 4 lavados en tampón cacodilato (0,1 mol L^{-1} pH 7,4) de 10 min a 4 °C
5. Serie de 2 lavados en agua bidestilada de 10 min a temperatura ambiente
6. Solución de acetona 30 % durante 15 min a temperatura ambiente
7. Solución de acetona 50 % durante 15 min a temperatura ambiente
8. Solución de acetona 70 % durante 15 min a temperatura ambiente
9. Solución de acetona 90 % durante 15 min a temperatura ambiente
10. Solución de acetona 95 % durante 15 min a temperatura ambiente
11. Serie de tres cambios de acetona 100 % de 15 min cada uno a temperatura ambiente

A partir de este punto el protocolo varió en función de que las muestras fuesen usadas para microscopía electrónica de transmisión o para microscopía electrónica de barrido. Ambas técnicas se llevaron a cabo en las instalaciones de los servicios de los Centros Científicos y Tecnológicos de la Universitat de Barcelona (CCiTUB), localizadas en el Hospital Clinic de Barcelona.

Microscopía electrónica de transmisión (*TEM*). Las muestras fueron embebidas en "resina Spurr". Este material es un tipo de resina epoxy de viscosidad reducida que debe ser infiltrada en los tejidos, es una resina líquida a temperatura ambiente que solidifica tras un proceso de polimerización que ocurre a una temperatura de 70 °C (Spurr, 1969; Wallis y Griffin, 1973). Las muestras infiltradas y solidificadas en bloques sólidos de "resina Spurr" son a continuación cortadas en láminas finas. En el presente estudio esto se llevó a cabo mediante un ultramicrotomo Leica UCT. En primer lugar, la muestra fue laminada en cortes de pocas micras de espesor denominadas "semifinos", dichas láminas fueron teñidas con un tinte básico denominado azul de toluidina, con el objetivo de estudiar la estructura básica de dicha muestra a nivel histológico (Ross y Pawlina, 2016). Estas observaciones permiten precisar qué área del bloque resulta interesante para su observación en microscopía electrónica.

Una vez seleccionada el área a cortar, se realizaron nuevas láminas empleando el mismo ultramicrotomo, solo que esta vez el espesor fue de entre 50 y 70 nanómetros. Previamente a su observación, las muestras fueron sometidas a un tratamiento con acetato de uranilo ($UO_2(CH_3COO)_2 \cdot 2H_2O$) y citrato de plomo ($C_{12}H_{10}O_{14}Pb_3$), esta combinación interactúa con las preparaciones aumentando su contraste y resolución para su observación en el microscopio electrónico de transmisión (Frasca y Parks, 1965; Ross y Pawlina, 2016; Stempak y Ward, 1964). Las observaciones fueron realizadas en un microscopio electrónico de transmisión JEOL EM-1010 con filamento de tungsteno a una potencia de 80 kV (Fig. 9.4.5A).

Microscopía electrónica de barrido o scanning (*SEM*).

Las muestras fueron sometidas a la técnica de secado de punto crítico (más conocida por su nombre en inglés "critical-point-drying"). El objetivo de este procedimiento es eliminar totalmente el contenido líquido de las muestras manteniendo su estructura inalterada. Este es un paso necesario ya que en un microscopio de barrido las muestras están sometidas a condiciones de vacío, por lo que si las muestras contuviesen líquidos, estos tenderían a abandonar las muestras, deformándolas en el proceso debido a las fuerzas de tensión superficial. Para ello las muestras, previamente deshidratadas en acetona, son transferidas a una cámara que permite el drenaje de la acetona ya que es alternativamente llenada y vaciada con CO_2 líquido. El objetivo es eliminar por completo la acetona sustituyéndola por CO_2. Una vez que la muestra ha sido totalmente infiltrada de CO_2, la cámara es llevada a una temperatura y presión donde las fases líquida y gaseosa del CO_2 alcanzan el equilibrio anulando la tensión superficial, entonces la presión es gradualmente reducida liberando paulatinamente el CO_2 gaseoso, hasta que la muestra queda por completo seca (Bray, 2000). Después de este proceso, las muestras son adheridas a unos soportes de aluminio diseñados para microscopía electrónica de barrido, la adhesión de la muestras a dichos soportes se realizó mediante una pegatina adhesiva. El funcionamiento del microscopio electrónico de barrido se basa en el escaneo de la superficie de la muestra mediante un haz de electrones, los electrones reflejados por la muestra son recolectados por detectores y procesados para formar imágenes tridimensionales. Para ello es preciso que las muestras estén recubiertas por una capa capaz de reflejar los electrones (Ross y Pawlina, 2016). En el presente caso dicha capa consistió en una fina película de carbono. Una de las ventajas que tiene el carbono frente los recubrimientos metálicos, es que al no tratarse de un compuesto conductor a temperatura ambiente, se evitan problemas de carga eléctrica que disminuirían la resolución de las imágenes (Brink et al., 1998; Larson et al., 2011). Las observaciones fueron realizadas en un microscopio electrónico de barrido JEOL JSM-7001F a una potencia de 15 kV (Fig. 9.4.5B).

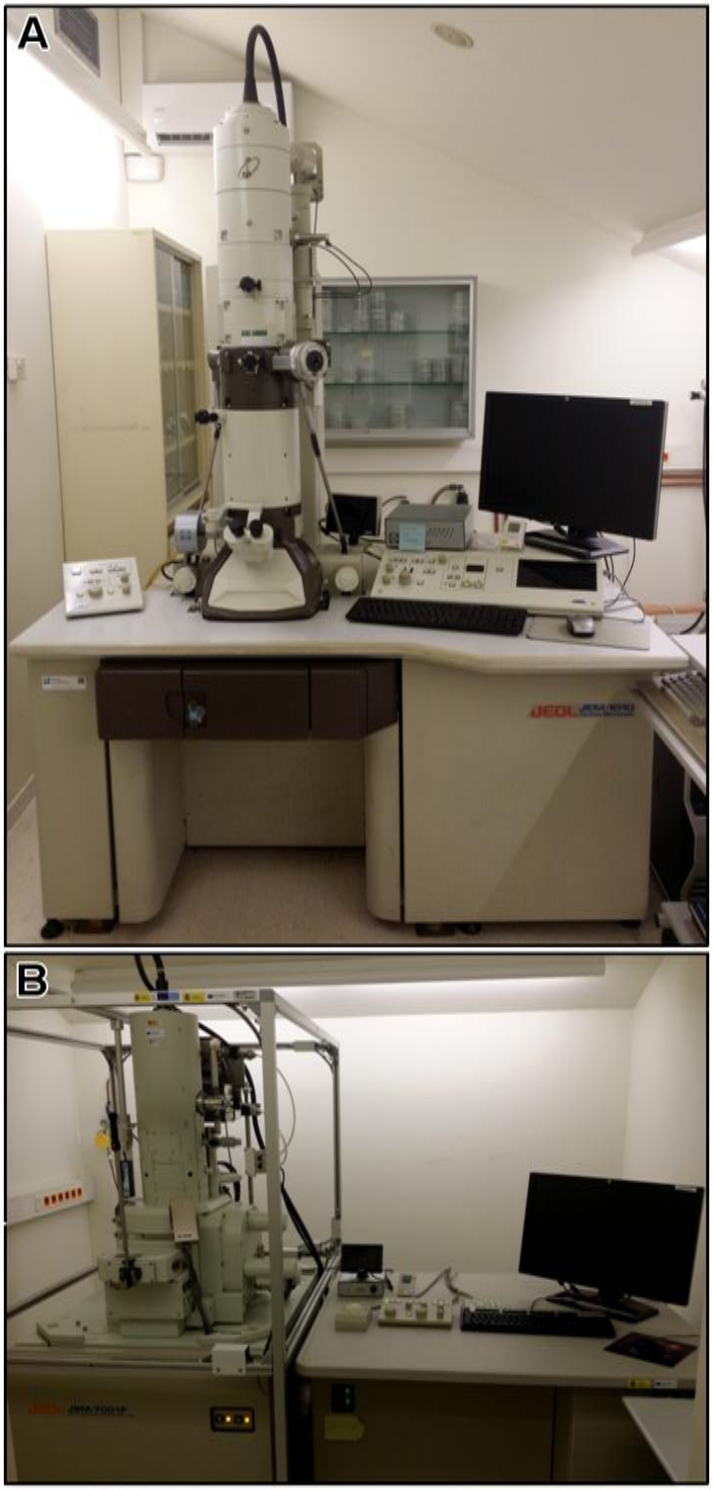

Figura 9.4.5. Microscopio electrónico de transmisión JEOL EM-1010 (A). Microscopio electrónico de barrido JEOL JSM-7001F (B). Instalaciones del CCiTUB del Hospital Clinic de Barcelona, 2012-2016. Imágenes publicadas con permiso de los Centros Científicos y Tecnológicos de la Universidad de Barcelona (CCiTUB).

9.4.6 Tomografía y micro-tomografía computarizada

Los rayos X penetran en una gran diversidad de materiales, tanto orgánicos como inorgánicos. Determinados rayos X son especialmente útiles para los estudios biológicos, ya que poseen una elevada penetración y gracias a las propiedades de su espectro de absorción contrastan muy bien con diversas estructuras biológicas (Haddad et al., 1994). Estas propiedades han permitido el desarrollo de la **tomografía computarizada** (abreviada como CT), una técnica basada en el uso de rayos X para escanear una muestra dada en rotación (la rotación es llevada a cabo por la propia fuente de rayos X o por la muestra en sí); las imágenes obtenidas, las sombras de radiación de rayos X no absorbida por la muestra, son superpuestas mediante un software especializado para formar una imagen tridimensional (Haddad et al., 1994; Ritman, 2004; Schambach et al., 2010). La micro-tomografía computarizada (abreviada como micro-CT o μCT) representa la evolución de la técnica anterior llevada hasta una escala de micrómetros (Ritman, 2004; Schambach et al., 2010). Esta técnica permite estudiar con gran nivel de detalle la estructura tridimensional de animales de una talla de milímetros, representando una ventaja sobre las técnicas de microscopía de barrido en el sentido de poder estudiar los animales desde cualquier ángulo, tanto a nivel externo como interno, sin necesidad de diseccionar la muestra (Alba-Tercedor, 2014; Alba-Tercedor y Sáinz-Cantero, 2012).

En el presente estudio se analizaron por tomografía computarizada (CT) especímenes adultos y por micro-tomografía computarizada (micro-CT) especímenes larvarios de la especie objeto de estudio, *Maja brachydactyla* Balss, 1922.

Tomografía Computarizada. *Adultos*. El análisis de los adultos se hizo con individuos congelados de ambos sexos. El escaneo de los especímenes se llevó a cabo en las instalaciones del IRTA localizadas en Monells (Girona). El equipamiento empleado consistió en un tomógrafo "General Electric HiSpeedZx/I". El protocolo de adquisición fue: adquisición helicoidal, pitch de 1, voltaje de 140 kV, corriente de 150 mA, campo de visión de 250 mm, grosor de 3 mm, algoritmo de reconstrucción STD+. La reconstrucción obtenida fue empleada para el estudio de la glándula digestiva (Fig. 9.4.6).

Micro-Tomografía Computarizada, *Larvas*. Fueron analizados los estadios larvarios zoea I y megalopa. Las larvas fueron sometidas a dos procedimientos de fijación. El primero fue el protocolo descrito para microscopía electrónica, basado en la fijación con paraformaldehído 2 % y glutaraldehído 2,5 % y en la post-fijación con tetraóxido de osmio (para más detalles ver sección "7.6.5 *Estudio ultra-estructural: microscopía electrónica*"). La parte final de dicho protocolo fue modificada, de modo que la deshidratación se llevó a cabo con isopropanol en lugar de acetona. El segundo protocolo empleado consistió en la fijación de las larvas en etanol 70 %, después fueron deshidratadas en soluciones de concentración creciente de isopropanol y se conservaron en isopropanol 100 %.

Las muestras fueron enviadas al Departamento de Zoología de la Facultad de Ciencias de la Universidad de Granada, donde se llevó a cabo el resto del protocolo. Las larvas conservadas en isopropanol 100 % fueron transferidas a una solución de yodo 1 % en etanol absoluto durante 72 horas, a continuación fueron sumergidas en hexametildisilazano durante 4 horas y secadas durante la noche. La técnica empleada para montar la muestra en los soportes varió con el estadio larvario, ya que su tamaño determina qué tipo de soporte y fijación es el más eficiente (Alba-Tercedor y Sáinz-Cantero, 2012). En el estadio de zoea, el telson fue pegado al extremo de un filamento de nylon de 200 µm de diámetro obtenido de un sedal de pesca, como agente adherente se usó cianoacrilato. En el estadio de megalopa, fueron montados en un soporte de BASOTECT® (espuma de resina de melanina, BASF). Las muestras se emplazaron en el interior de tubos de plástico para evitar cualquier movimiento provocado por los movimientos de aire que pueden darse durante el escaneo (Fig. 9.4.7).

Se empleó un micro-tomógrafo de alta resolución "SkyScan 1172", con una Hamamatsu 80/250 como fuente y una cámara VDS 1,3Mp. Los parámetros de escaneo fueron:

- *Zoea*: tamaño de voxel isotrópico de 1,48 µm por pixel; voltaje de 49 kV, corriente de 78 µA; escaneo de 180 ° con pasos de 0,3 °.
- *Megalopa*: tamaño de voxel isotrópico de 1,47 µm por pixel; voltaje de 54 kV, corriente de 84 µA; escaneo de 180 ° con pasos de 0,5 °.

Las reconstrucciones preliminares y el proceso de "limpieza" para obtener las bases de datos de imágenes en sección transversal se realizaron con las últimas versiones del software libre Bruker micro-CT Skyscan (www.skyscan.be; NRecon, DataViewer, CTAnalyser). El renderizado en volumen se obtuvo usando el software libre Skyscan's CTVox. La renderización de las figuras se obtuvo empleando el software FEI's Amirav.6.2 (Amira, 2016). El resumen del proceso se detalla en la Fig. 9.4.7, para una descripción más detallada se recomienda revisar Alba-Tercedor (2014).

Figura 9.4.6. Tomografía computarizada del adulto. Instalaciones del IRTA localizadas en Monells (Girona), por la Dra. María Font i Furnols.

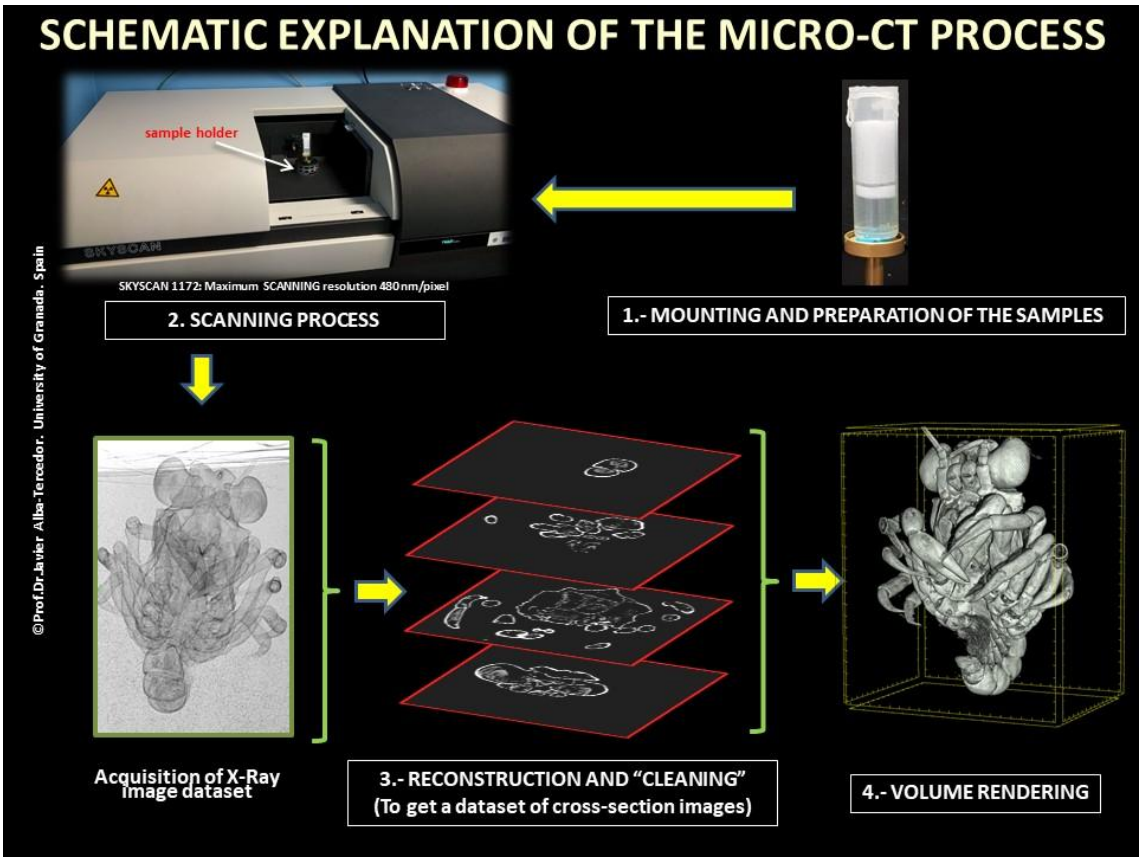

Figura 9.4.7. Resumen esquemático del proceso de micro-tomografía computarizada. Publicada con el permiso del Dr. Javier Alba-Tercedor, Universidad de Granada.

9.5 Bibliografía.

Abrunhosa FA, Kittaka J. 1997. Morphological changes in the midgut, midgut gland and hindgut during the larval and postlarval development of the red king crab *Paralithodes camtschaticus*. Fisheries Science 63(5):746-754.

Al-Mohanna SY, Nott JA. 1989. Functional cytology of the hepatopancreas of *Penaeus semisulcatus* (Crustacea: Decapoda) during the moult cycle. Marine Biology 101(4):535-544.

Al-Mohanna SY, Nott JA, Lane DJW. 1985. M-'Midget' cells in the hepatopancreas of the shrimp, *Penaeus semisulcatus* De Hann, 1844 (Decapoda, Natantia). Crustaceana 48(3):260-268.

Alba-Tercedor J. 2014. From the sample preparation to the volume rendering images of small animals: A step by step example of a procedure to carry out the micro-CT study of the leafhopper insect *Homalodisca vitripennis* (Hemiptera: Cicadellidae). In: Skyscan, editor. Bruker microCT Users Meeting 2014. Kontich, Belgium. p 260-288.

Alba-Tercedor J, Sáinz-Cantero CE. 2012. Volume rendering reconstructions of the anatomy of small aquatic beetles (Insecta : Coleoptera) scanned with the Skyscan 1172 high resolution micro-CT. In: Skyscan, editor. Micro-CT Users Meeting 2012. Kontich, Belgium. p 75-84.

Altner H, Hatt H, Altner I. 1986. Structural and functional properties of the mechanoreceptors and chemoreceptors in the anterior oesophageal sensilla of the crayfish, *Astacus astacus*. Cell and Tissue Research 244(3):537-547.

Alves STM, Abrunhosa FA, Lima JdF. 2010. Foregut morphology of Pseudothelphusidae and Trichodactylidae (Decapoda: Brachyura) from northeastern Pará, Brazil. Zoologia (Curitiba) 27(2):228-244.

Amira. 2016. 3D Visualization and Analysis Software. Hillsboro, Oregon, USA.

Anger K. 2001. The Biology of Decapod Crustacean Larvae. Rotterdam: A.A. Balkema Publishers. 419 p.

Anger K, Hayd L. 2009. From lecithotrophy to planktotrophy: ontogeny of larval feeding in the Amazon River prawn *Macrobrachium amazonicum*. Aquatic Biology 7:19-30.

Bancroft JD. 2008. Theory and Practice of Histological Techniques. Bancroft JD, Gamble M, editors: Elsevier Health Sciences.

Barker PL, Gibson R. 1977. Observations on the feeding mechanism, structure of the gut, and digestive physiology of the european lobster *Homarus gammarus* (L.) (Decapoda: Nephropidae). J Exp Mar Biol Ecol 26(3):297-324.

Barker PL, Gibson R. 1978. Observations on the structure of the mouthparts, histology of the alimentary tract, and digestive physiology of the mud crab *Scylla serrata* (Forskål) (Decapoda: Portunidae). J Exp Mar Biol Ecol 32(2):177-196.

Bell TA, Lightner DV. 1988. A handbook of normal penaeid shrimp histology. Society WA, editor. 114 p.

Bray D. 2000. Critical Point Drying of Biological Specimens for Scanning Electron Microscopy. In: Williams JR, Clifford AA, editors. Supercritical Fluid Methods and Protocols. Totowa, NJ: Humana Press. p 235-243.

Brink, Gross, Tittmann, Sherman, Chiu. 1998. Reduction of charging in protein electron cryomicroscopy. Journal of Microscopy 191(1):67-73.

Brösing A. 2010. Recent developments on the morphology of the brachyuran foregut ossicles and gastric teeth. Zootaxa 2510:1-44.

Brösing A. 2014. Foregut structures of freshly moulted exuviae from *Maja crispata*, *Cancer pagurus* and *Pseudosesarma moeschi* (Decapoda: Brachyura). Journal of Natural History 48(9-10):543-555.

Brösing A, Richter S, Scholtz G. 2002. The foregut-ossicle system of *Dromia wilsoni*, *Dromia personata* and *Lauridromia intermedia* (Decapoda, Brachyura, Dromiidae), studied with a new staining method. Arthropod Structure & Development 30(4):329-338.

Brösing A, Richter S, Scholtz G. 2007. Phylogenetic analysis of the Brachyura (Crustacea, Decapoda) based on characters of the foregut with establishment of a new taxon. Journal of Zoological Systematics and Evolutionary Research 45(1):20-32.

Brösing A, Türkay M. 2011. Gastric teeth of some thoracotreme crabs and their contribution to the brachyuran phylogeny. J Morphol 272(9):1109-1115.

Brusca RC, Brusca GJ. 2003. Invertebrates, 2nd Edition. 922 p.

Bullock GR. 1984. The current status of fixation for electron microscopy: A review. Journal of Microscopy 133(1):1-15.

Bunt AH. 1968. An ultrastructural study of the hepatopancreas of *Procambarus clarkii* (Girard) (Decapoda, Astacidea). Crustaceana 15(3):282-288.

Caceci T, Neck KF, Lewis DDH, Sis RF. 1988. Ultrastructure of the hepatopancreas of the Pacific white shrimp, *Penaeus vannamei* (Crustacea: Decapoda). Journal of the Marine Biological Association of the United Kingdom 68(02):323-337.

Ceccaldi HJ. 1989. Anatomy and physiology of digestive tract of Crustaceans Decapods reared in aquaculture. Advances in Tropical Aquaculture, Workshop at Tahiti, French Polynesia. Tahiti, French Polynesia: Actes de colloques Ifremer. p 243-259.

Cervellione F, McGurk C, Silva P, Owen MAG, Van den Broeck W. 2017a. Optimization of fixation methods for image analysis of the hepatopancreas in whiteleg shrimp, *Penaeus vannamei* (Boone). Journal of Fish Diseases 40(4):517-527.

Cervellione F, McGurk C, Van den Broeck W. 2017b. "Perigastric organ": a replacement name for the "hepatopancreas" of Decapoda. Journal of Crustacean Biology 37(3):353-355.

Cooper JE. 2011. Anesthesia, Analgesia and Euthanasia of Invertebrates. ILAR Journal 52(2):196-204.

Cuartas EI, Díaz AC, Petriella AM. 2002. Estudio morfológico e histológico del hepatopáncreas del langostino *Pleoticus muelleri* (Bate) (Crustacea, Penaeoidea). Revista de Investigación y Desarrollo Pesquero 15:5-13.

Chisaka H, Ueno M, Futaesaku Y. 1999. Spines in the hindgut of the crayfish *Procambarus clarkii* (Decapoda): their distribution and correlation with hindgut muscles. Journal of Crustacean Biology 19(2):337-343.

Dall W. 1967. The functional anatomy of the digestive tract of a shrimp *Metapenaeus bennettae* Racek & Dall (Crustacea : Decapoda : Penaeidae). Australian Journal of Zoology 15(4):699-714.

Davie PJF, Guinot D, Ng PKL. 2015. Anatomy and functional morphology of Brachyura. In: Castro P, Davie PJF, Guinot D, Schram F, Von Vaupel Klein C, editors. Treatise on Zoology - Anatomy Taxonomy Biology The Crustacea Volume 9 Part C: Brill. p 11-163.

Davolos D, L. P, Accordi F, De Matthaeis E. 2010. Morphology and histology of the mouthparts and gut system of *Macarorchestia remyi* (Schellenberg, 1950) (Amphipoda, Talitridae). Zoologia Baetica 21:151-178.

de La Barra P, Narvarte M, Williner V. 2017. Functional morphology of the gastric mill of the swimming crab *Ovalipes trimaculatus* (Decapoda: Portunidae). Journal of the Marine Biological Association of the United Kingdom:1-8.

Díaz AC, Sousa LG, Petriella AM. 2010. Functional cytology of the hepatopancreas of *Palaemonetes argentinus* (Crustacea, Decapoda, Caridea) under osmotic stress. Brazilian Archives of Biology and Technology 53:599-608.

Durfort i Coll M. 2006. Iniciació a les tècniques histològiques vegetals y animals i note sobre les técniques de transparentats. Barcelona: Institut D'Estudis Catalans.

Elzinga RJ. 1998. Microspines in the alimentary canal of arthropoda, onychophora, annelida. International Journal of Insect Morphology and Embryology 27(4):341-349.

Elzinga RJ, Hopkins TL. 1994. Foregut microspines in four families of cockroaches (Blattaria). International Journal of Insect Morphology and Embryology 23(3):253-260.

Elzinga RJ, Hopkins TL. 1995. Microspine variation in hindgut regions of four families of cockroaches (Blattaria). International Journal of Insect Morphology and Embryology 24(2):203-211.

Erri Babu D, Shyamasundari K, Hanumantha Rao K. 1979. The structure and histochemistry of the oesophageal glands in the crab *Menippe rumphii* (Frabricius) (Crustacea : Brachyura). Proceedings: Animal Sciences 88(4):277-285.

Erri Babu D, Shyamasundari K, Rao KH. 1982. Studies on the digestive system of the crab *Menippe rumphii* (Fabricius) (Crustacea:Brachyura). J Exp Mar Biol Ecol 58(2):175-191.

Factor JR. 1981. Development and metamorphosis of the digestive system of larval lobsters, *Homarus americanus* (Decapoda: Nephropidae). J Morphol 169:225-242.

Felgenhauer BE. 1992. Chapter 3. Internal Anatomy of the Decapoda: An Overview. In: Harrison FW, Humes AG, editors. Microscopic Anatomy of Invertebrates Volume 10: Decapod Crustacea: Wiley-Liss, Inc. p 45-75.

Fox CH, Johnson FB, Whiting J, Roller PP. 1985. Formaldehyde fixation. Journal of Histochemistry & Cytochemistry 33(8):845-853.

Frasca JM, Parks VR. 1965. A routine technique for double-staining ultrathin sections using uranyl and lead salts. The Journal of Cell Biology 25(1):157-161.

Garvey W. 1984. Modified Elastic Tissue-Masson Trichrome Stain. Stain Technology 59(4):213-216.

Gibson R, Barker PL. 1979. The Decapod Hepatopancreas. Oceanography and Marine Biology - An Annual Review 17:285-346.

Guerao G, Pastor E, Martin J, Andrés M, Estévez A, Grau A, Duran J, Rotllant G. 2008. The larval development of *Maja squinado* and *M. brachydactyla* (Decapoda, Brachyura, Majidae) described from plankton collected and laboratory-reared material. Journal of Natural History 42(33-34):2257-2276.

Haddad WS, McNulty I, Trebes JE, Anderson EH, Levesque RA, Yang L. 1994. Ultrahigh-Resolution X-ray Tomography. Science 266(5188):1213-1215.

Herrera-Alvarez L, Fernández I, Benito J, Pardos F. 2000. Ultrastructure of the midgut and hindgut of *Derocheilocaris remanei* (Crustacea, Mystacocarida). J Morphol 244(3):177-189.

Hinton DJ, Corey S. 1979. The mouthparts and digestive tract in the larval stages of *Homarus americanus*. Canadian Journal of Zoology 57(7):1413-1423.

Hobbs KH, Hooper SL. 2009. High-resolution computed tomography of lobster (*Panulirus interruptus*) stomach. J Morphol 270(9):1029-1041.

Holdich DM. 1973. The Midgut/Hindgut Controversy in Isopods. Crustaceana 24(2):211-214.

Holliday CW, Mykles DL, Terwilliger RC, Dangott LJ. 1980. Fluid secretion by the midgut caeca of the crab, *Cancer magister*. Comparative Biochemistry and Physiology Part A: Physiology 67(2):259-263.

Huxley TH. 1880. The Crayfish; an Introduction to the Study of Zoology. Series TIS, editor: New York: D. Appleton and Company.

Icely JD, Nott JA. 1992. Digestion and absorption: digestive system and associated organs. In: Harrison FW, Humes AG, editors. Microscopic anatomy of invertebrates: decapod Crustacea. New York: Wiley-Liss. p 147-201.

Johnston D. 2007. Feeding Morphology and Digestive System of Slipper Lobsters. The Biology and Fisheries of the Slipper Lobster: CRC Press. p 111-132.

Karnovsky MJ. 1965. A Formaldehyde-Glutaraldehyde Fixative of high osmolality for use in Electron Microscopy. The Journal of Cell Biology 27:137A.

Kaushik N, Kumar S. 1998. Midgut pathology of aldrin, monocrotophos, and carbaryl in the freshwater crab, *Paratelphusa masoniana* (Henderson). Bulletin of Environmental Contamination and Toxicology 60(3):480-486.

Komuro T, Yamamoto T. 1968. Fine structure of the epithelium of the gut in the crayfish (*Procambarus clarkii*) with special reference to the cytoplasmic microtutubles. Archivum histologicum japonicum 30(1):17-32.

Kubaryk J, Harper C. 2001. Optimizing waterless shipping conditions for *Macrobrachium rosenbergii*. In: Paust BC, Rice AA, editors. Marketing and shipping live aquatic products: Proceedings of the Second International Conference and Exhibition, November 1999, Seattle, WA: University of Alaska Sea Grant College Program. p 131-140.

Kunze J, Anderson D. 1979. Functional morphology of the mouthparts and gastric mill in the Hermit Crabs *Clibanarius taeniatus* (Milne Edwards), *Clibanarius virescens* (Krauss), *Paguristes squamosus* McCulloch and *Dardanus setifer* (Milne-Edwards) (Anomura: Paguridae). Marine and Freshwater Research 30(5):683-722.

Larson DM, Downing KH, Glaeser RM. 2011. The surface of evaporated carbon films is an insulating, high-bandgap material. Journal of structural biology 174(2):420-423.

Lehane MJ. 1997. Peritrophic matrix structure and function. Annual Review of Entomology 42(1):525-550.

Lev R, Spicer SS. 1964. Specific staining of sulphate groups with Alcian blue at low pH. Journal of Histochemistry & Cytochemistry 12:309.

Lima-Gomes RC, Lima JdF, Magalhães C. 2017. Description of ten additional ossicles in the foregut of the freshwater crabs *Sylviocarcinus pictus* and *Valdivia serrata* (Decapoda: Trichodactylidae). Zoologia (Curitiba) 34.

Loizzi RF. 1971. Interpretation of crayfish hepatopancreatic function based on fine structural analysis of epithelial cell lines and muscle network. Zeitschrift für Zellforschung und Mikroskopische Anatomie 113(3):420-440.

Longo MV, Díaz AO. 2015. Histological and histochemical study of the hepatopancreas of two estuarine crab species, *Cyrtograpsus angulatus* and *Neohelice granulata* (Grapsoidea, Varunidae): influence of environmental salinity. Zoological Science 32(2):163-170.

Longshaw M, Stebbing P. 2016. Biology and Ecology of Crayfish: CRC Press.

Lovett DL, Felder DL. 1989. Ontogeny of gut morphology in the white shrimp *Penaeus setiferus* (Decapoda, Penaeidae). J Morphol 201(3):253-272.

Lovett DL, Felder DL. 1990. Ontogeny of kinematics in the gut of the white shrimp *Penaeus setiferus* (Decapoda: Peneidae). Journal of Crustacean Biology 10(1):53-68.

Loya-Javellana GN, Fielder DR, Thorne MJ. 1994. Ontogeny of foregut in the tropical freshwater crayfish, *Cherax quadricarinatus* Von Martens, 1868 (Parasticidae: Decapoda). Invertebrate Reproduction and Development 25(1):49-58.

Lumasag GJ, Quinitio ET, Aguilar RO, Baldevarona RB, Saclauso CA. 2007. Ontogeny of feeding apparatus and foregut of mud crab *Scylla serrata* Forsskål larvae. Aquaculture Research 38(14):1500-1511.

Mallory FB. 1900. A contribution to staining methods. I. A differential stain for connective-tisse fibrillae and reticulum. II. Chloride of iron haematoxylin for nuclei and fibrin. III. Phosphotungstic acid haematoxylin for neuroglia fibers. Journal of Experimental Medicine 5:15-20.

Martin GG, Simcox R, Nguyen A, Chilingaryan A. 2006. Peritrophic membrane of the penaeid shrimp *Sicyonia ingentis*: structure, formation, and permeability. The Biological Bulletin 211(3):275-285.

McDowell EM, Trump BF. 1976. Histologic fixatives suitable for diagnostic light and electron microscopy. Archives of Pathology & Laboratory Medicine 100(8):405-414.

McGaw IJ, Stillman JH. 2010. Cardiovascular system of the Majidae (Crustacea: Decapoda). Arthropod Structure & Development 39(5):340-349.

Meiss DE, Norman RS. 1977. Comparative study of the stomatogastric system of several decapod crustacea. I. Skeleton. J Morphol 152(1):21-53.

Mets RD. 1962. Submicroscopic structure of the peritrophic membrane in arthropods. Nature 196:77-78.

Milne-Edwards H. 1834a. Histoire naturelle des crustacés, comprenant l'anatomie, la physiologie et la classification de ces animaux: Libraire Encyclopédique de Roret.

Milne-Edwards H. 1834b. Histoire naturelle des crustacés: atlas: Libraire Encyclopédique de Roret.

Minagawa M, Takashima F. 1994. Developmental changes in larval mouthparts and foregut in the red frog crab, *Ranina ranina* (Decapoda: Raninidae). Aquaculture 126(1-2):61-71.

Muhammad F, Zhang ZF, Shao MY, Dong YP, Muhammad S. 2012. Ontogenesis of digestive system in *Litopenaeus vannamei* (Boone, 1931) (Crustacea: Decapoda). Italian Journal of Zoology 79(1):77-85.

Murray MJ. 2008. Appendix 3: Euthanasia. In: Lewbart GA, editor. Invertebrate Medicine: Blackwell Publishing Professional. p 303-304.

Mykles DL. 1977. The ultrastructure of the posterior midgut caecum of *Pachygrapsus crassipes* (Decapoda, Brachyura) adapted to low salinity. Tissue and Cell 9(4):681-691.

Mykles DL. 1979. Ultrastructure of alimentary epithelia of lobsters, *Homarus americanus* and *H. gammarus*, and crab, *Cancer magister*. Zoomorphologie 92(3):201-215.

Nakamura K, Takemoto T. 1986. Morphology of stomach ossicles in Brachyura. Memoirs of Faculty of Fisheries Kagoshima University 35(1):7-15.

Nielsen LF, Moe D, Kirkeby S, Garbarsch C. 1998. Sirius Red and Acid Fuchsin staining mechanisms. Biotechnic & Histochemistry 73(2):71-77.

Nishida S, Takahashi Y, Kittaka J. 1995. Structural changes in the hepatopancreas of the rock lobster, *Jasus edwardsii* (Crustacea: Palinuridae) during development from the puerulus to post-puerulus. Marine Biology 123(4):837-844.

Nunes ET, Braga AA, Camargo-Mathias MI. 2014. Histochemical study of the hepatopancreas in adult females of the pink-shrimp *Farfantepenaeus brasiliensis* Latreille, 1817. Acta Histochemica 116(1):243-251.

Papathanassiou E, King PE. 1984. Effects of starvation on the fine structure of the hepatopancreas in the common prawn *Palaemon serratus* (pennant). Comparative Biochemistry and Physiology Part A: Physiology 77(2):243-249.

Patwardhan SS. 1935. On the structure and mechanism of the gastric mill in Decapoda. Proceedings of the Indian Academy of Sciences - Section B 1(11):693-704.

Puchtler H, Meloan SN, Terry MS. 1969. On the history and mechanism of Alizarin Red S stains for calcium. Journal of Histochemistry & Cytochemistry 17(2):110-124.

Pugh JE. 1962. A contribution toward a knowledge of the hind-gut of fiddler crabs (Decapoda, Grapsidae). Transactions of the American Microscopical Society 81(4):309-320.

Ramadevi KRLS, Shyamasundari K, Hanumantha Rao K. 1990. Observation of the hepatopancreas of *Ocypoda platytarsis* (Milne-Edwards) (Crustacea, Brachyura). Bolletino di zoologia 57(3):261-265.

Reddy AR. 1937. The physiology of digestion and absorption in the crab *Paratelphusa* (*Oziotelphusa*) *hydrodromus* (Herbst). Proceedings of the Indian Academy of Sciences - Section B 6(3):170-193.

Ritman EL. 2004. Micro-Computed Tomography — Current Status and Developments. Annual Review of Biomedical Engineering 6:185-208.

Robertson RM, Laverack MS. 1979. Oesophageal sensors and their modulatory influence on oesophageal peristalsis in the lobster, *Homarus gammarus*. Proceedings of the Royal Society of London Series B Biological Sciences 206(1163):235-263.

Ross MH, Pawlina W. 2016. Histology: A Text and Atlas, with correlated Cell and Molecular Biology: Wolters Kluwer Health.

Rotllant G, González-Gurriarán E, Fernández L, Benhalima K, Ribes E. 2007. Ovarian maturation of the multi-spawning spider crab *Maja brachydactyla* (Decapoda: Majidae) with special reference to yolk formation. Marine Biology 152(2):383-394.

Schaefer N. 1970. The functional morphology of the foregut of three species of decapod Crustacea: *Cyclograpsus punctatus* Milne-Edwards, *Diogenes brevirostris* Stimpson, and *Upogebia africana* (Ortmann). Zoologica Africana 5(2):309-326.

Schambach SJ, Bag S, Schilling L, Groden C, Brockmann MA. 2010. Application of micro-CT in small animal imaging. Methods 50(1):2-13.

Schlegel C. 1911. Anatomie sommaire de la première zoé de *Maja squinado* Latr. (Note préliminaire à des recherches sur l'Organogénese des Décapodes brachyoures). Archives de Zoologie Experimentale et Générale 5º Série T. VIII.(2):29-40.

Schmitz EH, Scherrey PM. 1983. Digestive anatomy *Hyalella azteca* (Crustacea, Amphipoda). J Morphol 175:91-100.

Sharman A, Hirji R, Birmingham JT, Govind CK. 2000. Crab stomach pyloric muscles display not only excitatory but inhibitory and neuromodulatory nerve terminals. J Comp Neurol 425(1):70-81.

Simeó CG. 2012. Estudi de la biologia reproductiva de la cabra de mar, *Maja brachydactyla*: aparell reproductor i qualitat de les postes en captivitat [Doctoral Dissertation]. Barcelona (Spain): Universitat de Barcelona. 254 p.

Simeó CG, Kurtz K, Chiva M, Ribes E, Rotllant G. 2010. Spermatogenesis of the Spider Crab *Maja brachydactyla* (Decapoda: Brachyura). J Morphol 271(4):394-406.

Simeó CG, Kurtz K, Rotllant G, Chiva M, Ribes E. 2009a. Sperm ultrastructure of the spider crab *Maja brachydactyla* (Decapoda: Brachyura). J Morphol 271(4):407-417.

Simeó CG, Ribes E, Rotllant G. 2009b. Internal anatomy and ultrastructure of the male reproductive system of the spider crab *Maja brachydactyla* (Decapoda: Brachyura). Tissue and Cell 41(5):345-361.

Smith RI. 1978. The Midgut Caeca and the Limits of the Hindgut of Brachyura: A Clarification. Crustaceana 35(2):195-205.

Sousa L, Petriella AM. 2006. Morphology and histology of *P. argentinus* (Crustacea, Decapoda, Caridea) digestive tract. Biocell 30:287-294.

Sousa LG, Petriella AM. 2007. Functional morphology of the hepatopancreas of *Palaemonetes argentinus* (Crustacea: decapoda) : Influence of environmental pollution. Espagnol 55:79-85, SUP71.

Spurr AR. 1969. A low-viscosity epoxy resin embedding medium for electron microscopy. Journal of Ultrastructure Research 26(1):31-43.

Stanier JE, Woodhouse MA, Griffin RL. 1968. The Fine Structure of the Hepatopancreas of *Carcinus maenas* (L.) (Decapoda Brachyura). Crustaceana 14(1):56-66.

Stempak JG, Ward RT. 1964. An improved staining method for electron microscopy. The Journal of Cell Biology 22(3):697-701.

Storch V, Anger K. 1983. Influence of starvation and feeding on the hepatopancreas of larval *Hyas araneus* (Decapoda, Majidae). Helgoländer Meeresuntersuchungen 36(1):67-75.

Suljak SW, Rose CM, Sabatier C, Le T, Trieu Q, Verley DR, Lewis AM, Birmingham JT. 2010. Enhancement of Muscle Contraction in the Stomach of the Crab *Cancer borealis*: a Possible Hormonal Role for GABA. The Biological Bulletin 218(3):293-302.

Titford M. 2005. The long history of hematoxylin. Biotechnic & Histochemistry 80(2):73-78.

To TH, Brenner TL, Cavey MJ, Wilkens JL. 2004. Histological organization of the intestine in the crayfish *Procambarus clarkii*. Acta Zoologica 85(2):119-130.

Trinadha Babu B, Shyamasundari K, Hanumantha Rao K. 1989. Observations on the morphology and histology of the foregut of *Portunus sanguinolentus* (Crustacea: Brachyura). Folia Morphologica 37(4):364-372.

Tziouveli V, Bastos-Gomez G, Bellwood O. 2011. Functional morphology of mouthparts and digestive system during larval development of the cleaner shrimp *Lysmata amboinensis* (de Man, 1888). J Morphol 272(9):1080-1091.

Van Weel PB. 1974. Hepatopancreas? Comparative Biochemistry and Physiology Part A: Physiology 47(1):1-9.

Vogt G. 1996. Morphology and physiology of digestive epithelia in Decapod crustaceans. Pflügers Archiv 431(6):R239-R240.

Wallis MA, Griffin RL. 1973. A routine method for embedding animal tissues in Spurr resin for electron microscopy. Journal of Clinical Pathology 26(1):77-78.

Wang L, Li F, Wang B, Xiang J. 2012. Structure and partial protein profiles of the peritrophic membrane (PM) from the gut of the shrimp *Litopenaeus vannamei*. Fish & Shellfish Immunology 33(6):1285-1291.

Woods CMC. 1995. Morphology of the foregut of the Spider Crab *Notomithrax ursus* (Brachyura:Majidae) Journal of Crustacean Biology 15(2):220-227.

Yonge CM. 1924. Studies on the comparative physiology of digestion II. - The mechanism of feeding, digestion, and assimilation in *Nephrops norvegicus*. British Journal of Experimental Biology 1:343-389.

Yonge CM. 1932. On the nature and permeability of Chitin. I.--The Chitin lining the Foregut of Decapod Crustacea and the function of the Tegumental Glands. Proceedings of the Royal Society B: Biological Sciences 111(772):298-329.

Zambonino-Infante JL, Gisbert E, Sarasquete C, Navarro I, Gutiérrez J, Cahu CL. 2008. Ontogeny and Physiology of the Digestive System of Marine Fish Larvae. In: Cyrino JEP, editor. Feeding and Digestive Functions in Fishes: CRC Press.

CHAPTER 10.

Exploring the internal morphology of the larvae digestive system of *Maja brachydactyla* Balss, 1922 using micro computed tomography:

Assessment of spatial resolution

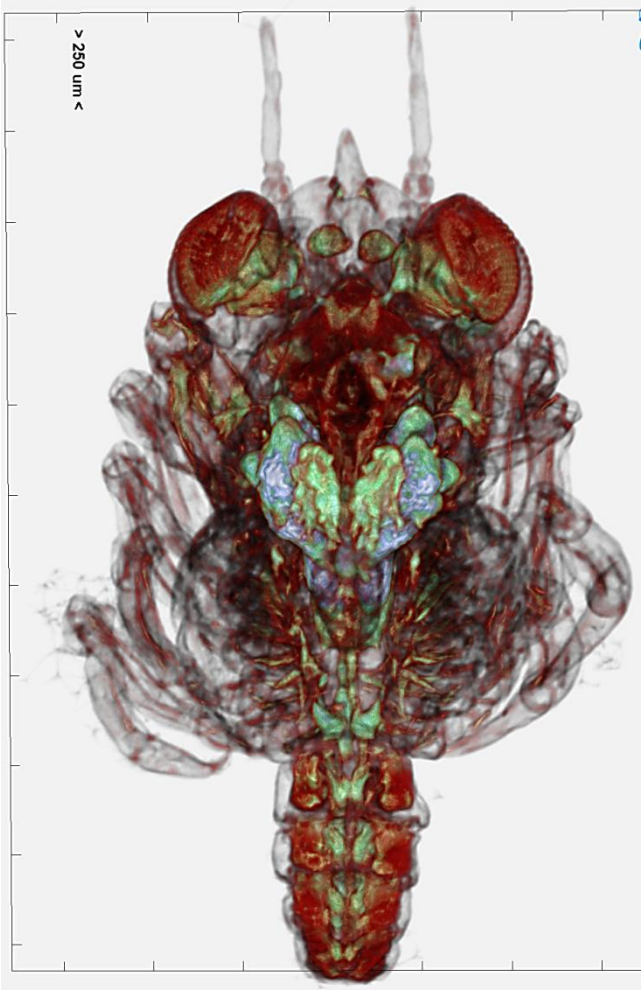

Exploring the internal morphology of the larvae digestive system of *Maja brachydactyla* Balss, 1922 using micro computed tomography: Assessment of spatial resolution

Diego Castejón[1*], Javier Alba-Tercedor[2], Guiomar Rotllant[3], Enric Ribes[4], Mercè Durfort[4], and Guillermo Guerao[5]

[1]IRTA, Centre d'Aqüicultura, Ctra. del Poble Nou Km 5.5., 43540 Sant Carles de la Ràpita, Tarragona, Spain.

[2]Departamento de Zoología, Facultad de Ciencias, Universidad de Granada, Av. de Fuente Nueva s/n, 18071 Granada, Spain.

[3]CSIC, Institut de Ciències del Mar, Passeig Marítim de la Barceloneta 37-49, 08003 Barcelona, Spain.

[4]Unitat de Biologia Cel·lular, Departament de Biologia Cel·lular, Fisiologia i Immunologia, Facultat de Biologia, Universitat de Barcelona, Diagonal 645, 08028Barcelona,Spain.

[5]PS Fabra i Puig 344, 08028 Barcelona, Spain.

Short title: Micro-CT for *Maja brachydactyla*: digestive anatomy of the larvae

***Corresponding author:** Diego Castejón. E-mail: diego.castejon.dcb@gmail.com; phone: +34 681 154 398; postal address: IRTA, Subprogram Cultius Aqüàtics, Ctra. Poble Nou, Km 5.5, 43540 Sant Carles de la Ràpita, Tarragona, Spain.

Abstract.

The study of the internal morphology of Malacostraca larvae is traditionally based on histological methods. The preparation of serial sections resolve structures at cellular level but means the irreversible loss of the animal and it is time-consuming, while micro computed tomography (micro-CT) provides high quality three-dimensional images. The present study describes the larval internal morphology, with special focus on the digestive system, of the brachyuran crab *Maja brachydactyla* Balss, 1922 combining micro-CT and optical microscopy techniques. The anatomical features of the zoeal and megalopa stages are similar and follow the typical pattern described in the adult Decapoda. The digestive system comprises a foregut subdivided into esophagus and stomach; a midgut subdivided into midgut tract, midgut caeca and midgut gland ("hepatopancreas"); and a large hindgut. The circulatory system includes a compact heart located dorsally and various main arteries: "anterior aorta" and "anterolateral arteries" projected anteriorly, "posterior aorta" projected posteriorly and "ventral abdominal artery" beneath the ventral nerve cord. The nervous system is located beneath the digestive system and includes: an anterior syncerebrum ("brain"), nervous connectives around the esophagus, thoracic ganglionic mass and ventral nerve cord. The muscular system is highly developed. The major glands has been identified adjacent to the mouthparts and esophagus; and antennal glands on the basis of the antennae. The main changes occurred on the metamorphosis to the megalopa stage include the development of the ossicles and gastric mill on the stomach, the shortening of the abdominal nerve cord, as well the development of functional pereiopods, pleopods and lamellate gills.

Keywords: Eucrustacea; Decapoda; larval development; ontogeny; 3D imaging anatomy

1. Introduction

The decapods are the richest malacostracan group with ca. 15,000 described species [1, 2] and a major component of the marine and freshwater communities [3]. The decapods are also an important economic resource that mobilize billions on dollars in fishery and aquaculture production (www.fao.org). To understand the biology of the decapods the knowledge of the larval stages is crucial, since they are the most vulnerable phases of development and its role in population dynamics, species dispersal, settlement and recruitment [3]. A key element to understand the biology of the Decapoda larval stages rely on their morphology and anatomy, in this sense numerous studies have been focused on their morphological diversity but less information is available in relation to their anatomy [3-5]. A detailed knowledge of the anatomical features (including relative size, shape and location of the organs and other structures) is crucial to comprehend the physiology and development of these organisms in a functional and evolutionary perspective [6-8].

Classically, the study of the inner anatomy of small-sized animals required procedures based on the dissection or physical sectioning of the specimens as prerequisite for their observation under stereo-, optical or scanning electron microscope. The dissection permit to examine directly the inner structures but it is a very invasive technique that implies drastic alterations (since many organs cannot be examined until other anatomical structures were retired) leading to the specimen destruction [9]. The studies based on the optical microscopy techniques permit to examine the anatomy at cellular level preserving the location of the inner structures. The anatomical studies received a significant advance with the arrival of the confocal laser scanning microscopy (CLSM) technology, that permit the realization of anatomical studies

employing non-invasive techniques avoiding the physical alteration of the specimens [10-12], for this purpose image stacks of two-dimensional sections are used to reconstruct three-dimensional models [10, 12]. In non-insect pancrustaceans this approach have been applied for the study of embryos and larvae of decapods and copepods [13-15]. However, this technique is limited for their requirements of transparent body structures [7] and the dye absorptive properties of these structures [7, 13-15].

The next advance was achieved by the development of the micro computed tomography (micro-CT), a technology based on the X-Ray absorption properties of the tissues to obtain the two-dimensional sections required for the three-dimensional model reconstruction [9, 16-19]. This technology provides higher resolution and deeper penetration level than the CLSM giving improved virtual models. According to Betz et al. [7]: "*it allows biologists and material scientists to section samples virtually in any direction, with submicrometer resolution, in their natural state and without elaborate and time-consuming dissection or histology*". The usefulness of this technology has been demonstrated innumerous morphological and developmental studies [7, 16-18], being widely used in insects [6, 7, 20-25]. Few studies applied this technology in Decapoda taxa, e.g. the ossicle organization of the adult spiny lobster stomach[26], the adult caridean alimentary tract [27], the female reproductive system of an adult brachyuran species [28] and the general anatomy of an adult brachyuran species [29]. Recently, also it has been used to describe the invasiveness of the parasitic rhizocephalans inside the adult Decapoda host [30]. To our knowledge micro-CT has not yet used on the studies focused on the anatomy of decapod larval stages.

The main objective of the present study is the assessment of the potential of micro-CT technology for the study of the internal morphology of the larvae of the Atlantic spider crab *Maja brachydactyla* Balss, 1922. The optical microscopy observations will be used to obtain complementary information and to compare the resolution of the micro-CT techniques. The investigation is mainly focused on the digestive system, although other systems are also described briefly.

2. Material and methods

2.1 Animal culture

The larvae were obtained by a design successfully employed in previous culture experiences [31-33]. In brief, groups of adult specimens (six females and one male) were maintained in 2,000 L cylindrical tanks with water renewal rate of 3.5 m^3 h^{-1}, temperature of 18 ± 1 °C, salinity of 35 ± 1 psu, photoperiod of 12 h light: 12 h dark and diet based on fresh and frozen *Mytilus* sp. mussels. The larvae hatched in the adult tanks were drained into special 35 L PVC collector baskets. Following a previous study [34], the larvae within ca. 15 hours after hatch (zoeae) were cultured in 600 mL glass beakers placed inside 360 L tanks (96 x 96 x 40 cm) used as incubation chambers. The conditions were temperature of 21 ± 1 °C, salinity of 35 ± 1 psu, photoperiod of 12 h light: 12 h dark and diet was based on *Artemia* sp. Kellogg, 1906 nauplii. Daily the living specimens were carefully pipetted to glass beakers with clean water and fresh food. The megalopae were obtained in six days.

2.2 Optical microscopy study

The whole larvae, either newly molted zoeae I (ZI) or megalopa (M),were directly fixed in Davidson's fixative (ethanol absolute: filtered seawater: formaldehyde 37%: glycine: glacial acetic acid in proportion 3: 3: 2: 1: 1) during 24 h. Then, samples

were dehydrated in an ethanol and xylene series and infiltrated with paraffin using an automatic tissue processor (Myr, Spain). The paraffin blocks were realized in a paraffin processor composed by a dispensing module for heated liquid paraffin and a table-top cooling plate as paraffin cooling module (AP208-1, AP208-2 and AP208-3; Myr, Spain). The paraffin blocks were cut into 2 µm sheets using a microtome Leica RM2155 (Leica Microsystems, Wetzlar, Germany). The paraffin sheets were stained with Hematoxylin and Eosin (HE). The optical microscopy observations were realized under an optical microscope (Leica LB30T 111/97) connected to a camera (Olympus DP70 1.45 Mpx; Olympus Corporation, Germany) and an image analyzing system (DP Controller 2.1.1.83 and DP Manager 2.1.1.163; Olympus Corporation, Germany).

2.2 Micro computed tomography (micro-CT) study

Zoeae fixation was realized by a solution of 2 % paraformaldehyde - 2.5 % glutaraldehyde in cacodylate buffer (0.1 mol L^{-1} pH 7.4) for ca. 12 h at 4 °C in constant darkness conditions. Then ZI samples were rinsed twice in the same buffer and post-fixed in 1 % osmium tetroxide solution in cacodylate buffer (0.1 mol L^{-1} pH 7.4).The megalopae fixation was realized by a solution of ethanol 70 %.The larvae (ZI and M) were rinsed, dehydrated and preserved in 100% isopropanol, at continuation the megalopae were transferred to a solution of 1 % iodine in ethanol absolute during 72 h. Following previous studies [35], previously to the scanning, the larvae were submerged in hexamethyldisilazane for 4-5 hours and overnight air dried. The dried specimens were placed in holders specially designed for small sized animals following Alba-Tercedor and Sáinz-Cantero [20].The zoeae were mounted on the tip of a nylon filament line (200 µm diameter, fishing line) and glued using cyanoacrylate. The megalopae were mounted in a piece of BASOTECT® (melamine resin foam, Chemical Company

BASF), whose very low density gives low absorptive properties for the X-Ray and consequently can be easily eliminated during the segmentation procedure [36]. All samples were enclosed inside a plastic straw to avoid any movement caused by the air refrigerating forced air during the scan process.

The larvae were scanned in a SkyScan 1172 high resolution microtomographer (Bruker microCT, Kontich, Belgium), with a Hamamatsu 80/250 source and a VDS 1.3 Mp camera. The scanning parameters for the zoea were setup as: isotropic voxel size = 1.48 µm per pixel; source voltage = 49 KV; source current = 78 µA; image rotation scan of 180° with 0.3° rotation step. The scanning parameters for the megalopa were setup as: isotropic voxel size = 1.47 µm per pixel; source voltage = 54 KV; source current = 85 µA; image rotation scan of 180° with 0.5° rotation step.

The latest versions of the free Bruker micro-CT Skyscan (www.skyscan.be) software (NRecon, DataViewer, CTAnalyser) was used for primary reconstructions and the "cleaning" process to obtain the datasets of cross-sectional images (slices). The volume renderings images were obtained with the free Skyscan's software CTVox (color volume rendering images were obtained varying the color transfer function curves, conjunction with the lighting and shadowing options) and the FEI's Amira software v.6.2 [37]. For a more detailed description of the process see Alba-Tercedor [38]. Micro-CT analyses were realized at the Department of Zoology of the University of Granada, Spain.

3. Results

The combined use of micro-CT and optical microscopy permit to observe the internal anatomy of *M. brachydactyla* larvae. The main structures resolved by micro-CT were the digestive, nervous and muscular systems. The internal anatomy is conserved

between the stages of zoea and megalopa, including the digestive organs with the exception of the stomach. The digestive system is located medially, between the main structures of the circulatory system (positioned dorsally) and the main structures of the nervous system (positioned ventrally). It is composed by: esophagus, stomach, midgut tract, midgut caeca, midgut gland (also known as "hepatopancreas") and hindgut (Fig. 1-3; 7-9; S1, 3-6, 8-10). The circulatory system includes a dorsal heart with associated main arteries; the nervous system is composed by an anterior syncerebrum ("brain"), ventral thoracic ganglions and abdominal nerve cord (Fig. 1-10); the respiratory system increases in complexity in the megalopal stage with the appearance of lamellate gills located in the branchial chamber (Fig. 6; 8D-F; S11). The reproductive system has not been identified in any larval stage. The different elements of the digestive system will be described below.

Esophagus. The esophagus is a short tube that communicates the mouth opening with the stomach: the mouth opening is located ventrally on the anterior part of the head, then the esophagus appear as a vertical tube, being the juncture between the esophagus and the stomach located on the ventral wall of the cardiac stomach (Fig. 1; 2; 7A-C; S1, 3, 6). The esophagus is surrounded by a continuous band of wide rings of circular muscles (Fig. 1B; S1), and contains internal folds. By micro-CT a narrowing of the esophagus on the juncture with the stomach can be observed (Fig. 1C; 2C; 7C); while the optical microscopy reveal a lumen lined by a simple epithelium whose cells are vacuolated and covered by a cuticle(Fig. 7B; S3).

The esophagus is laterally surrounded by the nervous system. The basic organization of the nervous system includes an external and basophil cortical layer formed by the main neural bodies; and an internal and acidophil central neuropil formed

by neural extensions (Fig. 1A-B). Between the esophagus and the anterior tegument of the head the syncerebrum is present. The syncerebrum is connected with the thoracic ganglions through nervous connectives that surrounds both lateral sides of the esophagus (Fig. 7A-C; S3). Some small masses of tegumental (or rosette) glands associated with the mouth opening and mouthparts have been identified on the labrum and between the esophagus and the thoracic ganglionic mass (Fig. 1-2; S1, 6). Additionally, on the basis of the antennae appear the antennal glands as sac like structures lined by a simple epithelium with cuboidal to squamous cells and microvillous border, this structure surround a small globular formation composed by plain cells (Fig. 7A-C; S3).

Stomach. The next component of the foregut is the stomach. This organ is subdivided into cardiac and pyloric stomach, separated by the cardio-pyloric valve (Fig. 1-4; S1, 3, 6). The stomach of the zoeae has an anterior, short and simple cardiac stomach like a wider and vertical continuation of the underlying esophagus. By micro-CT and optical microscopy were observed internal folds and the optical microscope reveal as well the absence of the vacuolated epithelial cells and circular muscles observed in the esophagus (Fig. 1, 3; S1, 3). The cardio-pyloric valve separates the cardiac from the pyloric stomach; in the zoeae sustains strong thick setae (S2, 3). The lateral sides of the cardio-pyloric valve have ventral folds forming channels connected to the posterior pyloric filters. The pyloric stomach sustains a pair of ventro-posterior folds inflated as pouches, inside these pouches are located the pyloric filters (Fig. 3B, 7B; S3). The pyloric filters are parallel and longitudinal channels formed by laminar cuticle projections presenting large and thin setae organized as a thin sieve that remember to a filtering system (Fig. 7A-C; S3).

The stomach undergoes the most drastic change in the metamorphosis to megalopa (Fig. 1-4; S1, 2, 6, 7). The cardiac stomach of the megalopa enlarges anterior and laterally acquiring a sac-like shape forming the called cardiac sacs. Simultaneously, the ossicle armature that supports the stomach structure is developed concomitantly with the gastric mill. Some ossicles are easily observed by micro-CT: the single propyloric and urocardiac ossicles, as well the paired pterocardiacs and zygocardiacs ossicles (Fig. 6). The gastric mill appears as ossicles transformed into teeth like structures projected toward the lumen (Fig. 2B, 3; S1, 2). The cardio-pyloric valve lost the large and thick setae observed in the zoeae but maintain thin setae. The pyloric stomach of the megalopa is similar to their zoea counterpart (Fig. 2, 4,7D- F).

The larval stomach is associated with thick, vertical, striated muscle bundles attached dorsally to the dorsal tegument and basally to the lateral walls and basis of the stomach (Fig. 3-5, 7; S2, 3, 7, 8). In the zoeae these major bundles are attached to the dorsal tegument located anteriorly to the dorsal spine (Fig. 1, 3; S1-3), and projected downward to both sides of the stomach at the cardio-pyloric valve level (Fig. 7A-C; S3). In the megalopae, these major muscle bundles are displaced backward at the level of the pyloric stomach (Fig. 3, 5; S7, 8). Additional and numerous thin muscle bundles are attached to the stomach walls and extended from the cardiac to the pyloric stomach (Fig. 7; S3, 8). In both zoeae and megalopae, a single anterior aorta located on the middle line of the body over the stomach was observed, as well a pair of anterolateral arteries located laterally crossing between major muscle bundles (Fig. 1-2, 6A-E, 7D-E; S3, 8).

Midgut tract. In both zoeae and megalopae, it is a short cylindrical tube. The lumen is generally smooth with sparse small folds. By optical microscopy we identified a simple, short, columnar and microvillous epithelium. The anterior extreme of the midgut tract is connected forwardly with the pyloric stomach, dorsally with a pair of short anterior caeca and ventrally with the main tubes of the midgut gland. The posterior extreme of the midgut tract is connected backwardly to the midgut-hindgut junction and dorso-laterally with a short and single posterior caecum (Fig. 1 - 5; S1, 2, 4, 6, 7, 9).

Midgut caeca. The digestive system of the *M. brachydactyla* larvae has three midgut caeca: a pair of anterior caeca projected forward from the dorso-anterior extreme of the midgut tract and a single posterior caecum projected dorso-laterally from the midgut side of the midgut - hindgut junction. The caeca are very similar among them and between larval stages, but larger in the megalopae. The caeca are short blind-end tubules with a finger like shape as observed by micro-CT (Fig. 3C, 6B). The lumen is smooth and without any type of folding, by optical microscopy is observed a simple and microvillous epithelium formed by short-columnar cells (Fig. 1- 3; S1, 6).

The midgut tract and associated caeca are located below the pericardium and heart, in turn the pericardium and heart are located between the posterior dorsal tegument and the digestive system in the zoeae (Fig. 1,8B; S1, 3) and megalopae (Fig. 2-3; S6). The pericardium and heart are structures easily observable by optical microscopy but difficult to observe by micro-CT. The pericardium and heart walls are intimately associated (Fig. 1B, 2B, 4B): the pericardium is a voluminous and single sac like structure that surround the heart by a single layer of plain cells (Fig. 1B, 2B, 4B); while the heart is lined by a thin layer of plain cells, showing numerous muscular fibers crossing the heart cavity as trabeculae like structures (Fig. 2B, 3, 4B; S1, 6).

Midgut gland (MGG). It is the most voluminous organ of the digestive system and occupies an important volume of the cephalothoracic cavity. This organ is observed in great detail under micro-CT: it is composed by a pair of similar halves, each one located in a lateral side of the pyloric stomach and midgut tract. Each half is constituted by a lower sub-lobule positioned below the level of the midgut tract and an upper sub-lobule that nearly cover their lateral sides. Each sub-lobule is formed by few blind-end tubules projected anteriorly toward the lateral sides of the pyloric stomach, laterally toward the lateral sides of the carapace walls and backwardly toward the anterior part of the hindgut (Fig. 3, 6A, B, 7F, 8F). By optical microscopy we observed a simple, short, microvillous epithelium composed by different cell types that correspond to the R (resorptive), F (fibrillar) and B (blister like) cells identified in other Decapoda taxa (Fig. 1B, 2B, 4B, 5B, 7B, E, 8b, E; S1 - 4, 6 - 9).

Underlying the midgut tract are located the lower sub-lobules of the MGG, and beneath these sub-lobules is located the thoracic ganglions (Fig. 1- 3, 7 - 8; S1, 4 - 6, 8, 9). Their tridimensional organization is one of the most visible structures under micro-CT. The thoracic ganglions are a long structure located ventrally in the middle line of the animal body presenting a pair of ganglions in each segment. In the zoeae, it is extended from the esophagus to the last thoracic segment (Fig. 1; S1). In the megalopae, it is extended from the esophagus to the junction between the third and fourth thoracic segment (Fig. 2, 3). The height of the thoracic ganglions is approximately constant, but internally the neuropile expand and shrink inside each segment and between segments, respectively (Fig. 1-2). The thoracic ganglionic mass is expanded laterally acquiring a plate like shape, from which extends some fiber like nerves toward the pereiopods (Fig. 6C).

The branchial chambers of de megalopa contains lamellate gills. By optical microscopy the gills shows a simple, squamous epithelium covered by a thin cuticle (Fig. 8E; S9). By micro-CT the gills shows the typical phyllobranchiate structure of the brachyurans: the gill comprises a central filament with extended parallel lamellae (Fig. 8D -F; S9, 11).

Hindgut. It includes the hindgut tract and the anus. The hindgut morphology is similar among the zoeae and megalopae: it is a long tube extended from the midgut - hindgut junction (located beneath the posterior margin of the carapace) toward the last abdominal segment (Fig. 1-2; S1, 6). The micro-CT technique allows to observe that the hindgut tract has an external tubular shape with smooth margins, being the hindgut diameter smaller than the midgut tract diameter (Fig. 1C, 3, 6). Cross-sections observed by optical microscopy reveal five longitudinal infolds projected toward the center of the hindgut lumen, it is lined by a simple epithelium composed by squamous cells covered by a cuticle (Fig. 2B, 9B, E; S1, 5, 6, 10).

The hindgut is extended backward along the middle line of the body. Above the hindgut is present a single and parallel vessel (posterior aorta) following the middle line of the pleon (Fig. 5, 9; S5, 7, 10). Beneath the hindgut we observed the abdominal nerve cord. In the zoeae, the abdominal nerve cord is thin and extended from the first to the fourth abdominal segments, the diameter increases inside each segment due to the presence of a ganglia (Fig. 1; S1). In the megalopa, the micro-CT reveal that the abdominal nerve cord is displaced anteriorly, compressed and composed by four ganglia. Due to this displacement and compression, the abdominal nerve cord of the megalopa is extended only reach the first or second abdominal segment (Fig. 2, 6, 8F; S6). By optical microscopy, in cross section, the abdominal nerve cord has an

ellipsoidal shape, but the neuropile has a butterfly wingspan shape that remember to the fusion of a pair of nerves (Fig. 8, 9). The micro-CT reveals a high development of the pleon musculature, observation that is confirmed by the optical microscopy.

4. Discussion

The combination of optical microscopy (OM) and micro computed tomography (micro-CT) techniques permit to insight in detail into the anatomy of a given Decapoda larval stage. The OM techniques has been largely used for studying the anatomy of decapods showing a detailed two-dimensional vision where different tissues can be identified and described, as the digestive system detailed as an example in the present study [39-41]. The non-invasiveness of the micro-CT has the advantage to allow the anatomical study retaining a three-dimensional image and the natural disposition of the inner structures [26-29]. Previous attempts to fulfill this objective in small marine pancrustaceans employed confocal laser scanning microscopy [13, 14, 42]. However, this technology requires transparent structures and tissues with staining affinity, as well a minimal thickness for the optical image sectioning to allow the reconstruction of the models. These requirements influence the resolution and light penetration capacity, limiting the study of the innermost structures [13-15, 42]. By contrast, the micro-CT technology is based on the X-ray absorptive properties of the tissues, increasing the resolution and penetration level, allowing the obtaining of higher quality three-dimensional models [6, 20, 38, 43]. Nevertheless, the micro-CT also has some limitations: it is difficult to identify adjacent structures with similar X-ray absorptive properties, moreover the technological limitations could difficult to resolve very small or thin structures. To solve this problem, this study shows the usefulness of the OM techniques as complementary tool to confirm the structure identity, providing

simultaneously information about the cellular organization of these structures. Therefore, OM techniques are complementary and irreplaceable. In fact, Betz et al. [7] suggested the combined use of micro-CT and OM for microanatomical investigations in arthropods.

The present study demonstrates that the study of small Decapoda larvae can be realized using micro-CT to obtain good resolution 3D images of the nervous system (ganglionic medullas of the eyestalk, syncerebrum, thoracic ganglions and abdominal nerve cord), digestive system (esophagus, stomach, midgut tract, midgut gland, midgut caeca and hindgut) and body musculature. In other small arthropods the micro-CT proven heavily his utility to study the neuroanatomy [7, 8, 23, 44-46], digestive organs [7, 23, 24, 45, 46] and body musculature [6, 7, 17, 23, 45]. Apparently, the structures with the highest resolution are large and robust [9], with a thick cuticle and/or large cells [24]. By contrast, the structures with less visibility are the circulatory system (pericardium, heart and vessels), respiratory system (gills) and diverse glands. These tissues are thin and delicate and therefore they have reduced X-ray absorptive capacity and contrast.

The present study found numerous similarities with previous descriptions of the inner anatomy of other brachyuran larvae, including the first zoeal of a *Maja* species [39], the zoeal stages of the portunid *Portunus trituberculatus* [40], the megalopae of the cancrid *Metacarcinus anthonyi* [47] and the megalopae of the portunid *Carcinus maenas* [48]. The external morphology of the *M. brachydactyla* larvae changes drastically after the metamorphosis to megalopa: the main spines of the cephalotorax (rostral, dorsal and lateral) disappear, the maxillipeds are transformed from large swimming appendages into short and compact appendages required for the food

grasping and processing, and the pereiopods and pleopods becomes fully functional as walking and swimming appendages [49]. However, despite the external transformation, the internal morphology suffer few changes that can be resumed in the development of the ossicles and gastric mill of the stomach, the relative shortening of the abdominal ventral nerve cord, the development of lamellate gills and the development of a fully functional musculature on pereiopods and pleopods. In the larvae, the organ shape and location coincides to the described in the adults [50, 51], differing mainly in their major simplicity. The distribution of the internal organs also follows the general pattern described in others decapods, including some advanced larval stages [3, 52, 53].

In relation to the digestive system, coinciding to previous studies, the larval esophagus is a short tube that connects the mouth with the stomach [52, 54-57], surrounded by circular muscles responsible of the peristaltic movements and food ingestion [52, 55, 58-60], but lacking the rosette glands observed in adults [54, 55, 60-62]. By micro-CT we observed a smooth and folded lumen, while the OM shows details as the vacuolated epithelium and the circular muscle fibers. The stomach of *M. brachydactyla* larvae has the typical subdivision into cardiac and pyloric regions separated by the cardio-pyloric valve [52, 59, 63-65]. As it has been observed in other brachyurans, the ossicles and gastric mill are formed in the megalopa stage [64-70]. The gastric mill, including some ossicles, are directly identified by micro-CT, when previous studies required the dissection and staining of this organ for the ossicle identification [64, 65, 71, 72].

The midgut tract of *M. brachydactyla* larvae is a tube anteriorly attached to the stomach, the pair of anterior caeca and the main ducts of the midgut gland; while posteriorly is attached to the midgut - hindgut junction and a single posterior caecum.

This organization is shared with other decapods [55, 56, 61, 62, 73, 74]. The micro-CT reveal the general morphology as a short cylindrical tube, while the OM shows a short columnar and microvillous epithelium sustained by a very thin connective, as occur in the larvae of achelatans [75], astacids [74, 76], other brachyurans [66] and carideans [77]. The midgut caeca of the adult brachyurans are very large and coiled blind-end tubules [55, 78], lined by a simple and microvillous epithelium [55, 62]. The *M. brachydactyla* larvae share the same caeca but they are very short buds that enlarge from the first zoeal to the megalopa stage, as in other brachyurans [40, 66]; but differing from other decapods as dendrobranchiatans and astacids, whose anterior caeca shrink and fuse into a single caecum [74, 76, 79-81].

The midgut gland of the decapods(commonly known as "hepatopancreas"), is a massive organ composed by "countless" blind-end tubules occupying a great volume of the cephalothorax cavity [52, 58, 82-85]. The larval MGG of *M. brachydactyla* is composed by few blind-end tubules as has been proposed for other brachyuran larvae in basis of OM observations [40, 47, 66]. The micro-CT reconstruction allows to appreciate in detail the shape of the organ, avoiding other techniques more invasive such as dissections or scanning electron microscopy: the ventral sub-lobules forms a basis where the pyloric stomach settles, while the dorsal sub-lobules surround the lateral sides of the pyloric stomach. This basic morphology coincides to the observed in the dissected midgut gland of the anomuran *Paralithodes camtschaticus* during their larval stages [86]. Using OM we appreciated a simple epithelium composed by short columnar cells with microvillous border, being identified different cell types (R-, F- and B-cells) observed in other brachyurans [40, 47, 66, 87], as well other decapods as anomurans [86, 88], achelatans [75, 89], and astacids [90] during their larval stages.

The larval hindgut of *M. brachydactyla* is presented in the micro-CT reconstructions as a thin tube extended from the midgut-hindgut junction to the anus, occupying a minute volume of the pleon cavity but representing more than the half of the post-gastric tract length as it has been observed in other brachyurans [50, 55, 62]. Similarly to other Decapoda taxa, the OM allowed the identification of a cuticle covering internally the hindgut [52, 58, 59], and an stellate lumen formed by longitudinal infolds [56, 62, 73, 78, 91-93]. The general description of the hindgut of the adult decapods generally includes a highly developed connective tissue with thick longitudinal and circular muscle bundles and rosette glands [55, 56, 61, 62, 73, 94, 95], but in the larval hindgut of *M. brachydactyla* these structures were not observed.

Despite the focus of the present study on the digestive system, the micro-CT combined with the OM also provides information about other organ systems. The heart is shown as a globular and dorsal structure with numerous internal trabeculae like formations; similar trabeculae have been identified in the heart of other decapods forming internal sub-chambers [52, 96-98]. The vessels are more visible by OM than by micro-CT. The larvae of *M. brachydactyla* hatch with a functional circulatory system to supply their organ systems of nutrients and energy, coinciding the location of their heart and main arteries to the described in other Decapoda species [96-101], including the megalopa of the brachyuran *M. anthonyi* [47]. The main nervous system structures are well reconstructed in the micro-CT models. The larvae of *M. brachydactyla* have an anterior syncerebrum, term suggested by Richter et al. [102] instead of brain. In decapods, the syncerebrum innervates the eyestalk (protocerebrum), first antennae (deutocerebrum) and second antennae (tritocerebum) [102-109]. In *M. brachydactyla* zoeae ganglionic masses are identified by micro-CT and OM, located at both sides of the esophagus , that could correspond to posterior extensions of the deuto- or

tritocerebrum [110]. In brachyurans the thoracic, and ventral nerve cord is modified into a long and wide plate-like ganglion mass [105, 107] that innervates maxillipeds [106] and pereiopods [107]. This structure is clearly visible in the micro-CT reconstructions of the *M. brachydactyla* megalopae, its morphology coincides to previous reports realized in other brachyuran larvae [40, 48, 110]. By micro-CT and OM, the abdominal nerve cord of *M. brachydactyla* during the zoeal stages is present as a large nerve cord, as occur with the first zoeal stage of the brachyuran *Pachygrapsus marmoratus* [110]. By contrast, according to the micro-CT reconstructions, the abdominal nerve cord of the megalopa is a very short chain displaced forwardly and composed by few ganglia. In other brachyuran larvae the morphology of the abdominal nerve cord is controversial. Nakamura [40] reported three abdominal neuropiles in the megalopa of *P. trituberculatus*, but contrary to our observations also mentioned the absence of ventral nerve cord in earlier stages. Trask [47] mentioned an abdominal nerve cord extended up to the anus in the megalopa of *M.anthonyi*. Harzsch and Dawirs [48] described in the megalopa of *C. maenas* a structure with six ganglions displaced in relation to their correspondent abdominal segment, similarly to the present study.

All together, this information shows that *M. brachydactyla* larvae are anatomically prepared for a free life style as pelagic animals, since all the main organ systems (digestive, nervous, circulatory, muscular) are fully developed from hatching. Few ontogenic changes occurred on these organ systems during the larval development, and then major anatomical modifications must occur during the juvenile development. The micro-CT techniques resulted especially useful to insight into the morphological shape of the organs, as well their location in the context of other body structures. The OM was decisive to distinguish between some structures not clearly identifiable by micro-CT and to discern the histological organization of the body structures. Then, the

combination of micro-CT and OM techniques has been proven to be a better tool to study the microanatomy of Decapoda larvae that each technique separately.

5. Acknowledgements

Financial support provided by the Spanish Ministry of Economy and Competitiveness through the INIA project [grant number RTA2011-00004-00-00] to G.G. and a predoctoral fellowship to D.C. (FPI-INIA). The authors would like to thank to the technicians at IRTA Sant Carles de la Ràpita for their assistance, in special David Carmona, GlòriaMacià, Magda Monllaó, Francesc X. Ingla and Olga Bellot. We also thank Bruker–Skyscan staff for their effectiveness and fast support, and for their constant improvements to the software and in implementing new options we requested. In this respect, we are especially indebted to Alexander Sasov, Stephan Boons, Xuan Liu, Phil Salmon, Jeroen Hostens, and Vladimir Kharitonov.

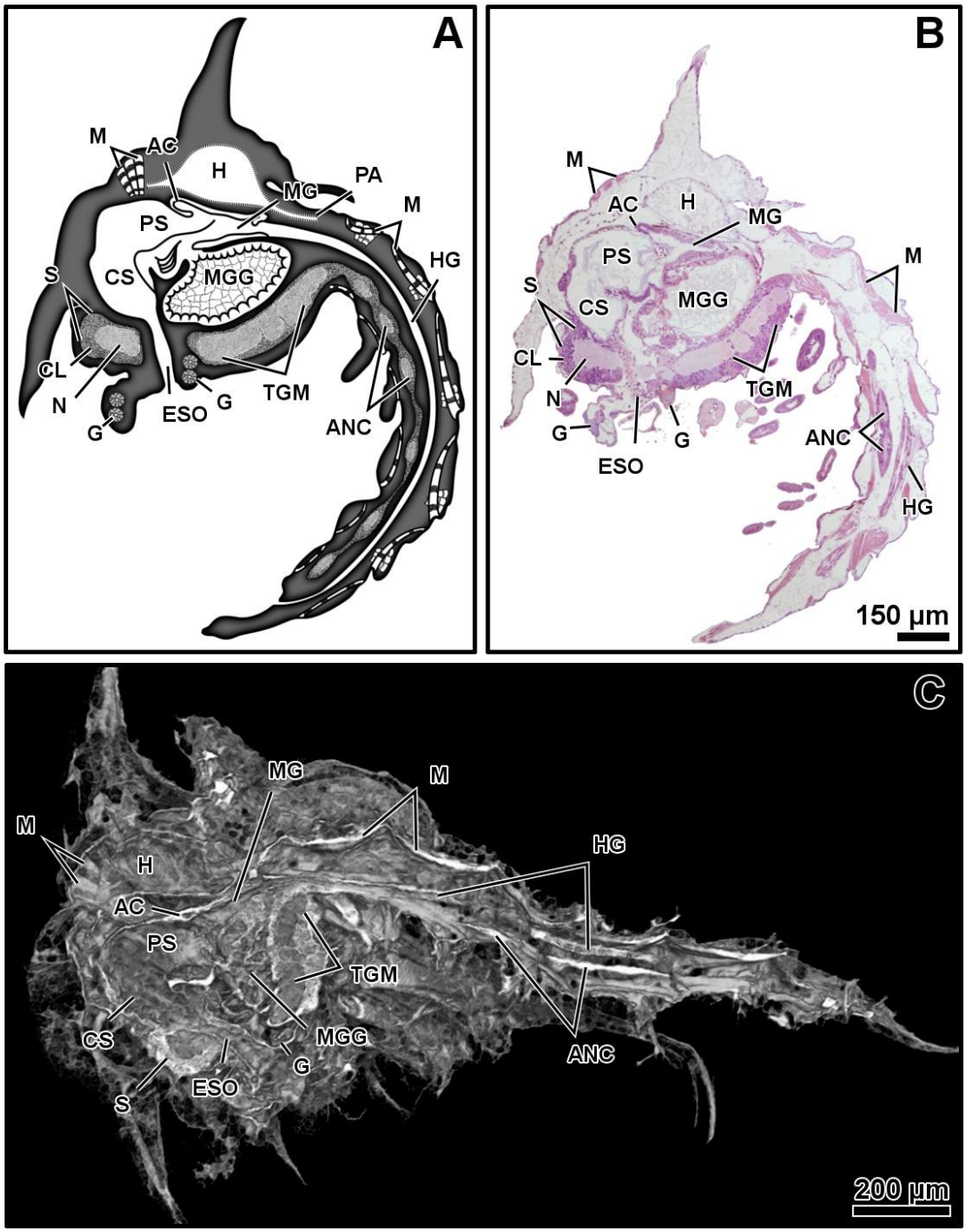

Figure 1. *Maja brachydactyla*. Zoea I, sagittal plane. General diagram (A). Optical microscopy, Hematoxylin - Eosin (B). Micro-CT reconstruction (C). Abbreviations: AC, anterior caeca; CL, cortical layer of the ganglion; CS, cardiac stomach; ESO, esophagus; G, glands; H, heart; HG, hindgut tract; M, muscles; MG, midgut tract; MGG, midgut gland; N, neuropile of the ganglion; PA, posterior aorta; PS, pyloric stomach; TGM, thoracic ganglionic mass; S, syncerebrum.

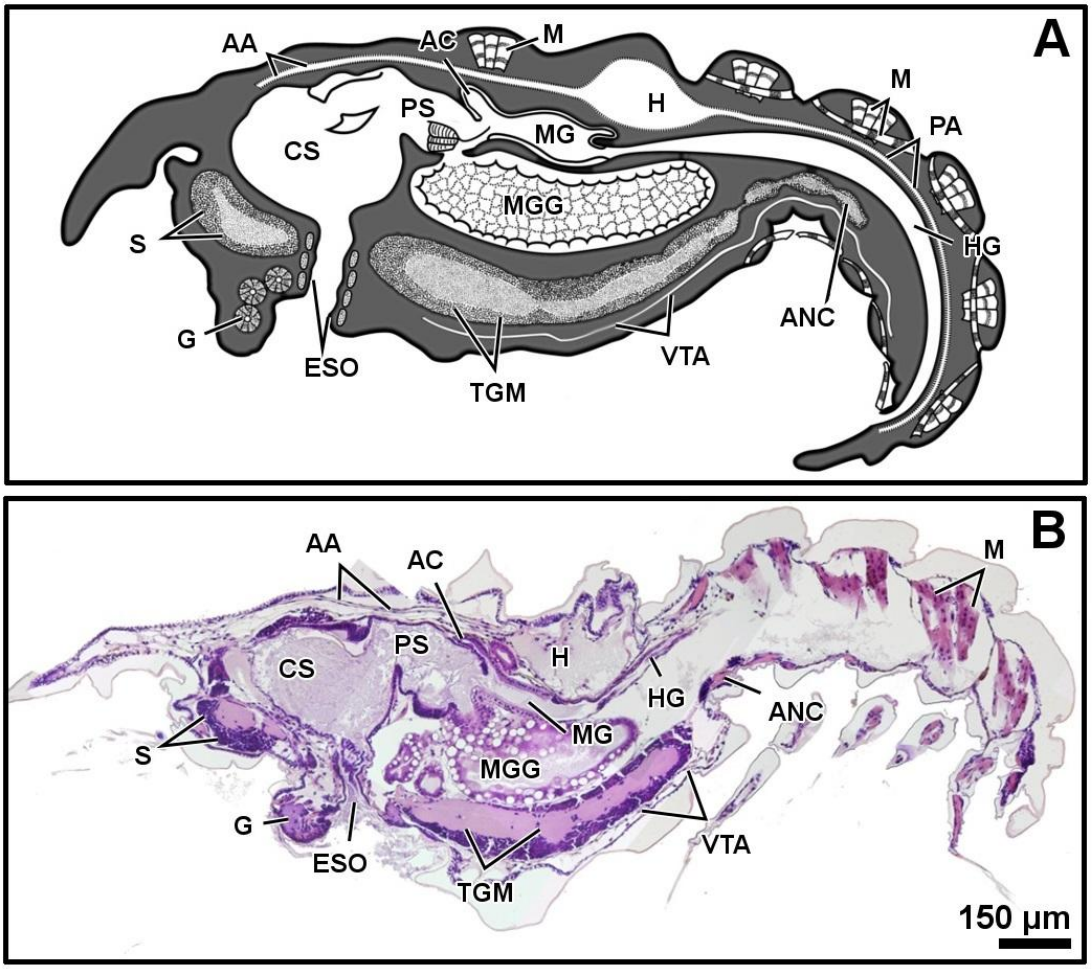

Figure 2. *Maja brachydactyla*. Megalopa, sagittal plane. General diagram (A). Optical microscopy, Hematoxylin - Eosin (B). Abbreviations: AA, anterior aorta; AC, anterior caeca; ANC, abdominal nerve cord; CS, cardiac stomach; ESO, esophagus; G, glands; H, heart; HG, hindgut tract; M, muscles; MG, midgut tract; MGG, midgut gland; PA, posterior aorta; PS, pyloric stomach; TGM, thoracic ganglionic mass; S, syncerebrum; VTA, ventral thoracic artery.

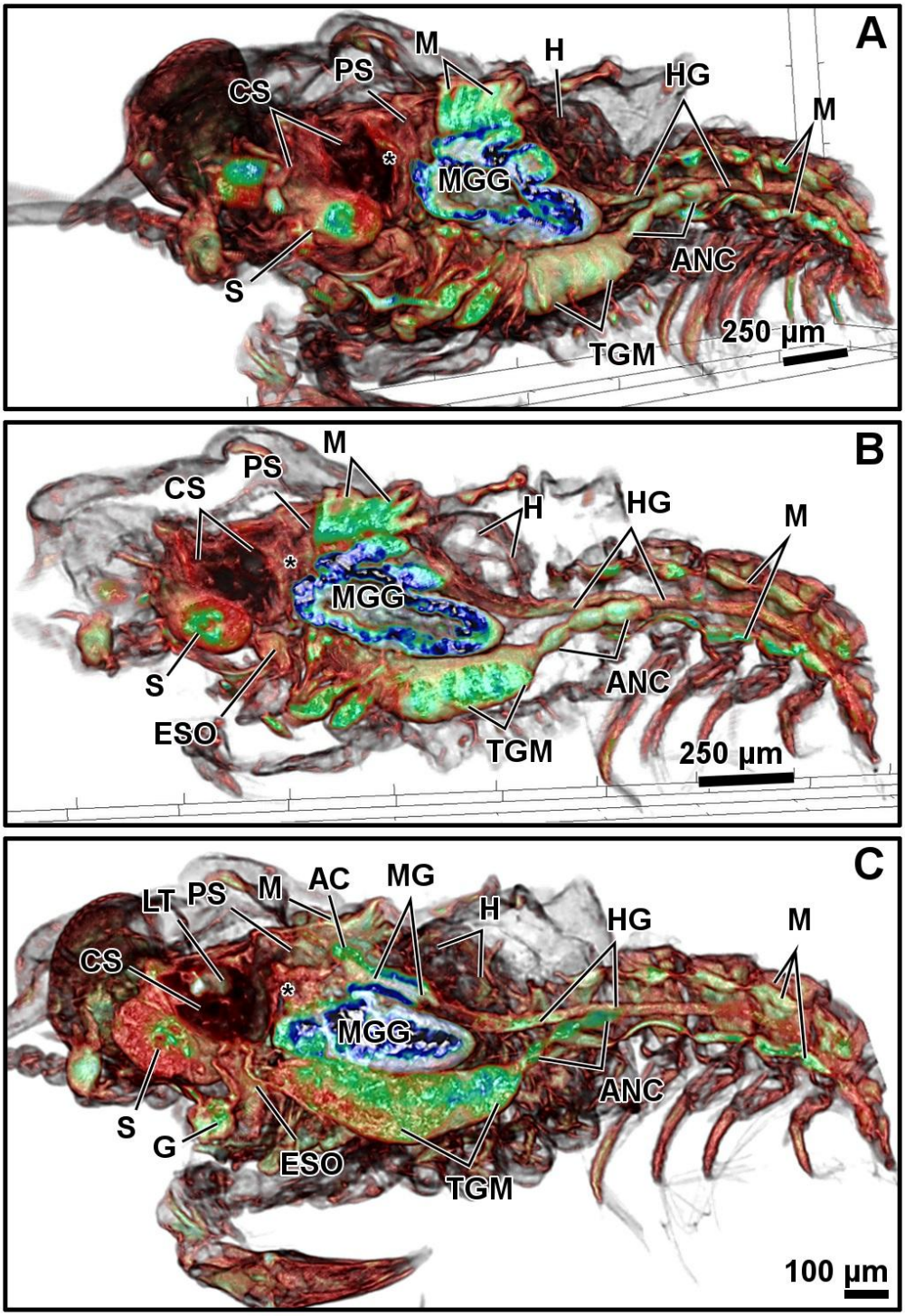

Figure 3. *Maja brachydactyla*. Megalopa, different sagittal planes. Micro-CT reconstruction (A-C). Abbreviations: (*), cardio-pyloric valve; AC, anterior caeca; ANC, abdominal nerve cord; CS, cardiac stomach; ESO, esophagus; G, glands; H, heart; HG, hindgut tract; LT, lateral tooth of the gastric mill; M, muscles; MG, midgut tract; MGG, midgut gland; PS, pyloric stomach; TGM, thoracic ganglionic mass; S, syncerebrum.

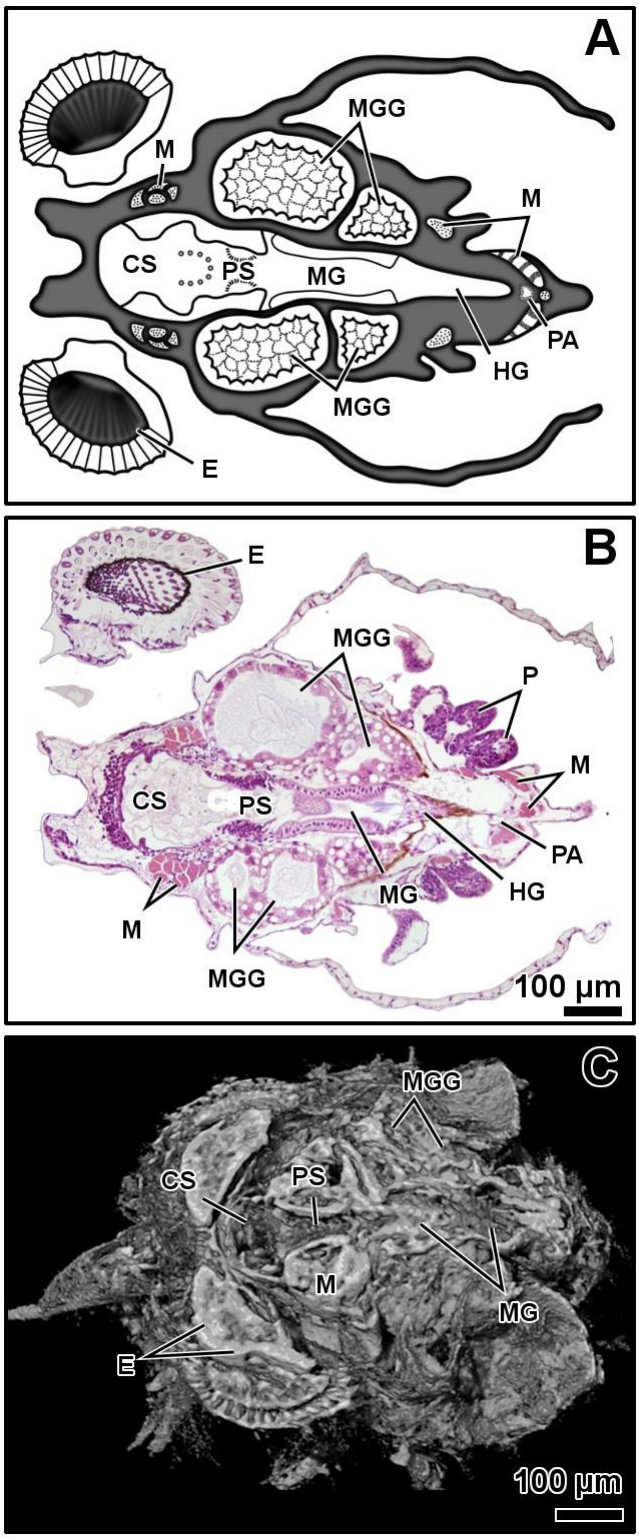

Figure 4. *Maja brachydactyla*. Zoea I, dorso-ventral plane of the digestive system. General diagram (A). Optical microscopy, Hematoxylin - Eosin (B). Micro-CT reconstruction (C). Abbreviations: CS, cardiac stomach; E, eye; HG, hindgut tract; M, muscles; MG, midgut tract; MGG, midgut gland; P, pereiopods, PA, posterior aorta; PS, pyloric stomach.

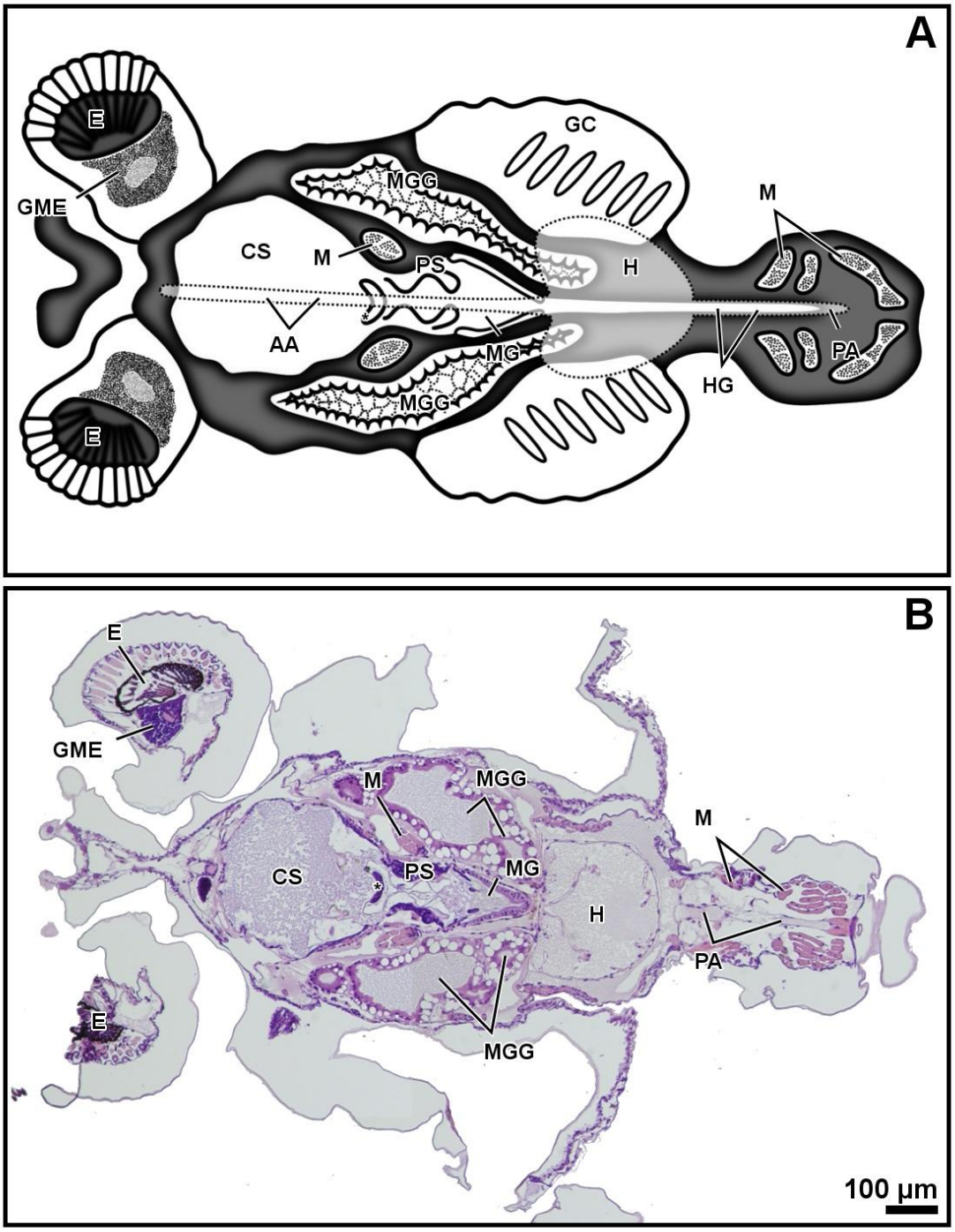

Figure 5. *Maja brachydactyla*. Megalopa, dorso-ventral plane of the digestive system. General diagram (A). Optical microscopy, Hematoxylin - Eosin (B). Abbreviations: (*), cardio-pyloric valve; AA, anterior aorta; CS, cardiac stomach; GME, ganglionic mass of the eye peduncle; E, eye; GC, gill chamber; H, heart; HG, hindgut tract; M, muscles; MG, midgut tract; MGG, midgut gland; PA, posterior aorta; PS, pyloric stomach.

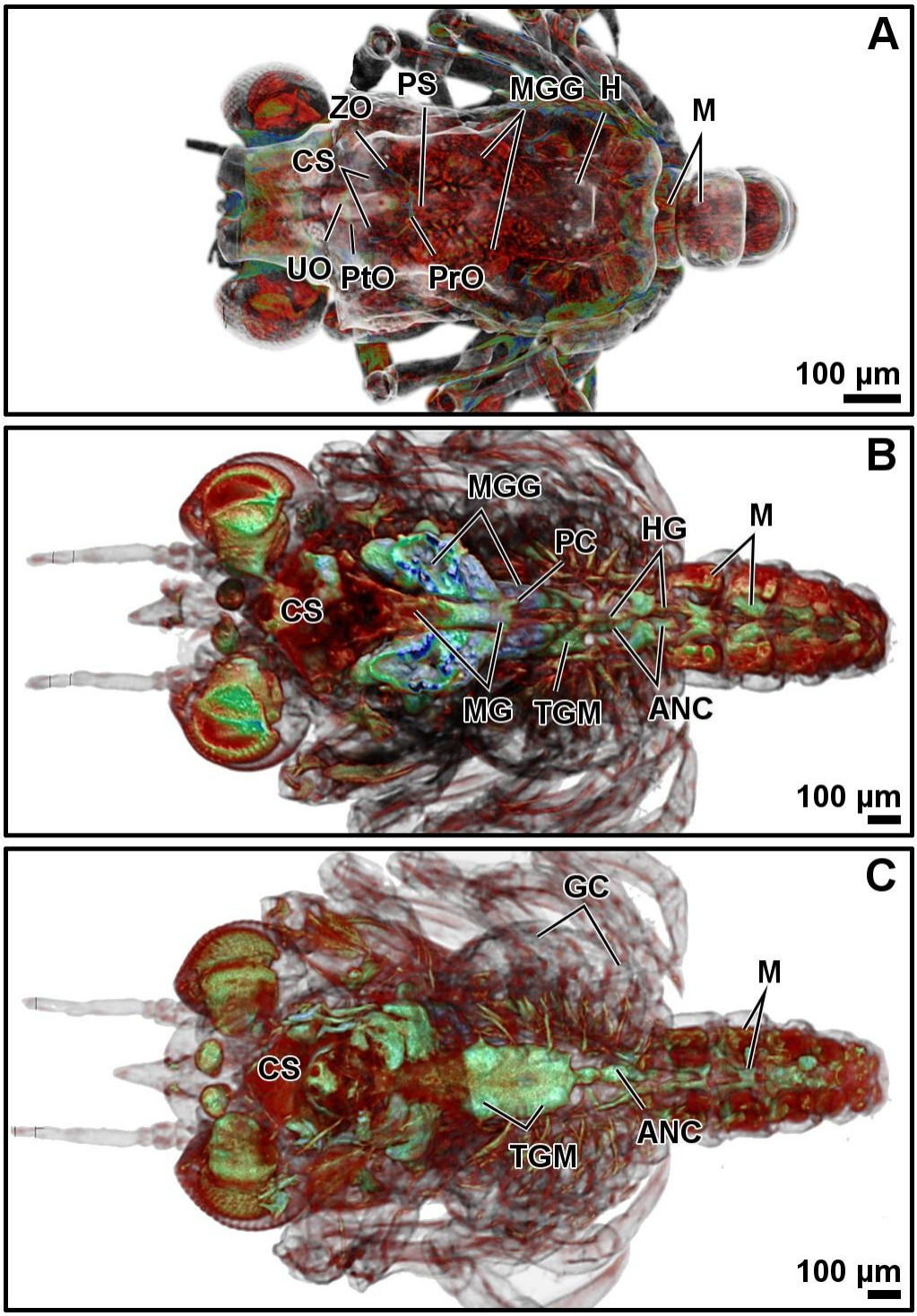

Figure 6. *Maja brachydactyla*. Megalopa, dorsal and ventral view. Micro-CT reconstruction. Dorsal view (A). Dorso-ventral plane of the digestive system (B). Ventral view (C). Abbreviations: ANC, abdominal nerve cord; CS, cardiac stomach; GC, gill chamber; H, heart; HG, hindgut tract; M, muscles; MG, midgut tract; MGG, midgut gland; Pro, propyloric ossicle; Pto, pterocardiac ossicle; PC, posterior caecum; PS, pyloric stomach; TGM, thoracic gangionic mass; UO, urocardiac ossicle; ZO, zygocardiac ossicle.

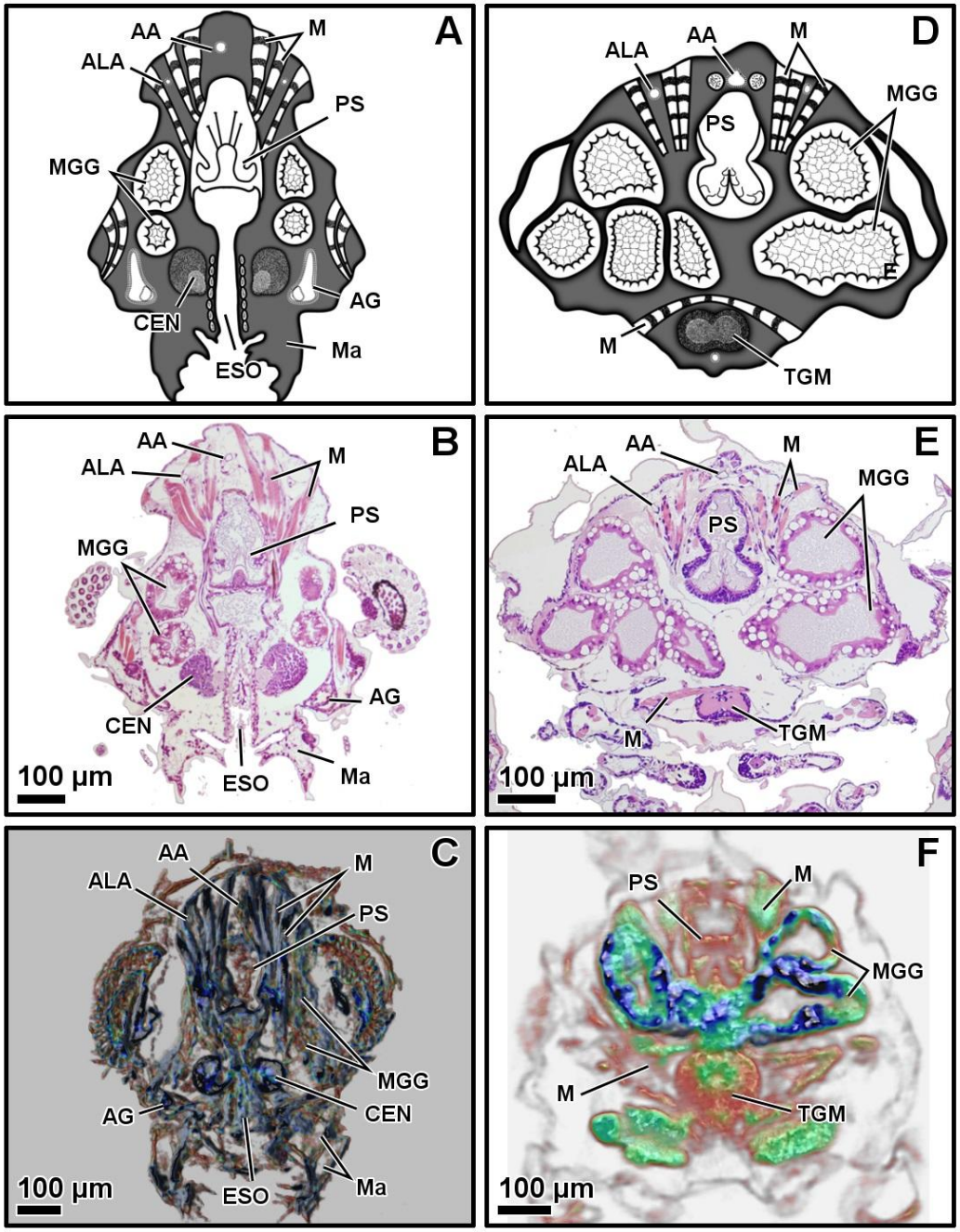

Figure 7. *Maja brachydactyla*. Transversal section at the pyloric stomach plane. Zoea I (A-C): general diagram (A); optical microscopy, Hematoxylin - Eosin (B); micro-CT reconstruction (C). Megalopa (D-F): general diagram (D); optical microscopy, Hematoxylin - Eosin (E); micro-CT reconstruction (F). Abbreviations: AA, anterior aorta; AG, antennal gland; ALA, anterolateral artery; CEN, circumesophageal nervous ring; ESO, esophagus; M, muscle; Ma, mandible; MGG, midgut gland; PS, pyloric stomach; TGM, thoracic ganglionic mass.

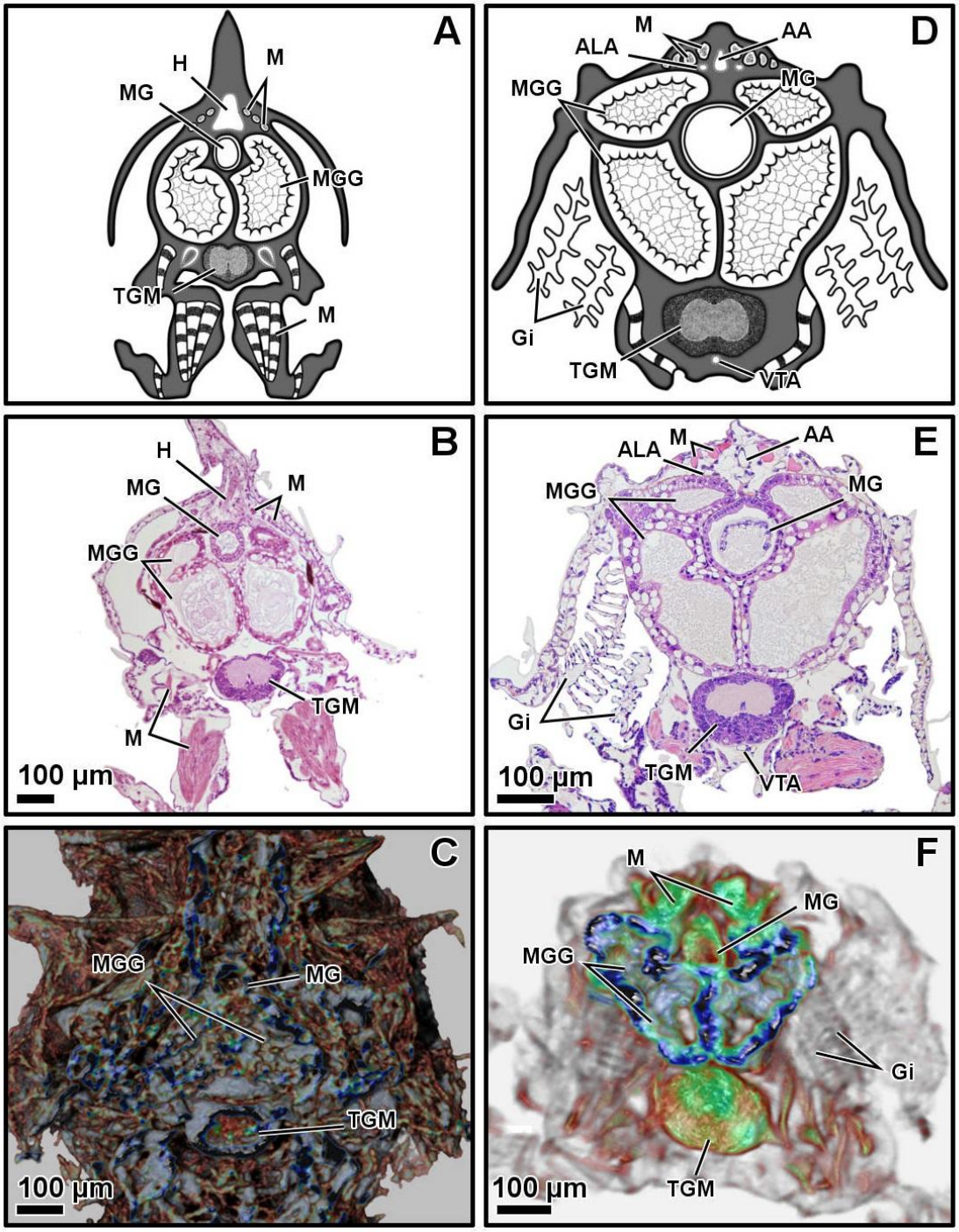

Figure 8. *Maja brachydactyla*. Transversal section at the midgut tract plane. Zoea I (A-C): general diagram (A); optical microscopy, Hematoxylin - Eosin (B); micro-CT reconstruction (C). Megalopa (D-F): general diagram (D); optical microscopy, Hematoxylin - Eosin (E); micro-CT reconstruction (F). Abbreviations: AA, anterior aorta; ALA, anterolateral artery; CEC, circumesophageal connective; Gi, gills; H, heart; M, muscle; MG, midgut tract; MGG, midgut gland; TGM, thoracic ganglionic mass; VTA, ventral thoracic arteria.

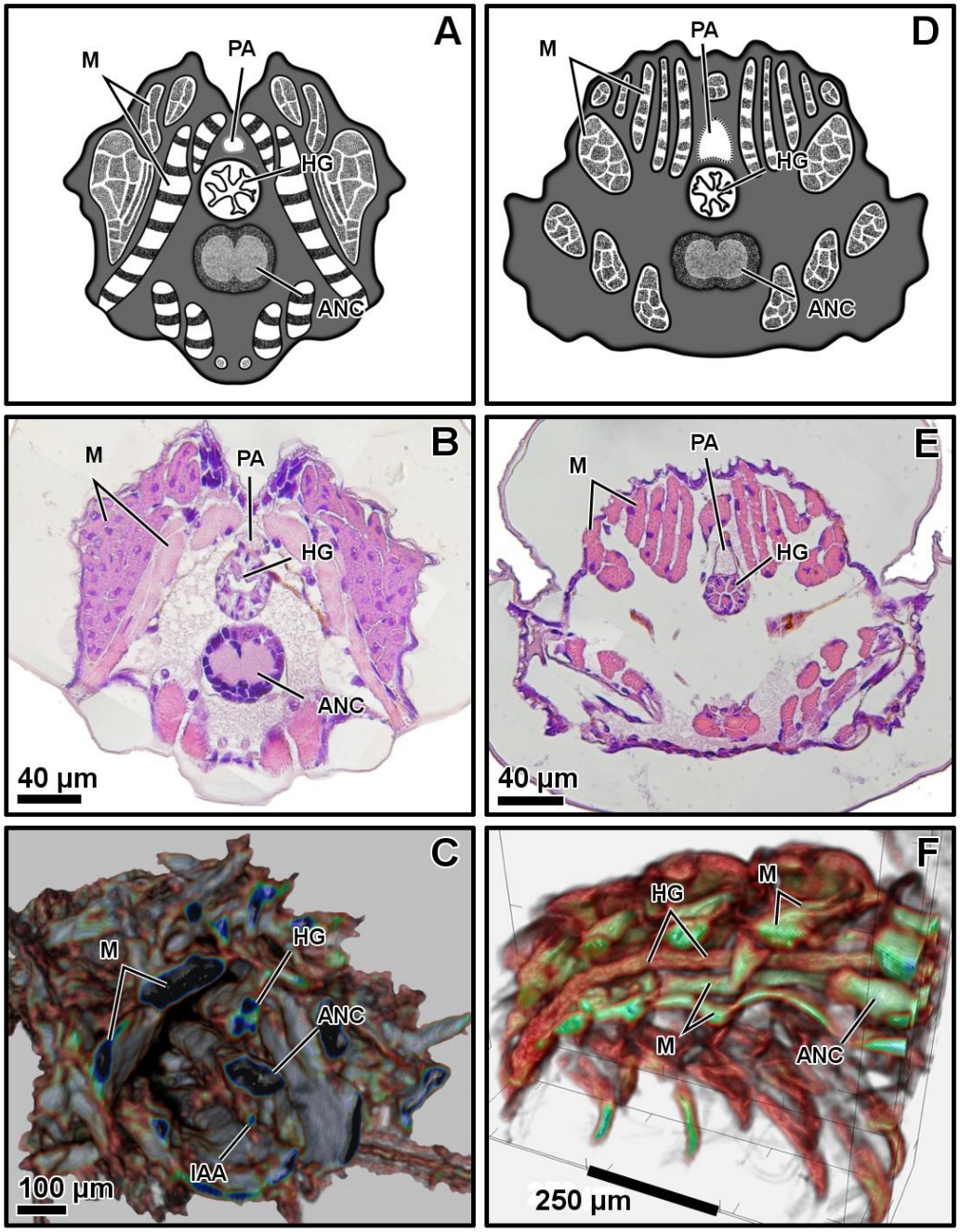

Figure 9. *Maja brachydactyla*. Transversal section at the hindgut tract plane. Zoea I (A-C): general diagram (A); optical microscopy, Hematoxylin - Eosin (B); micro-CT reconstruction (C). Megalopa (D-F): general diagram (D); optical microscopy, Hematoxylin - Eosin (E); micro-CT reconstruction (F). Abbreviations: ANC, abdominal nervous cord; HG, hindgut tract; IAA, inferior abdominal artery; PA, posterior aorta; VNC, ventral nerve cord.

Supplementary Material 1 (S1). *Maja brachydactyla*. Zoea I. Sagittal section. Hematoxylin - Eosin.

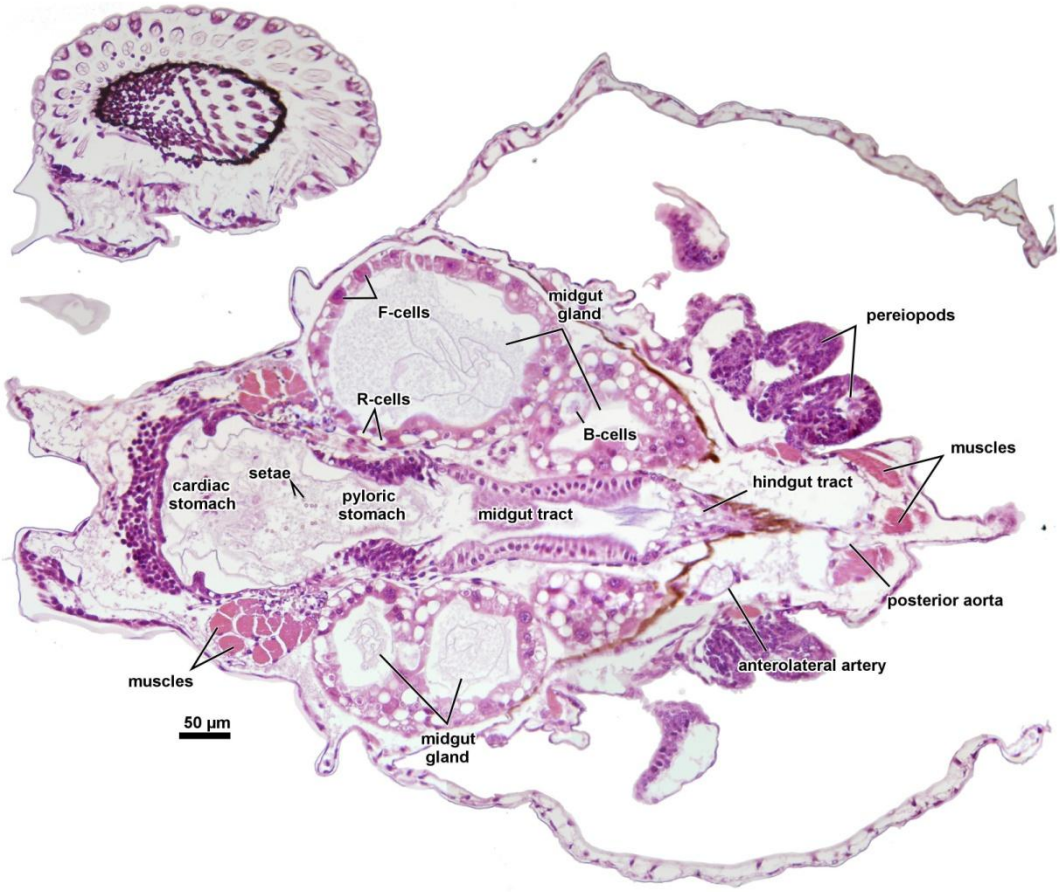

Supplementary Material 2 (S2). *Maja brachydactyla*. Zoea I. Dorso-ventral section at digestive system plane. Hematoxylin - Eosin.

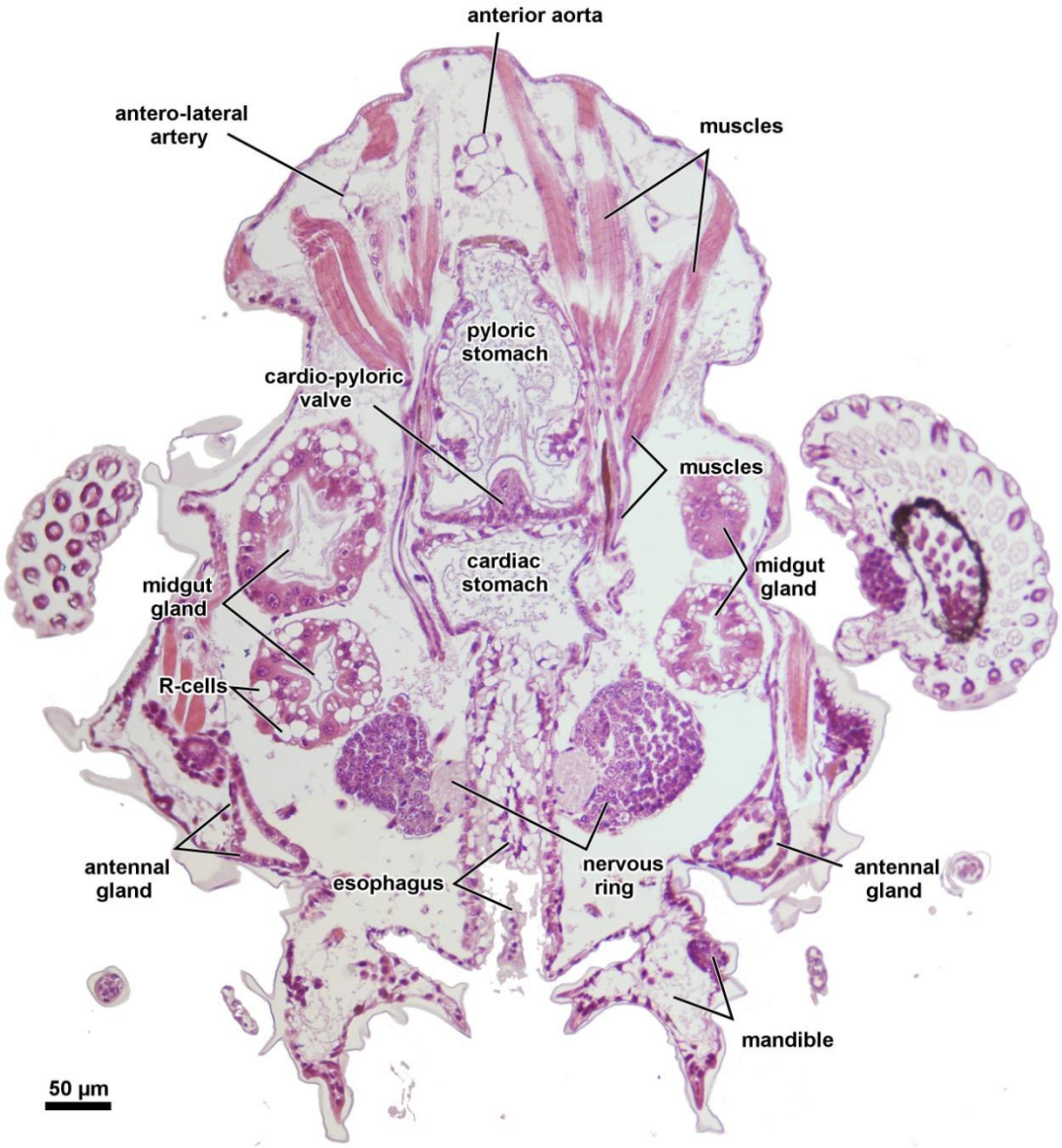

Supplementary Material 3 (S3). *Maja brachydactyla*. Zoea I. Transversal section at cardio-pyloric valve plane. Hematoxylin - Eosin.

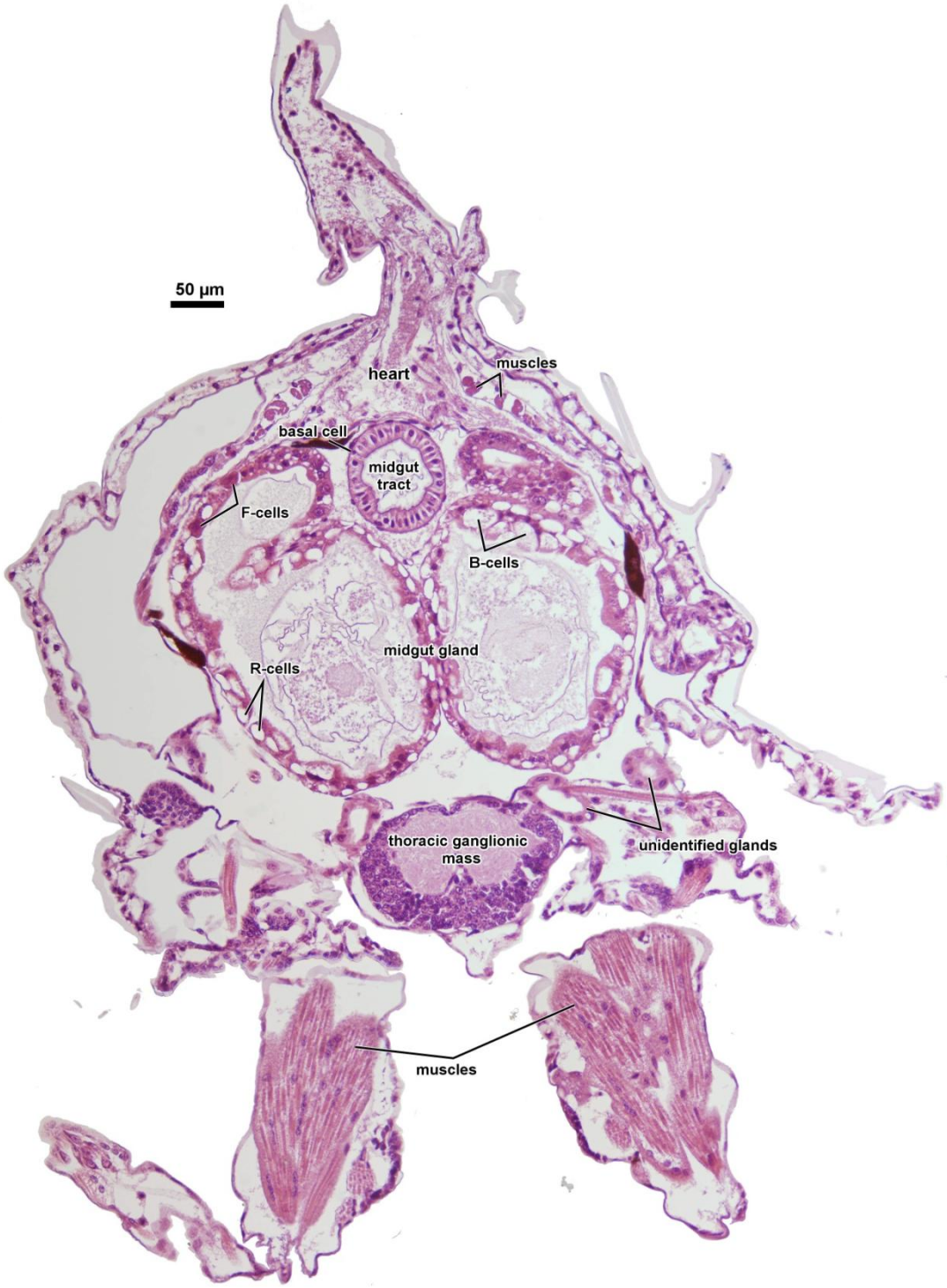

Supplementary Material 4 (S4). *Maja brachydactyla*. Zoea I. Transversal section at midgut tract plane. Hematoxylin - Eosin.

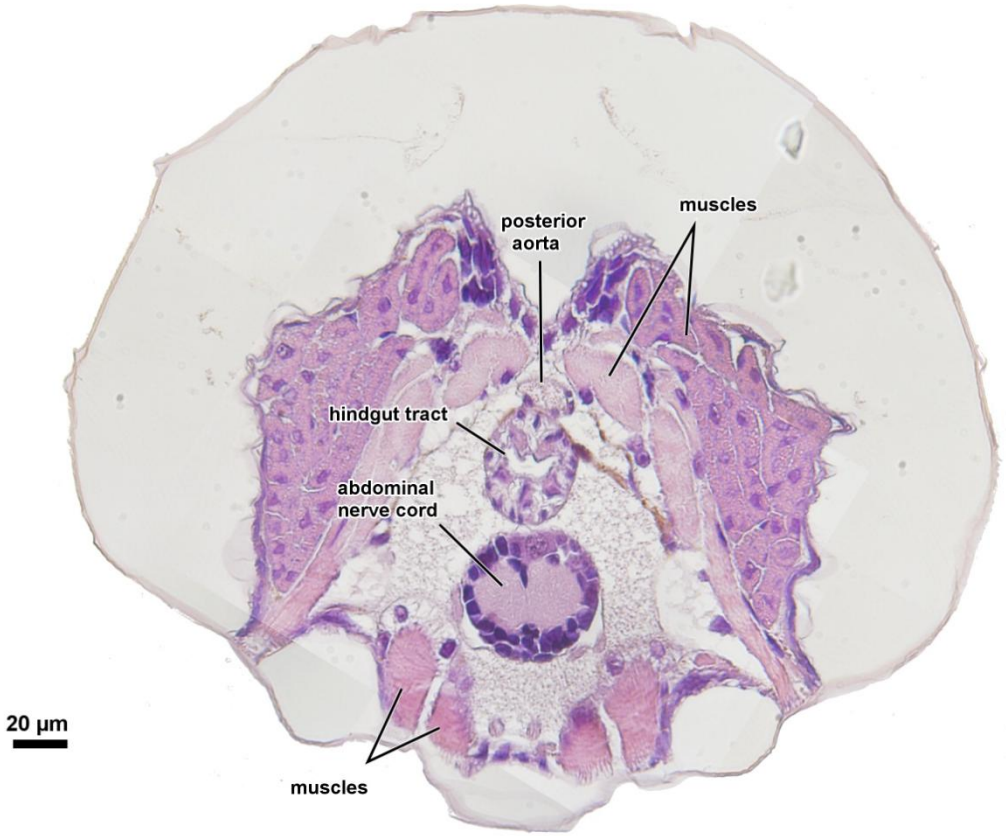

Supplementary Material 5 (S5). *Maja brachydactyla*. Zoea I. Transversal section at hindgut tract plane. Hematoxylin - Eosin.

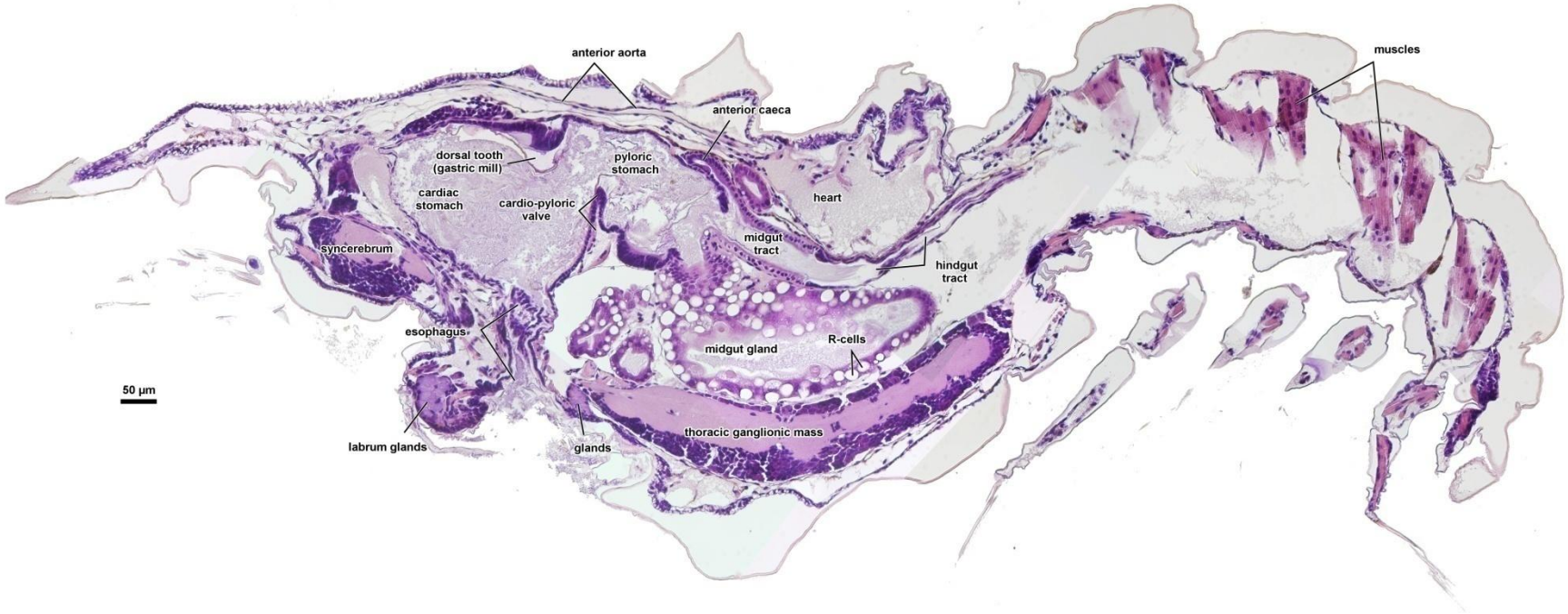

Supplementary Material 6 (S6). *Maja brachydactyla*. Megalopa. Sagittal section. Hematoxylin - Eosin.

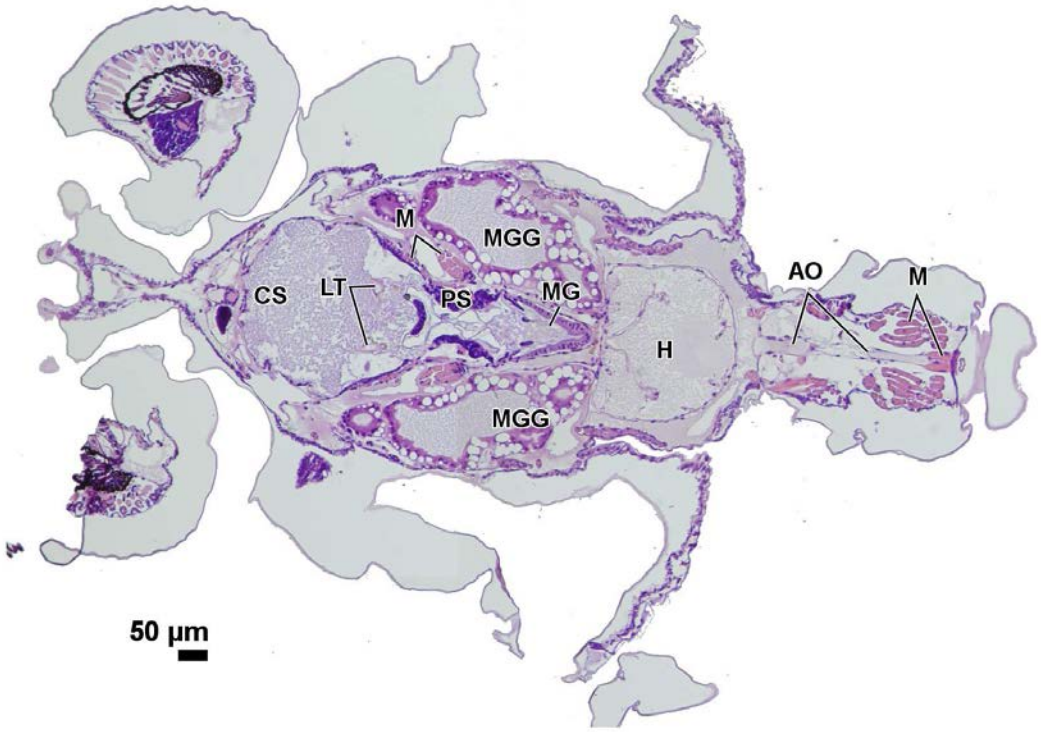

Supplementary Material 7 (S7). *Maja brachydactyla*. Megalopa. Dorso-ventral section at digestive system plane. Hematoxylin - Eosin. Abbreviations: AO, abdominal aorta; CS, cardiac stomach; LT, lateral teeth of the gastric mill; M, muscles; MG, midgut tract; PO, perigastric organ; PS, pyloric stomach.

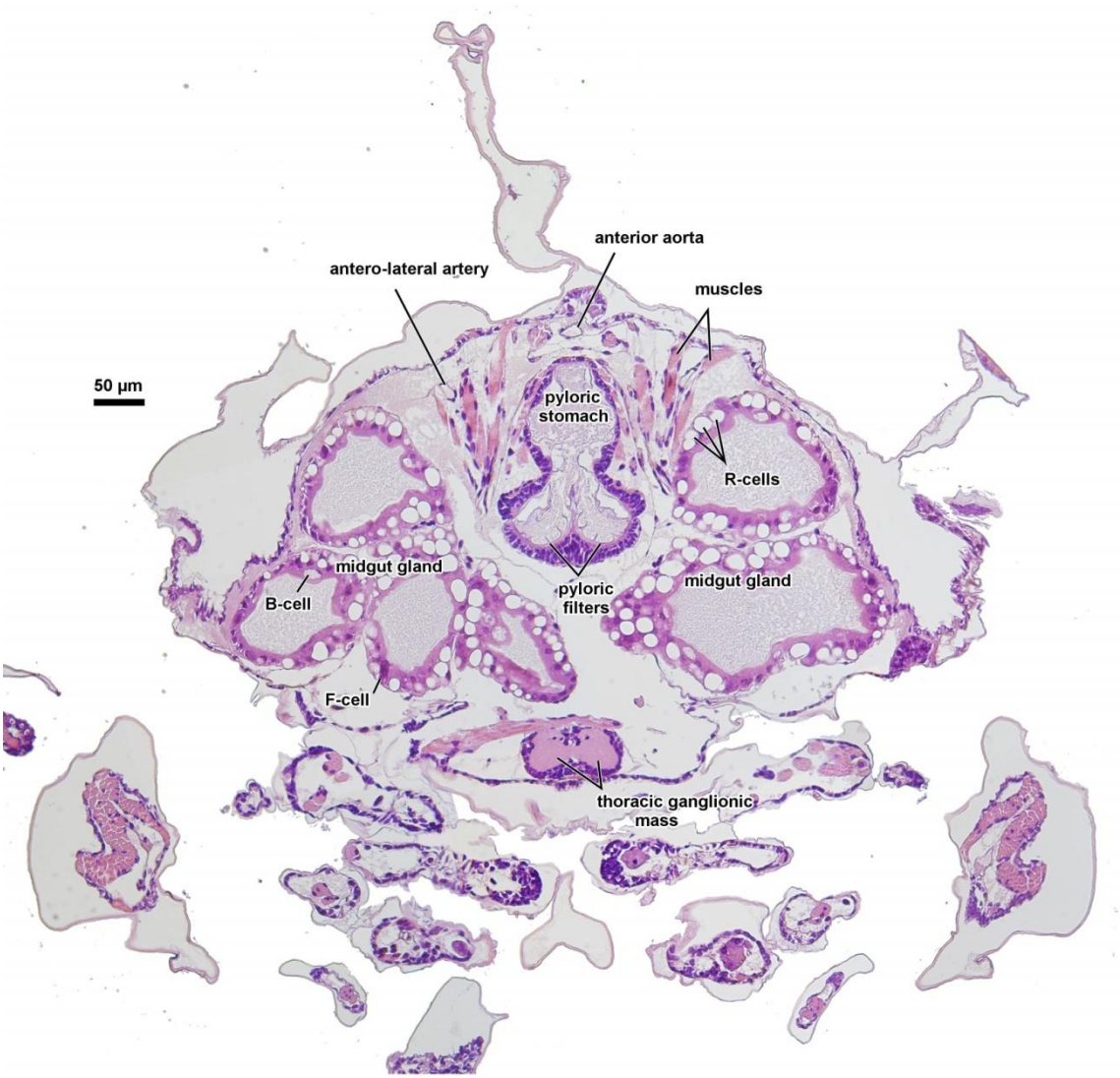

Supplementary Material 8 (S8). *Maja brachydactyla*. Megalopa. Transversal section at pyloric filters plane. Hematoxylin - Eosin.

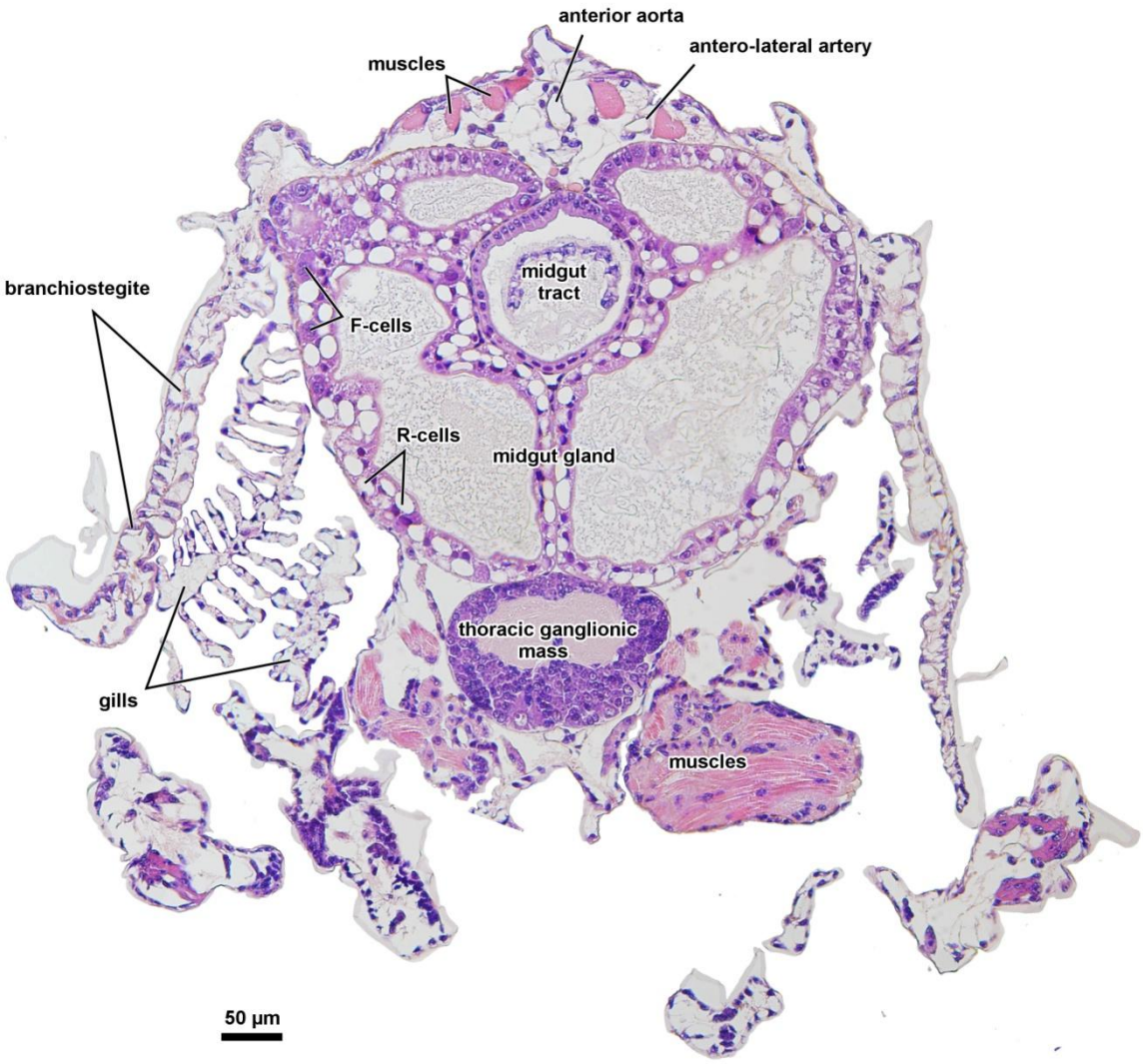

Supplementary Material 9 (S9). *Maja brachydactyla*. Megalopa. Transversal section at midgut tract plane. Hematoxylin - Eosin.

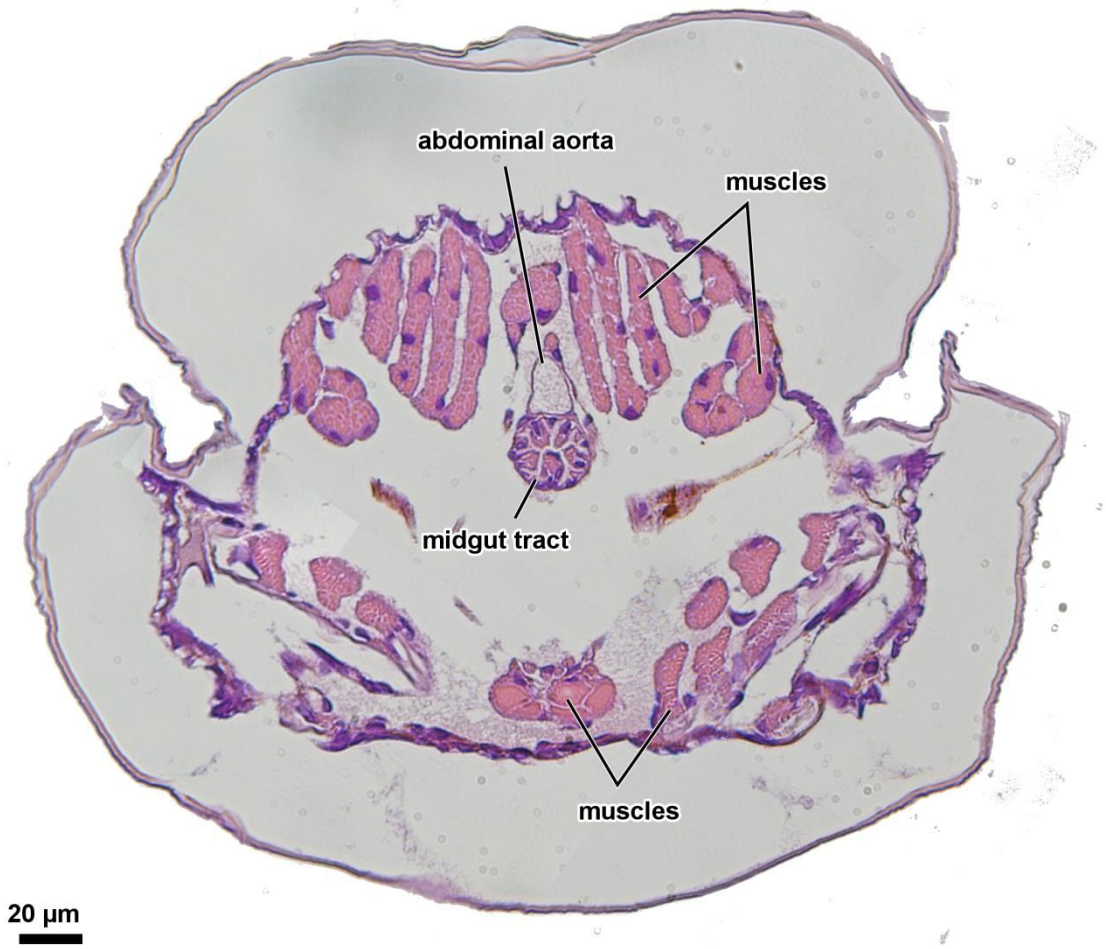

Supplementary Material 10 (S10). *Maja brachydactyla*. Megalopa. Transversal section at hindgut tract plane. Hematoxylin - Eosin.

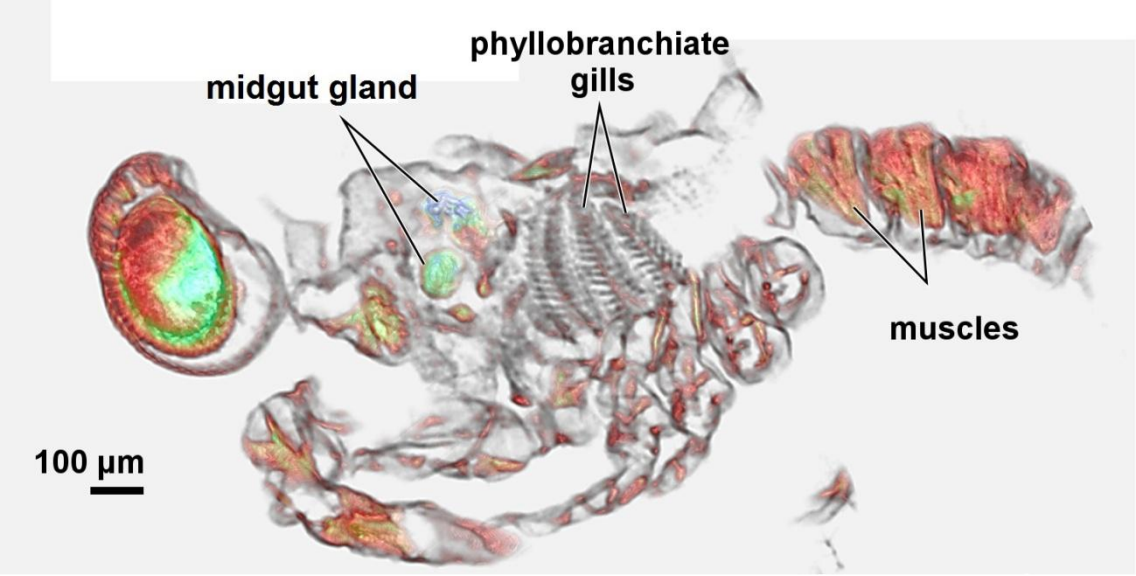

Supplementary Material 11 (S11). *Maja brachydactyla*. Megalopa. Lateral view. Micro-CT reconstruction showing the gills.

6. Bibliography

1. Bracken HD, Toon A, Felder DL, Martin JW, Finley M, et al. (2009) The Decapod Tree of Life: Compiling the data and moving toward a consensus of Decapod Evolution. Arthropod Systematics & Phylogeny 67: 99-116.

2. De Grave S, Pentcheff ND, Ahyong ST, Chan T-Y, Crandall KA, et al. (2009) A Classification of Living and Fossil Genera of Decapod Crustaceans. Raffles Bulletin of Zoology Supplement No. 21: 1-109.

3. Anger K (2001) The Biology of Decapod Crustacean Larvae. Rotterdam: A.A. Balkema Publishers. 419 p.

4. Martin JW, Olesen J, Høeg JT (2014) Atlas of Crustacean Larvae. Baltimore: Johns Hopkins University Press.

5. Clark PF, Cuesta JA (2015) Larval systematics of Brachyura. In: Castro P, Davie P, Guinot D, Schram F, Klein CV, editors. Treatise on Zoology - Anatomy Taxonomy Biology The Crustacea Volume 9 Part C 2 vols: Brill. pp. 981-1048.

6. Socha JJ, De Carlo F. Use of synchrotron tomography to image naturalistic anatomy in insects; 2008. pp. 70780A-70780A-70787.

7. Betz O, Wegst U, Weide D, Heethoff M, Helfen L, et al. (2007) Imaging applications of synchrotron X-ray phase-contrast microtomography in biological morphology and biomaterials science. I. General aspects of the technique and its advantages in the analysis of millimetre-sized arthropod structure. Journal of Microscopy 227: 51-71.

8. Sombke A, Lipke E, Michalik P, Uhl G, Harzsch S (2015) Potential and limitations of X-Ray micro-computed tomography in arthropod neuroanatomy: A methodological and comparative survey. Journal of Comparative Neurology 523: 1281-1295.

9. Dinley J, Hawkins L, Paterson G, Ball AD, Sinclair I, et al. (2010) Micro-computed X-ray tomography: a new non-destructive method of assessing sectional, fly-through and 3D imaging of a soft-bodied marine worm. Journal of Microscopy 238: 123-133.

10. Wanninger AWG (2007) The application of confocal microscopy and 3D imaging software in Functional, Evolutionary, and Developmental Zoology: reconstructing myo- and neurogenesis in space and time. In: Méndez-Vilas A, Diaz J, editors. Modern research and educational topics in microscopy Vol 1: Applications in Biology and Medicine. Badajoz, Spain: FORMATEX. pp. 353-361.

11. Shotton DM (1989) Confocal scanning optical microscopy and its applications for biological specimens. Journal of Cell Science 94: 175-206.

12. Klaus AV, Schawaroch V (2006) Novel methodology utilizing confocal laser scanning microscopy for systematic analysis in arthropods (Insecta). Integrative and Comparative Biology 46: 207-214.

13. Zupo V, Buttino I (2001) Larval development of decapod crustaceans investigated by confocal microscopy: an application to *Hippolyteinermis* (Natantia). Marine Biology 138: 965-973.

14. Buttino I, Ianora A, Carotenuto Y, Zupo V, Miralto A (2003) Use of the confocal laser scanning microscope in studies on the developmental biology of marine crustaceans. Microscopy Research and Technique 60: 458-464.

15. Kamanli SA, Kihara TC, Ball AD, Morritt D, Clark PF (2017) A 3D imaging and visualization workflow, using confocal microscopy and advanced image processing for brachyuran crab larvae. Journal of Microscopy: n/a-n/a.

16. Metscher BD (2009) MicroCT for developmental biology: A versatile tool for high-contrast 3D imaging at histological resolutions. Developmental Dynamics 238: 632-640.

17. Metscher BD (2009) MicroCT for comparative morphology: simple staining methods allow high-contrast 3D imaging of diverse non-mineralized animal tissues. BMC Physiology 9: 11.

18. Metscher B (2013) Biological applications of X-ray microtomography: imaging micro-anatomy, molecular expression and organismal diversity. Microscopy and Analysis 27: 13-16.

19. Nesteruk T, Wiśniewski Ł (2015) Microtomography in morphological studies of small invertebrates. Teka Komisji Ochrony i Kształtowania Środowiska Przyrodniczego OL PAN 12: 62-70.

20. Alba-Tercedor J, Sáinz-Cantero CE (2012) Volume rendering reconstructions of the anatomy of small aquatic beetles (Insecta : Coleoptera) scanned with the Skyscan 1172 high resolution micro-CT. In: Skyscan, editor. Micro-CT Users Meeting 2012. Kontich, Belgium. pp. 75-84.

21. Wecker S, Hörnschemeyer T, Hoehn M (2002) Investigation of insect morphology by MRI: assessment of spatial and temporal resolution. Magnetic Resonance Imaging 20: 105-111.

22. Tanisako A, Tsuruta S, Hori A, Okumura A, Miyata C, et al. Micro-CT of small insects by projection x-ray microscopy; 2006. pp. 63180B-63180B-63188.

23. Ge S-Q, Hua Y, Ren J, Slipinski A, Beutel R, et al. (2015) Transformation of head structures during the metamorphosis of *Chrysomela populi* (Coleoptera, Chrysomelidae). Arthropod Systematics & Phylogeny 73: 129-152.

24. Lowe T, Garwood RJ, Simonsen TJ, Bradley RS, Withers PJ (2013) Metamorphosis revealed: time-lapse three-dimensional imaging inside a living chrysalis. Journal of The Royal Society Interface 10.

25. Greco M, Bell D, Woolnough L, Laycock S, Corps N, et al. (2014) 3-D visualisation, printing, and volume determination of the tracheal respiratory system in the adult desert locust, *Schistocerca gregaria*. Entomologia Experimentalis et Applicata 152: 42-51.

26. Hobbs KH, Hooper SL (2009) High-resolution computed tomography of lobster (*Panulirus interruptus*) stomach. Journal of Morphology 270: 1029-1041.

27. Sonakowska L, Włodarczyk A, Poprawa I, Binkowski M, Śróbka J, et al. (2015) Structure and Ultrastructure of the endodermal region of the alimentary tract in the freshwater shrimp *Neocaridina heteropoda* (Crustacea, Malacostraca). PLOS ONE 10: e0126900.

28. Hayer S, Köhnk S, Boretius S, Brandis D (2016) Ever more complex: a new type of organization of reproductive organs in female *Dorippe sinica* Chen, 1980 (Decapoda: Brachyura: Dorippidae). Zoology 119: 455-463.

29. Köhnk S, Baudewig J, Brandis D, Boretius S (2017) What's in this crab? MRI providing high-resolution three-dimensional insights into recent finds and historical collections of Brachyura. Zoology 121: 1-9.

30. Nagler C, Hörnig MK, Haug JT, Noever C, Høeg JT, et al. (2017) The bigger, the better? Volume measurements of parasites and hosts: Parasitic barnacles (Cirripedia, Rhizocephala) and their decapod hosts. PLOS ONE 12: e0179958.

31. Andrés M, Rotllant G, Sastre M, Estevez A (2011) Replacement of live prey by formulated diets in larval rearing of spider crab *Maja brachydactyla*. Aquaculture 313: 50-56.

32. Rotllant G, Moyano FJ, Andrés M, Estévez A, Díaz M, et al. (2010) Effect of delayed first feeding on larval performance of the spider crab *Maja brachydactyla* assessed by digestive enzyme activities and biometric parameters. Marine Biology 157: 2215-2227.

33. Andrés M, Estévez A, Rotllant G (2007) Growth, survival and biochemical composition of spider crab *Maja brachydactyla* (Balss, 1922) (Decapoda: Majidae) larvae reared under different stocking densities, prey:larva ratios and diets. Aquaculture 273: 494-502.

34. Castejón D, Rotllant G, Giménez L, Torres G, Guerao G (2015) The effects of temperature and salinity on the survival, growth and duration of the larval development of the common spider crab *Maja brachydactyla* (Balss, 1922) (Brachyura: Majidae). Journal of Shellfish Research 34: 1073-1083.

35. Alba-Tercedor J (2016) Microtomographic study on the anatomy of adult male eyes of two mayfly species. Zoosymposia 11: 101–120.

36. Alba-Tercedor J, Alba-Alejandre I (2017) Comparing micro-CT results of insects with classical anatomical studies: The European honey bee (*Apis mellifera* Linnaeus, 1758) as a benchmark (Insecta: Hymenoptera, Apidae). In: Skyscan, editor. Micro-CT User Meeting 2017. Kontich, Belgium. pp. 147-167.

37. Amira (2016) 3D Visualization and Analysis Software. Hillsboro, Oregon, USA.

38. Alba-Tercedor J (2014) From the sample preparation to the volume rendering images of small animals: A step by step example of a procedure to carry out the micro-CT study of the leafhopper insect *Homalodisca vitripennis* (Hemiptera: Cicadellidae). In: Skyscan, editor. Bruker microCT Users Meeting 2014. Kontich, Belgium. pp. 260-288.

39. Schlegel C (1911) Anatomie sommaire de la première zoé de *Maja squinado* Latr. (Note préliminaire à des recherches sur l'Organogénese des Décapodes brachyoures). Archives de Zoologie Experimentale et Générale 5º Série T. VIII.: 29-40.

40. Nakamura K (1990) Organogenesis during metamorphosis in the swimming crab *Portunus trituberculatus*. Nippon Suisan Gakkaishi 56: 1561-1564.

41. Heeren T, Mitchell BD (1997) Morphology of the mouthparts, gastric mill and digestive tract of the giant crab, *Pseudocarcinus gigas* (Milne Edwards) (Decapoda: Oziidae). Marine and Freshwater Research 48: 7-18.

42. Michels J (2007) Confocal laser scanning microscopy: using cuticular autofluorescence for high resolution morphological imaging in small crustaceans. Journal of Microscopy 227: 1-7.

43. Handschuh S, Beisser CJ, Ruthensteiner B, Metscher BD (2017) Microscopic dual-energy CT (microDECT): a flexible tool for multichannel ex vivo 3D imaging of biological specimens. Journal of Microscopy: n/a-n/a.

44. Ribi W, Senden TJ, Sakellariou A, Limaye A, Zhang S (2008) Imaging honey bee brain anatomy with micro-X-ray-computed tomography. Journal of Neuroscience Methods 171: 93-97.

45. Antunes-Carvalho C, Yavorskaya M, Gnaspini P, Ribera I, Hammel JU, et al. (2017) Cephalic anatomy and three-dimensional reconstruction of the head of *Catops ventricosus* (Weise, 1877) (Coleoptera: Leiodidae: Cholevinae). Organisms Diversity & Evolution 17: 199-212.

46. Franz-Guess S, Klußmann-Fricke B-J, Wirkner CS, Prendini L, Starck JM (2016) Morphology of the tracheal system of camel spiders (Chelicerata: Solifugae) based on micro-CT and 3D-

reconstruction in exemplar species from three families. Arthropod Structure & Development 45: 440-451.

47. Trask T (1974) Laboratory-reared larvae of *Cancer anthonyi* (Decapoda: Brachyura) with a brief description of the internal anatomy of the megalopa. Marine Biology 27: 63-74.

48. Harzsch S, Dawirs RR (1993) On the morphology of the central nervous system in larval stages of *Carcinus maenas* L. (Decapoda, Brachyura). Helgoländer Meeresuntersuchungen 47: 61-79.

49. Guerao G, Pastor E, Martin J, Andrés M, Estévez A, et al. (2008) The larval development of *Maja squinado* and *M. brachydactyla* (Decapoda, Brachyura, Majidae) described from plankton collected and laboratory-reared material. Journal of Natural History 42: 2257-2276.

50. Milne-Edwards H (1834) Histoire naturelle des crustacés: atlas: Libraire Encyclopédique de Roret.

51. Milne-Edwards H (1834) Histoire naturelle des crustacés, comprenant l'anatomie, la physiologie et la classification de ces animaux: Libraire Encyclopédique de Roret.

52. Felgenhauer BE (1992) Chapter 3. Internal Anatomy of the Decapoda: An Overview. In: Harrison FW, Humes AG, editors. Microscopic Anatomy of Invertebrates Volume 10: Decapod Crustacea: Wiley-Liss, Inc. pp. 45-75.

53. Davie PJF, Guinot D, Ng PKL (2015) Anatomy and functional morphology of Brachyura. In: Castro P, Davie PJF, Guinot D, Schram F, Von Vaupel Klein C, editors. Treatise on Zoology - Anatomy Taxonomy Biology The Crustacea Volume 9 Part C: Brill. pp. 11-163.

54. Trinadha Babu B, Shyamasundari K, Hanumantha Rao K (1989) Observations on the morphology and histology of the foregut of *Portunus sanguinolentus* (Crustacea: Brachyura). Folia Morphologica 37: 364-372.

55. Erri Babu D, Shyamasundari K, Rao KH (1982) Studies on the digestive system of the crab *Menippe rumphii* (Fabricius) (Crustacea:Brachyura). Journal of Experimental Marine Biology and Ecology 58: 175-191.

56. Yonge CM (1924) Studies on the comparative physiology of digestion II. - The mechanism of feeding, digestion, and assimilation in *Nephrops norvegicus*. British Journal of Experimental Biology 1: 343-389.

57. Patwardhan SS (1935) On the structure and mechanism of the gastric mill in Decapoda. Proceedings of the Indian Academy of Sciences - Section B 1: 693-704.

58. Ceccaldi HJ (1989) Anatomy and physiology of digestive tract of Crustaceans Decapods reared in aquaculture. Advances in Tropical Aquaculture, Workshop at Tahiti, French Polynesia. Tahiti, French Polynesia: Actes de colloques Ifremer. pp. 243-259.

59. Icely JD, Nott JA (1992) Digestion and absorption: digestive system and associated organs. In: Harrison FW, Humes AG, editors. Microscopic anatomy of invertebrates: decapod Crustacea. New York: Wiley-Liss. pp. 147-201.

60. Erri Babu D, Shyamasundari K, Hanumantha Rao K (1979) The structure and histochemistry of the oesophageal glands in the crab *Menippe rumphii* (Frabricius) (Crustacea : Brachyura). Proceedings: Animal Sciences 88: 277-285.

61. Reddy AR (1937) The physiology of digestion and absorption in the crab *Paratelphusa* (*Oziotelphusa*) *hydrodromus* (Herbst). Proceedings of the Indian Academy of Sciences - Section B 6: 170-193.

62. Barker PL, Gibson R (1978) Observations on the structure of the mouthparts, histology of the alimentary tract, and digestive physiology of the mud crab *Scylla serrata* (Forskål) (Decapoda: Portunidae). Journal of Experimental Marine Biology and Ecology 32: 177-196.

63. Schaefer N (1970) The functional morphology of the foregut of three species of decapod Crustacea: *Cyclograpsus punctatus* Milne-Edwards, *Diogenes brevirostris* Stimpson, and *Upogebia africana* (Ortmann). Zoologica Africana 5: 309-326.

64. Castejón D, Ribes E, Durfort M, Rotllant G, Guerao G (2015) Foregut morphology and ontogeny of the mud crab *Dyspanopeus sayi* (Smith, 1869) (Decapoda, Brachyura, Panopeidae). Arthropod Structure & Development 44: 33-41.

65. Castejón D, Rotllant G, Ribes E, Durfort M, Guerao G (2015) Foregut morphology and ontogeny of the spider crab *Maja brachydactyla* (Brachyura, Majoidea, Majidae). Journal of Morphology 276: 1109-1122.

66. Jantrarotai PN, Sawanyatiputi SA (2005) Histological study on the development of digestive system in zoeal stages of mud crab (*Scylla olivacea*). Kasetsart Journal 39: 666-671.

67. Melo MA, Abrunhosa F, Sampaio I (2006) The morphology of the foregut of larvae and postlarva of *Sesarma curacaoense* De Man, 1892: a species with facultative lecithotrophy during larval development. Acta Amazonica 36: 375-380.

68. Abrunhosa FA, Melo MA, Abrunhosa JP (2003) Development and functional morphology of the foregut of larvae and postlarva of *Ucides cordatus* (Decapoda, Ocypodidae). Nauplius 11: 37-43.

69. Abrunhosa FA, Melo M (2008) Development and functional morphology of the foreguts of larvae and postlarvae of three crustacean decapods. Brazilian Journal of Biology 68: 221-228.

70. Abrunhosa FA, Simith DJB, Monteiro JRC, de Souza Junior AN, Oliva PAC (2011) Development and functional morphology of the larval foregut of two brachyuran species from Northern Brazil. Anais da Academia Brasileira de Ciências 83: 1269-1278.

71. Brösing A (2010) Recent developments on the morphology of the brachyuran foregut ossicles and gastric teeth. Zootaxa 2510: 1-44.

72. Brösing A, Richter S, Scholtz G (2002) The foregut-ossicle system of *Dromia wilsoni*, *Dromia personata* and *Lauridromia intermedia* (Decapoda, Brachyura, Dromiidae), studied with a new staining method. Arthropod Structure & Development 30: 329-338.

73. Barker PL, Gibson R (1977) Observations on the feeding mechanism, structure of the gut, and digestive physiology of the european lobster *Homarus gammarus* (L.) (Decapoda: Nephropidae). Journal of Experimental Marine Biology and Ecology 26: 297-324.

74. Hinton DJ, Corey S (1979) The mouthparts and digestive tract in the larval stages of *Homarus americanus*. Canadian Journal of Zoology 57: 1413-1423.

75. Mikami S, Greenwood JG, Takashima F (1994) Functional morphology and cytology of the phyllosomal digestive system of *Ibacus ciliatus* and *Panulirus japonicus* (Decapoda, Scyllaridae and Palinuridae). Crustaceana 67: 212-225.

76. Factor JR (1981) Development and metamorphosis of the digestive system of larval lobsters, *Homarus americanus* (Decapoda: Nephropidae). Journal of Morphology 169: 225-242.

77. Tziouveli V, Bastos-Gomez G, Bellwood O (2011) Functional morphology of mouthparts and digestive system during larval development of the cleaner shrimp *Lysmata amboinensis* (de Man, 1888). Journal of Morphology 272: 1080-1091.

78. Smith RI (1978) The Midgut Caeca and the Limits of the Hindgut of Brachyura: A Clarification. Crustaceana 35: 195-205.

79. Abubakr MA, Jones DA (1992) Functional morphology and ultrastructure of the anterior mid-gut diverticulae of larvae of *Penaeus monodon* Fabricius, 1798 (Decapoda, Natantia). Crustaceana 62: 142-158.

80. Muhammad F, Zhang ZF, Shao MY, Dong YP, Muhammad S (2012) Ontogenesis of digestive system in *Litopenaeus vannamei* (Boone, 1931) (Crustacea: Decapoda). Italian Journal of Zoology 79: 77-85.

81. Lovett DL, Felder DL (1990) Ontogenetic changes in enzyme distribution and midgut function in developmental stages of *Penaeus setiferus* (Crustacea, Decapoda, Penaeidae). The Biological Bulletin 178: 160-174.

82. Gibson R, Barker PL (1979) The Decapod Hepatopancreas. Oceanography and Marine Biology - An Annual Review 17: 285-346.

83. Loizzi RF (1971) Interpretation of crayfish hepatopancreatic function based on fine structural analysis of epithelial cell lines and muscle network. Zeitschrift für Zellforschung und Mikroskopische Anatomie 113: 420-440.

84. Van Weel PB (1974) Hepatopancreas? Comparative Biochemistry and Physiology Part A: Physiology 47: 1-9.

85. Vogt G (1996) Morphology and physiology of digestive epithelia in Decapod crustaceans. Pflügers Archiv 431: R239-R240.

86. Abrunhosa FA, Kittaka J (1997) Morphological changes in the midgut, midgut gland and hindgut during the larval and postlarval development of the red king crab *Paralithodes camtschaticus*. Fisheries Science 63: 746-754.

87. Storch V, Anger K (1983) Influence of starvation and feeding on the hepatopancreas of larval *Hyas araneus* (Decapoda, Majidae). Helgoländer Meeresuntersuchungen 36: 67-75.

88. Williams RL (1944) The pre-zoea stage of *Porcellana platycheles* (Pennant). Preliminary anatomical and histological notes. Journal of the Royal Microscopical Society 64: 1-15.

89. Nishida S, Takahashi Y, Kittaka J (1995) Structural changes in the hepatopancreas of the rock lobster, *Jasus edwardsii* (Crustacea: Palinuridae) during development from the puerulus to post-puerulus. Marine Biology 123: 837-844.

90. Anger K, Storch V, Anger V, Capuzzo JM (1985) Effects of starvation on moult cycle and hepatopancreas of stage I lobster (*Homarus americanus*) larvae. Helgoländer Meeresuntersuchungen 39: 107-116.

91. Pugh JE (1962) A contribution toward a knowledge of the hind-gut of fiddler crabs (Decapoda, Grapsidae). Transactions of the American Microscopical Society 81: 309-320.

92. Mykles DL (1979) Ultrastructure of alimentary epithelia of lobsters, *Homarus americanus* and *H. gammarus*, and crab, *Cancer magister*. Zoomorphologie 92: 201-215.

93. Huxley TH (1880) The Crayfish; an Introduction to the Study of Zoology; Series TIS, editor: New York: D. Appleton and Company.

94. To TH, Brenner TL, Cavey MJ, Wilkens JL (2004) Histological organization of the intestine in the crayfish *Procambarus clarkii*. Acta Zoologica 85: 119-130.

95. Komuro T, Yamamoto T (1968) Fine structure of the epithelium of the gut in the crayfish (*Procambarus clarkii*) with special reference to the cytoplasmic microtutubles. Archivum histologicum japonicum 30: 17-32.

96. Maynard DM (1960) Circulation and Heart Function. In: Waterman TH, editor. The Physiology of Crustacea. New York: Academic Press. pp. 161-225.

97. McMahon BR, Burnett LE (1990) The Crustacean Open Circulatory System: A Reexamination. Physiological Zoology 63: 35-71.

98. Keiler J, Richter S, Wirkner CS (2013) Evolutionary morphology of the hemolymph vascular system in hermit and king crabs (Crustacea: Decapoda: Anomala). Journal of Morphology 274: 759-778.

99. Davidson GW, Taylor HH (1995) Ventilatory and vascular routes in a sand-burying swimming crab, *Ovalipes catharus* (White, 1843) (Brachyura: Portunidae). Journal of Crustacean Biology 15: 605-624.

100. McGaw IJ (2005) The Decapod crustacean circulatory system: a case that is neither open nor closed. Microscopy and Microanalysis 11: 18-36.

101. McGaw IJ, Stillman JH (2010) Cardiovascular system of the Majidae (Crustacea: Decapoda). Arthropod Structure & Development 39: 340-349.

102. Richter S, Loesel R, Purschke G, Schmidt-Rhaesa A, Scholtz G, et al. (2010) Invertebrate neurophylogeny: suggested terms and definitions for a neuroanatomical glossary. Frontiers in Zoology 7: 29.

103. Scholtz G, Edgecombe GD (2006) The evolution of arthropod heads: reconciling morphological, developmental and palaeontological evidence. Development Genes and Evolution 216: 395-415.

104. Richter S, Stein M, Frase T, Szucsich NU (2013) The Arthropod Head. In: Minelli A, Boxshall G, Fusco G, editors. Arthropod Biology and Evolution: Molecules, Development, Morphology. Berlin, Heidelberg: Springer Berlin Heidelberg. pp. 223-240.

105. Brusca RC, Brusca GJ (2003) Invertebrates, 2nd Edition. 922 p.

106. Heath JP (1941) The nervous system of the kelp crab, *Pugettia producta*. Journal of Morphology 69: 481-498.

107. Sandeman DC (1982) Organization of the Central Nervous System. In: Meurant G, editor. The Biology of Crustacea: Volume 3: Neurobiology, Structure and Function: Academic Press. pp. 1-62.

108. Sandeman D, Sandeman R, Derby C, Schmidt M (1992) Morphology of the brain of crayfish, crabs, and spiny lobsters: a common nomenclature for homologous structures. The Biological Bulletin 183: 304-326.

109. Krieger J, Sombke A, Seefluth F, Kenning M, Hansson BS, et al. (2012) Comparative brain architecture of the European shore crab *Carcinus maenas* (Brachyura) and the common hermit crab *Pagurus bernhardus* (Anomura) with notes on other marine hermit crabs. Cell and Tissue Research 348: 47-69.

110. Geiselbrecht H, Melzer RR (2013) Nervous systems in 3D: A comparison of caridean, anomuran, and brachyuran zoea-I (Decapoda). Journal of Experimental Zoology Part B: Molecular and Developmental Evolution 320: 511-524.

CHAPTER 11.

Morphology and ultrastructure of the esophagus during the ontogeny of the spider crab *Maja brachydactyla* (Decapoda, Brachyura, Majidae)

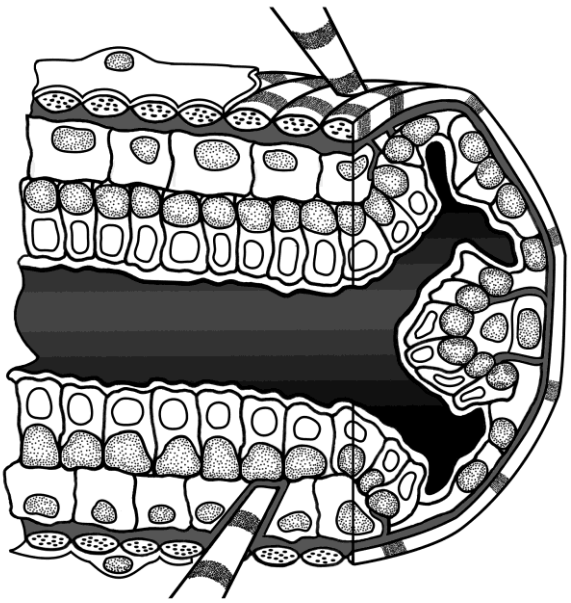

Morphology and ultrastructure of the esophagus during the ontogeny of the spider crab *Maja brachydactyla* (Decapoda, Brachyura, Majidae).

Diego Castejón[1*], Guiomar Rotllant[2], Enric Ribes[3], Mercè Durfort[3], and Guillermo Guerao[4]

[1] IRTA, Centre d'Aqüicultura, Ctra. de Poble Nou Km 5.5. 43540 Sant Carles de la Ràpita, Tarragona (Spain)

[2] CSIC, Institut de Ciències del Mar, Passeig Marítim de la Barceloneta 37-49. 08003 Barcelona (Spain)

[3] Unitat de Biologia Cel·lular, Departament de Biologia Cel·lular, Fisiologia i Immunologia, Facultat de Biologia, Universitat de Barcelona, Diagonal 645. 08028 Barcelona (Spain)

[4] PS Fabra i Puig 344. 08028 Barcelona (Spain)

Short title: *Maja brachydactyla* esophagus morphology and ontogeny

***Corresponding author:** Diego Castejón. E-mail: diego.castejon.dcb@gmail.com; phone: +34 681 154 398; postal address: IRTA, Subprogram Cultius Aqüàtics, Ctra. Poble Nou, Km 5.5. 43540 Sant Carles de la Ràpita, Tarragona (Spain).

Abstract.

The esophagus of the eucrustaceans is known as a short tube that connects the mouth with the stomach but has generally received little attention by the carcinologists, especially during the larval stages. By this reason, the present study is focused on the morphology and ultrastructure of the esophagus in the brachyuran *Maja brachydactyla* Balss, 1922 during the larval development and adult stage. The esophagus shows internally four longitudinal folds. The simple columnar epithelium is covered by a thick cuticle. The epithelial cells of the adults are heavily interdigitated and show abundant apical mitochondria and bundles of filamentous structures. The cuticle surface has microspines and mutually exclusive pores. Three muscle types surrounded by the connective tissue are reported: circular muscles forming a broad continuous band, longitudinal muscle bundles adjacent to the circular muscles, and dilator muscles crossing the connective tissue vertically toward the epithelium. The connective tissue has rosette glands. The esophagus of the larvae have epithelial cells with big vesicles but poorly developed interdigitations and filamentous structures, the cuticle is formed by a procuticle without differentiated exocuticle and endocuticle, the connective layer is thin and the rosette glands are absent. The observed features can be explained by his role in the swallowing of the food.

Keywords: Eucrustacea sensu Walossek 1999; larval development; epithelium; microspines; rosette glands

1. Introduction

The comprehension of the digestive process is fundamental to the understanding of the nutrition of decapods (Ceccaldi, 1989; Vogt, 1996) and it is a crucial step for the production of aquaculture species (Zambonino-Infante et al., 2008). The foregut of decapods derives from the embryonary ectoderm and it is lined by a chitinous cuticle. It is constituted by two organs: the esophagus and the stomach (Ceccaldi, 1989; Felgenhauer, 1992; Icely and Nott, 1992; McLaughlin, 1983). The study of the foregut of the decapods has been overshadowed by the stomach (Felgenhauer, 1992; Icely and Nott, 1992) and comparatively little attention has been realized on the esophagus. Henry Milne-Edwards (1834a; b) published one of the earliest descriptions using crabs of the genus *Maja* (presumably *M. brachydactyla*) and other species as models. The first sentence that describes the esophagus indicated that "*l'oesophage ne présenterien de remarquable*" (the esophagus does not show anything remarkable). This impression was maintained during the next decades, being described as a simple, short, vertical tube that connects the mouth with the stomach (Ceccaldi, 1989; Felgenhauer, 1992).

However, in fact the esophagus comprises different structures: longitudinal folds (Felgenhauer, 1992; McLaughlin, 1983); internal cuticle surfaces covered by microspines or setae (Elzinga, 1998; Elzinga and Hopkins, 1994; 1995; McLaughlin, 1983) and pierced by pore-like structures (Robertson and Laverack, 1979); epithelium surrounded by a connective tissue with rosette or "tegumental" glands (Barker and Gibson, 1977; 1978; Erri Babu et al., 1979; Trinadha Babu et al., 1989) and strong circular and longitudinal muscles (Barker and Gibson, 1977; 1978; Erri Babu et al., 1979; Felgenhauer, 1992; McLaughlin, 1983; Trinadha Babu et al., 1989). However, few publications have focused on this organ (Altner et al., 1986; Erri Babu et al., 1979;

Robertson and Laverack, 1979; Spirito, 1975), and the study of the esophagus during the larval stages has been largely neglected in studies focused on the foregut or on the general digestive anatomy (Johnston and Ritar, 2002; Minagawa and Takashima, 1994; Schlegel, 1911; Tziouveli et al., 2011).

We consider the esophagus an important organ involved in the swallowing of the food pieces provided by the mouth appendages, with the knowledge of their morphology being important for understanding this role. The main objective of this study is a detailed description of the esophagus of a representative Decapoda species from hatching to the first juvenile stage, as well during the adult stage employing morphological, histological and ultrastructural approaches. The species selected for this study was the spider crab *Maja brachydactyla* Balss, 1922. It is a commercial brachyuran species with fisheries located on the NW of the Iberian Peninsula, Denmark, France, Ireland, Portugal, and United Kingdom (FAO, 2012). In *M. brachydactyla*, the larval development has two zoeal stages (zoea I and zoea II) and one megalopa stage (Guerao et al., 2008). Previous studies focused on the feeding and digestive system of *M. brachydactyla* during their larval development, in which the mouthparts (Guerao et al., 2008), the general morphology of the stomach (Castejón et al., 2015), and the ontogeny of the digestive enzymatic capacity were described (Andrés et al., 2010), as well as the tolerance to starvation and refeeding on the success of the larval development (Guerao et al., 2012; Rotllant et al., 2010).

2. Material and methods

2.1 Adult and larval culture system

The adult specimens of *M. brachydactyla* were captured along the coasts of the Northwest Iberian Peninsula and Ireland (CADEMAR & LONXANET), and transported to the Institut de Recerca i Tecnologia Agroalimentàries (IRTA, Sant Carles de la Ràpita, Tarragona, Spain). The adult specimens were euthanatized and dissected to obtain the foregut, or employed for reproductive purposes, maintaining a sex ratio of six females and one male per tank. In this last case, the specimens were maintained in 2,000 L cylindrical tanks with a renewal rate of 3.5 m^3 h^{-1}. The environmental parameters were: 18 ± 1 °C, 35 ± 1 psu, and photoperiod 12 h light: 12 h dark provided by fluorescent tubes at 25 lux. The feeding consisted on fresh and frozen mussels (*Mytilus* sp. Linnaeus, 1758). Under these conditions continuous larval hatches can be obtained yearly during 5-6 months (Simeó et al., 2015). The larvae ca. 12 hours after hatch were recovered from the broodstock tanks by the water drainage into 35 L PVC baskets. Then, the larvae were put directly in 600 mL glass beakers placed inside 360 L tanks (96 x 96 x 40 cm) used as incubation chambers. The environmental parameters were: 21 ± 1 °C, 35 ± 1 psu, and photoperiod 12 h light: 12 h dark provided by white LED lights at 1,000 lux. The feeding consisted of fresh *Artemia* sp. Kellogg, 1906 nauplii (INVE Aquaculture Nutrition, Salt Lake UT, USA). Daily, the living specimens were carefully pipetted to glass beakers with clean water and fresh food. The specimens were sampled at each larval stage: zoea I ca. 15 hours after hatching, zoea II at 3-4 days after hatching (dah), megalopa at 6-7 dah, and first juvenile at 12-13 dah, and fixed according to the required procedure (see next sections).

2.2 Optical microscopy study

In the present study the stages of zoea I, zoea II, megalopa and first juvenile will be considered together as "immature stages". For the gross morphology observations, entire specimens of immature stages were fixed in formaldehyde 4 %. Then, these specimens were dissected and the foregut extracted and cleaned by their immersion in a solution of 10 % KOH at 80 °C during 15-20 min. The cleaned foreguts were mounted in microscope slides for their observation without staining. In the case of the adults, a fresh foregut was obtained and the pictures were taken with a digital camera. The esophagus of three specimens of each immature stage were measured; by contrast, the length of the adult esophagus is an approximation because it is strongly attached to the mouth opening and can break when extracted.

To study the tissue organization of the esophagus in immature stages the specimens were fixed as a whole; in the case of the adults the fresh foreguts were extracted and the esophagus sectioned with a scalpel into longitudinal and transversal sections before fixation. Thereafter, Davidson's fixative (ethanol absolute: seawater: formaldehyde 37 %: glycine: glacial acetic acid in proportion 3: 3: 2: 1: 1) was employed as fixative during 24 h. An automatic tissue processor was used for the dehydration and embedding in paraffin, then a paraffin processor was used to prepare the paraffin blocks (AP208, Myr, Spain). A microtome (Leica RM2155, Wetzlar, Germany) was employed to cut 2 µm sections. The staining techniques used were: 1) Hematoxylin and Eosin (H-E) to show the general morphology of the tissue; 2) Periodic Acid–Schiff (PAS) to reveal substances with affinity to neutral polysaccharides and mucopolysaccharides; and 3) Mallory's trichrome stain (Acid Fuchsine, Orange G and Aniline Blue stains) to visualize the structure of the muscular and connective tissues.

The observations were realized under an optical microscope (Leica LB30T 111/97, Wetzlar, Germany) connected to a camera (Olympus DP70 1.45 Mpx) and an image analyzing system (DP Controller 2.1.1.83 and DP Manager 2.1.1.163; Olympus).

2.3 Transmission and scanning electron microscopy study

Zoea I specimens and pieces of the esophagus of the adults were fixed with 2 % paraformaldehyde - 2.5 % glutaraldehyde in cacodylate buffer (0.1 mol L^{-1} pH 7.4) in total darkness at 4 °C for 12 h. Then, the samples were rinsed twice with cacodylate buffer and post-fixed in 1 % osmium tetroxide solution in cacodylate buffer. After the post-fixation the samples were dehydrated in a graded series of acetone. For the transmission electron microscopy post-fixed samples were embedded in Spurr's resin and cut into semi-thin (0.5 µm) and ultrathin (50-70 nm) sections with an ultramicrotome (Leica UCT, Wetzlar, Germany). Before observation, grids were counterstained with uranyl acetate and lead citrate. The observations were realized in a JEOL EM-1010 electron microscope at 80 kV equipped with an image analysis system (AnalySIS, SIS, Münster, Germany), a single zoea I specimen and two adult specimens were observed. For scanning electron microscopy, post-fixed samples were critical-point-dried, mounted on SEM stubs with self-adhesive stickers and coated with carbon. Observations were made with a JEOL JSM-7001F scanning electron microscope. The post-fixative treatment and TEM and SEM observations were realized at CCiTUB (Hospital Clinic, University of Barcelona, Spain).

3. Results

The mouth of *M. brachydactyla* open ventrally, while the stomach is positioned dorsally (Fig. 1C). The esophagus is a short, almost vertical tube that connects the mouth with the ventral floor of the cardiac stomach (Fig. 1A-C). The esophagus length has been measured during development: 233 ± 5 µm in zoea I, 265 ± 20 µm in zoea II, 265 ± 17 µm in megalopa, 297 ± 24 µm in juvenile 1, and between 15 and 25 mm in the adult (Fig. 1A-C). The cross-section is quadrate; however the lumen has an X- or H-like shape due to the presence of four main internal longitudinal folds or evaginations located on the lateral walls (Fig. 2A-B; 3A, C, E).

The basic structure of the esophagus is similar in all the life stages, but it is more complex in the adults than in the immature stages (Fig. 2-3). The basic structure comprises an epithelium covered by a cuticle. Below the basal lamina a layer of connective tissue is present: in the adults the connective layer is wide and contain groups of rosette glands (Fig. 2A-D; 8A), while in the immature stages it is very thin and glands were not observed (Fig. 3B-C). Three orientations of striated muscle fibers have been observed: circular, longitudinal and dilator muscles (Fig. 2A-D; 3A-D). The circular muscles form a continuous band that wrap the connective tissue and the epithelium along the longitudinal axis of the esophagus (Fig. 2A-C). In the adults, this muscle layer is highly developed and associated with blood vessels (Fig. 2B) and constitutes the most prominent muscle layer of the immature stages (Fig. 3A-C). The bundles of longitudinal muscles of the adults are located in the connective layer, adjacently to the circular muscle band (Fig. 2A-B), but in the immature stages the longitudinal muscles were not identified. The dilator muscles of the adults are identified crossing vertically the connective tissue to reach perpendicularly the epithelium (Fig.

2A-B, D), while in the immature stages they connect the epithelium of the esophagus with the epithelial cells of the tegument located behind the mandibles (Fig. 3A-D).

Epithelial cells. The epithelium of the esophagus is composed of a single cell type and is covered by a cuticle. The morphology of the epithelium differs between adults and immature stages. The adults have a simple columnar epithelium, measuring around 47 ± 19 µm in height (Fig. 2E). In the immature stages, the invaginations have a simple squamous epithelium (3-5 µm in height), while the evaginations have a stratified epithelium composed by basal irregular cells and distal short columnar (25-30 µm in height) cells (Fig. 3E; 5B-C).

The adult epithelial cells have a marked polarity (Fig. 4A, B, D); whereas in zoea I no polarity has been observed (Fig. 3E; 5A-B). The apical cell membrane contains a structure denominated by us as an "apical complex": these are irregular electron-dense infolds intracellularly connected to bundles of filamentous structures (Fig. 4F). In the adults, the lateral cell membranes are heavily interdigitated; the number of interdigitations increases toward the cell basis (Fig. 4B, D). By contrast, in the zoeae I the lateral cell membranes are smoothly undulated and lateral interdigitations are marginal (Fig. 5A-C). The cells are joined by cell-to-cell junctions, but their extension is not yet well defined (Fig. 4F; Suppl. Mat. 1). The basal membrane of the adults is heavily infolded (Fig. 4D); while in the zoeae I the basal membrane is generally smooth (Fig. 5B-C).

Neither adults nor immature stages showed PAS positive granules in their cytoplasm (Suppl. Mat. 3). In the adults, the cytoplasm is generally lucent, containing sparse ribosomes, small lucent vesicles and multivesicular bodies (Fig. 4A-F). In the immature stages the majority of the cytoplasm can be occupied by a giant vesicle

without affinity to the staining techniques used (Fig. 3A-C). By electron microscopy this vesicle is lined by a single membrane and contains aggregations of electron-dense matter (Fig. 3E; 5A-B; Suppl. Mat. 1-2). In the adults the cell nucleus is located medial to basally (Fig. 2E; 4A, D); while in immature stages the cell nucleus can be located from the cell basis to the cell apex (Fig. 3E; 5A-B).

The mitochondria concentrate at the cell apex of the adult cells, but in the zoeae I they do not show such a distribution pattern (Fig. 4A, B, F; 5A-B; Suppl. Mat. 1-2). The rough endoplasmic reticulum is composed by thin, short and dispersed cisternae (Fig. 4D-E; 5D). Golgi bodies are scarce (Fig. 4E). One of the most important features of the epithelial cells is the presence of bundles of filamentous structures (Fig. 4C), whose identity is unclear. The bundles of filamentous structures are more prominent in the adults (Fig. 4B-D, F) than in the zoeae I (Fig. 5D; Suppl. Mat. 1). In the adults they cross the cell from the basis (Fig. 4D) to the apex (Fig. 4B, F). The apical extreme of the filamentous structures are attached to the "apical complex" of the apical membrane (Fig. 4F).

Cuticle organization. The epithelial cells are apically covered by a cuticle layer. In the adults the cuticle thickness is 86 ± 18 µm. The adult cuticle shows the typical layers of the arthropod cuticle: epicuticle, exocuticle and endocuticle (Fig. 2D-E; Suppl. Mat. 3). The epicuticle is the outmost cuticle layer, and represents ca. 10 ± 1 % of the cuticle thickness. It is strongly stained by Orange G and Eosin, and it can be subdivided into three sub-layers: 1) the outermost sub-layer is a thin refractory coat; 2) the next sub-layer shows affinity to Eosin and acquires a yellow color with Orange G, it is composed by fibers without a defined orientation; and 3) the most basal epicuticle sub-layer shows affinity to Hematoxylin and acquires an orange color with Orange G, and is

composed of fibers with a vertical orientation that protrudes toward the underlying exocuticle (Fig. 2D-F; 6A-B). The next layers are the exocuticle and the endocuticle. Both layers differentiate from the epicuticle due to their lamellar structure and their homogeneous staining affinity to Hematoxylin and Aniline Blue (Fig. 2D-E). PAS staining is slightly stronger in the exocuticle than in the endocuticle (Suppl. Mat. 3). The exocuticle represents ca. 30-40 % of the cuticle thickness and it is composed of wide lamellae (5.8 ± 1.1 μm), while the endocuticle represents ca. 50-55 % of the cuticle thickness and it is composed by thin lamellae (2.5 ± 0.6 μm) (Fig. 6B-C). Concomitantly with the proximity to the cell basis the lamellae of the endocuticle gradually lose definition and become extensively wider (Fig. 6D).

The cuticle of the immature stages is much thinner and the typical layers of the arthropod cuticle cannot be identified by optical microscopy (Fig. 3B-C). The cuticle of the zoeal stage is around 570 ± 70 nm, it has an epicuticle that represents ca. 20 ± 5 % of the cuticle thickness and a lamellate procuticle (Fig. 7B; Suppl. Mat. 1-2).

The cuticle surface shows two types of structures: microspines and pores. The microspines appear in all the life stages. The microspines are projected from the epicuticle (Fig. 7B) as hair-like structures difficult to observe by optical microscopy (Fig. 7A). The microspines of the adults form groups of one to three microspines attached to each other, occasionally some groups include more than three microspines (Fig. 7C-D), with the density of groups of microspines calculated to be ca. 0.7 per 10 μm^2. Each microspine is approximately 4 ± 1 μm in length (Fig. 7C). The distribution pattern of the microspines is unclear; we observed areas rich in microspines and areas where the microspines are absent. In the zoeae I, the microspines are shorter (540 ± 180

nm in ZI) and each microspine is individually separated from each other (Suppl. Mat. 4).

The pores have been observed on the adult cuticle but not in the zoeae I. The pores are aggregated in "pore areas", they are microspine free areas with a circular to elliptical shape, slightly elevated in comparison to the surrounding cuticle and pierced by pores (Fig.7F). Two types of pores have been identified. The "large pores" are 2 µm in diameter or more, the cross section is circular and are surrounded by a smooth elevation of the cuticle (Fig. 7G). The "small pores" have around 1 µm in diameter or less, the cross section is horseshoe-like and are surrounded by an abrupt elevation of the cuticle (Fig. 7H).

Rosette glands. In the adults, the connective tissue of the esophagus contains rosette glands (Fig. 2D; 7E; 8A). The rosette glands are absent from the esophagus of the immature stages, but appear below the tegument of the mouthparts and the anterior distal portion of the thoracic ganglionic mass, nevertheless they seem more associated with the mouth and mouthparts than with the esophagus itself (Fig. 1C). The rosette glands are clusters of secretory cells aggregated into acinar like structures with a diameter of 75-100 µm. The secretory cells surround a central tube that channel the secretions outside the glands (Fig. 8A). The cuticle is pierced by tube-like structures located above some gland agglomerations, showing a possible secretion pathway of the products released by the secretory cells (Fig. 7E). There is only a single type of secretory cell in the rosette glands. These cells have a pyramidal shape and measure ca. 35 µm in height (Fig. 8A). The cytoplasm is filled by vesicles of 865 ±118 nm in diameter, however many vesicles are fused into larger structures (Fig. 8B-C). The vesicles contain a dense fibrillar-like matrix with a variable electron-density (Fig.8B-E).

Some secretory cells contain a cytoplasm occupied by vesicles that are similar in appearance and size to a "vacuole" (Fig. 8A). The nucleus is located basally (Fig.8A). Mitochondria are usually located around the Golgi bodies (Fig. 8B). Golgi bodies are abundant, large and highly developed (Fig. 8B). The rough endoplasmic reticulum forms a thin layer located adjacent to the nucleus and the basal membrane (Fig. 8D-E).

4. Discussion

The esophagus of *M. brachydactyla* is a short vertical tube that connects the mouth with the stomach as has been described in other decapods (Ceccaldi, 1989; Felgenhauer, 1992; Icely and Nott, 1992), including larval stages such as the zoeae of the brachyuran crabs *Maja* sp. (Schlegel, 1911), *Ranina ranina* (Minagawa and Takashima, 1994), and *Scylla olivacea* (Jantrarotai and Sawanyatiputi, 2005), the zoeae of the caridean shrimp *Lysmata amboinensis* (Tziouveli et al., 2011) and the phyllosomata of the achelatan rock lobster *Panulirus ornatus* (Johnston et al., 2008).

The esophagus is the organ responsible for the transport of the ingested food from the mouth opening to the stomach. The passage of the food into the stomach requires the dilation of the esophageal walls. For this reason, when relaxed the esophagus of *M. brachydactyla* shows four internal longitudinal folds from hatching to the adult stage, which provide capacity for elastic expansion of the esophagus and passage of food to the stomach. Similar infoldings have been described in brachyurans (Erri Babu et al., 1982; Minagawa and Takashima, 1994; Trinadha Babu et al., 1989), astacideans (Factor, 1981; Loya-Javellana et al., 1994; Yonge, 1924), penaeids (Dall, 1967), achelatans (Johnston and Alexander, 1999) and carideans (Patwardhan, 1935; Pillai, 1960; Sousa and Petriella, 2006).

To realize the peristaltic movements required to swallow the food requires a powerful set of muscles. The adult esophagus of *M. brachydactyla* shares with other brachyuran crabs such as *Menippe rumphii* (Erri Babu et al., 1982), *Portunus sanguinolentus* (Trinadha Babu et al., 1989), *Scylla serrata* (Barker and Gibson, 1978), and *Spiralothelphusa hydrodroma* (referred as *Parathelphusa hydrodromus*) (Reddy, 1937), caridean shrimps as *Caridina laevis* (Pillai, 1960), and astacideans such as the Norway lobster *Nephrops norvegicus* (Yonge, 1924) and the European lobster *Homarus gammarus* (Barker and Gibson, 1977), the presence of a wide band of circular muscles associated with longitudinal muscles. Another set of muscles observed in *M. brachydactyla* receive names such as "dilator muscles" (Erri Babu et al., 1979; Erri Babu et al., 1982; Pillai, 1960; Reddy, 1937; Yonge, 1924), "extrinsic muscles" (Schmitz and Scherrey, 1983) and "radial muscles" (Barker and Gibson, 1977; 1978). Their function has been associated with the expansive efforts required to swallow the food in amphipods (Schmitz and Scherrey, 1983) and the present study suggests the same function for *M. brachydactyla*: the contraction of the "dilator muscles" could press the epithelium toward the connective tissue facilitating the expansion of the lumen. In the case of the larval stages of *M. brachydactyla*, we observed circular and dilator muscles but longitudinal muscles were not identified. Similarly, Schlegel (1911) in the zoea I of the same genus described circular muscle fibers (as "constrictor muscles") and similar "dilator muscles". The circular muscles also were described in the esophagus of *R. ranina* zoeae (Minagawa and Takashima, 1994). The role of the muscles of the larvae must be similar to their adult counterpart.

Epithelial cells. The simple columnar epithelium of the adult esophagus of *M. brachydactyla* is covered by a cuticle, as has been reported in other brachyurans: e.g. *M. rumphii* (Erri Babu et al., 1982), *P. sanguinolentus* (Trinadha Babu et al., 1989), *S.*

serrata (Barker and Gibson, 1978) and *S. hydrodroma* (Reddy, 1937). The esophageal epithelium is also described as columnar in astacideans (Barker and Gibson, 1977; Yonge, 1924) and carideans (Pillai, 1960). By contrast, in the brachyuran crab *Pseudocarcinus gigas* the epithelium is cuboidal (Heeren and Mitchell, 1997). This information suggests that the epithelium of the esophagus is generally conserved among the decapods during the adulthood. The epithelial cells of the larvae differs from their adult counterpart, varying from plane to short columnar cells. Schlegel (1911) in his study of the first zoeal stage of a *Maja* species, described an esophageal epithelium composed of big cells with basal nuclei and covered by a cuticle. In other Decapoda larvae the epithelium is considered short columnar, as in *R. ranina* zoeae (Minagawa and Takashima, 1994) and *P. ornatus* phyllosomata (Johnston et al., 2008), or cuboidal as in *L. amboinensis* zoeae (Tziouveli et al., 2011). The current data are not enough to evaluate if these cell morphologies are related with a functional role, the phylogeny, or a consequence of the molt cycle.

The esophageal epithelium must be able to support the expansive and contractive efforts required for the swallowing of the food. In this sense, one of the most distinctive characteristics of the epithelial cells of *M. brachydactyla* are their richness in interdigitations and bundles of filamentous structures, coinciding with the esophageal epithelial cells of the cirolanid isopod *Natatolana obtusata* (Storch et al., 2002). The filamentous structures have been reported as microtubules in the esophagus and/or hindgut tract of diverse malacostracans, including the brachyuran *Metacarcinus magister* (Mykles, 1979), and astacideans such as the lobsters *Homarus americanus* and *Homarus gammarus* (Mykles, 1979), and the crayfish *Procambarus clarkii* (Komuro and Yamamoto, 1968), as well diverse isopod species (Holdich and Mayes, 1975; Vernon et al., 1974; Witkus et al., 1969). Some authors suggested that the microtubules

could help to maintain the cell structure through the support of the expansive and contractive efforts realized by these organs (Komuro and Yamamoto, 1968; Mykles, 1979; Witkus et al., 1969). Similarly, the interdigitations could help to avoid the tearing of the epithelium through the expansive waves. By contrast, the epithelial cells of the larvae are very different from their adult counterpart. Many larval epithelial cells show highly developed vesicles (feature not observed in the adults), while the bundles of filamentous structures and interdigitations are poorly developed. These large vesicles have not been reported previously and their role is unknown, but tentatively could be considered as having a structural role, maybe maintaining the cell shape.

Cuticle organization. The cuticle surface is rich in small hair-like structures named "microspines" by Elzinga and Hopkins (1994; 1995). These microspines are cuticle specializations observed in ectoderm derivatives such as the foregut and hindgut (Elzinga, 1998; Elzinga and Hopkins, 1994; 1995). They have been reported in the esophagus of the Malacostraca as small aggregations or rows projected toward the stomach (De Jong and Casanova, 1997; Elzinga, 1998; Friesen et al., 1986; Icely and Nott, 1984; Johnston et al., 2004; Storch et al., 2002). Few studies mentioned the presence of microspines in the esophagus of the larval stages. Johnston et al. (2008) mentioned "short spines" in the esophageal lumen of *P. ornatus* phyllosomata. By contrast, in *L. amboinensis* the larval esophagus project dense and thick setae, a feature not observed in *M. brachydactyla* (Tziouveli et al., 2011). The role of the esophageal microspines is unknown. In the hindgut, they have been associated with the grasping of the peritrophic membrane to avoid their backward movement due to anti-peristaltic waves (Felder and Felgenhauer, 1993; Hopkin and Nott, 1980). Other authors suggested a role such as a supporting surface for symbiotic microorganisms (Elzinga, 1998; Harris, 1993). In the case of the esophagus none of these hypotheses looks probable,

since no peritrophic membrane or microorganism have been observed. Perhaps the microspines could help to grasp the food for their ingestion.

Other cuticle specializations are the areas devoid from microspines but pierced by "small" (ca. 1 µm diameter) and "large" (ca. 2 µm diameter) pores. In *S. serrata* the cuticle is also pierced by tubes ca. 3 µm in width (Barker and Gibson, 1978). Small (1-3 µm diameter) and large (5-8 µm diameter) pores have been identified in the esophagus of *H. gammarus*, but differs from our study since they are restricted to the esophagus - stomach junction and are associated with long filaments (Robertson and Laverack, 1979). The "pore areas" can appear at the distal side of cuticle tubes located over the rosette glands, which make it is possible that these pores constitute a release pathway for the gland secretions. An alternative hypothesis suggests that the pores and channels could be "sensors" of the rosette glands, but this hypothesis require confirmation of the presence of nervous structures, i.e. the axons observed in the connective that surrounds rosette glands in carideans such as the common prawn *Palaemon serratus* (Alexander, 1989) and the daggerblade grass shrimp *Palaemonetes pugio* (Doughtie and Rao, 1982).

Rosette glands. The rosette glands received numerous names based on their location ("tegumental", "esophageal", or "intestinal glands"), shape ("rosette glands") or hypothetical function ("salivary glands", or "cement glands"), but has not yet been an agreement in their denomination (Gorvett, 1946; Reddy, 1937; Trinadha Babu et al., 1989; Yonge, 1924). The rosette glands have been described in the adult esophagus of diverse brachyurans (Barker and Gibson, 1978; Erri Babu et al., 1979; Erri Babu et al., 1982; Heeren and Mitchell, 1997; Reddy, 1937; Trinadha Babu et al., 1989), astacideans (Barker and Gibson, 1977; Yonge, 1924; 1932), achelatans (Johnston and Alexander, 1999), carideans (Pillai, 1960) and penaeids (Dall, 1967; Sousa and

Petriella, 2006). Although the rosette glands appear to be absent in the esophagus of the immature specimens, they appear near to the mouth opening and mouthparts, coinciding with observations realized in the zoeal stages of *S. olivacea* (Jantrarotai and Sawanyatiputi, 2005) and the pre-zoeal stage of the anomuran *Porcellana platycheles* (Williams, 1944). The rosette glands of *M. brachydactyla* are very active: the cytoplasm of the secretory cells is filled by vesicles and the Golgi bodies are highly developed. Moreover, the secretory cells can be stained by Alcian blue and PAS coinciding to previous studies realized in other brachyurans (Barker and Gibson, 1978; Erri Babu et al., 1982; Trinadha Babu et al., 1989). These stain affinities reveal a possible composition based on acid mucopolysaccharides (including sulphated mucopolysaccharides, sulphated sialomucins and hyaluronic acid), as well neutral mucopolysaccharides (Erri Babu et al., 1979; Trinadha Babu et al., 1989). Other studies discarded the presence of glycogen (Erri Babu et al., 1979), lipids and phospholipids (Trinadha Babu et al., 1989). Yonge (1932) mentioned numerous possible roles for the rosette glands: "salivary glands" that help the passage and digestion of the food, "slime glands" with no mentioned role, "secretory organs" with a midgut gland-like role, or "cement glands" involved on the oviposition. Considering all the mentioned roles and their location, a probable function for the esophageal rosette glands in *M. brachydactyla* could be comparable to the "salivary glands": the acid compounds could help in digestive processes, while the mucous nature is useful to entangle and lubricate the lumen surface allowing the passage of the food (Barker and Gibson, 1977; Erri Babu et al., 1979; Hunt et al., 1992; Shyamasundari and Hanumantha Rao, 1977; 1978; Yonge, 1924).

The role of the esophagus can explain their histological and ultrastructural characteristics: the internal folds allow the expansion of the lumen, the epithelial cells have numerous interdigitations and filamentous structures to presumably avoid its tearing, the epithelium is covered by a cuticle that protects the epithelial cells and it is covered by microspines that could help to grasp the food, while the connective tissue contains highly developed muscles to realize the peristaltic movements required for these efforts. The rosette glands found in the connective tissue could act as "salivary glands". The esophagus of the larval stages has numerous differences from their adult counterpart: the epithelial cells can contain big vesicles, and the connective tissue and cuticle are thinner than in the adults, lacking rosette glands and blood vessels. The esophagus of the adults is much wider than in the larvae, with the distance between tissues being greatly increased. Consequently, the esophagus of the adult requires additional structures for their maintenance (such as extended connective tissue, blood vessels and glands) and a more complex organization.

5. Acknowledgements

Financial support provided by the Spanish Ministry of Economy and Competitiveness through the INIA project [grant number RTA2011-00004-00-00] to G.G and a predoctoral fellowship to D.C. [FPI-INIA]. The authors would like to thank Karl B. Andree for their revision of the language, as well to anonymous reviewers whose suggestions have greatly improved the article. The authors would like to thank the technicians at IRTA, Sant Carles de la Ràpita (David Carmona, Glòria Macià, Magda Monllaó, Francesc X. Ingla and Olga Bellot) and CCiTUB Hospital Clinic, Barcelona (Adriana Martínez, Almudena García, José Manuel Rebled and Rosa Rivera) for their assistance.

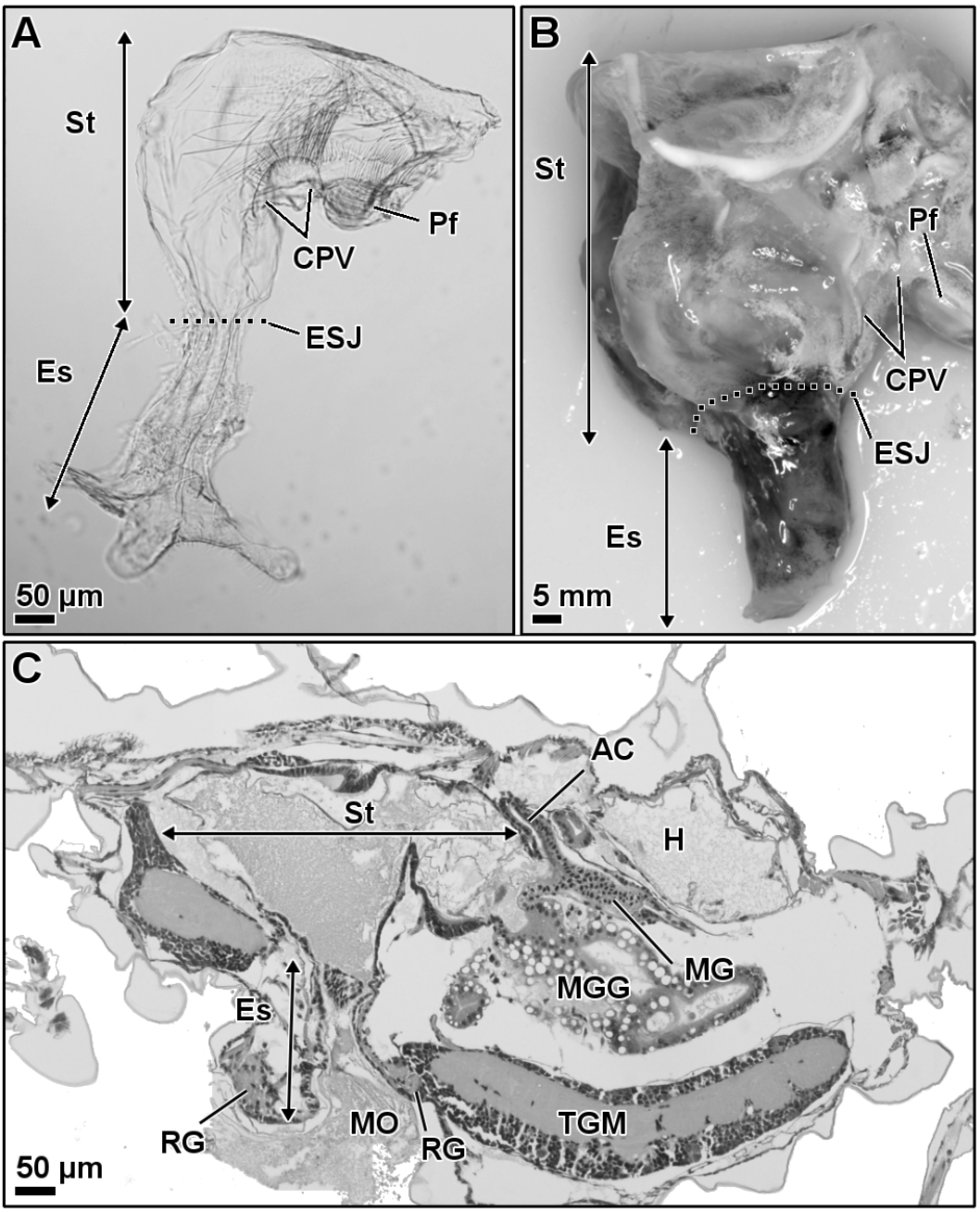

Figure 1. *Maja brachydactyla*. Esophagus, gross morphology and location. Zoea II, optical microscope (A). Adult, digital camera (B). Megalopa, H-E, optical microscope (C). Abbreviations: AC, anterior caeca; CPV, cardio-pyloric valve; Es, esophagus; ESJ, esophagus - stomach junction; H, heart; Pf, pyloric filter; MG, midgut tract; MGG, midgut gland (hepatopancreas); MO, mouth opening; RG, rosette glands; St, stomach; TGM, thoracic ganglionic mass.

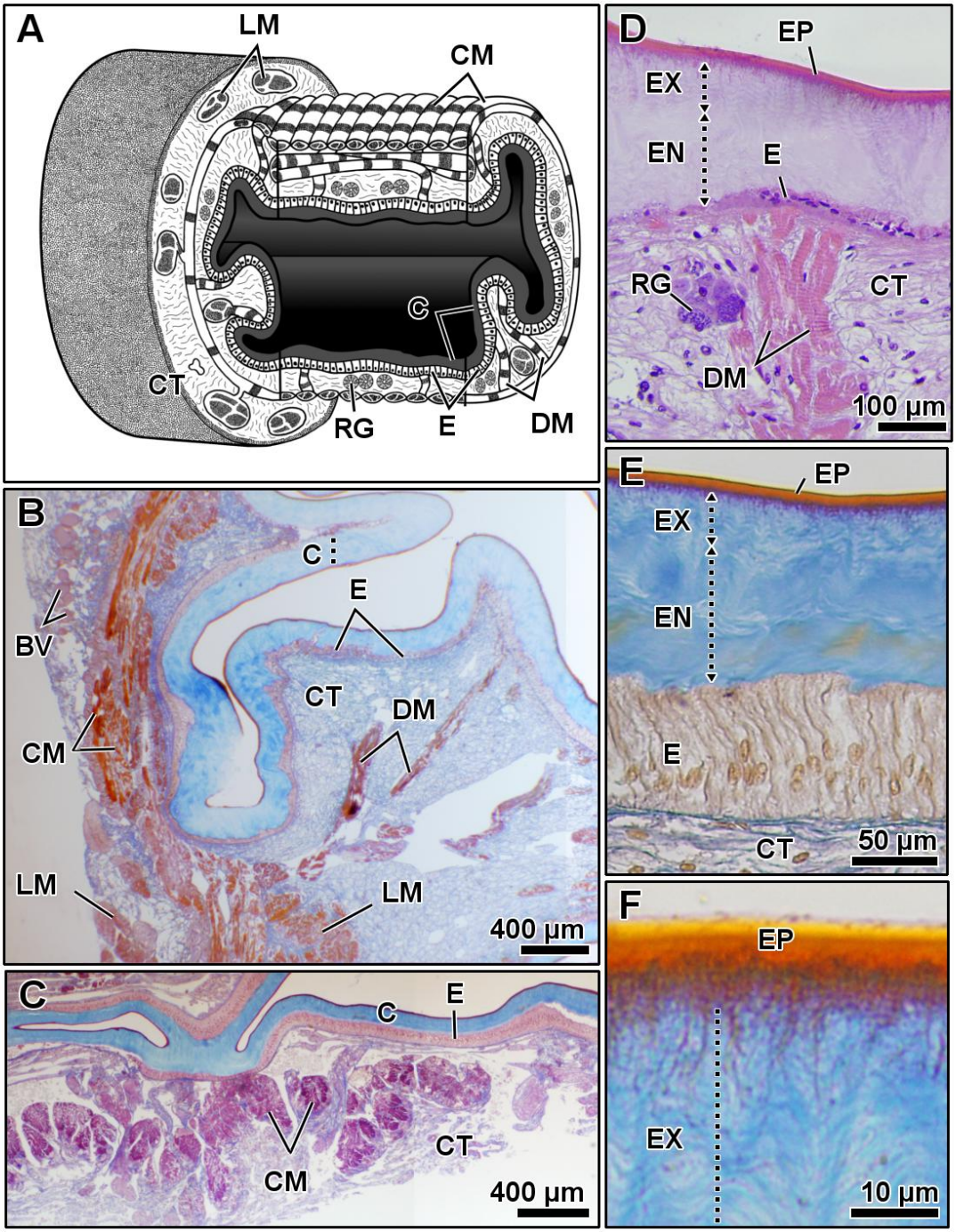

Figure 2. *Maja brachydactyla*. Adult. Esophagus, histological organization. Optical microscopy. General diagram (A). General view, Mallory's trichrome (B-C): transversal (B) and longitudinal sections (C). Epithelium and connective tissue, H-E (D). Close view of the epithelium, Mallory's trichrome (E). Exocuticle and epicuticle, Mallory's trichrome (F). Abbreviations: BV, blood vessels; C, cuticle; CT, connective tissue; CM, circular muscles; DM, dilator muscles; EN, endocuticle; EP, epicuticle; EX, exocuticle; RG, rosette glands; LM, longitudinal muscles.

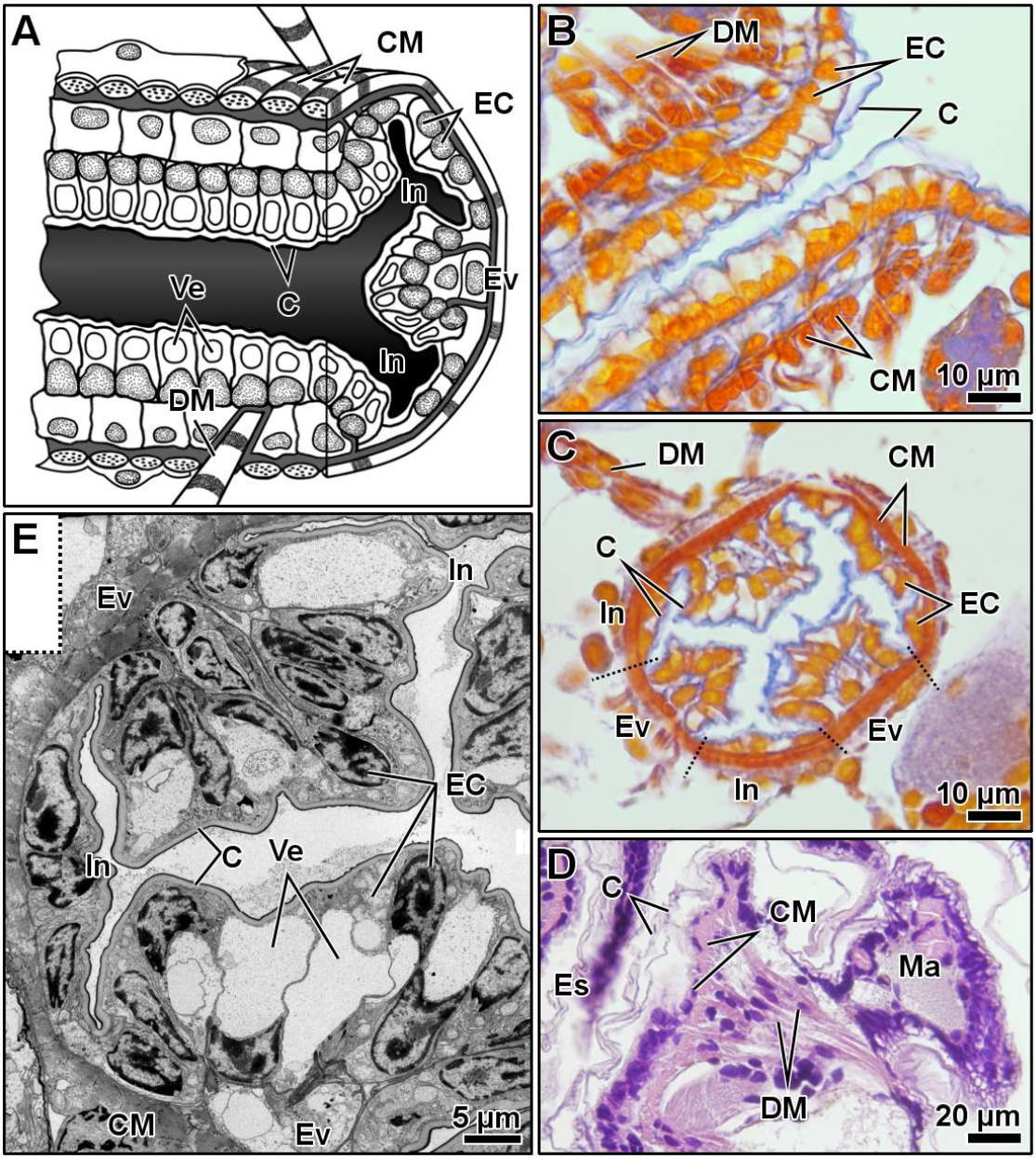

Figure 3. *Maja brachydactyla*. Larvae. Esophagus, histological organization. Optical microscopy. General diagram (A). Megalopa, Mallory's trichrome (B-C): longitudinal (B) and transversal sections (C). Megalopa, close view of the dilator muscles, HE (D). Zoea I, transversal section, TEM. Abbreviations: C, cuticle; CM, circular muscles; DM, dilator muscles; EC, epithelial cells; Es, esophagus; Ev, evaginations; If, infold; In, invaginations; Ma, mandible; Ve, vesicles.

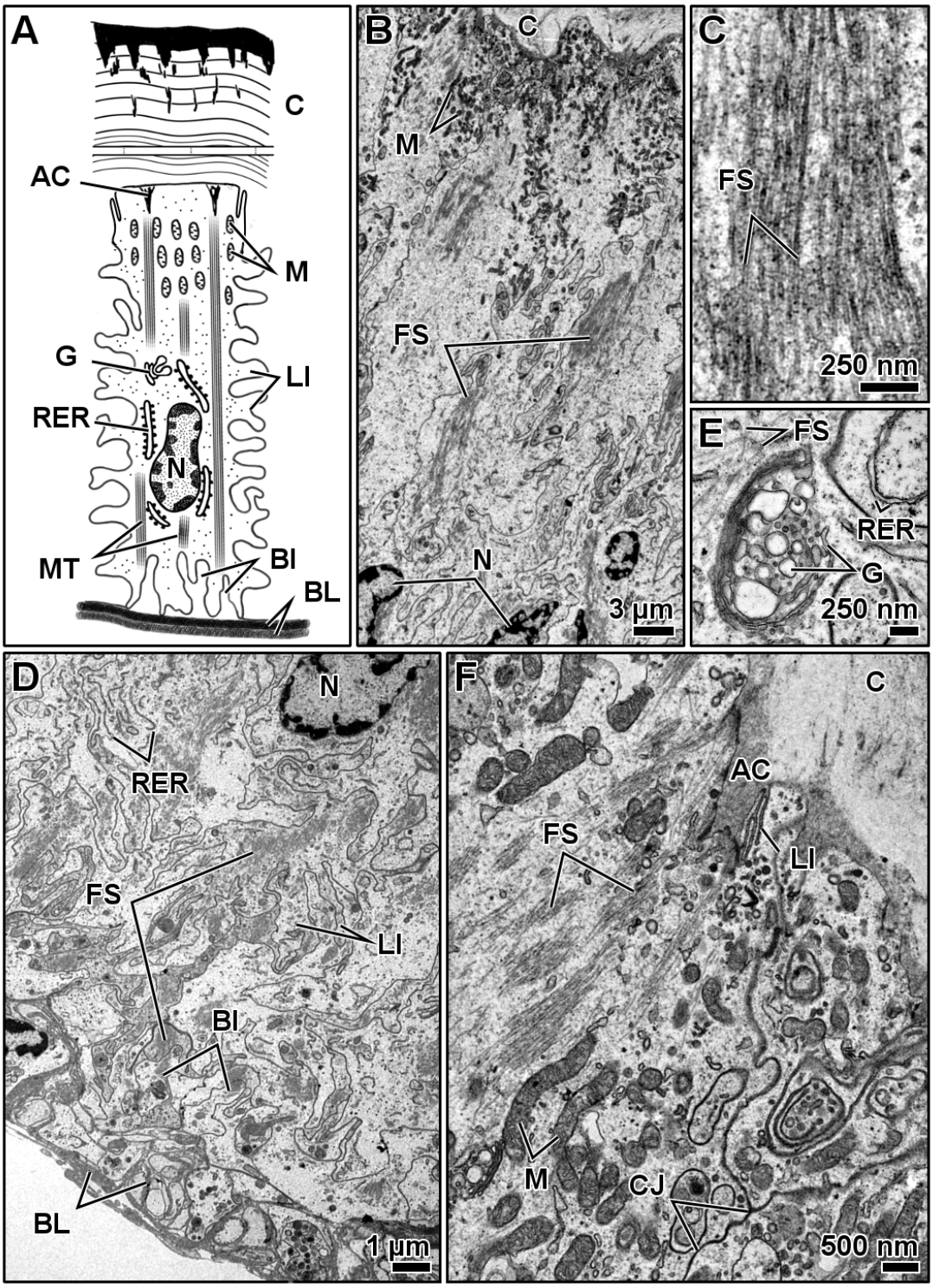

Figure 4. *Maja brachydactyla*. Adult. Esophagus. Epithelial cells. TEM. General diagram (A). Apex of the epithelial cell (B). Close view of the filamentous structures (C). Basis of the epithelial cell (D). Close view of a Golgi body (E). Cell apex showing the cell-to-cell junctions and the "apical complex" (F). Abbreviations: AC, apical complex; AI, apical infolds; BI, basal infolds; BL, basal lamina; C, cuticle; CJ, cell-to-cell junctions; FS, filamentous structures; G, Golgi body; LI, lateral interdigitations; M, mitochondria; N, nucleus; RER, rough endoplasmic reticulum.

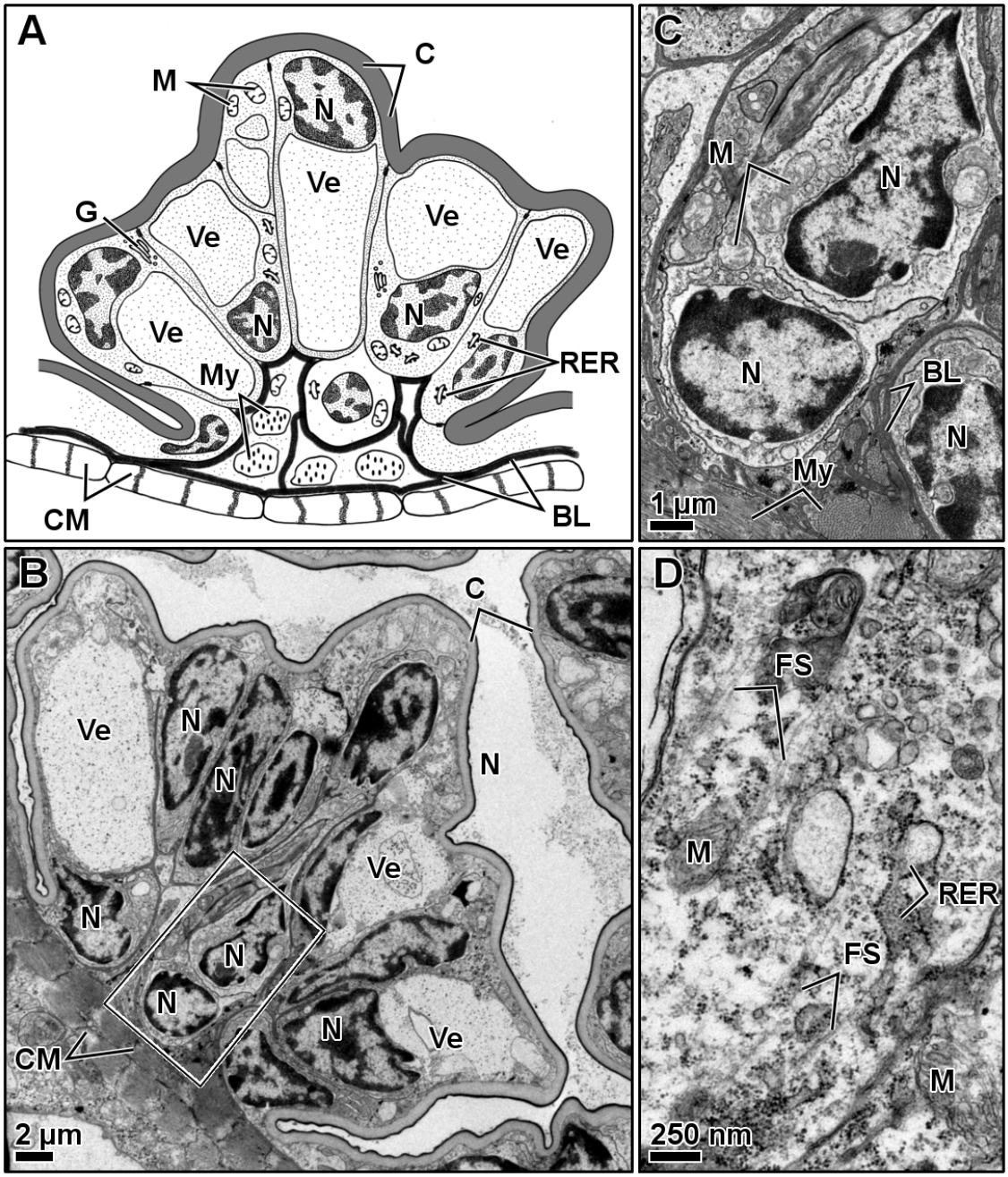

Figure 5. *Maja brachydactyla*. Zoea I. Esophagus. Epithelial fold. TEM. General diagram (A). General view, the rectangle marks the epithelial cells located on the fold center (B). Detailed view of the rectangle marked in B (C). Close view of the filamentous structures (D). Abbreviations: BL, basal lamina; C, cuticle; CM, circular muscles; EC, epithelial cell; FS, filamentous structures; G; Golgi body; M, mitochondria; My, myofibrils; N, nucleus; RER, rough endoplasmic reticulum; Ve, vesicles.

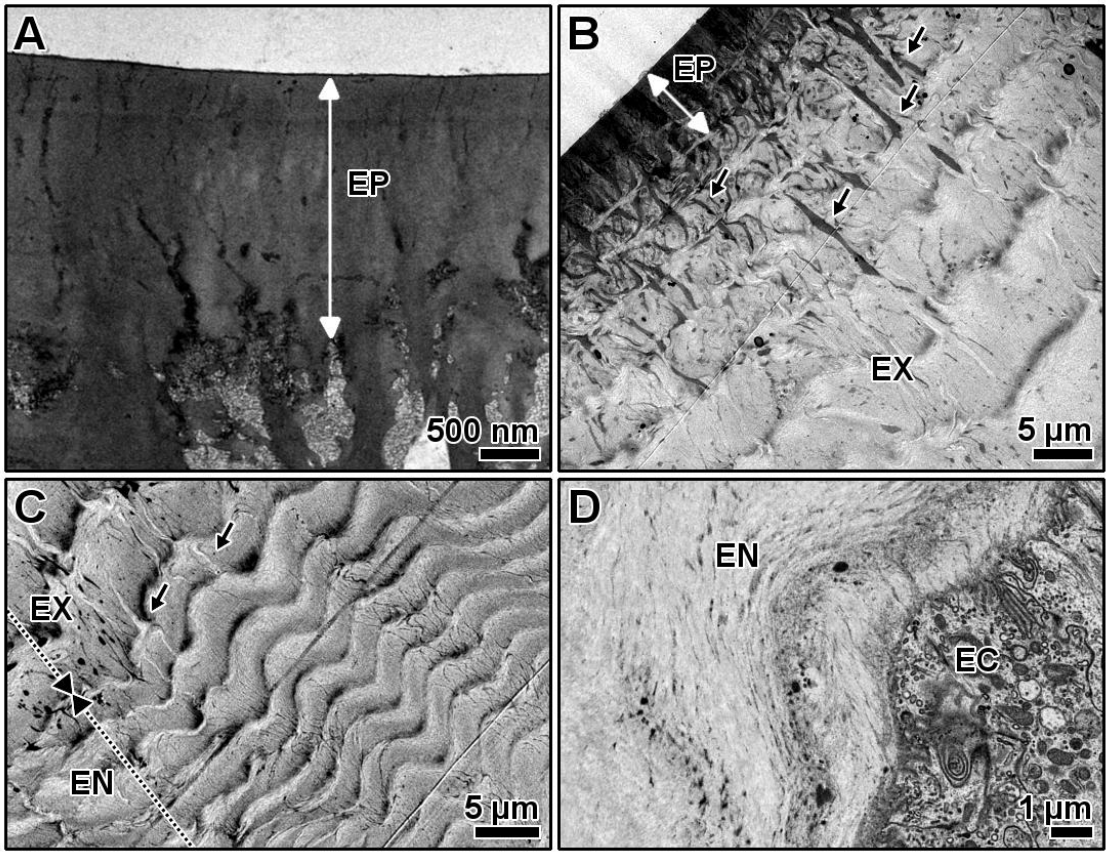

Figure 6. *Maja brachydactyla*. Adult. Esophagus. Cuticle. TEM. Epicuticle (A). Epicuticle, exocuticle and protrusions of epicuticle crossing the exocuticle (arrows) (B). Transition from the exocuticle to the endocuticle, pore canals (arrows) are showed (C). Basal endocuticle and apex of the epithelial cell (D). Abbreviations: EC; epithelial cell; EN, endocuticle; EP, epicuticle; EX, exocuticle.

Figure 7 (next page). *Maja brachydactyla*. Esophagus, superficial structures of the cuticle. Adult, microspines (arrows), Mallory's trichrome (A). Zoea I, microspines protruding from the cuticle, TEM (B). Adult, microspines, SEM (C-D): close view (C) and field of microspines (D). Rosette glands associated with duct-like structures and pores, Mallory's trichrome (E). "Pore area" with elongated shape, SEM (F). Close view of the cuticle pores, SEM (G-H): "large pore" surrounded by "small pores" (G) and "small pore" (H). Abbreviations: D, duct-like structure; EC, epithelial cells; EN, endocuticle; EP, epicuticle; EX, exocuticle; LP, "large pore"; MS, microspines; P, pores; PC, procuticle; RG, rosette glands; SP, "small pore".

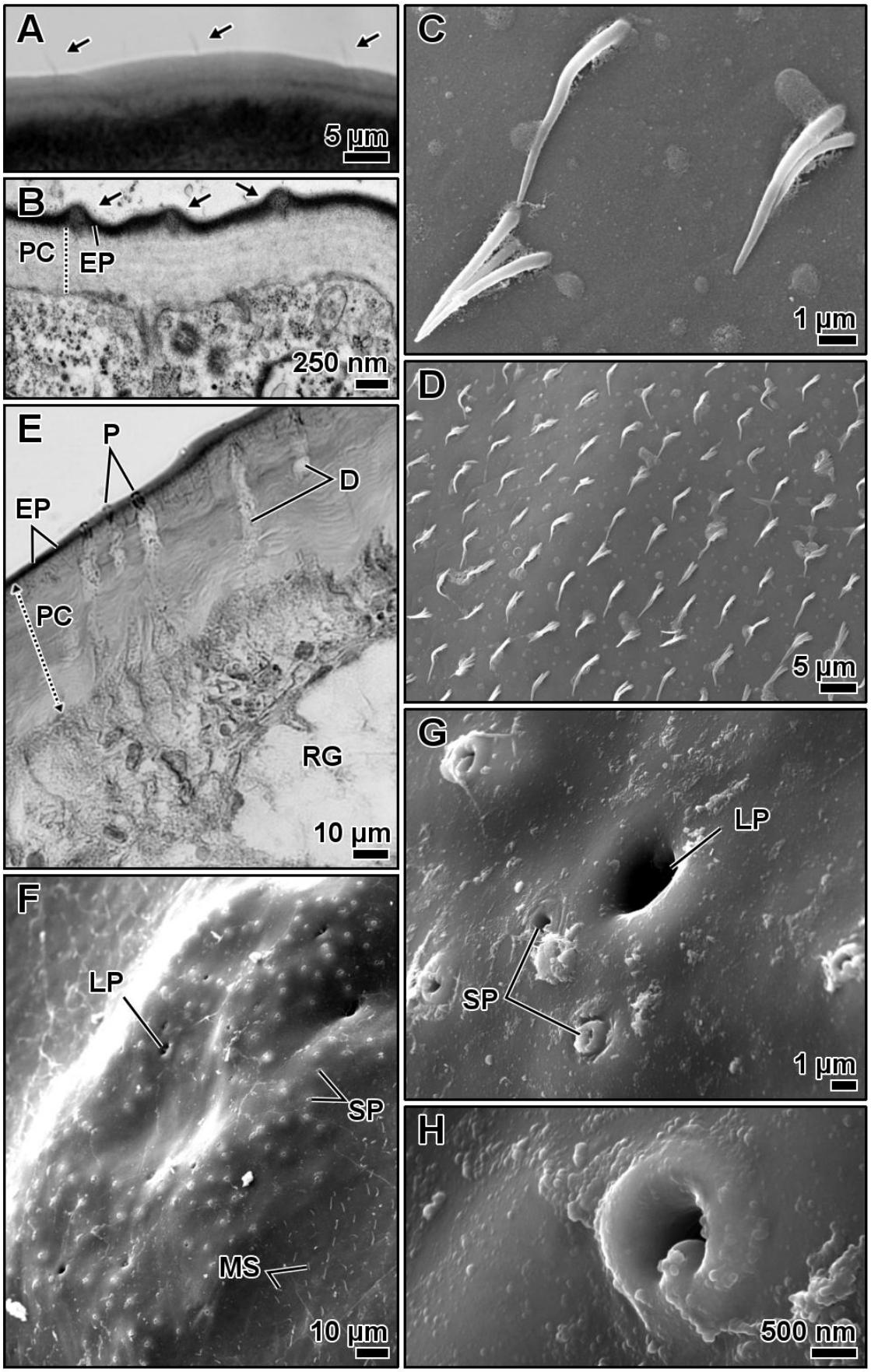
A
5 µm
B
PC
EP
250 nm
C
1 µm
D
5 µm
E
P
D
EP
PC
RG
10 µm
F
LP
SP
MS
10 µm
G
LP
SP
1 µm
H
500 nm

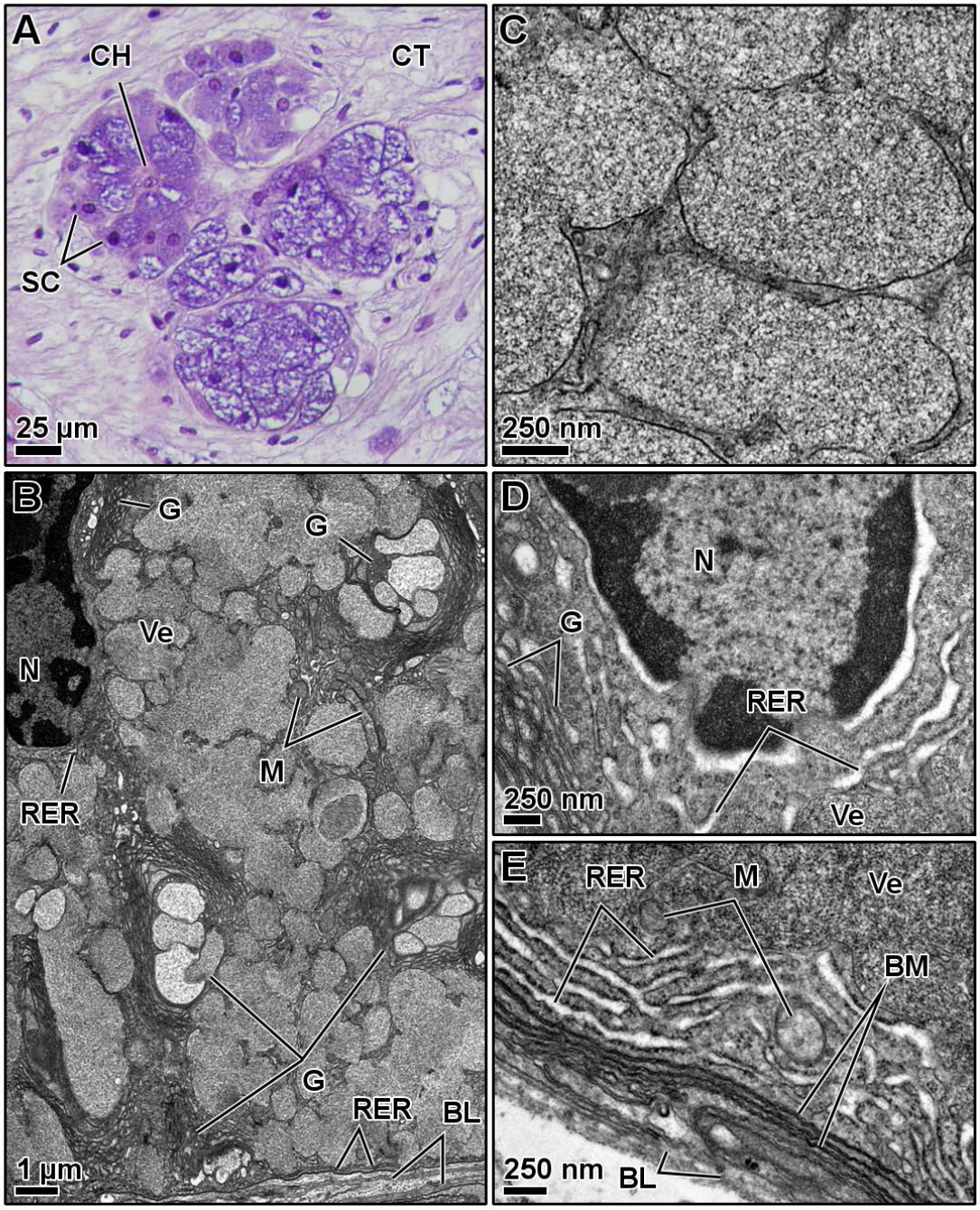

Figure 8. *Maja brachydactyla*. Adult. Esophagus, rosette glands. General view of the rosette glands, H-E (A). General view of the gland cells, TEM (B). Close view of the secretory vesicles (C). Close view of the nucleus and rough endoplasmic reticulum (D). Close view of the basal layer of rough endoplasmic reticulum. Abbreviations: BL, basal lamina; BM, basal membrane; CH, central channel; CT, connective tissue; G, Golgi bodies; N, nucleus; RER, rough endoplasmic reticulum; RG, rosette glands; SC, secretory cells; Ve, vesicles.

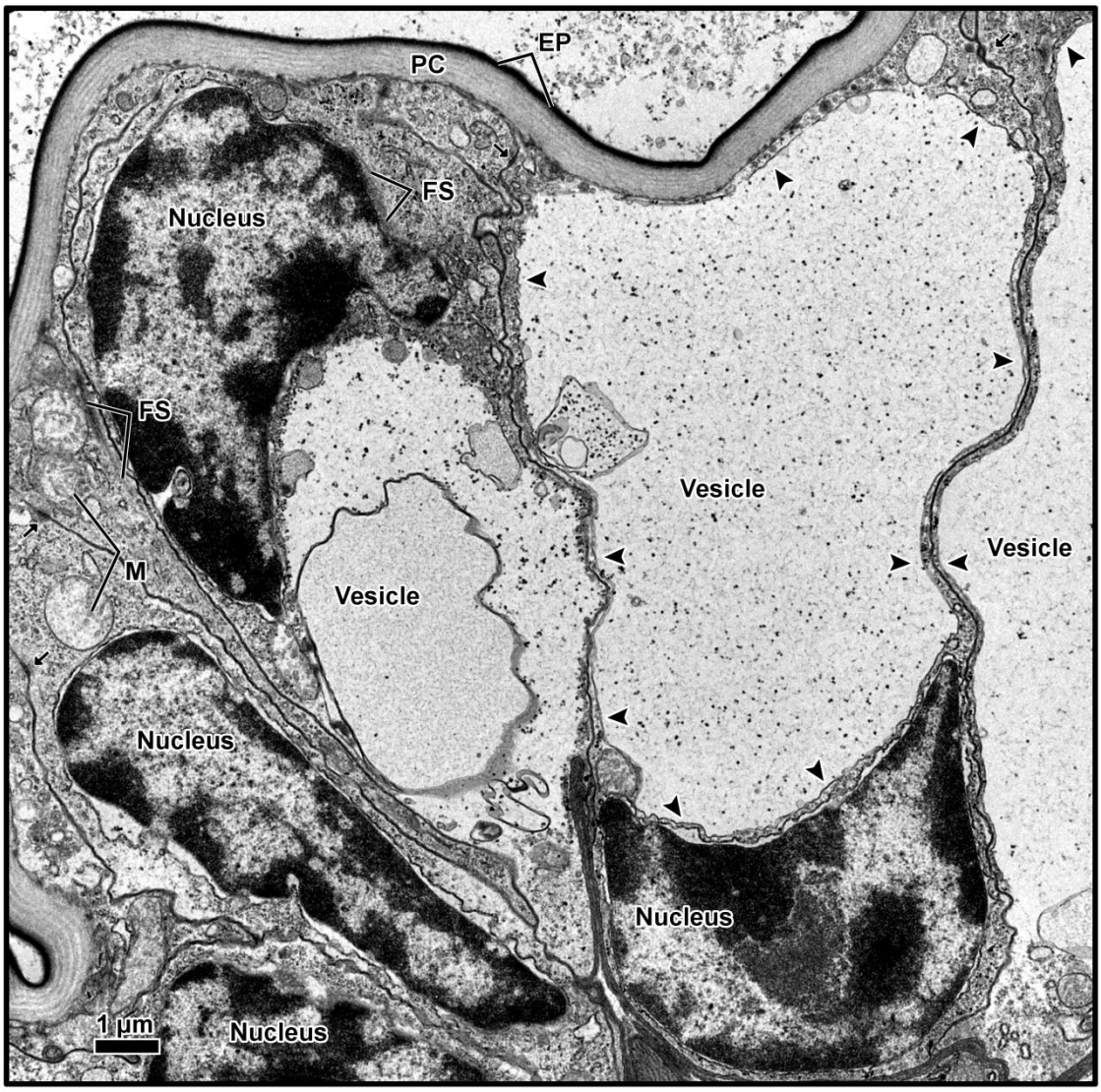

Supplementary Material 1 (Suppl. Mat 1). *Maja brachydactyla*. Zoea I. Esophagus, epithelial cells. TEM. The cell-to-cell junctions are marked by arrows and the single membrane of the vesicles by arrow-heads. Abbreviations: EC, epicuticle; FS, filamentous structures; M, mitochondria; PC, procuticle.

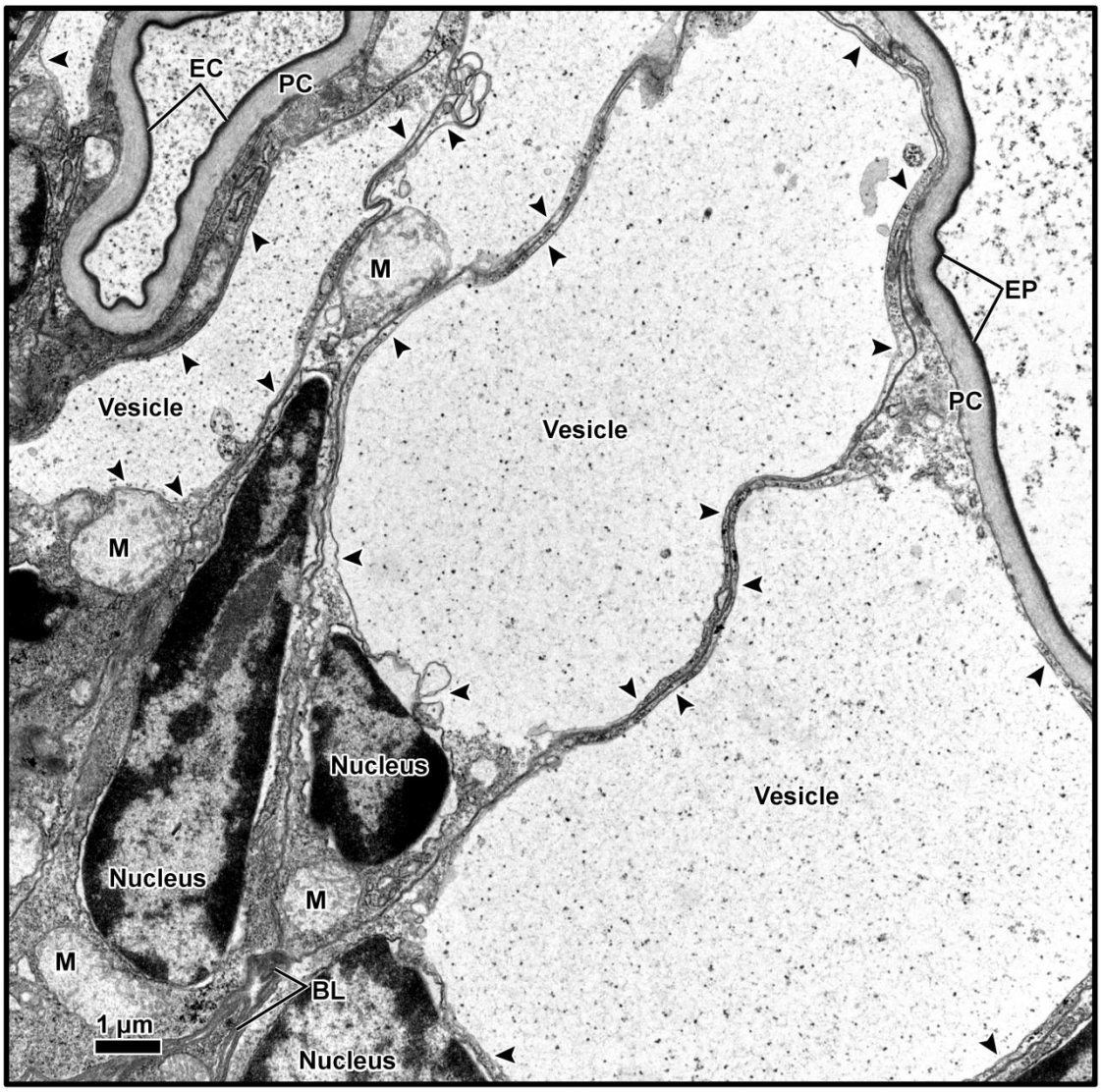

Supplementary Material 2 (Suppl. Mat 2). *Maja brachydactyla*. Zoea I. Esophagus, epithelial cells. TEM. The single membrane of the vesicles are marked by arrow-heads. Abbreviations: EC, epicuticle; M, mitochondria; PC, procuticle.

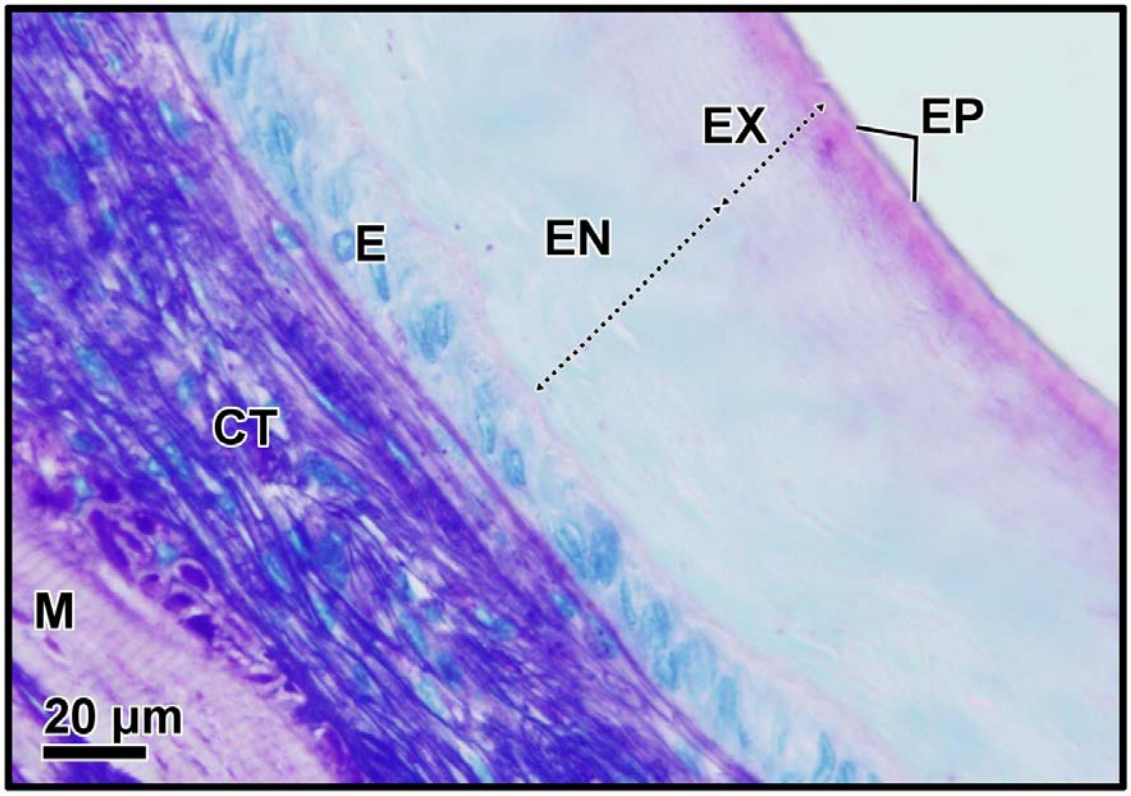

Supplementary Material 3 (Suppl. Mat 3). *Maja brachydactyla*. Adult. Esophagus. Close view of the epithelium, PAS and Methylene Blue. Abbreviations: CT, connective tissue; E, epithelium; EN, endocuticle; EP, epicuticle; EX, exocuticle; M, muscle.

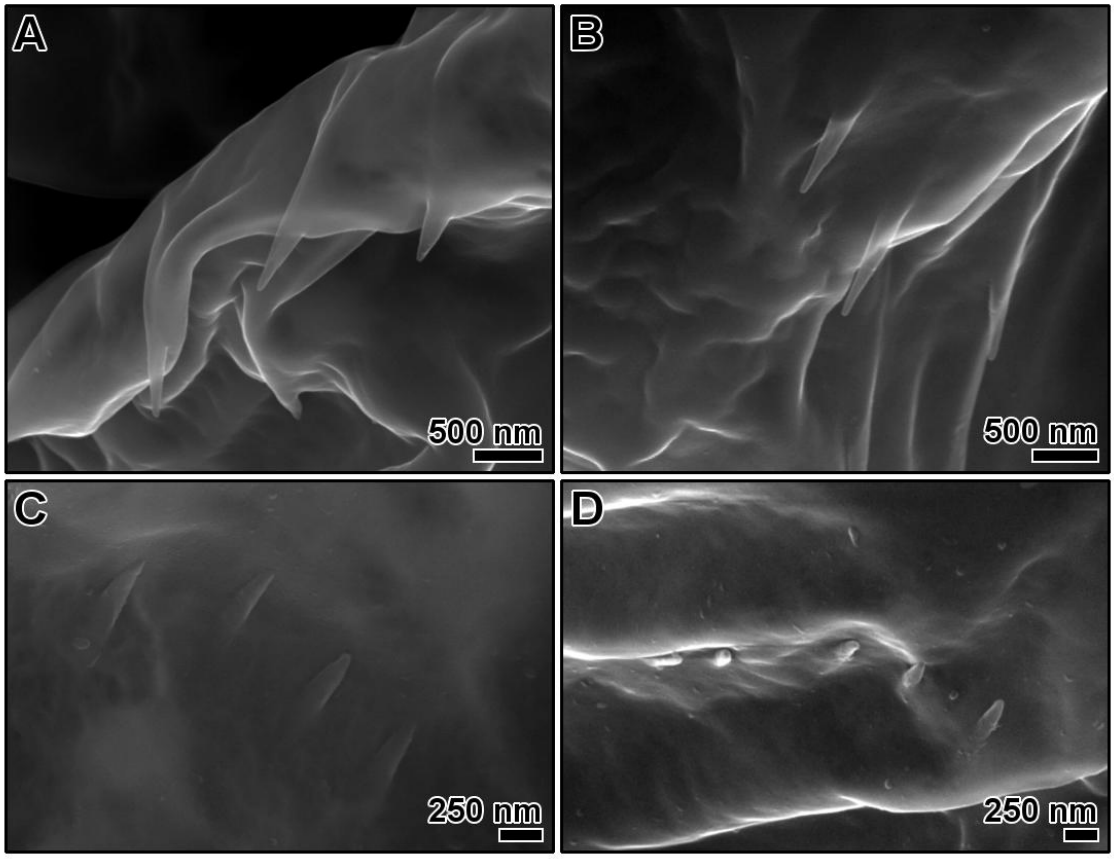

Supplementary Material 4 (Suppl. Mat 4). *Maja brachydactyla*. Zoea I. Esophagus, microspines of the cuticle surface (A-D): three microspines (A), three microspines (B), four microspines (C) and five microspines (D).

6. Bibliography

Alexander CG. 1989. Tegumental glands in the paragnaths of *Palaemon serratus* (Crustacea: Natantia). Journal of the Marine Biological Association of the United Kingdom 69(01):53-63.

Altner H, Hatt H, Altner I. 1986. Structural and functional properties of the mechanoreceptors and chemoreceptors in the anterior oesophageal sensilla of the crayfish, *Astacus astacus*. Cell and Tissue Research 244(3):537-547.

Andrés M, Gisbert E, Díaz M, Moyano FJ, Estévez A, Rotllant G. 2010. Ontogenetic changes in digestive enzymatic capacities of the spider crab, *Maja brachydactyla* (Decapoda: Majidae). J Exp Mar Biol Ecol 389(1-2):75-84.

Barker PL, Gibson R. 1977. Observations on the feeding mechanism, structure of the gut, and digestive physiology of the european lobster *Homarus gammarus* (L.) (Decapoda: Nephropidae). J Exp Mar Biol Ecol 26(3):297-324.

Barker PL, Gibson R. 1978. Observations on the structure of the mouthparts, histology of the alimentary tract, and digestive physiology of the mud crab *Scylla serrata* (Forskål) (Decapoda: Portunidae). J Exp Mar Biol Ecol 32(2):177-196.

Castejón D, Rotllant G, Ribes E, Durfort M, Guerao G. 2015. Foregut morphology and ontogeny of the spider crab *Maja brachydactyla* (Brachyura, Majoidea, Majidae). J Morphol 276(9):1109-1122.

Ceccaldi HJ. 1989. Anatomy and physiology of digestive tract of Crustaceans Decapods reared in aquaculture. Advances in Tropical Aquaculture, Workshop at Tahiti, French Polynesia. Tahiti, French Polynesia: Actes de colloques Ifremer. p 243-259.

Dall W. 1967. The functional anatomy of the digestive tract of a shrimp *Metapenaeus bennettae* Racek & Dall (Crustacea : Decapoda : Penaeidae). Australian Journal of Zoology 15(4):699-714.

De Jong L, Casanova B. 1997. Comparative morphology of the foregut of three *Eucopia* species (Crustacea, Mysidacea, Lophogastrida). Journal of Natural History 31(3):389-402.

Dillaman RM, Roer R, Shafer T, Modla S. 2012. The Crustacean Integument: Structure and Function. In: Watling L, Thiel M, editors. The Natural History of the Crustacea, vol 1 Functional Morphology and Diversity: Oxford University Press. p 140-165.

Doughtie DG, Rao KR. 1982. Rosette glands in the gills of the grass shrimp, *Palaemonetes pugio*. I. Comparative morphology, cyclical activity, and innervation. J Morphol 171(1):41-67.

Elzinga RJ. 1998. Microspines in the alimentary canal of arthropoda, onychophora, annelida. International Journal of Insect Morphology and Embryology 27(4):341-349.

Elzinga RJ, Hopkins TL. 1994. Foregut microspines in four families of cockroaches (Blattaria). International Journal of Insect Morphology and Embryology 23(3):253-260.

Elzinga RJ, Hopkins TL. 1995. Microspine variation in hindgut regions of four families of cockroaches (Blattaria). International Journal of Insect Morphology and Embryology 24(2):203-211.

Erri Babu D, Shyamasundari K, Hanumantha Rao K. 1979. The structure and histochemistry of the oesophageal glands in the crab *Menippe rumphii* (Frabricius) (Crustacea : Brachyura). Proceedings: Animal Sciences 88(4):277-285.

Erri Babu D, Shyamasundari K, Rao KH. 1982. Studies on the digestive system of the crab *Menippe rumphii* (Fabricius) (Crustacea:Brachyura). J Exp Mar Biol Ecol 58(2):175-191.

Factor JR. 1981. Development and metamorphosis of the digestive system of larval lobsters, *Homarus americanus* (Decapoda: Nephropidae). J Morphol 169:225-242.

FAO. 2012. B-42 Crabs, sea-spiders. Capture production by species, fishing areas and countries or areas. In: FAO, editor. FAO yearbook Fishery and aquaculture statistics. Rome: FAO.

Felder DL, Felgenhauer BE. 1993. Morphology of the midgut–hindgut juncture in the ghost shrimp *Lepidophthalmus louisianensis* (Schmitt) (Crustacea: Decapoda: Thalassinidea). Acta Zoologica 74(4):263-276.

Felgenhauer BE. 1992. Chapter 3. Internal Anatomy of the Decapoda: An Overview. In: Harrison FW, Humes AG, editors. Microscopic Anatomy of Invertebrates Volume 10: Decapod Crustacea: Wiley-Liss, Inc. p 45-75.

Friesen JA, Mann KH, Willison JHM. 1986. Gross anatomy and fine structure of the gut of the marine mysid shrimp *Mysis stenolepis* Smith. Canadian Journal of Zoology 64(2):431-441.

Gorvett H. 1946. The Tegumental Glands in the Land Isopoda A. The Rosette Glands. Quarterly Journal of Microscopical Science s2-87:209-235.

Guerao G, Pastor E, Martin J, Andrés M, Estévez A, Grau A, Duran J, Rotllant G. 2008. The larval development of *Maja squinado* and *M. brachydactyla* (Decapoda, Brachyura, Majidae) described from plankton collected and laboratory-reared material. Journal of Natural History 42(33-34):2257-2276.

Guerao G, Simeo CG, Anger K, Urzua A, Rotllant G. 2012. Nutritional vulnerability of early zoea larvae of the crab *Maja brachydactyla* (Brachyura, Majidae). Aquatic Biology 16(3):253-264.

Harris J. 1993. The presence, nature, and role of gut microflora in aquatic invertebrates: A synthesis. Microbial Ecology 25(3):195-231.

Heeren T, Mitchell BD. 1997. Morphology of the mouthparts, gastric mill and digestive tract of the giant crab, *Pseudocarcinus gigas* (Milne Edwards) (Decapoda: Oziidae). Marine and Freshwater Research 48(1):7-18.

Holdich DM, Mayes KR. 1975. A Fine-Structural Re-Examination of the so-called 'Midgut' of the isopod *Porcellio*. Crustaceana 29(2):186-192.

Hopkin SP, Nott JA. 1980. Studies on the digestive cycle of the shore crab *Carcinus maenas* (L.) with special reference to the b cells in the hepatopancreas. Journal of the Marine Biological Association of the United Kingdom 60(04):891-907.

Hunt MJ, Winsor H, Alexander CG. 1992. Feeding by penaeid prawns: the role of the anterior mouthparts. J Exp Mar Biol Ecol 160(1):33-46.

Icely JD, Nott JA. 1984. On the morphology and fine structure of the alimentary canal of *Corophium volutator* (Pallas) (Crustacea: Amphipoda). Philosophical Transactions of the Royal Society of London B, Biological Sciences 306(1126):49-78.

Icely JD, Nott JA. 1992. Digestion and absorption: digestive system and associated organs. In: Harrison FW, Humes AG, editors. Microscopic anatomy of invertebrates: decapod Crustacea. New York: Wiley-Liss. p 147-201.

Jantrarotai PN, Sawanyatiputi SA. 2005. Histological study on the development of digestive system in zoeal stages of mud crab (*Scylla olivacea*). Kasetsart Journal 39(4):666-671.

Johnston DJ, Alexander CG. 1999. Functional morphology of the mouthparts and alimentary tract of the slipper lobster *Thenus orientalis* (Decapoda : Scyllaridae). Marine and Freshwater Research 50(3):213-223.

Johnston DJ, Ritar A. 2002. Mouthpart and foregut ontogeny in phyllosoma larvae of the spiny lobster *Jasus edwardsii* (Decapoda: Palinuridae). Marine and Freshwater Research 52(8):1375-1386.

Johnston M, Johnston D, Knott B. 2008. Ontogenetic changes in the structure and function of the mouthparts and foregut of early and late stage *Panulirus ornatus* (Fabricius, 1798) phyllosomata (Decapoda: Palinuridae). Journal of Crustacean Biology 28(1):46-56.

Johnston MD, Johnston DJ, Richardson AMM. 2004. Mouthpart and digestive tract structure in four talitrid amphipods from a translittoral series in Tasmania. Journal of the Marine Biological Association of the United Kingdom 84(4):717-726.

Komuro T, Yamamoto T. 1968. Fine structure of the epithelium of the gut in the crayfish (*Procambarus clarkii*) with special reference to the cytoplasmic microtutubles. Archivum histologicum japonicum 30(1):17-32.

Loya-Javellana GN, Fielder DR, Thorne MJ. 1994. Ontogeny of foregut in the tropical freshwater crayfish, *Cherax quadricarinatus* Von Martens, 1868 (Parasticidae: Decapoda). Invertebrate Reproduction and Development 25(1):49-58.

McLaughlin PA. 1983. 1. Internal Anatomy. In: Mantel LH, editor. The Biology of Crustacea Vol 5 Internal Anatomy and Physiological Regulation: Academic Press. p 1-52.

Milne-Edwards H. 1834a. Histoire naturelle des crustacés, comprenant l'anatomie, la physiologie et la classification de ces animaux: Libraire Encyclopédique de Roret.

Milne-Edwards H. 1834b. Histoire naturelle des crustacés: atlas: Libraire Encyclopédique de Roret.

Minagawa M, Takashima F. 1994. Developmental changes in larval mouthparts and foregut in the red frog crab, *Ranina ranina* (Decapoda: Raninidae). Aquaculture 126(1-2):61-71.

Mykles DL. 1979. Ultrastructure of alimentary epithelia of lobsters, *Homarus americanus* and *H. gammarus*, and crab, *Cancer magister*. Zoomorphologie 92(3):201-215.

Patwardhan SS. 1935. On the structure and mechanism of the gastric mill in Decapoda. Proceedings of the Indian Academy of Sciences - Section B 1(11):693-704.

Pillai RS. 1960. Studies on the shrimp *Caridina laevis* (Heller) 1. The Digestive System. Journal of the Marine Biological Association of India 2(1):57-74.

Reddy AR. 1937. The physiology of digestion and absorption in the crab *Paratelphusa* (*Oziotelphusa*) *hydrodromus* (Herbst). Proceedings of the Indian Academy of Sciences - Section B 6(3):170-193.

Robertson RM, Laverack MS. 1979. Oesophageal sensors and their modulatory influence on oesophageal peristalsis in the lobster, *Homarus gammarus*. Proceedings of the Royal Society of London Series B Biological Sciences 206(1163):235-263.

Rotllant G, Moyano FJ, Andrés M, Estévez A, Díaz M, Gisbert E. 2010. Effect of delayed first feeding on larval performance of the spider crab *Maja brachydactyla* assessed by digestive enzyme activities and biometric parameters. Marine Biology 157(10):2215-2227.

Schlegel C. 1911. Anatomie sommaire de la première zoé de *Maja squinado* Latr. (Note préliminaire à des recherches sur l'Organogénese des Décapodes brachyoures). Archives de Zoologie Experimentale et Générale 5º Série T. VIII.(2):29-40.

Schmitz EH, Scherrey PM. 1983. Digestive anatomy *Hyalella azteca* (Crustacea, Amphipoda). J Morphol 175:91-100.

Shyamasundari K, Hanumantha Rao K. 1977. Studies on the alimentary canal of amphipods: morphology and histology of cephalic mucous glands. Crustaceana 33(2):149-153.

Shyamasundari K, Hanumantha Rao K. 1978. Studies on the Indian sand lobster *Thenus orientalis* (Lund): mucopolysaccharides of the tegumental glands. Folia Histochemica et Cytochemica 16(3):247-254.

Simeó CG, Andrés M, Estévez A, Rotllant G. 2015. The effect of male absence on the larval production of the spider crab *Maja brachydactyla* Balss, 1922. Aquaculture Research 46(4):937-944.

Sousa L, Petriella AM. 2006. Morphology and histology of *P. argentinus* (Crustacea, Decapoda, Caridea) digestive tract. Biocell 30:287-294.

Spirito CP. 1975. The organization of the crayfish oesophageal nervous system. Journal of comparative physiology 102(3):237-249.

Storch V, Strus J, Brandt A. 2002. Microscopic anatomy and ultrastructure of the digestive system of *Natatolana obtusata* (Vanhöffen, 1914) (Crustacea, Isopoda). Acta Zoologica 83(1):1-14.

Trinadha Babu B, Shyamasundari K, Hanumantha Rao K. 1989. Observations on the morphology and histology of the foregut of *Portunus sanguinolentus* (Crustacea: Brachyura). Folia Morphologica 37(4):364-372.

Tziouveli V, Bastos-Gomez G, Bellwood O. 2011. Functional morphology of mouthparts and digestive system during larval development of the cleaner shrimp *Lysmata amboinensis* (de Man, 1888). J Morphol 272(9):1080-1091.

Vernon GM, Herold L, Witkus ER. 1974. Fine structure of the digestive tract epithelium in the terrestrial isopod. *Armadillidium vulgare*. J Morphol 144(3):337-359.

Vogt G. 1996. Morphology and physiology of digestive epithelia in Decapod crustaceans. Pflügers Archiv 431(6):R239-R240.

Williams RL. 1944. The pre-zoea stage of *Porcellana platycheles* (Pennant). Preliminary anatomical and histological notes. Journal of the Royal Microscopical Society 64(1-2):1-15.

Witkus ER, Grillo RS, Smith WJ. 1969. Microtubule bundles in the hindgut epithelium of the woodlouse *Oniscus ascellus*. Journal of Ultrastructure Research 29(3):182-190.

Yonge CM. 1924. Studies on the comparative physiology of digestion II. - The mechanism of feeding, digestion, and assimilation in *Nephrops norvegicus*. British Journal of Experimental Biology 1:343-389.

Yonge CM. 1932. On the nature and permeability of Chitin. I.--The Chitin lining the Foregut of Decapod Crustacea and the function of the Tegumental Glands. Proceedings of the Royal Society B: Biological Sciences 111(772):298-329.

Zambonino-Infante JL, Gisbert E, Sarasquete C, Navarro I, Gutiérrez J, Cahu CL. 2008. Ontogeny and Physiology of the Digestive System of Marine Fish Larvae. In: Cyrino JEP, editor. Feeding and Digestive Functions in Fishes: CRC Press.

CHAPTER 12.

Foregut Morphology and Ontogeny of the Spider Crab *Maja brachydactyla* (Brachyura, Majoidea, Majidae)

Published in:

Journal of Morphology 276 (9): 1109–1122

Impact factor: 1.521

Foregut morphology and ontogeny of the spider crab *Maja brachydactyla* (Brachyura, Majoidea, Majidae)

Diego Castejón[1*], Guiomar Rotllant[2], Enric Ribes[3], Mercè Durfort[3], and Guillermo Guerao[4]

[1]IRTA, Centre d'Aqüicultura, Ctra. del Poble Nou Km 5.5. 43450, Sant Carles de la Ràpita, Tarragona (Spain).

[2]CSIC, Institut de Ciències del Mar, Passeig Marítim de la Barceloneta 37-49. 08003 Barcelona (Spain).

[3]Dept. Biologia Cel·lular, Fac. Biologia, Universitat de Barcelona, Gran Via de les Corts Catalanes 585. 08007 Barcelona (Spain).

[4]PS Fabra i Puig 344.08028 Barcelona (Spain).

Short title: *Maja brachydactyla* foregut ontogeny

***Corresponding author:** Diego Castejón. E-mail: diego.castejon@irta.cat; phone: +34 681 154 398; postal address: IRTA, Aqüicultura, Cultius Aqüàtics, Ctra. Poble Nou, Km 5.5, 43540 Sant Carles de la Ràpita, Tarragona, Spain.

Abstract

We describe the morphology of the foregut of the spider crab *Maja brachydactyla* Balss, 1922, from first larval stage to adult, with detailed stage-specific documentation using light and scanning electron microscopy. A total of 40 ossicles have been identified in the foregut of adults of *M. brachydactyla* using Alizarin-Red staining. The morphological pattern of the ossicles and gastric mill is very similar to other Majoidea species with only a few variations. The foregut of the zoeae stages appeared as a small and simple cavity, with a cardio-pyloric valve that separates the stomach into cardiac and pyloric regions. The pyloric filter is present from the first zoea, in contrast to the brachyuran species which have an extended larval development. Calcified structures have been identified in the cardio-pyloric valve and pyloric region of the zoeal stages. The most significant changes in foregut morphology take place after the metamorphosis from ZII to megalopa, including the occurrence of the gastric mill. In the megalopa stage, the foregut ossicles are recognizable by their organization and general morphology, but are different from the adult phase in shape and number. Moreover, the gastric teeth show important differences: the cusps of the lateral teeth are sharp (no molariform); the dorsal tooth have a small, dentate cusp (not a well-developed quadrangular cusp); and the accessory teeth are composed of one sharp peak (instead of four sharp peaks). The gastric mill ontogeny from megalopa to adult reveals intermediate morphologies during the earlier juvenile stages. The relationship between gastric mill structures with food preferences and their contribution to the brachyuran phylogeny are briefly discussed.

Keywords: Crustacea; stomach; ossicles; gastric mill; larval development

1. Introduction

The brachyuran foregut, like in other decapods, occupies the anterior part of the cephalothorax. The foregut comprises various structures that carry out specialized functions related to the processing of ingested food: esophagus (swallowing of the food from the mouth to the stomach), cardiac sac (food storage), gastric mill (chewing of the ingested food) and pyloric filter (filtering and transport of chewed food to midgut gland and coarse material to intestines). Traditionally, the esophagus and the anterior part of the stomach (the cardiac sac and gastric mill, inclusive) together were called the "cardiac foregut", while the posterior part of the stomach (that includes pylorus and pyloric filter) was called the "pyloric foregut". These compartments, the cardiac foregut and pyloric foregut are separated by the cardio-pyloric valve (Felgenhauer, 1992; Icely and Nott, 1992; Schaefer, 1970; Stein, 2009; Woods, 1995). According to Felgenhauer (1992) and Lin (2000), the pyloric filters are composed of a complicated setal network organized in ampullary chambers.

The ossicles are structurally relevant features of the decapod foregut. They are calcified structures derived from the cuticle that cover the internal walls of the foregut, whose main role is the shaping and stabilization of the stomach for the correct functioning of the gastric mill and pyloric filter (Felgenhauer, 1992; Icely and Nott, 1992; Schaefer, 1970). A total of 41 ossicles have been described in the brachyuran foregut (Brösing, 2010), organized in a phylogenetically conservative pattern recognizable in other decapod taxa (Meiss and Norman, 1977). The ossicle system of the different brachyuran taxa show variations in the number, shape and position of the ossicles; these variations have been demonstrated to be useful for the study of phylogenetic relationships (Brösing, 2010; Brösing et al., 2007; Brösing and Türkay,

2011; Huespe et al., 2008). The gastric mill is another interesting foregut structure, composed of an unpaired dorsal tooth and paired lateral and accessory teeth, it can provide information about to food resources and the phylogenetic relationships among different taxa (Skilleter and Anderson, 1986).

Major changes have been observed during the ontogeny of the brachyuran foregut morphology: the zoeae foregut lacks the gastric mill and the ossicles, these structures appear for the first time after the metamorphosis to megalopa (Abrunhosa et al., 2003; Castejón et al., 2015; Lumasag et al., 2007; Melo et al., 2006). The knowledge of the morphological development of the foreguts and feeding appendages might assist in identifying appropriate prey characteristics, or in developing diets that meet the nutritional requirements for each life stage of important aquaculture organisms (Abrunhosa and Melo, 2008).

The spider crab, *Maja brachydactyla* is a marine brachyuran of commercial interest widely distributed from the Açores and British Isles to the Sahara, Canary Islands and south-western Mediterranean Sea (Abelló et al., 2014). Many studies have focused on different aspects of their biology: e.g., description of larval stages and molt cycles (Guerao et al., 2008; Guerao and Rotllant, 2010; Guerao et al., 2010), growth patterns (Andrés et al., 2008), biochemistry of the ontogeny (Andrés et al., 2007; Andrés et al., 2010), ovarian maturation (Rotllant et al., 2007), spermatogenesis and histological description of the male reproductive system (Simeó et al., 2010; Simeó et al., 2009a; Simeó et al., 2009b), and aspects of animal production (Alaminos, 2011; Alaminos and Domingues, 2008; Andrés et al., 2011; Domingues and Alaminos, 2008; Domingues et al., 2012; Palma et al., 2008; Verísimo et al., 2011). The larval development of *M. brachydactyla* is abbreviated (like in all known Majoidea) and

consists of two zoeal stages (zoea I and zoea II) and one megalopa stage; the morphology of the larval mouthparts is known in detail (Guerao et al., 2008), but the foregut morphology in larval and postlarval stages has not been previously described.

The main objective of this study was to describe *M. brachydactyla* larval, juvenile and adult foregut morphology; emphasizing the most important changes during ontogeny. The usefulness of the morphology of the ossicle-system as a tool for brachyuran taxonomy and the relationship between gastric mill morphology and food preferences are briefly discussed.

2. Material and Methods

The broodstock of *Maja brachydactyla* Balss, 1922 was captured from the NW Iberian Peninsula coast (Galicia, Spain) and transported to the Institut de Recerca i Tecnologia Agroalimentàries facilities (Tarragona, Spain) in December 2012. The broodstock were kept in 2,000 L cylindrical tanks connected to a recirculation unit maintained at controlled conditions of temperature (18 ± 1ºC), salinity (35 ± 1‰) and photoperiod (12 h light:12 h dark cycle). The broodstock was daily fed with a combination of fresh mussels (*Mytilus* sp. four times per week), frozen mussels (*Mytilus* sp, twice per week) and frozen crabs (*Liocarcinus depurator*, once per week).

The active, newly hatched zoeae I (ZI) were collected from broodstock tanks after hatching and transferred to the culture vessels (600 mL glass beakers filled with 500 mL of filtered seawater) and reared to obtain zoeae II (ZII) and megalopae (M). Larval density was 60 zoeae L^{-1} and 20 megalopae L^{-1}, respectively. The larvae were kept at constant conditions of temperature (18 ± 1 °C), salinity (35 ± 1 ‰) and photoperiod (12 h light: 12 h dark cycle). Water was changed daily and the larvae were

fed with *Artemia* sp. nauplii and metanauplii (INVE Aquaculture Nutrition, Salt Lake UT, USA). The first juveniles (C1) obtained were transferred to 50 L aquarium and raised to juveniles with a cephalothorax length of 8 mm (C_{CL8}). The same environmental conditions (salinity, temperature and photoperiod) used for the larvae were maintained in juvenile culture. The juveniles were fed five times per week with fresh mussels (*Mytilus* sp.).

Adult Foregut

Five adults were dissected the foregut and cleaned by heating in a 10% KOH solution at 80 ºC for 30-60 min. The foreguts were then stained with Alizarin-Red 1% KOH solution according to Brösing (2002; 2010), for revealing calcified structures. After staining, the foreguts were stored in ethanol 70% for posterior observations. The foregut ossicles were described according to the nomenclature of Brösing (2002; 2010; 2014). Observations of the foregut were taken with a Nikon SMZ800 stereomicroscope equipped with an image analyzing system (AnalySIS, SIS, Münster, Germany).

Foregut of the Larvae and Juveniles

Ten fresh individuals of ZI, ZII, M, C1 and five fresh individuals of C_{CL8} were dissected and the foreguts were cleaned by immersion in a 10% KOH solution at 80ºC for 10-15 min and sonicated for 3-5 min in an ultrasonic cleaner. The foreguts of all stages were stained by adding Alizarin-Red 1% KOH solution for 10-15 min. The larvae and juvenile foreguts were observed using either a Nikon SMZ800 stereomicroscope or a LB30T Leica DMLB light microscope (Leica Microsystems GmbH, Wetzlar, Germany) connected to a 12.5 megapixel Olympus DP70 Digital Microscope Camera (Olympus America Inc., New York, USA). The stereo and light

microscopes were equipped with an image analyzing system (AnalySIS, SIS, Münster, Germany). The measurements taken from the foregut of the larvae and juveniles were: foregut length (FL) as the distance from the anterior margin of the cardiac chamber to the posterior margin of the pyloric chamber; and foregut width (FW) as the foregut maximum width of the cardiac chamber.

For the scanning electron microscopy (SEM), the gastric mill of the M, C1 and C_{CL8} were dissected using a Nikon SMZ800 stereomicroscope. The dissected foreguts were immediately sonicated for 2-3 min for removal of surface debris and dehydrated in a graded ethanol series (70%, 90%, and 100%). After the critical-point-drying, individuals were mounted on SEM stubs with self-adhesive carbon stickers and were coated in gold. The dried structures were observed with a Hitachi H-4100 FE SEM in the Barcelona University (UB, Barcelona, Spain).

3. Results

Adult foregut

It has been identified 40 ossicles in the adult foregut of *M. brachydactyla*. The cardiac foregut forms a short esophagus and a sack-like structure with four unpaired and thirteen paired ossicles that support the gastric mill. The cardio-pyloric valve is a rigid structure with one paired and three unpaired ossicles. The pyloric foregut is smaller than the cardiac foregut and contains three unpaired and sixteen paired ossicles as well as the pyloric filter. It is connected to the intestines and midgut gland. A complete list of identified ossicles is given in the Table 1 and their positions are documented in the figures 1A-E.

Ossicles of the dorsal gastric mill

The mesocardiac ossicle (I; Fig. 1E) is a half-moon shaped dorsal plate posteriorly fused to the urocardiac ossicle (VII) and laterally connected to the pterocardiac ossicles (II). The pterocardiac ossicles (II; Fig. 1E) are large, thin plates extending perpendicularly to the longitudinal axis; the Alizarin Red stain reveals anterior parallel plates that could be interpreted as the pre-pterocardiac ossicles (IIa) and posterior parallel plates considered as the post-pterocardiac ossicles (IIb).

The pyloric ossicle (III; Fig. 1D) is an unpaired U-shaped ossicle anteriorly attached to the propyloric ossicle (VI) and laterally to the exopyloric ossicles (IV). The exopyloric ossicles (IV; Fig. 1A, D) are bar shaped structures that connect the pyloric ossicle (III) with the zygocardiac ossicles (V). The zygocardiac ossicles (V; Fig. 1A, E) are large subtriangular plates that carry the lateral teeth of the gastric mill. These heavily sclerotized teeth have a large anterior cusp and two well-developed lateral cusps, the surface of the lateral teeth are smooth and clean (Fig. 4A, F). Externally, the zygocardiac ossicle articulates posteriorly with the exopyloric (IV) and the subdentate (XIV) ossicles (Fig. 1A).

The propyloric ossicle (VI; Fig. 1D) is located dorsally between the urocardiac ossicle (VII) and the pyloric ossicle (III). The length of the urocardiac ossicle (VII; Fig. 1E) is three times the width, with the anterior edge fused to the mesocardiac ossicle (I) and the posterior edge connected to the propyloric ossicle (VI). The postero-ventral portion of the urocardiac ossicle supports a well-developed quadrangular dorsal median tooth with two lateral and smooth cusps on its posterior margin (Fig 4A, J and 5D).

Ossicles of the lateral gastric mill

The pectineal ossicles (VIII; Fig. 1A) are U-shaped ossicles and support the accessory teeth; comprising four or five small, sharp peaks (Fig. 4A and 5H). The pectineal ossicles (VIII) are connected anteriorly with the hook-shaped pre-pectineal ossicles (IX; Fig. 1A), joined in turn with the zygocardiac ossicle (V). Posteriorly, the pectineal ossicles are connected with the fusion of the post-pectineal ossicles (X) and the J-shaped "quill" of the post-pectineal ossicles (Xa); the post-pectineal ossicles (X) (Fig. 1A) are long ossicles parallel to the inferior lateral cardiac ossicles (XIII).

The anterior lateral cardiac plates (XI; Fig. 1A) are half-moon-shaped structures connected posteriorly by an uncalcified cuticle with the ear-shaped posterior lateral cardiac plates (XII). The posterior lateral plates (XII; Fig. 1A) are dorsally and posteriorly connected by the pre-pectineal (IX), the pectineal (VIII), the post-pectineal (X) and the "quill" of the post-pectineal ossicles (Xa).

The inferior lateral cardiac ossicles (XIII; Fig. 1A) are large structures with their anterior margin attached in parallel to the post-pectineal (X) and "quill" of the post-pectineal ossicles (Xa). Their posterior-dorsal margin is connected to the lateral cardio-pyloric ossicle (XV) and the lateral ossicle of the cardio-pyloric valve (XVIII). The subdentate ossicle (XIV; Fig. 1A) connects dorsally with the zygocardiac ossicle (V) and ventrally with the post-pectineal (X) and inferior lateral cardiac ossicles (XIII).

Ossicles of the cardio-pyloric valve

The cardio-pyloric valve is seen as a hemispherical structure in lateral view, sub-triangular in frontal view and "U"-shaped in dorsal view; with a concave anterior

margin and a convex posterior margin. Interiorly it is covered by numerous and small setae (Fig. 5K).

The lateral cardio-pyloric ossicle (XV; Fig. 1A) is a small structure connected dorsally with the anterior supra-ampullary ossicle (XXVIII), posteriorly with the lateral ossicle of the cardio-pyloric valve (XVIII) and ventrally with the inferior lateral cardiac ossicle (XIII). The anterior ossicle of the cardio-pyloric valve (XVI; Fig. 1A) forms a fine plate marked by a calcified line in the middle. The unpaired "U"-shaped posterior ossicle of the cardio-pyloric valve (XVII; Fig. 1B) is fused posteriorly with the anterior inferior pyloric ossicle (XXIII) and anteriorly connects with the lateral ossicles of the cardio-pyloric valve (XVIII). The "paired" lateral ossicle of the cardio-pyloric valve (XVIII) appears fused ventrally (Fig. 1A, B).

Ossicles of the dorsal pyloric foregut

The small, dorsal, bean-shaped anterior mesopyloric ossicles (XIX; Fig. 1A, C and D) are located between the pyloric ossicle (III) and the posterior mesopyloric ossicles (XX). The lateral mesopyloric ossicles (XIXa; Fig. 1A, D) appear as a curved rod structure located below the anterior mesopyloric ossicle (XIX). The posterior mesopyloric ossicles (XX; Fig. 1A, C and D) are half-moon-shaped structures attached laterally to the middle pleuropyloric ossicles (XXXI) and posteriorly with the uropyloric ossicle (XXI).

The uropyloric ossicle (XXI; Fig. 1C, D) is thin and slightly bent, perpendicular to the longitudinal axis in dorsal view and parallel to the longitudinal axis in lateral view. The infra-uropyloric fragments (XXIa; Fig. 1C, D) are located below the uropyloric ossicle (XXI) forming a slightly curved rod over the posterior pleuropyloric

ossicles (XXXIII). The uropyloric ossicle (XXI) continues dorsally with the large stick shaped posterior uropyloric ossicles (XXIb; Fig. 1C).

Ossicles of the lateral and ventral pyloric foregut

The pre-ampullary ossicles (XXII; Fig. 1B) are small ventral plates surrounded by the middle supra-ampullary ossicles (XXIX), the fused unpaired posterior ossicle of the cardio-pyloric valve (XVII) and anterior inferior pyloric ossicle (XXIII), the lateral ossicle of the cardio-pyloric valve (XVIII) and the inferior ampullary ossicles (XXIV). The anterior inferior pyloric ossicle (XXIII; Fig. 1B) is an unpaired oval plate anteriorly fused to the posterior ossicle of the cardio-pyloric valve (XVII) and posteriorly connected to the inferior ampullary ossicles (XXIV).

The inferior ampullary ossicles (XXIV; Fig. 1B, C) appear as pair of fine convex plates that protect the pyloric filter, posterioly are fused to the ampullary roof ossicles (XXVII). The ampullary roof ossicles (XXVII; Fig. 1B, C) are unpaired, large “V”-shaped ossicles connected posteriorly with the supra-ampullary ossicles (XXX).

Both lower portions and upper portions of the ampullary roof ossicles (XXV-XXVI) are fused as enlarged plates (Fig. 1C), connected anteriorly with the anterior process of the ampullary roof ossicles (XXVIa), inverted “L”-shaped ossicles in turn connected with the anterior pleuropyloric ossicles (XXXI). Ventrally the lower and upper portions of the ampullary roof ossicles (XXV-XXVI) are joined to the inferior ampullary ossicle (XXIV), the posterior inferior pyloric ossicle (XXVII) and the supra-ampullary ossicles (XXX).

Supporting ossicles of the lateral pyloric foregut

The anterior supra-ampullary ossicle (XXVIII) is a slightly calcified plate, connected dorsally to the anterior pleuropyloric ossicles (XXXI), ventrally to the lateral cardio-pyloric (XV), and the lateral ossicle of the cardio-pyloric valve (XVIII) and posteriorly with the middle supra-ampullary ossicles (XXIX).

The middle supra-ampullary ossicles (XXIX; Fig. 1B, C) are fine plates projecting from the cuticle as a semicircular plate ventrally attached to the pre-ampullary ossicles (XXII) and the inferior ampullary ossicles (XXIV). Their posterior margin linked to the fused lower and upper portion of the ampullary roof ossicles (XXV-XXVI) and the anterior process of the ampullary-roof-ossicles (XXVIa).

The posterior supra-ampullary ossicles (XXX; Fig. 1B, C) are "T"-shaped structures connected with the terminal margin of upper portion of the ampullary roof ossicles (XXVII) and dorsally attached to the middle pleuropyloric ossicles (XXXII). The anterior pleuropyloric ossicles (XXXI; Fig. 1C, D) are compound by an elongated and curved vertical bar connected with an horizontal, narrow and drop shape plate slightly calcified; the dorsal margin is connected to the posterior mesopyloric ossicles (XX), while ventrally it is attached to the anterior process of the ampullary roof ossicles (XXVIa) and the anterior process of the supra-ampullary ossicles (XXVIII).

The middle pleuropyloric ossicles (XXXII; Fig. 1C) are wide, horizontal plates joined anteriorly with the anterior processes of the ampullary roof ossicles (XXVIa) and posteriorly with the posterior pleuropyloric ossicles (XXXIII). The posterior pleuropyloric ossicles (XXXIII; Fig. 1C) are large subtriangular plates, located behind

the lateral mesopyloric ossicles (XIXa), and posteriorly to the uropyloric ossicles (XXIb).

Foregut of the Zoeal Stages

The foregut of the zoeae of *Maja brachydactyla* has two chambers: the cardiac foregut and the pyloric foregut separated by the cardio-pyloric valve (FL = 750-800 µm in ZI and FL= 900-1,000 µm in ZII). The morphology of the foregut is nearly similar in both zoeal stages, being characterized by the simplicity of the cardiac chamber and the absence of the ossicle system and the gastric mill (Fig. 2A-D).

The morphology of the cardio-pyloric valve is similar to that of the adult: hemispherical in lateral view, sub-triangular in frontal view, and "U"-shaped in dorsal view; with a concave anterior margin and a convex posterior margin (Fig. 2A-E). The cardio-pyloric valve presents tiny setae grouped in small clusters in the anterior margin, fine spinous setae in the lateral margin and long thickened setae crowned by small sharp protuberances in the posterior-lateral margin (Fig. 2E, F). The Alizarin Red staining reveals that the cardio-pyloric valve is a calcified structure with a calcium-rich basin (Fig. 2A, B, and D).

The pyloric foregut supports an inter-ampullary septum with a row of elongate medium setae. A well-developed pyloric filter is present from the ZI stage, filling the entire inferior portion of the chamber. In the ZI stage 3-4 ampullary chambers are visible and in the ZII stage there are 5-6 ampullary chambers (Fig. 2B, C). The Alizarin Red staining reveals a pair of terminal calcified "supra-ampullary ossicles-like" structures (Fig. 2D).

Foregut of the Megalopa Stage

The foregut of the megalopa stage (Fig. 3A, B) is more developed and more complex as compared to the zoeal stages. Important changes are observed in the general shape and size (approximate FL = 1,500 µm; approximate FW = 950 µm). The cardiac foregut is enlarged laterally, acquiring the adult sac-like morphology (Fig. 3B). The ossicle system and gastric mill appear for the first time. However compared to the adult, many ossicles have a different shape and position and others are missing. Therefore, we describe only the ossicles we can clearly identify. The ossicles of the gastric mill show a pronounced adult-like morphology, while the gastric mill teeth are markedly different: the mesocardiac ossicle (I) appears laterally connected with pterocardiacs ossicles (II) and it is posteriorly fused with urocardiac ossicles (VII; Fig. 3B). The zygocardiac ossicles (V; Fig 3B) are large subtriangular plates, although the highly calcified margins contrast with the poorly calcified central area, resulting in a "V"-shaped appearance. The lateral teeth associated to the zygocardiac ossicles have three small lateral dentate cusps surrounded by small peaks, crowned posteriorly by 13-15 partially scaly setae (Fig. 4B, C). The propyloric ossicle (VI) differs from the adult, in that it is a "Y"-shaped structure ventrally connected to the posterior edge of the urocardiac ossicle (VII; Fig. 3B). Similarly as in the adults, the length of the urocardiac ossicle (VII) is nearly three times the width and bears the dorsal tooth in the posterior edge; however, unlike the adult, this dorsal tooth contains one small, dentate cusp and 7-12 long lateral spines (Fig. 4G and 5A). The pectineal ossicles (VIII) are small ossicles that support the accessory teeth, composed by one forked peak surrounded laterally by 5-6 large scaly setae (Fig. 5E). The pectineal ossicles (VIII) are connected anteriorly with the curved

rod-shaped prepectineal ossicles (IX) and posteriorly with the enlarged rod-shape post-pectineal ossicles (X; Fig. 3A).

The cardio-pyloric valve is intensively calcified and its morphology is similar to that of the juveniles and adults. The anterior margin of the cardio-pyloric valve is covered by numerous clusters of tiny setae; the posterior and lateral margins lack the long thickened setae characteristic of the zoeae while presenting numerous long and scaly setae (Fig. 5I). The pyloric filter has a high number of food grooves. The inter-ampullary net is composed of rows of elongate setae, and a minimum of seven ampullary chambers have been identified (Fig. 3A). The anterior ossicle of the cardio-pyloric valve (XVI) has a similar shape and position as in the adult (Fig. 3A). However, in the megalopa the majority of the ossicles of the pyloric foregut have a shape that differs from the adult. The inferior ampullar ossicles (XXIV) appear as thin plates poorly calcified that ventrally cover the pyloric filter (Fig. 3A). Ventral to the posterior edge of the cardio-pyloric valve we found structures that resemble the adult middle supra-ampullary-like ossicles (XXIX-like; Fig. 3A). The anterior pleuropyloric ossicles (XXXI; Fig 3A, B) are vertical and curved bars connected posteriorly with the middle pleuropyloric-like ossicles (XXXII-like; Fig. 3A). The posterior supra-ampullary ossicles (XXX; Fig. 3A, B) appear in the posterior-ventral margin as a curved rod whose morphology is similar to the adults and the calcified structures seen during the zoeal stages. In the pyloric foregut, some unidentified ossicles with a thin rod-shape have been observed in the posterior-dorsal margin, that have been named the uropyloric-like (XXI-like) and posterior pleuropyloric-like (XXXIII-like) ossicles (Fig. 3B).

Foregut of the C1 stage

The morphology of the foregut at juvenile stage is more similar to that of the adult than to the megalopa (Fig. 3C, D). New ossicles appear for the first juvenile, and there are others that are identifiable. In relation to the cardiac foregut and gastric mill associated ossicles, the inferior lateral cardiac (XIII; Fig. 3C) and the subdentate ossicles (XIV; Fig. 3C) appear with an adult shape and position. Also the anterior lateral cardiac plates (XI) and the posterior lateral cardiac plates (XII) can be observed as slightly calcified structures (Fig. 3C). The gastric mill teeth are retained and acquire an intermediate morphology between the megalopa and the C_{CL8} juvenile. The dorsal tooth bears one small and dentate cusp whose relative size is higher than in the megalopa stage, the lateral spines become thicker and their number is reduced to seven (Fig. 4H and 5B). The lateral teeth show three big lateral dentate and conical cusps; posteriorly there appear approximately 20 spinous setae (Fig. 4D). The accessory teeth are composed of two peaks surrounded by 5-6 long lateral setae (Fig. 5F).

The cardio-pyloric valve is similar to that of the adult. The anterior margin is covered by fine setae, while the posterior and lateral margins show long and scaly setae similar as in the megalopae (Fig. 5J). New ossicles appear in the dorsal pyloric foregut: the small, fine and enlarged anterior mesopyloric ossicles (XIX; 3C, D) are attached posteriorly with the bean-shaped mesopyloric ossicles (XX; 3C, D), which are in turn connected laterally to the middle pleuropyloric ossicles (XXXI; Fig. 3C). Like in the adults, the uropyloric ossicle (XXI; 3C, D) is thin and slightly bent perpendicular to longitudinal axis. Ventrally are identifiable the lateral ossicles of the cardio-pyloric valve (XVIII; Fig. 3C) and the small, paired pre-ampullary-like ossicles (XXII-like). At

this stage of development the middle supra-ampullary ossicles (XXIX) are most notable (Fig. 3C).

Foregut of the C_{CL8} stage

The morphology of the foregut at this stage is adult-like in shape (Fig. 3E, F). All the cardiac and gastric mill associated ossicles have an adult morphology; these being: the mesocardiac (I), pterocardiacs (II), zygocardiacs (V), propyloric (VI), urocardiac (VII), pectineal (VIII), prepectineal (IX), postpectineal (X), anterior lateral cardiac plates (XI), posterior lateral cardiac plates (XII), lateral cardiac (XIII) and subdentate (XIV) ossicles (Fig. 3E, F). The C_{CL8} juvenile gastric mill shows an intermediate morphology between the C1 and adult gastric mill. The dorsal tooth supports a well-developed quadrangular dorsal median tooth with two lateral conical cusps on its posterior margin (Fig. 4I and 5C). The lateral teeth show a large anterior and two well-developed ventral cusps more conical than in the adult stage, the surface of the lateral teeth are smooth and clean; no terminal setae have been found posteriorly (Fig. 4E). The accessory teeth are composed of four peaks surrounded laterally by more than 20 large spinous setae (Fig. 5G). Also, the unpaired pyloric ossicle (III; Fig. 3F) has an adult shape, i.e., as a broad dorsal plate posterior to the propyloric ossicle (VI). The exopyloric ossicles (IV) were located between the pyloric (III) and the zygocardiac (V) ossicles (Fig. 3F).

The pyloric foregut ossicles also show an adult shape and position. Different to the foregut of C1 stage, however, the foregut of C_{CL8} stage has the lateral mesopyloric (XIXa), the infra-uropyloric fragments (XXIa) and the posterior uropyloric ossicles (XXIb) in dorsal position as thin bar-shaped ossicles parallel to the longitudinal axis (Fig. 3E, F). In the cardio-pyloric valve it also can be observed the lateral cardio-pyloric

ossicle (XV) dorsal to the anterior supra-ampullary ossicle (XXVIII; Fig. 3E). Dorsal to the pyloric filters and in a similar position as in the adults, there appears the lower and upper portion of the ampullary roof ossicles (XXV-XXVI) fused with the anterior processes of the ampullary roof ossicles (XXVIa).

4. Discussion

The Adult Foregut

The first description of the foregut morphology in the genus *Maja* (identified as *Maja squinado*) was published by Milne-Edwards (1840). His description included the traditional subdivision in the cardiac and pyloric foregut, the gastric mill and some ossicles that according to Brösing et al. (2002) could be named as: mesocardiac (I), pterocardiacs (II), pyloric (III), zygocardiacs (V), urocardiac (VII), inferior ampullary (XXIV) and two additional unidentified pyloric ossicles. We present a more detailed description of the foregut of *M. brachydactyla*. The foregut ossicles have a relatively constant morphology previously described among species of Majoidea: *Libinia emarginata* Leach, 1815 (Epialtidae) (Meiss and Norman, 1977); *Inachus dorsettensis* (Pennant, 1777) (Inachidae) (Brösing, 2010); and *Maja crispata* Risso, 1827 (Majidae) (Brösing, 2014). Although the morphological pattern of the ossicle system is similar within these species, the similarities are higher between the congeneric majid species *M. brachydactyla* and *M. crispata* (Brösing, 2014). However, our interpretation of the dorsal ossicles is different when compared to the description of *M. crispata* (Brösing, 2014). The pyloric ossicle (III) appears paired in *M. crispata* while in *M. brachydactyla* it appears unpaired, like in *L. emarginata* and *I. dorsettensis*. Also, the anterior mesopyloric ossicles (XIX) and the posterior mesopyloric ossicles (XX) of *M. crispata* are interpreted in the present work as the lateral mesopyloric ossicles (XIXa) and the

anterior mesopyloric ossicles (XIX), respectively; while the posterior mesopyloric ossicles (XX) of *M. brachydactyla* appears in *M. crispata* scheme as a unlabelled ossicle located anteriorly to the uropyloric ossicle (XXI) in the dorsal view, in the same position as in *I. dorsettensis*. Additionally, the pre-pterocardiac and post-pterocardiac ossicles (IIa and IIb) and the anterior lateral cardiac plates (XI) have been described for the first time in the genus *Maja*. The brachyuran foregut possesses a conservative pattern among the species of one family or among the species of close-related families, which makes them useful for phylogenetic reconstructions (Brösing, 2010; Brösing et al., 2002; Brösing et al., 2007; Reimann et al., 2011). In this sense, our data support the structure of the superfamily Majoidea (Brösing et al., 2007) based in the phylogenetic analysis of the ossicle system: *Hyas araneus* Linnaeus, 1758, *Hyas coarctatus* Leach, 1815 and *Libinia dubia* H. Milne Edwards, 1834 comprising a monophyletic clade with *Inachus dorsettensis* (Pennant, 1777) as a sister group. The monophyly of the Majoidea superfamily, including the family Inachidae, is supported by larval morphology and genetic studies (Hultgren and Stachowicz, 2008). All these data support the usefulness of the general morphology of the ossicle-system for the phylogenetic studies (Brösing, 2010; Brösing et al., 2002; Brösing et al., 2007; Reimann et al., 2011).

The gastric mill is a cardiac structure whose function is to bite and grind the food particles (Nakamura and Takemoto, 1986). In the carnivorous and omnivorous species the medial tooth possessed a large, rounded posterior process which in action with the smooth surface of the lateral teeth act like a mortar and pestle useful to crush and mill calcified shells (Allardyce and Linton, 2010). We found a similar morphology in the gastric mill of *M. brachydactyla*, and therefore the ability to crush the mollusc shells, operculi fragments, echinodermata dermic plates and calcareous seaweeds

revealed in the stomach content of wild specimens (Bernárdez et al., 2000) could be expected. However, as *M. brachydactyla* (Bernárdez et al., 2000), some marine brachyuran species studied have opportunistic feeding habits (Cannicci et al., 2007; Norman and Jones, 1992; Vannini et al., 1989). In this sense, the morphology of the gastric mill teeth of these brachyuran crabs will be more closely related to phylogeny rather than to their feeding behaviour. Huespe et al. (2008) and Sakai et al. (2006) noted the relevance and utility of the dorsal and lateral gastric mill teeth morphology in taxonomical studies. The morphology of the gastric mill teeth of other species of the superfamily Majoidea belonging to the genera *Inachus* (Brösing, 2010) is clearly different to that of *Maja brachydactyla*. These data support the potential utility of the gastric mill for the study of the brachyuran phylogenetic relationships.

The Zoeae Foregut

Like in other Majoidea species, *M. bracydactyla* larval development is abbreviated to two zoeae and one megalopa (Guerao et al., 2008). The description of the morphology of the *M. brachydactyla* zoeae foregut is in agreement with the traditional description for the zoeae foregut among the brachyuran species: a simple structure that lacks the gastric mill and ossicles; with cardiac and pyloric foregut separated by the cardio-pyloric valve, a well-developed structure covered by large thickened setae with a poorly understood role in the processing of food (Abrunhosa and Melo, 2008; Abrunhosa et al., 2003; Abrunhosa et al., 2011; Castejón et al., 2015; Lumasag et al., 2007; Melo et al., 2006). The present work described for first time the presence of a calcified cardio-pyloric valve and paired “supra-ampullary ossicle-like” structures in the ZI and ZII stages.

The first zoea of *M. brachydactyla* also has a well-developed pyloric filter. This situation is rather different as compared to other brachyuran species with extended larval development, where their first zoea lacks the pyloric filter or it is undeveloped as in *Ucides cordatus* (Linnaeus, 1763) (Abrunhosa et al., 2003), *Uca vocator* (Herbst, 1804) (Abrunhosa et al., 2011) and *Dyspanopeus sayi* (Smith, 1869) (Castejón et al., 2015). Abbreviated larval development affect the timing of appearance and rate of development of many larval features. These changes in the development can be attributed to heterochronic processes resulting from the dissociation of age, size, and shape between ancestral and descendant ontogeny (Clark, 2005; Clark et al., 2005; Gerber and Hopkins, 2011; Raff and Raff, 2000; Reilly et al., 1997). In *M. brachydactyla*, heterochrony during embryonic development could affect the onset of the pyloric filter, whose appearance is earlier relative to the ancestral condition.

Additionally, some authors (Abrunhosa et al., 2003; Abrunhosa et al., 2011; Icely and Nott, 1992; Meiss and Norman, 1977; Melo et al., 2006) suggest that the presence of a pyloric filter in the first zoeae of brachyurans with abbreviated larval development could be related to the life-strategy and feeding behavior; numerous setae and a well-developed pyloric filter are necessary for the processing and mixing of soft food particles. Melo et al. (2006) observed that the first zoea of the brachyuran *Sesarma curacaoense* De Man, 1892 is a facultative lecithotrophic, lacking the pyloric filter; while the first zoea of *M. brachydactyla* is an obligatory planktotroph that must feed to achieve the next stage of development (Guerao et al., 2012). Therefore, we suggest that the pyloric filter is necessary in the zoeae stages to avoid those large food particles that are introduced into the digestive gland and the intestines.

The Megalopae and Juvenile Foregut

After the metamorphosis to megalopa, major changes occur in the foregut with the appearance of the main foregut ossicles and a functional gastric mill. This foregut metamorphosis has been observed in other brachyuran species as *Dyspanopeus sayi* (Smith, 1869) (Panopeidae) (Castejón et al., 2015), *Menippe mercenaria* Say, 1818 (Oziidae) (Factor, 1982), *Panopeus occidentalis* De Saussure, 1857 (Panopeidae) (Abrunhosa et al., 2011), *Sesarma rectum* Randall, 1840 (Sesarmidae) (Abrunhosa and Melo, 2008), *Uca vocator* (Herbst, 1804) (Ocypodidae) (Abrunhosa et al., 2011) and *Ucides cordatus* (Linnaeus, 1763) (Ucididae) (Abrunhosa et al., 2003).

As a consequence of the zoeal metamorphosis of the brachyuran crabs, Factor (1981; 1982) suggests that the mastication of food shifts from the mandibles to the gastric mill. These morphological changes from the zoea foregut to the megalopa foregut could correspond to changes in the environment and diet that take place at metamorphosis, when the previously planktonic larvae begin their benthic life and there is a need to process food more efficiently in this new environment. In this sense, some authors also described an inverse relation in complexity between gastric mill and mouthparts, where in many taxa the increase of complexity in the gastric mill is parallel to a decrease of complexity in mouthparts (Guillaume and Ceccaldi, 2011; Meiss and Norman, 1977). In *M. brachydactyla*, Guerao et al. (2008) also observed that mandibles morphology was simplified after metamorphosis and in the present study we observed the complexity of the gastric mill after the metamorphosis.

In the present study, the ontogenetic changes in the morphology of the ossicle-system and gastric mill teeth from megalopa to adult stage are described for the first time in brachyuran crabs. The megalopa cardiac foregut ossicles are similar to their

counterparts in the juveniles and adult stages. A similar situation has been observed in the megalopa foregut of *D. sayi* (Castejón et al., 2015). We suggest that the advanced adult-like morphology of the megalopa cardiac foregut could be related with the functional requirements of the gastric mill (Factor, 1982; Nakamura and Takemoto, 1986; Woods, 1995). On the contrary, as has been observed in *D. sayi* (Castejón et al., 2015), the megalopa pyloric foregut lacks many adult ossicles and show other ossicles that cannot be identify properly in the juvenile or adult foregut: the middle supra-ampullary-like (XXIX-like), the posterior uropyloric-like (XXIb-like), the middle pleuropyloric-like (XXXII-like) and the posterior pleuropyloric-like ossicles (XXXIII-like). The definitive adult-shape ossicles gradually appear during the postlarval development. This gradual development could be explained if the pyloric foregut did not require highly specialized associated ossicles during the earlier developmental stages, as has been observed in the zoeal phase. The present results also reveals that the morphology of megalopa gastric mill teeth of *M. brachydactyla* is rather different from the adult gastric mill teeth, as was described previously in *D. sayi* (Castejón et al., 2015). Additionally, in both species the dorsal tooth of the megalopa gastric mill showed a similar structure: lateral spines and a small and dentate cusp. The first juvenile gastric mill is similar to the megalopa gastric mill, remaining different to that of the adult in shape and morphometric structure, while the gastric mill of the C_{CL8} juveniles have an intermediate morphology between that of the first juvenile and the adult. Factor (1982) also showed that the juvenile gastric mill of the stone crab *M. mercenaria* has a slightly different morphology from the adult gastric mill, but no details about the age or size of juveniles were provided.

These changes in gastric mill morphology could be related to modifications in prey preferences and/or prey availability in the new environments. Relationship between the diet and crab size has been described in many brachyuran species: the small individuals of *Matuta lunaris* (Forskål, 1775) fed primarily on small crustaceans (sergestids and copepods) while large individuals fed primarily on anomurans and gastropods (Perez and Bellwood, 1988); the predation over the polychaetes increases with the size of the crab in *Chionoecetes opilio* (O. Fabricius, 1788) (Kolts et al., 2013); the juveniles of *Callinectes sapidus* (Rathbun, 1896) ingest more polychaetes and less bivalves and crustaceans than the adults (Seitz et al., 2011). Additionally, prey size selection in relation to corporal size has been observed in the brachyuran *Carcinus maenas* (Linnaeus, 1758) and *Cancer pagurus* Linnaeus, 1758 (Mascaró and Seed, 2001). The ontogenetic change in the diet also has been reported in other decapoda groups, e.g., the Caridea *Palaemon serratus* (Pennat, 1777) (Guerao and Ribera, 1996), the Achelata *Jasus lalandii* (H. Milne-Edwards, 1837) (Haley et al., 2011) or the Achelata *Panulirus argus* Latreille, 1804 (Briones-Fourzán et al., 2003). Therefore, we suggest that the morphology of the teeth (with sharper and less crushing cusps) of the megalopae and earlier juveniles could be related with a soft prey diet such as copepods and amphipods; while the molariform structure of the adult teeth is suitable for crushing food pieces protected by hard shells (bivalves, gastropods, echinoderms and calcareous seaweeds) as feeding studies have demonstrated (Bernárdez et al., 2000). For elucidation of this hypothesis, further studies on the relation of the natural diet of the megalopa and earlier juvenile stages of *M. brachydactyla* are needed.

5. Acknowledgements

Bench fees were funded by the INIA (RTA2011-00004-00-00) to G.G. Funding to D. C. (FPI-INIA predoctoral fellowship, RTA2011-00004-00-00) was provided by the Spanish Ministry of Economy and Competitiveness. The authors would like to thank Karl B. Andree and Alicia Estevez for their comments that have greatly improved the paper. The authors are grateful to the personnel of the Scientific Technical Services of Barcelona University for their support in sample preparation for SEM observations. We thank hatchery technician at IRTA in Sant Carles de la Ràpita.

IMPORTANT NOTE: The size of the stomach during the larval and first juvenile stages is erroneous, as well the scales of the Fig. 2 and 3. These data has been corrected in the next chapter (see chapter 13).

Table 1. Nomenclature of the identified ossicles in adults of *M. brachydactyla*.

	Ossicles of dorsal gastric mill	
I	mesocardiac ossicle	unpaired
II	pterocardiac ossicles	paired
IIa	pre-pterocardiac ossicles	paired
IIb	post-pterocardiac ossicles	paired
III	pyloric ossicle	unpaired
IV	exopyloric ossicles	paired
V	zygocardiac ossicles	paired
VI	propyloric ossicle	unpaired
VII	urocardiac ossicle	unpaired
	Ossicles of the lateral gastric mill	
VIII	pectineal ossicles	paired
IX	pre-pectineal ossicles	paired
X	post-pectineal ossicles	paired
Xa	“quill” of the post-pectineal ossicles	paired
XI	anterior lateral cardiac plates	paired
XII	posterior lateral cardiac plates	paired
XIII	inferior lateral cardiac ossicles	paired
XIV	subdentate ossicles	paired
	Ossicles of the cardio-pyloric valve	
XV	lateral cardio-pyloric ossicles	paired
XVI	anterior ossicle of the cardio-pyloric valve	unpaired
XVII	posterior ossicle of the cardio-pyloric valve	unpaired
XVIII	lateral ossicle of the cardio-pyloric valve	unpaired

Table 1 (continuation). Nomenclature of the identified ossicles in adults of *M. brachydactyla*.

	Ossicles of the dorsal pyloric foregut	
XIX	anterior mesopyloric ossicle	paired
XIXa	lateral mesopyloric ossicles	paired
XX	posterior mesopyloric ossicles	paired
XXI	uropyloric ossicle	unpaired
XXIa	infra-uropyloric fragments	paired
XXIb	posterior uropyloric ossicles	paired
	Ossicles of the lateral & ventral pyloric foregut	
XXII	pre-ampullary ossicles	paired
XXIII	anterior inferior pyloric ossicle	unpaired
XXIV	inferior ampullary ossicles	paired
XXV	ampullary-roof-ossicles, lower portion	paired
XXVI	ampullary-roof-ossicles, upper portion	paired
XXVIa	anterior process of the ampullary roof ossicles, upper portion	paired
XXVII	posterior inferior pyloric ossicle	unpaired
	Supporting ossicles of the lateral foregut	
XXVIII	anterior supra-ampullary ossicles	paired
XXIX	middle supra-ampullary ossicles	paired
XXX	posterior supra-ampullary ossicles	paired
XXXI	anterior pleuropyloric ossicles	paired
XXXII	middle pleuropyloric ossicles	paired
XXXIII	posterior pleuropyloric ossicles	paired

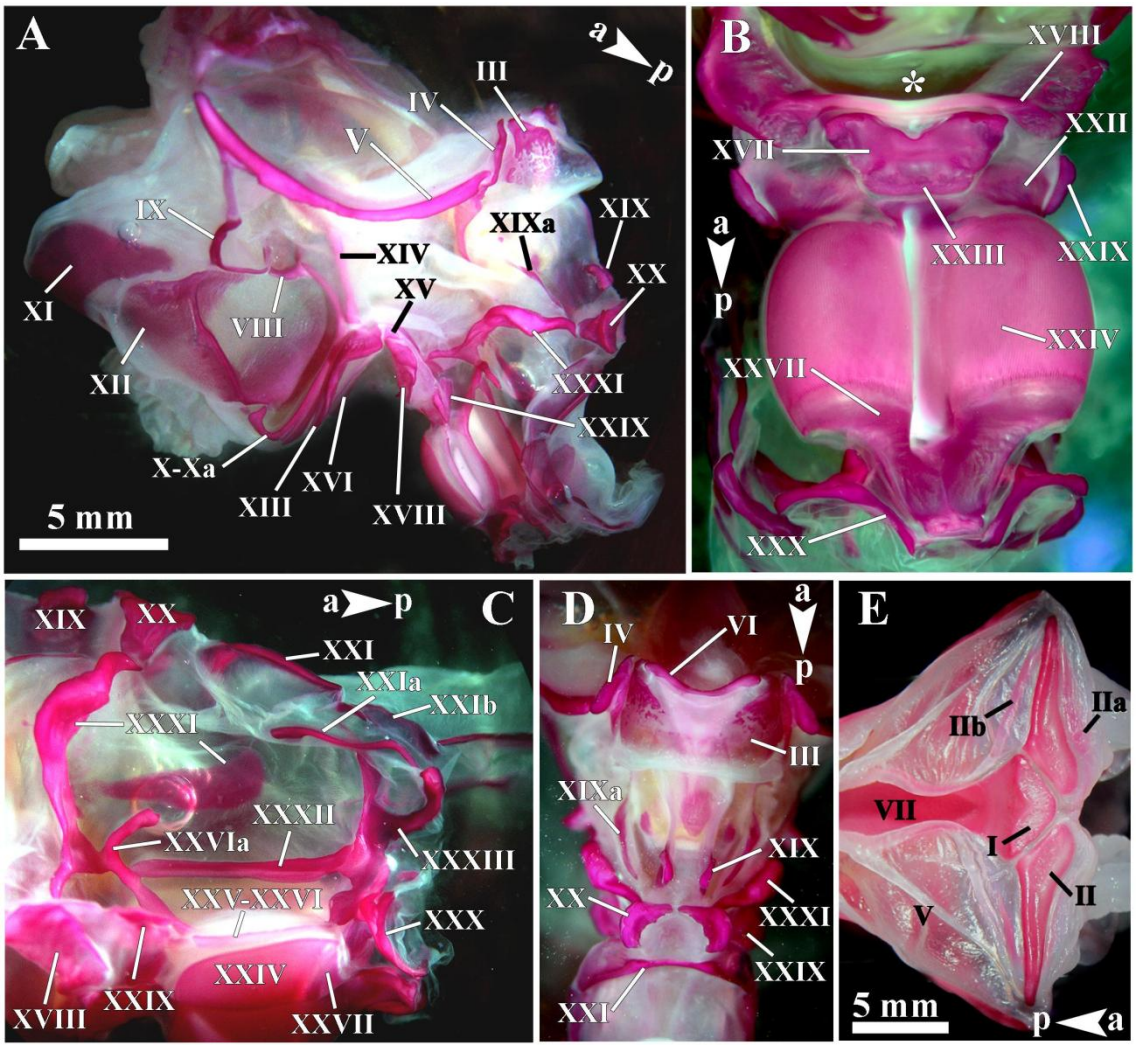

Figure 1. *Maja brachydactyla*. Foregut of the adult stained with Alizarin Red. Foregut lateral view, stereo microscope image (A). Pyloric foregut ventral view, stereo microscope image (B). Pyloric foregut lateral view, stereo microscope image (C). Pyloric foregut dorsal view, stereo microscope image (D). Cardiac foregut dorsal view, stereo microscope image (E). Abbreviations: (*), position of the cardio-pyloric valve; a > p, anterior to posterior margin. For ossicles nomenclature sees Table 1.

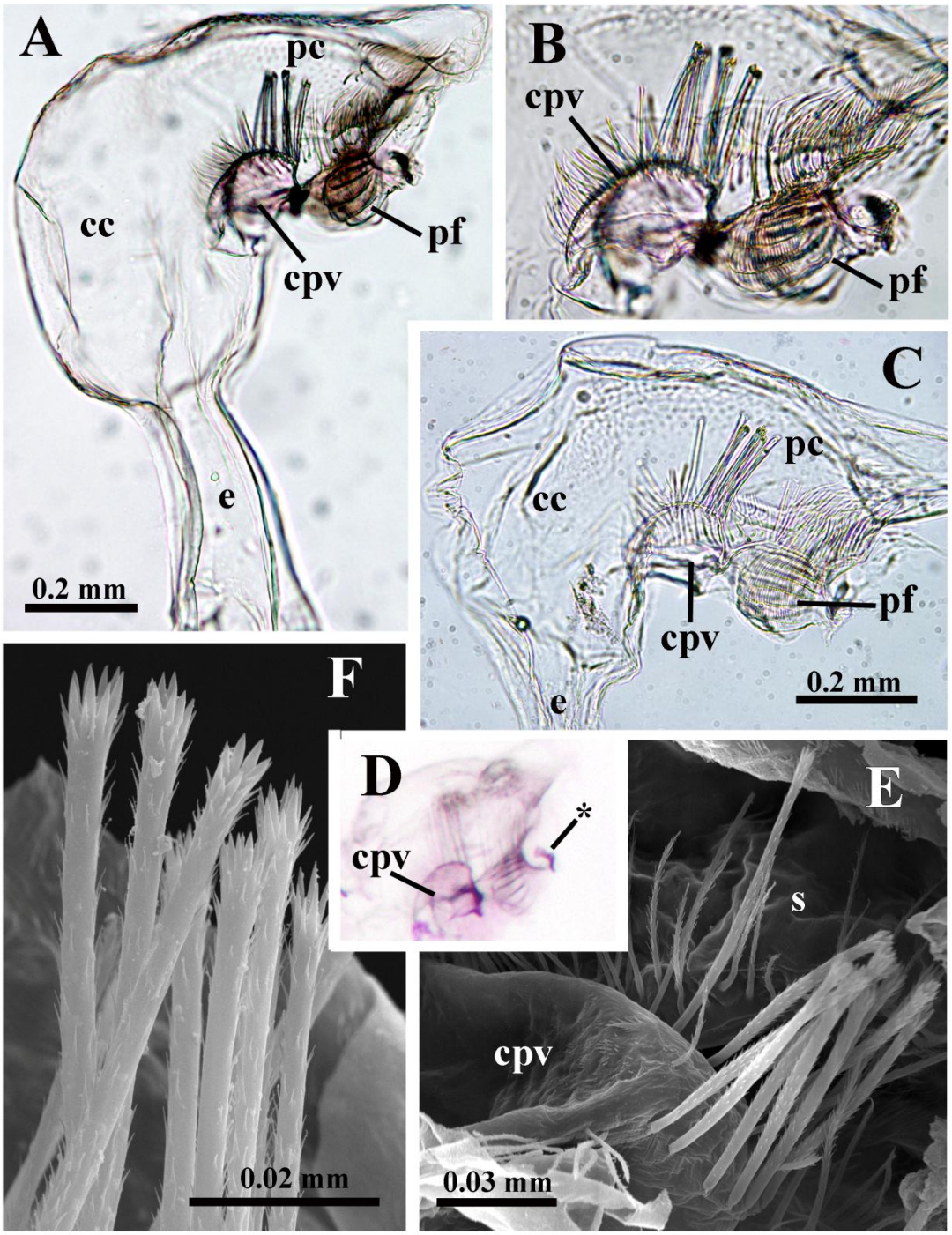

Figure 2. *Maja brachydactyla*. Foregut of the zoeal stages. Zoea I, stained with Alizarin Red, light microscope image (A). Close view of 2A (B). Zoea II, without staining, light microscope image (C). Zoea I, stained with Alizarin Red, stereo microscope image (D). Close view of zoea I cardio-pyloric valve, SEM image (E). Close view of the long thickened setae of the cardio-pyloric valve, SEM image (F). Abbreviations: (*),"supra-ampullary ossicles-like" structures; cc, cardiac chamber; cpv, cardio-pyloric valve; e, esophagus; pc, pyloric chamber; pf, pyloric filter; s, long thickened setae.

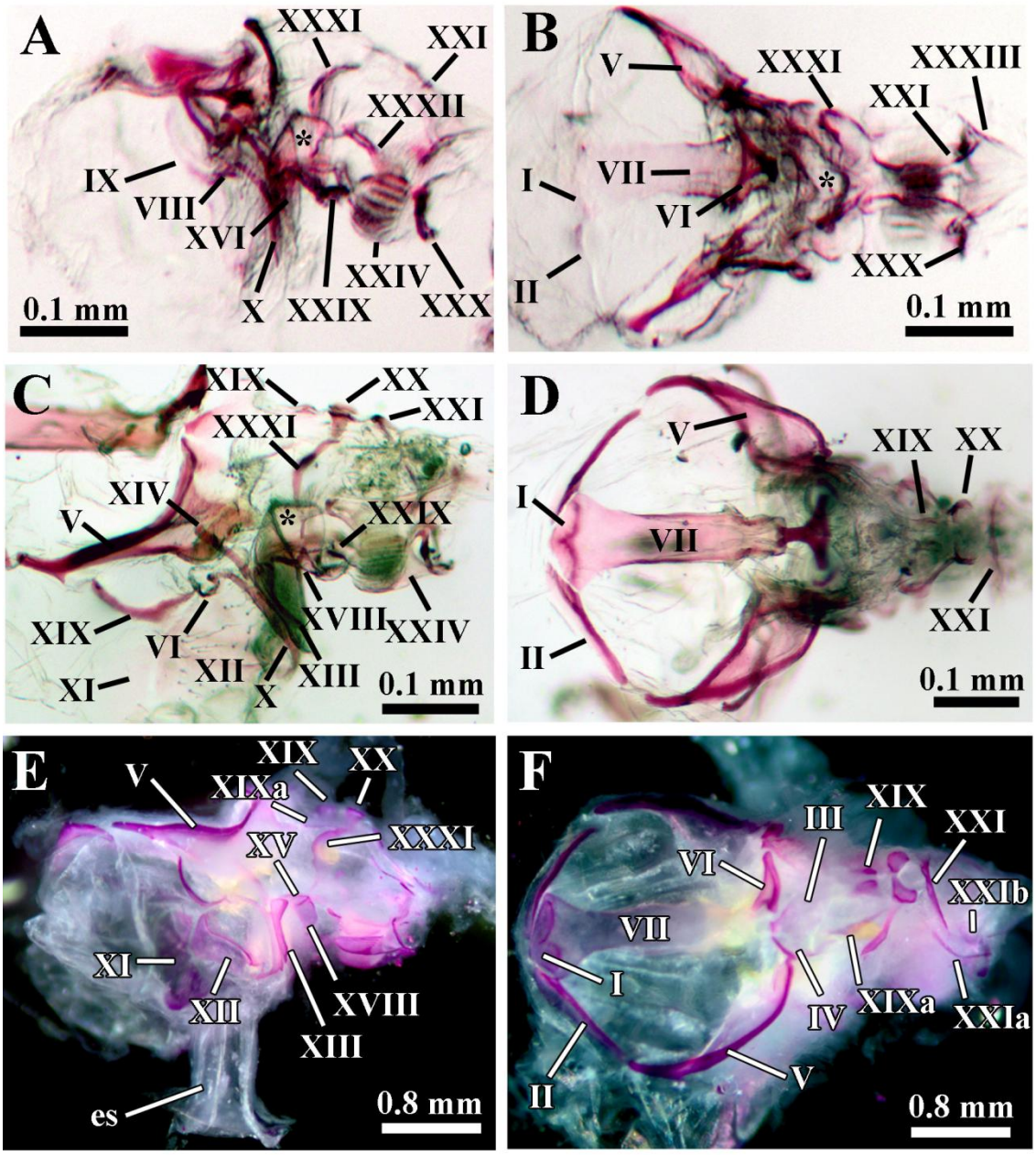

Figure 3. *Maja brachydactyla*. Foregut of the megalopa and juveniles; stained with Alizarin Red. Lateral view of megalopa foregut, light microscope image (A). Dorsal view of megalopa foregut, light microscope image (B). Lateral view of C1 foregut, light microscope image (C). Dorsal view of C1 foregut, light microscope image (D). Lateral view of C_{CL8} foregut, stereo microscope image (E). Dorsal view of C_{CL8} foregut, stereo microscope image (F). Abbreviations: (*), cardio-pyloric valve. For ossicles nomenclature sees Table 1.

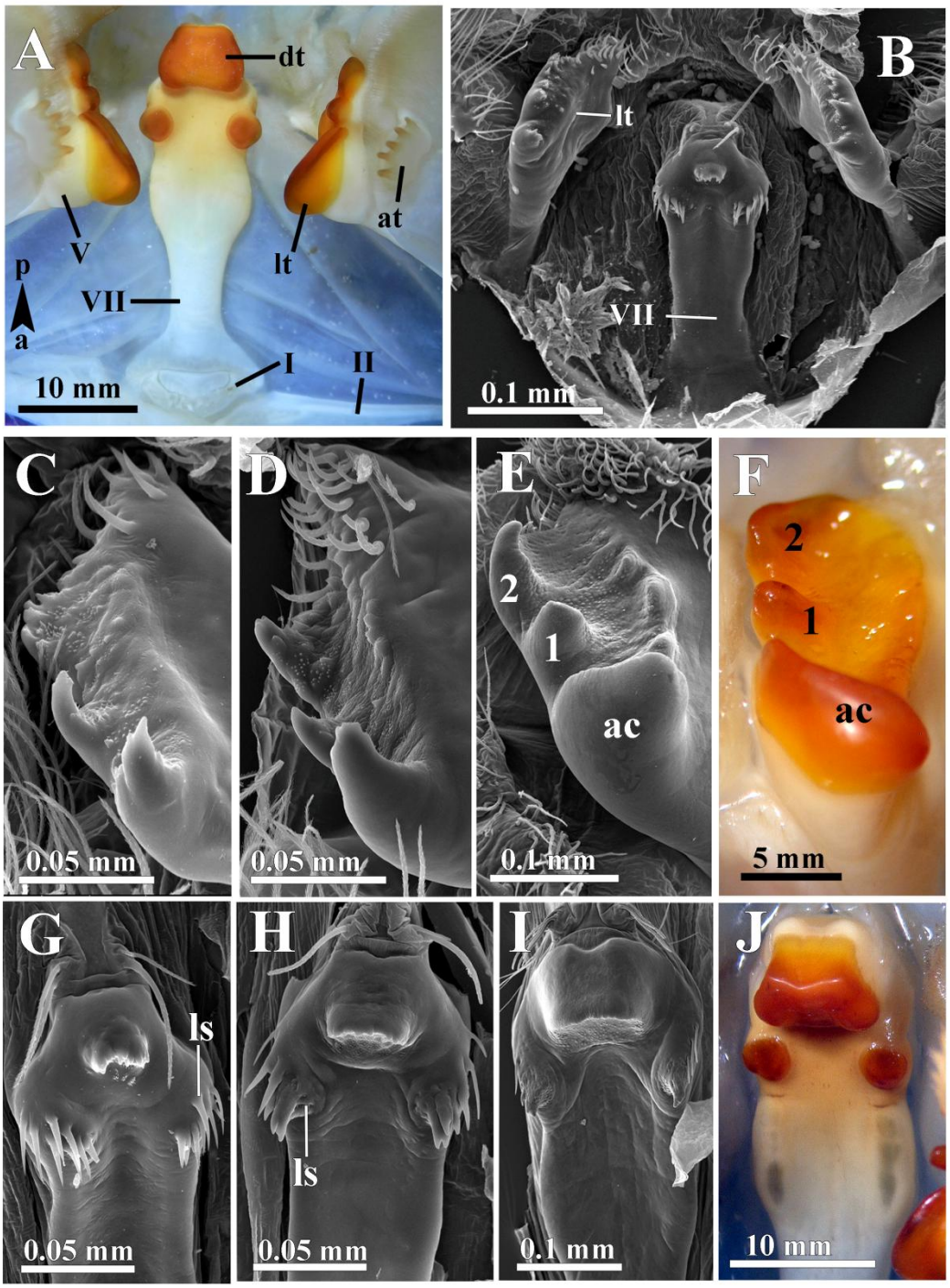

Figure 4. *Maja brachydactyla*. Gastric mill and associated teeth. Adult gastric mill, stereo microscope image (A). Megalopa gastric mill, SEM image (B). Megalopa lateral tooth, SEM image (C). C1 lateral tooth, SEM image (D). C_{CL8} lateral tooth, SEM image (E). Adult lateral tooth, stereo microscope image (F). Megalopa dorsal tooth, SEM image (G). C1 dorsal tooth, SEM image (H). CC_{L8} dorsal tooth, SEM image (I). Adult dorsal tooth, stereo microscope image (L). Abbreviations: ac, anterior cusp; at, accessory tooth; dt, dorsal tooth; lt, lateral tooth; ls, lateral spines. Numbers: lateral cusps. For ossicles nomenclature sees Table 1.

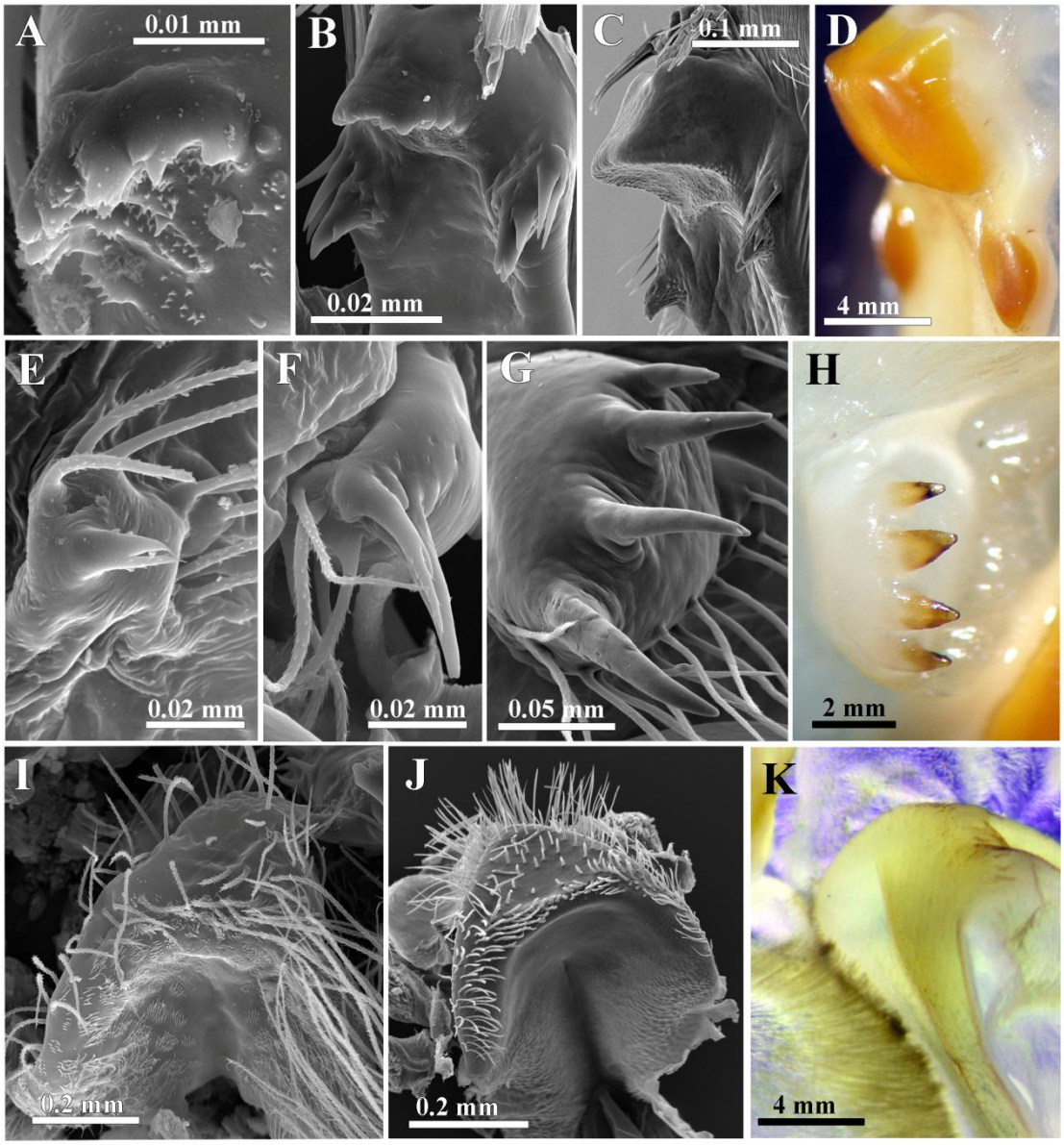

Figure 5. *Maja brachydactyla*. Gastric mill teeth and cardio-pyloric valve. Megalopa dorsal tooth median cusp, SEM image (A). C1 dorsal tooth median cusp, SEM image (B). C_{CL8} dorsal tooth median cusp, SEM image (C). Adult dorsal tooth median cusp, stereo microscope image (D). Megalopa accessory tooth, SEM image (E). C1 accessory tooth, SEM image (F). C_{CL8} accessory tooth, SEM image (G). Adult accessory tooth, stereo microscope image (H). Megalopa cardio-pyloric valve, SEM image (I). C1 cardio-pyloric valve, SEM image (J). Adult cardio-pyloric valve, stereo microscope image (K).

6. References

Abelló P, García Raso JE, Guerao G, Salmerón F. 2014. *Maja brachydactyla* (Brachyura: Majidae) in the western Mediterranean. Marine Biodiversity Records 7(e77).

Abrunhosa FA, Melo M. 2008. Development and functional morphology of the foreguts of larvae and postlarvae of three crustacean decapods. Brazilian Journal of Biology 68:221-228.

Abrunhosa FA, Melo MA, Abrunhosa JP. 2003. Development and functional morphology of the foregut of larvae and postlarva of *Ucides cordatus* (Decapoda, Ocypodidae). Nauplius 11(1):37-43.

Abrunhosa FA, Simith DJB, Monteiro JRC, de Souza Junior AN, Oliva PAC. 2011. Development and functional morphology of the larval foregut of two brachyuran species from Northern Brazil. Anais da Academia Brasileira de Ciências 83:1269-1278.

Alaminos J. 2011. Efecto del confinamiento en espacios reducidos sobre el crecimiento de juveniles de centollo, *Maja brachydactyla*, y su repercusión en la madurez. Revista de biología marina y oceanografía 46(2):219-230.

Alaminos J, Domingues P. 2008. Effects of different natural or prepared diets on growth and survival of juvenile spider crabs, *Maja brachydactyla* (Balss, 1922). Aquaculture International 16(5):417-425.

Allardyce BJ, Linton SM. 2010. Functional Morphology of the Gastric Mills of Carnivorous, Omnivorous, and Herbivorous Land Crabs. J Morphol 271(1):61-72.

Andrés M, Estévez A, Anger K, Rotllant G. 2008. Developmental patterns of larval growth in the edible spider crab, *Maja brachydactyla* (Decapoda: Majidae). J Exp Mar Biol Ecol 357(1):35-40.

Andrés M, Estévez A, Rotllant G. 2007. Growth, survival and biochemical composition of spider crab *Maja brachydactyla* (Balss, 1922) (Decapoda: Majidae) larvae reared under different stocking densities, prey:larva ratios and diets. Aquaculture 273(4):494-502.

Andrés M, Gisbert E, Díaz M, Moyano FJ, Estévez A, Rotllant G. 2010. Ontogenetic changes in digestive enzymatic capacities of the spider crab, *Maja brachydactyla* (Decapoda: Majidae). J Exp Mar Biol Ecol 389(1-2):75-84.

Andrés M, Rotllant G, Sastre M, Estevez A. 2011. Replacement of live prey by formulated diets in larval rearing of spider crab *Maja brachydactyla*. Aquaculture 313(1-4):50-56.

Bernárdez C, Freire J, González-Gurriarán E. 2000. Feeding of the spider crab *Maja squinado* in rocky subtidal areas of the Ría de Arousa (north-west Spain). Journal of the Marine Biological Association of the United Kingdom 80(01):95-102.

Briones-Fourzán P, Castañeda-Fernández de Lara V, Lozano-Álvarez E, Estrada-Olivo J. 2003. Feeding ecology of the three juvenile phases of the spiny lobster *Panulirus argus* in a tropical reef lagoon. Marine Biology 142(5):855-865.

Brösing A. 2010. Recent developments on the morphology of the brachyuran foregut ossicles and gastric teeth. Zootaxa 2510:1-44.

Brösing A. 2014. Foregut structures of freshly moulted exuviae from *Maja crispata*, *Cancer pagurus* and *Pseudosesarma moeschi* (Decapoda: Brachyura). Journal of Natural History 48(9-10):543-555.

Brösing A, Richter S, Scholtz G. 2002. The foregut-ossicle system of *Dromia wilsoni*, *Dromia personata* and *Lauridromia intermedia* (Decapoda, Brachyura, Dromiidae), studied with a new staining method. Arthropod Structure & Development 30(4):329-338.

Brösing A, Richter S, Scholtz G. 2007. Phylogenetic analysis of the Brachyura (Crustacea, Decapoda) based on characters of the foregut with establishment of a new taxon. Journal of Zoological Systematics and Evolutionary Research 45(1):20-32.

Brösing A, Türkay M. 2011. Gastric teeth of some thoracotreme crabs and their contribution to the brachyuran phylogeny. J Morphol 272(9):1109-1115.

Cannicci S, Gomei M, Dahdouh-Guebas F, Rorandelli R, Terlizzi A. 2007. Influence of seasonal food abundance and quality on the feeding habits of an opportunistic feeder, the intertidal crab *Pachygrapsus marmoratus*. Marine Biology 151(4):1331-1342.

Castejón D, Ribes E, Durfort M, Rotllant G, Guerao G. 2015. Foregut morphology and ontogeny of the mud crab *Dyspanopeus sayi* (Smith, 1869) (Decapoda, Brachyura, Panopeidae). Arthropod Structure & Development 44(1):33-41.

Clark PF. 2005. The evolutionary significance of heterochrony in the abbreviated zoeal development of pilumnine crabs (Crustacea: Brachyura: Xanthoidea). Zoological Journal of the Linnean Society 143(3):417-446.

Clark PF, Ng PKL, Noho H, Shokita S. 2005. The first-stage zoeas of *Carpilius convexus* (Forskål, 1775) and *Carpilius maculatus* (Linnaeus, 1758) (Crustacea: Decapoda: Brachyura: Xanthoidea: Carpiliidae): an example of heterochrony. Journal of Plankton Research 27(2):211-219.

Domingues P, Alaminos J. 2008. Efectos de la densidad de cultivo y de elementos de refugio en el crecimiento y supervivencia de juveniles de centollo, *Maja brachydactyla* (Balss, 1922). Revista de biología marina y oceanografía 43(1):121-127.

Domingues P, Alaminos J, García-Garrido S, Hachero-Cruzado I, Rosas C. 2012. Growth and survival of juvenile spider crabs, *Maja brachydactyla* (Balss, 1922), fed with fresh or frozen mussels. Aquaculture Research 43(2):167-177.

Factor JR. 1981. Development and Metamorphosis of the Digestive System of Larval Lobsters, *Homarus americanus* (Decapoda: Nephropidae). J Morphol 169:225-242.

Factor JR. 1982. Development and metamorphosis of the feeding apparatus of the stone crab, *Menippe mercenaria* (brachyura, xanthidae). J Morphol 172(3):299-312.

Felgenhauer BE. 1992. Chapter 3. Internal Anatomy of the Decapoda: An Overview. In: Harrison FW, Humes AG, editors. Microscopic Anatomy of Invertebrates: Wiley-Liss, Inc.

Gerber S, Hopkins MJ. 2011. Mosaic heterochrony and evolutionary modularity: the trilobite genus *Zacanthopsis* as a case study. Evolution 65(11):3241-3252.

Guerao G, Pastor E, Martin J, Andrés M, Estévez A, Grau A, Duran J, Rotllant G. 2008. The larval development of *Maja squinado* and *M. brachydactyla* (Decapoda, Brachyura, Majidae) described from plankton collected and laboratory-reared material. Journal of Natural History 42(33-34):2257-2276.

Guerao G, Ribera C. 1996. Locomotor Activity Patterns and Feeding Habits in the Prawn *Palaemon serratus* (Pennant, 1777) (Decapoda, Palaemonidae) in the Alfacs Bay, Ebro Delta, Spain. Crustaceana 69(1):101-112.

Guerao G, Rotllant G. 2010. Development and growth of the early juveniles of the spider crab *Maja squinado* (Brachyura: Majoidea) in an individual culture system. Aquaculture 307(1-2):105-110.

Guerao G, Rotllant G, Anger K. 2010. Characterization of larval moulting cycles in *Maja brachydactyla* (Brachyura, Majidae) reared in the laboratory. Aquaculture 302(1-2):106-111.

Guerao G, Simeó CG, Anger K, Urzúa Á, Rotllant G. 2012. Nutritional vulnerability of early zoea larvae of the crab *Maja brachydactyla* (Brachyura, Majidae). Aquatic Biology 16(3):253-264.

Guillaume J, Ceccaldi HJ. 2011. Digestive physiology of shrimps. In: Guillaume J, Kaushik S, Bergot P, Metailler R, editors. Nutrition and Feeding of Fish and Crustaceans. Chichester: Springer-Praxis.

Haley CN, Blamey LK, Atkinson LJ, Branch GM. 2011. Dietary change of the rock lobster *Jasus lalandii* after an 'invasive' geographic shift: Effects of size, density and food availability. Estuarine, Coastal and Shelf Science 93(2):160-170.

Huespe AV, Gámez-Simes E, Pastor-de-Ward CT. 2008. Gastric mill morphology in the genus *Cyrtograpsus* (Crustacea: Decapoda: Grapsoidea: Varunidae). Journal of the Marine Biological Association of the United Kingdom 88(02):311-319.

Hultgren KM, Stachowicz JJ. 2008. Molecular phylogeny of the brachyuran crab superfamily Majoidea indicates close congruence with trees based on larval morphology. Molecular Phylogenetics and Evolution 48(3):986-996.

Icely JD, Nott JA. 1992. Digestion and absorption: digestive system and associated organs. In: Harrison FW, Humes AG, editors. Microscopic anatomy of invertebrates: decapod Crustacea. New York: Wiley-Liss. p 147-201.

Kolts JM, Lovvorn JR, North CA, Grebmeier JM, Cooper LW. 2013. Effects of body size, gender, and prey availability on diets of snow crabs in the northern Bering Sea. Marine Ecology Progress Series 483:209-+.

Lin F-Y. 2000. Scanning Electron Microscopic Observations on the Gland Filters of the Pyloric Stomach of *Penaeus monodon* and *Metapenaeus ensis* (Decapoda, Penaeidae). Crustaceana 73(2):163-174.

Lumasag GJ, Quinitio ET, Aguilar RO, Baldevarona RB, Saclauso CA. 2007. Ontogeny of feeding apparatus and foregut of mud crab *Scylla serrata* Forsskål larvae. Aquaculture Research 38(14):1500-1511.

Mascaró M, Seed R. 2001. Foraging behavior of juvenile *Carcinus maenas* (L.) and *Cancer pagurus* L. Marine Biology 139(6):1135-1145.

Meiss DE, Norman RS. 1977. Comparative study of the stomatogastric system of several decapod crustacea. I. Skeleton. J Morphol 152(1):21-53.

Melo MA, Abrunhosa F, Sampaio I. 2006. The morphology of the foregut of larvae and postlarva of *Sesarma curacaoense* De Man, 1892: a species with facultative lecithotrophy during larval development. Acta Amazonica 36:375-380.

Milne-Edwards H. 1840. Histoire naturelle des crustacés: atlas: Libraire Encyclopédique de Roret.

Nakamura K, Takemoto T. 1986. Morphology of Stomach Ossicles in Brachyura. Memoirs of Faculty of Fisheries Kagoshima University 35(1):7-15.

Norman CP, Jones MB. 1992. Influence of depth, season and moult stage on the diet of the velvet swimming crab *Necora puber* (brachyura, portunidae). Estuarine, Coastal and Shelf Science 34(1):71-83.

Palma J, Correia M, Andrade JP. 2008. Usefulness of flat bottom tanks on the settlement of spider crab (*Maja squinado*, Herbst) larvae. Aquaculture Research 39(9):1005-1008.

Perez O, Bellwood D. 1988. Ontogenetic changes in the natural diet of the sandy shore crab, *Matuta lunaris* (Forskål) (Brachyura : Calappidae). Marine and Freshwater Research 39(2):193-199.

Raff EC, Raff RA. 2000. Dissociability, modularity, evolvability. Evolution & Development 2(5):235-237.

Reilly SM, Wiley EO, Meinhardt DJ. 1997. An integrative approach to heterochrony: the distinction between interspecific and intraspecific phenomena. Biological Journal of the Linnean Society 60(1):119-143.

Reimann A, Richter S, Scholtz G. 2011. Phylogeny of the Anomala (Crustacea, Decapoda, Reptantia) based on the ossicles of the foregut. Zoologischer Anzeiger - A Journal of Comparative Zoology 250(4):316-342.

Rotllant G, González-Gurriarán E, Fernández L, Benhalima K, Ribes E. 2007. Ovarian maturation of the multi-spawning spider crab *Maja brachydactyla* (Decapoda: Majidae) with special reference to yolk formation. Marine Biology 152(2):383-394.

Sakai K, Türkay M, Yang S-L. 2006. Revision of the *Helice*/*Chasmagnathus* complex (Crustacea: Decapoda: Brachyura). Abhandlungen der Senckenbergischen Naturforschenden Gesellschaft 565:1-76.

Schaefer N. 1970. The functional morphology of the foregut of three species of decapod Crustacea: *Cyclograpsus punctatus* Milne-Edwards, *Diogenes brevirostris* Stimpson, and *Upogebia africana* (Ortmann). Zoologica Africana 5(2):309-326.

Seitz RD, Knick KE, Westphal M. 2011. Diet Selectivity of Juvenile Blue Crabs (*Callinectes sapidus*) in Chesapeake Bay. Integrative and Comparative Biology 51(4):598-607.

Simeó CG, Kurtz K, Chiva M, Ribes E, Rotllant G. 2010. Spermatogenesis of the Spider Crab *Maja brachydactyla* (Decapoda: Brachyura). J Morphol 271(4):394-406.

Simeó CG, Kurtz K, Rotllant G, Chiva M, Ribes E. 2009a. Sperm ultrastructure of the spider crab *Maja brachydactyla* (Decapoda: Brachyura). J Morphol 271(4):407-417.

Simeó CG, Ribes E, Rotllant G. 2009b. Internal anatomy and ultrastructure of the male reproductive system of the spider crab *Maja brachydactyla* (Decapoda: Brachyura). Tissue and Cell 41(5):345-361.

Skilleter G, Anderson D. 1986. Functional morphology of the Chelipeds, mouthparts and gastric mill of *Ozius truncatus* (Milne Edwards) (Xanthidae) and *Leptograpsus variegatus* (Fabricius) (Grapsidae) (Brachyura). Marine and Freshwater Research 37(1):67-79.

Sotelo G, Morán P, Posada D. 2009. Molecular phylogeny and biogeographic history of the European *Maja* spider crabs (Decapoda, Majidae). Molecular Phylogenetics and Evolution 53(1):314-319.

Stein W. 2009. Modulation of stomatogastric rhythms. Journal of Comparative Physiology A 195(11):989-1009.

Vannini M, Chelazzi G, Gherardi F. 1989. Feeding habits of the pebble crab *Eriphia smithi* (Crustacea, Brachyura, Menippidae). Marine Biology 100(2):249-252.

Verísimo P, Bernárdez C, González-Gurriarán E, Freire J, Muino R, Fernández L. 2011. Changes between consecutive broods in the fecundity of the spider crab, *Maja brachydactyla*. ICES J Mar Sci 68(3):472-478.

Woods CMC. 1995. Morphology of the Foregut of the Spider Crab *Notomithrax ursus* (Brachyura:Majidae). Journal of Crustacean Biology 15(2):220-227.

CHAPTER 13.

Morphology of the stomach cuticle during the ontogeny of the spider crab *Maja brachydactyla* (Decapoda, Brachyura, Majidae)

Morphology of the stomach cuticle during the ontogeny of the spider crab *Maja brachydactyla* (Decapoda, Brachyura, Majidae).

Diego Castejón[1*], Guiomar Rotllant[2], Enric Ribes[3], Mercè Durfort[3], and Guillermo Guerao[4]

[1] IRTA, Centre d' Aqüicultura, Ctra. de Poble Nou Km 5.5. 43540 Sant Carles de la Ràpita, Tarragona (Spain)

[2] CSIC, Institut de Ciències del Mar, Passeig Marítim de la Barceloneta 37-49. 08003 Barcelona (Spain)

[3] Unitat de Biologia Cel·lular, Departament de Biologia Cel·lular, Fisiologia i Immunologia, Facultat de Biologia, Universitat de Barcelona, Diagonal 645. 08028 Barcelona, Spain

[4] PS Fabra i Puig 344.08028 Barcelona (Spain)

Short title: *Maja brachydactyla* morphology stomach cuticle

***Corresponding author:** Diego Castejón. E-mail: diego.castejon.dcb@gmail.com; phone: +34 681 154 398; postal address: IRTA, Subprogram Cultius Aqüàtics, Ctra. Poble Nou, Km 5.5. 43540 Sant Carles de la Ràpita, Tarragona (Spain).

Abstract

The stomach of the decapods is mainly known by the morphology of the ossicle armature and gastric mill, by contrast the tissular and cellular details are less known. The present study explores the cuticle that lines the stomach during the larval, first juvenile and adult stages of the brachyuran crab *Maja brachydactyla*. During the larval stages, employing optical microscopy none cuticle layer can be identified, excepting the epicuticle observed in the gastric teeth of the megalopae. By electron microscopy, the cuticle thickness varies from very thin (ca. 0.5 µm) to relatively thick (8 µm), the procuticle varies from clearly organized in layers to unidentifiable exocuticle and endocuticle. The medial tooth of the first juveniles shows a procuticle which endocuticle gradually disappears in the lateral sides of the medial tooth. During adulthood, the stomach is lined by a cuticle always subdivided into epicuticle, exocuticle, and endocuticle. The cuticle thickness, structure and composition vary: in the cardiac sacs the simple columnar epithelium sustains a flexible cuticle; in the ossicles and cardio-pyloric valve the simple epithelium varies from squamous to columnar, the more rigid cuticle shows variations in thickness, morphology and differential staining; in the pyloric filters the simple columnar epithelium sustains a cuticle which trabeculae-like structure is extended into ridges and long setae forming filtering surfaces. These cuticle variations could respond to the functional role of these stomach structures.

Keywords: Eucrustacea; larval development; cuticle; ossicles; epithelium

1. Introduction

The foregut of the decapods comprises the esophagus and the stomach, both organs derive from the embryonic ectoderm and are lined by a chitinous cuticle (Davie et al., 2015a; Felgenhauer, 1992; Icely and Nott, 1992). The stomach is a complex structure supported by numerous calcified thickenings of the cuticle named ossicles (Alves et al., 2010; Brösing et al., 2002; Davie et al., 2015a; Hobbs and Hooper, 2009; McLaughlin, 1983; Meiss and Norman, 1977). This organ is subdivided into different specialized structures: expansive cardiac sacs for the storage of food; a gastric mill composed by thickened teeth-like ossicles with grinding function; the cardio-pyloric valve supports numerous setae and separates the cardiac from the pyloric stomach, it acts as primary filters; the pyloric stomach presents setae that lead the ingested food to the ventral pyloric filters, which as secondary filters permit the finest material to enter into the midgut gland or hepatopancreas, while the rejected material is moved dorsally towards the midgut tract (Davie et al., 2015a; Icely and Nott, 1992; McLaughlin, 1983; Woods, 1995).

In decapods, the study of the stomach has been largely focused on the morphology of the ossicle armature and gastric mill (Alves et al., 2010; Brösing, 2010; 2014; Brösing et al., 2002; Brösing et al., 2007; Brösing and Türkay, 2011; de La Barra et al., 2017), on the functional physiology of the stomach and his relation with feeding specializations (Allardyce and Linton, 2010; Heinzel et al., 1993; Hobbs and Hooper, 2009; Martin et al., 1998; Woods, 1995). Other studies describe the morphological change of the stomach during the larval development (Abrunhosa and Melo, 2008; Abrunhosa et al., 2003; Abrunhosa et al., 2011; Castejón et al., 2015a; Castejón et al., 2015c; Jantrarotai and Sawanyatiputi, 2005; Melo et al., 2006). However, the above

cited studies generally neglected the cytological description and ultrastructure including the cuticle and the underlying epithelium.

The cuticle that covers the decapod integument has specializations depending of its role, e.g. carapace, chelae coating, arthrodial membrane or gills (Boßelmann et al., 2007; Dillaman et al., 2012; Mary and Krishnan, 1974; Welinder, 1974). The stomach contain numerous specialized structures, then it is congruent to consider that his cuticle must reflect these specializations, e.g. the features observed in the cuticle of the medial tooth (Chisaka and Kozawa, 2003; Nesbit and Roer, 2016; Vatcher et al., 2015). In this sense, the main objective for the present study is to describe the cuticle of different structures of the stomach, including larval and adult stages.

The species selected for this purpose was the common spider crab *Maja brachydactyla* Balss, 1922. As other majids, this species realizes the terminal molt, i.e. the animal cease to molt when the adult stage is reached (Corgos et al., 2011; Davie et al., 2015b; Fahy, 2001; González-Gurriarán et al., 1993). Then, the cuticle of the adults is not influenced by the molting cycle. Similarly to other majoids (Davie et al., 2015b; Hultgren and Stachowicz, 2008), the larval development is abbreviated and includes two zoeal stages, zoea I and zoea II, and one megalopa stage; then the megalopa metamorphoses into the first juvenile (Clark, 1986; Guerao et al., 2008). Previous studies realized in this species describe the morphological changes occurring during the larval development in the mouthparts and other appendages (Guerao et al., 2008), as well in the gastric mill and ossicle armature (Castejón et al., 2015c).

2. Material and methods

Fishing enterprises (CADEMAR & LONXANET) provided the adult specimens of *M. brachydactyla* employed in this study. The specimens were captured in the coasts of the Northwest Iberian Peninsula and Ireland and translated to the Institut de Recerca i Tecnologia Agroalimentàries facilities (IRTA, Tarragona, Spain). The adult specimens used for broodstock were placed inside 2,000 L cylindrical tanks: 3.5 m^3 h^{-1}, 18 ± 1 °C, 35 ± 1 psu, 12 h light per day provided by fluorescent tubes at 25 lux. The feeding consisted on fresh and frozen mussels of the genus *Mytilus*. The larvae ca. 12 hours after hatch were introduced directly in 600 mL glass beakers placed inside 360 L tanks (96 x 96 x 40 cm) used as incubation chambers: 21 ± 1 °C, 35 ± 1 psu, 12 h light per day provided by white LED lights at 1,000 lux. The feeding consisted on fresh *Artemia* sp. Kellogg, 1906 nauplii and metanauplii (INVE Aquaculture Nutrition, Salt Lake UT, USA). The larvae reached the zoea II stage in 3-4 days, the megalopa stage in 6-7 days and the first juvenile stage in 12-13 days.

The general morphology of the stomach during the stages of zoea, megalopa and first juvenile required the fixation of entire specimens in formaldehyde 4%. The foreguts were extracted using dissecting needles and cleaned by immersion in 10 % KOH at 80 °C during 15-20 min. The cleaned foreguts were mounted and observed without staining under a Leica LB30T 111/97 optical microscope (Wetzlar, Germany). Three foreguts per stage were examined.

The study of the stomach histology required the fixation of entire specimens in the case of larval and first juvenile stages, while in the adults only specific regions of the stomach were fixed: cardiac sacs, dorsal tooth of the gastric mill (urocardiac ossicle), cardio-pyloric valve and pyloric filters. The fixation process employed

Davidson's fixative during 24 h. The Davidson's fixative consisted in a solution of ethanol absolute: seawater: formaldehyde 37 %: glycine: glacial acetic acid in proportion 3: 3: 2: 1: 1. The fixed samples were processed to form paraffin blocks that were cut into 2 µm sections using a Leica RM2155 microtome (Wetzlar, Germany). The staining techniques used include Hematoxylin and Eosin (H–E), Periodic Acid–Schiff (PAS) contrasted with Methylene Blue, and Mallory's trichrome (Acid Fuchsine, Orange G and Aniline Blue). The observations were done with a Leica LB30T 111/97 optical microscope (Wetzlar, Germany). The published material was obtained from several larval specimens: 4 zoeae (Fig. 3) and 5 megalopae (Fig. 5), and two adult specimens (Figs. 7 and 8, Suppl. Mat. 1A-C).

The study of the stomach ultrastructure required the fixation of entire larval and first juvenile specimens, and small pieces of the cardiacs sacs in the adults. The fixative used was 2 % paraformaldehyde and 2.5 % glutaraldehyde in cacodylate buffer (0.1 mol L^{-1} pH 7.4) and post-fixed using 1 % osmium tetroxide solution in cacodylate buffer. Then, the samples were dehydrated in acetone, mounted in Spurr's resin and cut using a Leica UCT ultramicrotome (Wetzlar, Germany). The grids were stained with uranyl acetate and lead citrate and the observations were performed in a JEOL EM-1010 electron microscope at 80 kV equipped with an image analysis system. The post-fixative treatment and observations were performed at CCiTUB (Hospital Clinic, University of Barcelona). The published material was obtained from a single specimen per stage: zoea II (Figs. 4 and 9), first juvenile (Fig. 6) and adult (Fig. 10).

3. Results

Gross morphology of the stomach through the ontogeny. During the zoeal stages, the mean length of the stomach of the zoea I and II is respectively 369 ± 36 µm and 445 ± 30 µm, differing considerably from previous measures that must be considered erroneous (Castejón et al., 2015c). The cardiac stomach is narrow and simple (Figs. 1A; 2A; 3A). The cardio-pyloric valve has a "crescent-moon" shape with the concave side oriented anteriorly, this structure sustains thickened large setae that are lost in subsequent stages (Figs. 1A; 2). The pyloric stomach has a pair of pyloric filters located on postero-ventral pouches (Figs. 1A; 2B-C, F). The cuticle of the zoeal stomach is folded: the lateral walls of the cardiac stomach are laterally folded toward the thick setae of the cardio-pyloric valve forming a narrow channel (Figs. 2B-C, E; 3B, D); the lateral walls of the pyloric stomach also form lateral folds projected toward the pyloric filters (Figs. 2C, E-F; 3B). The zoeal stomach undergoes a major transformation during the molt to the megalopa stage, the gastric mill is formed underlying the old zoeae II cuticle in advanced premolt specimens (Fig. 1B).

The stomach of *M. brachydactyla* from the megalopa to the adult stage shares a common morphology which differs from the stomach of the zoeae. The mean length is 647 ± 36 µm in the megalopa stage and 771 ± 72 µm in the first juvenile stage, differing considerably from previous measures that must be considered erroneous (Castejón et al., 2015c). The cardiac stomach is expanded forming a pair of lateral sac-like structures termed "cardiac sacs" and characterized by elastic walls (Fig. 1C-D). The cardiac stomach sustains dorsally and posteriorly the "gastric mill", it is composed by specialized ossicles transformed into internal teeth (Figs. 1C-D; 5C, F-I). The pyloric stomach presents a pair of ventral pouches that maintains the pyloric filters, they are in

turn connected with the midgut gland or "hepatopancreas". The pyloric stomach connects dorsally with the midgut tract (Figs. 1C-D; 3A; 5E).

Stomach of the zoeal stages. During the zoeal stages the stomach walls are lined by a simple squamous epithelium, excepting the lateral folds, the cardio-pyloric valve and the ventral pouches of the pyloric filters, which are lined by a cuboidal to short columnar epithelium (Fig. 3A-D). Some epithelial cells show an unstained cytoplasm (Fig. 3D). The cuticle is extremely thin and the typical cuticle layers (epicuticle, exocuticle and endocuticle) cannot be identified by optical microscopy (Fig. 3). However, by electron microscopy can be observed more details on the cuticle, including variations in the same ultrathin slice of a given specimen (Fig. 4A-E). The cuticle is generally extremely thin (480 ± 32 nm) and composed by two layers: an electron-dense epicuticle and an underlying procuticle without a clear lamellate structure (Fig. 4C). In other stomach regions (probably folds) the cuticle varies in thickness (from 1-2 to 8-9 μm) and shows the typical cuticle layers (Fig. 4A): the epicuticle is a thin electron-dense layer (2-4 % cuticle thickness), the exocuticle (45- 85 % cuticle thickness) has a lamellar or pseudo-lamellar organization, the endocuticle (5-45 % cuticle thickness) shows well defined lamellae (Fig. 4A). The exocuticle and endocuticle can merge into a lamellate procuticle without clearly identifiable layers (Fig. 4B). The tubular setae are composed by fibers oriented concentrically around a central core filled by an extracellular amorphous matrix layer (AML, Fig. 4D-E).

Stomach of the megalopa and first juvenile. The cardiac sacs are lined by a simple squamous epithelium (Fig. 5A-B); while the gastric mill teeth and the pyloric stomach are lined by a simple cuboidal to short columnar epithelium, which cells often show an unstained cytoplasm (Fig. 5C-D). By optical microscopy, the structure of the

cuticle is similar than during the zoeal stages (Fig. 5A-E). The exception is the cuticle of the gastric mill teeth, it is thicker and shows a predominant epicuticle with differential staining (yellowish to orange color) by Mallory's trichrome (Fig. 5C, F-I). By electron microscopy, the cuticle of the medial tooth (gastric mill) varies from a cuticle which procuticle cannot be subdivided into exocuticle and endocuticle (Fig. 6A-B), to a cuticle with the typical layers (Fig. 6A, C): the epicuticle is the outmost and electron-dense layer (10-15 % cuticle thickness); the exocuticle (30-40 % cuticle thickness) is formed by few lamellae (800 ± 200 nm per lamellae) and it is crossed by lucent arc-like formations (probably pore channels); the endocuticle (40-50 % cuticle thickness) is composed by thinner and well defined lamellae (310 ± 100 nm per lamellae). In some regions (probably stomach folds) the cuticle occasionally acquires an appearance that remember to the observed during the zoeal phase in the Fig. 4A.

Stomach of the adults. In adults, the cuticle of the stomach differs considerably from the previous stages with variations in the thickness, structure and composition depending of its location. The composition of the cuticle cannot be solved by the staining techniques used, however the variation in composition can be reflected by the differential staining observed in a single slice, and corroborated when the pattern of the differential staining is repeated in sequential slices. The cuticle lining of different structures will be described below:

1. Cardiac sacs (Figs. 1C-D; 7E; Suppl. Mat. 1A-C). The cardiac sacs are flexible expansions of the stomach walls to allow storing food inside the stomach (Fig. 1C-D). The cuticle width is approximately 140 µm and can reach up to 300 µm in some folds (Fig. 5E). The epicuticle is thin (ca. 1-5 % of the cuticle thickness) and differentially stained by H–E and Mallory's trichrome stains, while the exocuticle and

endocuticle are homogeneously stained by these stains (Fig. 7E; Suppl. Mat. 1A, C). The PAS staining is stronger in the exocuticle than in the endocuticle (Suppl. Mat. 1B). The exocuticle represents ca. 6-10 % of the cuticle thickness, the lamellae in the exocuticle are twice to three times wider than in the endocuticle (Suppl. Mat. 1A-C). The cardiac sacs have a simple columnar epithelium (Fig.7E; Suppl. Mat. 1A-C). The cuticle of the cardiac sacs was studied by electron microscopy as example of the adult cuticle (Fig. 10A-C). The epicuticle is highly electron-dense and around 1.9 ± 0.1 µm in thickness (Fig. 10A). The exocuticle is extensive and constituted by lamellae with 3.5 ± 0.3 µm in thickness, but this thickness decreases quickly with the proximity to the epicuticle and endocuticle. (Fig. 10A-B). The lamellae of the endocuticle measure around 1.4 ± 0.2 µm in thickness (Fig. 10B). The lamellae of the endocuticle loss gradually their organization and the size and quantity of patches of disorganized fibers increases toward the cuticle basis (Fig. 10C).

2. Ossicles and gastric teeth (Fig. 7A-D). The ossicles are rigid and hardened cuticle thickenings that constitute the stomach armature and the gastric mill. As example, we describe the medial tooth of the gastric mill, it is located dorsally in the midline of the cardiac stomach and formed by the urocardiac ossicle, see Castejón et al. (2015c) for details. The cross section of the medial tooth is an elliptical ring with three main layers (Fig. 7A): the outmost layer is the cuticle, beneath appears a simple epithelium, the innermost layer is connective tissue filling the "internal core" of the ossicle. The cuticle varies in thickness, structure and staining of the layers. The cuticle of one side resembles to the cuticle of the cardiac sacs (Fig. 7A-B), it has approximately 110 ± 30 µm in thickness. The epicuticle is thin (ca. 2-4 % of the cuticle thickness) and differentially stained by H–E and Mallory's trichrome stains, while the exocuticle and endocuticle are homogeneously stained by these stains. The PAS staining is stronger in

the exocuticle than in the endocuticle. The exocuticle represents ca. 20-30 % of the cuticle thickness and its lamellae are up to three times wider than the endocuticle. The cuticle is lined by a simple short columnar epithelium (Fig. 7B).

In the opposite side, the cuticle has approximately 220 ± 27 µm in thickness and probably represents the cuticle of the tooth itself (Fig. 7A, C). The epicuticle is wider representing ca. 10-12 % of the cuticle thickness. The epicuticle shows two differentiated layers with similar thickness (Fig. 7A, C-D): the outmost layer is unstained by H–E but light yellow by orange G, while the innermost layer is strongly stained by Eosin and orange by orange G and can penetrate into the exocuticle (Fig. 7C-D). The exocuticle and endocuticle are differently stained by H–E (Fig. 7C), but similarly stained by the Mallory's trichrome. The PAS staining is stronger in the exocuticle than in the endocuticle. The exocuticle and endocuticle represent ca. 35-40 % and ca. 45-50 % of the cuticle thickness, respectively. The cuticle is lined by a simple squamous epithelium (Fig. 7B, D).

3. Cardio-pyloric valve (Figs. 1D; 8A, C-D). The cardio-pyloric valve is a ventral structure that separates the cardiac from the pyloric stomach, it has a crescent-moon shape and its very rich in setae. The cuticle thickness, structure and staining varies along the cardio-pyloric valve (Fig. 8A, C-D). In one side the cuticle measures 77 ± 12 µm in thickness (Fig. 8A, C). The epicuticle is relatively thick (ca. 6-12 % of the cuticle thickness) and shows two layers: the outmost layer represents a third of the thickness and it is more stained by Hematoxylin than the innermost layer. The exocuticle and endocuticle are differently stained by H–E but homogeneously stained by PAS and Mallory's trichrome. The exocuticle and endocuticle represent ca. 50-60 % and ca. 30-40 % of the cuticle thickness, respectively. The exocuticle lamellae are four

to five times wider than the endocuticle lamellae. The cuticle is lined by a simple columnar epithelium (Fig. 8A, C).

The cuticle of the opposite side measures 117 ± 5 μm in thickness (Fig. 8A, D). The epicuticle represents ca. 9-12 % of the cuticle thickness. It presents two layers with similar thickness (Fig. 8D): the outmost layer is not stained by H–E but yellow by Mallory's trichrome, while the innermost layer is stained by Eosin and orange by Mallory's trichrome. The exocuticle is more stained by Hematoxylin but less stained by PAS than the endocuticle (Fig. 8D). Differing from the exocuticle, the endocuticle shows yellowish orange patches when stained by Mallory's trichrome (Suppl. Mat. 2). The exocuticle and endocuticle represents ca. 50-60 % and ca. 30-40 % of the cuticle thickness, respectively. The exocuticle shows wide and undulate lamellae, while in the endocuticle the lamellae are not clearly visible. The cuticle is lined by a simple squamous epithelium (Fig. 8A, D).

4. Pyloric filters (Fig. 6B, E-H). The pyloric filters are located on ventral pouches of the pyloric stomach, both pouches are united by a continuous W shaped floor (in transversal section) whose medial line is elevated into a central ridge (Fig. 6B). The cuticle of the pyloric filters is highly specialized. The roof is lined by a cuticle with a variable thickness (Fig. 6B). The epicuticle is strongly stained by eosin (Fig. 6F). The exocuticle and endocuticle cannot be easily distinguished by differential staining affinity or the structure of the lamellae. The cuticle shows tubular channels ended in setae stained as the epicuticle. The density of setae is very high (Fig. 6F). The cuticle of the floor forms numerous and parallel ridges ended in setae organized in a net-like structure (Fig. 6B). In cross section, these setae are Y-shaped and its size decreases toward the distal extreme (Fig. 6H). The exocuticle and endocuticle are not

distinguishable by differential staining affinity or a differential structure of the lamellae. The cuticle has a trabeculae-like organization (Fig. 6E, G). The pyloric filters have a simple columnar epithelium (Fig. 6G).

Ultrastructure of the epithelial cells. The ultrastructure of the epithelial cells was described in the zoea II and should be considered as an example, since its morphology can be influenced by the molt cycle. The cell membrane is polarized (Fig. 9A, D): the apical membrane shows infolds (Fig. 9D), the lateral membranes form interdigitations (Fig. 9A, D), while the basal membrane has strong cell-to-cell junctions if below appear muscle cells (Fig. 9B, D). The apical membrane contains highly electron-dense invaginations denominated in this study as "apical complexes", they are attached to the filamentous structures that cross the cytoplasm (Fig. 9A-B). The cytoplasm contains a high density of ribosomes, rough endoplasmic reticulum and mitochondria (Fig. 9C).

The ultrastructure was also described in adult specimens using the epithelial cells of the cardiac sacs as example, in this case the cell morphology cannot be affected by the molt cycle because this species cease molting following maturity. The epithelial cells have a polarized organization (Fig. 10D). The apical membrane is generally smooth (Fig. 10D-E), the lateral membranes form extensive interdigitations (Fig. 10D-E), and the basal membrane is smooth (Fig. 10D, F). The "apical complexes" are larger than during the zoeal stage and appear attached to bundles of filamentous structures (Fig. 10D-E, G-H). Following upward the "apical complexes" can be observed electron-dense formations in the cuticle (Fig. 10E, H). The bundles of filamentous structures cross vertically the epithelial cells (Fig. 10D-E, G). The cytoplasm is lucent and the organelles are dispersed and rare, including mitochondria, ribosomes and rough endoplasmic reticulum (Fig. 10E-F).

4. Discussion

The stomach of the brachyurans during the zoeal stages is relatively simple. Coinciding to our observations and a previous research (Castejón et al., 2015c), Schlegel (1911) illustrated the stomach of the first zoea of *Maja* divided into cardiac stomach ("*cardia*") and pyloric stomach ("*pylore*"), both separated by a cardio-pyloric valve ("*valvule cardiopylorique*") with long thick setae, the pyloric stomach has "*chambres latéro-ventrales*" that could correspond to the pouches of the pyloric filters. This description coincides with numerous brachyuran species (Abrunhosa and Melo, 2008; Abrunhosa et al., 2003; Abrunhosa et al., 2011; Castejón et al., 2015a; Jantrarotai and Sawanyatiputi, 2005; Lumasag et al., 2007; Melo et al., 2006). The biggest ontogenetic change occur during the molt to megalopa involving the emergence of the ossicle armature and gastric mill (Abrunhosa and Melo, 2008; Abrunhosa et al., 2003; Abrunhosa et al., 2011; Castejón et al., 2015a; Castejón et al., 2015c; Jantrarotai and Sawanyatiputi, 2005; Lumasag et al., 2007; Melo et al., 2006). By contrast, Minagawa and Takashima (1994) using histological techniques observed in *Ranina ranina* a "dorsal tooth" located in the cardiac stomach of the zoea VII, which shape and thickness coincides to the dorsal tooth of the megalopa of the same species. This observation contradicts the present and previous studies (cited before) where none gastric mill teeth appear before the molt to megalopa. Maybe Minagawa and Takashima (1994) observed specimens in advanced premolt where the gastric teeth underlie the old cuticle (Fig. 1B). As alternative hypothesis, the emergence of the gastric mill in basal brachyurans could occur in advanced zoeal stages, the confirmation requires the study of the stomach ontogeny in these taxa (including raninids), being recommended the use of dissecting and SEM techniques.

The cuticle of the malacostracans is basically composed by a matrix of chitin and proteins reinforced by calcium and phosphate minerals (Coffey et al., 2017; Dillaman et al., 2012; Giraud-Guille, 1984; Lignon, 1987; Mary and Krishnan, 1974; Mrak et al., 2017; Pires et al., 2017; Roer et al., 2015; Willis, 1999). The affinity to the Hematoxylin and Aniline Blue stains can be explained by the protein content. The chitin itself gives a PAS negative reaction (Hackman, 1954; Muzzarelli, 1977; Skinner, 1962). Then, the observed PAS positive reaction has been explained by the presence of glycoproteins with hydroxyl groups (Skinner, 1962). The staining techniques used in this study cannot provide a deep insight into the cuticle composition. However, the differential staining reveal that composition varies, especially when the pattern of differential staining of a single slice is repeated along sequential slices. This hypothesis is strengthen by the fact that each cuticle layer can have a particular composition (Giraud-Guille, 1984; Green and Neff, 1972; Hegdahl et al., 1977a; b; Hegdahl et al., 1977c; Welinder, 1975) and each structure can have a cuticle with a particular composition and organization (Dillaman et al., 2012; Huber et al., 2014; Huber et al., 2015).

Castejón et al. (2015c) studying the stomach of *M. brachydactyla* observed that the cardiac sac walls are elastic and lack calcification, while the ossicles (gastric teeth inclusive) are rigid and calcified. Ceccaldi (1989) also differentiated between the anterior cuticle of the cardiac stomach (thin and flexible) and the cuticle of the ossicles and gastric mill (thick and calcareous). Similarly, Heeren and Mitchell (1997) studying the brachyuran *Pseudocarcinus gigas* indicated some sort of variation among the cuticle of different stomach regions: cardiac sacs (non-calcicified), mid-region of the cardiac stomach (rich in setae), gastric mill (thick and irregular) and pyloric stomach (thick and non-calcified). Coincidentally, in the present study histological differences were found

among the cardiac sacs, dorsal tooth, cardio-pyloric valve and pyloric stomach. The variation in morphology and composition could respond to functional specializations. This situation occurs with the external exoskeleton: the carapace cuticle has hardness and fracture resistance for protection against predation (Boßelmann et al., 2007; Dillaman et al., 2012), the dactyl and propodus are extra hardened to support high mechanical efforts (Welinder, 1974), specially when they form chelae (Boßelmann et al., 2007; Dillaman et al., 2012); the arthrodial membrane is extremely thin and flexible articulating the animal (Dillaman et al., 2012; Hepburn and Chandler, 1976; Williams et al., 2003); while the gill cuticle is also very thin, non-mineralized and non-sclerotized permitting the diffusion of respiratory gases and ions (Dillaman et al., 2012; Mary and Krishnan, 1974).

It is reasonable to consider the same structure and function relationship for the cuticle of the stomach. The cardiac sacs have thin and elastic walls for storage and processing of food (McGaw and Curtis, 2013). Similar properties (relative thinness, elasticity and none mineral content) are found in the arthrodial membrane (Dillaman et al., 2012; Hepburn and Chandler, 1976; Williams et al., 2003) and similarity at histological level can be found between the cardiac sacs (Fig. 7E, Suppl. Mat. 1A-C) and the arthrodial membrane (Williams et al., 2003). The ossicles and gastric teeth are skeletal and chewing elements (Allardyce and Linton, 2010; de La Barra et al., 2017; Hobbs and Hooper, 2009; Icely and Nott, 1992; Lima-Gomes et al., 2017; Lima et al., 2016; McGaw and Curtis, 2013; Nakamura and Takemoto, 1986; Skilleter and Anderson, 1986). Common properties (relative high thickness, rigidity and mineral content) are found in the carapace (Boßelmann et al., 2007; Dillaman et al., 2012), and certain similarity can be observed between the medial tooth (Fig. 7A, C) and the mineralized exoskeleton at histological level (Williams et al., 2003). Moreover, the

cuticle variation observed in the medial tooth of the first juvenile (Fig. 6A) remember to the transition between the arthrodial membrane and the joint head cuticle in isopods (Ruangchai et al., 2013), maybe corresponding to the transition between flexible and rigid regions of the medial tooth. In this sense, one of the most studied stomach structures is the medial tooth, which role explain his particular composition and morphology (Chisaka and Kozawa, 2003; Nesbit and Roer, 2016; Vatcher et al., 2015). In the present study the cuticle of the medial tooth shows an highly developed epicuticle in the megalopa, while in the adults varies between the ventral and dorsal sides, possibly due to different roles: i.e. the dorsal side acting as supportive structure and the ventral side as grinding molar. The dorsal tooth of the brachyuran *Callinectes sapidus* shows a variation in the relative thickness of the cuticle layers (epicuticle, exocuticle, and endocuticle) along the longitudinal axis (Vatcher et al., 2015), while in the astacidean *Procambarus clarkii* the exocuticle thickness varies with the type of teeth-like process (Chisaka and Kozawa, 2003). Nesbit and Roer (2016) suggest that epicuticle is specialized since maintains silicon during the entire molt cycle.

The cardio-pyloric valve is able to block the access toward the pyloric filters regulating the pass of the ingested content into the pyloric stomach (Icely and Nott, 1992; Kunze and Anderson, 1979; McGaw and Curtis, 2013). Maybe his cuticle variation is a compromise between the flexibility and rigidity required for this valve-like role. The cuticle of the pyloric stomach is highly specialized and transformed into a filtering system composed by screens of setae (Icely and Nott, 1992; McGaw and Curtis, 2013; Salindeho and Johnston, 2003; Simon et al., 2012). This role explain the transformation of the pyloric cuticle into ridges, channels and Y-shaped setae.

Generally, the histological organization of the brachyuran stomach during the larval stages is not described but appears similar to our observations, e.g. the brachyurans *Portunus trituberculatus* (Nakamura, 1990), *Scylla serrata* (Lumasag et al., 2007) and *R. ranina* (Minagawa and Takashima, 1994). The epithelium is described as simple cuboidal or simple columnar (Johnston et al., 2008; Tziouveli et al., 2011). Williams (1944) mentioned a stratified columnar epithelium in the anomuran *Porcellana platycheles* prezoeae, but this information has not been confirmed by posterior studies. The stomach of the adult *M. brachydactyla* has a simple squamous to columnar epithelium, coinciding to descriptions realized in other brachyurans (Erri Babu et al., 1982; Mykles, 1979; Reddy, 1937), astacids (Reddy, 1937) and penaeids (Dall, 1967). Sousa and Petriella (2006) mentioned that the epithelium of the caridean *Palaemonetes argentinus* varies from simple to squamous.

The TEM observations reveal highly developed interdigitations and bundles of filamentous structures crossing the cytoplasm and attached to the apical complex. Mykles (1979) describes these features in the foregut of *Metacarcinus magister, Homarus americanus* and *Homarus gammarus*, but were also described in the hindgut of other malacostracans (Holdich and Mayes, 1975; Komuro and Yamamoto, 1968; Mykles, 1979; Vernon et al., 1974; Witkus et al., 1969). These features are associated with the capacity to support contractive and expansive efforts associated with the pass of the ingested material (Komuro and Yamamoto, 1968; Mykles, 1979; Witkus et al., 1969). The interdigitations could help to avoid tearing the epithelium. The filamentous structures also could have a transport role, this hypothesis is congruent with the electro-dense formations extended into the cuticle from the apical complex. The strong cell-to-cell junctions that attach the epithelial and muscle cells probably ensure a stomach response to the muscular action. The organelles are abundant in the larvae but scarce in

the adults. This situation can be explained by the molting cycle: in the larvae the molt cycle requires few days (Castejón et al., 2015b; Guerao et al., 2010), while this species cease to molt when sexual maturity is reached (Corgos et al., 2011; Corgos López-Prado et al., 2005; González-Gurriarán et al., 1993). The high density of organelles observed in the larvae could be a sign of activity (Ziegler, 1997), by contrast the cytoplasm of the adult cells could reveal inactivity.

As concluding remarks, is tentative to consider the stomach as a Pandora's box waiting to be open. Numerous authors revealed the complexity of this organ: cardiac sacs, ossicle armature, gastric mill, cardio-pyloric valve, screens of setae, pyloric filters. The present study reveal an even higher complexity considering that each structure is supported by a specialized cuticle that varies at smaller scales. The possibility of important but hidden cuticle diversity must be considered for future studies.

5. Acknowledgements

Financial support provided by the Spanish Ministry of Economy and Competitiveness through the INIA project [grant number RTA2011-00004-00-00] to G.G and a predoctoral fellowship to D.C. [FPI-INIA]. The authors would like to thank to the technicians at IRTA, Sant Carles de la Ràpita (David Carmona, Glòria Macià, Magda Monllaó, Francesc X. Ingla and Olga Bellot) and CCiTUB Hospital Clinic, Barcelona (Adriana Martínez, Almudena García, José Manuel Rebled and Rosa Rivera) for their assistance.

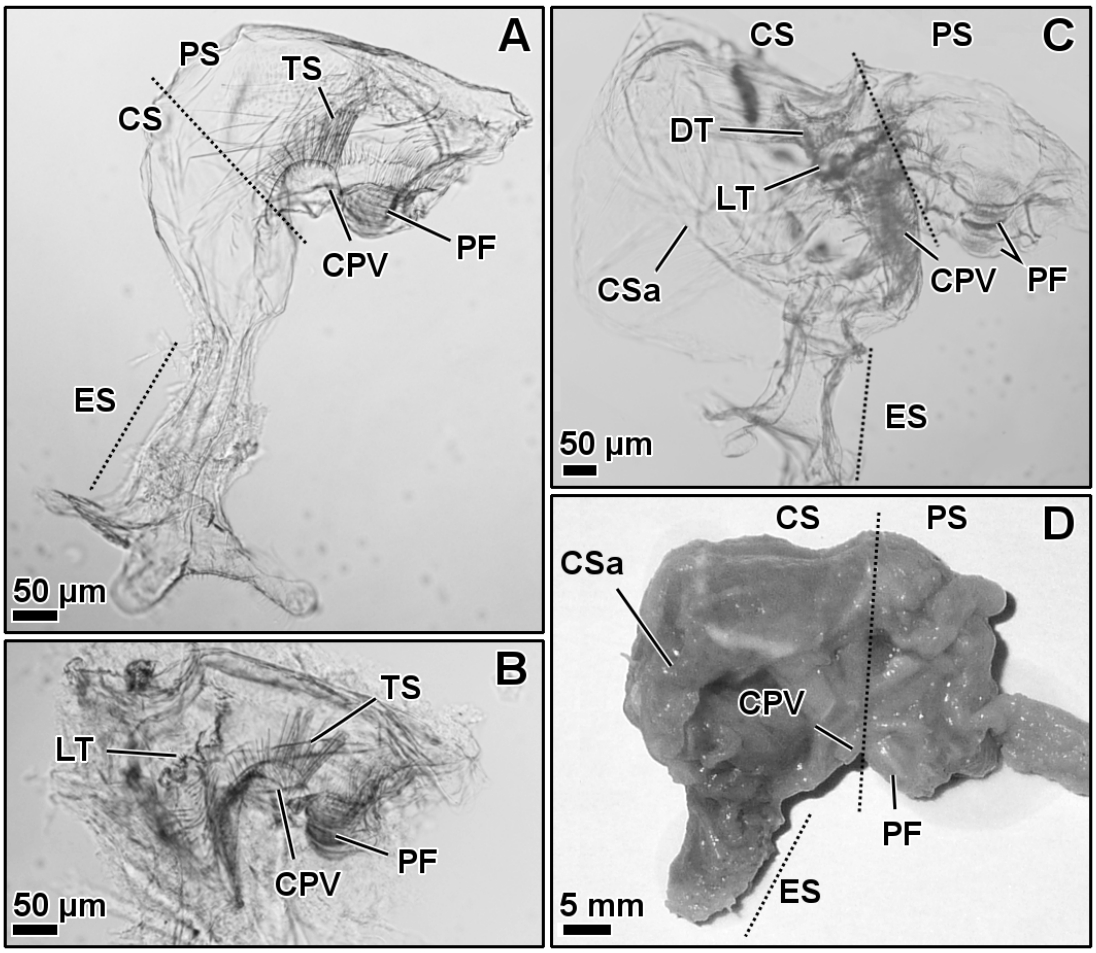

Figure 1. *Maja brachydactyla*. Foregut. General morphology. Zoea II, 4 days after hatching (4 dah) (A). Zoea II (6 dah), gastric mill teeth below the old cuticle (B). First juvenile (12 dah) (C). Adult (D). Abbreviations: CPV, cardio-pyloric valve; CS, cardiac stomach; CSa, cardiac sacs; DT, dorsal tooth; ES esophagus; LT, lateral teeth; PF, pyloric filters; PS, pyloric stomach; TS, thick setae of the cardio-pyloric valve.

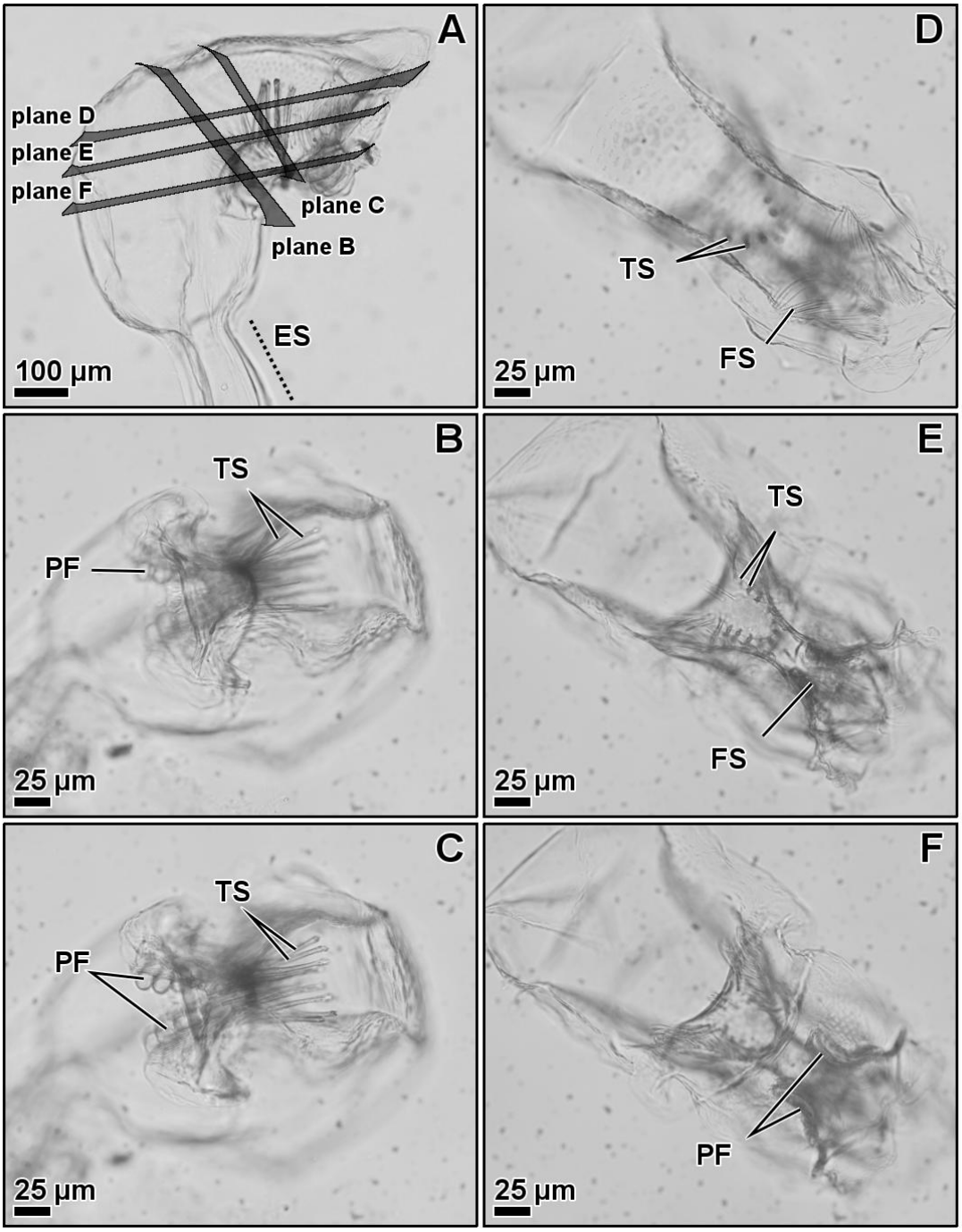

Figure 2. *Maja brachydactyla*. Foregut. General morphology. Zoeal I (ca. 12 h after hatching). Lateral view (A), each letter represents a plane showed in the present figure: antero-posterior planes (B-C) and dorso-ventral planes (D-F). Abbreviations: FS, fine setae; PF, pyloric filters; TS, thickened setae of the cardio-pyloric valve.

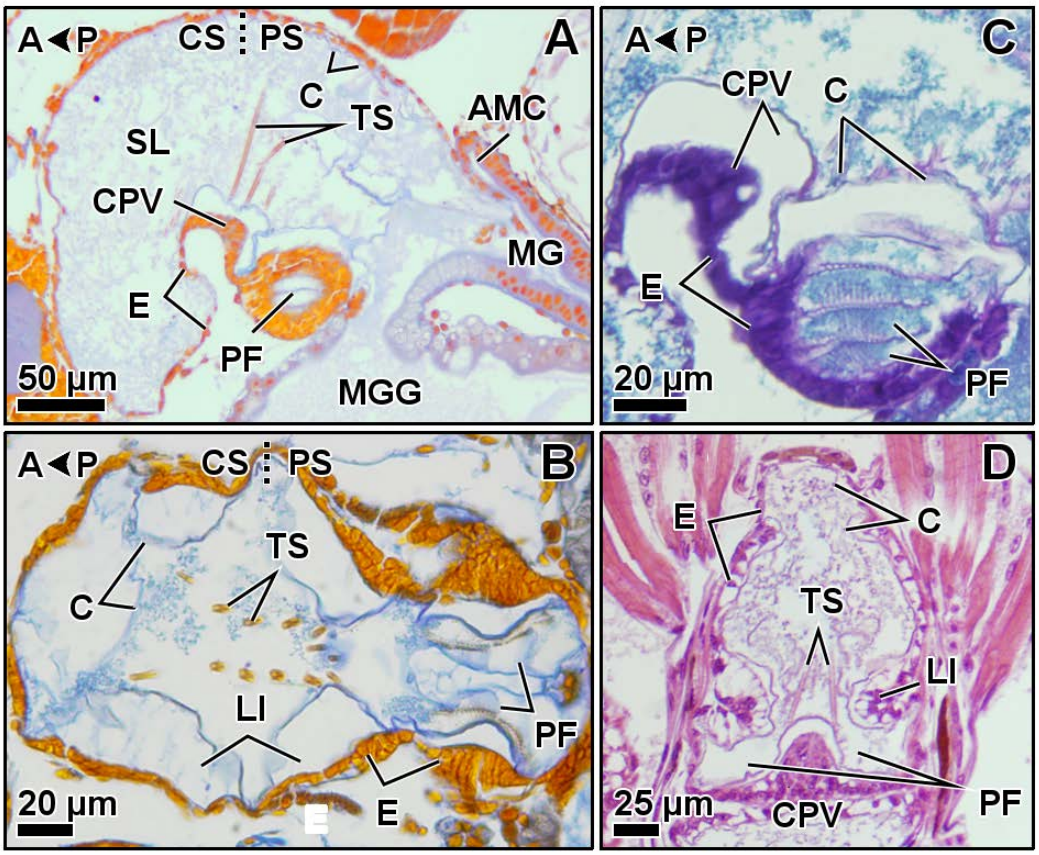

Figure 3. *Maja brachydactyla*. Stomach. Histology. Zoea II (5 dah), Mallory's trichrome (A-B): sagittal (A) and dorso-ventral section (B). Zoea II (6 dah), cardio-pyloric valve and pyloric filters, lateral view, PAS and Alcian Blue contrasted with Hematoxylin (C). Zoea I (ca. 12 h after hatching), cardio-pyloric valve, transversal section, H-E (D). The direction from anterior (A) to posterior (P) is marked by the symbol A ◀ P. Abbreviations: AMC, anterior midgut caeca; C, cuticle; CS, cardiac stomach; CPV, cardio-pyloric valve; E, epithelium; LI, lateral infolds; MG, midgut tract; MGG, midgut gland (hepatopancreas); PF, pyloric filters; PS, pyloric stomach; SL, stomach lumen; TS, thickened setae of the cardio-pyloric valve.

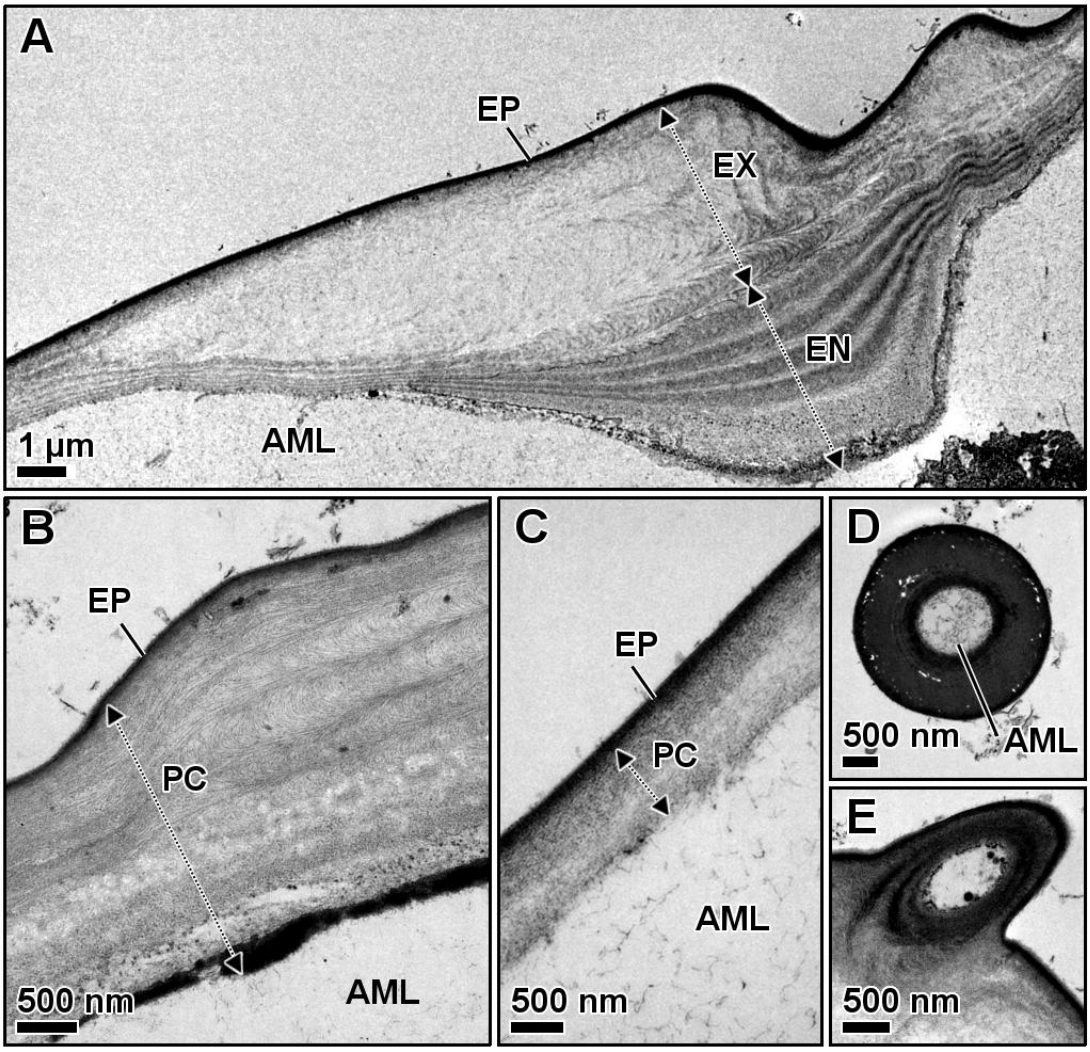

Figure 4. *Maja brachydactyla*. Stomach. Cuticle. Zoea II. TEM. Variation in thickness and morphology, observed in a single specimen (A-C). Setae, cross section (D-E). Abbreviations: AML, amorphous matrix layer; EN, endocuticle; EP, epicuticle; EX, exocuticle; PC, procuticle.

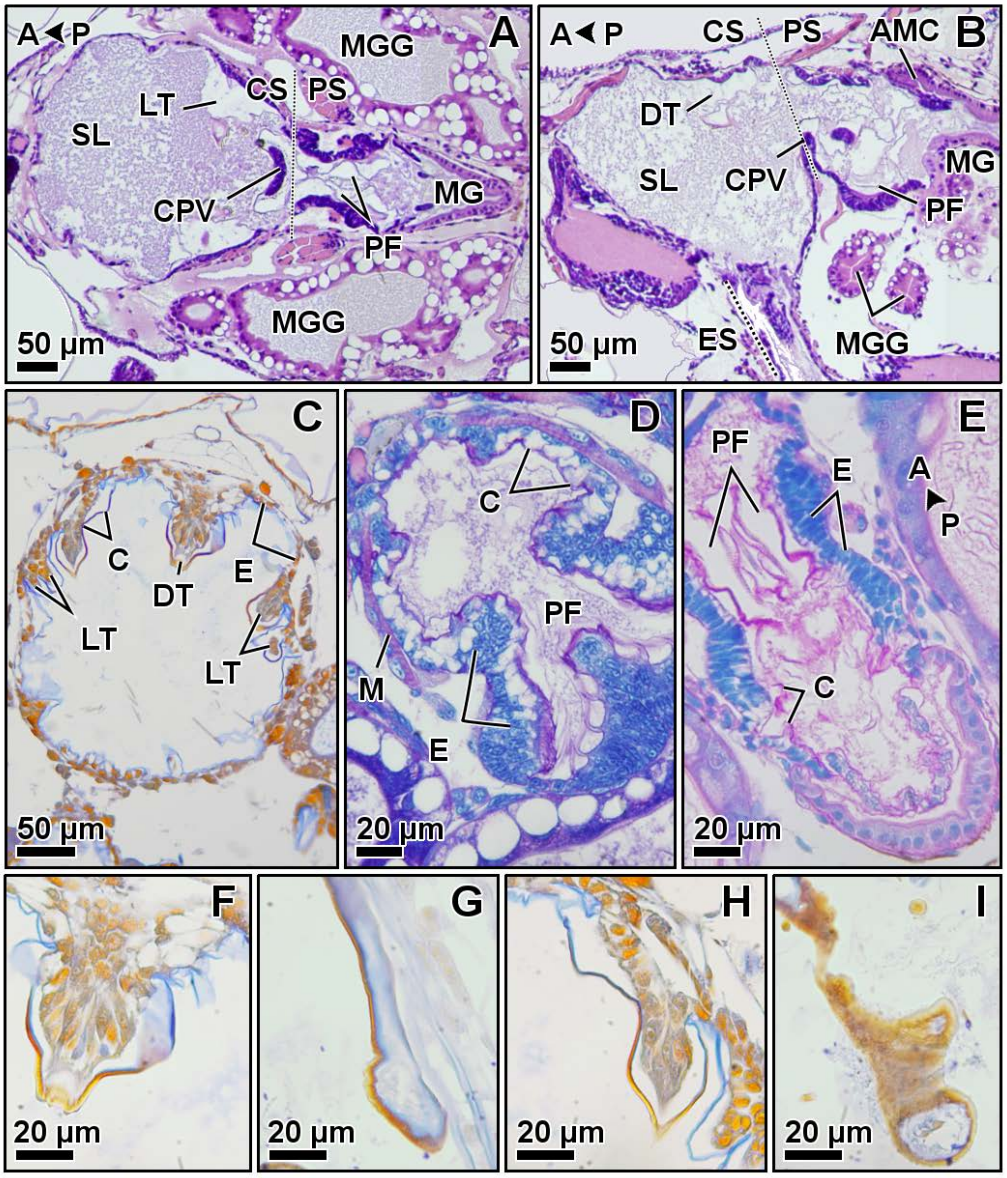

Figure 5. *Maja brachydactyla*. Stomach and gastric mill. Histology. Megalopa. General view (9 dah), HE (A-B): dorso-ventral (A) and sagittal section (B). Gastric mill (6 dah), transversal section, Mallory's trichrome (C). Pyloric stomach (6 dah), PAS and Methylene Blue (D-E): transversal (D) and dorso-ventral section (E). Medial tooth of the gastric mill (urocardiac ossicle, 6 dah), Mallory's trichrome (F-G): transversal (F) and longitudinal section (G). Lateral teeth of the gastric mill (zygocardiac ossicles, 6 dah), Mallory's trichrome (H-I): transversal (H) and longitudinal section (I). The direction from anterior (A) to posterior (P) is marked by the symbol A ◀ P. Abbreviations: AMC, anterior midgut caeca; C, cuticle; CS, cardiac stomach; CPV, cardio-pyloric valve; E, epithelium; ES, esophagus; DT, dorsal tooth; LS, lumen stomach; LT, lateral teeth; MG, midgut tract; MGG, midgut gland; PF, pyloric filters; PS, pyloric stomach; SL, stomach lumen.

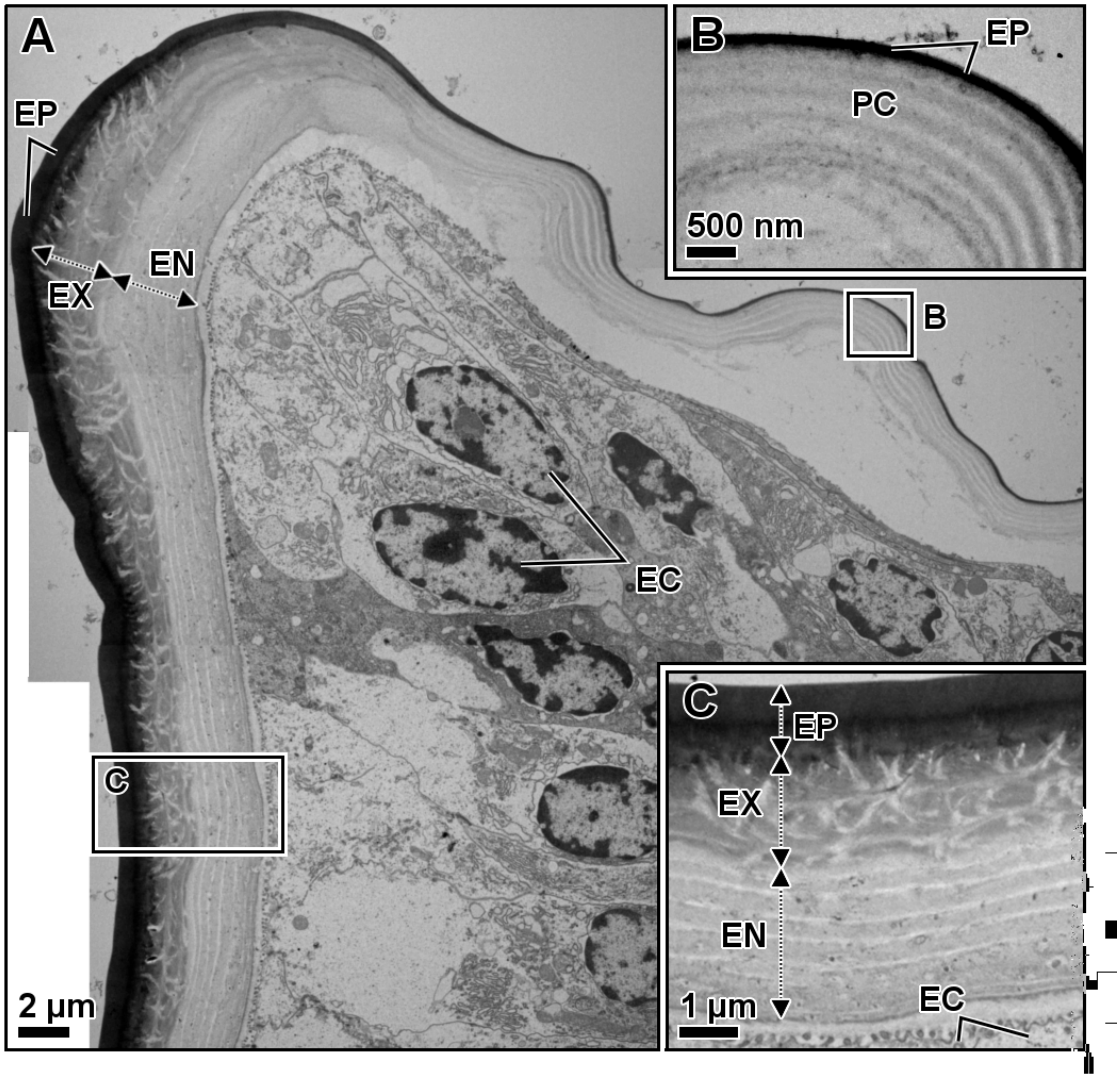

Figure 6. *Maja brachydactyla*. Stomach. Cuticle. First juvenile. TEM. Medial tooth, urocardiac ossicle, the squares correspond to the pictures B and C (A). Close view of the square B (B). Close view of the square C (C). Abbreviations: EC, epithelial cells; EN, endocuticle; EP, epicuticle; EX, exocuticle; PC, procuticle.

Figure 7 (next page). *Maja brachydactyla*. Stomach. Cuticle and epithelium. Adult. Medial tooth, H-E (A-C). General view, the squares correspond to the pictures B and C (A). Close view of the square B (B). Close view of the square C (C). Close view of the square C, epicuticle, Mallory's trichrome (D). Cardiac sacs, H-E (E). Abbreviations: CT, connective tissue; E, epithelium; EN, endocuticle; EP, epicuticle; EP1 and EP2, sublayers of the epicuticle; EX, exocuticle; M, muscles.

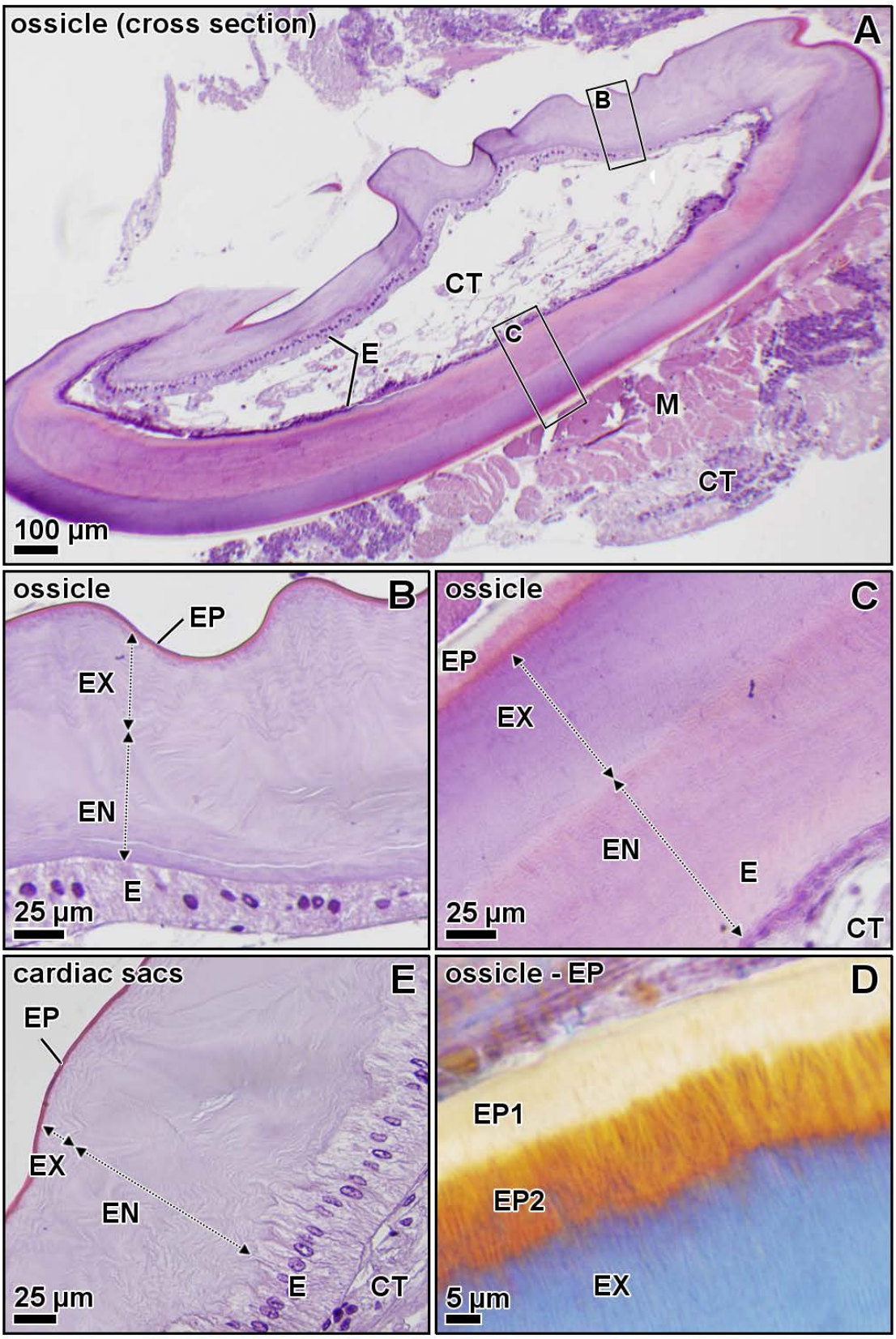
ossicle (cross section)
A
B
CT
C
E
M
CT
100 µm
ossicle
B
EP
EX
EN
E
25 µm
ossicle
C
EP
EX
EN
E
25 µm
CT
cardiac sacs
E
EP
EX
EN
E
CT
25 µm
ossicle - EP
D
EP1
EP2
EX
5 µm

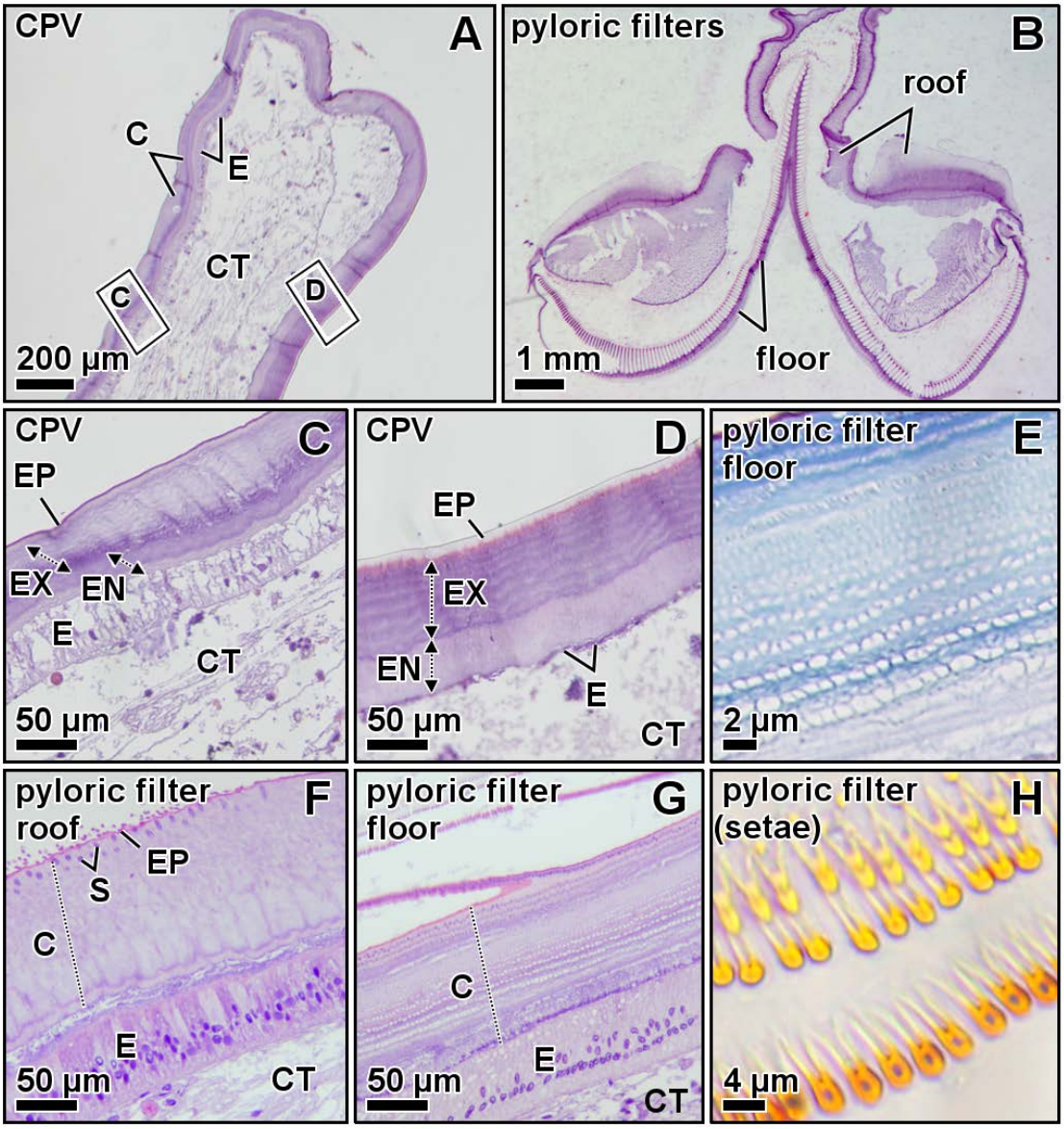

Figure 8. *Maja brachydactyla*. Stomach. Cuticle and epithelium. Adult. Cardio-pyloric valve, H-E (A, C-D). General view (A). Close view of the square C (C). Close view of the square D (D). Pyloric filters, H-E (B, F-G). General view (B). Roof of the pyloric filters (F). Floor of the pyloric filters (G). Roof of the pyloric filters, close view of the cuticle, Mallory's trichrome (E). Pyloric filters, close view of the setae, Mallory's trichrome (H). Abbreviations: C, cuticle; CPV, cardio-pyloric valve; CT, connective tissue; E, epithelium; EN, endocuticle; EP, epicuticle; EX, exocuticle; S, setae.

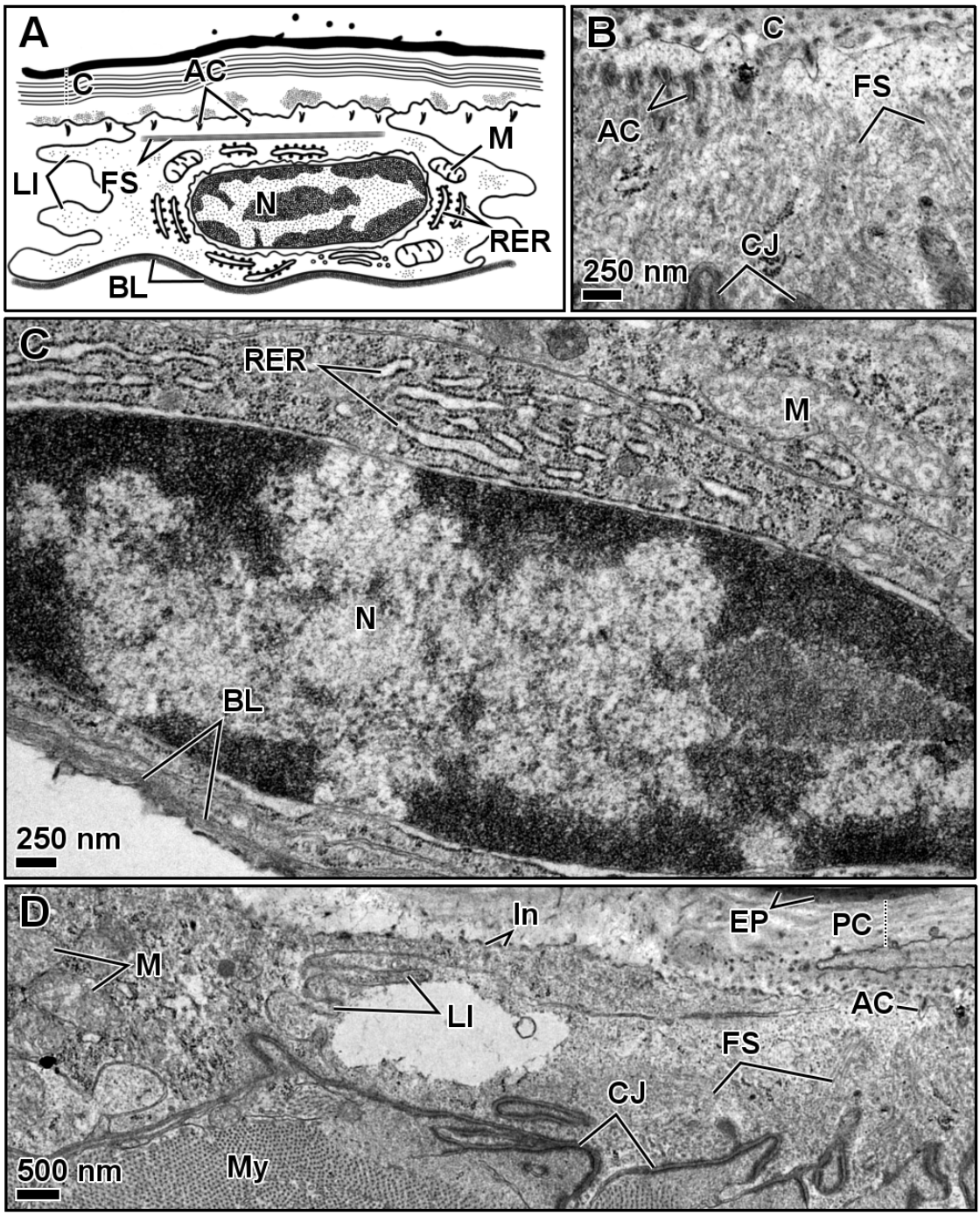

Figure 9. *Maja brachydactyla*. Stomach. Epithelial cell. Zoea II. TEM. General diagram (A). Cell apex, close view showing the "apical complex" (B). General view (C). General view showing the specializations of the membrane (D). Abbreviations: AC, apical complex; BL, basal lamina; C, cuticle; electron-dense formations; CJ, cell-to-cell junctions; EP, epicuticle; FS, filamentous structures; In, infolds; LI, lateral interdigitations; M, mitochondria; My, myofibrils; N, nucleus; PC, procuticle; RER, rough endoplasmic reticulum.

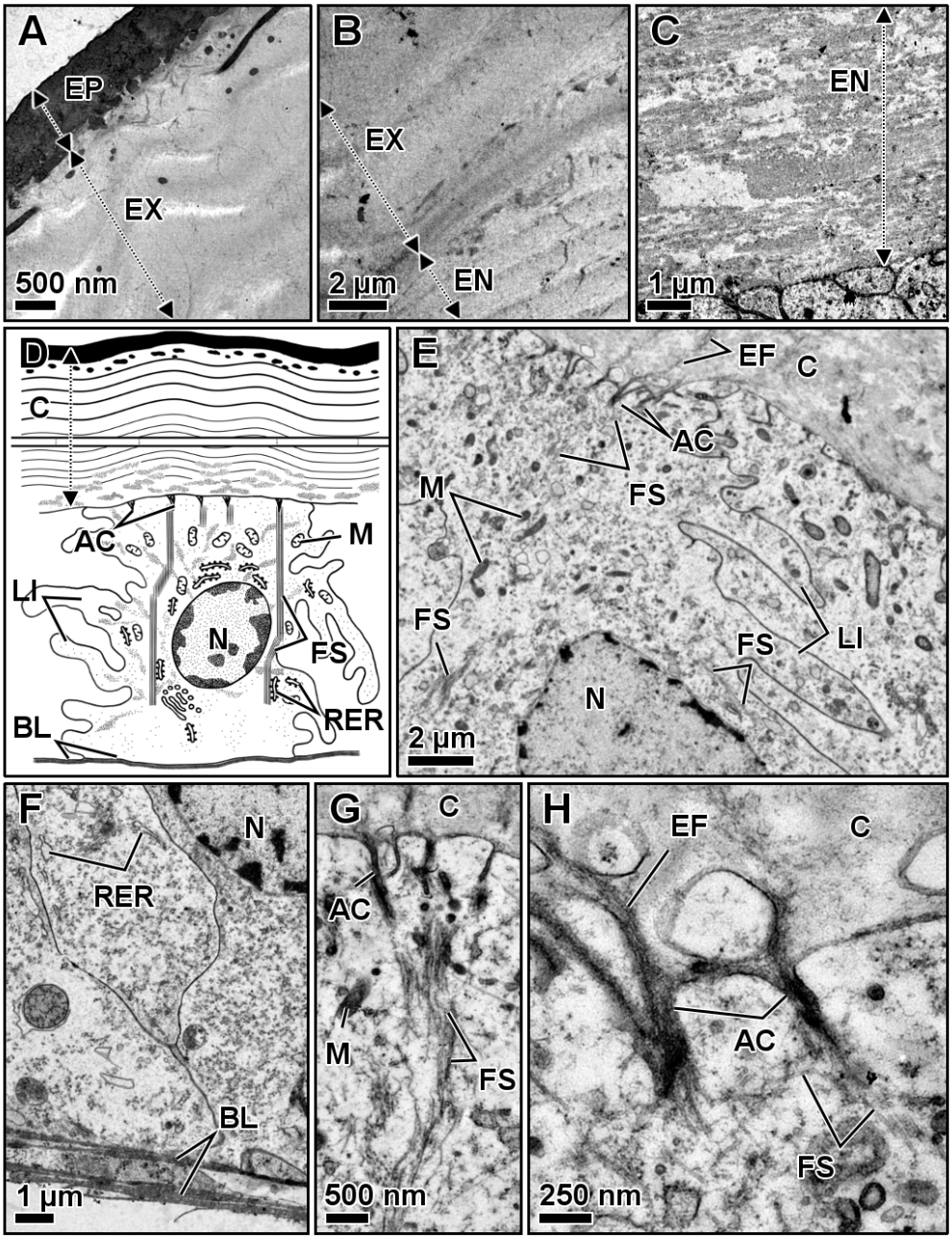

Figure 10. *Maja brachydactyla*. Stomach. Cuticle and epithelial cell. Adult. TEM. Cuticle (A-C): epicuticle and exocuticle (A), exocuticle and endocuticle (B), basis of the endocuticle (C). General diagram (D). Cell apex showing the apical complex (E). Cell basis (F). Cell apex, close view of the apical complex and filamentous structures (G). Cell apex, close view of the electron-dense formations, as well the attachment between the filamentous structures and the apical complex (H). Abbreviations: AC, apical complex; BL, basal lamina; C, cuticle; EF, electron-dense formations; EN, endocuticle; EP, epicuticle; EX, exocuticle; FS, filamentous structures; LI, lateral interdigitations; M, mitochondria; RER, rough endoplasmic reticulum.

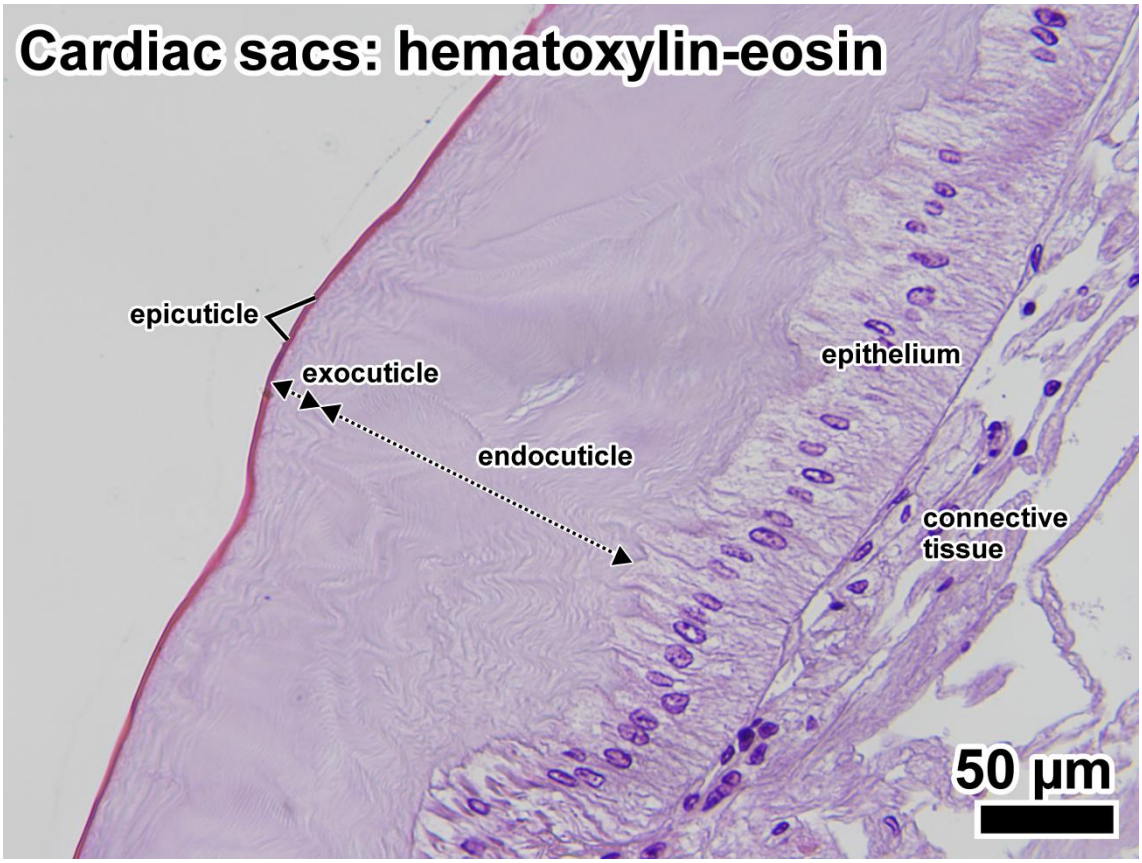

Supplementary Material 1A (Suppl. Fig. 1A). *Maja brachydactyla*. Stomach. Cardiac sacs. Adult. Cuticle and epithelium. Stained with Hematoxylin-Eosin.

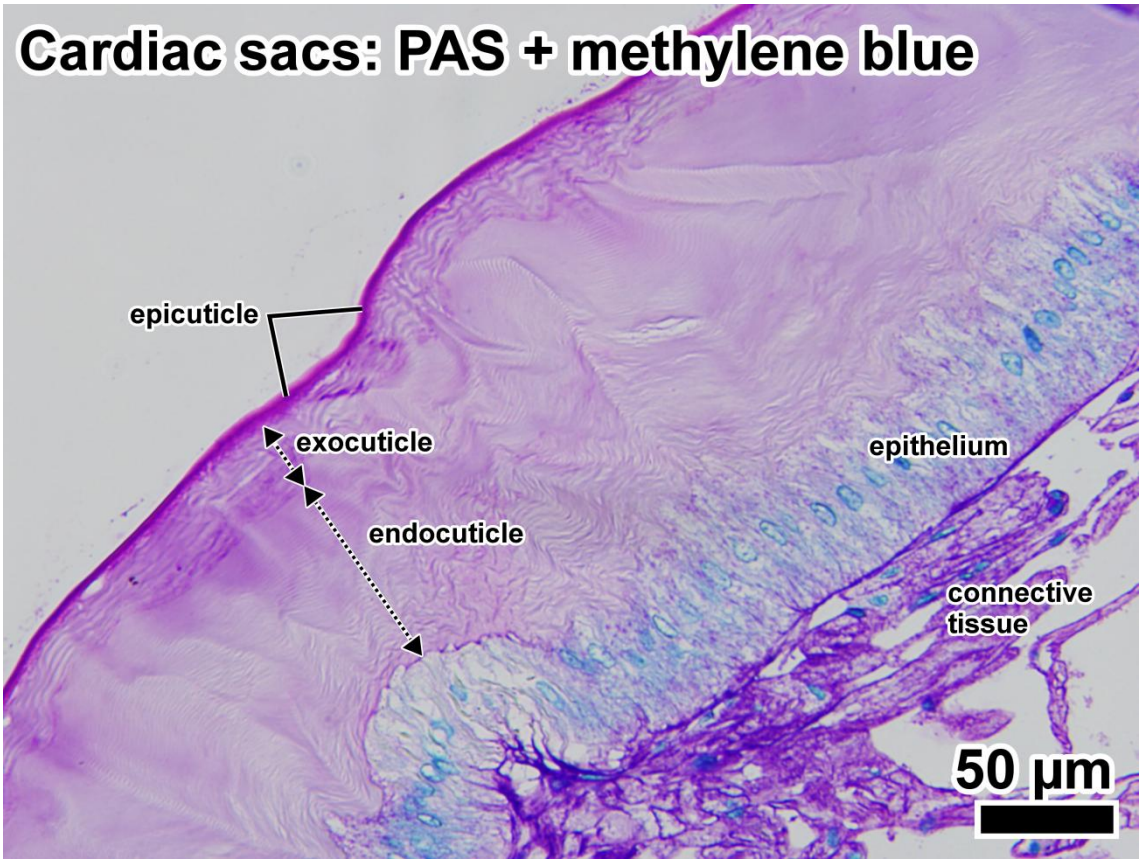

Supplementary Material 1B (Suppl. Fig. 1B). *Maja brachydactyla*. Stomach. Cardiac sacs. Adult. Cuticle and epithelium. Stained with PAS and Methylene Blue.

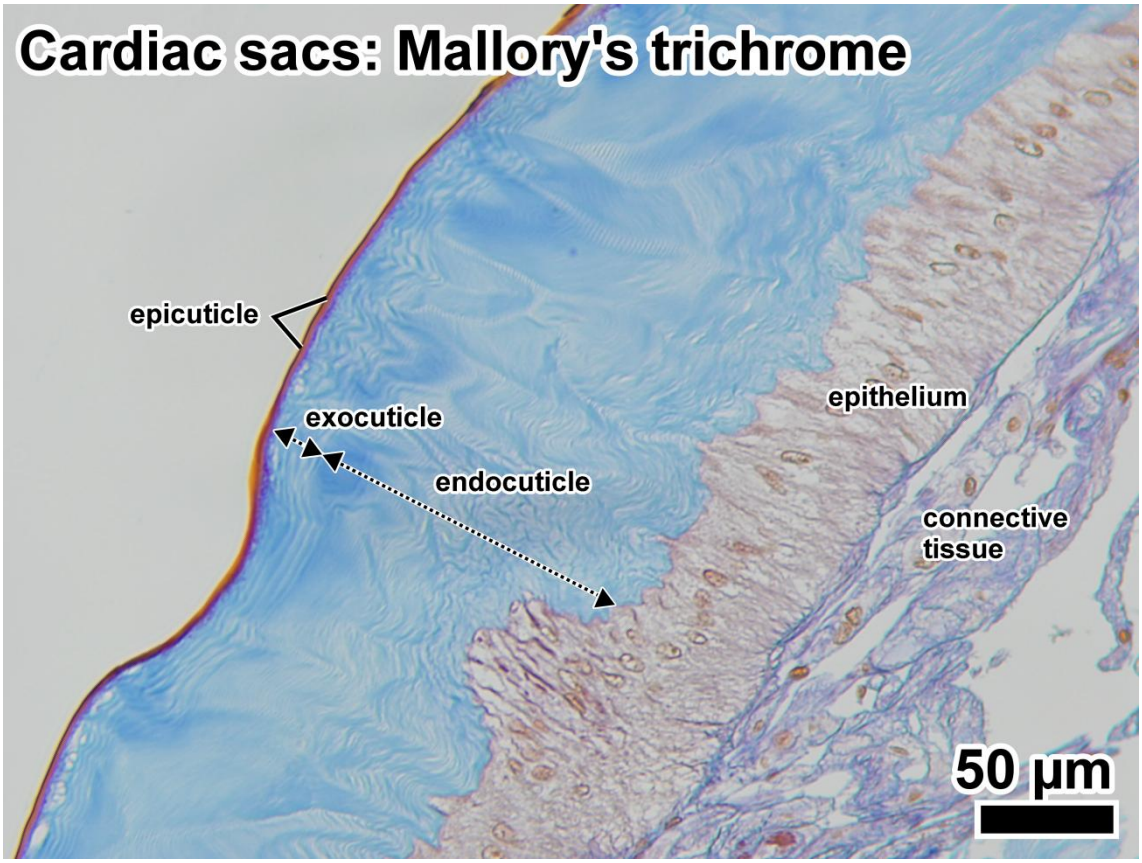

Supplementary Material 1C (Suppl. Fig. 1C). *Maja brachydactyla*. Stomach. Cardiac sacs. Adult. Cuticle and epithelium. Stained with Mallory's Trichrome.

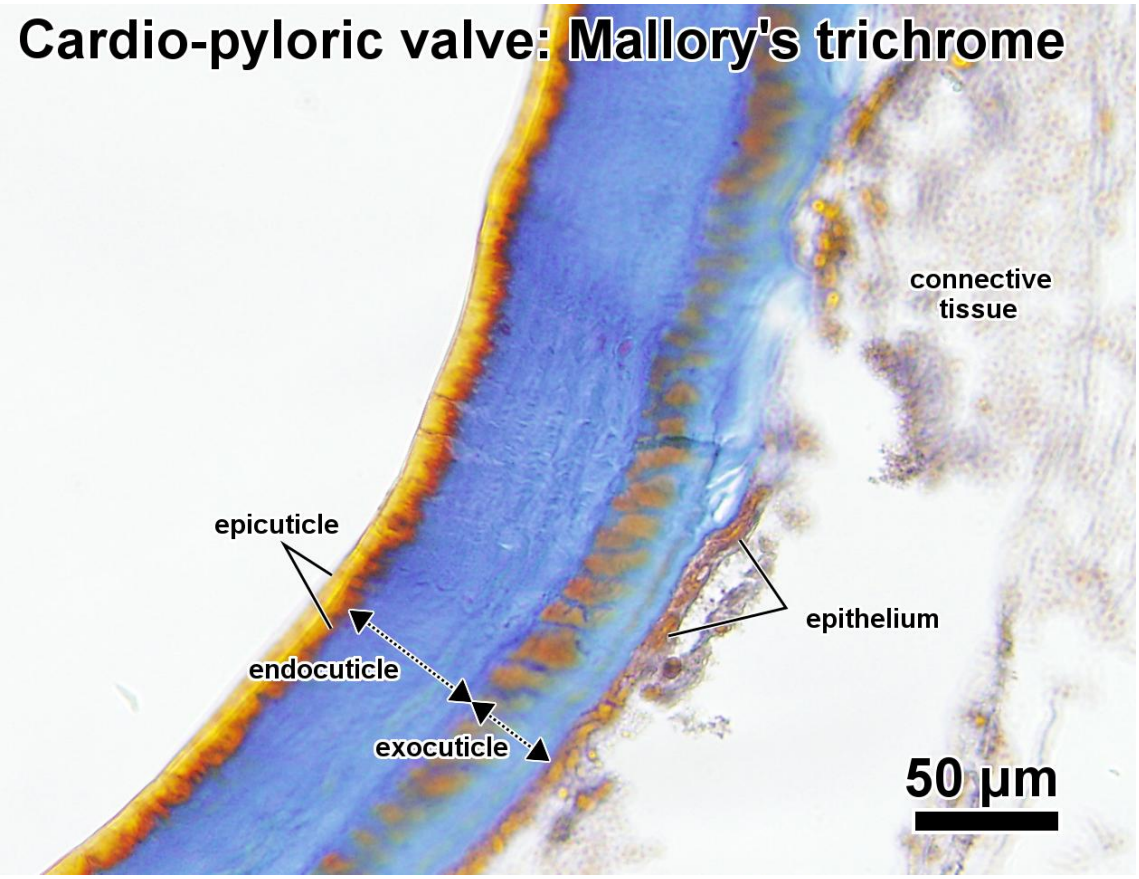

Supplementary Material 2 (Suppl. Fig. 2). *Maja brachydactyla*. Stomach. Cardio-pyloric valve. Adult. Region equivalent to the Fig. 8D. Cuticle and epithelium. Stained with Mallory's Trichrome.

6. Bibliography

Abrunhosa FA, Melo M. 2008. Development and functional morphology of the foreguts of larvae and postlarvae of three crustacean decapods. Brazilian Journal of Biology 68:221-228.

Abrunhosa FA, Melo MA, Abrunhosa JP. 2003. Development and functional morphology of the foregut of larvae and postlarva of *Ucides cordatus* (Decapoda, Ocypodidae). Nauplius 11(1):37-43.

Abrunhosa FA, Simith DJB, Monteiro JRC, de Souza Junior AN, Oliva PAC. 2011. Development and functional morphology of the larval foregut of two brachyuran species from Northern Brazil. Anais da Academia Brasileira de Ciências 83:1269-1278.

Alves STM, Abrunhosa FA, Lima JdF. 2010. Foregut morphology of Pseudothelphusidae and Trichodactylidae (Decapoda: Brachyura) from northeastern Pará, Brazil. Zoologia (Curitiba) 27(2):228-244.

Allardyce BJ, Linton SM. 2010. Functional Morphology of the Gastric Mills of Carnivorous, Omnivorous, and Herbivorous Land Crabs. J Morphol 271(1):61-72.

Boßelmann F, Romano P, Fabritius H, Raabe D, Epple M. 2007. The composition of the exoskeleton of two crustacea: The American lobster *Homarus americanus* and the edible crab *Cancer pagurus*. Thermochimica Acta 463(1):65-68.

Brösing A. 2010. Recent developments on the morphology of the brachyuran foregut ossicles and gastric teeth. Zootaxa 2510:1-44.

Brösing A. 2014. Foregut structures of freshly moulted exuviae from *Maja crispata*, *Cancer pagurus* and *Pseudosesarma moeschi* (Decapoda: Brachyura). Journal of Natural History 48(9-10):543-555.

Brösing A, Richter S, Scholtz G. 2002. The foregut-ossicle system of *Dromia wilsoni*, *Dromia personata* and *Lauridromia intermedia* (Decapoda, Brachyura, Dromiidae), studied with a new staining method. Arthropod Structure & Development 30(4):329-338.

Brösing A, Richter S, Scholtz G. 2007. Phylogenetic analysis of the Brachyura (Crustacea, Decapoda) based on characters of the foregut with establishment of a new taxon. Journal of Zoological Systematics and Evolutionary Research 45(1):20-32.

Brösing A, Türkay M. 2011. Gastric teeth of some thoracotreme crabs and their contribution to the brachyuran phylogeny. J Morphol 272(9):1109-1115.

Castejón D, Ribes E, Durfort M, Rotllant G, Guerao G. 2015a. Foregut morphology and ontogeny of the mud crab *Dyspanopeus sayi* (Smith, 1869) (Decapoda, Brachyura, Panopeidae). Arthropod Structure & Development 44(1):33-41.

Castejón D, Rotllant G, Giménez L, Torres G, Guerao G. 2015b. The effects of temperature and salinity on the survival, growth and duration of the larval development of the common spider crab *Maja brachydactyla* (Balss, 1922) (Brachyura: Majidae). Journal of Shellfish Research 34(3):1073-1083.

Castejón D, Rotllant G, Ribes E, Durfort M, Guerao G. 2015c. Foregut morphology and ontogeny of the spider crab *Maja brachydactyla* (Brachyura, Majoidea, Majidae). J Morphol 276(9):1109-1122.

Ceccaldi HJ. 1989. Anatomy and physiology of digestive tract of Crustaceans Decapods reared in aquaculture. Advances in Tropical Aquaculture, Workshop at Tahiti, French Polynesia. Tahiti, French Polynesia: Actes de colloques Ifremer. p 243-259.

Clark PF. 1986. The larval stages of *Maja squinado* (Herbst, 1788) (Crustacea: Brachyura: Majidae) reared in the laboratory. Journal of Natural History 20(4):825-836.

Coffey WD, Nardone JA, Yarram A, Long WC, Swiney KM, Foy RJ, Dickinson GH. 2017. Ocean acidification leads to altered micromechanical properties of the mineralized cuticle in juvenile red and blue king crabs. J Exp Mar Biol Ecol 495:1-12.

Corgos A, Bernárdez C, Sampedro P, Verísimo P, Freire J. 2011. Spatial structure of the spider crab, *Maja brachydactyla* population: Evidence of metapopulation structure. Journal of Sea Research 66(1):9-19.

Corgos López-Prado A, Verísimo Amor P, Freire Botana JM. 2005. Estacionalidad de la muda terminal y la migración reproductiva en la centolla, *Maja brachydactyla*: evidencias de estrategias de apareamiento alternativas. Repositorio Universidade da Coruña.

Chisaka H, Kozawa Y. 2003. Fine structure and mineralization of the gastric mill in the crayfish during intermolt stage. Journal of Crustacean Biology 23(2):371-379.

Dall W. 1967. The functional anatomy of the digestive tract of a shrimp *Metapenaeus bennettae* Racek & Dall (Crustacea : Decapoda : Penaeidae). Australian Journal of Zoology 15(4):699-714.

Davie PJF, Guinot D, Ng PKL. 2015a. Anatomy and functional morphology of Brachyura. In: Castro P, Davie PJF, Guinot D, Schram F, Von Vaupel Klein C, editors. Treatise on Zoology - Anatomy Taxonomy Biology The Crustacea Volume 9 Part C: Brill. p 11-163.

Davie PJF, Guinot D, Ng PKL. 2015b. Phylogeny of Brachyura. In: Castro P, Davie PJF, Guinot D, Schram F, Von Vaupel Klein C, editors. Treatise on Zoology - Anatomy Taxonomy Biology The Crustacea Volume 9 Part C: Brill, Leiden and Boston. p 922-979.

de La Barra P, Narvarte M, Williner V. 2017. Functional morphology of the gastric mill of the swimming crab *Ovalipes trimaculatus* (Decapoda: Portunidae). Journal of the Marine Biological Association of the United Kingdom:1-8.

Dillaman RM, Roer R, Shafer T, Modla S. 2012. The Crustacean Integument: Structure and Function. In: Watling L, Thiel M, editors. The Natural History of the Crustacea, vol 1 Functional Morphology and Diversity: Oxford University Press. p 140-165.

Erri Babu D, Shyamasundari K, Rao KH. 1982. Studies on the digestive system of the crab *Menippe rumphii* (Fabricius) (Crustacea:Brachyura). J Exp Mar Biol Ecol 58(2):175-191.

Fahy E. 2001. The Magharees spider crab *Maja squinado* fishery in 2000. Irish Fisheries Investigations 9. 21 + appendix p.

Felgenhauer BE. 1992. Chapter 3. Internal Anatomy of the Decapoda: An Overview. In: Harrison FW, Humes AG, editors. Microscopic Anatomy of Invertebrates Volume 10: Decapod Crustacea: Wiley-Liss, Inc. p 45-75.

Giraud-Guille MM. 1984. Fine structure of the chitin-protein system in the crab cuticle. Tissue and Cell 16(1):75-92.

González-Gurriarán E, Fernández L, Freire J, Muiño R, Parapar J. 1993. Reproduction of the spider crab *Maja squinado* (Brachyura: Majidae) in the southern Galician coast (NW Spain). International Council for the Exploration of the Sea: Shellfish Committe ICES C.M. 1993/K:19.

Green JP, Neff MR. 1972. A survey of the fine structure of the integument of the fiddler crab. Tissue and Cell 4(1):137-171.

Guerao G, Pastor E, Martin J, Andrés M, Estévez A, Grau A, Duran J, Rotllant G. 2008. The larval development of *Maja squinado* and *M. brachydactyla* (Decapoda, Brachyura, Majidae) described from plankton collected and laboratory-reared material. Journal of Natural History 42(33-34):2257-2276.

Guerao G, Rotllant G, Anger K. 2010. Characterization of larval moulting cycles in *Maja brachydactyla* (Brachyura, Majidae) reared in the laboratory. Aquaculture 302(1-2):106-111.

Hackman R. 1954. Studies on Chitin I. Enzymic degradation of chitin and chitin esters. Australian Journal of Biological Sciences 7(2):168-178.

Heeren T, Mitchell BD. 1997. Morphology of the mouthparts, gastric mill and digestive tract of the giant crab, *Pseudocarcinus gigas* (Milne Edwards) (Decapoda: Oziidae). Marine and Freshwater Research 48(1):7-18.

Hegdahl T, Gustavsen F, Silness J. 1977a. The structure and mineralization of the carapace of the crab (*Cancer pagurus* L.) 2. The exocuticle. Zoologica Scripta 6(2):101-105.

Hegdahl T, Gustavsen F, Silness J. 1977b. The structure and mineralization of the carapace of the crab (*Cancer pagurus* L.) 3. The epicuticle. Zoologica Scripta 6(3):215-220.

Hegdahl T, Silness J, Gustavsen F. 1977c. The structure and mineralization of the carapace of the crab (*Cancer pagurus* L.) 1. The endocuticle. Zoologica Scripta 6(2):89-99.

Heinzel HG, Weimann JM, Marder E. 1993. The behavioral repertoire of the gastric mill in the crab, *Cancer pagurus*: an in situ endoscopic and electrophysiological examination. The Journal of Neuroscience 13(4):1793-1803.

Hepburn HR, Chandler HD. 1976. Material properties of arthropod cuticles: The arthrodial membranes. Journal of comparative physiology 109(2):177-198.

Hobbs KH, Hooper SL. 2009. High-resolution computed tomography of lobster (*Panulirus interruptus*) stomach. J Morphol 270(9):1029-1041.

Holdich DM, Mayes KR. 1975. A Fine-Structural Re-Examination of the so-called 'Midgut' of the isopod *Porcellio*. Crustaceana 29(2):186-192.

Huber J, Fabritius H-O, Griesshaber E, Ziegler A. 2014. Function-related adaptations of ultrastructure, mineral phase distribution and mechanical properties in the incisive cuticle of mandibles of *Porcellio scaber* Latreille, 1804. Journal of Structural Biology 188(1):1-15.

Huber J, Griesshaber E, Nindiyasari F, Schmahl WW, Ziegler A. 2015. Functionalization of biomineral reinforcement in crustacean cuticle: Calcite orientation in the partes incisivae of the mandibles of *Porcellio scaber* and the supralittoral species *Tylos europaeus* (Oniscidea, Isopoda). Journal of Structural Biology 190(2):173-191.

Hultgren KM, Stachowicz JJ. 2008. Molecular phylogeny of the brachyuran crab superfamily Majoidea indicates close congruence with trees based on larval morphology. Molecular Phylogenetics and Evolution 48(3):986-996.

Icely JD, Nott JA. 1992. Digestion and absorption: digestive system and associated organs. In: Harrison FW, Humes AG, editors. Microscopic anatomy of invertebrates: decapod Crustacea. New York: Wiley-Liss. p 147-201.

Jantrarotai PN, Sawanyatiputi SA. 2005. Histological study on the development of digestive system in zoeal stages of mud crab (*Scylla olivacea*). Kasetsart Journal 39(4):666-671.

Johnston M, Johnston D, Knott B. 2008. Ontogenetic changes in the structure and function of the mouthparts and foregut of early and late stage *Panulirus ornatus* (Fabricius, 1798) phyllosomata (Decapoda: Palinuridae). Journal of Crustacean Biology 28(1):46-56.

Komuro T, Yamamoto T. 1968. Fine structure of the epithelium of the gut in the crayfish (*Procambarus clarkii*) with special reference to the cytoplasmic microtutubles. Archivum histologicum japonicum 30(1):17-32.

Kunze J, Anderson D. 1979. Functional morphology of the mouthparts and gastric mill in the Hermit Crabs *Clibanarius taeniatus* (Milne Edwards), *Clibanarius virescens* (Krauss), *Paguristes squamosus* McCulloch and *Dardanus setifer* (Milne-Edwards) (Anomura: Paguridae). Marine and Freshwater Research 30(5):683-722.

Lignon JM. 1987. Structure and permeability of Decapod Crustacea cuticle. In: Kirsch R, Lahlou B, editors. Adaptations to Salinity and Dehydration 8th Conference of the European Society for Comparative Physiology and Biochemistry (ESCP). Strasbourg: Karger, Basel. p 178-187.

Lima-Gomes RC, Lima JdF, Magalhães C. 2017. Description of ten additional ossicles in the foregut of the freshwater crabs *Sylviocarcinus pictus* and *Valdivia serrata* (Decapoda: Trichodactylidae). Zoologia (Curitiba) 34.

Lima JdF, Garcia JdS, Tavares M. 2016. Foregut morphology of *Macrobrachium carcinus* (Crustacea, Decapoda, Palaemonidae). Acta Amazonica 46(2):209-218.

Lumasag GJ, Quinitio ET, Aguilar RO, Baldevarona RB, Saclauso CA. 2007. Ontogeny of feeding apparatus and foregut of mud crab *Scylla serrata* Forsskål larvae. Aquaculture Research 38(14):1500-1511.

Martin JW, Jourharzadeh P, Fitterer PH. 1998. Description and comparison of major foregut ossicles in hydrothermal vent crabs. Marine Biology 131(2):259-267.

Mary RF, Krishnan G. 1974. On the nature and role of protein constituents of the cuticle of crustaceans in relation to permeability of the cuticle. Marine Biology 25(4):299-309.

McGaw IJ, Curtis DL. 2013. A review of gastric processing in decapod crustaceans. Journal of Comparative Physiology B 183(4):443-465.

McLaughlin PA. 1983. 1. Internal Anatomy. In: Mantel LH, editor. The Biology of Crustacea Vol 5 Internal Anatomy and Physiological Regulation: Academic Press. p 1-52.

Meiss DE, Norman RS. 1977. Comparative study of the stomatogastric system of several decapod crustacea. I. Skeleton. J Morphol 152(1):21-53.

Melo MA, Abrunhosa F, Sampaio I. 2006. The morphology of the foregut of larvae and postlarva of *Sesarma curacaoense* De Man, 1892: a species with facultative lecithotrophy during larval development. Acta Amazonica 36:375-380.

Minagawa M, Takashima F. 1994. Developmental changes in larval mouthparts and foregut in the red frog crab, *Ranina ranina* (Decapoda: Raninidae). Aquaculture 126(1-2):61-71.

Mrak P, Bogataj U, Štrus J, Ţnidaršič N. 2017. Cuticle morphogenesis in crustacean embryonic and postembryonic stages. Arthropod Structure & Development 46(1):77-95.

Muzzarelli RAA. 1977. Chapter 3 - Chitin Chemistry. Chitin: Pergamon. p 87-154.

Mykles DL. 1979. Ultrastructure of alimentary epithelia of lobsters, *Homarus americanus* and *H. gammarus*, and crab, *Cancer magister*. Zoomorphologie 92(3):201-215.

Nakamura K. 1990. Organogenesis during metamorphosis in the swimming crab *Portunus trituberculatus*. Nippon Suisan Gakkaishi 56(10):1561-1564.

Nakamura K, Takemoto T. 1986. Morphology of stomach ossicles in Brachyura. Memoirs of Faculty of Fisheries Kagoshima University 35(1):7-15.

Nesbit KT, Roer RD. 2016. Silicification of the medial tooth in the blue crab *Callinectes sapidus*. J Morphol 277(12):1648-1660.

Pires C, Marques A, Carvalho ML, Batista I. 2017. Chemical Characterization of *Cancer Pagurus*, *Maja Squinado*, *Necora Puber* and *Carcinus Maenas* Shells. Poultry, Fisheries & Wildlife Sciences 5:181.

Reddy AR. 1937. The physiology of digestion and absorption in the crab *Paratelphusa* (*Oziotelphusa*) *hydrodromus* (Herbst). Proceedings of the Indian Academy of Sciences - Section B 6(3):170-193.

Roer R, Abehsera S, Sagi A. 2015. Exoskeletons across the Pancrustacea: Comparative Morphology, Physiology, Biochemistry and Genetics. Integrative and Comparative Biology 55(5):771-791.

Ruangchai S, Reisecker C, Hild S, Ziegler A. 2013. The architecture of the joint head cuticle and its transition to the arthrodial membrane in the terrestrial crustacean Porcellio scaber. Journal of Structural Biology 182(1):22-35.

Salindeho IR, Johnston DJ. 2003. Functional morphology of the mouthparts and proventriculus of the rock crab *Nectocarcinus tuberculosus* (Decapoda: Portunidae). Journal of the Marine Biological Association of the United Kingdom 83(04):821-834.

Schlegel C. 1911. Anatomie sommaire de la première zoé de *Maja squinado* Latr. (Note préliminaire à des recherches sur l'Organogénese des Décapodes brachyoures). Archives de Zoologie Experimentale et Générale 5º Série T. VIII.(2):29-40.

Simon CJ, Carter CG, Battaglene SC. 2012. Development and function of the filter-press in spiny lobster, *Sagmariasus verreauxi*, phyllosoma. Aquaculture 370-371(0):68-75.

Skilleter G, Anderson D. 1986. Functional morphology of the Chelipeds, mouthparts and gastric mill of *Ozius truncatus* (Milne Edwards) (Xanthidae) and *Leptograpsus variegatus* (Fabricius) (Grapsidae) (Brachyura). Marine and Freshwater Research 37(1):67-79.

Skinner DM. 1962. The structure and metabolism of a crustacean integumentary tissue during a molt cycle. The Biological Bulletin 123(3):635-647.

Sousa L, Petriella AM. 2006. Morphology and histology of *P. argentinus* (Crustacea, Decapoda, Caridea) digestive tract. Biocell 30:287-294.

Tziouveli V, Bastos-Gomez G, Bellwood O. 2011. Functional morphology of mouthparts and digestive system during larval development of the cleaner shrimp *Lysmata amboinensis* (de Man, 1888). J Morphol 272(9):1080-1091.

Vatcher HE, Roer RD, Dillaman RM. 2015. Structure, molting, and mineralization of the dorsal ossicle complex in the gastric mill of the blue crab, *Callinectes sapidus*. J Morphol 276(11):1358-1367.

Vernon GM, Herold L, Witkus ER. 1974. Fine structure of the digestive tract epithelium in the terrestrial isopod. *Armadillidium vulgare*. J Morphol 144(3):337-359.

Welinder BS. 1974. The crustacean cuticle—I. Studies on the composition of the cuticle. Comparative Biochemistry and Physiology Part A: Physiology 47(2):779-787.

Welinder BS. 1975. The crustacean cuticle - III. Composition of the individual layers in *Cancer pagurus* cuticle. Comparative Biochemistry and Physiology Part A: Physiology 52(4):659-663.

Williams CL, Dillaman RM, Elliott EA, Gay DM. 2003. Formation of the arthrodial membrane in the blue crab, *Callinectes sapidus*. J Morphol 256(3):260-269.

Williams RL. 1944. The pre-zoea stage of *Porcellana platycheles* (Pennant). Preliminary anatomical and histological notes. Journal of the Royal Microscopical Society 64(1-2):1-15.

Willis JH. 1999. Cuticular proteins in insects and crustaceans. American Zoologist 39(3):600-609.

Witkus ER, Grillo RS, Smith WJ. 1969. Microtubule bundles in the hindgut epithelium of the woodlouse *Oniscus ascellus*. Journal of Ultrastructure Research 29(3):182-190.

Woods CMC. 1995. Morphology of the foregut of the Spider Crab *Notomithrax ursus* (Brachyura:Majidae) Journal of Crustacean Biology 15(2):220-227.

Ziegler A. 1997. Ultrastructural changes of the anterior and posterior sternal integument of the terrestrial isopod *Porcellio scaber* Latr. (Crustacea) during the moult cycle. Tissue and Cell 29(1):63-76.

CHAPTER 14.

Morphology and ontogeny of the midgut gland ("hepatopancreas") of the Atlantic spider crab *Maja brachydactyla* Balss, 1922 (Brachyura, Majidae)

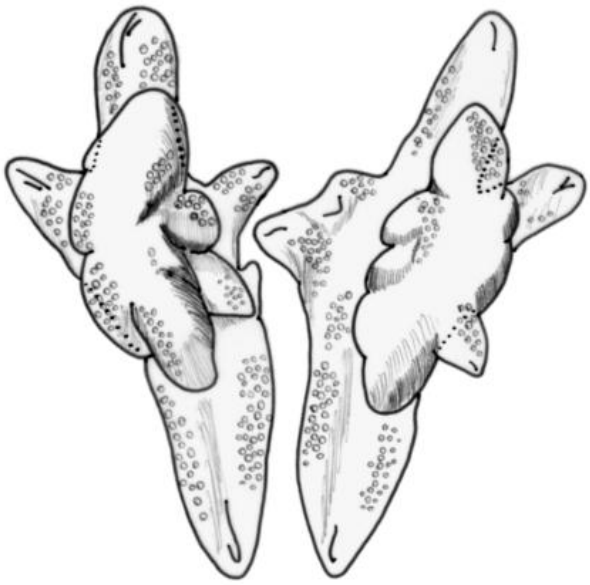

Morphology and ontogeny of the midgut gland ("hepatopancreas") of the Atlantic spider crab *Maja brachydactyla* Balss, 1922 (Brachyura, Majidae).

Diego Castejón[1*], Guiomar Rotllant[2], Javier Alba-Tercedor[3], María Font i Furnols[4], Enric Ribes[5], Mercè Durfort[5], and Guillermo Guerao[6]

[1]IRTA, Centre d"Aqüicultura, Ctra. del Poble Nou Km 5.5. 43540 Sant Carles de la Ràpita, Tarragona (Spain).

[2]CSIC, Institut de Ciències del Mar, Passeig Marítim de la Barceloneta 37-49. 08003 Barcelona (Spain).

[3]Departamento de Zoología, Facultad de Ciencias, Universidad de Granada, Av. de Fuente Nueva s/n. 18071 Granada (Spain).

[4]IRTA, Qualitat del Producte, Finca Camps i Armet. 17121 Monells, Girona (Spain).

[5]Unitat de Biologia Cel·lular, Departament de Biologia Cel·lular, Fisiologia i Immunologia, Facultat de Biologia, Universitat de Barcelona, Diagonal 645. 08028 Barcelona (Spain).

[6]PS Fabra i Puig 344.08028 Barcelona (Spain).

Short title: *Maja brachydactyla* midgut gland morphology and ontogeny

***Corresponding author:** Diego Castejón. E-mail: diego.castejon.dcb@gmail.com; phone: +34 681 154 398; postal address: IRTA, Subprogram Cultius Aqüàtics, Ctra. Poble Nou, Km 5.5, 43540 Sant Carles de la Ràpita, Tarragona, Spain.

Abstract.

The midgut gland (MGG), also called "hepatopancreas", is the most important digestive organ of Decapoda. It occupies a great volume of the cephalothoracic cavity and has an important digestive and absorptive role. The studies focused on the MGG ontogeny still are scarce, then this study describes the MGG morphology of the brachyuran *Maja brachydactyla* Balss, 1922 in larval, first juvenile and adult stages. The techniques employed include the stereomicroscopy, optical and scanning electron microscopy, as well as computed tomography and micro computed tomography (micro-CT). The adult MGG of *M. brachydactyla* resulted similar to other decapods. It is a massive organ with orange-yellowish to brownish coloration that occupies the cephalothoracic cavity. It is composed by tens of thousands blind-end tubules. The larval MGG is much simpler and formed by fourteen blind-end tubules whose number do not increase until the late megalopa/early juvenile stages. The most important morphological change observed along the larval development is the lengthening of the blind-end tubules. The muscles fibers forms a network that surround the blind-end tubules: the circular fibers are wider and forms rings around the tubule, these rings are connected by thin and spaced longitudinal muscle fibers oriented longitudinally with the tubule axis.

Keywords: Crustacea; larval development; allometric growth; blind-end tubules; muscle network; Micro-computed tomography (micro-CT)

1. Introduction

The midgut gland (MGG) of decapods is an organ that received numerous names since its early description on the 19th Century: "anterior caeca", "digestive diverticula", "digestive gland", "digestive organ", "enteric organ", "gastric gland", "glandula media intestini", "liver", "mid-intestinal gland", "midgut gland", "pancreas" or "principal digestive gland" among others, but the most popular denomination for this organ is "hepatopancreas" (Davie et al., 2015; Gibson and Barker, 1979; Milne-Edwards, 1834a, b; Schlegel, 1911; Van Weel, 1974). Nevertheless, we agree with Cervellione et al. (2017), that “hepatopancreas” is inappropriate because this organ inherently differs from the liver and pancreas of vertebrates. In this study the term used is "midgut gland". The MGG of the decapods is a pair of large and compact glandular masses occupying the majority of the volume of the cephalothoracic cavity, covering partially the stomach and midgut tract. Each half of the MGG is composed by two to three lobes ramified into numerous blind-end tubules. The entire structure is surrounded by a slender syncytial or connective tissue and a network of muscle fibers (Ceccaldi, 1989; Davie et al., 2015; Felgenhauer, 1992; Gibson and Barker, 1979). The MGG is a very important digestive organ, main functions are nutrient storage (Gibson and Barker, 1979; Loizzi, 1971; Vogt, 1994) and synthesis and secretion of digestive enzymes (Ceccaldi, 1989; Felgenhauer, 1992; Gibson and Barker, 1979). The morphology and role of the MGG has been extensively studied and reviewed in adult decapods (Ceccaldi, 1989; Cervellione et al., 2017; Felgenhauer, 1992; Gibson and Barker, 1979; Loizzi, 1971; Van Weel, 1974; Vogt, 1996). On the contrary, in the case of the larvae the general morphology and ontogeny of the MGG received little attention (Abrunhosa and Kittaka, 1997; Nakamura, 1990; Trask, 1974), and therefore the information available is still scarce.

The Atlantic spider crab *Maja brachydactyla* Balss, 1922 is distributed from the Açores and British Isles to the Sahara, including the Canary Islands and south-western Mediterranean Sea (Abelló et al., 2014), and it is an important fishery species in Europe (FAO, 2012). The larval development is abbreviated; to hatch to the first juvenile stage the animal require two zoeal stages (zoea I and zoea II) and one megalopa stage (Guerao et al., 2008; Lebour, 1927). Milne-Edwards (1834b) illustrated in detail the MGG shape in adult *Maja* specimens, and some notes of the MGG in the first zoeal stage were mentioned by Schlegel (1911). However, a detailed description of the general morphology of the MGG during the larval stages and the changes occurred during the development is still missing.

The present study focus on the gross morphology and ontogeny of the MGG in *M. brachydactyla* comparing with it is up to now known in others decapods, employing stereomicroscopy, optical and electron microscopy, computed tomography and micro computed tomography.

2. Material and methods

2.1 Origin of the adult specimens. Broodstock culture system.

The adult specimens were caught in Atlantic waters by order to fishery companies (LONXANET, CADEMAR) and transported to the Institut de Recerca i Tecnologia Agroalimentàries facilities (IRTA, Sant Carles de la Ràpita, Tarragona, Spain). These animals were dissected at their arrival or used as broodstock. Broodstock animals were kept in 2,000 L cylindrical tanks connected to a recirculation unit (renewal rate = 3.5 m^3 h^{-1}) in a sex-ratio of six females and one male per tank. Constant conditions were: temperature =18 ± 1 °C, salinity = 35 ± 1 psu (filtered seawater), photoperiod = 12 h light: 12 h dark, and light intensity = 25 lux (fluorescent tubes). The

animals were feed with a combination of fresh and frozen mussels (*Mytilus* sp.). The broodstock animals were used to obtain the larvae required for the study of the MGG during the larval stages.

2.2 Larval culture system

The larvae obtained from the broodstock animals were reared in 600 mL glass beakers placed inside 360 L tanks (96 x 96 x 40 cm) used as incubation chambers. The environmental parameters were maintained constants: temperature = 21 ± 1 °C, salinity = 35 ± 1 psu, photoperiod = 12 h light: 12 h and light intensity = 1,000 lux (LED lights). The larvae were fed daily *ad libitum* with fresh *Artemia* sp. nauplii and metanauplii (INVE Aquaculture Nutrition, Salt Lake UT, USA). Daily, the living specimens were carefully transferred to other glass beakers with clean water and fresh food. Newly hatched larvae within ca. 15 hours were collected from the broodstock tanks and placed in the culture glass beakers without previous acclimation. The animals reached the zoea II stage at day 3, the megalopa stage at day 6 and metamorphosed to first juvenile at day 11-13.

2.3 Gross morphology

The morphometric study required the dissection of six adult specimens. The entire fresh midgut gland (MGG) of each specimen was weighed. Then samples of each MGG were taken, weighed and fixed in 4 % formaldehyde. The fixed samples were weighed again to calculate the relative weight variation due to the fixative process, then subsamples with known weight (between 15 and 60 mg) were taken to count the number of blind-end tubules. Only the tips of the blind-end tubules have been counted since the tubules broke easily. The previous data were employed to calculate the density as number of tubules per mass unity, this value was extrapolated to calculate the number

of tubules per MGG. The weight measures were realized using a Mettler Toledo AE200 balance (range: 0 - 205 g, precision: 0.1mg). The observations were realized under a Nikon SMZ800 stereomicroscope.

The larvae were sampled daily from hatching to the first juvenile stage. The sampled specimens were immediately fixed in 4 % formaldehyde. After the fixation, the specimens were dissected under a Nikon SMZ800 stereomicroscope using teasing needles. For the morphometric study, specimens at the start of each stage were selected and between 4 and 6 MGGs per stage were measured. Several measures were taken as described below (see Fig. 5). The photographs and length measures were realized employing the AnalySIS® software tools (Soft Imaging System, Münster, Germany) properly calibrated.

2.3.1. Measures realized on the ventral sub-lobule (VSL): total length (TL) and maximum width (MW), these measures are important since this central tubule represents the main volume of the larval MGG.

2.3.2. Measures of the lateral tubules have been differentiated between external (ET) and internal tubules (IT) in relation to their location in the larval MGG. In the case of the ET the following measures were taken: total length (ETl) and width (ETw); while in the case of the IT the measures were: total length (ITl) and width (ITw). The lateral tubules are projected in diverse angles, so to take standardized measures we proceed to consider the width as the basal line that separates the lateral tubule from the central tubule; then, the total length has been measured as the maximum perpendicular height from the basal line to the tip of the lateral tubule.

2.3.3.Measures of the dorsal sub-lobule (DSL): total length (DSl), width (DSw) and height (DSh).

The data obtained were analyzed using R version 3.2.0 (R Development Core Team, 2015). One way ANOVA was performed using as factor one measure value (TL, MW, DSl, DSw, DSh, ETl, ETw, ITl, or ITw) per analysis. Comparisons among life stages (zoea I, zoea II, megalopa, first juvenile) after finding significant differences were performed by Tukey-HSD test. Normality and homogeneity were tested by Shapiro-Wilk and Levene tests. The critical level (α) to reject the null hypothesis was 0.05.

For optical microscopy, the fixative employed was Davidson's (ethanol absolute: seawater: formaldehyde 37 %: glycine: glacial acetic acid in proportion 3: 3: 2: 1: 1). The material fixed were pieces of adult MGG (2 - 5 g) and entire larval specimens. The samples were maintained in the fixative during ca. 24 h. The samples were dehydrated, embedded in paraffin, cut into 2 µm sections using a microtome (Leica RM2155) and stained with Mallory's trichrome (acid fuchsine, orange G and aniline blue stain) to reveal the structure of the muscular and connective tissues. The histological observations were realized under an optical microscope (Leica LB30T 111/97) connected to a camera (Olympus DP70 1.45 Mpx; Olympus Corporation, Germany) and an image analyzing system (DP Controller 2.1.1.83 and DP Manager 2.1.1.163; Olympus Corporation, Germany).

In the case of the electron microcopy, the fixative employed was 2 % paraformaldehyde - 2.5 % glutaraldehyde in cacodylate buffer (0.1 mol L^{-1} pH 7.4). The material fixed were small pieces of adult MGG and entire MGGs of first zoeae and megalopa. The samples were maintained in the fixative during ca. 12 h at 4 °C and constant darkness, then they were rinsed twice with cacodylate buffer and post-fixed in 1 % osmium tetroxide solution in cacodylate buffer (0.1 mol L^{-1} pH 7.4). The next step

was the dehydration in a graded series of acetone. For scanning electron microscopy (SEM), the post-fixed samples after the critical-point-drying were mounted on SEM stubs with self-adhesive carbon stickers and covered by carbon coating. Observations were made with a JEOL JSM-7001F scanning electron microscope (15 kV). For transmission electron microscopy (TEM), the samples were embedded in Spurr‟s resin, semi-thin sections were obtained using a Leica UCT ultra-microtome and stained by Bromophenol Blue. Then the ultra-thin sections (50 - 70nm) were made using the same ultra-microtome and counterstained with uranyl acetate and lead citrate. Observations were made with a JEOLEM-1010 transmission electron microscope (tungsten filament, 80 kV). The post-fixative treatment and TEM and SEM observations were realized at CCiTUB (Hospital Clinic, University of Barcelona, Barcelona).

Two protocols were employed for the computed tomography. In the case of the adults, specimens (one male and one female) were scanned with the computed tomography equipment General Electric HiSpeedZx/I (GE Healthcare, Boston, Massachusetts, USA). The scanning parameters were setup as: helical acquisition, pitch 1, 140 kV, 150 mA, displayed field of view 250 mm, 3 mm thickness and reconstruction algorithm STD+. Image analysis was performed with the Centricity Radiology RA600 v.7 software (GE Medical Systems Information Technologies, Inc., 8200 W, Tower Ave Milkwaukee, WI, USA). This activity was realized at the Institut de Recerca i Tecnologia Agroalimentàries facilities (IRTA) of Monells (Girona, Spain).

In the case of the larvae, zoeae fixed in 2 % paraformaldehyde - 2.5 % glutaraldehyde in cacodylate buffer (0.1 mol L^{-1} pH 7.4) and megalopae fixed in ethanol 70 % were preserved into isopropanol 100 %. At continuation, the specimens were transferred to a solution of iodine 1 % in ethanol absolute during 72 h, then submerged

in hexamethyldisilazane for 4 h and overnight air dried. To maintain the animals on the sample holder, different methods have been essayed (Alba-Tercedor and Sáinz-Cantero, 2012). For tiny samples such as the zoea larvae, the best results were obtained by gluing the animal with cyanoacrylate to the tip of a nylon filament line, of 200 µm diameter. The megalopa were mounted inside of a holed piece of BASOTECT® (melamine resin foam, created by the Chemical Company BASF). All samples were enclosed inside a plastic straw, to avoid any movement provoqued by the air refrigerating forced air during the scan process. The Basotect‟s material results of very low density, and thereafter very transparent to X-Ray and therefore it can be easily eliminated during the segmentation procedure (Alba-Tercedor and Alba-Alejandre, 2017). A SkyScan 1172 high resolution microtomographer (Bruker microCT,Kontich, Belgium), with a Hamamatsu 80/250 source and a VDS 1.3Mp camera was used. The scanning parameters for the zoea were setup as: isotropic voxel size of 1.48 µm per pixel, 49 kV, 78µA, rotation step of 0.3° and 180º of rotation scan. The scanning parameters for the megalopa were setup as: isotropic voxel size of 1.47 µm per pixel, 54 kV, 85 µA, rotation step of 0.5° and 180º of rotation scan.

For primary reconstructions and the "cleaning" process to obtain the datasets of cross-sectional images („slices‟), we used the latest versions of the free Bruker micro-CT Skyscan (www.skyscan.be) software (NRecon, DataViewer, CTAnalyser); then volume renderings were obtained using Skyscan‟s software CTVox. For a more detailed description of the process see Alba-Tercedor (2014). This activity was realized at the Department of Zoology of the University of Granada, Spain.

3. Results

General morphology in adult. The midgut gland (MGG) of the adult *M. brachydactyla* is a large and massive organ that occupies a great volume of the cephalothoracic cavity (Fig. 1A). The MGG distribution is quite ubiquitous, occupying the majority of the spaces of the cephalothoracic cavity, excepting those occupied by other organs. The observations realized by helical tomography reveal that the adult MGG occupies approximately the 62 % of the cephalothoracic cavity at the stomach plane, the 49 % at the heart plane and the 19 % at the terminal midgut tract plane (Fig. 2A-B). The MGG is directly connected to the pyloric filters of the stomach and the anterior extreme of the midgut tract. It is divided in right and left lobes, each one extended inside the cephalothorax into anterior, lateral and posterior projections (Fig. 1A). The MGG is composed with a large quantity of blind-end tubules (Fig. 1A-B), compacted at a mean density of 2.3 ± 0.8 tubules per mg of fresh MGG. The mean number of tubules is 46,000 per MGG, although values ranged from 35,000 to 60,000 tubules in specimens with a mean carapace length of 135 ± 8 mm. The mean length of the tubules is 2.5 mm, but can oscillate from 0.8 to 4.5 mm (Fig. 1C-D). The blind-end tubules have a finger-like shape at low magnification (Fig. 1A-B), but are organized in a branched structure where numerous tubules of different size are originated from multiple points along the length of a longer tubule, remembering the growing scheme of the coral branches (Fig. 1C-D). The tubules are tubular structures with circular cross section (Fig. 1E); the opaque and translucent longitudinal bands observed under the stereomicroscope (Fig. 1C) correspond to an internal variation in the epithelium height that gives an "X" shape to the lumen cross section (Fig. 1 E). The scanning microscopy also permit to identify some epithelial cell types as the R- and B- cells (Fig. 1E). The

blind-end tubules are surrounded by fine rings of circular muscle fibers (Fig. 1D; 8B; 9D-E); see the "Muscle organization" section for more details.

General morphology in larvae and first juvenile. Similarly to the adults, the MGG of the larvae and first juvenile occupies an important volume of the cephalothoracic cavity. The micro computed tomography and optical microscopy observations reveal that the MGG occupies at the pyloric stomach and heart planes around the 11 % and 46 % of the cephalothoracic cavity in the first zoeal stage and around the 43 % and 59 % in the megalopa stage, respectively (Fig. 2C-D). The MGG, from hatching to late megalopa stage (the major part of the larval development) is composed by fourteen blind-end tubules (Fig. 3-6; S1A-C), contrasting with the thousands of blind-end tubules that forms the adult MGG. The description of the larvae MGG is schematized in the Fig. 5. This organ presents two lobules, right and left, both lobules are mirrored but asymmetrical. Each lobule is in turn subdivided in dorsal and ventral sub-lobules. The dorsal sub-lobule is flattened laterally and shorter than the ventral sub-lobule; it is composed by a single anterior blind end-tubule and a pair of posterior blind-end tubules parallel to the vertical plane. The ventral sub-lobule represents the maximum length of the lobe, this sub-lobule has a "trident-like" shape, being composed by a single posterior blind-end tubule and three anterior blind-end tubules parallel to the horizontal plane. The three anterior blind-end tubules of the ventral sub-lobule have been denominated external, central and interior tubules in relation to their position (Fig. 5). The pyloric stomach rest over a basement formed by the internal tubules, while the lateral walls of the pyloric stomach are covered by the dorsal sub-lobules, but at difference to the adults the posterior caecum remain uncovered (Fig. 3-4). In total, each lobule has seven blind-end tubules and the entire

organ has fourteen blind-end tubules. The number of tubules of the MGG vary after the late megalopa stage. Few days before the metamorphosis to juvenile (around the ninth or tenth day of development at 21°C), the megalopa presents a few buds that will develop into new end tubules. Therefore, the MGG of the newly metamorphosed juveniles can show from two to five additional buds / short blind-end tubules and these buds are only developed on the dorsal sub-lobule (Fig. 6, Juvenile; S1A-C, Juvenile).

Although no new tubules are formed until the late larval development, the size of the MGG tubules varies from hatching to the first juvenile stage (Fig. 3, 6-7; S1A-C). The results of the morphometric study of the MGG during the larval development are showed in Table 1. These results reveal that all the blind-end tubules have a general tend to grow in length while the growth in width is marginal in comparison (Table 1, Fig. 7A-C), demonstrating that the MGG growth is allometric prioritizing the increment in length over the increment in width (right lobule: $F_{3,13}= 8.79$ $p < 0.01$; left lobule: $F_{3,13} = 10.88$ $p < 0.001$). In this sense, the relation between length and width increases from 2.7 ± 0.5 in the newly hatched zoeae to 4.1 ± 0.4 in the newly molted juvenile.

Muscle organization. Despite the differences observed on the MGG morphology between the adult and the larval / first juvenile stages, the muscle organization at tubule level is very similar. The muscle fibers are striated (Fig. 8B). We observed two orientations on the muscle fibers: circular and longitudinal muscle fibers (Fig. 9D-E). In both cases the muscle fibers are separated from the epithelial cells by a very thin basal lamina. The intimate relation between epithelial cells and muscle fibers imply that the epithelium forms basal folds that fit with the muscle fiber width (Fig. 8A; 9C, F). In both adult and larval stages the circular muscle fibers are wider and most visible than the longitudinal muscle fibers, these forms rings that wrap the blind-end tubule (Fig.

1D; 9A-B, D-E). In the adults the circular muscle fibers are 6.95 ± 3.31 µm in width. The rings of circular muscle fibers are parallel among them and separated by intervals of 47.58 ± 8.33 µm along the tubule length (Fig. 1D; 8B; 9D-E). In the larvae, the fibers of the circular muscles are thinner and more difficult to observe (Fig. 8C), they are separated by intervals of around 9 ± 2 µm (Fig. 9A-B). The longitudinal muscle fibers connect the rings of circular muscle fibers, these longitudinal fibers are oriented parallel to the longitudinal axis of the tubule and perpendicularly to the circular muscle fibers, so both circular and longitudinal muscles forms an rectangular network highly connected. The longitudinal muscle fibers are thinner (measuring around the half of the circular muscle fiber width) and are also separated among them by less distance than the circular muscle fibers (Fig. 9D-E). In general terms, the circular and longitudinal muscle fibers are much bigger and richer in myofibrils in adults than in larvae, the bundle of myofibrils is delimited by a thin membrane. Surrounding the muscle fibers appear a thin basal lamina (Fig. 9C, F).

4. Discussion

Milne-Edwards in his historical document "Histoire naturelle des crustacés" (1834a, b) described for first time the adult midgut gland (MGG), named foie ("*liver*"), of a species of the genus *Maja*. This organ was described as a pair of big, yellowish, glandular masses occupying the cephalothoracic cavity, subdivided into three main lobes (anterior, posterior and dorsal), in turn composed by numerous small "vesicles" (probable reference to the "blind-end tubules") united by tubes that converge into a pair of main ducts located on the lateral sides of the pyloric stomach. This description coincides greatly to our study of the adult MGG of *M. brachydactyla*: it is an organ composed by a pair of enormous glandular masses, orange to brownish, that occupy an

important volume of the cephalotorax cavity. The MGG is connected to the midgut by a pair of main ducts, can be subdivided into three main lobules (anterior, posterior and dorsal), in turn composed by tens of thousands short blind-end tubules. Other brachyurans present a similar description of the MGG, e.g. the eriphiid *Menippe rumphii* (Erri Babu et al., 1982), the gecarcinucid *Spiralothelphusa hydrodroma* (as *Parathelphusa hydrodromus*) (Reddy, 1937), the portunid *Scylla serrata* (Barker and Gibson, 1978), the ocypodids *Ocypode platytarsis* (Ramadevi et al., 1990) and *Uca uruguayensis* (Cuartas and Petriella, 2002), as well the varunids *Neohelice granulata* and *Cyrtograpsus angulatus* (Cuartas and Petriella, 2002).

In the astacids the MGG is quite similar with scarce morphological variability. The historical monograph of Huxley (1880) dedicated to the crayfish *Astacus astacus* (as *Astacus fluviatilis*) described the MGG (named "liver") as a pair of large glands, yellowish or brownish, with tri-lobular structure and composed by countless small caeca. These MGG features are shared by other crayfishes species, as *Orconectes virilis*, *Procambarus blandingii* and *P. clarkii* (Davis and Burnett, 1964; Kouichi, 1959; Loizzi, 1966). Yonge (1924) studied extensively the digestive system of the Norway Lobster *Nephrops norvegicus* and the MGG (named "hepatopancreas") is described as a pair of brownish glands with tri-lobular structure (anterior, posterior and dorsal) and composed by numerous small tubules, the author also noted that the main ducts of the MGG connect with the midgut. In *Homarus gammarus* the MGG is also a yellowish green, massive, paired organ subdivided into three main lobes composed by numerous blind-end tubules covered by connective tissue and discrete muscle fibers, it is connected to the midgut-stomach junction by primary lateral ducts (Barker and Gibson, 1977). In Anomura as *Pagurus bernhardus* and *Clibanarius longitarsus* the MGG main ducts are connected ventrally to the stomach at the junction level to the midgut tract, the organ is

composed by numerous blind-end tubules (Erri Babu and Manjulatha, 1995). A similar morphology was reported among the Dendrobranchiata: in the green tiger prawn *Penaeus semisulcatus* it is a large compact organ formed by a pair of lobes that occupy the majority of the cephalothoracic cavity(Al-Mohanna et al., 1985); and in the red shrimp *Pleoticus muelleri* it is composed by numerous and enlarged tubules surrounded by connective tissue and the haemocoel (Cuartas et al., 2002). The MGG of the caridean *Macrobrachium amazonicum* is also a paired yellowish-brown compact organ which occupies much of the cephalothoracic cavity and connected ventrally to the midgut at the junction with the stomach, as in the previous examples the basic unit of the MGG is a blind-end tubule surrounded by laminar connective tissue and myoepithelial cells (Franceschini-Vicentini et al., 2009). Similar MGG morphology is reported in other carideans as *Caridina laevis* (Pillai, 1960) and *Neocaridina heteropoda* (Sonakowska et al., 2015). In Axiidea and Gebiidea species, also known as "ghost/mud shrimps", the MGG is described as a large mass composed by numerous blind-end tubules extended along the cephalotorax length (Pinn et al., 1999). All the above suggest that the morphology of the MGG is highly conserved among the Decapoda (Ceccaldi, 1989; Gibson and Barker, 1979; McLaughlin, 1983; Pillai, 1960; Reddy, 1938).

Schlegel (1911) described the MGG of the first larval stage of *Maja* sp. as a big multi-lobed visceral mass. These lobes should correspond to the blind-end tubules observed in this study. In the cancrid *Metacarcinus anthonyi* (as *Cancer anthonyi*) the MGG of the megalopa is also described as tubular in shape (Trask, 1974). According to our observations, the larval MGG of *M. brachydactyla* contains fourteen tubules and does not develop additional tubules until the late megalopa stage, so the main growth is due to an increase in the length of the existing tubules. In this sense, in the portunids *Scylla olivacea* (Jantrarotai and Sawanyatiputi, 2005) and *Portunus trituberculatus*

(Nakamura, 1990) the number of tubules increases earlier, during the last zoeal stages. The general morphology of the MGG in brachyuran larvae is similar to anomurans, maybe because they are close relatives. In the *Porcellana platycheles* pre-zoeae the MGG (termed "liver") each half is formed by three or four structures termed "lobes" that might correspond to blind-end tubules (Williams, 1944). In the red king crab *Paralithodes camtschaticus* the MGG is subdivided into dorsal sub-lobule with anterior and posterior tubules, and ventral sub-lobule with a single posterior tubule and two anterior tubules (Abrunhosa and Kittaka, 1997). However the development differs from *M. brachydactyla*, these authors observed that after late glaucothoe (equivalent to the megalopa in *M. brachydactyla*), the dorsal sub-lobule and one of the ventral tubules become vestigial, then new tubules are developed during the juvenile growth.

In the astacids the larval MGG is more complex than in the brachyurans. In the American Lobster *Homarus americanus* the larval MGG is similar to their adult counterpart, being divided into anterior, posterior, and dorsal lobules ramified into numerous blind-end tubules (Biesiot and McDowell, 1995; Factor, 1981). In the achelatans, as *Panulirus ornatus*, the MGG during the phyllosoma stages also comprises anterior, lateral and posterior lobules composed by numerous blind-end tubules (Johnston, 2006). A complex MGG during the zoeal stages was also reported in the caridean *Lysmata amboinensis*: it is a massive organ that occupies the majority of the cephalotorax cavity, it is composed by numerous tubules whose number increases during the larval development (Tziouveli et al., 2011). The contrary has been observed in the Dendrobranchiata, a group whose extended and gradual larval development start with the nauplius stage. In the northern white shrimp *Penaeus setiferus* the MGG appears in the first protozoeal stage as a pair of short lateral tubules, the subdivision into three tubules occur in the third protozoeal stage, and the complexity increases during the

subsequent larval and juvenile stages (Lovett and Felder, 1989). This pattern remember to the Pacific white shrimp *Penaeus vannamei*, where the MGG is identifiable in the sixth nauplius stage as a pair of tubules, the number of tubules increases gradually during the subsequent development (Muhammad et al., 2012). Nevertheless, in the kuruma prawn *Penaeus japonicus* the MGG maintain a simple structure during the protozoea and mysis stage and the complexity increases significantly during the juvenile development (Nakamura and Tshuru, 1987), i.e. latter than in *P. vannamei*. These result seem to indicate that the growth of the MGG is species-specific.

The tubules of the MGG in *M. brachydactyla*, beneath the basal lamina, are surrounded by a network of muscle fibers fitted in thin epithelial folds with a quadrate to rectangular pattern. The presence of a network formed by longitudinal and circular muscles has been described in numerous Decapoda species (Ceccaldi, 1989; Icely and Nott, 1992). In *S. serrata* the tubules are covered by a meshwork of circular fibers apparently linked by the longitudinal fibers (Barker and Gibson, 1978). Initially, the muscle fibers in *Carcinus maenas*, termed myoepithelial cells, were described as fine bundles located externally to the basement membrane and oriented in all directions (Stanier et al., 1968), but posterior studies revealed a rectangular pattern formed by circular fibers linked by longitudinal muscle fibers (Hopkin and Nott, 1979), closely similar to the observed in *M. brachydactyla*. Yonge (1924) observed the blind-tubules of the crayfish *P. clarkii* wrapped by a network formed by simple or branched circular muscle fibers and longitudinal muscle fibers occasionally branched. Latter, Loizzi (1971) in the crayfishes *O.virilis* and *P.clarkii* reported a muscle network surrounding each tubule, considered "myoepithelial", and formed by circular muscle fibers located regularly along the tubule length and connected by very fine longitudinal muscles occasionally branched. The network of muscle fibers also have been observed in the

adult *Penaeus semisulcatus* (Al-Mohanna and Nott, 1989), and the juveniles of *P. vannamei* (Caceci et al., 1988). In carideans also have been cited "myoepithelial cells" surrounding the blind-end tubules (Franceschini-Vicentini et al., 2009); as well in other malacostraca taxa as the isopods (Hopkin and Martin, 1982).

The contraction of the muscles causes the shrinkage of the tubules, while their relaxation causes their expansion (Correia et al., 2002; Lovett and Felder, 1990; Yonge, 1924). The coordination of these movements generates peristaltic and anti-peristaltic waves that permit the entry and exit of the digestive fluids into the blind tubules (Ceccaldi, 1989; Correia et al., 2002; Hopkin and Nott, 1979).Therefore, the tubule muscle fibers (circular and longitudinal) are responsible for the movement of fluids throughout the organ (Ceccaldi, 1989). These movements could help to the movement of the digestive fluids in and out from the MGG, being mixed with the midgut tract and midgut caeca content. Then, the presence of a muscle fiber network from hatching in *M. brachydactyla* reveals an active MGG able to participate in the digestive processes. This observation is congruent with feeding requirements of the first zoeal stage of this species, that it is unable to continue the larval development without feeding (Rotllant et al., 2010).

The earliest studies of the Decapoda digestive system compared their organs with the Vertebrata digestive system. Milne-Edwards (1834a) directly considered the MGG as a "liver", naming this organ "*foie*" in his study of the crustacean anatomy in the early 19th Century. Later, Huxley (1880) mentioned that the "liver" of the crayfishes is "in position to the glands termed liver and pancreas in the higher animals". This comparison to the liver and pancreas become highly popular, being the term "hepatopancreas" standardized an employed in the majority of the studies (Gibson and

Barker, 1979; Van Weel, 1974; Vogt, 1996; Yonge, 1924). However, the term "hepatopancreas" maybe is not accurate as it is supposed to be, being considered inappropriate and inaccurate by some authors (Cervellione et al., 2017; Van Weel, 1974). Morphologically the liver of vertebrates is a massive, reddish-organ organ highly vascularized, whose parenchyma is formed by lobules with a central vein connected radially to vascular sinusoids, in turn intercalated to tubules of hepatocytes connected with peripherical bile ducts (Bruslé and Gonzàlez i Anadon, 1996; Ross and Pawlina, 2016); and the mammal pancreas is an elongated organ with tubulo-acinar glands and vascularized islets (Ross and Pawlina, 2016). By contrast, according to the present and previous studies, the MGG morphology is completely different. It is an enormous aggregation of blind end tubules whose epithelium vary along the tubule length, in this organ the digestive fluids entry and exit thanks to the external network of muscle fibers (Al-Mohanna and Nott, 1989; Ceccaldi, 1989; Gibson and Barker, 1979; Loizzi, 1971).

In a functional perspective, Gibson and Barker (1979) defended the term "hepatopancreas", considering that as the pancreas it is involved in the synthesis of digestive enzymes and carbohydrate metabolism; while as the livers it is involved in the synthesis of emulsifiers and storage of nutrients. However, this idea could be discussed. Van Weel (1974) considered the term "hepatopancreas" incorrect because this organ is not able to regulate the sugar concentration in blood or to produce "true" bile acids. Later, Phillips et al. (1977) rejected the term "hepatopancreas" since activities as gluconeogenesis and ketogenesis were not found in the MGG. Besides the biochemical activity, also functional differences are reported. In the MGG the digestive process occur on the organ lumen, being the nutrients directly absorbed by specialized epithelial cells (Al-Mohanna and Nott, 1989; Ceccaldi, 1989; Gibson and Barker, 1979; Loizzi, 1971). This function has been neither observed in vertebrata liver or pancreas, but could

be analogous to the vertebrata intestine (Ross and Pawlina, 2016). Recently, Cervellione et al. (2017) resumed numerous cellular and physiological features of the vertebrata "hepatopancreas" that are absent in the MGG. Then, Cervellione et al. (2017) recommended the name "perigastric organ" or "perigaster" since "defines its location without reference to its physiological functions". In a evolutionary perspective, the MGG is not homologous with the vertebrata liver or pancreas and the coincidence in particular roles could be assumed as a case of evolutionary convergence.

5. Acknowledgements

Financial support provided by the Spanish Ministry of Economy and Competitiveness through the INIA project [grant number RTA2011-00004-00-00] to G.G and a predoctoral fellowship to D.C. [FPI-INIA]. The authors would like to thank to the technicians at IRTA, SantCarles de la Ràpita (David Carmona, Glòria Macià, Magda Monllaó, Francesc X. Ingla and Olga Bellot) and CCiTUB Hospital Clinic, Barcelona (Adriana Martínez, Almudena García, José Manuel Rebled and Rosa Rivera) for their assistance.We thank Bruker–Skyscan staff for their effectiveness and fast support, and for their constant improvements to the software and in implementing new options we requested, and kindness in providing to Prof. Dr. J. Alba-Tercedor fast and effective suggestions and answers to queries. In this respect, we are especially indebted to Alexander Sasov, Stephan Boons, Xuan Liu, Phil Salmon, Jeroen Hostens, and Vladimir Kharitonov.

Table 1. *Maja brachydactyla*. Growth of the midgut gland from hatching to the first juvenile stage. The size of each structure (mean ± SD) at the age of newly hatched zoea (ZI_0) and newly metamorphosed first juvenile (J_0), as well the results of the statistical analysis, are showed.

Structure		ZI_0 (µm)	J_0 (µm)	Statistical significance per lobule	
				right	left
Total length	TL	621 ± 60	848 ± 139	$F_{3,13}$= 16.23 $p < 0.001$	$F_{3,13}$= 12.62 $p < 0.001$
Maximum width	MW	235 ± 36	206 ± 23	$F_{3,13}$ = 0.50 $p = 0.69$	$F_{3,13}$ = 2.21 $p = 0.14$
Dorsal sub-lobule, length	DSl	368 ± 40	588 ± 80	$F_{3,13}$ = 25.83 $p < 0.001$	$F_{3,13}$ = 12.23 $p < 0.001$
Dorsal sub-lobule, width	DSw	223 ± 43	351 ± 44	$F_{3,13}$ = 19.17 $p < 0.001$	$F_{3,13}$ = 13.17 $p < 0.001$
Dorsal sub-lobule, height	DSh	204 ± 23	281 ± 11	$F_{3,13}$ = 3.25 $p = 0.06$	$F_{3,13}$ = 5.17 $p = 0.01$
External tubule, length	ETl	118 ± 13	168 ± 48	$F_{3,13}$ = 11.76 $p < 0.001$	$F_{3,13}$ = 13.27 $p < 0.001$
External tubule, width	ETw	139 ± 20	129 ± 33	$F_{3,13}$ = 1.89 $p = 0.18$	$F_{3,13}$ = 4.76 $p < 0.05$
Internal tubule, length	ITl	87 ± 13	91 ± 20	$F_{3,13}$ = 1.63 $p = 0.23$	$F_{3,13}$ = 11.28 $p < 0.001$
Internal tubule, width	ITw	131 ± 16	146 ± 15	$F_{3,13}$ = 4.72 $p = 0.02$	$F_{3,13}$ = 3.03 $p = 0.07$

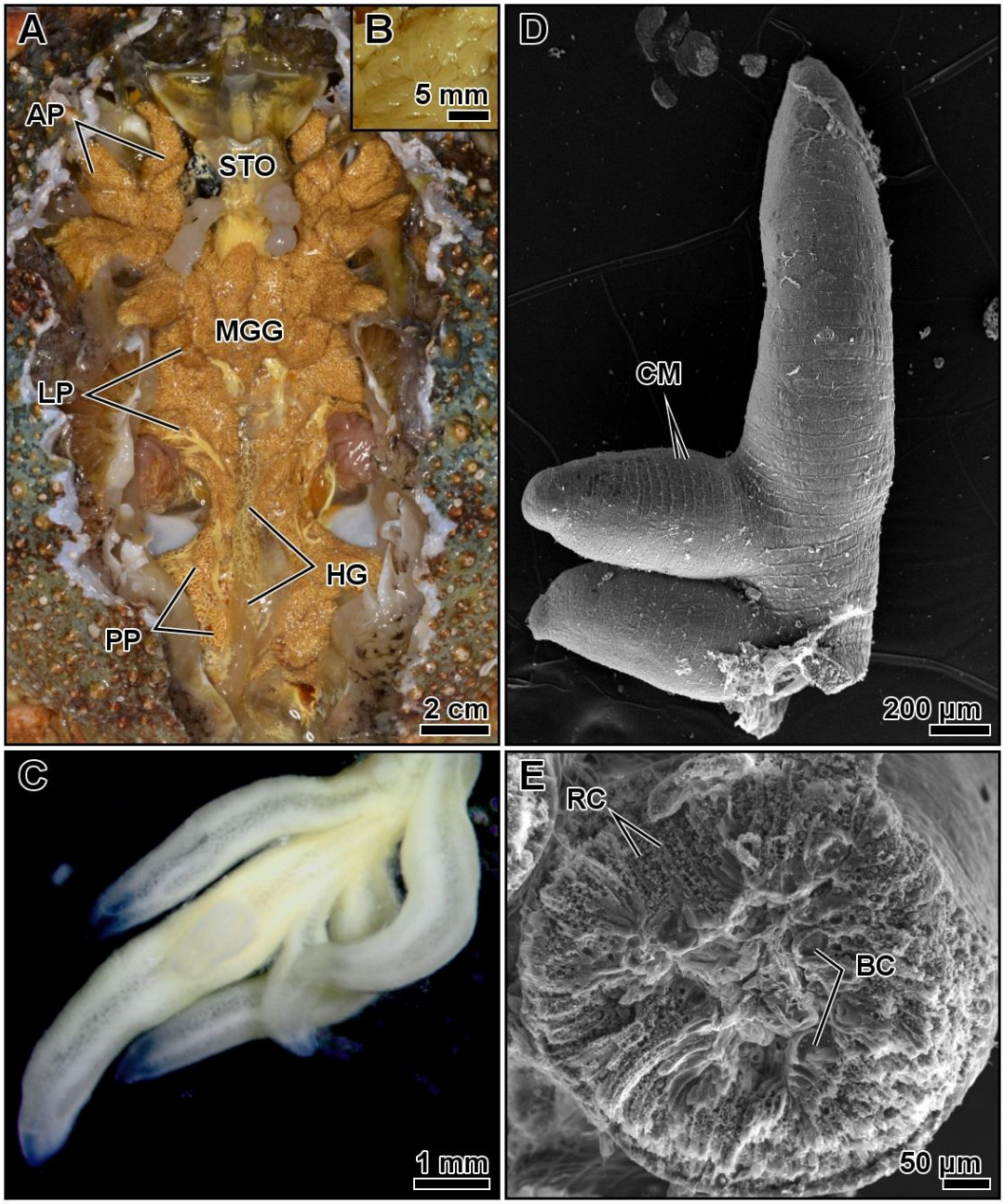

Figure 1. *Maja brachydactyla*. Adult . Midgut gland. General morphology. Fresh entire organ, digital camera (A). Blind-end tubules of the midgut-gland, fixed with 4 % formaldehyde, digital camera (B). Close view of the blind-end tubules of the midgut gland, fixed with 4 % formaldehyde, stereomicroscope (C). Blind-end tubules of the midgut gland, fixed with 2 % paraformaldehyde - 2.5 % glutaraldehyde, SEM (D-E): general view (D) and transversal section (E). Abbreviations: AP: anterior projections; BC: B-cells; CM: circular muscle fibers; HG: hindgut; MGG, midgut gland; LP: lateral projections; RC: R-cells; PP: posterior projections; STO: stomach.

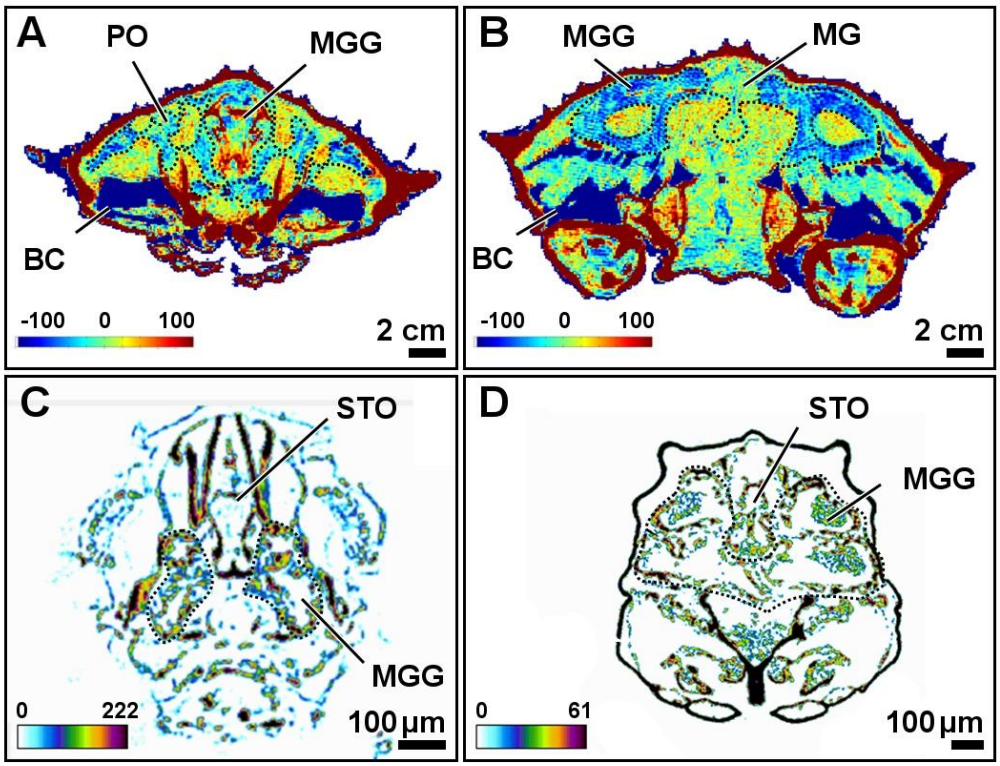

Figure 2. *Maja brachydactyla*. Midgut gland. Tomographic and microtomographic cross section images. Adult, tomography, the midgut gland is marked by the dotted line (A-B): anatomical area of the stomach (A); and anatomical area of the heart (B). Larvae, Micro-CT Data Viewer‟s cross section images, the midgut gland is marked by the dotted line (C-D): zoea I, anatomical area of the pyloric stomach (C); and megalopa, anatomical area of the pyloric stomach (D). Abbreviations: BC: branchial chamber; MG: midgut tract; MGG, midgut gland; STO: stomach.

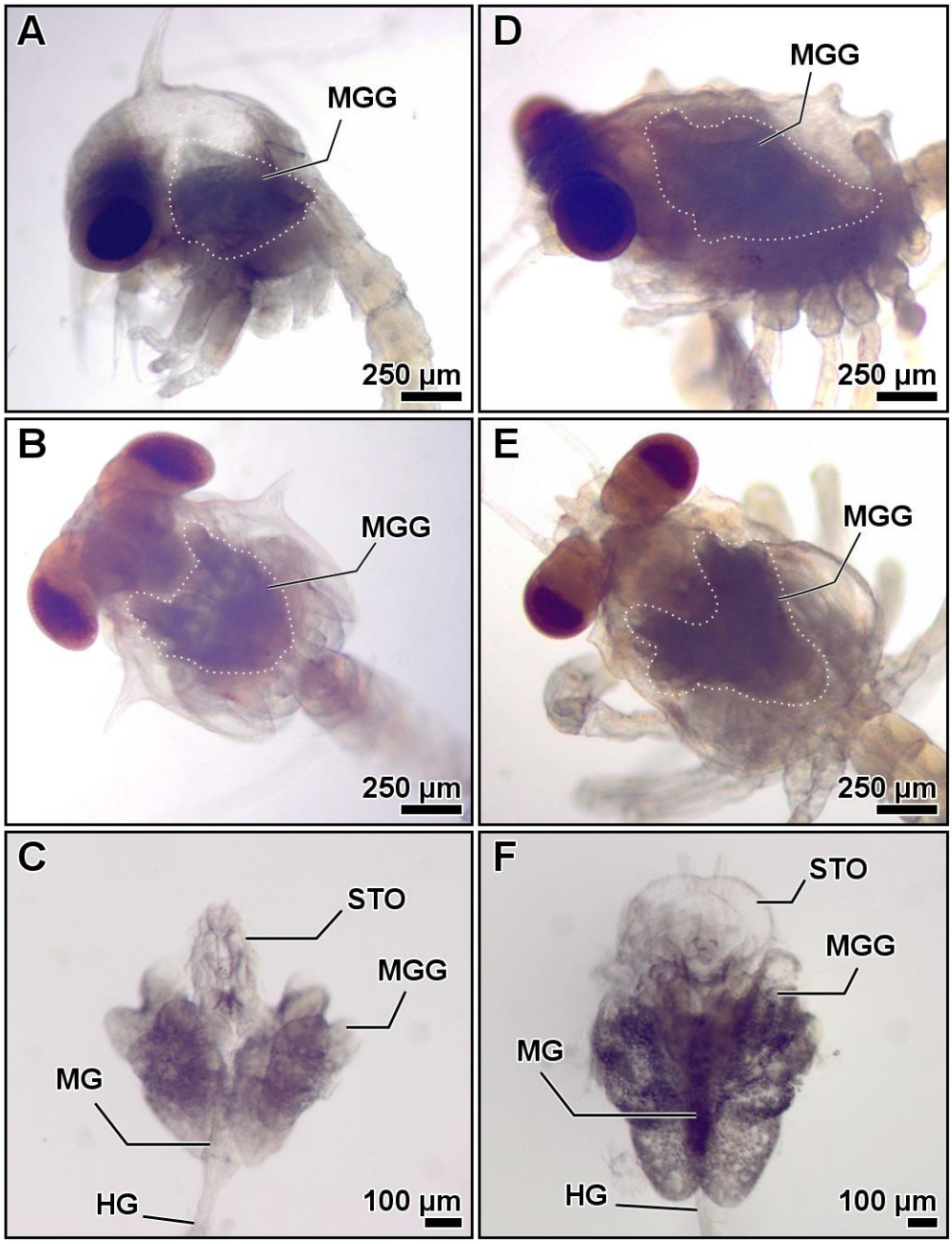

Figure 3. *Maja brachydactyla*. Larvae. Location of the midgut gland. Stereomicroscope. Zoea I, 2 dah (days after hatch), lateral view (A). Zoea II, 3 dah, dorsal view (B). Zoea I organs, 0 dah, dissected midgut gland and adjacent organs (C). Megalopa, 6 dah, lateral view (D). Megalopa, 11 dah, dorsal view (E). Megalopa organs, 6 dah, dissected midgut gland and adjacent organs (F). Abbreviations: HG, hindgut; MG, midgut; MGG, midgut gland; STO, stomach.

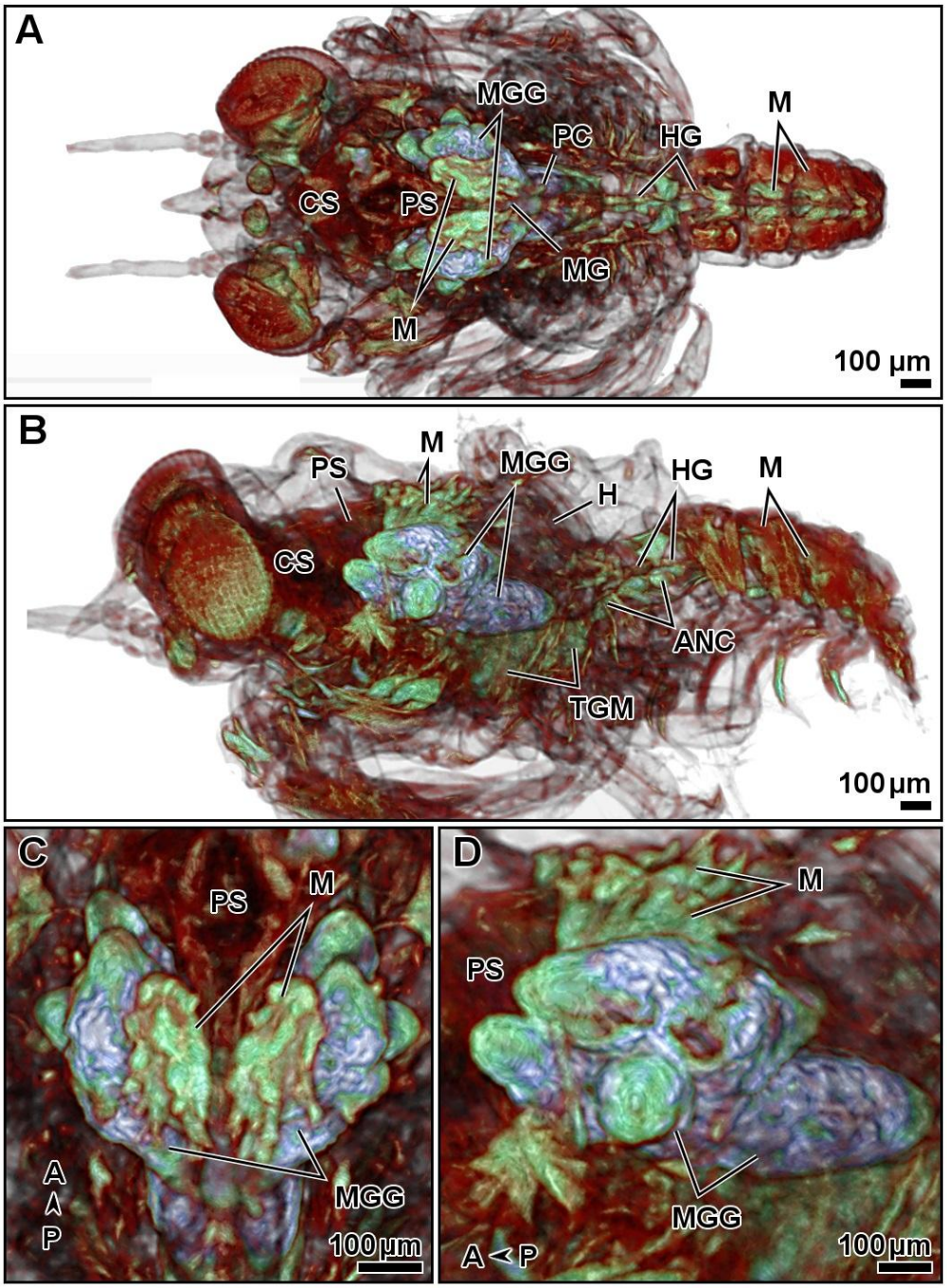

Figure 4. *Maja brachydactyla*. Megalopa. Micro-CT Vox"s volume rendering reconstruction images. Entire specimen (A-B): dorsal view (A); lateral view (B). Close view of the midgut gland (C-D): dorsal view (C); lateral view (D). Abbreviations: A < P: anterior < posterior; ANC: abdominal nerve cord; CS: cardiac stomach; H: heart; HG: hindgut tract; M: muscles; MG: midgut tract; PC: posterior caecum; MGG, midgut gland; PS: pyloric stomach; TGM: thoracic ganglionic mass.

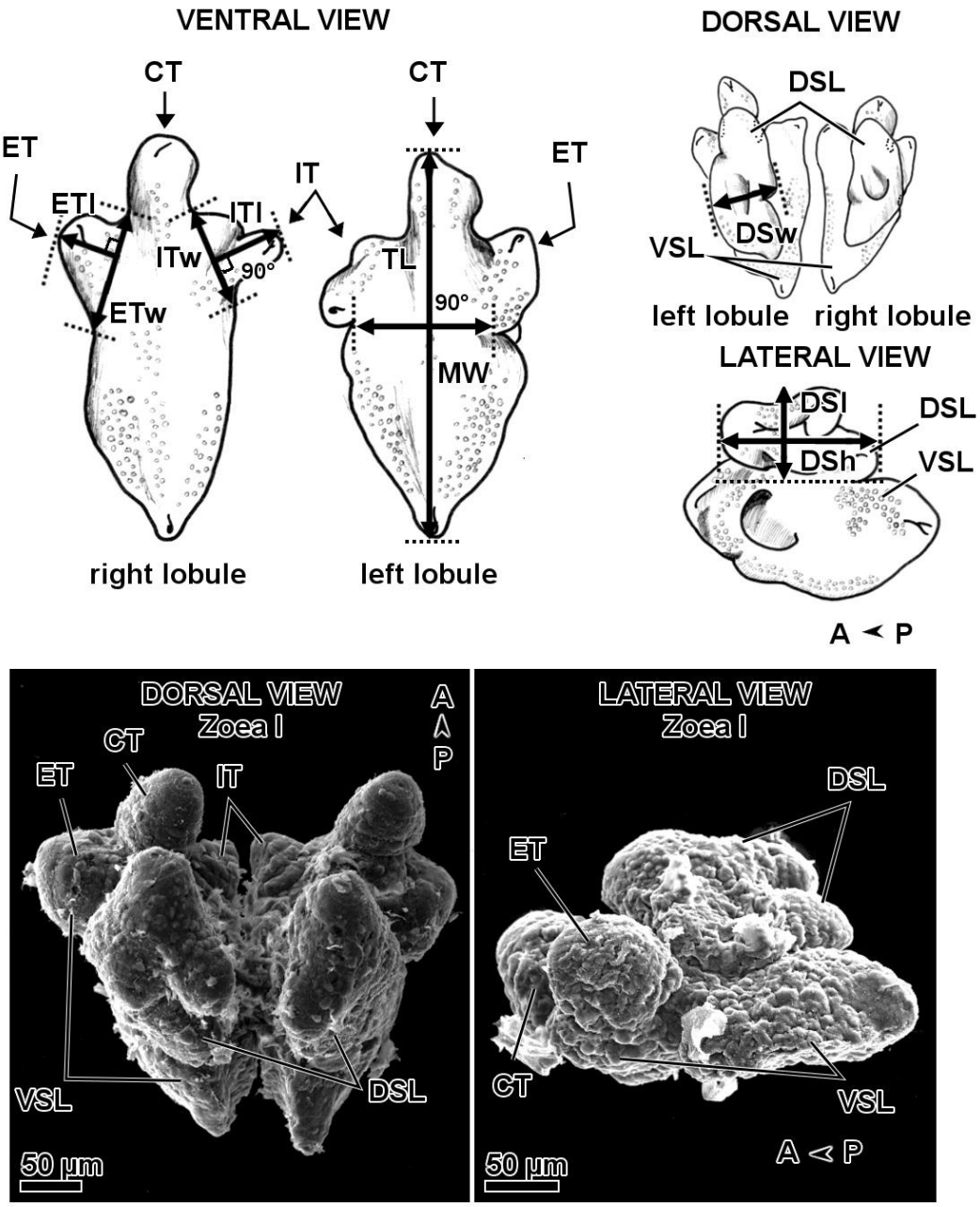

Figure 5. *Maja brachydactyla*. Zoeae. Midgut gland. Diagram showing the morphology and location of the main lobules, sub-lobules and blind-end tubules. The measures taken for the morphometric study are indicated by a double arrow (up). Dorsal and lateral view by SEM (down). Abbreviations: A < P: anterior < posterior; CT: central tubule; DSL: dorsal sub-lobule; DSh: dorsal sub-lobule height; DSl: dorsal sub-lobule length; DSw: dorsal sub-lobule width; ET: external tubule; ETl: external tubule length; ETw: external tubule width; IT: internal tubule; ITl: internal tubule length; ITw: internal tubule length; MW: maximum width; TL: total length; VSL: ventral sub-lobule.

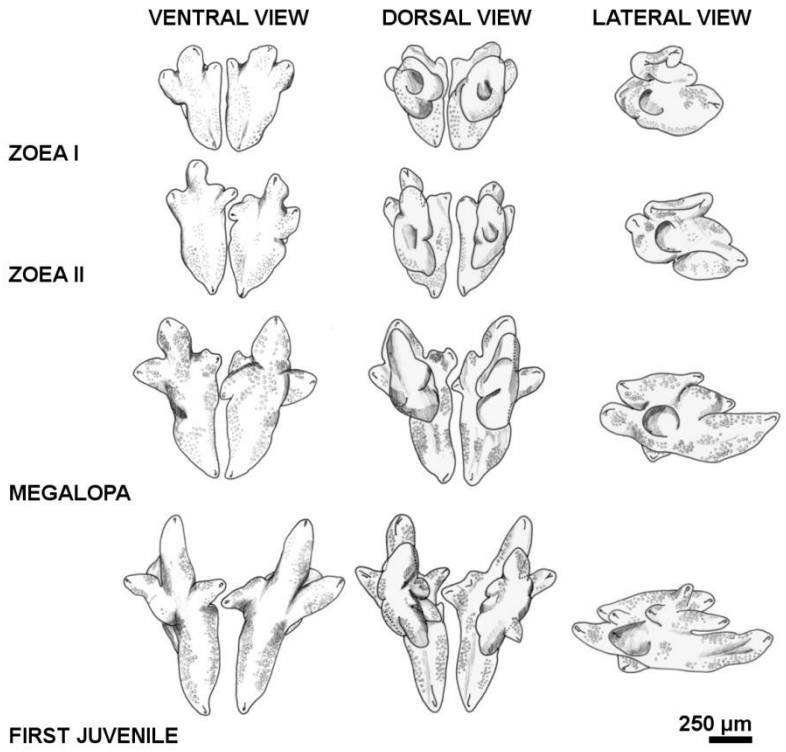

Figure 6. *Maja brachydactyla*. Diagrams showing different views (ventral, dorsal and lateral) of the larval midgut gland and at the start of different stages (zoea I, zoea II, megalopa and first juvenile). All the diagrams are at scale (250 µm).

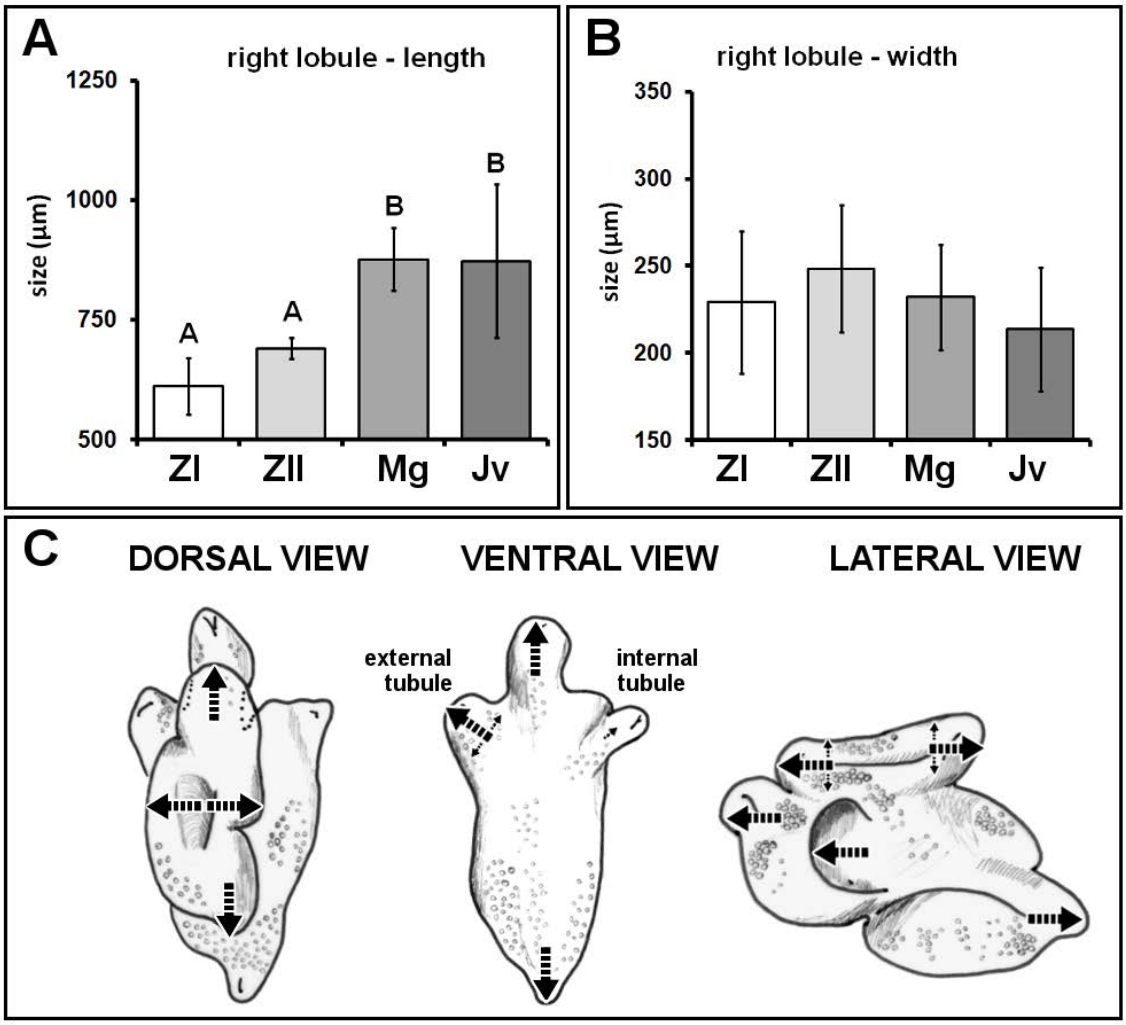

Figure 7. *Maja brachydactyla*. Growth of the midgut gland during the larval development, using the right lobule as example. Total length of the lobule at each larval and first juvenile stage (A). Maximum width of the lobule at each larval and first juvenile stage (B). Growth trends of the different midgut gland tubules during the larval development (C). The big sized arrows indicated an important growth, while the small sized arrows indicated a marginal growth. Abbreviations: Jv: juvenile; Mg: megalopa; ZI: zoea I; ZII: zoea II.

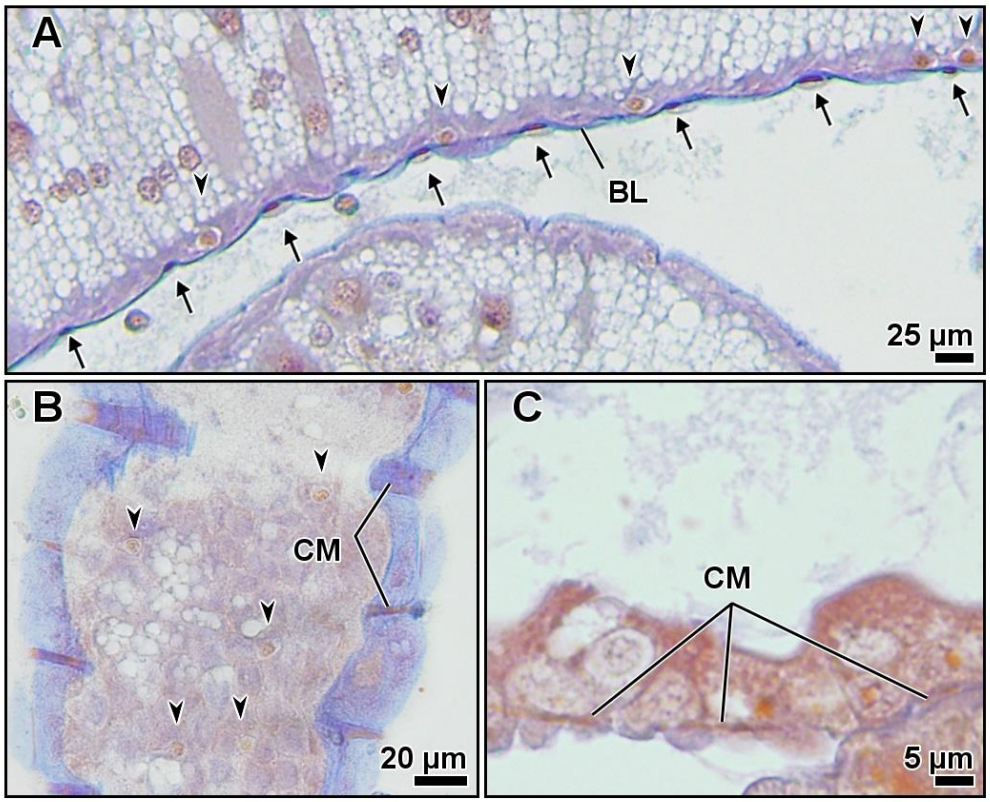

Figure 8. *Maja brachydactyla*. Midgut gland. Histology of the muscle fibers that surround the blind-end tubules. Mallory's trichrome. Optical microscopy. Adult, longitudinal section, circular muscle fibers (arrows) showing some M-cells (arrow-heads), Mallory's trichrome (A-B). Zoea I, close view of the circular muscle fibers, located below the midgut gland epithelium (C). Abbreviations: BL: basal lamina; CM: circular muscle fibers.

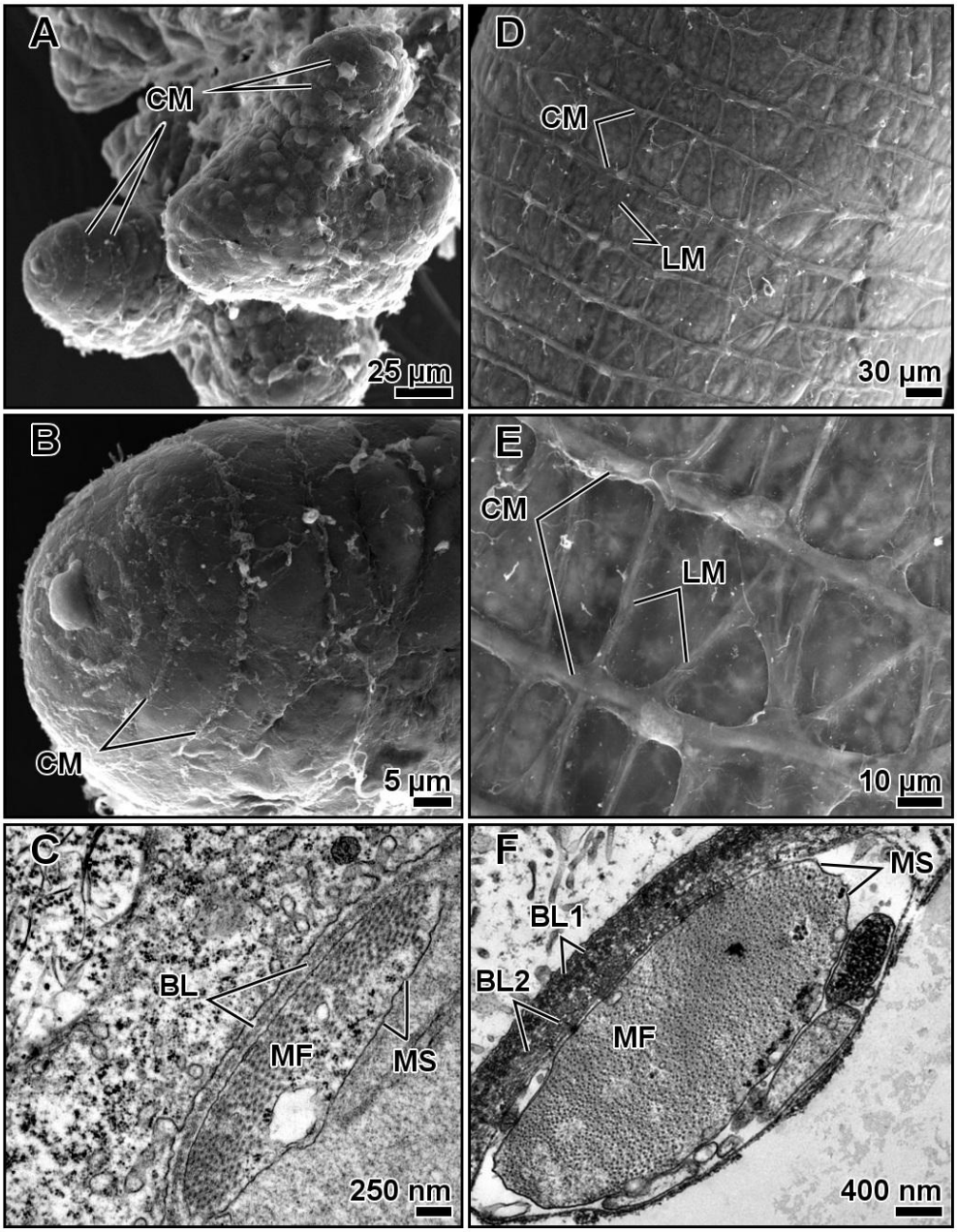

Figure 9. *Maja brachydactyla*. Midgut gland. Ultrastructure of the muscle fibers that surround the blind-end tubules. Newly hatched zoea, muscle fibers, SEM (A-B): general (A) and close view (B). Megalopa, muscle fiber, transversal section, TEM (C). Adult, muscle fibers, SEM (D-E): general (D) and close view (E). Adult, muscle fiber, transversal section, TEM (F). Abbreviations: BL: basal lamina; BL1: first layer of the basal lamina; BL2: second layer of the basal lamina; CM: circular muscle fibers; LM: longitudinal muscle fibers; MF: muscle fiber in transversal view; MS: membrane that surround the bundle of myofibrils.

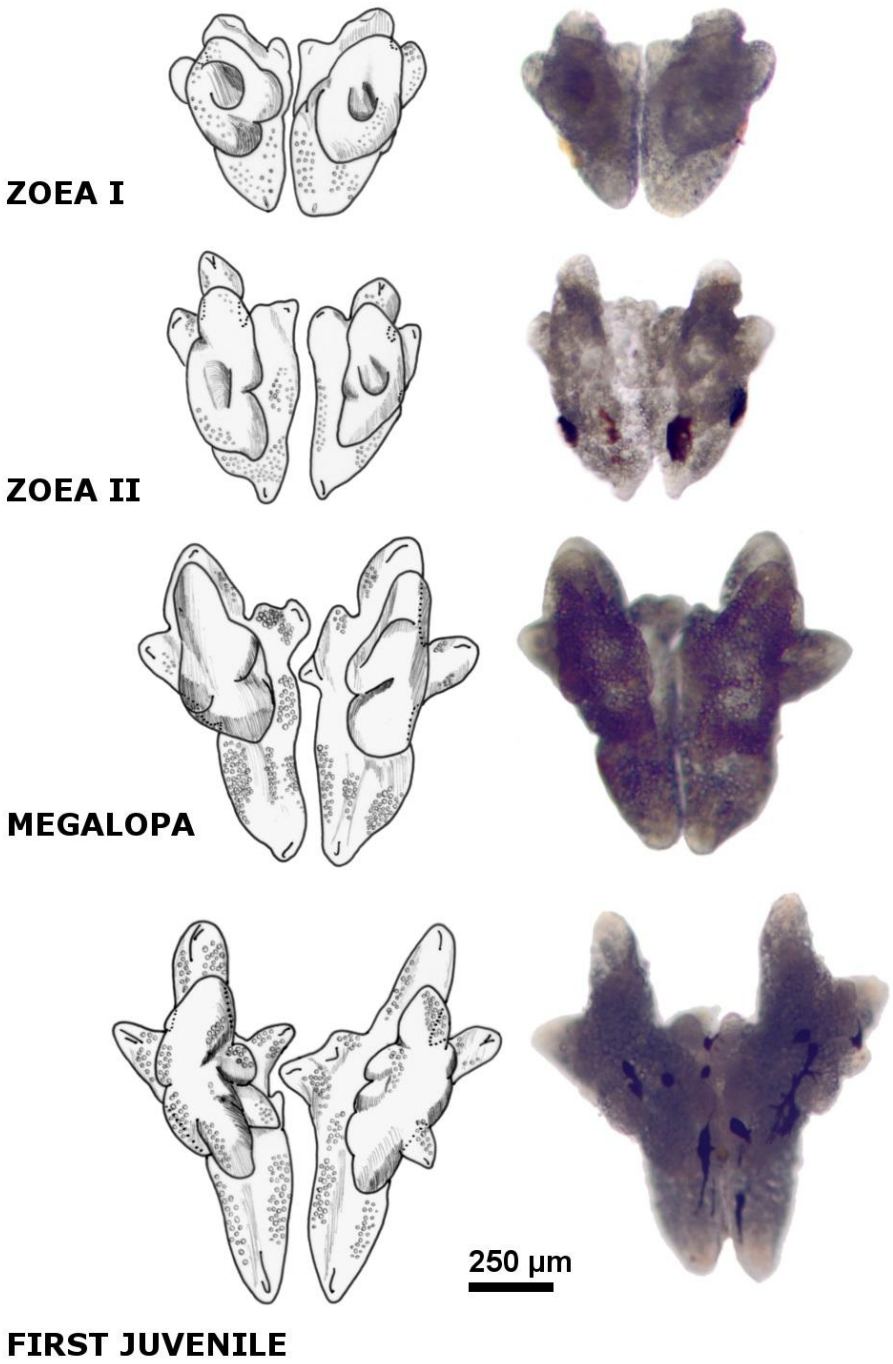

Supplementary Material 1A (S1A). *Maja brachydactyla*. Ontogeny of the midgut gland through the larval development. Dorsal view. General diagram (left) and dissected midgut gland (right).

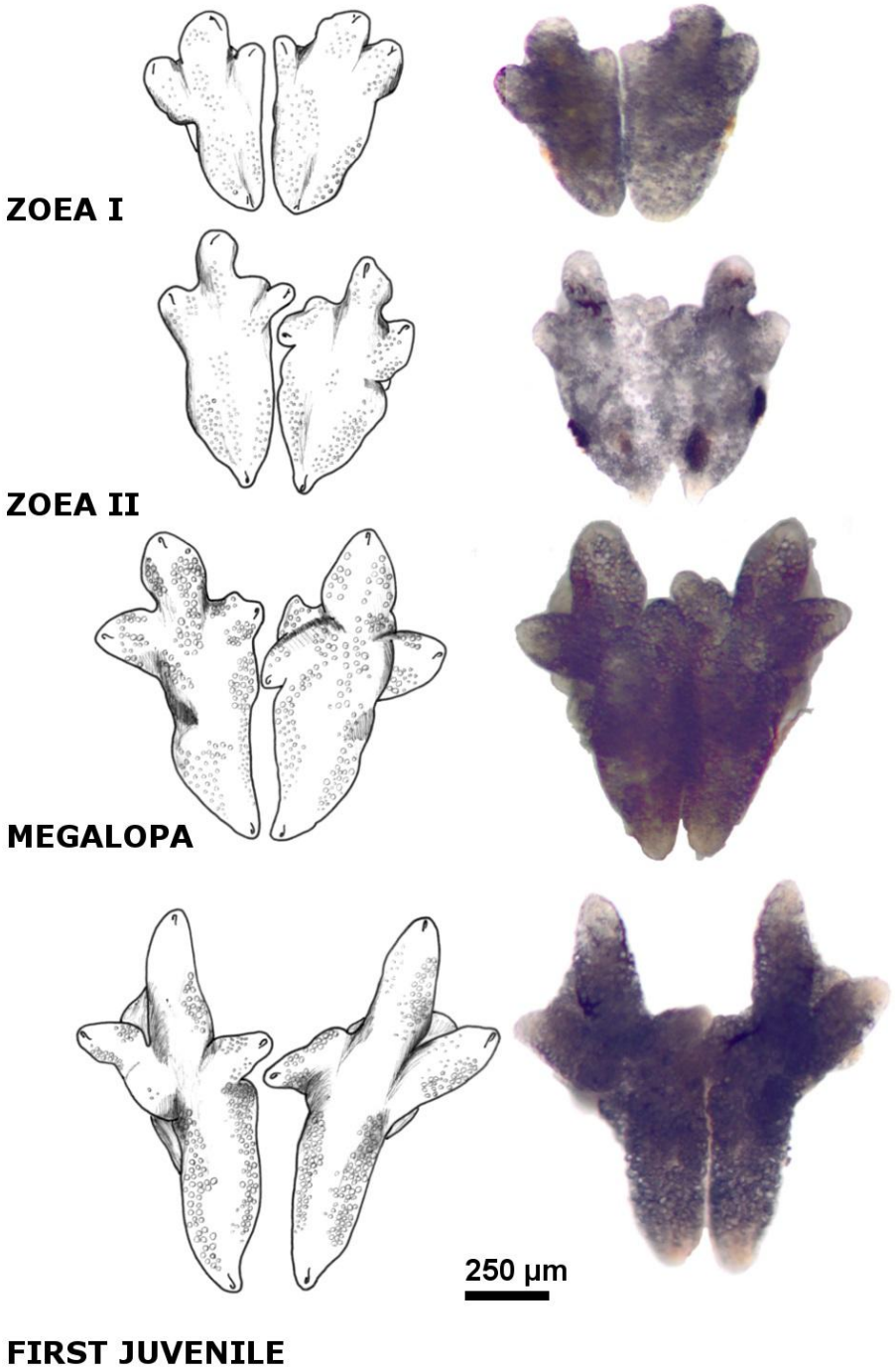

Supplementary Material 1B (S1B). *Maja brachydactyla*. Ontogeny of the midgut gland through the larval development. Ventral view. General diagram (left) and dissected midgut gland (right).

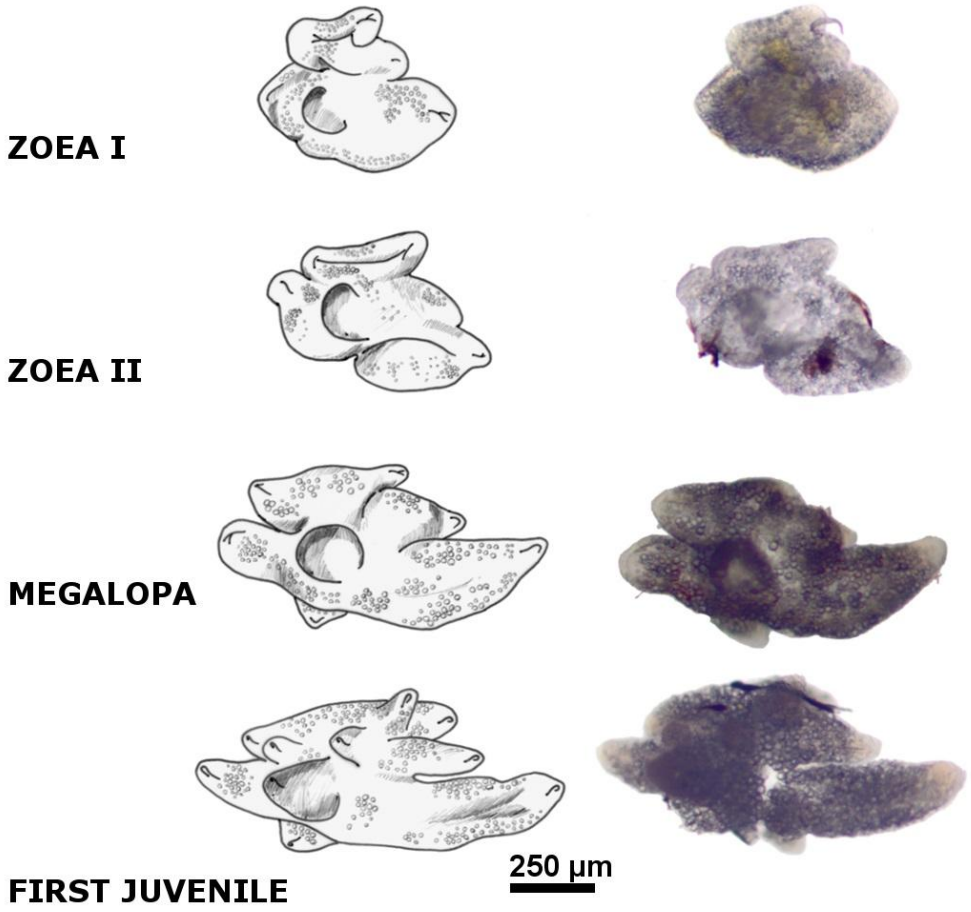

Supplementary Material 1C (S1C). *Maja brachydactyla*. Ontogeny of the midgut gland through the larval development. Lateral view. General diagram (left) and dissected midgut gland (right).

6. Bibliography

Abelló, P., García Raso, J.E., Guerao, G., Salmerón, F., 2014. *Maja brachydactyla* (Brachyura: Majidae) in the western Mediterranean. Marine Biodiversity Records 7.

Abrunhosa, F.A., Kittaka, J., 1997. Morphological changes in the midgut, midgut gland and hindgut during the larval and postlarval development of the red king crab *Paralithodes camtschaticus*. Fisheries Science 63, 746-754.

Al-Mohanna, S.Y., Nott, J.A., 1989. Functional cytology of the hepatopancreas of *Penaeus semisulcatus* (Crustacea: Decapoda) during the moult cycle. Marine Biology 101, 535-544.

Al-Mohanna, S.Y., Nott, J.A., Lane, D.J.W., 1985. M-'Midget' cells in the hepatopancreas of the shrimp, *Penaeus semisulcatus* De Hann, 1844 (Decapoda, Natantia). Crustaceana 48, 260-268.

Alba-Tercedor, J., 2014. From the sample preparation to the volume rendering images of small animals: A step by step example of a procedure to carry out the micro-CT study of the leafhopper insect *Homalodisca vitripennis* (Hemiptera: Cicadellidae), in: Skyscan (Ed.), Bruker microCT Users Meeting 2014, Kontich, Belgium, pp. 260-288.

Alba-Tercedor, J., Alba-Alejandre, I., 2017. Comparing micro-CT results of insects with classical anatomical studies: The European honey bee (*Apis mellifera* Linnaeus, 1758) as a benchmark (Insecta: Hymenoptera, Apidae), in: Skyscan (Ed.), Micro-CT User Meeting 2017, Kontich, Belgium, pp. 147-167.

Alba-Tercedor, J., Sáinz-Cantero, C.E., 2012. Volume rendering reconstructions of the anatomy of small aquatic beetles (Insecta : Coleoptera) scanned with the Skyscan 1172 high resolution micro-CT, in: Skyscan (Ed.), Micro-CT Users Meeting 2012, Kontich, Belgium, pp. 75-84.

Barker, P.L., Gibson, R., 1977. Observations on the feeding mechanism, structure of the gut, and digestive physiology of the european lobster *Homarus gammarus* (L.) (Decapoda: Nephropidae). Journal of Experimental Marine Biology and Ecology 26, 297-324.

Barker, P.L., Gibson, R., 1978. Observations on the structure of the mouthparts, histology of the alimentary tract, and digestive physiology of the mud crab *Scylla serrata* (Forskål) (Decapoda: Portunidae). Journal of Experimental Marine Biology and Ecology 32, 177-196.

Biesiot, P.M., McDowell, J.E., 1995. Midgut-gland development during early life-history of the American Lobster *Homarus americanus*. Journal of Crustacean Biology 15, 679-685.

Bruslé, J., Gonzàlez i Anadon, G., 1996. The structure and function of fish liver, In: Dutta, H.M., Datta-Mushi, J.S. (Eds.), Fish morphology : horizon of new research. CRC Press, pp. 77-93.

Caceci, T., Neck, K.F., Lewis, D.D.H., Sis, R.F., 1988. Ultrastructure of the hepatopancreas of the Pacific white shrimp, *Penaeus vannamei* (Crustacea: Decapoda). Journal of the Marine Biological Association of the United Kingdom 68, 323-337.

Ceccaldi, H.J., 1989. Anatomy and physiology of digestive tract of Crustaceans Decapods reared in aquaculture, Advances in Tropical Aquaculture, Workshop at Tahiti, French Polynesia. Actes de colloques Ifremer, Tahiti, French Polynesia, pp. 243-259.

Cervellione, F., McGurk, C., Van den Broeck, W., 2017. “Perigastric organ”: a replacement name for the “hepatopancreas” of Decapoda. Journal of Crustacean Biology 37, 353-355.

Correia, A.D., Pereira, A.L., Costa, M.H., Carrapiço, F., 2002. Functional anatomy of the midgut gland of *Gammarus locusta* (Crustacea: Amphipoda). Journal of the Marine Biological Association of the United Kingdom 82, 201-204.

Cuartas, E., Petriella, A.M., 2002. Cytoarchitecture of the hepatopancreas of three species of crabs from Mar Chiquita Lagoon, Argentina, In: Escobar-Briones, E., Alvarez, F. (Eds.), Modern Approaches to the Study of Crustacea. Springer US, Boston, MA, pp. 39-44.

Cuartas, E.I., Díaz, A.C., Petriella, A.M., 2002. Estudio morfológico e histológico del hepatopáncreas del langostino *Pleoticus muelleri* (Bate) (Crustacea, Penaeoidea). Revista de Investigación y Desarrollo Pesquero 15, 5-13.

Davie, P.J.F., Guinot, D., Ng, P.K.L., 2015. Anatomy and functional morphology of Brachyura, in: Castro, P., Davie, P.J.F., Guinot, D., Schram, F., Von Vaupel Klein, C. (Eds.), Treatise on Zoology - Anatomy Taxonomy Biology. The Crustacea Volume 9 Part C. Brill, pp. 11-163.

Davis, L.E., Burnett, A.L., 1964. A study of growth and cell differentiation in the hepatopancreas of the crayfish. Developmental Biology 10, 122-153.

Erri Babu, D., Manjulatha, C., 1995. Zymogen secreting cells in the hepatopancreatic duct of *Pagurus bernhardus* (Linnaeus, 1758) and *Clibanarius longitarsus* (De Haan, 1849) (Anomura). Crustaceana 68, 616-628.

Erri Babu, D., Shyamasundari, K., Rao, K.H., 1982. Studies on the digestive system of the crab *Menippe rumphii* (Fabricius) (Crustacea:Brachyura). Journal of Experimental Marine Biology and Ecology 58, 175-191.

Factor, J.R., 1981. Development and metamorphosis of the digestive system of larval lobsters, *Homarus americanus* (Decapoda: Nephropidae). Journal of Morphology 169, 225-242.

FAO, 2012. B-42 Crabs, sea-spiders. Capture production by species, fishing areas and countries or areas, In: FAO (Ed.), FAO yearbook. Fishery and aquaculture statistics. FAO, Rome.

Felgenhauer, B.E., 1992. Chapter 3. Internal Anatomy of the Decapoda: An Overview, In: Harrison, F.W., Humes, A.G. (Eds.), Microscopic Anatomy of Invertebrates. Wiley-Liss, Inc.

Franceschini-Vicentini, I.B., Ribeiro, K., Papa, L.P., Marques Junior, J., Vicentini, C.A., Valenti, P.M.C.M., 2009. Histoarchitectural features of the hepatopancreas of the Amazon River Prawn *Macrobrachium amazonicum*. International Journal of Morphology 27, 121-128.

Gibson, R., Barker, P.L., 1979. The Decapod Hepatopancreas. Oceanography and Marine Biology - An Annual Review 17, 285-346.

Guerao, G., Pastor, E., Martin, J., Andrés, M., Estévez, A., Grau, A., Duran, J., Rotllant, G., 2008. The larval development of *Maja squinado* and *M. brachydactyla* (Decapoda, Brachyura, Majidae)

described from plankton collected and laboratory-reared material. Journal of Natural History 42, 2257-2276.

Hopkin, S.P., Martin, M.H., 1982. The distribution of zinc, cadmium, lead and copper within the hepatopancreas of a woodlouse. Tissue and Cell 14, 703-715.

Hopkin, S.P., Nott, J.A., 1979. Some observations on concentrically structured, intracellular granules in the hepatopancreas of the shore crab *Carcinus maenas* (L.). Journal of the Marine Biological Association of the United Kingdom 59, 867-877.

Huxley, T.H., 1880. The Crayfish; an Introduction to the Study of Zoology. New York: D. Appleton and Company.

Icely, J.D., Nott, J.A., 1992. Digestion and absorption: digestive system and associated organs, In: Harrison, F.W., Humes, A.G. (Eds.), Microscopic anatomy of invertebrates: decapod Crustacea. Wiley-Liss, New York, pp. 147-201.

Jantrarotai, P.N., Sawanyatiputi, S.A., 2005. Histological study on the development of digestive system in zoeal stages of mud crab (*Scylla olivacea*). Kasetsart Journal 39, 666-671.

Johnston, M.D., 2006. Feeding and digestion in the phyllosoma larvae of Ornate Spiny Lobster, *Panulirus ornatus* (Fabricius) and the implications for their culture, Zoology. The University of Western Australia, p. 146.

Kouichi, O., 1959. Midgut Gland cells accumulating iron or copper in the crayfish, *Procambarus clarkii*. 日本動物学彙報 = Annotationes zoologicae Japonenses 32, 133-142.

Lebour, M.V., 1927. Studies of the Plymouth Brachyura. I. The rearing of crabs in captivity, with a description of the larval stages of *Inachus dorsettensis*, *Macropodia longirostris* and *Maia squinado*. Journal of the Marine Biological Association of the United Kingdom 14, 795-821.

Loizzi, R.F., 1966. Cellular and physiological changes during secretion in crayfish hepatopancreas, Zoology. Iowa State University of Science and Technology, Ames, Iowa, p. 190.

Loizzi, R.F., 1971. Interpretation of crayfish hepatopancreatic function based on fine structural analysis of epithelial cell lines and muscle network. Zeitschrift für Zellforschung und Mikroskopische Anatomie 113, 420-440.

Lovett, D.L., Felder, D.L., 1989. Ontogeny of gut morphology in the white shrimp *Penaeus setiferus* (Decapoda, Penaeidae). Journal of Morphology 201, 253-272.

Lovett, D.L., Felder, D.L., 1990. Ontogeny of kinematics in the gut of the white shrimp *Penaeus setiferus* (Decapoda: Peneidae). Journal of Crustacean Biology 10, 53-68.

McLaughlin, P.A., 1983. 1. Internal Anatomy, In: Mantel, L.H. (Ed.), The Biology of Crustacea Vol. 5. Internal Anatomy and Physiological Regulation. Academic Press, pp. 1-52.

Milne-Edwards, H., 1834a. Histoire naturelle des crustacés, comprenant l'anatomie, la physiologie et la classification de ces animaux. Libraire Encyclopédique de Roret.

Milne-Edwards, H., 1834b. Histoire naturelle des crustacés: atlas. Libraire Encyclopédique de Roret.

Muhammad, F., Zhang, Z.F., Shao, M.Y., Dong, Y.P., Muhammad, S., 2012. Ontogenesis of digestive system in *Litopenaeus vannamei* (Boone, 1931) (Crustacea: Decapoda). Italian Journal of Zoology 79, 77-85.

Nakamura, K., 1990. Organogenesis during metamorphosis in the swimming crab *Portunus trituberculatus*. Nippon Suisan Gakkaishi 56, 1561-1564.

Nakamura, K., Tshuru, H., 1987. Organogenesis of the Midgut Gland in the Prawn *Penaeus japonicus*. Memoirs of Faculty of Fisheries Kagoshima University 36, 12-25.

Phillips, J.W., McKinney, R.J.W., Hird, F.J.R., Macmillan, D.L., 1977. Lactic acid formation in crustaceans and the liver function of the midgut gland questioned. Comparative Biochemistry and Physiology Part B: Comparative Biochemistry 56, 427-433.

Pillai, R.S., 1960. Studies on the shrimp *Caridina laevis* (Heller) 1. The Digestive System. Journal of the Marine Biological Association of India 2, 57-74.

Pinn, E.H., Nickell, L.A., Rogerson, A., Atkinson, R.J.A., 1999. Comparison of gut morphology and gut microflora of seven species of mud shrimp (Crustacea: Decapoda: Thalassinidea). Marine Biology 133, 103-114.

R Development Core Team, 2015. R: A language and environment for statistical computing. R Foundation for Statistical Computing, Vienna, Austria.

Ramadevi, K.R.L.S., Shyamasundari, K., Hanumantha Rao, K., 1990. Observation of the hepatopancreas of *Ocypoda platytarsis* (Milne-Edwards) (Crustacea, Brachyura). Bolletino di zoologia 57, 261-265.

Reddy, A.R., 1937. The physiology of digestion and absorption in the crab *Paratelphusa* (*Oziotelphusa*) *hydrodromus* (Herbst). Proceedings of the Indian Academy of Sciences - Section B 6, 170-193.

Reddy, A.R., 1938. The cytology of digestion and absorption in the crab *Paratelphusa* (*Oziotelphusa*) *hydrodromus* (Herbst). Proceedings of the Indian Academy of Sciences - Section B 8, 171-181.

Ross, M.H., Pawlina, W., 2016. Histology: A Text and Atlas, with correlated Cell and Molecular Biology. Wolters Kluwer Health.

Rotllant, G., Moyano, F.J., Andrés, M., Estévez, A., Díaz, M., Gisbert, E., 2010. Effect of delayed first feeding on larval performance of the spider crab *Maja brachydactyla* assessed by digestive enzyme activities and biometric parameters. Marine Biology 157, 2215-2227.

Schlegel, C., 1911. Anatomie sommaire de la première zoé de *Maja squinado* Latr. (Note préliminaire à des recherches sur l'Organogénese des Décapodes brachyoures). Archives de Zoologie Experimentale et Générale 5º Série T. VIII., 29-40.

Sonakowska, L., Włodarczyk, A., Poprawa, I., Binkowski, M., Śróbka, J., Kamińska, K., Kszuk-Jendrysik, M., Chajec, Ł., Zajusz, B., Rost-Roszkowska, M.M., 2015. Structure and Ultrastructure of the endodermal region of the alimentary tract in the freshwater shrimp *Neocaridina heteropoda* (Crustacea, Malacostraca). PLoS ONE 10, e0126900.

Stanier, J.E., Woodhouse, M.A., Griffin, R.L., 1968. The Fine Structure of the Hepatopancreas of *Carcinus maenas* (L.) (Decapoda Brachyura). Crustaceana 14, 56-66.

Trask, T., 1974. Laboratory-reared larvae of *Cancer anthonyi* (Decapoda: Brachyura) with a brief description of the internal anatomy of the megalopa. Marine Biology 27, 63-74.

Tziouveli, V., Bastos-Gomez, G., Bellwood, O., 2011. Functional morphology of mouthparts and digestive system during larval development of the cleaner shrimp *Lysmata amboinensis* (de Man, 1888). Journal of Morphology 272, 1080-1091.

Van Weel, P.B., 1974. Hepatopancreas? Comparative Biochemistry and Physiology Part A: Physiology 47, 1-9.

Vogt, G., 1994. Life-cycle and functional cytology of the hepatopancreatic cells of *Astacus astacus* (Crustacea, Decapoda). Zoomorphology 114, 83-101.

Vogt, G., 1996. Morphology and physiology of digestive epithelia in Decapod crustaceans. Pflügers Archiv 431, R239-R240.

Williams, R.L., 1944. The pre-zoea stage of *Porcellana platycheles* (Pennant). Preliminary anatomical and histological notes. Journal of the Royal Microscopical Society 64, 1-15.

Yonge, C.M., 1924. Studies on the comparative physiology of digestion II. - The mechanism of feeding, digestion, and assimilation in *Nephrops norvegicus*. British Journal of Experimental Biology 1, 343-389.

CHAPTER 15.

Histology and ultrastructure of the adult and larval midgut gland ("hepatopancreas") of the Atlantic spider crab *Maja brachydactyla* Balss, 1922 (Brachyura, Majidae)

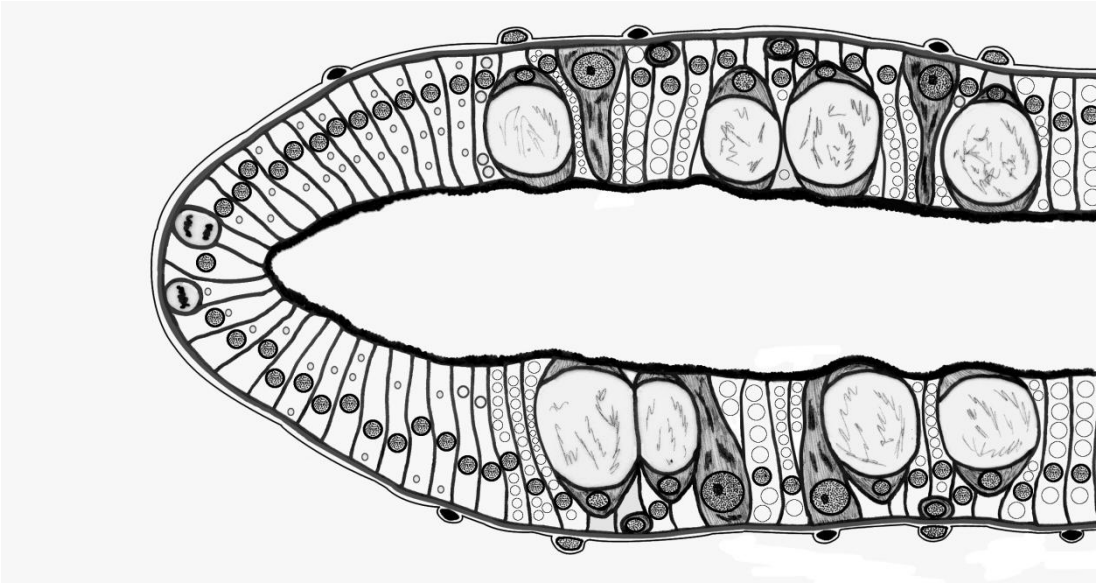

Histology and ultrastructure of the adult and larval midgut gland ("hepatopancreas") of the Atlantic spider crab *Maja brachydactyla* Balss, 1922 (Brachyura, Majidae).

Diego Castejón[1*], Guiomar Rotllant[2], Enric Ribes[3], Mercè Durfort[3], and Guillermo Guerao[4]

[1] IRTA, Centre d'Aqüicultura, Ctra. del Poble Nou Km 5.5. 43540 Sant Carles de la Ràpita, Tarragona (Spain).

[2] CSIC, Institut de Ciències del Mar, Passeig Marítim de la Barceloneta 37-49. 08003 Barcelona (Spain).

[3] Unitat de Biologia Cel·lular, Departament de Biologia Cel·lular, Fisiologia i Immunologia, Facultat de Biologia, Universitat de Barcelona, Diagonal 645. 08028 Barcelona (Spain).

[4] PS Fabra i Puig 344. 08028 Barcelona (Spain).

Short title: *Maja brachydactyla* midgut gland histology and ultrastructure

***Corresponding author:** Diego Castejón. E-mail: diego.castejon.dcb@gmail.com; phone: +34 681 154 398; postal address: IRTA, Subprogram Cultius Aqüàtics, Ctra. Poble Nou, Km 5.5, 43540 Sant Carles de la Ràpita, Tarragona (Spain).

Abstract.

The midgut gland (MGG) of the decapods is a major organ of the digestive system. This study delve into the histology and ultrastructure of the MGG of the brachyuran *Maja brachydactyla* Balss, 1922, comparing both larval and adult specimens using optical and transmission electron microscopy. The MGG histology and ultrastructure is very similar between larval and adult specimens, being the main difference the shorter height of the larval epithelium. From hatching, five types of epithelial cells have been identified: E, R, F, B and M. The mitotic and differentiation function occurs in E-cells. The main absorptive role has been observed on the R-cells since cytoplasmic lipid droplets are usually observed. The secretive role has been observed in R-cells (apocrine secretion from the cell apex and the microvilli tips) and B-cells (vacuole release by apocrine or holocrine secretion and apocrine secretion from microvilli tips). The F-cells are extremely rich in rough endoplasmic reticulum and Golgi bodies, features of cells typically involved in active synthesis of enzymes. Transitional F-cells into B-cells were observed as F-cells with a giant supranuclear vacuole. The M-cells abundance and role is discussed, probably they have mitotic and differentiating functions.

Keywords: Crustacea; ontogeny; larval development; digestive system; cell types; apocrine and holocrine secretion

1. Introduction

The midgut gland (MGG) is a major digestive organ among the Malacostraca, formed by a pair of enormous glandular masses that occupy a great volume on the cephalothoracic cavity. This organ is traditionally known as "hepatopancreas", but according to Cervellione et al. (2017b) this organ lacks features of the "vertebrata hepatopancreas". Then, in this study we used the term "midgut gland". The MGG is implied in numerous functions: synthesis and secretion of digestive enzymes, absorption and storage of nutrients, lipid and carbohydrate metabolism, as well excretion, molting cycle and storage of inorganic reserves (Ceccaldi, 1989; Felgenhauer, 1992; Gibson and Barker, 1979). More recently have been suggested additional roles involved with the synthesis of hemocyanin (Kusche and Burmester, 2001; Sellos et al., 1997) and the immune system (Rőszer, 2014). The MGG is ramified into numerous blind-end tubules, each one internally lined by a simple, columnar epithelium with microvillous border, the basal lamina is surrounded by a thin connective tissue and a network of muscle fibers (Castejón et al., this issue; Icely and Nott, 1992). The MGG is constituted by different cell types, classified into E-cells (embryonic) located on the distal tips and responsible of cell division and differentiation, F-cells (fibrillar) with basophilic and "striated" cytoplasm, R-cells (resorptive) rich in lipid vacuoles and glycogen granules, B-cells (blister like) characterized by a giant supra-nuclear vacuole (Al-Mohanna and Nott, 1989; Felgenhauer, 1992; Icely and Nott, 1992; Loizzi, 1971), and short M-cells (midget) that are located adjacently to the basal lamina and cannot reach the lumen (Al-Mohanna et al., 1985a). The function of each cell type in adult Malacostraca, as well the models of cellular differentiation, have been largely discussed by different authors during decades (Gibson and Barker, 1979; Hu and Leung, 2007; Van Weel, 1974; Vogt,

1996). However, information available in relation to larval stages, and particularly in brachyuran crabs, is still scarce.

In relation to the spider crabs of the genus *Maja*, the general morphology of the MGG was previously described by Milne-Edwards (1834) for the adults and by Schlegel (1911) for the first zoeal stage. However, in these studies a detailed cellular description of this organ is missing as well as the function of the different cell types. In this sense, this paper continues the study of the MGG of the Atlantic spider crab *Maja brachydactyla* Balss 1922 along different life stages. The main objective of this study is the description of the histology and ultrastructure of the MGG, providing detailed information about each epithelial cell type in the larvae and adults, whose role is discussed.

2. Material and methods

2.1 Broodstock and larval culture systems

The acquisition and maintenance of the adult broodstock, as well the culture system and sampling design of the larvae, were described in a previous study (Castejón et al., this issue).

2.2 Optical microscopy

The fixative employed for all samples was Davidson's (ethanol absolute: seawater: formaldehyde 37 %: glycine: glacial acetic acid in proportion 3: 3: 2: 1: 1). The material fixed were entire specimens of each larval stage, first juvenile and small pieces of adult MGG. The fixation process required 24 h, and then the fixed tissues were preserved in ethanol 70 %. The dehydration and paraffin infiltration was realized using an automatic tissue processor (Myr, Spain). The paraffin blocks were realized in a

paraffin processor (Myr, Spain) and a microtome (Leica RM2155) was employed to obtain 2 µm sections. The staining procedures were: 1. Hematoxylin-Eosin (HE), to show the general morphology of the tissue. 2. Periodic Acid–Schiff (PAS) contrasted with Methylene Blue, to reveal the presence of polysaccharides, neutral mucopolysaccharides and the structure of the cuticle line. 3. Periodic Acid–Schiff (PAS) and Alcian Blue pH 2.5 contrasted with Hematoxylin, to reveal the presence of acid mucopolysaccharides. 4. Mallory's trichrome stain (Acid Fuchsine, Orange G and Aniline Blue stains), to reveal the structure of the muscular and connective tissues. The stained sections were observed under an optical microscope (Leica LB30T 111/97). The pictures were taken using a camera (Olympus DP70) and image analyzing system software: DP Controller 2.1.1.83 with DP Manager 2.1.1.163 (Olympus Corporation, Germany).

2.3 Transmission electron microscopy (TEM)

Entire specimens of the larval and first juvenile stages, and small pieces of the adult MGG, were fixed in 2 % paraformaldehyde - 2.5 % glutaraldehyde in cacodylate buffer (0.1 mol L^{-1} pH 7.4). The fixation process required ca. 12 h at 4 °C and constant darkness. Fixed samples were rinsed twice with cacodylate buffer (0.1 mol L^{-1} pH 7.4), post-fixed in 1 % osmium tetroxide, and then dehydrated in a graded series of acetone. The post-fixed samples were embedded in Spurr's resin. Semi-thin sections (0.5–1 µm) and ultra-thin sections (50–70 nm) were made using a Leica UCT ultramicrotome. Semi-thin sections were stained with Bromophenol Blue and ultra-thin sections were counterstained with uranyl acetate and lead citrate. Semi-thin sections were observed under an OlympusBX61 light microscope and ultra-thin sections were viewed and photographed with a JEOL EM-1010 transmission electron microscope (tungsten

filament, 80 kV) equipped with a camera (CCD GATAN ORIUS) and AnalySIS® image software (Soft Imaging System, Münster, Germany). The post-fixative treatment and TEM observations were realized at CCiTUB (Hospital Clinic, University of Barcelona, Barcelona).

3. Results

General morphology. The MGG of the adult *M. brachydactyla* is composed by numerous blind-end tubules, while the larval MGG is composed by fourteen blind-end tubules. These blind-end tubules are the basic unit of the MGG as elongated and tubular structures (Fig. 1A-B), which lumen is "X" shaped in the adults (Fig. 1C), and rounded to irregular in the larvae (Fig. 3D, F). The MGG of the adults is lined by a simple tall columnar epithelium (Fig. 1-2), the height of the epithelial cells varies from 27.02 ± 3.52 µm to 96.20 ± 5.96 µm (Fig. 1C). The epithelium of the larvae and first juvenile is similar, then for simplicity they will be referred as "immature". The immature specimens have a simple epithelium which cell shape varies from cuboidal to short columnar, the height varies from 13 to 37 µm (Fig. 3). Under the epithelium there is a thin basal lamina and a network of muscle fibers (Figs. 1D; 2B, F). These muscle fibers are less evident in the larvae than in the adult. The basal lamina is formed by at least two distinguishable layers, being the layer located adjacent to the basis of the epithelial cells more electron-dense than the layer located immediately below (Fig. 2C).

Five cell types have been identified in the MGG epithelium of *M. brachydactyla* from ca. 15 h after hatching to the adult stage (Fig. 1-3): *E-cells* (embryonic), *R-cells* (resorptive), *F-cells* (fibrillar), *B-cells* (blister-like) and *M-cells* (midget). The different cell types are heterogeneously distributed through the length of the tubule. The distal tip of the blind-end tubule is the "E-cells region" since it is mainly occupied by the E-cells,

some of them can be observed in mitosis (Figs. 1A-B, E; 3B). The E-cells are followed by the "transitional region", composed by sparse F-cells and numerous R-cells characterized by a dense and poorly vacuolated cytoplasm. The next region is the "mature" or "B-cells region", it is dominated by fully developed R-cells with cytoplasm rich in lipid vacuoles, as well abundant B and F-cells. The M-cells are predominately distributed in the medial and proximal parts of the blind-end tubule (Fig. 1-2). The mentioned cell types will be described in detail below:

E-cells. The E-cells are hard to find, so our observations are restricted to the observations realized by optical microscopy. The E-cells of the adult and larval specimens are very similar and located on the distal tip of the blind-end tubules. The E-cell shape vary from short columnar to slightly pyramidal. The nucleus is oval and big in comparison with the cell width. The cytoplasm is homogeneously stained, not showing PAS positive inclusions or other relevant characteristic (Figs. 1B, E; 3B). The cytoplasm is less stained in comparison to adjacent epithelial cells (Fig. 3B). Several E-cells can be observed in active mitotic activity (Fig. 1E).

R-cells. The R-cells of the adult and larval specimens are very similar (Figs. 1-3). They are the main cell type of the MGG epithelium, representing the 76 ± 6 % and the 85 ± 7 % of the cell population in adult and immature stages, respectively. The adult R-cells are narrow and tall columnar with a brush border (Figs. 1-2). The cytoplasm varies depending of the position of the R-cell along the tubule length: the cells located in the "transitional region" have a cytoplasm homogeneously stained with a reduced or null number of vacuoles; on the contrary, the R-cells located in the "B-cells region" have a cytoplasm with numerous PAS positive inclusions and abundant lipid vacuoles. The cytoplasm becomes scarce when it is occupied by infranuclear and supranuclear

lipid vacuoles, whose diameter can be large as the cell width (Figs. 1A-B; 3B). Due to the organization of the vacuoles along the vertical axis, under optical microscopy the adult R-cells resemble to a "tower" of globular vesicles (Figs. 1C-D; 2A, D-F). By contrast, the larval R-cells are cuboidal to short columnar cells with a single lipid vacuole generally located below the nucleus, occasionally there are R-cells lacking this vacuole or presenting two or more vacuoles, including supranuclear vacuoles (Fig. 3D-G). The nucleus is located along the first basal third of the cell in both adults and larvae (Fig. 1-3).

The ultrastructural study reveal a marked polarity in the cell membrane and cytoplasm organization (Figs. 4A-C; 5A-D). The apical membrane forms numerous undulated and slender microvilli, the tip of each microvillus shows a dome shaped electron-dense coat (Fig. 4B). The lateral membranes are generally straight and smooth with sporadic slight undulations (Figs. 4A-C; 5A); short lateral interdigitations have been only observed near to the base of the cells (Fig. 4C). The adjacent cells are attached by cell-to-cell junctions in the apical part of the cell (Fig. 4A-B). These junctions are shorter in the larval R-cells (Fig. 5A-B, D). The basal membrane is generally straight and smooth, but in the adults forms occasional short basal infolds (Fig. 4A, C).

The cytoplasm is lucent, containing generally a low density of free ribosomes (Figs. 4B, 5B). In the cytoplasm can appear vesicular structures of variable size which content varies from lucent to electron-dense and amorphous (Fig. 4B-C), as well as multivesicular and multilamellar bodies. In the adults, the cell apex appear poor in organelles (Fig. 4A-B) and contains vertical filamentous formations composed by associations of filaments and RER-like cisternae projected from the basis of the microvilli to 3 µm downward (FF, Figs. 4A, B, F). On the contrary, in the larvae the cell

apex is very rich in mitochondria and rough endoplasmic reticulum (Fig. 5A-B). The adult cells contains filamentous structures (Fig. 4D), but these were not observed in the larvae (Fig. 5A-B). The adult mitochondria are generally rare and sparse but concentrated on the cell basis, these organelles are short (approximately between 1 and 2 µm length) and generally rounded to rod shaped (Fig. 4A-C). In the larvae the mitochondria are abundant, appear along the entire cell and are larger than in the adults (up to 6 µm length), showing from spherical to cylindrical-conical shape (Fig. 5A-E). The rough endoplasmic reticulum is composed by numerous, thin and short chained cisternae located preferentially above the nucleus (Figs. 4A; 5A-E). In adults, these cisternae do not show a clear arrangement (Fig. 4A, B). In the immature, the cisternae appear scattered around the cytoplasm like in adults and adjacent to the mitochondria (Fig. 5E). The Golgi bodies do not show a clear distribution pattern, they are dispersed and formed by flattened and stacked cisternae (Figs. 4G; 5F).

One of the most important features of the R-cells is the presence of highly developed lipid vacuoles distributed from the basis to the cell apex in adult and immature stages. The shape of these vacuoles is spherical, the borders are regular and smooth, the content is homogeneous, and the size is highly variable, being able to reach the cell width (Figs. 4A, H; 5A, C-D). The R-cells have an apocrine secretory activity based on the formation and release of big vesicles and "micro-vesicles". During the formation of the bigger vesicles, the microvilli are apparently pushed away concomitantly to the increment of the vesicle diameter. When the vesicle is completely formed, it is directly released to the MGG lumen (Fig. 4F). The secretion of the "micro-vesicles" is based on the formation and release of small vesicles from the microvilli. We observed that each micro-vesicle is formed from the microvillus membrane as a lucent

bulge that acquires a globular shape, when the vesicle is completed it is released to the MGG lumen (Fig. 4E).

The cell basis contains a band, adjacent to the basal lamina, composed by smooth endoplasmic reticulum and mitochondria. The smooth endoplasmic reticulum is an electron-dense, branched and tubular net. Some of these tubules fuse with the basal membrane. This band of smooth endoplasmic reticulum is much thicker in the adults than in the larvae. (Figs. 4C; 5C-D).

The nucleus is located in the first basal third of the cell, but can be displaced due to the presence of adjacent lipid vacuoles (Fig. 5A, D).The majority of the nucleoplasm is occupied by heterochromatin. The euchromatin is extremely electron-dense, but restricted to small clusters attached to the nucleus membrane and the nucleoplasm (Figs. 4A, I; 5A, D).

F-cells. The F-cells of the adult and immature stages are very similar, being mainly differentiated by the shorter size of the immature cells. The F-cells are identified by three key features: pyramidal shape, highly stained cytoplasm with some marks and big nucleus (Figs. 2A, D, F; 3A, D-G). The F-cells represent 10 ± 2 % and 7 ± 3 % of the cell population in adult and immature stages, respectively. In both immature and adult stages the height of the F-cells is comparable to the height of the R-cells. The F-cells are pyramidal cells which basis is wider than the apex, thus only a small proportion of the cell apex contact to the free surface of the organ forming a short brush border (Figs. 2D, F; 3D-G). The cytoplasm is perhaps the most stained cytoplasm among the MGG epithelial cells and by optical microscopy shows marks as dense aggregates with fibrillar-like appearance (Figs. 2D, F; 3E, G). The presence of PAS

positive inclusions is rare. The nucleus of the F-cells is the biggest among the epithelial cells, it is usually located close to the cell basis (Figs. 2D, F; 3D-G).

The ultrastructure reveal a marked polarity in the F-cell organization (Figs. 6-7). The apical membrane forms numerous undulated and slender microvilli (Figs. 6B; 7B). The lateral membranes vary from smooth and straight, to slightly undulated. The adjacent cells are attached by an elongated cell-to-cell junctions that arises from the cell apex to few µm down (Figs. 6A-B; 7A). The basal membrane is generally straight with sporadic undulations and infolds, it is attached to an extracellular basal lamina (Figs. 6D; 7C, E).

The most apical cytoplasm of the adult cells forms a thin band devoid from rough endoplasmic reticulum, mitochondria and Golgi bodies (Fig. 6B). This area contains a lucent cytoplasm, sparse lucent or electron-dense rounded vesicles with less than 200 nm diameter, some short undulated membranes, and vertical filamentous formations that resembles to an association of filaments and rough endoplasmic reticulum, these filamentous formations are similar to the observed in the R-cells (Fig. 6A-B). Similarly, the most apical cytoplasm of the larval F-cells forms a thin lucent band with a low density of organelles (Fig. 7B). The cytoplasm of the F-cells is generally lucent, but generally contains a high density of ribosomes (Figs. 6A, C; 7A-D). Moreover, other structures as multi-vesicular bodies (numerous and small rounded vesicles surrounded by a membrane) have been detected as well. The main feature of the F-cells is the extraordinary abundance of rough endoplasmic reticulum, mitochondria and Golgi bodies. In general terms, these organelles are highly developed and are very abundant, distributed widespread in the cell cytoplasm without any regional preference. The rough endoplasmic reticulum is composed by numerous cisternae located almost everywhere on the cell cytoplasm, showing supranuclear and infranuclear distribution. The cisternae

of rough endoplasmic reticulum show three main organizations: short and globular cisternae without a clearly structured organization (Fig. 6A, C), long and wide cisternae stacked in long and parallel chains (Figs. 7A-B; 11A-B), as well long and wide cisternae structured in concentric layers (Fig. 6D; 11A-B). The mitochondria are abundant and scattered in the cytoplasm. The mitochondria are generally small and their shape varies from spherical to elongated (Figs. 6A, C-D; 7A-B, E). The Golgi bodies are abundant and distributed widespread thorough the cytoplasm, their morphology is distinctive for this cell type: the cisternae are very expanded and wide, acquiring a globular appearance; these globular cisternae can be stacked in columns or in zigzag (Figs. 6A, C; 7A, B, D).

The cell basis is characterized by the presence of a thin band composed by tubular smooth endoplasmic reticulum (SEM). It is branched in numerous tubules forming a basal electron-dense net that occasionally fuses with the basal cell membrane. In the F-cells, the height of the band of smooth endoplasmic reticulum is around three times minor than in the R-cells (Figs. 6D; 7C, E).

The nucleus is very big, spherical and located on the first basal third of the cell. The majority of the nucleoplasm is occupied by heterochromatin. The euchromatin is scarce and extremely electron-dense, but restricted to small clusters attached to the nucleus membrane and nucleoplasm (Figs. 6A, C; 7A, C).

B-cells. The B-cells of the immature stages are shorter than during the adult stage, otherwise B-cells present a similar morphology and ultrastructure. The key character of the B-cells is the presence of a giant central vacuole that occupies the majority of the cytoplasmic cell volume. The B-cells represent the 12 ± 5 % and the 8 ± 5 % of the cell population in adult and immature stages, respectively. In the larvae the

B-cells height is higher than the adjacent epithelial cells, then the cell apex protrudes toward the cytoplasm (Fig. 3C); but in the adults the B-cell height is inferior than the adjacent R and F-cells height (Figs. 1A-B; 2D-F). The B-cells of the adults reach a width of 46 ± 7 µm, comparable to three-five times the width of a R- or F-cell (Fig. 2A, D-F), while in the larvae they have 36 ± 7 µm in width. In all the life stages, the diameter of the B-cells is occupied by a single giant central vacuole. The shape of the central vacuole is generally rounded, ovoid or ellipsoidal, although in the larvae irregular forms also have been observed. The B-cell vacuole is unique, not multiple as occur in the R-cells. The B-cell vacuole is always located over the cell nucleus, never below as occur with some vacuoles of the R-cells (Figs. 2A, D-F; 3C). The main difference rely on the internal content: the vacuoles of the R-cells have an homogeneous content that cannot be stained by the histological techniques used; while the B-cells the vacuole has an heterogeneous content similarly stained than the lumen of the MGG (Figs. 2D-F; 3C). The apical cytoplasm is concentrated over the central vacuole forming an "apical dome", and then the cell apex is crowned by a brush border. The nucleus shape varies from ellipsoidal to plane and it is located basally, below the giant central vacuole. Similarly to the cell apex, the cell basis also contains cytoplasm highly concentrated (Figs. 2A, E; 3C).

The ultrastructure reveal a marked polarity in the cell membrane and cytoplasm organization (Figs. 8; 9A-B). The apical membrane forms abundant undulated microvilli which tip is covered by a dome shaped electron-dense coat, basally each microvillus is sustained by a "root-like" filaments laterally organized into a "terminal web"-like structure (Fig. 8C). In the larvae, the apical membrane also shows deep infolds between the microvilli (Fig. 9C). The lateral membranes are smooth. The adjacent cells are attached by elongated cell-to-cell junctions that arises from the cell

apex to down to ca. 8 µm (Fig. 8A-B). The lateral membranes converges until forms a cone shaped cell basis (Figs. 8A, E; 9B). The cytoplasm of the cell apex forms the "apical dome": an electron-dense concentration of cytoplasm filled by numerous and lucent vesicles which shape varies from spherical to ellipsoidal. It is unclear if these vesicles are originated from the disintegration of the giant central vacuole, or by the contrary are merging into the giant central vacuole: the bigger vesicles are partially fused with the apical border of the giant central vacuole, then the vesicle diameter decrease concomitantly with the upward distance from the giant central vacuole, finally some vesicles fuse with the apical membrane (Figs. 8B-C; 9C).

The content of the central vacuole is highly heterogeneous, varying from areas with sparse content and lucent matrix, to areas filled by heavily electron-dense and big sized particulate agglomerations; also can appear fibrillar and lamellate structures composed by thin membranes densely packed, as well flocculent material and vesicles (Figs. 8A-B, F; 9A-B, D). In both larvae and adults the shape of the cell basis varies from inverted cone to inverted dome, being not observed a basal membrane clearly attached to the basal lamina as occur with the other epithelial cell types (Figs. 8A, E; 9B). Similarly to the cell apex, the cytoplasm of the cell basis is highly electron-dense due to the presence of an high density of ribosomes and/or amorphous and disorganized granular matter (Figs. 8E; 9B, E). Few mitochondria are present and their shape varies from slender rods to rounded globules (Figs. 8A; 9A, E). The rough endoplasmic reticulum can appear as enlarged cisternae concentrated around the nucleus (Fig. 9A, E), in other cases the rough endoplasmic reticulum is difficult to identify (Fig. 8B, E). The abundance of Golgi bodies varies from very rare to relatively common, the cisternae vary from very thin and regularly packed to wider and irregularly packed (Figs. 8D; 9E).

Two types of secretory activity have been observed. The most characteristic secretion type of the B-cells consists on the total release of the giant central vacuole toward the MGG lumen, but according to our observations it is unclear if the vacuole is released by apocrine or holocrine secretion. Additionally, the B-cells show apocrine secretion from small lucent bulges formed in the microvilli tip, these bulges acquires a globular shape before their separation and release toward the lumen (Fig. 9C).

The nucleus is mainly constituted by heterochromatin. The heterochromatin is heavily electron-dense, contrasting to the other MGG epithelial cells. The euchromatin is located adjacently to the nuclear membrane, although can form scattered clusters on the nucleoplasm (Figs. 8A, E; 9A-B, E).

M-cells. They are the smallest cell type of the epithelium. Due to this feature this cell type is more easily identified in the adults (Figs. 1D; 2B) than in the immatures, which shorter height makes this cell type more difficult to identify. However, we have identified M-cells in larval stages as zoea I (Fig. 3E) and megalopa (Fig. 10C). The M-cells have an ellipsoidal to rounded shape. In comparison to other epithelial cell types, the M-cells are very small: 11.53 ± 1.50 μm in width and 7.14 ± 0.48 μm in height. They are located basally and attached to the basal lamina, never reaching the MGG lumen (Figs. 1D; 2A-B; 3E). The cytoplasm is a thin layer located around the nucleus with affinity to PAS, the nucleus is small and central (Fig. 1D; 2B).

The similarity of the M-cells in adult and immature stages is confirmed by its ultrastructure (Fig. 10B-C). The M-cells do not show polarity, differing from the other cell types previously described. The cell shape varies from rounded to elongated, including slightly irregular shapes. The cell membrane varies from smooth to slightly undulated. The cytoplasm is lucent; the ribosomes are scattered around the cytoplasm

forming granular aggregations (Fig. 10A-C). In general, the density of organelles is low. The mitochondria are dispersed around the nucleus. The mitochondria size is generally small, rarely exceeding 1 µm length (Fig. 10E-F). The presence of endoplasmic reticulum is unclear: numerous undulated and short tubules lined by a single membrane have been observed forming tubular or globular structures, these appear sometimes as lucent vesicles filled by an extremely low dense matrix of fibers, reaching up to 1 µm diameter or even more. The association of these tubules with ribosomes is unclear, since it was not possible to demonstrate that the ribosomes are attached or merely adjacent to these membranes. One of the most interesting features of the M-cells is the presence of smooth and rounded "electron-dense vesicles", which diameter oscillates between 0.5 and 1.0 µm. The content varies from homogeneous to highly heterogeneous and granular (Fig. 10A-C, F). The Golgi bodies are scarce and small (Fig. 10D). Another interesting feature is the occasional presence of stacks of packed annulate lamellae roaming on the cytoplasm but physically separated from the nucleus (Fig. 10E). The nucleus is located centrally. The quantity of euchromatin is generally high (Fig. 10A-C).

4. Discussion

One of the earliest histological descriptions of the MGG in malacostracans was realized by Thomas Henry Huxley (1880). In his extensive study of the crayfish *Astacus astacus* (as *A. fluviatilis*) the MGG (termed "*liver*") is described as an organ composed by numerous "*caeca*" (in reference to the blind-end tubules), each tubule is lined by a cellular layer termed "*epithelium*" formed by "*nucleated cells*". Huxley identified two types of epithelial cells: distal cells as young cells without "*fat globules*" (probable reference to the lipid vacuoles), as well cells rich in lipid vacuoles located medial and proximally. Moreover, Huxley also observed that the epithelial cells release secretions

into the lumen. Since then, the studies focused on the Malacostraca MGG revealed a complex organ lined by a simple, columnar and microvillous epithelium with diverse (four to five) cell types: embryonary (E-) cells, resorptive (R-) cells, fibrillar (F-) cells, blister like (B-) cells, and midget (M-) cells (to delve into the historical study of the MGG, see the extensive review published by Gibson and Barker, 1979). The identification of these cell types in various Malacostraca taxa is summarized in Table 1.

The present study reveal that the tubules of the MGG of *M. brachydactyla* have all the previously mentioned cell types since hatching. We also observed that the different cell types are differentially located in regions (or zones) along the longitudinal axis of the tubule. Loizzi (1971) subdivided the tubule length into four zones: "distal tip" with E-cells, "transitional zone" with developing R- and F-cells, "B-cell zone" where mature R-, F- and B-cells are intercalated, and "proximal zone" zone where R- and F-cells degenerate. This regionalization has been widely reported in numerous Decapoda taxa (Al-Mohanna and Nott, 1989; Gibson and Barker, 1979; Hopkin and Nott, 1979; Icely and Nott, 1992; Pillai, 1960) and coincides with the observations realized in larvae and adults of *M. brachydactyla*, excepting the degenerative "proximal zone" that has not been identified. This zone also was not observed in *Carcinus maenas* (Hopkin and Nott, 1980). In *M. brachydactyla*, underlying the MGG epithelium we observed a basal lamina divided into an electron-dense innermost layer adjacent to the cellular basal membrane and an outermost layer located beneath the previous one; this description coincides with the basal lamina of *C. maenas* (Stanier et al., 1968). The cellular types and their role are discussed below and compared to observations reported in other decapods:

E-cells. In *M. brachydactyla* E-cells are located in the distal tip of the blind-end tubules and undeveloped, similarly to those described in other Decapoda species (Felgenhauer, 1992; Gibson and Barker, 1979; Icely and Nott, 1992; Li and Li, 1998; Paquet et al., 1993). The E-cell role looks like restricted to the cell division and differentiation, being not involved in the digestive process (Al-Mohanna et al., 1985b).

R-cells. Coinciding to our observations, as reported previously in other Decapoda, the R-cells are the most abundant cell type of the MGG epithelium. At ultrastructural level the R-cells typically contains apical and straight filamentous formations projected from the apical membrane downward the cytoplasm, also contains apical mitochondria, poorly developed rough endoplasmic reticulum, Golgi bodies formed by flattened membranes and smooth endoplasmic reticulum located basal and apically (Al-Mohanna and Nott, 1987; Bunt, 1968; Felgenhauer, 1992; Gibson and Barker, 1979; Li and Li, 1998; Loizzi, 1971; Paquet et al., 1993; Vogt, 1994).The only feature not observed in *M. brachydactyla* was the presence of smooth endoplasmic reticulum on the cell apex, this absence could be related to the phase of the digestive cycle when individuals were sampled (Al-Mohanna and Nott, 1987; Icely and Nott, 1992; Vogt, 1994). Although the low density of mitochondria observed in the cell apex could be related with the phase of the digestive cycle, this relation was not found in previous studies (Al-Mohanna and Nott, 1987). In all the life stages, the R-cells of *M. brachydactyla* show lipid vacuoles and PAS positive inclusions that could correspond to glycogen granules. In this sense, the R-cells are typically associated with the storage of lipid droplets/vacuoles and glycogen granules (Caceci et al., 1988; Felgenhauer, 1992; Icely and Nott, 1992; Vogt, 1994). In other brachyurans, as *C. maenas* and *Scylla serrata*, were reported calcium deposits (Barker and Gibson, 1978; Stanier et al., 1968) as well granules concentrically structured (Hopkin and Nott, 1979), but in this study

they were not noticed. We observed apocrine secretory activity from the R-cell apex and microvilli. Caceci et al. (1988) also observed in the R-cells of *Penaeus vannamei* the extrusion of apical cell fragments by apocrine like secretion. The enzymatic activity has been detected on the microvilli of the R-cells, including esterases, acid and alkaline phosphatases, ATPase and lipolytic enzymes (Barker and Gibson, 1977). Hence, it can be suggested that the R-cells not only might have some digestive activities, but also could release these enzymes into the organ lumen. In fact, previous studies detected similar enzymes on *M. brachydactyla* larvae (Andrés et al., 2010b).

F-cells. The F-cells of decapods, including *M. brachydactyla*, are characterized by the extensive development of the rough endoplasmic reticulum that gives the "striated/fibrillar" appearance under optical microscopy. As observed in other species, the cytoplasm is characterized by their abundance in ribosomes, mitochondria, and Golgi bodies formed by highly dilated membranes; as well the high development of the rough endoplasmic reticulum (Al-Mohanna et al., 1985b; Caceci et al., 1988; Felgenhauer, 1992; Gibson and Barker, 1979; Hopkin and Nott, 1979; Icely and Nott, 1992; Li and Li, 1998; Loizzi, 1971; Paquet et al., 1993; Vogt, 1994). In *M. brachydactyla* the F-cells also have vertical filamentous formations penetrating downward into the cytoplasm from the apical membrane, as observed previously in some crayfish species, e.g. *Astacus astacus*, *Orconectes virilis* and *Procambarus clarkii* (Loizzi, 1971; Vogt, 1994). In *M. brachydactyla* we observed a thin band located in the cell basis and composed by mitochondria and smooth endoplasmic reticulum that was not reported previously by Paquet et al. (1993).

B-cells. In *M. brachydactyla* this globular cell type has a volume comparable to various R- or F-cells. Due to this high volume, the B-cells are considered the largest cell

type of the MGG (Icely and Nott, 1992). Our observations does not differ from previous studies: the B-cells contain a vacuole that occupies the majority of the cell cytoplasm, as well apical microvilli, numerous pynocitic vesicles and channels, dense cytoplasm concentrated basal and apically and packs of rough endoplasmic reticulum (Al-Mohanna and Nott, 1986; Li and Li, 1998; Loizzi, 1971; Paquet et al., 1993). Coinciding with our study, Hopkin and Nott (1979) also observed "vesicles of increasing size occur between the microvillous border and the large vacuole", that were interpreted as a process of pynocitosis. Similar observations were realized by other authors (Li and Li, 1998; Paquet et al., 1993). The basal region contains the nucleus, sparse mitochondria, rough endoplasmic reticulum, and Golgi bodies formed by narrow and flattened membranes (Icely and Nott, 1992). As in previous studies, the supranuclear vacuole is filled by heterogeneous content, including fine and flocculent material, myelin figures, filaments, and dense clumps of particulate matter (Gibson and Barker, 1979; Loizzi, 1971). In the present study, the vacuole secretion mode (apocrine or holocrine) is unclear. In some decapods is holocrine, e.g. the brachyuran *Ocypode platytarsis* (Ramadevi et al., 1990) and the astacid *Homarus gammarus* (Barker and Gibson, 1977); while in others is apocrine, e.g. the brachyuran *Menippe rumphii* (Erri Babu et al., 1982), the palinurid *Panulirus argus* (Travis, 1955) and the caridean *Macrobrachium amazonicum* (Franceschini-Vicentini et al., 2009). Caceci et al. (1988) proposed that the B-cell vacuole can be released by both apocrine or holocrine secretion. We also observed apocrine secretory activity from the B-cell microvilli, as occur with the R-cells. The role of this secretion mode is unknown, but in insects its associated with the release of digestive and other enzymes (Bolognesi et al., 2001; Silva et al., 2013).

M-cells. The "Midget (M-) cells" observed in *M. brachydactyla* are distributed along the tubule length, as in other decapods (Franceschini-Vicentini et al., 2009; Icely and Nott, 1992; Vogt, 1994). In the present study, the M-cells are short, rounded cells in contact with the basal lamina, unable to reach the tubule lumen. The M-cells have a low density of organelles: small mitochondria, short cisternae of endoplasmic reticulum and Golgi bodies. A similar description was reported in previous studies (Al-Mohanna et al., 1985a; Icely and Nott, 1992; Paquet et al., 1993; Vogt, 1994). An important feature of the M-cells is the presence of electron-dense, pleomorphic granules in adults and larvae. Some authors pointed that the number of granules increases concomitantly with the digestive progress until various granules fuse into a massive dense body in the final stages of digestion (Al-Mohanna et al., 1985a; Icely and Nott, 1992). These granules are composed by neutral glycoproteins and might be presumably formed by the accumulation of Golgi bodies products (Icely and Nott, 1992; Vogt, 1994). The role of the M-cells is not yet elucidated. Some authors hypothesize that their role is probably related with storage of proteins or enzymes (Al-Mohanna et al., 1985a; Nunes et al., 2014). Other authors suggested that the M-cells could be endocrine cells since are adjacently located to the hemolymph, where hormones could be excreted (Vogt, 1994); by the same reason they were interpreted as "blood cells" involved in the synthesis of hemocyanin or with a phagocytic role (Paquet et al., 1993). According to our observations, the ultrastructure of the M-cells is close to the basal cells observed on the midgut tract and the midgut caeca of *M. brachydactyla* and other decapods (Komuro and Yamamoto, 1968; Pugh, 1962). The basal cells are related with processes of division and differentiation. Hence, we suggest that M-cells are in fact basal cells and true point of cell regeneration of the MGG tubules. This hypothesis is also supported by the formation of new tubules as branches of older tubules, in other zones but the tubule

tip where E-cells are restricted. Early authors also described this cell type as "basal cells" (Reddy, 1938) or "replacement cells" (Pillai, 1960). Supporting our hypothesis, some authors proposed that the M-cells could replace the B-cell space after their extrusion toward the tubule lumen by the generation of other cell types (Hu and Leung, 2007; Reddy, 1938).

One traditional and central theme of discussion is the origin of the different MGG cell types. It is generally accepted that the R- and F-cells are directly originated from the E-cells, but is unclear if the B-cells differentiate from R- or F-cells (Gibson and Barker, 1979). The most accepted model postulates that the F-cells gradually transform into B-cells (Al-Mohanna et al., 1985b). Vogt (1994) discarded this hypothesis suggesting that the origin of the supranuclear vacuole differs between the cell types: in the F-cells it is an autophagosome formed by the digestion of cell organelles, while in the B-cells is an heterophagosome originated by the fusion of vesicles. By contrast, other authors mentioned that the supranuclear vacuole is originated from the fusion of numerous small vacuoles produced during the F-cell stage (Stanier et al., 1968); being recognized a progressive transition from F-cells to B-cells. In this sense, we observed F-cells maintaining a supranuclear B-cell like vacuole (Fig. 11). Similar F-cell supranuclear vacuoles (which content resembling the B-cell vacuole) have been observed in the crayfishes *O. virilis* y *P. clarkii* (Loizzi, 1971). We observed that the content of the B-vacuole has affinity to the PAS stain, this affinity also has been observed in the supranuclear vacuole of the F-cells by Barker and Gibson (1978). Some authors suggested that the B-cell vacuole is originated by the fusion of electron dense granules ("digestive bodies") formed during the F-cell stage (Al-Mohanna and Nott, 1986). An additional support to the F-cells as precursors of the B-cells was the detection of cathepsin L (CatL) mRNA in F-cells and B-cells vacuole, but absent in E-, M- and R-

cells (Hu and Leung, 2007). Furthermore, it has been suggested that the F-cells produce digestive enzymes that are accumulated on the vacuole and released during the B-cell phase (Icely and Nott, 1992), between 12 and 24 h after feeding (Hopkin and Nott, 1980).

The MGG of the Decapoda larval stages generally has been less studied in comparison to the adult stages. Moreover, these studies generally identified less cell types (see summarized information provided in Table 2). The global view provided by these studies shows that the cell types observed in the larval MGG of *M. brachydactyla* coincides with the cell types reported in other decapods during their larval stages. In general, the adult and larval cells are very similar, excepting pointed differences. Coinciding to our study, it has been reported that the larval R-cells have generally less vacuoles than the adult R-cells, being described from none to few rounded vacuoles in their cytoplasm (Biesiot and McDowell, 1995; Factor, 1995; Li and Li, 1998). Maybe the greatest divergences have been observed with members of the Achelata group: during the phyllosoma stage the abundant R-cells accumulates unknown spherical globules (Mikami et al., 1994), although other authors reported lipid vacuoles (Johnston, 2006); while in the most advanced puerulus stage this cell type start to accumulate lipids from the hemolymph coinciding with the accumulation of pigments on the animal, these lipids droplets where reabsorbed during the post-puerulus stages (Nishida et al., 1995).

The data obtained in this study demonstrates that the first larval stage has the cellular machinery required for a exogenous nutrition. The newly hatched zoeae of *M. brachydactyla* are obligate feeders from hatching: they lack enough nutritional reserves to reach the next larval stage in starving conditions and an initial food deprivation delay

the larval development and increases the mortality rate (Guerao et al., 2012; Rotllant et al., 2010). The digestion and assimilation of the matter and energy provided by the live preys require a powerful enzymatic battery with the ability to sustain the digestive process. In this sense, previous studies demonstrates that the *M. brachydactyla* larvae are able to digest proteins, carbohydrates and lipids as soon as they hatch, being detected proteolytic, amylase, maltase, chitinase and esterase activities in newly hatched larvae (Andrés et al., 2010b; Rotllant et al., 2008); the variety of enzymes detected in the digestive gland suggest an omnivore pattern. Since the majority of these enzymes are produced by the MGG in Malacostraca (Barker and Gibson, 1977), our data show that the MGG of *M. brachydactyla* is ready for the enzyme production and food digestion as soon as they hatch, since the epithelial cells of the larval MGG have an adult like shape and ultrastructure.

The MGG of the newly hatched zoeae of *M. brachydactyla* is rich in lipid vacuoles that occupy most of the cellular cytoplasm, similar observation has been realized in the newly hatched larvae of *H. araneus* (Storch and Anger, 1983). Moreover, the *M. brachydactyla* larvae in good nutritional condition accumulate lipids during the larval development, specially neutral lipids as triacylglycerols, waxes and sterol esters, including cholesterol (Andrés et al., 2010a); on the contrary, the number of lipid vacuoles of the R-cells decrease significantly in starving conditions (Guerao et al., 2012). Similarly, in the relative *H. araneus* the quantity of lipid vacuoles decreases gradually in starving conditions, being the MGG depleted from lipids after four days without feeding (Storch and Anger, 1983). Also, in newly hatched *Homarus americanus* larvae, R-cells become depleted or nearly depleted of lipid vacuoles after three days of food deprivation (Anger et al., 1985) and in the juvenile *Penaeus vannamei* the lipid content of the MGG decreases significantly in starving conditions (Cervellione et al.,

2017a; Sánchez-Paz et al., 2007). These data demonstrates a correlation between the density of lipid vacuoles and the nutritional condition of the larvae. In addition, the density of lipid vacuoles on the R-cells also varies with the molting cycle in *U. cordatus* (Marcolin et al., 2008). We suggest that this lipid storage could act as energy reserve to support survival, so the lipid droplets observed in the MGG could help to sustain the animal until new preys were captured. Hence, the digestive gland of *M. brachydactyla* is formed and functional from hatching and during the ontogeny the MGG mainly increases in size and digestive capacities.

5. Acknowledgements

Financial support provided by the Spanish Ministry of Economy and Competitiveness through the INIA project [grant number RTA2011-00004-00-00] to G.G and a predoctoral fellowship to D.C. [FPI-INIA]. The authors would like to thank to the technicians at IRTA in Sant Carles de la Ràpita (David Carmona, Glòria Macià, Magda Monllaó, Francesc X. Ingla and Olga Bellot) and CCiTUB in Hospital Clinic, Barcelona (Adriana Martínez, Almudena García, José Manuel Rebled, Rosa Rivera) for their assistance.

Table 1. Types of midgut gland epithelial cells identified in different Malacostraca taxa during the adult stage. The question mark (?) indicate the presence of a cell type whose description have some similarities to the marked type, the superscript indicate the denomination of this cell type in the original reference. CNE: Identified cell types non equivalent to the described in other Malacostraca (E-, R-, F-, B- and M-cells).

Species	Taxa	E-cells	R-cells	F-cells	B-cells	M-cells	Reference:
Carcinus maenas (Linnaeus, 1758)	Brachyura	X	X	X	X		(Hopkin and Nott, 1979; Stanier et al., 1968)
Cyrtograpsus angulatus Dana, 1851	Brachyura	X	X	X	X		(Cuartas and Petriella, 2002; Longo and Díaz, 2015)
Eriocheir sinensis H. Milne Edwards, 1853	Brachyura	X	X	X	X		(Zhang et al., 2017)
Menippe rumphii (Fabricius, 1798)	Brachyura	X	X	X	X		(Erri Babu et al., 1982)
Neohelice granulata (Dana, 1851)	Brachyura	X	X	X	X		(Bianchini and Monserrat, 2007; Cuartas and Petriella, 2002)
Ocypode platytarsis H. Milne Edwards, 1852	Brachyura	X	X	X	X	X	(Ramadevi et al., 1990)
Scylla paramamosain Estampador, 1950	Brachyura	X	X	X	X		(Zeng et al., 2010)
Scylla serrata (Forskål, 1775)	Brachyura	X	X	X	X		(Barker and Gibson, 1978)
Sinopotamon honanense Dai et al. 1975	Brachyura		X	X	X		(Liu et al., 2013)
Spiralothelphusa hydrodroma (Herbst, 1974)	Brachyura		X		X		(Reddy, 1937)
Ucides cordatus (Linnaeus, 1763)	Brachyura	X	X	X	X		(Marcolin et al., 2008)
Uca uruguayensis Nobili 1901	Brachyura	X	X	X	X		(Cuartas and Petriella, 2002)
Astacus astacus (Linnaeus, 1758)	Astacidae	X	X	X	X	X	(Vogt, 1994)
Homarus americanus H. Milne Edwards, 1837	Astacidae	X	X	X	X		(Biesiot and McDowell, 1995)

Table 1 (continuation). Types of midgut gland epithelial cells identified in different Malacostraca taxa during the adult stage. The question mark (?) indicate the presence of a cell type whose description have some similarities to the marked type, the superscript indicate the denomination of this cell type in the original reference. CNE: Identified cell types non equivalent to the described in other Malacostraca (E-, R-, F-, B- and M-cells).

Species	Taxa	E-cells	R-cells	F-cells	B-cells	M-cells	Reference:
Homarus gammarus (Linnaeus, 1758)	Astacidae	X	X	X	X	X	(Barker and Gibson, 1977; Paquet et al., 1993)
Nephrops norvegicus (Linnaeus, 1758)	Astacidae		X	X	X		(Yonge, 1924)
Orconectes virilis (Hagen, 1870)	Astacidae	X	X	X	X		(Loizzi, 1971)
Procambarus clarkii (Girard, 1852)	Astacidae	X	X	X	X		(Bunt, 1968; Loizzi, 1971)
Farfantepenaeus brasiliensis (Latreille, 1817)	Dendrobranchiata	X	X	X	X	X	(Nunes et al., 2014)
Metapenaeus bennettae Racek and Dall, 1965	Dendrobranchiata		X	X			(Dall, 1967)
Penaeus japonicus Spence Bate, 1888	Dendrobranchiata	X	X	X	X		(Zilli et al., 2003)
Penaeus semisulcatus De Haan, 1844	Dendrobranchiata	X	X	X	X	X	(Al-Mohanna and Nott, 1989; Al-Mohanna et al., 1985)
Penaeus vannamei Boone, 1931	Dendrobranchiata		X	X	X		(Caceci et al., 1988)
Pleoticus muelleri (Bate, 1888)	Dendrobranchiata	X	X	X	X		(Cuartas et al., 2002)
Caridina laevis Heller, 1862	Caridea	X	X	X	X	X	(Pillai, 1960)
Lysmata amboinensis De Man, 1888	Caridea	X	X	X	X	X	(Tziouveli et al., 2011)
Macrobrachium amazonicum (Heller, 1862)	Caridea	X	X	X	X	X	(Franceschini-Vicentini et al., 2009; Ribeiro et al., 2016)
Macrobrachium borellii (Nobili, 1896)	Caridea		X	X	X		(Collins, 2010)
Macrobrachium rosenbergii (de Man, 1879)	Caridea	X	X	X	X		(Li et al., 2006)

Table 1 (continuation). Types of midgut gland epithelial cells identified in different Malacostraca taxa during the adult stage. The question mark (?) indicate the presence of a cell type whose description have some similarities to the marked type, the superscript indicate the denomination of this cell type in the original reference. CNE: Identified cell types non equivalent to the described in other Malacostraca (E-, R-, F-, B- and M-cells).

Species	Taxa	E-cells	R-cells	F-cells	B-cells	M-cells	Reference:
Neocaridina heteropoda Liang, 2002	Caridea	X	?$^{\text{type II}}$	?$^{\text{type I}}$	?$^{\text{type II}}$		(Sonakowska et al., 2015)
Palaemon argentinus (Nobili, 1901)	Caridea	X	X	X	X		(Sousa et al., 2005; Sousa and Petriella, 2007)
Palaemon serratus (Pennant, 1777)	Caridea		X	X	X	?^{E}	(Papathanassiou and King, 1984)
Mysis stenolepis S.I. Smith, 1873	Mysida	?^{S}	X	X	X		(Friesen et al., 1986)
Gammarus locusta (Linnaeus 1758)	Amphipoda	X	X	X	X		(Correia et al., 2002)
Gammarus minus Say, 1818	Amphipoda	X	X	X	X		(Schultz, 1976)
Hyalella azteca Saussure, 1858	Amphipoda	X	X	X			(Schmitz and Scherrey, 1983)
Macarorchestia remyi (Schellenberg, 1950)	Amphipoda	X	X	X	X	X	(Davolos et al., 2010)
Armadillidium nasatum Budde-Lund, 1885	Isopoda		?				(Schmitz and Schultz, 1969)
Armadillidium vulgare (Latreille, 1804)	Isopoda		?				(Schmitz and Schultz, 1969)
Oniscus asellus Linnaeus, 1758	Isopoda	CNE: termed "B-cells" and "S-cells"					(Hopkin and Martin, 1982)
Porcellio scaber Latreille, 1804	Isopoda	CNE: termed "B-cells" and "S-cells"					(Ņnidarńič et al., 2003)

Table 2. Types of midgut gland epithelial cells identified during the larval stages of different Decapoda taxa. The question mark (?) indicate the description of cells with resemblances to the marked type.

Species	Taxa	Larval stages	E-cells	R-cells	F-cells	B-cells	M-cells	Reference:
Hyas araneus (Linnaeus, 1758)	Brachyura	Zoeae - Megalopa	X	X	X	X		(Storch and Anger, 1983)
Maja sp. Lamarck, 1801	Brachyura	First zoea		X				(Schlegel, 1911)
Metacarcinus anthonyi Rathbun 1897	Brachyura	Megalopa				X		(Trask, 1974)
Portunus trituberculatus (Miers, 1876)	Brachyura	Megalopa		X		X		(Nakamura, 1990)
Scylla olivacea (Herbst, 1796)	Brachyura	Zoeae		X		X		(Jantrarotai and Sawanyatiputi, 2005)
Scylla serrata (Forskål, 1775)	Brachyura	Zoeae	X	X	X	X		(Li and Li, 1998)
Paralithodes camtschaticus (Tilesius, 1815)	Anomura	Zoeae - Glaucothoe	X	X	X	X		(Abrunhosa and Kittaka, 1997)
Porcellana platycheles (Pennant, 1777)	Anomura	Pre-zoea		X	X	X	?	(Williams, 1944)
Homarus americanus H. Milne Edwards, 1837	Astacidae	First zoea	X	X	X	X		(Anger et al., 1985; Biesiot and McDowell, 1995)
Ibacus ciliatus (Von Siebold, 1824)	Achelata	Phyllosoma		X	X	X		(Mikami et al., 1994)
Jasus edwardsii (Hutton, 1875)	Achelata	Puerulus		X	X	X		(Nishida et al., 1995)
Panulirus japonicus (Von Siebold, 1824)	Achelata	Phyllosoma		X	X	X		(Mikami et al., 1994)
Panulirus ornatus (Fabricius, 1798)	Achelata	Phyllosoma		X	X	X		(Johnston, 2006)

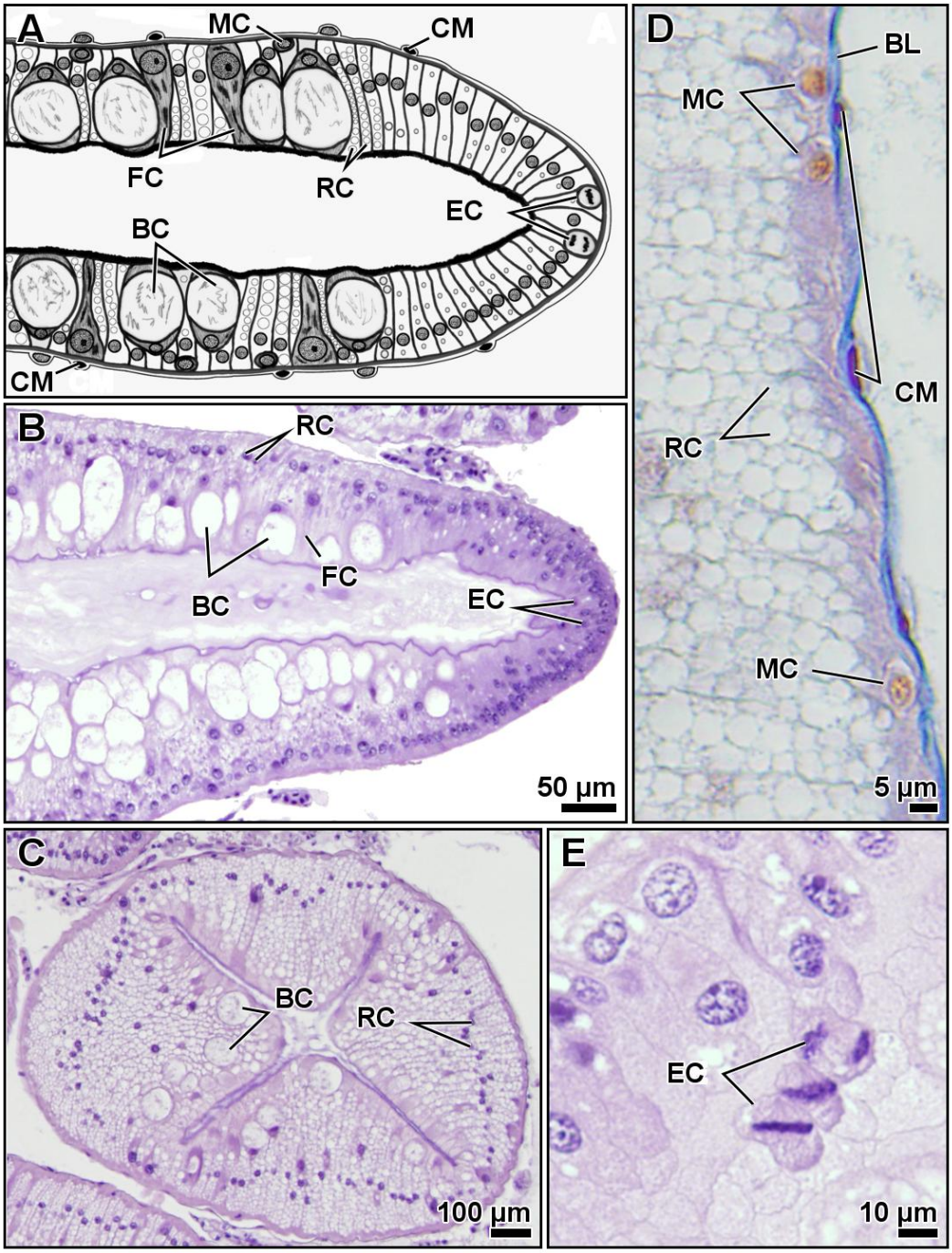

Figure 1. *Maja brachydactyla*. Midgut gland. Histological organization of the blind-end tubules, optical microscopy. General diagram (A). General view, Hematoxylin-Eosin (B-C): longitudinal (B) and transversal section (C). Basis of the epithelial cells showing some M-cells (MC), Mallory's trichrome (D). E-cells in different stages of mitosis, Hematoxylin-Eosin (E). Abbreviations: BC: B-cells; BL: basal lamina; CM: circular muscle fibers; EC: E-cells; BC: B-cells; FC: F-cells; MC: M-cells; RC: R-cells.

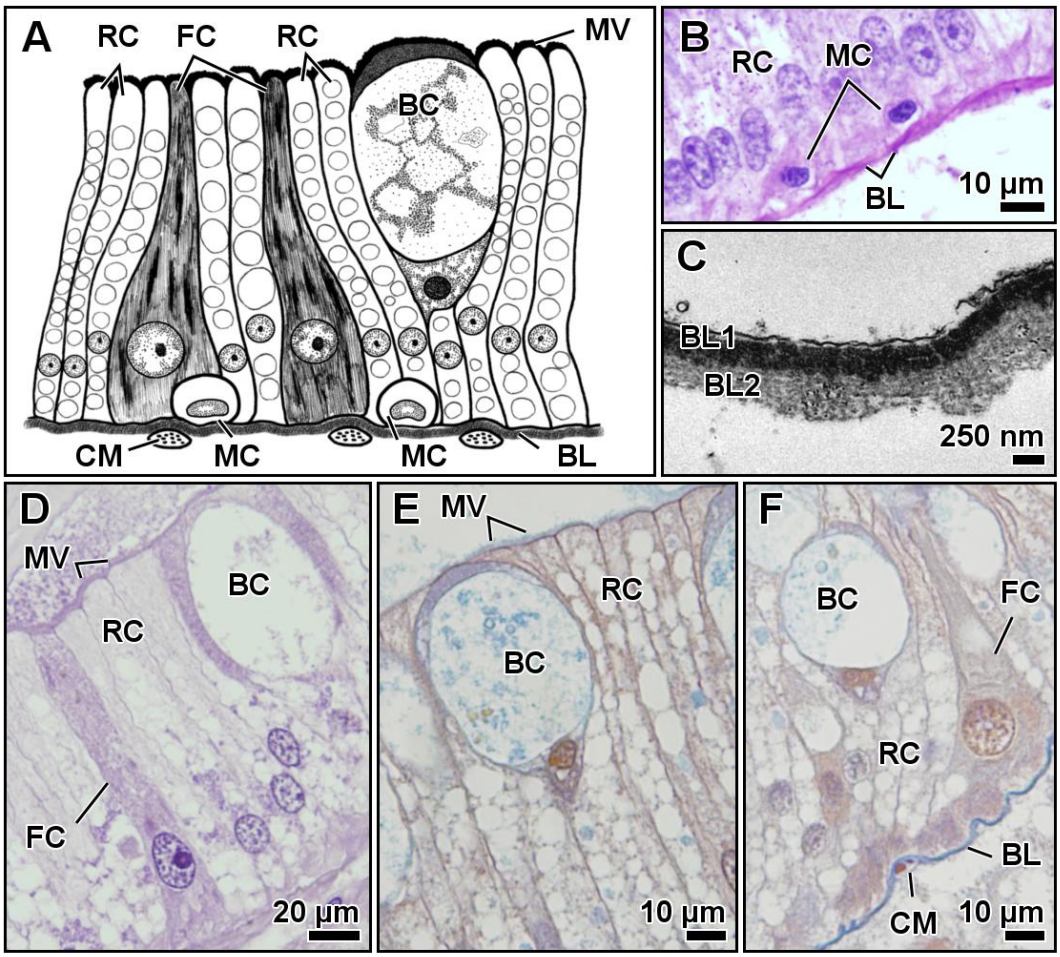

Figure 2. *Maja brachydactyla*. Adult. Midgut gland. Epithelial cells. General diagram (A). Epithelium basis showing the M-cells (MC), PAS and Alcian Blue contrasted with Hematoxylin (B). Close view of the basal lamina, TEM (C). Epithelial cells, Hematoxylin-Eosin (D). Epithelial cells, Mallory's trichrome (E-F). Abbreviations: BC: B-cells; BL: basal lamina; BL1: first layer of the basal lamina; BL2: second layer of the basal lamina; CM: circular muscle fibers; FC: F-cells; MC: M-cells; RC: R-cells.

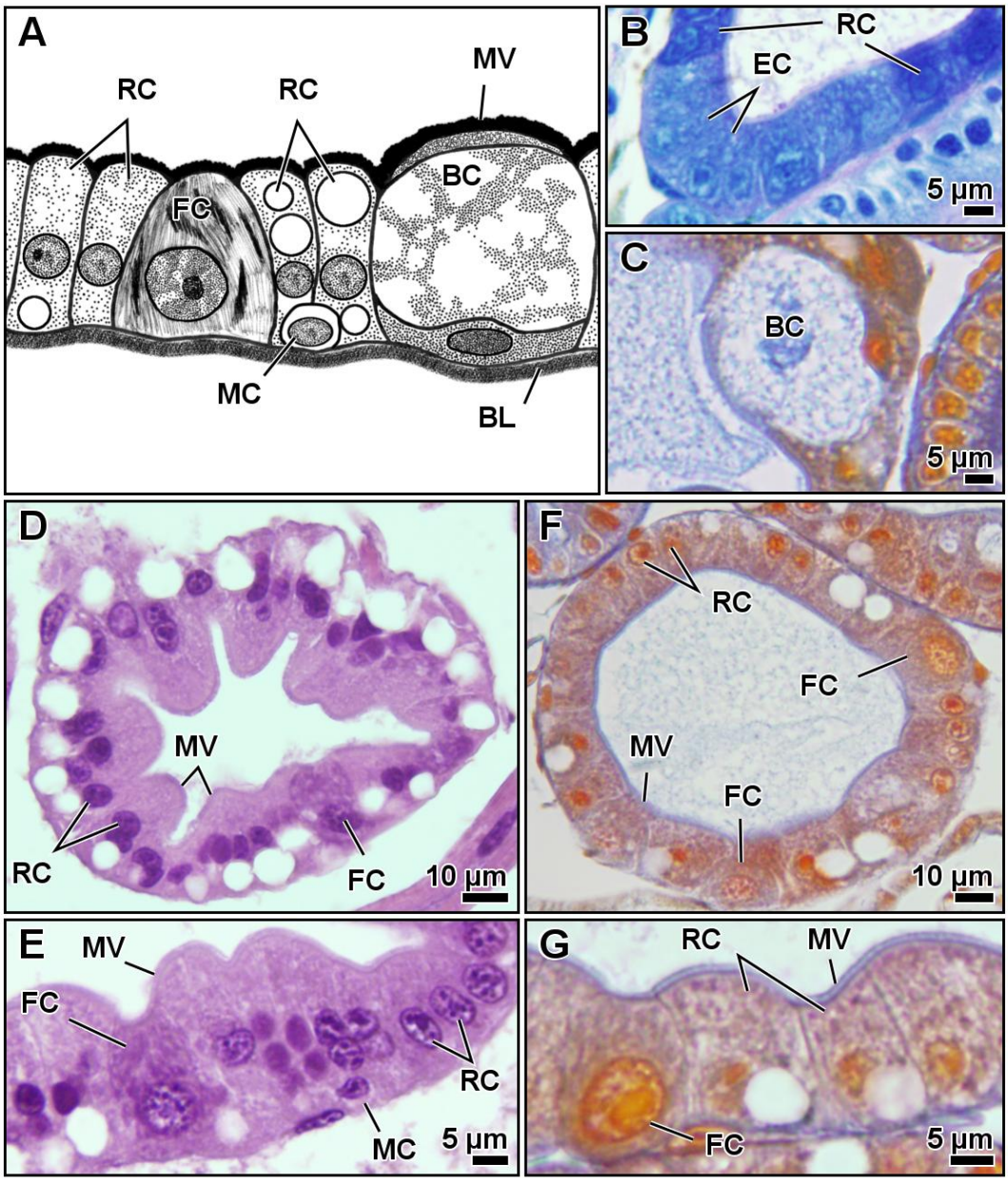

Figure 3. *Maja brachydactyla*. Larvae. Midgut gland. Epithelial cells. General diagram (A). Megalopa, 6 days after hatching (dah), distal tip of the blind-end tubule, PAS contrasted with Methylene Blue (B). Zoea II, 6 dah, close view of the B-cell, Mallory's trichrome (C). Newly hatched zoeae, Hematoxylin-Eosin (D-E): transversal section (D) and detailed view (E). Megalopa, 6 dah, Mallory's trichrome (F-G): transversal section (F) and detailed view (G). Abbreviations: BC: B-cells; BL, basal lamina; EC: E-cells; FC: F-cells; MC: M-cells; MV: microvilli; RC: R-cells.

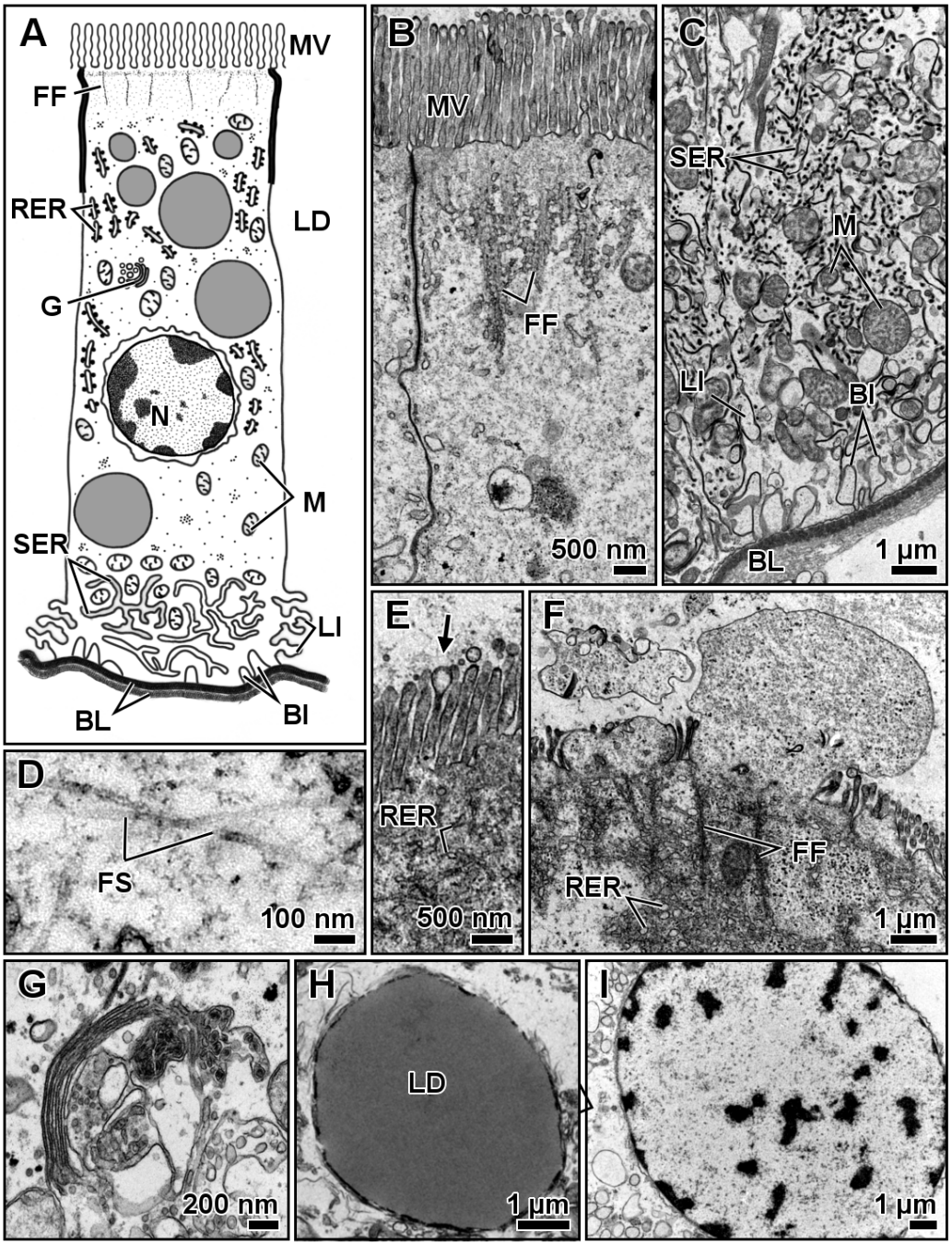

Figure 4. *Maja brachydactyla*. Adult. Midgut gland. Ultrastructure of the R-cells. General diagram (A). Cell apex, supranuclear region (B). Cell basis, infranuclear region (C). Close view of the filamentous structures (D). Apocrine secretion of micro-vesicles from the microvilli (arrow) (E). Apocrine secretion from the cell apex (F). Close view of a Golgi body (G). Lipid droplet (H). Nucleus (I). Abbreviations: BL: basal lamina; BI: basal infolds; FF, filamentous formation; FS, filamentous structures; G: Golgi bodies; LD, lipid droplets; LI: lateral interdigitations; M: mitochondria; MV: microvilli; N: nucleus; RER: rough endoplasmic reticulum; SER: smooth endoplasmic reticulum.

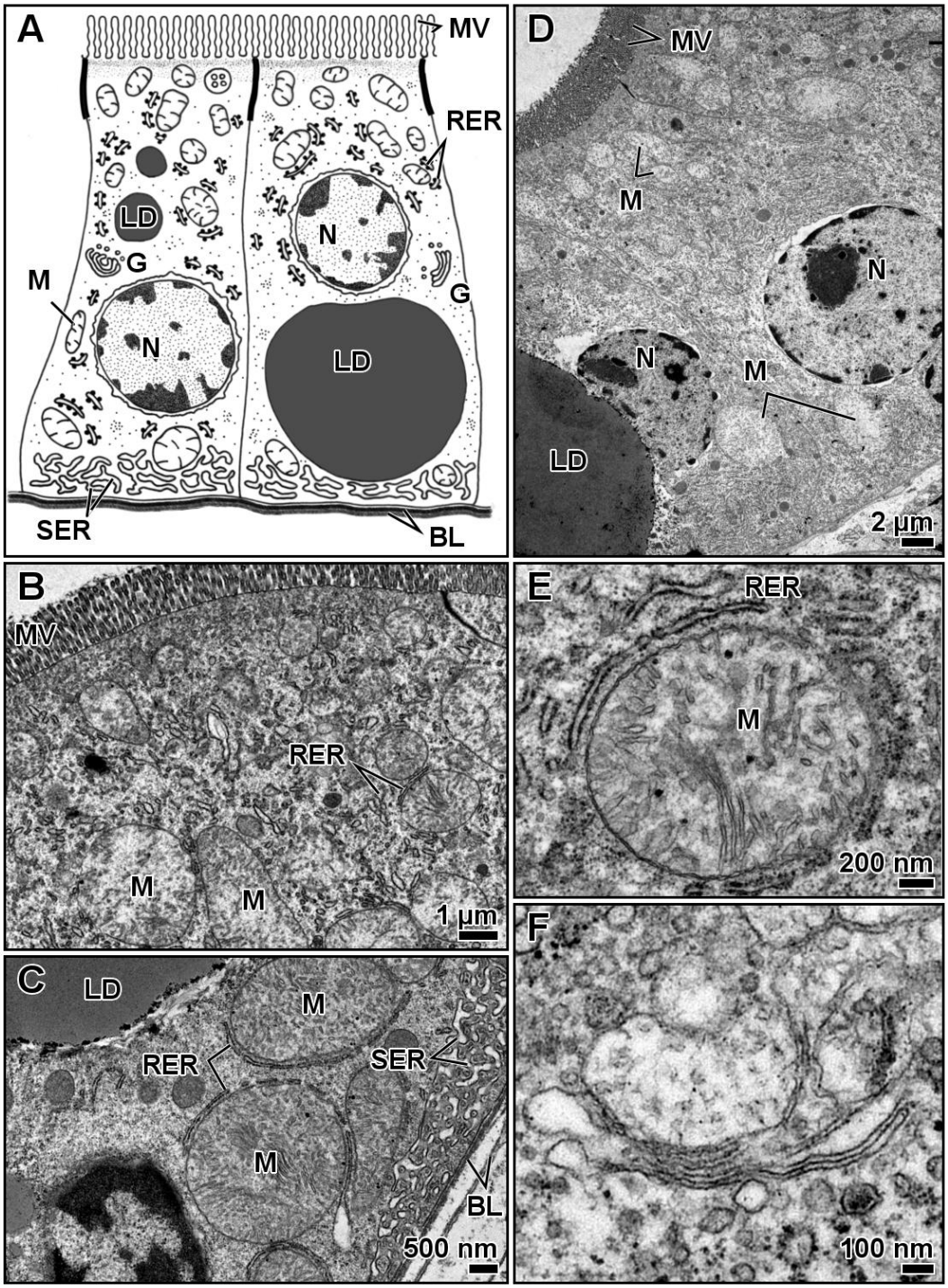

Figure 5. *Maja brachydactyla*. Megalopa, 10 days after hatching. Midgut gland. Ultrastructure of the R-cells. General diagram (A). Cell apex, supranuclear region (B). Cell basis, nucleus and infranuclear region (C). General view of the R-cells (D). Close view of the mitochondria and RER (E). Close view of a Golgi body (F). Abbreviations: BL: basal lamina; G: Golgi bodies; LD, lipid droplets; M: mitochondria; MV: microvilli; N: nucleus; RER: rough endoplasmic reticulum; SER: smooth endoplasmic reticulum.

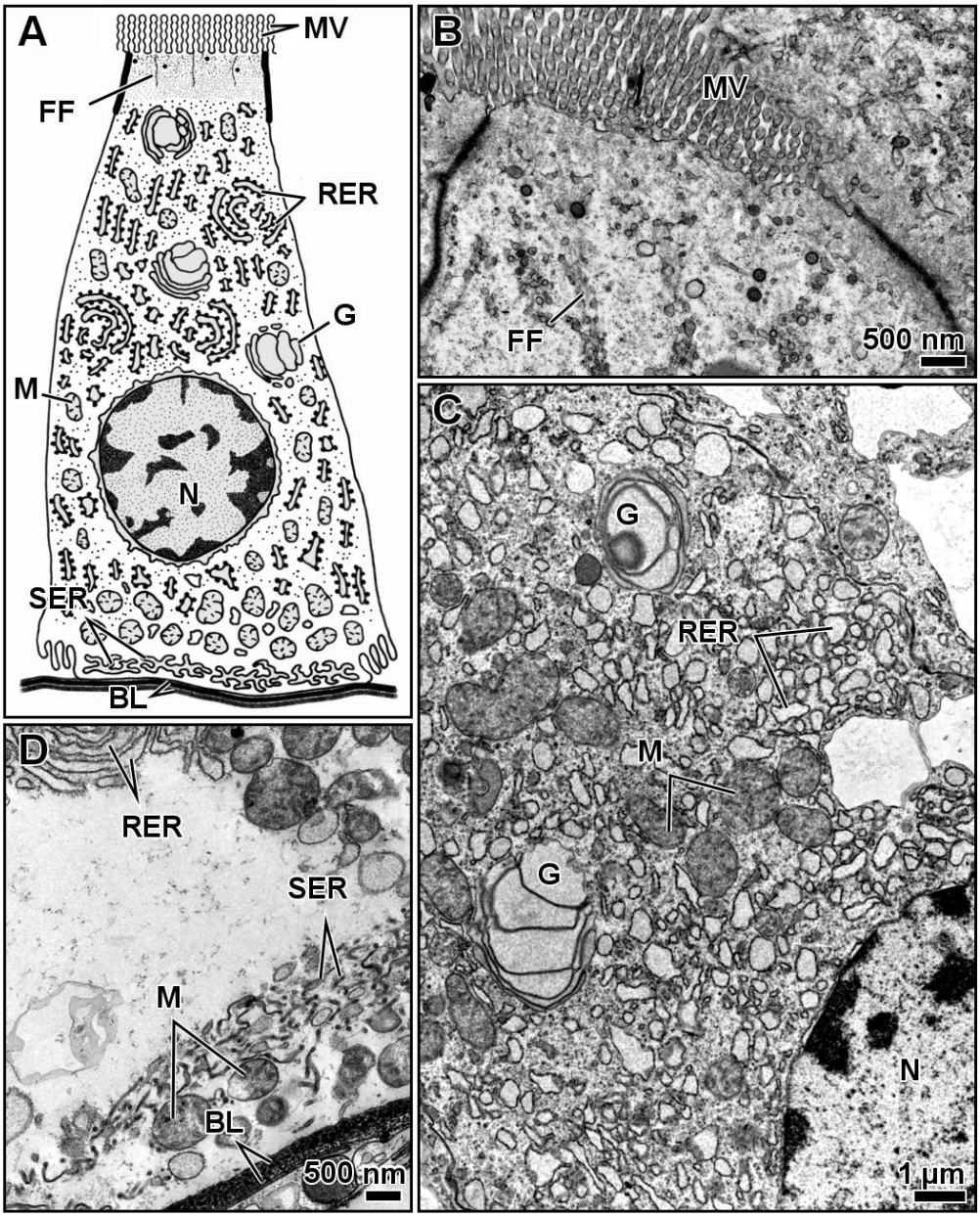

Figure 6. *Maja brachydactyla*. Adult. Midgut gland. Ultrastructure of the F-cells. General diagram (A). Close view of the cell apex and microvilli (B). Nucleus and supranuclear region (C). Close view the cell basis, infranuclear region (D). Abbreviations: BL: basal lamina; FF: filamentous formations; G, Golgi bodies; M: mitochondria; MV: microvilli; N: nucleus; RER: rough endoplasmic reticulum; SER: smooth endoplasmic reticulum.

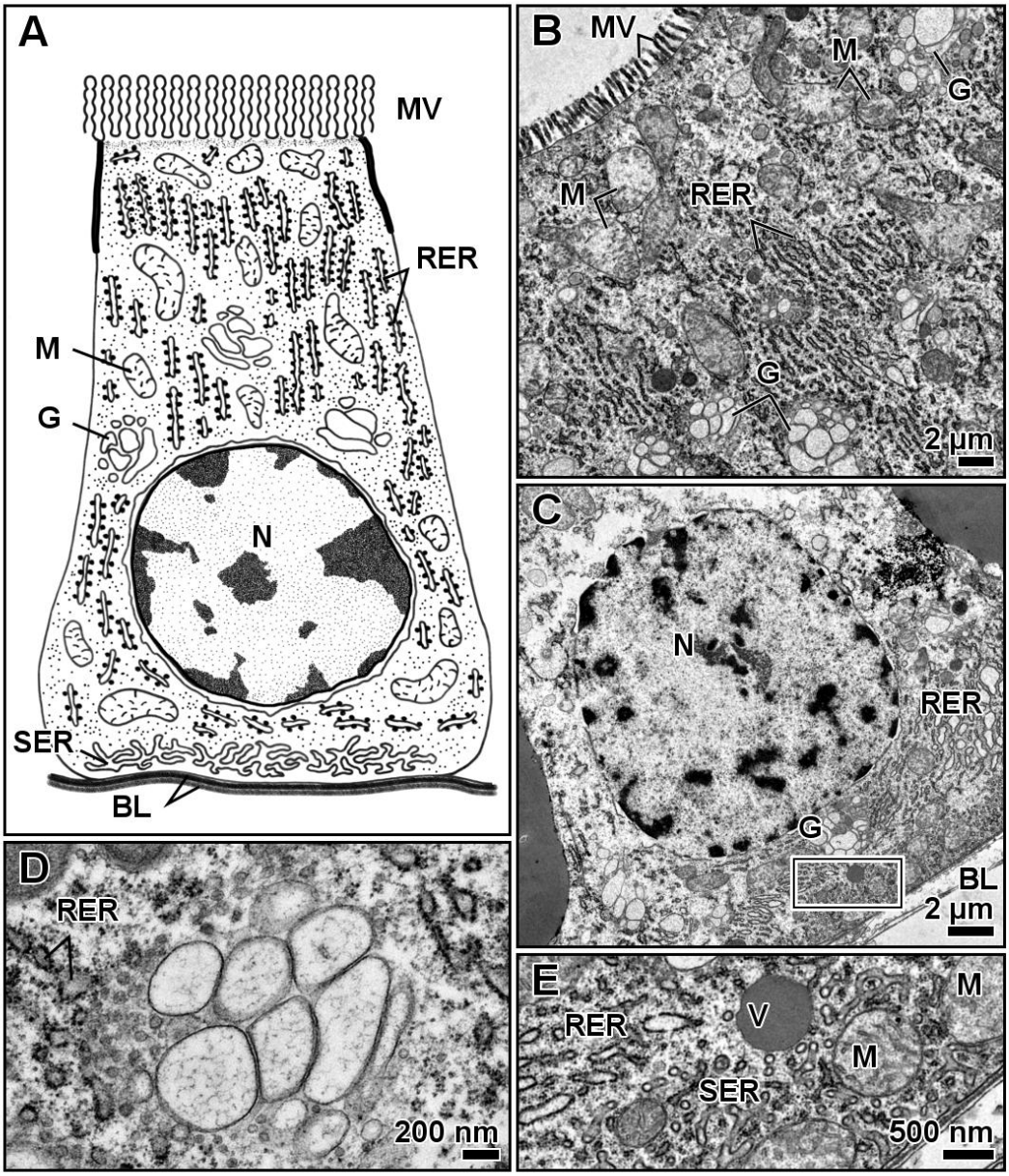

Figure 7. *Maja brachydactyla*. Megalopa, 10 days after hatching. Midgut gland. Ultrastructure of the F-cells. General diagram (A). Cell apex, supranuclear region (B). Nucleus and cell basis (C). Close view of a Golgi body (D). Close view of the cell basis, marked in C (E). Abbreviations: BL: basal lamina; M: mitochondria; MV: microvilli; N: nucleus; RER: rough endoplasmic reticulum; SER: smooth endoplasmic reticulum; V, vacuole.

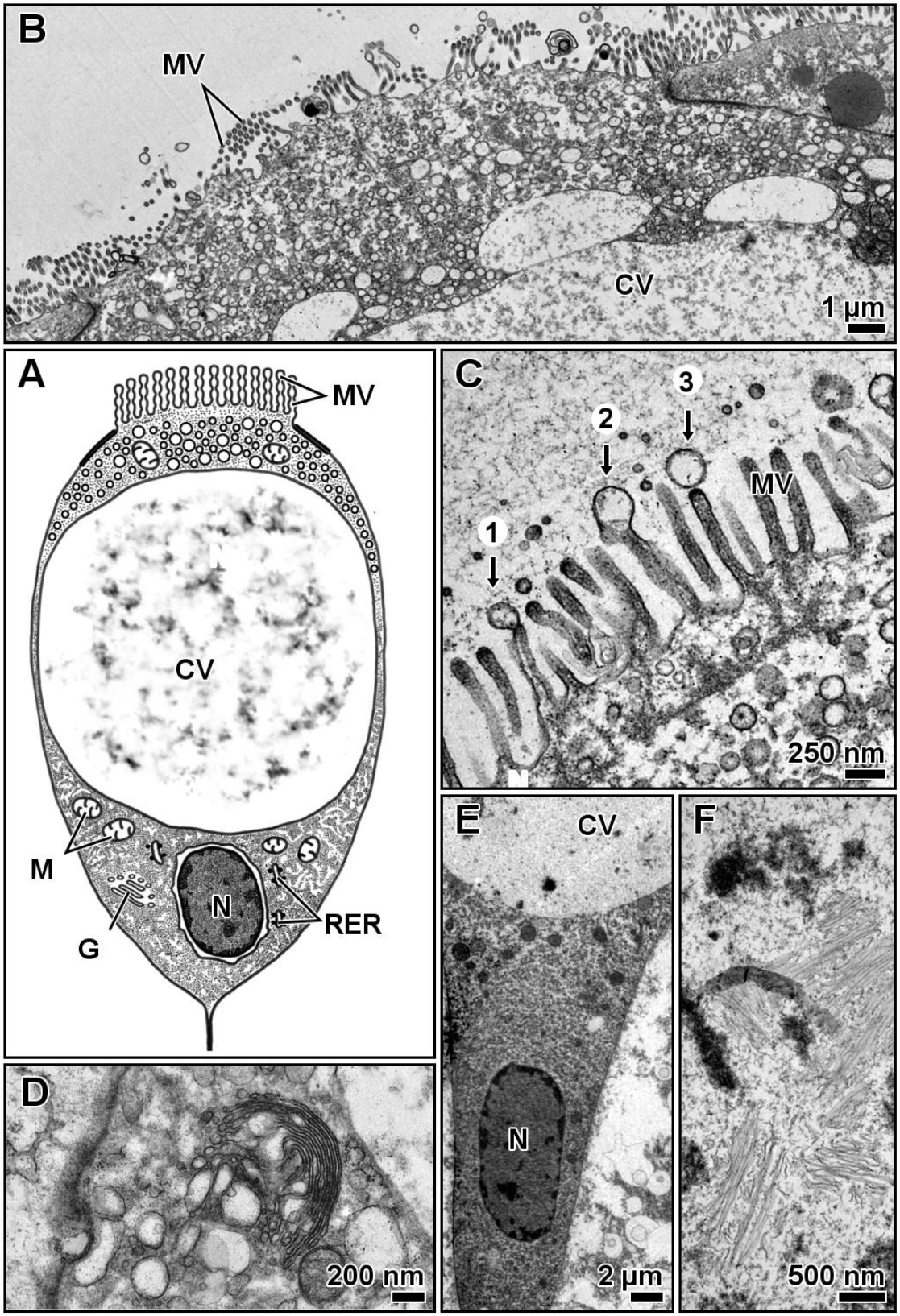
B
MV
CV
1 µm
A
MV
CV
M
N
RER
G
C
3
2
1
MV
250 nm
E
CV
N
2 µm
F
500 nm
D
200 nm

Figure 8 (previous page). *Maja brachydactyla*. Adult. Midgut gland. Ultrastructure of the B-cells. General diagram (A). Cell apex, supra-vacuolar region (B). Secretory activity of the microvilli (numbered arrows) (C). Close view of a Golgi body (D). Nucleus and cell basis, infra-vacuolar region (E). Content of the central vacuole (F). Abbreviations: CV: central vacuole; G: Golgi bodies; M: mitochondria; MV: microvilli; N: nucleus; RER: rough endoplasmic reticulum.

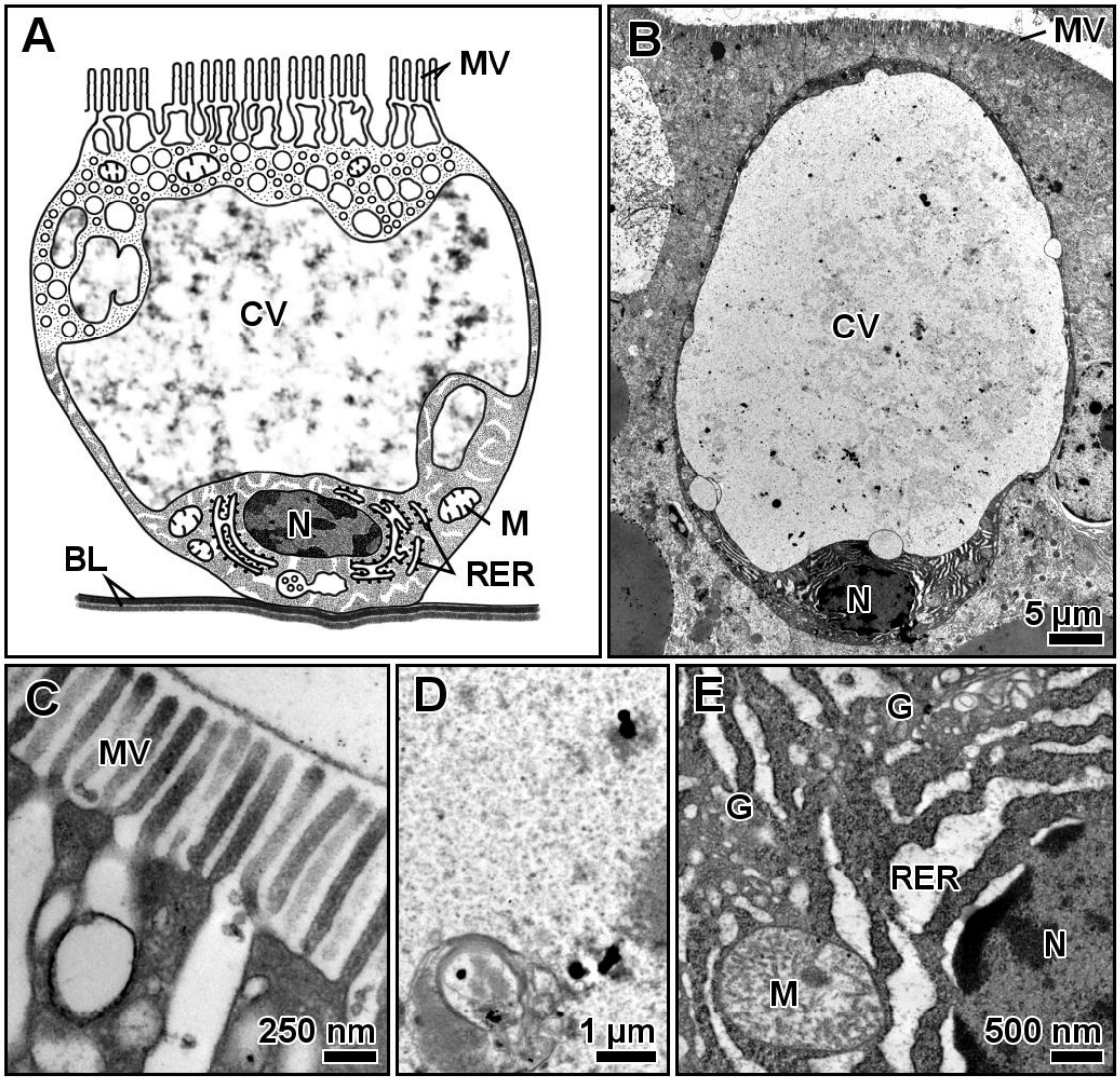

Figure 9. *Maja brachydactyla*. Megalopa, 10 days after hatching. Midgut gland. Ultrastructure of the B - cells. General diagram (A). General view (B). Close view of the microvilli (C). Content of the central vacuole (D). Close view of the nucleus and cell basis, infra-nuclear region (E). Abbreviations: BL: basal lamina; CV: central vacuole; G: Golgi bodies; M: mitochondria; N: nucleus; RER: rough endoplasmic reticulum.

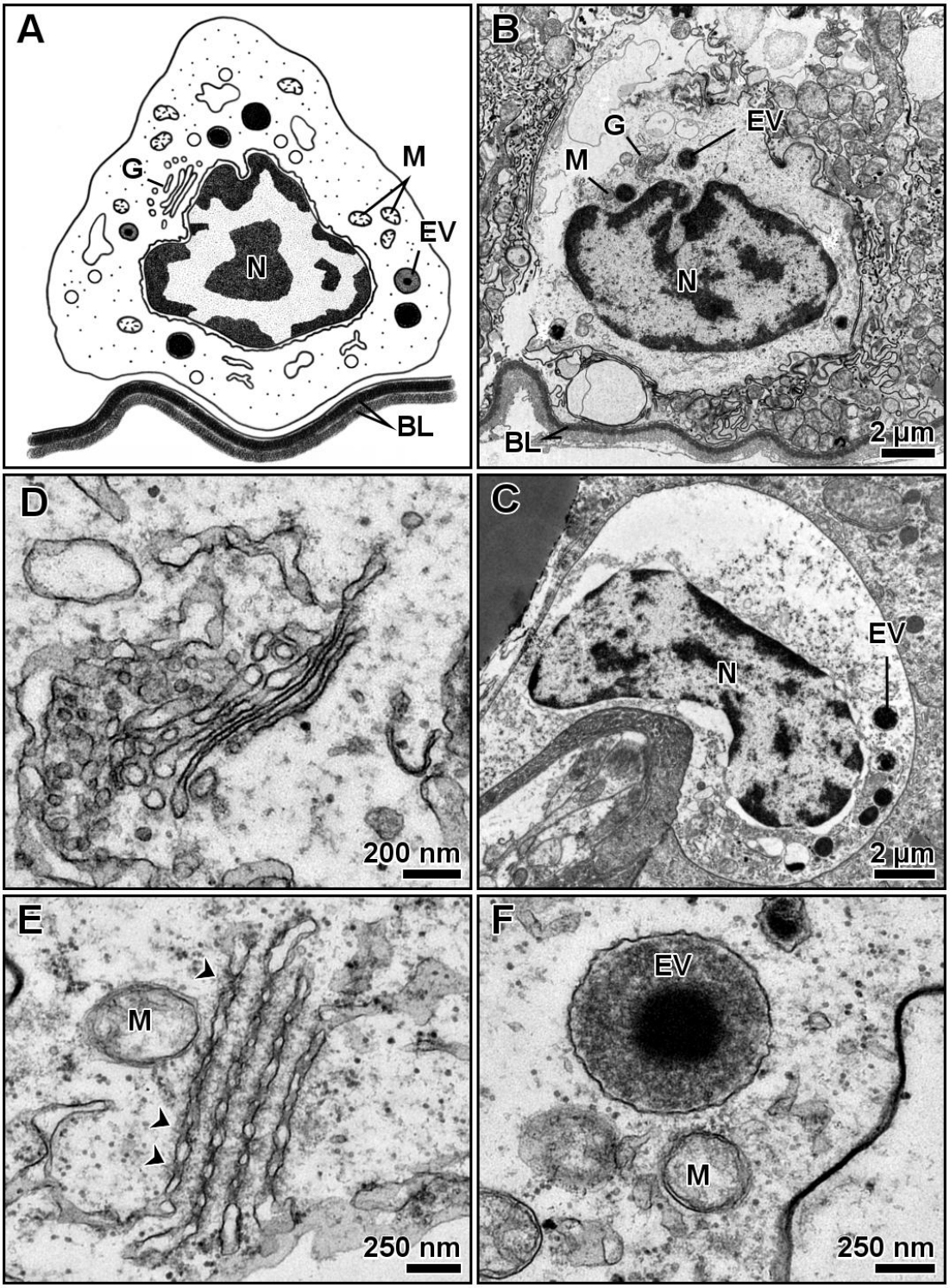

Figure 10. *Maja brachydactyla*. Midgut gland. Ultrastructure of the M - cells. General diagram (A). General view of the M-cells (B-C): adult (B) and megalopa, 10 days after hatching (C). Close view of a Golgi body (D). Close view of the annulate lamellae (E). Close view of a electron-dense vesicle (F). Abbreviations: BL: basal lamina; EV: electron-dense vesicles; G: Golgi bodies; M: mitochondria; N: nucleus.

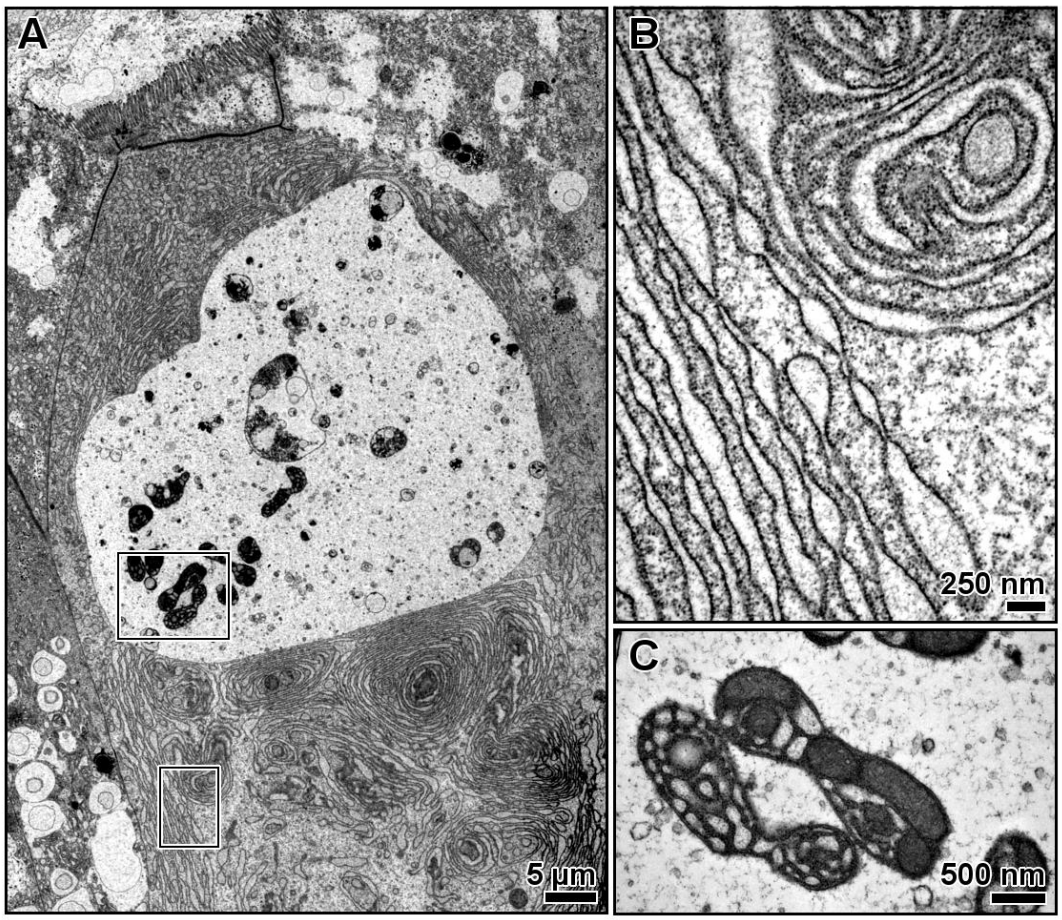

Figure 11. *Maja brachydactyla*. Adult. Midgut gland. Ultrastructure of an F-cell with features of B-cell (A-C): general view (A), close view of the rough endoplasmic reticulum (B), and detailed view of the giant central vacuole content (C).

6. References.

Abrunhosa, F.A., Kittaka, J., 1997. Morphological changes in the midgut, midgut gland and hindgut during the larval and postlarval development of the red king crab *Paralithodes camtschaticus*. Fisheries Science 63, 746-754.

Al-Mohanna, S.Y., Nott, J.A., 1986. B-cells and digestion in the hepatopancreas of *Penaeus semisulcatus* (Crustacea: Decapoda). Journal of the Marine Biological Association of the United Kingdom 66, 403-414.

Al-Mohanna, S.Y., Nott, J.A., 1987. R-cells and the digestive cycle in *Penaeus semisulcatus* (Crustacea: Decapoda). Marine Biology 95, 129-137.

Al-Mohanna, S.Y., Nott, J.A., 1989. Functional cytology of the hepatopancreas of *Penaeus semisulcatus* (Crustacea: Decapoda) during the moult cycle. Marine Biology 101, 535-544.

Al-Mohanna, S.Y., Nott, J.A., Lane, D.J.W., 1985a. M-'Midget' cells in the hepatopancreas of the shrimp, *Penaeus semisulcatus* De Hann, 1844 (Decapoda, Natantia). Crustaceana 48, 260-268.

Al-Mohanna, S.Y., Nott, J.A., Lane, D.J.W., 1985b. Mitotic E- and secretory F-cells in the hepatopancreas of the shrimp *Penaeus semisulcatus* (Crustacea: Decapoda). Journal of the Marine Biological Association of the United Kingdom 65, 901-910.

Andrés, M., Estévez, A., Hontoria, F., Rotllant, G., 2010a. Differential utilization of biochemical components during larval development of the spider crab *Maja brachydactyla* (Decapoda: Majidae). Marine Biology 157, 2329-2340.

Andrés, M., Gisbert, E., Díaz, M., Moyano, F.J., Estévez, A., Rotllant, G., 2010b. Ontogenetic changes in digestive enzymatic capacities of the spider crab, *Maja brachydactyla* (Decapoda: Majidae). Journal of Experimental Marine Biology and Ecology 389, 75-84.

Anger, K., Storch, V., Anger, V., Capuzzo, J.M., 1985. Effects of starvation on moult cycle and hepatopancreas of stage I lobster (*Homarus americanus*) larvae. Helgoländer Meeresuntersuchungen 39, 107-116.

Barker, P.L., Gibson, R., 1977. Observations on the feeding mechanism, structure of the gut, and digestive physiology of the european lobster *Homarus gammarus* (L.) (Decapoda: Nephropidae). Journal of Experimental Marine Biology and Ecology 26, 297-324.

Barker, P.L., Gibson, R., 1978. Observations on the structure of the mouthparts, histology of the alimentary tract, and digestive physiology of the mud crab *Scylla serrata* (Forskål) (Decapoda: Portunidae). Journal of Experimental Marine Biology and Ecology 32, 177-196.

Bianchini, A., Monserrat, J.M., 2007. Effects of methyl parathion on *Chasmagnathus granulatus* hepatopancreas: Protective role of Sesamol. Ecotoxicology and Environmental Safety 67, 100-108.

Biesiot, P.M., McDowell, J.E., 1995. Midgut-gland development during early life-history of the American Lobster *Homarus americanus*. Journal of Crustacean Biology 15, 679-685.

Bolognesi, R., Ribeiro, A.F., Terra, W.R., Ferreira, C., 2001. The peritrophic membrane of *Spodoptera frugiperda*: Secretion of peritrophins and role in immobilization and recycling digestive enzymes. Archives of Insect Biochemistry and Physiology 47, 62-75.

Bunt, A.H., 1968. An ultrastructural study of the hepatopancreas of *Procambarus clarkii* (Girard) (Decapoda, Astacidea). Crustaceana 15, 282-288.

Caceci, T., Neck, K.F., Lewis, D.D.H., Sis, R.F., 1988. Ultrastructure of the hepatopancreas of the Pacific white shrimp, *Penaeus vannamei* (Crustacea: Decapoda). Journal of the Marine Biological Association of the United Kingdom 68, 323-337.

Ceccaldi, H.J., 1989. Anatomy and physiology of digestive tract of Crustaceans Decapods reared in aquaculture, Advances in Tropical Aquaculture, Workshop at Tahiti, French Polynesia. Actes de colloques Ifremer, Tahiti, French Polynesia, pp. 243-259.

Cervellione, F., McGurk, C., Silva, P., Owen, M.A.G., Van den Broeck, W., 2017a. Optimization of fixation methods for image analysis of the hepatopancreas in whiteleg shrimp, *Penaeus vannamei* (Boone). Journal of Fish Diseases 40, 517-527.

Cervellione, F., McGurk, C., Van den Broeck, W., 2017b. “Perigastric organ”: a replacement name for the “hepatopancreas” of Decapoda. Journal of Crustacean Biology 37, 353-355.

Collins, P., 2010. Environmental stress upon hepatopancreatic cells of freshwater prawns (Decapoda: Caridea) from the floodplain of Paraná River. Natural Science 2, 748-759.

Correia, A.D., Pereira, A.L., Costa, M.H., Carrapiço, F., 2002. Functional anatomy of the midgut gland of *Gammarus locusta* (Crustacea: Amphipoda). Journal of the Marine Biological Association of the United Kingdom 82, 201-204.

Cuartas, E., Petriella, A.M., 2002. Cytoarchitecture of the hepatopancreas of three species of crabs from Mar Chiquita Lagoon, Argentina, In: Escobar-Briones, E., Alvarez, F. (Eds.), Modern Approaches to the Study of Crustacea. Springer US, Boston, MA, pp. 39-44.

Cuartas, E.I., Díaz, A.C., Petriella, A.M., 2002. Estudio morfológico e histológico del hepatopáncreas del langostino *Pleoticus muelleri* (Bate) (Crustacea, Penaeoidea). Revista de Investigación y Desarrollo Pesquero 15, 5-13.

Dall, W., 1967. The functional anatomy of the digestive tract of a shrimp *Metapenaeus bennettae* Racek & Dall (Crustacea : Decapoda : Penaeidae). Australian Journal of Zoology 15, 699-714.

Davolos, D., L., P., Accordi, F., De Matthaeis, E., 2010. Morphology and histology of the mouthparts and gut system of *Macarorchestia remyi* (Schellenberg, 1950) (Amphipoda, Talitridae). Zoologia Baetica 21, 151-178.

Erri Babu, D., Shyamasundari, K., Rao, K.H., 1982. Studies on the digestive system of the crab *Menippe rumphii* (Fabricius) (Crustacea:Brachyura). Journal of Experimental Marine Biology and Ecology 58, 175-191.

Factor, J.R., 1995. The Digestive System, In: Factor, J.R. (Ed.), Biology of the Lobster *Homarus americanus*. Academic Press, pp. 395-440.

Felgenhauer, B.E., 1992. Chapter 3. Internal Anatomy of the Decapoda: An Overview, In: Harrison, F.W., Humes, A.G. (Eds.), Microscopic Anatomy of Invertebrates. Volume 10: Decapod Crustacea. Wiley-Liss, Inc., pp. 45-75.

Franceschini-Vicentini, I.B., Ribeiro, K., Papa, L.P., Marques Junior, J., Vicentini, C.A., Valenti, P.M.C.M., 2009. Histoarchitectural features of the hepatopancreas of the Amazon River Prawn *Macrobrachium amazonicum*. International Journal of Morphology 27, 121-128.

Friesen, J.A., Mann, K.H., Willison, J.H.M., 1986. Gross anatomy and fine structure of the gut of the marine mysid shrimp *Mysis stenolepis* Smith. Canadian Journal of Zoology 64, 431-441.

Gibson, R., Barker, P.L., 1979. The Decapod Hepatopancreas. Oceanography and Marine Biology - An Annual Review 17, 285-346.

Guerao, G., Simeó, C.G., Anger, K., Urzúa, Á., Rotllant, G., 2012. Nutritional vulnerability of early zoea larvae of the crab *Maja brachydactyla* (Brachyura, Majidae). Aquatic Biology 16, 253-264.

Hopkin, S.P., Martin, M.H., 1982. The distribution of zinc, cadmium, lead and copper within the hepatopancreas of a woodlouse. Tissue and Cell 14, 703-715.

Hopkin, S.P., Nott, J.A., 1979. Some observations on concentrically structured, intracellular granules in the hepatopancreas of the shore crab *Carcinus maenas* (L.). Journal of the Marine Biological Association of the United Kingdom 59, 867-877.

Hopkin, S.P., Nott, J.A., 1980. Studies on the digestive cycle of the shore crab *Carcinus maenas* (L.) with special reference to the b cells in the hepatopancreas. Journal of the Marine Biological Association of the United Kingdom 60, 891-907.

Hu, K.-J., Leung, P.-C., 2007. Food digestion by cathepsin L and digestion-related rapid cell differentiation in shrimp hepatopancreas. Comparative Biochemistry and Physiology Part B: Biochemistry and Molecular Biology 146, 69-80.

Huxley, T.H., 1880. The Crayfish; an Introduction to the Study of Zoology. New York: D. Appleton and Company.

Icely, J.D., Nott, J.A., 1992. Digestion and absorption: digestive system and associated organs, In: Harrison, F.W., Humes, A.G. (Eds.), Microscopic anatomy of invertebrates: decapod Crustacea. Wiley-Liss, New York, pp. 147-201.

Jantrarotai, P.N., Sawanyatiputi, S.A., 2005. Histological study on the development of digestive system in zoeal stages of mud crab (*Scylla olivacea*). Kasetsart Journal 39, 666-671.

Johnston, M.D., 2006. Feeding and digestion in the phyllosoma larvae of Ornate Spiny Lobster, *Panulirus ornatus* (Fabricius) and the implications for their culture, Zoology. The University of Western Australia, p. 146.

Komuro, T., Yamamoto, T., 1968. Fine structure of the epithelium of the gut in the crayfish (*Procambarus clarkii*) with special reference to the cytoplasmic microtutubles. Archivum histologicum japonicum 30, 17-32.

Kusche, K., Burmester, T., 2001. Molecular cloning and evolution of lobster hemocyanin. Biochemical and Biophysical Research Communications 282, 887-892.

Li, F., Li, S., 1998. Studies on the hepatopancreas of larval *Scylla serrata*. Oceanologia Et Limnologia Sinica 29, 29-34.

Li, N., Zhao, Y., Yang, J., 2006. Impact of waterborne copper on the structure of gills and hepatopancreas and its impact on the content of metallothionein in juvenile Giant Freshwater Prawn *Macrobrachium rosenbergii* (Crustacea: Decapoda). Archives of Environmental Contamination and Toxicology 52, 73.

Liu, D., Yang, J., Wang, L., 2013. Cadmium induces ultrastructural changes in the hepatopancreas of the freshwater crab *Sinopotamon henanense*. Micron 47, 24-32.

Loizzi, R.F., 1971. Interpretation of crayfish hepatopancreatic function based on fine structural analysis of epithelial cell lines and muscle network. Zeitschrift für Zellforschung und Mikroskopische Anatomie 113, 420-440.

Longo, M.V., Díaz, A.O., 2015. Histological and histochemical study of the hepatopancreas of two estuarine crab species, *Cyrtograpsus angulatus* and *Neohelice granulata* (Grapsoidea, Varunidae): influence of environmental salinity. Zoological Science 32, 163-170.

Marcolin, C.d.R., Carqueija, C.R.G., Tozetto, S.d.O., Oliveira, D.C.d., Côrrea, A.M.A., 2008. Alterações morfológicas do hepatopâncreas de *Ucides cordatus* (Linnaeus, 1763) (Crustacea, Decapoda, Ocypodidae) em relação aos estádios de intermuda e pré-muda inicial. Zoociências 10, 97-104.

Mikami, S., Greenwood, J.G., Takashima, F., 1994. Functional morphology and cytology of the phyllosomal digestive system of *Ibacus ciliatus* and *Panulirus japonicus* (Decapoda, Scyllaridae and Palinuridae). Crustaceana 67, 212-225.

Milne-Edwards, H., 1834. Histoire naturelle des crustacés: atlas. Libraire Encyclopédique de Roret.

Nakamura, K., 1990. Organogenesis during metamorphosis in the swimming crab *Portunus trituberculatus*. Nippon Suisan Gakkaishi 56, 1561-1564.

Nishida, S., Takahashi, Y., Kittaka, J., 1995. Structural changes in the hepatopancreas of the rock lobster, *Jasus edwardsii* (Crustacea: Palinuridae) during development from the puerulus to post-puerulus. Marine Biology 123, 837-844.

Nunes, E.T., Braga, A.A., Camargo-Mathias, M.I., 2014. Histochemical study of the hepatopancreas in adult females of the pink-shrimp *Farfantepenaeus brasiliensis* Latreille, 1817. Acta Histochemica 116, 243-251.

Papathanassiou, E., King, P.E., 1984. Effects of starvation on the fine structure of the hepatopancreas in the common prawn *Palaemon serratus* (pennant). Comparative Biochemistry and Physiology Part A: Physiology 77, 243-249.

Paquet, F., Germain, P., Fritsch, P., 1993. Étude ultra-structurale de la glande digestive du homard *Homarus gammarus*. Rôle des divers types cellulaires dans les processus digestifs. Cahiers de Biologie Marine 35, 15-37.

Pillai, R.S., 1960. Studies on the shrimp *Caridina laevis* (Heller) 1. The Digestive System. Journal of the Marine Biological Association of India 2, 57-74.

Pugh, J.E., 1962. A contribution toward a knowledge of the hind-gut of fiddler crabs (Decapoda, Grapsidae). Transactions of the American Microscopical Society 81, 309-320.

Ramadevi, K.R.L.S., Shyamasundari, K., Hanumantha Rao, K., 1990. Observation of the hepatopancreas of *Ocypoda platytarsis* (Milne-Edwards) (Crustacea, Brachyura). Bolletino di zoologia 57, 261-265.

Reddy, A.R., 1937. The physiology of digestion and absorption in the crab *Paratelphusa* (*Oziotelphusa*) *hydrodromus* (Herbst). Proceedings of the Indian Academy of Sciences - Section B 6, 170-193.

Reddy, A.R., 1938. The cytology of digestion and absorption in the crab *Paratelphusa* (*Oziotelphusa*) *hydrodromus* (Herbst). Proceedings of the Indian Academy of Sciences - Section B 8, 171-181.

Ribeiro, K., Papa, L.P., Vicentini, C.A., Franceschini-Vicentini, I.B., 2016. The ultrastructural evaluation of digestive cells in the hepatopancreas of the Amazon River prawn, *Macrobrachium amazonicum*. Aquaculture Research 47, 1251-1259.

Rőszer, T., 2014. The invertebrate midintestinal gland ("hepatopancreas") is an evolutionary forerunner in the integration of immunity and metabolism. Cell and Tissue Research 358, 685-695.

Rotllant, G., Moyano, F.J., Andrés, M., Díaz, M., Estévez, A., Gisbert, E., 2008. Evaluation of fluorogenic substrates in the assessment of digestive enzymes in a decapod crustacean *Maja brachydactyla* larvae. Aquaculture 282, 90-96.

Rotllant, G., Moyano, F.J., Andrés, M., Estévez, A., Díaz, M., Gisbert, E., 2010. Effect of delayed first feeding on larval performance of the spider crab *Maja brachydactyla* assessed by digestive enzyme activities and biometric parameters. Marine Biology 157, 2215-2227.

Sánchez-Paz, A., García-Carreño, F., Hernández-López, J., Muhlia-Almazán, A., Yepiz-Plascencia, G., 2007. Effect of short-term starvation on hepatopancreas and plasma energy reserves of the Pacific white shrimp (*Litopenaeus vannamei*). Journal of Experimental Marine Biology and Ecology 340, 184-193.

Schlegel, C., 1911. Anatomie sommaire de la première zoé de *Maja squinado* Latr. (Note préliminaire à des recherches sur l'Organogénese des Décapodes brachyoures). Archives de Zoologie Experimentale et Générale 5º Série T. VIII., 29-40.

Schmitz, E.H., Scherrey, P.M., 1983. Digestive anatomy *Hyalella azteca* (Crustacea, Amphipoda). Journal of Morphology 175, 91-100.

Schmitz, E.H., Schultz, T.W., 1969. Digestive anatomy of terrestrial isopoda: *Armadillidium vulgare* and *Armadillidium nasatum*. The American Midland Naturalist 82, 163-181.

Schultz, T.W., 1976. The ultrastructure of the hepatopancreatic caeca of *Gammarus minus* (crustacea, amphipoda). Journal of Morphology 149, 383-399.

Sellos, D., Lemoine, S., Van Wormhoudt, A., 1997. Molecular cloning of hemocyanin cDNA from *Penaeus vannamei* (Crustacea, Decapoda): structure, evolution and physiological aspects 1. FEBS Letters 407, 153-158.

Silva, W., Cardoso, C., Ribeiro, A.F., Terra, W.R., Ferreira, C., 2013. Midgut proteins released by microapocrine secretion in *Spodoptera frugiperda*. Journal of Insect Physiology 59, 70-80.

Sonakowska, L., Włodarczyk, A., Poprawa, I., Binkowski, M., Śróbka, J., Kamińska, K., Kszuk-Jendrysik, M., Chajec, Ł., Zajusz, B., Rost-Roszkowska, M.M., 2015. Structure and Ultrastructure of the endodermal region of the alimentary tract in the freshwater shrimp *Neocaridina heteropoda* (Crustacea, Malacostraca). PLoS ONE 10, e0126900.

Sousa, L.G., Cuartas, E.I., Petriella, A.M., 2005. Fine structural analysis of the epithelial cells in the hepatopancreas of *Palaemonetes argentinus* (Crustacea, Decapoda, Caridea) in intermoult. Biocell 29, 25-31.

Sousa, L.G., Petriella, A.M., 2007. Functional morphology of the hepatopancreas of *Palaemonetes argentinus* (Crustacea: decapoda) : Influence of environmental pollution. Revista de biología tropical 55, 79-85, SUP71.

Stanier, J.E., Woodhouse, M.A., Griffin, R.L., 1968. The Fine Structure of the Hepatopancreas of *Carcinus maenas* (L.) (Decapoda Brachyura). Crustaceana 14, 56-66.

Storch, V., Anger, K., 1983. Influence of starvation and feeding on the hepatopancreas of larval *Hyas araneus* (Decapoda, Majidae). Helgoländer Meeresuntersuchungen 36, 67-75.

Trask, T., 1974. Laboratory-reared larvae of *Cancer anthonyi* (Decapoda: Brachyura) with a brief description of the internal anatomy of the megalopa. Marine Biology 27, 63-74.

Travis, O.F., 1955. The molting cycle of the spiny lobster, *Panulirus argus* Latreille. II. Pre-ecdysial histological and histochemical changes in the hepatopancreas and integumental tissues. The Biological Bulletin 108, 88-112.

Tziouveli, V., Bastos-Gomez, G., Bellwood, O., 2011. Functional morphology of mouthparts and digestive system during larval development of the cleaner shrimp *Lysmata amboinensis* (de Man, 1888). Journal of Morphology 272, 1080-1091.

Van Weel, P.B., 1974. Hepatopancreas? Comparative Biochemistry and Physiology Part A: Physiology 47, 1-9.

Vogt, G., 1994. Life-cycle and functional cytology of the hepatopancreatic cells of *Astacus astacus* (Crustacea, Decapoda). Zoomorphology 114, 83-101.

Vogt, G., 1996. Morphology and physiology of digestive epithelia in Decapod crustaceans. Pflügers Archiv 431, R239-R240.

Williams, R.L., 1944. The pre-zoea stage of *Porcellana platycheles* (Pennant). Preliminary anatomical and histological notes. Journal of the Royal Microscopical Society 64, 1-15.

Yonge, C.M., 1924. Studies on the comparative physiology of digestion II. - The mechanism of feeding, digestion, and assimilation in *Nephrops norvegicus*. British Journal of Experimental Biology 1, 343-389.

Zeng, H., Ye, H., Li, S., Wang, G., Huang, J., 2010. Hepatopancreas cell cultures from mud crab, *Scylla paramamosain*. In Vitro Cellular & Developmental Biology - Animal 46, 431-437.

Zhang, H., Zhong, S., Fan, Q., Yu, P., Ge, T., Peng, S., Zhou, Z., Guo, X., 2017. The epithelial cytotypes of hepatopancreas in the Chinese mitten crab (Decapoda, Varunidae). Crustaceana 90, 253-262.

Zilli, L., Schiavone, R., Scordella, G., Zonno, V., Verri, T., Storelli, C., Vilella, S., 2003. Changes in cell type composition and enzymatic activities in the hepatopancreas of *Marsupenaeus japonicus* during the moulting cycle. Journal of Comparative Physiology B 173, 355-363.

Ņnidarńič, N., Ńtrus, J., Drobne, D., 2003. Ultrastructural alterations of the hepatopancreas in *Porcellio scaber* under stress. Environmental Toxicology and Pharmacology 13, 161-174.

CHAPTER 16.

Morphology and ontogeny of the midgut tract in the spider crab *Maja brachydactyla* (Brachyura, Majidae)

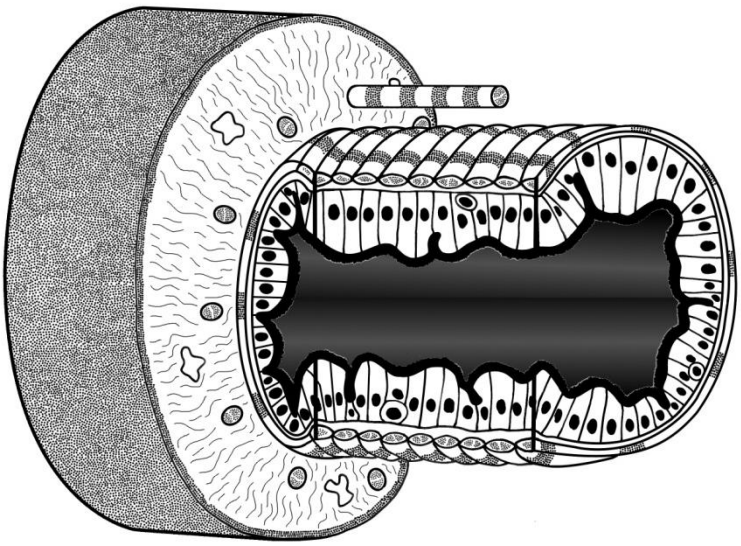

Morphology and ontogeny of the midgut tract in the spider crab *Maja brachydactyla* (Brachyura, Majidae).

Diego Castejón[1*], Guiomar Rotllant[2], Enric Ribes[3], Mercè Durfort[3], and Guillermo Guerao[4]

[1] IRTA, Centre d'Aqüicultura, Ctra. del Poble Nou Km 5.5. 43540 Sant Carles de la Ràpita, Tarragona (Spain).

[2] CSIC, Institut de Ciències del Mar, Passeig Marítim de la Barceloneta 37-49. 08003 Barcelona (Spain).

[3] Unitat de Biologia Cel·lular, Departament de Biologia Cel·lular, Fisiologia i Immunologia, Facultat de Biologia, Universitat de Barcelona, Diagonal 645. 08028 Barcelona (Spain).

[4] PS Fabra i Puig 344. 08028 Barcelona (Spain).

Short title: *Maja brachydactyla* midgut tract morphology & ontogeny

***Corresponding author:** Diego Castejón. E-mail: diego.castejon.dcb@gmail.com; phone: +34 681 154 398; postal address: IRTA, Subprogram Cultius Aqüàtics, Ctra. Poble Nou, Km 5.5. 43540 Sant Carles de la Ràpita, Tarragona(Spain).

Abstract.

The present study is focused on the morphology and ontogeny of the midgut tract in the brachyuran *Maja brachydactyla* Balss, 1922. The midgut tract has been studied from newly hatched zoeae to first juvenile, and the adult stage. The methodology includes: the morphometric study by stereomicroscopy, the histological study by optical microscopy, and the ultrastructural study by transmission and scanning electron microscopy. The midgut tract is a short tube anteriorly connected with the stomach, the midgut gland and a pair of anterior caeca; while posteriorly it is connected to the hindgut tract and a single posterior caecum. The junction between midgut and hindgut is also described. During the larval development, the midgut tract only changes significantly in length, while changes in diameter or morphology were not observed. In all the stages it is lined by a simple columnar epithelium with microvillous borders and basal cells. In adults, beneath the basal lamina appears a wide layer of connective surrounding a thin continuous layer of circular muscles and a discontinuous layer of longitudinal muscles. During the larval stages the musculature and connective are poorly developed. The epithelial cells have a polarized organization: the cell apex contains a band of mitochondria and numerous electron-dense secretory vesicles; while the cell basis contains a basal layer of mitochondria and smooth endoplasmic reticulum which tubules can fuse with the basal membrane. The epithelial cells can contain lipid droplets. The peritrophic membrane was observed from hatching and its possible association with the secretory vesicles of the midgut tract epithelium is discussed.

Keywords: Crustacea; larval development; secretion; peritrophic membrane; midgut-hindgut junction; epithelium

1. Introduction

The midgut of the Malacostraca derives from the embryonary endoderm, considered as a whole, the midgut includes the midgut tract itself, one or more associated additional caeca and the midgut gland, usually termed "hepatopancreas" (Ceccaldi, 1989; Factor, 1995; Felgenhauer, 1992; Gibson and Barker, 1979; Icely and Nott, 1992). The midgut tract of the decapods is anteriorly connected to the stomach, the main ducts of the midgut gland and one or more blind end tubules termed "caeca" or "diverticula"; while posteriorly it is connected to the hindgut by a valve-like structure denominated "midgut-hindgut junction" and one or more blind end tubules or caeca protruding from the midgut portion (Erri Babu et al., 1982; Factor, 1995; Felgenhauer, 1992; Hopkin and Nott, 1980; Icely and Nott, 1992; Smith, 1978). The midgut tract is specialized on the synthesis of the peritrophic membrane: an extracellular sheet-like matrix composed by numerous chitinous membranes wrapped around the ingested matter (Georgi, 1969; Holliday et al., 1980; Martin et al., 2006). The midgut tract is also involved on the transport of the alimentary bolus (Ceccaldi, 1989; Felgenhauer, 1992; Gibson and Barker, 1979; Icely and Nott, 1992). Other authors also suggested a role related with the nutrient absorption (Talbot et al., 1972).

The knowledge of the morphology and role of the midgut tract during the larval development is useful to differentiate between non-feeding and feeding stages (Lovett and Felder, 1989; Nakamura and Seki, 1990), as well to differentiate between healthy and sick states in histopathological studies (Kaushik and Kumar, 1998; Martin et al., 2004). By similar reasons, the knowledge of the digestive system morphology is mandatory to develop commercial diets since their composition can alter the

histological structure of the digestive system into healthy or unhealthy traits (Bonaldo et al., 2006; Fontagné et al., 1998; Øverland et al., 2009).

Despite its importance, morphology and ultrastructure of the midgut tract of the malacostracans is still poorly known. This situation is even more noticeable in the case of the larval stages. Hence, the objective of this study is the description of the midgut tract during the larval development and adult stage employing stereo, optical and electron microscopy. The role of the midgut tract during the larval stages is also discussed.

The species selected for this purpose was the common spider crab *Maja brachydactyla* Balss, 1922. It is a marine brachyuran widely distributed from the Açores to the Sahara and SW Mediterranean Sea (Abelló et al., 2014) and a valuable species in various European countries (FAO, 2014). It is somewhat considered as a potential aquaculture species, since the female fecundity is high, between 100,000 and 500,000 eggs per female (Rotllant et al., 2015; Verísimo et al., 2011); and the larval development is abbreviated, being completed in approximately two weeks at 21 °C (Castejón et al., 2015a). Various studies have been focused on its larval development, including the larval growth patterns and molting cycles (Andrés et al., 2008; Guerao et al., 2010), the external morphology (including mouthparts) of the larval stages (Guerao et al., 2008), the ontogeny and morphology of the foregut (Castejón et al., 2015b) and the ontogenetic changes occurred on the digestive enzymatic capacities during the larval development (Andrés et al., 2010; Rotllant et al., 2010).

2. Material and methods

2.1 Culture system

The adult specimens of *M. brachydactyla* were acquired from fisheries located on the Northwest Iberian Peninsula and Ireland coasts. The specimens were transported to the Institut de Recerca i Tecnologia Agroalimentàries (IRTA) facilities, located on the Ebro Delta (Sant Carles de la Ràpita, Tarragona, Spain), in polystyrene boxes covered by seawater-soaked rags in cooler conditions to maintain the humidity and improve the survival. The adult specimens were dissected or kept in 2,000 L cylindrical tanks connected to a recirculation unit (renewal rate = 3.5 m^3 h^{-1}) to establish a broodstock, whose rearing conditions were: 18 ± 1 °C, 35 ± 1 psu, photoperiod of 12 h light: 12 h dark provided by fluorescent tubes at 25 lux. The diet consisted on of fresh and frozen mussels (*Mytilus* sp.).

The larvae hatched on the broodstock tanks were transferred to a modified version of a culture system designed for the larval culture at small and laboratory scale (Castejón et al., 2015a). The larval culture system consisted on 600 mL glass beakers placed inside 360 L tanks (96 x 96 x 40 cm). The culture conditions were: 18 ± 1 °C, 35 ± 1 psu, photoperiod of 12 h light: 12 h dark provided by LED lights tubes at 1000 lux. The diet was based on fresh *Artemia* sp. Kellogg, 1906 nauplii and metanauplii (INVE Aquaculture Nutrition, Salt Lake UT, USA). The living specimens were carefully transferred each day to glass beakers with clean water and fresh food. The larvae reached the zoea II stage in 3-4 days, the megalopa stage in the 6-7 days and metamorphosed to first juvenile in 11-13 days. The larvae and juvenile were sampled daily for further processes.

2.2 Stereomicroscopy

Entire larvae and first juvenile specimens were fixed in formaldehyde 4 % and dissected under a Nikon SMZ800 stereomicroscope (Nikon Instruments Inc., Melville, NY, U.S.A.) using teasing needles. The total length and diameter of 4-6 organs per life day, including 2 organs of newly molted juveniles were measured using image analysis software (AnalySIS, SIS, Münster, Germany) properly calibrated. The midgut length and diameter at the start of each larval stage were analyzed using R version 3.2.0 (R Development Core Team, 2015) performing One way ANOVA (total length and diameter as factors) analyses. The comparisons among groups (zoea I, zoea II, megalopa and first juvenile) after finding significant differences were performed by post-hoc Tukey-HSD test. Normality and homogeneity were tested by Shapiro-Wilk and Levene tests, respectively. The critical level (α) to reject the null hypothesis was 0.05.

2.3 Optical microscopy

The fixation was realized in entire larvae and first juvenile specimens, as well longitudinal and transversal sections of the adult organ, employing Davidson's fixative (ethanol absolute: seawater: formaldehyde 37 %: glycine: glacial acetic acid in proportion 3: 3: 2: 1: 1) during 24 h. The samples were dehydrated and embedded with paraffin using an automatic tissue processor (Myr, Spain), and the paraffin blocks were realized using a paraffin processor (Myr, Spain). The paraffin blocks were cut in 2 µm sections employing a Leica RM2155 microtome (Leica, Wetzlar, Germany). The stains used were: Hematoxylin & Eosin stain (H–E), to show the general morphology of the tissues; Periodic Acid–Schiff (PAS) contrasted with Methylene Blue, to reveal the presence of polysaccharides and mucopolysaccharides; Periodic acid–Schiff (PAS) combined with Alcian Blue (pH 2.5) and contrasted with Hematoxylin, to reveal the

presence of acid mucopolysaccharides; Mallory's trichrome stain (Acid Fuchsine, Orange G and Aniline Blue stains), to reveal the structure of the muscular and connective tissues. The observations were realized in a Leica LB30T 111/97 optical microscope (Leica, Wetzlar, Germany) connected to a camera (Olympus DP70 1.45 Mpx; Olympus Corporation, Germany) and an image analysis software (DP Controller 2.1.1.83 and DP Manager 2.1.1.163; Olympus Corporation, Germany).

2.4 Electron microscopy

The ultrastructure was studied using entire larvae and first juvenile specimens, as well small portions of the organ in adult specimens. The fixation required a bath in a solution of 2 % paraformaldehyde and 2.5 % glutaraldehyde in cacodylate buffer (0.1 mol L^{-1} pH 7.4) during ca. 12 h at 4 °C and constant darkness. The post-fixation used 1 % osmium tetroxide solution in cacodylate buffer (0.1 mol L^{-1} pH 7.4). The samples were dehydrated in a graded series of acetone. For scanning electron microscopy, post-fixed samples were critical-point-dried, mounted on SEM stubs with self-adhesive carbon stickers and covered by carbon coating. Observations were made with a JEOL JSM-7001F scanning electron microscope (15 kV). For transmission electron microscopy, samples were embedded in Spurr's resin. The ultra-thin sections were obtained using a Leica UCT ultramicrotome (Leica, Wetzlar, Germany) and counterstained with uranyl acetate and lead citrate. Observations were made with a Jeol EM-1010 transmission electron microscope (tungsten filament, 80 kV). The treatment realized after the post-fixation in osmium tetroxide and the TEM and SEM observations were realized at CCiTUB (Hospital Clinic, University of Barcelona, Barcelona).

3. Results

Gross morphology. The midgut tract of *M. brachydactyla* is a short cylindrical tube (Figs. 1A-D; 2A-D), located dorso-anteriorly in the cephalothoracic cavity (Fig. 1A). The anterior extreme is connected forwardly with the stomach, ventrally to the midgut gland (also called "hepatopancreas") and dorsally with a pair of anterior midgut caeca that are projected toward the stomach walls (Figs. 1A-D; 2A-D). The posterior extreme of the midgut tract is connected backwardly with the hindgut tract through the "midgut-hindgut junction" and dorsally with a single and unpaired posterior caecum (Figs. 1A-D; 2A-D). The length of the midgut tract increases significantly from hatching (302 ± 41 µm) to the metamorphosis to first juvenile (466 ± 86 µm) (ANOVA, $F_{3,13} = 10.88$ $p < 0.001$; Fig. 2A-E), maintaining a logarithmic growth trend (Fig. 2F). By contrast, the midgut tract diameter does not changed significantly from the newly hatched zoea (158 ± 11 µm) to the first juvenile (169 ± 12 µm) (ANOVA, $F_{3,13} = 0.92$ $p = 0.46$). Consequently, the midgut tract shows an allometric growth, length: diameter ratio increased from 2.0 ± 0.3 at hatching to 2.7 ± 0.2 in the first juvenile (ANOVA, $F_{3,13} = 4.90$ $p < 0.05$). The adult midgut tract have ca. 23 ± 2 mm length and ca. 4-6 mm diameter.

The midgut tract is a cylindrical tube, in cross-section the external borders are circular but the luminal borders are undulated (Figs. 3A; 4C-D). The midgut tract is structured in different tissular layers which complexity increases during ontogeny (Figs. 3A-D; 4A-F). The basic structure comprises a simple columnar epithelium with a well-developed brush border and an underlying basal lamina (Fig. 3E-F), the epithelial cells are larger in the adult stage than during the larval and first juvenile stages (Fig. 4A-D). The epithelium has two cell types: main epithelial cells and basal cells (Figs. 3E; 4B-C).

In adults, the midgut tract epithelium detach from the basal lamina, then the separation between them is an artifact (Fig. 3B-D). Many detached epithelial cells are not apparently deformed and show the typical columnar shape and microvillous border observed in attached cells (Fig. 3B, E-F). The basal lamina is surrounded by a layer of connective tissue. This layer is extremely thin in the larval and first juvenile stages (Fig. 4A-F), but in adults it is extensive and surrounds bundles of different muscle fibers (Fig. 3A-D, F). The musculature is organized in inner circular muscles and outer longitudinal muscles fibers. The inner circular muscles are located adjacently to the basal lamina, surrounding the midgut tract as a thin and continuous layer; while the outer longitudinal muscles form a discontinuous layer located at short distance from the circular muscles (Fig. 3A, C, D, F). The musculature in larval stages is formed by an extremely thin layer only observable by electron microscopy. The midgut tract of the adult specimens contains abundant hemocytes extended from the basal lamina to beyond the outer layer of longitudinal muscles (Fig. 3C-D).

Epithelial cells. The main epithelial cells of the adults are tall columnar cells which height is superior to 50 µm (Fig. 3E-F), while in larvae and first juvenile they are cuboidal to short columnar with ca. 10-20 µm height (Fig. 4). The organization of the epithelial cells is polarized (Fig. 5A-C). The apical membrane forms numerous undulated, slender and long microvilli (Fig. 5B) whose tips can be covered by a semi-spherical electron-dense coat (Fig. 7A, C). The microvilli have similar or higher electron-density than the cell cytoplasm (Fig. 7B), the basis of each microvillus can show "root-like" filaments, but the presence of a "terminal web" is unclear (Fig. 5A-B; 7B). The lateral membranes are smooth, showing only slightly undulations but none interdigitation; the cell-to-cell junctions are elongated and arise from the cell apex to down to 4-5 µm (Figs. 5A-B; 7B). The cell basis is highly undulated and forms

numerous folds (Figs. 3C-D, F; 5C; 6B). Underlying the basal membrane, a basal lamina is present showing a high electron-dense outmost layer (Fig. 6B).

The cell apex shows a band which staining affinity remember to the peritrophic membrane (Fig. 4C-D). This apical band is observed by electron microscopy as a layer composed by numerous secretory vesicles whose diameter oscillates from 200 to 500 nm (Fig. 5B). The vesicle shape varies from rounded to ovoid or rod-like, while the content varies from homogeneous and highly electron-dense to heterogeneous and less electron-dense (Figs. 5B; 7B). The cytoplasm is rich in PAS positive granules (Fig. 3E). By electron microscopy, the cytoplasm appears generally lucent (Figs. 5-6), sporadically cells with highly electron-dense cytoplasm was observed. The cytoplasm contains some ribosomes, sparse small lucent vesicles and multi-vesicular bodies composed by numerous small and rounded vesicles surrounded by a membrane. The nucleus is usually ellipsoidal and located medial to basally (Figs. 3E-F; Fig. 4C-D). The euchromatin is scarce and attached to the nuclear membrane and nucleus center (Figs. 5C; 6B).

The mitochondria are generally rod shaped organelles (0.9 to 3 μm in length) generally concentrated beneath the apical band of secretory vesicles, some mitochondria appear in other cell sites, e.g. adjacently to the rough endoplasmic reticulum, below the nucleus and surrounded by smooth endoplasmic reticulum in the cell basis (Figs. 5B-C, E; 6B). The rough endoplasmic reticulum is composed by numerous, enlarged and mutually interconnected cisternae, mainly located above the nucleus (Fig. 5A-D). The smooth endoplasmic reticulum forms a band near to the cell basis, this band is composed by numerous branched tubules (some of them fused with the basal cell membrane) and mitochondria (Figs. 5A, C; 6B). The Golgi bodies are abundant and

distributed from the cell basis to the cell apex (Fig. 5B-C). The Golgi bodies combine stacks of thin and globular cisternae (Fig. 5F), but in the cells with electron-dense cytoplasm the Golgi bodies are more abundant and formed by globular and highly expanded cisternae. The cytoplasm of the epithelial cells occasionally contain lipid vacuoles which size is big as the cell diameter. The lipid vacuoles usually have a supranuclear location (Fig. 5A, C).

Basal cells. The basal cells are the less abundant cell type of the epithelium. They are small and rounded cells (4-6 μm diameter) located near to the basal lamina, due to their small size the basal cells never reach the midgut lumen (Figs. 3E; 4A-C). The basal cells were observed in all the life stages, from larvae within ca. 15 hours after hatching (Fig. 6B) to megalopa (Fig. 4C) and adult stage (Fig. 3E). The cell shape varies from rounded to ellipsoidal and they do not show polarity in their organization (Fig. 6A-B). The cytoplasm is lucent containing very low density of organelles: scarce ribosomes and sparse lucent and pleomorphic vesicles with variable size and shape (from rounded to highly irregular), whose content is amorphous and filamentous. The most characteristic feature is the presence of rounded vesicles filled by highly electron-dense and granular content. The nucleus is rounded, central and very big in comparison to the cell size. The euchromatin is located adjacently to the cell membranes and nucleus center, it can be as abundant as the heterochromatin. The mitochondria are scarce and small. None other cell organelle has been identified (Fig. 6A-B).

Peritrophic membrane. The peritrophic membrane has been identified in all the life stages, from ca. 15 hours after hatching to the adult stage (Figs. 3B; 4C-E; 7). It is an acellular and extracellular secretion that forms delicate and translucent sheets that wrap the ingested matter along their pass through the midgut and hindgut tract, as well

the fecal matter when excreted outside the body. The peritrophic membrane is composed by numerous membranous layers, it can be stained with PAS, Hematoxylin, Alcian Blue (pH 2.5) and Aniline Blue (Fig. 4B-E). The electron microscopy confirms the presence of secretory waves of peritrophic membrane from the apex of the epithelial cells (Fig. 7A). The presence of these waves coincides with the fusion of the apical electron-dense secretory vesicles with the apical membrane and the release of their content (Fig. 7B). The layer of peritrophic membrane located adjacently to the microvilli is thinner and more electron-dense than the layers separated from the microvilli (Fig. 7C). The scanning microscope reveals that the peritrophic membrane forms a reticulate pattern that resembles to a polygonal to hexagonal mesh (Fig. 7D).

Midgut-hindgut junction. The midgut-hindgut junction is the substitution of the midgut tract by the hindgut tract. This transition is observed in all the life stages (Figs. 1B-D; 2A-D). The midgut-hindgut junction of the immature stages is characterized by the invagination of the midgut and hindgut epithelium toward the basal lamina (Fig. 4B). The epithelium of the midgut tract is directly substituted by the hindgut tract epithelium and true transitional cells with mixed features between midgut and hindgut tracts were not observed (Fig. 8A-B). In this sense, the transition can be considered abrupt since each organ maintain its identity. Nevertheless, the epithelial cells of the midgut tract suffer some modifications toward the hindgut proximity: the gradual reduction of the cell height (especially noticeable in the pair of cells immediately adjacent to the hindgut), the gradual shrink of the microvilli height until their disappearance and the gradual drop of the density of apical electron-dense vesicles. The last epithelial cell of the midgut tract has the most divergent shape: it is not columnar but sub-triangular or trapezoidal, the electron-dense secretory vesicles are almost absent and the nucleus is very reduced in size (Fig. 8A-C). Similarly, the epithelial cells of the

hindgut tract also suffer some modifications with the proximity toward the midgut tract. The main features of the epithelial cells of the hindgut tract during the larval stages include: squamous shape, nucleus ellipsoidal and central, cell apex covered by a cuticle and cytoplasm lucent, rich in ribosomes but with sparse vesicles and rounded mitochondria. However, the epithelial cells immediately adjacent to the midgut tract are highly divergent: the cell shape is not squamous but varies from cuboidal to rounded, the cell nucleus is surrounded by a thin layer of cytoplasm, the density of organelles decreases and the cuticle become thinner toward the midgut proximity (Fig. 8A-C). In addition, the hindgut cuticle most adjacent to the midgut tract is extremely thin and lacks distinguishable layers (Fig. 8C).

4. Discussion

The French zoologist Henri Milne-Edwards (1834a; b) described the midgut tract ("*duodénium*") of the decapods as a smooth tube enclosed between the anterior stomach and the posterior hindgut ("*rectum*"). His anatomical description of the midgut tract in the genus *Maja* coincides to our study: a short tube anteriorly connected with the stomach, a pair of anterior caeca and the midgut gland; and posteriorly with the hindgut and a single posterior caecum. The same description has been reported in other brachyurans (Barker and Gibson, 1978; Erri Babu et al., 1982; Reddy, 1937; Trinadha Babu et al., 1989). The relative length of the midgut tract is highly variable among the malacostracans. In *M. brachydactyla* represents ca. 10 % of the digestive system length. In crayfishes as *Astacus astacus* and *Procambarus clarkii* the midgut tract is very short (Chisaka et al., 1999; Huxley, 1880), near to an order of magnitude shorter than the hindgut (Komuro and Yamamoto, 1968). By contrast, in other astacids as *Homarus gammarus* and *Nephrops norvegicus* the midgut tract is several times larger than the

hindgut tract and reach the sixth pleonite (Barker and Gibson, 1977; Factor, 1995; Hinton and Corey, 1979; Milne-Edwards, 1834a; b; Yonge, 1924), as occur in some penaeids (Dall, 1967; Martin and Chiu, 2003; Sousa and Petriella, 2006). The most extreme case is observed in certain terrestrial isopods that lacks the midgut tract: the digestive tract is originated by the fusion of the embryonary stomodeum and proctodeum (Goodrich, 1939; Ńtrus et al., 2008) and it is lined by a continuous cuticle from the foregut to the hindgut (Holdich, 1973; Holdich and Mayes, 1975; Ńtrus et al., 1995; Ńtrus et al., 2008).

The midgut tract of *M. brachydactyla* has the typical histological organization observed in the decapods (tall columnar epithelium with microvillous border and short basal cells, thick connective, inner circular muscles and outer longitudinal muscles), coinciding to studies realized in other brachyurans (Barker and Gibson, 1978; Erri Babu et al., 1982; Kaushik and Kumar, 1998; Reddy, 1937; Trinadha Babu et al., 1989), as well astacideans (Barker and Gibson, 1977; Komuro and Yamamoto, 1968; Yonge, 1924) and carideans, although in this later case the connective and muscle layers are proportionally thinner (Sonakowska et al., 2015). The simple columnar epithelium observed during the larval stages coincides with the observations realized by Schlegel (1911) in the first zoeal stage of *Maja* sp. By contrast, the midgut tract of the brachyuran *Pseudocarcinus gigas* is lined by a pseudostratified epithelium and non-striated muscles (Heeren and Mitchell, 1997), but this information was not confirmed by later studies. Another interesting feature of the midgut tract of *P. gigas* is the presence of hematopoietic cells (Heeren and Mitchell, 1997). Similarly, in the shrimps of the genus *Sicyonia* (Dendrobranchiata) is described a "hemocyte layer" located beneath the basal lamina and composed by granulocytes (Martin and Chiu, 2003). In *M.*

brachydactyla, the hemocyte layer has been identified in adults but not in larval specimens.

The absence of significant changes in the midgut tract (excepting in length) during the larval development has been reported in other brachyurans as *Scylla olivacea* (Jantrarotai and Sawanyatiputi, 2005), as well other decapods including achelatans (Mikami et al., 1994), carideans (Tziouveli et al., 2011) and penaeids after the protozoeal and mysis stage (Abubakr and Jones, 1992; Lovett and Felder, 1990; Muhammad et al., 2012; Talbot et al., 1972). The morphology and ultrastructure of the main epithelial cells of the midgut tract of *M. brachydactyla* during the larval stages is similar to the described in other decapods: brachyurans (Moon and Kim, 1999; Mykles, 1979), astacideans (Komuro and Yamamoto, 1968; Mykles, 1979) and penaeids (Abubakr and Jones, 1992; Lovett and Felder, 1990; Talbot et al., 1972). Few differences were pointed out for three species: the septum that separates the midgut and hindgut tract in the anomuran *Porcellana platycheles* pre-zoeae (Williams, 1944), the anterior yolk reserves described in the astacidean *Homarus gammarus* (Factor, 1981; Hinton and Corey, 1979), and the absence of secretory vesicles and reserve materials as glycogen or lipids in the caridean *Neocaridina heteropoda* (Sonakowska et al., 2015). Similar basal cells to the described in the present study were observed in the epithelium of the midgut tract of *Procambarus clarkii* (Komuro and Yamamoto, 1968) and *N. heteropoda* (Sonakowska et al., 2015). The role of the basal cells is unknown, but could be involved with processes of mitosis and differentiation for the regeneration of the organ. In fact, Sonakowska et al. (2015) mentioned mitotic activity in basal cells (referred as "regenerative cells").

The main role of the midgut tract epithelium is probably the secretion of the peritrophic membrane, an extracellular secretion widespread among the malacostracans (McLaughlin, 1983), including Amphipoda (Davolos et al., 2010), Astacidea (Factor, 1981; Georgi, 1969), Brachyura (Mets, 1962), Caridea (Forster, 1953) and Dendrobranchiata (Martin and Chiu, 2003; Martin et al., 2006; Wang et al., 2012). In Isopoda, the peritrophic membrane has been identified in taxa with midgut tract, e.g. *Dynamene bidentata* (Holdich and Ratcliffe, 1970), but it is absent in those taxa that lacks the midgut tract, e.g. *Armadillidium vulgare* (Vernon et al., 1974) and *Porcellio scaber* (Holdich and Mayes, 1975). The peritrophic membrane is produced by both starved and nourished animals, then its synthesis is independent of the feeding regime (Forster, 1953; Martin et al., 2006). In *M. brachydactyla* the peritrophic membrane is produced since hatching as previously observed in *H. americanus* (Factor, 1981). The peritrophic membrane is composed by translucent sheets folded into a tube that wrap completely the fecal matter. In *M. brachydactyla*, the surface of the peritrophic membrane forms a polygonal-like pattern, coinciding to observations realized in the brachyuran *Eriocherir sinensis* (Mets, 1962). However this pattern is highly variable among other arthropods, including rhomboidal, hexagonal and square-like patterns (Georgi, 1969; Lehane, 1997; Mets, 1962). These patterns have been associated with the distribution of the microvilli during the formation of the peritrophic membrane (Lehane, 1997). The main role of the peritrophic membrane is probably to be a protective barrier against pathogens and abrasive particles (Martin et al., 2006; Wang et al., 2012). Other authors proposed a protective role against toxic substances (Barbehenn and Martin, 1992; Hegedus et al., 2009; Lehane, 1997; Terra, 2001).

The role of the midgut tract epithelial cells for the secretion of peritrophic membrane is supported by our observations: the epithelial cells have high density of

mitochondria, rough endoplasmic reticulum and Golgi bodies, features of secretory cells observed in other decapods (Komuro and Yamamoto, 1968; Mykles, 1979). Moreover, these cells have an apical band which staining affinity is similar to the peritrophic membrane, this band coincides with the location of the band of secretory vesicles. Georgi (1969) mentioned that the peritrophic membrane of the decapods is polymerized among the microvilli. Martin et al. (2006) supported this hypothesis, but rejected the role of the secretory vesicles in the formation of the peritrophic membrane due to its absence of chitin. However, in *M. brachydactyla* the peritrophic membrane is stained by PAS, Alcian Blue and Aniline Blue, suggesting the presence of mucopolysaccharides and probable peptides. In this sense, previous studies identified proteins and mucopolysaccharides in the peritrophic membrane (Georgi, 1969). This protein content includes digestive enzymes (carboxypeptidase, trypsin and peptidase), as well immune related and antioxidant proteins (Wang et al., 2012). Therefore, in our opinion the secretory vesicles might contain non chitinous elements present in the peritrophic membrane.

Beside the secretion of the peritrophic membrane and/or other products, the lipid droplets observed in the epithelium of the midgut tract of *M. brachydactyla* suggest an ability to absorb and/or storage lipids from the lumen. This activity can be enhanced by microvilli (increasing the absorptive surface) and apical mitochondria (for the ATP production). The absorptive role has special sense in species with a relatively large midgut tract as penaeids (Talbot et al., 1972) and carideans, where cytoplasmic globules appear after feeding (Tziouveli et al., 2011). On the contrary, in species with vestigial midgut tract the absorptive role can be discarded. Komuro and Yamamoto (1968) pointed that despite the presence of microvilli and small vesicles, the midgut tract of *P. clarkii* is too short for a significant absorptive role. The relative length of the midgut

tract of *M. brachydactyla* is intermediate between the previous examples, then a complementary absorptive role is possible. Lovett and Felder (1990) mentioned that in *Penaeus setiferus* the midgut tract process the yolk reserves during the larval development and this function shift to the synthesis and secretion of enzymes after the yolk depletion. The midgut tract also has been associated with osmoregulatory processes due to the presence of basal mitochondria and smooth endoplasmic reticulum, features observed in osmoregulatory cells located on the gill filaments and urinary tubules (Komuro and Yamamoto, 1968; Talbot et al., 1972). In *M. brachydactyla*, we do not have enough information to support this last hypothesis.

In *M. brachydactyla* the midgut-hindgut junction is a short transition from the midgut tract to the hindgut, as previously observed in the brachyuran *Carcinus maenas* (Hopkin and Nott (1980), the anomuran *Paralithodes camtschaticus* (Abrunhosa and Kittaka, 1997), the astacidean *H. americanus* (Factor, 1981) and the penaeid *Metapenaeus bennettae* (Dall, 1967). Barker and Gibson (1978) described epithelial cells with mixed features of midgut and hindgut tracts, but these mixed features were not observed in *M. brachydactyla*. By contrast, our study revealed that the epithelial cells located adjacently to this "frontier" show general reduction in size, the microvillous border terminates in the connection with the hindgut tract while the hindgut cuticle is remarkably thin and simplified adjacently to the midgut tract. These key changes were also described in the midgut - hindgut junction of *Lepidophthalmus louisianensis* (Axiidea) by Felder and Felgenhauer (1993).

5. Acknowledgements

Financial support provided by the Spanish Ministry of Economy and Competitiveness through the INIA project [grant number RTA2011-00004-00-00] to G.G. and a pre-doctoral fellowship to D.C. [FPI-INIA]. The authors would like to thank to the technicians at IRTA, SantCarles de la Ràpita (David Carmona, Glòria Macià, Magda Monllaó, Francesc X. Ingla and Olga Bellot) and CCiTUB Hospital Clinic, Barcelona (Adriana Martínez, Almudena García, José Manuel Rebled and Rosa Rivera) for their assistance.

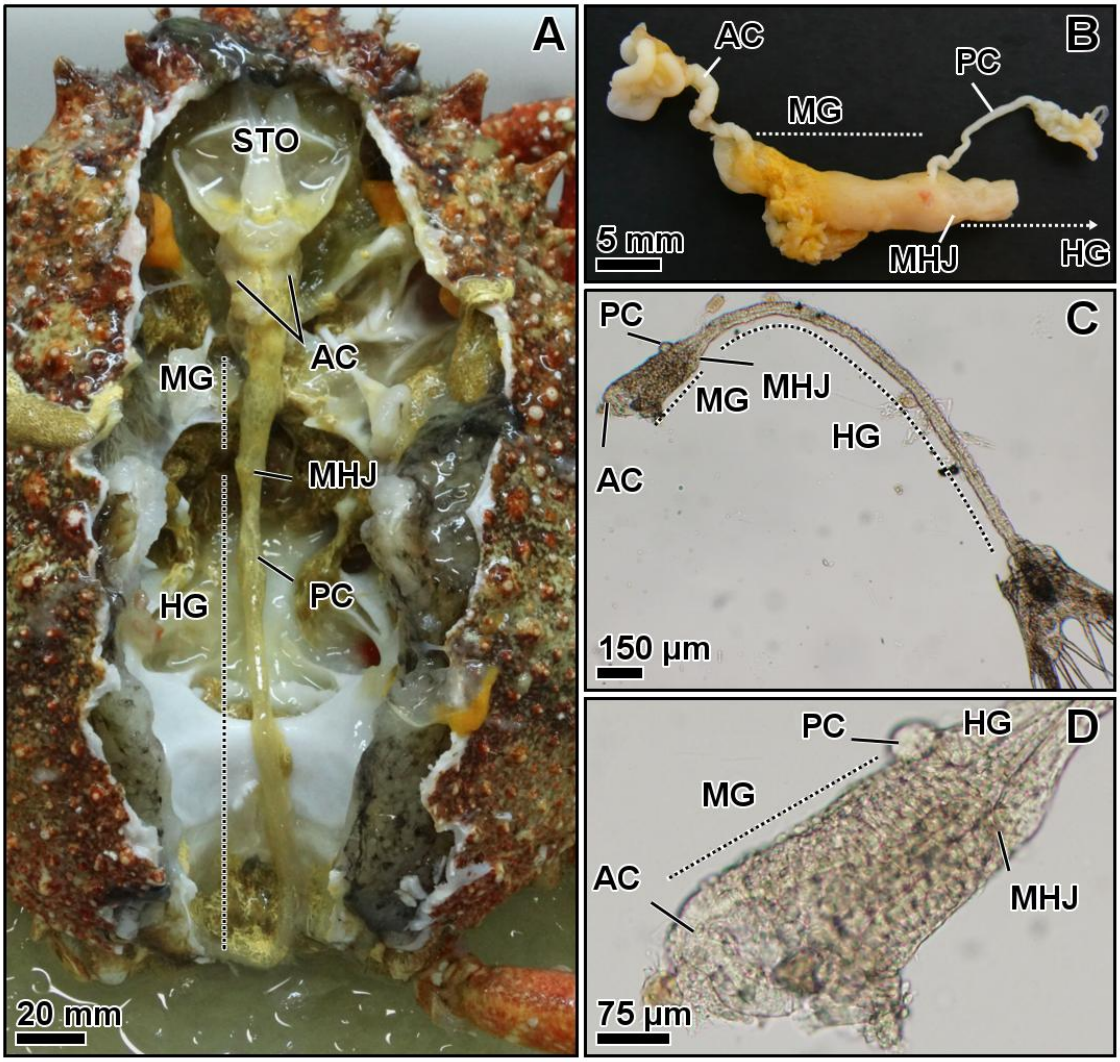

Figure 1. *Maja brachydactyla*. Midgut tract. Morphology. Adult, cephalothoracic cavity and digestive organs exposed, the midgut gland ("hepatopancreas") has been removed, fresh specimen (A). Adult, midgut tract and associated caeca, fixed in 4 % formaldehyde (B). Zoea I (ca. 15 hours after hatching), midgut tract and associated caeca (the foregut and midgut gland have been removed), fixed in 4 % formaldehyde (C-D): general view of the digestive system (C) and close view of the midgut tract and associated caeca (D). Abbreviations: AC, anterior midgut caeca; HG, hindgut tract; MG, midgut tract; MHJ, midgut-hindgut junction; PC, posterior midgut caecum; STO, stomach.

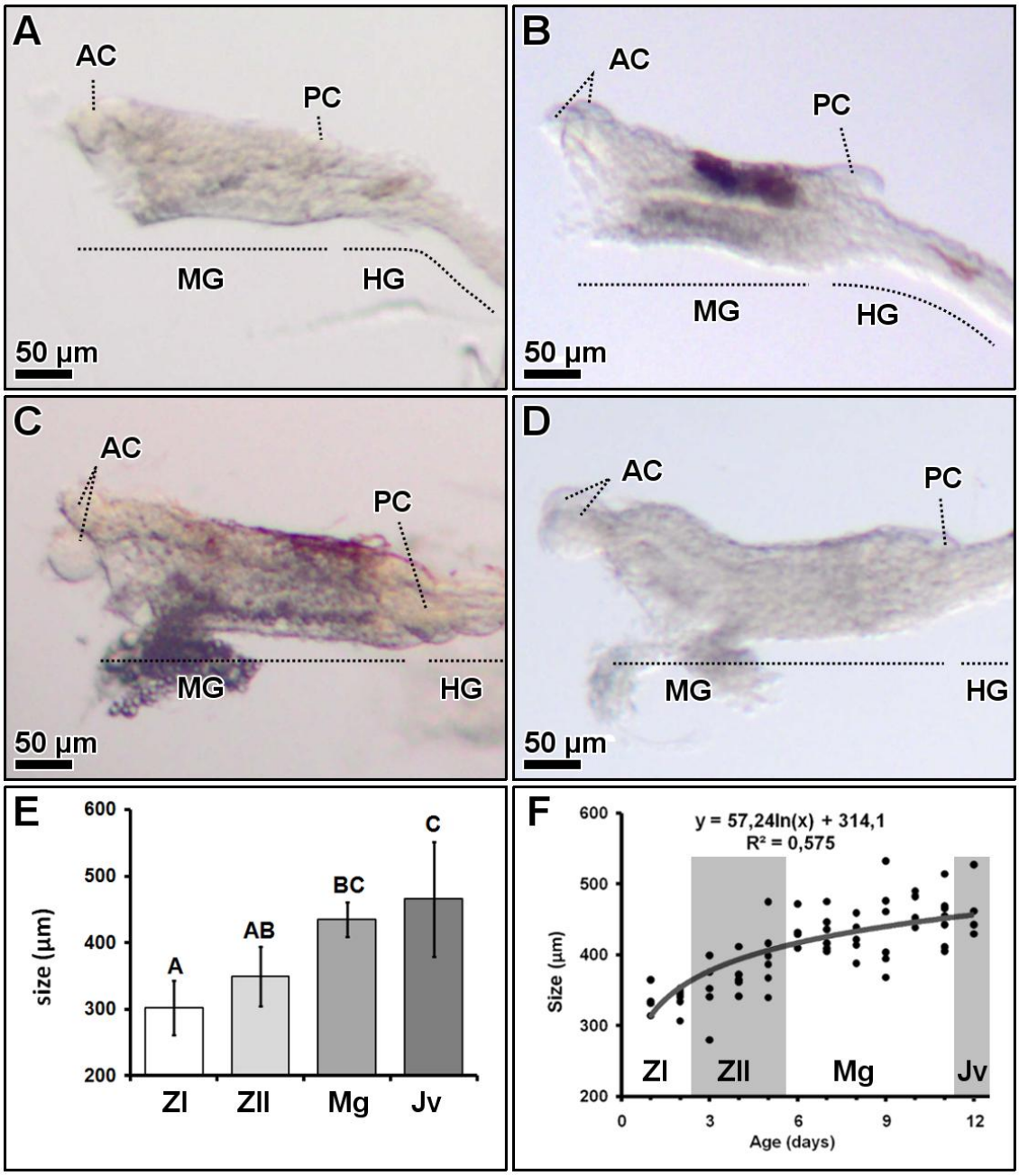

Figure 2. *Maja brachydactyla*. Midgut tract. Ontogeny. Fixed in 4 % formaldehyde, stereomicroscope (A-D): zoea I, 0 days after hatching (0 dah) (A); zoea II, 3 dah (B); megalopa, 7 dah (C); first juvenile, 12 dah (D). Comparative length of the midgut tract at the start of each larval and first juvenile stage, mean ± SD (E). Length of the midgut tract during the larval development (F). Abbreviations: AC, anterior midgut caeca; Mg, megalopa, MG, midgut tract; HG, hindgut tract; Jv, juvenile; PC, posterior midgut caecum; ZI, zoea I; ZII, zoea II.

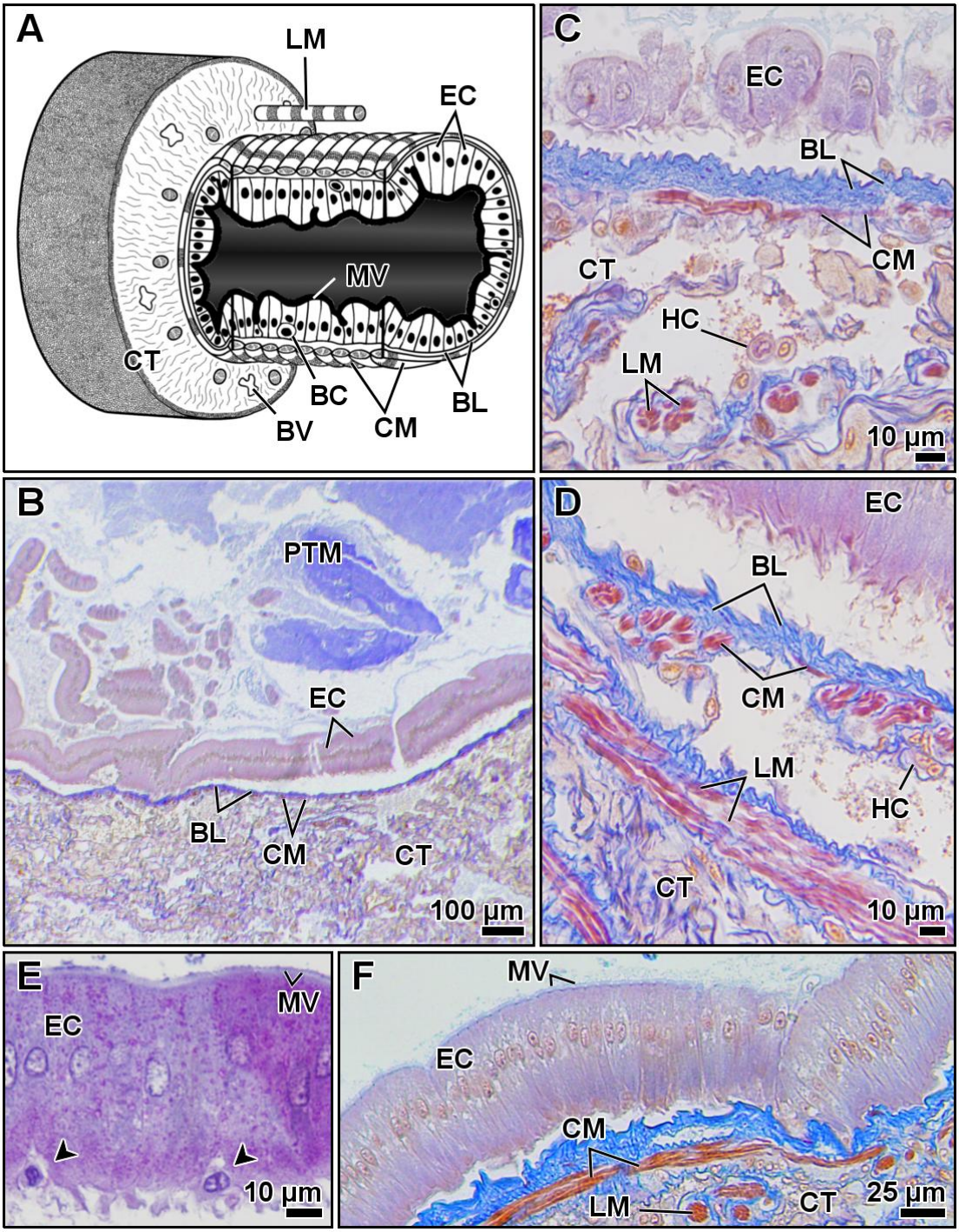

Figure 3. *Maja brachydactyla*. Midgut tract. Histological organization. Adult. General diagram (A). General view of the midgut tract, transversal section, Mallory's trichrome (B). Muscle organization, Mallory's trichrome (C-D): transversal (C) and longitudinal section (D). Epithelial and basal (marked with arrow-heads) cells (E-F): PAS and Alcian Blue contrasted with Hematoxylin (E), and Mallory's trichrome (F). Abbreviations: BC, basal cells; BL, basal lamina; BV, blood vessel; CM, circular muscle bundles; CT, connective tissue; EC, epithelial cells; HC, hemocytes; LM, longitudinal muscle bundles; MV, microvilli; PTM, peritrophic membrane.

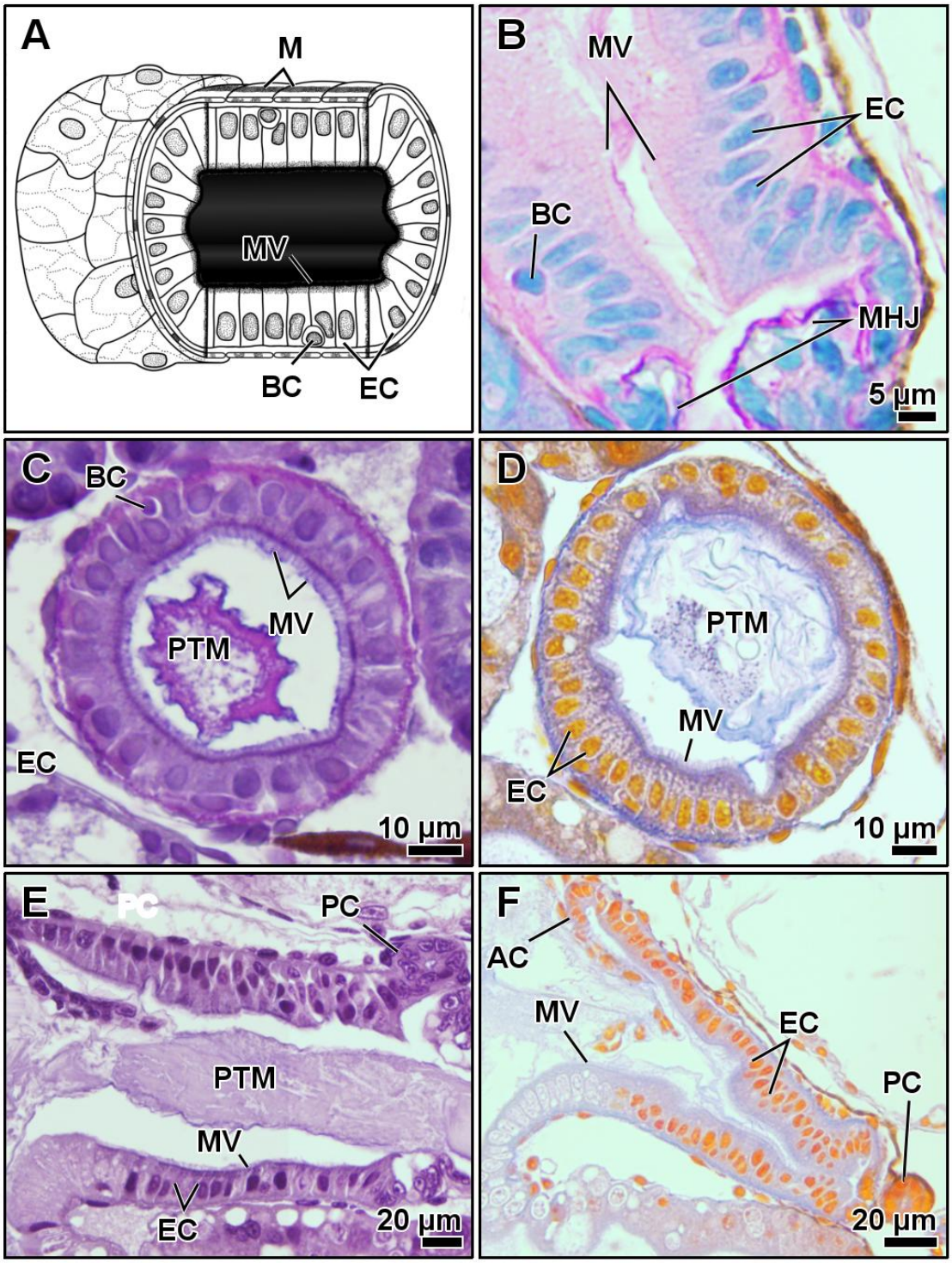

Figure 4. *Maja brachydactyla*. Midgut tract. Histological organization. Larvae. General diagram (A). Zoea II, 6 days after hatching (6 dah), close view of the midgut-hindgut junction, longitudinal section, PAS contrasted with Methylene Blue (B). Midgut tract, H-E (C, E): megalopa, 6 dah, transversal section (C) and zoea I, 0 dah, longitudinal section (E). Midgut tract, Mallory's trichrome (D, F): megalopa, 6 dah, transversal section (C) and zoea II, 6 dah, longitudinal section (E). Abbreviations: AC, anterior midgut caecum; BC, basal cell; EC, epithelial cells; M, muscle cells; MV, microvilli; PC, posterior midgut caeca; PTM, peritrophic membrane.

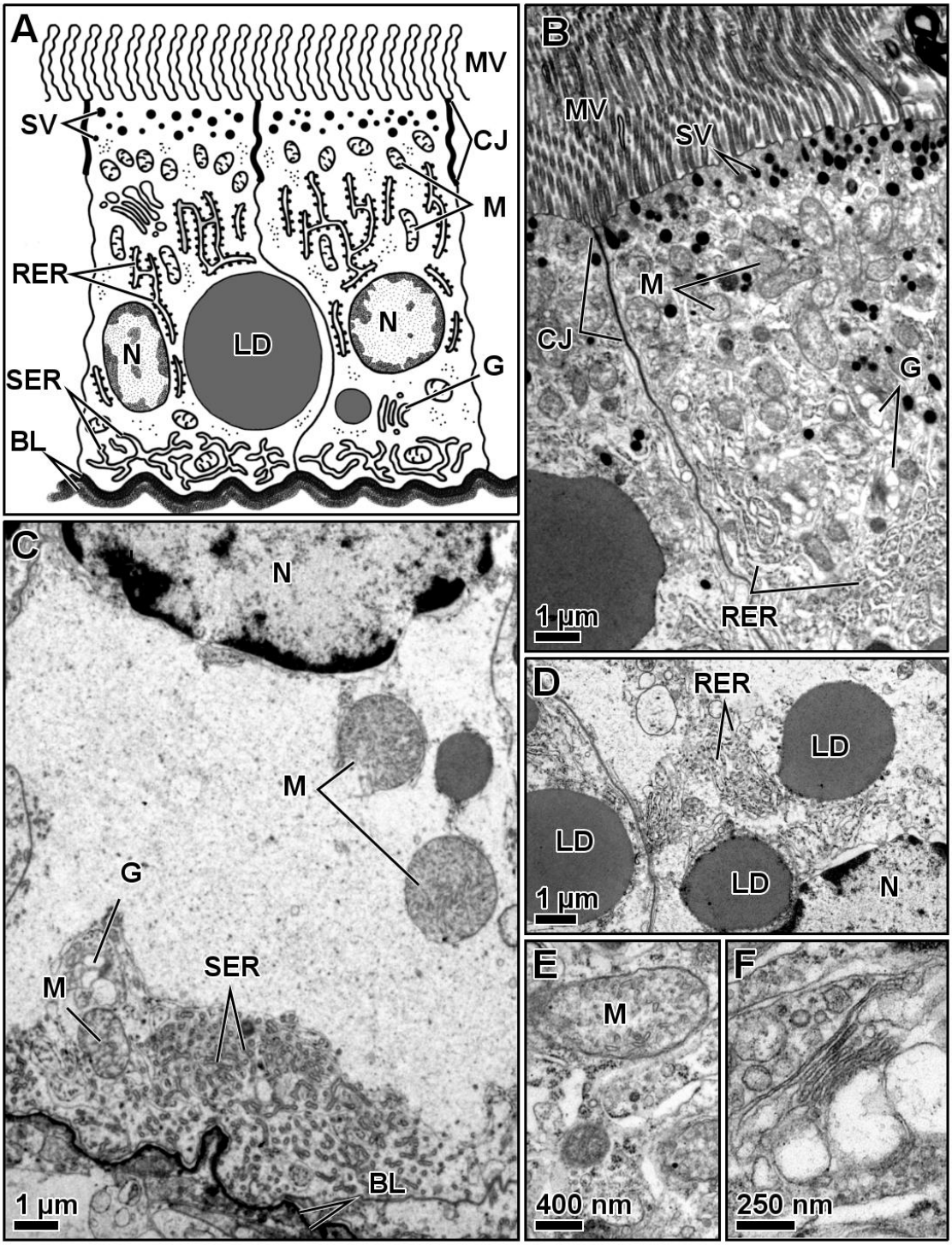

Figure 5. *Maja brachydactyla*. Midgut tract. Epithelial cells. Megalopa, 10 days after hatching. Ultrastructure. TEM. General diagram (A). Cell apex, supranuclear region (B). Cell basis, infranuclear region (C). General view, lipid droplets (D). Mitochondria, close view (E). Golgi body, close view (F). Abbreviations: BL, basal lamina; CJ, cell-to-cell junction; G, Golgi bodies; LD, lipid droplets; M, mitochondria; MV, microvilli; N, nucleus; RER, rough endoplasmic reticulum; SER, smooth endoplasmic reticulum; SV, secretory vesicles

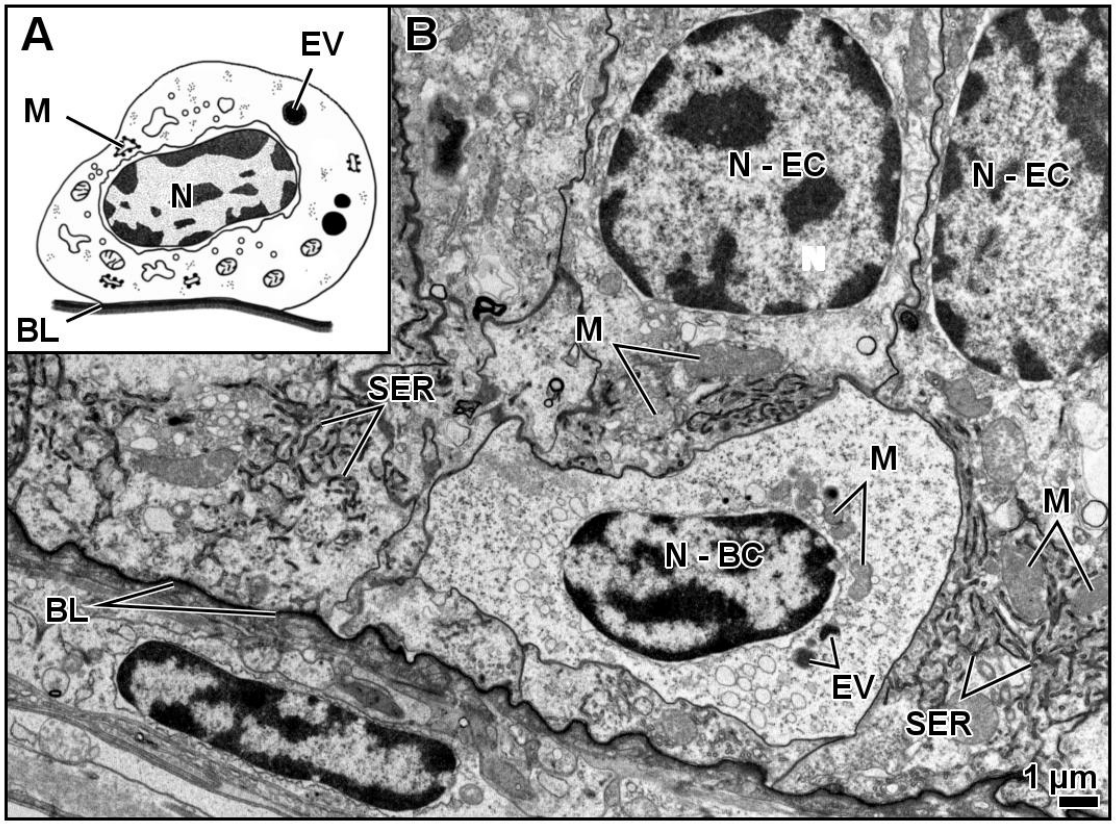

Figure 6. *Maja brachydactyla*. Midgut tract. Basal cells and basis of the epithelial cells. Zoea I (ca. 15 h after hatching). Ultrastructure. TEM. General diagram (A). General view, basal cell surrounded by epithelial cells (B). Abbreviations: BL, basal lamina; EV, electron-dense vesicle; M, mitochondria; N, nucleus; N - BC, nucleus of the basal cell; N - EC, nucleus of the epithelial cells; SER, smooth endoplasmic reticulum.

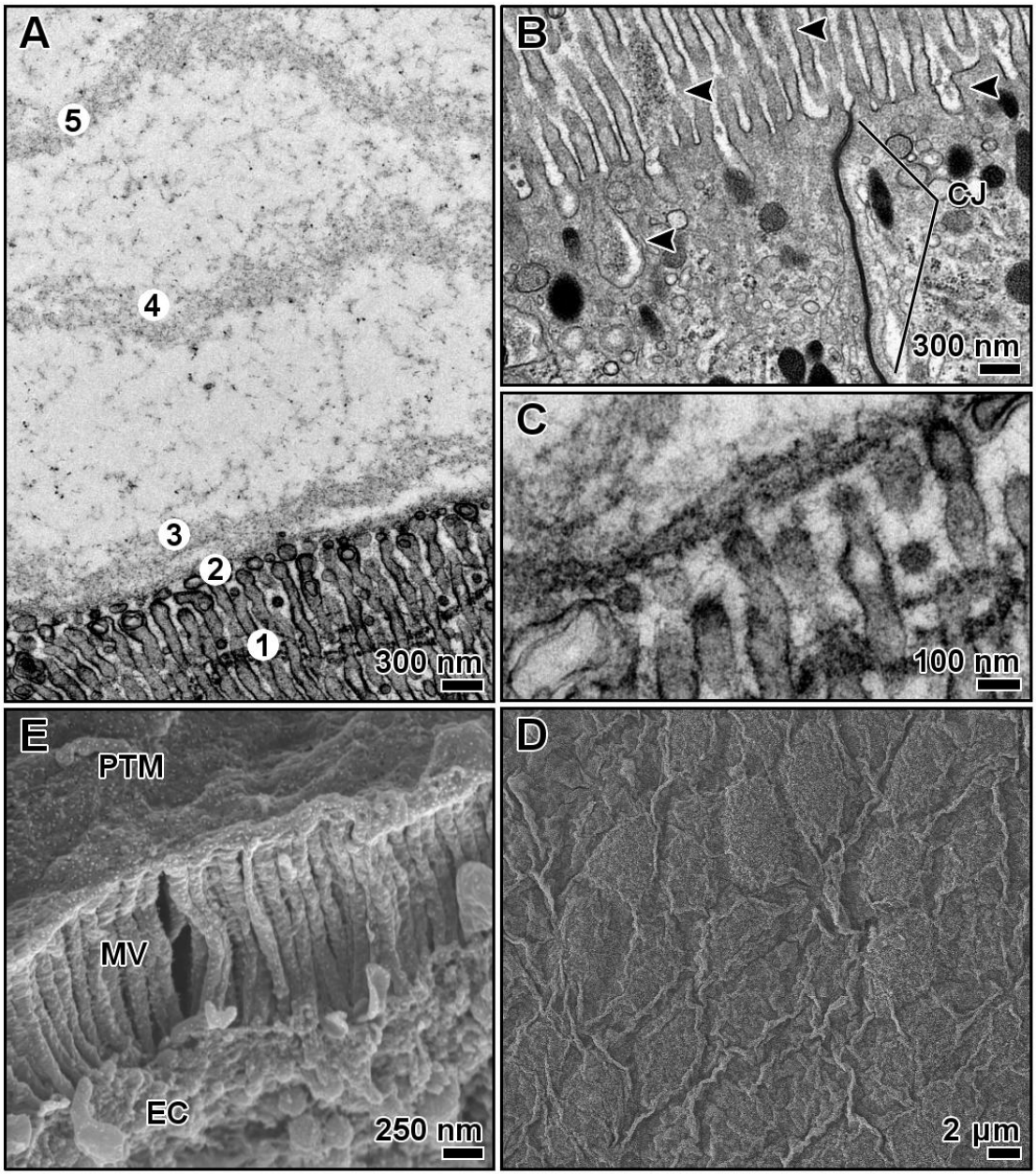

Figure 7. *Maja brachydactyla*. Midgut tract. Peritrophic membrane. Ultrastructure. Zoea I (ca. 15 h after hatching), TEM (A-C): waves of secretion (numbered) of peritrophic membrane (A); release of the secretory vesicle content by merocrine secretion toward the microvilli (arrow-heads) (B); and close view of the peritrophic membrane attached to the microvilli tips (C). Adult, SEM (D-E): apical view of the peritrophic membrane (D) and peritrophic membrane attached to the microvilli tips (E). Abbreviations: EC, epithelial cells; CJ, cell-to-cell junction; MV, microvilli; PTM, peritrophic membrane.

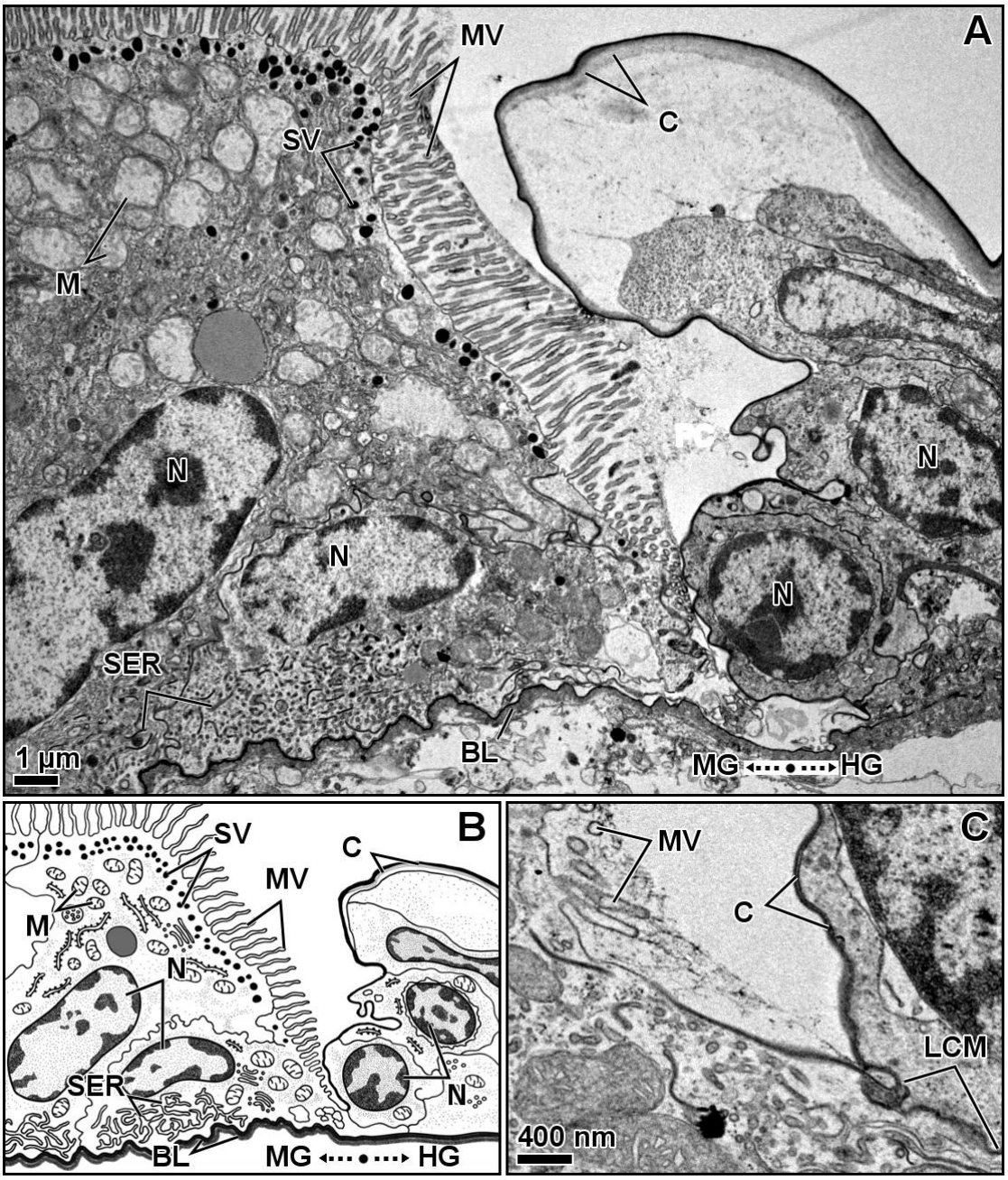

Figure 8. *Maja brachydactyla*. Midgut-hindgut junction. Megalopa, 10 days after hatching. Ultrastructure. TEM. General view (A). General diagram (B). Transition from the midgut tract to the hindgut tract, close view (C). Abbreviations: BL, basal lamina; C, cuticle; HG, hindgut tract; LCM, lateral cell membrane; M, mitochondria; MG, midgut tract; MV, microvilli; N, nucleus; SER, smooth endoplasmic reticulum; SV, secretory vesicles.

6. References.

Abelló P, García Raso JE, Guerao G, Salmerón F. 2014. *Maja brachydactyla* (Brachyura: Majidae) in the western Mediterranean. Marine Biodiversity Records 7(e77).

Abrunhosa FA, Kittaka J. 1997. Morphological changes in the midgut, midgut gland and hindgut during the larval and postlarval development of the red king crab *Paralithodes camtschaticus*. Fisheries Science 63(5):746-754.

Abubakr MA, Jones DA. 1992. Functional morphology and ultrastructure of the anterior mid-gut diverticulae of larvae of *Penaeus monodon* Fabricius, 1798 (Decapoda, Natantia). Crustaceana 62(2):142-158.

Andrés M, Estévez A, Anger K, Rotllant G. 2008. Developmental patterns of larval growth in the edible spider crab, *Maja brachydactyla* (Decapoda: Majidae). J Exp Mar Biol Ecol 357(1):35-40.

Andrés M, Gisbert E, Díaz M, Moyano FJ, Estévez A, Rotllant G. 2010. Ontogenetic changes in digestive enzymatic capacities of the spider crab, *Maja brachydactyla* (Decapoda: Majidae). J Exp Mar Biol Ecol 389(1-2):75-84.

Barbehenn RV, Martin MM. 1992. The protective role of the peritrophic membrane in the tannin-tolerant larvae of *Orgyia leucostigma* (Lepidoptera). Journal of Insect Physiology 38(12):973-980.

Barker PL, Gibson R. 1977. Observations on the feeding mechanism, structure of the gut, and digestive physiology of the european lobster *Homarus gammarus* (L.) (Decapoda: Nephropidae). J Exp Mar Biol Ecol 26(3):297-324.

Barker PL, Gibson R. 1978. Observations on the structure of the mouthparts, histology of the alimentary tract, and digestive physiology of the mud crab *Scylla serrata* (Forskål) (Decapoda: Portunidae). J Exp Mar Biol Ecol 32(2):177-196.

Bonaldo A, Roem AJ, Pecchini A, Grilli E, Gatta PP. 2006. Influence of dietary soybean meal levels on growth, feed utilization and gut histology of Egyptian sole (*Solea aegyptiaca*) juveniles. Aquaculture 261(2):580-586.

Castejón D, Rotllant G, Giménez L, Torres G, Guerao G. 2015a. The effects of temperature and salinity on the survival, growth and duration of the larval development of the common spider crab *Maja brachydactyla* (Balss, 1922) (Brachyura: Majidae). Journal of Shellfish Research 34(3):1073-1083.

Castejón D, Rotllant G, Ribes E, Durfort M, Guerao G. 2015b. Foregut morphology and ontogeny of the spider crab *Maja brachydactyla* (Brachyura, Majoidea, Majidae). J Morphol 276(9):1109-1122.

Ceccaldi HJ. 1989. Anatomy and physiology of digestive tract of Crustaceans Decapods reared in aquaculture. Advances in Tropical Aquaculture, Workshop at Tahiti, French Polynesia. Tahiti, French Polynesia: Actes de colloques Ifremer. p 243-259.

Chisaka H, Ueno M, Futaesaku Y. 1999. Spines in the hindgut of the crayfish *Procambarus clarkii* (Decapoda): their distribution and correlation with hindgut muscles. Journal of Crustacean Biology 19(2):337-343.

Dall W. 1967. The functional anatomy of the digestive tract of a shrimp *Metapenaeus bennettae* Racek & Dall (Crustacea : Decapoda : Penaeidae). Australian Journal of Zoology 15(4):699-714.

Davolos D, L. P, Accordi F, De Matthaeis E. 2010. Morphology and histology of the mouthparts and gut system of *Macarorchestia remyi* (Schellenberg, 1950) (Amphipoda, Talitridae). Zoologia Baetica 21:151-178.

Erri Babu D, Shyamasundari K, Rao KH. 1982. Studies on the digestive system of the crab *Menippe rumphii* (Fabricius) (Crustacea:Brachyura). J Exp Mar Biol Ecol 58(2):175-191.

Factor JR. 1981. Development and metamorphosis of the digestive system of larval lobsters, *Homarus americanus* (Decapoda: Nephropidae). J Morphol 169:225-242.

Factor JR. 1995. The Digestive System. In: Factor JR, editor. Biology of the Lobster *Homarus americanus*: Academic Press. p 395-440.

FAO. 2014. B-42 Crabs, sea-spiders. Capture production by species, fishing areas and countries or areas. In: FAO, editor. FAO yearbook Fishery and aquaculture statistics. Rome: FAO.

Felder DL, Felgenhauer BE. 1993. Morphology of the midgut–hindgut juncture in the ghost shrimp *Lepidophthalmus louisianensis* (Schmitt) (Crustacea: Decapoda: Thalassinidea). Acta Zoologica 74(4):263-276.

Felgenhauer BE. 1992. Chapter 3. Internal Anatomy of the Decapoda: An Overview. In: Harrison FW, Humes AG, editors. Microscopic Anatomy of Invertebrates Volume 10: Decapod Crustacea: Wiley-Liss, Inc. p 45-75.

Fontagné S, Geurden I, Escaffre A-M, Bergot P. 1998. Histological changes induced by dietary phospholipids in intestine and liver of common carp (*Cyprinus carpio* L.) larvae. Aquaculture 161(1–4):213-223.

Forster GR. 1953. Peritrophic membranes in the Caridea (Crustacea Decapoda). Journal of the Marine Biological Association of the United Kingdom 32(2):315-318.

Georgi R. 1969. Bildung peritrophischer Membranen von Decapoda. Zeitschrift für Zellforschung und Mikroskopische Anatomie 99(4):570-607.

Gibson R, Barker PL. 1979. The Decapod Hepatopancreas. Oceanography and Marine Biology - An Annual Review 17:285-346.

Goodrich AL. 1939. The origin and fate of the entoderm elements in the embryogeny of *Porcellio laevis* Latr. and *Armadillidium nasatum* B. L. (Isopoda). J Morphol 64(3):401-429.

Guerao G, Pastor E, Martin J, Andrés M, Estévez A, Grau A, Duran J, Rotllant G. 2008. The larval development of *Maja squinado* and *M. brachydactyla* (Decapoda, Brachyura, Majidae) described from plankton collected and laboratory-reared material. Journal of Natural History 42(33-34):2257-2276.

Guerao G, Rotllant G, Anger K. 2010. Characterization of larval moulting cycles in *Maja brachydactyla* (Brachyura, Majidae) reared in the laboratory. Aquaculture 302(1-2):106-111.

Heeren T, Mitchell BD. 1997. Morphology of the mouthparts, gastric mill and digestive tract of the giant crab, *Pseudocarcinus gigas* (Milne Edwards) (Decapoda: Oziidae). Marine and Freshwater Research 48(1):7-18.

Hegedus D, Erlandson M, Gillott C, Toprak U. 2009. New Insights into peritrophic matrix synthesis, architecture, and function. Annual Review of Entomology 54:285-302.

Hinton DJ, Corey S. 1979. The mouthparts and digestive tract in the larval stages of *Homarus americanus*. Canadian Journal of Zoology 57(7):1413-1423.

Holdich DM. 1973. The Midgut/Hindgut Controversy in Isopods. Crustaceana 24(2):211-214.

Holdich DM, Mayes KR. 1975. A Fine-Structural Re-Examination of the so-called 'Midgut' of the isopod *Porcellio*. Crustaceana 29(2):186-192.

Holdich DM, Ratcliffe NA. 1970. A light and electron microscope study of the hindgut of the herbivorous isopod, *Dynamene bidentata* (Crustacea: Peracarida). Zeitschrift für Zellforschung und Mikroskopische Anatomie 111(2):209-227.

Holliday CW, Mykles DL, Terwilliger RC, Dangott LJ. 1980. Fluid secretion by the midgut caeca of the crab, *Cancer magister*. Comparative Biochemistry and Physiology Part A: Physiology 67(2):259-263.

Hopkin SP, Nott JA. 1980. Studies on the digestive cycle of the shore crab *Carcinus maenas* (L.) with special reference to the b cells in the hepatopancreas. Journal of the Marine Biological Association of the United Kingdom 60(04):891-907.

Huxley TH. 1880. The Crayfish; an Introduction to the Study of Zoology. Series TIS, editor: New York: D. Appleton and Company.

Icely JD, Nott JA. 1992. Digestion and absorption: digestive system and associated organs. In: Harrison FW, Humes AG, editors. Microscopic anatomy of invertebrates: decapod Crustacea. New York: Wiley-Liss. p 147-201.

Jantrarotai PN, Sawanyatiputi SA. 2005. Histological study on the development of digestive system in zoeal stages of mud crab (*Scylla olivacea*). Kasetsart Journal 39(4):666-671.

Kaushik N, Kumar S. 1998. Midgut pathology of aldrin, monocrotophos, and carbaryl in the freshwater crab, *Paratelphusa masoniana* (Henderson). Bulletin of Environmental Contamination and Toxicology 60(3):480-486.

Komuro T, Yamamoto T. 1968. Fine structure of the epithelium of the gut in the crayfish (*Procambarus clarkii*) with special reference to the cytoplasmic microtutubles. Archivum histologicum japonicum 30(1):17-32.

Lehane MJ. 1997. Peritrophic matrix structure and function. Annual Review of Entomology 42(1):525-550.

Lovett DL, Felder DL. 1989. Ontogeny of gut morphology in the white shrimp *Penaeus setiferus* (Decapoda, Penaeidae). J Morphol 201(3):253-272.

Lovett DL, Felder DL. 1990. Ontogenetic changes in enzyme distribution and midgut function in developmental stages of *Penaeus setiferus* (Crustacea, Decapoda, Penaeidae). The Biological Bulletin 178(2):160-174.

Martin GG, Chiu A. 2003. Morphology of the midgut trunk in the penaeid shrimp, *Sicyonia ingentis*, highlighting novel nuclear pore particles and fixed hemocytes. J Morphol 258(2):239-248.

Martin GG, Rubin N, Swanson E. 2004. *Vibrio parahaemolyticus* and *V. harveyi* cause detachment of the epithelium from the midgut trunk of the penaeid shrimp *Sicyonia ingentis*. Diseases of Aquatic Organisms 60:21-29.

Martin GG, Simcox R, Nguyen A, Chilingaryan A. 2006. Peritrophic membrane of the penaeid shrimp *Sicyonia ingentis*: structure, formation, and permeability. The Biological Bulletin 211(3):275-285.

McLaughlin PA. 1983. 1. Internal Anatomy. In: Mantel LH, editor. The Biology of Crustacea Vol 5 Internal Anatomy and Physiological Regulation: Academic Press. p 1-52.

Mets RD. 1962. Submicroscopic structure of the peritrophic membrane in arthropods. Nature 196:77-78.

Mikami S, Greenwood JG, Takashima F. 1994. Functional morphology and cytology of the phyllosomal digestive system of *Ibacus ciliatus* and *Panulirus japonicus* (Decapoda, Scyllaridae and Palinuridae). Crustaceana 67(2):212-225.

Milne-Edwards H. 1834a. Histoire naturelle des crustacés, comprenant l'anatomie, la physiologie et la classification de ces animaux: Libraire Encyclopédique de Roret.

Milne-Edwards H. 1834b. Histoire naturelle des crustacés: atlas: Libraire Encyclopédique de Roret.

Moon YW, Kim HH. 1999. Morphological study of the digestive tract of the mud crab (*Hemigrapsus penicillatus* De Haan) and the symbiotic crab (*Pinnotheres cyclinus* Shen). Korean Journal of Biological Sciences 3(4):407-412.

Muhammad F, Zhang ZF, Shao MY, Dong YP, Muhammad S. 2012. Ontogenesis of digestive system in *Litopenaeus vannamei* (Boone, 1931) (Crustacea: Decapoda). Italian Journal of Zoology 79(1):77-85.

Mykles DL. 1979. Ultrastructure of alimentary epithelia of lobsters, *Homarus americanus* and *H. gammarus*, and crab, *Cancer magister*. Zoomorphologie 92(3):201-215.

Nakamura K, Seki K. 1990. Organogenesis during metamorphosis in the prawn *Penaeus japonicus*. Nippon Suisan Gakkaishi 56(9):1413-1417.

Øverland M, Sørensen M, Storebakken T, Penn M, Krogdahl Å, Skrede A. 2009. Pea protein concentrate substituting fish meal or soybean meal in diets for Atlantic salmon (*Salmo salar*)—Effect on growth performance, nutrient digestibility, carcass composition, gut health, and physical feed quality. Aquaculture 288(3–4):305-311.

R Development Core Team. 2015. R: A language and environment for statistical computing. Vienna, Austria: R Foundation for Statistical Computing.

Reddy AR. 1937. The physiology of digestion and absorption in the crab *Paratelphusa* (*Oziotelphusa*) *hydrodromus* (Herbst). Proceedings of the Indian Academy of Sciences - Section B 6(3):170-193.

Rotllant G, Moyano FJ, Andres M, Estevez A, Diaz M, Gisbert E. 2010. Effect of delayed first feeding on larval performance of the spider crab *Maja brachydactyla* assessed by digestive enzyme activities and biometric parameters. Mar Biol 157(10):2215-2227.

Rotllant G, Simeó CG, Macià G, Estévez A. 2015. High environmental salinity reduces the reproductive potential of the spider crab *Maja brachydactyla* (Decapoda, Majidae). Marine Ecology 36(3):496-505.

Schlegel C. 1911. Anatomie sommaire de la première zoé de *Maja squinado* Latr. (Note préliminaire à des recherches sur l'Organogénese des Décapodes brachyoures). Archives de Zoologie Experimentale et Générale 5º Série T. VIII.(2):29-40.

Smith RI. 1978. The Midgut Caeca and the Limits of the Hindgut of Brachyura: A Clarification. Crustaceana 35(2):195-205.

Sonakowska L, Włodarczyk A, Poprawa I, Binkowski M, Śróbka J, Kamińska K, Kszuk-Jendrysik M, Chajec Ł, Zajusz B, Rost-Roszkowska MM. 2015. Structure and Ultrastructure of the endodermal region of the alimentary tract in the freshwater shrimp *Neocaridina heteropoda* (Crustacea, Malacostraca). PLOS ONE 10(5):e0126900.

Sousa L, Petriella AM. 2006. Morphology and histology of *P. argentinus* (Crustacea, Decapoda, Caridea) digestive tract. Biocell 30:287-294.

Ńtrus J, Drobne D, Ličar P. 1995. Comparative anatomy and functional aspects of the digestive system in amphibious and terrestrial isopods (Isopoda: Oniscidea). In: Alikkhan MA, editor. Crustacean Issues "Terrestrial Isopod Biology". Rotterdam, Netherlands: Balkema Publishers. p 13-23.

Ńtrus J, Klepal W, Repina J, Tuńek-Ņnidarič M, Milatovič M, Pipan Ņ. 2008. Ultrastructure of the digestive system and the fate of midgut during embryonic development in *Porcellio scaber* (Crustacea: Isopoda). Arthropod Structure & Development 37(4):287-298.

Talbot P, Clark WH, Lawrence AL. 1972. Fine structure of the midgut epithelium in the developing brown shrimp, *Penaeus aztecus*. J Morphol 138(4):467-485.

Terra WR. 2001. The origin and functions of the insect peritrophic membrane and peritrophic gel. Archives of Insect Biochemistry and Physiology 47(2):47-61.

Trinadha Babu B, Shyamasundari K, Hanumantha Rao K. 1989. Observations on the morphology and histochemistry of the midgut and hindgut of *Portunus sanguinolentus* (Herbst) (Crustaceans: Brachyura). Folia Morphologica 37(4):373-381.

Tziouveli V, Bastos-Gomez G, Bellwood O. 2011. Functional morphology of mouthparts and digestive system during larval development of the cleaner shrimp *Lysmata amboinensis* (de Man, 1888). J Morphol 272(9):1080-1091.

Verísimo P, Bernárdez C, González-Gurriarán E, Freire J, Muino R, Fernández L. 2011. Changes between consecutive broods in the fecundity of the spider crab, *Maja brachydactyla*. ICES J Mar Sci 68(3):472-478.

Vernon GM, Herold L, Witkus ER. 1974. Fine structure of the digestive tract epithelium in the terrestrial isopod. *Armadillidium vulgare*. J Morphol 144(3):337-359.

Wang L, Li F, Wang B, Xiang J. 2012. Structure and partial protein profiles of the peritrophic membrane (PM) from the gut of the shrimp *Litopenaeus vannamei*. Fish & Shellfish Immunology 33(6):1285-1291.

Williams RL. 1944. The pre-zoea stage of *Porcellana platycheles* (Pennant). Preliminary anatomical and histological notes. Journal of the Royal Microscopical Society 64(1-2):1-15.

Yonge CM. 1924. Studies on the comparative physiology of digestion II. - The mechanism of feeding, digestion, and assimilation in *Nephrops norvegicus*. British Journal of Experimental Biology 1:343-389.

CHAPTER 17.

Morphology and ontogeny of the midgut caeca in the spider crab *Maja brachydactyla* Balss, 1922 (Brachyura, Majidae)

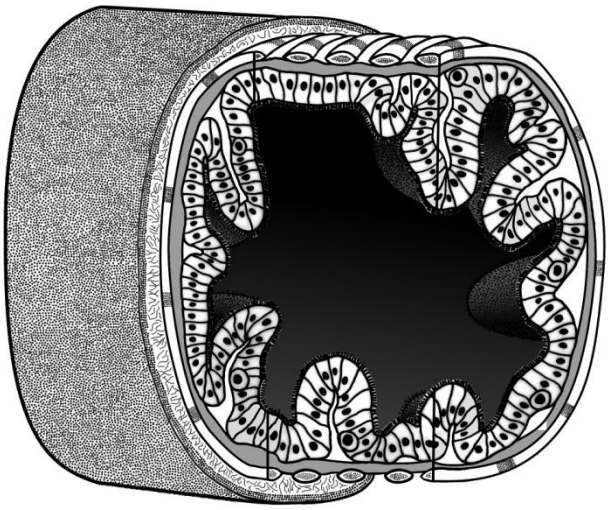

Morphology and ontogeny of the midgut caeca in the spider crab *Maja brachydactyla* Balss, 1922 (Brachyura, Majidae).

Diego Castejón[1*], Guiomar Rotllant[2], Enric Ribes[3], Mercè Durfort[3], and Guillermo Guerao[4]

[1]IRTA, Centre d'Aqüicultura, Ctra. del Poble Nou Km 5.5. 43540 Sant Carles de la Ràpita, Tarragona (Spain).

[2]CSIC, Institut de Ciències del Mar, Passeig Marítim de la Barceloneta 37-49. 08003 Barcelona (Spain).

[3]Unitat de Biologia Cel·lular, Departament de Biologia Cel·lular, Fisiologia i Immunologia, Facultat de Biologia, Universitat de Barcelona, Diagonal 645.08028 Barcelona (Spain).

[4]PS Fabra i Puig 344.08028 Barcelona (Spain).

Short title: *Maja brachydactyla* midgut caeca morphology & ontogeny

***Corresponding author:** Diego Castejón. E-mail: diego.castejon.dcb@gmail.com; phone: +34 681 154 398; postal address: IRTA, Subprogram Cultius Aqüàtics, Ctra. Poble Nou, Km 5.5, 43540 Sant Carles de la Ràpita, Tarragona(Spain).

Abstract

The common spider crab *Maja brachydactyla* Balss, 1922 have two types of midgut caeca: anterior and posterior midgut caeca. The pair of anterior midgut caeca protrudes dorsally from the anterior midgut tip and are projected toward the stomach walls. The single posterior midgut caecum protrudes before the midgut-hindgut junction and it is projected toward the hindgut tract and haemocoel. Both midgut caeca are large blind-end tubules highly coiled. The larval midgut caeca are small buds that elongate significantly during the larval development. The anatomy and ultrastructure of the anterior and posterior midgut caeca are similar. The caeca are composed by a simple microvillous epithelium folded toward the lumen. Two cell types have been identified: epithelial and basal cells. The epithelial cells have a polarized cell organization: the cell apex is rich in microvilli, mitochondria and parallel membranes of rough endoplasmic reticulum while below the nucleus a band of tubular smooth endoplasmic reticulum is present with some mitochondria and abundant vesicles. The basal cells are rounded, short and never reach the caeca lumen; they are associated with processes of mitosis and cell differentiation. The midgut caeca are wrapped by a thin connective tissue and a network of muscle fibers. The midgut caeca realize an important secretory activity observed in larval and adult stages. The main secretory activity is apocrine, based on the formation of enormous vesicles on the cell apex that are released into the caeca lumen. An additional microapocrine secretion is based on the formation small vesicles on the microvilli tip, this type of secretion is described for first time in decapods. The role of the midgut caeca is discussed.

Keywords: Crustacea; larvae; anterior caeca; posterior caecum; microvillous; apocrine secretion

1. Introduction

The digestive system of the malacostracans comprises the foregut, the midgut and the hindgut. The midgut includes numerous endoderm-derived organs: the midgut tract, the midgut gland (also known as "hepatopancreas") and the midgut caeca (Ceccaldi, 1989; Erri Babu et al., 1982; Felgenhauer, 1992; Icely and Nott, 1992; McLaughlin, 1983). The midgut caeca are blind-end tubules projected from the midgut tract whose length varies among different Decapoda taxa, from very short finger-like projections in astacids (Factor, 1981; Hinton and Corey, 1979) to very long and coiled tubules in brachyurans (Smith, 1978). One of the most divergent caeca is described in some penaeid shrimps where the posterior midgut caeca exhibits a complex cauliflower-like shape (Lovett and Felder, 1989; 1990b; Muhammad et al., 2012). The midgut caeca are located at both extremes of the midgut tract. In brachyurans, the anterior midgut caeca (AMC) protrude dorsally from the anterior extreme of the midgut tract; while the single posterior caecum (PMC) protrudes dorso-laterally from the midgut tract immediately before the midgut-hindgut junction (Erri Babu et al., 1982; Smith, 1978). The role of the midgut caeca on the crustacean physiology and/or on the digestive process is unclear, however certain secretory activity has been documented (Holliday et al., 1980; Pinn et al., 1999; Pugh, 1962).

The information available in relation to the midgut caeca of the Decapoda digestive system is scarce and fewer studies are focused on their ontogeny and development (Abubakr and Jones, 1992). The majority of the studies focused on the digestive system describe with higher detail other organs as the stomach or the midgut gland (Abrunhosa and Kittaka, 1997; Factor, 1981; Hinton and Corey, 1979; Lovett and Felder, 1990a; Muhammad et al., 2012).

The species selected for this study is the common spider crab *Maja brachydactyla* Balss, 1922. It is a marine brachyuran distributed in the eastern Atlantic coast from the British Isles to the Sahara and SW Mediterranean Sea (Abelló et al., 2014), with important fisheries located on European countries (FAO, 2014). The larval development consists in two zoeal stages, zoea I (ZI) and zoea II (ZII), and one megalopa stage (M) before the metamorphosis to first juvenile (J1) (Clark, 1986; Guerao et al., 2008). Regarding the ontogeny of the digestive system of *M. brachydactyla,* previous studies focuses on the description of mouth appendixes (Guerao et al., 2008), stomach (Castejón et al., 2015) and enzymes (Andrés et al., 2010; Rotllant et al., 2010).

The main objective of the present study is to describe the anterior and posterior midgut caeca of the brachyuran *M. brachydactyla* during the larval, first juvenile and adult stages. This study insight into the external morphology of the organ by their observation under stereomicroscopy and internal anatomy by optical and electron microscopy, emphasizing on the changes occurred during the ontogeny. The role of the midgut caeca is discussed.

2. Material and methods

Animal origin, sample collection, dissection, general morphology, optical and electron microscopy techniques (transmission and scanning) were described in a previous study dedicated to the study of the midgut tract (Castejón et al. this issue).

3. Results

The midgut of *M. brachydactyla* has two types of caeca from hatching to the adult stage: a pair of anterior caeca and a single posterior caecum. Both anterior and posterior caeca shares some features: they are long, thin and coiled blind-end tubules

projected from the midgut tract (Fig. 1A, C-D). These organs are very delicate and susceptible to break when manipulated. Besides their similarities, the AMC and PMC show some differences. The AMC are a pair of organs extended forward from the antero-dorsal tip of the midgut tract toward the stomach walls, where in adults they coil forming a disc-shaped structure (Fig. 1A-C; 2A-D). By contrast, the PMC is a single organ, thinner than the AMC, extended backward from the midgut side of the midgut-hindgut junction toward the hindgut tract (Fig. 1A-B, D; 3A-D). In adults, the proximal section of the PMC is undulated and attached to the hindgut walls; while the distal portion is narrow, coiled and located on the haemocoel (Fig. 1A, D).

The AMC of the newly hatched zoeae are short buds (Fig. 1B; 2A), these buds enlarges quickly in the next days to simple and short blind-end tubules whose length increases through the larval development (Fig. 2B-D). The total length increases significantly from 22 ± 4 µm in the newly hatched zoeae to 131 ± 1 µm in the newly molted juvenile (ANOVA, $F_{3,11} = 140$ $p < 0.001$; Fig. 2E) following a linear trend (Fig. 2F). The diameter varies from 62 ± 7 µm in the newly hatched zoeae to 78 ± 10 µm in the newly molted juvenile, the significant differences were marginal (ANOVA, $F_{3,7} = 4.94$ $p = 0.04$). Consequently, the AMC have a clear allometric growth where the relation length: diameter increases from 0.35 in ZI to 1.7 in J1 (ANOVA, $F_{3,7} = 65.2$ $p < 0.001$).

The PMC of the newly hatched zoeae is a very short blind-end tubule (Fig. 1B; 3A). The total length increases through the larval development (Fig. 3A-D), from 53 ± 10 µm in the newly hatched zoeae to 137 ± 1 µm in the newly molted juvenile (ANOVA, $F_{3,10} = 21.0$ $p < 0.001$; Fig. 3E) following a linear trend (Fig. 3F). The diameter varies from 42 ± 5 µm in the newly hatched zoeae to 57 ± 3 µm in the newly

molted juvenile, as occur with the AMC significant variation in the diameter was marginal (ANOVA, $F_{3,10} = 5.31$ $p = 0.02$). Then, the PMC has a clear allometric growth where the relation length: diameter varies approximately from 1.3 in ZI to 2.4 in J1 (ANOVA, $F_{3,10} = 7.96$ $p < 0.01$).

The anatomical organization of the AMC and PMC is very similar and therefore we describe it altogether (Fig. 4; 5). During the larval and first juvenile stages, the lumen of the midgut caeca is smooth and lined by a simple epithelium formed by short columnar to pyramidal cells crowned by short microvilli (Fig. 5). By contrast, the adult midgut caeca are internally folded (Fig. 4A-D, F; 9E). The epithelium is simple, tall columnar and large number of microvilli are present (Fig. 4A-D). The folds are internally filled by an extracellular matrix (Fig. 4D). The basal lamina is continued by a very thin layer of connective and muscles forms a network of myofibrils (Fig. 4A, D, G). The circular muscles forms helicoidal or diagonal rings of muscle fibers that surrounds the midgut caeca (Fig. 4G). The longitudinal muscles have not been identified.

Epithelial cells. Two cell types have been observed on the epithelium: epithelial cells and basal cells, although the basal cells only have been identified on the adults and represent less than the 10 % of the cell population (Fig. 4A-E; 5). During the larval and J1 stages, the height of the epithelial cells from the AMC measures 13 ± 2 μm (ranging from 10 to 17μm); while in the PMC their height is 7 ± 2 μm (ranging from 4 to 10 μm). The epithelial cells of the adults are taller, in the AMC they have a mean height of 54 ± 16 μm (ranging from 27 to 78 μm) while in the PMC the mean height is 77 ± 21 μm (ranging from 43 to 101 μm).

The epithelial cells have a polarized organization (Fig. 6A-C; 7A-D). The apical membrane forms slender and slightly undulated microvilli with an electron-dense apex, the microvilli are short during the larval stages and long during the adult stage (Fig. 6A-B; 7A-C; 9A-D, F). The microvilli are anchored by filaments that forms a terminal web like apical band (Fig. 6A-B; 7C; 9A-B). The lateral membranes are smooth and straight. In the cell apex, there are important cell-to-cell junctions extended up to 4-5 µm (Fig. 6A-B; 9A); these junctions are shorter on the larval stages (Fig. 7C). Near to the cell basis, the lateral membranes forms short interdigitations with the neighbor cells (Fig. 6A, C, F). The basal membrane is generally smooth with intercalated folds (Fig. 6C-F).

In all the life stages the cytoplasm of the epithelial cells is homogenously stained (Fig. 4B-C; 5C-F). Underlying the microvillous border of the adult cells there is a thin band of deeply stained cytoplasm (Fig. 4B, D). The cell apex contains small vesicles whose content varies from lucent to highly electron-dense (Fig. 6B; 7C), as well small multivesicular and multilamellar bodies. The cytoplasm has PAS positive granules (Fig. 4D). The cytoplasm of the epithelial cells varies from lucent and rich in ribosomes (Fig. 6B-C) to electron-dense and "saturated" in ribosomes (Fig. 9A-B). The nucleus is rounded to ellipsoidal and it is located medial to basally (Fig. 4B-C; 5). The nucleus generally contains less euchromatin than heterochromatin, and the euchromatin is distributed in patches adjacently to the nuclear membrane forming irregular clusters close to the nucleus center (Fig. 6B; 7D).

The density of cytoplasmic organelles is high, specially ribosomes, mitochondria and rough endoplasmic reticulum. The mitochondria are concentrated on the cell apex and basis (Fig. 6A-C; 7C-D). They are short, cylindrical rod to peanut-like organelles (ca. 1 µm in the adults and up to 3.5 µm in the larvae), whose matrix is more lucent in

the larvae than in the adults (Fig. 6B-C, E; 7C-D). In the larvae, the rough endoplasmic reticulum is composed by short and elongated cisternae that surround the mitochondria and nucleus (Fig. 7C-D); while in the adults it is composed by slender and large cisternae organized in parallel stacks aligned to the vertical cell axis (Fig. 6B) or in concentric rings. The smooth endoplasmic reticulum forms a band of branched, electron-dense tubules located near to the basal membrane, this band surrounds vesicles and mitochondria (Fig. 6C; 7D). Some tubules are fused with the basal membrane (Fig. 7D). The Golgi bodies are widely distributed on the cytoplasm and are very similar between larval and adult stages: the trans-cisternae are thin and packed stacks of lamellae while the cis-cisternae are globular, expanded and associated with numerous vesicles (Fig. 6D; 7E). In adults, the first basal third of the cell contains numerous diverse types of vesicles: small lucent vesicles, multivesicular bodies, multilamellar bodies and vesicles with double membrane whose content varies from lucent to electron-dense, including granulose matter.

Basal cells. The basal cells are small (ca. 7-10 µm diameter), rounded to ellipsoidal cells located adjacently to the basal lamina. Due to their small size (3-10 times smaller than the main epithelial cells) never reach the midgut lumen (Fig. 4E). The basal cells do not have any polarization on their cell membrane or cytoplasm. The cell membranes are smooth with sparse short undulations or irregularities (Fig. 8B). The nucleus is rounded and located centrally (Fig. 4E; 8A-B). The euchromatin is abundant and located adjacently to the nuclear membrane and on the nucleus center (Fig. 8A-B).The mitochondria are located around the nucleus, they are small (ca. 500 nm diameter) and rounded organelles. The presence of rough or smooth endoplasmic reticulum is unclear. Basal cells are characterized by the presence of medium sized vesicles whose diameter oscillates between 0.5 and 1.0 µm; the content of these vesicles

is highly electron-dense and varies from homogeneous to granular (Fig. 8D). Sparse lucent vesicles were occasionally observed (Fig. 8D).

The basal cells divide and differentiate into the epithelial cells. We observed a basal cell in advanced telophase stage of mitosis: the cell showed two nuclei located on opposite cell sides, as well as organelles with a mirrored distribution. Moreover, the same cell showed mixed features of both basal and epithelial cells: the cell size is small and the cytoplasm is lucent as in the basal cells; while the mitochondria and smooth endoplasmic reticulum are similar to the observed in the epithelial cells (Fig. 8C).

Secretory Activity of the Midgut Caeca. The adult midgut caeca have an important apocrine secretory activity based on the production of big vesicles from the cell apex and the production of small vesicles from the microvilli (Fig. 9A-B, D-G). The lumen of the larval caeca is filled by secretory vesicle like content, indicating that the secretory activity must be important during the larval stages although it has not been directly observed in the epithelial cells (Fig. 9C).The apocrine secretion from the cell apex starts as a bud in the apical membrane, this bud increases in volume while pushes aside the adjacent microvilli, acquiring a globular to columnar shape (Fig. 9A). The secretory vesicles usually contains one or more vesicles lined by a single membrane, the content of the vesicles varies from lucent to electron-dense depending of the density of granular aggregations.(Fig. 9A-B). Two types of vesicle release have been observed: the entire vesicle is released toward the caeca lumen or the vesicle break releasing content into the caeca lumen, this last case includes the secretion of small vesicles (Fig. 9B). The space occupied by the vesicle during their formation is maintained after its release as "empty spaces" or "holes" on the microvillous border(Fig. 9F). According to our

observations, the apocrine secretion occur on the entire epithelium of the midgut caeca, but the density of secretory vesicles is concentrated in the caeca folders(Fig. 9E).

The most interesting secretory activity observed in the adult midgut caeca is theapocrineactivity realized from the microvilli. This secretion consist on the formation and release of small vesicles from the microvilli;this process is observed more clearly on the microvilli tip. The vesicle formation startsas a reduction of the electron-density in the cytoplasm on a given microvillus tip, then this lucent area expand reaching a globular shape. This globular bud increases in diameter before their release into the caeca lumen (Fig. 9D, G; see numbered sequence).In the midgut caeca surface, this secretion type occur simultaneously with the apocrine secretionof big vesicles from the cell apex(Fig. 9F).

Discussion

The common spider crab has two types of long and coiled caeca with similar morphology but different location: a pair of anterior caeca projected from the antero-dorsal midgut tip and a single posterior caeca projected from the midgut side of the midgut-hindgut junction. Henri Milne-Edwards (1834a; b) illustrated the digestive system of the genus *Maja* sp. with similar caeca in the same location (AMC as "coecums pyloriques" and PMC as "coecums postérieurs") and considered the three caeca as secretory organs. The caeca number, morphology and location described in *M. brachydactyla* is shared and widespread among the brachyurans as reviewed by Smith (1978), but varies among higher Malacostraca taxa (Table 1).

The AMC of the malacostracans received numerous names since their description: "anterior diverticula", "appendices pyloriques", "coeca anteriores dorsalia", "coecums pyloriques", "dorsal caecum", "midgut caeca" or "pyloric caeca" (Barker and

Gibson, 1977; Milne-Edwards, 1834a; Pugh, 1962; Reddy, 1937; Smith, 1978; Yonge, 1924). The AMC of the adult *M. brachydactyla* are long blind-end tubules projected forward and coiled toward the pyloric stomach walls forming disc-shaped structures, as they have been typically observed in other brachyurans species (Barker and Gibson, 1978; Reddy, 1937; Smith, 1978; Trinadha Babu et al., 1989). However, the shape of the AMC varies among the malacostracans. In astacids as *Homarus gammarus* they fused into a short bud (Barker and Gibson, 1977), while in the amphipods one of the three AMC is a projection longer than the other two (Davolos et al., 2010; Schmitz and Scherrey, 1983). Similarly to the AMC, the PCM also received numerous names: "appendice coecal", "coecums postérieurs", "dorsal diverticulum", "hindgut caecum", "intestinal caecum", "posterior diverticulum", "rectal caecum" or "tubular gland" (Barker and Gibson, 1977; Milne-Edwards, 1834a; Pugh, 1962; Reddy, 1937; Smith, 1978; Yonge, 1924). The PMC of *M. brachydactyla* is a single and unpaired long blind-end tubule that arises from the midgut side of the midgut-hindgut junction, as it has been described in numerous brachyurans (Smith, 1978; Trinadha Babu et al., 1989). Reddy (1937) and Pugh (1962) termed the PMC as "hindgut caecum" since considered that it is originated from the hindgut side of the midgut-hindgut junction. However, our observations confirm that the PMC is originated in the midgut side. Moreover, the anatomical and ultrastructural features of the PMC coincide to the observed in the midgut tract (microvilli, secretory activity and smooth lateral membranes) rather than to the hindgut (cuticle, bundles of filament-like structures and large interdigitations) (Komuro and Yamamoto, 1968; Mykles, 1979; Witkus et al., 1969). Smith (1978) in his study of the brachyuran midgut caeca also concluded the PMC arise from the midgut side. The PMC shape also varies among taxa, while in *M. brachydactyla* the first part of the PMC is parallel to the hindgut tract, in astacids the PMC wraps the hindgut tract

(Barker and Gibson, 1977; Yonge, 1924) and in penaeids acquires a cauliflower-like shape (Lovett and Felder, 1989; 1990b; Muhammad et al., 2012).

The newly hatched larvae (first zoeal stage) of *M. brachydactyla* have a pair of anterior buds that will develop into a pair of short AMC few days later, as well a single posterior caecum with finger like appearance. This description coincides with the anatomical study realized by C. Schlegel (1911) in a given species of the genus *Maja* during the first zoeal stage: none reference to the AMC was reported, but a small and single caecum is mentioned in the posterior end of the midgut (termed "intestine"). The presence of a pair of AMC during the zoeal stages also have been noticed in other brachyurans as *Portunus trituberculatus* (Nakamura, 1990) and *Scylla olivacea* (Jantrarotai and Sawanyatiputi, 2005). In *M. brachydactyla*, during the larval development the morphology of the midgut caeca do not change, only a length increment was observed, the AMC of the anomuran *Paralithodes camtschaticus* also enlarges during the larval development (Abrunhosa and Kittaka, 1997). In other decapods, the midgut caeca development is different. The newly hatched larvae have a pair of active AMC, but during the development the caeca degenerate and fuse into a single short caecum in *Homarus americanus* (Factor, 1981; Hinton and Corey, 1979), *Penaeus setiferus* (Lovett and Felder, 1989) and *Penaeus vannamei* (Muhammad et al., 2012). For some authors, the degeneration of the larval AMC occur after the depletion of their yolk reserves (Factor, 1981; Hinton and Corey, 1979). In *M. brachydactyla,* the PMC was observed since hatching and it elongates gradually during the larval development. Similarly, the PCM is a small bud that increases in length with the larval development in *H. americanus* (Factor, 1981; Hinton and Corey, 1979) and the animal growth in the fiddler crabs of the genus *Uca* (Pugh, 1962). In *P. camtschaticus* the PMC appears in the late glaucothoe stage (Abrunhosa and Kittaka, 1997). By contrast, the

"midgut caecum" described in the pre-zoeal stage of *Porcellana platycheles* presumably correspond to the PMC (Williams, 1944). In peneids during the juvenile growth the PMC acquires a sac-like structure and shortly develop the adult cauliflower-like shape (Lovett and Felder, 1989; 1990b; Muhammad et al., 2012). These data suggest that the caeca ontogeny is species specific.

The simple epithelium of the midgut caeca of *M. brachydactyla* form short longitudinal folds composed by sparse short basal cells and columnar epithelial cells with microvillous border. These features are shared with other brachyurans (Barker and Gibson, 1978; Erri Babu et al., 1982). In the genus *Uca* the epithelium is described as pseudostratified (Pugh, 1962). The epithelium of *M. brachydactyla* rest over a basal lamina, surrounded in turn by a connective layer encircled by a thin network of muscle fibers. Similar description is presented in the brachyuran *Menippe rumphii* (Erri Babu et al., 1982). In *Scylla serrata* muscle bands were considered "absent" (Barker and Gibson, 1978).

In *M. brachydactyla*, the epithelial cells have a cell apex rich in microvilli and mitochondria, the rough endoplasmic reticulum is mainly supranuclear, the Golgi bodies are well developed, the rounded nucleus is medial to basal and the cell basis has mitochondria, diverse vesicles and smooth endoplasmic reticulum. A similar ultrastructure has been observed in the midgut caeca of the grapsid *Pachygrapsus crassipes*, but differs from our description by the presence of apical smooth endoplasmic reticulum (Mykles, 1977). In the crayfish *Procambarus clarkii* the epithelial cell ultrastructure is also similar, being observed a basal "unusual membranous structure" that could correspond to smooth endoplasmic reticulum (Komuro and Yamamoto, 1968). The epithelium of this crayfish species also contains

sparse basal cells as short rounded cells that does not reach the caeca lumen (Komuro and Yamamoto, 1968). Similar cells have been observed on the midgut tract and midgut gland of *M. brachydactyla* (unpublished data). Pugh (1962) described similar cells in the midgut of the fiddler crabs, the author postulated a role involved in division and regeneration processes and mentioned basal cells in various degrees of mitosis. This hypothesis is also supported by our data, since we observed a basal cell in advanced stage of division and differentiation.

The function of the midgut caeca is currently subject of controversy. As above mentioned, during the larval development of *H. americanus* the AMC are involved in the yolk digestion and absorption and degenerate shortly after the yolk depletion (Factor, 1981; Hinton and Corey, 1979). In other decapods the role of the midgut caeca shift during the development. In the protozoeal and mysis stages of *P. monodon* the AMC apparently realizes the midgut gland function until this organ is fully developed in the juvenile stages (Abubakr and Jones, 1992). Similarly, in *P. setiferus* the production of enzymes by the AMC cease during the juvenile development (Lovett and Felder, 1990a). These examples differ from our observations in *M. brachydactyla*, where none yolk reserve was observed and the midgut caeca are not vestigial organs. On the contrary, they increases in length during the development until they become long and coiled blind-end tubules with important secretory activity. The epithelial cells of the midgut caeca of *M. brachydactyla* have features that suggest a secretory role, as the abundance of apical mitochondria, rough endoplasmic reticulum and Golgi bodies. Moreover, our observations show a high secretory activity that probably occur during the larval stages, since the lumen of the larval midgut caeca is filled by vesicles similar to the observed in the adults.

The epithelial cells of the midgut caeca of *M. brachydactyla* show an important secretory activity by the production and release of big secretory vesicles from the cell apex. Pugh (1962) did not observed apocrine but merocrine secretory activity in the midgut caeca of the *Uca* sp. fiddler crabs; while Dall (1967) did not mentioned apocrine activity but observed numerous vesicles in the caeca lumen of *P. bennettae*. Pinn et al. (1999) described in Axiidea and Gebiidea numerous "coccoid bodies" similar to the big secretory vesicles observed by scanning microscopy in this study, as well "pores" similar to the "vesicle holes". Another interesting secretory activity is the production of micro-vesicles realized from the microvilli. The midgut caeca of *M. brachydactyla* have an important secretory activity that consists on the extrusion of small vesicles from the microvilli (sides and tips). This type of secretion has been widely reported in the insect midgut tract and usually receives the name of the "microapocrine mechanism" or "microapocrine route" (Cristofoletti et al., 2001; Ferreira et al., 1990; Monteiro et al., 2014; Silva et al., 2013). Our observations realized in *M. brachydactyla* are the first report of this type of secretion in a Decapoda midgut organ. Sonakowska et al. (2015) mentioned "microapocrine" secretion in the midgut tract epithelial cells of the caridean *Neocaridina heteropoda* as "small bulges of microvilli", however their observations correspond to the "common" microvilli shape. In Coleoptera and Lepidoptera larvae these small vesicles contain digestive enzymes, including amylase, lipase and peptidases/proteases that can associate to the peritrophic membrane (Bolognesi et al., 2001; Cristofoletti et al., 2001; Silva et al., 2013). In this sense, amylolytic and proteolytic activity has been detected in a brachyuran caeca fluids (Holliday et al., 1980). Then, it is possible that the midgut caeca have a role in the digestive process.

Another potential role of the midgut tract is the production of peritrophic membrane. The peritrophic membrane is an extracellular secretion that surrounds the

digested/fecal matter during their pass through the midgut and hindgut tract (Lehane, 1997; Martin et al., 2006). Nevertheless, Holliday et al. (1980) demonstrated that the ligation of the AMC did not affected the production of peritrophic membrane in the brachyuran *Metacarcinus magister* (as *Cancer magister*). Other hypothesis suggest that the midgut caeca are involved with the absorption and storage of nutrients but Smith (1978) did not observed charcoal in the midgut caeca of *Carcinus* sp. after feeding them with powered charcoal and Dall (1967) in *P. bennettae* did not found food matter on the midgut caeca. Further hypothesis suggest that the midgut are involved with osmoregulatory processes, but in the grapsid *Pachygrapsus crassipes* the physiological response of the PMC to hyposaline conditions was more associated with degenerative stress rather than with an osmoregulatory response (Mykles, 1977). Moreover, in *M. magister* the AMC did not show a osmoregulatory associated response after exposition to osmotic stress (Holliday et al., 1980).

Acknowledgements

Financial support provided by the Spanish Ministry of Economy and Competitiveness through the INIA project [grant number RTA2011-00004-00-00] to G.G. and a predoctoral fellowship to D.C. [FPI-INIA]. The authors would like to thank to the technicians at IRTA, Sant Carles de la Ràpita (David Carmona, Glòria Macià, Magda Monllaó, Francesc X. Ingla and Olga Bellot) and CCiTUB Hospital Clinic, Barcelona (Adriana Martínez, Almudena García, José Manuel Rebled and Rosa Rivera) for their assistance.

Table 1. Presence and number of anterior midgut caeca (AMC) and posterior midut caeca (PMC) in different Malacostraca taxa.

Species	Taxa	AMC	PMC	References
Hyalella azteca Saussure, 1858	Amphipoda	3	2	(Schmitz and Scherrey, 1983)
Macarorchestia remyi (Schellenberg, 1950)	Amphipoda	3	2	(Davolos et al., 2010)
Galathea squamifera Leach, 1815	Anomura	0	0	(Smith, 1978)
Lithodes maja (Linnaeus, 1758)	Anomura	2	1	(Smith, 1978)
Paralithodes camtschaticus (Tilesius, 1815)	Anomura	2	1	(Abrunhosa and Kittaka, 1997)
Homarus gammarus (Linnaeus, 1758)	Astacidea	1	1	(Barker and Gibson, 1977)
Nephrops norvegicus (Linnaeus, 1758)	Astacidea	1	1	(Smith, 1978)
Crangon crangon (Linnaeus, 1758)	Caridea	0	0	(Smith, 1978)
Neocaridina heteropoda Liang, 2002	Caridea	0	0	(Sonakowska et al., 2015)
Palaemonetes argentinus Nobili, 1901	Caridea	0	0	(Sousa and Petriella, 2007)
Cancer pagurus Linnaeus, 1758	Brachyura	2	1	(Smith, 1978)
Carcinus maenas (Linnaeus, 1758)	Brachyura	2	1	(Smith, 1978)
Hyas araneus (Linnaeus, 1758)	Brachyura	2	1	(Smith, 1978)
Macropipus depurator (Linnaeus, 1758)	Brachyura	2	1	(Smith, 1978)
Maja brachydactyla Balss, 1922	Brachyura	2	1	Present study
Metacarcinus magister Dana, 1852	Brachyura	2	1	(Mykles, 1979)
Oziothelphusa senex (Fabricius, 1798)	Brachyura	2	1	(Smith, 1978)
Parathelphusa convexa De Man, 1879	Brachyura	2	1	(Smith, 1978)
Scylla serrata (Forskål, 1775)	Brachyura	2	1	(Barker and Gibson, 1978)
Spiralothelphusa hydrodroma (Herbst, 1794)	Brachyura	2	1	(Reddy, 1937)
Penaeus bennettae R. & D., 1965	Dendrobranchiata	2	1	(Dall, 1967)
Penaeus setiferus (Linnaeus, 1767)	Dendrobranchiata	1	1	(Lovett and Felder, 1990a)
Penaeus vannamei (Boone, 1931)	Dendrobranchiata	1	1	(Muhammad et al., 2012)
Armadillidium arnasus Budde-Lund, 1885	Isopoda	0	0	(Schmitz and Schultz, 1969)
Armadillidium vulgare (Latreille, 1804)	Isopoda	0	0	(Schmitz and Schultz, 1969)

Table 1 (continuation). Presence and number of anterior midgut caeca (AMC) and posterior midut caeca (PMC) in different Malacostraca taxa.

Species	Taxa	AMC	PMC	References
Axius stirhynchus Leach, 1815	Axiidea	0	1	(Pinn et al., 1999)
Callianassa subterranea (Montagu, 1808)	Axiidea	0	1	(Pinn et al., 1999)
Calocaris macandreae Bell, 1853	Axiidea	0	1	(Pinn et al., 1999)
Jaxea nocturna Nardo, 1847	Gebiidea	0	1	(Pinn et al., 1999)
Upogebia pusilla (Petagna, 1792)	Gebiidea	0	1	(Pinn et al., 1999)

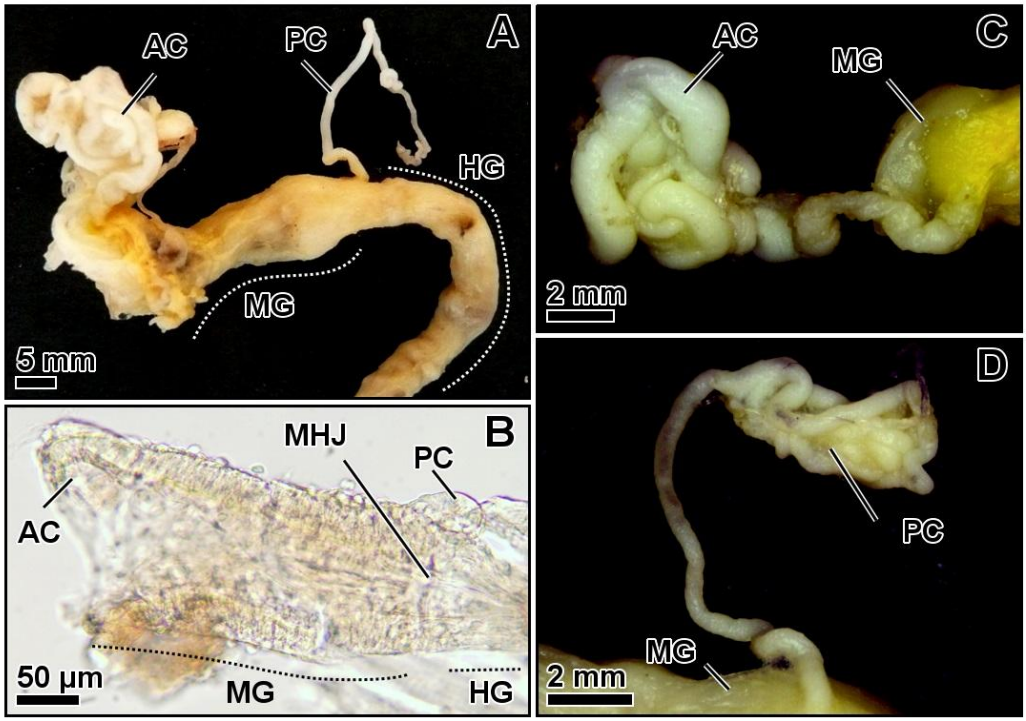

Figure 1. *Maja brachydactyla*. Midgut caeca, fixed with 4 % formaldehyde. Adult, midgut tract and associated caeca (A). Zoea I, newly hatched zoeae, midgut tract and associated caeca (B). Adult, close view of the midgut tract caeca (C-D): anterior midgut caeca (C) and posterior midgut caecum (D). Abbreviations: AC, anterior midgut caeca; HG, hindgut tract; MG, midgut tract; MHJ, midgut-hindgut junction; PC, posterior midgut caecum.

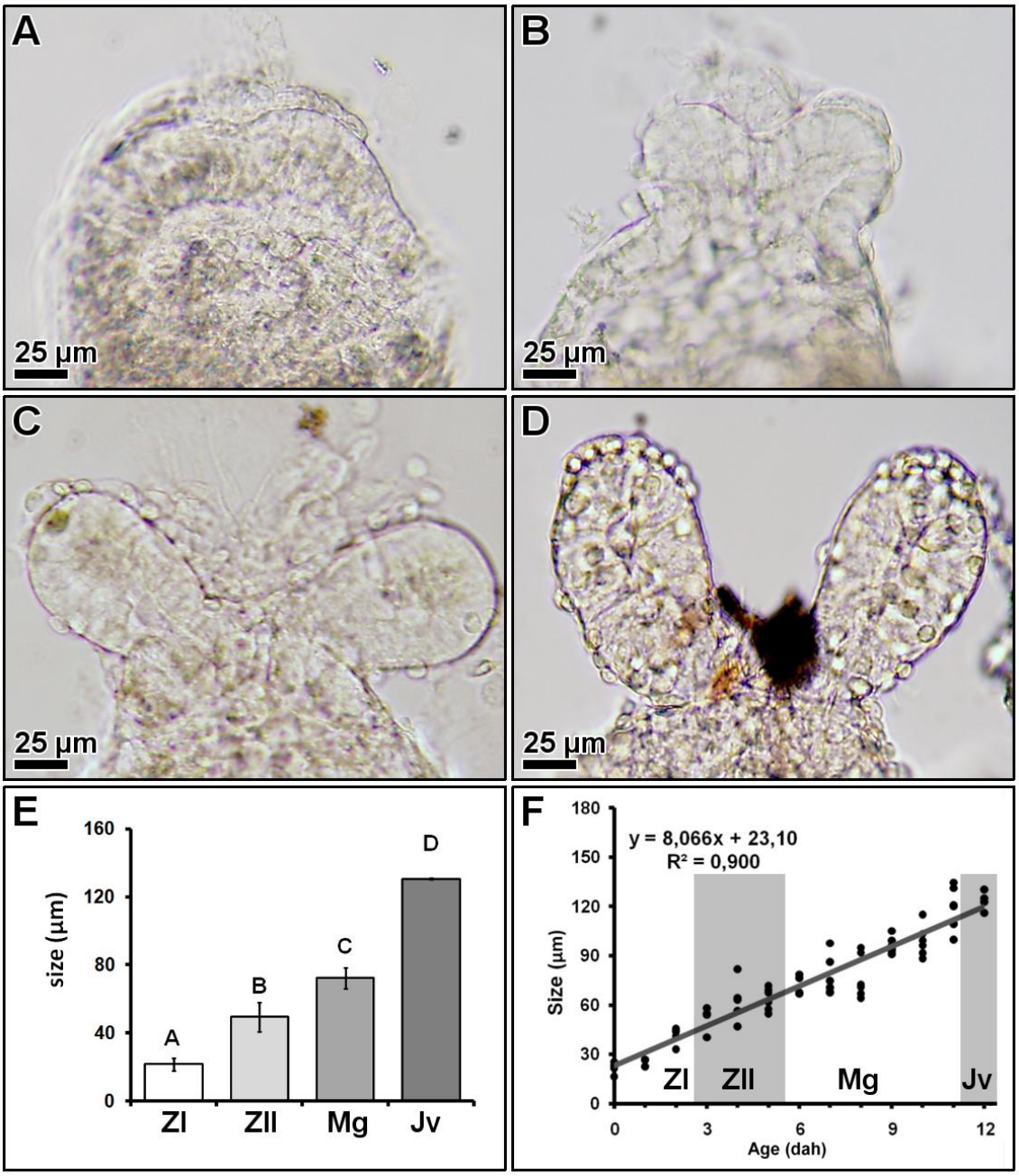

Figure 2. *Maja brachydactyla*. Ontogeny of the anterior midgut caeca, optical microscope (A-D): zoea I, 0 days after hatching (dah) (A); zoea II, 3 dah (B); megalopa, 7 dah (C); first juvenile, 12 dah (D). Length of the anterior midgut caeca at the start of each larval stage (E). Growth of the anterior midgut caeca in length during the larval development, mean ± SD (F). Increment of the mean anterior caeca length through the larval development.

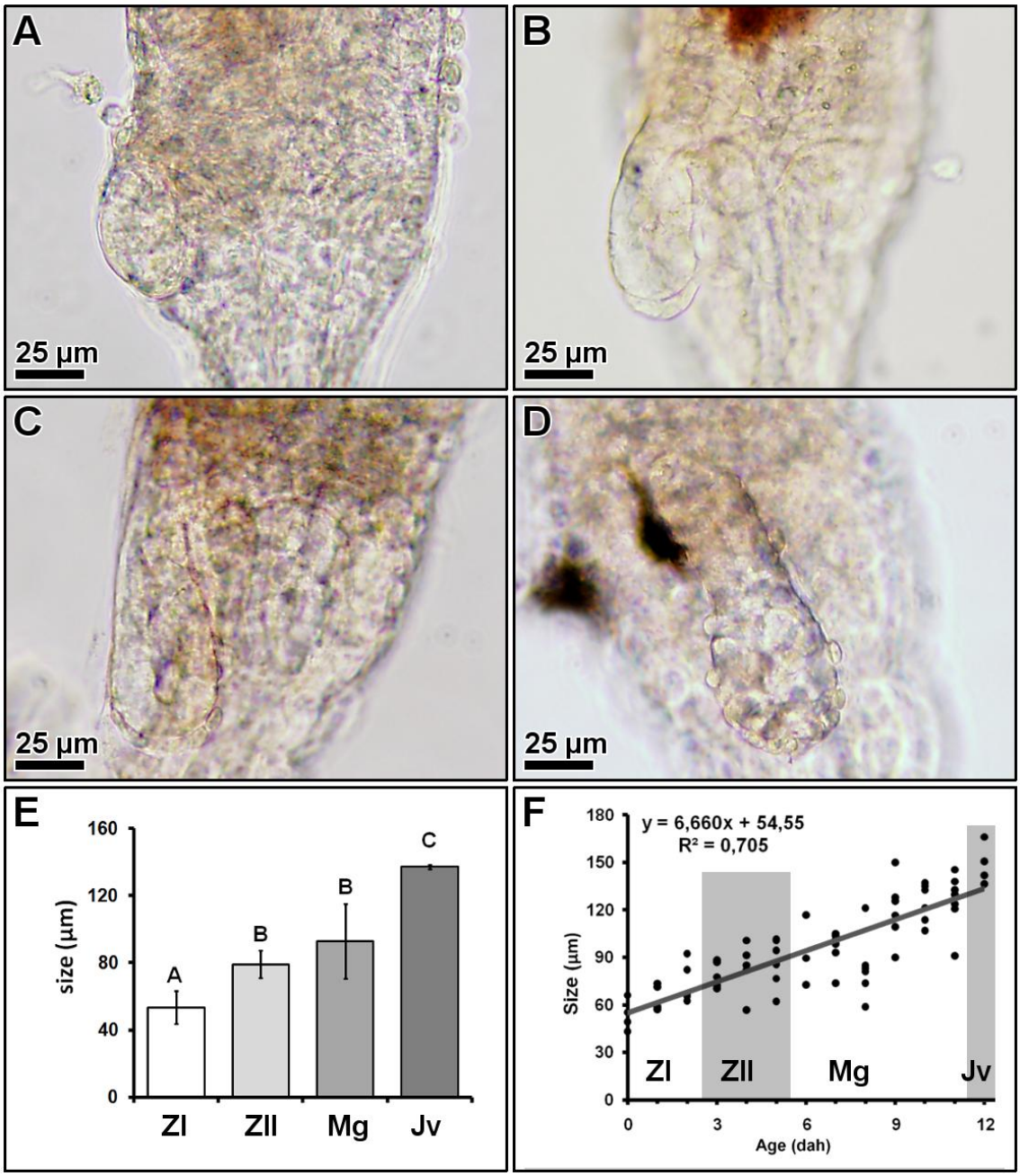

Figure 3. *Maja brachydactyla*. Ontogeny of the posterior midgut caeca, optical microscope (A-D): zoea I, 0 days after hatching (dah) (A); zoea II, 3 dah (B); megalopa, 7 dah (C); first juvenile, 12 dah (D). Length of the anterior midgut caeca at the start of each larval stage, mean ± SD (E). Growth of the anterior midgut caeca in length during the larval development (F). Increment of the mean anterior caeca length through the larval development.

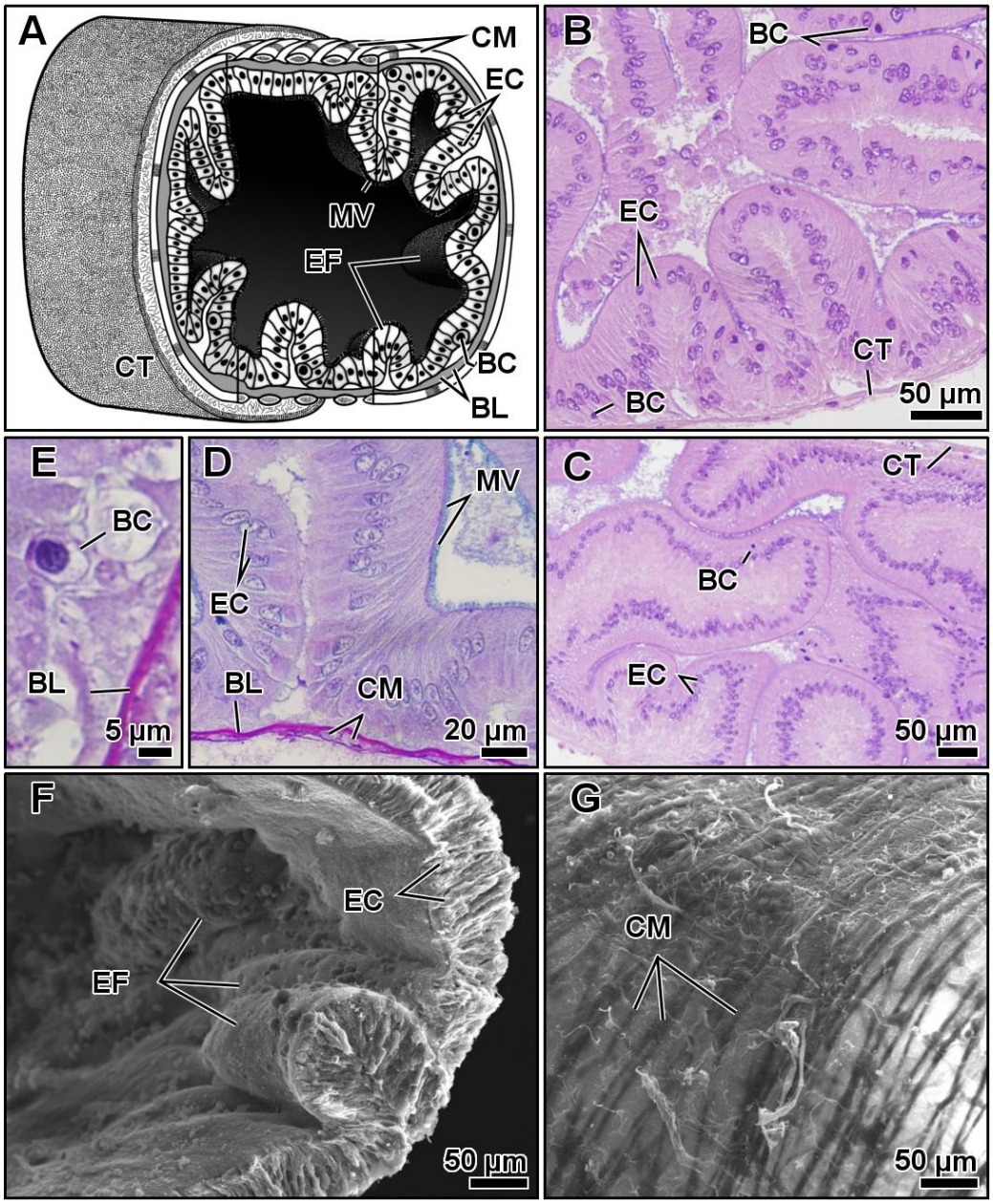

Figure 4. *Maja brachydactyla*. Adult. Midgut caeca, histology and morphology. General diagram (A). Histological organization of the midgut caeca, Hematoxylin-Eosin (B-C): anterior midgut caeca (B) and posterior midgut caecum (C). Close view of the epithelium, anterior midgut caeca, PAS and Alcian Blue contrasted with Hematoxylin (D). Close view of basal cell, anterior midgut caeca, PAS and Alcian Blue contrasted with Hematoxylin (E). Morphology of the anterior midgut caeca, SEM (F-G): lumen showing some folds (F) and surrounding muscle fibers (G). Abbreviations: BC, basal cell; CM, circular muscle fiber; CT, connective tissue; EC, epithelial cells; EF, epithelial folds; MV, microvilli.

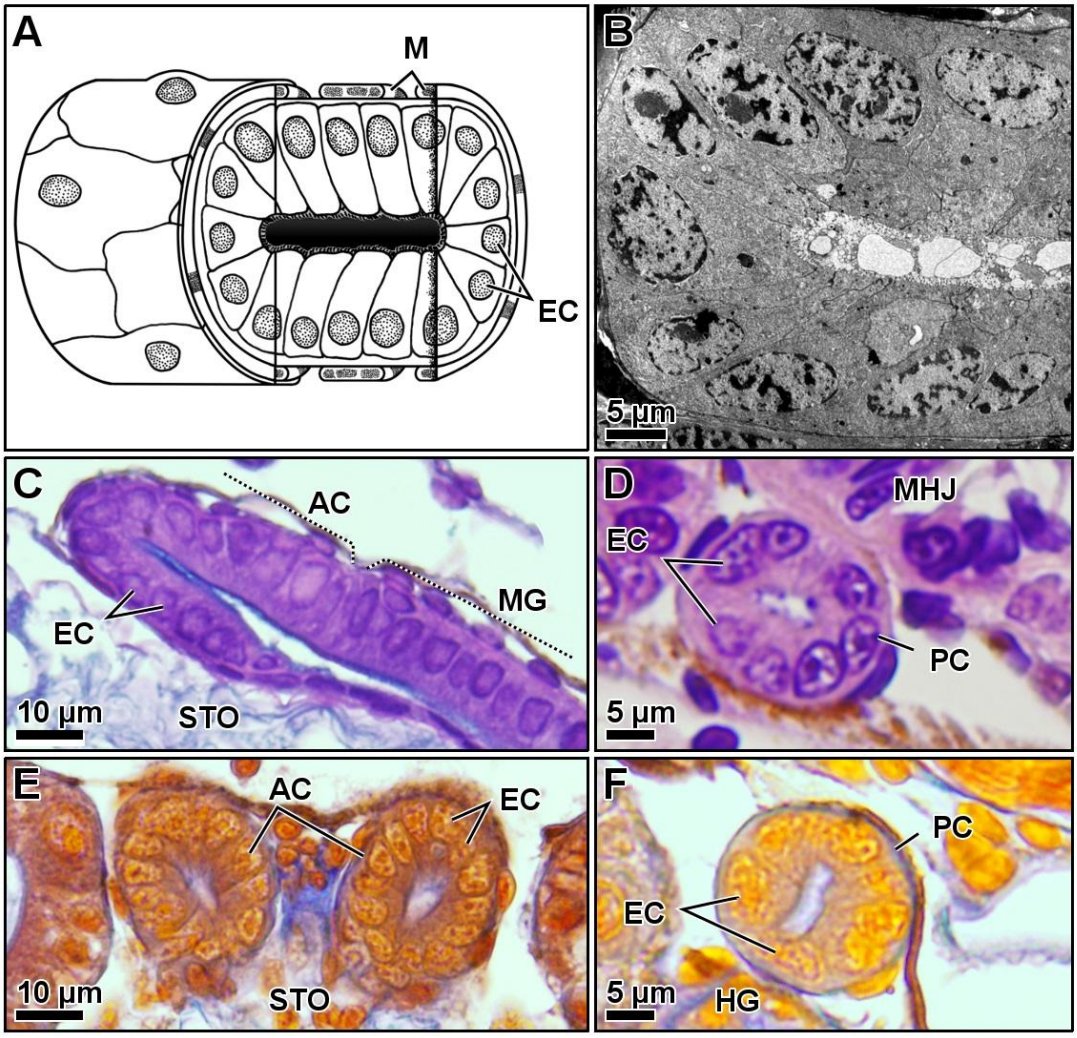

Figure 5. *Maja brachydactyla*. Larvae. Midgut caeca, histology. General diagram (A). Zoea II, 6 days after hatching (dah), transversal section of the anterior midgut caeca, TEM (B). Anterior midgut caeca (C, E): Zoea II, 5 dah, longitudinal section, Hematoxylin-Eosin (C); megalopa, 6 dah, transversal section, Mallory's trichrome (E). Posterior midgut caecum, transversal section (D, F): megalopa, 6 dah, Hematoxylin-Eosin (C); megalopa, 10 dah, Mallory's trichrome (E). Abbreviations: AC, anterior midgut caeca; EC, epithelial cells; HG, hindgut tract; MHJ, midgut-hindgut junction; M, muscles; MG, midgut tract; PC, posterior midgut caecum; STO, stomach.

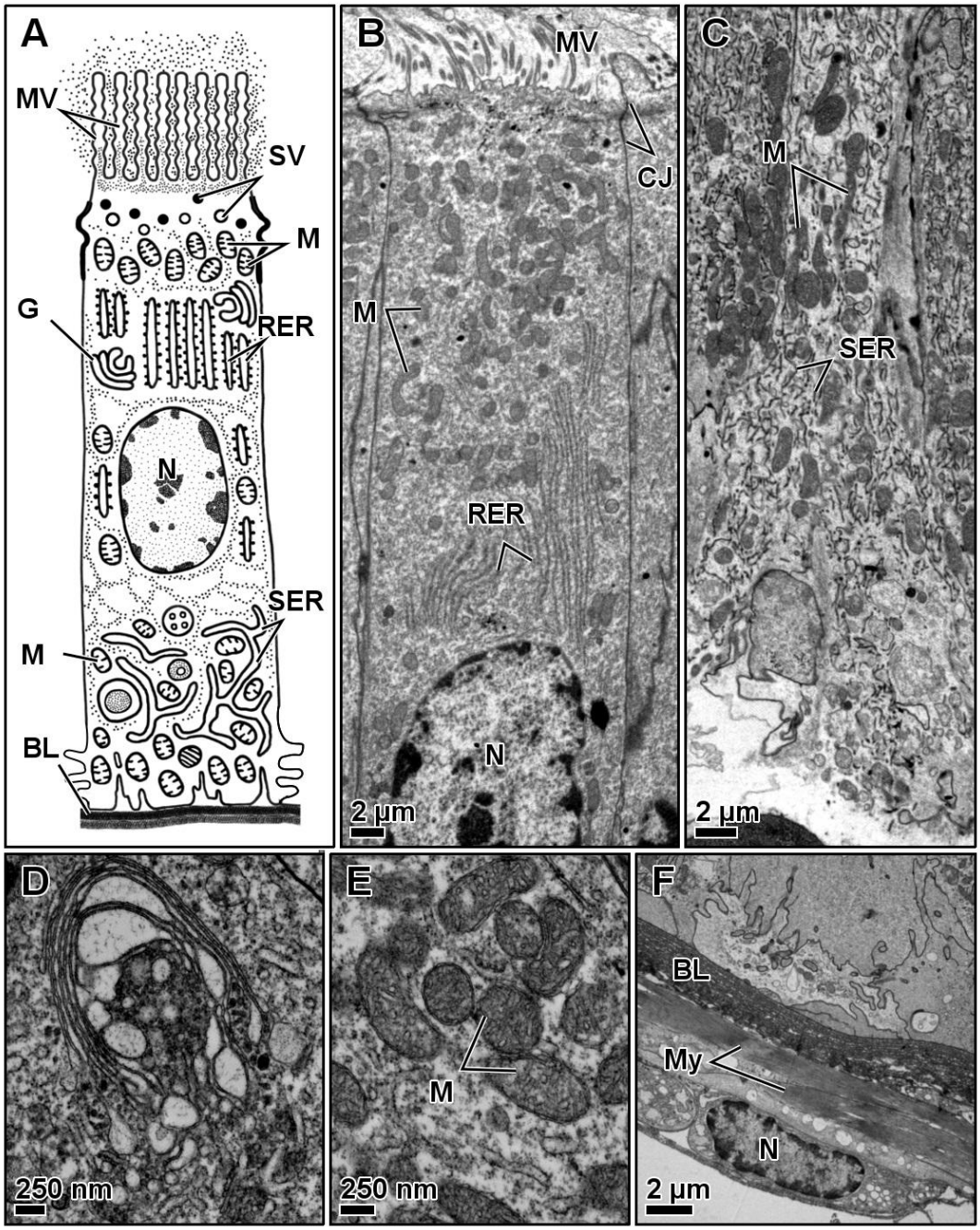

Figure 6. *Maja brachydactyla*. Adult. Midgut caeca. Ultrastructure of the epithelial cells. General diagram (A). Cell apex, supranuclear region (B). Cell basis, infranuclear region (C). Close view of a Golgi body (D). Close view of the mitochondria (E). Basal lamina and muscle fibers (F). Abbreviations: BL, basal lamina; CJ, cell-to-cell junction; G, Golgi body; M, mitochondria; MV, microvilli; My, myofibrils; N, nucleus; RER, rough endoplasmic reticulum; SER, smooth endoplasmic reticulum.

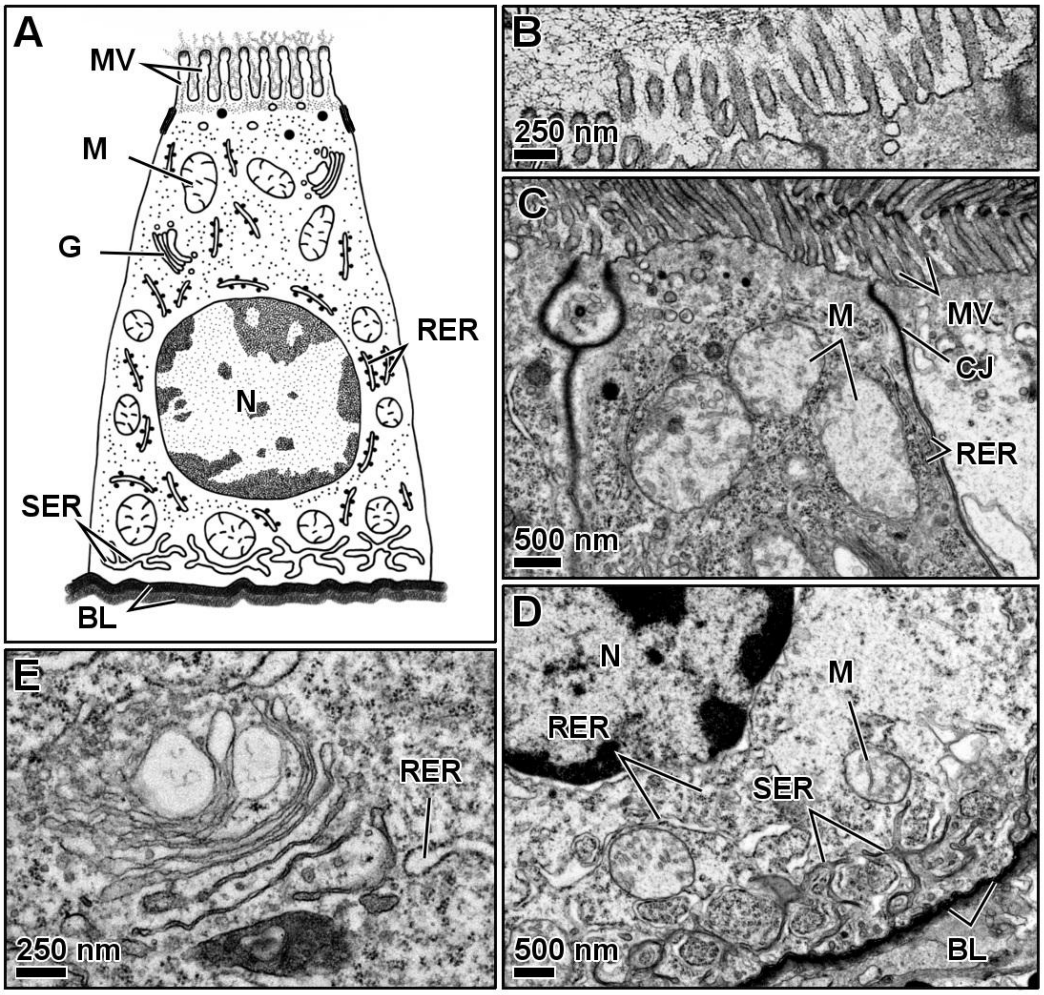

Figure 7. *Maja brachydactyla*. Larvae. Midgut caeca. Ultrastructure of the epithelial cells. General diagram (A). Cell apex, supranuclear region (B-C): close view of the microvilli (B) and general view (C). Cell basis, infranuclear region (D). Close view of a Golgi body (E). Abbreviations: BL, basal lamina; CJ, cell-to-cell junction; G, Golgi body; M, mitochondria; MV, microvilli; N, nucleus; RER, rough endoplasmic reticulum; SER, smooth endoplasmic reticulum.

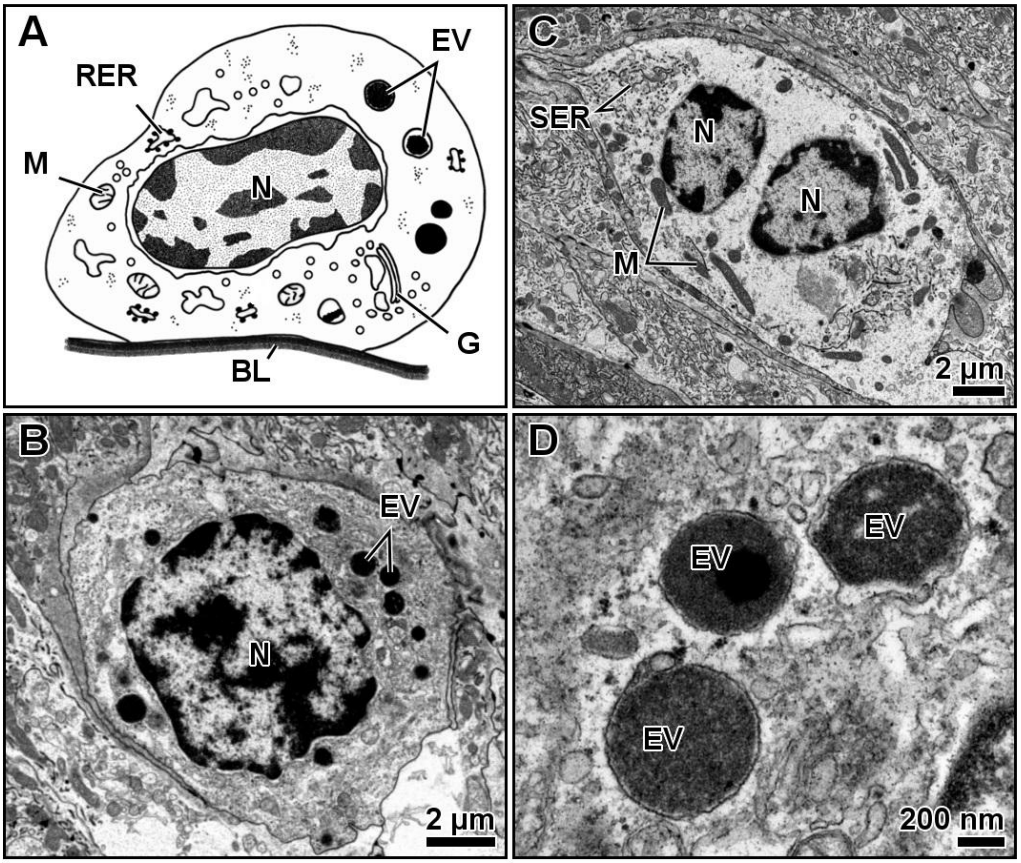

Figure 8. *Maja brachydactyla*. Adult. Midgut caeca. Ultrastructure of the basal cells. General diagram (A). General view (B). Basal cells in advanced stage of division and differentiation (C). Close view of the electron-dense vesicles (D). Abbreviations: BL, basal lamina; EV, electron-dense vesicles; G, Golgi body; M, mitochondria; N, nucleus; RER, rough endoplasmic reticulum; SER, smooth endoplasmic reticulum.

Figure 9 (next page). *Maja brachydactyla*. Midgut caeca. Adult anterior midgut caeca, apocrine secretion of the epithelial cells, TEM (A-B): formation of the vesicles (A); release of the vesicles (B). Anterior midgut caeca of the larvae, lumen filled by secretory vesicles, TEM (C). Adult, anterior midgut caeca, production of micro-vesicles by the microvilli (numbered), TEM (D). Adult, anterior midgut caeca, epithelial fold filled by secretory vesicles, SEM (E). Adult, posterior midgut caecum, apocrine secretion, SEM (F-G): secretory vesicles produced from the cell apex (F); production of micro-vesicles by the microvilli (numbered) (G). Abbreviations: CJ, cell-to-cell junction; SV, secretory vesicles; VH, vesicle "hole".

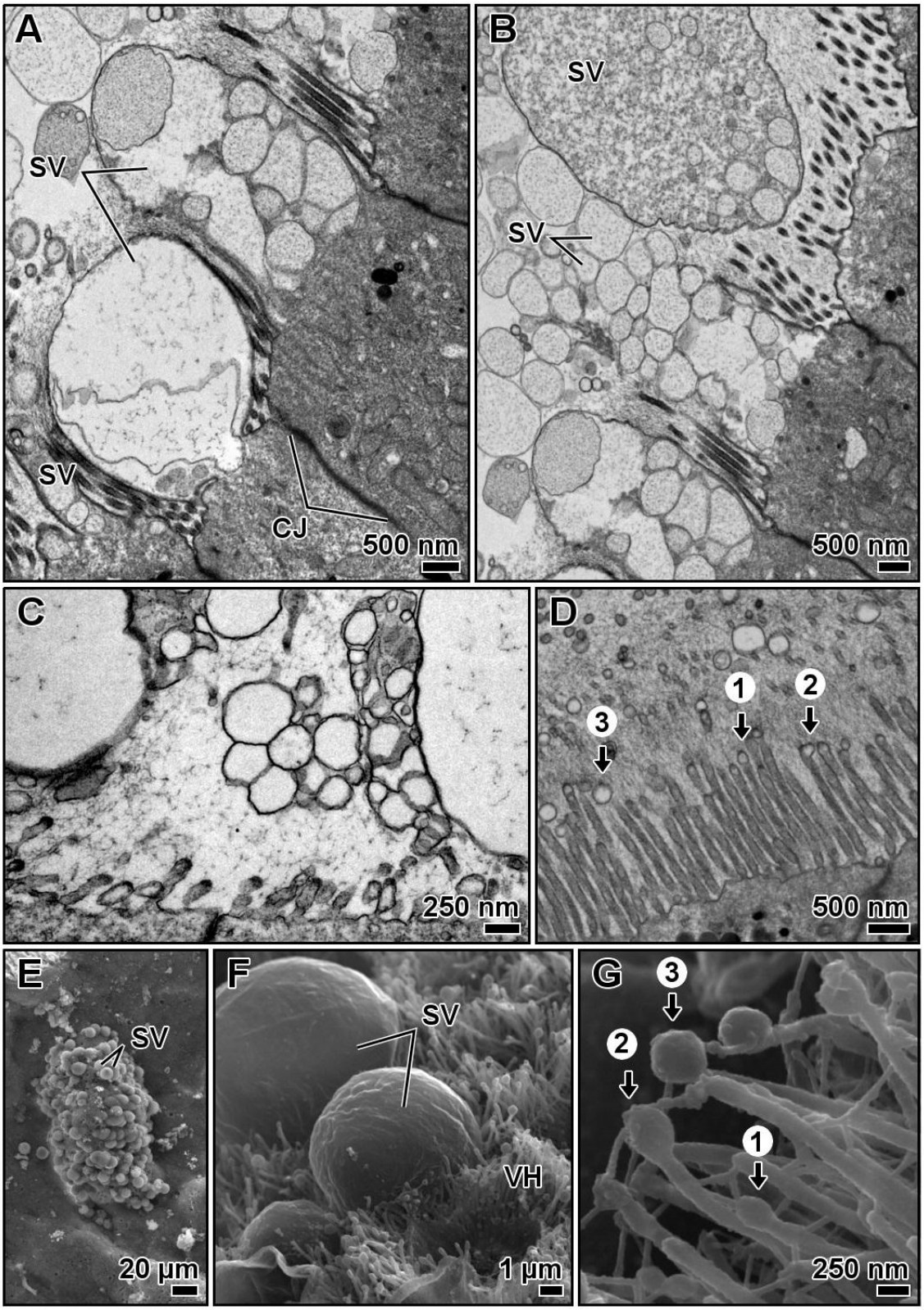
A
SV
SV
CJ
500 nm
B
SV
SV
500 nm
C
250 nm
D
1
2
3
500 nm
E
SV
20 µm
F
SV
VH
1 µm
G
3
2
1
250 nm

Bibliography.

Abelló P, García Raso JE, Guerao G, Salmerón F. 2014. *Maja brachydactyla* (Brachyura: Majidae) in the western Mediterranean. Marine Biodiversity Records 7(e77).

Abrunhosa FA, Kittaka J. 1997. Morphological changes in the midgut, midgut gland and hindgut during the larval and postlarval development of the red king crab *Paralithodes camtschaticus*. Fisheries Science 63(5):746-754.

Abubakr MA, Jones DA. 1992. Functional morphology and ultrastructure of the anterior mid-gut diverticulae of larvae of *Penaeus monodon* Fabricius, 1798 (Decapoda, Natantia). Crustaceana 62(2):142-158.

Andrés M, Gisbert E, Díaz M, Moyano FJ, Estévez A, Rotllant G. 2010. Ontogenetic changes in digestive enzymatic capacities of the spider crab, *Maja brachydactyla* (Decapoda: Majidae). J Exp Mar Biol Ecol 389(1-2):75-84.

Barker PL, Gibson R. 1977. Observations on the feeding mechanism, structure of the gut, and digestive physiology of the european lobster *Homarus gammarus* (L.) (Decapoda: Nephropidae). J Exp Mar Biol Ecol 26(3):297-324.

Barker PL, Gibson R. 1978. Observations on the structure of the mouthparts, histology of the alimentary tract, and digestive physiology of the mud crab *Scylla serrata* (Forskål) (Decapoda: Portunidae). J Exp Mar Biol Ecol 32(2):177-196.

Bolognesi R, Ribeiro AF, Terra WR, Ferreira C. 2001. The peritrophic membrane of *Spodoptera frugiperda*: Secretion of peritrophins and role in immobilization and recycling digestive enzymes. Archives of Insect Biochemistry and Physiology 47(2):62-75.

Castejón D, Rotllant G, Ribes E, Durfort M, Guerao G. 2015. Foregut morphology and ontogeny of the spider crab *Maja brachydactyla* (Brachyura, Majoidea, Majidae). J Morphol 276(9):1109-1122.

Ceccaldi HJ. 1989. Anatomy and physiology of digestive tract of Crustaceans Decapods reared in aquaculture. Advances in Tropical Aquaculture, Workshop at Tahiti, French Polynesia. Tahiti, French Polynesia: Actes de colloques Ifremer. p 243-259.

Clark PF. 1986. The larval stages of *Maja squinado* (Herbst, 1788) (Crustacea: Brachyura: Majidae) reared in the laboratory. Journal of Natural History 20(4):825-836.

Cristofoletti PT, Ribeiro AF, Terra WR. 2001. Apocrine secretion of amylase and exocytosis of trypsin along the midgut of *Tenebrio molitor* larvae. Journal of Insect Physiology 47(2):143-155.

Dall W. 1967. The functional anatomy of the digestive tract of a shrimp *Metapenaeus bennettae* Racek & Dall (Crustacea : Decapoda : Penaeidae). Australian Journal of Zoology 15(4):699-714.

Davolos D, L. P, Accordi F, De Matthaeis E. 2010. Morphology and histology of the mouthparts and gut system of *Macarorchestia remyi* (Schellenberg, 1950) (Amphipoda, Talitridae). Zoologia Baetica 21:151-178.

Erri Babu D, Shyamasundari K, Rao KH. 1982. Studies on the digestive system of the crab *Menippe rumphii* (Fabricius) (Crustacea:Brachyura). J Exp Mar Biol Ecol 58(2):175-191.

Factor JR. 1981. Development and metamorphosis of the digestive system of larval lobsters, *Homarus americanus* (Decapoda: Nephropidae). J Morphol 169:225-242.

FAO. 2014. B-42 Crabs, sea-spiders. Capture production by species, fishing areas and countries or areas. In: FAO, editor. FAO yearbook Fishery and aquaculture statistics. Rome: FAO.

Felgenhauer BE. 1992. Chapter 3. Internal Anatomy of the Decapoda: An Overview. In: Harrison FW, Humes AG, editors. Microscopic Anatomy of Invertebrates Volume 10: Decapod Crustacea: Wiley-Liss, Inc. p 45-75.

Ferreira C, Bellinello GL, Ribeiro AF, Terra WR. 1990. Digestive enzymes associated with the glycocalyx, microvillar membranes and secretory vesicles from midgut cells of *Tenebrio molitor* larvae. Insect Biochemistry 20(8):839-847.

Guerao G, Pastor E, Martin J, Andrés M, Estévez A, Grau A, Duran J, Rotllant G. 2008. The larval development of *Maja squinado* and *M. brachydactyla* (Decapoda, Brachyura, Majidae) described from plankton collected and laboratory-reared material. Journal of Natural History 42(33-34):2257-2276.

Hinton DJ, Corey S. 1979. The mouthparts and digestive tract in the larval stages of *Homarus americanus*. Canadian Journal of Zoology 57(7):1413-1423.

Holliday CW, Mykles DL, Terwilliger RC, Dangott LJ. 1980. Fluid secretion by the midgut caeca of the crab, *Cancer magister*. Comparative Biochemistry and Physiology Part A: Physiology 67(2):259-263.

Icely JD, Nott JA. 1992. Digestion and absorption: digestive system and associated organs. In: Harrison FW, Humes AG, editors. Microscopic anatomy of invertebrates: decapod Crustacea. New York: Wiley-Liss. p 147-201.

Jantrarotai PN, Sawanyatiputi SA. 2005. Histological study on the development of digestive system in zoeal stages of mud crab (*Scylla olivacea*). Kasetsart Journal 39(4):666-671.

Komuro T, Yamamoto T. 1968. Fine structure of the epithelium of the gut in the crayfish (*Procambarus clarkii*) with special reference to the cytoplasmic microtutubles. Archivum histologicum japonicum 30(1):17-32.

Lehane MJ. 1997. Peritrophic matrix structure and function. Annual Review of Entomology 42(1):525-550.

Lovett DL, Felder DL. 1989. Ontogeny of gut morphology in the white shrimp *Penaeus setiferus* (Decapoda, Penaeidae). J Morphol 201(3):253-272.

Lovett DL, Felder DL. 1990a. Ontogenetic changes in enzyme distribution and midgut function in developmental stages of *Penaeus setiferus* (Crustacea, Decapoda, Penaeidae). The Biological Bulletin 178(2):160-174.

Lovett DL, Felder DL. 1990b. Ontogeny of kinematics in the gut of the white shrimp *Penaeus setiferus* (Decapoda: Peneidae). Journal of Crustacean Biology 10(1):53-68.

Martin GG, Simcox R, Nguyen A, Chilingaryan A. 2006. Peritrophic membrane of the penaeid shrimp *Sicyonia ingentis*: structure, formation, and permeability. The Biological Bulletin 211(3):275-285.

McLaughlin PA. 1983. 1. Internal Anatomy. In: Mantel LH, editor. The Biology of Crustacea Vol 5 Internal Anatomy and Physiological Regulation: Academic Press. p 1-52.

Milne-Edwards H. 1834a. Histoire naturelle des crustacés, comprenant l'anatomie, la physiologie et la classification de ces animaux: Libraire Encyclopédique de Roret.

Milne-Edwards H. 1834b. Histoire naturelle des crustacés: atlas: Libraire Encyclopédique de Roret.

Monteiro EC, Tamaki FK, Terra WR, Ribeiro AF. 2014. The digestive system of the “stick bug” *Cladomorphus phyllinus* (Phasmida, Phasmatidae): A morphological, physiological and biochemical analysis. Arthropod Structure & Development 43(2):123-134.

Muhammad F, Zhang ZF, Shao MY, Dong YP, Muhammad S. 2012. Ontogenesis of digestive system in *Litopenaeus vannamei* (Boone, 1931) (Crustacea: Decapoda). Italian Journal of Zoology 79(1):77-85.

Mykles DL. 1977. The ultrastructure of the posterior midgut caecum of *Pachygrapsus crassipes* (Decapoda, Brachyura) adapted to low salinity. Tissue and Cell 9(4):681-691.

Mykles DL. 1979. Ultrastructure of alimentary epithelia of lobsters, *Homarus americanus* and *H. gammarus*, and crab, *Cancer magister*. Zoomorphologie 92(3):201-215.

Nakamura K. 1990. Organogenesis during metamorphosis in the swimming crab *Portunus trituberculatus*. Nippon Suisan Gakkaishi 56(10):1561-1564.

Pinn EH, Nickell LA, Rogerson A, Atkinson RJA. 1999. Comparison of gut morphology and gut microflora of seven species of mud shrimp (Crustacea: Decapoda: Thalassinidea). Marine Biology 133:103-114.

Pugh JE. 1962. A contribution toward a knowledge of the hind-gut of fiddler crabs (Decapoda, Grapsidae). Transactions of the American Microscopical Society 81(4):309-320.

Reddy AR. 1937. The physiology of digestion and absorption in the crab *Paratelphusa* (*Oziotelphusa*) *hydrodromus* (Herbst). Proceedings of the Indian Academy of Sciences - Section B 6(3):170-193.

Rotllant G, Moyano FJ, Andrés M, Estévez A, Díaz M, Gisbert E. 2010. Effect of delayed first feeding on larval performance of the spider crab *Maja brachydactyla* assessed by digestive enzyme activities and biometric parameters. Marine Biology 157(10):2215-2227.

Schlegel C. 1911. Anatomie sommaire de la première zoé de *Maja squinado* Latr. (Note préliminaire à des recherches sur l'Organogénese des Décapodes brachyoures). Archives de Zoologie Experimentale et Générale 5º Série T. VIII.(2):29-40.

Schmitz EH, Scherrey PM. 1983. Digestive anatomy *Hyalella azteca* (Crustacea, Amphipoda). J Morphol 175:91-100.

Schmitz EH, Schultz TW. 1969. Digestive anatomy of terrestrial isopoda: *Armadillidium vulgare* and *Armadillidium nasatum*. The American Midland Naturalist 82(1):163-181.

Silva W, Cardoso C, Ribeiro AF, Terra WR, Ferreira C. 2013. Midgut proteins released by microapocrine secretion in *Spodoptera frugiperda*. Journal of Insect Physiology 59(1):70-80.

Smith RI. 1978. The Midgut Caeca and the Limits of the Hindgut of Brachyura: A Clarification. Crustaceana 35(2):195-205.

Sonakowska L, Włodarczyk A, Poprawa I, Binkowski M, Śróbka J, Kamińska K, Kszuk-Jendrysik M, Chajec Ł, Zajusz B, Rost-Roszkowska MM. 2015. Structure and Ultrastructure of the endodermal region of the alimentary tract in the freshwater shrimp *Neocaridina heteropoda* (Crustacea, Malacostraca). PLOS ONE 10(5):e0126900.

Sousa LG, Petriella AM. 2007. Functional morphology of the hepatopancreas of *Palaemonetes argentinus* (Crustacea: decapoda) : Influence of environmental pollution. Espagnol 55:79-85, SUP71.

Trinadha Babu B, Shyamasundari K, Hanumantha Rao K. 1989. Observations on the morphology and histochemistry of the midgut and hindgut of *Portunus sanguinolentus* (Herbst) (Crustaceans: Brachyura). Folia Morphologica 37(4):373-381.

Williams RL. 1944. The pre-zoea stage of *Porcellana platycheles* (Pennant). Preliminary anatomical and histological notes. Journal of the Royal Microscopical Society 64(1-2):1-15.

Witkus ER, Grillo RS, Smith WJ. 1969. Microtubule bundles in the hindgut epithelium of the woodlouse *Oniscus ascellus*. Journal of Ultrastructure Research 29(3):182-190.

Yonge CM. 1924. Studies on the comparative physiology of digestion II. - The mechanism of feeding, digestion, and assimilation in *Nephrops norvegicus*. British Journal of Experimental Biology 1:343-389.

CHAPTER 18.

Morphology and ontogeny of the hindgut tract in the spider crab *Maja brachydactyla* Balss, 1922 (Brachyura, Majidae)

Morphology and ontogeny of the hindgut tract in the spider crab *Maja brachydactyla* Balss, 1922 (Brachyura, Majidae).

Diego Castejón[1*], Guiomar Rotllant[2], Enric Ribes[3], Mercè Durfort[3], and Guillermo Guerao[4]

[1] IRTA, Centre d'Aqüicultura, Ctra. del Poble Nou Km 5.5. 43540 Sant Carles de la Ràpita, Tarragona (Spain).

[2] CSIC, Institut de Ciències del Mar, Passeig Marítim de la Barceloneta 37-49. 08003 Barcelona (Spain).

[3] Unitat de Biologia Cel·lular, Departament de Biologia Cel·lular, Fisiologia i Immunologia, Facultat de Biologia, Universitat de Barcelona, Diagonal 645. 08028 Barcelona (Spain).

[4] PS Fabra i Puig 344. 08028 Barcelona (Spain).

Short title: *Maja brachydactyla* hindgut tract morphology & ontogeny

***Corresponding author:** Diego Castejón. E-mail: diego.castejon.dcb@gmail.com; phone: +34 681 154 398; postal address: IRTA, Subprogram Cultius Aqüàtics, Ctra. Poble Nou, Km 5.5. 43540 Sant Carles de la Ràpita, Tarragona (Spain).

Abstract

The hindgut tract of the spider crab *Maja brachydactyla* Balss, 1922 has been described in the larval, first juvenile and adult stages. The study employed stereomicroscopy, light microscopy and electron microscopy. The hindgut tract is a dorsal, tubular organ that crosses the animal length from the midgut - hindgut junction to the anus. The hindgut has internally five longitudinal folds, lined by a simple epithelium and a cuticle. Each fold contains bundles of longitudinal muscle fibers. The connective is surrounded by a layer of outer circular muscles. The epithelial cells have numerous lateral interdigitations, apical mitochondria and are vertically crossed by thick bundles of filamentous structures. The cuticle surface contains aggregations of microspines organized in parallel bands crossing the hindgut length. The adults have rosette glands forming important masses beneath the epithelium; they are globular and composed by pyramidal secretory cells grouped around a central cellular tube. During the larval development the hindgut decreases significantly in length and presents the same basic morphology than in the adults, but the connective and muscles are relatively thinner and rosette glands were not observed. The role of the different structures is discussed.

Keywords: Crustacea; larval development; epithelium; cuticle; rosette glands; microspines; filamentous structures

1. Introduction

The hindgut of the Malacostraca comprises the hindgut tract and the anus. The hindgut tract of the malacostracans is a dorsal, tubular organ that cross the animal length from the midgut - hindgut junction to the anus, that open ventrally in the telson (Ceccaldi, 1989; Holdich, 1973; Icely and Nott, 1992; Smith, 1978). The hindgut derives from the embryonary ectoderm and consequently it is internally covered by a chitinous cuticle (Felgenhauer, 1992; Holdich, 1973; Holdich and Mayes, 1975). The cuticle surface usually has microspines projected toward the anus, whose size and shape varies among taxa and along the hindgut length (Elzinga, 1998; Erri Babu et al., 1982; Felgenhauer, 1992; Harris, 1993b). The hindgut tract can contain rosette glands that produce mucopolysaccharides but whose role is unknown (Barker and Gibson, 1978; To et al., 2004; Yonge, 1924; 1932). The main role of the hindgut is the defecation (transport and excretion of the residual waste matter as fecal pellets), but it is also involved in the osmoregulation and anal water intake (Ceccaldi, 1989; Davie et al., 2015; Holdich and Ratcliffe, 1970; Icely and Nott, 1992; Mykles, 1979).

The majority of the studies focused on the digestive system of the Malacostraca described in detail the stomach and/or the midgut gland ("hepatopancreas"), but the hindgut tract received comparatively less attention (Davolos et al., 2010; Johnston, 2007a; Pillai, 1960; Tziouveli et al., 2011). Few studies have been focused exclusively on the morphology (or other features) of the hindgut tract (Chisaka et al., 1999; Felder and Felgenhauer, 1993; Holdich, 1973; Witkus et al., 1969). This situation is reflected in the extensive reviews dedicated to the Malacostraca digestive system, where the hindgut tract is mentioned in few short paragraphs contrasting to the extensive discussion of the stomach or the midgut gland morphology and function (Ceccaldi,

1989; Davie et al., 2015; Felgenhauer, 1992; Icely and Nott, 1992; McLaughlin, 1983). The studies that describe the features of the hindgut tract during the larval stages and its ontogeny are even more scarce. In general terms, these studies mentioned some resemblances between the adult and the larval hindgut (Abrunhosa and Kittaka, 1997; Factor, 1981; Hinton and Corey, 1979; Lovett and Felder, 1989). The similarities and differences of the morphology of the hindgut tract between the adult and larval stages would be useful to understand the role of this organ during the ontogeny.

The aim of this study is to solve some of these gaps in our knowledge of the hindgut tract of the decapods. For this purpose, we describe the hindgut tract of *M. brachydactyla* during larval development and compare it with the adult stage. The role of the different hindgut tract structures will be discussed and compared with previous studies realized in other malacostracans species. The species selected for this purpose is the majid crab *Maja brachydactyla* Balss, 1922. This marine brachyuran species is exploited commercially in the European coast (FAO, 2014) and presents an abbreviated larval development: zoea I, zoea II and megalopa, before the metamorphosis to first juvenile (Clark, 1986; Guerao et al., 2008). In this species, the foregut morphology and ontogeny has been recently described (Castejón et al., 2015).

2. Material and methods

The animal origin and culture, sample collection, methodology employed for the dissection of the specimen and the protocols employed for the optical and electron microscopy techniques (transmission and scanning) were described in a previous study dedicated to the study of the midgut tract (see chapter 11).

3. Results

Gross morphology. In all the life stages (from hatching to the adult stage), the hindgut tract of *M. brachydactyla* is a large tube that cross the animal length from the midgut-hindgut junction (located approximately at the middle of the cephalothorax length) to the anus, located ventrally on the telson (Fig. 1A-D). The cross-section of the hindgut tract is externally circular, but the lumen present radial symmetry and stellate shape due to the presence of five longitudinal evaginations separated by their respective invaginations, in turn subdivided in dichotomic or trichotomic branches (Figs. 3A-B, D-F; 4A, C). Despite the length of the hindgut tract decreases significantly from 1710 ± 80 μm in the newly hatched zoea I to 1495 ± 75 μm in newly molted first juvenile (ANOVA, $F_{3,13} = 8.14$ $p < 0.01$; Fig. 2A), this result is not reflected by the mean length of the hindgut tract at each life day (Fig. 2B). The hindgut diameter was significantly smaller in the first zoeal stage with 51 ± 5 μm comparing to other stages: 63 ± 8 μm in zoea II, 63 ± 1 μm in megalopa and 71 ± 10 μm in first juvenile ($F_{3,13} = 6.83$ $p < 0.01$).

The histological organization of the hindgut tract was constant during all the larval development. During these stages it is lined by a simple squamous epithelium covered by a very thin cuticle (Figs. 3A-F; 5A-C). The basal lamina is not visible under optical microscopy but by TEM (Figs. 3A-B; 5A, D). Two types of muscles were identified: outer circular muscles and inner longitudinal muscles. The outer circular muscles are very thin and surround the external perimeter of the hindgut tract (Figs. 3A-B; 5D; 11C). The cells of the inner longitudinal muscles are columnar in transversal section, they are located in the center of each invagination and surrounded by a simple layer of squamous epithelial cells (Figs. 3B; 5A-B; 11C-D). The myofibrils of the longitudinal muscle cells occupy the cell apex (Figs. 3B; 11C-D).

The hindgut tract of the adult specimens shares with the larval stages the same tissue layers and their location, but each tissue layer suffer great changes due to a high increment in size and complexity. The hindgut tract is lined by a simple columnar epithelium covered by a cuticle which layers can be identified (Figs. 4A-D; 8A). The cuticle form undulations with a variable degree in size (Fig. 4B). The basal lamina is very thin (Fig. 6A, C). The connective tissue is very wide and contains numerous rosette glands that were absent during the larval stages (Figs. 4A-D; 9B). The same muscle types observed in the larvae were identified: outer circular muscles and inner longitudinal muscles (Fig. 4A, C-D). The bundles of circular muscles surround the hindgut perimeter and are thinner than the bundles of longitudinal muscles, while the bundles of longitudinal muscles are and surrounded by a wide layer of connective tissue (Fig. 4A, C-D). The muscle cells of the adults include a central nucleus surrounded by densely packed mitochondria, in turn surrounded by packs of myofibrils (Fig. 11A-B).

Epithelial cells. During the larval development the epithelial cells are generally squamous (Figs. 5A-B; 11C). The cell membrane has some degree of polarization, the apical membrane forms short microvilli with electron-dense apex and small conical or dome-like infolds where filamentous structures are attached, these infolds were termed "apical complex" (Fig. 5B-C). The lateral membranes form lateral interdigitations (Fig. 5C). Some cell-to-cell junctions were observed: very short cell-to-cell junctions attaching adjacent epithelial cells (CEJ, Fig. 5B-C) and large and highly developed cell-to-cell junctions attaching epithelial and muscle cells (CMJ, Fig. 5B). The basal membrane is generally smooth with some infolds (Fig. 5D). The cytoplasm is generally lucent and contains a variable density of ribosomes and single membrane vesicles (Fig. 5B-C). The mitochondria are lucent and globular (Fig. 5B). The rough endoplasmic reticulum is scarce and composed by short globular cisternae dispersed thorough to the

cytoplasm (Fig. 5B). Some bundles of filamentous structures were observed (Fig. 5B-C). The nucleus shape is variable: rounded, conical, rhomboidal or irregular (Fig. 3B; 6A-B).

The epithelial cells of the adult specimens differs considerably from the larvae. They are tall columnar cells (ca. 30-40 μm height, Fig. 4B) and show polarized organization (Fig. 6A-C). The apical membrane is smooth, the "apical complexes" are more developed (larger and more electron-dense) than in the larvae, showing more clearly the attachment to the filamentous structures (Fig. 6D). The lateral membranes show short apical cell-to-cell junctions and numerous interdigitations which number, size and complexity increases toward the cell basis (Fig. 6A-C). The basal membrane is highly infolded (Fig. 6C). The cytoplasm of the adult epithelial cells is homogeneously stained by Hematoxylin and Mallory's trichrome, but it is poorly stained by Methylene Blue (Fig. 4B-D). The cytoplasm is rich in PAS positive granules. By electron microscopy, the cytoplasm is lucent and contains sparse ribosomes and single membrane vesicles (Fig. 6B-F). The mitochondria are abundant and elongated (ca. 2-3 μm length and 200-300 nm width); they are concentrated above the nucleus as highly electron-dense organelles (Fig. 6B, F). The rough endoplasmic reticulum is composed by cisternae with variable length and mainly located around the nucleus. The Golgi bodies are scarce and composed by few, flattened, parallel stacks of cisternae (Fig. 6F). The nucleus is rounded to ellipsoidal and located medially. The euchromatin is scarce and distributed as patches attached to the nuclear membrane (Fig. 6B). The adult epithelial cells are crossed by well developed bundles of filamentous structures from the cell basis (Fig. 6C) to the cell apex (Fig. 6B, D), where they attach to the "apical complex" (Fig. 6D). These filaments usually appear near to the lateral membranes, some mitochondria are oriented parallel to these filamentous structures (Fig. 6E).

Cuticle. The epithelial cells are covered by a cuticle layer. During the larval and first juvenile stages the cuticle is very thin and it is not possible to identify any layer by optical microscopy (Fig. 3C-F). By electron-microscopy can be distinguished an outer electron-dense epicuticle and a less electron-dense procuticle without a clear lamellate organization (Figs. 5B-D; 7B). The cuticle of the adults represents approximately a third of the epithelial cell height (ca. 12 μm height; Fig. 4B) and shows the typical cuticle layers: epicuticle, exocuticle and endocuticle (Fig. 8A). The epicuticle is the outmost layer, it is stained by orange G and represents ca. 9 ± 1 % of the cuticle thickness (Fig. 4B; 8A). The exocuticle and the endocuticle are lamellate layers highly difficult to identify by light microscopy due to their similarity in structure and staining affinity (Fig. 4B). By TEM, the exocuticle lamellae are more electron-dense, wider and folded than the endocuticle lamellae (Fig. 8A).

The external surface of the cuticle is very rich in different types of microspines (Figs. 7C-D; 8C-G). The microspines are formations derived from the epicuticle (Fig. 7B). Occasionally, some bacillus-shaped bacteria appear over the micropines (Fig. 8E, F). During the larval stages, the microspines are very short (ca. 0.5-1 μm length) and simple fang-like structures projected backward in the hindgut; they are organized in longitudinal bands that cross the hindgut length (7A, C). The morphology of the microspines change during the juvenile growth, being observed adult-like microspines in juveniles with 7 mm carapace length (Fig. 7D). The adult microspines differs considerably from the larval stages, they are aggregated in hexagonal cells formed by the folding of the cuticle (Fig. 8D-G). We identify two types of aggregations that differ in their composition and distribution:

Aggregation type I (Figs. 7D; 8E-F). They are composed by elongated microspines and midget microspines. The elongated microspines are large (ca. 4-6 μm) and typically aggregated in groups from one to four microspines (Fig. 8E-F), groups with higher number of microspines are occasionally observed (Fig. 7D). The midget microspines are small (less than 1μm) and blunt, they are showed as an "halo" up to 200 microspines that surrounds the elongated microspines (Fig. 8F). The aggregations type I form longitudinal bands located in the tip and lateral sides of the hindgut tract evaginations (Fig. 7B-D).

Aggregation type II (Fig. 8G). They are only composed by midget microspines similar to the previously described, being observed more than 200 microspines in a single aggregation (Fig. 8G). The aggregations type II are typically located between two parallel aggregations type I in the lateral and basal sides of the evaginations (Fig. 8B-D).

Rosette glands. The rosette glands are absent during the larval development (Fig. 3A-F), but they are very abundant in the adult stage (Figs. 4A, C; 9B). Their presence is individual or as huge glandular masses located in the connective tissue (Fig. 9B). The rosette glands are globular clusters of cells composed by gland cells (GC) surrounding an slender central duct (CD), formed by one or more duct cells (DC) (Fig. 9A, C-E). Each gland is surrounded by a thin envelope of connective tissue. The gland cells are pyramidal in shape (Fig. 9A, C-E; 10A-B), the thin apex pierces the duct cells to reach the central duct through the "collector ducts" (*, Fig. 10A-B, E-F). The cytoplasm has a foamy appearance due to the high abundance of vesicles (Figs. 9C-E; 10A-C). The staining affinity of the vesicle content vary between the cells of the same gland: from completely stained by PAS to completely stained by Alcian Blue, including all the

intermediate stages (Fig. 9C). The cytoplasm contain from a myriad of tiny small vesicles to a single and non-stained vesicle occupying the majority of the cell volume (Fig. 9C). The vesicles are filled by fibrillar matter condensed at a variable electron-density (Fig. 10B-C). The nucleus is basal and irregular (Figs. 9C-E; 10A-B). The Golgi bodies are abundant and composed by numerous, narrow and elongated electron-dense cisternae densely packed (Fig. 10B, D). The central duct of the rosette glands is short and formed by one or more cells (Figs. 9A, C-E; 10A-B). The duct cells does not show a clear polarization in their organization. The cytoplasm is highly electron-dense and contains a high density of filamentous structures oriented concomitantly with the cell shape. The nucleus shape varied from spherical to ovoid. The remain cell organelles are very scarce (Fig. 10A-B).

4. Discussion

The hindgut tract of the genus *Maja* was illustrated for the first time by Milne-Edwards (1834a; b), showing a large hindgut tract ("rectum") distinct from the midgut tract ("duodénium") and prolonged to the anus. In this study the hindgut tract represents six seventh of the post-gastric tract. Similar descriptions were realized in other brachyuran species (Barker and Gibson, 1978; Erri Babu et al., 1982; Reddy, 1937). However, the length of the hindgut tract is highly variable among the malacostracans. In some astacideans as *Homarus gammarus* (Barker and Gibson, 1977) and *Nephrops norvegicus* (Yonge, 1924) is very short starting at the sixth pleonite; while in others as *Procambarus clarkii* is around ten times longer than the midgut tract (Chisaka et al., 1999; Huxley, 1880; Komuro and Yamamoto, 1968). The hindgut tract starts in the sixth pleonite in penaeids (Dall, 1967; Martin and Chiu, 2003) and carideans (Pillai, 1960; Sousa and Petriella, 2006). On the contrary, in terrestrial isopods (*Trachelipus*

illyricus, *Porcellio* sp. and *Armadillidium* sp.) the foregut and hindgut fuse during the embryonic development, then the midgut tract and associated caeca are absent (Holdich, 1973; Holdich and Mayes, 1975; Štrus et al., 1995; Štrus et al., 2008). The presence of five longitudinal folds (or evaginations) is typical among the brachyurans (Barker and Gibson, 1978; Mykles, 1979; Pugh, 1962; Smith, 1978), being observed six longitudinal folds in other taxa as astacideans (Barker and Gibson, 1977; Huxley, 1880; Komuro and Yamamoto, 1968; To et al., 2004; Yonge, 1924) and penaeids (Dall, 1967). Moreover, in *P. clarkii* the longitudinal folds are in turn folded into secondary folds (Chisaka et al., 1999; To et al., 2004) that could correspond to the "papillae" mentioned by Huxley (1880) in *Astacus astacus* (as *A. fluviatilis*). In *M. brachydactyla*, the cuticular undulations could be interpreted as a secondary folds.

The description of the hindgut tract during the first zoeal stage realized originally by Schlegel (1911) coincides with the present study (stellate lumen, simple epithelium and a cuticle). The hindgut tract during the larval stages was described in similar terms in anomurans (Abrunhosa and Kittaka, 1997; Williams, 1944), carideans (Tziouveli et al., 2011) and achelatans (Mikami et al., 1994). Jantrarotai and Sawanyatiputi (2005) reported major differences in the larval hindgut tract of the brachyuran *Scylla olivacea*: six longitudinal folds (instead of five) and columnar epithelium (instead of squamous). Other differences include the rosette glands reported in the midgut -hindgut junction of *Homarus americanus* larvae (Hinton and Corey, 1979) and the differentiation of the hindgut tract during the larval development as occur in penaids (Lovett and Felder, 1989).

The histological organization of the hindgut tract of *M. brachydactyla* during the adult stage resembles to the hindgut tract described in other brachyurans (Barker and

Gibson, 1978; Erri Babu et al., 1982; Heeren and Mitchell, 1997; Moon and Kim, 1999; Pugh, 1962; Reddy, 1937; Trinadha Babu et al., 1989a) and astacideans (Barker and Gibson, 1977; Komuro and Yamamoto, 1968; To et al., 2004; Yonge, 1924). Some differences are found in other malacostracans: in the isopods the musculature forms a square mesh with inner circular muscles and outer longitudinal muscles (Holdich and Mayes, 1975; Holdich and Ratcliffe, 1970), while in the amphipods the presence of longitudinal muscles is not described (Davolos et al., 2010; Schmitz and Scherrey, 1983).

The epithelial cells of the adult *M. brachydactyla* shares many features with the epithelial cells of the adult brachyuran *Cancer magister* and the astacideans *H. americanus* and *H. gammarus*, including the richness of infolds/evaginations and mitochondria, as well the scarcity of other cell organelles (Mykles, 1979). In several isopods the epithelial cells also are rich in mitochondria but their microvilli differs from the observed in the *M. brachydactyla* larvae (Holdich and Mayes, 1975; Holdich and Ratcliffe, 1970; Vernon et al., 1974; Witkus et al., 1969). One interesting feature are the well developed bundles of filamentous structures crossing vertically the cell. These structures were interpreted as microtubules in other decapods (Komuro and Yamamoto, 1968; Mykles, 1979) and isopods (Holdich and Mayes, 1975; Vernon et al., 1974; Witkus et al., 1969); being proposed as structural support for the contractive and expansive efforts associated with the movement of the matter through the lumen (Komuro and Yamamoto, 1968; Mykles, 1979; Witkus et al., 1969). Other hypothesis proposes a role associated with the movement of water, ions or other intra-cytoplasmic elements trough the cell, due to the apparent association between the filaments and the mitochondria (Komuro and Yamamoto, 1968; Vernon et al., 1974; Witkus et al., 1969). Moreover, Witkus et al. (1969) also suggested that these filaments are responsible of the

alignment of the mitochondria and other cellular components in the cytoplasm. This type of association was also observed in *M. brachydactyla*, but we have not enough data to support any of these hypothesis.

The epithelial cells are covered by the typical crustacean cuticle (Dillaman et al., 2012; Roer and Dillaman, 1984), described in the hindgut of other brachyurans (Pugh, 1962) and astacideans (Komuro and Yamamoto, 1968; To et al., 2004). By contrast, in adult isopods the cuticle has an outer epicuticle and an amorphous endocuticle (Holdich and Mayes, 1975; Holdich and Ratcliffe, 1970; Vernon et al., 1974); resembling to the cuticle observed in larval specimens. The cuticle is considered a protection against the abrasion and proteolytic enzymes (Komuro and Yamamoto, 1968). Maybe smaller animals can afford simpler cuticles, since they manage smaller pieces of matter.

In all the life stages of *M. brachydactyla* the cuticle is rich in hair like projections called microspines. These structures have been reported in numerous euarthropods (Elzinga, 1998; Elzinga and Hopkins, 1995; Miyoshi et al., 2005; Schlüter, 1980) and are common in the hindgut tract of brachyurans (Erri Babu et al., 1982; Harris, 1993b; Hopkin and Nott, 1980; Moon and Kim, 1999; Pugh, 1962), astacideans (Elzinga, 1998; Felgenhauer, 1992), scyllarids (Johnston, 2007b), gebiideans and axiideans (Felder and Felgenhauer, 1993; Harris, 1993b; Pinn et al., 1999). Only in few taxa as *Palaemonetes argentinus* the microspines are absent (Sousa and Petriella, 2006). This study also describes for first time the microspines of a given brachyuran during the larval stages. Previously, in larvae they have been only identified in *Paralithodes camtschaticus* (Abrunhosa and Kittaka, 1997). We also identified two types of microspine aggregations. A variation was also observed in other taxa, Moon

and Kim (1999) observed in *Hemigrapsus penicillatus* the reduction in number but increment in size toward the anus; Chisaka et al. (1999) observed in *P. clarkii* an influence of the hindgut region (anterior, medial, posterior) over the size and density. The different types of aggregations of the microspines in the hindgut tract might be related with functional requirements.

The role of the hindgut microspines is unknown. The most suggestive hypothesis proposes a role involved in the defecation process (Ceccaldi, 1989; Davie et al., 2015; Felgenhauer, 1992; Icely and Nott, 1992). The feces of the decapods are wrapped by the peritrophic membrane (Davie et al., 2015; Felgenhauer, 1992; Forster, 1953), an extracellular secretion organized as sheets composed by a fibrillar matrix of proteins and chitin (Martin et al., 2006; Wang et al., 2012). In this sense, the microspines could grasp the peritrophic membrane helping to move the fecal matter by peristaltic waves (Felder and Felgenhauer, 1993; Hopkin and Nott, 1980) and avoiding the forward movement due to the antiperistaltic waves that sustain the anal water intake (Felder and Felgenhauer, 1993). Other hypothesis postulates that the microspines shreds the peritrophic membrane to release its content for the water and ion absorption (Byers and Bond, 1971). This late hypothesis has not sense in *M. brachydactyla* since the peritrophic membrane is excreted undamaged. A third hypothesis consider the microspines as attachments for symbiotic microorganisms involved in the digestive process (Elzinga, 1998; Harris, 1993a). We observed some bacteria attached to the microspines, but this situation is not enough to support this hypothesis since the identity of these bacteria is unknown.

The hindgut tract of *M. brachydactyla* is very rich in rosette glands, at least during the adulthood. The hindgut of other decapods (including brachyurans) is also rich in rosette glands (Barker and Gibson, 1978; To et al., 2004; Trinadha Babu et al., 1989a; Yonge, 1924; 1932), although in certain species the rosette glands are restricted to the proximal and distal extremes of the hindgut (Pugh, 1962). These glands appear in other ectoderm derived organs (esophagus, stomach, hindgut and anus) and associated with the gill chambers, gills itself and mouthparts (Doughtie and Rao, 1982; Gorvett, 1946; Yonge, 1932). *M. brachydactyla* has huge glandular masses located in the connective tissue, similarly to those described in many malacostracans (Barker and Gibson, 1977; 1978; Gorvett, 1946; Pugh, 1962; To et al., 2004; Yonge, 1924; 1932). However, despite the massive size of these agglomerations we did not observed a clear communication between the rosette glands and the hindgut lumen. Similar situation have been noticed in brachyurans (Barker and Gibson, 1978), astacideans (Barker and Gibson, 1977; To et al., 2004) and isopods (Holdich and Ratcliffe, 1970).

By contrast, pore like structures have been reported near to the midgut-hindgut junction of other brachyuran species (Harris, 1993b; Heeren and Mitchell, 1997). The rosette glands can either be stained by PAS or alcian blue pH 2.5 stains coinciding with other decapods (Barker and Gibson, 1978; Erri Babu et al., 1979; Heeren and Mitchell, 1997; Trinadha Babu et al., 1989b). This staining affinity suggest a content based on neutral and acid mucopolysaccharides, including sulphated mucopolysaccharides, sulphated sialomucins and hyaluronic acid (Erri Babu et al., 1979; Trinadha Babu et al., 1989b). The role of these glands is unknown, being proposed: lubrication of the cuticle surface to help the movement of the peritrophic membrane movement, maintenance of the cuticle or peritrophic membrane, or protection against pathogens or noxious

substances. To test any of these hypotheses is crucial to identify the exact composition and destiny of the gland secretions.

5. Acknowledgements

Financial support provided by the Spanish Ministry of Economy and Competitiveness through the INIA project [grant number RTA2011-00004-00-00] to G.G and a predoctoral fellowship to D.C. [FPI-INIA]. The authors would like to thank to the technicians at IRTA, Sant Carles de la Ràpita (David Carmona, Glòria Macià, Magda Monllaó, Francesc X. Ingla and Olga Bellot) and CCiTUB Hospital Clinic, Barcelona (Adriana Martínez, Almudena García, José Manuel Rebled and Rosa Rivera) for their assistance.

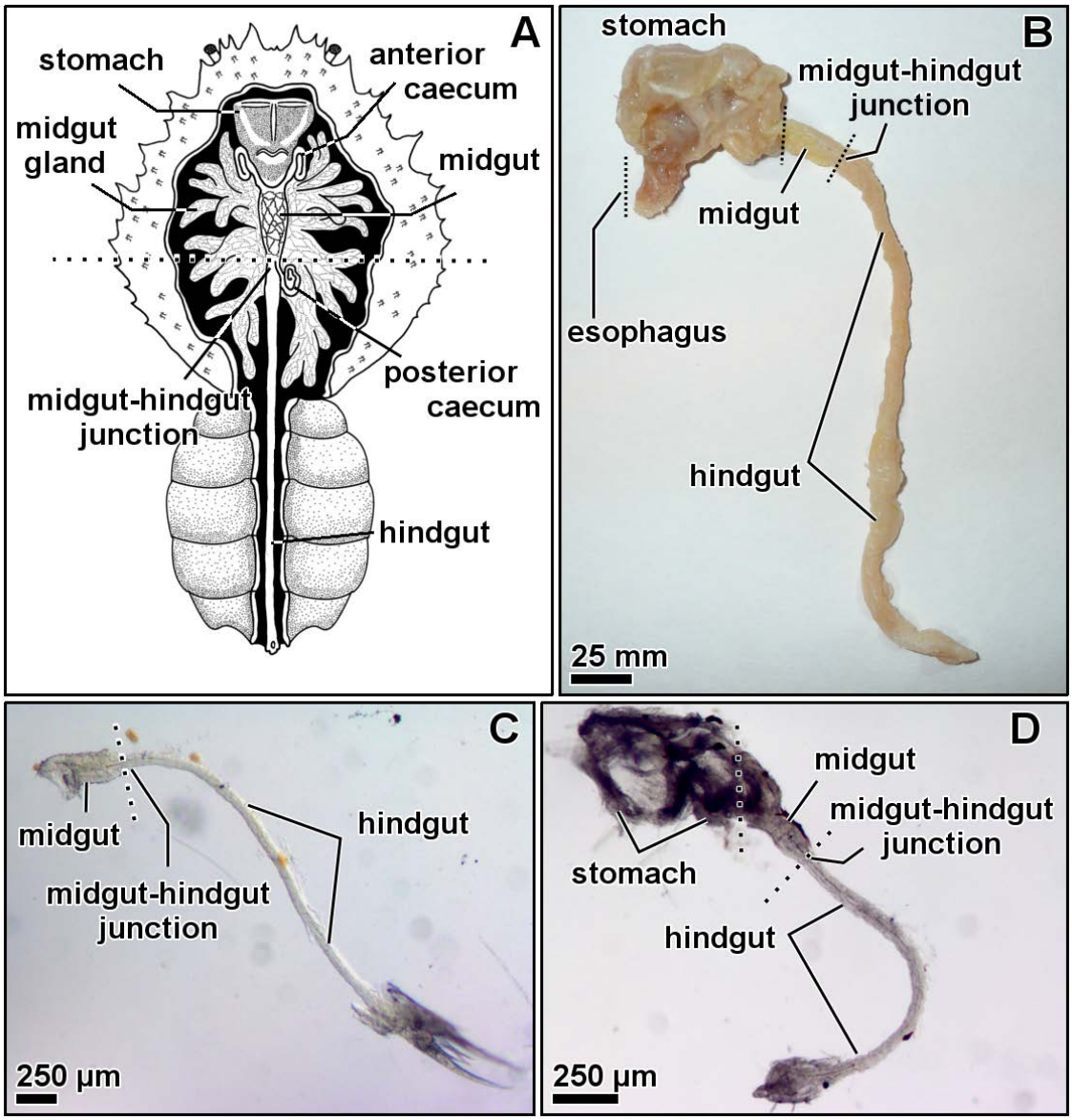

Figure 1. *Maja brachydactyla*. Digestive System, fixed in 4 % formaldehyde. General diagram (A). Adult, the midgut gland ("hepatopancreas") has been removed (B). Zoea I (ca. 15 h after hatching), the foregut and midgut gland have been removed (C). First juvenile (12 days after hatching), the midgut gland has been removed (D).

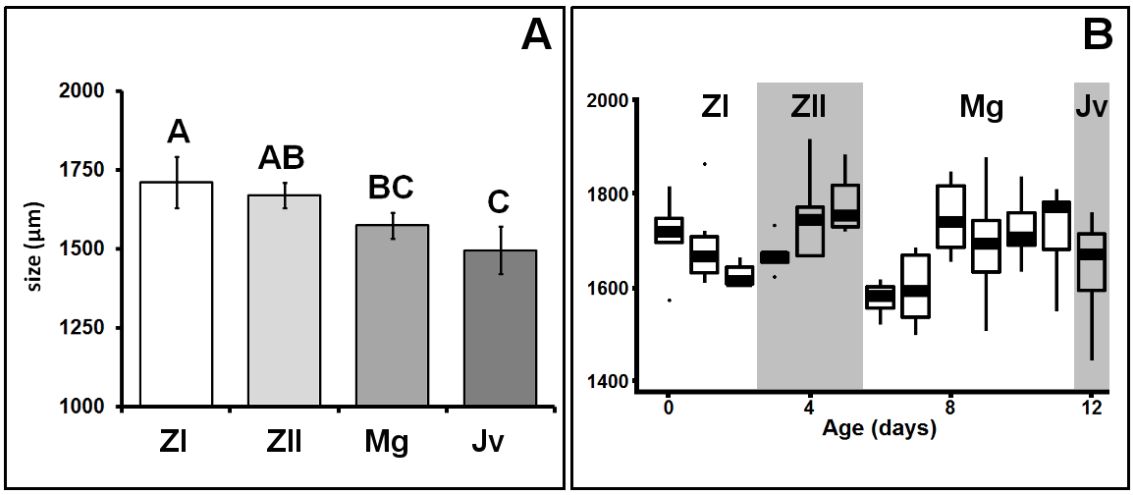

Figure 2. *Maja brachydactyla.* Hindgut tract through the larval development. Length (mean ± SD) at the start of each stage (A). Length (mean ± SD) at each life day (B). Abbreviations: Jv, juvenile; Mg, megalopa; ZI, zoea I; ZII, zoea II.

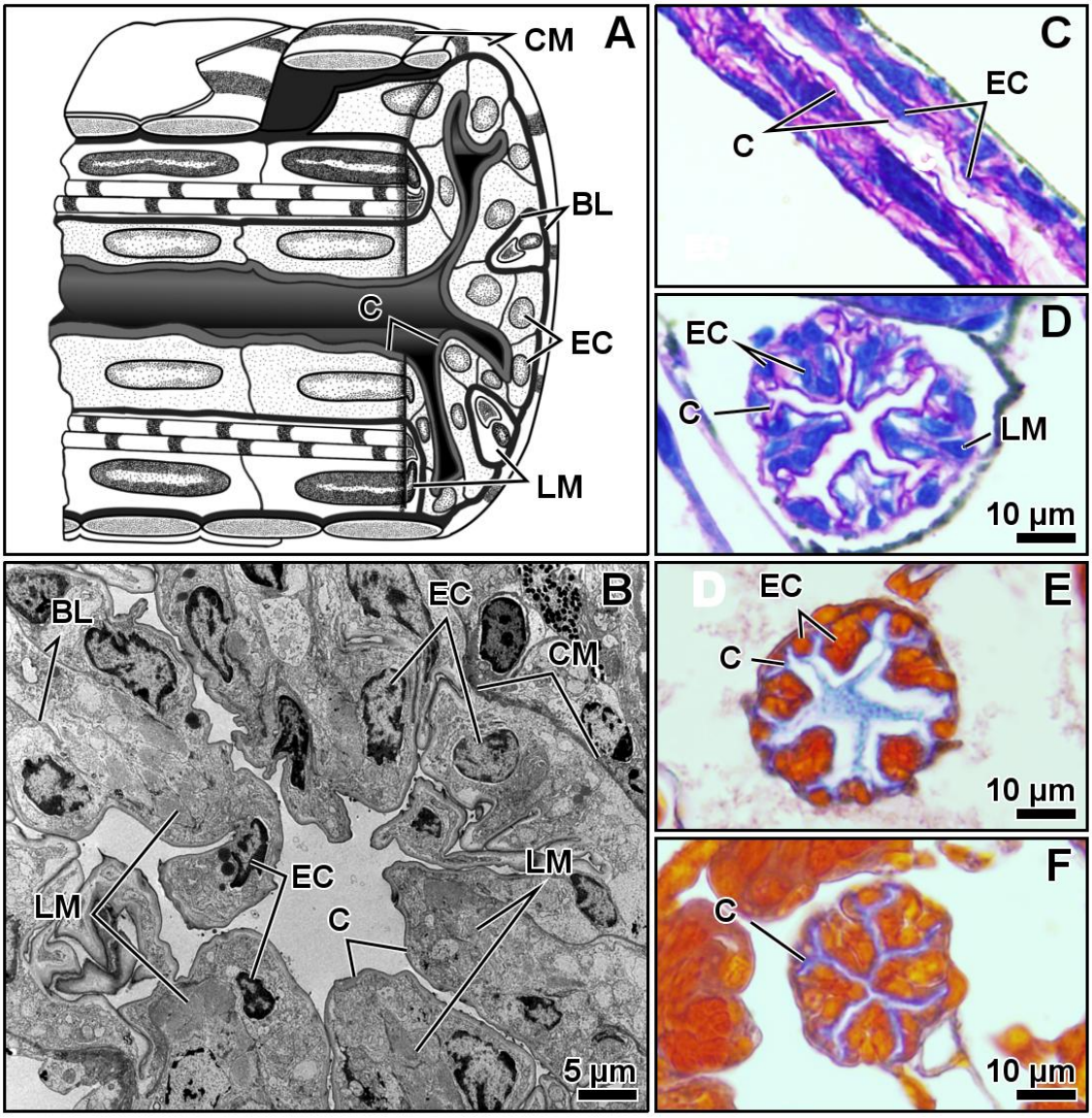

Figure 3. *Maja brachydactyla*. Hindgut tract. Morphology and histology. Larvae. General diagram (A). Megalopa, 10 days after hatching (10 dah), general view in transversal section, TEM (B). Zoea II (6 dah), hindgut tract, PAS contrasted with Methylene Blue (C-D): longitudinal (C) and transversal section (D). Megalopa (6 dah), hindgut tract, Mallory's trichrome (E-F): lumen expanded showing an stellate shape (E) and lumen contracted (F). Abbreviations: C, cuticle; CM, circular muscle fibers; EC, epithelial cells; LM, longitudinal muscle fibers.

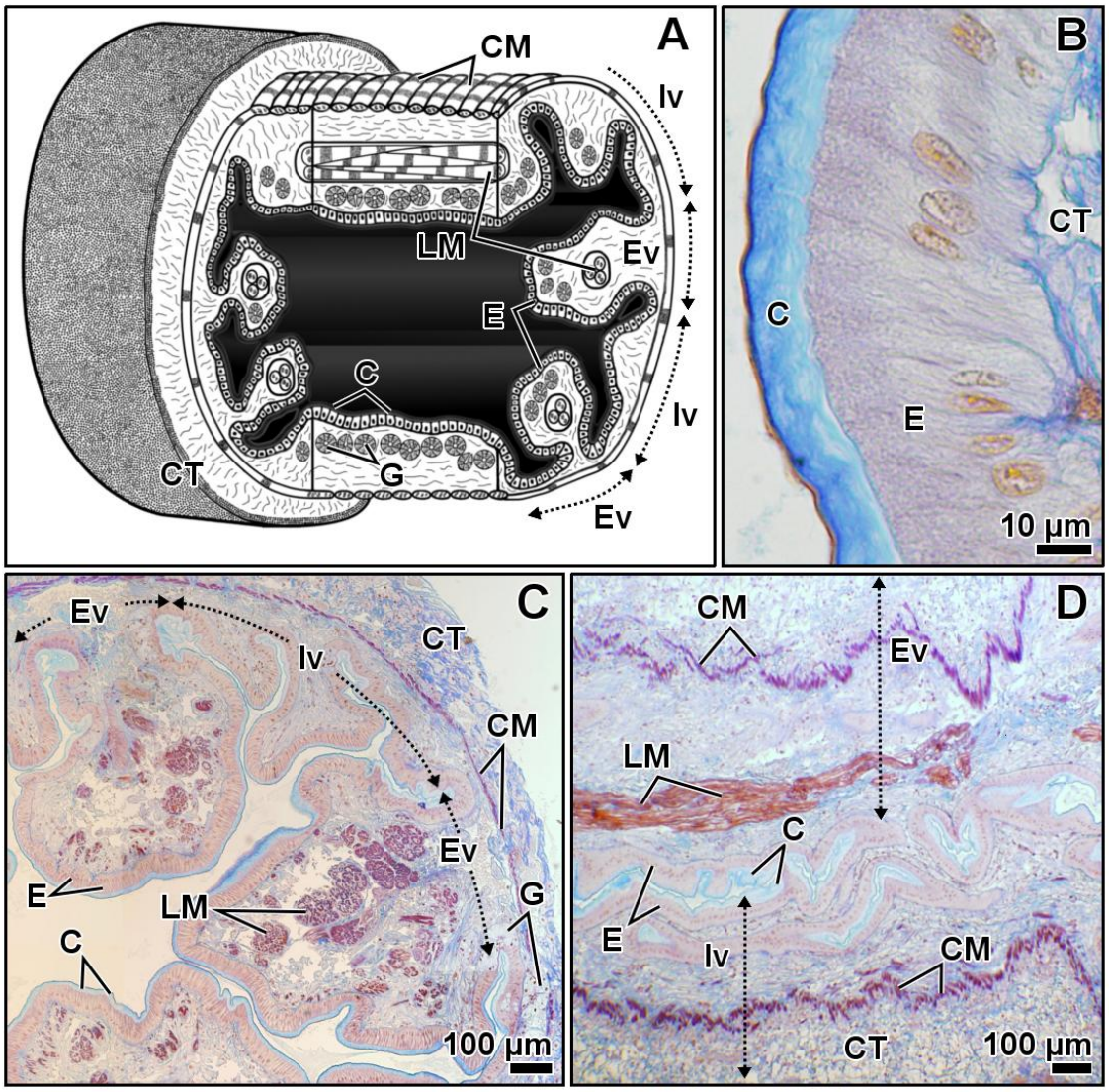

Figure 4. *Maja brachydactyla*. Hindgut tract. Morphology and histology. Adult. General diagram (A). Epithelium, close view (B). General view, Mallory's trichrome (C-D): transversal (C) and longitudinal section (D). Abbreviations: C, cuticle; CM, circular muscle fibers; CT, connective tissue; E, epithelium; Ev, evagination; G, Glands; Iv, invagination; LM, longitudinal muscle fibers.

Figure 5 (next page). *Maja brachydactyla*. Hindgut tract. Epithelial and muscle cells. Ultrastructure. TEM. Megalopa (10 days after hatching). General diagram (A). General view (B). Cell apex, close view (C). Longitudinal muscle, transversal view, close view (D). Abbreviations: AC, "apical complex"; BL, basal lamina; C, cuticle; CEJ, cell-to-cell (epithelial) junction; CMJ, cell-to-cell (muscle) junction; EC, epithelial cell; EP, epicuticle; Ev, evagination; FS, filamentous structures; G, Golgi body; Iv, invagination; LI, lateral invaginations; M, mitochondria; MC, longitudinal muscle cell; MS, microspines; MV, microvilli; My, myofibrils; N, nucleus; PC, procuticle; RER, rough endoplasmic reticulum.

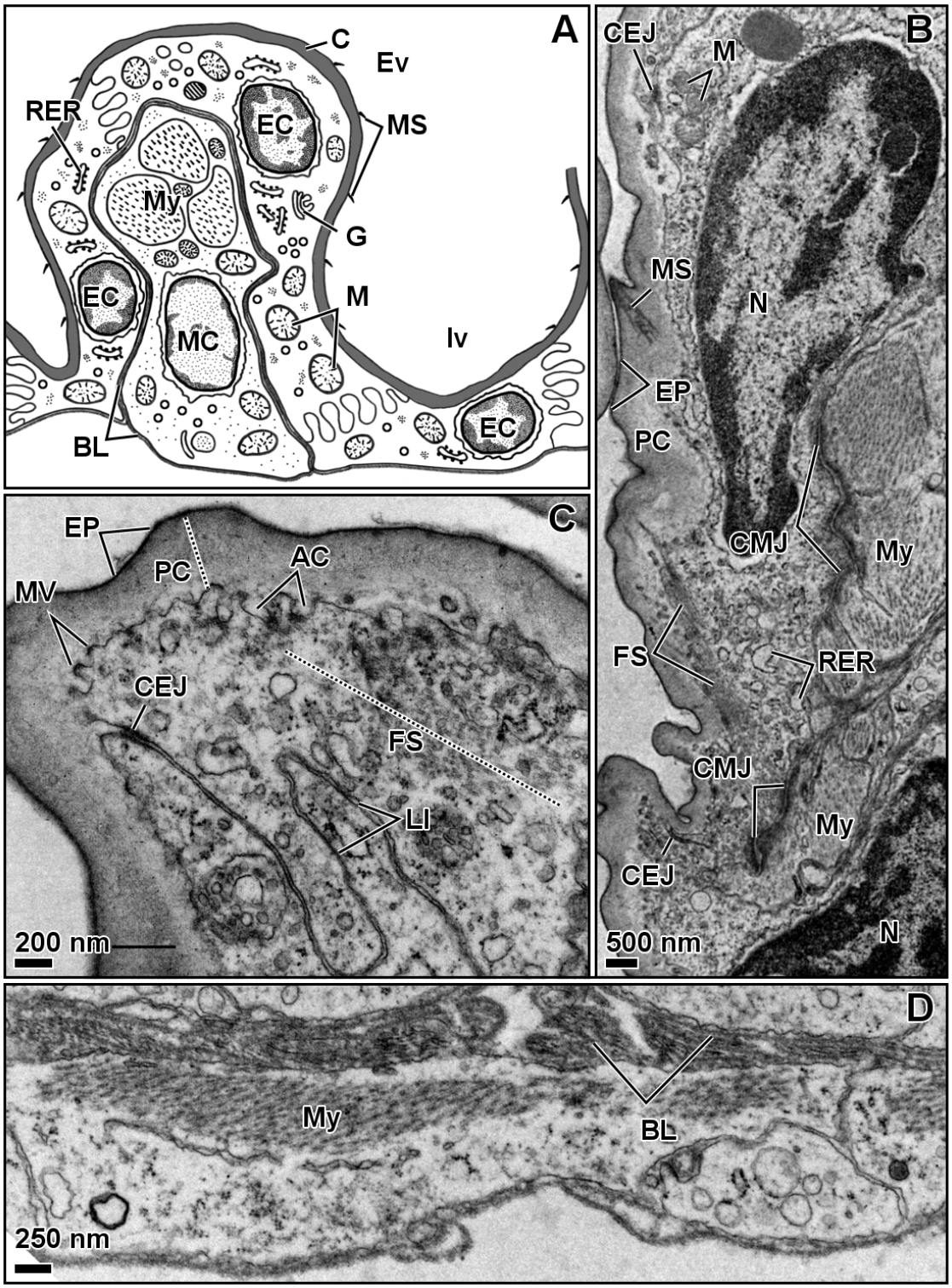
A
C
Ev
RER
EC
MS
My
G
EC
M
MC
lv
EC
BL
B
CEJ
M
MS
N
EP
PC
CMJ
My
FS
RER
CMJ
My
CEJ
N
500 nm
C
EP
PC
AC
MV
CEJ
FS
LI
200 nm
D
My
BL
250 nm

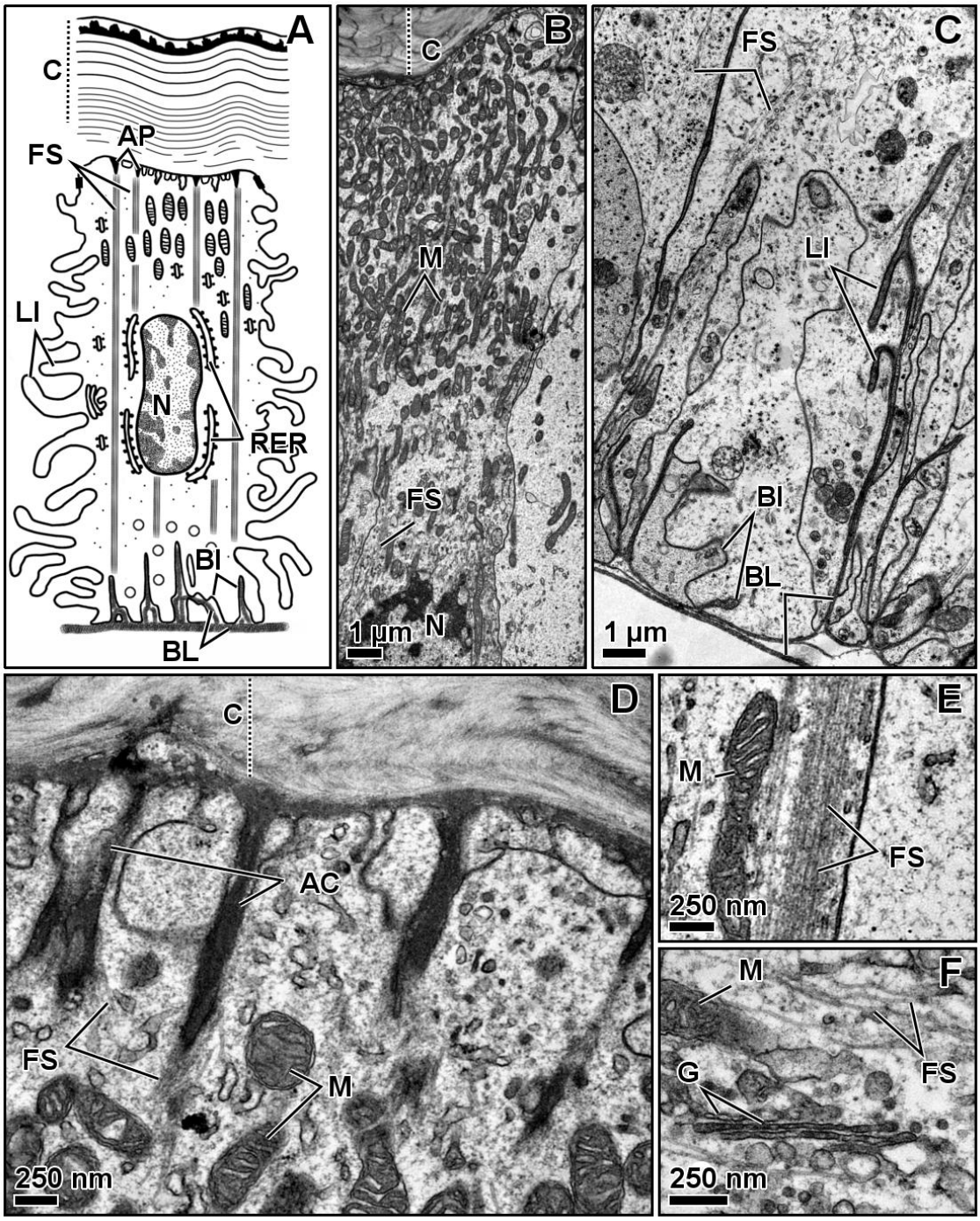

Figure 6. *Maja brachydactyla*. Hindgut tract. Epithelial cells. Ultrastructure. TEM. Adult. General diagram (A). General view (B-C): cell apex, supranuclear region (B) and cell basis, infranuclear region (C). "Apical complex", close view (D). Mitochondria and filamentous structures, close view (E). Golgi body, close view (F). Abbreviations: AC, "apical complex"; BI, basal infolds; BI, basal invaginations; BL, basal lamina; C, cuticle; LI, lateral interdigitations lateral; FS, filamentous structures; M, mitochondria; N, nucleus; RER, rough endoplasmic reticulum.

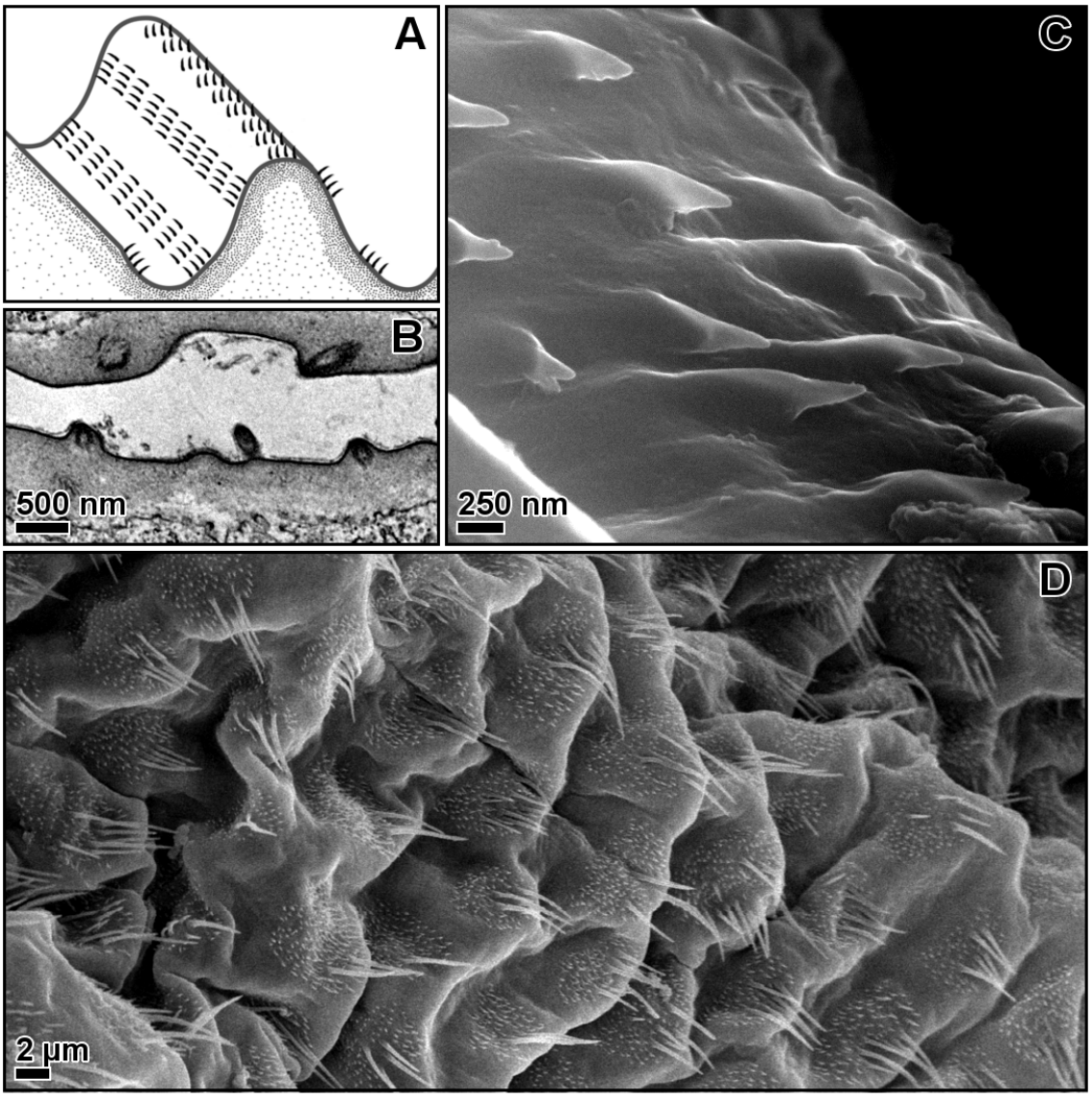

Figure 7. *Maja brachydactyla*. Hindgut tract. Cuticle surface. Ultrastructure. Larvae and juvenile. General diagram, hypothetical location of the microspines (A). Microspines (arrows), megalopa (10 days after hatching), close view, TEM (B). Microspines, zoea I (ca. 15 h after hatching), SEM (C). Microspines, juvenile (7 mm carapace length), SEM (D).

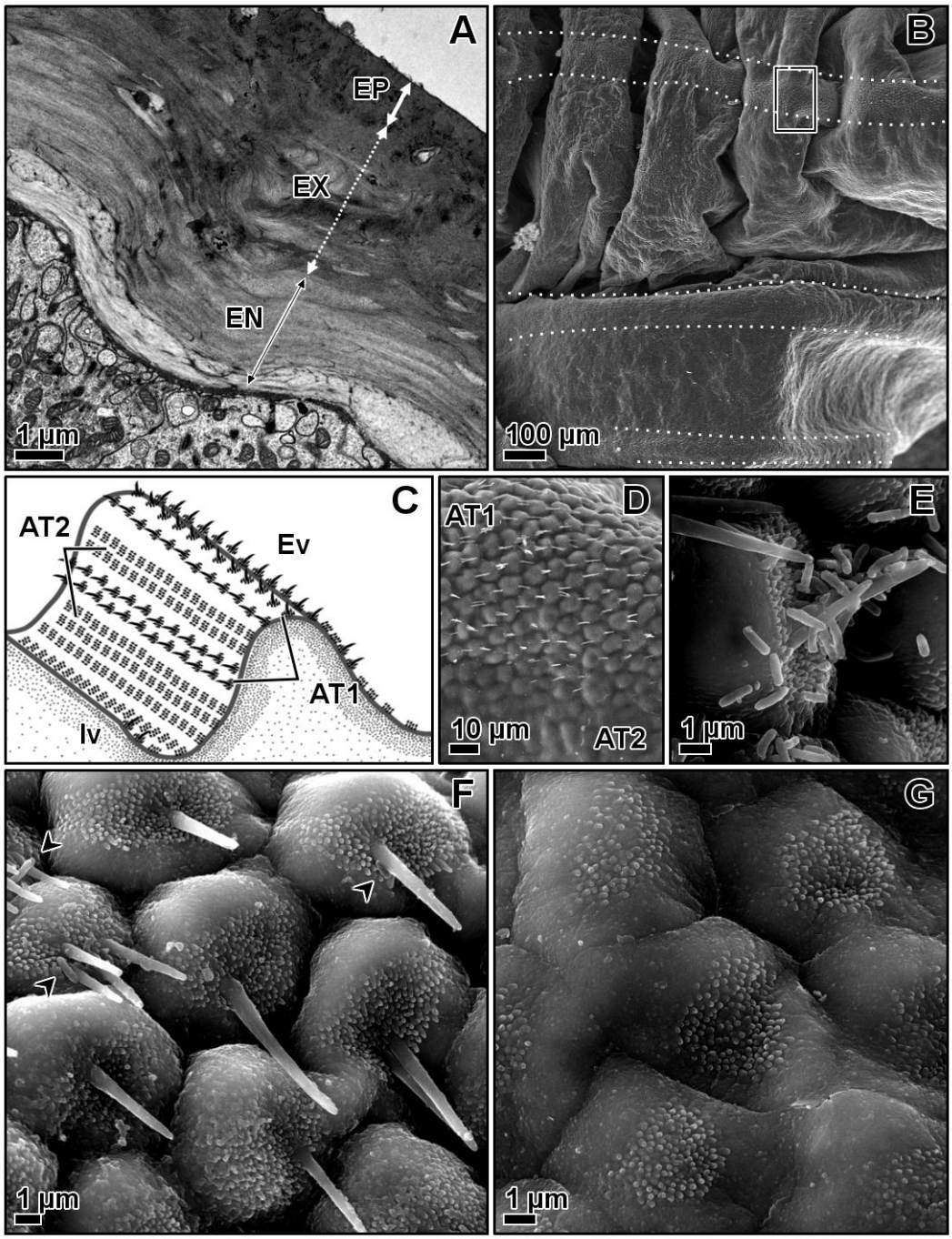

Figure 8. *Maja brachydactyla*. Hindgut tract. Cuticle structures. Ultrastructure. Adult. Cuticle layers, general view, TEM (A). Microspines, distribution of the different aggregations, SEM (B-D): general view (B), general diagram (C) and frontier between aggregations type 1 and 2 marked in B (D). Aggregation type 1 covered by bacillus-shaped bacteria, SEM (E). Microspine aggregations, close view, SEM (F-G): aggregation type 1 with sparse bacteria (arrow-heads) (F) and aggregation type 2 (G). Abbreviations: AT1, aggregation type 1; AT2, aggregation type 2; EN, endocuticle; EP, epicuticle; EX, exocuticle; Ev, evagination; Iv, invagination.

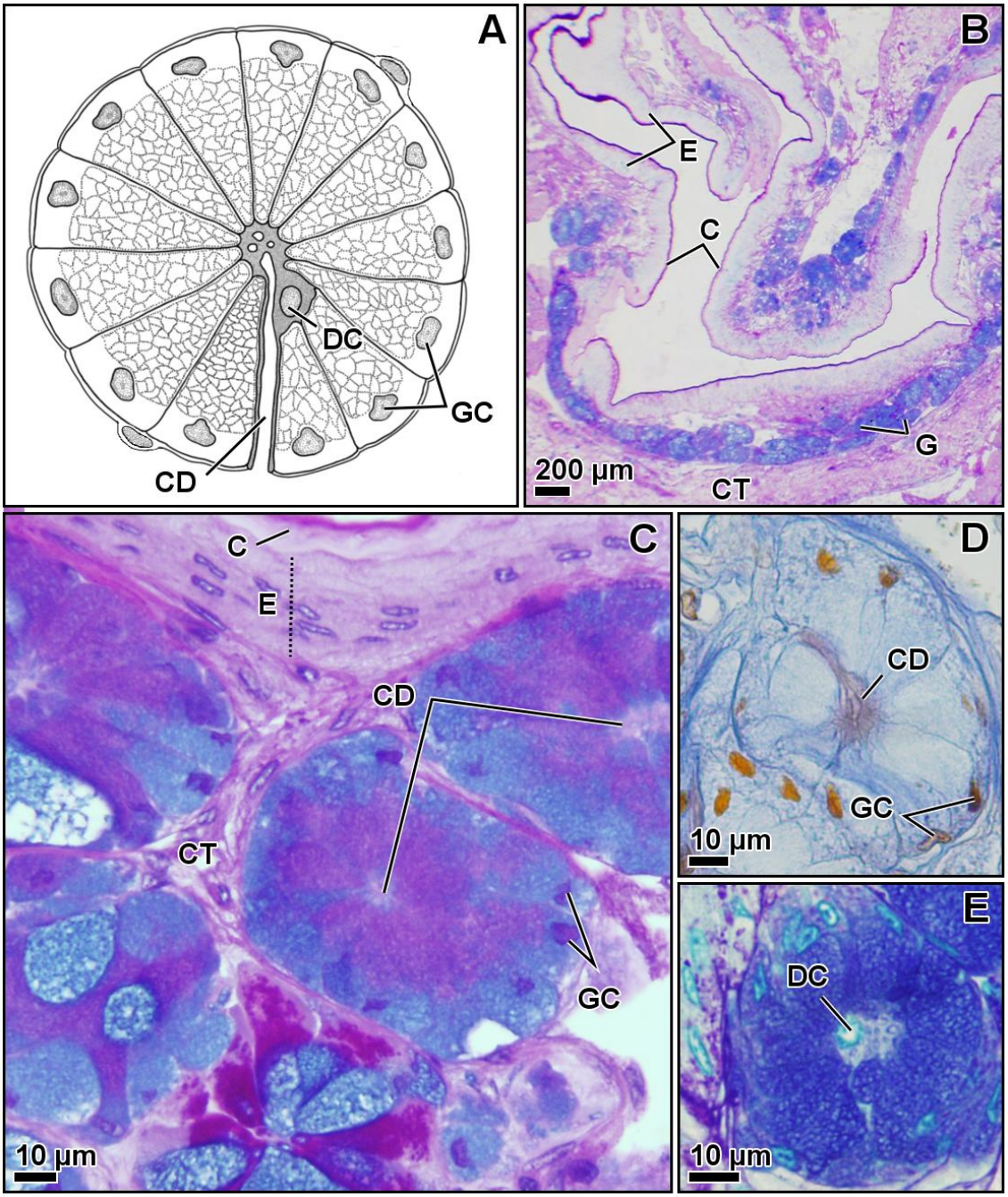

Figure 9. *Maja brachydactyla*. Hindgut tract. Rosette glands. Morphology and histology. Adult. General diagram (A). Extension of the glandular masses (bluish), general view, PAS contrasted with Methylene Blue (B). Rosette glands, close view (C-E): PAS and Alcian Blue contrasted with Hematoxylin (C), Mallory's trichrome (D) and PAS contrasted with Methylene Blue (E). Abbreviations: C, cuticle; CD, central ducts; CT, connective tissue; DC, duct cells; E, epithelium; G, rosette glands; GC, gland cells.

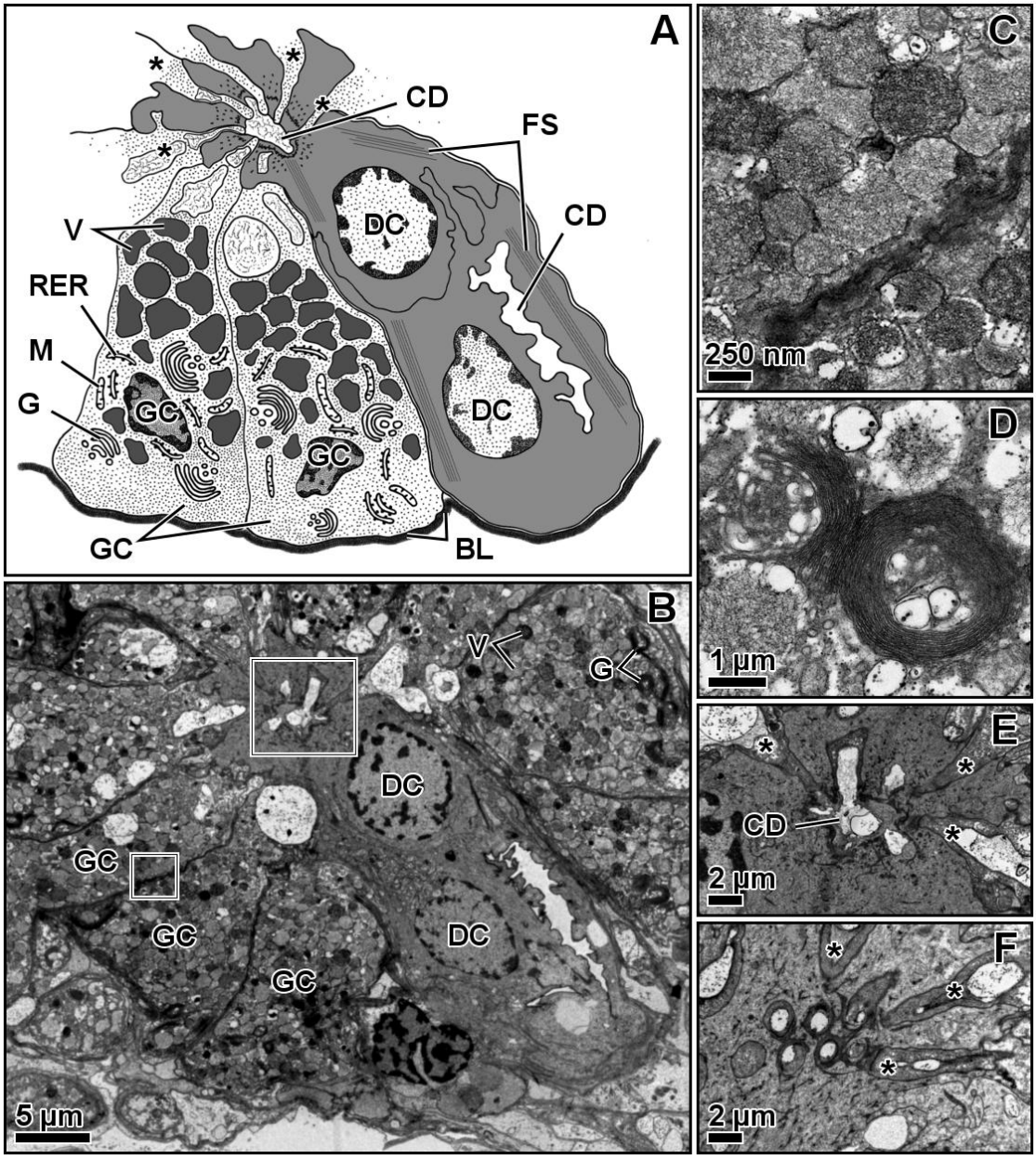

Figure 10. *Maja brachydactyla*. Hindgut tract. Rosette glands. Ultrastructure. Adult. TEM. General diagram (A). General view (B). Secretory vesicles, close view (C). Golgi bodies, close view (D). Central duct and associated collector ducts, close view (E-F). Abbreviations: (asterisk), collector ducts; BL, basal lamina; CD, central duct; DC, duct cells; G, Golgi bodies; GC, gland cells; FS, filamentous structures; M, mitochondria; RER, rough endoplasmic reticulum; V, vesicles of the gland cells.

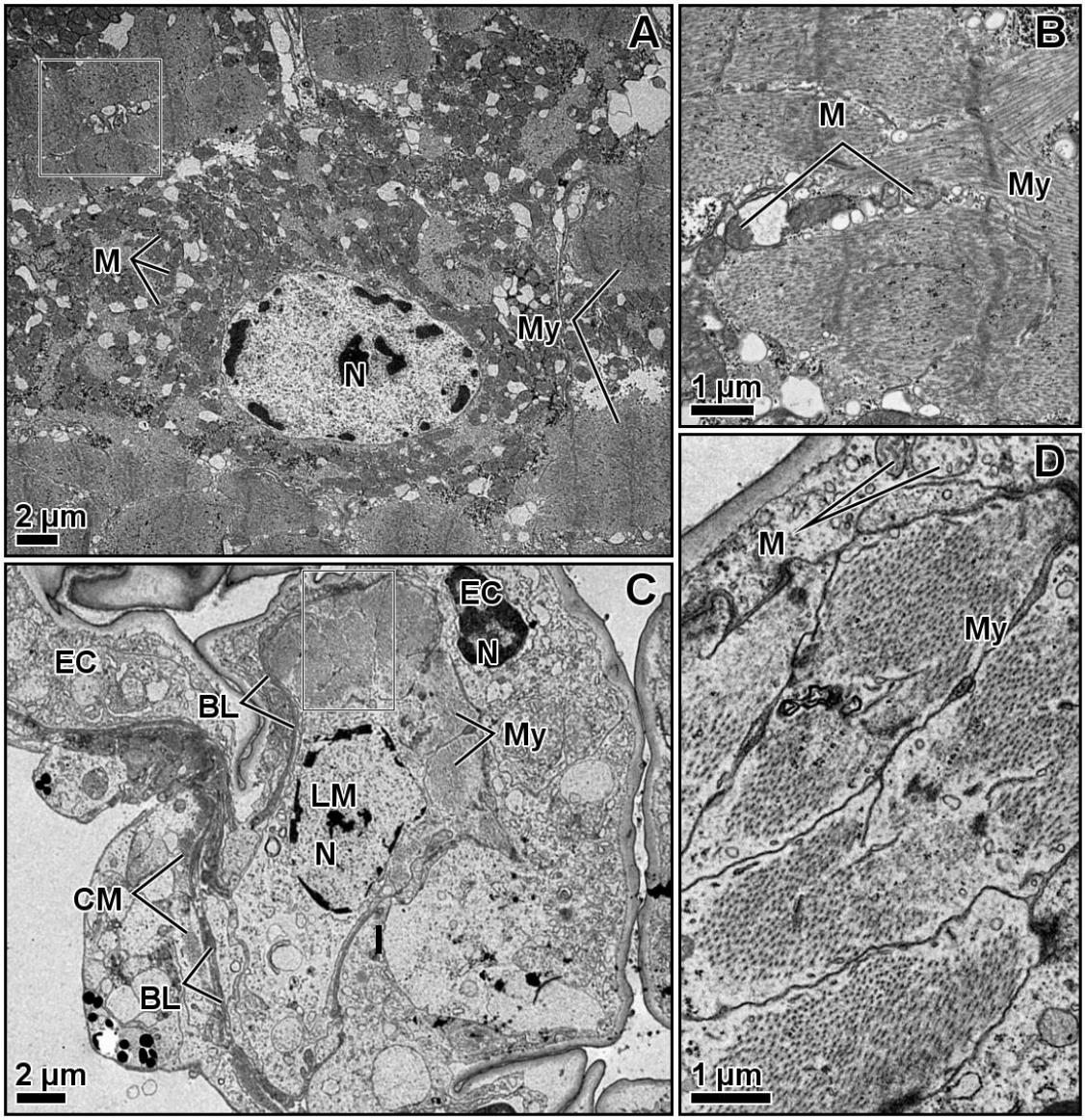

Figure 11. *Maja brachydactyla*. Hindgut tract. Muscle cells. Ultrastructure. TEM. Adult (A-B): general view (A) and close view of the myofibrils (B). Megalopa (10 days after hatching), longitudinal muscle cell located within the hindgut evagination (C-D): general view (C) and close view of the myofibrils (D). Abbreviations: BL, basal lamina; CM, circular muscle fibers; EC, epithelial cells; LM, longitudinal muscle cell; M, mitochondria; MC, muscle cell; My, myofibrils; N, nucleus.

6. References

Abrunhosa FA, Kittaka J. 1997. Morphological changes in the midgut, midgut gland and hindgut during the larval and postlarval development of the red king crab *Paralithodes camtschaticus*. Fisheries Science 63(5):746-754.

Barker PL, Gibson R. 1977. Observations on the feeding mechanism, structure of the gut, and digestive physiology of the european lobster *Homarus gammarus* (L.) (Decapoda: Nephropidae). J Exp Mar Biol Ecol 26(3):297-324.

Barker PL, Gibson R. 1978. Observations on the structure of the mouthparts, histology of the alimentary tract, and digestive physiology of the mud crab *Scylla serrata* (Forskål) (Decapoda: Portunidae). J Exp Mar Biol Ecol 32(2):177-196.

Byers JR, Bond EF. 1971. Surface specializations of the hindgut cuticle of lepidopterous larvae. Canadian Journal of Zoology 49(6):867-876.

Castejón D, Rotllant G, Ribes E, Durfort M, Guerao G. 2015. Foregut morphology and ontogeny of the spider crab *Maja brachydactyla* (Brachyura, Majoidea, Majidae). J Morphol 276(9):1109-1122.

Ceccaldi HJ. 1989. Anatomy and physiology of digestive tract of Crustaceans Decapods reared in aquaculture. Advances in Tropical Aquaculture, Workshop at Tahiti, French Polynesia. Tahiti, French Polynesia: Actes de colloques Ifremer. p 243-259.

Clark PF. 1986. The larval stages of *Maja squinado* (Herbst, 1788) (Crustacea: Brachyura: Majidae) reared in the laboratory. Journal of Natural History 20(4):825-836.

Chisaka H, Ueno M, Futaesaku Y. 1999. Spines in the hindgut of the crayfish *Procambarus clarkii* (Decapoda): their distribution and correlation with hindgut muscles. Journal of Crustacean Biology 19(2):337-343.

Dall W. 1967. The functional anatomy of the digestive tract of a shrimp *Metapenaeus bennettae* Racek & Dall (Crustacea : Decapoda : Penaeidae). Australian Journal of Zoology 15(4):699-714.

Davie PJF, Guinot D, Ng PKL. 2015. Anatomy and functional morphology of Brachyura. In: Castro P, Davie PJF, Guinot D, Schram F, Von Vaupel Klein C, editors. Treatise on Zoology - Anatomy Taxonomy Biology The Crustacea Volume 9 Part C: Brill. p 11-163.

Davolos D, L. P, Accordi F, De Matthaeis E. 2010. Morphology and histology of the mouthparts and gut system of *Macarorchestia remyi* (Schellenberg, 1950) (Amphipoda, Talitridae). Zoologia Baetica 21:151-178.

Dillaman RM, Roer R, Shafer T, Modla S. 2012. The Crustacean Integument: Structure and Function. In: Watling L, Thiel M, editors. The Natural History of the Crustacea, vol 1 Functional Morphology and Diversity: Oxford University Press. p 140-165.

Doughtie DG, Rao KR. 1982. Rosette glands in the gills of the grass shrimp, *Palaemonetes pugio*. I. Comparative morphology, cyclical activity, and innervation. J Morphol 171(1):41-67.

Elzinga RJ. 1998. Microspines in the alimentary canal of arthropoda, onychophora, annelida. International Journal of Insect Morphology and Embryology 27(4):341-349.

Elzinga RJ, Hopkins TL. 1995. Microspine variation in hindgut regions of four families of cockroaches (Blattaria). International Journal of Insect Morphology and Embryology 24(2):203-211.

Erri Babu D, Shyamasundari K, Hanumantha Rao K. 1979. The structure and histochemistry of the oesophageal glands in the crab *Menippe rumphii* (Frabricius) (Crustacea : Brachyura). Proceedings: Animal Sciences 88(4):277-285.

Erri Babu D, Shyamasundari K, Rao KH. 1982. Studies on the digestive system of the crab *Menippe rumphii* (Fabricius) (Crustacea:Brachyura). J Exp Mar Biol Ecol 58(2):175-191.

Factor JR. 1981. Development and metamorphosis of the digestive system of larval lobsters, *Homarus americanus* (Decapoda: Nephropidae). J Morphol 169:225-242.

FAO. 2014. B-42 Crabs, sea-spiders. Capture production by species, fishing areas and countries or areas. In: FAO, editor. FAO yearbook Fishery and aquaculture statistics. Rome: FAO.

Felder DL, Felgenhauer BE. 1993. Morphology of the midgut–hindgut juncture in the ghost shrimp *Lepidophthalmus louisianensis* (Schmitt) (Crustacea: Decapoda: Thalassinidea). Acta Zoologica 74(4):263-276.

Felgenhauer BE. 1992. Chapter 3. Internal Anatomy of the Decapoda: An Overview. In: Harrison FW, Humes AG, editors. Microscopic Anatomy of Invertebrates Volume 10: Decapod Crustacea: Wiley-Liss, Inc. p 45-75.

Forster GR. 1953. Peritrophic membranes in the Caridea (Crustacea Decapoda). Journal of the Marine Biological Association of the United Kingdom 32(2):315-318.

Gorvett H. 1946. The Tegumental Glands in the Land Isopoda A. The Rosette Glands. Quarterly Journal of Microscopical Science s2-87:209-235.

Guerao G, Pastor E, Martin J, Andrés M, Estévez A, Grau A, Duran J, Rotllant G. 2008. The larval development of *Maja squinado* and *M. brachydactyla* (Decapoda, Brachyura, Majidae)

described from plankton collected and laboratory-reared material. Journal of Natural History 42(33-34):2257-2276.

Harris J. 1993a. The presence, nature, and role of gut microflora in aquatic invertebrates: A synthesis. Microbial Ecology 25(3):195-231.

Harris JM. 1993b. Widespread occurrence of extensive epimural rod bacteria in the hindguts of marine Thalassinidae and Brachyura (Crustacea: Decapoda). Marine Biology 116(4):615-629.

Heeren T, Mitchell BD. 1997. Morphology of the mouthparts, gastric mill and digestive tract of the giant crab, *Pseudocarcinus gigas* (Milne Edwards) (Decapoda: Oziidae). Marine and Freshwater Research 48(1):7-18.

Hinton DJ, Corey S. 1979. The mouthparts and digestive tract in the larval stages of *Homarus americanus*. Canadian Journal of Zoology 57(7):1413-1423.

Holdich DM. 1973. The Midgut/Hindgut Controversy in Isopods. Crustaceana 24(2):211-214.

Holdich DM, Mayes KR. 1975. A Fine-Structural Re-Examination of the so-called 'Midgut' of the isopod *Porcellio*. Crustaceana 29(2):186-192.

Holdich DM, Ratcliffe NA. 1970. A light and electron microscope study of the hindgut of the herbivorous isopod, *Dynamene bidentata* (Crustacea: Peracarida). Zeitschrift für Zellforschung und Mikroskopische Anatomie 111(2):209-227.

Hopkin SP, Nott JA. 1980. Studies on the digestive cycle of the shore crab *Carcinus maenas* (L.) with special reference to the b cells in the hepatopancreas. Journal of the Marine Biological Association of the United Kingdom 60(04):891-907.

Huxley TH. 1880. The Crayfish; an Introduction to the Study of Zoology. Series TIS, editor: New York: D. Appleton and Company.

Icely JD, Nott JA. 1992. Digestion and absorption: digestive system and associated organs. In: Harrison FW, Humes AG, editors. Microscopic anatomy of invertebrates: decapod Crustacea. New York: Wiley-Liss. p 147-201.

Jantrarotai PN, Sawanyatiputi SA. 2005. Histological study on the development of digestive system in zoeal stages of mud crab (*Scylla olivacea*). Kasetsart Journal 39(4):666-671.

Johnston D. 2007a. Feeding Morphology and Digestive System of Slipper Lobster. In: Lavalli KL, Spanier E, editors. The Biology and Fisheries of the Slipper Lobster: CRC Press. p 111-132.

Johnston D. 2007b. Feeding Morphology and Digestive System of Slipper Lobsters. The Biology and Fisheries of the Slipper Lobster: CRC Press. p 111-132.

Komuro T, Yamamoto T. 1968. Fine structure of the epithelium of the gut in the crayfish (*Procambarus clarkii*) with special reference to the cytoplasmic microtutubles. Archivum histologicum japonicum 30(1):17-32.

Lovett DL, Felder DL. 1989. Ontogeny of gut morphology in the white shrimp *Penaeus setiferus* (Decapoda, Penaeidae). J Morphol 201(3):253-272.

Martin GG, Chiu A. 2003. Morphology of the midgut trunk in the penaeid shrimp, *Sicyonia ingentis*, highlighting novel nuclear pore particles and fixed hemocytes. J Morphol 258(2):239-248.

Martin GG, Simcox R, Nguyen A, Chilingaryan A. 2006. Peritrophic membrane of the penaeid shrimp *Sicyonia ingentis*: structure, formation, and permeability. The Biological Bulletin 211(3):275-285.

McLaughlin PA. 1983. 1. Internal Anatomy. In: Mantel LH, editor. The Biology of Crustacea Vol 5 Internal Anatomy and Physiological Regulation: Academic Press. p 1-52.

Mikami S, Greenwood JG, Takashima F. 1994. Functional morphology and cytology of the phyllosomal digestive system of *Ibacus ciliatus* and *Panulirus japonicus* (Decapoda, Scyllaridae and Palinuridae). Crustaceana 67(2):212-225.

Milne-Edwards H. 1834a. Histoire naturelle des crustacés, comprenant l'anatomie, la physiologie et la classification de ces animaux: Libraire Encyclopédique de Roret.

Milne-Edwards H. 1834b. Histoire naturelle des crustacés: atlas: Libraire Encyclopédique de Roret.

Miyoshi AR, Gabriel VA, Fantazzini ER, Fontanetti CS. 2005. Microspines in the pylorus of *Pseudonannolene tricolor* and *Rhinocricus padbergi* (Arthropoda, Diplopoda). Iheringia Série Zoologia 95:183-187.

Moon YW, Kim HH. 1999. Morphological study of the digestive tract of the mud crab (*Hemigrapsus penicillatus* De Haan) and the symbiotic crab (*Pinnotheres cyclinus* Shen). Korean Journal of Biological Sciences 3(4):407-412.

Mykles DL. 1979. Ultrastructure of alimentary epithelia of lobsters, *Homarus americanus* and *H. gammarus*, and crab, *Cancer magister*. Zoomorphologie 92(3):201-215.

Pillai RS. 1960. Studies on the shrimp *Caridina laevis* (Heller) 1. The Digestive System. Journal of the Marine Biological Association of India 2(1):57-74.

Pinn EH, Nickell LA, Rogerson A, Atkinson RJA. 1999. Comparison of gut morphology and gut microflora of seven species of mud shrimp (Crustacea: Decapoda: Thalassinidea). Marine Biology 133:103-114.

Pugh JE. 1962. A contribution toward a knowledge of the hind-gut of fiddler crabs (Decapoda, Grapsidae). Transactions of the American Microscopical Society 81(4):309-320.

Reddy AR. 1937. The physiology of digestion and absorption in the crab *Paratelphusa* (*Oziotelphusa*) *hydrodromus* (Herbst). Proceedings of the Indian Academy of Sciences - Section B 6(3):170-193.

Roer R, Dillaman RM. 1984. The structure and calcification of the crustacean cuticle. American Zoologist 24(4):893-909.

Schlegel C. 1911. Anatomie sommaire de la première zoé de *Maja squinado* Latr. (Note préliminaire à des recherches sur l'Organogénese des Décapodes brachyoures). Archives de Zoologie Experimentale et Générale 5º Série T. VIII.(2):29-40.

Schlüter U. 1980. Ultrastruktur der Pyloruszähnchen zweier Tausendfüßler (*Tachypodoiulus niger*, *Polydesmus angustus*)*. Acta Zoologica 61(3):171-178.

Schmitz EH, Scherrey PM. 1983. Digestive anatomy *Hyalella azteca* (Crustacea, Amphipoda). J Morphol 175:91-100.

Smith RI. 1978. The Midgut Caeca and the Limits of the Hindgut of Brachyura: A Clarification. Crustaceana 35(2):195-205.

Sousa L, Petriella AM. 2006. Morphology and histology of *P. argentinus* (Crustacea, Decapoda, Caridea) digestive tract. Biocell 30:287-294.

Štrus J, Drobne D, Ličar P. 1995. Comparative anatomy and functional aspects of the digestive system in amphibious and terrestrial isopods (Isopoda: Oniscidea). In: Alikkhan MA, editor. Crustacean Issues "Terrestrial Isopod Biology". Rotterdam, Netherlands: Balkema Publishers. p 13-23.

Štrus J, Klepal W, Repina J, Tušek-Ţnidarič M, Milatovič M, Pipan Ţ. 2008. Ultrastructure of the digestive system and the fate of midgut during embryonic development in *Porcellio scaber* (Crustacea: Isopoda). Arthropod Structure & Development 37(4):287-298.

To TH, Brenner TL, Cavey MJ, Wilkens JL. 2004. Histological organization of the intestine in the crayfish *Procambarus clarkii*. Acta Zoologica 85(2):119-130.

Trinadha Babu B, Shyamasundari K, Hanumantha Rao K. 1989a. Observations on the morphology and histochemistry of the midgut and hindgut of *Portunus sanguinolentus* (Herbst) (Crustaceans: Brachyura). Folia Morphologica 37(4):373-381.

Trinadha Babu B, Shyamasundari K, Hanumantha Rao K. 1989b. Observations on the morphology and histology of the foregut of *Portunus sanguinolentus* (Crustacea: Brachyura). Folia Morphologica 37(4):364-372.

Tziouveli V, Bastos-Gomez G, Bellwood O. 2011. Functional morphology of mouthparts and digestive system during larval development of the cleaner shrimp *Lysmata amboinensis* (de Man, 1888). J Morphol 272(9):1080-1091.

Vernon GM, Herold L, Witkus ER. 1974. Fine structure of the digestive tract epithelium in the terrestrial isopod. *Armadillidium vulgare*. J Morphol 144(3):337-359.

Wang L, Li F, Wang B, Xiang J. 2012. Structure and partial protein profiles of the peritrophic membrane (PM) from the gut of the shrimp *Litopenaeus vannamei*. Fish & Shellfish Immunology 33(6):1285-1291.

Williams RL. 1944. The pre-zoea stage of *Porcellana platycheles* (Pennant). Preliminary anatomical and histological notes. Journal of the Royal Microscopical Society 64(1-2):1-15.

Witkus ER, Grillo RS, Smith WJ. 1969. Microtubule bundles in the hindgut epithelium of the woodlouse *Oniscus ascellus*. Journal of Ultrastructure Research 29(3):182-190.

Yonge CM. 1924. Studies on the comparative physiology of digestion II. - The mechanism of feeding, digestion, and assimilation in *Nephrops norvegicus*. British Journal of Experimental Biology 1:343-389.

Yonge CM. 1932. On the nature and permeability of Chitin. I.--The Chitin lining the Foregut of Decapod Crustacea and the function of the Tegumental Glands. Proceedings of the Royal Society B: Biological Sciences 111(772):298-329.

BLOQUE 2.

SISTEMA DIGESTIVO. DISCUSIÓN.

"*Being clothed in a hard exoskeleton, devoid of cilia, and with limited ability to produce mucus but with seemingly limitless capacity to mold and reconfigure the features of their mouth appendages, crustaceans have evolved so that they can feed on almost anything*"

Les Watling 2013

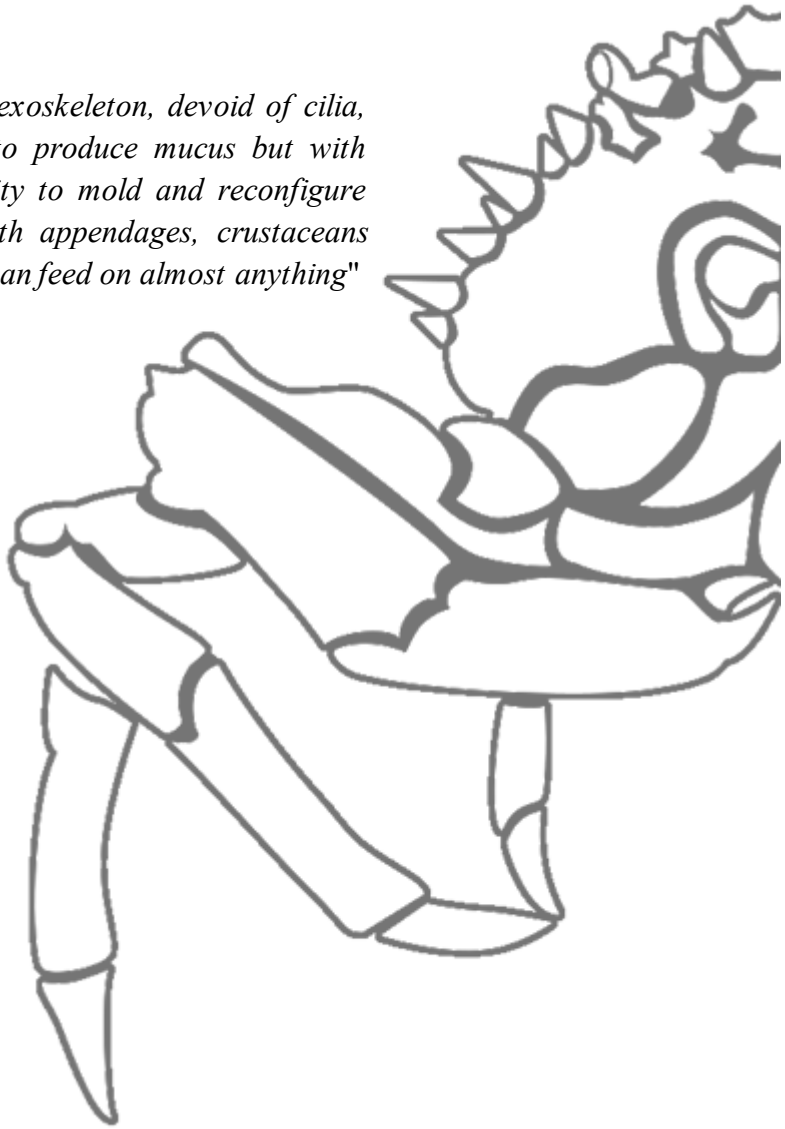

En el presente capítulo se discuten de manera global aquellos aspectos sobre el sistema digestivo que han sido tratados de forma individualizada en los artículos previos que componen este bloque. Previamente, es preciso clarificar la nomenclatura empleada. Para ello se ha realizado la siguiente tabla, la cual ha sido realizada en base a las revisiones realizadas por McLaughlin (1983), Icely y Nott (1992) y Cervellione et al. (2017).

Tabla 1. Nomenclatura empleada en relación a los órganos digestivos de los malacostráceos.

Denominación traducida	**Denominación inglesa**	**Otras denominaciones**
esófago	*esophagus*	buccal cavity, oesophagus
estómago cardiaco	*cardiac stomach*	anterior foregut, anterior region, cardiac chamber, gizzard, proventriculus (anterior)
estómago pilórico	*pyloric stomach*	posterior foregut, posterior region, posterior chamber, proventriculus (posterior), pylorus
glándula digestiva	*midgut gland*	branched diverticula, digestive gland, digestive diverticula, hepatopancreas, hepatic caeca, hepatic gland, intestinal caecum, lateral caecum, midgut diverticula, perigastric organ, racemose gland, pancreas, perigastric organ
tracto digestivo medio	*midgut*	intestine, midgut trunk, stomach
ciegos anteriores	*anterior midgut caeca*	accessory gland, anterior midgut cecum/a, blind pouch of midgut, dorsal cecum/a, hepatic cecum, pyloric cecum/a,
ciego posterior	*posterior midgut caeca*	excretory caecum, hindgut caecum, hindgut gland, posterior midgut cecum, posterior diverticulum, posterior midgut diverticulum, renal gland, rectal cecum, rectal gland
tracto digestivo posterior	*hindgut*	midgut (isopods)

19.1 Iniciación en el estudio morfológico de las larvas de decápodos.

Una primera aproximación para estudiar la morfología interna es la disección de los especímenes. Realizar una correcta disección requiere destreza y conocimientos previos sobre la anatomía interna de la especie que se desea estudiar. El proceder durante la disección varía de acuerdo a la etapa vital y los órganos que se desean extraer o visualizar, de modo que cada etapa vital y sistema de órganos puede requerir una estrategia distinta. La disección precisa de gran cantidad de ejemplares, especialmente durante el aprendizaje inicial, por lo que es recomendable disponer de abundancia de especímenes a la hora de abordar este tipo de estudios. Las estrategias descritas en este apartado están enfocadas al estudio anatómico del sistema digestivo de *M. brachydactyla* (quizás podrían extrapolarse a los braquiuros en general), por lo que podrían no ser aplicables para otros sistemas de órganos u otros taxones.

Los estadios larvarios de *M. brachydactyla* tienen una talla de entre 0,5 y 2,2 mm (Andrés et al., 2008). La disección se realizó bajo la lupa binocular usando de agujas hipodérmicas 25 G unidas a jeringas usadas como mango. Durante la disección los especímenes deben estar en solución acuosa para evitar la deshidratación y el colapso de estructuras, lo que dificultaría de forma importante la disección. Es más difícil diseccionar especímenes frescos que fijados, ya que la fijación otorga mayor consistencia a las estructuras corporales. Quien desee iniciarse en la disección de este tipo de animales debe estar prevenido de que cada etapa vital tiene una morfología diferente que obliga a abordar la disección de un modo específico:

Zoeas. El caparazón dorsal es una delicada lámina dividida tras la espina dorsal en dos extensiones laterales que recubren parcialmente los pereiópodos (Fig. 19.1.1A-B). Retirarlo requiere hacer un corte longitudinal en el caparazón usando la aguja a modo de bisturí, para ello la aguja es introducida desde la región posterior en sentido anterior hacia el espacio dorsal existente entre el caparazón y los órganos internos. Este corte permite retirar el caparazón dorsal como si fuesen un par de "valvas". El caparazón cefálico es más complicado de retirar ya que la aplicación de una presión mínima puede separar el estómago de la glándula digestiva y el tracto digestivo medio. La estrategia más exitosa requiere romper cuidadosamente la musculatura de la región mandibular, ya que está firmemente unida al esófago. Una vez se ha logrado la retirada de la parte cefálica del caparazón, los maxilípedos y pereiópodos pueden separarse fácilmente del sistema digestivo "tirando" de ellos, esto también retirará la masa ganglionar torácica. En cuanto al pleon, basta presionar y estirar en sentido opuesto los laterales de un segmento para "abrirlo" exponiendo los órganos, es difícil dañar al tracto digestivo posterior dado el menor diámetro de este último en comparación con el diámetro del pleon.

Megalopas. El caparazón dorsal "cierra" la región dorso-lateral (Fig. 19.1.1C-D). Como primer paso se recomienda eliminar los pereiópodos dado que entorpecen la disección debido a su mayor tamaño. A continuación, se recomienda voltear el espécimen para cortar y retirar las paredes laterales del caparazón, eliminadas estas puede quitarse la pared dorsal del mismo. Durante este proceder la mayor dificultad reside en conservar intacta la glándula digestiva, cuyo mayor tamaño incrementa las probabilidades de dañarla durante el proceso de disección. El resto del proceder es similar al de la zoea, si bien resulta mucho más fácil separar el esófago de la región mandibular sin romper la unión del estómago con el tracto digestivo medio.

Primer juvenil. En el caso de los juveniles, el caparazón dorsal es semejante al de las megalopas (Fig. 19.1.1E-F), si bien al estar más endurecido quiebra con mayor facilidad. El proceso de disección es similar al descrito en las megalopas.

Adultos. El caparazón dorsal de los adultos es una estructura mucho más endurecida y calcificada que en cualquiera de las etapas anteriormente mencionadas. Como en los juveniles, el caparazón cubre por completo la región dorsal y está unido a los escleritos ventrales por una fina membrana pleural. Inicialmente se pensó en retirar el caparazón dorsal cortando la membrana pleural con un bisturí, pero pronto descubrimos que resulta inviable: cortar la membrana pleural es un proceso lento e ineficiente dado que el estrecho espacio existente entre el caparazón dorsal y los escleritos apenas permite la entrada y el movimiento del bisturí, además se percibió que cortar gran parte de la membrana pleural no basta para separar el caparazón dorsal. También se comprobó que retirar el caparazón dorsal forzadamente daña los órganos internos: rompe la unión del estómago con el tracto digestivo posterior así como la glándula digestiva y los ciegos asociados al tracto digestivo. Por estas razones se adoptó una estrategia distinta basada en el empleo de alicates de punta plana. Esta idea puede parecer contra-intuitiva dado el aspecto tosco de dicha herramienta, pero ha resultado sorpresivamente útil. Comenzando desde el borde posterior, el caparazón fue troceado cuidadosamente evitando contacto con los órganos internos, para ello la punta inferior de los alicates se apretó contra la cara interna del caparazón. Con los alicates presionando el caparazón el esfuerzo se realizó hacia el exterior. Mediante este proceso fue posible eliminar la mayor parte del caparazón dorsal y exponer intactos los órganos internos.

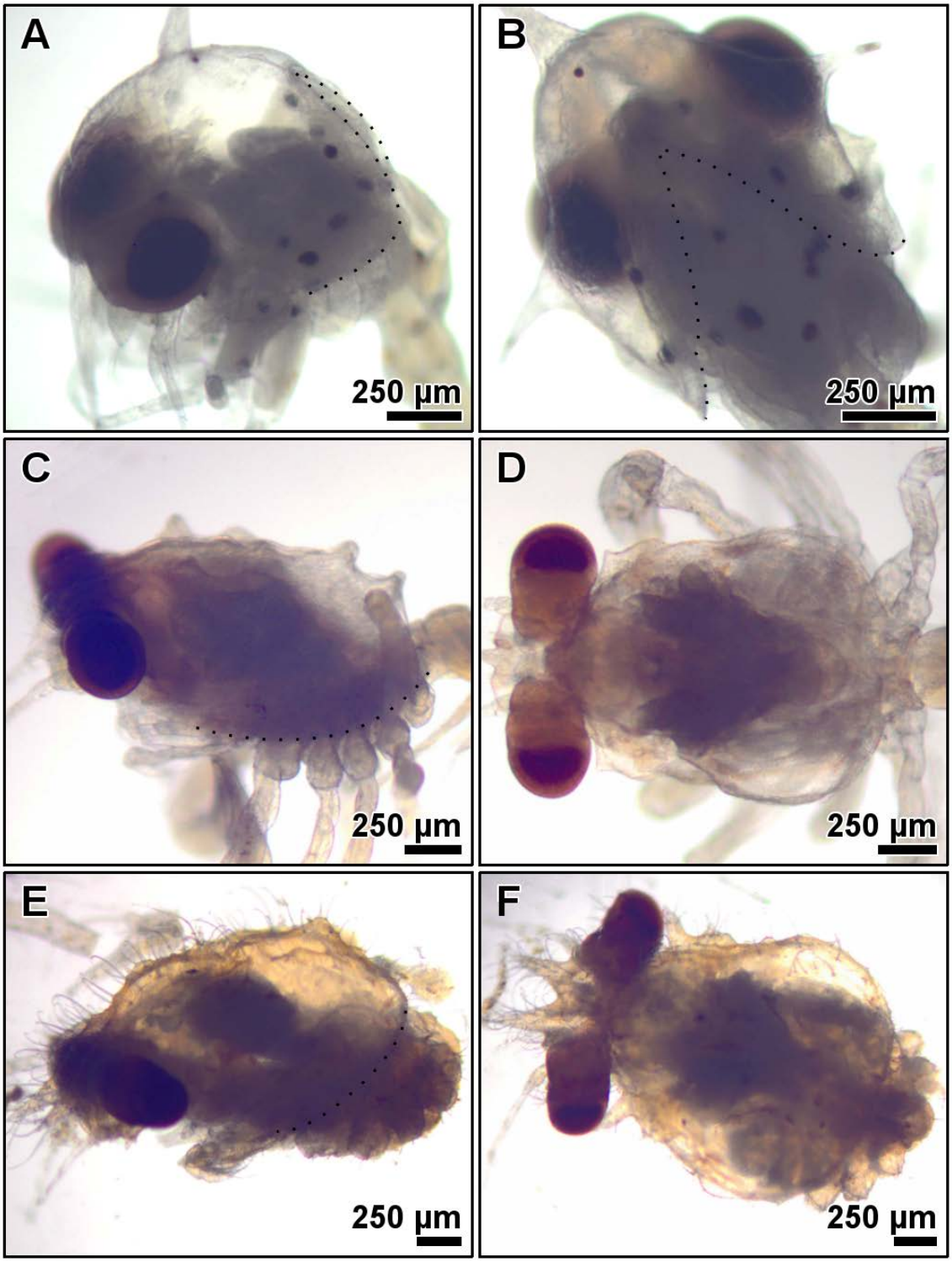

Figura 19.1.1. Estadios de zoea, megalopa y juvenil. Zoea I (A-B): vista lateral (A) y posterior (B). Megalopa (C-D): vista lateral (C) y dorsal (D). Juvenil, sin pereiópodos (E-F): vista lateral (E) y dorsal (F). En algunas imágenes el caparazón ha sido marcado con línea discontinua (A, B, C, E).

La disección permite la observación directa de numerosas estructuras anatómicas. Sin embargo, también implica la destrucción de los especímenes estudiados, ya que el acceso a determinadas estructuras requiere la eliminación de otras. Adicionalmente, ciertas estructuras son difíciles de estudiar debido a su reducido tamaño y nivel de transparencia. Por ello no resulta posible estudiar todos los órganos internos en su localización original. Sin embargo, existe una técnica que permite visualizar los distintos órganos en su localización original: los estudios histológicos realizados mediante técnicas de microscopía óptica, que permiten explorar la anatomía larvaria en secciones bidimensionales cuyo nivel de detalle alcanza el nivel tisular. Sin embargo, la microscopía óptica no carece de desventajas, la más notoria es la limitación de las observaciones a dos dimensiones y la necesidad de realizar gran cantidad de cortes seriados para poder elaborar un modelo tridimensional, un trabajo que requiere de una gran cantidad de especímenes, tiempo y material (Dinley et al., 2010; Wanninger, 2007).

La observación de estructuras larvarias bajo el microscopio electrónico de barrido (MEB) es otro reto debido al pequeño tamaño y fragilidad de dichas estructuras, características que dificultan su manipulación así como el tratamiento requerido para su observación en MEB. Las observaciones realizadas en MEB ayudan de forma inestimable a interpretar correctamente las observaciones histológicas. En ese sentido, las observaciones de MEB han resultado cruciales para estudiar la forma y organización de las espinas del esófago y tracto digestivo posterior (Fig. 19.6.1-3; 19.6.4B), la morfología del molino gástrico durante distintos estadios (Fig. 19.3.5E; 19.6.4E-F), el aspecto de los pliegues presentes en los ciegos digestivos y su actividad secretora (Fig. 19.9.4E-F; 19.9.5E-F), así como la organización muscular de los túbulos de la glándula digestiva (Fig. 19.3.4E-F). Todos estos detalles anatómicos habrían sido interpretados de un modo distinto o bien pasados por alto de no utilizar la MEB.

Otro avance crucial para los estudios anatómicos ha sido el desarrollo de una técnica que permite observar directamente la estructura tridimensional de los órganos (como en la disección y la microscopía electrónica de barrido) conservando al mismo tiempo la disposición original de los mismos (como en las técnicas histológicas). Se trata de la micro tomografía computarizada (micro-CT por sus siglas en inglés, «*micro computed tomography*»). Esta tecnología reconstruye de forma virtual los especímenes estudiados, tanto a nivel de morfología externa como de anatomía interna (Alba-Tercedor, 2014; Alba-Tercedor y Sáinz-Cantero, 2012; Betz et al., 2007; Handschuh et al., 2017; Socha y De Carlo, 2008). El carácter virtual implica que los modelos pueden ser manipulados mediante software especializado, permitiendo su examen desde cualquier ángulo y profundidad. Por ello, la micro-CT permite disponer de modelos virtuales que permiten estudiar directamente la anatomía interna sin alterarla.

En los modelos de micro-CT las estructuras más visibles son la cutícula, las masas musculares, los órganos del sistema digestivo y las principales formaciones del sistema nervioso (Fig. 19.1.2-3); situación similar a la observada en insectos (Antunes-Carvalho et al., 2017; Betz et al., 2007; Franz-Guess et al., 2016; Ge et al., 2015; Lowe et al., 2013). Todas estas estructuras tienen en común su organización como densas agregaciones celulares (como el tejido muscular o los ganglios nerviosos) o bien se caracterizan por poseer células epiteliales altas y/o están cubiertas por cutícula (como sucede con los órganos del sistema digestivo). Los estudios realizados por otros autores también aventuran que esta tecnología revela con mayor facilidad aquellas estructuras grandes y robustas o bien provistas de gruesas células o cutícula (Dinley et al., 2010; Lowe et al., 2013), debido a su mayor capacidad de absorción de rayos X.

Por el contrario, las estructuras asociadas al sistema circulatorio (pericardio, corazón y vasos) y respiratorio (branquias) tienen menor contraste debido a que están delimitadas por células y/o cutícula muy delgadas. En el mismo sentido, ciertas estructuras como los nervios de menor diámetro no son observables ya que están por debajo del límite de resolución de esta tecnología. Estas limitaciones pueden solventarse si la micro-CT se combina con el estudio histológico, el cual permite identificar aquellas estructuras no observables por su reducido tamaño así como identificar aquellas estructuras cuya identificación es incierta. Por esa razón, Betz et al. (2007) ya sugirieron que deberían de combinarse los modelos de micro-CT con las observaciones histológicas con objeto de obtener resultados óptimos en los estudios anatómicos. Nuestros resultados demuestran dicha afirmación, ya que las técnicas histológicas permiten resolver la identidad de aquellas estructuras que no se identifican fácilmente mediante micro-CT, además las técnicas histológicas también permiten la visualización de aquellas estructuras que debido a su tamaño no aparecen (al menos con claridad) en los modelos de micro-CT.

Los modelos de micro-CT del estadio de zoea no han sido obtenidos con la misma calidad que los estudios del estadio de megalopa. En dichos modelos el exoesqueleto muestra cierto nivel de degradación, mientras que los órganos internos no presentan la misma calidad de resolución, siendo comparativamente más difícil identificar numerosas estructuras. Las causas de este resultado son desconocidas. Las zoeas fueron tratadas de forma distinta a las megalopas, ya que fueron fijadas en una solución de aldehídos y post-fijadas con tetraóxido de osmio. Sin embargo este tratamiento no tendría por qué afectar a la calidad de las observaciones, por el contrario se ha recomendado el uso de agentes de contraste para estudiar tejidos blandos mediante técnicas de micro-CT (Holdsworth y Thornton, 2002), siendo el tetraóxido de osmio uno de los agentes recomendados (Metscher, 2009a; b). Por lo tanto, el uso de este tratamiento fijador debería de ser descartado como causante de tales resultados. Sin pruebas ni datos adicionales, no podemos aseverar la causa (o causas) de dicha degradación.

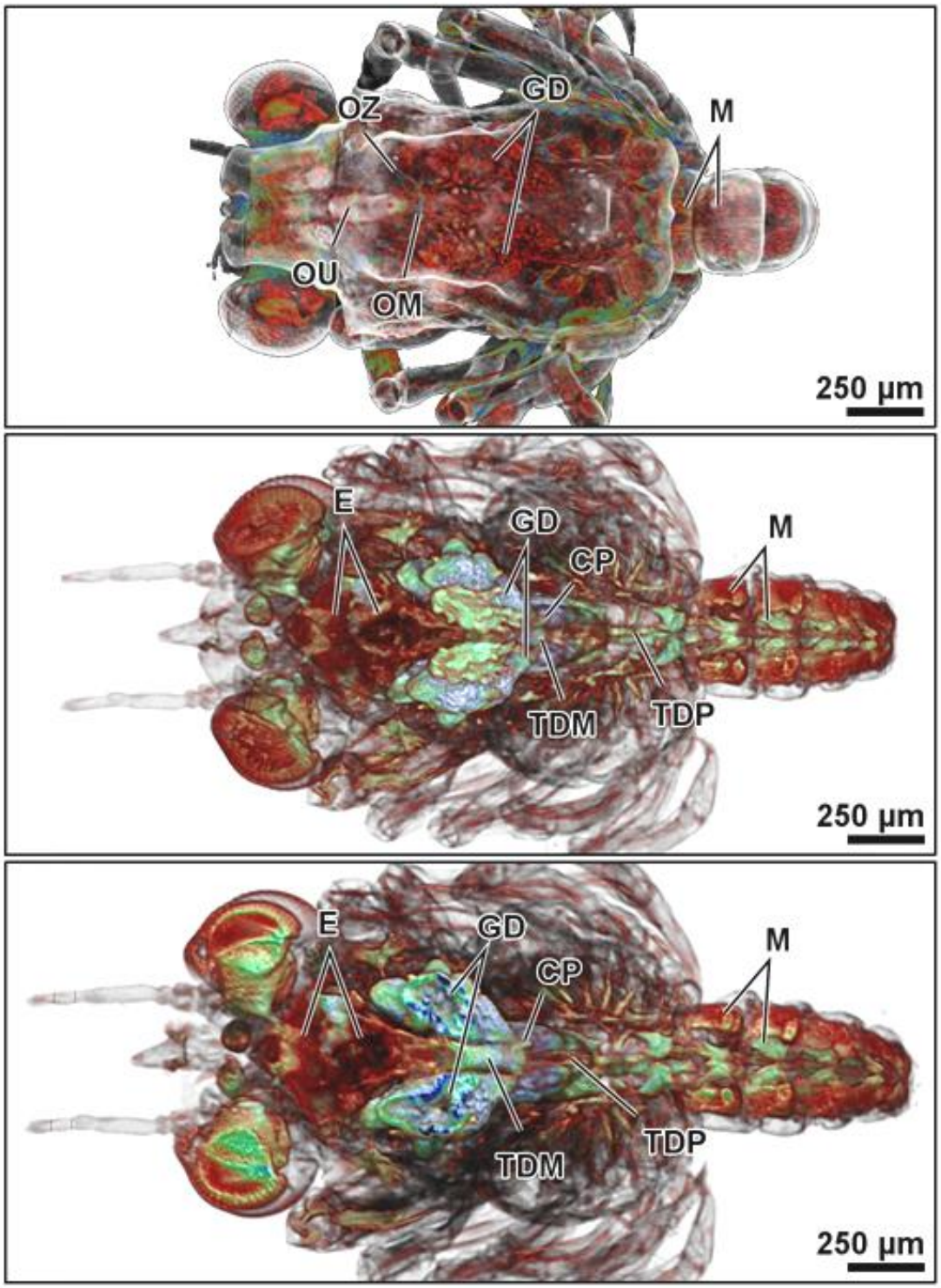

Figura 19.1.2. Megalopa. Modelo tridimensional obtenido mediante micro-CT. Distintas secciones dorso-ventrales. Abreviaciones: CP, ciego posterior; E, estómago; GD, glándula digestiva; M, musculatura; TDM, tracto digestivo medio; TDP, tracto digestivo posterior; OM, osículo mesocárdico del estómago; OU, osículo urocárdico del estómago; OZ, osículos zigocárdicos del estómago.

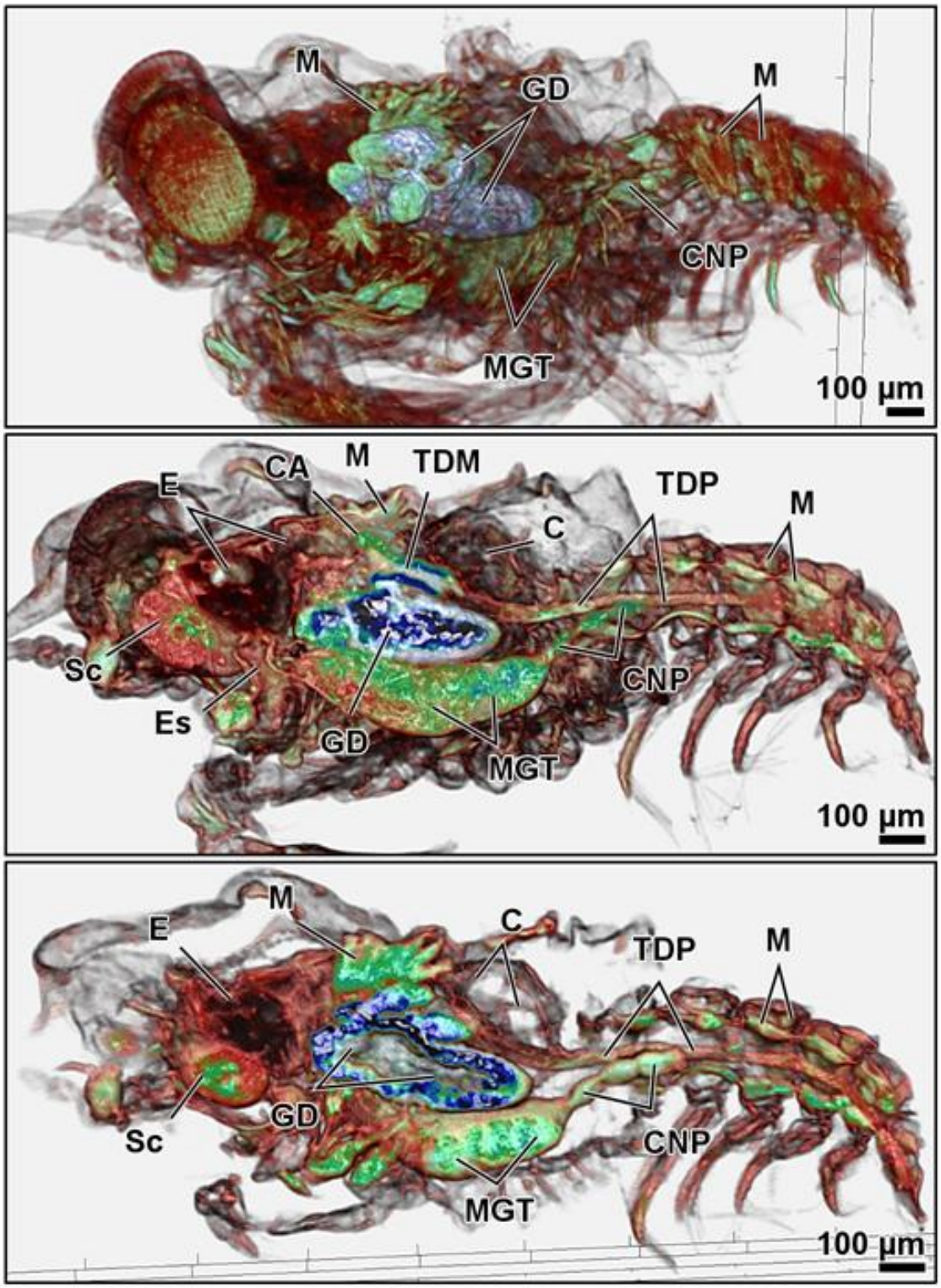

Figura 19.1.3. Megalopa. Modelo tridimensional obtenido mediante micro-CT. Distintas secciones sagitales. Abreviaciones: CA, ciegos anteriores; CNP, cordón nervioso posterior; C, corazón; Es, esófago; E, estómago; GD, glándula digestiva; M, musculatura; MGT, masa ganglionar torácica; Sc, sincerebro; TDM, tracto digestivo medio; TDP, tracto digestivo posterior.

19.2 Sobre los epitelios derivados del ectodermo y endodermo.

Los distintos órganos que conforman el sistema digestivo tienen características propias relacionadas con su localización y su rol especializado. Sin embargo, a pesar de dichas diferencias es posible observar que los órganos del sistema digestivo tienen características comunes que permiten diferenciarlos en dos grandes grupos: derivados del ectodermo embrionario y derivados del endodermo embrionario.

En los malacostráceos, los órganos digestivos derivados del ectodermo embrionario incluyen al esófago, estómago, tracto digestivo posterior y ano (Anger, 2001; Felgenhauer, 1992; Icely y Nott, 1984; Icely y Nott, 1992; McLaughlin, 1983; Soonthornchai et al., 2015; Ńtrus et al., 2008). Son órganos caracterizados por estar revestidos internamente por una cutícula quitinosa que debe de ser mudada periódicamente (Anger, 2001; Icely y Nott, 1992; McLaughlin, 1983), la presencia de dicha cutícula ha sido confirmada en el presente estudio (Fig. 19.2.1). Teniendo en cuenta únicamente a la etapa adulta, el grosor de la cutícula es muy variable, desde varias veces inferior a la altura de la célula epitelial (Fig. 19.2.1C) hasta varias veces superior a dicha altura (Fig. 19.2.1B). La cutícula es la característica más destacable, pero además se han encontrado otros paralelismos entre los epitelios del esófago, estómago y tracto digestivo posterior: las células son generalmente altas y prismáticas (si bien otras morfologías celulares se han identificado en el estómago) y presentan un núcleo esférico a elipsoidal situado en posición media a basal (Fig. 19.2.1).

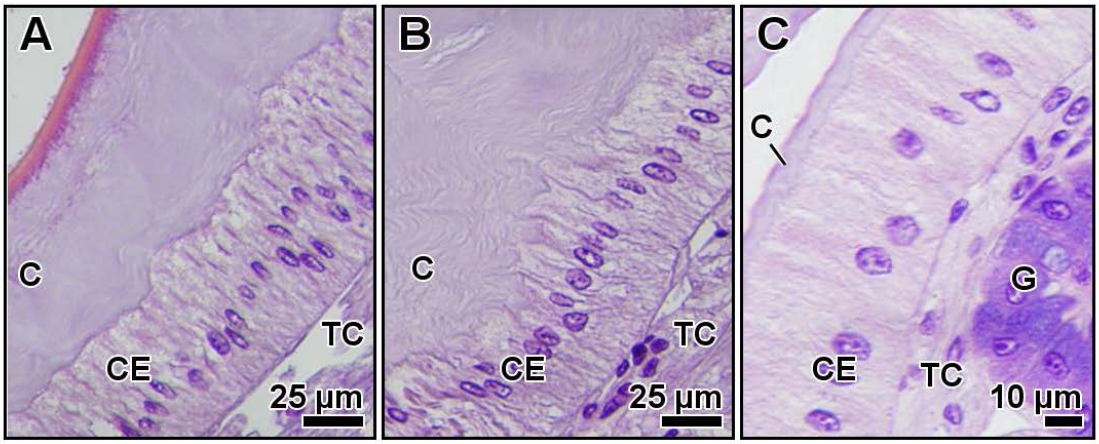

Figura 19.2.1. Adulto. Epitelio de los órganos digestivos derivados del ectodermo embrionario. Tinción de Hematoxilina - Eosina. Esófago (A). Estómago, saco cardiaco (B). Tracto digestivo posterior (C). Abreviaciones: C, cutícula; CE, células epiteliales; G, glándulas de roseta; TC, tejido conectivo.

Aún más interesante es el hecho de que las células epiteliales de los órganos digestivos derivados del ectodermo embrionario tienen características ultra-estructurales comunes. Una de las más prominentes son los gruesos paquetes de estructuras filamentosas, de naturaleza incierta. Estas recorren el eje vertical de las células, desde la región basal hasta la apical (Fig. 19.2.2D-F) y se anclan a los "complejos apicales": invaginaciones electrodensas de la membrana apical (Fig. 19.2.2A-C). Tanto los filamentos como los "complejos apicales" han sido descritos en braquiuros (Mykles, 1979), astacídeos (Komuro y Yamamoto, 1968; Mykles, 1979) e isópodos (Holdich y Mayes, 1975; Holdich y Ratcliffe, 1970; Storch et al., 2002; Vernon et al., 1974; Witkus et al., 1969).

Se ha postulado que estos filamentos podrían proporcionar rigidez a las células y que conectarían a las fibras musculares con la cutícula (Komuro y Yamamoto, 1968; Mykles, 1979). También se postula que podrían actuar como elementos de transporte intracelular (Komuro y Yamamoto, 1968); así como alinearían y organizarían las mitocondrias y otros orgánulos, ya que estas suelen orientarse paralelas a dichos filamentos (Vernon et al., 1974; Witkus et al., 1969). Sin embargo, su verdadero rol sigue siendo desconocido.

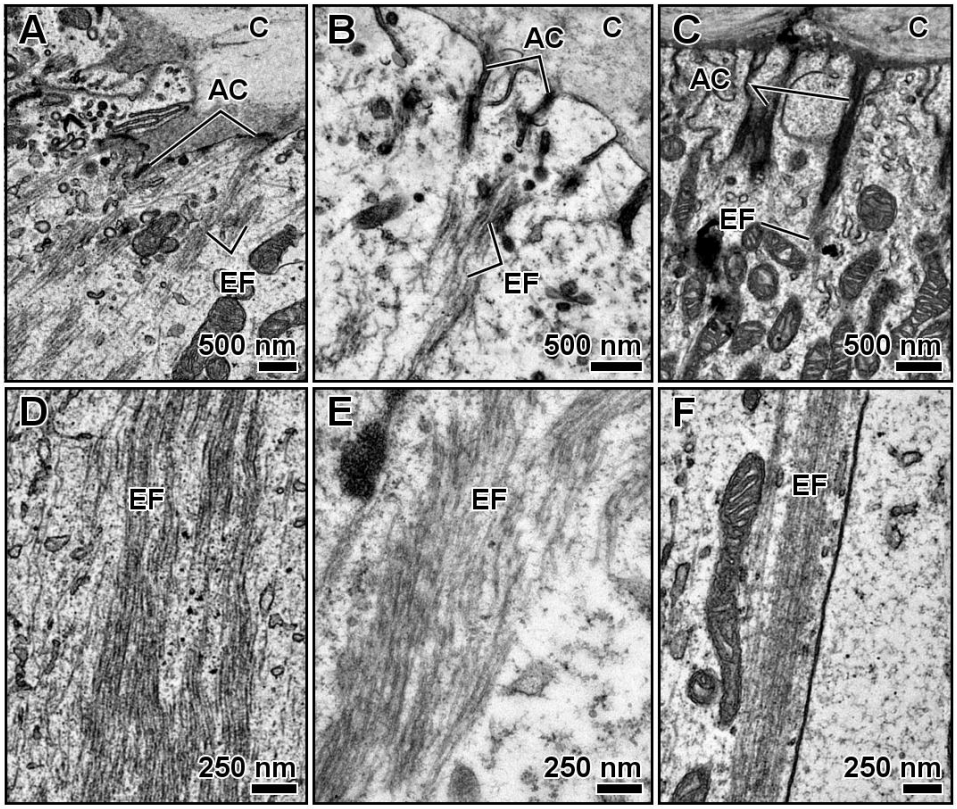

Figura 19.2.2. Adulto. Células epiteliales de los órganos digestivos derivados del ectodermo embrionario. MET. Complejo apical (A-C): esófago (A), estómago (B) y tracto digestivo posterior (C). Estructuras filamentosas (D-F): esófago (D), estómago (E) y tracto digestivo posterior (F). Abreviaciones: C, cutícula; AC, complejo apical; EF, estructuras filamentosas.

Otros rasgos comunes son: región apical rica en mitocondrias (Fig. 19.2.3A-C) y citoplasma con reducida densidad de otros orgánulos (Fig. 19.2.3D-F). La abundancia de mitocondrias apicales ha sido observada en otros braquiuros (Moon y Kim, 1999; Mykles, 1979) y astacídeos (Komuro y Yamamoto, 1968; Mykles, 1979) y se han asociado con células muy activas. En este caso se ha sugerido un rol asociado al transporte iónico, mientras que actividades secretoras se han descartado por falta de evidencia (Komuro y Yamamoto, 1968).

Adicionalmente, las membranas laterales de estas células epiteliales suelen estar muy extendidas formando abundantes y complejas interdigitaciones (Fig. 19.2.3D-F). Similares observaciones se han realizado en isópodos (Holdich y Ratcliffe, 1970; Storch et al., 2002). Mykles (1979) interpreta que el gran desarrollo de las interdigitaciones permite que las células adyacentes estén unidas con mucha firmeza, protegiendo la integridad del epitelio ante los esfuerzos expansivos que acompañan al paso del material ingerido.

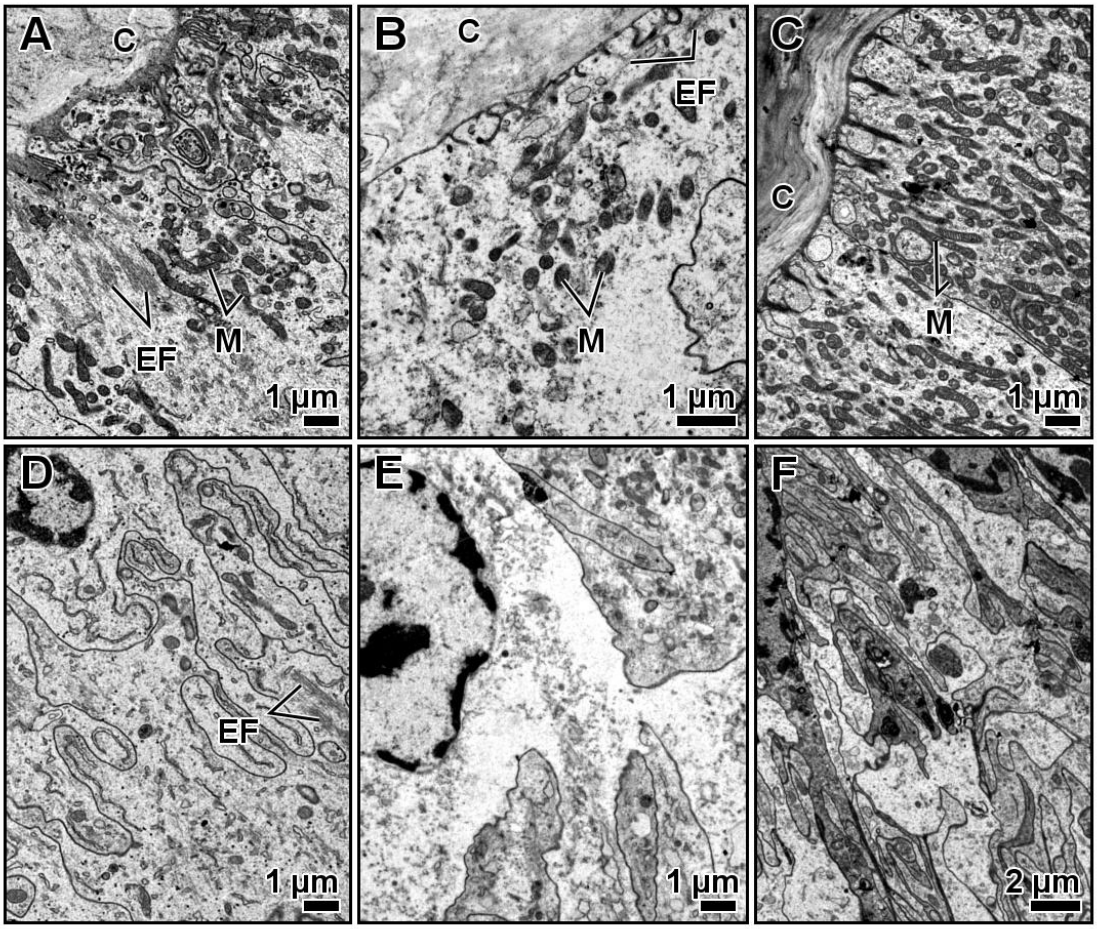

Figura 19.2.3. Adulto. Células epiteliales de los órganos digestivos derivados del ectodermo embrionario. MET. Mitocondrias apicales (A-C): esófago (A), estómago (B) y tracto digestivo posterior (C). Interdigitaciones de la membrana lateral (D-F): esófago (D), estómago (E) y tracto digestivo posterior (F). Abreviaciones: C, cutícula; EF, estructuras filamentosas; M, mitocondrias.

En los malacostráceos, los órganos del sistema digestivo derivados del endodermo embrionario incluyen al tracto digestivo medio, los ciegos asociados al mismo y la glándula digestiva, también llamada hepatopáncreas u órgano perigástrico (Anger, 2001; Cervellione et al., 2017; Felgenhauer, 1992; Icely y Nott, 1984; Icely y Nott, 1992; McLaughlin, 1983; Soonthornchai et al., 2015; Ńtnus et al., 2008). A diferencia de los órganos digestivos derivados del ectodermo embrionario, ninguno de los órganos digestivos derivados del endodermo presenta cutícula (Anger, 2001; Felgenhauer, 1992; Icely y Nott, 1992; McLaughlin, 1983).

El epitelio de estos órganos se caracteriza por estar formado por células generalmente prismáticas (si bien la glándula digestiva posee diversos tipos celulares con morfologías especializadas), coronadas por microvilli y cuyos núcleos se localizan medial a basalmente (Fig. 19.2.4). También pueden aparecer células redondeadas de pequeño tamaño adyacentes a la lámina basal, denominadas células basales en el tracto digestivo medio y los ciegos asociados, y células M en la glándula digestiva. La naturaleza de dichas células será discutida en un apartado posterior ("19.8 Células M de la glándula digestiva como posibles células basales").

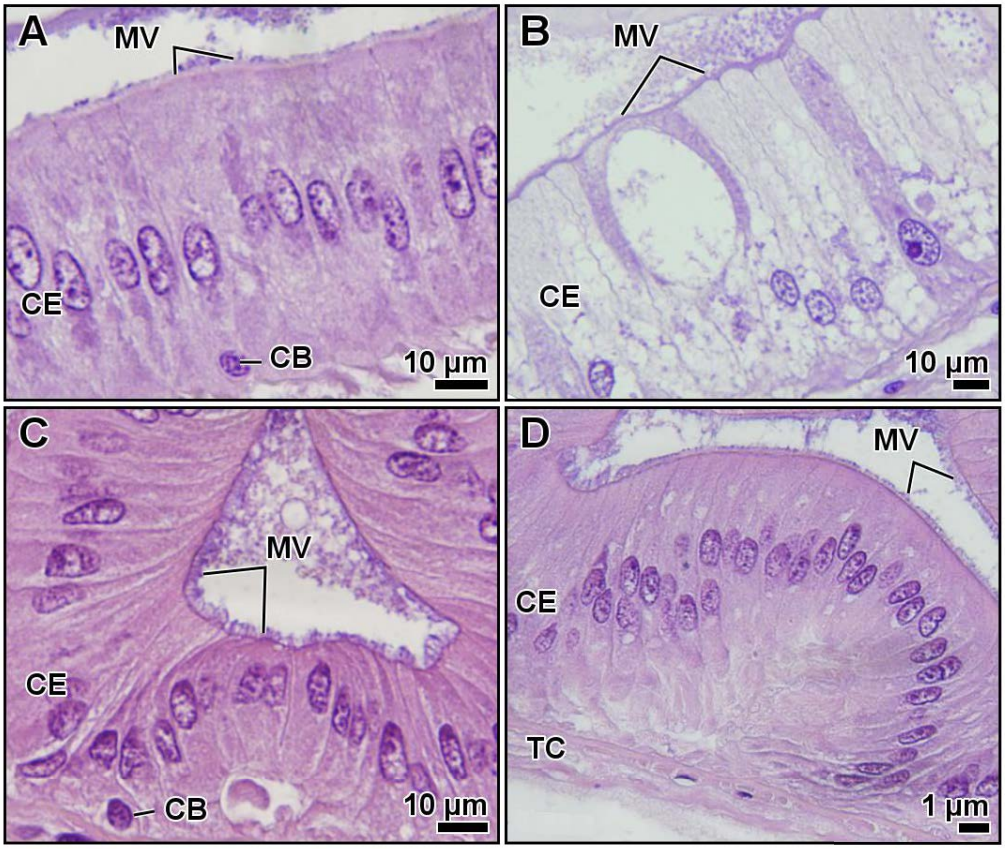

Figura 19.2.4. Adulto. Epitelio de los órganos digestivos derivados del endodermo embrionario. Tinción de Hematoxilina - Eosina. Tracto digestivo medio (A). Glándula digestiva (B). Ciegos anteriores (C). Ciego posterior (D). Abreviaciones: CB, células basales; CE, células epiteliales; MV, microvilli; TC, tejido conectivo.

La región apical de dichos epitelios se caracteriza por la presencia apical de microvilli festoneados, mitocondrias, estructuras filamentosas verticales extendidas desde la membrana apical hacia el interior celular y vesículas de electro-densidad variable (Fig. 19.2.5). En los decápodos los microvilli son un rasgo típico de todos estos epitelios (Felgenhauer, 1992; Icely y Nott, 1992; Mykles, 1979). Son estructuras generalmente asociadas a un papel involucrado con la absorción y secreción, esta hipótesis se ve reforzada por la presencia habitual de mitocondrias en la región apical (Moon y Kim, 1999; Talbot et al., 1972).

Las estructuras filamentosas se han hallado en todos los epitelios derivados del endodermo, pero son notorias en el epitelio de la glándula digestiva ya que se asocian a estructuras membranosas que recuerdan al retículo. Similares estructuras se han observado en astacídeos (Loizzi, 1971; Mykles, 1979) y dendrobranquiados (Martin y Chiu, 2003). De acuerdo con nuestras observaciones y las de otros autores (Loizzi, 1971), estas estructuras se anclan a la base de los microvilli. En relación a las presuntas vesículas de secreción, su papel será discutido en un apartado posterior ("19.9 Actividad secretora en el sistema digestivo").

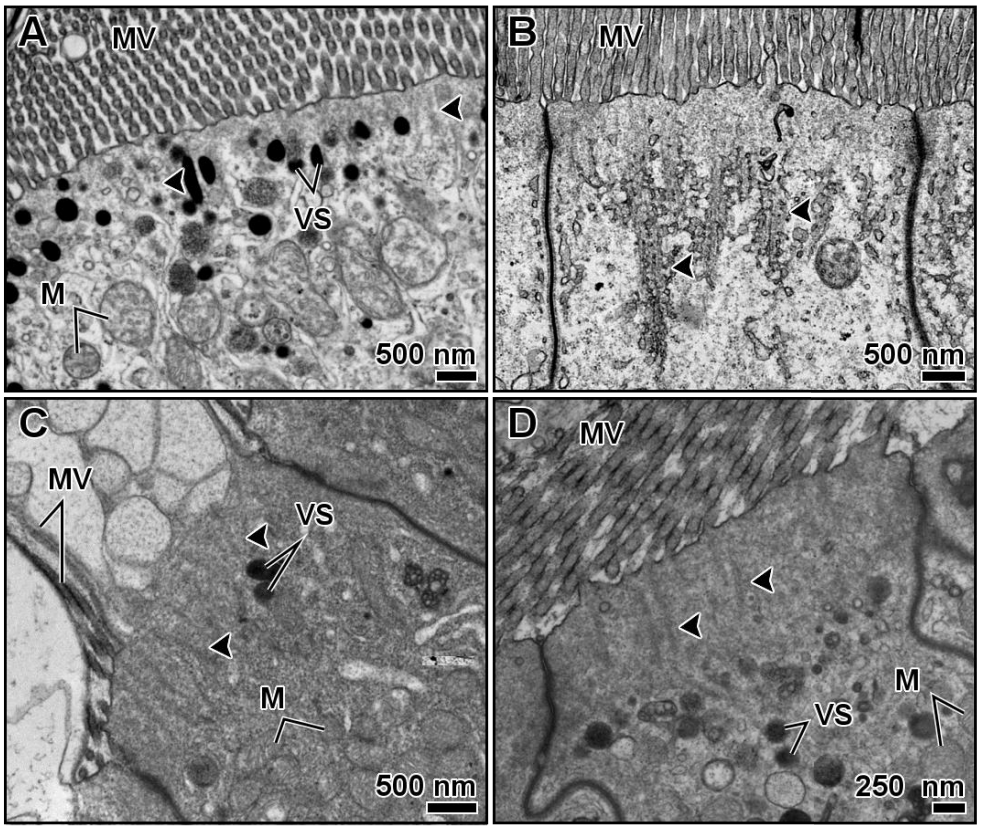

Figura 19.2.5. Adulto. Región apical del epitelio de los órganos digestivos derivados del endodermo embrionario. MET. Tracto digestivo medio (A). Glándula digestiva (B). Ciegos anteriores (C). Ciego posterior (D). Abreviaciones: ➤, estructuras filamentosas; M, mitocondrias; MV, microvilli; VS, vesícula de secreción.

La región basal se caracteriza por la presencia de una banda de retículo endoplasmático liso (REL) que rodea a mitocondrias y vesículas de diversa índole (Fig. 19.2.6). Esta banda se localiza adyacente a la membrana basal (Fig. 19.2.6A - B). Sin embargo, sus dimensiones son variables: puede extenderse desde unas escasas micras (Fig. 19.2.6A) hasta ocupar toda la región infranuclear (Fig. 19.2.6C-D). El REL es una red de túbulos electro-densos fusionados ocasionalmente con la membrana basal (Fig. 19.2.6A). Una región basal de aspecto similar se ha identificado en braquiuros (Mykles, 1977; 1979; Storch y Anger, 1983), astacídeos (Komuro y Yamamoto, 1968; Mykles, 1979; Paquet et al., 1993) y dendrobranquiados (Al-Mohanna y Nott, 1987; Martin y Chiu, 2003; Talbot et al., 1972).

Se ha considerado que la asociación entre las invaginaciones de la membrana basal, las mitocondrias y el REL es similar a la presente en las células de cloruro de las branquias de los teleósteos, sugiriéndose un papel similar relacionado con la osmoregulación y el transporte de agua y electrolitos (Komuro y Yamamoto, 1968; Mykles, 1977; 1979; Talbot et al., 1972). Otros autores han sugerido que dichos túbulos podrían transportar metabolitos desde la hemolinfa hacia el interior celular, en ese sentido se ha demostrado que el dióxido de torio inyectado en la hemolinfa se acumula en vesículas basales (Al-Mohanna y Nott, 1987).

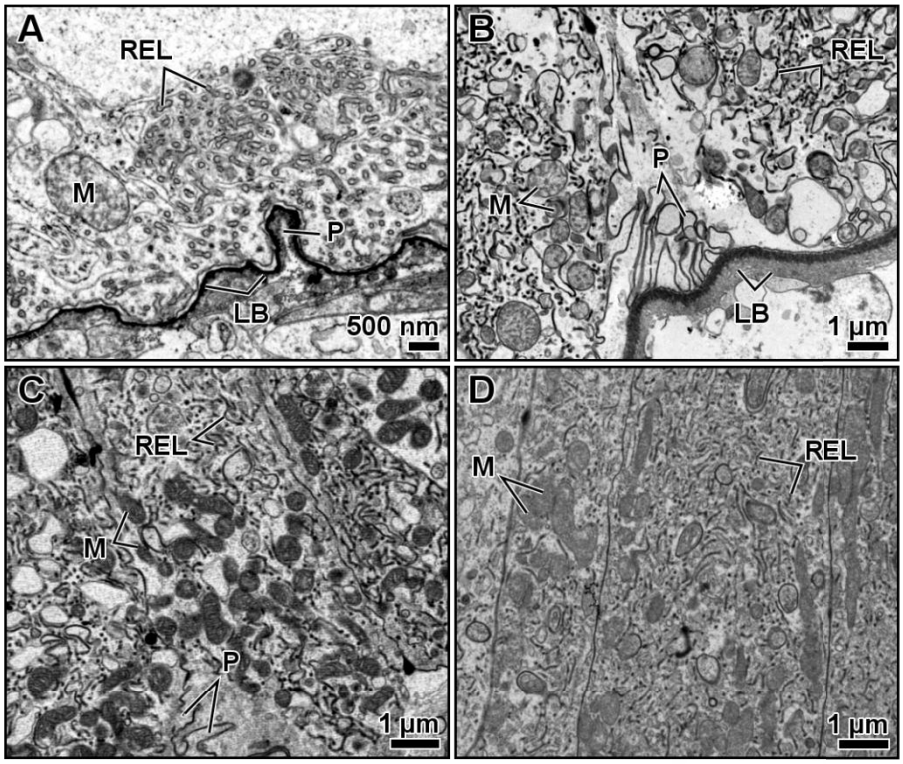

Figura 19.2.6. Adulto. Región basal del epitelio de los órganos digestivos derivados del endodermo embrionario. MET. Tracto digestivo medio (A). Glándula digestiva (B). Ciegos anteriores (C). Ciego posterior (D). Abreviaciones: LB, lámina basal; M, mitocondria; P, pliegues; REL, retículo endoplasmático liso.

19.3 Sistema digestivo adulto y larvario: semejanzas y diferencias.

Las larvas de *M. brachydactyla* eclosionan con un sistema digestivo desarrollado y preparado para la ingesta y procesado del alimento. La funcionalidad de este sistema es un requisito fundamental para la supervivencia temprana de estos animales, ya que se ha demostrado que en condiciones de inanición las larvas recién eclosionadas son incapaces de alcanzar el siguiente estadio larvario de zoea II (Guerao et al., 2012; Rotllant et al., 2010). Dada esta circunstancia, no es de extrañar que las larvas de *M. brachydactyla* también posean la maquinaria enzimática requerida para la digestión del alimento (Andrés et al., 2010; Rotllant et al., 2008), cuya actividad tiende a incrementarse a lo largo del desarrollo larvario (Andrés et al., 2010).

Los órganos del sistema digestivo de *M. brachydactyla* son los mismos que se pueden observar en el estadio adulto. Las mayores similitudes entre órganos adultos y larvarios se encuentran en aquellos que tienen forma tubular: esófago, tracto digestivo medio y tracto digestivo posterior. Son órganos de lumen provisto de pliegues internos recubiertos por un epitelio simple (revestido de cutícula en el esófago y tracto digestivo posterior, coronado por microvilli en el tracto digestivo medio). En las larvas el tejido conectivo y la musculatura asociada son capas más delgadas que las propias células epiteliales, mientras que en los adultos el conectivo es grueso, aloja glándulas de roseta y rodea grandes paquetes musculares y estructuras semejantes a vasos (Fig. 19.3.1).

La escasa presencia de conectivo y musculatura no solo se ha observado en los estadios larvarios de *M. brachydactyla*, sino también en adultos de carideos (Pillai, 1960), misidáceos (Friesen et al., 1986), anfípodos (Icely y Nott, 1984; Schmitz y Scherrey, 1983) e isópodos (Hames y Hopkin, 1989; Holdich y Ratcliffe, 1970; Schmitz y Scherrey, 1983; Schmitz y Schultz, 1969). Todos los mencionados son animales de pequeño tamaño. Por ello, es posible que el factor determinante de la complejidad de tales órganos sea el tamaño del animal: un animal de mayor tamaño tenderá a tener en términos absolutos órganos de mayor tamaño, que requerirán para su movimiento una musculatura que deberá ser más potente y que requerirá un mayor mantenimiento, que será solventado a través de vasos y glándulas presentes en el tejido conectivo. Esto también explicaría por qué los mismos órganos del sistema digestivo tienen mayor complejidad en animales de mayor tamaño (Erri Babu et al., 1982; Georgi, 1969; Pugh, 1962; Reddy, 1937; To et al., 2004; Yonge, 1924).

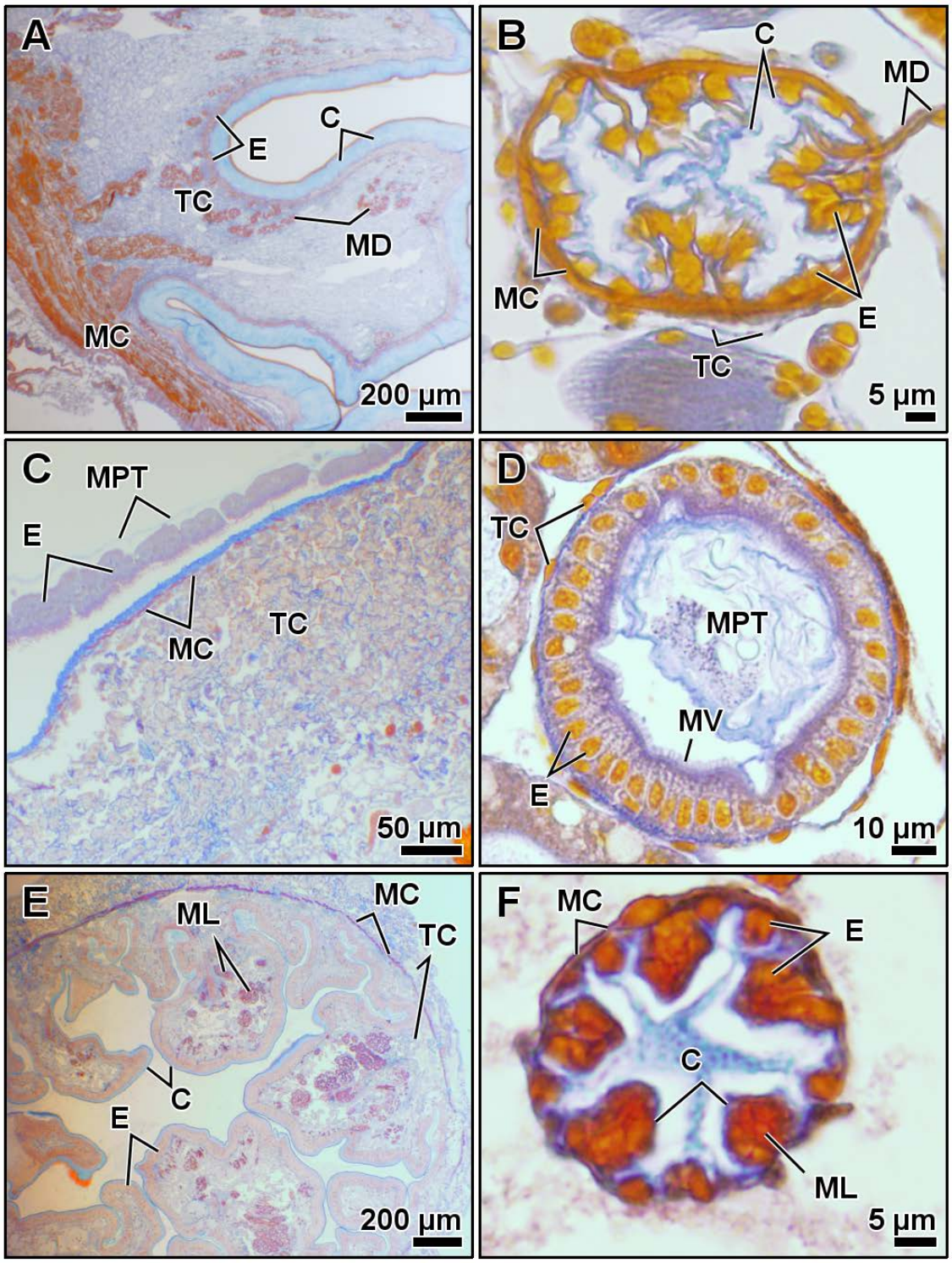

Figura 19.3.1. Esófago, tracto digestivo medio y tracto digestivo posterior. Comparación entre estadios adulto y larvarios. Sección transversal. Tricrómico de Mallory. Esófago (A-B): adulto (A) y larvario (B). Tracto digestivo medio (C-D): adulto (C) y larvario (D). Tracto digestivo posterior (E-F): adulto (E) y larvario (F). Abreviaciones: C, cutícula; E, epitelio; MC, musculatura circular; MD, musculatura "dilatadora"; ML, musculatura longitudinal; MV; microvilli; MPT, membrana peritrófica; TC, tejido conectivo.

En relación al propio epitelio, en el tracto digestivo medio las células epiteliales son similares tanto en adultos como en larvas y juveniles: prismáticas y coronadas de microvilli (Fig. 19.2.4A; 19.3.1D). En relación al esófago y tracto digestivo posterior la situación es diferente: mientras que en el estadio adulto las células epiteliales de ambos órganos son prismáticas (Fig. 19.2.1A, C), las células epiteliales del esófago larvario tienen una morfología variable de plana a prismática (estas últimas suelen contener una gran vesícula que ocupa la mayoría del volumen celular, dichas vesículas no aparecen en el epitelio adulto); por su parte, en el caso del tracto digestivo posterior, las células epiteliales larvarias son generalmente planas (Fig. 19.3.1B, F; 19.3.2).

Mientras que la forma larvaria de los órganos de *M. brachydactyla* recuerda a la forma adulta de los mismos en otras especies de malacostráceos, lo mismo no ocurre con el epitelio, el cual suele variar de cuboidal a prismática en lugar de plano (Friesen et al., 1986; Holdich y Ratcliffe, 1970; Schmitz y Schultz, 1969; Schultz, 1973; Wägele et al., 1981). ¿La forma celular cuboidal o prismática responde a un requisito funcional del órgano? ¿La forma celular sea un resultado evolutivo no adaptativo (Gould (1982)? ¿O más bien en dichos estudios se estudiaron animales en otro momento del ciclo de muda? ¿El proceso digestivo puede alterar la forma de las células epiteliales? Por el momento, se poseen más preguntas que respuestas.

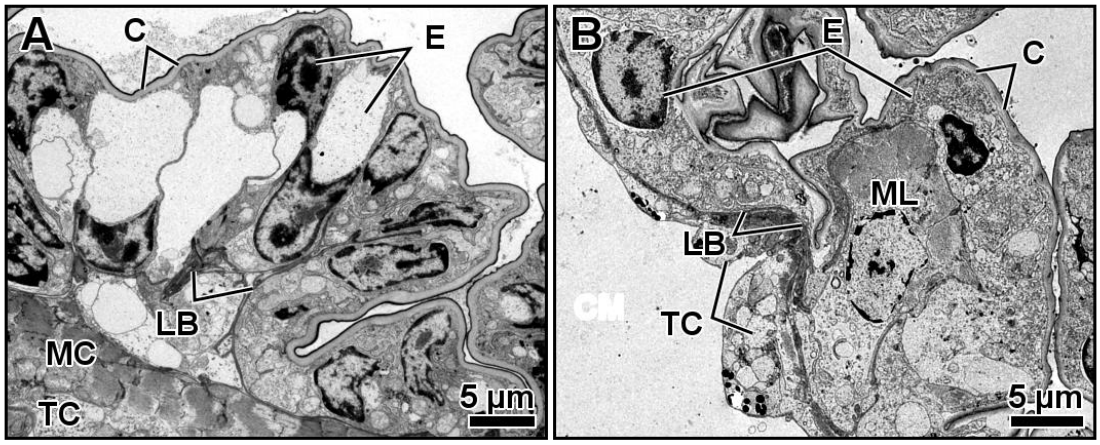

Figura 19.3.2. Digestivo larvario. Epitelio del esófago (A) y del tracto digestivo posterior (B). MET. Abreviaciones: C, cutícula; CE, células epiteliales; LB, lámina basal; MC, musculatura circular; ML, musculatura longitudinal; TC, tejido conectivo.

Los ciegos asociados al tracto digestivo medio (tanto el par de ciegos anteriores como el único ciego posterior) difieren si se comparan larvas y adultos. En el estadio adulto son tubos ciegos extremadamente largos y enrollados sobre sí mismos, con un lumen rico en pliegues (Fig. 19.3.3A-B). Sin embargo, en el momento de la eclosión, los ciegos anteriores son sencillas yemas que apenas sobresalen del extremo anterior del tracto digestivo medio, por su parte el ciego posterior es un tubo ciego muy corto. Durante el desarrollo larvario la longitud de dichos órganos se incrementará, pero conservarán un lumen sencillo sin pliegues ni ondulaciones (Fig. 19.3.3C-F).

A nivel histológico los ciegos adultos y larvarios son muy similares: se componen de un epitelio simple coronado por microvilli, formado por células prismáticas en los adultos (Fig. 19.2.4C-D) y por células más cortas y piramidales en las larvas (Fig. 19.3.3C-F). El epitelio está rodeado por una lámina basal, a su vez rodeada por un fino conectivo asociado a delgadas fibras musculares. La ultra-estructura de las células larvarias y adultas es también similar y sigue el patrón típico de las células derivadas del endodermo descritas en el apartado anterior ("19.2 Sobre los epitelios derivados del ectodermo y endodermo").

Los braquiuros cuentan con ciegos extremadamente largos (Erri Babu et al., 1982; Smith, 1978), mientras que otros decápodos (como los astacídeos y dendrobranquiados) poseen ciegos muy cortos (Abubakr y Jones, 1992; Factor, 1981; Lovett y Felder, 1989). Le Vay et al. (2001) asocian los ciegos largos con una dieta herbívora. Desde nuestro punto de vista, dicha hipótesis no se sostiene. Durante el estadio adulto, tanto los astacídeos como los braquiuros son principalmente omnívoros oportunistas (Bernárdez et al., 2000; Choy, 1986; Elner y Campbell, 1987; Griffen y Mosblack, 2011; MacArthur et al., 2011; Sainte-Marie y Chabot, 2002; Williams, 1981). Sin embargo, a pesar de tener una dieta parecida, los ciegos asociados al tracto digestivo medio son muy cortos en astacídeos y muy largos en braquiuros. No cabe duda que dada la gran longitud que tienen los ciegos asociados al tracto digestivo de *M. brachydactyla*, estos deben de desempeñar un papel biológico relevante. Sobre el posible rol de dichos ciegos se discutirá en el apartado "19.9 Actividad secretora en el sistema digestivo".

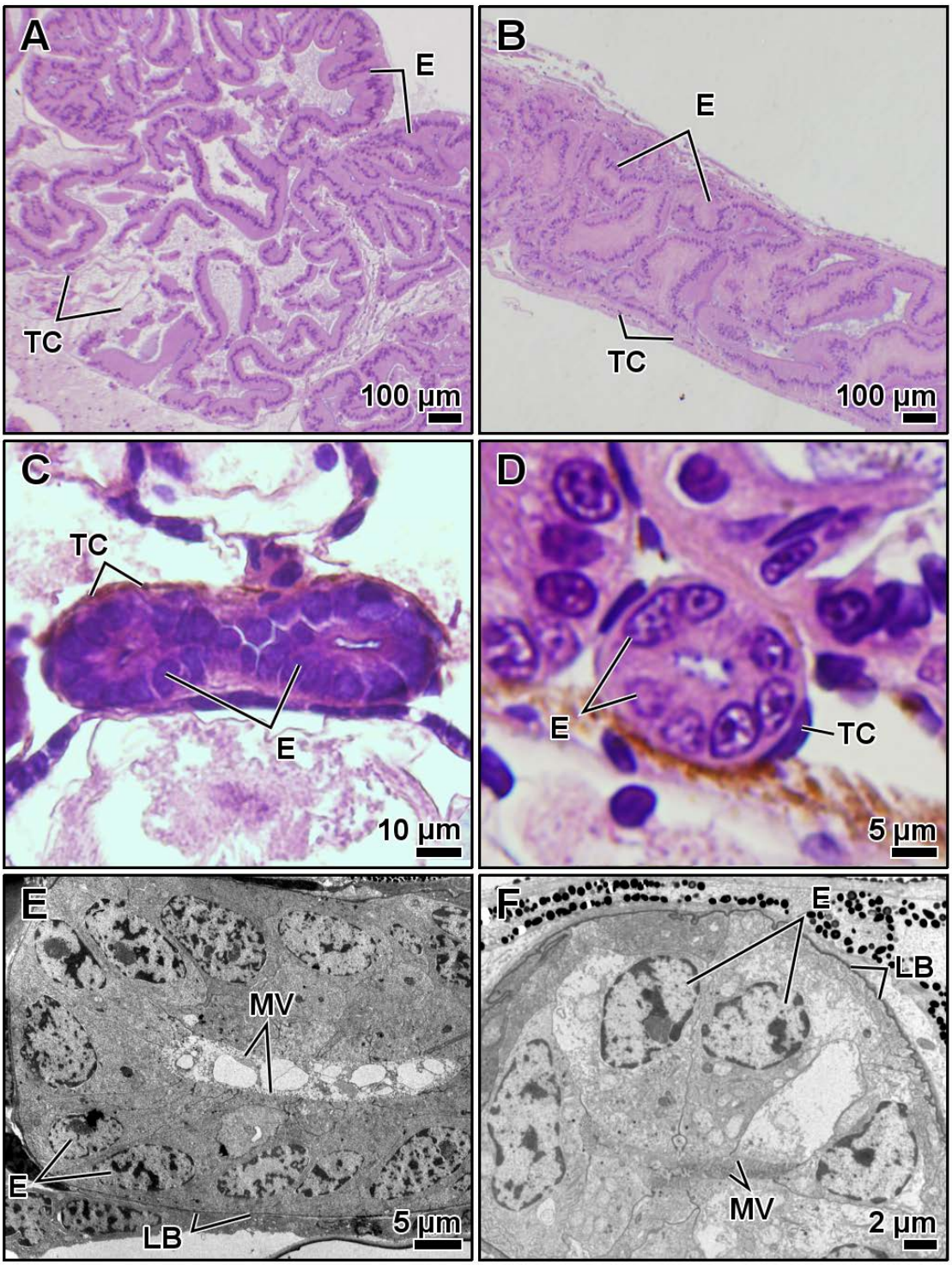

Figura 19.3.3. Ciegos asociados al tracto digestivo medio. Comparación entre estadios adulto y larvarios. Adulto, Hematoxilina - Eosina (A-B): ciegos anteriores (A) y posterior (B). Megalopa, Hematoxilina - Eosina (C-D): ciegos anteriores (C) y posterior (D). Zoea, MET (E-F): ciegos anteriores (E) y posterior (F). Abreviaciones: E, epitelio; LB, lámina basal; MV, microvilli; TC, tejido conectivo.

En relación a la glándula digestiva u órgano perigástrico, los principales cambios ontogénicos ocurren a nivel de morfología general, no mostrando grandes diferencias a nivel de túbulos, tejidos o células. En todos los estadios la unidad básica es el túbulo ciego delimitado por un epitelio simple, coronado por microvilli y formado por cinco tipos celulares (Fig. 19.3.4C-D): células E (embrionarias), células F (fibrilares), células R (de absorción), células B ("hinchadas") y células M (enanas). Los mismos tipos celulares han sido descritos en especímenes adultos de otras especies de decápodos (Al-Mohanna y Nott, 1989; Al-Mohanna et al., 1985a; Gibson y Barker, 1979; Nunes et al., 2014; Ramadevi et al., 1990; Ribeiro et al., 2016; Tziouveli et al., 2011; Vogt, 1994). En la mayoría de los estudios publicados, las células M no han sido identificados en los estadios larvarios (Abrunhosa y Kittaka, 1997; Anger et al., 1985; Biesiot y McDowell, 1995; Li y Li, 1998; Mikami et al., 1994; Nishida et al., 1995; Storch y Anger, 1983), pero tales células si han sido identificadas en los estadios larvarios de *M. brachydactyla*. Las células epiteliales de larvas y adultos son muy similares a nivel ultra-estructural, dicha morfología también coincide con la publicada en estudios previos (Nishida et al., 1995; Storch y Anger, 1983). Debido a tales similitudes, es razonable pensar que la función de cada tipo celular se conserva durante la vida del animal. La distribución de las células epiteliales en el túbulo ciego también sigue el mismo patrón descrito en otros decápodos (Al-Mohanna y Nott, 1989; Icely y Nott, 1992; Loizzi, 1971): región distal provista de células E; región medial con abundancia de células R y F; región proximal con células R ricas en vacuolas lipídicas, así como células F y B; y células M dispersas tanto por la región medial como proximal (Fig. 19.3.4A-B).

El epitelio de los túbulos descansa sobre una lámina basal, rodeada por una fina capa de tejido conjuntivo asociado a fibras musculares, las cuales forman un patrón reticulado formado por anillos de fibras musculares circulares unidas por fibras musculares longitudinales; este patrón también se ha observado en larvas recién eclosionadas (Fig. 19.3.4E-F). Loizzi (1971) describe una organización muscular muy similar en sendas especies de cangrejos de río (*Orconectes virilis* y *Procambarus clarkii*). Lo mismo hace Al-Mohanna y Nott (1989) con respecto al langostino *Penaeus semisulcatus*. Es posible que la organización de la musculatura de los túbulos ciegos esté conservada en todos los decápodos.

Los principales cambios ontogénicos de la glándula digestiva ocurren a nivel de morfología general, principalmente en el número de túbulos ciegos: mientras que durante los estadios larvarios cuenta con catorce túbulos, en los adultos este número se incrementa hasta 35.000 a 60.000 túbulos, implicando un aumento extraordinario de la complejidad y volumen del órgano. Este patrón de desarrollo ha sido observado en otros decápodos (Abrunhosa y Kittaka, 1997; Anger, 2001; Lovett y Felder, 1989; Nakamura y Tshuru, 1987).

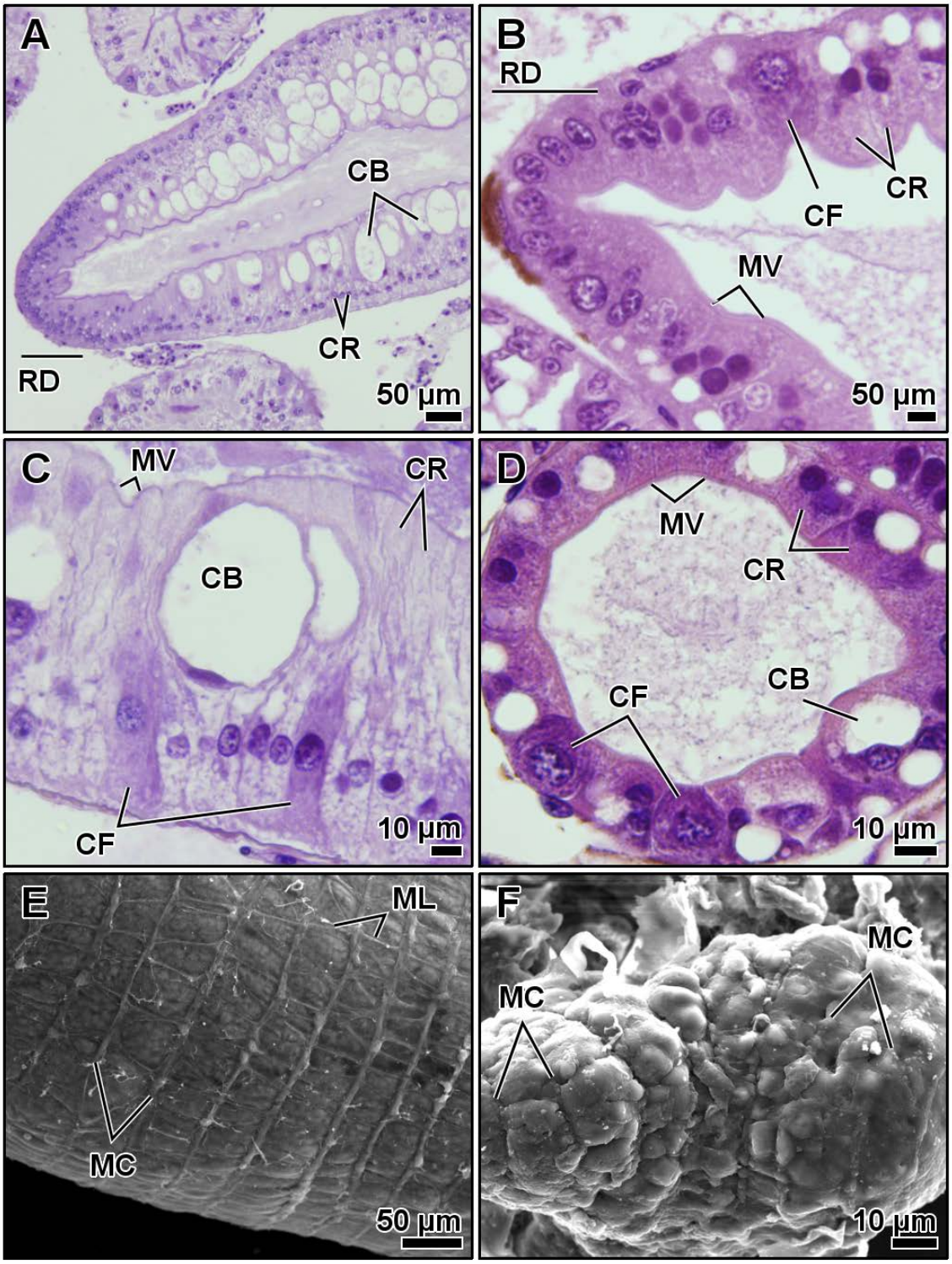

Figura 19.3.4. Glándula digestiva. Comparación entre estadios adulto y larvarios. Sección longitudinal, Hematoxilina - Eosina (A-B): adulto (A) y zoea I (B). Detalle de las células epiteliales, Hematoxilina - Eosina (C-D): adulto (C) y megalopa (D). Detalle de las fibras musculares, MEB (E-F): adulto (E) y zoea I (F). Abreviaciones: CB, células B; CF, células F; CR, células R; MC, musculatura circular; ML, musculatura longitudinal; MV, microvilli; RD, región distal.

El estómago es el órgano que sufre más cambios durante el desarrollo larvario aunque conserva la misma organización básica: una región anterior denominada estómago cardiaco, una región posterior denominada estómago pilórico y una estructura denominada válvula cardio-pilórica que separa a ambas cámaras (Fig. 19.3.5). La principal transformación del estómago ocurre durante la metamorfosis a megalopa: durante los estadios de zoea el estómago cardiaco es pequeño y compacto (Fig. 19.3.5A-B), pero tras la muda al estadio de megalopa incrementa su tamaño, la región cardiaca se expande formando los "sacos cardiacos" y aparecen por primera vez el sistema de osículos y el molino gástrico (Fig. 19.3.5C-F). Es posible que la aparición del molino gástrico refleje un cambio en la dieta como adaptación al nuevo estilo de vida intermedio entre pelágico y bentónico (Anger, 2001; Factor, 1989).

El nuevo sistema de osículos y el molino gástrico adquirirán el aspecto adulto en subsecuentes mudas que ocurrirán durante la fase de juvenil (Fig. 19.3.5E-F). La válvula cardio-pilórica conserva su forma de media luna durante todos los estadios vitales, con una cara cóncava anterior y una cara convexa posterior; el mayor cambio es la desaparición en el estadio de megalopa de las setas largas y gruesas que están presentes durante la fase de zoea (Fig. 19.3.5A-B).

A nivel histológico también ocurren cambios destacables. Durante los estadios de zoea el epitelio varía de plano en la región cardiaca a cuboidal - prismático en la válvula cardio-pilórica, mientras que la cutícula es muy delgada y no muestra zonas diferenciadas bajo microscopía óptica. El estómago de la megalopa, muy diferente a nivel morfológico, es muy similar a nivel tisular, solo la cutícula de los dientes del molino gástrico muestra modificaciones significativas bajo microscopía óptica, como la aparición de una capa adicional que podría identificarse con una epicutícula muy desarrollada. Por su parte, a nivel tisular el estómago adulto es muy distinto al de los estadios de zoea y megalopa, ya que muestra una gran diversidad de epitelios (plano, cuboidal, prismático) y cutículas (distintos grosores y morfología de las capas), cuya complejidad es mayor que la observada en los estadios larvarios. El impacto de estos cambios en la funcionalidad del estómago se discutirá en el apartado "19.5 El estómago y especializaciones de la cutícula".

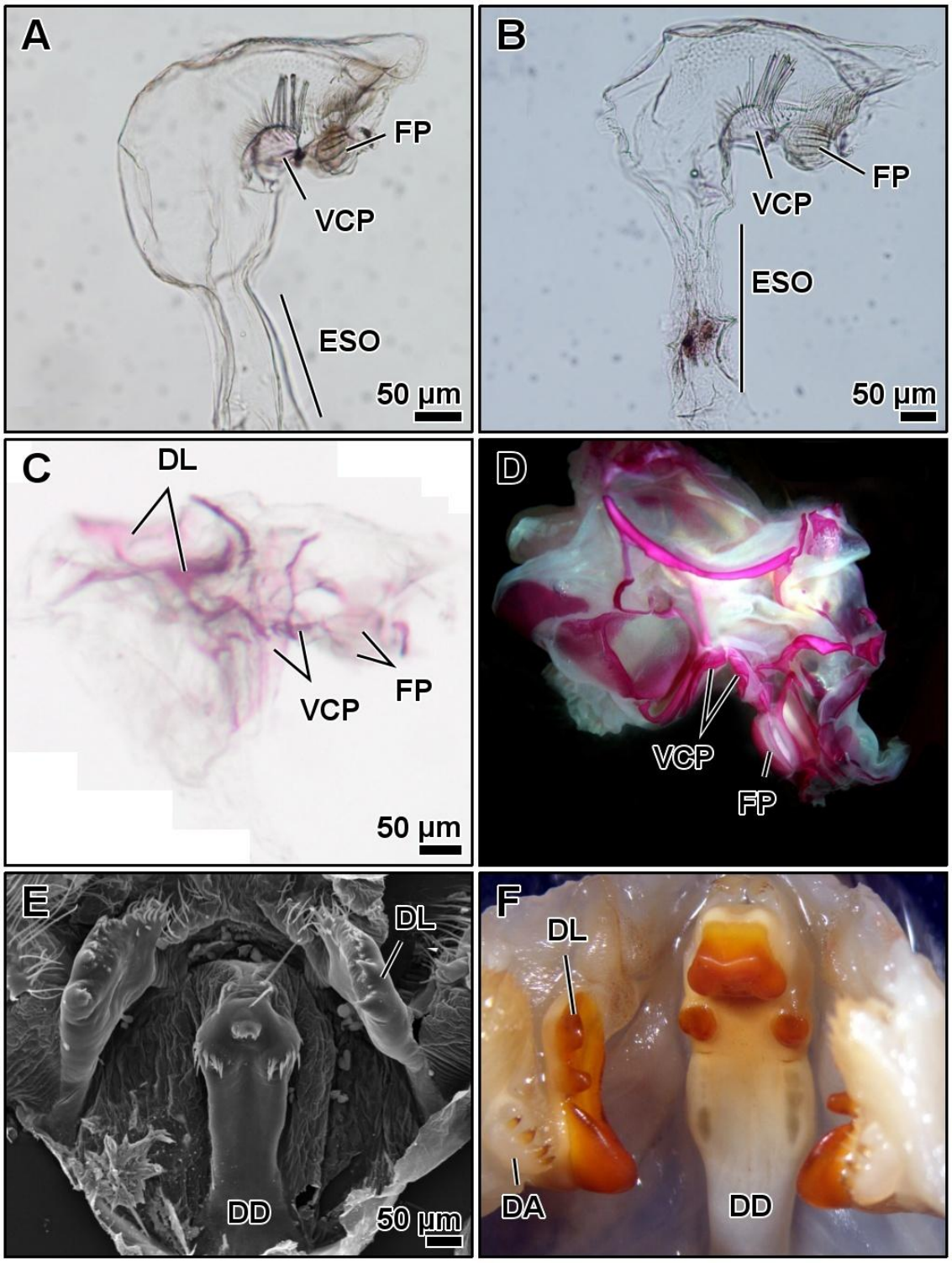

Figura 19.3.5. Estómago. Morfología general, Rojo de Alizarina (A-D): zoea I, (A), zoea II (B), megalopa (C) y adulto (D). Molino gástrico (E-F): megalopa, MEB (E) y adulto, lupa binocular (F). Abreviaciones: DA, diente accesorio; DD, diente dorsal; DL, diente dorsal; ESO, esófago; FP, filtros pilóricos; VCP, válvula cardio-pilórica.

19.4 El sistema digestivo durante el desarrollo larvario.

Durante el desarrollo larvario ocurren cambios morfológicos externos muy remarcables (Fig. 19.1.1), sobre todo cuando el animal muda a megalopa (Guerao et al., 2008). Esta transformación morfológica es acompañada por un crecimiento alométrico y linear con predominancia del crecimiento en longitud sobre el de anchura (Andrés et al., 2008). De acuerdo con Guerao y Rotllant (2009a; b), la metamorfosis a primer juvenil también implica numerosos cambios. Durante el desarrollo post-larvario, cada muda implica el aumento de la longitud del caparazón entre un 21 y un 37 %, también se incrementa el número de setas y tubérculos, la relación entre longitud/anchura del caparazón decrece y los caracteres sexuales secundarios se observan a partir de la cuarta muda post-larvaria (Guerao y Rotllant, 2009a; b). El patrón de desarrollo de los juveniles de *M. brachydactyla* es muy similar al descrito en la especie hermana *M. squinado* (Guerao y Rotllant, 2010).

Sin embargo, la morfología interna de los diferentes estadios larvarios no experimenta cambios profundos. La gran mayoría de los órganos que componen el sistema digestivo no sufre ningún cambio que modifique su organización tisular o celular, su forma y/o su función. La única excepción es el estómago, que como se ha discutido en el apartado anterior, es el único órgano del sistema digestivo que sufre cambios mayores durante el desarrollo larvario, adquiriendo nuevas funciones y estructuras (Fig. 19.3.5C).

Nuestros resultados muestran un patrón general donde los órganos del sistema digestivo crecen de forma alométrica favoreciendo la longitud. En lo que respecta a otros decápodos, los pocos estudios anatómicos realizados no dan cuenta de este aspecto del desarrollo morfológico. Sin embargo, en aquellas publicaciones que ilustran mediante diagramas con escala el desarrollo de los órganos digestivos, puede apreciarse una tendencia similar donde el crecimiento en longitud está favorecido frente al de anchura, como en el peneido *Penaeus setiferus* y el anomuro *Paralithodes camtschaticus* (Abrunhosa y Kittaka, 1997; Lovett y Felder, 1989).

La conservación de la similitud de los órganos digestivos a lo largo de todo el desarrollo larvario concuerda con la hipótesis planteada anteriormente, que propone al tamaño del animal como el factor determinante de la morfología del órgano. Esta hipótesis también explicaría porque la mayor parte de los cambios morfológicos que sufren los órganos digestivos ocurren durante el desarrollo de los juveniles, en la que el volumen de los animales y su consiguiente organización interna aumenta exponencialmente en subsecuentes mudas.

19.5 El estómago y especializaciones de la cutícula.

La cutícula que reviste la cavidad interna del estómago en los decápodos forma una serie de engrosamientos especializados denominados osículos, que distribuidos simétricamente actúan como soporte estructural o "esqueleto" (Brösing, 2010; 2014; Brösing et al., 2002; Ceccaldi, 1989; Factor, 1982; Felgenhauer, 1992; Icely y Nott, 1992; Kunze y Anderson, 1979; Maynard y Dando, 1974; McLaughlin, 1983; Meiss y Norman, 1977; Salindeho y Johnston, 2003; Suthers, 1984). Brösing (2010) ha identificado un máximo de 41 osículos en braquiuros. Lima-Gomes et al. (2017) aumentan este valor a 48 en determinadas especies de la familia Trichodactylidae. Típicamente, este valor es menor en varios taxones: entre 36 y 38 osículos en la familia Pseudothelphusidae (Alves et al., 2010), 38 osículos en el panopeido *Dyspanopeus sayi* (Castejón et al., 2015) y 40 osículos en la familia Dromiidae (Brösing et al., 2002). En *M. brachydactyla* ha sido posible identificar 40 osículos, los cuáles se resumen en la tabla 1 del capítulo 9 "Foregut Morphology and Ontogeny of the Spider Crab *Maja brachydactyla* (Brachyura, Majoidea, Majidae)". Los osículos de *M. brachydactyla* son muy similares a los de especies congénericas como *Maja crispata* Risso, 1827 (Brösing, 2014) u otros majoides como *Inachus dorsettensis* (Pennant, 1777) (Brösing, 2010) o *Libinia emarginata* Leach, 1815 (Meiss y Norman, 1977). Por el contrario, la mayoría de osículos de *M. brachydactyla* posee una morfología que difiere de la de taxones menos emparentados de braquiuros, aunque dichos osículos compartan una localización similar (Brösing, 2010; Brösing et al., 2002; de La Barra et al., 2017; Meiss y Norman, 1977).

El estómago cardiaco se caracteriza por sostener el molino gástrico, una estructura constituida por osículos engrosados y transformados en estructuras similares a dientes: un diente dorsal derivado del osículo urocárdico, un par de dientes laterales derivados de sendos osículos zigocárdicos y un par de pequeños dientes laterales derivados de los osículos pectineales (Alves et al., 2010; Allardyce y Linton, 2010; Brösing et al., 2002; Brösing y Türkay, 2011; Ceccaldi, 1989; Factor, 1982; Felgenhauer, 1992; Frick et al., 2011; Huespe et al., 2008; Icely y Nott, 1992; Kunze y Anderson, 1979; McLaughlin, 1983; Meiss y Norman, 1977; Nakamura y Takemoto, 1986; Salindeho y Johnston, 2003; Skilleter y Anderson, 1986). El molino gástrico es una estructura masticadora responsable de triturar el alimento ingerido hasta reducirlo a finas partículas (Allardyce y Linton, 2010; Ceccaldi, 1989; Factor, 1982; Icely y Nott, 1992; Kunze y Anderson, 1979; McLaughlin, 1983; Nakamura y Takemoto, 1986; Salindeho y Johnston, 2003; Skilleter y Anderson, 1986).

Tabla 19.5.1. Osículos identificados en el estómago de los decápodos, cada osículo tiene asignado un número romano (Nº) identificativo, empleado generalmente en las figuras e ilustraciones. Clasificación según Maynard y Dando (1974) y Meiss y Norman (1977).

Nº	Nombre traducido	Nombre original	Distribución
Molino gástrico cardiaco / *Cardiac gastric mill*			
I	mesocardiaco	*mesocardiac*	impar
II	pterocardiaco	*pterocardiac*	par
III	pilórico	*pyloric*	impar
IV	exopilórico	*exopyloric*	par
V	zigocardiaco	*zygocardiac*	par
VI	propilórico	*propyloric*	impar
VII	urocardiaco	*urocardiac*	impar
Osículos cardiacos de soporte lateral / *Lateral supporting cardiac ossicles*			
VIII	pectineal	*pectineal*	par
IX	prepectineal	*prepectineal*	par
X	postpectineal	*postpectineal*	par
Xa	'quilla' del osículo postpectineal	*'quill' of postpectineal ossicle*	par
XI	placa cardiaca lateral anterior	*anterior lateral cardiac plate*	par
XII	placa cardiaca lateral posterior	*posterior lateral cardiac plate*	par
XIII	placa cardiaca lateral inferior	*inferior lateral cardiac plate*	par
XIV	subdentado	*subdentate*	par
XV	cardio-pilórico lateral	*lateral cardio-pyloric*	par
Osículos de la válvula cardio-pilórica / *Ossicles of the cardio-pyloric valve*			
XVI	osículo anterior de la válvula cardio-pilórica	*anterior ossicle of cardio-pyloric valve*	impar
XVII	osículo posterior de la válvula cardio-pilórica	*posterior ossicle of cardio-pyloric valve*	impar
XVIII	osículo lateral de la válvula cardio-pilórica	*lateral ossicle of cardio-pyloric valve*	par
Osículos de soporte del estómago pilórico / *Supporting ossicles of the dorsal pyloric stomach*			
XIX	mesopilórico anterior	*anterior mesopyloric*	par
XX	mesopilórico posterior	*posterior mesopyloric*	impar
XXI	uropilórico	*uropyloric*	variable
XXIa	fragmento infra-uropilórico	*infra-uropyloric fragment*	par

Tabla 19.5.1 (continuación y final). Osículos identificados en el estómago de los decápodos, cada osículo tiene asignado un número romano (Nº) identificativo, empleado generalmente en las figuras e ilustraciones. Clasificación según Maynard y Dando (1974) y Meiss y Norman (1977).

Nº	**Nombre traducido**	**Nombre original**	**Distribución**
Osículos de soporte del píloro ventral y las ampullae / *Supporting ossicles of the ventral pylorus and ampullae*			
XXII	pre-ampular	*preampullary*	par
XXIII	pilórico inferior anterior	*anterior inferior pyloric*	impar
XXIV	ampular inferior	*inferior ampullary*	par
XXV	techo ampular, porción inferior	*ampullary roof, lower portion*	par
XXVI	techo ampular, porción superior	*ampullary roof, upper portion*	par
XXVII	pilórico inferior posterior	*posterior inferior pyloric*	impar
Osículos cardiacos de soporte lateral / *Lateral supporting cardiac ossicles*			
XXVIII	supra-ampular anterior	*anterior supra-ampullary*	par
XXIX	supra-ampular medio	*middle supra-ampullary*	par
XXX	supra-ampular posterior	*posterior supra-ampullary*	par
Osículos de la válvula cardio-pilórica / *Ossicles of the cardio-pyloric valve*			
XXXI	pleuropilórico anterior	*anterior pleuropyloric*	par
XXXII	pleuropilórico medio	*middle pleuropyloric*	par
XXXIII	pleuropilórico posterior	*posterior pleuropyloric*	par

Nakamura y Takemoto (1986) sugirieron que la similitud compartida del molino gástrico por tantos taxones es consecuencia de un fenómeno de convergencia evolutiva, ya que su forma podría responder a un requisito funcional. También se ha postulado una correlación inversa entre la complejidad del molino gástrico y las piezas bucales (Meiss y Norman, 1977), así como que la morfología de los dientes del molino gástrico podría explicarse por la dieta de la especie (Icely y Nott, 1992). En ese sentido, Icely y Jones (1978) concluyen que determinados caracteres del molino gástrico de los ocipódidos (abundancia y número de crestas y setas) varía a nivel específico en función del tamaño de las partículas de los sedimentos componen la dieta. Por su parte, Allardyce y Linton (2010) relacionan cada dieta con un tipo de morfología dentaria: las especies carnívoras cuentan con dientes suaves, romos y con superficies cóncavas, ya que actúan como un mortero útil para romper piezas duras como conchas; las especies herbívoras cuentan con dientes provistos de crestas afiladas con objeto de cortar las fibras vegetales; mientras que las especies omnívoras poseen dientes que varían desde una combinación de superficies romas y crestas afiladas hasta totalmente romos. Skilleter y Anderson (1986) también adjudican superficies más crestadas a las especies herbívoras, pero consideran que la razón es debida a que el alimento es ingerido como piezas de menor tamaño.

La morfología del molino gástrico de *M. brachydactyla* corresponde a una dieta que incluye diversas especies de macrófitos (incluyendo algas coralinas), poríferos, corales, anélidos, diversos tipos de moluscos (bivalvos y gasterópodos), eucrustáceos y equinodermos (Bernárdez et al., 2000; Freire et al., 2009). Esta dieta es rica en organismos con protecciones duras y calcificadas, por ello el molino gástrico cuenta con dientes laterales suaves, romos y cóncavos, de acuerdo con la hipótesis de Allardyce y Linton (2010).

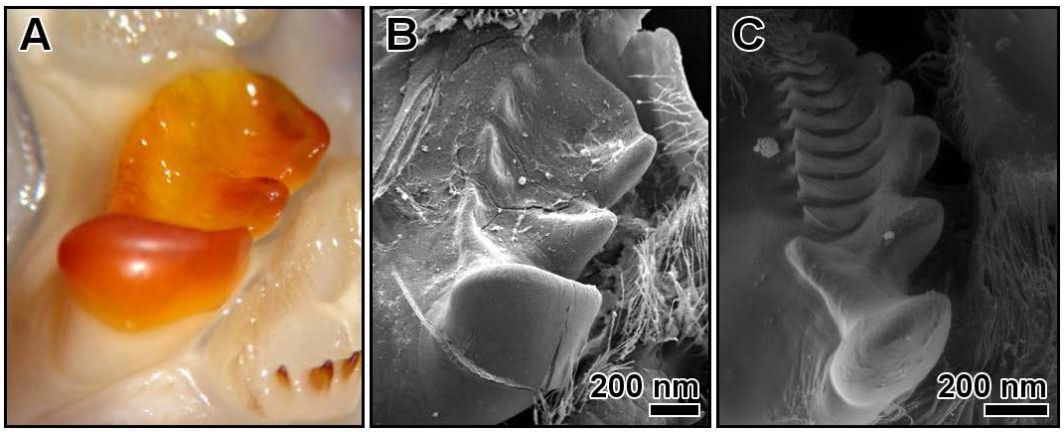

Figura 19.5.2. Diente lateral del molino gástrico de *M. brachydactyla*, nótese las superficies romas y suaves (B). Diente lateral del molino gástrico de *Maja crispata* Risso, 1827, nótese las similitud con *M. brachydactyla* (B). Diente lateral del molino gástrico de *D. sayi*, nótese la gran abundancia de crestas (C).

Sin embargo, el tipo de dieta no es el único factor determinante de la morfología del molino gástrico. Brösing y Türkay (2011) observaron que el braquiuro *Heloecius cordiformis* ingiere materia animal y vegetal a pesar de tener un molino gástrico similar al de especies suspensívoras. Según Icely y Nott (1992), la morfología del molino gástrico está fuertemente determinada por la filogenia. En ese sentido, el molino gástrico de *M. brachydactyla* es muy similar al de *M. crispata* (Fig. 19.5.2B). Lo mismo ocurre en otros géneros como *Cyrtograpsus* (Huespe et al., 2008) y *Planes* (Frick et al., 2011): las diferencias interespecíficas son mínimas. Brösing et al. (2007) utilizó la estructura del molino gástrico y el sistema de osículos para reconstruir la filogenia de los braquiuros, la cual no concuerda en todos los detalles con las filogenias moleculares (Ahyong et al., 2007; Bracken et al., 2009; Spears et al., 1992; Tsang et al., 2014), pero es capaz de agrupar géneros y familias de forma coherente. Similares resultados han sido obtenidos al reconstruir la filogenia de los anomuros empleando la morfología del sistema de osículos (Reimann et al., 2011). Por tanto, la morfología del molino gástrico está fuertemente influida por la filogenia. Es probable, como han sugerido otros autores (de La Barra et al., 2017), que la morfología del molino gástrico represente un compromiso entre requisitos funcionales, herencia filogenética y ligeras modificaciones adaptativas relacionadas con la dieta.

Las especializaciones de la cutícula no se restringen a los osículos. El estómago de los decápodos posee otras estructuras cuticulares como micro-espinas, espinas y setas. Pero sin duda también ha de tenerse en cuenta que la propia cutícula es modificada de acuerdo con la función que debe realizar la región estomacal donde se localiza dicha cutícula.

La cutícula es una secreción extracelular con un contenido de agua del 50 % (Lignon, 1987). El contenido seco es una matriz constituida por α-quitina, un polímero formado por residuos de N-acetil-D-glucosamina unidos mediante enlaces β-1,4 (Dillaman et al., 2012; Lignon, 1987) y numerosos tipos de proteínas (Mary y Krishnan, 1974; Roer et al., 2015; Willis, 1999), que incluyen artropodinas y esclerotinas (Lignon, 1987), así como enzimas implicadas en procesos de síntesis, mineralización y esclerotización (Roer et al., 2015). La quitina se organiza en fibrillas que rodean a las proteínas, formando filamentos embebidos a su vez en una matriz proteica (Dillaman et al., 2012; Lignon, 1987). La cutícula puede contener minerales de calcio, los cuáles llegan a suponer entre el 60 y el 90 % del peso seco (Lignon, 1987; Welinder, 1974). La porción más importantes es carbonato cálcico ($CaCO_3$) en forma de calcita o de cristal amorfo (Boßelmann et al., 2007; Lignon, 1987; Roer y Dillaman, 1984), con asociaciones de fosfato de calcio y magnesio (Becker et al., 2005; Boßelmann et al., 2007). La cutícula de los malacostráceos es también endurecida por procesos de esclerotización (Dillaman et al., 2012; Lignon, 1987; Roer et al., 2015). También se han detectado fosfolípidos (Erri Babu et al., 1985), pero su importancia es marginal (Lignon, 1987).

La cutícula se divide en capas, denominadas epicutícula, exocutícula, endocutícula y capa membranosa (Dillaman et al., 2012; Erri Babu et al., 1985), cada una con estructura y composición propias (Welinder, 1975). Nosotros solo identificamos las tres primeras capas (Fig. 19.5.3). La epicutícula es la capa más externa y delgada. Se subdivide en dos (Erri Babu et al., 1985; Hegdahl et al., 1977b; Roer y Dillaman, 1984; Travis, 1955; Welinder, 1975) o tres subcapas: cubierta superficial, cuticulina y epicutícula interna (Compère, 1995; Dillaman et al., 2012; Roer et al., 2015). La epicutícula carece de organización laminar (Roer y Dillaman, 1984), contiene lipoproteínas (Roer y Dillaman, 1984; Travis, 1955; Welinder, 1975) pero carece de lípidos (Erri Babu et al., 1985). Es una capa mineralizada, esclerotizada y estabilizada por puentes cruzados (Roer y Dillaman, 1984; Travis, 1955; Welinder, 1975).

La exocutícula o "*capa pigmentada*" (Travis, 1955) se sitúa entre la epicutícula y la endocutícula (Roer y Dillaman, 1984). Representa 1/3 del grosor (Hegdahl et al., 1977a; Travis, 1955) y casi el 20 % del peso relativo (Welinder, 1975). Los filamentos de proteína y quitina forman láminas apiladas en un patrón de giro helicoidal formando cada 180° una banda observable bajo microscopía (Dillaman et al., 2012; Roer et al., 2015; Roer y Dillaman, 1984). La quitina representa alrededor del 34 % del peso seco descalcificado (Welinder, 1975). La exocutícula contiene lípidos (Erri Babu et al., 1985) y minerales de calcio (Hegdahl et al., 1977a; Roer y Dillaman, 1984). Está esclerotizada por puentes cruzados derivados de la tirosina (Welinder et al., 1976) y quinonas producidas por la enzima fenol oxidasa (Dillaman et al., 2012; Roer et al., 2015; Travis, 1955).

La endocutícula o "*capa principal*" (Travis, 1955) se sitúa entre la endocutícula y la capa membranosa (si está presente) o el ápice de las células epiteliales (si la capa membranosa está ausente). Representa entre 2/3 y 3/4 del grosor (Hegdahl et al., 1977a; Travis, 1955) y 3/4 del peso relativo (Welinder, 1975). Los filamentos de proteínas y quitina se organizan en láminas como en la exocutícula (Dillaman et al., 2012; Hegdahl et al., 1977c; Roer et al., 2015; Roer y Dillaman, 1984). La quitina representa alrededor del 73 % del peso seco descalcificado (Welinder, 1975), contiene fosfolípidos (Erri Babu et al., 1985) y minerales de calcio (Hegdahl et al., 1977c; Roer y Dillaman, 1984; Travis, 1955).

La capa membranosa es la capa más basal, se sitúa entre la endocutícula y el ápice de las células epiteliales. Su reducido tamaño representa aproximadamente el 6 % del peso relativo. Como en la exocutícula y endocutícula, los filamentos se organizan en láminas. La quitina representa 3/4 del peso seco, pero a diferencia de las anteriores capas, la capa membranosa no está esclerotizada ni calcificada (Welinder, 1975).

La estructura y composición de la cutícula varían dependiendo de su localización y de los requisitos funcionales de cada estructura corporal (Mary y Krishnan, 1974). En ese sentido, la cutícula del caparazón debe resistir esfuerzos de compresión y de fracturación como medio de protección frente a los depredadores (Dillaman et al., 2012), pero conservando al mismo tiempo la flexibilidad necesaria para permitir los movimientos del animal (Boßelmann et al., 2007). Por su parte, la cutícula de aquellas estructuras que deben resistir un elevado esfuerzo mecánico poseen un contenido mineral mucho más elevado, tal y como se ha observado en el dactilopodio y propodio (Welinder, 1974). En el caso de las quelas de *Homarus americanus* y *Cancer pagurus*, la cutícula además debe de ser capaz de cortar o romper el caparazón de otros animales (Boßelmann et al., 2007). Otros ejemplos de cutícula altamente especializada son la membrana artrodial y la cutícula branquial. La membrana artrodial articula al animal, por ello es fina y flexible (Dillaman et al., 2012; Hepburn y Chandler, 1976) y no está mineralizada (Williams et al., 2003) ni esclerotizada (Hepburn y Chandler, 1976). La cutícula de las branquias es muy delgada (de dos a menos de una micra de espesor), carece de epicutícula y tampoco está esclerotizada ni mineralizada (Dillaman et al., 2012; Mary y Krishnan, 1974), ya que debe de ser permeable a gases, agua e iones (Dillaman et al., 2012; Mary y Krishnan, 1974).

La cutícula estomacal es similar a la del tegumento (Fig. 19.5.3). Sin embargo, se han observado diferencias en el plano bioquímico. Por ejemplo, Mary y Krishnan (1974) en su estudio del braquiuro *Ocypode platytarsis* mencionan que la cutícula del tegumento posee una epicutícula con componentes lipídicos (lipoproteínas) y esclerotizada, por el contrario la cutícula del estómago tiene una epicutícula que carece de lípidos y no está esclerotizada. Los autores sospechan que estas diferencias se deben a que en el estómago la cutícula debe de ser permeable para permitir el intercambio iónico y/o la absorción de agua. En el presente estudio hemos observado que la cutícula que reviste el estómago también varía de una región a otra del mismo. Sospechamos que tales variaciones son funcionales: sacos cardiacos, osículos y molino gástrico, válvula cardio-pilórica y filtros pilóricos.

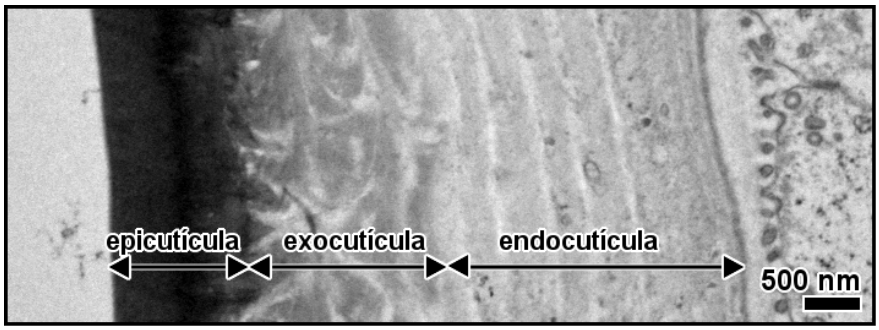

Figura 19.5.3. Cutícula estomacal del primer juvenil de *M. brachydactyla*. MET.

Los sacos cardiacos se localizan en las paredes laterales del estómago cardiaco (Alves et al., 2010; McGaw y Curtis, 2013; Meiss y Norman, 1977), poseen paredes finas y elásticas capaces de dilatarse (Ceccaldi, 1989), ya que almacenan el alimento (McGaw y Curtis, 2013) y permiten la mezcla del alimento con fluidos digestivos (Hobbs y Hooper, 2009). Los sacos cardiacos tienden a expandirse en sentido anterior o lateral, pero en carideos también se expanden en sentido posterior (Lima et al., 2014; Lima et al., 2016). Por el contrario, los osículos y dientes del molino gástrico son estructuras rígidas dada su función esquelética y masticadora, respectivamente (Allardyce y Linton, 2010; Ceccaldi, 1989; Factor, 1982; Hobbs y Hooper, 2009; Icely y Nott, 1992; Kunze y Anderson, 1979; McGaw y Curtis, 2013; McLaughlin, 1983; Nakamura y Takemoto, 1986; Salindeho y Johnston, 2003; Skilleter y Anderson, 1986). Estos dos ejemplos tan dispares (una cutícula elástica y distensible y una cutícula rígida y resistente) tienen un aspecto muy diferente a nivel histológico. La cutícula de los sacos cardiacos se caracteriza por tener una epicutícula muy fina y capas laminares (exo- y endocutícula) muy similares entre sí (Fig. 19.5.4B). Por su parte, la cutícula de los osículos varía localmente (Fig. 19.5.4A): en sección transversal, la cutícula de una de las caras es similar a la del estómago cardiaco (Fig. 19.5.4C), mientras que la cara opuesta presenta una epicutícula muy engrosada y gruesa y de láminas aparentemente compactadas (Fig. 19.5.4D-E).

La cutícula de los sacos cardiacos es similar a la cutícula de la membrana artrodial descrita en *Callinectes sapidus* por Williams et al. (2003), ambas son finas, elásticas y no están mineralizadas (Fig. 19.3.5D). Por su parte, la cutícula de los osículos recuerda a la del caparazón (Ruangchai et al., 2013; Williams et al., 2003) y como este está fuertemente calcificada. Desde un punto de vista funcional, tanto los osículos como el caparazón son estructuras de tipo esquelético. En el caso del molino gástrico, además deben de resistir los esfuerzos requeridos para triturar el material ingerido, por ello su composición incluye sílice así como minerales de calcio y fosfato (Nesbit y Roer, 2016; Vatcher et al., 2015). También encontramos variación entre la cutícula de la cara ventral y la cara dorsal de un diente del molino gástrico. Quizás la cara dorsal actúa de soporte o requiera elasticidad para amortiguar los esfuerzos del diente, mientras que la ventral debe actuar como una muela de gran resistencia y capaz de realizar actividades de molienda. Trabajos previos también observaron variaciones en la estructura y composición de la cutícula en un mismo osículo. El espesor relativo de las capas cuticulares (epi-, exo- y endocutícula) de los dientes del molino gástrico de *C. sapidus* varía a lo largo del eje longitudinal del mismo (Vatcher et al., 2015). Por su parte, Chisaka y Kozawa (2003) estudiaron los dientes gástricos de *Procambarus clarkii* y observaron que la forma y espesor de la exocutícula varía según el tipo y morfología del diente. En un plano funcional, la región anterior de un diente gástrico debe de actuar como soporte, mientras que la región posterior debe actuar como una muela propiamente dicha.

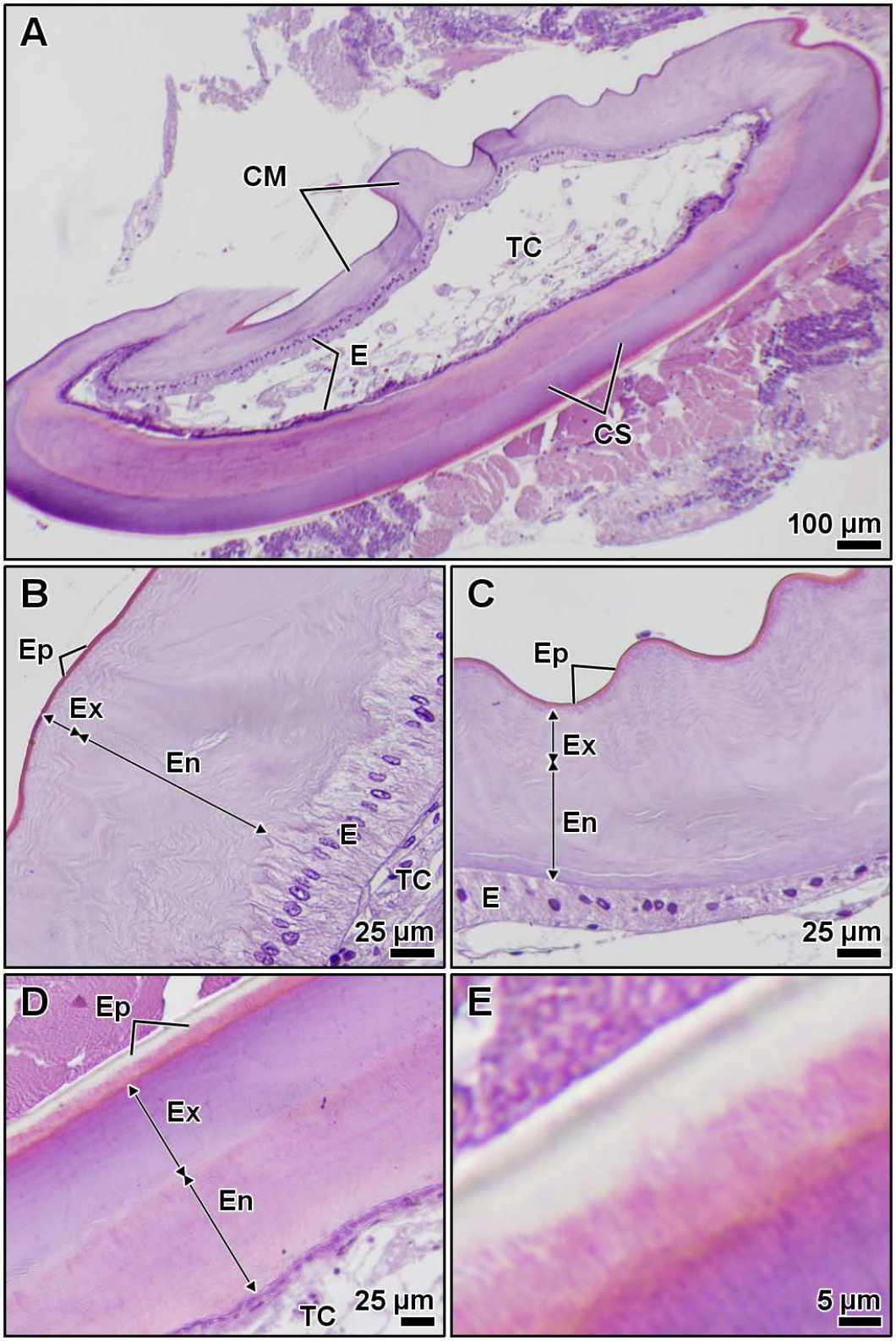

Figura 19.5.4. Adulto. Cutícula estomacal. Hematoxilina - Eosina. Sacos cardiacos (B). Osículo urocárdico, diente dorsal del molino gástrico: vista general (A), variación de la cutícula (C-D), detalle de la epicutícula de D (E). Abreviaciones: CM, cutícula "similar a la cutícula de la membrana artrodial"; CS, cutícula "similar a la cutícula de los escleritos"; E, epitelio; En, endocutícula; Ep, epicutícula; Ex, exocutícula; TC, tejido conectivo.

La válvula cardio-pilórica separa el estómago cardiaco del estómago pilórico (Barker y Gibson, 1978; Icely y Nott, 1992; Kunze y Anderson, 1979). Es un pliegue ventral soportado por varios osículos y puede presentar crestas esclerotizadas poco flexibles (Icely y Nott, 1992; Kunze y Anderson, 1979). La válvula cardio-pilórica también presenta superficies con abundante setación (Icely y Nott, 1992; Salindeho y Johnston, 2003) y paquetes musculares (Maynard y Dando, 1974). Esta estructura puede bloquear el acceso al estómago pilórico ventral y los filtros pilóricos, redirigiendo el movimiento del contenido estomacal al estómago pilórico dorsal (Icely y Nott, 1992; Kunze y Anderson, 1979). La válvula cardio-pilórica actúa como una barrera primaria de filtración, retiene el alimento en el molino gástrico y solo permite que los fluidos y las partículas más finas alcancen los filtros pilóricos (Barker y Gibson, 1978; Salindeho y Johnston, 2003), también impide que el contenido del estómago pilórico retroceda al estómago cardiaco (Salindeho y Johnston, 2003). La rigidez de la válvula cardio-pilórica podría explicar la similitud de la cutícula de esta con la de los osículos (Fig. 19.5.5A-C). Si bien las diferencias observadas podrían representar un compromiso entre rigidez y flexibilidad, ya que la válvula cardio-pilórica debe ser capaz de ocluir el paso a los filtros pilóricos cuando es preciso.

Los filtros pilóricos son estructuras altamente especializadas. Coincidiendo con otros autores (Abbott, 1971; Icely y Nott, 1992; Kunze y Anderson, 1979; Lin, 1996; 2000; Salindeho y Johnston, 2003), están subdivididos en cámara superior e inferior. La cutícula que forma el "techo" de la cámara superior es una densa matriz de setas (Fig. 19.5.6A-C), mientras que la cutícula de la cámara inferior forma canales estrechos, longitudinales y paralelos mediante crestas ventrales, paralelas y orientadas en sentido antero-posterior, desde las que se proyectan crestas largas setas imbricadas entre sí (Fig. 19.5.6A, D-E). El estómago pilórico posee un complejo armazón de osículos, pero además está musculado e inervado (Maynard y Dando, 1974), por ello puede realizar movimientos que permiten la oclusión de la cámara superior exprimiendo su contenido contra las setas de la cámara inferior, provocando la filtración de fluidos y partículas muy finas hacia los canales inferiores (Kunze y Anderson, 1979; Salindeho y Johnston, 2003). El rol de los filtros pilóricos es permitir que solo fluidos y partículas muy finas puedan entrar en la glándula digestiva, donde continuará la digestión y absorción de nutrientes (Icely y Nott, 1992; McGaw y Curtis, 2013).

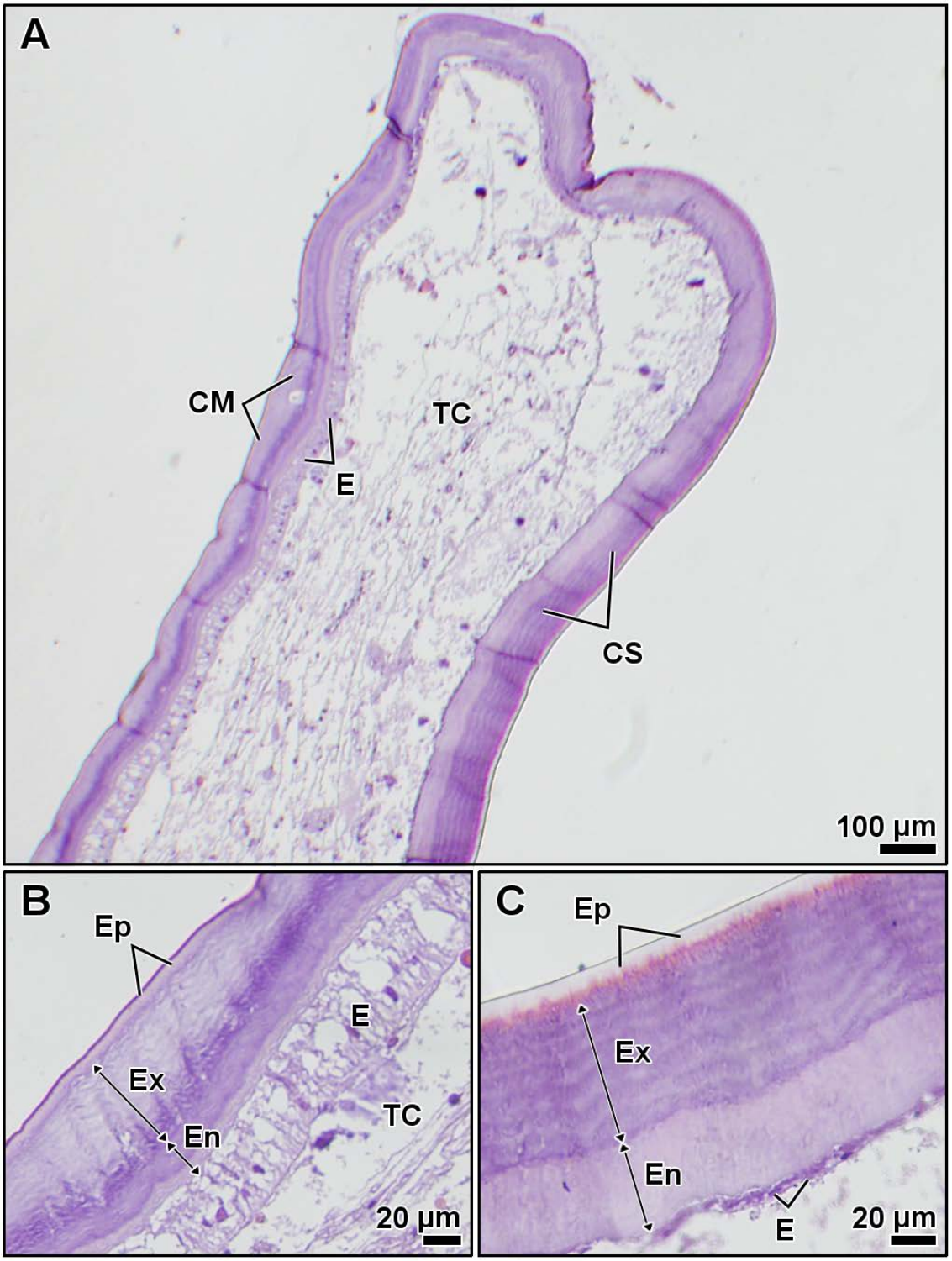

Figura 19.5.5. Adulto. Cutícula estomacal. Válvula cardio-pilórica. Hematoxilina - Eosina. Vista general (A). Variación de la cutícula (B-C). Abreviaciones: CM, cutícula "similar a la cutícula de la membrana artrodial"; CS, cutícula "similar a la cutícula de los escleritos"; E, epitelio; En, endocutícula; Ep, epicutícula; Ex, exocutícula; TC, tejido conectivo.

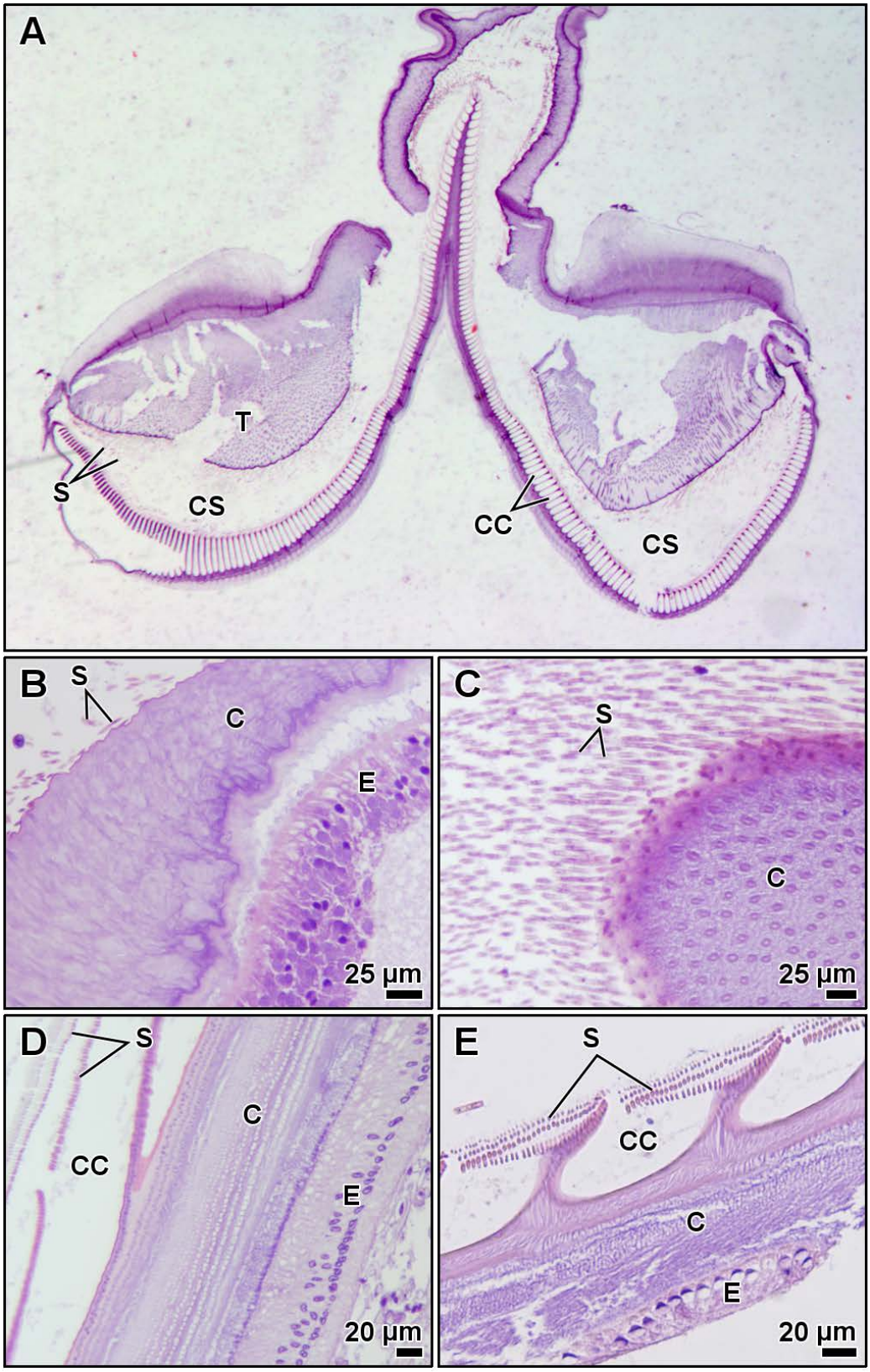

Figura 19.5.6. Adulto. Cutícula estomacal. Filtros pilóricos. Hematoxilina - Eosina. Vista general, corte transversal (A). Cutícula del "techo de la cámara superior" (B-C). Cutícula de los "canales de la cámara inferior" (D-E). Abreviaciones: C, cutícula; CC, canales de la cámara inferior; CS, cámara superior; E, epitelio; S, setas; T, "techo" de la cámara superior.

19.6 Micro-espinas en órganos derivados del ectodermo.

La cutícula proyecta diversos tipos de estructuras: micro-espinas, espinas, tubérculos y setas. En el presente estudio nos centramos en las micro-espinas que se han identificado en el esófago, estómago y tracto digestivo posterior, tanto en larvas como en juveniles y adultos. Las micro-espinas son pequeñas proyecciones no articuladas de la cutícula con forma de pelo o colmillo. Según Elzinga (1998), la presencia de micro-espinas en el tracto digestivo de los euartrópodos es reconocida desde hace dos siglos, por ello han recibido numerosos nombres: "*acanthae*", "*dentículos*", "*espículas*", "*micro-espinas*" y "*setas*". También se han denominado "*espínulas*" (Pillai, 1960), "*microtricas*" (Pugh, 1962) y "*tricromas*" (Schlüter, 1980). De todos ellos, el término "micro-espina" es el que decidimos emplear, dada su morfología equivalente a espinas únicamente observables bajo microscopía.

El esófago adulto presenta grupos compactos de una a tres micro-espinas (raramente más) parcialmente unidas entre sí y de 4 ± 1 µm de longitud (Fig. 19.6.1C), aunque se han observado de hasta 14 µm (Fig. 19.6.1D). Los grupos son equidistantes entre sí (Fig. 19.6.1A). El esófago también presenta áreas en forma de elipse o circulo atravesadas por poros que excluyen a las micro-espinas (Fig. 19.6.1B), el esófago también presenta otras áreas extensas carentes de micro-espinas y de poros pero su distribución no ha podido ser determinada. El esófago de las larvas recién eclosionadas también posee micro-espinas, las cuales difieren de las adultas por su menor tamaño (~0,5 µm) y porque forman grupos dispersos donde las micro-espinas de forma individual están separadas entre sí (Fig. 19.6.1E-F).

En el estómago de la zoea las micro-espinas se han observado en las paredes laterales y en las paredes de la válvula cardio-pilórica (Fig. 19.6.4C-D). Estas agrupaciones se componen de micro-espinas cortas (entre 1 y 2 µm) y delgadas. En la megalopa y primer juvenil también se observan micro-espinas localizadas en los dientes del molino gástrico (Fig. 19.6.4E-F).

El tracto digestivo posterior del adulto presenta una cutícula con un relieve pentagonal o hexagonal. Las micro-espinas ocupan las celdas identificándose dos tipos de agregaciones (Fig. 19.6.2A, D-E): un halo de más de 200 micro-espinas de punta roma e inferiores a 1 µm (Fig. 19.6.2E) y un tipo de agregación que combina el tipo anterior con micro-espinas de punta aguda de 4 a 6 µm de longitud (Fig. 19.6.2D). Sendos tipos de agregaciones se intercalan entre sí como bandas longitudinales (Fig. 19.6.2A-C). En la zoea I la cutícula carece de relieve, mientras que las micro-espinas son de un solo tipo y de 0,5 a 1 µm de longitud (Fig. 19.6.3E-F). Como en el adulto, las micro-espinas forman bandas paralelas al eje longitudinal del tracto digestivo posterior, cada banda está separada de las demás por una extensión carente de micro-espinas. Micro-espinas similares a las adultas se observan en juveniles de 7 mm (Fig. 19.6.4A-B).

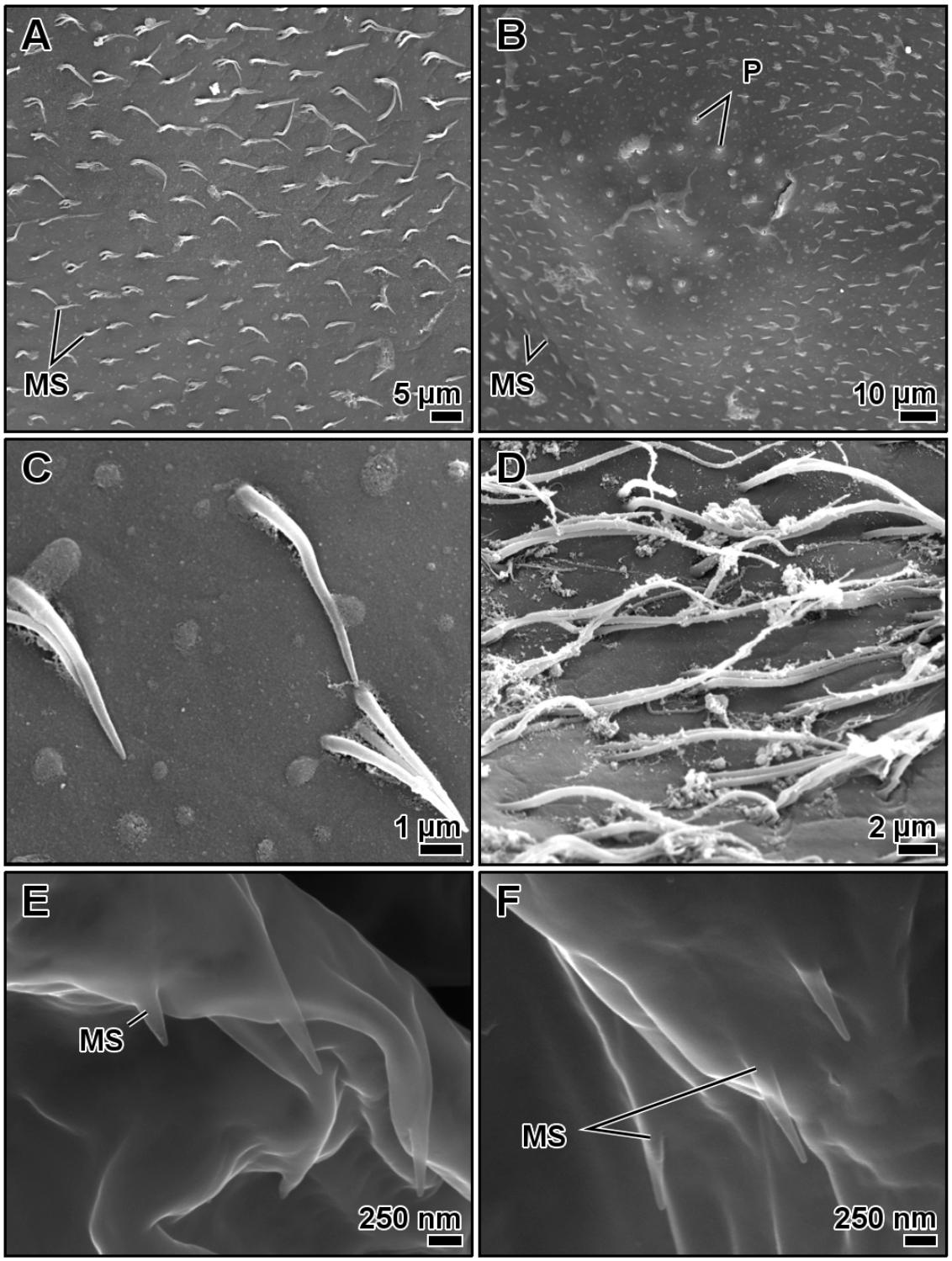

Figura 19.6.1. Esófago. Micro-espinas. MEB. Adulto (A-D). Extensión de micro-espinas (A). "Área con poros" rodeada de micro-espinas (B). Detalle de las micro-espinas, nótese como en cada agrupación están parcialmente unidas (en contacto) entre sí (C). Detalle de micro-espinas de gran longitud (alrededor de 14 µm) (D). Zoea I (E-F). Abreviaciones: MS, micro-espinas; P, poros.

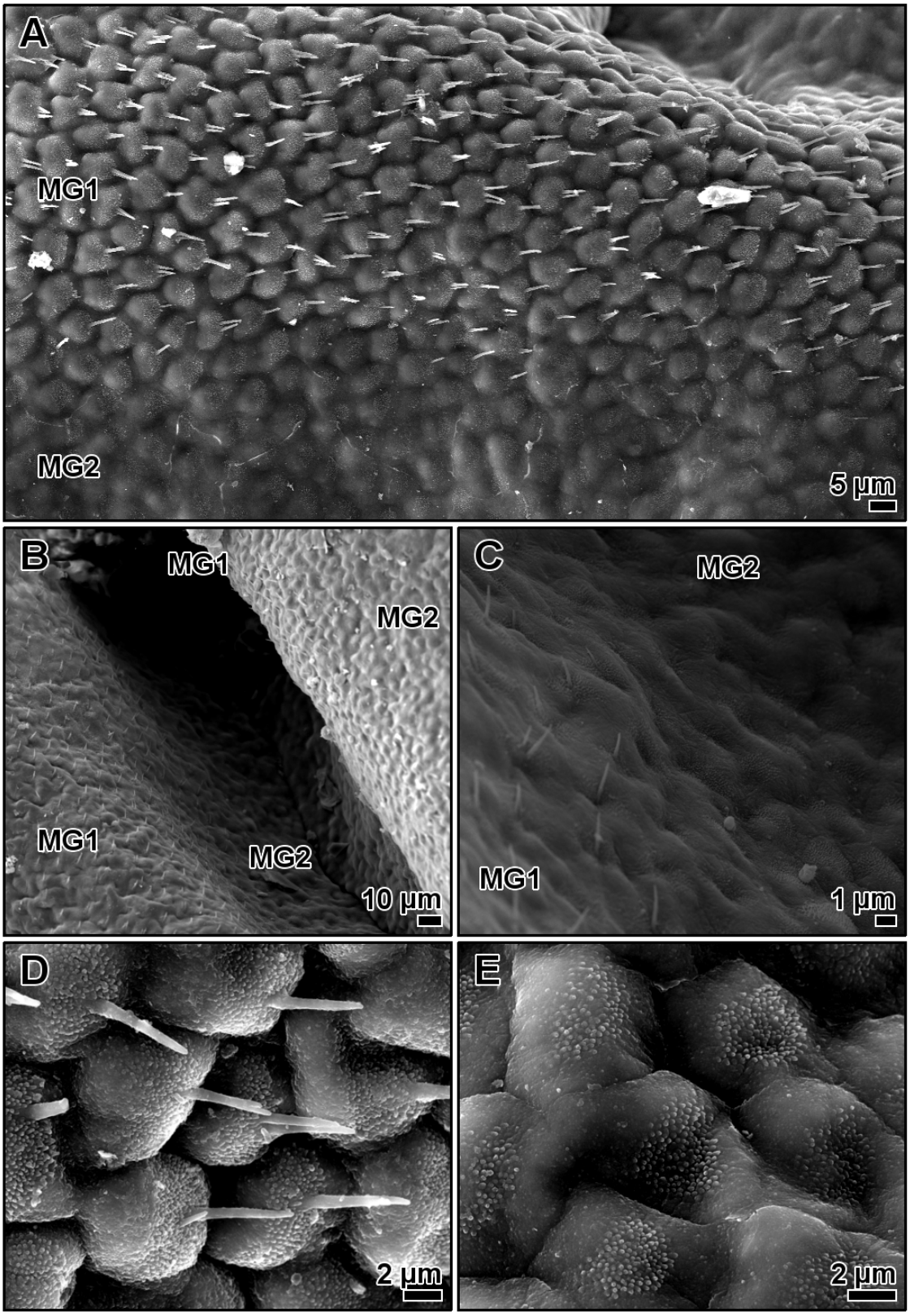

Figura 19.6.2. Adulto. Tracto digestivo posterior. Micro-espinas. MEB. Vista general (A-B). Detalle de la transición entre la agregación de micro-espinas tipo 1 y 2 (C). Agregación de tipo 1 (D). Agregación de tipo 2 (E). Abreviaciones: AT1, agregación de micro-espinas tipo 1; AG2, agregación de micro-espinas tipo 2.

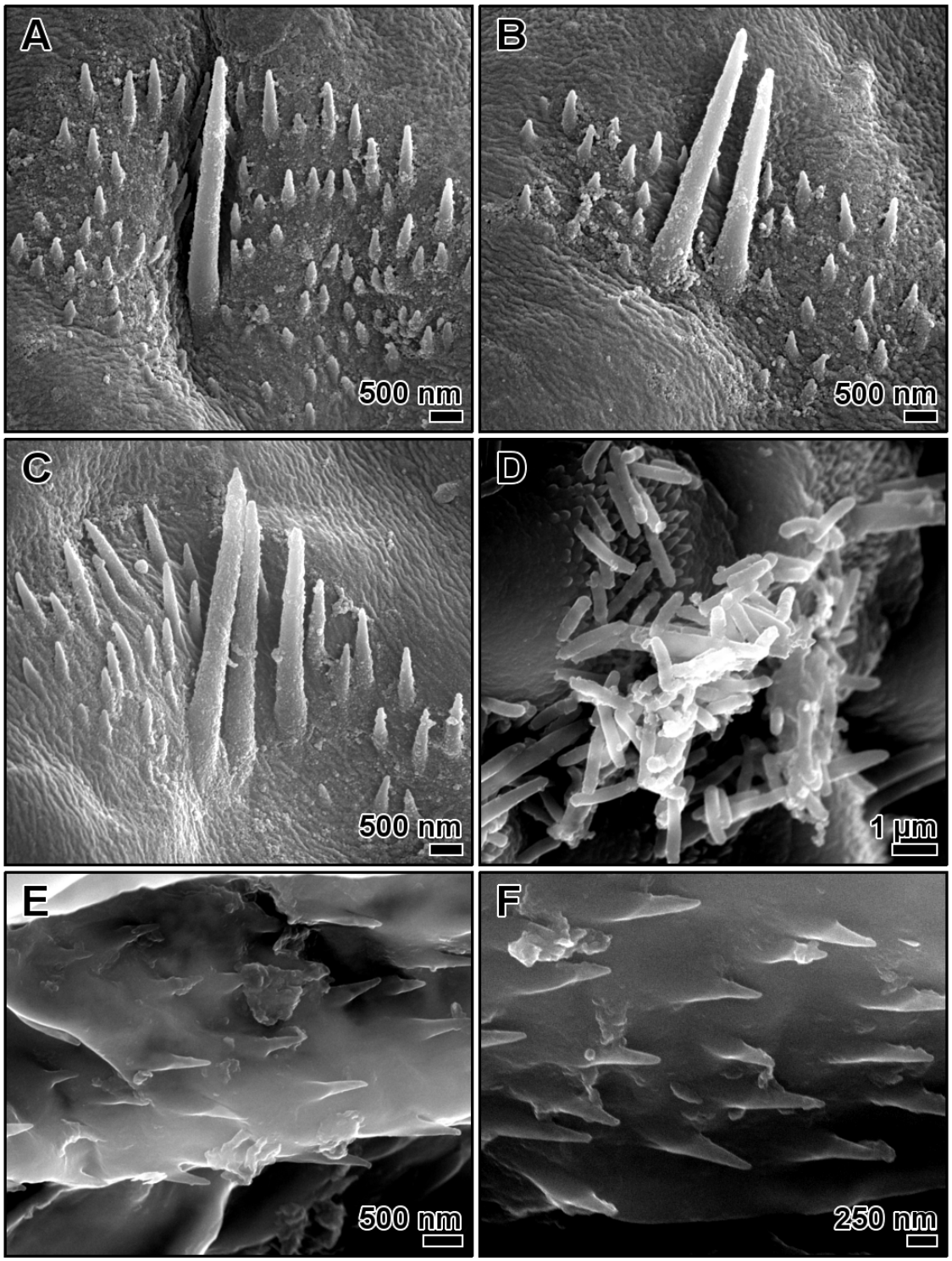

Figura 19.6.3. Tracto digestivo posterior. Micro-espinas. MEB. Adulto (A-D). Distintas variaciones de la agregación de tipo 1 (A-C). Agregación tipo 1 cubierta por microorganismos (D). Zoea I (E-F).

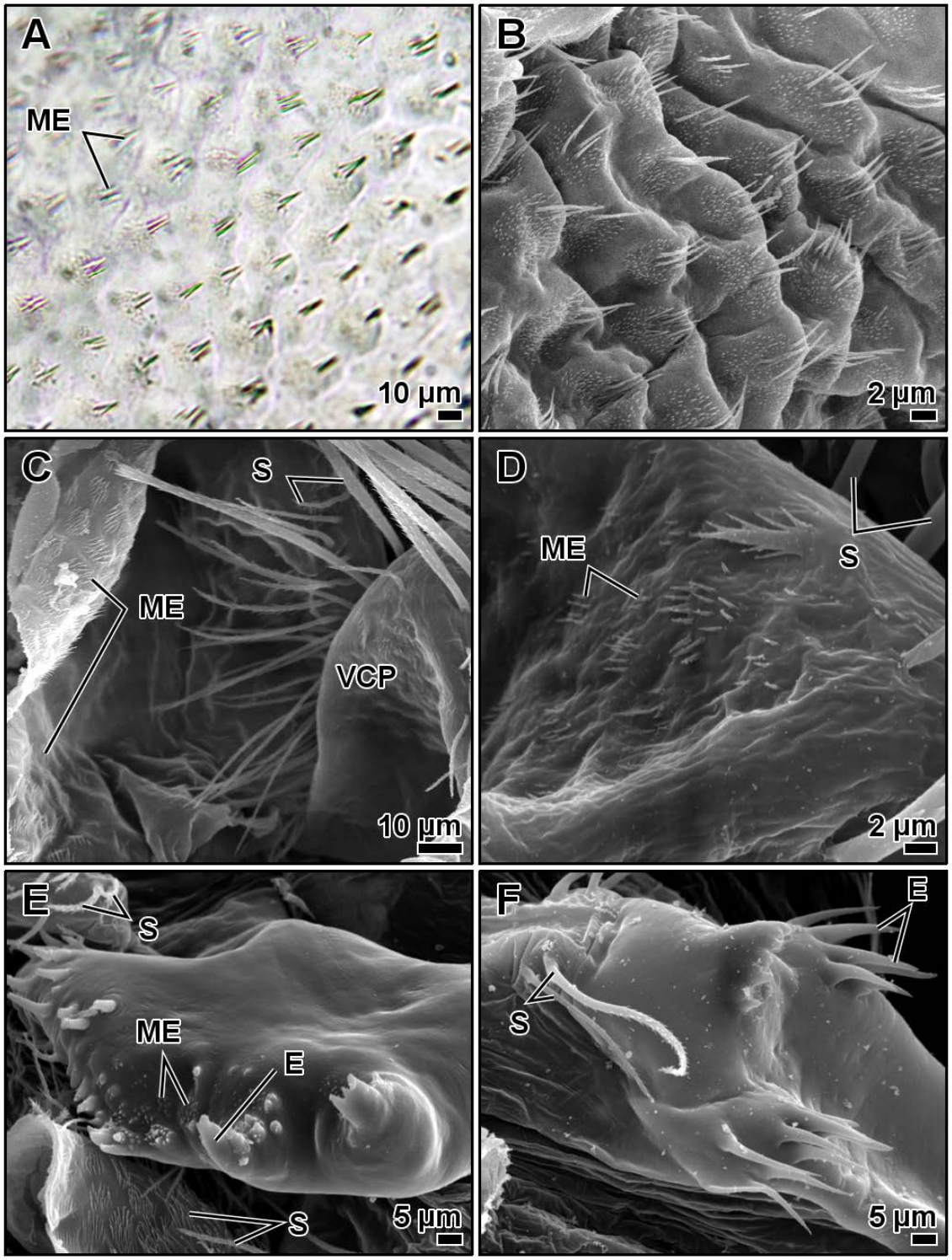

Figura 19.6.4. Micro-espinas y espinas. MEB. Tracto digestivo posterior, juvenil de caparazón de 7 mm (A-B). Vávula cardio-pilórica (C-D): zoea I (C) y zoea II (D). Molino gástrico, megalopa (E-F): diente lateral (E) y diente dorsal (F).

Las presencia de micro-espinas en los órganos derivados del ectodermo embrionario no es exclusivo de *M. brachydactyla*, sino común a varios taxones de euartrópodos tal y como se resume en la tabla 19.6.1. Raramente se ha reportado de forma explícita la carencia de micro-espinas, pero este es el caso del carideo *Palaemonetes argentinus* (Sousa y Petriella, 2006) y de los "camarones fantasma" del género *Upogebia* (Pinn et al., 1999). En un sentido biológico, si una estructura está tan distribuida en distintos taxones, órganos y estadios vitales, cabe suponer que cumple una importante función.

En el caso del esófago se ha hipotetizado que las micro-espinas podrían prevenir la regurgitación del bolo alimenticio (Dapples y Lea, 1974; Elzinga, 1998). Otros autores han propuesto que las micro-espinas facilitarían el desplazamiento de las piezas de alimento al favorecer su agarre (Chisaka et al., 1999; Elzinga, 1998; Felder y Felgenhauer, 1993; Icely y Nott, 1984; Moon y Kim, 1999; Pillai, 1960; Pinn et al., 1999; Schlüter, 1980). En ambos casos, las micro-espinas aumentarían el rozamiento contra la superficie del esófago y su orientación hacia el estómago facilitaría el desplazamiento en ese sentido en lugar del contrario.

En relación al tracto digestivo posterior, la hipótesis más popular sugiere que las micro-espinas sujetan la membrana peritrófica para facilitar el transporte de materia fecal (Chisaka et al., 1999; Elzinga, 1998; Felder y Felgenhauer, 1993; Icely y Nott, 1984; Moon y Kim, 1999; Pillai, 1960; Pinn et al., 1999; Schlüter, 1980). Esta sujeción también prevendría el desplazamiento en sentido anterior cuando tienen lugar los movimientos anti-peristálticos que permiten la ingesta anal de agua (Chisaka et al., 1999; Felder y Felgenhauer, 1993; Hopkin y Nott, 1980; Pinn et al., 1999). La compactación de las heces también se facilitaría por esta sujeción (Felder y Felgenhauer, 1993; Pillai, 1960). Otros autores proponen que las micro-espinas rasgan la membrana peritrófica liberando su contenido y facilitando la absorción de aguas e iones (Byers y Bond, 1971; Elzinga y Hopkins, 1995; Miyoshi et al., 2005; Schlüter, 1980), pero en *M. brachydactyla* esto no es factible ya que la membrana peritrófica es excretada conservando su integridad. Otros autores sugieren que las micro-espinas permiten el anclaje de comunidades de microorganismos mutualistas (Elzinga, 1998; Elzinga y Hopkins, 1995). En *M. brachydactyla* se han observado microorganismos asociados a las micro-espinas (Fig. 19.6.3E), pero su presencia no basta para considerarlas una comunidad de endosimbiontes.

En el tracto digestivo posterior las micro-espinas se proyectan desde formaciones con aspecto de celda. Observaciones similares han sido realizadas en otros braquiuros como los cangrejos violinista de la familia Ocypodidae (Pugh, 1962), así como en el anomuro *Munidopsis andamanica* (Hoyoux et al., 2009). Pugh (1962) menciona que los bordes de dichas celdas coincide con los bordes de las células epiteliales localizadas debajo, por lo que su aspecto de celda podría ser una mera consecuencia de su formación.

Tabla 19.6.1 Distintas especies de euartrópodos en los que ha sido descrita la presencia de micro-espinas en órganos digestivos derivados del ectodermo embrionario: esófago (ES), estómago (ES) y tracto digestivo posterior (TP).

Especie	Taxón	ES	ET	TP	Referencias
Armases cinereum (Bosc, 1802)	Brachyura			X	Harris (1993)
Callinectes sapidus Rathbun, 1896	Brachyura			X	Harris (1993)
Carcinus maenas (Linnaeus, 1758)	Brachyura			X	Hopkin y Nott (1980)
Hemigrapsus penicillatus (De Haan, 1835)	Brachyura			X	Moon y Kim (1999)
Leptuca pugilator (Bosc, 1802)	Brachyura			X	Harris (1993), Pugh (1962)
Mictyris longicarpus Latreille, 1806	Brachyura			X	Harris (1993)
Minuca minax (LeConte, 1855)	Brachyura			X	Harris (1993), Pugh (1962)
Minuca pugnax (Smith, 1870)	Brachyura			X	Harris (1993), Pugh (1962)
Ovalipes punctatus (De Haan, 1833)	Brachyura			X	Harris (1993)
Parasesarma catenatum (Ortmann, 1897)	Brachyura			X	Harris (1993)
Panopeus herbstii H. Milne Edwards, 1834	Brachyura			X	Harris (1993)
Pinnotheres cyclinus Shen, 1932	Brachyura			X	Moon y Kim (1999)
Scylla serrata (Forskål, 1775)	Brachyura			X	Harris (1993)
Munidopsis andamanica MacGilchrist, 1905	Anomura		X	X	Hoyoux et al. (2009)
[L]*Paralithodes camtschaticus* (Tilesius, 1815)	Anomura			X	Abrunhosa y Kittaka (1997)
Procambarus clarkii (Girard, 1852)	Astacidea			X	Chisaka et al. (1999)
Orconectes sp. Cope, 1872	Astacidea		X	X	Elzinga (1998)
Ibacus ciliatus (von Siebold, 1824)	Achelata	X[?]	X		Mikami y Takashima (1993)
Thenus orientalis (Lund, 1793)	Achelata			X	Johnston y Alexander (1999)
[L]*Panulirus ornatus* (Fabricius, 1798)	Achelata	X			Johnston et al. (2008)
Caridina laevis Heller, 1862	Caridea		X	X	Pillai (1960)

([L]): estudio basado en estadios larvarios; (S): presuntas micro-espinas, estas estructuras son denominadas "setas" en la publicación original; (X): Presencia de micro-espinas; (X[a]): Micro-espinas ausentes en la mayor parte del órgano exceptuando una región o área muy concreta, se recomienda ver bibliografía. (X[?]): Presunta presencia según ilustraciones, pero no se describe explícitamente en el texto.

Tabla 19.6.1 (continuación). Distintas especies de eurtrópodos en los que ha sido descrita la presencia de micro-espinas en órganos digestivos derivados del ectodermo embrionario: esófago (ES), estómago (ES) y tracto digestivo posterior (TP).

Especie	Taxón	ES	ET	TP	Referencias
Género *Eucopia* Dana, 1852	Lophogastrida		X		De Jong y Casanova (1997)
Mysis stenolepis S.I. Smith, 1873	Mysida	X	X		Friesen et al. (1986)
Armadillidium vulgare (Latreille, 1804)	Isopoda	X	X	X	Elzinga (1998)
Natatolana obtusata Vanhöffen, 1914	Isopoda	X	X		Storch et al. (2002)
Bellorchestia marmorata (Haswell, 1880)	Amphipoda	X[a]		X	Johnston et al. (2004)
Corophium volutator (Pallas, 1766)	Amphipoda	S		S	Icely y Nott (1984)
Hyperiidea Milne Edwards, 1830: 8 especies	Amphipoda	X	X		Coleman (1994)
Axius stirhynchus Leach, 1816	Axiidea			X	Pinn et al. (1999)
Callianassa subterranea (Montagu, 1808)	Axiidea			X	Pinn et al. (1999)
Callichirus kraussi (Stebbing, 1900)	Axiidea			X	Harris (1993)
Calocaris macandreae Bell, 1853	Axiidea			X	Pinn et al. (1999)
Neotrypaea californiensis (Dana, 1854)	Axiidea			X	Harris (1993)
Lepidophthalmus louisianensis (Schmitt, 1935)	Axiidea			X	Felder y Felgenhauer (1993)
Trypaea australiensis Dana, 1852	Axiidea			X	Harris (1993)
Jaxea nocturna Nardo, 1847	Gebiidea			X	Pinn et al. (1999)
Aedes aegypti (Linnaeus 1762)	Insecta	X		X	Dapples y Lea (1974)
Anax junius (Drury, 1773)	Insecta	X	X	X[a]	Elzinga (1998)
[L]*Calopteryx maculata*Palisot de Beauvois, 1807	Insecta	X	X	X[a]	Elzinga (1998)
[L]*Gomphoides*sp. Selys, 1854	Insecta	X	X	X[a]	Elzinga (1998)
[L]*Hexagenia limbata* (Serville, 1829)	Insecta			X	Elzinga (1998)
[L]*Lestes*sp. Leach, 1815	Insecta	X	X	X[a]	Elzinga (1998)

([L]): estudio basado en estadios larvarios; (S): presuntas micro-espinas, estas estructuras son denominadas "setas" en la publicación original; (X): Presencia de micro-espinas; (X[a]): Micro-espinas ausentes en la mayor parte del órgano exceptuando una región o área muy concreta, se recomienda ver bibliografía.

Tabla 19.6.1 (continuación y final). Distintas especies de eurtrópodos en los que ha sido descrita la presencia de micro-espinas en órganos digestivos derivados del ectodermo embrionario: esófago (ES), estómago (ES) y tracto digestivo posterior (TP).

Especie	Taxón	ES	ET	TP	Referencias
Libellula lydia (Drury, 1773)	Insecta	X	X	X[a]	Elzinga (1998)
Locusta migratoria (Linnaeus, 1758)	Insecta		X		Hochuli et al. (1992)
Petrobius brevistylis Carpenter, 1913	Insecta	X			Elzinga (1998)
Thermobia domestica (Packard, 1873)	Insecta	X	X		Elzinga (1998)
Blattodea: 10 especies de 4 familias	Insecta	X	X	X	Elzinga y Hopkins (1994; 1995)
[L]Lepidoptera: 30 especies de 19 familias	Insecta	X		X	Byers y Bond (1971)
Orthoptera: 17 especies de 5 familias	Insecta	X	X	X	Elzinga (1996)
Triops longicaudatus (LeConte, 1846)	Branchiopoda		X	X	Elzinga (1998)
Scolopendra viridis Say 1821	Chilopoda	X		X	Elzinga (1998)
Scolopocryptops rubiginosus L. Koch 1878	Chilopoda	X			Elzinga (1998)
Polydesmus angustus Latzel, 1884	Diplopoda			X	Schlüter (1980)
Rhinocricus padbergi Verhoeff, 1938	Diplopoda			X	Miyoshi et al. (2005)
*Orthoporus*sp. Silvestri, 1897	Diplopoda			X	Elzinga (1998)
Pseudonannolene tricolor Brölemann, 1901	Diplopoda			X	Miyoshi et al. (2005)
*Spirobolus*sp. (Wood, 1865)	Diplopoda			X	Elzinga (1998)
Tachypodoiulus niger (Leach, 1814)	Diplopoda			X	Schlüter (1980)
Aphonopelma chalcodes Chamberlin, 1940	Arachnida	X			Elzinga (1998)
Mastigoproctus giganteus (Lucas, 1835)	Arachnida	X[a]			Elzinga (1998)
Nephila clavipes (Linnaeus, 1767)	Arachnida	X			Elzinga (1998)
Uroctonus mordax Thorell, 1876	Arachnida			X	Elzinga (1998)
Limulus polyphemus (Linnaeus, 1758)	Xiphosurida	X		X[a]	Elzinga (1998)

([L]): estudio basado en estadios larvarios; (S): presuntas micro-espinas, estas estructuras son denominadas "setas" en la publicación original; (X): Presencia de micro-espinas; (X[a]): Micro-espinas ausentes en la mayor parte del órgano exceptuando una región o área muy concreta, se recomienda ver bibliografía.

19.7 Glándulas de roseta, más preguntas que respuestas.

Por el nombre de "glándulas de roseta" entendemos un tipo glandular caracterizado por su morfología: son una agrupación acinar de células secretoras rodeadas de tejido conectivo, las células secretoras tienen forma piramidal y disponen de núcleo medial o basal, vierten sus productos en un canal central, el cual también está constituido por una o más células (Gorvett, 1946; Ikeda et al., 2004; Pugh, 1962; Yonge, 1924). La presencia de este tipo de glándulas en los malacostráceos es conocida desde hace mucho tiempo, por lo que han recibido diversos nombres por los autores que las han estudiado. Dichos nombres se asocian a su posible función, localización o morfología (Tabla 19.7.1).

Tabla 19.7.1. Nombres dados a las "glándulas de roseta" en los malacostráceos.

Nombre traducido	Nombre original	Referencias
Asociado a una función		
Glándulas cementantes	Cement glands	Aiken y Waddy (1982); Erri Babu et al. (1979);Talbot et al. (1991); Yonge (1932)
Glándulas salivares	Salivary glands	Erri Babu et al. (1979); Reddy (1937);Yonge (1924)
Asociado a una localización		
Glándulas abdominales	Abdominal glands	Aiken y Waddy (1982)
Glándulas de los pleópodos	Pleopodal glands	Aiken y Waddy (1982)
Glándulas del esófago	Oesophageal glands	Erri Babu et al. (1979), Yonge (1924)
Glándulas del tegumento	Tegumental / Tegumentary glands	Alexander (1989); Barker y Gibson (1977); Ikeda et al. (2004); Jalaja-Kumari et al. (1983); McKenzie y Alexander (1989); Reddy (1937); Talbot et al. (1991); Yonge (1924; 1932)
Glándulas intestinales	Intestinal glands	Reddy (1937)
Glándulas labiales	Labial glands	Yonge (1924)
Glándulas mucosas cefálicas	Cephalic mucous glands	Shyamasundari y Hanumantha Rao (1977)
Asociado a la morfología		
Glándulas de roseta	Rosette glands	Gorvett (1946); Ikeda et al. (2004)

En el presente estudio preferimos usar el nombre "glándulas de roseta". Los nombres basados en la posible función se descartaron ya que esta resulta desconocida; mientras que los nombres basados en la localización (como por ejemplo, "glándulas del tegumento") no nos parecieron correctos porque bajo tal denominación se pueden englobar varios tipos glandulares que difieren de la morfología "roseta" (Gorvett, 1946; 1951; Ikeda et al., 2004).

En el estadio adulto de *M. brachydactyla* las "glándulas de roseta" se han identificado en el tejido conectivo del esófago y del tracto digestivo posterior, en este último órgano resultan especialmente llamativas las grandes formaciones glandulares, sobre las que pueden aparecer canales atravesando la cutícula y terminados en poros (Fig. 19.7.1A-C). La misma localización se ha reportado en otras especies de braquiuros (Erri Babu et al., 1979; Pugh, 1962) y astacídeos (Barker y Gibson, 1977; Shyamasundari y Hanumantha Rao, 1978; Yonge, 1924), reportándose grandes masas glandulares en el extremo anterior del tracto digestivo posterior así como canales atravesando la cutícula (Erri Babu et al., 1979; Pugh, 1962); si bien otros estudios mencionan expresamente no haber identificado tales canales (Barker y Gibson, 1977). En cambio, durante los estadios larvarios de *M. brachydactyla* las "glándulas de roseta" han sido identificadas en la región oral (asociadas al labro y otras piezas bucales) y adyacentes al extremo anterior de la masa ganglionar torácica, pero no en el tejido conectivo del esófago o tracto digestivo posterior (Fig. 19.7.1D-E). La misma disposición de las glándulas de roseta se ha reportado en isópodos y anfípodos: asociadas a las piezas bucales y extremo anterior del cordón nervioso torácico ventral, pero no en el conectivo del esófago o del tracto digestivo posterior (Gorvett, 1946; Jalaja-Kumari et al., 1983; Shyamasundari y Hanumantha Rao, 1977). También aparecen en la región oral y paragnatos del carideo *Palaemon serratus* (Alexander, 1989) y del dendrobranquiado *Penaeus merguiensis* (Hunt et al., 1992; McKenzie y Alexander, 1989), contactando con el medio externo a través de poros (McKenzie y Alexander, 1989).

En realidad, en los decápodos las glándulas de roseta tienen una distribución variada. En las familias Sesarmidae y Ocypodidae se han identificado bajo la espina dorsal de embriones y zoeas, mientras que en las familias Grapsidae, Portunidae y Xanthidae las glándulas con dicha localización tienen otra morfología (Ikeda et al., 2004). También aparecen en el raquis de las branquias del carideo *Palaemonetes pugio* (Doughtie y Rao, 1982); en los pereiópodos de los calianásidos donde permitirían reforzar los túneles excavados por estos animales (Dworschak, 1998); así como en el quinto par de pereiópodos del anomuro *Aegla platensis* (Almerão et al., 2007) y en los pleópodos del astácido *Homarus americanus* (Aiken y Waddy, 1982; Talbot et al., 1991), cuyo rol se ha asociado a la adhesión de las puestas. Recientemente se han identificado abundantes "glándulas de roseta" en la base de las sensilas del flagelo de las anténulas de *Panulirus argus* (Schmidt et al., 2006).

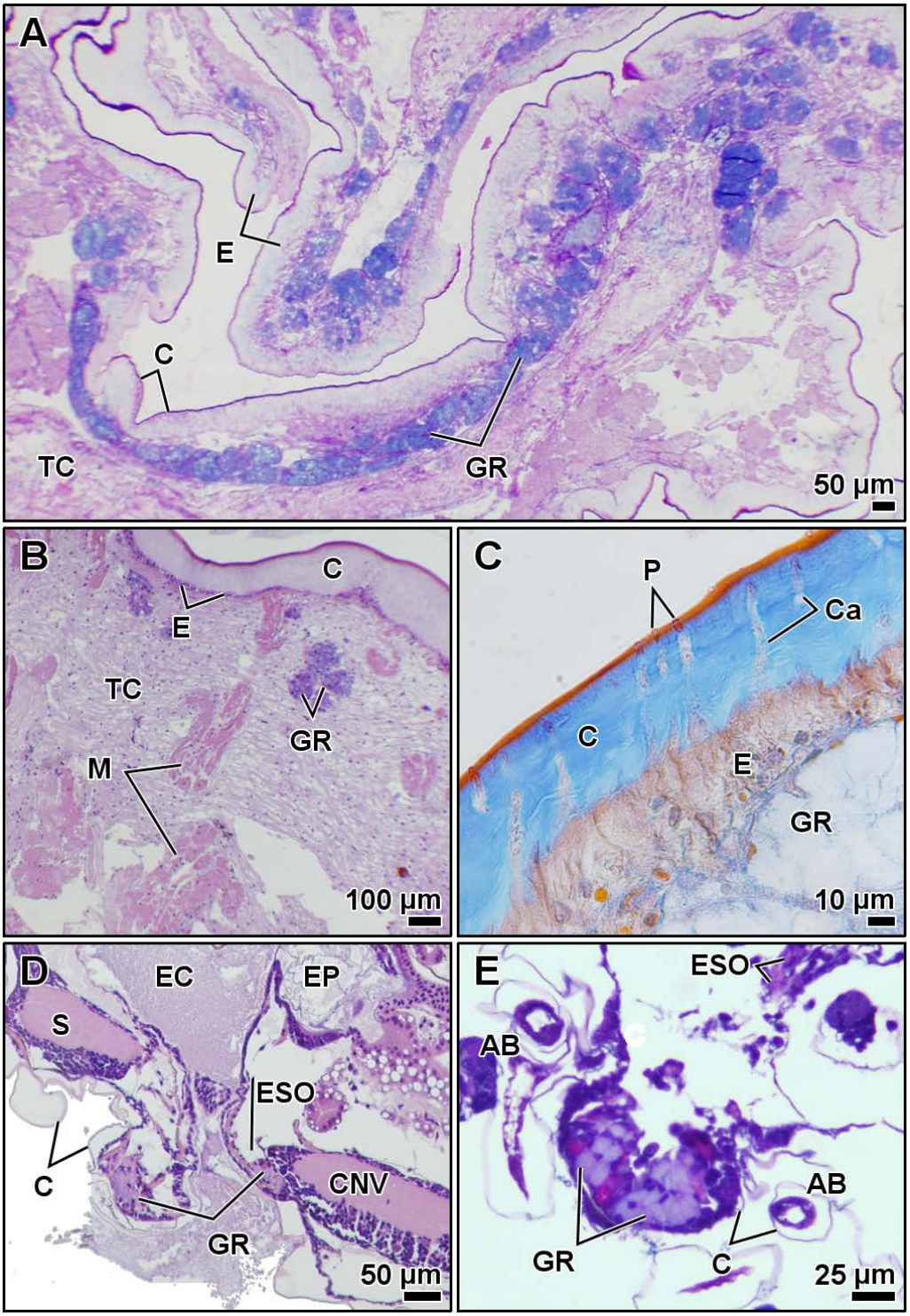

Figura 19.7.1. Glándulas de roseta. Adulto (A-C): tracto digestivo posterior, nótese la abundancia de glándulas (azul), PAS con contraste Azul de Metileno (A); esófago, Hematoxilina - Eosina (B) y tracto digestivo posterior, tricrómico de Mallory (C). Megalopa, glándulas asociadas a piezas bucales (D-E): adyacentes al esófago, Hematoxilina - Eosina (D) y localizadas en el labro, PAS con Azul Alcián y contraste de Hematoxilina (E). Abreviaciones: AB, apéndices bucales; C, cutícula; Ca, canales; CNV, cordón nervioso ventral; E, epitelio; EC, estómago cardiaco; EP, estómago pilórico; ESO, esófago; GR, glándulas de roseta; M, musculatura; P, poros; S, syncerebro; TC, tejido conectivo.

Las células secretoras tienen afinidad por PAS y Azul de Alcián, tinciones específicas de mucopolisacáridos neutros y ácidos (Fig. 19.7.2C - F). Estas células también tienen afinidad por Hematoxilina, Azul de Metileno y Azul de Anilina, por lo que contienen componentes ácidos y probablemente proteicos. La afinidad por dichas tinciones también se ha observado en las "glándulas de roseta" del braquiuro *Menippe rumphii* (Erri Babu et al., 1979), del dendrobranquiado *Penaeus merguiensis* (McKenzie y Alexander, 1989), del isópodo *Ligia exotica* (Jalaja-Kumari et al., 1983) y de ciertos anfípodos (Shyamasundari y Hanumantha Rao, 1977). Según distintos estudios el contenido de las vesículas incluye mucopolisacáridos neutros, ácidos y sulfatados, ácido hialurónico, así como mucinas sulfatadas y/o asociadas al ácido siálico (Barker y Gibson, 1977; Erri Babu et al., 1979; Jalaja-Kumari et al., 1983; McKenzie y Alexander, 1989; Shyamasundari y Hanumantha Rao, 1977; 1978; Stevenson y Murphy, 1967). También aparecen lípidos y fosfolípidos como demuestra su afinidad por Sudan Black B y Ftalocianina de Cobre (Jalaja-Kumari et al., 1983). En las células secretoras la afinidad por PAS y Azul de Alcián es variable, incluso si son células de la misma glándula. Es posible que esta variabilidad sea debida al ciclo de producción de las células secretoras, donde el contenido vesicular inicialmente afín a PAS gradualmente gana afinidad por Azul de Alcián desde la región basal hasta la región apical (probablemente a causa de la acidificación y/o sulfatación del contenido vesicular), entonces el volumen celular empieza a ser sustituido por vesículas de gran tamaño, las cuales probablemente representen el final del ciclo de secreción. Otros autores interpretan las vesículas de gran tamaño de forma opuesta. Pugh (1962) asocia la presencia de vesículas con el estado activo de las células secretoras, mientras que Yonge (1924) las asocia con el estado "durmiente" de las mismas.

A nivel ultra-estructural, uno de los rasgos más notorios es la saturación del citoplasma por vesículas de secreción cuyo contenido recuerda a una maraña amorfa de filamentos de electrodensidad variable (Fig. 19.7.3; 19.7.4A-B). Los principales orgánulos son los grandes y abundantes aparatos de Golgi y el retículo endoplasmático rugoso localizado adyacentemente a la membrana basal (Fig. 19.7.3; 19.7.4C-D). Dicha descripción es similar a la de las "glándulas de roseta" de los paragnatos de *Palaemon serratus* (Alexander, 1989), de las branquias de *Palaemonetes pugio* (Doughtie y Rao, 1982), del quinto pereiópodo del anomuro *Aegla platensis* (Almerão et al., 2007) y las de la base de la espina dorsal de embriones y zoeas del braquiuro *Chiromantes haematocheir* (como *Sesarma haematocheir*) (Ikeda et al., 2004). Si bien, una diferencia importante es que tanto Alexander (1989) como Doughtie y Rao (1982) describen axones en el tejido conectivo de las glándulas, lo que sugiere un control nervioso de la actividad secretora. En *M. brachydactyla* no se han identificado estructuras nerviosas, pero no por ello descartamos su presencia.

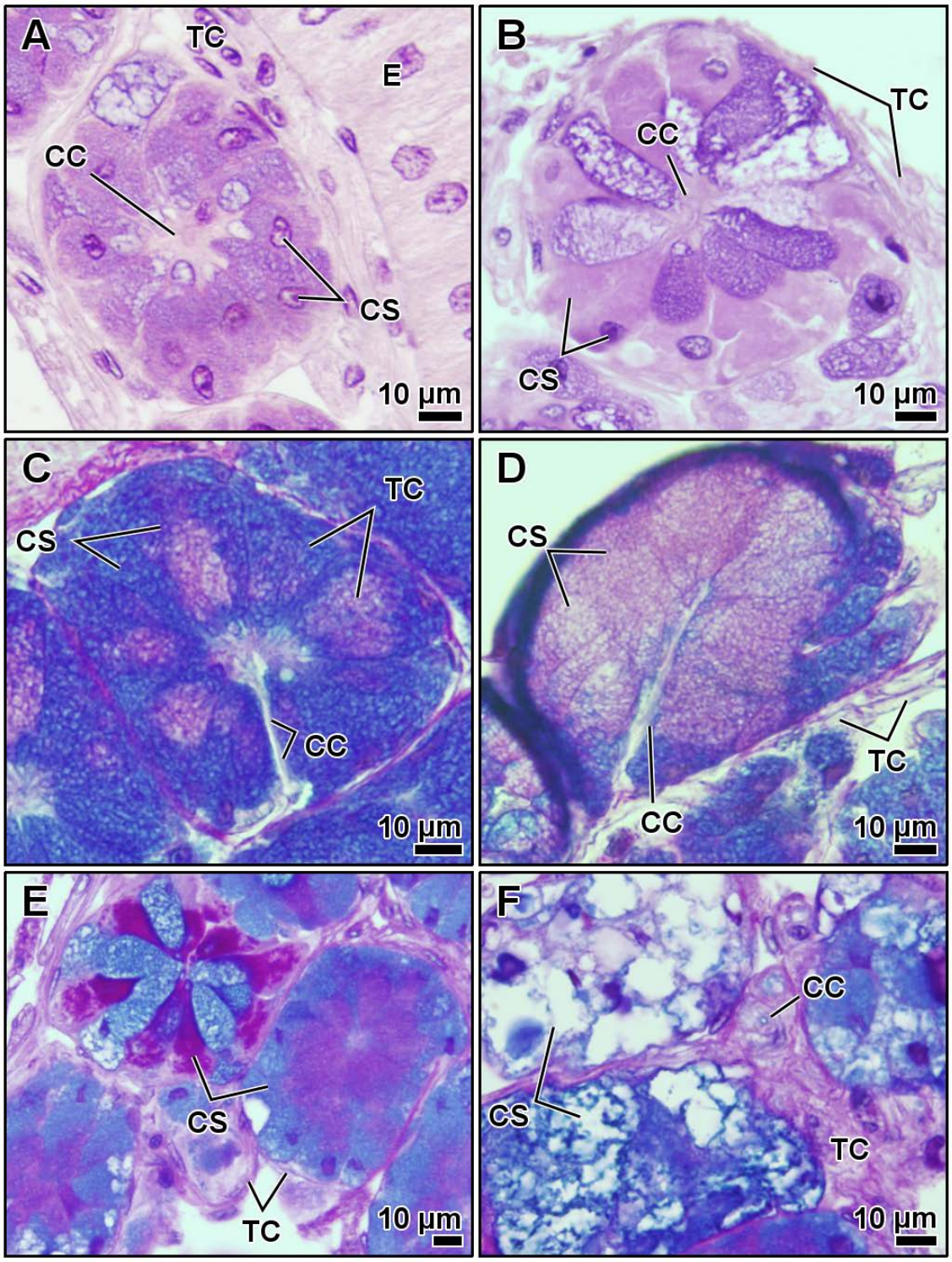

Figura 19.7.2. Detalle de las glándulas de roseta. Tracto digestivo posterior. Nótese las células secretoras en distintos estadios, Hematoxilina-Eosina (A-B). PAS con Azul de Alcián y contraste de Hematoxilina, nótese el canal central y células en distintos estadios (C-E). Células secretoras, posiblemente en el último estadio (F). Abreviaciones: CC, célula del canal ("canal central"); CS, células secretoras; E, epitelio; TC, tejido conectivo.

Las secreciones son recolectadas por un canal central formado por las "células del canal". Coincidiendo con Ikeda et al. (2004), el citoplasma es electrodenso y rico en estructuras filamentosas que constituyen el citoesqueleto, el canal también parece revestido por una cutícula extremadamente delgada (19.7.4F). Estudios previos afirman que dichas estructuras filamentosas están constituidas por microtúbulos con un probable rol de soporte estructural y posiblemente de transporte (Talbot et al., 1991). Doughtie y Rao (1982) también describen "células del canal" con características similares, incluyendo la fina cutícula quitinosa.

El rol de las "glándulas de roseta" ha sido incierto desde su descubrimiento en el siglo XIX. Las diversas propuestas se han basado en su localización y productos de secreción. Dada su asociación a las piezas bucales se ha sugerido un rol como glándulas salivares (Barker y Gibson, 1977; Erri Babu et al., 1979; Hunt et al., 1992; Shyamasundari y Hanumantha Rao, 1977; 1978; Yonge, 1924). Otros autores no están de acuerdo ya que consideran que el estómago y la glándula digestiva son más que suficientes para la función digestiva (Gorvett, 1946; Yonge, 1924; 1932). Sin embargo, puede contra-argumentarse que en otros organismos las glándulas salivares y sistemas digestivos eficientes no son mutuamente excluyentes.

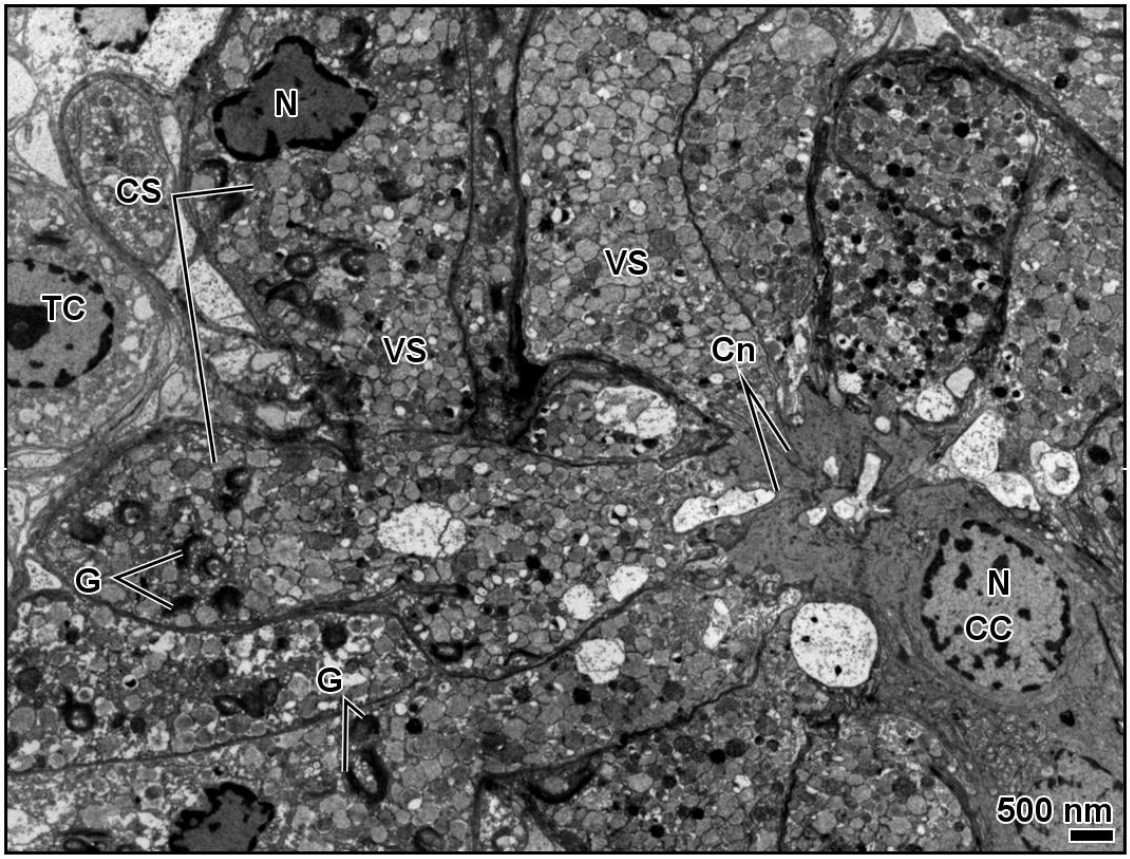

Figura 19.7.3. *M. brachydactyla*. "Glándula de roseta", células secretoras y células del canal central. MET. Abreviaciones: CC, células del canal; Cn, "canalículos"; CS, células secretoras; G, aparatos de Golgi; N, núcleo; TC, tejido conectivo; VS, vesículas de secreción.

Para muchos autores, las "glándulas de roseta" no participan en la digestión, pero son responsables de lubricar las paredes del esófago y unir el material ingerido para evitar su disgregación y facilitar su desplazamiento (Barker y Gibson, 1977; Erri Babu et al., 1979; Felder y Felgenhauer, 1993; Hunt et al., 1992; Jalaja-Kumari et al., 1983; Pugh, 1962; Reddy, 1937; Salindeho y Johnston, 2003; Shyamasundari y Hanumantha Rao, 1977; 1978; Yonge, 1924). Otros autores proponen que tales secreciones mucosas atrapan las partículas de alimento y los microorganismos en animales suspensívoros (McKenzie y Alexander, 1989). Para otros autores, en el tracto digestivo posterior se encargan de ayudar a digerir el alimento (Erri Babu et al., 1979) o bien ayudan al mantenimiento de comunidades mutualistas de microorganismos (Felder y Felgenhauer, 1993).

Dado que las secreciones de estas glándulas se han hallado en el tracto digestivo de animales en condiciones de inanición (Barker y Gibson, 1977), también es posible que su rol sea conservar y mantener en buen estado la cutícula del esófago (Yonge, 1924). En ese sentido, otros autores proponen que las "glándulas de roseta" participan en la secreción de la cutícula, sosteniendo esta hipótesis en la similitud entre algunos componentes de la cutícula y el contenido de los conductos glandulares (Gorvett, 1946; Yonge, 1932) y en cierta correlación entre la actividad glandular y el ciclo de muda (Gorvett, 1946), como las "glándulas de roseta" tipo A de las branquias de *P. pugio*, que son activas durante la pre-muda tardía y muestran máxima actividad poco después de la ecdisis (Doughtie y Rao, 1982). Sin embargo, McKenzie y Alexander (1989) aventuran que algunas "glándulas de roseta" no tendrían este papel, así el ciclo de las glándulas de los paragnatos y maxilípedos no muestra asociación con el ciclo de muda. Las "glándulas de roseta" de los pleópodos se asocian con la adhesión de los huevos a los pleópodos (Aiken y Waddy, 1982; Talbot et al., 1991; Yonge, 1932) y existe correlación entre el máximo nivel de desarrollo glandular y la maduración de los ovarios (Aiken y Waddy, 1982). Por su parte, las "glándulas de roseta" de los pereiópodos de los calianásidos se asocian con el refuerzo de los túneles mediante mucosidades (Dworschak, 1998).

Visto en perspectiva, es posible que el término "glándulas de roseta" abarque varios tipos de glándulas cuya morfología es similar. Por ejemplo, en el isópodo *Armadillidium vulgare* las "glándulas de roseta" de los pereiópodos producen polifenol oxidasa, involucrada en la esclerotización de la cutícula (Stevenson, 1961); mientras que las "glándulas de roseta" de los maxilípedos no secretan esta enzima pero sí mucopolisacáridos (Stevenson y Murphy, 1967), relacionados con la ingesta y lubricación del tracto digestivo. Otra hipótesis a considerar es que ciertas familias de compuestos, como ciertos mucopolisacáridos, podrían tener múltiples roles no excluyentes: atrapar y compactar el alimento, lubricación de los órganos internos, protección de la cutícula y adhesión de las puestas.

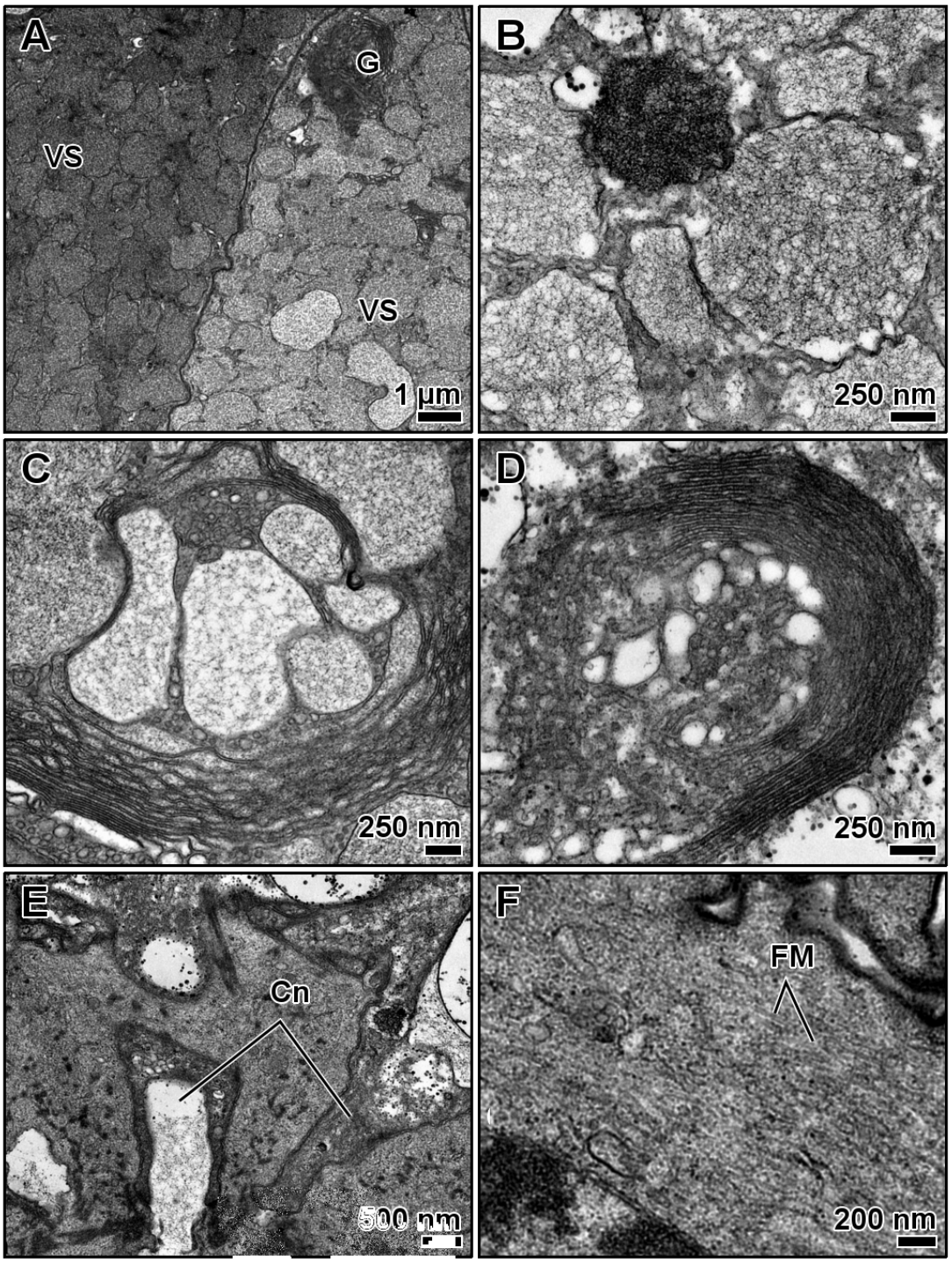

Figura 19.7.4. Detalles de las "glándulas de roseta". MET. Vesículas de secreción (A-B): esófago (A) y tracto digestivo posterior (B). Aparato de Golgi (C-D): esófago (C) y tracto digestivo posterior (D). Tracto digestivo posterior (E-F): detalle de los "canalículos" (conexión entre las células secretoras y las células del canal) (E) y detalle de las estructuras filamentosas de las células del canal (F). Abreviaciones: Cn, "canalículo"; G, aparato de Golgi; VS, vesículas de secreción.

19.8 Células M de la glándula digestiva como posibles células basales.

Las células M ("*midget*", de significado "muy pequeño") son inconfundibles cuando se comparan con otras células epiteliales de la glándula digestiva. Se caracterizan por su pequeño tamaño, se reducen a poco más que un núcleo rodeado de citoplasma, nunca alcanzan el lumen de la glándula digestiva y carecen de microvilli (Fig. 19.8.1B). Por el contrario, el resto de células epiteliales son mucho más altas (células R prismáticas, células F piramidales y células B globulares) y están coronadas por microvilli. A nivel ultra-estructural, en las células M destaca el núcleo central, citoplasma poco electrodenso, reducida densidad de orgánulos, así como la presencia de vesículas esféricas de contenido granular a homogéneo de elevada electro-densidad (Fig. 19.8.2C-D).

El consenso actual adjudica una función principal para cada tipo celular del epitelio de la glándula digestiva (Al-Mohanna y Nott, 1987; 1989; Al-Mohanna et al., 1985b; Gibson y Barker, 1979; Hopkin y Nott, 1979; 1980; Icely y Nott, 1992): las células E realizan procesos de división y diferenciación celular; las células R acumulan reservas de lípidos y glucógeno, así como depósitos minerales (calcio, fósforo y magnesio) y metales (cobre y zinc); mientras que las células F sintetizan activamente enzimas digestivas y se consideran una etapa previa de las células B. Según Hopkin y Nott (1980), las células B acumulan en su vacuola central las enzimas sintetizadas durante su etapa como células F. Al-Mohanna y Nott (1986) postulan que las células B adquieren material mediante pinocitosis y es digerido en las vacuolas.

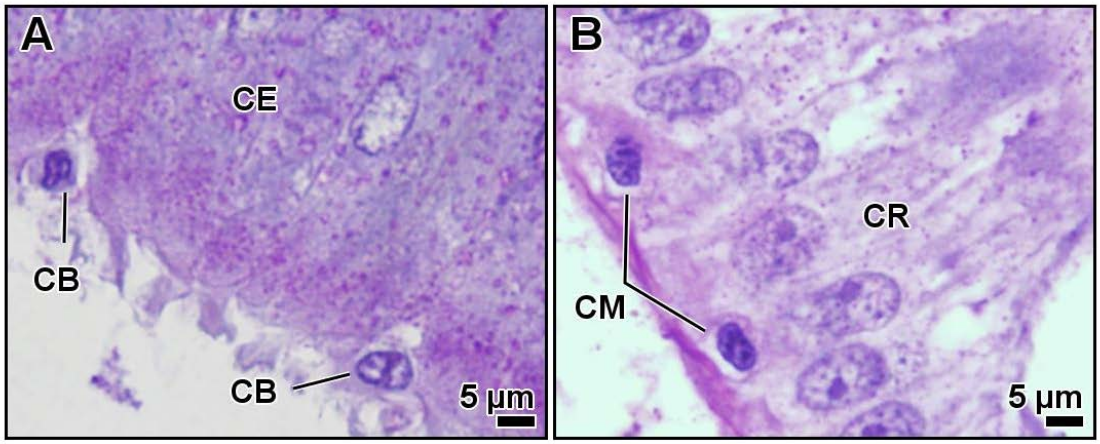

Figura 19.8.1. Adulto. Similitudes entre células basales y células M de la glándula digestiva. PAS con Azul de Alcián y contraste de Hematoxilina. Epitelio del tracto digestivo medio, células basales (A). Epitelio de la glándula digestiva, células M (B). Abreviaciones: CB, células basales; CE, células epiteliales, CM, células M; CR, células R.

Por el contrario, la función de las células M nunca ha sido clara. Entre las diversas hipótesis, se ha propuesto que las células M absorben y almacenan metabolitos y nutrientes, quizás a través de la hemolinfa o de las células epiteliales cercanas (Al-Mohanna y Nott, 1987; Al-Mohanna et al., 1985a; Nunes et al., 2014). Por su parte, Vogt (1994) propuso que las células M podrían ser células endocrinas que regulan la actividad de las células epiteliales adyacentes o de la red muscular subyacente, dada la distribución de estas células y su situación adyacente al sistema de transporte de la hemolinfa.

En la presente memoria, se propone un rol distinto para las células M. Un rasgo común del tracto digestivo medio y de los ciegos asociados es la presencia de células basales: células de reducido tamaño caracterizadas por ser un núcleo rodeado por una delgada capa de citoplasma, no alcanzan el lumen y carecen de microvilli (Fig. 19.8.1A). El citoplasma de las células basales es poco electrodenso, contiene una densidad variable de orgánulos celulares y presenta vesículas esféricas cuyo contenido es de elevada electro-densidad (Fig. 19.8.2A-B). En el epitelio del tracto digestivo medio de otras especies de decápodos se han identificado células similares, como por ejemplo los braquiuros del género *Uca* (Pugh, 1962) y el astacídeo *Procambarus clarkii* (Komuro y Yamamoto, 1968). Mykles (1979) describe células similares en el tracto digestivo medio del braquiuro *Metacarcinus magister* (denominado *Cancer magister*) y de astacídeos del género *Homarus*, pero dichas células son consideradas "hemocitos".

La idea de considerar a las células M como "células basales" no es realmente nueva. Los primeros histólogos que estudiaron la glándula digestiva denominaban con este nombre a las células M. En ese sentido, Reddy (1938) menciona la presencia de "células basales" en el tracto digestivo medio, ciegos asociados y glándula digestiva del braquiuro *Spiralothelphusa hydrodroma* (denominado *Parathelphusa hydrodromus*), como células pequeñas y adyacentes a la lámina basal. Similarmente, Pillai (1960) describe en el carideo *Caridina laevis* la presencia de "células basales" en el tracto digestivo medio y ciegos asociados, y "células de repuesto" en la glándula digestiva. Se puede proponer a las células M como células basales en base a varios argumentos: las células basales son comunes y fáciles en el tracto digestivo medio y en los ciegos asociados, por ello resulta curioso que no "aparezcan" en la descripción de la glándula digestiva (Al-Mohanna y Nott, 1989; Icely y Nott, 1992; Ramadevi et al., 1990; Vogt, 1994), especialmente cuando los órganos digestivos derivados del endodermo embrionario son tan similares entre sí. Esta situación se soluciona si se considera a las células M como basales. Además, las células M tienen muchas similitudes con las células basales de los demás órganos digestivos: tamaño, localización (dispersa pero adyacente a la lámina basal), forma (globular a achatada), organización (núcleo central rodeado de una fina película de citoplasma), así como ultra-estructura (que incluye la presencia de gránulos de elevada electro-densidad).

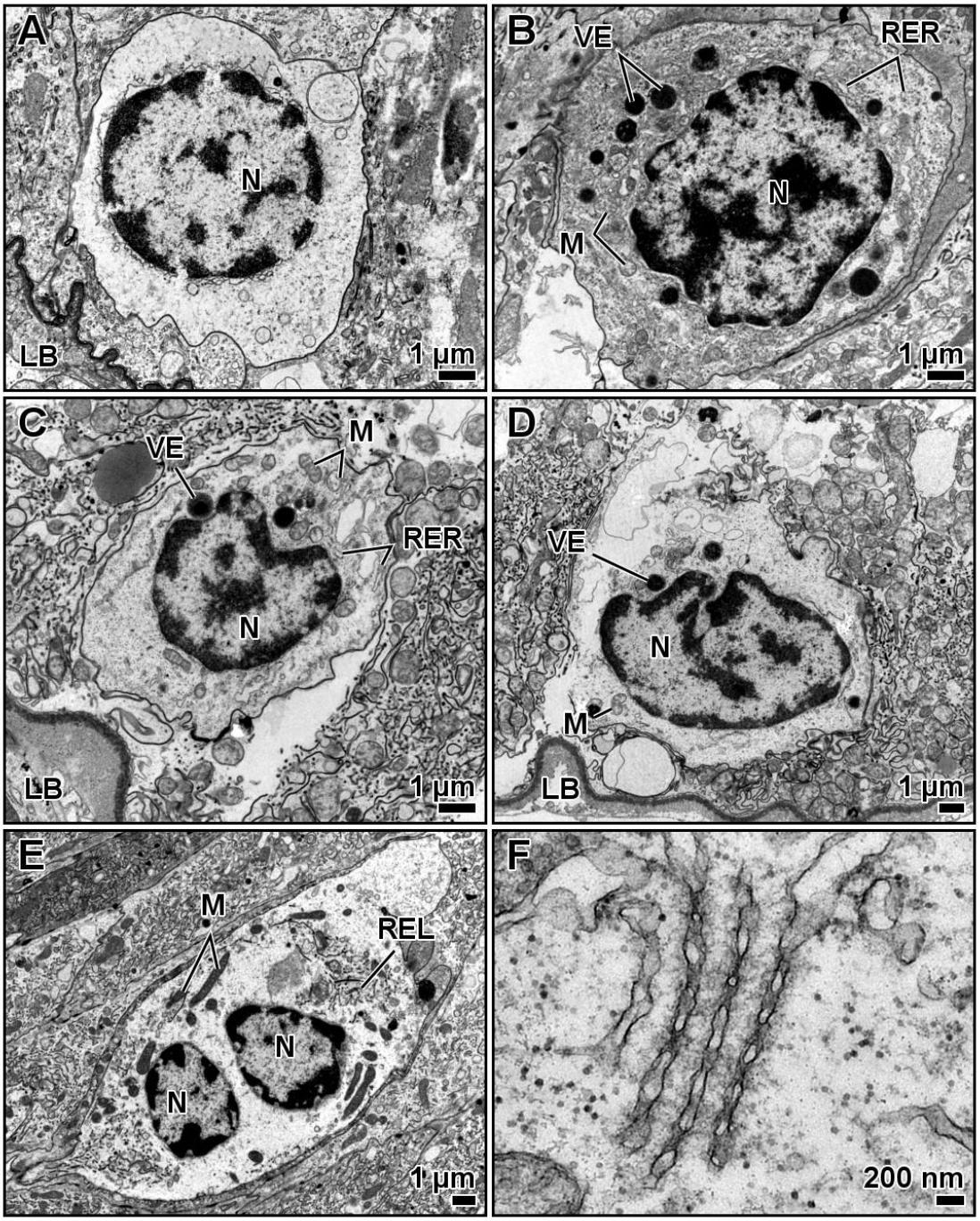

Figura 19.8.2. Similitudes ultra-estructurales entre células basales y células M de la glándula digestiva. MET. Zoea I, tracto digestivo medio, célula basal (A). Adulto, ciego anterior, célula basal (B). Adulto, glándula digestiva, célula M (C-D). Adulto, ciego anterior, células basales en telofase y parcialmente diferenciadas (E). Adulto, glándula digestiva, láminas anilladas localizadas en el citoplasma de una célula M (F). Abreviaciones: LB, lámina basal; N, núcleo; M, mitocondria; RER, retículo endoplasmático rugoso; VE, vesícula electro-densa.

Por todo ello, se propone que las células M de la glándula digestiva son las células basales de dicho órgano. Esta hipótesis también explicaría la "ausencia" de células basales en la glándula digestiva, ya que no estarían ausentes, sino que estas serían las propias células M. Las células basales desempeñan un papel relacionado con los procesos de mitosis, diferenciación y regeneración celular, ya que se encargarían de reemplazar las células epiteliales que han degenerado tras su periodo de actividad, así como a las células B tras la extrusión de su gran vesícula (Hu y Leung, 2007; Pillai, 1960; Pugh, 1962; Reddy, 1938). Otros autores han reportado células basales en distintos estadios de mitosis (Pugh, 1962) y su aumento numérico tras la extrusión de las células B (Pillai, 1960). En el presente trabajo se ha aportado la presencia de una célula basal en telofase avanzada con rasgos de células epiteliales (Fig. 19.8.2E). Otra observación interesante es la presencia de láminas anilladas en el citoplasma de las células M (Fig. 19.8.2F), las cuales se asocian a procesos de división celular (Cordes et al., 1996; Hampoelz et al., 2016).

19.9 Actividad secretora en el sistema digestivo.

Los órganos digestivos derivados del endodermo embrionario (tracto digestivo medio, ciegos asociados y glándula digestiva) realizan una notable actividad secretora desde el primer estadio larvario hasta la edad adulta. Los procesos de secreción observados incluyen: merocrina, donde la membrana de las vesículas de secreción se fusiona con la membrana apical de las células epiteliales; apocrina, donde las vesículas se forman desde el ápice celular o los microvilli; holocrina, donde la gran mayoría del volumen celular está ocupado por una única y gran vacuola que es liberada enteramente al lumen del órgano.

La secreción merocrina parece relacionarse con la producción de membrana peritrófica. Esta se observa desde el tracto digestivo medio hasta el ano y es excretada como componente de las heces. Es una lámina translúcida que envuelve la materia fecal separándola de los microvilli del tracto digestivo medio y de la cutícula del tracto digestivo posterior (Fig. 19.9.2). Diversos datos señalan a las células epiteliales del tracto digestivo como las probables productoras de la membrana peritrófica: la secreción merocrina solo ha sido observada en las células epiteliales del tracto digestivo medio, el mismo órgano a partir del cual empieza a observarse la membrana peritrófica (Fig. 19.9.2B-C); el ápice de las células epiteliales muestra una banda cuya afinidad de tinción es similar a la de la membrana peritrófica (Fig. 19.9.2A, C); la localización de dicha banda coincide con la localización de las vesículas de secreción (Fig. 19.9.1A); por lo que podría existir correspondencia entre el contenido de las vesículas de secreción y la composición de la membrana peritrófica en formación (Fig. 19.9.1C-D).

La membrana peritrófica es una estructura típica de artrópodos, habiéndose identificado en pancrustáceos, miriápodos y xifosuros, así en grupos emparentados como los onicóforos (Lehane, 1997; Mets, 1962). Entre los grupos de malacostráceos de mayor importancia, la membrana peritrófica ha sido observada en Achelata (Irvin y Tabrett, 2005; Kamio et al., 2016), Amphipoda (Davolos et al., 2010; Lautenschlager et al., 1978), Anomura (Greenaway y Morris, 1989; Wilde et al., 2004), Astacidea (Chisaka et al., 1999; Factor, 1981), Brachyura (Heeren y Mitchell, 1997; Hopkin y Nott, 1980; McGaw y Reiber, 2000), Caridea (Forster, 1953; Pillai, 1960), Dendrobranchiata (Dall, 1967; Martin y Chiu, 2003; Martin et al., 2006; Wang et al., 2012) e Isopoda (Holdich y Ratcliffe, 1970). En *M. brachydactyla*la membrana peritrófica está presente durante toda la vida del animal desde al menos 15 horas tras la eclosión (Fig, 19.9.2C). También es descrita en el primer estadio de zoea del género *Homarus* (Factor, 1981) y en los primeros estadios de filosoma del escilárido *Ibacus novemdentatus* (Kamio et al., 2016).

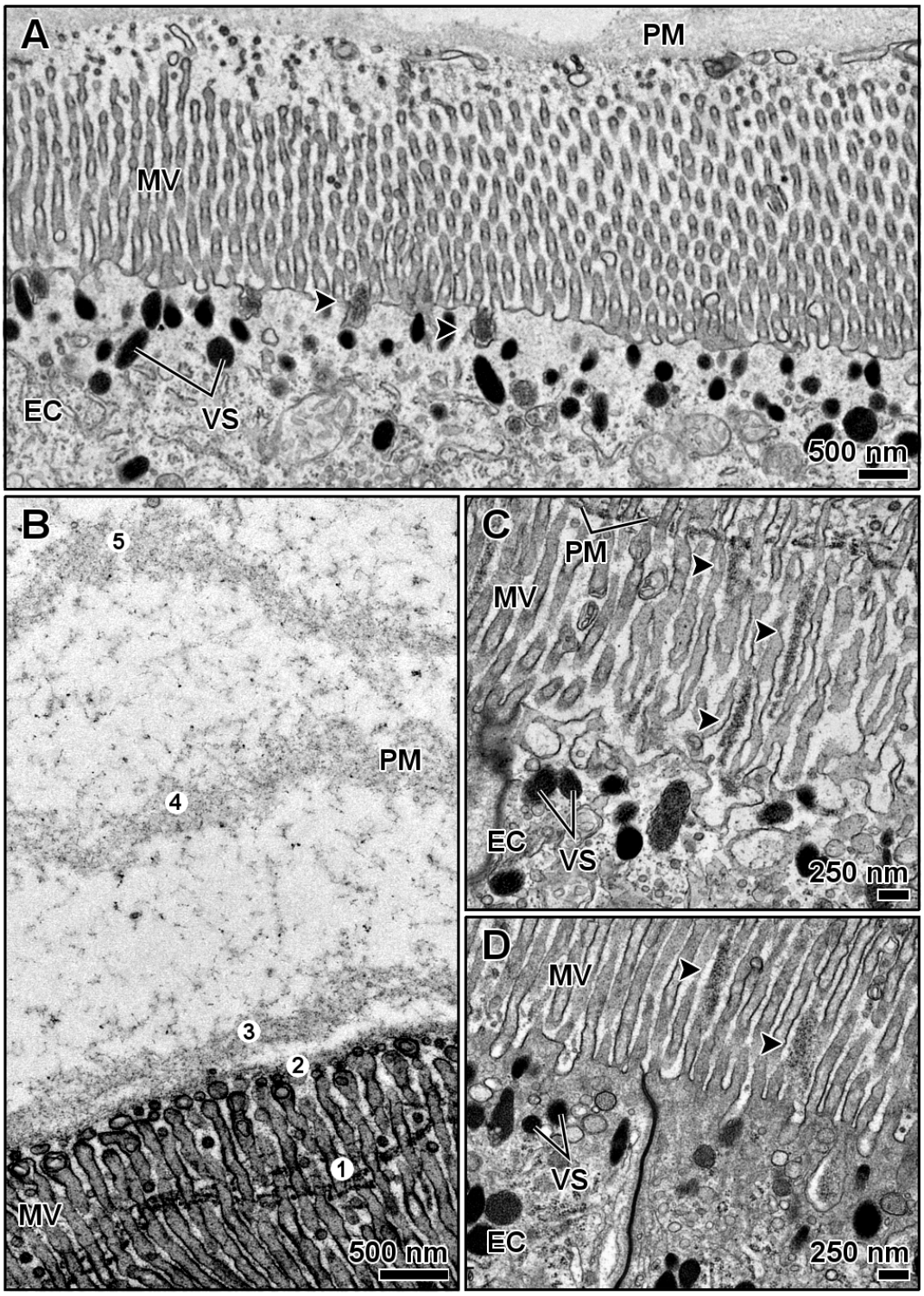

Figura 19.9.1. Actividad secretora merocrina de las células epiteliales del tracto digestivo medio. MET. Megalopa, zona apical de las células epiteliales y vesículas de secreción (A). Zoea I (B-D). Oleadas de producción (o secreción) de la membrana peritrófica (cada oleada ha recibido un número) (B). Detalle de la liberación del contenido de las vesículas de secreción entre los microvilli (puntas de flecha) (C-D). Abreviaciones: EC, células epiteliales; MV, microvilli; PM, membrana peritrófica; VS, vesículas de secreción.

La membrana peritrófica tiene afinidad por las tinciones de Hematoxilina y Azul de Anilina (Fig. 19.9.2), posiblemente debido a la presencia de sustancias de tipo peptídico. También es teñida por la tinción de PAS (Fig. 19.9.2A) desvelando la presencia de aldehídos. Esto concuerda con los estudios enfocados en la composición de la membrana peritrófica. En insectos esta incluye entre un 3 y un 13 % de quitina, un polímero formado por monómeros de N-acetil-glucosamina unidos por enlaces β-D 1-4; mientras que la porción restante es una combinación de varios tipos de proteínas, glicoproteínas y proteoglicanos (Lehane, 1997). La membrana peritrófica de los malacostráceos es similar: fibras de quitina (Forster, 1953; Georgi, 1969) rodeadas de una matriz de proteínas y mucopolisacáridos (Georgi, 1969). Sin embargo, en estos la quitina es el componente mayoritario (Martin et al., 2006; Wang et al., 2012) y el contenido proteico solo representa alrededor del 3,5 % del peso seco (Martin et al., 2006). Este contenido proteico incluye enzimas digestivas (carboxipeptidasa, tripsina y peptidasa) y proteínas relacionadas con el sistema inmune y proteínas antioxidantes, pero no proteínas estructurales (Wang et al., 2012).

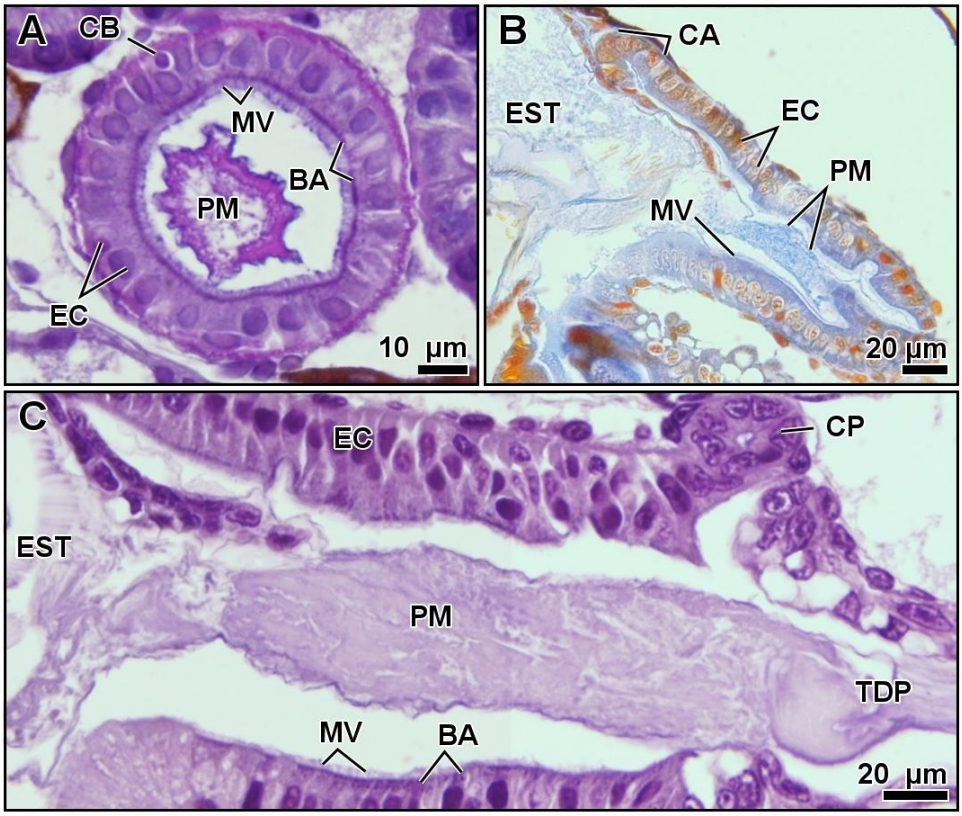

Figura 19.9.2. Membrana peritrófica. Zoea II (A-B). Sección transversal tracto digestivo medio, PAS con contraste de Hematoxilina (A). Sección longitudinal del tracto digestivo medio, tricrómico de Mallory (B). Zoea I, sección longitudinal del tracto digestivo medio, Hematoxilina-Eosina (C). Abreviaciones: BA, banda apical; CA, ciego anterior; CB, célula basal; CP, ciego posterior; EC, células epiteliales; EST, estómago; MV, microvilli; PM, membrana peritrófica; TDP, tracto digestivo posterior.

Las proteínas y la quitina que componen la membrana peritrófica están organizadas en fibras formando capas laminares (Wang et al., 2012). En *M. brachydactyla* la superficie de la membrana peritrófica puede presentar un aspecto no fibrilar y carente de relieves (Fig. 19.9.3B) o bien el de una maraña de fibras sin patrón determinado (Fig. 19.9.3C). Adang y Spence (1981) también describen dos morfologías de membrana peritrófica en las larvas del lepidóptero *Trichoplusia ni*: 1) no fibrilar y considerada inmadura y 2) fibrilar y considerada madura. Por tanto, es posible que las variaciones observadas en la membrana peritrófica de *M. brachydactyla* puedan corresponderse con distintos estadios de maduración de la misma. En *M. brachydactyla* también se ha observado una membrana peritrófica no fibrilar con un relieve de fibras de aspecto poligonal (Fig. 19.9.3D). Una membrana peritrófica con aspecto similar ha sido descrita en el braquiuro *Eriocherir sinensis* (Mets, 1962). En otros artrópodos este patrón varía: romboidal en el astácido *Homarus gammarus* (Georgi, 1969), poligonal en el dendrobranquiado *Sicyonia ingentis* (Martin et al., 2006), hexagonal en el xifosuro *Limulus polyphemus* (Mets, 1962), poligonal a romboidal en las larvas del insecto *Tipula* sp. (Lehane, 1997) y con forma de malla provista de ángulos rectos en los diplópodos *Glomeris marginata* (Martin y Kirkham, 1989) y *Tachypodoiulus niger* (como *Iulus albipes*) (Mets, 1962). Se ha sugerido que dichos patrones son moldeados por los microvilli durante la formación de la membrana peritrófica (Harper y Hopkins, 1997; Kawakita et al., 2016; Lehane, 1997).

La membrana peritrófica es producida en oleadas (Fig. 19.9.1B) e independientemente del régimen alimentario, ya que es producida tanto por animales con régimen continuo de alimentación como de inanición (Forster, 1953; Martin et al., 2006). Su producción continua desde edades tempranas, indican que es un elemento importante del proceso digestivo, pero su rol no ha podido ser determinado. En insectos se considera una barrera de protección del epitelio digestivo frente microorganismos y virus patógenos (Brandt et al., 1978; Hegedus et al., 2009; Lehane, 1997; Terra, 2001; Wang y Granados, 1998), así como frente compuestos nocivos (Barbehenn y Martin, 1992; Hegedus et al., 2009; Lehane, 1997; Terra, 2001). En contraste, se ha observado que la eliminación de la membrana peritrófica no aumenta la tasa de infección por ingesta del virus del síndrome la mancha blanca en el langostino *Penaeus vannamei* (Van Thuong et al., 2016). También se ha propuesto que podría aumentar la eficiencia de la digestión al retener material y ser capaz de movilizar enzimas (Hegedus et al., 2009; Lehane, 1997; Terra, 2001). La membrana peritrófica también facilitaría la expulsión de los desechos al embutirlos en una única estructura fácil de eliminar (Dall, 1967; Sousa y Petriella, 2006).

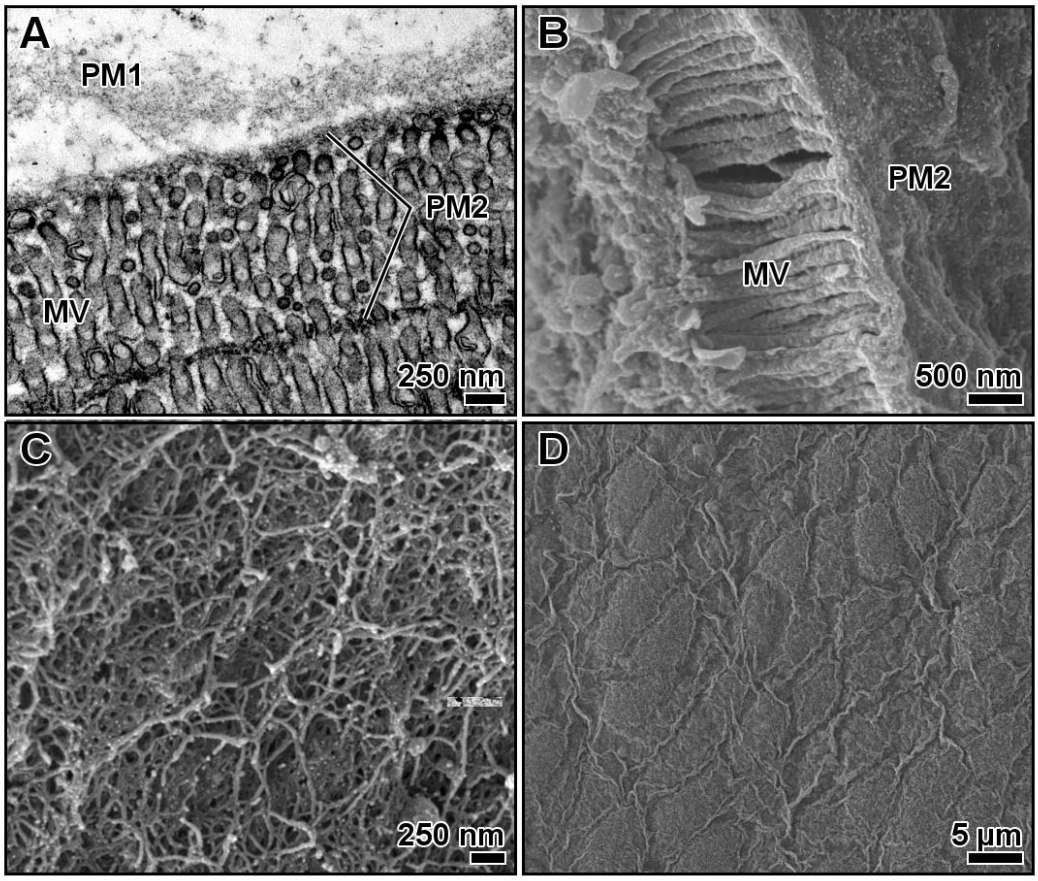

Figura 19.9.3. Membrana peritrófica. Variación en la membrana peritrófica, MET (A). Membrana peritrófica no fibrilar, MEB (B). Membrana peritrófica fibrilar, MEB (C). Membrana peritrófica mixta, MEB (D). Abreviaciones: MV, microvilli; PM1, membrana peritrófica "libre"; PM2, membrana peritrófica adherida/adyacente a los microvilli.

La secreción apocrina se define como aquella que libera los productos se secreción junto con parte del citoplasma (Farkań, 2015; Gesase y Satoh, 2003). Farkań (2015) menciona que en las glándulas salivares de *Drosophila* este tipo de secreción libera grandes fragmentos celulares delimitados por una membrana, cuyo contenido incluye citoesqueleto, ribosomas, mitocondrias y proteínas nucleares (Gesase y Satoh, 2003). En *M. brachydactyla* se han observado dos tipos de secreción apocrina: producción de vesículas de gran tamaño desde el ápice celular y producción de vesículas de pequeño tamaño desde los microvilli (Fig. 19.9.4-5). La producción de vesículas de gran tamaño desde el ápice celular ha sido observada en las células R de la glándula digestiva y en el epitelio de los ciegos del tracto digestivo medio. En sus primeras etapas se forma una protrusión más o menos globular de la membrana apical, que al aumentar de tamaño desplaza a los microvilli que la rodean (Fig. 19.9.4A).

Coincidiendo con nuestras observaciones, esta secreción se ha observado en la glándula digestiva del astácido *Orconectes virilis* (Loizzi, 1966) y del braquiuro *Ocypode platytarsis* (Ramadevi et al., 1990), en las células R del camarón *Penaeus vannamei* (Caceci et al., 1988) y en las células B del braquiuro *Menippe rumphii* (Erri Babu et al., 1982), del palinúrido *Panulirus argus* (Travis, 1955) y del misidáceo *Mysis stenolepis* (Friesen et al., 1986), así como en los conductos de la glándula digestiva de los anomuros *Pagurus bernhardus* y *Clibanarius longitarsus* (Erri Babu y Manjulatha, 1995) y las células epiteliales del tracto digestivo medio del carideo *Neocaridina laevis* (Sonakowska et al., 2015).

En el caso de los ciegos del tracto digestivo medio, la bibliografía es escasa y no se han reportado ejemplos explícitos de secreción apocrina que puedan considerarse equivalentes a los observados en *M. brachydactyla*. Pugh (1962) observó en los braquiuros del género *Uca* secreción merocrina pero no apocrina. Dall (1967) describe en los ciegos del dendrobranquiado *Metapenaeus bennettae* gran abundancia de vesículas en el lumen pero no las asocia a ningún tipo de secreción. Finalmente, Pinn et al. (1999) publica ilustraciones de microscopía electrónica de barrido del epitelio de los ciegos de Axiidea y Gebiidea, observándose "coccoid bodies" similares a las protrusiones observadas en *M. brachydactyla* y "poros" similares a los "huecos" dejados por estas, pero tampoco hace referencia a ningún tipo de secreción.

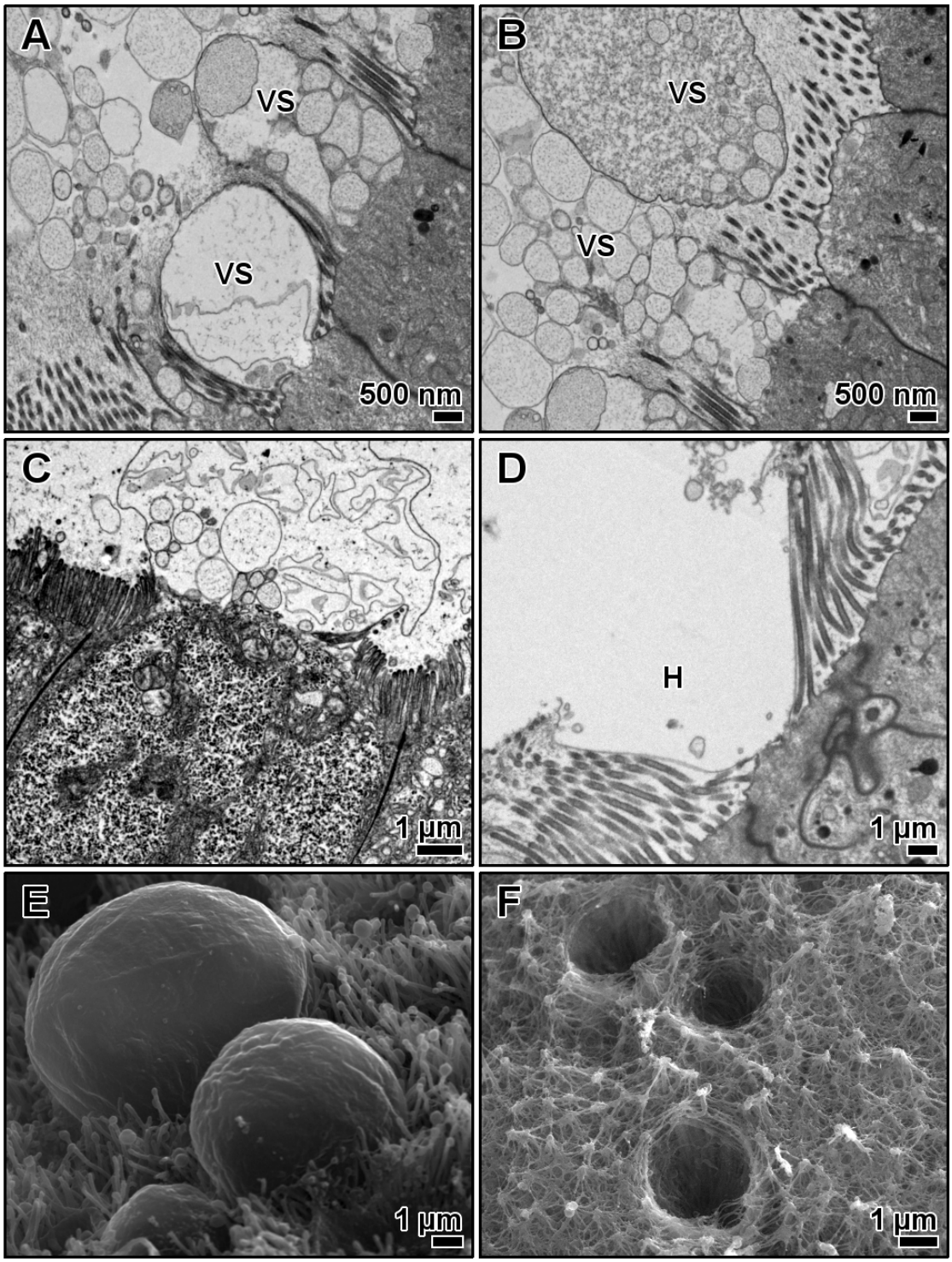

Figura 19.9.4. *M. brachydactyla*. Adulto. Actividad secretora apocrina. Células epiteliales de los ciegos anteriores, MET (A-B). Células R de la glándula digestiva, MET (C). Células epiteliales del ciego posterior, "hueco" (H) dejado tras la liberación de la protrusión apical, MET (D). Secreción apocrina en el ciego posterior, MEB (E-F): protrusiones de las células epiteliales del ciego posterior (E) y "huecos" dejados tras la liberación de la protrusión apical (F). Abreviaciones: H, "hueco" dejado tras la secreción; VS, vesícula de secreción.

El otro tipo de secreción apocrina es denominada micro-apocrina ("*microapocrine*") por varios autores (Cristofoletti et al., 2001; Ferreira et al., 1990; Monteiro et al., 2014; Silva et al., 2013; Sonakowska et al., 2015). En *M. brachydactyla* se ha observado en las células R y B de la glándula digestiva y en las células epiteliales de los ciegos. Este tipo de secreción comienza como una protrusión luciente en la membrana de los microvilli, la cual se expande hasta formar una formación globular, que se separará de los microvilli como una vesícula esférica y libre de muy pequeño tamaño. La secreción micro-apocrina tradicionalmente ha sido descrita en el tracto digestivo de los insectos y definida como la liberación de pequeñas vesículas (con única o doble membrana) desde los microvilli (Cristofoletti et al., 2001).

Entre las especies en cuyo tracto digestivo esta secreción ha sido descrita se incluyen el fásmido *Cladomorphus phyllinus* (Monteiro et al., 2014), los himenópteros *Spodoptera frugiperda* (Bolognesi et al., 2001; Silva et al., 2013) y *Apis melifera* (Jimenez y Gilliam, 1990) y el lepidóptero *Anticarsia gemmatalis* (Gomes et al., 2013). En el isóptero *Cubitermes severus* se han observado protrusiones en los microvilli que se han relacionado con este tipo de secreción (Bignell et al., 1982). En el caso de los decápodos se menciona por primera vez en una publicación dedicada al tracto digestivo del carideo *Neocaridina laevis*, pero dicha identificación parece corresponderse con un error de interpretación de la morfología de los microvilli (Sonakowska et al., 2015). Por lo tanto, en la presente memoria se describe por primera vez este tipo de secreción en los decápodos.

La secreción "micro-apocrina" también ha sido descrita recientemente en vertebrados. McConnell et al. (2009) y Shifrin Jr et al. (2012) describen la producción de vesículas desde los microvilli de los enterocitos del intestino de ratón, identificándose en dichas vesículas enzimas catalíticas que parecen ser responsables de proteger la mucosa intestinal. Estudios realizados posteriormente han identificado diversas proteínas (incluyendo enzimas digestivas) y ácidos nucleicos asociados con procesos de transporte, comunicación celular y procesos metabólicos e inmunológicos (Maas et al., 2016; Tricarico et al., 2016).

En los insectos el rol de las vesículas producidas mediante secreción micro-apocrina parece directamente relacionado con los procesos digestivos. En las larvas del coleóptero *Tenebrio molitor* se han asociado con la movilización de amilasa (Cristofoletti et al., 2001) y en las larvas del lepidóptero *S. frugiperda* se ha reportada tripsina y amilasa (Bolognesi et al., 2001). Estudios más extensos han detectado la presencia de diversas enzimas digestivas (incluyendo amilasa, lipasas, peptidasas y proteasas, entre otras), así como proteínas de función protectora o formadora de la membrana peritrófica (Silva et al., 2013). En relación a *M. brachydactyla*, es posible que el contenido de las vesículas sea similar al de insectos, pero se requieren nuevos estudios para demostrarlo.

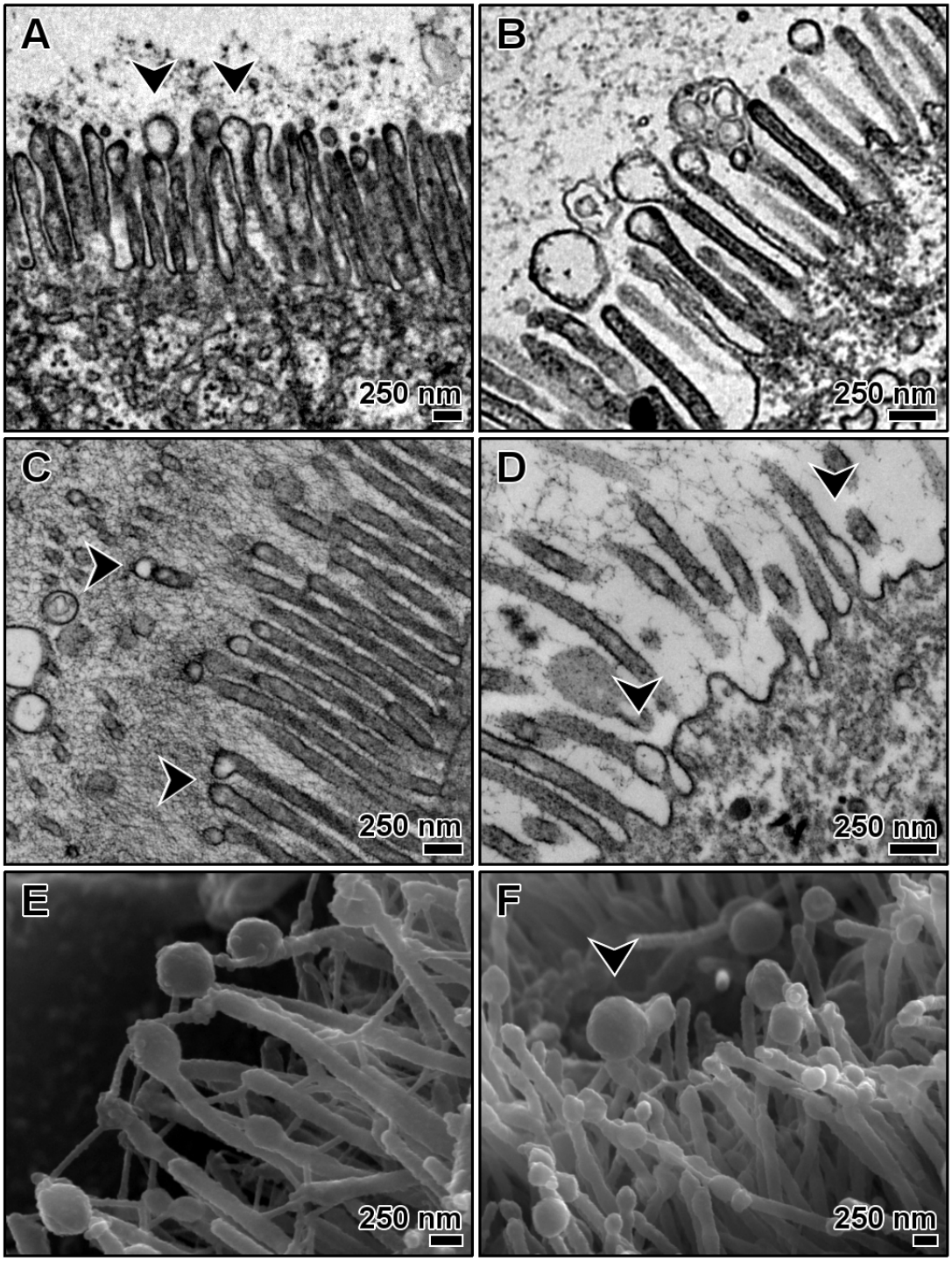

Figura 19.9.5. *M. brachydactyla*. Adulto. Actividad secretora micro-apocrina. Célula R de la glándula digestiva, MET (A). Célula B de la glándula digestiva, MET (B). Células epiteliales del tracto digestivo anterior, MET (C-D). Células epiteliales del tracto digestivo posterior, MEB (E-F). Las puntas de flecha indican microvilli donde están ocurriendo protrusiones que originarán las micro-vesículas.

La secreción holocrina consiste en la liberación o secreción de todo el contenido citoplasmático de la célula secretora en el lumen del órgano (Gesase y Satoh, 2003). En el presente estudio la secreción holocrina solo se habría identificado en las células B de la glándula digestiva (Fig. 19.9.6). Este tipo celular se caracteriza por la presencia de una gran vacuola que ocupa una importante proporción del volumen citoplasmático, exceptuando la zona apical y basal. El contenido vacuolar es heterogéneo: formaciones de tipo filamentoso y particulado, vesículas de tamaño variable y agregaciones de membranas. El contenido vacuolar de las células B es liberado al citoplasma, pero no ha sido posible determinar si dicha secreción es de tipo apocrino u holocrino: en ocasiones la vacuola ha sido hallada en el lumen de la glándula digestiva conservando el núcleo celular (Fig. 19.9.6B) y ninguna estructura celular es hallada en el espacio en el que debía de encontrarse originalmente la célula B (Fig. 19.9.6C), por lo que podría considerarse secreción holocrina; pero en otras ocasiones la vacuola de la célula B aparece en el lumen del órgano sin estar asociada a ninguna estructura celular reconocible (Fig. 19.9.6A) o bien aparecen estructuras celulares en el espacio previamente ocupado por la célula B (Fig. 19.9.6D), por lo que podría ser secreción de tipo apocrino.

No solo en el presente estudio se plantean dudas acerca del tipo de secreción realizado por las células B, ya que se describen distintos tipos de secreción según el estudio realizado. La secreción holocrina ha sido citada en el braquiuro *Ocypode platytarsis* dado que sus células B aparecen en el lumen conservando el núcleo (Ramadevi et al., 1990), en el astácido *Homarus gammarus* donde no existe evidencia de que este tipo celular realice otro tipo de secreción (Barker y Gibson, 1977) y en diversas especies de anfípodos ya que las células B conservan el núcleo en el lumen (Shyamasundari y Varghese, 1973). La secreción holocrina también ha sido descrita en el epitelio del tracto digestivo medio del carideo *Caridina laevis* (Pillai, 1960).

Por otro lado, en otros taxa el contenido vacular de las células B es liberado mediante secreción apocrina. Erri Babu et al. (1982) describe esta secreción en el braquiuro *Menippe rumphii*, donde el contenido de las células B es vertido mediante la ruptura de la región apical. Travis (1955) en el palinúrido *Panulirus argus*observa que el contenido vacuolar es secretado de forma apocrina ya que la zona basal de las células B es conservada. En las células B del carideo *Macrobrachium amazonicum* también se ha descrito que el contenido vacuolar es liberado de este modo (Franceschini-Vicentini et al., 2009). Según otros autores, la actividad secretora de las células B puede ser tanto apocrina como holocrina, siendo las células B una fuente adicional de liberación de enzimas digestivas (Caceci et al., 1988), dicha secreción ocurre en la fase terminal del proceso de digestión y asimilación intracelular (Al-Mohanna y Nott, 1986; 1987). En el caso de *M. brachydactyla* se requerieren observaciones adicionales para concretar si el contenido de las células B es liberado de forma apocrina, holocrina o ambas.

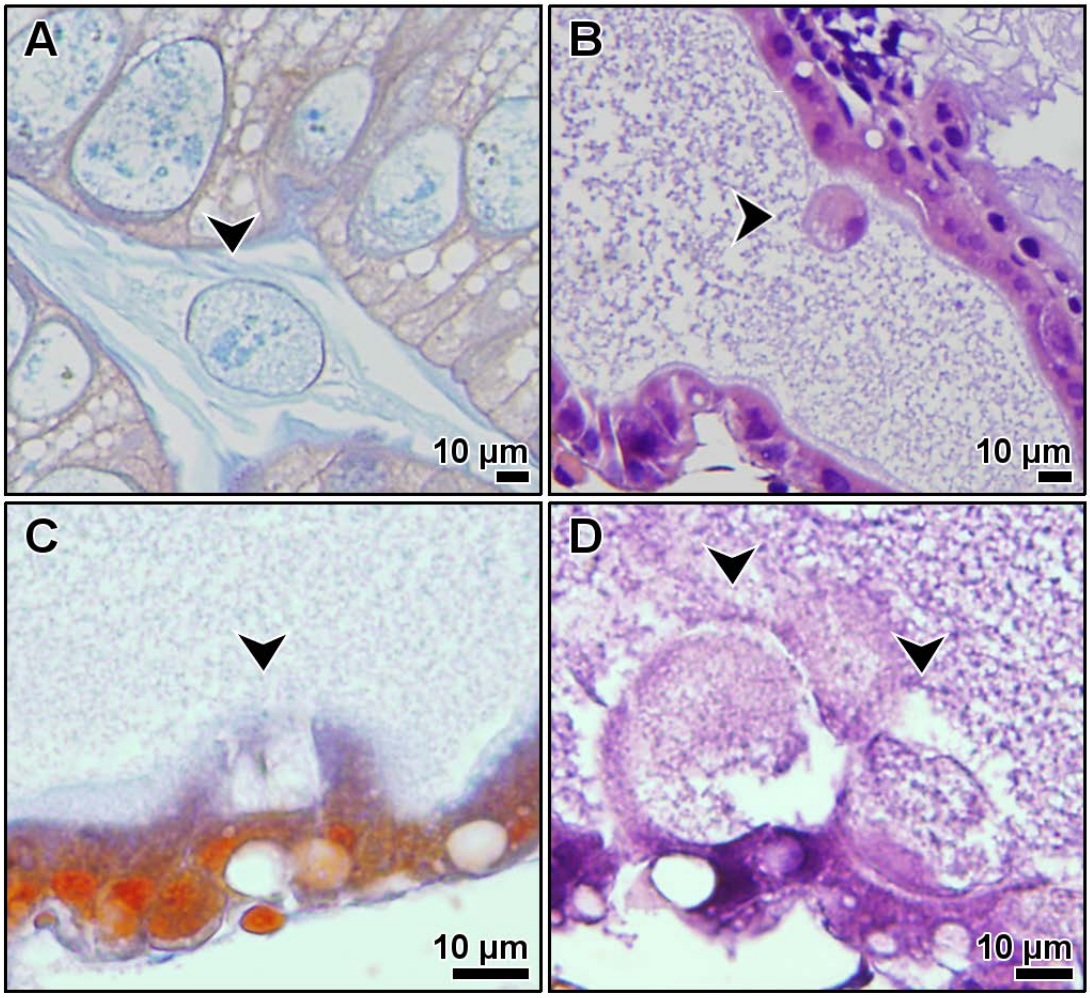

Figura 19.9.6. Actividad secretora holocrina. Adulto, vacuola de célula B en el lumen de la glándula digestiva, tricrómico de Mallory (A). Megalopa (B-D): célula B en el lumen de la glándula digestiva, Hematoxilina - Eosina (B), hipotético "hueco" dejado por una célula B tras su secreción, tricrómico de Mallory (C) y células B parcialmente secretadas (D). Las puntas de flecha indican los huecos dejados por las células B.

19.10 Conclusiones y nuevas preguntas.

Después de todo lo observado, se puede afirmar que el esquema básico del proceso digestivo es similar entre las distintas fases vitales (zoea, megalopa, juvenil y adulto):

El alimento es manipulado por las piezas bucales e introducido en la cavidad oral. La acción muscular del esófago desplazará el alimento hasta el estómago, durante este proceso el epitelio del esófago es protegido de la acción abrasiva de ciertos materiales por la cutícula que lo recubre, mientras que las micro-espinas podrían ayudar a la ingesta. Las glándulas de roseta del esófago secretan productos que podrían ser análogos a la saliva, lubricantes o protectores del esófago. Las mandíbulas de las zoeas cuentan con un proceso molar que realiza la función masticadora, pero tras la muda a megalopa la mandíbula de las zoeas se simplifica ya que el proceso molar desaparece y la función masticadora es realizada por el molino gástrico.

El alimento triturado pasa una serie de filtros consistentes en pantallas de setas hasta alcanzar el estómago pilórico. Una vez en el estómago pilórico, el material ingerido llega a los filtros pilóricos, los cuales solo son atravesados por las partículas más finas y los fluidos que serán transportados a la glándula digestiva. Por otro lado, el material ingerido que no puede atravesar los filtros pilóricos es reconducido hacia el tracto digestivo medio. Para llevar a cabo estas acciones el estómago dispone de una cutícula regionalmente especializada.

En la glándula digestiva el material que ha atravesado los filtros pilóricos es bombeado hacia los túbulos ciegos mediante la acción coordinada de los anillos de musculatura circular y de las tiras de musculatura longitudinal. En este órgano el material es procesado y digerido extra- e intracelularmente mediante acción enzimática, seguramente llevada a cabo por las células F y B, asimismo diversos nutrientes tanto orgánicos como inorgánicos son asimilados y almacenados por las células R. Finalizada la acción de la glándula digestiva, la acción de los mismos músculos bombea el contenido del lumen desde los túbulos ciegos hasta el tracto digestivo medio. En el tracto digestivo medio el material procesado por la glándula digestiva y el material que no ha podido atravesar los filtros pilóricos es rodeado por una estructura laminar denominada membrana peritrófica, sintetizada por el epitelio de este órgano. Es posible que en el tracto digestivo medio sigan teniendo lugar procesos de acción digestiva, así también de asimilación de nutrientes, dada la presencia de inclusiones lipídicas en el epitelio. Los tres ciegos asociados al tracto digestivo medio (un par de ciegos anteriores y un único ciego posterior) están muy desarrollados y poseen una gran actividad secretora, sin embargo ni la naturaleza ni el destino de dichas secretoras es conocido, si bien parece probable que estas sean vertidas en el tracto digestivo medio.

El material rodeado de membrana peritrófica es conducido al tracto digestivo posterior. Este es un largo tubo que ha sido asociado un rol de formación y compactación de las heces, incluyendo la absorción de agua e iones, si bien no ha sido posible determinar estas actividades en el presente estudio. El tracto digestivo posterior está cubierto por una cutícula provista de micro-espinas que podrían ayudar al desplazamiento de la materia fecal mediante el agarre de la membrana peritrófica, evitando su movimiento en sentido posterior. El tracto digestivo posterior presenta abundantes glándulas de rol desconocido.

En el presente estudio ha sido posible determinar la morfología, estructura histológica y ultra-estructura de los distintos órganos del sistema digestivo. Esto nos ha permitido indagar en las capacidades digestivas de cada etapa larvaria y compararla con la adulta, así como pronosticar el posible rol de cada uno de dichos órganos en relación a los conocimientos adquiridos en otras especies. Sin embargo, todo el trabajo desarrollado a lo largo de esta Tesis es solo un preámbulo, o mejor dicho, un requisito inicial para entender el proceso digestivo de los braquiuros desde sus etapas larvarias. Por ello no es casualidad que este estudio haya terminado generando más preguntas que respuestas, las cuales deben de ser exploradas mediante otras vías de investigación. Entre ellas se resumen las siguientes:

1. Los principales cambios del sistema digestivo ocurren durante el desarrollo de los juveniles. En ese sentido, sería interesante indagar en la estructura del sistema digestivo durante el desarrollo de los juveniles, durante los cuales el sistema digestivo se transforma desde la morfología larvaria a la adulta.

2. El esófago larvario cuenta con vesículas en las células epiteliales que dan forma a los pliegues del mismo. ¿Qué contenido poseen dichas vesículas? ¿Cómo se forman y cuál es su rol? El conocimiento de su composición podría ayudar a descubrir su origen y función. Sería interesante relacionarlas con el ciclo de muda y/o el ciclo de digestión.

3. El esófago y el tracto digestivo posterior presentan micro-espinas orientadas en sentido posterior, estas se hallan presentes desde el momento de la eclosión hasta la edad adulta. La abundancia y distribución de dichas micro-espinas, tanto en estos órganos como entre distintos taxa, implican que deben de realizar un rol importante en estos animales. Para ello sería interesante estudiar dichos órganos en el momento en el que el alimento, procesado o no, esté atravesando el lumen.

4. Las glándulas de roseta son estructuras presentes en el tejido conectivo del esófago y extremadamente abundantes en el tracto digestivo posterior. Es probable que la composición de las secreciones consista principalmente en mucopolisacáridos. Sin embargo, la composición de dichas secreciones resulta desconocida. La identificación del contenido podría realizarse en base a la disección de las glándulas y el aislamiento y purificación de sus distintas fracciones. El uso de técnicas de transcriptómica podría resolver qué genes están actuando en un momento dado, lo que podría dar idea de los productos que están siendo sintetizados. Una vez identificados los productos de secreción, el empleo de técnicas inmunohistoquímicas será fundamental para determinar su localización *in situ*, no solo en las mismas glándulas, sino también en el destino de dichas secreciones en el tracto digestivo.

5. El estómago cuenta con una gran diversidad de tipos de cutícula cuya especialización parece ser congruente con la función de la región del estómago en la que se encuentran. Si bien, los datos obtenidos son muy preliminares y es preciso profundizar en este apartado. En este caso, el objetivo sería realizar un estudio más metódico de la cutícula estomacal, la cual debería ser estudiada a nivel de cada tipo de estructura (sacos cardiacos, osículos diversos, válvula cardio-pilórica, filtros pilóricos, etc) en varias orientaciones (longitudinal, transversal, dorso-ventral...), empleando técnicas para determinar su composición (minerales, quitina, proteínas, nivel de esclerotización...) al detalle de capa por capa (epicutícula, exocutícula, endocutícula, capa membranosa). Esta información determinaría hasta qué punto la cutícula puede llegar a especializarse.

6. La glándula digestiva (hepatopáncreas, órgano perigástrico) es poco conocida a pesar de la gran diversidad de estudios y publicaciones que se han enfocado en este órgano. En el presente estudio hemos observado diversos tipos de secreción, por lo que sería interesante descubrir el contenido y destino de dichas secreciones, así como su ciclo de formación y aparición en relación del ciclo digestivo. Estas preguntas podrían ser solventadas si se realizan los estudios sugeridos en el punto 4.

7. Se desconoce el papel que juegan las células M de la glándula digestiva. Como se ha discutido previamente, su rol se ha relacionado con el transporte de nutrientes, síntesis hormonal o enzimática o, como en el presente estudio, son consideradas células basales. Demostrar esta última hipótesis requiere de un gran número de observaciones sobre túbulos en distintos estadios de desarrollo con objeto de encontrar células M en diferentes estadios de desarrollo o de actividad. De modo que si la hipótesis planteada en esta memoria es correcta, debería ser posible encontrar células M en proceso de mitosis o de diferenciación hacia otros tipos celulares.

8. En relación al tracto digestivo medio de los especímenes adultos, sería interesante realizar un estudio a nivel morfológico con mayor nivel de detalle. Es preciso conseguir fijar con mayor éxito dicho órgano con objeto de poder estudiar la ultra-estructura de las células epiteliales. Asimismo, el tejido conectivo presenta vasos o estructuras equivalentes a estos, cuya distribución es interesante conocer en profundidad para determinar hasta qué punto está irrigado este órgano y su rol en la nutrición de los braquiuros.

9. El epitelio del tracto digestivo medio parece ser el principal responsable de la síntesis de membrana peritrófica. Las observaciones realizadas han permitido observar que las células epiteliales presentan abundantes vesículas de secreción de carácter electro-denso. Para discernir el nivel de involucración de dichas vesículas en la síntesis de la membrana peritrófica, así como el proceso mismo su síntesis, es preciso aislarlas e identificar su composición. Las técnicas de transcriptómica resolverían qué genes están actuando en las células epiteliales del tracto digestivo, lo que ayudaría a estimar qué productos están siendo sintetizados, con objeto de identificar *a posteriori* su localización mediante técnicas inmunohistoquímicas.

10. Los ciegos digestivos son estructuras muy desarrolladas, de gran longitud y con una gran actividad secretora. Dadas estas características deben de ser órganos con un rol importante en el proceso digestivo, el cual es desconocido. En ese sentido es preciso describir la naturaleza bioquímica de las secreciones, así como el destino final y función de las mismas. Con este fin podrían emplearse las técnicas descritas en los puntos 4 y 9.

11. No ha sido posible estudiar ni profundizar en la morfología y organización tisular del tracto final del tracto digestivo posterior o ano. Este tramo del sistema digestivo posterior debe de poseer ciertas especializaciones, ya que debe de finalizar la expulsión de materia fecal así como cerrar el paso al medio externo cuando es preciso, en otros estudios también se hace mención de la ingesta anal de agua. Por ello, considero que debe de ser interesante indagar en la estructura del ano durante todos los estadios vitales. Para cumplir este objetivo podrían utilizarse las técnicas empleadas en el presente estudio. Se aventura de que debe de tratarse de una estructura fuertemente musculada.

Llegados a estas líneas finales, soy consciente de que muchas otras preguntas se han quedado en el tintero y que son necesarias de responder para entender la fisiología digestiva de *M. brachydactyla* en particular y de los braquiuros en general. Después de todo, los braquiuros son animales de los que todavía se desconocen muchas facetas de su biología. La presente Tesis también ha dado lugar a una situación habitual del trabajo científico: obtener una respuesta abre las puertas a varias y nuevas preguntas. Esta situación se podría resumir en cuatro palabras, son requeridos más estudios.

19.11 Bibliografía.

Abbott NJ. 1971. The organization of the cerebral ganglion in the shore crab, *Carcinus maenas*. II. The relation of intracerebral blood vessels to other brain elements. Zeitschrift für Zellforschung und Mikroskopische Anatomie 120(3):401-419.

Abrunhosa FA, Kittaka J. 1997. Morphological changes in the midgut, midgut gland and hindgut during the larval and postlarval development of the red king crab *Paralithodes camtschaticus*. Fisheries Science 63(5):746-754.

Abubakr MA, Jones DA. 1992. Functional morphology and ultrastructure of the anterior mid-gut diverticulae of larvae of *Penaeus monodon* Fabricius, 1798 (Decapoda, Natantia). Crustaceana 62(2):142-158.

Adang MJ, Spence KD. 1981. Surface morphology of peritrophic membrane formation in the cabbage looper, *Trichoplusia ni*. Cell and Tissue Research 218(1):141-147.

Ahyong ST, Lai JCY, Sharkey D, Colgan DJ, Ng PKL. 2007. Phylogenetics of the brachyuran crabs (Crustacea: Decapoda): The status of Podotremata based on small subunit nuclear ribosomal RNA. Molecular Phylogenetics and Evolution 45(2):576-586.

Aiken DE, Waddy SL. 1982. Cement gland development, ovary maturation, and reproductive cycles in the American Lobster *Homarus americanus*. Journal of Crustacean Biology 2(3):iii-327.

Al-Mohanna SY, Nott JA. 1986. B-cells and digestion in the hepatopancreas of *Penaeus semisulcatus* (Crustacea: Decapoda). Journal of the Marine Biological Association of the United Kingdom 66(2):403-414.

Al-Mohanna SY, Nott JA. 1987. R-cells and the digestive cycle in *Penaeus semisulcatus* (Crustacea: Decapoda). Marine Biology 95(1):129-137.

Al-Mohanna SY, Nott JA. 1989. Functional cytology of the hepatopancreas of *Penaeus semisulcatus* (Crustacea: Decapoda) during the moult cycle. Marine Biology 101(4):535-544.

Al-Mohanna SY, Nott JA, Lane DJW. 1985a. M-'Midget' cells in the hepatopancreas of the shrimp, *Penaeus semisulcatus* De Hann, 1844 (Decapoda, Natantia). Crustaceana 48(3):260-268.

Al-Mohanna SY, Nott JA, Lane DJW. 1985b. Mitotic E- and secretory F-cells in the hepatopancreas of the shrimp *Penaeus semisulcatus* (Crustacea: Decapoda). Journal of the Marine Biological Association of the United Kingdom 65(4):901-910.

Alba-Tercedor J. 2014. From the sample preparation to the volume rendering images of small animals: A step by step example of a procedure to carry out the micro-CT study of the leafhopper insect

Homalodisca vitripennis (Hemiptera: Cicadellidae). In: Skyscan, editor. Bruker microCT Users Meeting 2014. Kontich, Belgium. p 260-288.

Alba-Tercedor J, Sáinz-Cantero CE. 2012. Volume rendering reconstructions of the anatomy of small aquatic beetles (Insecta : Coleoptera) scanned with the Skyscan 1172 high resolution micro-CT. In: Skyscan, editor. Micro-CT Users Meeting 2012. Kontich, Belgium. p 75-84.

Alexander CG. 1989. Tegumental glands in the paragnaths of *Palaemon serratus* (Crustacea: Natantia). Journal of the Marine Biological Association of the United Kingdom 69(01):53-63.

Almerão MP, Faccioni-Heuser MC, Bond-Buckup G. 2007. An ultrastructural study of tegumental glands of the fifth pereiopods of *Aegla platensis* (Anomura: Aeglidae). Journal of Crustacean Biology 27(4):529-533.

Alves STM, Abrunhosa FA, Lima JdF. 2010. Foregut morphology of Pseudothelphusidae and Trichodactylidae (Decapoda: Brachyura) from northeastern Pará, Brazil. Zoologia (Curitiba) 27(2):228-244.

Allardyce BJ, Linton SM. 2010. Functional Morphology of the Gastric Mills of Carnivorous, Omnivorous, and Herbivorous Land Crabs. J Morphol 271(1):61-72.

Andrés M, Estévez A, Anger K, Rotllant G. 2008. Developmental patterns of larval growth in the edible spider crab, *Maja brachydactyla* (Decapoda: Majidae). J Exp Mar Biol Ecol 357(1):35-40.

Andrés M, Gisbert E, Díaz M, Moyano FJ, Estévez A, Rotllant G. 2010. Ontogenetic changes in digestive enzymatic capacities of the spider crab, *Maja brachydactyla* (Decapoda: Majidae). J Exp Mar Biol Ecol 389(1-2):75-84.

Anger K. 2001. The Biology of Decapod Crustacean Larvae. Rotterdam: A.A. Balkema Publishers. 419 p.

Anger K, Storch V, Anger V, Capuzzo JM. 1985. Effects of starvation on moult cycle and hepatopancreas of stage I lobster (*Homarus americanus*) larvae. Helgoländer Meeresuntersuchungen 39:107-116.

Antunes-Carvalho C, Yavorskaya M, Gnaspini P, Ribera I, Hammel JU, Beutel RG. 2017. Cephalic anatomy and three-dimensional reconstruction of the head of *Catops ventricosus* (Weise, 1877) (Coleoptera: Leiodidae: Cholevinae). Organisms Diversity & Evolution 17(1):199-212.

Barbehenn RV, Martin MM. 1992. The protective role of the peritrophic membrane in the tannin-tolerant larvae of *Orgyia leucostigma* (Lepidoptera). Journal of Insect Physiology 38(12):973-980.

Barker PL, Gibson R. 1977. Observations on the feeding mechanism, structure of the gut, and digestive physiology of the european lobster *Homarus gammarus* (L.) (Decapoda: Nephropidae). J Exp Mar Biol Ecol 26(3):297-324.

Barker PL, Gibson R. 1978. Observations on the structure of the mouthparts, histology of the alimentary tract, and digestive physiology of the mud crab *Scylla serrata* (Forskål) (Decapoda: Portunidae). J Exp Mar Biol Ecol 32(2):177-196.

Becker A, Ziegler A, Epple M. 2005. The mineral phase in the cuticles of two species of Crustacea consists of magnesium calcite, amorphous calcium carbonate, and amorphous calcium phosphate Dalton Transactions(10):1814–1820.

Bernárdez C, Freire J, González-Gurriarán E. 2000. Feeding of the spider crab *Maja squinado* in rocky subtidal areas of the Ría de Arousa (north-west Spain). Journal of the Marine Biological Association of the United Kingdom 80(01):95-102.

Betz O, Wegst U, Weide D, Heethoff M, Helfen L, Lee W-K, Cloetens P. 2007. Imaging applications of synchrotron X-ray phase-contrast microtomography in biological morphology and biomaterials science. I. General aspects of the technique and its advantages in the analysis of millimetre-sized arthropod structure. Journal of Microscopy 227(1):51-71.

Biesiot PM, McDowell JE. 1995. Midgut-gland development during early life-history of the American Lobster *Homarus americanus*. Journal of Crustacean Biology 15(4):679-685.

Bignell DE, Oskarsson H, Anderson JM. 1982. Formation of membrane-bounded secretory granules in the midgut epithelium of a termite, *Cubitermes severus*, and a possible intercellular route of discharge. Cell and Tissue Research 222(1):187-200.

Bolognesi R, Ribeiro AF, Terra WR, Ferreira C. 2001. The peritrophic membrane of *Spodoptera frugiperda*: Secretion of peritrophins and role in immobilization and recycling digestive enzymes. Archives of Insect Biochemistry and Physiology 47(2):62-75.

Boßelmann F, Romano P, Fabritius H, Raabe D, Epple M. 2007. The composition of the exoskeleton of two crustacea: The American lobster *Homarus americanus* and the edible crab *Cancer pagurus*. Thermochimica Acta 463(1):65-68.

Bracken HD, Toon A, Felder DL, Martin JW, Finley M, Rasmussen J, Palero F, Crandall KA. 2009. The Decapod Tree of Life: Compiling the data and moving toward a consensus of Decapod Evolution. Arthropod Systematics & Phylogeny 67(1):99-116.

Brandt CR, Adang MJ, Spence KD. 1978. The peritrophic membrane: Ultrastructural analysis and function as a mechanical barrier to microbial infection in *Orgyia pseudotsugata*. Journal of Invertebrate Pathology 32(1):12-24.

Brösing A. 2010. Recent developments on the morphology of the brachyuran foregut ossicles and gastric teeth. Zootaxa 2510:1-44.

Brösing A. 2014. Foregut structures of freshly moulted exuviae from *Maja crispata*, *Cancer pagurus* and *Pseudosesarma moeschi* (Decapoda: Brachyura). Journal of Natural History 48(9-10):543-555.

Brösing A, Richter S, Scholtz G. 2002. The foregut-ossicle system of *Dromia wilsoni*, *Dromia personata* and *Lauridromia intermedia* (Decapoda, Brachyura, Dromiidae), studied with a new staining method. Arthropod Structure & Development 30(4):329-338.

Brösing A, Richter S, Scholtz G. 2007. Phylogenetic analysis of the Brachyura (Crustacea, Decapoda) based on characters of the foregut with establishment of a new taxon. Journal of Zoological Systematics and Evolutionary Research 45(1):20-32.

Brösing A, Türkay M. 2011. Gastric teeth of some thoracotreme crabs and their contribution to the brachyuran phylogeny. J Morphol 272(9):1109-1115.

Byers JR, Bond EF. 1971. Surface specializations of the hindgut cuticle of lepidopterous larvae. Canadian Journal of Zoology 49(6):867-876.

Caceci T, Neck KF, Lewis DDH, Sis RF. 1988. Ultrastructure of the hepatopancreas of the Pacific white shrimp, *Penaeus vannamei* (Crustacea: Decapoda). Journal of the Marine Biological Association of the United Kingdom 68(02):323-337.

Castejón D, Ribes E, Durfort M, Rotllant G, Guerao G. 2015. Foregut morphology and ontogeny of the mud crab *Dyspanopeus sayi* (Smith, 1869) (Decapoda, Brachyura, Panopeidae). Arthropod Structure & Development 44(1):33-41.

Ceccaldi HJ. 1989. Anatomy and physiology of digestive tract of Crustaceans Decapods reared in aquaculture. Advances in Tropical Aquaculture, Workshop at Tahiti, French Polynesia. Tahiti, French Polynesia: Actes de colloques Ifremer. p 243-259.

Cervellione F, McGurk C, Van den Broeck W. 2017. ―Perigastric organ": a replacement name for the ―hepatopancreas" of Decapoda. Journal of Crustacean Biology 37(3):353-355.

Coleman CO. 1994. Comparative anatomy of the alimentary canal of hyperiid amphipods Journal of Crustacean Biology 14(2):346-370.

Compère P. 1995. Fine structure and morphogenesis of the sclerite epicuticle in the Atlantic shore crab *Carcinus maenas*. Tissue and Cell 27(5):525-538.

Cordes VC, Reidenbach S, Franke WW. 1996. Cytoplasmic annulate lamellae in cultured cells: composition, distribution, and mitotic behavior. Cell and Tissue Research 284(2):177-191.

Cristofoletti PT, Ribeiro AF, Terra WR. 2001. Apocrine secretion of amylase and exocytosis of trypsin along the midgut of *Tenebrio molitor* larvae. Journal of Insect Physiology 47(2):143-155.

Chisaka H, Kozawa Y. 2003. Fine structure and mineralization of the gastric mill in the crayfish during intermolt stage. Journal of Crustacean Biology 23(2):371-379.

Chisaka H, Ueno M, Futaesaku Y. 1999. Spines in the hindgut of the crayfish *Procambarus clarkii* (Decapoda): their distribution and correlation with hindgut muscles. Journal of Crustacean Biology 19(2):337-343.

Choy SC. 1986. Natural diet and feeding habits of the crabs *Liocarcinus puber* and *L. holsatus* (Decapoda, Brachyura, Portunidae). Marine Ecology Progress Series 31:97-99.

Dall W. 1967. The functional anatomy of the digestive tract of a shrimp *Metapenaeus bennettae* Racek & Dall (Crustacea : Decapoda : Penaeidae). Australian Journal of Zoology 15(4):699-714.

Dapples CC, Lea AO. 1974. Inner surface morphology of the alimentary canal in *Aedes aegypti* (L.) (diptera: culicidae). International Journal of Insect Morphology and Embryology 3(3):433-442.

Davolos D, L. P, Accordi F, De Matthaeis E. 2010. Morphology and histology of the mouthparts and gut system of *Macarorchestia remyi* (Schellenberg, 1950) (Amphipoda, Talitridae). Zoologia Baetica 21:151-178.

De Jong L, Casanova B. 1997. Comparative morphology of the foregut of three *Eucopia* species (Crustacea, Mysidacea, Lophogastrida). Journal of Natural History 31(3):389-402.

de La Barra P, Narvarte M, Williner V. 2017. Functional morphology of the gastric mill of the swimming crab *Ovalipes trimaculatus* (Decapoda: Portunidae). Journal of the Marine Biological Association of the United Kingdom:1-8.

Dillaman RM, Roer R, Shafer T, Modla S. 2012. The Crustacean Integument: Structure and Function. In: Watling L, Thiel M, editors. The Natural History of the Crustacea, vol 1 Functional Morphology and Diversity: Oxford University Press. p 140-165.

Dinley J, Hawkins L, Paterson G, Ball AD, Sinclair I, Sinnett-Jones P, Lanham S. 2010. Micro-computed X-ray tomography: a new non-destructive method of assessing sectional, fly-through and 3D imaging of a soft-bodied marine worm. Journal of Microscopy 238(2):123-133.

Doughtie DG, Rao KR. 1982. Rosette glands in the gills of the grass shrimp, *Palaemonetes pugio*. I. Comparative morphology, cyclical activity, and innervation. J Morphol 171(1):41-67.

Dworschak PC. 1998. The role of tegumental glands in burrow construction of two Mediterranean callianassid shrimp. Senckenbergiana maritima 28(4/6):143-149.

Elner RW, Campbell A. 1987. Natural diets of lobster *Homarus americanus* from barren ground and macroalgal habitats off southwestern Nova Scotia, Canada Marine Ecology Progress Series 37:131-140.

Elzinga RJ. 1996. A comparative study of microspines in the alimentary canal of five families of Orthoptera (Saltatoria). International Journal of Insect Morphology and Embryology 25(3):249-260.

Elzinga RJ. 1998. Microspines in the alimentary canal of arthropoda, onychophora, annelida. International Journal of Insect Morphology and Embryology 27(4):341-349.

Elzinga RJ, Hopkins TL. 1994. Foregut microspines in four families of cockroaches (Blattaria). International Journal of Insect Morphology and Embryology 23(3):253-260.

Elzinga RJ, Hopkins TL. 1995. Microspine variation in hindgut regions of four families of cockroaches (Blattaria). International Journal of Insect Morphology and Embryology 24(2):203-211.

Erri Babu D, Manjulatha C. 1995. Zymogen secreting cells in the hepatopancreatic duct of *Pagurus bernhardus* (Linnaeus, 1758) and *Clibanarius longitarsus* (De Haan, 1849) (Anomura). Crustaceana 68(5):616-628.

Erri Babu D, Rao KH, Shyamasundari K, Uma Devi DV. 1985. Histochemistry of the cuticle of the crab *Menippe rumphii* (Fabricius) (Crustacea: Brachyura) in relation to moulting. J Exp Mar Biol Ecol 88(2):129-144.

Erri Babu D, Shyamasundari K, Hanumantha Rao K. 1979. The structure and histochemistry of the oesophageal glands in the crab *Menippe rumphii* (Frabricius) (Crustacea : Brachyura). Proceedings: Animal Sciences 88(4):277-285.

Erri Babu D, Shyamasundari K, Rao KH. 1982. Studies on the digestive system of the crab *Menippe rumphii* (Fabricius) (Crustacea:Brachyura). J Exp Mar Biol Ecol 58(2):175-191.

Factor JR. 1981. Development and metamorphosis of the digestive system of larval lobsters, *Homarus americanus* (Decapoda: Nephropidae). J Morphol 169:225-242.

Factor JR. 1982. Development and metamorphosis of the feeding apparatus of the stone crab, *Menippe mercenaria* (Brachyura, Xanthidae). J Morphol 172(3):299-312.

Factor JR. 1989. Development of the feeding apparatus in decapod crustaceans. In: Felgenhauer BE, Watling L, Thistle AB, editors. Crustacean Issues 6 Functional morphology of feeding and grooming in Crustacea. Rotterdam, Balkema: CRC Press. p 185-203.

Farkań R. 2015. Apocrine secretion: New insights into an old phenomenon. Biochimica et Biophysica Acta (BBA) - General Subjects 1850(9):1740-1750.

Felder DL, Felgenhauer BE. 1993. Morphology of the midgut–hindgut juncture in the ghost shrimp *Lepidophthalmus louisianensis* (Schmitt) (Crustacea: Decapoda: Thalassinidea). Acta Zoologica 74(4):263-276.

Felgenhauer BE. 1992. Chapter 3. Internal Anatomy of the Decapoda: An Overview. In: Harrison FW, Humes AG, editors. Microscopic Anatomy of Invertebrates Volume 10: Decapod Crustacea: Wiley-Liss, Inc. p 45-75.

Ferreira C, Bellinello GL, Ribeiro AF, Terra WR. 1990. Digestive enzymes associated with the glycocalyx, microvillar membranes and secretory vesicles from midgut cells of *Tenebrio molitor* larvae. Insect Biochemistry 20(8):839-847.

Forster GR. 1953. Peritrophic membranes in the Caridea (Crustacea Decapoda). Journal of the Marine Biological Association of the United Kingdom 32(2):315-318.

Franceschini-Vicentini IB, Ribeiro K, Papa LP, Marques Junior J, Vicentini CA, Valenti PMCM. 2009. Histoarchitectural features of the hepatopancreas of the Amazon River Prawn *Macrobrachium amazonicum*. International Journal of Morphology 27:121-128.

Franz-Guess S, Klußmann-Fricke B-J, Wirkner CS, Prendini L, Starck JM. 2016. Morphology of the tracheal system of camel spiders (Chelicerata: Solifugae) based on micro-CT and 3D-reconstruction in exemplar species from three families. Arthropod Structure & Development 45(5):440-451.

Freire J, Carabel S, Verísimo P, Bernárdez C, Fernández L. 2009. Patterns of juvenile habitat use by the spider crab *Maja brachydactyla* as revealed by stable isotope analyses. Sci Mar 73(1):39-49.

Frick M, Kopitsky K, Bolten A, Bjorndal K, Martins H. 2011. Sympatry in grapsoid crabs (genera *Planes* and *Plagusia*) from olive ridley sea turtles (*Lepidochelys olivacea*), with descriptions of crab diets and masticatory structures. Marine Biology 158(8):1699-1708.

Friesen JA, Mann KH, Willison JHM. 1986. Gross anatomy and fine structure of the gut of the marine mysid shrimp *Mysis stenolepis* Smith. Canadian Journal of Zoology 64(2):431-441.

Ge S-Q, Hua Y, Ren J, Slipinski A, Beutel R, Wipfler B. 2015. Transformation of head structures during the metamorphosis of *Chrysomela populi* (Coleoptera, Chrysomelidae). Arthropod Systematics & Phylogeny 73(1):129-152.

Georgi R. 1969. Bildung peritrophischer Membranen von Decapoda. Zeitschrift für Zellforschung und Mikroskopische Anatomie 99(4):570-607.

Gesase AP, Satoh Y. 2003. Apocrine secretory mechanism: recent findings and unresolved problems. Histology and Histopathology 18(2):597-608.

Gibson R, Barker PL. 1979. The Decapod Hepatopancreas. Oceanography and Marine Biology - An Annual Review 17:285-346.

Gomes FM, Carvalho DB, Machado EA, Miranda K. 2013. Ultrastructural and functional analysis of secretory goblet cells in the midgut of the lepidopteran *Anticarsia gemmatalis*. Cell and Tissue Research 352(2):313-326.

Gorvett H. 1946. The Tegumental Glands in the Land Isopoda A. The Rosette Glands. Quarterly Journal of Microscopical Science s2-87:209-235.

Gorvett H. 1951. The Tegumental Glands in the Land Isopoda B. The Lobed Glands: Structure and Distribution. Journal of Cell Science s3-92(19):275-296.

Gould SJ. 1982. Darwinism and the expansion of evolutionary theory. Science 216(4544):380-387.

Greenaway P, Morris S. 1989. Adaptations to a terrestrial existence by the robber crab, *Birgus latro* L.: III. Nitrogenous excretion. Journal of Experimental Biology 143(1):333-346.

Griffen BD, Mosblack H. 2011. Predicting diet and consumption rate differences between and within species using gut ecomorphology. Journal of Animal Ecology 80(4):854-863.

Guerao G, Pastor E, Martin J, Andrés M, Estévez A, Grau A, Duran J, Rotllant G. 2008. The larval development of *Maja squinado* and *M. brachydactyla* (Decapoda, Brachyura, Majidae) described from plankton collected and laboratory-reared material. Journal of Natural History 42(33-34):2257-2276.

Guerao G, Rotllant G. 2009a. Post-larval development and sexual dimorphism of the spider crab *Maja brachydactyla* (Brachyura: Majidae). Sci Mar 73:797-808.

Guerao G, Rotllant G. 2009b. Survival and growth of post-settlement juveniles of the spider crab *Maja brachydactyla* (Brachyura: Majoidea) reared under individual culture system. Aquaculture 289(1-2):181-184.

Guerao G, Rotllant G. 2010. Development and growth of the early juveniles of the spider crab *Maja squinado* (Brachyura: Majoidea) in an individual culture system. Aquaculture 307(1-2):105-110.

Guerao G, Simeó CG, Anger K, Urzúa Á, Rotllant G. 2012. Nutritional vulnerability of early zoea larvae of the crab *Maja brachydactyla* (Brachyura, Majidae). Aquatic Biology 16(3):253-264.

Hames CAC, Hopkin SP. 1989. The structure and function of the digestive system of terrestrial isopods. Journal of Zoology 217(4):599-627.

Hampoelz B, Mackmull M-T, Machado P, Ronchi P, Bui KH, Schieber N, Santarella-Mellwig R, Necakov A, Andrés-Pons A, Philippe JM, Lecuit T, Schwab Y, Beck M. 2016. Pre-assembled nuclear pores insert into the nuclear envelope during early development. Cell 166(3):664-678.

Handschuh S, Beisser CJ, Ruthensteiner B, Metscher BD. 2017. Microscopic dual-energy CT (microDECT): a flexible tool for multichannel ex vivo 3D imaging of biological specimens. Journal of Microscopy:n/a-n/a.

Harper MS, Hopkins TL. 1997. Peritrophic membrane structure and secretion in european corn borer larvae (*Ostrinia nubilalis*). Tissue and Cell 29(4):463-475.

Harris JM. 1993. Widespread occurrence of extensive epimural rod bacteria in the hindguts of marine Thalassinidae and Brachyura (Crustacea: Decapoda). Marine Biology 116(4):615-629.

Heeren T, Mitchell BD. 1997. Morphology of the mouthparts, gastric mill and digestive tract of the giant crab, *Pseudocarcinus gigas* (Milne Edwards) (Decapoda: Oziidae). Marine and Freshwater Research 48(1):7-18.

Hegdahl T, Gustavsen F, Silness J. 1977a. The structure and mineralization of the carapace of the crab (*Cancer pagurus* L.) 2. The exocuticle. Zoologica Scripta 6(2):101-105.

Hegdahl T, Gustavsen F, Silness J. 1977b. The structure and mineralization of the carapace of the crab (*Cancer pagurus* L.) 3. The epicuticle. Zoologica Scripta 6(3):215-220.

Hegdahl T, Silness J, Gustavsen F. 1977c. The structure and mineralization of the carapace of the crab (*Cancer pagurus* L.) 1. The endocuticle. Zoologica Scripta 6(2):89-99.

Hegedus D, Erlandson M, Gillott C, Toprak U. 2009. New Insights into peritrophic matrix synthesis, architecture, and function. Annual Review of Entomology 54:285-302.

Hepburn HR, Chandler HD. 1976. Material properties of arthropod cuticles: The arthrodial membranes. Journal of comparative physiology 109(2):177-198.

Hobbs KH, Hooper SL. 2009. High-resolution computed tomography of lobster (*Panulirus interruptus*) stomach. J Morphol 270(9):1029-1041.

Hochuli DF, Roberts B, Sanson GD. 1992. Anteriorly directed microspines in the foregut of *Locusta migratoria* (Orthoptera : Acrididae). International Journal of Insect Morphology and Embryology 21(1):95-97.

Holdich DM, Mayes KR. 1975. A Fine-Structural Re-Examination of the so-called 'Midgut' of the isopod *Porcellio*. Crustaceana 29(2):186-192.

Holdich DM, Ratcliffe NA. 1970. A light and electron microscope study of the hindgut of the herbivorous isopod, *Dynamene bidentata* (Crustacea: Peracarida). Zeitschrift für Zellforschung und Mikroskopische Anatomie 111(2):209-227.

Holdsworth DW, Thornton MM. 2002. Micro-CT in small animal and specimen imaging. Trends in Biotechnology 20(8):S34-S39.

Hopkin SP, Nott JA. 1979. Some observations on concentrically structured, intracellular granules in the hepatopancreas of the shore crab *Carcinus maenas* (L.). Journal of the Marine Biological Association of the United Kingdom 59(4):867-877.

Hopkin SP, Nott JA. 1980. Studies on the digestive cycle of the shore crab *Carcinus maenas* (L.) with special reference to the b cells in the hepatopancreas. Journal of the Marine Biological Association of the United Kingdom 60(04):891-907.

Hoyoux C, Zbinden M, Samadi S, Gaill F, Compère P. 2009. Wood-based diet and gut microflora of a galatheid crab associated with Pacific deep-sea wood falls. Marine Biology 156(12):2421-2439.

Hu K-J, Leung P-C. 2007. Food digestion by cathepsin L and digestion-related rapid cell differentiation in shrimp hepatopancreas. Comparative Biochemistry and Physiology Part B: Biochemistry and Molecular Biology 146(1):69-80.

Huespe AV, Gámez-Simes E, Pastor-de-Ward CT. 2008. Gastric mill morphology in the genus *Cyrtograpsus* (Crustacea: Decapoda: Grapsoidea: Varunidae). Journal of the Marine Biological Association of the United Kingdom 88(02):311-319.

Hunt MJ, Winsor H, Alexander CG. 1992. Feeding by penaeid prawns: the role of the anterior mouthparts. J Exp Mar Biol Ecol 160(1):33-46.

Icely JD, Jones DA. 1978. Factors affecting the distribution of the genus *Uca* (Crustacea: Ocypodidae) on an East African shore. Estuarine and Coastal Marine Science 6(3):315-325.

Icely JD, Nott JA. 1984. On the morphology and fine structure of the alimentary canal of *Corophium volutator* (Pallas) (Crustacea: Amphipoda). Philosophical Transactions of the Royal Society of London B, Biological Sciences 306(1126):49-78.

Icely JD, Nott JA. 1992. Digestion and absorption: digestive system and associated organs. In: Harrison FW, Humes AG, editors. Microscopic anatomy of invertebrates: decapod Crustacea. New York: Wiley-Liss. p 147-201.

Ikeda H, Hirano Y, Saigusa M. 2004. A pair of rosette glands in the embryo and zoeal larva of an estuarine crab *Sesarma haematocheir*, and classification of the tegumental glands in the embryos of other crabs. J Morphol 259(1):55-68.

Irvin SJ, Tabrett SJ. 2005. A novel method of collecting fecal samples from spiny lobsters. Aquaculture 243(1):269-272.

Jalaja-Kumari C, Kanumantha-Rao K, Shyamasundari K. 1983. Histology and histochemistry of the tegumental glands in *Ligia exotica* Roux (Crustacea: Isopoda). Proceedings of the Indian Academy of Sciences (Animal Sciences) 92(3):207-214.

Jimenez DR, Gilliam M. 1990. Ultrastructure of the ventriculus of the honey bee, *Apis mellifera* (L.): cytochemical localization of acid phosphatase, alkaline phosphatase, and nonspecific esterase. Cell and Tissue Research 261(3):431-443.

Johnston DJ, Alexander CG. 1999. Functional morphology of the mouthparts and alimentary tract of the slipper lobster *Thenus orientalis* (Decapoda : Scyllaridae). Marine and Freshwater Research 50(3):213-223.

Johnston M, Johnston D, Knott B. 2008. Ontogenetic changes in the structure and function of the mouthparts and foregut of early and late stage *Panulirus ornatus* (Fabricius, 1798) phyllosomata (Decapoda: Palinuridae). Journal of Crustacean Biology 28(1):46-56.

Johnston MD, Johnston DJ, Richardson AMM. 2004. Mouthpart and digestive tract structure in four talitrid amphipods from a translittoral series in Tasmania. Journal of the Marine Biological Association of the United Kingdom 84(4):717-726.

Kamio M, Wakabayashi K, Nagai H, Tanaka Y. 2016. Phyllosomas of smooth fan lobsters (*Ibacus novemdentatus*) encase jellyfish cnidae in peritrophic membranes in their feces. Plankton and Benthos Research 11(3):100-104.

Kawakita H, Miyamoto K, Wada S, Mitsuhashi W. 2016. Analysis of the ultrastructure and formation pattern of the peritrophic membrane in the cupreous chafer, *Anomala cuprea* (Coleoptera: Scarabaeidae). Applied Entomology and Zoology 51(1):133-142.

Komuro T, Yamamoto T. 1968. Fine structure of the epithelium of the gut in the crayfish (*Procambarus clarkii*) with special reference to the cytoplasmic microtutubles. Archivum histologicum japonicum 30(1):17-32.

Kunze J, Anderson D. 1979. Functional morphology of the mouthparts and gastric mill in the Hermit Crabs *Clibanarius taeniatus* (Milne Edwards), *Clibanarius virescens* (Krauss), *Paguristes squamosus* McCulloch and *Dardanus setifer* (Milne-Edwards) (Anomura: Paguridae). Marine and Freshwater Research 30(5):683-722.

Lautenschlager KP, Kaushik NK, Robinson JB. 1978. The peritrophic membrane and faecal pellets of *Gammarus lacustris* limnaeus Smith. Freshwater Biology 8(2):207-211.

Le Vay L, Jones DA, Puello-Cruz AC, Sangha RS, Ngamphongsai C. 2001. Digestion in relation to feeding strategies exhibited by crustacean larvae. Comparative Biochemistry and Physiology Part A: Molecular & Integrative Physiology 128(3):621-628.

Lehane MJ. 1997. Peritrophic matrix structure and function. Annual Review of Entomology 42(1):525-550.

Li F, Li S. 1998. Studies on the hepatopancreas of larval *Scylla serrata*. Oceanologia Et Limnologia Sinica 29:29-34.

Lignon JM. 1987. Structure and permeability of Decapod Crustacea cuticle. In: Kirsch R, Lahlou B, editors. Adaptations to Salinity and Dehydration 8th Conference of the European Society for Comparative Physiology and Biochemistry (ESCP). Strasbourg: Karger, Basel. p 178-187.

Lima-Gomes RC, Lima JdF, Magalhães C. 2017. Description of ten additional ossicles in the foregut of the freshwater crabs *Sylviocarcinus pictus* and *Valdivia serrata* (Decapoda: Trichodactylidae). Zoologia (Curitiba) 34.

Lima JdF, Garcia JdS, Silva TCd. 2014. Natural diet and feeding habits of a freshwater prawn (*Macrobrachium carcinus*: Crustacea, Decapoda) in the estuary of the Amazon River. Acta Amazonica 44:235-244.

Lima JdF, Garcia JdS, Tavares M. 2016. Foregut morphology of *Macrobrachium carcinus* (Crustacea, Decapoda, Palaemonidae). Acta Amazonica 46(2):209-218.

Lin F-Y. 1996. Structure of the gland filters in the pyloric stomach of *Penaeus japonicus* (Decapoda: Penaeidae). Journal of Crustacean Biology 16(3):515-521.

Lin F-Y. 2000. Scanning electron microscopic observations on the gland filters of the pyloric stomach of *Penaeus monodon* and *Metapenaeus ensis* (Decapoda, Penaeidae). Crustaceana 73(2):163-174.

Loizzi RF. 1966. Cellular and physiological changes during secretion in crayfish hepatopancreas. Ames, Iowa: Iowa State University of Science and Technology. 190 p.

Loizzi RF. 1971. Interpretation of crayfish hepatopancreatic function based on fine structural analysis of epithelial cell lines and muscle network. Zeitschrift für Zellforschung und Mikroskopische Anatomie 113(3):420-440.

Lovett DL, Felder DL. 1989. Ontogeny of gut morphology in the white shrimp *Penaeus setiferus* (Decapoda, Penaeidae). J Morphol 201(3):253-272.

Lowe T, Garwood RJ, Simonsen TJ, Bradley RS, Withers PJ. 2013. Metamorphosis revealed: time-lapse three-dimensional imaging inside a living chrysalis. Journal of The Royal Society Interface 10(84).

Maas SLN, Breakefield XO, Weaver AM. 2016. Extracellular vesicles: unique intercellular delivery vehicles. Trends in Cell Biology In Press, Corrected Proof.

MacArthur LD, Phillips DL, Hyndes GA, Hanson CE, Vanderklift MA. 2011. Habitat surrounding patch reefs influences the diet and nutrition of the western rock lobster. Marine Ecology Progress Series 436:191-205.

Martin GG, Chiu A. 2003. Morphology of the midgut trunk in the penaeid shrimp, *Sicyonia ingentis*, highlighting novel nuclear pore particles and fixed hemocytes. J Morphol 258(2):239-248.

Martin GG, Simcox R, Nguyen A, Chilingaryan A. 2006. Peritrophic membrane of the penaeid shrimp *Sicyonia ingentis*: structure, formation, and permeability. The Biological Bulletin 211(3):275-285.

Martin JS, Kirkham JB. 1989. Dynamic role of microvilli in peritrophic membrane formation. Tissue and Cell 21(4):627-638.

Mary RF, Krishnan G. 1974. On the nature and role of protein constituents of the cuticle of crustaceans in relation to permeability of the cuticle. Marine Biology 25(4):299-309.

Maynard DM, Dando MR. 1974. The structure of the stomatogastric neuromuscular system in *Callinectes sapidus*, *Homarus americanus* and *Panulirus argus* (Decapoda Crustacea). Philosophical Transactions of the Royal Society of London B, Biological Sciences 268(892):161-220.

McConnell RE, Higginbotham JN, Shifrin DA, Tabb DL, Coffey RJ, Tyska MJ. 2009. The enterocyte microvillus is a vesicle-generating organelle. The Journal of Cell Biology 185(7):1285-1298.

McGaw IJ, Curtis DL. 2013. A review of gastric processing in decapod crustaceans. Journal of Comparative Physiology B 183(4):443-465.

McGaw IJ, Reiber CL. 2000. Integrated physiological responses to feeding in the blue crab *Callinectes sapidus*. Journal of Experimental Biology 203(2):359-368.

McKenzie LJ, Alexander CG. 1989. Mucus-secreting glands in the paragnaths and second maxillipeds of the banana prawn, *Penaeus merguiensis* de Man Australian Journal of Marine and Freshwater Research 40:669-677.

McLaughlin PA. 1983. 1. Internal Anatomy. In: Mantel LH, editor. The Biology of Crustacea Vol 5 Internal Anatomy and Physiological Regulation: Academic Press. p 1-52.

Meiss DE, Norman RS. 1977. Comparative study of the stomatogastric system of several decapod crustacea. I. Skeleton. J Morphol 152(1):21-53.

Mets RD. 1962. Submicroscopic structure of the peritrophic membrane in arthropods. Nature 196:77-78.

Metscher BD. 2009a. MicroCT for comparative morphology: simple staining methods allow high-contrast 3D imaging of diverse non-mineralized animal tissues. BMC Physiology 9(1):11.

Metscher BD. 2009b. MicroCT for developmental biology: A versatile tool for high-contrast 3D imaging at histological resolutions. Developmental Dynamics 238(3):632-640.

Mikami S, Greenwood JG, Takashima F. 1994. Functional morphology and cytology of the phyllosomal digestive system of *Ibacus ciliatus* and *Panulirus japonicus* (Decapoda, Scyllaridae and Palinuridae). Crustaceana 67(2):212-225.

Mikami S, Takashima F. 1993. Development of the proventriculus in larvae of the slipper lobster, *Ibacus ciliatus* (Decapoda: Scyllaridae). Aquaculture 116(2â€–3):199-217.

Miyoshi AR, Gabriel VA, Fantazzini ER, Fontanetti CS. 2005. Microspines in the pylorus of *Pseudonannolene tricolor* and *Rhinocricus padbergi* (Arthropoda, Diplopoda). Iheringia Série Zoologia 95:183-187.

Monteiro EC, Tamaki FK, Terra WR, Ribeiro AF. 2014. The digestive system of the ―stick bug" *Cladomorphus phyllinus* (Phasmida, Phasmatidae): A morphological, physiological and biochemical analysis. Arthropod Structure & Development 43(2):123-134.

Moon YW, Kim HH. 1999. Morphological study of the digestive tract of the mud crab (*Hemigrapsus penicillatus* De Haan) and the symbiotic crab (*Pinnotheres cyclinus* Shen). Korean Journal of Biological Sciences 3(4):407-412.

Mykles DL. 1977. The ultrastructure of the posterior midgut caecum of *Pachygrapsus crassipes* (Decapoda, Brachyura) adapted to low salinity. Tissue and Cell 9(4):681-691.

Mykles DL. 1979. Ultrastructure of alimentary epithelia of lobsters, *Homarus americanus* and *H. gammarus*, and crab, *Cancer magister*. Zoomorphologie 92(3):201-215.

Nakamura K, Takemoto T. 1986. Morphology of stomach ossicles in Brachyura. Memoirs of Faculty of Fisheries Kagoshima University 35(1):7-15.

Nakamura K, Tshuru H. 1987. Organogenesis of the Midgut Gland in the Prawn *Penaeus japonicus*. Memoirs of Faculty of Fisheries Kagoshima University 36(1):12-25.

Nesbit KT, Roer RD. 2016. Silicification of the medial tooth in the blue crab *Callinectes sapidus*. J Morphol 277(12):1648-1660.

Nishida S, Takahashi Y, Kittaka J. 1995. Structural changes in the hepatopancreas of the rock lobster, *Jasus edwardsii* (Crustacea: Palinuridae) during development from the puerulus to post-puerulus. Marine Biology 123(4):837-844.

Nunes ET, Braga AA, Camargo-Mathias MI. 2014. Histochemical study of the hepatopancreas in adult females of the pink-shrimp *Farfantepenaeus brasiliensis* Latreille, 1817. Acta Histochemica 116(1):243-251.

Paquet F, Germain P, Fritsch P. 1993. Étude ultra-structurale de la glande digestive du homard *Homarus gammarus*. Rôle des divers types cellulaires dans les processus digestifs. Cahiers de Biologie Marine 35:15-37.

Pillai RS. 1960. Studies on the shrimp *Caridina laevis* (Heller) 1. The Digestive System. Journal of the Marine Biological Association of India 2(1):57-74.

Pinn EH, Nickell LA, Rogerson A, Atkinson RJA. 1999. Comparison of gut morphology and gut microflora of seven species of mud shrimp (Crustacea: Decapoda: Thalassinidea). Marine Biology 133:103-114.

Pugh JE. 1962. A contribution toward a knowledge of the hind-gut of fiddler crabs (Decapoda, Grapsidae). Transactions of the American Microscopical Society 81(4):309-320.

Ramadevi KRLS, Shyamasundari K, Hanumantha Rao K. 1990. Observation of the hepatopancreas of *Ocypoda platytarsis* (Milne-Edwards) (Crustacea, Brachyura). Bolletino di zoologia 57(3):261-265.

Reddy AR. 1937. The physiology of digestion and absorption in the crab *Paratelphusa* (*Oziotelphusa*) *hydrodromus* (Herbst). Proceedings of the Indian Academy of Sciences - Section B 6(3):170-193.

Reddy AR. 1938. The cytology of digestion and absorption in the crab *Paratelphusa* (*Oziotelphusa*) *hydrodromus* (Herbst). Proceedings of the Indian Academy of Sciences - Section B 8(3):171-181.

Reimann A, Richter S, Scholtz G. 2011. Phylogeny of the Anomala (Crustacea, Decapoda, Reptantia) based on the ossicles of the foregut. Zoologischer Anzeiger - A Journal of Comparative Zoology 250(4):316-342.

Ribeiro K, Papa LP, Vicentini CA, Franceschini-Vicentini IB. 2016. The ultrastructural evaluation of digestive cells in the hepatopancreas of the Amazon River prawn, *Macrobrachium amazonicum*. Aquaculture Research 47(4):1251-1259.

Roer R, Abehsera S, Sagi A. 2015. Exoskeletons across the Pancrustacea: Comparative Morphology, Physiology, Biochemistry and Genetics. Integrative and Comparative Biology 55(5):771-791.

Roer R, Dillaman RM. 1984. The structure and calcification of the crustacean cuticle. American Zoologist 24(4):893-909.

Rotllant G, Moyano FJ, Andrés M, Díaz M, Estévez A, Gisbert E. 2008. Evaluation of fluorogenic substrates in the assessment of digestive enzymes in a decapod crustacean *Maja brachydactyla* larvae. Aquaculture 282(1–4):90-96.

Rotllant G, Moyano FJ, Andrés M, Estévez A, Díaz M, Gisbert E. 2010. Effect of delayed first feeding on larval performance of the spider crab *Maja brachydactyla* assessed by digestive enzyme activities and biometric parameters. Marine Biology 157(10):2215-2227.

Ruangchai S, Reisecker C, Hild S, Ziegler A. 2013. The architecture of the joint head cuticle and its transition to the arthrodial membrane in the terrestrial crustacean Porcellio scaber. Journal of Structural Biology 182(1):22-35.

Sainte-Marie B, Chabot D. 2002. Ontogenetic shifts in natural diet during benthic stages of American lobster (*Homarus americanus*), off the Magdalen Islands. Fishery Bulletin 100(1):106-116.

Salindeho IR, Johnston DJ. 2003. Functional morphology of the mouthparts and proventriculus of the rock crab *Nectocarcinus tuberculosus* (Decapoda: Portunidae). Journal of the Marine Biological Association of the United Kingdom 83(04):821-834.

Schlüter U. 1980. Ultrastruktur der Pyloruszähnchen zweier Tausendfüßler (*Tachypodoiulus niger*, *Polydesmus angustus*)*. Acta Zoologica 61(3):171-178.

Schmidt M, Chien H, Tadesse T, Johns ME, Derby CD. 2006. Rosette-type tegumental glands associated with aesthetasc sensilla in the olfactory organ of the Caribbean spiny lobster, *Panulirus argus*. Cell and Tissue Research 325(2):369-395.

Schmitz EH, Scherrey PM. 1983. Digestive anatomy *Hyalella azteca* (Crustacea, Amphipoda). J Morphol 175:91-100.

Schmitz EH, Schultz TW. 1969. Digestive anatomy of terrestrial isopoda: *Armadillidium vulgare* and *Armadillidium nasatum*. The American Midland Naturalist 82(1):163-181.

Schultz TW. 1973. Digestive anatomy of *Lirceus fontinalis* Rafinesque (Crustacea: Isopoda). Transactions of the American Microscopical Society 92(1):13-25.

Shifrin Jr David A, McConnell Russell E, Nambiar R, Higginbotham James N, Coffey Robert J, Tyska Matthew J. 2012. Enterocyte microvillus-derived vesicles detoxify bacterial products and regulate epithelial-microbial interactions. Current Biology 22(7):627-631.

Shyamasundari K, Hanumantha Rao K. 1977. Studies on the alimentary canal of amphipods: morphology and histology of cephalic mucous glands. Crustaceana 33(2):149-153.

Shyamasundari K, Hanumantha Rao K. 1978. Studies on the Indian sand lobster *Thenus orientalis* (Lund): mucopolysaccharides of the tegumental glands. Folia Histochemica et Cytochemica 16(3):247-254.

Shyamasundari K, Varghese S. 1973. Holocrine secretion in the hepatopancreas of amphidods. Current Science 42(9):319-321.

Silva W, Cardoso C, Ribeiro AF, Terra WR, Ferreira C. 2013. Midgut proteins released by microapocrine secretion in *Spodoptera frugiperda*. Journal of Insect Physiology 59(1):70-80.

Skilleter G, Anderson D. 1986. Functional morphology of the Chelipeds, mouthparts and gastric mill of *Ozius truncatus* (Milne Edwards) (Xanthidae) and *Leptograpsus variegatus* (Fabricius) (Grapsidae) (Brachyura). Marine and Freshwater Research 37(1):67-79.

Smith RI. 1978. The Midgut Caeca and the Limits of the Hindgut of Brachyura: A Clarification. Crustaceana 35(2):195-205.

Socha JJ, De Carlo F. Use of synchrotron tomography to image naturalistic anatomy in insects; 2008. p 70780A-70780A-70787.

Sonakowska L, Włodarczyk A, Poprawa I, Binkowski M, Śróbka J, Kamińska K, Kszuk-Jendrysik M, Chajec Ł, Zajusz B, Rost-Roszkowska MM. 2015. Structure and Ultrastructure of the endodermal region of the alimentary tract in the freshwater shrimp *Neocaridina heteropoda* (Crustacea, Malacostraca). PLOS ONE 10(5):e0126900.

Soonthornchai W, Chaiyapechara S, Jarayabhand P, Söderhäll K, Jiravanichpaisal P. 2015. Interaction of *Vibrio* spp. with the inner surface of the digestive tract of *Penaeus monodon*. PLOS ONE 10(8):e0135783.

Sousa L, Petriella AM. 2006. Morphology and histology of *P. argentinus* (Crustacea, Decapoda, Caridea) digestive tract. Biocell 30:287-294.

Spears T, Abele LG, Kim W. 1992. The monophyly of brachyuran crabs: a phylogenetic study based on 18s rRNÅ. Systematic Biology 41(4):446-461.

Stevenson JR. 1961. Polyphenol Oxidase in the tegumental glands in relation to the molting cycle of the isopod crustacean *Armadillidium vulgare*. Biological Bulletin 121(3):554-560.

Stevenson JR, Murphy JC. 1967. Mucopolysaccharide glands in the isopod crustacean *Armadillidium vulgare*. Transactions of the American Microscopical Society 86(1):50-57.

Storch V, Anger K. 1983. Influence of starvation and feeding on the hepatopancreas of larval *Hyas araneus* (Decapoda, Majidae). Helgoländer Meeresuntersuchungen 36(1):67-75.

Storch V, Strus J, Brandt A. 2002. Microscopic anatomy and ultrastructure of the digestive system of *Natatolana obtusata* (Vanhöffen, 1914) (Crustacea, Isopoda). Acta Zoologica 83(1):1-14.

Ńtrus J, Klepal W, Repina J, Tuńek-Ņnidarič M, Milatovič M, Pipan Ņ. 2008. Ultrastructure of the digestive system and the fate of midgut during embryonic development in *Porcellio scaber* (Crustacea: Isopoda). Arthropod Structure & Development 37(4):287-298.

Suthers I. 1984. Functional morphology of the mouthparts and gastric mill in *Penaeus plebejus* Hess (Decapoda : Penaeidea). Marine and Freshwater Research 35(6):785-792.

Talbot P, Al-Hajj H, Demers D, Howard D. 1991. Distribution of microfilaments and microtubules in *Homarus* pleopod tegumental glands (Crustacea, Decapoda). Zoomorphology 110(6):329-338.

Talbot P, Clark WH, Lawrence AL. 1972. Fine structure of the midgut epithelium in the developing brown shrimp, *Penaeus aztecus*. J Morphol 138(4):467-485.

Terra WR. 2001. The origin and functions of the insect peritrophic membrane and peritrophic gel. Archives of Insect Biochemistry and Physiology 47(2):47-61.

To TH, Brenner TL, Cavey MJ, Wilkens JL. 2004. Histological organization of the intestine in the crayfish *Procambarus clarkii*. Acta Zoologica 85(2):119-130.

Travis OF. 1955. The molting cycle of the spiny lobster, *Panulirus argus* Latreille. II. Pre-ecdysial histological and histochemical changes in the hepatopancreas and integumental tissues. The Biological Bulletin 108(1):88-112.

Tricarico C, Clancy J, D'Souza-Schorey C. 2016. Biology and biogenesis of shed microvesicles. Small GTPases:1-13.

Tsang LM, Schubart CD, Ahyong ST, Lai JCY, Au EYC, Chan T-Y, Ng PKL, Chu KH. 2014. Evolutionary history of true crabs (Crustacea: Decapoda: Brachyura) and the origin of freshwater crabs. Molecular Biology and Evolution 31(5):1173-1187.

Tziouveli V, Bastos-Gomez G, Bellwood O. 2011. Functional morphology of mouthparts and digestive system during larval development of the cleaner shrimp *Lysmata amboinensis* (de Man, 1888). J Morphol 272(9):1080-1091.

Van Thuong K, Van Tuan V, Li W, Sorgeloos P, Bossier P, Nauwynck H. 2016. Per os infectivity of white spot syndrome virus (WSSV) in white-legged shrimp (*Litopenaeus vannamei*) and role of peritrophic membrane. Veterinary Research 47(1):39.

Vatcher HE, Roer RD, Dillaman RM. 2015. Structure, molting, and mineralization of the dorsal ossicle complex in the gastric mill of the blue crab, *Callinectes sapidus*. J Morphol 276(11):1358-1367.

Vernon GM, Herold L, Witkus ER. 1974. Fine structure of the digestive tract epithelium in the terrestrial isopod. *Armadillidium vulgare*. J Morphol 144(3):337-359.

Vogt G. 1994. Life-cycle and functional cytology of the hepatopancreatic cells of *Astacus astacus* (Crustacea, Decapoda). Zoomorphology 114(2):83-101.

Wägele J-W, Welsch U, Müller W. 1981. Fine structure and function of the digestive tract of *Cyathura carinata* (Krøyer) (Crustacea, Isopoda). Zoomorphology 98(1):69-88.

Wang L, Li F, Wang B, Xiang J. 2012. Structure and partial protein profiles of the peritrophic membrane (PM) from the gut of the shrimp *Litopenaeus vannamei*. Fish & Shellfish Immunology 33(6):1285-1291.

Wang P, Granados RR. 1998. Observations on the presence of the peritrophic membrane in larval *Trichoplusia ni* and its role in limiting Baculovirus infection. Journal of Invertebrate Pathology 72(1):57-62.

Wanninger AWG. 2007. The application of confocal microscopy and 3D imaging software in Functional, Evolutionary, and Developmental Zoology: reconstructing myo- and neurogenesis in space and time. In: Méndez-Vilas A, Diaz J, editors. Modern research and educational topics in microscopy Vol 1: Applications in Biology and Medicine. Badajoz, Spain: FORMATEX. p 353-361.

Welinder BS. 1974. The crustacean cuticle—I. Studies on the composition of the cuticle. Comparative Biochemistry and Physiology Part A: Physiology 47(2):779-787.

Welinder BS. 1975. The crustacean cuticle - III. Composition of the individual layers in *Cancer pagurus* cuticle. Comparative Biochemistry and Physiology Part A: Physiology 52(4):659-663.

Welinder BS, Roepstorff P, Andersen SO. 1976. The crustacean cuticle—IV. Isolation and identification of cross-links from Cancer pagurus cuticle. Comparative Biochemistry and Physiology Part B: Comparative Biochemistry 53(4):529-533.

Wilde JE, Linton SM, Greenaway P. 2004. Dietary assimilation and the digestive strategy of the omnivorous anomuran land crab *Birgus latro* (Coenobitidae). Journal of Comparative Physiology B 174(4):299-308.

Williams CL, Dillaman RM, Elliott EA, Gay DM. 2003. Formation of the arthrodial membrane in the blue crab, *Callinectes sapidus*. J Morphol 256(3):260-269.

Williams MJ. 1981. Methods for analysis of natural diet in portunid crabs (Crustacea:Decapoda:Portunidae). J Exp Mar Biol Ecol 52(1):103-113.

Willis JH. 1999. Cuticular proteins in insects and crustaceans. American Zoologist 39(3):600-609.

Witkus ER, Grillo RS, Smith WJ. 1969. Microtubule bundles in the hindgut epithelium of the woodlouse *Oniscus ascellus*. Journal of Ultrastructure Research 29(3):182-190.

Yonge CM. 1924. Studies on the comparative physiology of digestion II. - The mechanism of feeding, digestion, and assimilation in *Nephrops norvegicus*. British Journal of Experimental Biology 1:343-389.

Yonge CM. 1932. On the nature and permeability of Chitin. I.--The Chitin lining the Foregut of Decapod Crustacea and the function of the Tegumental Glands. Proceedings of the Royal Society B: Biological Sciences 111(772):298-329.

CONCLUSIONES

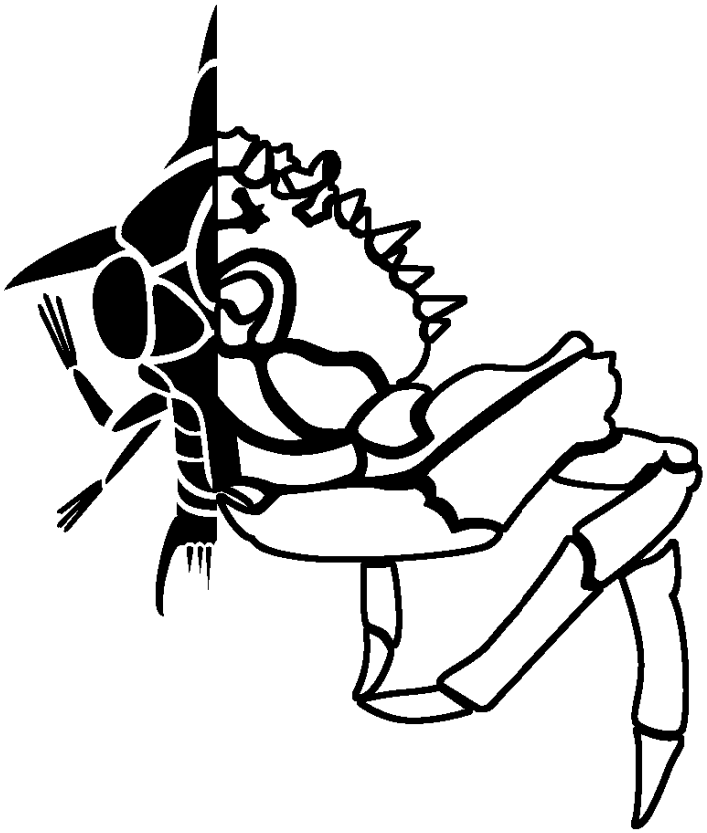

Las conclusiones de esta tesis permitirán mejorar el cultivo del centollo en dos frentes: cultivo larvario (bloque 1) a nivel de la optimización de los factores ambientales, y anatomía del sistema digestivo (bloque 2) permitiendo avanzar en los estudios de nutrición con objeto de incrementar la tasa de crecimiento y/o la reproducción en cautividad. Los objetivos específicos por cada uno de los bloques se describe a continuación.

BLOQUE 1. En lo que respecta a la optimización del cultivo larvario, los resultados más importantes pueden integrarse a lo largo de los siguientes puntos:

Temperatura. La óptima es 21 ± 1 °C. Desde la perspectiva del cultivo acuícola, no se recomiendan temperaturas inferiores o superiores. Temperaturas inferiores incrementan la duración del desarrollo larvario sin suponer un aumento significativo en la supervivencia. Por su parte, temperaturas superiores aumentan significativamente la mortalidad pero no reducen significativamente la duración del desarrollo larvario.

Salinidad. La óptima es 35 ± 1 psu. Nuestros ensayos han demostrado que *Maja brachydactyla* es una especie marcadamente estenohalina y vulnerable a los cambios de salinidad. Se ha demostrado que desviar la concentración salina más allá del óptimo implica un marcado aumento de la mortalidad, sin afectar claramente a la duración del desarrollo larvario.

Iluminación. En términos generales, *Maja brachydactyla* es poco sensitiva al régimen lumínico durante el desarrollo larvario, pero requiere un ciclo diario de luz-oscuridad. En ese sentido, debe evitarse un régimen de constante oscuridad ya que tiende a reducir la supervivencia y alargar la duración del desarrollo larvario.

Asentamiento. El asentamiento puede llevarse a cabo tanto en condiciones de cultivo individual como comunal. Nosotros obtuvimos mejores resultados con las condiciones de cultivo comunal (densidad inicial de 10 megalopas L^{-1}) en comparación con las condiciones de cultivo individual. Es una especie sin requerimientos especiales, no siendo necesario ningún tipo de sustrato y los exudados no tienen influencia en el cultivo.

BLOQUE 2. En relación a la descripción ontogénica del sistema digestivo, las observaciones más importantes pueden resumirse a lo largo de los siguientes puntos:

Morfología general. Resulta óptimo combinar la micro-CT con técnicas histológicas para estudiar la anatomía general de las larvas de decápodos. La micro-CT destaca el tracto digestivo, los ganglios nerviosos, la musculatura y estructuras cuticulares gruesas. Las técnicas histológicas permiten identificar estructuras finas más difíciles de observar mediante micro-CT, como glándulas, vasos y senos, así como el sistema branquial.

Esófago y tracto digestivo posterior. Epitelio simple columnar con células ricas en interdigitaciones y estructuras filamentosas. El epitelio está cubierto apicalmente por una cutícula que proyecta micro-espinas y rodeado basalmente por un tejido conectivo en el que aparecen gruesos paquetes musculares y glándulas de roseta. Se asume un rol de transporte.

Estómago. Posee estructuras especializadas: sacos cardiacos, osículos, molino gástrico, válvula-cardio pilórica y filtros pilóricos. Cada estructura posee un revestimiento cuticular distintivo, siendo posible que la cutícula se especialice de acuerdo con el rol de la estructura. El estómago tiene funciones de masticación y filtración.

Derivados del endodermo embrionario. Son la glándula digestiva, tracto digestivo medio y sus ciegos asociados. Poseen un epitelio simple columnar con células ricas en microvellosidades. La región basal posee retículo endoplásmático liso y mitocondrias. En estas células se ha observado una importante actividad secretora. Sus funciones se asocian con la digestión, absorción de nutrientes y síntesis de la membrana peritrófica.

Desarrollo ontogénico. La estructura básica de la mayoría de órganos es similar desde la eclosión hasta la etapa adulta, donde las principales diferencias son células epiteliales más altas y mayor grosor del conectivo y paquetes musculares, probablemente debido a sus mayores requisitos de mantenimiento y soporte. El estómago conserva su estructura desde el estadio de megalopa hasta la etapa adulta, con cambios menores en osículos y molino gástrico. Estos datos demuestran que el sistema digestivo es funcional desde el momento de la eclosión.

ANEXO

ARTÍCULOS PUBLICADOS

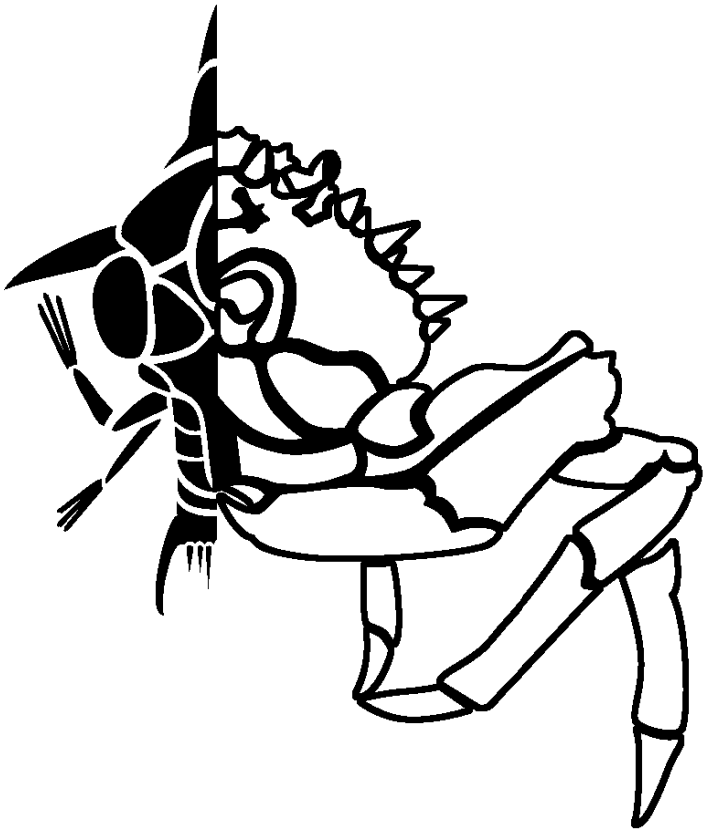

Journal of Shellfish Research, Vol. 34, No. 3, 1073–1083, 2015.

THE EFFECTS OF TEMPERATURE AND SALINITY ON THE SURVIVAL, GROWTH AND DURATION OF THE LARVAL DEVELOPMENT OF THE COMMON SPIDER CRAB *MAJA BRACHYDACTYLA* (BALSS, 1922) (BRACHYURA: MAJIDAE)

DIEGO CASTEJÓN,[1]* GUIOMAR ROTLLANT,[2] LUIS GIMÉNEZ,[3] GABRIELA TORRES[3] AND GUILLERMO GUERAO[4]

[1]*Subprograma Cultius Aquàtics, IRTA, Ctra. de Pobre Nou, Km 5.5, Sant Carles de la Ràpita 43540, Tarragona, Spain;* [2]*Departament de Recursos Marins Renovables, Institut de Ciències Del Mar, CSIC, Passeig Marítim de la Barceloneta 37-49, Barcelona 08003, Spain;* [3]*School of Ocean Sciences, Bangor University, Menai Bridge, Anglesey, LL59 5AB, United Kingdom;* [4]*PS Fabra i Puig 344, Barcelona 08031, Spain*

ABSTRACT The effect of temperature and salinity on the larval development of the common spider crab *Maja brachydactyla* (Balss, 1922) were studied in the laboratory. Larvae were reared at different salinities (0–45) at constant temperature, and under six different combinations of temperature (18 and 21°C) and salinity (30, 35, and 40). The survival and developmental time from newly hatched zoeae to the megalopa stage and from megalopa to the first juvenile stage was quantified; the 24 h median lethal salinity (LS_{50}) for first zoeal stage was calculated. Dry mass (DM), elemental body composition (Carbon, Hydrogen, Nitrogen) and carbon: nitrogen ratio (C:N) were determined in both starved and nourished zoeae. The lower and upper LS_{50} for *M. brachydactyla* first zoea in 24 h were 19.9 and 56.0, respectively; similar to other marine stenohaline brachyuran larvae. The megalopa stage was reached in a salinity range from 30 to 40. The highest survival rates to the first juvenile stage were observed at salinity: 35 and temperature: 21°C. Salinity was the key parameter for the survival to first juvenile, whereas the temperature had a higher effect over the duration of the larval development. The greatest loss of DM in starving and nourished zoeae was observed at low salinity (25). No differences were found in DM or C:N during the megalopa stage. The culture and ecological implications of the salinity tolerance of *M. brachydactyla* larvae are discussed.

KEY WORDS: *Maja brachydactyla*, Brachyura, growth, larval development, salinity, temperature

INTRODUCTION

The common spider crab *Maja brachydactyla* (Balss, 1922) is a brachyuran widely distributed in the eastern Atlantic, from the southern British Isles to the western Sahara (including Azores and Canary Islands), and southwestern Mediterranean (Abelló et al. 2014). This is a species of high commercial value whose main fisheries are located in France, United Kingdom, Ireland, and Spain, with an average of total annual captures of 5,600 and 7,000 tonnes between 2008 and 2012 (FAO 2012). This species shows an abbreviated larval development, consisting of a zoeal phase with two zoeal stages and a megalopa stage. The short larval duration makes *M. brachydactyla* a very attractive species for aquaculture (Guerao et al. 2008). Previous studies have covered the morphological description of larval stages and molt cycles (Guerao et al. 2008, Guerao & Rotllant 2010, Guerao et al. 2010), growth patterns (Andrés et al. 2008) and ontogenetic changes in biochemistry (Andrés et al. 2007, Andrés et al. 2010a).

In the Galician coast (NW Iberian Peninsula), the larval release and recruitment of *Maja brachydactyla* occur in nearshore waters (Corgos et al. 2011), where the larvae may be exposed to salinity fluctuations due to the coastal and estuarine influences (Cabanas et al. 1987, Gago et al. 2011). Since the salinity is one of the key factors affecting survival, growth, development, and distribution of aquatic crustacean larvae (Charmantier 1998, Anger 2003, Torres et al. 2011), the study of the salinity tolerance during the larval development is interesting for inferring the ecological adaptations of the larvae in the field. The range of salinities for survival and development of crustacean larvae depends on the ability and range of the osmoregulatory capacity, driven by adaptations to osmotic stress that can change drastically during the ontogeny (Charmantier 1998, Charmantier et al. 2001). According to Anger (2003), if salinity exceeds the tolerance range, there usually appears a stress response, characterized by reduced survival, prolongation of the developmental time, and a depression of the feeding and growth rates. Reductions in growth rates have also been correlated with the capacity to osmoregulate (Mikami & Kuballa 2007, Torres et al. 2011). In this sense, the precise knowledge of the range of salinity tolerance is necessary for both ecological and culture approaches.

Temperature is another factor with important implications for many ecological processes, including larval dispersal and mortality, population connectivity, and recruitment dynamics (O'Connor et al. 2007). Temperature is known to have significant influence on survival, molting intervals, and total duration of larval development (Anger 1983, Minagawa 1990, González-Ortegón & Giménez 2014). Many studies also have shown that temperature can modify the manner in which salinity can influence the survival and duration of the larval development of brachyuran species (Costlow Jr. et al. 1962, Costlow Jr. et al. 1966, Reed 1969, Baylon & Suzuki 2007, Nurdiani & Zeng 2007). Synergistic or other multiple stressors effects are likely to occur in coastal marine organisms as a consequence of natural variations in precipitation and estuarine discharge; they are currently an objective of intensive interest because variations caused by climate change and anthropogenic influence can also affect the capacity of organisms to cope with environmental stressors (González-Ortegón et al. 2013, Przeslawski et al. 2015). The larvae of *Maja brachydactyla* develop in coastal

*Corresponding author. E-mail: diego.castejon.dcb@gmail.com
DOI: 10.2983/035.034.0334

waters where freshwater flux, evaporation, and thermal radiance create dynamic changes in temperature and salinity, all of which can cause multiple stressor effects; such effects are also of importance for the optimization of techniques in aquaculture.

Hence, the main objective of this study was to determine the short- and long-term influence of salinity and the combined effects of temperature and salinity on larval development of *Maja brachydactyla* to better understand the likely conditions for larval recruitment in the field and obtain valuable information for the optimization of culture techniques.

MATERIAL AND METHODS

Broodstock Maintenance

The broodstock of *Maja brachydactyla* was captured with commercial fishery boats in the NW Iberian Peninsula coast (Ría de A Coruña, Galicia, Spain) and transported to the Institut de Recerca i Tecnologia Agroalimentàries facilities (Sant Carles de la Ràpita, Tarragona, Spain) in December 2012. The broodstock was kept in 2,000 l cylindrical tanks connected to a recirculation unit (renewal rate = 3.5 $m^3 \cdot h^{-1}$) maintained at controlled conditions of temperature (18 ± 1°C), salinity (35 ± 1), photoperiod (12 h light: 12 h dark), and light intensity (25 lux, fluorescent lights). The broodstock was fed daily with a combination of fresh mussels (*Mytilus* sp. four times per week), frozen mussels (*Mytilus* sp., twice per week), and frozen crabs (*Liocarcinus depurator*, once per week).

Larval Culture System

The designed larval culture system was a modification of a previous rearing system published by Anger et al. (1991) and Andrés et al. (2010b) for experimental and small-scale culture of brachyuran larvae. Each experiment was carried out in 200 l aquaria (100 × 40 × 50 cm) used as incubation chambers (Fig. 1). Experimental glass beakers with 600 ml capacity were located inside each aquarium. The temperature was maintained constant with calibrated submersible thermostat-controlled heaters (Eheim Jäger, Finsterrot, Germany) and distributed by an air lift. Daily the temperature was measured with portable meters (precision: 0.1°C; WTW ProfiLine Oxi 3210, Weilheim, Germany). The aquaria were illuminated from above with 1,000 lux LED lights; the light intensity was measured with a light meter (precision: 1 lux; Lx-101, Lutron Electronic Enterprise, Taipei, Taiwan). The photoperiod of 12 h light: 12 h dark was controlled with 24 h programmable timers.

Low salinities were obtained by diluting filtered seawater with distilled water and higher salinities by adding sea salt (Natural Salt Mix, Oceanic, Dallas, TX). The salinity of the experimental glass beakers was measured daily using a portable handheld salinity refractometer (precision: 1, range: 0–100; Shenzhen Handsome Technology Co. Ltd., Guandong, China). The glass beakers were filled with 500 ml of the test salinities according to each treatment.

The newly hatched larvae (ZI_0) were transferred by outflow pipe to special collectors (35 l fiberglass cylindroconical baskets opened by 12 × 18 cm windows covered with 150 μm mesh). Only actively swimming zoeae of the same hatch within a maximum ~15 h after hatching were selected for the experiments.

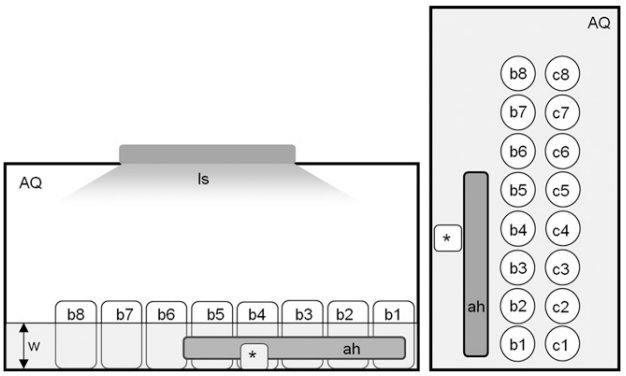

Figure 1. Experimental small-scale rearing system for *M. brachydactyla* larvae. Lateral view (left); upper view (right). Nomenclature: (AQ), 200 L aquarium (100 × 40 × 50 cm); (ah), submersible thermosthat-controlled heater; (b1 to b8), experimental glass beakers with larvae; (c1 to c8), reserve experimental vessels (without larvae, filled with clean filtered seawater); (ls), light source: LED lights; (w), water bath; (*) air lift.

Following Andrés et al. (2007, 2008), larvae were transferred to glass culture beakers at an initial density of 60 zoeae l^{-1} without prior adaptation, the experiment continued until all the larvae died or molted to megalopa. The newly molted megalopae (M_0) were transferred to new experimental glass beakers at an initial density of 20 megalopae l^{-1} and kept under the previous experimental conditions until all the animals died or reached the first juvenile instar (J_0). The confirmation of the death was carried out using a Nikon SMZ800 stereomicroscope; the total lack of movement of appendages and the immobility of the heart were used as criteria.

The larvae were fed daily *ad libitum* with fresh *Artemia* sp. Kellogg, 1906 nauplii and metanauplii (INVE Aquaculture Nutrition, Salt Lake, UT). Living larvae were collected daily by carefully pipetting to reserve glass beakers previously prepared at the same temperature and salinity conditions.

Experiments

Acute Osmotic Stress Tolerance

This first experiment used newly hatched zoeae in starving conditions to ascertain the range of salinity tolerance. The study used six salinity treatments ranging from 0 to 55 (0, 15, 25, 35, 45, and 55 ± 1) with four replicates per treatment. The total of living and dead specimens was counted after 3 days. Samples for dry mass (DM) and elemental body composition analysis were taken. The temperature was constant at 19.7 ± 0.2°C.

Median Lethal Salinity in 24 h

In this second experiment, newly hatched zoeae in starving conditions were used to obtain more detailed information on the range of tolerance. The upper and lower median lethal salinity (LS_{50}) were calculated through two separate experiments keeping larvae around the lower and upper range of tolerance: lower LS_{50} (15, 17, 19, 21, 23, and 25 ± 1); upper LS_{50} (51, 53, 55, 57, 59, and 61 ± 1). Three replicates per treatment were used. In both experimental sets, the total of living and dead specimens was counted after 24 h. The temperature was maintained constant at 19.7 ± 0.1°C.

Chronic Effects of Salinity on Survival and Growth

In this experiment, the long-term responses were studied within the range of salinities (20–45) that were tolerated by the starving zoea I (six salinity treatments: 20, 25, 30, 35, 40, and 45 ± 1). The survival and developmental time were tested using four replicates per treatment; additional replicates for DM and elemental body composition analysis were used. The temperature was constant at 22 ± 1°C. The following response variables were studied: (1) the duration of the zoeal phase, (2) the duration of the megalopa stage, (3) the survival to the megalopa stage, and (4) the survival from the megalopa to the first juvenile stage. Since the differentiation between zoeae stages required the individual examination of the larvae under the stereomicroscope, the study was decided to focus the research in the zoeal phase to reduce the manipulation and potential damage of the larvae and increase the chances of survival until M_0 and J_0.

Combined Effects of Salinity and Temperature on Survival and Growth

This experiment was used to understand how temperature may modulate the effect of salinity on survival and growth. The experiment used two temperature regimes: 18 and 21 ± 1°C combined with three salinity levels: 30, 35, and 40 ± 1, giving a total of six temperature–salinity combinations. Four replicates per treatment were used. The response variables measured were as stated in the previous experiment.

Dry Mass and Elemental Body Composition

The DM and elemental body composition [Carbon, Hydrogen, Nitrogen (CHN)] were analyzed in Acute Osmotic Stress Tolerance and Chronic Effects of Salinity on Survival and Growth experiments to study the acute and chronic effects of the salinity on the growth. Each treatment used five replicates per zoeae phase and megalopa stage. Each analysis (DM and CHN) required five zoeae and three megalopae, respectively. The zoeae were sampled as newly hatched (ZI_0) and in intermolt (ZI_{2-3}), whereas the megalopae were sampled when newly molted (M_0). The larvae were gently rinsed in distilled water for 10–20 sec and blotted dry on a metal sieve with filter paper. Subsequently, the larvae were transferred to preweighed tin capsules pressed for Elemental Microanalysis and stored at –20°C.

Analyses of DM and CHN were carried out at the School of Ocean Sciences (Bangor University, Menai Bridge, UK) following standard techniques (Anger & Harms 1990, D'Urban Jackson et al. 2014). Samples were freeze dried in a vacuum drier (Edwards Super Modulyo) for 24 h and DM was determined with a Mettler Toledo MX5 microbalance (precision: 1 μg, capacity: 5.1 g). Elemental Analysis was performed using a CHNS-O Analyzer (FlashEA 1112 Series).

Statistical Analysis

The statistical treatment of the data was performed using R version 3.2.0 (R Development Core Team 2015). The median lethal salinity was calculated using a general linear model with the «dosing.p» function of the R package «MASS 7.3-4» (Venables & Ripley 2002). One way analysis of variance (ANOVA) was performed using salinity as factor. The combined effects of temperature and salinity were tested through two-way Type III ANOVA applying R package «car 2.0-25» (Fox & Weisberg 2011). Comparisons between groups after finding significant differences were performed by Tukey's honest significant difference test. Normality and homogeneity were tested by Shapiro–Wilk and Levene tests, respectively. Kruskal–Wallis test was carried out when the data did not show normality or homogeneity of variance. The critical level (α) to reject the null hypothesis was 0.05.

RESULTS

Acute Osmotic Stress Tolerance

All larvae exposed to a salinity of 0 and 15 died in the first 24 h. In the salinity range from 25 to 55, the survival was higher than 90% without significant differences among treatments (Kruskal–Wallis: $X^2_3 = 2.76$, $P = 0.43$).

Salinity affected the DM and elemental body composition of the 3-day-old zoeae (ANOVA: $F_{3,15} = 32.01$, $P < 0.001$). The stronger effect in decreasing DM was produced by the low salinity (25); whereas only a minor DM reduction was produced by the higher salinities, 45 and 55 (Table 1). Larvae reared at low and seawater salinity (35) showed higher percent carbon and nitrogen than larvae reared at extremely high salinities (C: $F_{3,14} = 200.9$, $P < 0.001$; N: $F_{3,14} = 169.9$, $P < 0.001$). The carbon content per individual also decreased at higher salinity, but the nitrogen content per individual did not vary between treatments (C: $F_{3,14} = 6.11$, $P < 0.01$; N: $F_{3,14} = 0.82$, $P = 0.51$). The C:N ratio indicated that at high and low salinity, the losses of C were proportionally larger than losses of N ($F_{3,15} = 79.19$, $P < 0.001$; Table 1).

Median Lethal Salinity in 24 h

The lower LS_{50} was at 19.9, whereas the upper LS_{50} was at 56.0 (Fig. 2). The larvae exposed at 20 or lower salinities immediately sank passively to the bottom of the culture glass beakers; those larvae exposed at 56 or higher salinities remained swimming actively in the glass culture beakers until they died.

Chronic Effects of Salinity on Survival and Growth

Survival and Duration of Larval Development

Total mortality occurred after 24 h at salinity 20, after 5 days at salinity 45 and after 7 days at salinity 25, coinciding with the molt to megalopa stage (Fig. 3). The development until the megalopa stage only occurred in the salinity range from 30 to 40, but there were significant differences among treatments ($F_{2,9} = 16.52$, $P < 0.001$). The highest survival was observed at salinity 35 (51.7 ± 11.4%), followed by salinity 30 (39.2 ± 9.6%), and salinity 40 (11.4 ± 9.3%; Fig. 3). The molt to zoea II occurred between the 3rd and 4th day of culture from hatching (salinity range: 25–45). The duration of the zoeal phase until M_0 was on average 7.1 ± 0.8 days, but significant differences among salinity treatments were not observed ($F_{2,8} = 0.64$, $P = 0.55$).

The highest survival from megalopa to first juvenile occurred at salinity 35 (37.5 ± 4.8%); and the average duration of the megalopa stage was 6.2 ± 1.1 days. High mortality rates were observed at other salinities (100% of mortality at salinity 40;

TABLE 1.

Acute effects of salinity on growth under starving conditions in *Maja brachydactyla* zoeae I from ~15 h after hatch (0 day) and in intermoult (3 days from hatch).

Age (days)	Salinity	DM (μg)	Carbon (μg ind^{-1})	Carbon (%)	Nitrogen (μg ind^{-1})	Nitrogen (%)	C:N ratio
0	–	104 ± 1	35.7 ± 0.3	34.4 ± 0.1	9.20 ± 0.05	8.85 ± 0.08	3.89 ± 0.03
3	25	91 ± 1^{a}	28.3 ± 0.3^{a}	31.3 ± 0.2^{a}	7.37 ± 0.10	8.14 ± 0.04^{a}	3.84 ± 0.02^{ab}
	35	93 ± 1^{b}	28.2 ± 0.4^{a}	30.2 ± 0.2^{b}	7.28 ± 0.12	7.80 ± 0.05^{b}	3.87 ± 0.01^{a}
	45	96 ± 2^{c}	28.0 ± 0.2^{ab}	29.2 ± 0.3^{c}	7.32 ± 0.05	7.64 ± 0.04^{c}	3.82 ± 0.01^{b}
	55	97 ± 1^{c}	27.4 ± 0.4^{b}	28.2 ± 0.1^{d}	7.34 ± 0.09	7.56 ± 0.01^{c}	3.73 ± 0.02^{c}

Different letters indicate significant difference ($P < 0.05$) among the treatments.
Dry mass (DM, μg), carbon content (μg ind^{-1}), carbon percentage (%), nitrogen content (μg ind^{-1}), nitrogen percentage (%) and C:N ratio. Larvae were kept at constant 19.7 ± 0.2°C. Values are expressed as average ± SD.

only one individual reached the juvenile stage at salinity 30 after 5 days of megalopa stage).

Growth and Elemental Body Composition

Salinity had a significant effect on the larval growth and elemental body composition. Two-day-old zoeae showed a DM increment in all treatments except at salinity 25 ($F_{4,20} = 12.12$, $P < 0.001$; Table 2); the carbon and nitrogen content per individual also increased in all treatments except at 25 (C: $F_{4,20}$ 3.53, $P < 0.05$; N: $F_{4,20} = 3.58$, $P < 0.05$). The percent carbon and nitrogen was significantly lower at salinity of 40 and 45 (C: $F_{4,20} = 3.63$, $P < 0.05$; N: $F_{4,20} = 4.70$, $P < 0.01$). Although the C:N ratio differed significantly among treatments ($F_{4,19} = 4.65$, $P < 0.01$), a general trend was not observed (Table 2).

Megalopa from different salinity treatments did not show significant differences in DM ($F_{2,11} = 0.719$, $P = 0.51$), carbon and nitrogen content per individual (C: $F_{2,11} = 2.02$, $P = 0.18$; N: $F_{2,11} = 2.51$, $P = 0.13$), percent nitrogen ($F_{2,11} = 3.05$, $P = 0.09$), or C:N ratio ($F_{2,11} = 1.16$, $P = 0.35$). Only the percent carbon showed a significant response, consisting in decreased levels at higher salinity ($F_{2,11} = 6.98$, $P < 0.05$; Table 3).

Combined Effect of Temperature and Salinity

Survival and Duration of Development

The two-way ANOVA showed a significant interaction between temperature and salinity on survival from hatching to the megalopa stage ($F_{2,18} = 5.26$, $P < 0.05$): survival decreased at salinity 30 and 40 with the temperature increment, but increased at salinity 35. The lowest survival occurred at the combination: salinity 40 and 18°C (22.5 ± 22.3%); but it doubled in the remaining temperature–salinity combinations (Fig. 4). Survival to the juvenile stage was significantly affected by salinity ($F_{2,18} = 11.54$, $P < 0.001$), but not by temperature ($F_{1,18} = 2.08$, $P = 0.16$) or the interaction of both ($F_{2,18} = 0.31$, $P = 0.73$); the highest survival occurred at salinity 35 (average: 62.5 ± 21.2%; Fig. 5). In most cases, mortality occurred at the time of metamorphosis: most individuals failed to metamorphose or metamorphosed with deformities (syndrome of molt cycle).

The duration of the zoeal phase was significantly affected by temperature ($F_{1,17} = 87.71$, $P < 0.001$), but not by salinity ($F_{2,17} = 1.06$, $P = 0.36$) or their interaction ($F_{2,17} = 0.95$, $P = 0.40$).

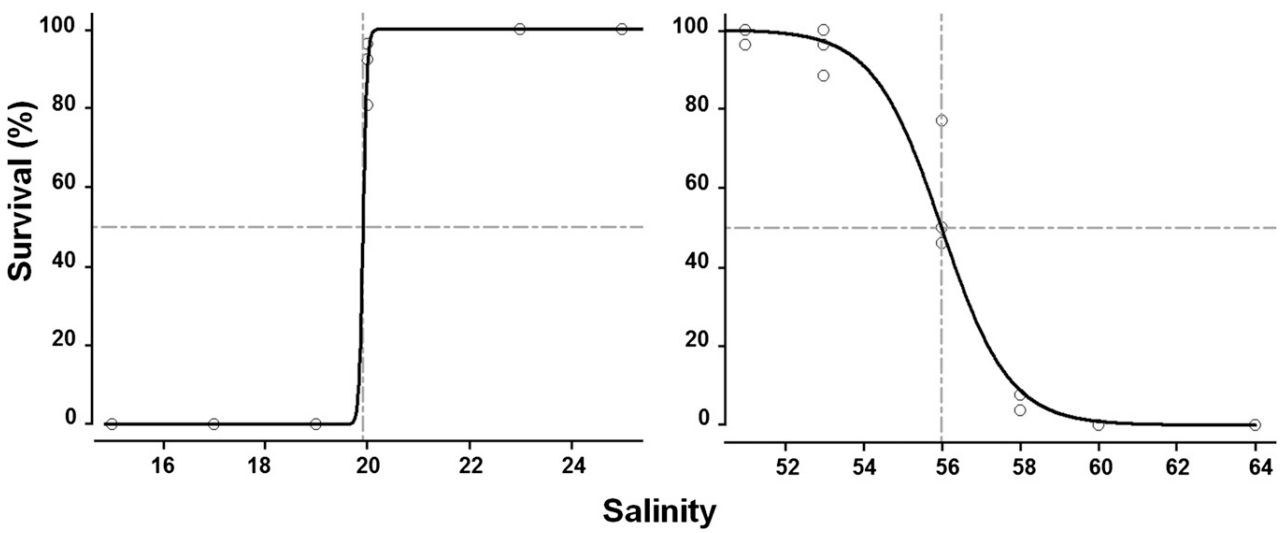

Figure 2. Median Lethal Salinity in *Maja brachydactyla*. Lower (left) and upper (right) median lethal salinity in newly hatched zoeae maintained during 24 h in starvation at 19.7°C.

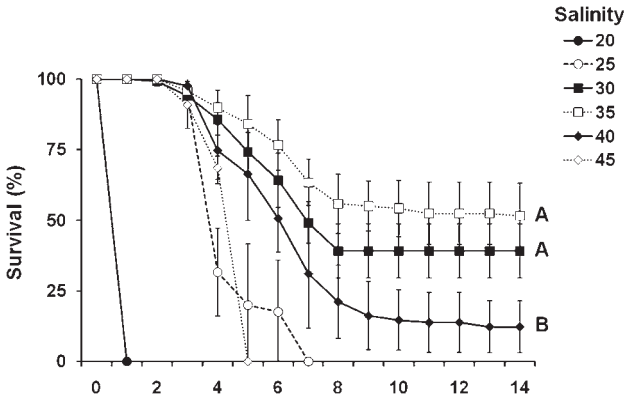

Figure 3. Chronic effect of the salinity on the survival to megalopa stage in *Maja brachydactyla*. Average survival (±SD) of the larvae from hatching to the megalopa stage at different salinity treatments at 22°C (n = 4 per treatment). Different letters indicate significant differences among the treatments (P < 0.05) at the end of the experiment.

The zoeal phase required less time at 21°C (average 7.6 ± 0.7 days) than at 18°C (average 10.2 ± 1.0 days) to complete (Fig. 6). The duration of the megalopa was also affected by temperature ($F_{1,14}$ = 89.7, P < 0.001), whereas salinity ($F_{2,14}$ = 1.62, P = 0.23) and the interaction between temperature and salinity was not significant ($F_{1,14}$ = 2.58, P = 0.13). The megalopa stage required less time to complete at 21°C (average: 6.0 ± 0.5 days) than at 18°C (average: 8.8 ± 1.0 days; Fig. 7).

DISCUSSION

The data showed that larvae of *Maja brachydactyla* are strictly stenohaline. The acute stress restricted the salinity tolerance range from 20 to 56 and outside this range the larvae died in less than 24 h. Larvae tolerated salinities of 25 and 45, but the growth rate was reduced and metamorphosis to megalopae did not occur. The most suitable range for development was between 30 and 40: larvae successfully metamorphosed to the first juvenile stage. Moreover, the highest survival from newly hatched zoeae to first juvenile stage was observed at salinity 35 ± 1. The duration of larval development was not affected by salinity. On the other hand, the highest temperature showed the shorter duration of the larval development (21°C). In general terms, the larval culture of this species required a constant salinity at 35 ± 1. Contrary to other brachyuran species of interest for culture such as *Scylla serrata* (Nurdiani & Zeng 2007), the larval stages of *M. brachydactyla* were not tolerant to salinity levels below 30. These restrictions must be taken into account in the selection of sites or water sources for the culture of this species.

Previous studies that have focused on the osmoregulatory physiology of the majid crabs showed that generally they are osmoconformers or weak regulators with high sensitivity to variations in salinity (Dakin 1912, Péqueux 1995). The vulnerability of *Maja brachydactyla* to low salinity is also reflected in the decrement of larvae production by adults (Rotllant et al. 2015) and a narrow range of acute salinity tolerance (LS_{50} in 24 h) in newly hatched zoeae (salinity range: 20–56). A similar LS_{50} range was observed in the larvae of other brachyurans such as the cancroid *Cancer irroratus* (salinity range: 15–46: Charmantier & Charmantier-Daures 1991) or the majoid *Chionoecetes opilio* (salinity range: 9.5–42.5: Charmantier & Charmantier-Daures 1995). Other brachyuran larvae have a broader salinity tolerance range: for example, the grapsoid *Armases miersii* and the xanthoid *Rhithropanopeus harrisii* can complete the larval development in a salinity range from 5 to 35 (Anger 1996; Forward Jr. 2009), whereas the first zoeae of *Armases ricordi* tolerate a salinity range from 5 to 55 during 6 days (Diesel & Schuh 1998). These differences in the salinity tolerance range correspond to adaptations to fluctuations in the salinity in the field (Anger 2001). Larvae with a narrow salinity tolerance inhabit waters with oceanic influence (Bigford 1979, Charmantier & Charmantier-Daures 1995) whereas those with broader salinity tolerance usually inhabit environments with high salinity fluctuations, such as rocky pools or estuaries (Costlow Jr. et al. 1966, Anger 1995, Forward Jr. 2009). The Table 4 summarizes the relationship between the range of salinity tolerance of brachyuran larvae and their habitat. In some taxa, there are specializations to some environments (e.g., estuarine environments in Grapsoidea and Portunoidea and nearshore/offshore in Majoidea); but exceptions are associated with habitat specialization (e.g., *Pachygrapsus transversus* in grapsoid or *Halicarcinus rostratus* in majoid crabs, see Table 4). Thus, it can be hypothesize that the larval tolerance to salinity is more influenced by adaptations to field conditions than by the phylogeny.

The optimal salinity for the larval development of *Maja brachydactyla* is 35 ± 1, coincides with the expected conditions

TABLE 2.

Acute effects of salinity on growth under feeding conditions in *Maja brachydactyla* zoeae I from ~15 h after hatch (0 days) and in intermoult (2 days from hatch).

Age (days)	Salinity	DM (μg)	Carbon (μg ind^{-1})	Carbon (%)	Nitrogen (μg ind^{-1})	Nitrogen (%)	C:N ratio
0	–	95 ± 1	30.6 ± 0.4	32.2 ± 0.3	8.01 ± 0.13	8.45 ± 0.10	3.82 ± 0.02
2	25	98 ± 3^{a}	32.1 ± 1.0^{a}	32.7 ± 0.4^{ab}	8.30 ± 0.26^{a}	8.45 ± 0.11^{ab}	3.87 ± 0.02^{ab}
	30	110 ± 4^{b}	36.5 ± 1.6^{ab}	33.2 ± 0.4^{a}	9.33 ± 0.41^{ab}	8.48 ± 0.09^{b}	3.91 ± 0.01^{a}
	35	110 ± 5^{b}	35.2 ± 2.5^{ab}	32.0 ± 0.7^{ab}	9.06 ± 0.56^{ab}	8.26 ± 0.15^{bc}	3.86 ± 0.02^{b}
	40	113 ± 2^{b}	35.6 ± 3.1^{ab}	31.5 ± 1.5^{b}	9.11 ± 0.73^{ab}	8.05 ± 0.32^{c}	3.91 ± 0.03^{a}
	45	118 ± 1^{b}	37.3 ± 2.9^{b}	31.5 ± 1.0^{b}	9.56 ± 0.70^{b}	8.08 ± 0.25^{ac}	3.90 ± 0.03^{ab}

Different letters indicate significant difference (P < 0.05) among the treatments.
Dry mass (DM, μg), carbon content (μg ind^{-1}), carbon percentage (%), nitrogen content (μg ind^{-1}), nitrogen percentage (%) and C:N ratio. Larvae were kept at constant 22 ± 1°C. Values are expressed as average ± SD.

TABLE 3.

Chronic effects of salinity on growth under feeding conditions in *Maja brachydactyla* megalopae from ~15 h after molt.

Salinity	DM (μg)	Carbon (μg ind^{-1})	Carbon (%)	Nitrogen (μg ind^{-1})	Nitrogen (%)	C:N ratio
30	168 ± 12	57.8 ± 4.4	34.3 ± 0.8^{a}	14.9 ± 1.0	8.82 ± 0.18	3.89 ± 0.07
35	171 ± 28	57.2 ± 10.1	33.4 ± 1.2^{ab}	15.0 ± 2.2	8.78 ± 0.36	3.81 ± 0.13
40	158 ± 8	50.9 ± 2.2	32.1 ± 0.8^{b}	13.3 ± 0.5	8.40 ± 0.34	3.83 ± 0.06

Different letters indicate significant difference ($P < 0.05$) among the treatments.
Dry mass (DM, μg), carbon content (μg ind^{-1}), carbon percentage (%), nitrogen content (μg ind^{-1}), nitrogen percentage (%) and C:N ratio. Larvae were kept at constant 22 ± 1°C. Values are expressed as average ± SD.

for development in the field: the outer coast of Galicia (NW Iberian Peninsula) shows a constant salinity of ~35, whereas in the inner coast the salinity fluctuates between the 30 in winter and the 35 in summer due to estuarine influence (Cabanas et al. 1987, Corgos et al. 2011, Gago et al. 2011). Exposure of larvae to this estuarine influence cannot be discarded, because the zoeae are released in nearshore areas (Corgos et al. 2011) and they will be distributed by the marine currents as occurs with other brachyuran larvae (Peliz et al. 2007). From the standpoint of salinity, moderate to high survival would be expected because zoeae reached the megalopa stage at 30. Survival might be also maximized as a consequence of the time of release (spring and summer: Corgos et al. 2011), when the fluctuations in salinity are reduced and the average salinity is nearest to the optimal range for this species (Gago et al. 2011).

When the larvae of *Maja brachydactyla* were exposed to very low salinities (near or under the LS_{50}), their immediate reaction was immobilization and dropping to the bottom of the glass culture beakers as observed in other brachyurans (Anger 1985, Kannupandi et al. 2000, Baylon & Suzuki 2007). Anger (1985) suggested that this behavior would enable larvae to reach the lower waters layers, where salinity is higher. This strategy may be useful for *M. brachydactyla* larvae, because in the Galician coast the salinity increases with depth until reaching a maximum of 35.5 (Gago et al. 2011).

The likely salinity conditions at the settlement habitat are still unknown, but the experiments suggest that megalopa would not settle in very shallow habitats, characterized by low or variable salinity. Le Foll (1993) found that juveniles (carapace length > 50 mm) of *Maja brachydactyla* (referred as *Maja squinado*) inhabit sand, mud-sand, gravel, rock, and maërl seafloors, mainly at 15 m depth; however, the habitat of younger juveniles was not found. Corgos et al. (2011) suggested that the recruitment may occur in more shallow habitats (<5 m depth). The same authors also noticed that both juveniles and adults inhabit seafloors with constant salinity around 35, in the range of optimal salinity as shown in this study. Hence, the study propose three possible hypotheses: (1) the megalopae avoid the estuarine influenced waters and their settlement occurs in coastal waters with oceanic characteristics; (2) because the settlement occurs during late spring and summer, the metamorphosis to first juvenile can take place in coastal waters with minimal estuarine influence (i.e., coinciding with a period when the drop in salinity is minimal); (3) the megalopae might tolerate short exposure to low salinity and they migrate shortly after metamorphosis into estuarine-influenced coastal areas. To evaluate these hypotheses, the settlement habitat of *M. brachydactyla* in the field must be determined.

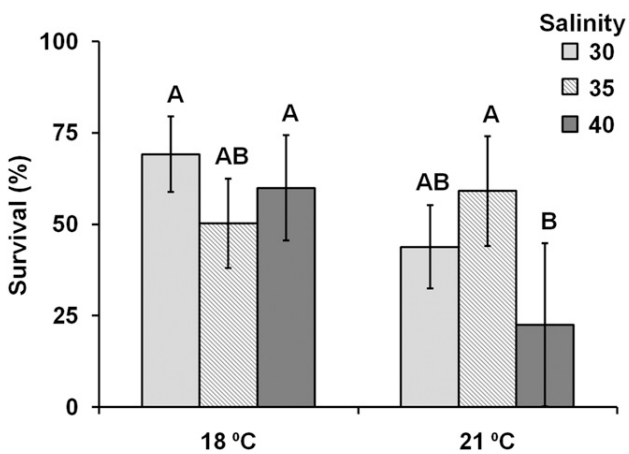

Figure 4. Combined effect of the temperature and salinity on the survival to megalopa stage in *Maja brachydactyla*. Average survival (±SD) of the larvae from hatching to the megalopa stage at different temperature (18 and 21°C) and salinity (30, 35, and 40) combinations (n = 4 per temperature-salinity combination). Different letters indicate significant differences among the treatments ($P < 0.05$).

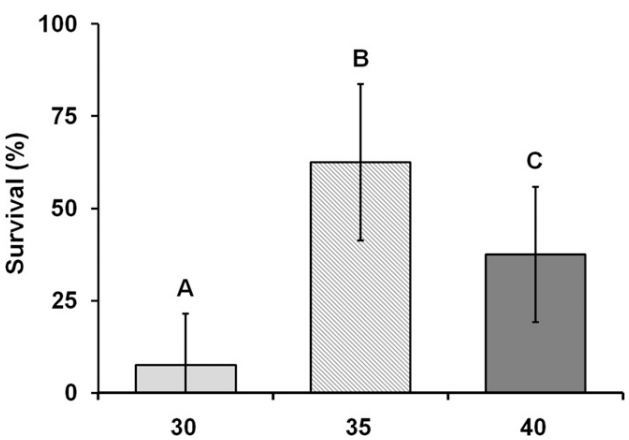

Figure 5. Combined effect of the temperature and salinity on the survival to juvenile stage in *Maja brachydactyla*. Average survival (±SD) of the larvae from megalopa to the juvenile stage at different salinity (30, 35, and 40) treatments (n = 8 per treatment). Different letters indicate significant differences among the treatments ($P < 0.05$).

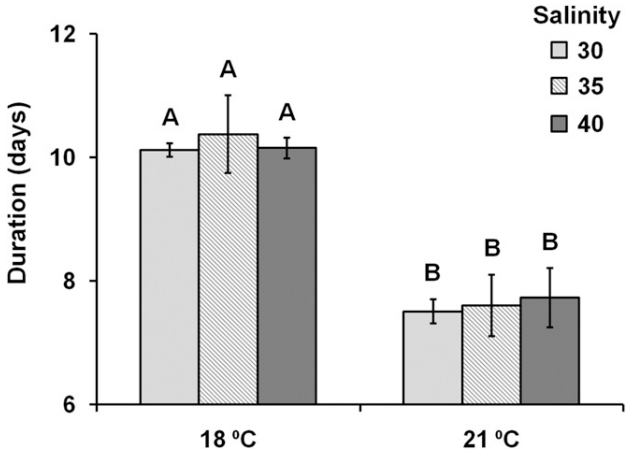

Figure 6. Effect of the temperature and salinity on the duration of the zoeal phase in *Maja brachydactyla*. Average developmental time (±SD) of the larvae from hatching to the megalopa stage at different temperature (18 and 21°C) and salinity (30, 35, and 40) combinations (n = 4 per temperature-salinity combination). Different letters indicate significant differences among the treatments (P < 0.05).

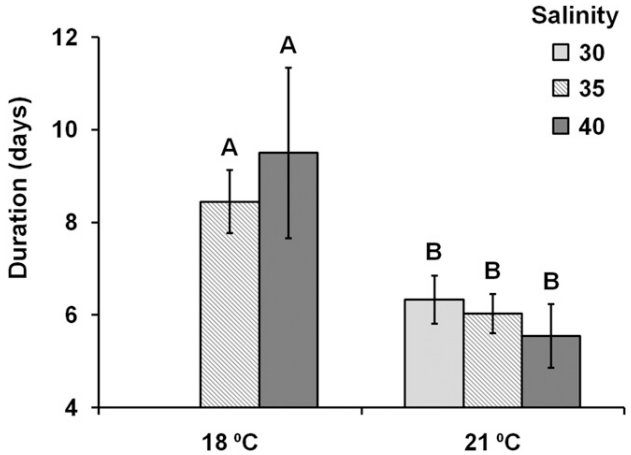

Figure 7. Combined effect of the temperature and salinity on the duration of the megalopa stage in *Maja brachydactyla*. Average developmental time (±SD) of the larvae from the megalopa to the juvenile stage at different temperature (18 and 21°C) and salinity (30, 35, and 40) combinations (n = 4 per temperature-salinity combination). Different letters indicate significant differences among the treatments (P < 0.05).

The temperature mainly influences the duration of the larval development of *Maja brachydactyla*: the duration was significantly shorter at higher temperatures (21 versus 18°C). Temperature increases the metabolic processes, accelerates the molting cycle and reduces the duration of larval development of brachyurans (Costlow et al. 1960, Costlow Jr. et al. 1966, Ong & Costlow 1970, Minagawa 1990, Anger 1991, Mene et al. 1991, Nagaraj 1992, Lárez et al. 2000, Anger 2001, Baylon & Suzuki 2007, Nurdiani & Zeng 2007, Spivak & Cuesta 2009, Hernández et al. 2012). Low salinities increased the duration of the larval development in some brachyuran species (Anger 1985, Mene et al. 1991, Minagawa 1992, Nagaraj 1992), however, the study did not observe this phenomenon in *M. brachydactyla* larvae. Beside the cited studies, the salinity evokes comparatively weak effects over the duration of decapods as reviewed by Anger (2003).

The DM and elemental body composition of the zoeae of *Maja brachydactyla* varied with the salinity. The larvae maintained at salinity 25 in starving conditions showed higher DM losses than the larvae maintained at salinity 35 although both groups maintained similar carbon levels. Because the carbon content is a reliable expression of the biomass content in the individuals (Anger & Dawirs 1982, Anger et al. 2000, Anger 2003), it can be considered that the higher DM losses at salinity 25 could be explained by mineral losses. The larvae of another majoid, *Hyas araneus*, show important mineral depletion under low salinities, probably due to the depression in the mineral accumulation rate and the osmotic loss of mineral content (Anger 2003). In this sense, the higher DM and lower carbon and nitrogen percentages observed in the larvae maintained at salinity 45 and 55 could be explained by a mineral accumulation. On the contrary, well-fed 2-day-old larvae increased their DM in all the salinity treatments except at salinity 25, although similar values of percentage carbon and nitrogen were observed. Short exposures (~50% molt cycle) to low salinities may also cause reduction of DM, lipid and/or protein content in marine brachyuran larvae such as *Cancer pagurus* (Torres et al. 2002) or *Hyas araneus* (Anger 2003, Torres et al. 2011). Similar results were also reported in astacideans larvae such as *Homarus gammarus* and *Nephrops norvegicus* (Torres et al. 2002, Torres et al. 2011). A reduction of feeding (Minagawa 1992), and food conversion (Anger 2003, Torres et al. 2011) has been proposed as an explanation for the reduction in growth at low salinity.

The C:N ratio has been widely applied as an indicator of the lipid:protein ratio in the decapod larvae (Anger & Dawirs 1981, Anger & Dawirs 1982, Anger & Harms 1990, Anger et al. 1998, D'Urban Jackson et al. 2014), including *Maja brachydactyla* (Andrés et al. 2008). Anger and Dawirs (1982) indicated that changes in the C:N ratio indicate shifts in the relative amounts of lipids (plus carbohydrates) and proteins (plus free amino acids); and a decrease in the C:N ratio can be interpreted as a degradation in lipid contents and/or a protein accumulation. In starved zoeae, the lowest C:N ratio occurred at salinity 55, intermediate values were observed at salinity 25 and 45. The reduction of the C:N ratio under unfavorable salinity conditions could be related with a degradation of the lipids due to extra energetic requirements. When larvae were fed, the C:N ratio did not show significant differences among the salinity concentrations tested.

In conclusion, the larvae of *Maja brachydactyla* are stenohaline with a rather narrow range of salinities where complete larval development is achieved. Such narrow limits should restrict the timing and sites of larval settlement, duration of the period of metamorphosis in coastal areas, and the water sources useful for their culture. Extreme salinities (low or high), influence the DM and the elemental body composition of the developing larvae, whereas the temperature can interact with salinity to influence the survival during the zoeal phase.

ACKNOWLEDGMENTS

The Spanish Ministry of Economy and Competitiveness funded bench fees through the INIA project (RTA2011-00004-00-00) to G.G. and a predoctoral fellowship to D.C.

TABLE 4.

Salinity tolerance in the larvae of the brachyuran clade.

Species	Family Superfamily	Saline range	Habitat	References
Cardisoma armatum (Herklots, 1851)	Gecarcinidae Grapsoidea	15–35	Nearshore¶ Estuaries	(Cuesta & Anger 2005)
Cardisoma guanhumi (Latreille, 1828)	Gecarcinidae Grapsoidea	20–40	Nearshore¶ Estuaries	(Costlow & Bookhout 1968)
Aratus pisonii (H. Milne Edwards, 1837)	Grapsidae Grapsoidea	25–35*†‡	Nearshore§¶ Estuaries§	(Díaz & Bevilacqua 1986)
Pachygrapsus gracilis (Saussure, 1858)	Grapsidae Grapsoidea	28–34*†	Nearshore§ Offshore§	(Brossi-Garcia & Rodrigues 1993)
Pachygrapsus transversus (Gibbes, 1850)	Grapsidae Grapsoidea	>32–35*†	Nearshore§ Offshore§	(Brossi-Garcia & Rodrigues 1997)
Armases (=*Sesarma*) *miersii* (Rathbun, 1897)	Sesarmidae Grapsoidea	15–45	Rocky pools	(Anger et al. 2000) (Schuh & Diesel 1995)
Armases ricordi (H. Milne Edwards, 1853)	Sesarmidae Grapsoidea	25–40	Nearshore§¶ Offshore§¶	(Diesel & Schuh 1998)
Armases roberti (H. Milne Edwards, 1853)	Sesarmidae Grapsoidea	20–40	Nearshore§¶ Estuaries §	(Diesel & Schuh 1998)
Armases (=*Metasesarma*) *rubripes* (Rathbun, 1897)	Sesarmidae Grapsoidea	>20–30*†	Nearshore§¶ Offshore§¶	(Luppi et al. 2003)
Selatium (=*Sesarma*) *brockii* (De Man, 1887)	Sesarmidae Grapsosidea	>20–30	Mangroves§	(Kannupandi et al. 2000)
Sesarma cinereum (Bosc, 1802)	Sesarmidae Grapsoidea	20–27	Nearshore§¶	(Costlow et al. 1960) (Seiple & Salmon 1987)
Sesarma curacaoense (De Man, 1982)	Sesarmidae Grapsoidea	15–32	Rocky pools Mangroves	(Anger & Charmantier 2000) (Diesel & Schuh 1998)
Acmaeopleura parvula (Stimpson, 1858)	Varunidae Graposidea	>27–34*†‡	Nearshore Offshore	(Kim & Jang 1987)
Eriocheir sinensis (H. Milne Edwards, 1853)	Varunidae Grapsoidea	15–32†	Nearshore¶ Estuaries	(Anger 1991)
Neohelice (=*Chasmagnathus*) *granulata* (Dana, 1851)	Varunidae Grapsoidea	15–32*†	Nearshore¶ Estuaries	(Anger et al. 2008) (Charmantier et al. 2002)
Pseudohelice subquadrata (Dana, 1851) (referred as *Helice leachi*)	Varunidae Grapsoidea	15–25	Mangroves§	(Mia & Shokita 2002)
Uca rapax (S. I. Smith, 1870)	Ocypodidae Ocypodoidea	25–35*†	Nearshore§¶ Offshore§¶	(Simith et al. 2014)
Uca subcylindrica (Stimpson, 1859)	Ocypodidae Ocypodoidea	0.08–45	Rainfall puddles	(Rabalais & Cameron 1985)
Uca tangeri (Eydoux 1835)	Ocypodidae Ocypodoidea	24–32*†	Nearshore§¶ Offshore§¶	(Spivak & Cuesta 2009)
Uca vocator (J. F. W. Herbst, 1804)	Ocypodidae Ocypodoidea	10–30*†	Nearshore§¶ Offshore§¶	(Simith et al. 2012)
Menippe mercenaria (Say, 1818)	Menippidae Xanthoidea	20–40†	Nearshore	(Ong & Costlow 1970)
Eurytium limosum (Say, 1818)	Panopeidae Xanthoidea	20–32†	Estuaries§	(Messerknecht et al. 1991)
Panopeus herbstii (H. Milne-Edwards, 1834)	Panopeidae Xanthoidea	20–31	Estuaries	(Costlow Jr. et al. 1962) (Dittel & Epifanio 1982)
Rhithropanopeus harrisii (Gould, 1841)	Panopeidae Xanthoidea	2.5–40	Estuaries	(Forward Jr. 2009)
Acheloüs (=*Portunus*) *spinicarpus* (Stimpson, 1871)	Portunidae Portunoidea	30–40	Nearshore Offshore	(Bookhout & Costlow Jr. 1974) (Brandão et al. 2015)
Callinectes sapidus (Rathbun, 1896)	Portunidae Portunoidea	20–31	Nearshore¶ Estuaries	(Costlow & Bookhout 1959) (Epifanio 1995)
Carcinus maenas (Linnaeus, 1758)	Portunidae Portunoidea	20–35*†‡	Nearshore¶ Estuaries	(Nagaraj 1993)
Charybdis feriata (Linnaeus, 1758)	Portunidae Portunoidea	25–35	Nearshore Estuaries	(Baylon & Suzuki 2007) (Fowler et al. 2011)
Necora puber (Linnaeus, 1767)	Portunidae Portunoidea	30–35	Nearshore Offshore	(Choy 1991) (Mene et al. 1991) (Nagaraj 1992)

continued on next page

TABLE 4.

continued

Species	Family Superfamily	Saline range	Habitat	References
Scylla serrata (Forskål, 1775)	Portunidae Portunoidea	20–30	Nearshore Offshore	(Dan & Hamasaki 2011)
Cancer irroratus (Say, 1817)	Cancridae Cancroidea	25–35†	Nearshore Offshore	(Sastry 1970) (Bigford 1979)
Metacarcinus (=*Cancer*) *magister* (Dana, 1852)	Cancridae Cancroidea	20–30*†	Nearshore Offshore	(Reed 1969)
Halicarcinus rostratus (Haswell, 1882) (referred as *H. australis*)	Hymenosomatidae Majoidea	6.4–19.3†	Estuaries	(Lucas & Hodgkin 1970)
Hymenosoma orbiculare (Desmarest, 1823)	Hymenosomatidae Majoidea	21–42	Estuaries Nearshore	(Papadopoulos et al. 2006)
Stenorhynchus seticornis (Herbst., 1788)	Inachidae Majoidea	30–40†‡	Nearshore§ Offshore§	(Hernández et al. 2012)
Mithrax caribbaeus (Rathbun, 1920)	Mithracidae Majoidea	32–38†‡	Nearshore Offshore	(Lárez et al. 2000)
Mithrax pleuracanthus (Stimpson, 1871)	Mithracidae Majoidea	30–35†	Nearshore Offshore	(Goy et al. 1981)
Mithrax verrucosus (H. Milne-Edwards, 1832)	Mithracidae Majoidea	25–35	Nearshore Offshore	(Rengel de Zambrano et al. 1993)
Chionoectes opilio (O. Fabricius, 1788)	Oregoniidae Majoidea	24–38†	Nearshore Offshore	(Yamamoto et al. 2015)
Hyas araneus (Linnaeus, 1758)	Oregoniidae Majoidea	25–35†	Nearshore Offshore	(Anger 1985)
Libinia emarginata (Leach, 1815)	Pisidae Majoidea	~30†	Nearshore Offshore	(Johns & Lang 1977)
Maja brachydactyla (Balss, 1922)	Majidae Majoidea	30–40	Nearshore§ Offshore§	Present study

Saline range suitable for the larval development from newly hatched zoeae to first juvenile stage. The habitat of the larvae also was included.
* The data only comprise the saline range suitable for the larval development from newly hatched zoeae to the megalopa stage.
† Salinity higher than the highest suitable salinity was not tested.
‡ Salinity lower than the lowest suitable salinity was not tested.
§ The habitat of the larvae is extrapolated from experimental data, confirmation with field data is required.
¶ The larvae migrate from the hatching habitat (estuaries, mangroves, rivers or brackish waters) to nearshore and/or offshore waters, i.e., "export strategy" (see Charmantier et al. 2002).

(FPI-INIA). We would like to thank Carles Alcaraz for his advice on the data analysis and Karl B. Andree for his improvement of the article. We thank hatchery technicians at IRTA in Sant Carles de la Ràpita (David Carmona, Glòria Macià, Magda Monllaó and Francesc X. Ingla) for the broodstock maintenance and the setup of the rearing culture system.

LITERATURE CITED

Abelló, P., J. E. García Raso, G. Guerao & F. Salmerón. 2014. *Maja brachydactyla* (Brachyura: Majidae) in the western Mediterranean. *Mar. Biodivers. Rec.* 7:e77.

Andrés, M., A. Estévez & G. Rotllant. 2007. Growth, survival and biochemical composition of spider crab *Maja brachydactyla* (Balss, 1922) (Decapoda: Majidae) larvae reared under different stocking densities, prey:larva ratios and diets. *Aquaculture* 273:494–502.

Andrés, M., A. Estévez, K. Anger & G. Rotllant. 2008. Developmental patterns of larval growth in the edible spider crab, *Maja brachydactyla* (Decapoda: Majidae). *J. Exp. Mar. Biol. Ecol.* 357:35–40.

Andrés, M., A. Estévez, F. Hontoria & G. Rotllant. 2010a. Differential utilization of biochemical components during larval development of the spider crab *Maja brachydactyla* (Decapoda: Majidae). *Mar. Biol.* 157:2329–2340.

Andrés, M., G. Rotllant & C. Zeng. 2010b. Survival, development and growth of larvae of the blue swimmer crab, *Portunus pelagicus*, cultured under different photoperiod conditions. *Aquaculture* 300:218–222.

Anger, K. 1983. Temperature and the larval development of *Hyas araneus* L. (Decapoda: Majidae); extrapolation of laboratory data to field conditions. *J. Exp. Mar. Biol. Ecol.* 69:203–215.

Anger, K. 1985. Influence of salinity on larval development of the spider crab, *Hyas araneus*, reared in the laboratory. In: Gray, J. S. & M. E. Christiansen, editors. Marine biology of polar regions and effects of stress on marine organisms. New York, NY: John Wiley & Sons. pp. 463–474.

Anger, K. 1991. Effects of temperature and salinity on the larval development of the chinese mitten crab *Eriocheir sinensis* (Decapoda: Grapsidae). *Mar. Ecol. Prog. Ser.* 72:103–110.

Anger, K. 1995. Developmental biology of *Armases miersii* (Grapsidae), a crab breeding in supratidal rock pools. I. Facultative lecithotrophy of larval stages. *Mar. Ecol. Prog. Ser.* 117:75–81.

Anger, K. 1996. Salinity tolerance of the larvae and first juveniles of a semiterrestrial grapsid crab, *Armases miersii* (Rathbun). *J. Exp. Mar. Biol. Ecol.* 202:205–223.

Anger, K. 2001. The biology of decapod crustacean larvae. Rotterdam, The Netherlands: A. A. Balkema Publishers.

Anger, K. 2003. Salinity as a key parameter in the larval biology of decapod crustaceans. *Invertebr. Reprod. Dev.* 43:29–45.

Anger, K. & G. Charmantier. 2000. Ontogeny of osmoregulation and salinity tolerance in a mangrove crab, *Sesarma curacaoense* (Decapoda: Grapsidae). *J. Exp. Mar. Biol. Ecol.* 251:265–274.

Anger, K. & R. R. Dawirs. 1981. Influence of starvation on the larval development of *Hyas araneus* (Decapoda, Majidae). *Helgol. Meersunters.* 34:287–311.

Anger, K. & R. R. Dawirs. 1982. Elemental composition (C, N, H) and energy in growing and starving larvae of *Hyas araneus* (Decapoda, Majidae). *Fish Bull.* 80:419–433.

Anger, K. & J. Harms. 1990. Elemental (CHN) and proximate biochemical composition of decapod crustacean larvae. *Comp. Biochem. Physiol.B* 97B:69–80.

Anger, K., K. Riesebeck & C. Püschel. 2000. Effects of salinity on larval and early juvenile growth of an extremely euryhaline crab species, *Armases miersii* (Decapoda: Grapsidae). *Hydrobiologia* 426:161–168.

Anger, K., E. Spivak & T. Luppi. 1998. Effects of reduced salinities on development and bioenergetics of early larval shore crab, *Carcinus maenas*. *J. Exp. Mar. Biol. Ecol.* 220:287–304.

Anger, K., E. Spivak, T. Luppi, C. Bas & D. Ismael. 2008. Larval salinity tolerance of the South American salt-marsh crab, *Neohelice* (*Chasmagnathus*) *granulata*: physiological constraints to estuarine retention, export and reimmigration. *Helgol. Mar. Res.* 62:93–102.

Baylon, J. & H. Suzuki. 2007. Effects of changes in salinity and temperature on survival and development of larvae and juveniles of the crucifix crab *Charybdis feriatus* (Crustacea:Decapoda:Portunidae). *Aquaculture* 269:390–401.

Bigford, T. E. 1979. Ontogeny of light and gravity responses in rock crab larvae (*Cancer irroratus*). *Mar. Biol.* 52:69–76.

Bookhout, C. G. & J. D. Costlow, Jr. 1974. Larval development of *Portunus spinicarpus* reared in the laboratory. *Bull. Mar. Sci.* 24:20–51.

Brandão, M. C., C. A. E. Garcia & A. S. Freire. 2015. Large-scale spatial variability of decapod and stomatopod larvae along the South Brazil Shelf. *Cont. Shelf Res.* 107:11–23.

Brossi-Garcia, A. L. & M. D. Rodrigues. 1993. Zoeal morphology of *Pachygrapsus gracilis* (Saussure, 1858) (Decapoda, Grapsidae) reared in the laboratory. *Invertebr. Reprod. Dev.* 24:197–205.

Brossi-Garcia, A. L. & M. D. Rodrigues. 1997. Zoeal morphology of *Pachygrapsus transversus* (Gibbes) (Decapoda, Grapsidae) reared in the laboratory. *Rev. Bras. Zool.* 14:803–819.

Cabanas, J. M., M. T. Nunes, M. L. Iglesias, N. González & R. Carballo. 1987. Oceanografía de la Bahía de La Coruña. *Bol. Inst. Esp. Oceanogr.* 4:21–28.

Charmantier, G. 1998. Ontogeny of osmoregulation in crustaceans: a review. *Invertebr. Reprod. Dev.* 33:177–190.

Charmantier, G. & M. Charmantier-Daures. 1991. Ontogeny of osmorregulation and salinity tolerance in *Cancer irroratus*; elements of comparison with *C. borealis* (Crustacea, Decapoda). *Biol. Bull.* 180:125–134.

Charmantier, G. & M. Charmantier-Daures. 1995. Osmoregulation and salinity tolerance in zoeae and juveniles of the snow crab *Chionoecetes opilio*. *Aquat. Living Resour.* 8:171–179.

Charmantier, G., C. Haond, J. Lignot & M. Charmantier-Daures. 2001. Ecophysiological adaptation to salinity throughout a life cycle: a review in homarid lobsters. *J. Exp. Biol.* 204:967–977.

Charmantier, G., L. Giménez, M. Charmantier-Daures & K. Anger. 2002. Ontogeny of osmoregulation, physiological plasticity, and larval export strategy in the grapsid crab *Chasmagnathus granulata* (Crustacea, Decapoda). *Mar. Ecol. Prog. Ser.* 229:185–194.

Choy, S. C. 1991. Embryonic and larval biology of *Liocarcinus holsatus* and *Necora puber* (Crustacea: Brachyura: Portunidae). *J. Exp. Mar. Biol. Ecol.* 148:77–92.

Corgos, A., C. Bernárdez, P. Sampedro, P. Verísimo & J. Freire. 2011. Spatial structure of the spider crab, *Maja brachydactyla* population: evidence of metapopulation structure. *J. Sea Res.* 66:9–19.

Costlow, J. D. & C. G. Bookhout. 1959. The larval development of *Callinectes sapidus* Rathbun reared in the laboratory. *Biol. Bull.* 116:373–396.

Costlow, J. D. & C. G. Bookhout. 1968. The effect of environmental factors on development of the land-crab, *Cardisoma guanhumi* Latreille. *Am. Zool.* 8:399–410.

Costlow, J. D., C. G. Bookhout & R. Monroe. 1960. The effect of salinity and temperature on larval development of *Sesarma cinereum* (Bosc) reared in the laboratory. *Biol. Bull.* 118:183–202.

Costlow, J. D., Jr., C. G. Bookhout & R. Monroe. 1962. Salinity-temperature effects on the larval development of the crab, *Panopeus herbstii* Milne-Edwards, reared in the laboratory. *Physiol. Zool.* 35:79–93.

Costlow, J. D., Jr., C. G. Bookhout & R. Monroe. 1966. Studies on the larval development of the crab, *Rhithropanopeus harrisii* (Gould). I. The effect of salinity and temperature on larval development. *Physiol. Zool.* 39:81–100.

Cuesta, J. A. & K. Anger. 2005. Larval morphology and salinity tolerance of a land crab from West Africa, *Cardisoma armatum* (Brachyura: Grapsoidea: Gecarcinidae). *J. Crustac. Biol.* 25:640–654.

D'Urban Jackson, T., G. Torres & L. Giménez. 2014. Survival and development of larvae of two decapod crustaceans under limited access to prey across a thermal range. *J. Plankton Res.* 36:1476–1487.

Dakin, W. M. J. 1912. Aquatic animals and their environment. The constitution of the external medium, and its effect upon the blood. *Int. Rev. Gesamten Hydrobiol. Hydrograph.* 5:53–80.

Díaz, H. & M. Bevilacqua. 1986. Larval development of *Aratus pisonii* (Milne Edwards) (Brachyura, Grapsidae) from marine and estuarine environments reared under different salinity conditions. *J. Coast. Res.* 2:43–49.

Diesel, R. & M. Schuh. 1998. Effects of salinity and starvation on larval development of the crabs *Armases ricordi* and *A. roberti* (Decapoda: Grapsidae) from Jamaica, with notes on the biology and ecology of adults. *J. Crustac. Biol.* 18:423–436.

Dittel, A. I. & C. E. Epifanio. 1982. Seasonal abundance and vertical distribution of crab larvae in Delaware Bay. *Estuaries* 5:197–202.

Drilhon, A. 1935. Etude biochimique de la mue chez les crustacés brachyoures (*Maïa squinado*). *Annales de Physiologie et de Physicochimie Biologique* 11:301–326.

Epifanio, C. E. 1995. Transport of blue crab (*Callinectes sapidus*) larvae in the waters of Mid-Atlantic States. *Bull. Mar. Sci.* 57:713–725.

FAO. 2012. B-42 Crabs, sea-spiders. Capture production by species, fishing areas and countries or areas. In: FAO, editor. FAO yearbook. Fishery and aquaculture statistics. Rome, Italy: FAO.

Forward, R. B., Jr. 2009. Larval biology of the crab *Rhithropanopeus harrisii* (Gould): a synthesis. *Biol. Bull.* 216:243–256.

Fowler, A. E., N. V. Gerner & M. A. Sewell. 2011. Temperature and salinity tolerances of Stage 1 zoeae predict possible range expansion of an introduced portunid crab, *Charybdis japonica*, in New Zealand. *Biol. Invasions* 13:691–699.

Fox, J. & S. Weisberg. 2011. An {R} companion to applied regression, 2nd edition. Thousand Oaks, CA: Sage.

Gago, J., J. M. Cabanas, G. Casas & A. Miranda. 2011. Thermohaline measurements in the continental shelf zone of the NWIberian Peninsula, 1994–2006. *Clim. Res.* 48:219–229.

González-Ortegón, E., J. Blasco, L. Le Vay & L. Giménez. 2013. A multiple stressor approach to study the toxicity and sub-lethal effects of pharmaceutical compounds on the larval development of a marine invertebrate. *J. Hazard. Mater.* 263(Part 1):233–238.

González-Ortegón, E. & L. Giménez. 2014. Environmentally mediated phenotypic links and performance in larvae of a marine invertebrate. *Mar. Ecol. Prog. Ser.* 502:185–195.

Goy, J. W., C. G. Bookhout & J. D. Costlow, Jr. 1981. Larval develoment of the spider crab *Mithrax pleuracanthus* Stimpson reared in the laboratory (Decapoda: Brachyura: Majidae). *J. Crustac. Biol.* 1:51–62.

Guerao, G., E. Pastor, J. Martin, M. Andrés, A. Estévez, A. Grau, J. Duran & G. Rotllant. 2008. The larval development of *Maja squinado* and *M. brachydactyla* (Decapoda, Brachyura, Majidae) described from plankton collected and laboratory-reared material. *J. Nat. Hist.* 42:2257–2276.

Guerao, G. & G. Rotllant. 2010. Development and growth of the early juveniles of the spider crab *Maja squinado* (Brachyura: Majoidea) in an individual culture system. *Aquaculture* 307:105–110.

Guerao, G., G. Rotllant & K. Anger. 2010. Characterization of larval moulting cycles in *Maja brachydactyla* (Brachyura, Majidae) reared in the laboratory. *Aquaculture* 302:106–111.

Hernández, J. E., J. L. Palazón-Fernández, G. Hernández & J. Bolaños. 2012. The effect of temperature and salinity on the larval development of *Stenorhynchus seticornis* (Brachyura: Inachidae) reared in the laboratory. *J. Mar. Biol. Ass. U.K.* 92:505–513.

Johns, M. D. & W. H. Lang. 1977. Larval development of the spider crab *Libinia emarginata* (Majidae). *Fish Bull.* 75:831–841.

Kannupandi, T., G. Vijayakumar & P. Soundarapandian. 2000. Influence of salinity on larval development of the mangrove crab *Sesarma brockii* De Man. *Indian J. Fish.* 47:343–348.

Kim, C. H. & I. K. Jang. 1987. The complete larval development of *Acmaeopleura parvula* Stimpson (Brachyura, Grapsidae) reared in the laboratory. *Bull. Korean Fish. Soc.* 20:543–560.

Lárez, M. B., J. L. Palazón-Fernández & C. J. Bolaños. 2000. The effect of salinity and temperature on the larval development of *Mithrax caribbaeus* Rathbun, 1920 (Brachyura: Majidae) reared in the laboratory. *J. Plankton Res.* 22:1855–1869.

Le Foll, D. 1993. Biologie et exploitation de l'araignée de mer *Maja squinado* Herbst en Manche Ouest. In: Ressources Halieutiques, IFREMER - Institut Français de Recherche pour l'Exploitation de la Mer. Plouzane (France): Université de Bretagne Occidentale. p. 517.

Lucas, J. S. & E. P. Hodgkin. 1970. Growth and reproduction of *Halicarcinus australis* (Haswell) (Crustacea, Brachyura) in the Swan Estuary Western Australia. II. Larval stages. *Mar. Freshw. Res.* 21:163–173.

Luppi, T. A., E. D. Spivak & C. C. Bas. 2003. The effects of temperature and salinity on larval development of *Armases rubripes* Rathbun, 1897 (Brachyura, Grapsoidea, Sesarmidae), and the southern limit of its geographical distribution. *Estuar. Coast. Shelf Sci.* 58:575–585.

Mene, L., M. T. Alvarez-Ossorio, E. González-Gurrián & L. Valdés. 1991. Effects of temperature and salinity on larval development of *Necora puber* (Brachyura: Portunidae). *Mar. Biol.* 108:73–81.

Messerknecht, I., M. Montu & K. Anger. 1991. Larval development and salinity tolerance of Brazilian *Eurytium limosum* (Say, 1818) (Brachyura: Xanthidae) reared in the laboratory. *Meeresforschung* 33:275–296.

Mia, M. D. Y. & S. Shokita. 2002. Early life history of an estuarine grapsid crab, *Helice leachi* Hess. *Indian J. Fish.* 49:23–28.

Mikami, S. & A. V. Kuballa. 2007. Factors important in larval and postlarval molting, growth, and rearing. In: Lavalli, K. L. & E. Spanier, editors. The biology and fisheries of the slipper lobster: Boca Raton, FL: CRC Press. pp. 91–110.

Minagawa, M. 1990. Influence of temperature on survival, feeding and development of larvae of the red frog crab, *Ranina ranina* (Crustacea, Decapoda, Raninidae). *Nippon Suisan Gakkaishi* 56:755–760.

Minagawa, M. 1992. Effects of salinity on survival, feeding and development of larvae of the red frog crab *Ranina ranina*. *Nippon Suisan Gakkaishi* 58:1855–1860.

Nagaraj, M. 1992. Combined effects of temperature and salinity on the zoeal development of the crab *Liocarcinus puber* (Decapoda: Portunidae). *Mar. Ecol. (Berl.)* 13:233–241.

Nagaraj, M. 1993. Combined effects of temperature and salinity on the zoeal development of the green crab, *Carcinus maenas* (Linnaeus, 1758) (Decapoda: Portunidae). *Sci. Mar.* 57:1–8.

Nurdiani, R. & C. Zeng. 2007. Effects of temperature and salinity on the survival and development of mud crab, *Scylla serrata* (Forsskål), larvae. *Aquacult. Res.* 38:1529–1538.

O'Connor, M. I., J. F. Bruno, S. D. Gaines, B. S. Halpern, S. E. Lester, B. P. Kinlan & J. M. Weiss. 2007. Temperature control of larval dispersal and the implications for marine ecology, evolution, and conservation. *Proc. Natl. Acad. Sci. USA* 104:1266–1271.

Ong, K. S. & J. Costlow. 1970. The effect of salinity and temperature on the larval development of the stone crab, *Menippe mercenaria* (Say), reared in the laboratory. *Chesap. Sci.* 11:16–29.

Papadopoulos, I., B. K. Newman, D. S. Schoeman & T. H. Wooldridge. 2006. Influence of salinity and temperature on the larval development of the crown crab, *Hymenosoma orbiculare* (Crustacea: Brachyura: Hymenosomatidae). *Afr. J. Aquat. Sci.* 31:43–52.

Peliz, A., P. Marchesiello, J. Dubert, M. Marta-Almeida, C. Roy & H. Queiroga. 2007. A study of crab larvae dispersal on the western Iberian shelf: physical processes. *J. Mar. Syst.* 68:215–236.

Péqueux, A. 1995. Osmotic regulation in crustaceans. *J. Crustac. Biol.* 15:1–60.

Przeslawski, R., M. Byrne & C. Mellin. 2015. A review and meta-analysis of the effects of multiple abiotic stressors on marine embryos and larvae. *Glob. Change Biol.* 21:2122–2140.

R Development Core Team. 2015. R: a language and environment for statistical computing. Vienna, Austria: R Foundation for Statistical Computing.

Rabalais, N. N. & J. N. Cameron. 1985. The effects of factors important in semi-arid environments on the early development of *Uca subcylindrica*. *Biol. Bull.* 168:147–160.

Reed, P. H. 1969. Culture methods and effects of temperature and salinity on survival and growth of Dungeness crab (*Cancer magister*) larvae in the laboratory. *J. Fish. Res. Board Can.* 26:389–397.

Rengel de Zambrano, I., K. Chung, J. Bolaños & J. Fermín. 1993. El efecto de la interacción entre el cadmio, la salinidad y la temperatura sobre el desarrollo larval de *Mithrax verrucosus* Milne Edwards 1832 (Crustacea, Decapoda, Majidae). *Ciencia* 1:13–25.

Rotllant, G., C. G. Simeó, G. Macià & A. Estévez. 2015. High environmental salinity reduces the reproductive potential of the spider crab *Maja brachydactyla* (Decapoda, Majidae). *Mar. Ecol.* 36:496–505.

Sastry, A. N. 1970. Culture of brachyuran crab larvae using a recirculating sea water system in the laboratory. *Helgol. Wiss. Meeresunters.* 20:406–416.

Schuh, M. & R. Diesel. 1995. Effects of salinity, temperature, and starvation on the larval development of *Armases* (=*Sesarma*) *miersii* (Rathbun, 1897), a semiterrestrial crab with abbreviated development (Decapoda: Grapsidae). *J. Crustac. Biol.* 15:205–213.

Seiple, W. H. & M. Salmon. 1987. Reproductive, growth and life-history contrasts between two species of grapsid crabs, *Sesarma cinereum* and *S. reticulatum*. *Mar. Biol.* 94:1–6.

Simith, D. J. B., A. S. de Souza, C. Maciel, F. Abrunhosa & K. Diele. 2012. Influence of salinity on the larval development of the fiddler crab *Uca vocator* (Ocypodidae) as an indicator of ontogenetic migration towards offshore waters. *Helgol. Mar. Res.* 66:77–85.

Simith, D. J. B., M. A. B. Pires, F. A. Abrunhosa, C. R. Maciel & K. Diele. 2014. Is larval dispersal a necessity for decapod crabs from the Amazon mangroves? Response of *Uca rapax* zoeae to different salinities and comparison with sympatric species. *J. Exp. Mar. Biol. Ecol.* 457:22–30.

Spivak, E. & J. A. Cuesta. 2009. The effect of salinity on larval development of *Uca tangeri* (Eydoux, 1835) (Brachyura: Ocypodidae) and new findings of the zoeal morphology. *Sci. Mar.* 73:297–305.

Torres, G., L. Giménez & K. Anger. 2002. Effects of reduced salinity on the biochemical composition (lipid, protein) of zoea 1 decapod crustacean larvae. *J. Exp. Mar. Biol. Ecol.* 277:43–60.

Torres, G., L. Giménez & K. Anger. 2011. Growth, tolerance to low salinity, and osmoregulation in decapod crustacean larvae. *Aquat. Biol.* 12:249–260.

Venables, W. N. & B. D. Ripley. 2002. Modern applied statistics with s. New York: Springer.

Yamamoto, T., T. Yamada, H. Fujimoto & K. Hamasaki. 2015. Effects of salinity on snow crab (*Chionoectes opilio*) larval survival and development under laboratory conditions. *J. Shellfish Res.* 34:499–504.

Foregut Morphology and Ontogeny of the Spider Crab *Maja brachydactyla* (Brachyura, Majoidea, Majidae)

Diego Castejón,[1]* Guiomar Rotllant,[2] Enric Ribes,[3] Mercè Durfort,[3] and Guillermo Guerao[4]

[1]*Subprograma Cultius Aquàtics, IRTA, Ctra. de Poble Nou, Km 5.5, Sant Carles de la Rápita 43540, Tarragona, Spain*
[2]*Departament de Recursos Marins Renovables, Institut De Ciències Del Mar, CSIC, Passeig Marítim de la Barceloneta 37-49, Barcelona, 08003 Spain*
[3]*Departament de Biologia Cel·lular, Facultat de Biologia, Universitat de Barcelona, Av Diagonal 643, Barcelona 08028, Spain*
[4]*PS Fabra i Puig 344, Barcelona 08031, Spain*

ABSTRACT We describe the morphology of the foregut of the spider crab *Maja brachydactyla* Balss, 1922, from first larval stage to adult, with detailed stage-specific documentation using light and scanning electron microscopy. A total of 40 ossicles have been identified in the foregut of adults of *M. brachydactyla* using Alizarin-Red staining. The morphological pattern of the ossicles and gastric mill is very similar to other Majoidea species with only a few variations. The foregut of the zoeae stages appeared as a small and simple cavity, with a cardio-pyloric valve that separates the stomach into cardiac and pyloric regions. The pyloric filter is present from the first zoea, in contrast to the brachyuran species which have an extended larval development. Calcified structures have been identified in the cardio-pyloric valve and pyloric region of the zoeal stages. The most significant changes in foregut morphology take place after the metamorphosis from ZII to megalopa, including the occurrence of the gastric mill. In the megalopa stage, the foregut ossicles are recognizable by their organization and general morphology, but are different from the adult phase in shape and number. Moreover, the gastric teeth show important differences: the cusps of the lateral teeth are sharp (no molariform); the dorsal tooth have a small, dentate cusp (not a well-developed quadrangular cusp); and the accessory teeth are composed of one sharp peak (instead of four sharp peaks). The gastric mill ontogeny from megalopa to adult reveals intermediate morphologies during the earlier juvenile stages. The relationship between gastric mill structures with food preferences and their contribution to the brachyuran phylogeny are briefly discussed. J. Morphol. 276:1109–1122, 2015. © 2015 Wiley Periodicals, Inc.

KEY WORDS: crustacea; stomach; ossicles; gastric mill; larval development

INTRODUCTION

The brachyuran foregut, like in other decapods, occupies the anterior part of the cephalothorax. The foregut comprises various structures that carry out specialized functions related to processing of ingested food: esophagus (swallowing of the food from the mouth to the stomach), cardiac sac (food storage), gastric mill (chewing of the ingested food), and pyloric filter (filtering and transport of chewed food to midgut gland and coarse material to intestines). Traditionally, the esophagus and the anterior part of the stomach (the cardiac sac and gastric mill, inclusive) together were called the "cardiac foregut," while the posterior part of the stomach (that includes pylorus and pyloric filter) was called the "pyloric foregut." These compartments, the cardiac foregut and pyloric foregut are separated by the cardio-pyloric valve (Schaefer, 1970; Felgenhauer, 1992; Icely and Nott, 1992; Woods, 1995; Stein, 2009). According to Felgenhauer (1992) and Lin (2000), the pyloric filters are composed of a complicated setal network organized in ampullary chambers.

The ossicles are structurally relevant features of the decapod foregut. They are calcified structures derived from the cuticle that cover the internal walls of the foregut, whose main role is the shaping and stabilization of the stomach for the correct functioning of the gastric mill and pyloric filter (Schaefer, 1970; Felgenhauer, 1992; Icely and Nott, 1992). A total of 41 ossicles have been described in the brachyuran foregut (Brösing, 2010), organized in a phylogenetically conservative pattern recognizable in other decapod taxa (Meiss and Norman, 1977). The ossicle system of the different brachyuran taxa show variations in the number, shape, and position

Contract grant sponsor: INIA, Spanish Ministry of Economy and Competitiveness (G.G.); Grant number: Project RTA2011-00004-00-00; Contract grant sponsor: INIA, Spanish Ministry of Economy and Competitiveness (D.C.); Grant number(s): FPI-INIA predoctoral fellowship, RTA2011-00004-00-00.

*Correspondence to: D. Castejón. IRTA, Cultius Aquàtics, Ctra. Poble Nou, Km 5.5, 43540 Sant Carles de la Ràpita, Tarragona, Spain. E-mail: diego.castejon@irta.cat

Received 21 November 2014; Revised 4 March 2015;
Accepted 27 April 2015.

Published online 1 July 2015 in
Wiley Online Library (wileyonlinelibrary.com).
DOI 10.1002/jmor.20404

© 2015 WILEY PERIODICALS, INC.

of the ossicles; these variations have been demonstrated to be useful for the study of phylogenetic relationships (Brösing et al., 2007; Huespe et al., 2008; Brösing, 2010; Brösing and Türkay, 2011). The gastric mill is another interesting foregut structure, composed of an unpaired dorsal tooth and paired lateral and accessory teeth, it can provide information about to food resources and the phylogenetic relationships among different taxa (Skilleter and Anderson, 1986).

Major changes have been observed during the ontogeny of the brachyuran foregut morphology: the zoeae foregut lacks the gastric mill and the ossicles, these structures appear for the first time after the metamorphosis to megalopa (Abrunhosa et al., 2003; Melo et al., 2006; Lumasag et al., 2007; Castejón et al., 2015). The knowledge of the morphological development of the foreguts and feeding appendages might assist in identifying appropriate prey characteristics, or in developing diets that meet the nutritional requirements for each life stage of important aquaculture organisms (Abrunhosa and Melo, 2008).

The spider crab, *Maja brachydactyla* is a marine brachyuran of commercial interest widely distributed from the Açores and British Isles to the Sahara, Canary Islands and south-western Mediterranean Sea (Abelló et al., 2014). Many studies have focused on different aspects of their biology: for example, description of larval stages and molt cycles (Guerao et al., 2008, 2010; Guerao and Rotllant, 2010), growth patterns (Andrés et al., 2008), biochemistry of the ontogeny (Andrés et al., 2007, 2010), ovarian maturation (Rotllant et al., 2007), spermatogenesis, and histological description of the male reproductive system (Simeó et al., 2009a, 2009b, 2010), and aspects of animal production (Alaminos and Domingues, 2008; Domingues and Alaminos, 2008; Palma et al., 2008; Alaminos, 2011; Andrés et al., 2011; Verísimo et al., 2011; Domingues et al., 2012). The larval development of *M. brachydactyla* is abbreviated (like in all known Majoidea) and consists of two zoeal stages (zoea I and zoea II) and one megalopa stage; the morphology of the larval mouthparts is known in detail (Guerao et al., 2008), but the foregut morphology in larval and postlarval stages has not been previously described.

The main objective of this study was to describe *M. brachydactyla* larval, juvenile and adult foregut morphology; emphasizing the most important changes during ontogeny. The usefulness of the morphology of the ossicle-system as a tool for brachyuran taxonomy and the relationship between gastric mill morphology and food preferences are briefly discussed.

MATERIAL AND METHODS

The broodstock of *M. brachydactyla* Balss, 1922 was captured from the NW Iberian Peninsula coast (Galicia, Spain) and transported to the Institut de Recerca i Tecnologia Agroalimentàries facilities (Tarragona, Spain) in December 2012. The broodstock was kept in 2,000 L cylindrical tanks connected to a recirculation unit maintained at controlled conditions of temperature (18 ± 1°C), salinity (35 ± 1‰), and photoperiod (12 h light:12 h dark cycle). The broodstock was daily fed with a combination of fresh mussels (*Mytilus* sp. four times per week), frozen mussels (*Mytilus* sp, twice per week) and frozen crabs (*Liocarcinus depurator*, once per week).

The active, newly hatched zoeae I (ZI) were collected from broodstock tanks after hatching and transferred to the culture vessels (600 ml glass beakers filled with 500 ml of filtered seawater) and reared to obtain zoeae II (ZII) and megalopae (M). Larval density was 60 zoeae L^{-1} and 20 megalopae L^{-1}, respectively. The larvae were kept at constant conditions of temperature (18 ± 1°C), salinity (35 ± 1‰) and photoperiod (12 h light:12 h dark cycle). Water was changed daily and the larvae were fed with *Artemia* sp. nauplii and metanauplii (INVE Aquaculture Nutrition, Salt Lake UT). The first juveniles (C1) obtained were transferred to 50 L aquarium and raised to juveniles with a cephalothorax length of 8 mm (C_{CL8}). The same environmental conditions (salinity, temperature and photoperiod) used for the larvae were maintained in juvenile culture. The juveniles were fed five times per week with fresh mussels (*Mytilus* sp.).

Adult Foregut

Five adults were dissected the foregut and cleaned by heating in a 10% KOH solution at 80°C for 30–60 min. The foreguts were then stained with Alizarin-Red 1% KOH solution according to Brösing (2002; 2010), for revealing calcified structures. After staining, the foreguts were stored in ethanol 70% for posterior observations. The foregut ossicles were described according to the nomenclature of Brösing (2002, 2010, 2014). Observations of the foregut were taken with a Nikon SMZ800 stereomicroscope equipped with an image analyzing system (AnalySIS, SIS, Münster, Germany).

Foregut of the Larvae and Juveniles

Ten fresh individuals of ZI, ZII, M, C1, and five fresh individuals of C_{CL8} were dissected and the foreguts were cleaned by immersion in a 10% KOH solution at 80°C for 10–15 min and sonicated for 3–5 min in an ultrasonic cleaner. The foreguts of all stages were stained by adding Alizarin-Red 1% KOH solution for 10–15 min. The larvae and juvenile foreguts were observed using either a Nikon SMZ800 stereomicroscope or a LB30T Leica DMLB light microscope (Leica Microsystems GmbH, Wetzlar, Germany) connected to a 12.5 megapixel Olympus DP70 Digital Microscope Camera (Olympus America, NY). The stereo and light microscopes were equipped with an image analyzing system (AnalySIS, SIS, Münster, Germany). The measurements taken from the foregut of the larvae and juveniles were: foregut length (FL) as the distance from the anterior margin of the cardiac chamber to the posterior margin of the pyloric chamber; and foregut width (FW) as the foregut maximum width of the cardiac chamber.

For the scanning electron microscopy (SEM), the gastric mill of the M, C1, and C_{CL8} were dissected using a Nikon SMZ800 stereomicroscope. The dissected foreguts were immediately sonicated for 2–3 min for removal of surface debris and dehydrated in a graded ethanol series (70, 90, and 100%). After the critical-point-drying, individuals were mounted on SEM stubs with self-adhesive carbon stickers and were coated in gold. The dried structures were observed with a Hitachi H-4100 FE SEM in the Barcelona University (UB, Barcelona, Spain).

RESULTS

Adult Foregut

It has been identified 40 ossicles in the adult foregut of *M. brachydactyla*. The cardiac foregut

TABLE 1. Nomenclature of the identified ossicles in adults of M. brachydactyla

	Ossicles of dorsal gastric mill	
I	mesocardiac ossicle	Unpaired
II	pterocardiac ossicles	Paired
IIa	prepterocardiac ossicles	Paired
IIb	postpterocardiac ossicles	Paired
III	pyloric ossicle	Unpaired
IV	exopyloric ossicles	Paired
V	zygocardiac ossicles	Paired
VI	propyloric ossicle	Unpaired
VII	urocardiac ossicle	Unpaired
	Ossicles of the lateral gastric mill	
VIII	pectineal ossicles	Paired
IX	prepectineal ossicles	Paired
X	postpectineal ossicles	Paired
Xa	"quill" of the postpectineal ossicles	Paired
XI	anterior lateral cardiac plates	Paired
XII	posterior lateral cardiac plates	Paired
XIII	inferior lateral cardiac ossicles	Paired
XIV	subdentate ossicles	Paired
	Ossicles of the cardio-pyloric valve	
XV	lateral cardio-pyloric ossicles	Paired
XVI	anterior ossicle of the cardio-pyloric valve	Unpaired
XVII	posterior ossicle of the cardio-pyloric valve	Unpaired
XVIII	lateral ossicle of the cardio-pyloric valve	Unpaired
	Ossicles of the dorsal pyloric foregut	
XIX	anterior mesopyloric ossicle	Paired
XIXa	lateral mesopyloric ossicles	Paired
XX	posterior mesopyloric ossicles	Paired
XXI	uropyloric ossicle	Unpaired
XXIa	Infra-uropyloric fragments	Paired
XXIb	posterior uropyloric ossicles	Paired
	Ossicles of the lateral & ventral pyloric foregut	
XXII	preampullary ossicles	Paired
XXIII	anterior inferior pyloric ossicle	Unpaired
XXIV	inferior ampullary ossicles	Paired
XXV	ampullary-roof-ossicles, lower portion	Paired
XXVI	ampullary-roof-ossicles, upper portion	paired
XXVIa	anterior process of the ampullary roof ossicles, upper portion	Paired
XXVII	posterior inferior pyloric ossicle	Unpaired
	Supporting ossicles of the lateral foregut	
XXVIII	anterior supra-ampullary ossicles	Paired
XXIX	middle supra-ampullary ossicles	Paired
XXX	posterior supra-ampullary ossicles	Paired
XXXI	anterior pleuropyloric ossicles	Paired
XXXII	middle pleuropyloric ossicles	Paired
XXXIII	posterior pleuropyloric ossicles	Paired

forms a short esophagus and a sack-like structure with four unpaired and thirteen paired ossicles that support the gastric mill. The cardio-pyloric valve is a rigid structure with one paired and three unpaired ossicles. The pyloric foregut is smaller than the cardiac foregut and contains three unpaired and 16 paired ossicles as well as the pyloric filter. It is connected to the intestines and midgut gland. A complete list of identified ossicles is given in the Table 1 and their positions are documented in the Figure 1A–E.

Ossicles of the dorsal gastric mill. The mesocardiac ossicle (I; Fig. 1E) is a half-moon shaped dorsal plate posteriorly fused to the urocardiac ossicle (VII) and laterally connected to the pterocardiac ossicles (II). The pterocardiac ossicles (II; Fig. 1E) are large, thin plates extending perpendicularly to the longitudinal axis; the Alizarin Red stain reveals anterior parallel plates that could be interpreted as the prepterocardiac ossicles (IIa) and posterior parallel plates considered as the postpterocardiac ossicles (IIb).

The pyloric ossicle (III; Fig. 1D) is an unpaired U-shaped ossicle anteriorly attached to the propyloric ossicle (VI) and laterally to the exopyloric ossicles (IV). The exopyloric ossicles (IV; Fig. 1A,D) are bar shaped structures that connect the pyloric ossicle (III) with the zygocardiac ossicles (V). The zygocardiac ossicles (V; Fig. 1A,E) are large subtriangular plates that carry the lateral teeth of the gastric mill. These heavily sclerotized teeth have a large anterior cusp and two well-developed lateral cusps, the surface of the lateral teeth are smooth and clean (Fig. 4A,F). Externally, the zygocardiac ossicle articulates posteriorly with the exopyloric (IV) and the subdentate (XIV) ossicles (Fig. 1A).

The propyloric ossicle (VI; Fig. 1D) is located dorsally between the urocardiac ossicle (VII) and the pyloric ossicle (III). The length of the urocardiac ossicle (VII; Fig. 1E) is three times the width, with the anterior edge fused to the mesocardiac ossicle (I) and the posterior edge connected to the propyloric ossicle (VI). The postero-ventral portion of the urocardiac ossicle supports a well-developed quadrangular dorsal median tooth with two lateral and smooth cusps on its posterior margin (Figs 4A,J and 5D).

Ossicles of the lateral gastric mill. The pectineal ossicles (VIII; Fig. 1A) are U-shaped ossicles and support the accessory teeth; comprising four or five small, sharp peaks (Fig. 4A and 5H). The pectineal ossicles (VIII) are connected anteriorly with the hook-shaped prepectineal ossicles (IX; Fig. 1A), joined in turn with the zygocardiac ossicle (V). Posteriorly, the pectineal ossicles are connected with the fusion of the postpectineal ossicles (X) and the J-shaped "quill" of the postpectineal ossicles (Xa); the postpectineal ossicles (X) (Fig. 1A) are long ossicles parallel to the inferior lateral cardiac ossicles (XIII).

The anterior lateral cardiac plates (XI; Fig. 1A) are half-moon-shaped structures connected

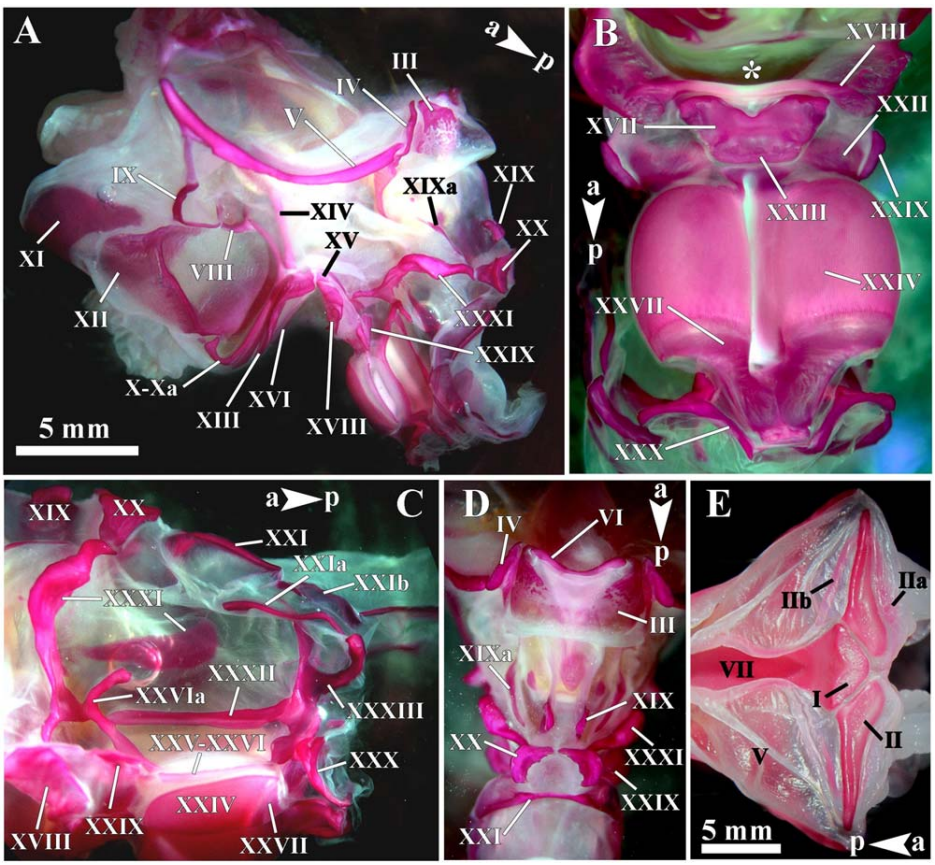

Fig. 1. *Maja brachydactyla* foregut of the adult stained with Alizarin Red. (**A**) foregut lateral view, stereo microscope image; (**B**) pyloric foregut ventral view, stereo microscope image; (**C**) pyloric foregut lateral view, stereo microscope image; (**D**) pyloric foregut dorsal view, stereo microscope image; (**E**) cardiac foregut dorsal view, stereo microscope image. (*), position of the cardio-pyloric valve; a > p, anterior to posterior margin. For ossicles nomenclature sees Table 1.

posteriorly by an uncalcified cuticle with the ear-shaped posterior lateral cardiac plates (XII). The posterior lateral plates (XII; Fig. 1A) are dorsally and posteriorly connected by the prepectineal (IX), the pectineal (VIII), the postpectineal (X), and the "quill" of the postpectineal ossicles (Xa).

The inferior lateral cardiac ossicles (XIII; Fig. 1A) are large structures with their anterior margin attached in parallel to the post-pectineal (X) and "quill" of the postpectineal ossicles (Xa). Their posterior-dorsal margin is connected to the lateral cardio-pyloric ossicle (XV) and the lateral ossicle of the cardio-pyloric valve (XVIII). The subdentate ossicle (XIV; Fig. 1A) connects dorsally with the zygocardiac ossicle (V) and ventrally with the postpectineal (X) and inferior lateral cardiac ossicles (XIII).

Ossicles of the cardio-pyloric valve. The cardio-pyloric valve is seen as a hemispherical structure in lateral view, subtriangular in frontal view and "U"-shaped in dorsal view; with a concave anterior margin and a convex posterior margin. Interiorly it is covered by numerous and small setae (Fig. 5K).

The lateral cardio-pyloric ossicle (XV; Fig. 1A) is a small structure connected dorsally with the anterior supra-ampullary ossicle (XXVIII), posteriorly with the lateral ossicle of the cardio-pyloric valve (XVIII), and ventrally with the inferior lateral cardiac ossicle (XIII). The anterior ossicle of the cardio-pyloric valve (XVI; Fig. 1A) forms a fine plate marked by a calcified line in the middle. The unpaired "U"-shaped posterior ossicle of the cardio-pyloric valve (XVII; Fig. 1B) is fused posteriorly with the anterior inferior pyloric ossicle (XXIII) and anteriorly connects with the lateral ossicles of the cardio-pyloric valve (XVIII). The "paired" lateral ossicle of the cardio-pyloric valve (XVIII) appears fused ventrally (Fig. 1A,B).

Ossicles of the dorsal pyloric foregut. The small, dorsal, bean-shaped anterior mesopyloric ossicles (XIX; Fig. 1A,C,D) are located between the pyloric ossicle (III) and the posterior mesopyloric ossicles (XX). The lateral mesopyloric ossicles (XIXa; Fig. 1A,D) appear as a curved rod structure located below the anterior mesopyloric ossicle (XIX). The posterior mesopyloric ossicles (XX; Fig. 1A,C,D) are

half-moon-shaped structures attached laterally to the middle pleuropyloric ossicles (XXXI) and posteriorly with the uropyloric ossicle (XXI).

The uropyloric ossicle (XXI; Fig. 1C,D) is thin and slightly bent, perpendicular to the longitudinal axis in dorsal view and parallel to the longitudinal axis in lateral view. The infrauropyloric fragments (XXIa; Fig. 1C,D) are located below the uropyloric ossicle (XXI) forming a slightly curved rod over the posterior pleuropyloric ossicles (XXXIII). The uropyloric ossicle (XXI) continues dorsally with the large stick shaped posterior uropyloric ossicles (XXIb; Fig. 1C).

Ossicles of the lateral and ventral pyloric foregut. The preampullary ossicles (XXII; Fig. 1B) are small ventral plates surrounded by the middle supra-ampullary ossicles (XXIX), the fused unpaired posterior ossicle of the cardio-pyloric valve (XVII) and anterior inferior pyloric ossicle (XXIII), the lateral ossicle of the cardio-pyloric valve (XVIII) and the inferior ampullary ossicles (XXIV). The anterior inferior pyloric ossicle (XXIII; Fig. 1B) is an unpaired oval plate anteriorly fused to the posterior ossicle of the cardio-pyloric valve (XVII) and posteriorly connected to the inferior ampullary ossicles (XXIV).

The inferior ampullary ossicles (XXIV; Fig. 1B,C) appear as pair of fine convex plates that protect the pyloric filter, posterioly are fused to the ampullary roof ossicles (XXVII). The ampullary roof ossicles (XXVII; Fig. 1B,C) are unpaired, large "V"-shaped ossicles connected posteriorly with the supra-ampullary ossicles (XXX).

Both lower portions and upper portions of the ampullary roof ossicles (XXV–XXVI) are fused as enlarged plates (Fig. 1C), connected anteriorly with the anterior process of the ampullary roof ossicles (XXVIa), inverted "L"-shaped ossicles in turn connected with the anterior pleuropyloric ossicles (XXXI). Ventrally the lower and upper portions of the ampullary roof ossicles (XXV-XXVI) are joined to the inferior ampullary ossicle (XXIV), the posterior inferior pyloric ossicle (XXVII), and the supra-ampullary ossicles (XXX).

Supporting ossicles of the lateral pyloric foregut. The anterior supra-ampullary ossicle (XXVIII) is a slightly calcified plate, connected dorsally to the anterior pleuropyloric ossicles (XXXI), ventrally to the lateral cardio-pyloric (XV), and the lateral ossicle of the cardio-pyloric valve (XVIII) and posteriorly with the middle supra-ampullary ossicles (XXIX).

The middle supra-ampullary ossicles (XXIX; Fig. 1B,C) are fine plates projecting from the cuticle as a semicircular plate ventrally attached to the preampullary ossicles (XXII) and the inferior ampullary ossicles (XXIV). Their posterior margin linked to the fused lower and upper portion of the ampullary roof ossicles (XXV-XXVI) and the anterior process of the ampullary-roof-ossicles (XXVIa).

The posterior supra-ampullary ossicles (XXX; Fig. 1B,C) are "T"-shaped structures connected with the terminal margin of upper portion of the ampullary roof ossicles (XXVII) and dorsally attached to the middle pleuropyloric ossicles (XXXII). The anterior pleuropyloric ossicles (XXXI; Fig. 1C,D) are compound by an elongated and curved vertical bar connected with an horizontal, narrow, and drop shape plate slightly calcified; the dorsal margin is connected to the posterior mesopyloric ossicles (XX), while ventrally they are attached to the anterior process of the ampullary roof ossicles (XXVIa) and the anterior process of the supra-ampullary ossicles (XXVIII).

The middle pleuropyloric ossicles (XXXII; Fig. 1C) are wide, horizontal plates joined anteriorly with the anterior processes of the ampullary roof ossicles (XXVIa) and posteriorly with the posterior pleuropyloric ossicles (XXXIII). The posterior pleuropyloric ossicles (XXXIII; Fig. 1C) are large subtriangular plates, located behind the lateral mesopyloric ossicles (XIXa), and posteriorly to the uropyloric ossicles (XXIb).

Foregut of the Zoeal Stages

The foregut of the zoeae of *M. brachydactyla* has two chambers: the cardiac foregut and the pyloric foregut separated by the cardio-pyloric valve (FL = 750–800 μm in ZI and FL = 900–1,000 μm in ZII). The morphology of the foregut is nearly similar in both zoeal stages, being characterized by the simplicity of the cardiac chamber and the absence of the ossicle system and the gastric mill (Fig. 2A–D).

The morphology of the cardio-pyloric valve is similar to that of the adult: hemispherical in lateral view, subtriangular in frontal view, and "U"-shaped in dorsal view; with a concave anterior margin and a convex posterior margin (Fig. 2A–E). The cardio-pyloric valve presents tiny setae grouped in small clusters in the anterior margin, fine spinous setae in the lateral margin and long thickened setae crowned by small sharp protuberances in the posterior-lateral margin (Fig. 2E,F). The Alizarin Red staining reveals that the cardio-pyloric valve is a calcified structure with a calcium-rich basin (Fig. 2A,B,D).

The pyloric foregut supports an interampullary septum with a row of elongate medium setae. A well-developed pyloric filter is present from the ZI stage, filling the entire inferior portion of the chamber. In the ZI stage 3–4 ampullary chambers are visible and in the ZII stage there are 5–6 ampullary chambers (Fig. 2B,C). The Alizarin Red staining reveals a pair of terminal calcified "supra-ampullary ossicles-like" structures (Fig. 2D).

Foregut of the Megalopa Stage

The foregut of the megalopa stage (Fig. 3A,B) is more developed and more complex as compared to the zoeal stages. Important changes are observed in the general shape and size (approximate

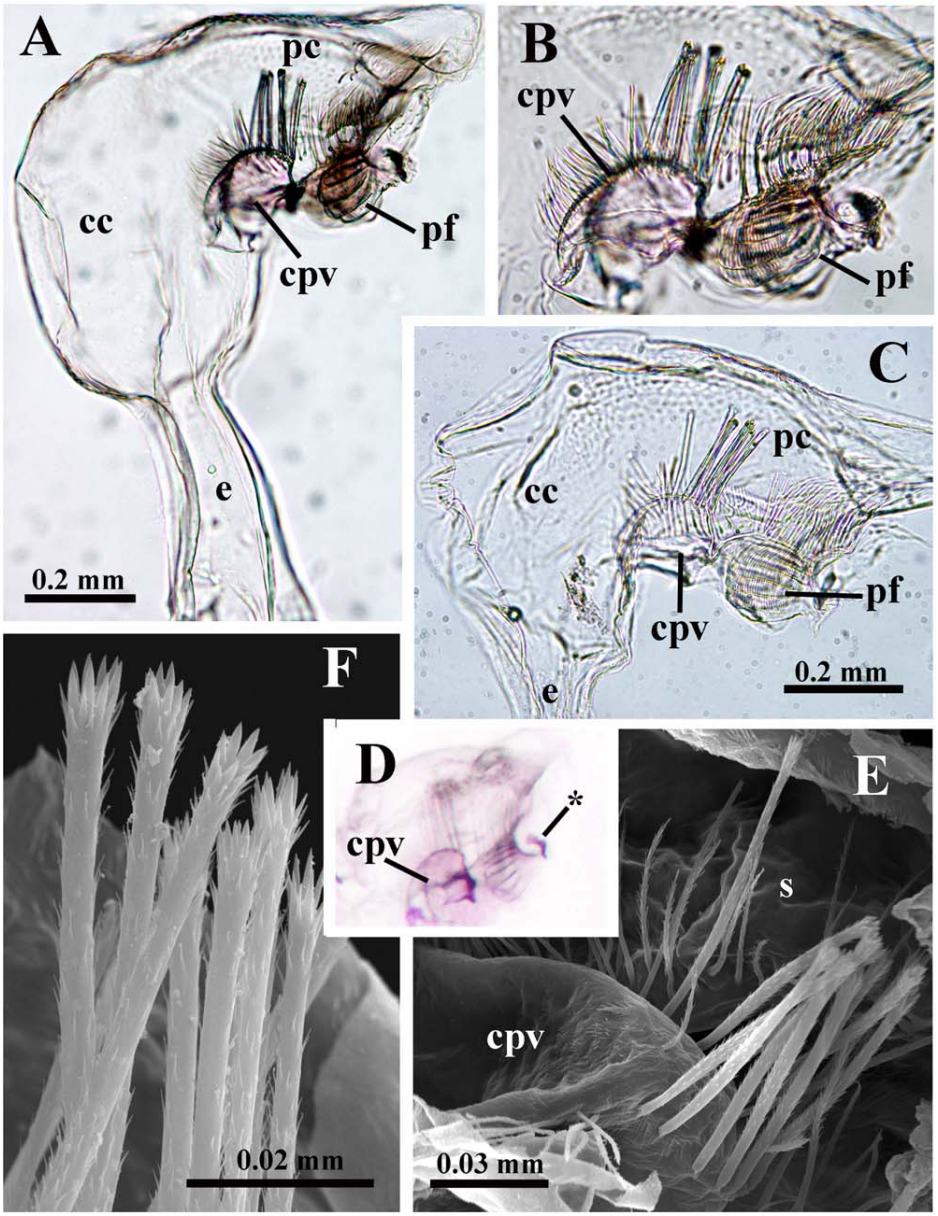

Fig. 2. *Maja brachydactyla* foregut of zoeae stages. (**A**) zoea I, stained with Alizarin Red, light microscope image; (**B**) close view of 2A; (**C**) zoea II, without staining, light microscope image; (**D**) zoea I, stained with Alizarin Red, stereo microscope image; (**E**) close view of zoea I cardio-pyloric valve, SEM image; (**F**) close view of the long thickened setae of the cardio-pyloric valve, SEM image. (*),"supra-ampullary ossicles-like" structures; cc, cardiac chamber; cpv, cardio-pyloric valve; e, esophagus; pc, pyloric chamber; pf, pyloric filter; s, long thickened setae.

FL = 1,500 μm; approximate FW = 950 μm). The cardiac foregut is enlarged laterally, acquiring the adult sac-like morphology (Fig. 3B). The ossicle system and gastric mill appear for the first time. However, compared to the adult, many ossicles have a different shape and position and others are missing. Therefore, we describe only the ossicles we can clearly identify. The ossicles of the gastric mill show a pronounced adult-like morphology, while the gastric mill teeth are markedly different: the mesocardiac ossicle (I) appears laterally connected with pterocardiacs ossicles (II) and it is posteriorly fused with urocardiac ossicles (VII; Fig. 3B). The zygocardiac ossicles (V; Fig 3B) are large subtriangular plates, although the highly calcified margins contrast with the poorly calcified central area, resulting in a "V"-shaped appearance. The lateral teeth associated to the zygocardiac ossicles have three small lateral dentate cusps surrounded by small peaks, crowned posteriorly by 13–15 partially scaly setae (Fig. 4B,C). The propyloric ossicle (VI) differs from the adult, in that it is a

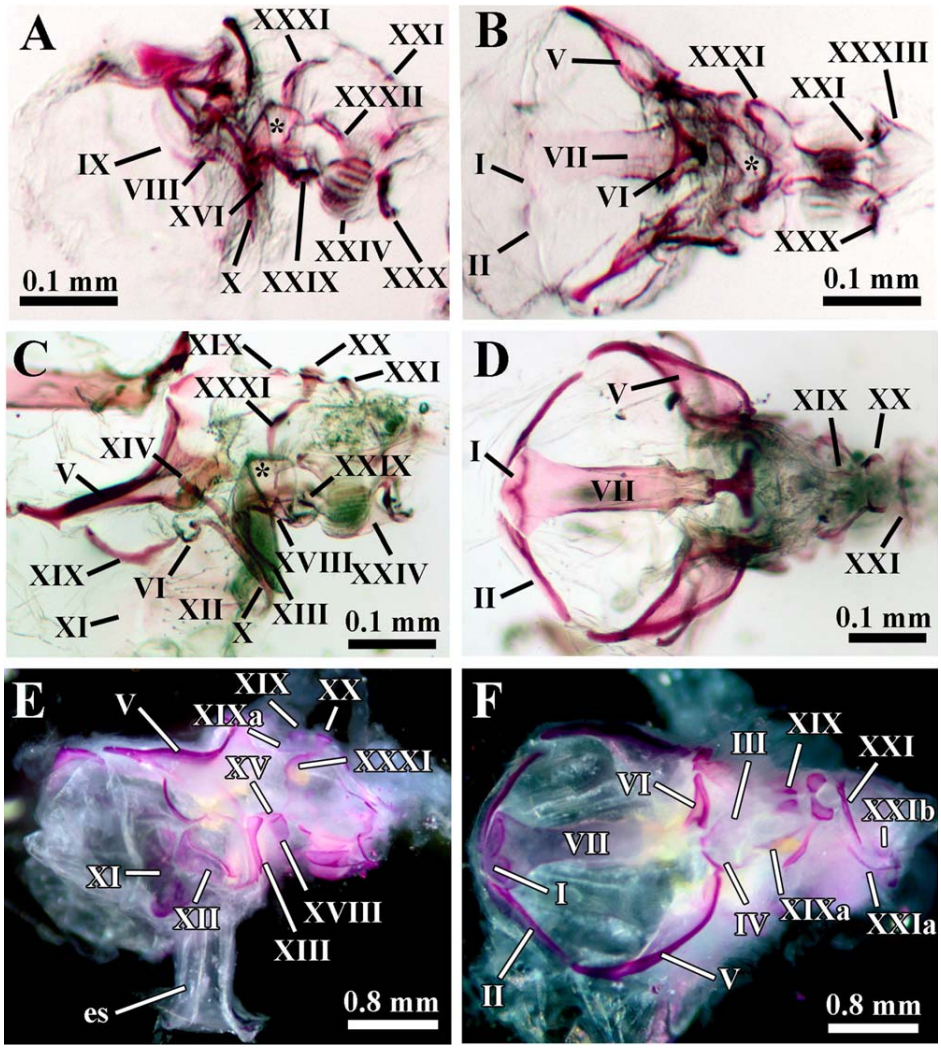

Fig. 3. *Maja brachydactyla* foregut of the megalopa and juveniles; stained with Alizarin Red. (**A**) lateral view of megalopa foregut, light microscope image; (**B**) dorsal view of megalopa foregut, light microscope image; (**C**) lateral view of C1 foregut, light microscope image; (**D**) dorsal view of C1 foregut, light microscope image; (**E**) lateral view of C_{CLS} foregut, stereo microscope image; (**F**) dorsal view of C_{CLS} foregut, stereo microscope image. (*), cardio-pyloric valve. For ossicles nomenclature sees Table 1.

"Y"-shaped structure ventrally connected to the posterior edge of the urocardiac ossicle (VII; Fig. 3B). Similarly as in the adults, the length of the urocardiac ossicle (VII) is nearly three times the width and bears the dorsal tooth in the posterior edge; however, unlike the adult, this dorsal tooth contains one small, dentate cusp and 7–12 long lateral spines (Figs. 4G and 5A). The pectineal ossicles (VIII) are small ossicles that support the accessory teeth, composed by one forked peak surrounded laterally by 5–6 large scaly setae (Fig. 5E). The pectineal ossicles (VIII) are connected anteriorly with the curved rod-shaped prepectineal ossicles (IX) and posteriorly with the enlarged rod-shape post-pectineal ossicles (X; Fig. 3A).

The cardio-pyloric valve is intensively calcified and its morphology is similar to that of the juveniles and adults. The anterior margin of the cardio-pyloric valve is covered by numerous clusters of tiny setae; the posterior and lateral margins lack the long thickened setae characteristic of the zoeae while presenting numerous long and scaly setae (Fig. 5I). The pyloric filter has a high number of food grooves. The interampullary net is composed of rows of elongate setae, and a minimum of seven ampullary chambers have been identified (Fig. 3A). The anterior ossicle of the cardio-pyloric valve (XVI) has a similar shape and position as in the adult (Fig. 3A). However, in the megalopa the majority of the ossicles of the pyloric foregut have a shape that differs from the adult. The inferior ampullar ossicles (XXIV) appear as thin plates poorly calcified that ventrally cover the pyloric filter (Fig. 3A). Ventral to the posterior edge of the cardio-pyloric valve we found

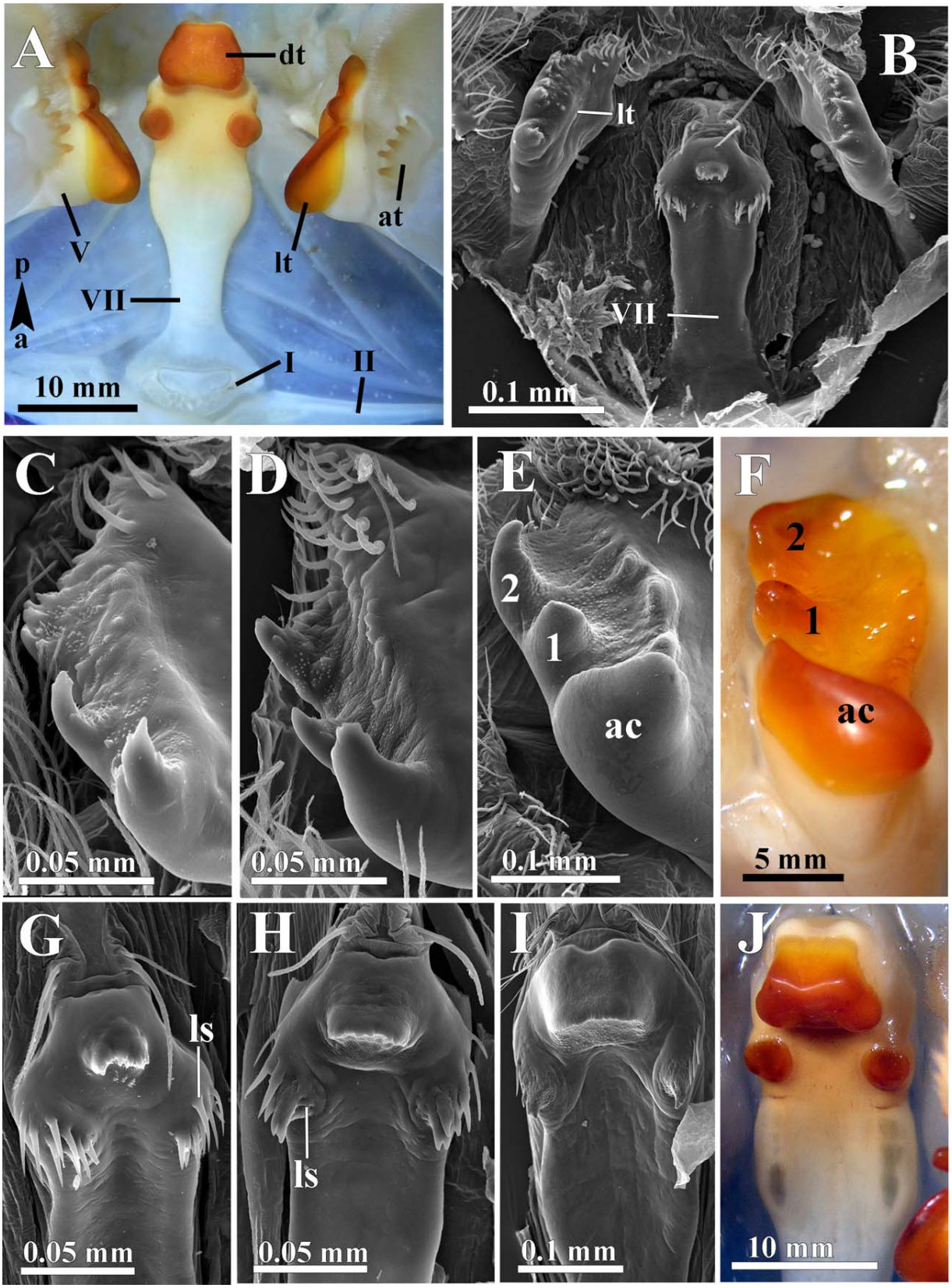

Fig. 4. *Maja brachydactyla*. Gastric mill and associated teeth; (**A**) adult gastric mill, stereo microscope image; (**B**) megalopa gastric mill, SEM image. (**C**) megalopa lateral tooth, SEM image; (**D**) C1 lateral tooth, SEM image; (**E**) C_{CLS} lateral tooth, SEM image; (**F**) adult lateral tooth, stereo microscope image; (**G**) megalopa dorsal tooth, SEM image; (**H**) C1 dorsal tooth, SEM image; (**I**) CC_{LS} dorsal tooth, SEM image; (**L**) adult dorsal tooth, stereo microscope image. ac, anterior cusp; at, accessory tooth; dt, dorsal tooth; lt, lateral tooth; ls, lateral spines. Numbers: lateral cusps. For ossicles nomenclature sees Table 1. [Color figure can be viewed in the online issue, which is available at wileyonlinelibrary.com.]

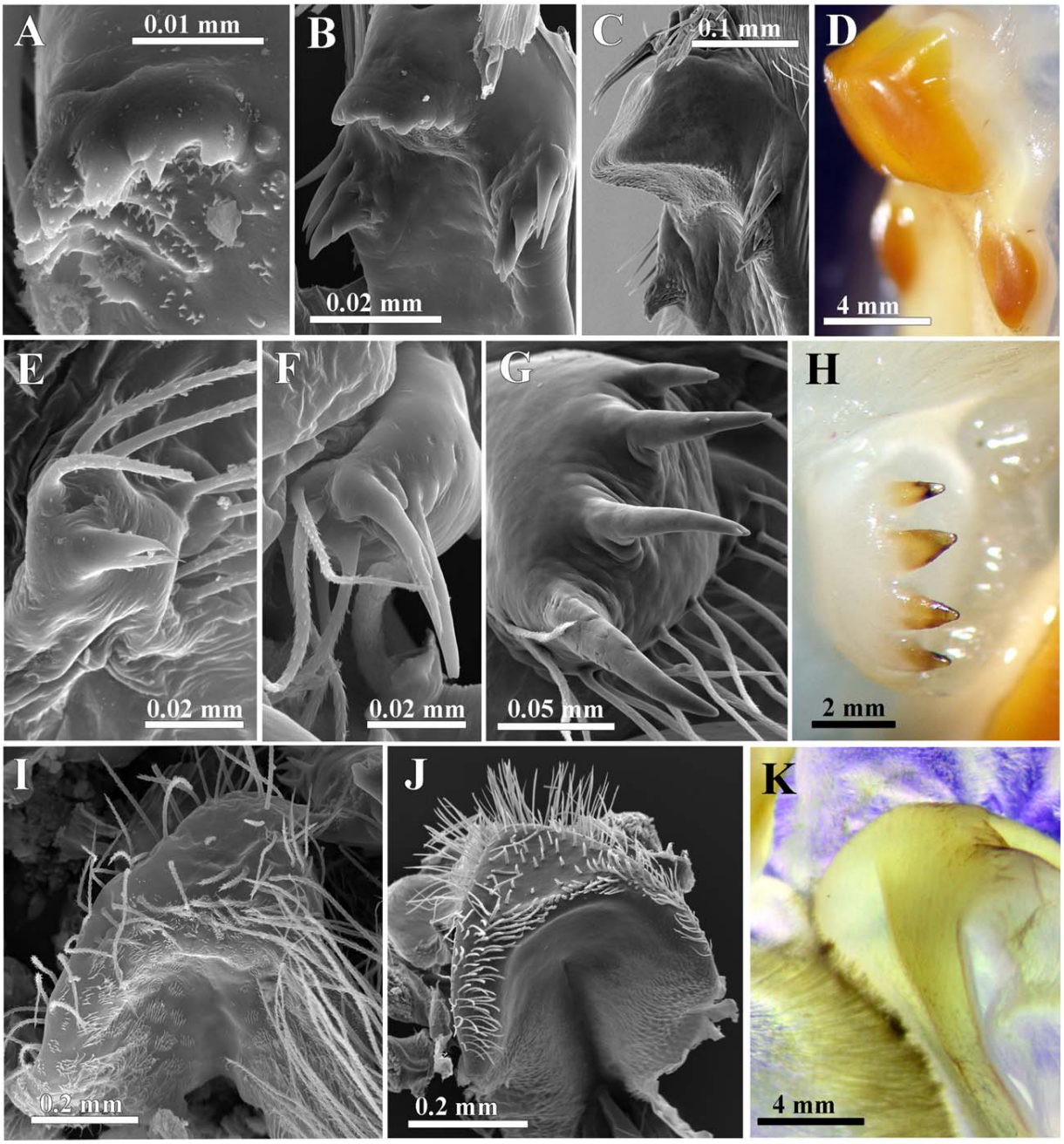

Fig. 5. *Maja brachydactyla* gastric mill teeth and cardio-pyloric valve. (**A**) megalopa dorsal tooth median cusp, SEM image; (**B**) C1 dorsal tooth median cusp, SEM image; (**C**) C_{CL8} dorsal tooth median cusp, SEM image; (**D**) adult dorsal tooth median cusp, stereo microscope image; (**E**) megalopa accessory tooth, SEM image; (**F**) C1 accessory tooth, SEM image; (**G**) C_{CL8} accessory tooth, SEM image; (**H**) adult accessory tooth, stereo microscope image; (**I**) megalopa cardio-pyloric valve, SEM image; (**J**) C1 cardio-pyloric valve, SEM image; (**K**) adult cardio-pyloric valve, stereo microscope image. [Color figure can be viewed in the online issue, which is available at wileyonlinelibrary.com.]

structures that resemble the adult middle supra-ampullary-like ossicles (XXIX-like; Fig. 3A). The anterior pleuropyloric ossicles (XXXI; Fig 3A,B) are vertical and curved bars connected posteriorly with the middle pleuropyloric-like ossicles (XXXII-like; Fig. 3A). The posterior supra-ampullary ossicles (XXX; Fig. 3A,B) appear in the posterior-ventral margin as a curved rod whose morphology is similar to the adults and the calcified structures seen during the zoeal stages. In the pyloric foregut, some unidentified ossicles with a thin rod-shape have been observed in the posterior-dorsal margin, that have been named the uropyloric-like (XXI-like) and posterior pleuropyloric-like (XXXIII-like) ossicles (Fig. 3B).

Foregut of the C1 Stage

The morphology of the foregut at juvenile stage is more similar to that of the adult than that of the megalopa (Fig. 3C,D). New ossicles appear for the first juvenile, and there are others that are identifiable. In relation to the cardiac foregut and gastric mill associated ossicles, the inferior lateral cardiac (XIII; Fig. 3C) and the subdentate ossicles (XIV; Fig. 3C) appear with an adult shape and position. Also the anterior lateral cardiac plates (XI) and the posterior lateral cardiac plates (XII) can be observed as slightly calcified structures (Fig. 3C). The gastric mill teeth are retained and acquire an intermediate morphology between the megalopa and the C_{CL8} juvenile. The dorsal tooth bears one small and dentate cusp whose relative size is higher than in the megalopa stage, the lateral spines become thicker and their number is reduced to seven (Figs. 4H and 5B). The lateral teeth show three big lateral dentate and conical cusps; posteriorly there appear approximately 20 spinous setae (Fig. 4D). The accessory teeth are composed of two peaks surrounded by 5–6 long lateral setae (Fig. 5F).

The cardio-pyloric valve is similar to that of the adult. The anterior margin is covered by fine setae, while the posterior and lateral margins show long and scaly setae similar as in the megalopae (Fig. 5J). New ossicles appear in the dorsal pyloric foregut: the small, fine and enlarged anterior mesopyloric ossicles (XIX; 3C, D) are attached posteriorly with the bean-shaped mesopyloric ossicles (XX; 3C, D), which are in turn connected laterally to the middle pleuropyloric ossicles (XXXI; Fig. 3C). Like in the adults, the uropyloric ossicle (XXI; 3C, D) is thin and slightly bent perpendicular to longitudinal axis. Ventrally are identifiable the lateral ossicles of the cardio-pyloric valve (XVIII; Fig. 3C) and the small, paired preampullary-like ossicles (XXII-like). At this stage of development the middle supra-ampullary ossicles (XXIX) are most notable (Fig. 3C).

Foregut of the C_{cl8} Stage

The morphology of the foregut at this stage is adult-like in shape (Fig. 3E,F). All the cardiac and gastric mill associated ossicles have adult morphology; these being: the mesocardiac (I), pterocardiacs (II), zygocardiacs (V), propyloric (VI), urocardiac (VII), pectineal (VIII), prepectineal (IX), postpectineal (X), anterior lateral cardiac plates (XI), posterior lateral cardiac plates (XII), lateral cardiac (XIII), and subdentate (XIV) ossicles (Fig. 3E,F). The C_{CL8} juvenile gastric mill shows an intermediate morphology between the C1 and adult gastric mill. The dorsal tooth supports a well-developed quadrangular dorsal median tooth with two lateral conical cusps on its posterior margin (Figs. 4I and 5C). The lateral teeth show a large anterior and two well-developed ventral cusps more conical than in the adult stage, the surface of the lateral teeth are smooth and clean; no terminal setae have been found posteriorly (Fig. 4E). The accessory teeth are composed of four peaks surrounded laterally by more than 20 large spinous setae (Fig. 5G). Also, the unpaired pyloric ossicle (III; Fig. 3F) has an adult shape, that is, as a broad dorsal plate posterior to the propyloric ossicle (VI). The exopyloric ossicles (IV) were located between the pyloric (III) and the zygocardiac (V) ossicles (Fig. 3F).

The pyloric foregut ossicles also show an adult shape and position. Different to the foregut of C1 stage, however, the foregut of C_{CL8} stage has the lateral mesopyloric (XIXa), the infrauropyloric fragments (XXIa) and the posterior uropyloric ossicles (XXIb) in dorsal position as thin bar-shaped ossicles parallel to the longitudinal axis (Fig. 3E,F). In the cardio-pyloric valve it also can be observed the lateral cardio-pyloric ossicle (XV) dorsal to the anterior supra-ampullary ossicle (XXVIII; Fig. 3E). Dorsal to the pyloric filters and in a similar position as in the adults, there appears the lower and upper portion of the ampullary roof ossicles (XXV-XXVI) appear, now fused with the anterior processes of the ampullary roof ossicles (XXVIa; Fig. 3E).

DISCUSSION

The Adult Foregut

The first description of the foregut morphology in the genus *Maja* (identified as *Maja squinado*) was published by Milne-Edwards (1840). His description included the traditional subdivision in the cardiac and pyloric foregut, the gastric mill and some ossicles that according to Brösing et al. (2002) could be named as: mesocardiac (I), pterocardiacs (II), pyloric (III), zygocardiacs (V), urocardiac (VII), inferior ampullary (XXIV), and two additional unidentified pyloric ossicles. We present a more detailed description of the foregut of *M. brachydactyla*. The foregut ossicles have a relatively constant morphology previously described among species of Majoidea: *Libinia emarginata* Leach, 1815 (Epialtidae) (Meiss and Norman, 1977); *Inachus dorsettensis* (Pennant, 1777) (Inachidae) (Brösing, 2010); and *Maja crispata* Risso, 1827 (Majidae) (Brösing, 2014). Although the morphological pattern of the ossicle system is similar within these species, the similarities are higher between the congeneric majid species *M. brachydactyla* and *M. crispata* (Brösing, 2014). However, our interpretation of the dorsal ossicles is different when compared to the description of *M. crispata* (Brösing, 2014). The pyloric ossicle (III) appears paired in *M. crispata* while in *M. brachydactyla* it appears unpaired, like in *L. emarginata* and

I. dorsettensis. Also, the anterior mesopyloric ossicles (XIX) and the posterior mesopyloric ossicles (XX) of *M. crispata* are interpreted in the present work as the lateral mesopyloric ossicles (XIXa) and the anterior mesopyloric ossicles (XIX), respectively; while the posterior mesopyloric ossicles (XX) of *M. brachydactyla* appears in *M. crispata* scheme as a unlabelled ossicle located anteriorly to the uropyloric ossicle (XXI) in the dorsal view, in the same position as in *I. dorsettensis*. Additionally, the prepterocardiac and postpterocardiac ossicles (IIa and IIb) and the anterior lateral cardiac plates (XI) have been described for the first time in the genus *Maja*. The brachyuran foregut possesses a conservative pattern among the species of one family or among the species of close-related families, which makes them useful for phylogenetic reconstructions (Brösing et al., 2002; Brösing et al., 2007; Brösing, 2010; Reimann et al., 2011). In this sense, our data support the structure of the superfamily Majoidea (Brösing et al., 2007) based in the phylogenetic analysis of the ossicle system: *Hyas araneus* Linnaeus, 1758, *Hyas coarctatus* Leach, 1815 and *Libinia dubia* H. Milne Edwards, 1834 comprising a monophyletic clade with *I. dorsettensis* (Pennant, 1777) as a sister group. The monophyly of the Majoidea superfamily, including the family Inachidae, is supported by larval morphology and genetic studies (Hultgren and Stachowicz, 2008). All these data support the usefulness of the general morphology of the ossicle-system for the phylogenetic studies (Brösing et al., 2002, 2007; Brösing, 2010; Reimann et al., 2011).

The gastric mill is a cardiac structure whose function is to bite and grind the food particles (Nakamura and Takemoto, 1986). In the carnivorous and omnivorous species, the medial tooth possessed a large, rounded posterior process which in action with the smooth surface of the lateral teeth act like a mortar and pestle useful to crush and mill calcified shells (Allardyce and Linton, 2010). We found a similar morphology in the gastric mill of *M. brachydactyla*, and therefore, the ability to crush the mollusc shells, operculi fragments, echinodermata dermic plates, and calcareous seaweeds revealed in the stomach content of wild specimens (Bernárdez et al., 2000) could be expected. However, as *M. brachydactyla* (Bernárdez et al., 2000), some marine brachyuran species studied have opportunistic feeding habits (Cannicci et al., 2007; Norman and Jones, 1992; Vannini et al., 1989). In this sense, the morphology of the gastric mill teeth of these brachyuran crabs will be more closely related to phylogeny rather than to their feeding behavior. Huespe et al. (2008) and Sakai et al. (2006) noted the relevance and utility of the dorsal and lateral gastric mill teeth morphology in taxonomical studies. The morphology of the gastric mill teeth of other species of the superfamily Majoidea belonging to the genera *Inachus* (Brösing, 2010) is clearly different to that of *M. brachydactyla*. These data support the potential utility of the gastric mill for the study of the brachyuran phylogenetic relationships.

The Zoeae Foregut

Like in other Majoidea species, *M. bracydactyla* larval development is abbreviated to two zoeae and one megalopa (Guerao et al., 2008). The description of the morphology of the *M. brachydactyla* zoeae foregut is in agreement with the traditional description for the zoeae foregut among the brachyuran species: a simple structure that lacks the gastric mill and ossicles; with cardiac and pyloric foregut separated by the cardio-pyloric valve, a well-developed structure covered by large thickened setae with a poorly understood role in the processing of food (Abrunhosa and Melo, 2008; Abrunhosa et al., 2003, 2011; Castejón et al., 2015; Lumasag et al., 2007; Melo et al., 2006). The present work described for first time the presence of a calcified cardio-pyloric valve and paired "supra-ampullary ossicle-like" structures in the ZI and ZII stages.

The first zoea of *M. brachydactyla* also has a well-developed pyloric filter. This situation is rather different as compared to other brachyuran species with extended larval development, where their first zoea lacks the pyloric filter or it is undeveloped as in *Ucides cordatus* (Linnaeus, 1763) (Abrunhosa et al., 2003), *Uca vocator* (Herbst, 1804) (Abrunhosa et al., 2011) and *Dyspanopeus sayi* (Smith, 1869) (Castejón et al., 2015). Abbreviated larval development affect the timing of appearance and rate of development of many larval features. These changes in the development can be attributed to heterochronic processes resulting from the dissociation of age, size, and shape between ancestral and descendant ontogeny (Reilly et al., 1997; Raff and Raff, 2000; Clark et al., 2005; Clark, 2005; Gerber and Hopkins, 2011). In *M. brachydactyla*, heterochrony during embryonic development could affect the onset of the pyloric filter, whose appearance is earlier relative to the ancestral condition.

Additionally, some authors (Meiss and Norman, 1977; Icely and Nott, 1992; Abrunhosa et al., 2003, 2011; Melo et al., 2006) suggest that the presence of a pyloric filter in the first zoeae of brachyurans with abbreviated larval development could be related to the life-strategy and feeding behavior; numerous setae and a well-developed pyloric filter are necessary for the processing and mixing of soft food particles. Melo et al. (2006) observed that the first zoea of the brachyuran *Sesarma curacaoense* De Man (1892) is a facultative lecithotrophic, lacking the pyloric filter; while the first zoea of *M. brachydactyla* is an obligatory planktotroph

that must feed to achieve the next stage of development (Guerao et al., 2012). Therefore, we suggest that the pyloric filter is necessary in the zoeae stages to avoid those large food particles that are introduced into the digestive gland and the intestines.

The Megalopae and Juvenile Foregut

After the metamorphosis to megalopa, major changes occur in the foregut with the appearance of the main foregut ossicles and a functional gastric mill. This foregut metamorphosis has been observed in other brachyuran species as *D. sayi* (Smith, 1869) (Panopeidae) (Castejón et al., 2015), *Menippe mercenaria* Say, 1818 (Oziidae) (Factor, 1982), *Panopeus occidentalis* De Saussure, 1857 (Panopeidae) (Abrunhosa et al., 2011), *Sesarma rectum* Randall, 1840 (Sesarmidae) (Abrunhosa and Melo, 2008), *U. vocator* (Herbst, 1804) (Ocypodidae) (Abrunhosa et al., 2011) and *U. cordatus* (Linnaeus, 1763) (Ucididae) (Abrunhosa et al., 2003).

As a consequence of the zoeal metamorphosis of the brachyuran crabs, Factor (1981, 1982) suggests that the mastication of food shifts from the mandibles to the gastric mill. These morphological changes from the zoea foregut to the megalopa foregut could correspond to changes in the environment and diet that take place at metamorphosis, when the previously planktonic larvae begin their benthic life and there is a need to process food more efficiently in this new environment. In this sense, some authors also described an inverse relation in complexity between gastric mill and mouthparts, where in many taxa the increase of complexity in the gastric mill is parallel to a decrease of complexity in mouthparts (Guillaume and Ceccaldi, 2001; Meiss and Norman, 1977). In *M. brachydactyla*, Guerao et al. (2008) also observed that mandibles morphology was simplified after metamorphosis and in the present study we observed the complexity of the gastric mill after the metamorphosis.

In the present study, the ontogenetic changes in the morphology of the ossicle-system and gastric mill teeth from megalopa to adult stage are described for the first time in brachyuran crabs. The megalopa cardiac foregut ossicles are similar to their counterparts in the juveniles and adult stages. A similar situation has been observed in the megalopa foregut of *D. sayi* (Castejón et al., 2015). We suggest that the advanced adult-like morphology of the megalopa cardiac foregut could be related with the functional requirements of the gastric mill (Factor, 1982; Nakamura and Takemoto, 1986; Woods, 1995). On the contrary, as has been observed in *D. sayi* (Castejón et al., 2015), the megalopa pyloric foregut lacks many adult ossicles and show other ossicles that cannot be identify properly in the juvenile or adult foregut: the middle supra-ampullary-like (XXIX-like), the posterior uropyloric-like (XXIb-like), the middle pleuropyloric-like (XXXII-like) and the posterior pleuropyloric-like ossicles (XXXIII-like). The definitive adult-shape ossicles gradually appear during the postlarval development. This gradual development could be explained if the pyloric foregut did not require highly specialized associated ossicles during the earlier developmental stages, as has been observed in the zoeal phase. These present results also reveals that the morphology of megalopa gastric mill teeth of *M. brachydactyla* is rather different from the adult gastric mill teeth, as was described previously in *D. sayi* (Castejón et al., 2015). Additionally, in both species the dorsal tooth of the megalopa gastric mill showed a similar structure: lateral spines and a small and dentate cusp. The first juvenile gastric mill is similar to the megalopa gastric mill, remaining different to that of the adult in shape and morphometric structure, while the gastric mill of the C_{CL8} juveniles have an intermediate morphology between that of the first juvenile and the adult. Factor (1982) also showed that the juvenile gastric mill of the stone crab *M. mercenaria* has a slightly different morphology from the adult gastric mill, but no details about the age or size of juveniles were provided.

These changes in gastric mill morphology could be related to modifications in prey preferences and/or prey availability in the new environments. Relationship between the diet and crab size has been described in many brachyuran species: the small individuals of *Matuta lunaris* (Forskål, 1775) fed primarily on small crustaceans (sergestids and copepods) while large individuals fed primarily on anomurans and gastropods (Perez and Bellwood, 1988); the predation over the polychaetes increases with the size of the crab in *Chionoecetes opilio* (Fabricius, 1788) (Kolts et al., 2013); the juveniles of *Callinectes sapidus* (Rathbun, 1896) ingest more polychaetes and less bivalves and crustaceans than the adults (Seitz et al., 2011). Additionally, prey size selection in relation to corporal size has been observed in the brachyuran *Carcinus maenas* (Linnaeus, 1758) and *Cancer pagurus* Linnaeus, 1758 (Mascaró and Seed, 2001). The ontogenetic change in the diet also has been reported in other decapoda groups, for example, the Caridea *Palaemon serratus* (Pennat, 1777) (Guerao and Ribera, 1996), the Achelata *Jasus lalandii* (Milne-Edwards, 1837) (Haley et al., 2011) or the Achelata *Panulirus argus* (Latreille, 1804) (Briones-Fourzán et al., 2003). Therefore, we suggest that the morphology of the teeth (with sharper and less crushing cusps) of the megalopae and earlier juveniles could be related with a soft prey diet such as copepods and amphipods; while the molariform structure of the

adult teeth is suitable for crushing food pieces protected by hard shells (bivalves, gastropods, echinoderms, and calcareous seaweeds) as feeding studies have demonstrated (Bernárdez et al., 2000). For elucidation of this hypothesis, further studies on the relation of the natural diet of the megalopa and earlier juvenile stages of *M. brachydactyla* are needed.

ACKNOWLEDGMENTS

The authors would like to thank Karl B. Andree and Alicia Estevez for their comments that have greatly improved the article. The authors are grateful to the personnel of the Scientific Technical Services of Barcelona University for their support in sample preparation for SEM observations. We thank hatchery technician at IRTA in Sant Carles de la Ràpita.

LITERATURE CITED

Abelló P, García Raso JE, Guerao G, Salmerón F. 2014. *Maja brachydactyla* (Brachyura: Majidae) in the western Mediterranean. Mar Biodivers Rec 7:e77

Abrunhosa FA, Melo M. 2008. Development and functional morphology of the foreguts of larvae and postlarvae of three crustacean decapods. Braz J Biol 68:221–228.

Abrunhosa FA, Melo MA, Abrunhosa JP. 2003. Development and functional morphology of the foregut of larvae and postlarva of *Ucides cordatus* (Decapoda, Ocypodidae). Nauplius 11:37–43.

Abrunhosa FA, Simith DJB, Monteiro JRC, dSouza AN Jr, Oliva PAC. 2011. Development and functional morphology of the larval foregut of two brachyuran species from Northern Brazil. An Acad Bras Cienc 83:1269–1278.

Alaminos J. 2011. Efecto del confinamiento en espacios reducidos sobre el crecimiento de juveniles de centollo, *Maja brachydactyla*, y su repercusión en la madurez. Rev Biol Mar Oceanogr 46:219–230.

Alaminos J, Domingues P. 2008. Effects of different natural or prepared diets on growth and survival of juvenile spider crabs, *Maja brachydactyla* (Balss, 1922). Aquaculture Int 16: 417–425.

Allardyce BJ, Linton SM. 2010. Functional morphology of the gastric mills of carnivorous, omnivorous, and herbivorous land crabs. J Morphol 271:61–72.

Andrés M, Estévez A, Rotllant G. 2007. Growth, survival and biochemical composition of spider crab *Maja brachydactyla* (balss, 1922) (Decapoda: Majidae) larvae reared under different stocking densities, prey: larva ratios and diets. Aquaculture 273:494–502.

Andrés M, Estévez A, Anger K, Rotllant G. 2008. Developmental patterns of larval growth in the edible spider crab, *Maja brachydactyla* (Decapoda: Majidae). J Exp Mar Biol Ecol 357: 35–40.

Andrés M, Gisbert E, Díaz M, Moyano FJ, Estévez A, Rotllant G. 2010. Ontogenetic changes in digestive enzymatic capacities of the spider crab, *Maja brachydactyla* (Decapoda: Majidae). J Exp Mar Biol Ecol 389:75–84.

Andrés M, Rotllant G, Sastre M, Estevez A. 2011. Replacement of live prey by formulated diets in larval rearing of spider crab *Maja brachydactyla*. Aquaculture 313:50–56.

Bernárdez C, Freire J, González-Gurriarán E. 2000. Feeding of the spider crab *Maja squinado* in rocky subtidal areas of the ría de arousa (North-West Spain). J Mar Biol Assoc UK 80: 95–102.

Briones-Fourzán P, Castañeda-Fernández de Lara V, Lozano-Álvarez E, Estrada-Olivo J. 2003. Feeding ecology of the three juvenile phases of the spiny lobster *Panulirus argus* in a tropical reef lagoon. Mar Biol 142:855–865.

Brösing A. 2010. Recent developments on the morphology of the brachyuran foregut ossicles and gastric teeth. Zootaxa 2510: 1–44.

Brösing A. 2014. Foregut structures of freshly moulted exuviae from *Maja crispata*, *Cancer pagurus* and *Pseudosesarma moeschi* (Decapoda: Brachyura). J Nat Hist 48:543–555.

Brösing A, Türkay M. 2011. Gastric teeth of some thoracotreme crabs and their contribution to the brachyuran phylogeny. J Morphol 272:1109–1115.

Brösing A, Richter S, Scholtz G. 2002. The foregut-ossicle system of *Dromia wilsoni*, *Dromia personata* and *Lauridromia intermedia* (Decapoda, Brachyura, Dromiidae), studied with a new staining method. Arthropod Struct Dev 30:329–338.

Brösing A, Richter S, Scholtz G. 2007. Phylogenetic analysis of the Brachyura (Crustacea, Decapoda) based on characters of the foregut with establishment of a new taxon. J Zool Syst Evol Res 45:20–32.

Cannicci S, Gomei M, Dahdouh-Guebas F, Rorandelli R, Terlizzi A. 2007. Influence of seasonal food abundance and quality on the feeding habits of an opportunistic feeder, the intertidal crab *Pachygrapsus marmoratus*. Mar Biol 151:1331–1342.

Castejón D, Ribes E, Durfort M, Rotllant G, Guerao G. 2015. Foregut morphology and ontogeny of the mud crab *Dyspanopeus sayi* (Smith, 1869) (Decapoda, Brachyura, Panopeidae). Arthropod Struct Dev 44:33–41.

Clark PF. 2005. The evolutionary significance of heterochrony in the abbreviated zoeal development of pilumnine crabs (Crustacea: Brachyura: Xanthoidea). Zool J Linn Soc 143: 417–446.

Clark PF, Ng PKL, Noho H, Shokita S. 2005. The first-stage zoeas of *Carpilius convexus* (Forskål, 1775) and *Carpilius maculatus* (Linnaeus, 1758) (Crustacea: Decapoda: Brachyura: Xanthoidea: Carpiliidae): An example of heterochrony. J Plankton Res 27:211–219.

Domingues P, Alaminos J. 2008. Efectos de la densidad de cultivo y de elementos de refugio en el crecimiento y supervivencia de juveniles de centollo, *Maja brachydactyla* (Balss, 1922). Rev Biol Mar Oceanogr 43:121–127.

Domingues P, Alaminos J, García-Garrido S, Hachero-Cruzado I, Rosas C. 2012. Growth and survival of juvenile spider crabs, *Maja brachydactyla* (Balss, 1922), fed with fresh or frozen mussels. Aquac Res 43:167–177.

Factor JR. 1981. Development and metamorphosis of the digestive system of larval lobsters, *Homarus americanus* (Decapoda: Nephropidae). J Morphol 169:225–242.

Factor JR. 1982. Development and metamorphosis of the feeding apparatus of the stone crab, *Menippe mercenaria* (Brachyura, Xanthidae). J Morphol 172:299–312.

Felgenhauer BE. 1992. Internal Anatomy of the Decapoda: An Overview, Chapter 3. In: Harrison FW, Humes AG, editors. Microscopic Anatomy of Invertebrates. Wiley-Liss Inc., 45–75.

Gerber S, Hopkins MJ. 2011. Mosaic heterochrony and evolutionary modularity: The trilobite genus *Zacanthopsis* as a case study. Evolution 65:3241–3252.

Guerao G, Ribera C. 1996. Locomotor activity patterns and feeding habits in the prawn *Palaemon serratus* (Pennant, 1777) (Decapoda, Palaemonidae) in the alfacs bay, ebro delta, Spain. Crustaceana 69:101–112.

Guerao G, Rotllant G. 2010. Development and growth of the early juveniles of the spider crab *Maja squinado* (Brachyura: Majoidea) in an individual culture system. Aquaculture 307:105–110.

Guerao G, Pastor E, Martin J, Andrés M, Estévez A, Grau A, Duran J, Rotllant G. 2008. The larval development of *Maja squinado* and *M. Brachydactyla* (Decapoda, Brachyura, Majidae) described from plankton collected and laboratory-reared material. J Nat Hist 42:2257–2276.

Guerao G, Rotllant G, Anger K. 2010. Characterization of larval moulting cycles in *Maja brachydactyla* (Brachyura, Majidae) reared in the laboratory. Aquaculture 302:106–111.

Guerao G, Simeó CG, Anger K, Urzúa Á, Rotllant G. 2012. Nutritional vulnerability of early zoea larvae of the crab *Maja brachydactyla* (Brachyura, Majidae). Aquat Biol 16:253–264.

Guillaume J, Ceccaldi HJ. 2001. Digestive physiology of shrimps. In: Guillaume J, Kaushik S, Bergot P, Metailler R, editors. Nutrition and Feeding of Fish and Crustaceans. Chichester: Springer-Praxis. p 239–263.

Haley CN, Blamey LK, Atkinson LJ, Branch GM. 2011. Dietary change of the rock lobster *Jasus lalandii* after an 'invasive' geographic shift: effects of size, density and food availability. Estuar Coast Shelf Sci 93:160–170.

Huespe AV, Gámez-Simes E, Pastor-de-Ward CT. 2008. Gastric mill morphology in the genus *Cyrtograpsus* (Crustacea: Decapoda: Grapsoidea: Varunidae). J Mar Biol Assoc UK 88:311–319.

Hultgren KM, Stachowicz JJ. 2008. Molecular phylogeny of the brachyuran crab superfamily Majoidea indicates close congruence with trees based on larval morphology. Mol Phylogenet Evol 48:986–996.

Icely JD, Nott JA. 1992. Digestion and absorption: Digestive system and associated organs. In: Harrison FW, Humes AG, editors. Microscopic Anatomy of Invertebrates: Decapod Crustacea. New York: Wiley-Liss. p 147–201.

Kolts JM, Lovvorn JR, North CA, Grebmeier JM, Cooper LW. 2013. Effects of body size, gender, and prey availability on diets of snow crabs in the Northern Bering sea. Mar Ecol Prog Ser 483:209–220.

Lin F-Y. 2000. Scanning electron microscopic observations on the gland filters of the pyloric stomach of *Penaeus monodon* and *Metapenaeus ensis* (Decapoda, Penaeidae). Crustaceana 73:163–174.

Lumasag GJ, Quinitio ET, Aguilar RO, Baldevarona RB, Saclauso CA. 2007. Ontogeny of feeding apparatus and foregut of mud crab *Scylla serrata* Forsskål larvae. Aquac Res 38:1500–1511.

Mascaró M, Seed R. 2001. Foraging behavior of juvenile *Carcinus maenas* (L.) and *Cancer pagurus* L. Mar Biol 139:1135–1145.

Meiss DE, Norman RS. 1977. Comparative study of the stomatogastric system of several decapod crustacea. I. Skeleton. J Morphol 152:21–53.

Melo MA, Abrunhosa F, Sampaio I. 2006. The morphology of the foregut of larvae and postlarva of *Sesarma curacaoense* De Man, 1892: A species with facultative lecithotrophy during larval development. Acta Amazon 36:375–380.

Milne-Edwards H. 1840. Histoire Naturelle des Crustacés: Atlas. Paris: Libraire Encyclopédique de Roret, Rue Hautefuille 10 bis. 132 p.

Nakamura K, Takemoto T. 1986. Morphology of stomach ossicles in Brachyura. Memoirs of Faculty of Fisheries Kagoshima University 35:7–15.

Norman CP, Jones MB. 1992. Influence of depth, season and moult stage on the diet of the velvet swimming crab *Necora puber* (Brachyura, Portunidae). Estuar Coast Shelf Sci 34:71–83.

Palma J, Correia M, Andrade JP. 2008. Usefulness of flat bottom tanks on the settlement of spider crab (*Maja squinado*, Herbst) larvae. Aquac Res 39:1005–1008.

Perez O, Bellwood D. 1988. Ontogenetic changes in the natural diet of the sandy shore crab, *Matuta lunaris* (Forskål) (Brachyura: Calappidae). Mar Freshw Res 39:193–199.

Raff EC, Raff RA. 2000. Dissociability, modularity, evolvability. Evol Dev 2:235–237.

Reilly SM, Wiley EO, Meinhardt DJ. 1997. An integrative approach to heterochrony: The distinction between interspecific and intraspecific phenomena. Biol J Linn Soc Lond 60: 119–143.

Reimann A, Richter S, Scholtz G. 2011. Phylogeny of the Anomala (Crustacea, Decapoda, Reptantia) based on the ossicles of the foregut. Zool Anz J Comp Zool 250:316–342.

Rotllant G, González-Gurriarán E, Fernández L, Benhalima K, Ribes E. 2007. Ovarian maturation of the multi-spawning spider crab *Maja brachydactyla* (Decapoda: Majidae) with special reference to yolk formation. Mar Biol 152:383–394.

Sakai K, Türkay M, Yang S-L. 2006. Revision of the *Helice*/*Chasmagnathus* complex (Crustacea: Decapoda: Brachyura). Abh Senckenb Naturforsch Ges 565:1–76.

Schaefer N. 1970. The functional morphology of the foregut of three species of decapod crustacea: *Cyclograpsus punctatus* Milne-edwards, *Diogenes brevirostris* Stimpson, and *Upogebia africana* (Ortmann). Zool Afr 5:309–326.

Seitz RD, Knick KE, Westphal M. 2011. Diet selectivity of juvenile blue crabs (*Callinectes sapidus*) in Chesapeake Bay. Integr Comp Biol 51:598–607.

Simeó CG, Kurtz K, Rotllant G, Chiva M, Ribes E. 2009a. Sperm ultrastructure of the spider crab *Maja brachydactyla* (Decapoda: Brachyura). J Morphol 271:407–417.

Simeó CG, Ribes E, Rotllant G. 2009b. Internal anatomy and ultrastructure of the male reproductive system of the spider crab *Maja brachydactyla* (Decapoda: Brachyura). Tissue Cell 41:345–361.

Simeó CG, Kurtz K, Chiva M, Ribes E, Rotllant G. 2010. Spermatogenesis of the spider crab *Maja brachydactyla* (Decapoda: Brachyura). J Morphol 271:394–406.

Skilleter G, Anderson D. 1986. Functional morphology of the chelipeds, mouthparts and gastric mill of *Ozius truncatus* (Milne Edwards) (Xanthidae) and *Leptograpsus variegatus* (Fabricius) (Grapsidae) (Brachyura). Mar Freshw Res 37:67–79.

Sotelo G, Morán P, Posada D. 2009. Molecular phylogeny and biogeographic history of the European *Maja* spider crabs (Decapoda, Majidae). Mol Phylogenet Evol 53:314–319.

Stein W. 2009. Modulation of stomatogastric rhythms. J Comp Physiol 195:989–1009.

Vannini M, Chelazzi G, Gherardi F. 1989. Feeding habits of the pebble crab *Eriphia smithi* (Crustacea, Brachyura, Menippidae). Mar Biol 100:249–252.

Verísimo P, Bernárdez C, González-Gurriarán E, Freire J, Muino R, Fernández L. 2011. Changes between consecutive broods in the fecundity of the spider crab, *Maja brachydactyla*. ICES J Mar Sci 68:472–478.

Woods CMC. 1995. Morphology of the foregut of the spider crab *Notomithrax ursus* (Brachyura: Majidae). J Crust Biol 15:220–227.

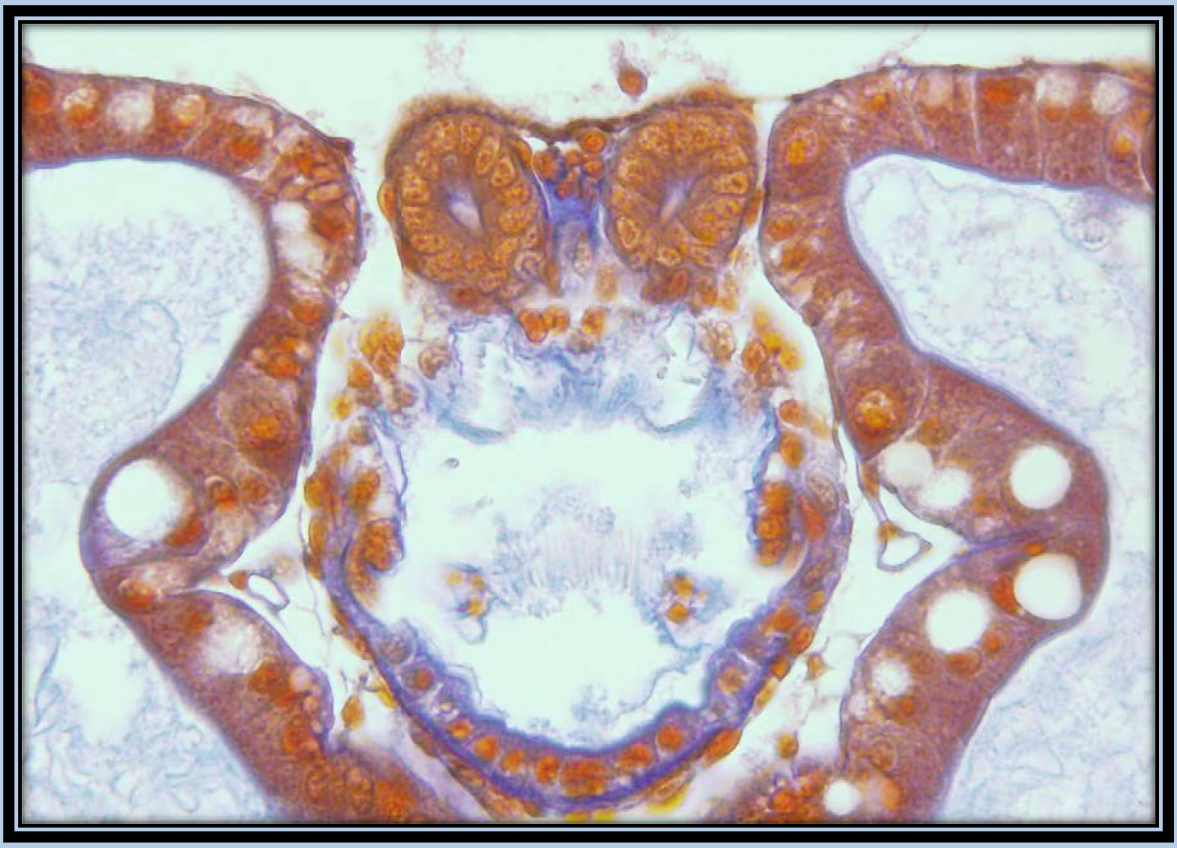

The present Doctoral Thesis is framed in the research toward the profitable culture of the common spider crab (*Maja brachydactyla* Balss, 1922) focusing in two topics: the improvement of the larval culture and the description of the digestive system. Our results conclude that the optimal parameters were: 21 ± 1 °C, 35 ± 1 psu and a daily light-dark cycle. Temperature influences the duration of the larval development, salinity the survival and light have a poor influence. This species does not have special requirements for settlement.

The basic morphology of the digestive system is conserved during all the life stages. The main differences rely on the higher development of connective and muscles in adult specimens comparing to larval stages. The biggest change occur in the stomach, since acquires cardiac sacs, ossicle system and gastric mill after the molt to megalopa. The caeca of the midgut gland (hepatopancreas) are very similar between larvae and adults, but their number increases from fourteen in the larvae to tens of thousands in the adults. The esophagus and hindgut tract are characterized by the presence of a cuticle with microspines and rosette glands in the connective. The midgut gland, midgut tract and midgut caeca are very rich in microvilli. The midgut gland realizes absorptive and secretory functions, the midgut tract secretes the peritrophic membrane and the midgut caeca realizes an important secretory activity. For first time, the "micro-apocrine" secretion is described in decapods.